frontiers | Research Topics

Management of rare oncological cases

Edited by
Dragos Eugen Georgescu, Lidia Castagneto Gissey and Ferdinando Agresta

Coordinated by
Mihai Teodor Georgescu

Published in
Frontiers in Oncology

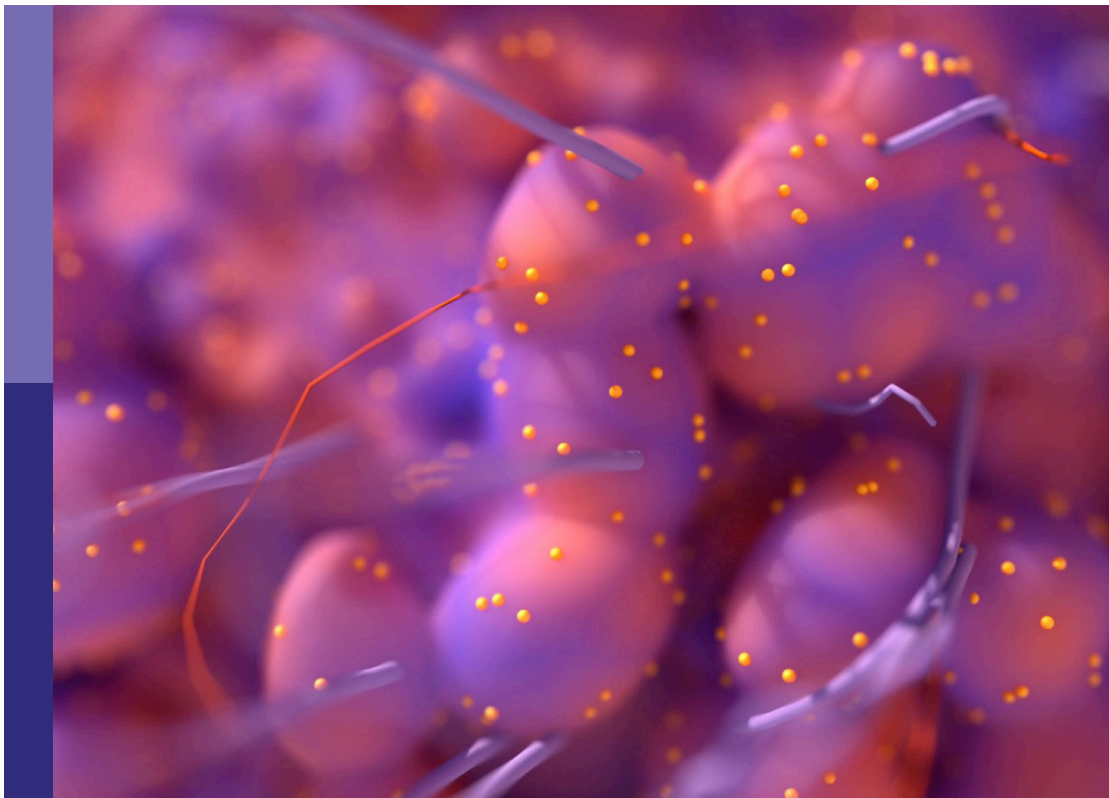

FRONTIERS EBOOK COPYRIGHT STATEMENT

The copyright in the text of individual articles in this ebook is the property of their respective authors or their respective institutions or funders. The copyright in graphics and images within each article may be subject to copyright of other parties. In both cases this is subject to a license granted to Frontiers.

The compilation of articles constituting this ebook is the property of Frontiers.

Each article within this ebook, and the ebook itself, are published under the most recent version of the Creative Commons CC-BY licence. The version current at the date of publication of this ebook is CC-BY 4.0. If the CC-BY licence is updated, the licence granted by Frontiers is automatically updated to the new version.

When exercising any right under the CC-BY licence, Frontiers must be attributed as the original publisher of the article or ebook, as applicable.

Authors have the responsibility of ensuring that any graphics or other materials which are the property of others may be included in the CC-BY licence, but this should be checked before relying on the CC-BY licence to reproduce those materials. Any copyright notices relating to those materials must be complied with.

Copyright and source acknowledgement notices may not be removed and must be displayed in any copy, derivative work or partial copy which includes the elements in question.

All copyright, and all rights therein, are protected by national and international copyright laws. The above represents a summary only. For further information please read Frontiers' Conditions for Website Use and Copyright Statement, and the applicable CC-BY licence.

ISSN 1664-8714
ISBN 978-2-8325-6903-0
DOI 10.3389/978-2-8325-6903-0

Generative AI statement
Any alternative text (Alt text) provided alongside figures in the articles in this ebook has been generated by Frontiers with the support of artificial intelligence and reasonable efforts have been made to ensure accuracy, including review by the authors wherever possible. If you identify any issues, please contact us.

About Frontiers

Frontiers is more than just an open access publisher of scholarly articles: it is a pioneering approach to the world of academia, radically improving the way scholarly research is managed. The grand vision of Frontiers is a world where all people have an equal opportunity to seek, share and generate knowledge. Frontiers provides immediate and permanent online open access to all its publications, but this alone is not enough to realize our grand goals.

Frontiers journal series

The Frontiers journal series is a multi-tier and interdisciplinary set of open-access, online journals, promising a paradigm shift from the current review, selection and dissemination processes in academic publishing. All Frontiers journals are driven by researchers for researchers; therefore, they constitute a service to the scholarly community. At the same time, the *Frontiers journal series* operates on a revolutionary invention, the tiered publishing system, initially addressing specific communities of scholars, and gradually climbing up to broader public understanding, thus serving the interests of the lay society, too.

Dedication to quality

Each Frontiers article is a landmark of the highest quality, thanks to genuinely collaborative interactions between authors and review editors, who include some of the world's best academicians. Research must be certified by peers before entering a stream of knowledge that may eventually reach the public - and shape society; therefore, Frontiers only applies the most rigorous and unbiased reviews. Frontiers revolutionizes research publishing by freely delivering the most outstanding research, evaluated with no bias from both the academic and social point of view. By applying the most advanced information technologies, Frontiers is catapulting scholarly publishing into a new generation.

What are Frontiers Research Topics?

Frontiers Research Topics are very popular trademarks of the *Frontiers journals series*: they are collections of at least ten articles, all centered on a particular subject. With their unique mix of varied contributions from Original Research to Review Articles, Frontiers Research Topics unify the most influential researchers, the latest key findings and historical advances in a hot research area.

Find out more on how to host your own Frontiers Research Topic or contribute to one as an author by contacting the Frontiers editorial office: frontiersin.org/about/contact

Management of rare oncological cases

Topic editors
Dragos Eugen Georgescu — Carol Davila University of Medicine and Pharmacy, Romania
Lidia Castagneto Gissey — Sapienza University of Rome, Italy
Ferdinando Agresta — ULSS2 Marca Trevigiana, Italy

Topic coordinator
Mihai Teodor Georgescu — Carol Davila University of Medicine and Pharmacy, Romania

Citation
Georgescu, D. E., Castagneto Gissey, L., Agresta, F., Georgescu, M. T., eds. (2025). *Management of rare oncological cases*. Lausanne: Frontiers Media SA.
doi: 10.3389/978-2-8325-6903-0

Table of contents

10 Editorial: Management of rare oncological cases
Lidia Castagneto-Gissey, Dragos Eugen Georgescu and Ferdinando Agresta

15 Gemcitabine combination therapies induce apoptosis in uterine carcinosarcoma patient-derived organoids
Matías J. Dahl, Kristopher A. Lofgren, Cleo Haugen, Gil E. Harmon, Sarah P. Hughes and Karen D. Cowden Dahl

28 Misleading clinical and imaging features in atypical aggressive angiomyxoma of the female vulvovaginal or perianal region: report of three cases and review of the literature
Ling Zhang, Rong Liu and Jian Peng

38 Corrigendum: Misleading clinical and imaging features in atypical aggressive angiomyxoma of the female vulvovaginal or perianal region: report of three cases and review of the literature
Ling Zhang, Rong Liu and Jian Peng

41 Paratesticular metastasis from colorectal adenocarcinoma presenting as hydrocele: a rare case report and literature review
XiaoJun Huang, KeLi Xu, Yin Zhao, MinHui Chen and ZheYang Li

47 Case report: Unusual breast cancer metastasis manifesting as a scalp lesion in a patient with invasive lobular carcinoma
Nam Hee Koh and Ha Yeun Oh

53 Successful application of chemosaturation with percutaneous hepatic perfusion in metastatic uveal melanoma patient progressing after systemic treatment options: a case report
Damla Gunenc, Ahmet Anil Ozluk, Utku Mahir Yıldırım, Paolo A. Ascierto and Burcak Karaca

60 Ewing sarcoma of the pancreas: a pediatric case report and narrative literature review
Zhensheng Liu, Jian Bian, Yong Yang, Decheng Wei and Shiqin Qi

70 Case report: Report of a rare encounter: metastasis of renal cell carcinoma to the thyroid
Siyi Xu, Jiawei Xu, Chengdong Yu, Ying Zeng, Lei Tang, Mu Tang, Tenghua Yu, Zhengkui Sun and Xiaofang Zhang

78 Epidemiology of the non-head and neck sebaceous carcinoma and implications for distant metastasis screening
Xi Chen, Yangyang Hao, Mengwei Chou and Jianqiang Yang

85 Myofibroblastic sarcoma in breast: a case report and literature review
Zixi Deng, Chuan Xia, Yuechong Li, Yongchao Luo and Songjie Shen

93 Prognostic factors in uterine adenosarcoma: subanalysis of the SARCUT study
Rosanna Mancari, Yildirim Yusuf, Ronalds Macuks, Patriciu Achimas-Cadariu, Jurgen Martinus Piek, Isabella Sperduti, Giacomo Corrado, Enrico Vizza and Ignacio Zapardiel

101 Breast metastasis from lung adenocarcinoma: a case report and review of the literature
Jialing Ding, Huayan Gu, Zhi Yang, Yiqiao Lu and Guilong Guo

106 Recurrent mucinous carcinoma with sarcomatoid and sarcomatous mural nodules: a case report and literature review
Simin Li, Jingyu Zhu, Na Jiang, Yanping Guo, Meng Hou, Xi Liu, Jin Yang and Xiaofeng Yang

115 Case report: An uncommon presentation of extramedullary plasmacytoma without a concurrent diagnosis of multiple myeloma
Katarzyna Stawarz, Adam Galazka, Anna Gorzelnik, Monika Durzynska, Karolina Bienkowska-Pluta and Jakub Zwolinski

122 Extranodal marginal zone lymphoma of mucosa-associated lymphoid tissue of the ileum in an adult presenting with intussusception: a case report and literature review
Binlin Da, Juanjuan Zhang, Feng Zhu, Zhiming Wang and Yanqing Diao

129 Ultrasonographic and clinicopathological features of pelvic yolk sac tumors in women: a single-center retrospective analysis
Mei Chen, Shengmin Zhang, Xiupeng Jia, Youfeng Xu, Yaping Wei and Shusheng Liao

141 Primary cervical malignant melanoma that was successfully treated with pembrolizumab: a case report and literature review
Mengpei Zhang, Rutie Yin, Liang Song, Lan Zhong and Ruiyu Wang

148 Primary retroperitoneal müllerian adenocarcinoma: a case report
Xiaohui Feng, Ping Zhang and Feng Gao

152 Case report: Magnetic resonance imaging findings of patients with diffuse uterine leiomyomatosis
Zanhua Zhang, Xianhui Lin, Xue Wang, Fang He, Weiwei Cai, Xiaoyan Min and Fei Xiang

158 Radiation and systemic immunotherapy for metastatic uveal melanoma: a clinical retrospective review
Danielle H. Tran, Ryan Shanley, Alessio Giubellino, Peter H. Tang, Dara D. Koozekanani, Jianling Yuan, Kathryn Dusenbery and Evidio Domingo-Musibay

167 Clinical and pathological characteristics of cervical clear cell carcinoma in patients not exposed to diethylstilbestrol: a comprehensive analysis of 49 cases
Jing Zeng, Wei Jiang, Kemin Li, Mengpei Zhang, Jinghong Chen, Yuanqiong Duan, Qingli Li and Rutie Yin

176 Testicular choriocarcinoma with pelvic and pulmonary metastases: a case report
Xin Bai, Xiao H. Liu, Hai W. Liang, Yi S. Li, Biao F. Shan and Jian M. Tang

181 Merkel cell carcinoma: updates in tumor biology, emerging therapies, and preclinical models
Elisabeth A. Pedersen, Monique E. Verhaegen, Mallory K. Joseph, Kelly L. Harms and Paul W. Harms

205 Unusual adult-onset cardiac rhabdomyomas in tuberous sclerosis complex: a case report
H. A. Nati-Castillo, Juan Manuel Quintero, Oswaldo Aguilar Molina, Marlon Arias-Intriago, Fernando P. Melgar Muñoz and Juan S. Izquierdo-Condoy

210 Regorafenib-related erythrocytosis in metastatic extra-gastrointestinal stromal tumor: a case report
Elena Fassi, Vito Amoroso, Deborah Cosentini, Vittorio Ferrari, Marta Laganà, Alfredo Berruti and Pierluigi di Mauro

215 Intraperitoneal spread in uterine sarcoma following unprotected laparoscopic transvaginal uterine morcellation: a case report and literature review
Jianhao Sun, Xinjuan Jiao, Zhenzhen Wu, Tingting Yao, Shumei Tuo, Yueyuan Wang, Ruirong Chen, Jing He, Jifang Qian, Shengfang Xu and Qing Liu

221 Case report: Ovarian mucinous tumor with a mural nodule of liposarcoma: a rare case
Jiezhen Li, Haijian Huang, Qiang Zeng, Xin Chen and Lingfeng Chen

229 Clinicopathological and molecular features of tubo-ovarian carcinosarcomas: a series of 51 cases
Fan Liang, Yue Shi, Yiqing Chen, Xiang Tao and Jingxin Ding

242 Letter to the editor regarding “Giant mucinous cystadenocarcinoma of ovary in a young woman: a case report and review of literature” Volume 14 2024
Lisa Feinstein

244 Case report: Clinicopathological characteristic of two cases of primary endometrial squamous cell carcinoma and review of the literature
Hui-Bin Zhang, Li-Hua Lin, Qiu-Ping Lin, Yuan-Qing Lin, Dan Luo and Shu-Xia Xu

251 A rare case of solitary plasmacytoma mimicking submucosal lesion of ascending colon: a case report and literature review
Alessandra Carella, Francesco Spannella, Sonia Morè, Riccardo Grifoni, Carlo Romano Settanni, Alessandra Mandolesi, Alessandra Filosa, Gaia Goteri, Gianfranco Boccoli and Giammarco Fava

256 Giant ovarian yolk sac tumor during late pregnancy: a case report and literature review
Qin Wang, Jianxin Zuo, Chong Liu, Huansheng Zhou, Wenjie Wang and Yankui Wang

263 Radiotherapy can improve overall survival in patients with lymph-node positive, high-grade neuroendocrine cervical cancer: construction of two prognostic nomograms to predict treatment outcome
Siying Zhang, Qinke Li, Xiping Ouyang, Ya Tang, Ji Cui and Zhu Yang

276 Case report: Report of a case of female adnexal malignant tumor of Wolffian origin
Shujun Ji, Xiao Yu, Yufang Xia, Yifan Yin, Tingting Ge, Lihua Cheng, Cui Tian and Yanhui Lou

282 Malignant granular cell tumor of chest wall: a case report
Fabiano Flauto, Alberto Servetto, Roberto Bianco and Luigi Formisano

289 Uterine inflammatory myofibroblastic tumor: a retrospective analysis
Liping Bai, Ling Han, Ai Zheng and Yali Chen

298 Case report: Conjunctival melanoma treated with relatlimab and nivolumab showing remarkable response
Mirona Attrash, Omar Badran, Yinon Shapira and Gil Bar-Sela

302 Urachal adenocarcinoma with cervical invasion misdiagnosed as primary cervical adenocarcinoma: a case report and literature review
Yiran Wang, Maomao Li, Kaixuan Yang, Qingli Li and Ping Wang

310 Recurrent giant cystic lymphangioma of peritoneum: a case report and literature review
Hongyan Lei, Jinxin Sun, Yongzhou Wang and Tao Ye

315 Case report: A case of intercostal intramuscular hemangioma with sternal invasion
Dongdong Liu, Yuchen Bao, Yanzhe Wang, Xiangjun Lu, Jian Shen, Siyuan Huang, Ming Zhao and Haitao Wang

321 Mullerian adenosarcoma accidentally detected and coexisting with cervical carcinoma *in situ*: a rare case report
Xuemei Qing, Min Xie, Hongying Guo, Liying Zhang, Jiatian Ye, Yong Zhang and Ying Ma

330 Clinicopathological correlations in 38 cases of gastroenteropancreatic high-grade neuroendocrine neoplasms
Na Li, Yanping Hu, Linguo Wu and Jianduo An

341 Case report: Advanced breast cancer with scalp metastases: a report of two cases
Jiaxuan Yu, Tianze Yao, Min Zhang, Bingxin Li and Yongqiang Yao

347 Case report: Long-term progression-free survival in advanced ovarian cancer treated with apatinib in first-line maintenance treatment
Ning Zan, Xuan Zhang, Danfei Yu, Juan Liu, Zhiyu Lin and Yanlin Zhu

352 Ultrasound findings of ovarian intravenous leiomyomatosis: a case report
Jin Li and Le Luo

358 Primary hepatoid adenocarcinoma of the lung in patient with silicosis: a case report and literature review
Lipeng Huang, Chaoyang Chen, Qingyu Sun, Zhichen Yu, Xiaoyan Wang, Xinle Wang, Shuoqi Yang, Luming Jin and Liang Bu

367 Perivascular epithelioid cell tumor of the uterus and pelvic cavity
Xiuzhang Yu, Ruiqi Duan, Bowen Yang, Liyan Huang, Minmin Hou and Mingrong Qie

377 Uterine smooth muscle tumors of uncertain malignant potential: a 13-year retrospective study
Liuliu Liu, Zhendong Xiao, Zhiwen Li, Jinyu Zheng, Xiaofeng Xu and Huaijun Zhou

390 A case of ovarian mesothelioma with VHL mutation diagnosed by immunohistochemistry and literature review
Ye Yao, Hao Yan, Jing Xiong and Yaqi Duan

400 Case report: Metastatic endocrine mucin-producing sweat gland carcinoma with features of mucinous carcinoma
Yuehua Sun, Yingchun Liu, Chuntao Li, Xiaodong Zhang, Lu Yin and Jun Niu

406 Undifferentiated endometrial carcinoma diagnosed during perimenopausal hormone therapy: a case report and literature review
Ying Wang, Yu-Tong Zheng, Ling Zhang, Xue-Quan Cao, Zhu Lin, Hong-Yu Liu and Qiong-Ying Hu

413 Case report: A successful live birth after *in vitro* fertilization and embryo transfer in a patient with endometrial cancer who was treated conservatively
Yifan Fan, Hui Song, Xu Chen, Pei Zhang, Jingwen Si and Hui Dong

420 Unveiling the hidden causal links: skin flora and cutaneous melanoma
Zexin Zhang, Wenfeng Wu, Jiajia Lin and Hongyi Li

429 Postoperative unexplained sigmoid stenosis in a patient with rectal cancer complicated with connective tissue disease: a case report and literature review
Deming Tong, Jian Li, Guangrong Gao and Cheng Zhang

436 Primary uterine non-Hodgkin's lymphoma:a rare case report and review of the literature
Jing Wu and Ting Liu

442 Changes in hormone receptor when breast cancer metastasizes to the colon: case report and literature review
Huimeng Li, Liying Yang, Xiqiang Sun, Zhuquan Wang, Shuangwei Qin, Chengcheng Li, Gongwu Liu, Fengming Xie and Weiwei Gao

452 Case report: Complete response of recurrent locally advanced basal cell carcinoma following addition of vismodegib to neoadjuvant cemiplimab therapy
Chalette Lambert-Swainston, Wolfram Samlowski, Brandon Reynolds and Amin Hedayat

457 High-grade serous cancer of left fallopian tube with right inguinal lymph node enlargement: a case report
Aizhi Zhou, Weiyong Gu, Yumei Yang, Xin Chen, Wenfeng Ye and Mei Wang

461 Gastric-type endocervical adenocarcinoma, superficial myofibroblastoma, sex cord-stromal tumors, and HSIL in Peutz–Jeghers syndrome: a rare case report, genetic characterization, and review of literature
Dongjin Sun, Yumei Li and Zhixing Cao

470 Solitary testicular metastasis post-prostatectomy for prostatic ductal adenocarcinoma: case report and literature review
Bo Chang, Manqing Zhang, Yifan Hou, Wenbin Li, Song Li, Jianhua Zhang, Chenyang Wang, Qiangqiang Zhang and Junqing Hou

479 Rectal neuroendocrine tumor during anorectal surgery: three case reports and a review of the literature
Ruoxi Dong, Jingen Lu, Hao Zhou, Qingjun Dong and Chen Wang

487 Cutaneous histiocytic sarcoma arising from soft tissue filler injections: a case report
Jangyoun Choi, Heeyang Park, Eun Jeong Ko, Jong Yun Choi, Suk-Ho Moon, Deuk Young Oh and Young-Joon Jun

492 Clinicopathological and imaging features of struma ovarii: a retrospective study
Mei Chen, Shusheng Liao, Youfeng Xu, Xianwang Ye, Xiupeng Jia and Shengmin Zhang

503 Fertility-sparing surgery in primary peritoneal serous borderline tumor: a case report
Tingting Li, Wei Jiang and Hongjing Wang

frontiers | Frontiers in Oncology

TYPE Editorial
PUBLISHED 11 September 2025
DOI 10.3389/fonc.2025.1668671

Check for updates

OPEN ACCESS

EDITED AND REVIEWED BY
Dana Kristjansson,
Norwegian Institute of Public Health (NIPH), Norway

*CORRESPONDENCE
Lidia Castagneto-Gissey
lidia.castagnetogissey@uniroma1.it

RECEIVED 18 July 2025
ACCEPTED 02 September 2025
PUBLISHED 11 September 2025

CITATION
Castagneto-Gissey L, Georgescu DE and Agresta F (2025) Editorial: Management of rare oncological cases.
Front. Oncol. 15:1668671.
doi: 10.3389/fonc.2025.1668671

COPYRIGHT
© 2025 Castagneto-Gissey, Georgescu and Agresta. This is an open-access article distributed under the terms of the Creative Commons Attribution License (CC BY). The use, distribution or reproduction in other forums is permitted, provided the original author(s) and the copyright owner(s) are credited and that the original publication in this journal is cited, in accordance with accepted academic practice. No use, distribution or reproduction is permitted which does not comply with these terms.

Editorial: Management of rare oncological cases

Lidia Castagneto-Gissey [1]*, Dragos Eugen Georgescu [2] and Ferdinando Agresta [3]

[1]Department of Surgery, Sapienza University of Rome, Rome, Italy, [2]Carol Davila University of Medicine and Pharmacy, Bucharest, Romania, [3]ULSS2 Marca Trevigiana, Treviso, Italy

KEYWORDS

melanoma, sarcoma, neuroendocrine tumor, gynecologic cancer, molecular immunotherapy

Editorial on the Research Topic
Management of rare oncological cases

The rapid evolution of oncology has brought new challenges and opportunities in the diagnosis and management of rare and complex tumors. Although infrequent in occurrence, these malignancies often carry poor prognoses due to diagnostic delays, limited treatment options, and lack of robust clinical trial data. The recent surge in detailed case reports, molecular analyses, and innovative treatment strategies contributes significantly to bridging these gaps. This editorial aims to synthesize recent findings from diverse rare tumor cases—spanning from gynecologic melanomas, to sarcomas, neuroendocrine neoplasms, and atypical metastases—and explore their implications for clinical practice and future research.

Rare soft tissue and mesenchymal tumors

The occurrence of malignant granular cell tumors (GCTs) outside their usual head and neck locations, such as the chest wall, exemplifies diagnostic challenges posed by atypical presentations (Flauto et al.). GCTs, typically benign and slow growing, occasionally demonstrate aggressive behavior with recurrence and metastasis, necessitating repeated surgical interventions and careful long-term monitoring. Similarly, the pediatric case of pancreatic Ewing sarcoma described by Liu et al. expands our understanding of rare extraskeletal manifestations in an uncommon anatomical site, demonstrating the value of molecular diagnostics and tailored chemotherapeutic regimens in improving outcomes in aggressive pediatric malignancies.

Soft tissue sarcomas and stromal tumors constitute a heterogeneous group of mesenchymal neoplasms often posing diagnostic and therapeutic challenges. Bai et al. present uterine inflammatory myofibroblastic tumor (UIMT) involving the female reproductive tract with uncertain malignant potential. These lesions straddle the border between reactive and neoplastic processes and require excision for definitive diagnosis. The discovery of ALK gene rearrangements in UIMT has enabled targeted therapy with ALK inhibitors in select cases.

Gastrointestinal schwannomas, although generally considered benign peripheral nerve sheath tumors, occasionally present in unusual locations such as the colon. Yu et al. present

a compelling case of a colonic schwannoma causing intestinal obstruction, an atypical clinical manifestation that underscores the importance of including mesenchymal tumors in the differential diagnosis of obstructive colorectal lesions.

The recurrence of benign tumors decades after surgery is another sobering reminder of the need for long-term surveillance. Lei et al. report a recurrent giant cystic lymphangioma of the peritoneum, which returned 20 years post-resection. The case raises important considerations regarding surveillance strategies and the latent potential for recurrence in ostensibly benign conditions.

Rare cutaneous and skin-associated malignancies

Cutaneous neoplasms with mixed histopathologic features, such as the endocrine mucin-producing sweat gland carcinoma with mucinous carcinoma components reported by Sun et al., illustrate the complexity of tumor classification and metastatic potential that can alter clinical course significantly.

Zhang et al. explore the potential causal relationship between skin flora and cutaneous melanoma using Mendelian Randomization analyses, suggesting a novel area for further research in cancer etiology. Lambert-Swainston et al. describe a locally advanced basal cell carcinoma achieving pathologic complete response after combined neoadjuvant cemiplimab and vismodegib, paving the way for innovative immunotherapy-hedgehog inhibitor combinations.

Chen et al. conducted a population-based study on sebaceous carcinoma arising outside the head and neck, a subset that remains poorly characterized in the literature. Their findings reveal that while overall prognosis is favorable for non-head and neck sebaceous carcinoma, patients with distant metastases experience significantly poorer outcomes. Independent predictors of survival included age, tumor size, and stage, while undifferentiated tumors of the trunk demonstrated a higher propensity for distant spread. These insights underscore the potential value of stratified metastasis screening in high-risk subset.

The review by Pedersen et al. provides a comprehensive overview of Merkel cell carcinoma (MCC) biology, focusing on tumor immunogenicity and the tumor microenvironment's role. MCC's strong association with Merkel cell polyomavirus (MCPyV) and UV-induced mutations positions it as a prime candidate for immunotherapy. The introduction of immune checkpoint inhibitors (ICI), particularly PD-1 and PD-L1 inhibitors, has transformed MCC management. Clinical trials demonstrate durable responses in metastatic MCC, yet not all patients benefit equally. Resistance mechanisms, including immune escape and tumor heterogeneity, limit efficacy. Pedersen et al. emphasize ongoing efforts to identify biomarkers predictive of response, such as tumor mutational burden and MCPyV status. Additionally, combining ICI with radiotherapy is an area of interest, leveraging radiation-induced immunogenic cell death to augment immune responses. Ongoing trials evaluating combination regimens may further improve patient outcomes.

Gynecologic and female reproductive tumors

The prognostic factors identified in uterine adenosarcoma through the SARCUT study subanalysis by Mancari et al. further refine risk stratification and guide postoperative treatment decisions in this rare uterine tumor.

Intravenous leiomyomatosis (IVL), a rare vascular smooth muscle tumor with potential for significant morbidity, is highlighted by Li et al. through the use of advanced ultrasound imaging techniques facilitating early diagnosis and successful surgical management. In parallel, Wang et al.'s case of urachal adenocarcinoma misdiagnosed as primary cervical adenocarcinoma draws attention to the critical need for accurate histopathological assessment in rare urologic malignancies and supports aggressive surgical interventions in advanced disease.

Feng et al.'s report on primary retroperitoneal müllerian adenocarcinoma (PRMA) introduces an exceptionally rare tumor entity, emphasizing the role of immunohistochemistry in distinguishing this diagnosis from other retroperitoneal masses and the importance of considering PRMA in differential diagnoses. Additionally, Zan et al. describe a long-term progression-free survival case in advanced ovarian cancer treated with apatinib as first-line maintenance therapy, offering promising insights into cost-effective alternatives to standard maintenance regimens.

Zhang et al. provide valuable prognostic models delineating patient subgroups with high-grade neuroendocrine cervical cancer who derive survival benefits from radiotherapy, advancing personalized treatment approaches for this aggressive malignancy.

Wu et al. review a rare case of primary uterine non-Hodgkin's lymphoma and provide valuable imaging-pathology correlation for diagnosis and treatment response assessment.

Liu et al. offer a comprehensive 13-year retrospective study on uterine smooth muscle tumors of uncertain malignant potential, revealing diagnostic difficulties and fertility implications, and highlighting myomectomy as a viable option in selected patients. Qing et al. described a synchronous presentation of cervical carcinoma *in situ* and Mullerian adenosarcoma diffusely involving the uterine cavity and cervix—an exceptionally rare co-occurrence. The diagnosis was established postoperatively, underscoring the diagnostic limitations posed by rare tumor types and the importance of histological reassessment. This case reinforces the imperative of considering multiple primary malignancies in gynecologic oncology, even in asymptomatic patients.

In a broader effort to characterize rare ovarian tumors, Chen et al. conduct a retrospective study of 40 cases of struma ovarii (SO), a rare ovarian teratoma composed predominantly of thyroid tissue. Their findings reveal that multimodal imaging—including ultrasound, contrast-enhanced ultrasound, and MRI—can significantly enhance diagnostic accuracy by identifying characteristic features such as cystic-solid components and distinctive signal patterns.

Uncommon gynecologic malignancies with unique histologies remain a diagnostic challenge. Zhang et al.'s report of primary cervical melanoma—a rare and aggressive neoplasm—underscores

the importance of early detection and novel treatments like immunotherapy.

Zeng et al. detail a clear cell carcinoma of the cervix occurring without prior diethylstilbestrol exposure, contrasting with the classic epidemiology. This report highlights the necessity of considering rare histotypes in differential diagnoses and tailoring treatment accordingly. Such rare tumors often have limited data guiding management, emphasizing the value of case reports and registries to accumulate knowledge.

Detailed pathology, supported by immunohistochemistry and molecular techniques, provides critical diagnostic and prognostic information. Liang et al. explore the molecular profile of tubo-ovarian carcinosarcoma, revealing complex genomic alterations that may inform targeted therapies.

Dahl et al. introduce the use of patient-derived organoids (PDOs) from uterine carcinosarcomas to evaluate drug sensitivity *in vitro*. This platform allows personalized testing of chemotherapy and targeted agents, accelerating therapy optimization. PDOs represent a promising tool for rare cancers, enabling rapid functional assays that reflect tumor heterogeneity and microenvironmental factors, potentially transforming clinical decision-making.

Zhang et al. describe neuroendocrine cervical cancer, characterized by aggressive behavior and unique histology. Molecular markers such as synaptophysin and chromogranin assist diagnosis, while identification of somatostatin receptors opens therapeutic options. This case highlights benefits of combining chemotherapy, radiation, and immunotherapy in neuroendocrine cervical cancer. Given the poor prognosis and aggressive course, integrating multimodal therapy offers hope for improved outcomes. Immunotherapy's expanding role across tumor types is evident from several reports, with checkpoint inhibitors inducing durable responses even in advanced disease. Radiotherapy's combination with systemic therapies emerges as a key strategy, enhancing immunogenicity and response rates.

Many rare tumors mimic benign conditions on imaging, complicating diagnosis. Li et al. highlight uterine leiomyomatosis, which may resemble fibroids or sarcomas on ultrasound and MRI. Differentiating benign from malignant lesions is critical to prevent unnecessary aggressive treatment or delays.

Finally, fertility preservation in the treatment of rare peritoneal tumors is illustrated by Li et al. in a case of primary peritoneal serous borderline tumor (PPSBT). The patient underwent multiple fertility-sparing surgeries, affirming the feasibility of this approach in well-selected patients and supporting the value of multidisciplinary care and personalized surgical planning.

Male genitourinary tumors

Huang et al. present a rare case of primary hepatoid adenocarcinoma of the lung in a patient with silicosis, demonstrating the aggressive nature of this tumor and the importance of early surgical intervention alongside emerging genetic testing approaches.

Furthermore, the report by Bai et al. on testicular choriocarcinoma with uncommon pelvic and pulmonary metastases highlights the aggressive clinical course in young males and the critical importance of early diagnosis and multidisciplinary care.

Unusual metastatic patterns

The rare occurrence of metastatic deposits in unusual locations can mislead clinicians and delay appropriate management. Koh et al. report a case of scalp metastasis originating from breast carcinoma. Scalp lesions are often benign and rarely biopsied, underscoring the need for suspicion in patients with cancer history presenting with atypical cutaneous nodules.

Likewise, rare metastatic patterns, including renal cell carcinoma spreading to the thyroid (Xu et al.) or breast metastases originating from lung adenocarcinoma (Ding et al.), remind clinicians to maintain vigilance for atypical metastatic sites and emphasize the role of comprehensive diagnostic workups.

Hormonal receptor status variability in metastatic breast cancer to the colon, as reported by Li et al., adds an additional layer of complexity in treatment selection, underscoring the dynamic nature of tumor biology and the necessity for repeat biopsies in metastatic disease management.

Rare gastrointestinal tumors

Therapeutic innovations and clinical management strategies are also a central theme. Fassi et al.'s report on regorafenib-associated erythrocytosis in metastatic extra-gastrointestinal stromal tumor (extra-GIST) presents a previously unrecognized adverse effect of a tyrosine kinase inhibitor, prompting closer hematologic monitoring during targeted therapy.

Carella et al. presented a rare case of primary solitary extraosseous plasmacytoma of the colon, mimicking a submucosal lesion. Notably, the lesion was detected during routine colonoscopy in a patient with minimal symptoms. Subsequent surgical and hematological workup confirmed the diagnosis. Given the tumor's rarity and the paucity of definitive endoscopic features, this case highlights the role of comprehensive postoperative evaluation and interdisciplinary diagnostics.

Dong et al. reported three cases of rectal neuroendocrine tumors (NETs) incidentally diagnosed during anorectal surgeries for presumed benign conditions. Each case was managed surgically, with subsequent histopathologic confirmation revealing one G1 and two G2 rectal NETs. The absence of recurrence on follow-up reinforces the efficacy of early, complete excision. These findings support increased vigilance during routine proctologic procedures, particularly when atypical tissue is encountered.

Similarly, in the context of hereditary cancer syndromes, Sun et al. highlight a rare instance of gastric adenocarcinoma in a patient with Peutz–Jeghers syndrome, a genetic disorder more commonly associated with polyposis and increased risk for other malignancies.

This case adds to the scarce but growing literature linking Peutz–Jeghers syndrome with gastric malignancy and raises questions about surveillance protocols in these patients.

Pulmonary and thoracic rare cancers

Huang et al. present a rare case of primary hepatoid adenocarcinoma of the lung in a patient with silicosis, demonstrating the aggressive nature of this tumor and the importance of early surgical intervention alongside emerging genetic testing approaches.

Immunotherapy and novel approaches

Uveal melanoma is the most common primary intraocular malignancy in adults but has limited treatment options when metastatic. Tran et al. present a case of metastatic uveal melanoma treated with combined radiotherapy and dual checkpoint blockade (nivolumab and relatlimab). The rationale involves radiation enhancing tumor antigen presentation and promoting T-cell infiltration, which checkpoint inhibitors can then amplify. Their report adds to emerging evidence supporting multimodal immunotherapy strategies in uveal melanoma. Despite historically poor responses to single-agent immunotherapy, combining checkpoint inhibitors with radiation may overcome immunosuppressive microenvironments. The observed durable partial response in this case underscores the potential of this approach and warrants further clinical investigation.

Several reports highlight the expanding role of immune checkpoint inhibitors in rare melanomas of mucosal and ocular origin. Gunenc et al. document effective use of combined relatlimab (anti-LAG3) and nivolumab (anti-PD-1) therapy in a conjunctival melanoma patient. These findings extend the success of immunotherapy beyond cutaneous melanoma, traditionally the most studied subtype. They emphasize the importance of molecular and immunologic profiling to identify candidates for checkpoint inhibition, particularly in tumors with low mutational burden but active immune microenvironments.

Concluding perspective

The aggregation of rare tumor cases in centralized databases enables pattern recognition, prognostication, and development of evidence-based guidelines. Enhanced collaboration across institutions is essential to overcome the limitations posed by rarity. Molecular profiling and PDO models exemplify the move toward personalized oncology. Identifying actionable mutations and immune biomarkers will expand therapeutic options and improve survival in rare tumors. Many rare tumors lack standardized management protocols. Prospective trials, translational research, and integration of real-world data are crucial to define optimal care pathways.

These contributions underscore the importance of case reporting, precision diagnostics, and novel therapies. The diversity and complexity in these cases drive innovation and collaborative research in rare cancer management. A unified global strategy must ensure every rare case enlightens future guidelines, clinical decisions, and research priorities.

As we move forward, integrating advanced genomic profiling, immunotherapy, and real-world evidence from rare tumors is crucial. The work included in this Research Topic reminds us that every single report contributes meaningfully to the literature. These insights can inform trial design, guide biomarker discovery, and promote global collaboration.

The diverse and complex spectrum of rare tumors demands vigilant diagnosis, innovative therapies, and personalized approaches. Recent advances in immunotherapy, molecular diagnostics, and preclinical modeling herald a new era in oncology, turning clinical challenges into opportunities for improved patient care. Continuous reporting and collaboration remain vital to deepen understanding and refine management of these uncommon yet impactful malignancies.

Collectively, these cases illuminate the multifaceted challenges in diagnosing and treating rare tumors, from atypical presentations and rare metastatic patterns to evolving molecular diagnostics and novel therapeutic interventions. They underline the indispensable value of meticulous histopathological examination, advanced imaging modalities, and multidisciplinary management in optimizing patient outcomes.

As the medical community continues to encounter rare tumors with unique clinical behaviors, these reports contribute to a growing body of knowledge that will apprise future clinical guidelines and foster more precise, individualized care. The heterogeneity and rarity of these conditions demand ongoing research and international collaboration to unravel their complexities and improve prognostication and treatment paradigms.

We encourage more institutions to document, publish, and contribute to rare oncology registries. With comprehensive molecular diagnostics and multidisciplinary treatment, outcomes for patients with rare tumors can continue to improve. Each study included here contributes a valuable thread in the larger fabric of rare oncology knowledge and care.

Author contributions

LC-G: Writing – original draft, Conceptualization, Writing – review & editing. DG: Writing – review & editing. FA: Writing – review & editing.

Conflict of interest

The authors declare that the research was conducted in the absence of any commercial or financial relationships that could be construed as a potential conflict of interest.

The author(s) declared that they were an editorial board member of Frontiers, at the time of submission. This had no impact on the peer review process and the final decision.

Generative AI statement

The author(s) declare that no Generative AI was used in the creation of this manuscript.

Any alternative text (alt text) provided alongside figures in this article has been generated by Frontiers with the support of artificial intelligence and reasonable efforts have been made to ensure accuracy, including review by the authors wherever possible. If you identify any issues, please contact us.

Publisher's note

All claims expressed in this article are solely those of the authors and do not necessarily represent those of their affiliated organizations, or those of the publisher, the editors and the reviewers. Any product that may be evaluated in this article, or claim that may be made by its manufacturer, is not guaranteed or endorsed by the publisher.

frontiers | Frontiers in Oncology

TYPE Original Research
PUBLISHED 13 March 2024
DOI 10.3389/fonc.2024.1368592

Check for updates

OPEN ACCESS

EDITED BY
Dragos Eugen Georgescu,
Carol Davila University of Medicine and Pharmacy, Romania

REVIEWED BY
Teodor Florin Georgescu,
Carol Davila University of Medicine and Pharmacy, Romania
Stergios Boussios,
Canterbury Christ Church University, United Kingdom
Iuliana Pantelimon,
Carol Davila University of Medicine and Pharmacy, Romania
Roberto Altamirano,
University of Chile, Chile

*CORRESPONDENCE
Karen D. Cowden Dahl
kdcowden@gundersenhealth.org

RECEIVED 10 January 2024
ACCEPTED 22 February 2024
PUBLISHED 13 March 2024

CITATION
Dahl MJ, Lofgren KA, Haugen C, Harmon GE, Hughes SP and Cowden Dahl KD (2024) Gemcitabine combination therapies induce apoptosis in uterine carcinosarcoma patient-derived organoids.
Front. Oncol. 14:1368592.
doi: 10.3389/fonc.2024.1368592

COPYRIGHT
© 2024 Dahl, Lofgren, Haugen, Harmon, Hughes and Cowden Dahl. This is an open-access article distributed under the terms of the Creative Commons Attribution License (CC BY). The use, distribution or reproduction in other forums is permitted, provided the original author(s) and the copyright owner(s) are credited and that the original publication in this journal is cited, in accordance with accepted academic practice. No use, distribution or reproduction is permitted which does not comply with these terms.

Gemcitabine combination therapies induce apoptosis in uterine carcinosarcoma patient-derived organoids

Matías J. Dahl[1], Kristopher A. Lofgren[1], Cleo Haugen[1], Gil E. Harmon[2], Sarah P. Hughes[3] and Karen D. Cowden Dahl[1]*

[1]Kabara Cancer Research Institute, Gundersen Medical Foundation, La Crosse, WI, United States, [2]Department of Hematology and Oncology, Gundersen Health Systems, La Crosse, WI, United States, [3]Department of Pathology, Gundersen Health Systems, La Crosse, WI, United States

Uterine carcinosarcoma (UCS) is a rare but aggressive endometrial cancer. Survival outcomes for women diagnosed with UCS remain poor with lower survival than those of endometrioid or high-grade serous uterine cancers. The histopathological hallmark of carcinosarcoma is the presence of both sarcomatous and carcinomatous elements. The survival rates for UCS have not improved for over 40 years; therefore, there is a profound need to identify new treatments. To investigate novel chemotherapy treatment combinations for UCS, we generated a UCS patient-derived organoid (PDO) cell line from a patient that received neoadjuvant treatment with paclitaxel and carboplatin. The PDO cell line (UCS1) was grown in three-dimensional domes. The PDO domes were treated with six individual chemotherapies or nine combinations of those six drugs. Cell death in response to chemotherapy was assessed. We found that the six monotherapies had minimal effectiveness at inducing cell death after 48 h of treatment. The combination of paclitaxel and carboplatin (which is the standard-of-care chemotherapy treatment for UCS) led to a small increase in apoptosis compared with the monotherapies. Importantly, when either carboplatin or paclitaxel was combined with gemcitabine, there was an appreciable increase in cell death. In conclusion, for the UCS1 patient-derived tumor cells, gemcitabine combinations were more effective than carboplatin/paclitaxel. Our data support the use of PDOs to predict responses to second-line chemotherapy.

KEYWORDS

uterine carcinosarcoma, patient-derived organoids, chemotherapy, apoptosis, carboplatin, paclitaxel, gemcitabine

1 Introduction

High-grade endometrial tumors are composed of FIGO grade 3 endometrioid, serous, clear cell, undifferentiated/dedifferentiated carcinomas and carcinosarcomas (1). While uterine serous carcinoma is rare compared with endometrioid carcinoma, patients with serous carcinomas have a higher incidence of recurrence and poorer prognosis (2). Uterine carcinosarcoma (UCS) is a high-grade and highly aggressive cancer, which represents roughly 5% of all endometrial malignancies. Survival outcomes for women diagnosed with UCS remain poor and worse than that of endometrioid or high-grade serous histologies (3). The median survival of patients with UCS is less than 2 years and the overall survival rate ~33% (4). Carcinosarcomas are characterized by the presence of both sarcomatous and carcinomatous elements. The carcinomatous component can range from low to high grade with the majority being high grade. The sarcomatous component is further characterized as being either homologous or heterologous. The homologous sarcoma has evidence of high-grade undifferentiated round or spindle-cell proliferation with features resembling leiomyosarcoma, endometrial stromal sarcoma, or fibrosarcoma. The heterologous sarcoma, which accounts for around half of the cases, can have histophenotypes resembling cartilaginous, rhabdosarcomatous, chondrosarcomatous, or osteosarcomatous differentiation (5). The percentage of carcinoma and sarcoma varies from patient to patient (6). The component invading the myometrium or metastatic in the lymph nodes is often the carcinomatous component. However, metastases can include both the carcinomatous and sarcomatous components or only the sarcomatous element, although this is less frequent (7). There are a number of factors in UCS that correlate with poorer prognosis. Some of these factors include lymph node metastasis, heterologous histopathology, higher than 25% stromal composition, elevated expression of vascular endothelial growth factor, and increased microvessel density (8–10). Therefore, due to the complicated nature and heterogeneity of UCS, responses to chemotherapy are currently difficult to predict.

The incidence of UCS is increasing in the USA (4). Optimal treatment for UCS is debated. Given that UCS is rare, it is a challenging tumor to investigate potential treatment options. Additionally, few clinical trials are applicable for UCS patients. When compared with uterine adenocarcinomas, UCS presents with a higher grade and frequency of metastasis, resulting in lower overall survival (4). The presence of two tumor histologies in UCS makes treatment and cure challenging. Importantly, the ratio of carcinoma to sarcoma impacts survival as sarcoma dominance (SD) (>50% of the tumor is sarcomatous) correlates with poorer prognosis (4). Most UCS patients receive carboplatin and paclitaxel with or without radiation following a debulking surgery. Surgery usually entails a hysterectomy with bilateral salpingo-oophorectomy and lymphadenectomy for staging. The response to chemotherapy in UCS depends on the grade of tumor, type of sarcoma, and if there is SD (11). The clinical data suggest that carcinoma and sarcoma tumor cells respond differently to therapy and implies that targeting the sarcoma tumor cells separately from the carcinoma may improve chemotherapy response rates. Currently, the median response rates for UCS to first- and second-line chemotherapy are 37.5% and 5.5%, respectively (4). Therefore, there is a crucial need to enhance our understanding about UCS progression in order to develop more effective therapies and improve survival.

Genetic evidence suggests that UCS is epithelial derived and that the sarcoma component arises from dedifferentiation of the epithelial/carcinoma precursor (12, 13). How UCS cells are programmed to become both carcinoma and sarcoma cells is unknown. Genetic analysis revealed that sarcoma and carcinoma components of UCS share the same driver mutations including TP53, PIK3CA FBXW7, PTEN, and KRAS (14). It is hypothesized that epithelial to mesenchymal transition (EMT) signals induce differentiation of the sarcomatous portion of the UCS. In particular, the sarcoma tumor cells have a higher EMT score (expression EMT markers) than the carcinoma cells (14–16). SD tumors tend to have a heterologous histology and express EMT markers (11, 17). Factors that may contribute to UCS EMT are repression of the miR-200 family of microRNAs (miRNAs) and TGFβ (18–20). Overexpression of miR-200 in UCS xenografts induced epithelial morphology and decreased tumor growth (20). TGFβ promotes EMT in UCS cells, and inhibition of TGFβ reduces viability and differentiation of UCS cells (18, 19). In support of this, TGFβ is demonstrated to promote EMT and a cancer stem cell (CSC) phenotype (21, 22). Additionally, adipocytes have the ability to induce EMT in cancer cells (23–25). These studies suggested that the UCS tumors exhibit plasticity and the tumor microenvironment (TME) influences UCS tumor differentiation.

Patient-derived organoid (PDO) cell lines have been generated for endometrial cancers including UCS (26). PDOs are tumor cells that are harvested directly from a fresh patient tumor or tumor cells such as ascites and cultured in 3D. By culturing the cells in a 3D matrix, the cells retain some of the structure and behavior as found in the original tumor and exhibit more accurate responses to treatments than established tumor cell lines. PDOs also enable us to study the physical properties of tumor cells and response to therapy of individual tumors *ex vivo* (27). These PDOs have the potential to determine chemotherapy sensitivities for first-line chemotherapy and subsequent rounds of chemotherapy (28). The goal of our study was to examine the impact of different chemotherapy treatments for UCS on a primary patient-derived organoid (PDO) line. The PDO line was generated from a primary tumor of a patient with UCS who had received neoadjuvant carboplatin and paclitaxel. We treated organoids with six different chemotherapy drugs and nine combinations of those drugs. We chose to use carboplatin and paclitaxel in our studies because this combination is the standard of care for UCS. Additionally, we used ifosfamide, docetaxel, doxorubicin, and gemcitabine since these drugs either alone or in combination are possible therapies for uterine sarcoma. According to the NCCN guidelines, doxorubicin is preferred; however, gemcitabine, ifosfamide, and docetaxel/gemcitabine can be used for sarcoma treatment. We assessed how the treatments impacted cell morphology and survival.

2 Results

2.1 Derivation of patient-derived organoid cell line UCS1

A patient with UCS was selected for the study. This patient had stage IVB at the time of diagnosis. The carcinoma component of the tumor was poorly differentiated serous carcinoma, and the sarcomatous portion was undifferentiated with a small amount of chondroid differentiation. The initial biopsy contained 95% carcinoma and 5% sarcoma. H&E staining demonstrated the UCS diagnosis (Figures 1A, B). Immunohistochemistry (IHC) cytokeratin AE1AE3 demonstrated cytokeratin in the carcinomatous portion of the tumor, whereas the sarcomatous portion was negative for cytokeratin (Figure 1C). IHC staining on the tumor found diffuse strong p53 positivity in both carcinomatous and sarcomatous tumor cells (Figure 1D). Tumor was also focally positive vimentin (not shown). Tempus sequencing on tumor biopsy found a loss of function mutation in TP53 at A159V. The patient was treated with three rounds of neoadjuvant carboplatin and paclitaxel. After the chemotherapy regime, the patient underwent a total abdominal hysterectomy with bilateral salpingo-oophorectomy, omentectomy, and tumor debulking. Response to therapy was CRS2 (moderate). At the time of surgery, a tumor specimen was collected and processed into a single-cell suspension. The single cells were suspended in a three-dimensional (3D) dome composed of an artificial basement membrane to generate a UCS organoid cell line (UCS1).

2.2 Characterization of UCS1

Following development of the UCS1 line, we conducted further characterization using immunofluorescence (IF) and fluorescent staining on UCS1 organoids to assess the expression or localization/organization of F-actin, p53, Pax8, vimentin, E-cadherin, and N-cadherin. Consistent with the pathology findings on the primary tumor, focal expression of p53 (Figure 2A) was identified in organoids. Texas Red phalloidin staining and DAPI staining demonstrate F-actin organization and nuclei in organoids (Figures 2B–D). Organoids also contained PAX8-positive cells, demonstrating the Mullerian origin of the cells (Figures 2E–G). Our next goal was to examine the morphology of the spheroids (referring to isolated 3D spheres of PDO cells) generated from UCS1 and determine if they exhibited epithelial and/or mesenchymal markers. IF for E-cadherin, N-cadherin, and vimentin was conducted. We found that individual UCS1 spheroids typically expressed either E-cadherin (Figures 3A, C) or N-cadherin (Figures 3B, D). Some individual live UCS1 spheroids expressed vimentin (Figures 4A, B) while others did

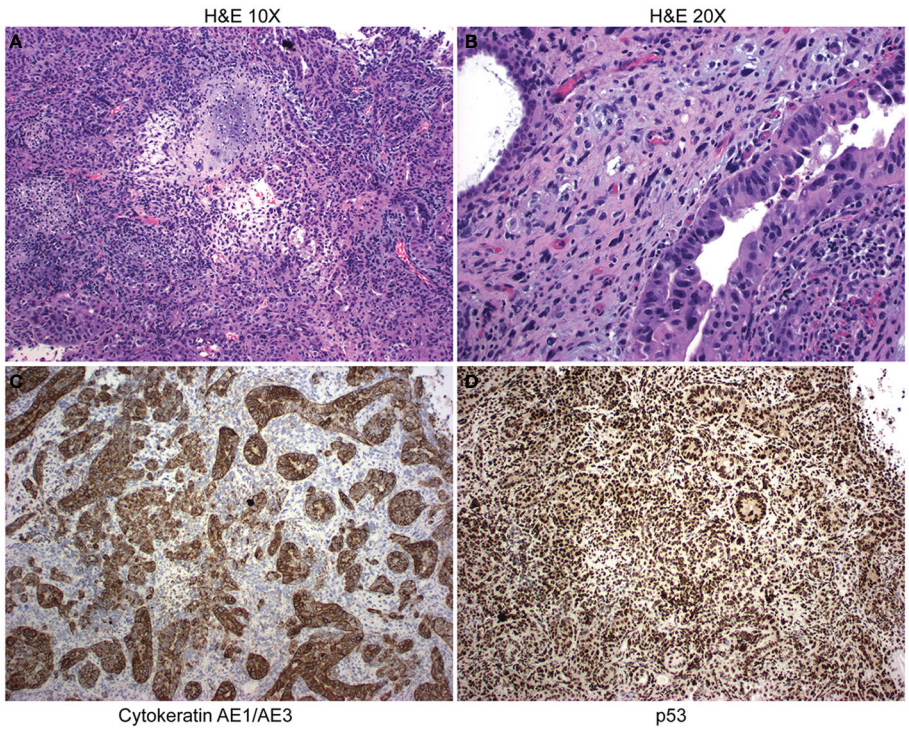

FIGURE 1
Pathology from uterine carcinosarcoma (UCS) patient tumor. **(A)** H&E staining at 10× demonstrates UCS tumor with serous carcinoma and chondroid sarcomatous differentiation. **(B)** H&E at 20× magnification. **(C)** Immunohistochemistry demonstrates staining for cytokeratin. **(D)** Immunohistochemistry demonstrates nuclear accumulation of p53.

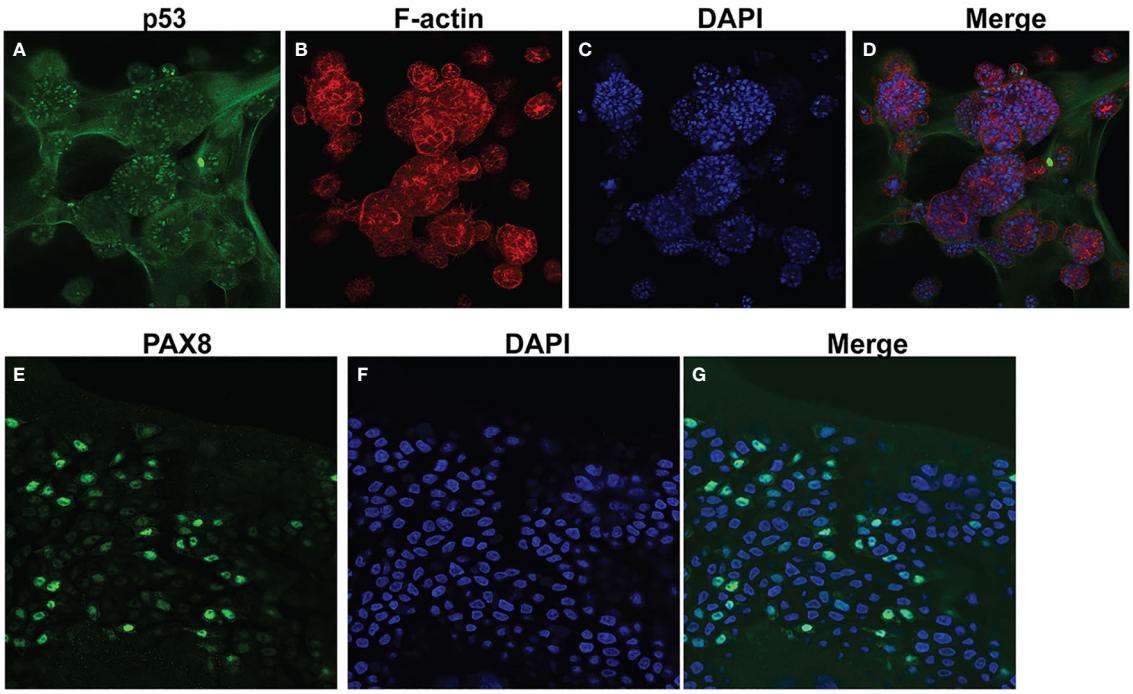

FIGURE 2
Characterization of UCS1 organoids by immunofluorescence and confocal microscopy. **(A–D)** Depicts staining for p53 **(A)**, Texas-Red phalloidin (F-actin) **(B)**, and DAPI **(C)** on UCS PDOs (10x magnification). **(D)** is the merged image of **(A–C)**. **(E–G)** Demonstrates nuclear expression of PAX8 in organoids (63× magnification).

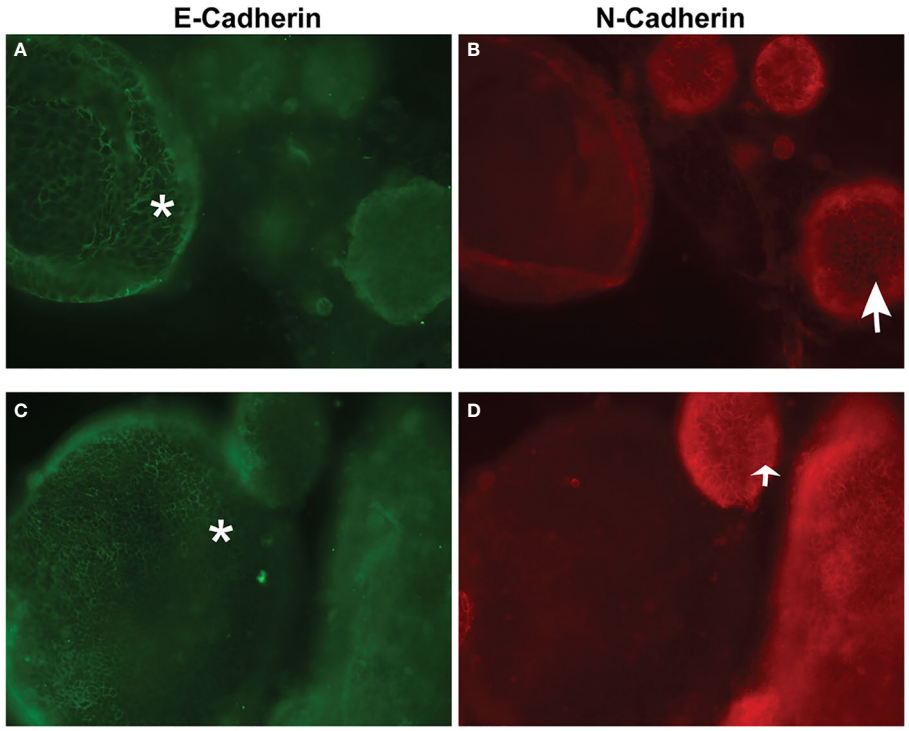

FIGURE 3
Immunofluorescence and confocal microscopy for E-cadherin and N-cadherin in UCS1 organoids. **(A, C)** are staining for E-cadherin, and **(B, D)** are staining for N-cadherin. **(A, B)** are different fields of cells than **(C, D)**. *: E-cadherin-positive cells; arrow: N-cadherin positive cells (63× magnification).

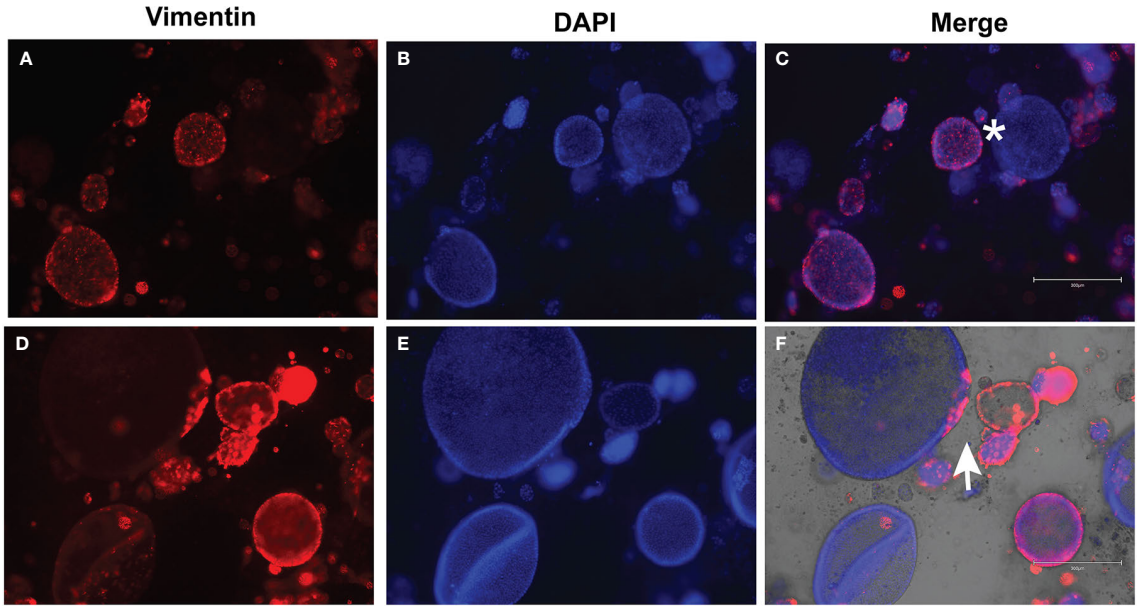

FIGURE 4
Immunofluorescence for vimentin on UCS1 organoids. UCS1 organoids were stained for vimentin **(A, D)** and DAPI **(B, E)**. **(A–C)** and **(D–F)** are two independent fields of spheroids. **(C, F)** are merged images. *: vimentin-negative cells; arrow: vimentin-positive cells (20× magnification).

not express vimentin (Figures 4B, C). Mixed morphology did occur in some organoid structures, but it was rare (Figures 4D–F). In our characterization of the organoids, we found that UCS1 cells formed spheroids with a variety of morphologies (Figures 5A–D). Figure 5 demonstrates the diversity in organoid organization. Texas Red phalloidin staining for F-actin demonstrated that some clusters had apical columnar organization (Figure 5A). Other spheroids were entirely cobblestone, exhibited a ring of cells on the surface of the sphere, or were unorganized (Figures 5B–D). On occasion, we had tumor cells migrate out from spheres (Figures 5E–N). These non-spheroid/differentiated cells could be epithelial as indicated through expression of E-cadherin (Figures 5I–K) or mesenchymal as indicated by vimentin expression (Figures 5L–N). Our characterization of the organoid morphology demonstrated that like UCS tumors, the organoids had diverse morphology and expression of epithelial and mesenchymal markers.

2.3 UCS1 organoid response to therapy

Due to the aggressive nature and poor survival associated with UCS, we hypothesized that UCS-derived PDOs may be used to identify alternate options for chemotherapy. We investigated the impacts of individual and combination chemotherapy treatments on the UCS1 line. We treated the UCS1 organoids with six different chemotherapy drugs and nine combinations of those drugs (Tables 1, 2).

We conducted dose curve analysis on organoids to identify appropriate ranges of drugs to be used in further experiments (Supplementary Figure 1). We treated UCS1 organoids with four doses of each of the six drugs (Table 1). We chose dose 4 (Bold concentrations in Table 1) for each of the individual therapies for further studies due to activation of CellEvent 3/7 and Annexin V staining. We analyzed the organoids for morphology, DNA integrity (DAPI staining), and apoptosis with Annexin V staining/flow cytometry. First, we stained with DAPI and assessed DAPI for nuclear integrity (Figure 6). We did not identify significant differences in nuclear appearance between the organoids treated with individual chemotherapies and DMSO treatment. Next, we conducted staining for Annexin V to determine if there was enhanced apoptosis in UCS1 organoids treated with the monotherapies (Figure 7). Each individual chemotherapy agent, except ifosfamide (Figure 7H), had a mild increase in Annexin V staining. Of the six drugs used, gemcitabine induced the most cell death, increasing cell death from 10.539% in DMSO-treated to 34% in gemcitabine-treated cultures (Figures 7B vs. 7E).

Next, we investigated the impact of chemotherapy combinations on organoid viability. We chose to use dose 4 from Table 1 for each drug for combination treatments (same as used for monotherapies). We compared eight combination chemotherapies (Table 2) to carboplatin/paclitaxel, which is the standard of care for UCS and the treatment regime that was given to the patient from which the UCS1 cell line was derived. Each of these combinations has been used to treat patients with various forms of cancer. Brightfield microscopy demonstrated compromised organoid structures for cultures treated with the C3, C7, and C8 combinations (Figure 8). The nuclear integrity of organoids treated with combinations 3, 7, and 8 was altered compared with treatment with carboplatin/paclitaxel and DMSO-treated cells (Figure 9). Nuclei in cultures 2, 7, and 8 culture were fragmented. Additionally, F-actin organization was abnormal in C3 and C7 (Supplementary Figure 2). Finally, we assessed by Annexin V staining the extent of apoptosis in UCS1 PDO cultures treated with the nine combinations of chemotherapy. In Figure 10, we compared combinations C2, C4, C5, C6, and C9 to treatment with carboplatin/paclitaxel. We stained cells with Annexin

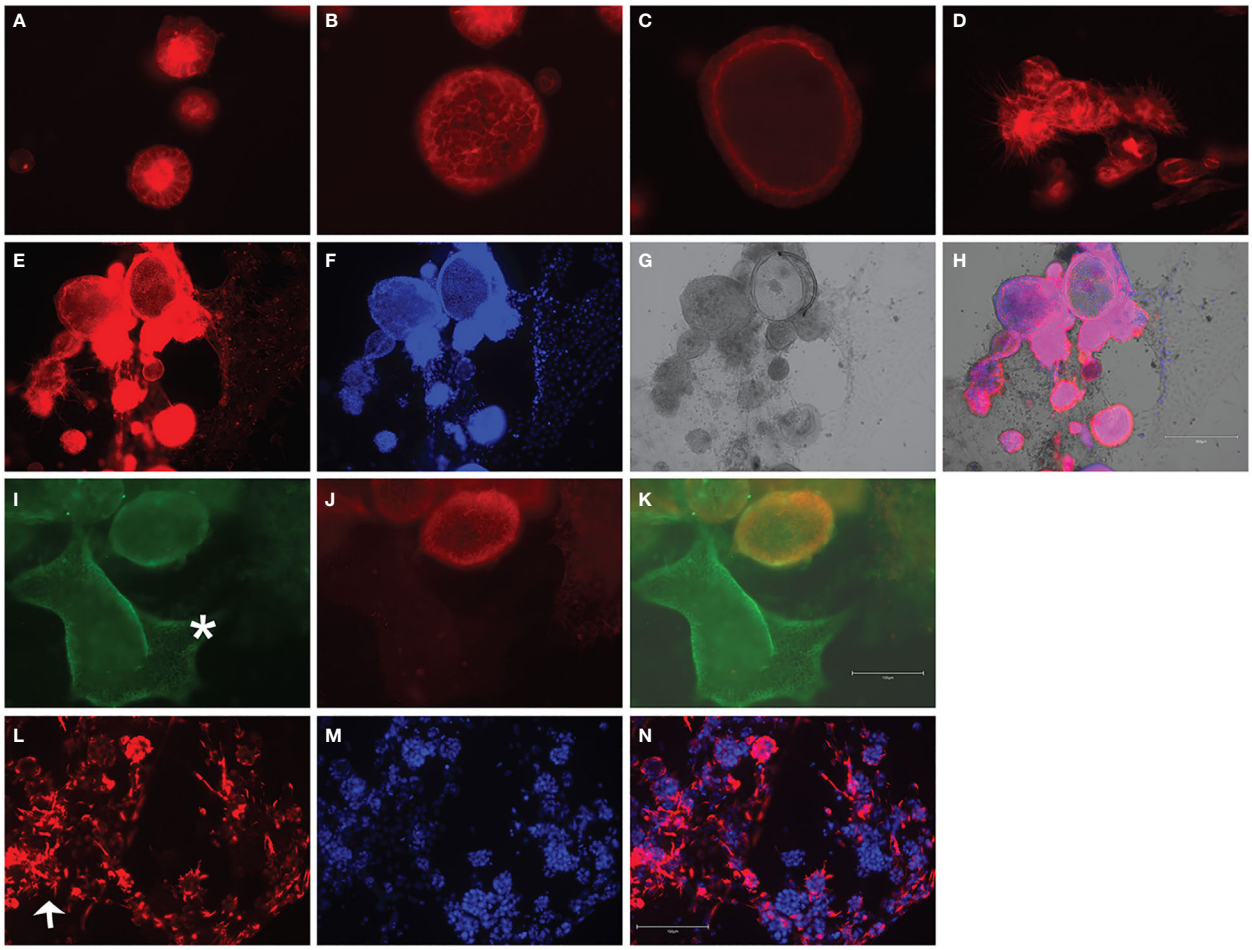

FIGURE 5
Fluorescent staining of UCS1 organoids demonstrates diverse morphologies. F-Actin staining in **(A–D)** denotes types of cellular organization observed in UCS1 cultures. Panels **(E–H)** demonstrate through F-actin staining in **(E)**, DAPI **(F)**, and brightfield **(G)** that tumor cells can differentiate and migrate/extend from spheroids. H is the merged image of **(E–G)**. Panels **(I–K)** demonstrate that migratory (non-spheroid) tumor cells can express E-cadherin (green staining in **I**, *E-cadherin-positive cells). **(J)** is N-cadherin, and **(K)** is a merge of **(I)** and **(J)**. Panel **(L)** is vimentin staining on non-spheroid tumor cells, and **(N)** is the merged image with DAPI in **(M)**. Arrow = vimentin-positive cells. 20× magnification.

V and performed flow cytometry to determine if the different combinations of chemotherapy induced apoptosis in UCS1 tumor organoids (Figure 10). We found that treatment with carboplatin/paclitaxel resulted in 31% of the cells staining for Annexin V (Figure 10). Each combination chemotherapy increased Annexin V staining/percent of apoptotic cells compared with DMSO treatment. However, combinations C2, C4, C5, C6, and C9 were equal or inferior at inducing apoptosis compared with carboplatin/paclitaxel. In Figure 11, we again treated cells with either carboplatin/paclitaxel or three different gemcitabine combinations C3, C7, and C8. In this experiment, we found that the C3 and C7 combinations resulted in more cell death than carboplatin/paclitaxel. The increase in Annexin V positivity in cultures treated with the C3 and C7 combinations agreed with the fragmented DNA integrity in Figure 9. The

TABLE 1 Doses of chemotherapy used in treating UCS1 organoids.

Drug	Dose 1	Dose 2	Dose 3	Dose 4	Dose 5
Carboplatin	Vehicle	25 nM	50 nM	**100 nM**	500 nM
Docetaxel	Vehicle	10 nM	50 nM	**100 nM**	10 µM
Doxorubicin	Vehicle	10 nM	100 nM	**1 µM**	50 µM
Gemcitabine	Vehicle	100 nM	1 µM	**10 µM**	100 µM
Ifosfamide	Vehicle	–	250 µM	**500 µM**	1mM
Paclitaxel	Vehicle	5 nM	50 nM	**500 nM**	5 µM

TABLE 2 Chemotherapy combinations used for treating UCS1 organoids.

Combination number	Drug combination
Combo 1: (C1)	100 nM carboplatin 500 nM paclitaxel
Combo 2: (C2)	100 nM carboplatin 100 nM docetaxel
Combo 3: (C3)	100 nM carboplatin 10 μM gemcitabine
Combo 4: (C4)	100 nM carboplatin 500 μM ifosfamide
Combo 5: (C5)	500 μM ifosfamide 500 nM paclitaxel
Combo 6: (C6)	100 nM doxorubicin 500 nM paclitaxel
Combo 7: (C7)	10 μM gemcitabine 500 nM paclitaxel
Combo 8: (C8)	100 nM doxorubicin 10 μM gemcitabine
Combo 9: (C9)	100 nM doxorubicin 100 nM docetaxel

combination of carboplatin/gemcitabine and paclitaxel/gemcitabine resulted in 83% and 80% of the cells labeling as Annexin V positive compared with 53.6% Annexin V-positive cells with carboplatin/paclitaxel treatment. Treatment with gemcitabine/doxorubicin resulted in 53% of the cells staining positive for Annexin V despite the abnormal appearance of the cultures and poor DNA integrity. These data suggest that the mechanism for gemcitabine/doxorubicin-induced cell death needs further investigation. Representative flow cytometry plots from four experiments were provided. Our data suggest that the UCS1 PDO exhibited increased susceptibility to gemcitabine combination therapies.

3 Discussion

Our goal was to generate a novel UCS organoid cell line that could be used to test currently unused combinations of chemotherapy since UCS has poor response rates to chemotherapy and radiation. We successfully generated UCS1, a PDO line that displays epithelial and mesenchymal morphologies. UCS1 was generated from a patient

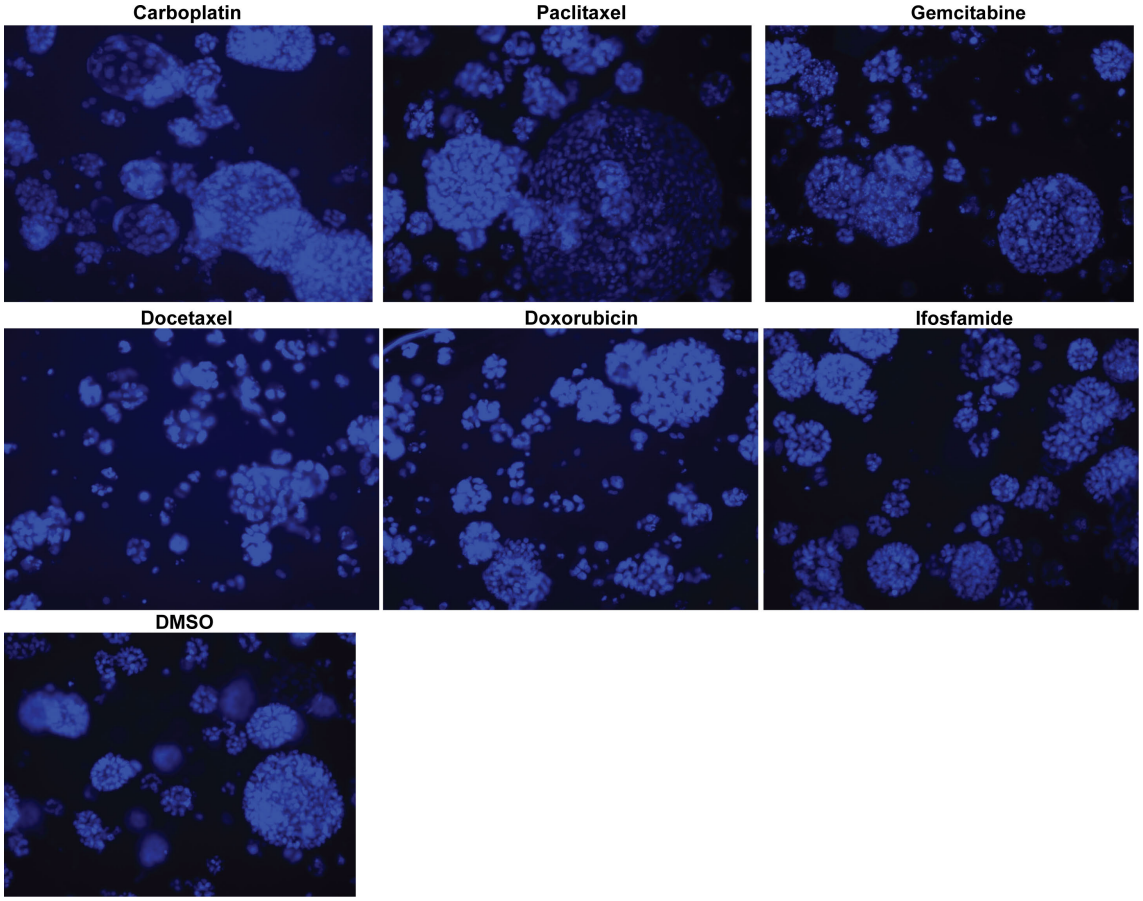

FIGURE 6
Monotherapy treatments of UCS1 organoids did not significantly alter nuclear integrity. DAPI staining was conducted on UCS1 cells treated with monotherapies listed in Table 1 for 48 h.

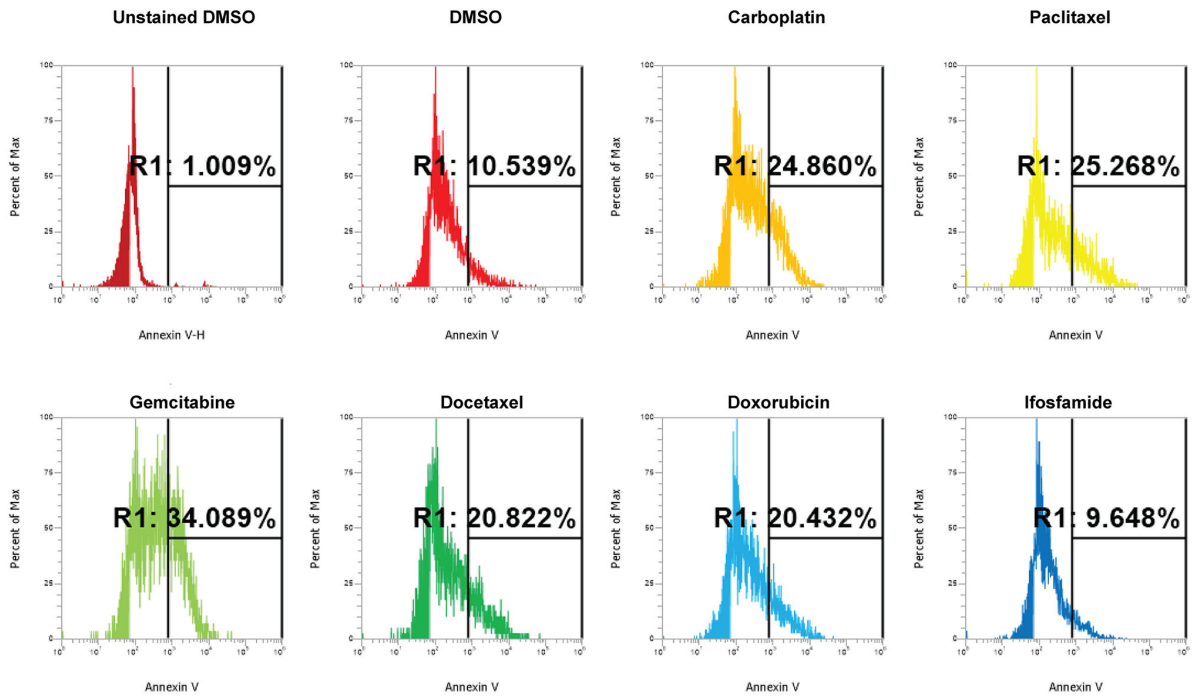

FIGURE 7
Induction of apoptosis by individual chemotherapy treatments in UCS1 organoids. UCS1 cells were treated for 48 h with DMSO, carboplatin, paclitaxel, gemcitabine, docetaxel, doxorubicin, or ifosfamide (at indicated doses in Table 1). Annexin V staining followed by flow cytometry was conducted. Percentages of Annexin V-positive cells are indicated as compared with unstained and untreated UCS1 cultures.

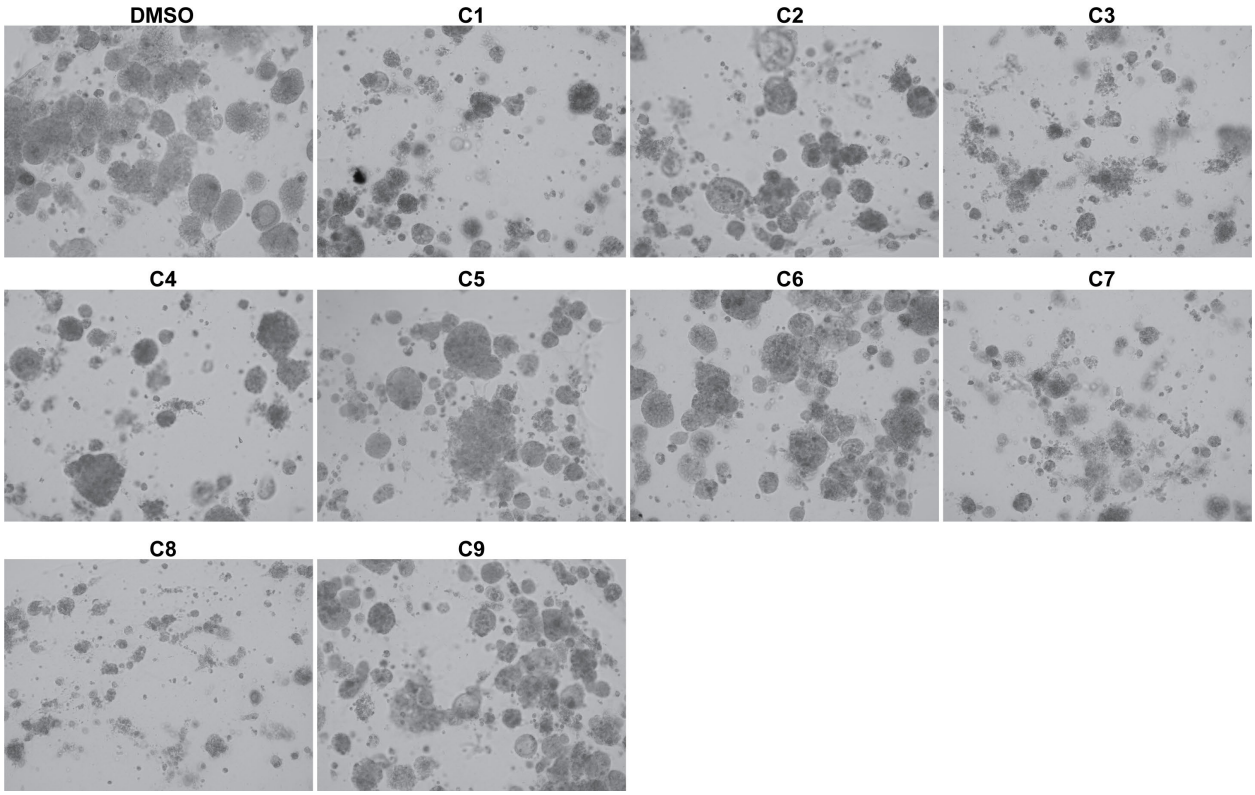

FIGURE 8
Brightfield morphology of UCS1 cells treated with combination chemotherapies. UCS1 cultures were treated with combination chemotherapy for 48 h or DMSO as a vehicle control. Brightfield images were collected to demonstrate cellular morphology. 10× magnification.

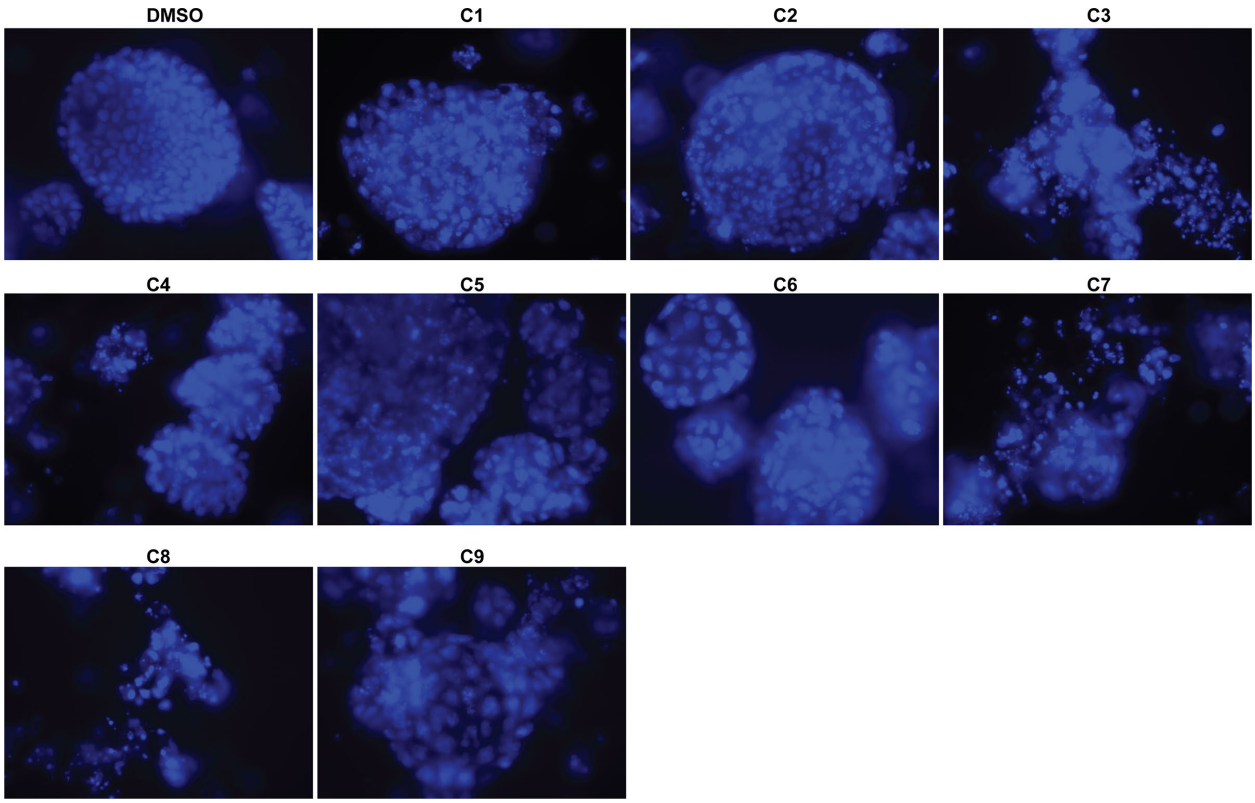

FIGURE 9
Nuclear morphology of UCS1 cells treated with combination chemotherapies. UCS1 cultures were treated with combination chemotherapy for 48 h or DMSO as a vehicle control and stained with DAPI as an indication of nuclear integrity. Fluorescent images were collected. 40× magnification.

that had received treatment with paclitaxel and carboplatin. Our UCS1 cell line enabled us to ask if the UCS organoids still exhibited a response to the combination of carboplatin and paclitaxel or if another chemotherapy regime would exhibit an improved response. Interestingly, we found that for our UCS1 PDO line, carboplatin/gemcitabine and paclitaxel/gemcitabine were superior to carboplatin/paclitaxel at inducing cell death. The improvement in cell killing with gemcitabine combinations may have occurred for a variety of reasons that have yet to be explored. Since the UCS1 line was derived from the tumor following the patient having received carboplatin/paclitaxel, the tumor may have acquired some level of chemoresistance to carboplatin/paclitaxel from the neoadjuvant therapy. We saw minimal response to carboplatin/paclitaxel. Future studies will explore how treatment-naïve tumors respond to combination chemotherapies such as those with gemcitabine. Moving forward, it will be critical to determine if PDOs can be used to predict response to first-line chemotherapy in addition to second-line chemotherapy and beyond. We hope to achieve this by creating PDOs from treatment-naïve tumors in addition to tumor cells derived for subsequent surgeries or procedures like paracentesis. Importantly, we identified two combinations of chemotherapy that effectively induced apoptosis in UCS1. Our data suggested that organoid-derived cell lines could be used to predict second-round chemotherapy options.

Current US National Comprehensive Cancer Network (NCCN) guidelines recommend carboplatin/paclitaxel for systemic UCS therapy. Ifosfamide, ifosfamide/paclitaxel, and cisplatin/ifosfamide are also recommended regimes for UCS. In our study, ifosfamide was not effective at inducing cell death in this UCS cell line. Our results are in alignment with a recent phase III trial demonstrating that carboplatin/paclitaxel is superior (or not inferior) to ifosfamide-based regimes (29). The study further concludes that carboplatin/paclitaxel should be used to treat UCS instead of ifosfamide (29). Surprisingly, gemcitabine combinations resulted in the most cell death in the UCS1 organoids. Gemcitabine alone had a mild increase in cell death, and combining gemcitabine with carboplatin and paclitaxel further increased apoptosis. However, there are few studies on gemcitabine and UCS. Perhaps with improvements in personalized medicine, we may find that some UCS patients may benefit from gemcitabine therapy. One *in vitro* study demonstrated that gemcitabine may have a potential for use in UCS when combined with other drugs. In the UCS cell line SK-UTI-B, combining gemcitabine with mTOR inhibition resulted in additive cell death (30). Other patient studies failed to show gemcitabine as effective in UCS. In a phase II study, the combination of docetaxel and gemcitabine was not active as a second-line chemotherapy in recurrent UCS (31). It is worth noting that the gemcitabine combinations we used are effective in other tumor types. Gemcitabine combined with carboplatin increased progression-free survival in ovarian cancer patients (32). Gemcitabine/carboplatin treatment was an effective second-line treatment in metastatic breast cancer (33). Additionally,

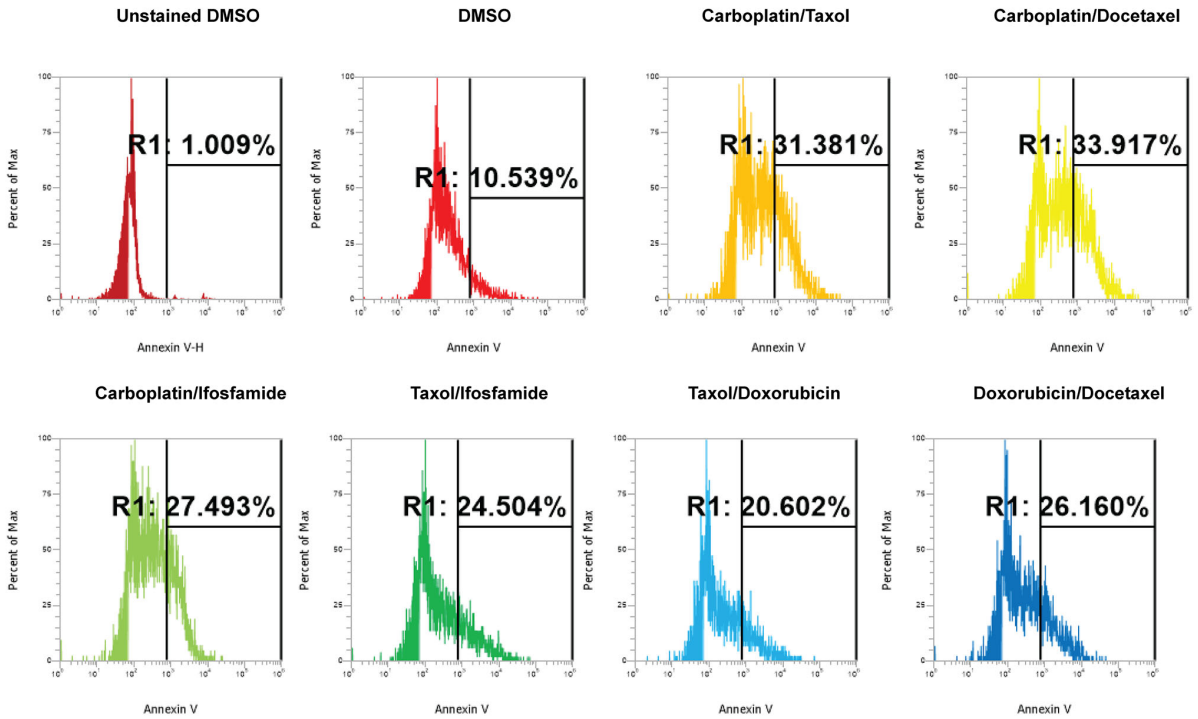

FIGURE 10
Induction of apoptosis by combination chemotherapy treatments in UCS1 PDOs. UCS1 cultures were treated with DMSO or the following combinations: C1, C2, C4, C5, C6, and C9. Annexin V staining followed by flow cytometry was conducted. Percentages of Annexin V-positive cells are indicated as compared with unstained and DMSO-treated UCS1 cultures.

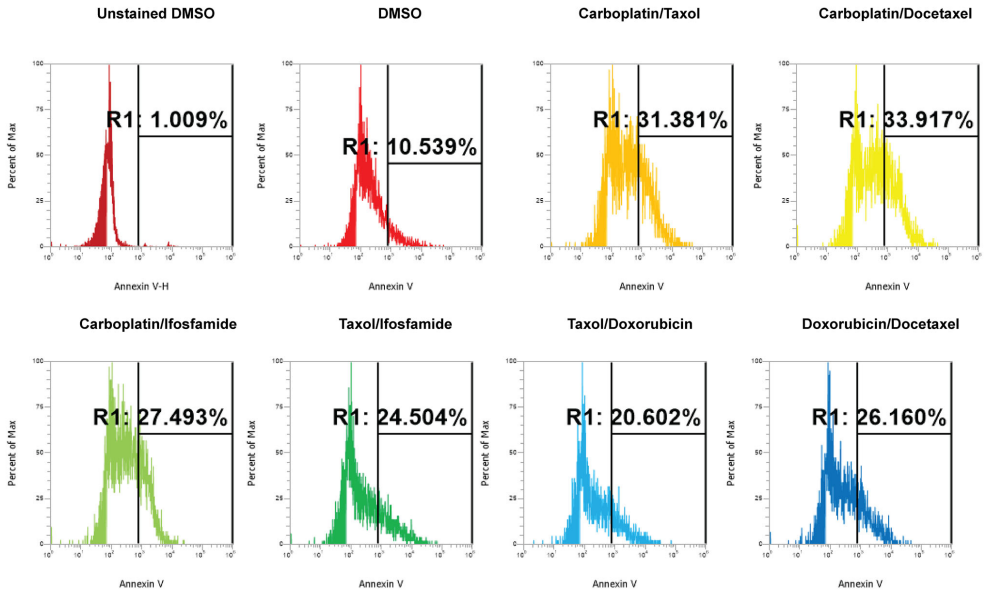

FIGURE 11
Comparison of apoptosis between UCS1 PDOs treated with carboplatin/paclitaxel (C1) or gemcitabine combinations (C3, C7, and C8). UCS1 cultures were treated with DMSO or the following combinations: C1, C3, C7, and C8. Annexin V staining followed by flow cytometry was conducted. Percentages of Annexin V-positive cells are indicated as compared with unstained and DMSO-treated UCS1 cultures.

gemcitabine when combined with paclitaxel has shown effective treatment in a variety of settings including lung cancer and urothelial cancer (34–36). A recent study found that endometrial and ovarian PDOs could be generated efficiently and predicted response to therapy (28). Moreover, in one PDO for serous (not UCS) endometrial cancer, gemcitabine was superior to carboplatin/paclitaxel at killing cells. Our data further support how useful PDOs can be in determining chemotherapy sensitivity.

Currently, the chemotherapy for UCS is often carboplatin/paclitaxel. However, given the poor survival rates of UCS, there may be better treatment options that have not been explored. It is important to note that whereas our results are *in vitro* and will require *in vivo* corroboration, preclinical, and clinical studies to validate changes to current UCS treatment practices, our PDO model highlights how *ex vivo* drug sensitivity screening could be used to improve personalized approaches to chemotherapy. An additional important step in determining if gemcitabine monotherapy and combination therapies might be efficacious for some UCS patients will be to generate patient-derived xenografts from multiple patients and additionally test gemcitabine combinations in preclinical mouse models (37–39). Importantly, our data suggest that some patients may benefit from gemcitabine combinations, particularly if they have acquired resistance to carboplatin/paclitaxel. However, we do not know if many patients or only a few would benefit from gemcitabine-based therapies until more PDOs have been generated and tested. Critically, our data found that using PDOs that identify effective combinations of therapies could lead to personalized treatment for UCS.

4 Materials and methods

4.1 Generating organoids from solid tumor

Patient UCS tumor specimen was obtained at Gundersen Heath Systems for patient-derived organoid (PDO) generation. Written consent was obtained for subjects under IRB approved protocol no. 2-20-10-004. The studies were conducted in accordance with the Belmont Report and U.S. Common Rule and approved by GHS IRB. Subsequently, the pathology department provided the tissue in Advanced Dulbecco's Modified Eagle Medium/Ham's F-12 (DMEM/F-12) (Thermo Fisher, Waltham, MA, USA). The medium was supplemented with 50 U/ml penicillin, 50 U/ml streptomycin, 1% GlutaMAX, and 10 mM HEPES. Cell culture additives were purchased from Thermo Fisher (Waltham, MA, USA). Tumor organoids were generated from tumor as described (40). Briefly, a single-cell suspension of tumor cells was generated by dicing tumor into small pieces and digesting with collagenase. Cells were then ACK lysed to remove erythrocytes, and cells were counted. Cells were resuspended in artificial Basement Membrane (Cultrex 3D Culture Matrix Reduced Growth Factor Basement Membrane Extract) (Bio-Techne, Minneapolis, MN, USA) and plated in domes on 48-well plates. Basement Membrane domes were incubated at 37°C for 5 min. Once the Basement Membrane solidified, defined media described in (40) were added to each well. Media on the organoids were changed every 3–4 days for maintenance.

4.2 Chemotherapy treatments

Organoids were collected from Basement Membrane by incubating organoids in TrypLE Express (Thermo Fisher, Waltham, MA, USA) followed by an incubation at 37°C for 5 min. Organoids were mechanically dislodged from the culture surface *via* pipetting up and down, incubated on ice for 1 h, and spun at 1,200 RPM for 10 min at 4°C. After supernatant was removed, cells were resuspended in Basement Membrane. Domes were plated on individual wells of 48-well plates at 10,000 cells per dome. Once gel polymerizes, media were added to each well. Organoids grew for 1 week before receiving chemotherapy treatments. At time of treatment, media were removed from the domes and replaced with media containing drugs as listed in Tables 1, 2.

4.3 Immunofluorescence

Organoids in Basement Membrane domes were plated on four-well chamber slides. Cells were fixed in warm 3.7% formaldehyde in PBS for 15 min at 37°C. Cells were permeabilized and blocked with bovine serum albumin (BSA) in Tris-buffered saline with 0.1% Tween (TBST). UCS1 organoids were incubated with primary antibodies and/or Texas Red phalloidin (Invitrogen, Carlsbad, CA) for 1 h at 37°C. Cells were washed with TBST thrice. For PAX8 and p53, cells were incubated with conjugated secondary antibodies for 1 h at 37°C followed by rinsing with TBST. Fluoromount-G with DAPI (Thermo Fisher, Waltham, MA, USA). Images were collected using an EVOS M5000 (Invitrogen, Carlsbad, CA) or the Leica STELLARIS 5 laser confocal microscope (Leica Microsystems, Inc., Deerfield, IL). IF was evaluated by KDCD and KAL.

4.4 Pathology

The Pathology Department at Gundersen Health Systems used standard H&E and immunohistochemistry (IHC) techniques were used to stain for p53 and cytokeratin AE1AE3 on the UCS patient tumor.

4.5 Annexin V flow cytometry

Organoids were collected from Basement Membrane by incubating organoids in TrypLE followed by an incubation at 37°C for 5 min. Organoids were mechanically dislodged from the culture surface *via* pipetting up and down, incubated on ice for 1 h, and then spun at 1,200 RPM for 10 min at 4°C. Cells were washed with PBS and Annexin V Binding Buffer (10 mM HEPES, 140 mM NaCl, 2.5 mM $CaCl_2$). Then, cells were incubated in Annexin V Binding Buffer with Annexin V-PE (BD Biosciences, Franklin Lakes, NJ) for 15 min at room temperature. Cells were washed with Annexin Binding Buffer. Finally, cells were spun down and resuspended in 0.1% BSA in PBS. Flow cytometry was performed on an Attune NTX flow cytometer (Thermo Fisher, Waltham, MA, USA).

46 Dose curve

To identify the optimal doses for each of the six chemotherapies that we used, we conducted a dose curve using the concentrations in Table 1. Briefly, we plated organoids (10,000 cells per dome) in Basement Membrane domes on individual wells of 48-well plates. Once gel polymerizes, media were added to each well. Organoids were grown for 1 week before receiving chemotherapy treatments. Each treatment was performed in triplicate. To measure cell death, we stained cells with CellEvent Caspase3/7 (Thermo Fisher, Waltham, MA, USA) according to instructions. Briefly, we added CellEvent Caspase3/7 to each culture for 30 min at 37°C along with NucBlue (Thermo Fisher, Waltham, MA, USA) to denote nuclei. We visualized dead cells (apoptotic) using fluorescence microscopy. We took images of each condition and scored cultures for the intensity of fluorescence. A score of 0 was no fluorescence and 3 was the highest intensity.

4.7 Chemicals

Texas Red phalloidin and Fluoromount-G with DAPI were purchased from Thermo Fisher (Waltham, MA, USA). Carboplatin, paclitaxel, gemcitabine, doxorubicin, docetaxel, and ifosfamide were all purchased from (Santa Cruz Biotechnology) (Dallas, TX, USA). Dimethyl Sulfoxide (DMSO) was purchased from Sigma-Aldrich (St. Louis, MO, USA).

4.8 Antibodies

The antibodies for Cytokeratin AE1AE3 (AE1/AE-601-L-CE) was purchased from Leica Biosystems (Deer Park, IL, USA), and p53 antibodies (Clone D0-7) are from (Dako/Agilent, Santa Clara, CA, USA). Anti-PAX8 and anti-Vimentin antibodies were purchased from Santa Cruz Biotechnologies (Dallas, TX, USA). We obtained antibodies against E-cadherin and N-Cadherin from BioLegend (San Diego, CA, USA).

Data availability statement

The original contributions presented in the study are included in the article/Supplementary Material, further inquiries can be directed to the corresponding author/s.

Ethics statement

The studies involving humans were approved by Gundersen Health Systems Institutional Review Board. The studies were conducted in accordance with the local legislation and institutional requirements. The participants provided their written informed consent to participate in this study.

Author contributions

MD: Investigation, Writing – original draft. KL: Data curation, Writing – review & editing. CH: Investigation, Writing – original draft. GH: Resources, Writing – review & editing. SH: Formal analysis, Resources, Writing – review & editing. KC: Conceptualization, Formal analysis, Investigation, Project administration, Writing – original draft, Writing – review & editing.

Funding

The author(s) declare financial support was received for the research, authorship, and/or publication of this article. Funding for this research was provided by the Kabara Cancer Research Institute.

Conflict of interest

The authors declare that the research was conducted in the absence of any commercial or financial relationships that could be construed as a potential conflict of interest.

Publisher's note

All claims expressed in this article are solely those of the authors and do not necessarily represent those of their affiliated organizations, or those of the publisher, the editors and the reviewers. Any product that may be evaluated in this article, or claim that may be made by its manufacturer, is not guaranteed or endorsed by the publisher.

Supplementary material

The Supplementary Material for this article can be found online at: https://www.frontiersin.org/articles/10.3389/fonc.2024.1368592/full#supplementary-material

SUPPLEMENTARY FIGURE 1
Dose curve on the six chemotherapies applied to UCS1 organoids. UCS1 organoids were treated with DMSO (Dose 1) or increasing concentrations of carboplatin, docetaxel, doxorubicin, gemcitabine, ifosfomide, or paclitaxel (See). Cells were stained with CellEvent Caspase 3/7 and intensity of caspase activation/fluorescence was scored on a scale of 0 (no fluorescence) to 3 most intense fluorescence. DMSO treatment was 0 (not shown on graph) as was Dose 2 of carboplatin.

SUPPLEMENTARY FIGURE 2
Nuclear and cellular morphology of UCS1 cells treated with gemcitabine combination chemotherapies. UCS1 cultures were treated with DMSO, Carboplatin/Paclitaxel (C1), Carboplatin/Gemcitabine (C3) or Gemcitabine/Paclitaxel (C7) for 48 hours or DMSO DAPI as an indication of nuclear integrity or Texas-Red Phalloidin. Fluorescent images were collected. 10x magnification.

References

1. Murali R, Davidson B, Fadare O, Carlson JA, Crum CP, Gilks CB, et al. High-grade endometrial carcinomas: morphologic and immunohistochemical features, diagnostic challenges and recommendations. *Int J Gynecol Pathol*. (2019) 38 Suppl 1: S40–63. doi: 10.1097/PGP.0000000000000491

2. Bogani G, Ray-Coquard I, Concin N, Ngoi NYL, Morice P, Enomoto T, et al. Uterine serous carcinoma. *Gynecol Oncol*. (2021) 162:226–34. doi: 10.1016/j.ygyno.2021.04.029

3. Raffone A, Travaglino A, Raimondo D, Maletta M, De Vivo V, Visiello U, et al. Uterine carcinosarcoma vs endometrial serous and clear cell carcinoma: A systematic review and meta-analysis of survival. *Int J Gynaecol Obstet*. (2022) 158:520–7. doi: 10.1002/ijgo.14033

4. Matsuzaki S, Klar M, Matsuzaki S, Roman LD, Sood AK, Matsuo K. Uterine carcinosarcoma: Contemporary clinical summary, molecular updates, and future research opportunity. *Gynecol Oncol*. (2021) 160:586–601. doi: 10.1016/j.ygyno.2020.10.043

5. Chen X, Arend R, Hamele-Bena D, Tergas AI, Hawver M, Tong GX, et al. Uterine carcinosarcomas: clinical, histopathologic and immunohistochemical characteristics. *Int J Gynecol Pathol*. (2017) 36:412–9. doi: 10.1097/PGP.0000000000000346

6. D'Angelo E, Prat J. Pathology of mixed Mullerian tumours. *Best Pract Res Clin Obstet Gynaecol*. (2011) 25:705–18. doi: 10.1016/j.bpobgyn.2011.05.010

7. Sreenan JJ, Hart WR. Carcinosarcomas of the female genital tract. A pathologic study of 29 metastatic tumors: further evidence for the dominant role of the epithelial component and the conversion theory of histogenesis. *Am J Surg Pathol*. (1995) 19:666–74. doi: 10.1097/00000478-199506000-00007

8. Athavale R, Thomakos N, Godfrey K, Kew F, Cross P, de Barros Lopes A, et al. The effect of epithelial and stromal tumor components on FIGO stages III and IV ovarian carcinosarcomas treated with primary surgery and chemotherapy. *Int J Gynecol Cancer*. (2007) 17:1025–30. doi: 10.1111/j.1525-1438.2007.00919.x

9. Ismail A, Choi S, Boussios S. Frontiers of ovarian carcinosarcoma. *Curr Treat Options Oncol*. (2023) 24:1667–82. doi: 10.1007/s11864-023-01138-4

10. Nayha V, Stenback F. Angiogenesis and expression of angiogenic agents in uterine and ovarian carcinosarcomas. *APMIS*. (2008) 116:107–17. doi: 10.1111/j.1600-0463.2008.00757.x

11. Matsuo K, Takazawa Y, Ross MS, Elishaev E, Podzielinski I, Yunokawa M, et al. Significance of histologic pattern of carcinoma and sarcoma components on survival outcomes of uterine carcinosarcoma. *Ann Oncol*. (2016) 27:1257–66. doi: 10.1093/annonc/mdw161

12. de Jong RA, Nijman HW, Wijbrandi TF, Reyners AK, Boezen HM, Hollema H. Molecular markers and clinical behavior of uterine carcinosarcomas: focus on the epithelial tumor component. *Mod Pathol*. (2011) 24:1368–79. doi: 10.1038/modpathol.2011.88

13. Leskela S, Perez-Mies B, Rosa-Rosa JM, Cristobal E, Biscuola M, Palacios-Berraquero ML, et al. Molecular basis of tumor heterogeneity in endometrial carcinosarcoma. *Cancers (Basel)*. (2019) 11. doi: 10.3390/cancers11070964

14. Zhao S, Bellone S, Lopez S, Thakral D, Schwab C, English DP, et al. Mutational landscape of uterine and ovarian carcinosarcomas implicates histone genes in epithelial-mesenchymal transition. *Proc Natl Acad Sci U S A*. (2016) 113:12238–43. doi: 10.1073/pnas.1614120113

15. Franceschi T, Durieux E, Morel AP, de Saint Hilaire P, Ray-Coquard I, Puisieux A, et al. Role of epithelial-mesenchymal transition factors in the histogenesis of uterine carcinomas. *Virchows Arch*. (2019) 475:85–94. doi: 10.1007/s00428-019-02532-w

16. Osakabe M, Fukagawa D, Sato C, Sugimoto R, Uesugi N, Ishida K, et al. Immunohistochemical analysis of the epithelial to mesenchymal transition in uterine carcinosarcoma. *Int J Gynecol Cancer*. (2019) 29:277–81. doi: 10.1136/ijgc-2018-000038

17. Cherniack AD, Shen H, Walter V, Stewart C, Murray BA, Bowlby R, et al. Integrated molecular characterization of uterine carcinosarcoma. *Cancer Cell*. (2017) 31:411–23. doi: 10.1016/j.ccell.2017.02.010

18. Dwivedi SK, McMeekin SD, Slaughter K, Bhattacharya R. Role of TGF-beta signaling in uterine carcinosarcoma. *Oncotarget*. (2015) 6:14646–55. doi: 10.18632/oncotarget.3711

19. Dwivedi SKD, Rao G, Dey A, Buechel M, Zhang Y, Zhang M, et al. Targeting the TGFbeta pathway in uterine carcinosarcoma. *Cell Stress*. (2020) 4:252–60. doi: 10.15698/cst2020.11.234

20. Tseng JH, Bisogna M, Hoang LN, Olvera N, Rodriguez-Aguayo C, Lopez-Berestein G, et al. miR-200c-driven mesenchymal-to-epithelial transition is a therapeutic target in uterine carcinosarcomas. *Sci Rep*. (2017) 7:3614. doi: 10.1038/s41598-017-03972-7

21. De Craene B, Berx G. Regulatory networks defining EMT during cancer initiation and progression. *Nat Rev Cancer*. (2013) 13:97–110. doi: 10.1038/nrc3447

22. Zhu H, Gu X, Xia L, Zhou Y, Bouamar H, Yang J, et al. A novel TGFbeta trap blocks chemotherapeutics-induced TGFbeta1 signaling and enhances their anticancer activity in gynecologic cancers. *Clin Cancer Res*. (2018) 24:2780–93. doi: 10.1158/1078-0432.CCR-17-3112

23. Gyamfi J, Lee YH, Eom M, Choi J. Interleukin-6/STAT3 signalling regulates adipocyte induced epithelial-mesenchymal transition in breast cancer cells. *Sci Rep*. (2018) 8:8859. doi: 10.1038/s41598-018-27184-9

24. Heldin CH, Landstrom M, Moustakas A. Mechanism of TGF-beta signaling to growth arrest, apoptosis, and epithelial-mesenchymal transition. *Curr Opin Cell Biol*. (2009) 21:166–76. doi: 10.1016/j.ceb.2009.01.021

25. Johansson J, Tabor V, Wikell A, Jalkanen S, Fuxe J. TGF-beta1-induced epithelial-mesenchymal transition promotes monocyte/macrophage properties in breast cancer cells. *Front Oncol*. (2015) 5:3. doi: 10.3389/fonc.2015.00003

26. Katcher A, Yueh B, Ozler K, Nizam A, Kredentser A, Chung C, et al. Establishing patient-derived organoids from human endometrial cancer and normal endometrium. *Front Endocrinol (Lausanne)*. (2023) 14:1059228. doi: 10.3389/fendo.2023.1059228

27. Spagnol G, Sensi F, De Tommasi O, Marchetti M, Bonaldo G, Xhindoli L, et al. Patient derived organoids (PDOs), extracellular matrix (ECM), tumor microenvironment (TME) and drug screening: state of the art and clinical implications of ovarian cancer organoids in the era of precision medicine. *Cancers (Basel)*. (2023) 15. doi: 10.3390/cancers15072059

28. Bi J, Newtson AM, Zhang Y, Devor EJ, Samuelson MI, Thiel KW, et al. Successful patient-derived organoid culture of gynecologic cancers for disease modeling and drug sensitivity testing. *Cancers (Basel)*. (2021) 13. doi: 10.3390/cancers13122901

29. Powell MA, Filiaci VL, Hensley ML, Huang HQ, Moore KN, Tewari KS, et al. Randomized phase III trial of paclitaxel and carboplatin versus paclitaxel and ifosfamide in patients with carcinosarcoma of the uterus or ovary: an NRG oncology trial. *J Clin Oncol*. (2022) 40:968–77. doi: 10.1200/JCO.21.02050

30. Bobinski M, Okla K, Luszczki J, Bednarek W, Wawruszak A, Moreno-Bueno G, et al. Gemcitabine and selected mTOR inhibitors in uterine sarcomas and carcinosarcoma cells- an isobolographic analysis. *Int J Med Sci*. (2020) 17:2987–97. doi: 10.7150/ijms.48187

31. Miller BE, Blessing JA, Stehman FB, Shahin MS, Yamada SD, Secord AA, et al. A phase II evaluation of weekly gemcitabine and docetaxel for second-line treatment of recurrent carcinosarcoma of the uterus: a gynecologic oncology group study. *Gynecol Oncol*. (2010) 118:139–44. doi: 10.1016/j.ygyno.2010.03.024

32. Ozols RF. Gemcitabine and carboplatin in second-line ovarian cancer. *Semin Oncol*. (2005) 32:S4–8. doi: 10.1053/j.seminoncol.2005.06.023

33. Nasr FL, Chahine GY, Kattan JG, Farhat FS, Mokaddem WT, Tueni EA, et al. Gemcitabine plus carboplatin combination therapy as second-line treatment in patients with relapsed breast cancer. *Clin Breast Cancer*. (2004) 5:117–22; discussion 23-4. doi: 10.3816/CBC.2004.n.015

34. Dazzi C, Cariello A, Casanova C, Verlicchi A, Montanari M, Papiani G, et al. Gemcitabine and paclitaxel combination as second-line chemotherapy in patients with small-cell lung cancer: a phase II study. *Clin Lung Cancer*. (2013) 14:28–33. doi: 10.1016/j.cllc.2012.03.003

35. Harada M, Tomisaki I, Minato A, Onishi R, Terado M, Inatomi H, et al. Combination therapy with paclitaxel and gemcitabine after platinum-based chemotherapy in patients with advanced urothelial cancer. *Int J Urol*. (2021) 28:970–4. doi: 10.1111/iju.14616

36. Suyama T, Ueda T, Fukasawa S, Imamura Y, Nakamura K, Miyasaka K, et al. Combination of gemcitabine and paclitaxel as second-line chemotherapy for advanced urothelial carcinoma. *Jpn J Clin Oncol*. (2009) 39:244–50. doi: 10.1093/jjco/hyp003

37. Cuppens T, Depreeuw J, Annibali D, Thomas D, Hermans E, Gomme E, et al. Establishment and characterization of uterine sarcoma and carcinosarcoma patient-derived xenograft models. *Gynecol Oncol*. (2017) 146:538–45. doi: 10.1016/j.ygyno.2017.06.005

38. Jeong SY, Cho YJ, Ryu JY, Choi JJ, Hwang JR, Kim B, et al. Establishment and preclinical application of a patient-derived xenograft model for uterine cancer. *Gynecol Oncol*. (2021) 162:173–81. doi: 10.1016/j.ygyno.2021.04.028

39. Yagishita S, Nishikawa T, Yoshida H, Shintani D, Sato S, Miwa M, et al. Co-clinical study of [fam-] trastuzumab deruxtecan (DS8201a) in patient-derived xenograft models of uterine carcinosarcoma and its association with clinical efficacy. *Clin Cancer Res*. (2023) 29:2239–49. doi: 10.1158/1078-0432.CCR-22-3861

40. Hill SJ, Decker B, Roberts EA, Horowitz NS, Muto MG, Worley MJ Jr., et al. Prediction of DNA repair inhibitor response in short-term patient-derived ovarian cancer organoids. *Cancer Discovery*. (2018) 8:1404–21. doi: 10.1158/2159-8290.CD-18-0474

frontiers | Frontiers in Oncology

TYPE Original Research
PUBLISHED 25 March 2024
DOI 10.3389/fonc.2024.1373607

Check for updates

OPEN ACCESS

EDITED BY
Dragos Eugen Georgescu,
Carol Davila University of Medicine and Pharmacy, Romania

REVIEWED BY
Teodor Florin Georgescu,
Carol Davila University of Medicine and Pharmacy, Romania
Mihai Emil Capilna,
George Emil Palade University of Medicine, Pharmacy, Sciences and Technology of Târgu Mureş, Romania
Mario Murguia-Perez,
Mexican Social Security Institute, Mexico

*CORRESPONDENCE
Rong Liu
liurongdoctor@tjh.tjmu.edu.cn

RECEIVED 20 January 2024
ACCEPTED 11 March 2024
PUBLISHED 25 March 2024

CITATION
Zhang L, Liu R and Peng J (2024) Misleading clinical and imaging features in atypical aggressive angiomyxoma of the female vulvovaginal or perianal region: report of three cases and review of the literature. *Front. Oncol.* 14:1373607. doi: 10.3389/fonc.2024.1373607

COPYRIGHT
© 2024 Zhang, Liu and Peng. This is an open-access article distributed under the terms of the Creative Commons Attribution License (CC BY). The use, distribution or reproduction in other forums is permitted, provided the original author(s) and the copyright owner(s) are credited and that the original publication in this journal is cited, in accordance with accepted academic practice. No use, distribution or reproduction is permitted which does not comply with these terms.

Misleading clinical and imaging features in atypical aggressive angiomyxoma of the female vulvovaginal or perianal region: report of three cases and review of the literature

Ling Zhang[1], Rong Liu[1,2]* and Jian Peng[3]

[1]Department of Obstetrics and Gynecology, National Clinical Research Center for Obstetrics and Gynecology, Tongji Hospital, Tongji Medical College, Huazhong University of Science and Technology, Wuhan, China, [2]Key Laboratory of Cancer Invasion and Metastasis (Ministry of Education), Hubei Key Laboratory of Tumor Invasion and Metastasis, Tongji Hospital, Tongji Medical College, Huazhong University of Science and Technology, Wuhan, China, [3]Department of Radiology, Tongji Hospital, Tongji Medical College, Huazhong University of Science and Technology, Wuhan, China

Objectives: Aggressive (deep) angiomyxoma (AAM) is a rare mesenchymal tumor that typically originates from the vulvovaginal region, perineum, and pelvis in adult women. The objective of this case report and literature review is to comprehensively analyze the clinical, imaging, and pathological characteristics of atypical AAM in the female lower genital tract and pelvic floor in order to minimize preoperative misdiagnosis or missed diagnosis and ultimately optimize the clinical management strategy.

Methods: The data of three cases with atypical AAM, which demonstrate similarities with other lesions observed in the female lower genital tract over the past 1.5 years, were retrospectively described. This description included clinical management, images and reports of ultrasonography (US) and magnetic resonance imaging (MRI), clinicopathological features, follow-up, and outcomes. In the Discussion section, a review of the literature on MEDLINE (PubMed) and Web of Science from the past 50 years was conducted.

Results: The three cases all underwent preoperative ultrasonography, and two of them also underwent preoperative MRI examination. Complete resection of the lesions was performed in all three cases, followed by postoperative pathological examination. The histopathology of these three cases revealed invasive angiomyxoma, as confirmed by immunohistochemical staining, which demonstrated positive expression of desmin, vimentin, estrogen, and progesterone receptors. The patients experienced a smooth postoperative recovery. Ultrasound had a diagnostic accuracy rate of 100% (3/3) for locating and determining the extent of the lesions; however, its specific diagnostic accuracy rate for identifying the pathological type was only 33% (1/3). In contrast, MRI had a diagnostic accuracy rate of 100% (2/2) for locating and determining the extent of lesions but did not show any specific diagnostic accuracy for identifying the pathological types.

Conclusions: Our findings indicate that even if a vulvovaginal lesion presents with a superficial location, small size, limited scope, and regular shape, suspicion of atypical AAM should arise when palpation reveals toughness, tensility, and deformability under pressure. US reveals a well-defined hypoechoic to anechoic mass with uniformly distributed coarse dot echoes, with or without detectable intratumoral blood flow signal. MRI shows prolonged T1 and T2 signals with inhomogeneous enhancement and evident diffusion restriction on diffusion-weighted imaging (DWI).

KEYWORDS

aggressive angiomyxoma, perineal soft tissue mass, vestibular gland cyst, vaginal wall prolapse, ultrasonography, magnetic resonance imaging

1 Introduction

Aggressive (deep) angiomyxoma (AAM) is a rare, benign mesenchymal tumor that almost exclusively occurs in the deep soft tissues of the genital area. It is considered aggressive due to its local infiltration and high rate of local recurrence after resection (1, 2). The latest edition of the World Health Organization Classification of Tumors of Soft Tissue and Bone defines deep angiomyxoma as a uniformly paucicellular myxoedematous tumor with infiltrative margins and a prominent vascular component (3). To our knowledge, since AAM was first described in 1983 by Steeper and Rosai, approximately 400 cases have been reported in the literature (1). The reported female-to-male ratio ranges from 6.6:1 to 9:1 (4, 5).

Due to its rare occurrence and non-specific clinical manifestations, clinical misdiagnosis is common, and imaging is helpful for the clinical management of AAM and follow-up. Based on typical imaging features, the radiologist was able to suspect that the lesion represented AAM initially. If there are no specific signs indicating AAM presence, this lesion might be mistaken for an AAM mimic like vestibular gland cysts, leiomyomas, inflammation, or other soft tissue tumors. Surgical resection remains a primary treatment option. Accurate evaluation of both the type and extent of this lesion plays a vital role in determining an appropriate surgical approach for tumor removal. Ultimately, pathological diagnosis confirms whether it is indeed an instance of AAM.

We conducted a retrospective study of three patients with AAM to assess the atypical clinical and imaging features that may lead to misdiagnosis. To our knowledge, there is a lack of literature regarding AAM, which often presents challenges for accurate diagnosis. We thoroughly reviewed all available images, including ultrasonography (US) and magnetic resonance imaging (MRI). Our aim was to provide a comprehensive description of radiological features in conjunction with clinical and histological findings, ultimately reducing preoperative misdiagnosis or missed diagnoses.

2 Materials and methods

2.1 Study design

This study is a retrospective and descriptive analysis of the data collected in routine medical records of three patients with AAM, including the clinical management, US and MRI images and reports, clinicopathological features, follow-up, and outcomes. In the Discussion section, a review of the literature on MEDLINE (PubMed) and Web of Science from the past 50 years was conducted.

2.2 Study population

These three cases were all referred to the Department of Obstetrics and Gynecology of Tongji Hospital, affiliated with Tongji Medical College of Huazhong University of Science and Technology, from other hospitals between February 2022 and August 2023. In the hospital, all patients underwent detailed preoperative imaging examination, surgical and pathological diagnosis, and regular postoperative follow-up. Clinical demographic information, gynecological examination, surgical data, follow-up information, patient clinicopathological features, and imaging features were retrieved from the original electronic hospital medical records and image reporting system.

2.3 Statistical analyses

The statistical software package SPSS26.0 (IBM SPSS Statistics for Windows, 26.0 version, Armonk, NY, USA) was used for data analysis. The classified variables are represented as n (%).

3 Results

3.1 Case 1

3.1.1 Clinical history

The patient, a 49-year-old woman, reported that she had been diagnosed with vaginal prolapse approximately 1 year ago. She experienced worsening symptoms when standing or being active, accompanied by urinary incontinence that worsened when sneezing. However, she did not have difficulty urinating and also experienced pain during urination. Initially, the patient received pelvic floor rehabilitation training for anterior vaginal wall prolapse at a local hospital; however, her symptoms did not improve. Subsequently, she was transferred to our department for further evaluation. Clinical gynecological examination revealed a multiparous and gravid vulva with a smooth vaginal canal and minimal secretions. During the Valsalva maneuver, there was an evident protrusion of the anterior vaginal wall extending beyond 3.0–4.0 cm of the hymen along with urinary retention. Mild cervical discharge was observed along with an anteverted uterus and no apparent abnormalities in the bilateral adnexa. The preliminary clinical diagnosis remained as anterior vaginal wall prolapse.

3.1.2 Imaging examinations

The transperineal pelvic floor ultrasound revealed a hypoechoic mass measuring 3.9 × 3.6 × 4.6 cm, which was located in the space between the urethra and the middle-lower segment of the vagina. The mass had clear boundaries and showed obvious protrusion toward the vagina (Figures 1A1–10). Blood flow signals were observed surrounding it with a resistance index (RI) of 0.64. Ultrasonographic diagnosis suggested that the solid mass in the urethrovaginal space originated from the vaginal wall and was a leiomyoma. The patient did not undergo an MRI examination.

3.1.3 Surgical findings

During the surgery, a palpable mass measuring approximately 4.0 × 5.0 cm in size was observed on the anterior vaginal wall under anesthesia, indicating evident protrusion (Figure 1B1). Notably, there was no discernible prolapse observed in the cervix or posterior vaginal wall. A longitudinal incision of approximately 1.0 cm was made in the mucosa and submucosal connective tissue of the anterior vaginal wall, located approximately 0.5 cm below the transverse sulcus of the urethra. A mass in the urethral space (Figure 1B2) was carefully dissected and completely excised, followed by transvaginal tension-free transobturator suburethral tape (TVT-O) surgery to suspend the middle part of the urethra. The excised tissue, measuring 4.0 × 5.0 cm and displaying an oval shape with a pink hue (Figure 1B3), exhibited a gray color and medium soft tissue consistency upon sectioning (Figure 1B4). Subsequently, it was sent for pathological examination. The vulva returned to its normal appearance after the surgical procedure (Figure 1B5).

3.1.4 Pathological examination results

Histopathological examination of the specimen revealed a tumor composed of fibroblasts and maternal muscle fiber cells, exhibiting characteristics consistent with a benign-intermediate type. Microscopically, mild cellular morphology was observed in the spindle cell proliferation against a background of extensive mucus degeneration; irregular hyperplasia of small vessels in the stroma was also observed (Figures 1C1,2). Immunohistochemical analysis of the specimen demonstrated strong positive staining for desmin (Figures 1C3,4), estrogen receptor (ER) (Figures 1C5,6), and progesterone receptor (PR) (Figures 1C7,8), as well as smooth muscle actin (SMA), caldesmon, and CD10. Partial positivity was observed for S-100, while negative staining was observed for CD34, β-catenin, and myogenin. The Ki-67 immunohistochemical index was estimated to be approximately 1%. No HMGA2 rearrangement, CTNNB1 gene mutations, or APC gene mutations were detected by molecular analysis. The final histopathological diagnosis indicated AAM with positive surgical margins.

3.1.5 Follow–up and outcomes

The patient reported no postoperative discomfort, and a postoperative ultrasound examination of the pelvic floor revealed no lesions. Therefore, there was no evidence of recurrence during the 1-month and 7-month follow-up visits.

3.2 Case 2

3.2.1 Clinical history

The patient was a 53-year-old woman who presented with a tumor in the left perineum that had persisted for 6 months without pain, fever, or other discomfort. She experienced urine leakage when coughing and had not received any related treatment. Clinical examination revealed a married and delivered vulva, as well as a cystic solid mass that could be observed and touched in the subcutaneous fossa of the left ischium. The preliminary clinical diagnosis was a vulvar mass.

3.2.2 Imaging examinations

The transvaginal and transperineal pelvic floor ultrasound showed an extremely irregular and uneven echo mass measuring 15.8 × 4.9 × 5.4 cm in the left ischiorectal fossa (Figures 2A1–4). The boundary was unclear, with no obvious capsule present. It extended upward below the plane of the hiatus of the levator ani muscle, and the inner boundary was close to the left external anal sphincter, left superficial perineal transverse muscle, and left anal levator muscle. The inferior margin reached a depth of 0.5 cm subcutaneously in the perineum. There were numerous corded high echoes, striped blood flow signals, and an RI of 0.74. The ultrasonographic diagnosis suggested the presence of a solid heterogeneous soft tissue tumor in the left perineum, ischiorectal fossa, and pelvic space, which could possibly be an AAM. The pelvic MRI (including a pelvic plain scan, perfusion imaging, diffusion, and multi-directional delay enhancement) revealed prolonged T1 and T2 signals in the left perineum, ischiorectal fossa, and pelvic space. The maximum dimensions measured approximately 3.4 × 10.0 × 9.6 cm (left–right diameter × anterior–posterior diameter × superior–inferior diameter). Inhomogeneous enhancement was observed with evident diffusion restriction on diffusion-weighted

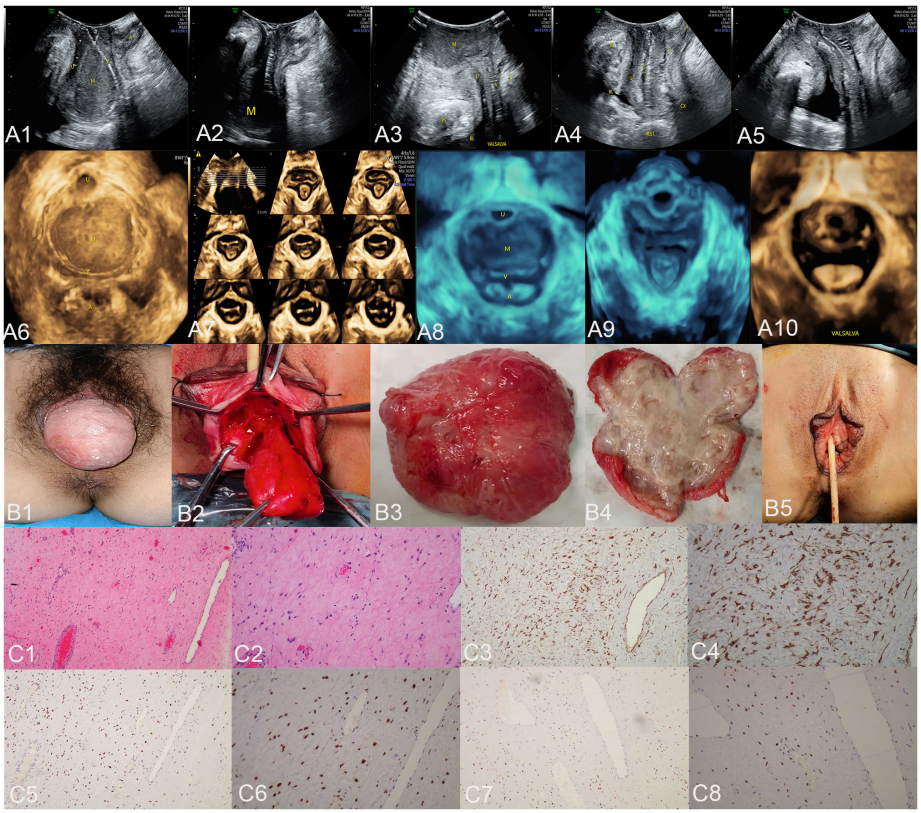

FIGURE 1
The ultrasound **(A1–A10)**, surgical **(B1–B5)**, and pathological images **(C1–C8)** of case 1. US: panels **(A1–A3)** respectively display the median sagittal sections of the transperineal ultrasound in the resting state, maximum contraction state, and maximum Valsalva state of the patient in the lithotomy position preoperatively. In panel **(A1)**, an AAM lesion is observed within the urethrovaginal space; it ascends to the posterior aspect of the bladder in panel **(A2)** and descends to the vaginal opening in panel **(A3)** (M represents the AAM lesion). All the lesions appeared as homogeneous hypoechoic masses with well-defined margins. Panels **(A4, A5)** show the median sagittal sections of perineal ultrasound in the resting state and maximum Valsalva state, respectively, of the patient 7 months post-surgery without any observed lesions. Panels **(A6, A8)** display the axial planes of HLAM reconstructed by three-dimensional ultrasound in the resting state preoperatively and during the Valsalva maneuver. Panel **(A7)** displays the axial plane of TUI during the maximum contraction state preoperatively. These axial planes provide information about the size, shape, and location of the AAM lesions. In panel **(A6)**, the lesion is observed protruding posteriorly from behind the urethra toward the vagina; in panel **(A7)**, the lesion has ascended completely above the HLAM; in panel **(A8)**, during the Valsalva maneuver, the lesion descends through the HLAM (M represents an AAM lesion). Panels **(A9, A10)** demonstrate the axial plane of the HLAM in the resting state and maximum Valsalva state, respectively, 7 months postsurgery for patient without any observed lesions. Surgery: panels **(B1, B2)** depict the lesion as an oval-shaped mass protruding from the anterior vaginal wall into the vaginal cavity. Panel **(B3)** displays the completely resected lesion, which is a soft tissue mass measuring 4.0 × 5.0 cm and exhibiting an oval shape with a pink appearance. Panel **(B4)** displays the lesion upon sectioning, which appears as a gray color with medium soft tissue consistency. Panel **(B5)** depicts the appearance of the vulva after the procedure has been completed. HE: Panel **(C1)**, at low magnification, shows that the tumor boundary appears indistinct, revealing a myxedema matrix interspersed with thin collagen fibers and blood vessels of varying thickness within the tumor. The tumor exhibits areas of loose and dense cellularity, with spindle cells uniformly scattered in dense regions without apparent organization (HE, ×100). As shown in panel **(C2)**, at high magnification, the tumor cells exhibited a low density and assumed a stellate or fusiform morphology without evident pleomorphism (HE, ×200). IHC: Tumor cells exhibited strong positive staining for desmin in panel **(C3)** (×100) and panel **(C4)** (×200), estrogen receptors in panel **(C5)** (×100) and panel **(C6)** (×200), and progesterone receptors in panel **(C7)** (×100) and panel **(C8)** (×200). US, ultrasonography; U, urethra; M, mass; V, vagina; A, anus; HLAM, hiatus of levator ani muscle; HE, histopathological examination; IHC, immunohistochemistry; AAM, aggressive angiomyxoma; TUI, tomographic ultrasound imaging.

imaging (DWI) (Figures 2B1–4). MRI revealed an abnormal signal in the left perineum, ischiorectal fossa, and pelvic space, differentiating the tumor from infection.

3.2.3 Surgical findings

During surgery, a 6.0 × 5.0 cm-sized cystic solid mass can be observed and palpated in the subcutaneous fossa of the left ischium, which was soft and non-tender and did not affect vaginal patency (Figure 2C1). A longitudinal incision of 7.0 cm was made on the lateral aspect of the left perineum, cutting through the perineal skin and subcutaneous fat layer by layer. It was observed that the left ischiorectal fossa was significantly enlarged with a non-mobile mass measuring approximately 12.0 × 10.0 × 3.0 cm. The edge of the lesion appeared extremely irregular with multiple pseudopodia-like extensions into the adipose space (Figure 2C2). The blunt and sharp dissection proceeded outward along the left side of the mass, up to the left anal levator muscle, outward to the left obturator muscle, inward to the left pubic rectal muscle, and deep into the left ischiorectal fossa. The mass was completely dissected, the perineal deep transverse muscle and superficial transverse muscle were partially ruptured during dissection, and the rectal mucosa was smooth on digital rectal examination. The excised tissue, measuring

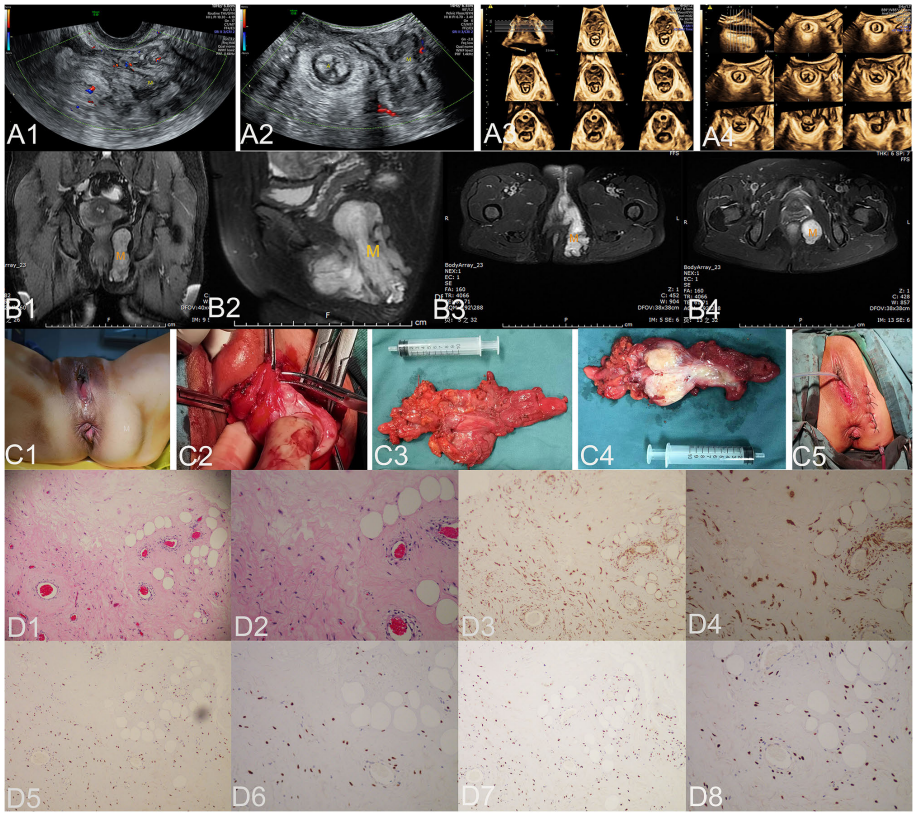

FIGURE 2
The ultrasound **(A1–A4)**, MRI **(B1–B4)**, surgical **(C1–C5)**, and pathological images **(D1–D8)** of case 2. US: In panel **(A1)**, a sagittal section of the left vulva obtained by transvaginal ultrasound reveals an irregular and uneven echo in the subcutaneous vulvar soft tissue, indicating the presence of an AAM lesion. The boundary is indistinct with no apparent capsule, extending upward below the HLAM plane and reaching 0.5 cm into the subcutaneous perineum (M represents AAM lesion). Panels **(A2)** and **(A4)** depict axial planes of the anus, while TUI axial planes of the anus are reconstructed by three-dimensional ultrasound. These images reveal that the lesion is located in the left ischiorectal fossa. The inner boundary was close to the left external anal sphincter, the left superficial perineal transverse muscle, and the left anal levator muscle. The outer boundary reached the pelvic wall (M represents the AAM lesion). Panel **(A3)** displays the TUI axial planes of HLAM reconstructed by three-dimensional ultrasound, demonstrating that the lesion does not extend to the anal levator plane. Panels **(A1)** and **(A2)** display the blood flow signals within the lesion. MRI: Panels **(B1–B4)** illustrate the pelvic coronal plane, the left sagittal plane of the pelvis, the axial plane of the high pelvic floor, and the axial plane of the low pelvic floor, respectively. These images reveal a prolonged T2 signal in the left perineum, ischiorectal fossa, and pelvic space, which define the boundaries of the lesions (M represents the AAM lesion), including their extent on both sides (left and right), upper and lower limits, and anterior and posterior extents. Surgery: Panel **(C1)** illustrates the lesion as a cystic solid mass measuring 6.0 × 5.0 cm, which is palpable in the subcutaneous fossa of the left ischium. Panel **(C2)** illustrates an irregular solid mass with multiple pseudopodia-like extensions infiltrating the adipose tissue in an extreme manner. The lesion, completely resected and displayed in panel **(C3)**, is a soft tissue mass measuring 12.0 × 10.0 × 3.0 cm. It exhibits an extremely irregular solid mass with multiple pseudopodia-like projections and a pink appearance. Panel **(C4)** displays the lesion upon sectioning, which appears as a gray color with medium soft tissue consistency. Panel **(C5)** illustrates the appearance of the vulva after the procedure is completed. HE: Under low magnification, panel **(D1)** shows a homogeneous distribution of spindle cells, blood vessels, and adipose tissue with varying diameters in the stroma of myxoid transformation (HE, ×100). Under high magnification in panel **(D2)**, the tumor cells were irregularly dispersed within the mucous stroma and infiltrated into the adipose tissue. These tumor cells exhibited a short fusiform and oval-shaped morphology without evident nuclear division, displaying mild characteristics (HE, ×200). IHC: Tumor cells exhibited strong positive staining for desmin in panel D3 (×100) and panel **(D4)** (×200), estrogen receptors in panel D5 (×100) and panel **(D6)** (×200), and progesterone receptors in panel **(D7)** (×100) and panel **(D8)** (×200). US, ultrasonography; MRI, magnetic resonance imaging; M, mass; A, anus; HLAM, hiatus of the levator ani muscle; HE, histopathological examination; IHC, immunohistochemistry; AAM, aggressive angiomyxoma; TUI, tomographic ultrasound imaging.

12.0 × 10.0 × 3.0 cm and displaying an extremely irregular shape with multiple pseudopodia-like projections and a pink appearance (Figure 2C3), exhibited a small amount of mucus and no obvious capsule upon sectioning (Figure 2C4) and was subsequently sent for pathological examination. The vulva returned to its normal appearance following the surgical procedure (Figure 2C5).

3.2.4 Pathological examination results

Histopathological examination of the specimen revealed a large number of thick-walled and thin-walled blood vessels in the tumor tissue, which were surrounded by oval and short fusiform cells. Cell atypia was not evident, and a small amount of collagen fibers and mucus were observed between the cells (Figures 2D1,2). Immunohistochemical analysis of the specimens showed strong positive staining for desmin (Figures 2D3,4), vimentin, ER (Figures 2D5,6), and PR (Figures 2D7,8); RB1 also exhibited strong positive staining. CD34 was expressed in small amounts; CD31 showed positive expression within blood vessels; CDK4 had scattered positivity; P16 showed mild positivity; MDM2 displayed partial positivity. SMA, S-100, and pan-cytokeratin exhibited

negative staining. The Ki-67 immunohistochemical index was approximately 2%. Molecular testing shows MDM2 negativity. The final histopathological diagnosis was AAM with positive surgical margins.

3.2.5 Follow–up and outcomes

The patient reported the absence of postoperative discomfort, and no recurrence was observed during the 3-month and 8-month telephone follow-up assessments.

3.3 Case 3

3.3.1 Clinical history

The patient, a 47-year-old woman, reported no specific discomfort and incidentally discovered a vulvar mass 6 months ago. She did not experience fever, abdominal pain, or vulvar pain. Regular evaluations were conducted at other medical facilities, which revealed a gradual increase in size over the past week. This led to the patient seeking treatment at our hospital. During the gynecological examination, a 4.0 × 3.0 cm mass was found in the right vulva with no tenderness and normal vaginal patency. The preliminary clinical diagnosis was a vulvar mass.

3.3.2 Imaging examinations

The transperineal pelvic floor ultrasound showed a well-defined, thick-walled mass measuring 3.7 × 1.1 × 2.9 cm located between 0.3 cm and 1.4 cm beneath the skin of the upper two-thirds of the right labia majora. The mass exhibited echogenicity ranging from echo-poor to hypoechoic with internal dense dot echoes and enhanced far-field echoes (Figures 3A1–4). No peripheral or internal blood flow signals were detected. Based on the ultrasound findings, it was suggested that the abnormal subcutaneous echo observed in the right labia majora could indicate either a lipoma or a mucinous cyst. The MRI revealed a well-defined, round lesion with prolonged T1 and T2 signals in the right vulva, which was diagnosed as a vestibular gland cyst (Figures 3B1–3).

3.3.3 Surgical findings

During the operation, a mass measuring 4.0 × 3.0 cm was identified in the right labia majora (Figure 3C1). A precise longitudinal incision measuring 2.5 cm was made on the surface of the mass, followed by careful blunt dissection to separate it (Figure 3C2). A cavity was formed by subcutaneous expansion and lesion growth (Figure 3C3). The resected lesion, measuring 4.0 × 3.0 cm and displaying an oval shape with a pink appearance (Figure 3C4), exhibited pink mucous soft tissue upon sectioning (Figure 3C5) and was subsequently sent for pathological examination.

3.3.4 Pathological examination results

Histopathological examination of the specimen revealed that the tumor was located in the dermis with unclear boundaries and consisted of fusiform cells, blood vessels of different sizes, and a myxoid matrix (Figures 3D1–3). Immunohistochemical analysis demonstrated strong positive staining for desmin (Figures 3D4,5), ER (Figures 3D6,7), and PR (Figures 3D8,9), as well as caldesmon and vimentin expression. CD34 showed mild positivity, caldesmon showed weak positivity, S-100 showed scattered positivity, and β-catenin staining was positive in the plasma membrane. SMA, SOX10, STAT6, and ALK-IA4 expression were negative. The Ki-67 immunohistochemical index was estimated to be approximately 2%. The final histopathological diagnosis was AAM with positive surgical margins.

3.3.5 Follow–up and outcomes

The patient reported no postoperative discomfort, and a postoperative ultrasound examination of the pelvic floor revealed no lesions. Therefore, there was no evidence of recurrence during the 1-month and 3-month follow-up visits.

3.4 Diagnostic accuracy of imaging

The overall diagnostic accuracy of ultrasound in locating and determining the extent of the lesion was 100% (3/3), but its specific diagnostic accuracy for identifying the pathological type of the lesion was 33% (1/3). However, MRI had a diagnostic accuracy of 100% (2/2) in locating and determining the extent of lesions, but its specific diagnostic accuracy for identifying pathological types of lesions was 0% (0/2).

4 Discussion

4.1 Clinical characteristics

AAM is a rare mesenchymal tumor that typically presents as a slow-growing soft tissue mass, occurring almost exclusively in the deep soft tissues of the vulvovaginal region, perineum, buttock, or pelvis of adult women. The reported age at presentation ranges from 9 months to 89 years, with the highest incidence observed during the fourth and fifth decades of life (6, 7). All three patients in this study were premenopausal women.

AAM lesions in women were primarily located in the vagina, vulva, perineal region, and extraperitoneal spaces of the pelvis (including the prevesical or retropubic, paravesical, paravaginal, pararectal, presacral, urethrovaginal, and rectovaginal spaces and the ischioanal fossa), with a wide range of involvement (8). Patients often visit the hospital due to a palpable, slow-growing, painless soft tissue mass in the vulvovaginal or perianal region or incidental findings of pelvic imaging without other discomfort. Some patients may experience symptoms related to local mass effects, such as dysuria, vaginal discomfort, or dyspareunia (9–15). Two out of the three cases included in this study presented with a gradually expanding and painless vulvar mass, while one exhibited significant anterior vaginal wall prolapse accompanied by urinary incontinence and dysuria. The initial clinical impressions may resemble other benign conditions like vestibular gland cysts, prolapse of the vaginal wall, obturator hernias, pelvic

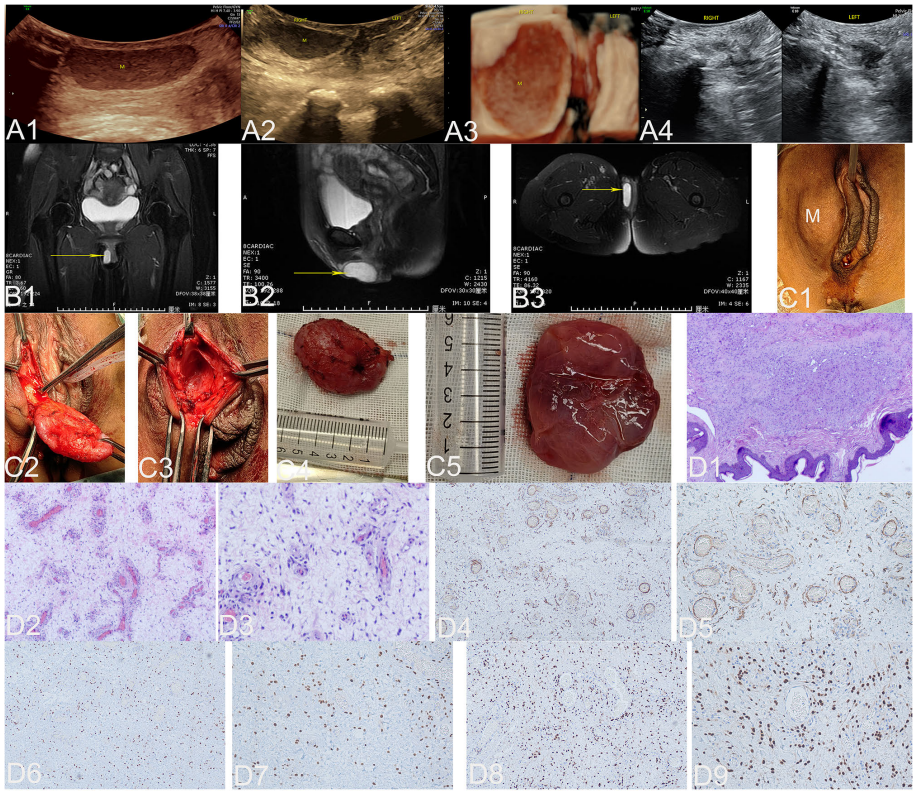

FIGURE 3
The ultrasound **(A1–A4)**, MRI **(B1–B3)**, surgical **(C1–C5)**, and pathological images **(D1–D9)** of case 3. US: The ultrasonic images in panels **(A1–A3)** depict the two-dimensional sagittal section of the right labia majora, the two-dimensional axial section, and the three-dimensional coronal section of both labia majora. These images clearly demonstrate a well-defined, thick-walled mass measuring 3.7 × 1.1 × 2.9 cm located between 0.3 cm and 1.4 cm beneath the skin of the upper two-thirds of the right labia majora (M represents an AAM lesion). The echogenicity of this mass varies from echo-poor to hypoechoic, with dense internal dot echoes and enhanced far-field echoes. Panel **(A4)** shows the sagittal section of the left and right labia majora 3 months after the operation, and no lesions were found. MRI: Panels **(B1–B3)** illustrate the pelvic coronal plane, the right sagittal plane of the pelvis, and the axial plane of the low pelvic floor, respectively. These images reveal a well-defined, round lesion with prolonged T1 and T2 signals in the right vulva (yellow arrow indicates the AAM lesion). Surgery: Panel **(C1)** illustrates a 4.0 × 3.0 cm mass located in the right labia majora (M represents the AAM lesion). Panel **(C2)** depicts an oval soft tissue mass, which is a lesion located on the skin of the right labia majora. Panel **(C3)** illustrates the cavity formed by the subcutaneous expansion and growth of the lesion. The lesion, completely resected and displayed in Panel **(C4)**, is an oval soft tissue mass measuring 4.0 × 3.0 cm with a pink appearance. Panel **(C5)** displays the lesion as pink, soft mucous tissue upon sectioning. HE: At low magnification, panel **(D1)** shows a tumor located within the dermis. The tumor has indistinct boundaries and is composed of spindle cells, blood vessels of varying sizes, and a myxoid matrix (HE, ×40). At low magnification in panel **(D2)**, an abundance of blood vessels can be observed within the backdrop of myxedema, ranging from noticeably slender-walled vessels to substantially thick-walled ones (HE, ×100). Upon high magnification, panel **(D3)** reveals neoplastic cells residing in the stroma of myxedema with reduced cellular density. These cells are characterized by abbreviated fusiform shape and occasional presence of atypical nuclei (HE, ×200). IHC: Tumor cells exhibited strong positive staining for desmin in panel **(D4)** (×100) and panel **(D5)** (×200), estrogen receptors in panel **(D6)** (×100) and panel **(D7)** (×200), and progesterone receptors in panel **(D8)** (×100) and panel **(D9)** (×200). US, ultrasonography; MRI, magnetic resonance imaging; M, mass; A, anus; HE, histopathological examination; IHC, immunohistochemistry; AAM, aggressive angiomyxoma.

inflammatory masses, and other perineal tumors. The initial clinical diagnosis of the three cases in this study was identified as anterior vaginal wall prolapse, vulvar mass, and vulvar mass.

4.2 Imaging diagnosis

An accurate preoperative diagnosis should alert the surgeon to the necessity of wide excision, which is crucial for preventing local recurrence (5). The preoperative clinical manifestations are non-specific, and imaging examinations play an important role in the preoperative diagnosis, including determining the nature and extent of the suspected lesion. Imaging techniques including ultrasonography, computed tomography (CT), and MRI can reveal characteristic features of typical AAM, such as a multilocular or polypoid mass extending across the pelvic diaphragm with a pelvic and perineal component, along with finger-like projections infiltrating the surrounding soft tissues without invasion. These imaging modalities also showed laminated or swirling patterns (16–20).

On ultrasonography, a typical AAM presents as an ill-defined hypoechoic or isoechoic solid mass that extends down the lateral pelvis. It is separated from the pelvic organs and has an irregular and multi-lobed morphology, with finger-like or lingual-like extensions to the surrounding soft tissue or vulvar surface. The mass pushes against adjacent structures or protrudes from the vulvar surface, showing a laminated or swirled appearance of inner echogenicity due to alternating high and low echo

intensities. Color Doppler imaging reveals abundant blood flow signals within and surrounding the tumor, while pulse Doppler imaging can detect arterial bloodstream spectrum. The obvious deformation of the lesion can be observed through probe pressure in real-time ultrasonography (21–24). In our study, one case occurred in the left rectal fossa and vulva with the typical ultrasound features described above, and AAM was accurately diagnosed by the sonographer. However, in the remaining two cases, the lesions were located in the urethrovaginal space and beneath the skin of the upper two-thirds of the right labia majora. Ultrasonographically, these lesions presented as oval hypoechoic to anechoic masses with well-defined margins, homogeneous distribution of coarse blip echoes, and no detectable intratumoral blood flow signal. The ultrasonic misdiagnosis was either a vaginal leiomyoma or a vulvar subcutaneous myxoma.

A typical AAM lesion is characterized by a well-defined mass that displaces adjacent structures on both CT and MRI. It exhibits hypoattenuation relative to the muscle on CT, hyperintense signal on T2-weighted MRI sequences, and hypointensity or isointensity on T1-weighted MRI sequences. Furthermore, both CT and MRI images exhibit avid and heterogeneous enhancement following intravenous contrast administration, potentially revealing a laminated or swirled appearance due to alternating high and low intensities (8, 17, 20, 24, 25). Two studies have documented the rare imaging characteristics of AAM, which include the presence of internal cystic degeneration, restricted diffusion, hemorrhage, and infiltration into adjacent organs (19, 24). However, due to its highly diverse morphological spectrum, AAM exhibits various imaging features, posing challenges for preoperative imaging diagnosis. Among our three cases, two patients underwent pelvic MRI. One patient exhibited prolonged T1 and T2 signals with inhomogeneous enhancement and evident diffusion restriction on DWI, suggesting a tumor or infection. The other patient presented a well-defined, round lesion with prolonged T1 and T2 signals in the right vulva, suggestive of a vestibular gland cyst.

4.3 Pathological characteristics

4.3.1 Gross pathology

During the operation, on gross examination, typical AAM is usually unencapsulated and poorly or vaguely circumscribed. It may blend imperceptibly with the surrounding soft tissue, extending like fingers or tongues into the adjacent soft tissue or vulvar surface. Most of the completely resected specimens were found to be anomalous and multilobed (14, 26, 27). In our study, the lesion in one case was located in the ischiorectal fossa and vulva, showing the typical growth pattern and shape described above. The lesions of the other two cases were oval with a clear envelope; they expanded into hemispherical protrusions within the vaginal cavity and on the surface of the labia majora. The tumor size varied, ranging from 1.5 to 60 cm in the greatest dimension (28). The maximum diameters of the three lesions in this study were 5 cm, 12 cm, and 4 cm. During sectioning, a typical AAM exhibits a tan-pink to tan-gray coloration. It presents as a voluminous mass with a resilient texture and displays a rubbery, lustrous, gelatinous appearance that is exclusively myxoid, fibro-myxoid, or predominantly fibrosclerotic (1, 26, 27, 29). Areas of congested blood vessels of various sizes, hemorrhage, small-to-large cystic foci, and fibrous tissue in the cord may be present (24, 26, 29). In our study, the incisions of two regular lesions showed small cystic foci in exclusively myxoid tissue ranging from tan-pink to grayish-brown, while the incision of the highly irregular lesion exhibited small cystic foci and cord-like fibrous tissue within the grayish-brown fibro-myxoid tissue.

4.3.2 Histopathological and immunohistochemical pathology

The combination of histopathological examination and immunohistochemical analysis can effectively establish a definitive diagnosis for AAM. The typical histological features of AAM include non-encapsulated lesions composed of small fusiform to stellate cells embedded in a loose mucoid matrix. This matrix contains a substantial number of small and medium blood vessels with varying wall thicknesses (1, 2, 4, 13, 15, 26, 27, 30, 31). On microscopic examination, all specimens from our three cases exhibited the typical features of AAM described above. Immunohistochemically, the tumor cells tested positive for desmin, vimentin, SMA, and CD34 and negative for S-100 and CK. The Ki-67 index was approximately 1%–3%. In most female patients, these characteristics were accompanied by strongly positive expression of ER and PR (15, 31–34). Immunohistochemically, the tumor cells in our three cases exhibited strong positive staining for desmin, vimentin, ER, and PR. SMA showed strong positivity in case 1 but was negative in cases 2 and 3. CD34 was negative in case 1, displayed a small amount of positive staining in case 2, and exhibited mild positivity in case 3. S-100 demonstrated partial positivity in case 1, was negative in case 2, and showed scattered positivity in case 3. The Ki-67 immunohistochemical indices for our three cases were approximately 1%, 2%, and 2%. During molecular testing, the rearrangement of the HMGA2 gene is commonly observed in vulvovaginal AAM, and it serves as a valuable diagnostic tool. This is because most mesenchymal lesions that closely resemble this condition exhibit negative results for this gene rearrangement, although some other mesenchymal lesions such as leiomyomas at this site may show positive results (35, 36). Two out of our three cases underwent molecular testing, one of which exhibited rearrangement in the HMGA2 gene. Additionally, our study identified other molecular markers such as CTNNB1, APC gene mutation, and MDM2 for differential diagnosis.

4.4 Follow-up and outcomes

AAM is characterized by a high recurrence rate of 36%–72% after surgery. Wide surgical excision is considered the gold standard treatment for AAM, and there is no universal consensus regarding hormonal therapy. Most studies (85%) describe successful surgical excision followed by either clinical or radiological (ultrasound or MRI) follow-up (37). The lesions in all three cases included in our study were completely resected, and there was no evidence of recurrence based on clinical and ultrasonographic follow-up for

cases 1 and 3 at the 7-month and 3-month visits, respectively. For case 2, no recurrence was observed during the telephone follow-ups at both the 3-month and 8-month marks, with the patient instructed to self-assess.

5 Conclusions

In conclusion, our findings indicate that due to the atypical clinical manifestations, imaging features, and gross appearance of some AAM, the presence of lesions in various extraperitoneal spaces of the pelvis (including the vagina, vulva, perineal region, prevesical or retropubic space, paravesical space, paravaginal space, pararectal space, presacral space, urethrovaginal space rectovaginal spaces, and ischioanal fossa), particularly when exhibiting extensive abdominal/perineal extension in reproductive-age female patients during the fourth to fifth decade, should raise suspicion for AAM. Even if a vulvovaginal lesion presents with a superficial location, small size, limited scope, and regular shape, suspicion of atypical AAM should arise when palpation reveals toughness, tensility, and deformability under pressure. US reveals a well-defined hypoechoic to anechoic mass with uniformly distributed coarse dot echoes, with or without detectable intratumoral blood flow signal. MRI shows prolonged T1 and T2 signals with inhomogeneous enhancement and evident diffusion restriction on DWI.

Data availability statement

The original contributions presented in the study are included in the article/supplementary material. Further inquiries can be directed to the corresponding author.

Ethics statement

The studies involving humans were approved by Medical Ethics Committee of Tongji Hospital Affiliated to Tongji Medical College of Huazhong University of Science and Technology (approval No. TJ-IRB20230834). The studies were conducted in accordance with the local legislation and institutional requirements. The participants provided their written informed consent to participate in this study. Written informed consent was obtained from the individual(s) for the publication of any potentially identifiable images or data included in this article.

Author contributions

LZ: Conceptualization, Data curation, Formal Analysis, Investigation, Methodology, Project administration, Resources, Software, Supervision, Writing – original draft, Writing – review & editing, Validation, Visualization. RL: Conceptualization, Data curation, Investigation, Methodology, Project administration, Resources, Supervision, Validation, Visualization, Writing – review & editing. JP: Investigation, Resources, Validation, Writing – review & editing.

Funding

The author(s) declare that no financial support was received for the research, authorship, and/or publication of this article.

Acknowledgments

We would like to express our gratitude to all those who helped during the case collection and writing of this manuscript, to the peer reviewers for their opinions and suggestions, and to the editors for their comments and guidance. We especially thank Professor Xi Wang (Department of Pathology of Tongji Hospital, Affiliated with Tongji Medical College of Huazhong University of Science and Technology) for providing pathological pictures and notes for our research.

Conflict of interest

The authors declare that the research was conducted in the absence of any commercial or financial relationships that could be construed as a potential conflict of interest.

Publisher's note

All claims expressed in this article are solely those of the authors and do not necessarily represent those of their affiliated organizations, or those of the publisher, the editors and the reviewers. Any product that may be evaluated in this article, or claim that may be made by its manufacturer, is not guaranteed or endorsed by the publisher.

References

1. Steeper TA, Rosai J. Aggressive angiomyxoma of the female pelvis and perineum. Report of nine cases of a distinctive type of gynecologic soft-tissue neoplasm. *Am J Surg Pathol.* (1983) 7:463–75. doi: 10.1097/00000478-198307000-00009

2. Begin LR, Clement PB, Kirk ME, Jothy S, McCaughey WT, Ferenczy A. Aggressive angiomyxoma of pelvic soft parts: a clinicopathologic study of nine cases. *Hum Pathol.* (1985) 16:621–8. doi: 10.1016/S0046-8177(85)80112-X

3. Kallen ME, Hornick JL. The 2020 WHO classification: what's new in soft tissue tumor pathology? Am. *J Surg Pathol.* (2021) 45:e1–23. doi: 10.1097/PAS.0000000000001552

4. Fetsch JF, Laskin WB, Lefkowitz M, Kindblom LG, Meis-Kindblom JM. Aggressive angiomyxoma: A clinicopathologic study of 29 female patients. *Cancer.* (1996) 78:79–90. doi: 10.1002/(ISSN)1097-0142

5. Wiser A, Korach J, Gotlieb WH, Fridman E, Apter S, Ben-Baruch G. Importance of accurate preoperative diagnosis in the management of aggressive angiomyxoma: report of three cases and review of the literature. *Abdominal Imaging*. (2006) 31:383–6. doi: 10.1007/s00261-005-0378-5

6. Ahmed MAM, Uehelie MA, Rage AMA, Mohey A, Noureldin YA. Aggressive angiomyxoma of the penis: the first case report in a 9-month-old infant. *Urology*. (2017) 104:187–90. doi: 10.1016/j.urology.2016.12.045

7. Amin A, El Badawy S, Bull A. Aggressive angiomyxoma of the vulva. *J Obstetrics Gynaecology*. (2013) 33:325–6. doi: 10.3109/01443615.2012.731456

8. Figueiredo G, O'Shea A, Neville GM, Lee SI. Rare mesenchymal tumors of the pelvis: imaging and pathologic correlation. *Radiographics*. (2022) 42:143–58. doi: 10.1148/rg.210049

9. Tseng Y-A, Lawrence WD, Slater SE. Nodular hyperplasia of the bartholin gland, A benign mimicker of aggressive angiomyxoma: A case series and literature review. *Int J Gynecological Pathol*. (2018) 37:554–8. doi: 10.1097/PGP.0000000000000456

10. Larouche M, Hague CJ, Masoudi H, Geoffrion R. Aggressive angiomyxoma presenting as massive irreducible vaginal prolapse. *Int Urogynecology J*. (2016) 27:1933–4. doi: 10.1007/s00192-016-3112-7

11. Boyd SS, Easwar A, Steinberg AC. Aggressive angiomyxoma presenting as posterior vaginal prolapse. *Int Urogynecology J*. (2019) 30:665–7. doi: 10.1007/s00192-018-3799-8

12. Yalav O, Topal U, Unal AG, Erdogan KE. Aggressive angiomyxoma of the pelvis presenting as an obturator hernia. *Ann Ital Chir*. (2019) 8.

13. Granter SRN. Aggressive angiomyxoma: reappraisal of its relationship to angiomyofibroblastoma in a series of 16 cases. *Histopathology*. (1997) 30:3–10. doi: 10.1046/j.1365-2559.1997.d01-556.x

14. Concepcion Cabanilla-Manuntag MC, Jose Lopez MP, Martin Tampo M, Louie Gaston C. Aggressive angiomyxoma presenting as an ischiorectal fossa tumour. *BMJ Case Rep*. (2020) 28:e234093. doi: 10.1136/bcr-2019-234093

15. Zhang J, Zhu C. Clinical experiences on aggressive angiomyxoma in China (Report of 93 cases). *Int J Gynecological Cancer*. (2010) 20:303–7. doi: 10.1111/IGC.0b013e3181cc339c

16. Davani M, Chablani VN, Saba PR. Aggressive angiomyxoma of pelvic soft tissues: MR imaging appearance. *Am J Roentgenology*. (1998) 170:1113–4. doi: 10.2214/ajr.170.4.9530081

17. Outwater BEM EK, Wagner BJ, Siegelman ES. Aggressive angiomyxoma: findings on CT and MR imaging. *Am J Roentgenology*. (1999) 172:435–8. doi: 10.2214/ajr.172.2.9930798

18. Sinha R, Verma R. Perineal angiomyxomas: Can a differential diagnosis be made with imaging studies? Response. *Radiology*. (2007) 245:612. doi: 10.1148/radiol.2452070211

19. Surabhi VR, Garg N, Frumovitz M, Bhosale P, Prasad SR, Meis JM. Aggressive angiomyxomas: A comprehensive imaging review with clinical and histopathologic correlation. *Am J Roentgenology*. (2014) 202:1171–8. doi: 10.2214/AJR.13.11668

20. Miguez Gonzalez J, Dominguez Oronoz R, Lozano Arranz P, Calaf Forn F, Barrios Sanchez P, Garcia Jimenez A. Aggressive angiomyxoma: imaging findings in 3 cases with clinicopathological correlation and review of the literature. *J Comput Assisted Tomography*. (2015) 39:914–21. doi: 10.1097/RCT.0000000000000305

21. Chien AJ, Freeby JA, Win TT, Gadwood KA. Aggressive angiomyxoma of the female pelvis: Sonographic, CT, and MR findings. *Am J Roentgenology*. (1998) 171:530–1. doi: 10.2214/ajr.171.2.9694499

22. Tariq R, Hasnain S, Siddiqui MT, Ahmed R. Aggressive angiomyxoma: swirled configuration on ultrasound and MR imaging. *J Pakistan Med Assoc*. (2014) 64:345–8.

23. Zhao CY, Su N, Jiang YX, Yang M. Application of ultrasound in aggressive angiomyxoma: Eight case reports and review of literature. *World J Clin cases*. (2018) 6:811–9. doi: 10.12998/wjcc.v6.i14.811

24. Kumar N, Goyal A, Manchanda S, Sharma R, Kumar A, Bansal VK. Aggressive pelvic angiomyxoma and its mimics: can imaging be the guiding light? *Br J Radiol*. (2020), 93. doi: 10.1259/bjr.20200255

25. Jeyadevan NN, Sohaib SAA, Thomas JM, Jeyarajah A, Shepherd JH, Fisher C. Imaging features of aggressive angiomyxoma. *Clin Radiol*. (2003) 58:157–62. doi: 10.1053/crad.2002.1127

26. Sutton BJ, Laudadio J. Aggressive angiomyxoma. *Arch Pathol Lab Med*. (2012) 136:217–21. doi: 10.5858/arpa.2011-0056-RS

27. Magro G, Angelico G, Michal M, Broggi G, Zannoni GF, Covello R, et al. The wide morphological spectrum of deep (Aggressive) angiomyxoma of the vulvo-vaginal region: A clinicopathologic study of 36 cases, including recurrent tumors. *Diagnostics (Basel)*. (2021) 11. doi: 10.3390/diagnostics11081360

28. Chan IM, Hon E, Ngai SW, Ng TY, Wong LC. Aggressive angiomyxoma in females: is radical resection the only option? *Acta Obstetricia Et Gynecologica Scandinavica*. (2000) 79:216–20. doi: 10.1080/j.1600-0412.2000.079003216.x

29. McCluggage WG. A review and update of morphologically bland vulvovaginal mesenchymal lesions. *Int J Gynecological Pathol*. (2005) 24:26–38.

30. Amezcua CA, Begley SJ, Mata N, Felix JC, Ballard CA. Aggressive angiomyxoma of the female genital tract: a clinicopathologic and immunohistochemical study of 12 cases. *Int J Gynecological Cancer*. (2005) 15:140–5. doi: 10.1111/j.1048-891x.2005.15015.x

31. Sun Y, Zhu L, Chang X, Chen J, Lang J. Clinicopathological features and treatment analysis of rare aggressive angiomyxoma of the female pelvis and perineum - a retrospective study. *Pathol Oncol Res*. (2017) 23:131–7. doi: 10.1007/s12253-016-0109-y

32. Zou R, Xu H, Shi Y, Wang J, Wang S, Zhu L. Retrospective analysis of clinicopathological features and prognosis for aggressive angiomyxoma of 27 cases in a tertiary center: a 14-year survey and related literature review. *Arch Gynecology Obstetrics*. (2020) 302:219–29. doi: 10.1007/s00404-020-05592-5

33. McCluggage WG, Patterson A, Maxwell P. Aggressive angiomyxoma of pelvic parts exhibits oestrogen and progesterone receptor positivity. *J Clin Pathol*. (2000) 53:603–5. doi: 10.1136/jcp.53.8.603

34. Bigby SM, Symmans PJ, Miller MV, Dray MS, Jones RW. Aggressive angiomyoma of the female genital tract and pelvis-clinicopathologic features with immunohistochemical analysis. *Int J Gynecological Pathol*. (2011) 30:505–13. doi: 10.1097/PGP.0b013e318211d56c

35. McCluggage WG, Connolly L, McBride HA. HMGA2 is a sensitive but not specific immunohistochemical marker of vulvovaginal aggressive angiomyxoma. *Am J Surg Pathol*. (2010) 34:1037–42. doi: 10.1097/PAS.0b013e3181e32a11

36. Harkness R, McCluggage WG. HMGA2 Is a Useful Marker of Vulvovaginal Aggressive Angiomyxoma but May Be Positive in Other Mesenchymal Lesions at This Site. *Int J Gynecological Pathol*. (2021) 40:185–9. doi: 10.1097/PGP.0000000000000689

37. Gulino FA, Gulisano M, Ettore C, Giorlandino A, Russo E, Ettore G. Aggressive angiomyxoma of the vulva: which is the best management strategy? Description of a case report and review of literature of the last ten years. *J Clin Med*. (2023) 12:1726. doi: 10.3390/jcm12051726

frontiers | Frontiers in Oncology

TYPE Correction
PUBLISHED 12 April 2024
DOI 10.3389/fonc.2024.1406876

Check for updates

OPEN ACCESS

EDITED AND REVIEWED BY
Dragos Eugen Georgescu,
Carol Davila University of Medicine and Pharmacy, Romania

*CORRESPONDENCE
Rong Liu
liurongdoctor@tjh.tjmu.edu.cn

RECEIVED 25 March 2024
ACCEPTED 02 April 2024
PUBLISHED 12 April 2024

CITATION
Zhang L, Liu R and Peng J (2024) Corrigendum: Misleading clinical and imaging features in atypical aggressive angiomyxoma of the female vulvovaginal or perianal region: report of three cases and review of the literature.
Front. Oncol. 14:1406876.
doi: 10.3389/fonc.2024.1406876

COPYRIGHT
© 2024 Zhang, Liu and Peng. This is an open-access article distributed under the terms of the Creative Commons Attribution License (CC BY). The use, distribution or reproduction in other forums is permitted, provided the original author(s) and the copyright owner(s) are credited and that the original publication in this journal is cited, in accordance with accepted academic practice. No use, distribution or reproduction is permitted which does not comply with these terms.

Corrigendum: Misleading clinical and imaging features in atypical aggressive angiomyxoma of the female vulvovaginal or perianal region: report of three cases and review of the literature

Ling Zhang[1], Rong Liu[1,2]* and Jian Peng[3]

[1]Department of Obstetrics and Gynecology, National Clinical Research Center for Obstetrics and Gynecology, Tongji Hospital, Tongji Medical College, Huazhong University of Science and Technology, Wuhan, China, [2]Key Laboratory of Cancer Invasion and Metastasis (Ministry of Education), Hubei Key Laboratory of Tumor Invasion and Metastasis, Tongji Hospital, Tongji Medical College, Huazhong University of Science and Technology, Wuhan, China, [3]Department of Radiology, Tongji Hospital, Tongji Medical College, Huazhong University of Science and Technology, Wuhan, China

KEYWORDS

aggressive angiomyxoma, perineal soft tissue mass, vestibular gland cyst, vaginal wall prolapse, ultrasonography, magnetic resonance imaging

A Corrigendum on

Misleading clinical and imaging features in atypical aggressive angiomyxoma of the female vulvovaginal or perianal region: report of three cases and review of the literature

By Zhang L, Liu R and Peng J. (2024). *Front. Oncol.* 14:1373607. doi: 10.3389/fonc.2024.1373607

In the published article, there was an error in Figure 1 as published. The presence of Figure 1B2 can be attributed to an oversight on the part of the authors, who mistakenly included the wrong image. The corrected Figure 1 and its caption Figure 1 "The ultrasound **(A1–A10)**, surgical **(B1–B5)**, and pathological images **(C1–C8)** of case 1. US: panels **(A1–A3)** respectively display the median sagittal sections of the transperineal ultrasound in the resting state, maximum contraction state, and maximum Valsalva state of the patient in the lithotomy position preoperatively. In panel **(A1)**, an AAM lesion is observed within the urethrovaginal space; it ascends to the posterior aspect of the bladder in panel **(A2)** and descends to the vaginal opening in panel **(A3)** (M represents the AAM lesion). All the lesions appeared as homogeneous hypoechoic masses with well-defined margins. Panels **(A4, A5)** show the median sagittal sections of perineal ultrasound in the resting state and maximum Valsalva state, respectively, of the patient 7 months post-surgery without any observed lesions. Panels **(A6, A8)** display the axial planes of HLAM reconstructed by three-dimensional ultrasound in the resting state preoperatively and during the Valsalva maneuver. Panel **(A7)** displays the axial plane of TUI during the maximum contraction state preoperatively. These axial planes provide information about the size, shape, and

10.3389/fonc.2024.1406876

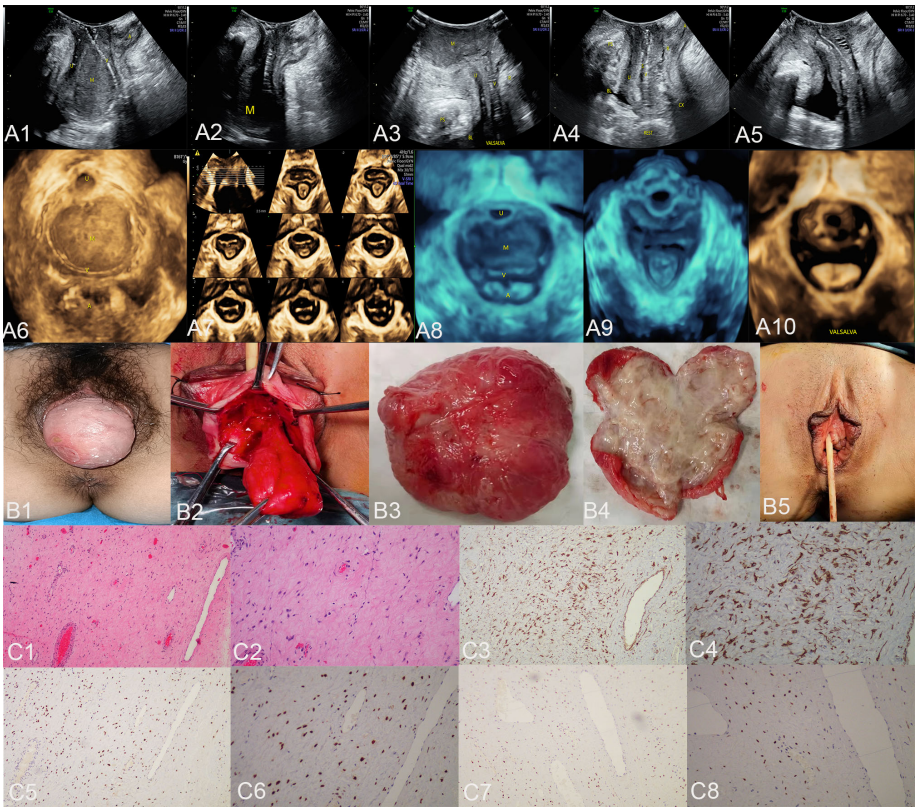

FIGURE 1
The ultrasound **(A1–A10)**, surgical **(B1–B5)**, and pathological images **(C1–C8)** of case 1. US: panels **(A1–A3)** respectively display the median sagittal sections of the transperineal ultrasound in the resting state, maximum contraction state, and maximum Valsalva state of the patient in the lithotomy position preoperatively. In panel **(A1)**, an AAM lesion is observed within the urethrovaginal space; it ascends to the posterior aspect of the bladder in panel **(A2)** and descends to the vaginal opening in panel **(A3)** (M represents the AAM lesion). All the lesions appeared as homogeneous hypoechoic masses with well-defined margins. Panels **(A4, A5)** show the median sagittal sections of perineal ultrasound in the resting state and maximum Valsalva state, respectively, of the patient 7 months post-surgery without any observed lesions. Panels **(A6, A8)** display the axial planes of HLAM reconstructed by three-dimensional ultrasound in the resting state preoperatively and during the Valsalva maneuver. Panel **(A7)** displays the axial plane of TUI during the maximum contraction state preoperatively. These axial planes provide information about the size, shape, and location of the AAM lesions. In panel **(A6)**, the lesion is observed protruding posteriorly from behind the urethra toward the vagina; in panel **(A7)**, the lesion has ascended completely above the HLAM; in panel **(A8)**, during the Valsalva maneuver, the lesion descends through the HLAM (M represents an AAM lesion). Panels **(A9, A10)** demonstrate the axial plane of the HLAM in the resting state and maximum Valsalva state, respectively, 7 months post-surgery for patient without any observed lesions. Surgery: panels **(B1, B2)** depict the lesion as an oval-shaped mass protruding from the anterior vaginal wall into the vaginal cavity. Panel **(B3)** displays the completely resected lesion, which is a soft tissue mass measuring 4.0 × 5.0 cm and exhibiting an oval shape with a pink appearance. Panel **(B4)** displays the lesion upon sectioning, which appears as a gray color with medium soft tissue consistency. Panel **(B5)** depicts the appearance of the vulva after the procedure has been completed. HE: Panel **(C1)**, at low magnification, shows that the tumor boundary appears indistinct, revealing a myxedema matrix interspersed with thin collagen fibers and blood vessels of varying thickness within the tumor. The tumor exhibits areas of loose and dense cellularity, with spindle cells uniformly scattered in dense regions without apparent organization (HE, ×100). As shown in panel **(C2)**, at high magnification, the tumor cells exhibited a low density and assumed a stellate or fusiform morphology without evident pleomorphism (HE, ×200). IHC: Tumor cells exhibited strong positive staining for desmin in panel **(C3)** (×100) and panel **(C4)** (×200), estrogen receptors in panel **(C5)** (×100) and panel **(C6)** (×200), and progesterone receptors in panel **(C7)** (×100) and panel **(C8)** (×200). US, ultrasonography; U, urethra; M, mass; V, vagina; A, anus; HLAM, hiatus of levator ani muscle; HE, histopathological examination; IHC, immunohistochemistry; AAM, aggressive angiomyxoma; TUI, tomographic ultrasound imaging.

location of the AAM lesions. In panel **(A6)**, the lesion is observed protruding posteriorly from behind the urethra toward the vagina; in panel **(A7)**, the lesion has ascended completely above the HLAM; in panel **(A8)**, during the Valsalva maneuver, the lesion descends through the HLAM (M represents an AAM lesion). Panels **(A9, A10)** demonstrate the axial plane of the HLAM in the resting state and maximum Valsalva state, respectively, 7 months post-surgery for patient without any observed lesions. Surgery: panels **(B1, B2)** depict the lesion as an oval-shaped mass protruding from the anterior vaginal wall into the vaginal cavity. Panel **(B3)** displays the completely resected lesion, which is a soft tissue mass measuring 4.0 × 5.0 cm and exhibiting an oval shape with a pink appearance. Panel **(B4)** displays the lesion upon sectioning, which appears as a gray color with medium soft tissue consistency. Panel **(B5)** depicts the appearance of the vulva after the procedure has been completed. HE: Panel **(C1)**, at low magnification, shows that the tumor boundary appears indistinct, revealing a myxedema matrix interspersed with thin collagen fibers and blood vessels of varying thickness within the tumor. The tumor exhibits areas of loose and dense cellularity, with spindle cells uniformly scattered in dense

regions without apparent organization (HE, ×100). As shown in panel **(C2)**, at high magnification, the tumor cells exhibited a low density and assumed a stellate or fusiform morphology without evident pleomorphism (HE, ×200). IHC: Tumor cells exhibited strong positive staining for desmin in panel **(C3)** (×100) and panel **(C4)** (×200), estrogen receptors in panel **(C5)** (×100) and panel **(C6)** (×200), and progesterone receptors in panel **(C7)** (×100) and panel **(C8)** (×200). US, ultrasonography; U, urethra; M, mass; V, vagina; A, anus; HLAM, hiatus of levator ani muscle; HE, histopathological examination; IHC, immunohistochemistry; AAM, aggressive angiomyxoma; TUI, tomographic ultrasound imaging." appear below.

The authors apologize for this error and state that this does not change the scientific conclusions of the article in any way. The original article has been updated.

Publisher's note

All claims expressed in this article are solely those of the authors and do not necessarily represent those of their affiliated organizations, or those of the publisher, the editors and the reviewers. Any product that may be evaluated in this article, or claim that may be made by its manufacturer, is not guaranteed or endorsed by the publisher.

frontiers | Frontiers in Oncology

TYPE Case Report
PUBLISHED 05 April 2024
DOI 10.3389/fonc.2024.1373760

Check for updates

OPEN ACCESS

EDITED BY
Lidia Castagneto Gissey,
Sapienza University of Rome, Italy

REVIEWED BY
Andee Dzulkarnaen Zakaria,
Universiti Sains Malaysia, Malaysia
Sanja Stifter-Vretenar,
Skejby Sygehus, Denmark

*CORRESPONDENCE
XiaoJun Huang
hxj258111@163.com

RECEIVED 25 January 2024
ACCEPTED 18 March 2024
PUBLISHED 05 April 2024

CITATION
Huang X, Xu K, Zhao Y, Chen M and Li Z (2024) Paratesticular metastasis from colorectal adenocarcinoma presenting as hydrocele: a rare case report and literature review.
Front. Oncol. 14:1373760.
doi: 10.3389/fonc.2024.1373760

COPYRIGHT
© 2024 Huang, Xu, Zhao, Chen and Li. This is an open-access article distributed under the terms of the Creative Commons Attribution License (CC BY). The use, distribution or reproduction in other forums is permitted, provided the original author(s) and the copyright owner(s) are credited and that the original publication in this journal is cited, in accordance with accepted academic practice. No use, distribution or reproduction is permitted which does not comply with these terms.

Paratesticular metastasis from colorectal adenocarcinoma presenting as hydrocele: a rare case report and literature review

XiaoJun Huang[1]*, KeLi Xu[2], Yin Zhao[2], MinHui Chen[2] and ZheYang Li[2]

[1]Department of Urology, The Second Affiliated Hospital Zhejiang University School of Medicine, Hangzhou, Zhejiang, China, [2]The Second school of Clinical Medicine, Second Clinical Medical College of Zhejiang Chinese Medical University, Hangzhou, Zhejiang, China

Colorectal cancer, with the liver being the most common site of distant metastasis, followed by the lungs and bones. Although reports of metastasis to the testis exist, paratesticular metastasis is extremely rare. A 37-year-old male presented with scrotal swelling. Ultrasound revealed hydrocele of the tunica vaginalis. The patient underwent routine surgical treatment, and postoperative pathology of the tunica vaginalis indicated adenocarcinoma of gastrointestinal origin. Colonoscopic biopsy confirmed adenocarcinoma of the sigmoid colon. After six months of systemic therapy, tumor reduction surgery was performed in conjunction with tunica vaginalis excision. Postoperative pathology suggested histological similarity in both sites, with immunohistochemistry results supporting the diagnosis of sigmoid colon adenocarcinoma metastasizing to the tunica vaginalis. We conducted a literature review, summarizing and discussing clinical presentations, metastatic pathways, and diagnostic approaches.

KEYWORDS

colorectal neoplasm, testicular neoplasm, paratesticular metastasis, testicular hydrocele, neoplasm metastasis, therapeutics, case report

Introduction

Hydrocele of the tunica vaginalis is a common urological condition with various etiologies. Despite its rarity, the impact of tumor-related hydrocele cannot be overlooked, as it significantly influences the overall diagnostic and therapeutic approach to the disease. Both testicular tumors and adjacent tumors can lead to hydrocele. In recent years, the incidence of colorectal cancer has been steadily rising in China, accompanied by an increase in mortality rates (1). Common sites of metastasis for colorectal cancer include the liver, lungs, and bones, while rare sites involve the testicles and adjacent tissues (spermatic cord,

tunica vaginalis, etc.). We conducted a literature search on PubMed regarding cases of colorectal cancer metastasizing to the adjacent testicular tissues and identified several relevant reports. This phenomenon is predominantly observed in elderly males, with mucinous adenocarcinoma being the primary histological type (2–7). Herein, we present a case involving a young male patient who presented with scrotal effusion as the initial symptom. Postoperative pathology revealed colorectal adenocarcinoma with metastasis to the testicular tunica vaginalis. We provide a detailed description of the diagnostic and therapeutic processes, and discuss the relevant aspects of symptom presentation, pathological type, metastatic pathways, and treatment modalities in this particular case.

Case report

A 37-year-old male with no underlying diseases presented with scrotal swelling for several months. He reported no significant discomfort in the medical history. Physical examination revealed positive transillumination test, and no palpable mass was detected, suggesting a possibility of tunica vaginalis fluid accumulation. Subsequent ultrasonography confirmed the diagnosis of testicular tunica vaginalis hydrocele, with no apparent occupancies in the testis, epididymis, or spermatic cord (Figure 1).

Following comprehensive preoperative examinations, the patient underwent surgery for the tunica vaginalis. During the procedure, a mass was identified in the right testicular tunica vaginalis, prompting pathological examination of bilateral testicular tunica vaginalis and the mass. Pathological results indicated a potential digestive tract metastatic carcinoma (Figure 2). we proceeded to inquire further into the medical history. The patient reported indeed experiencing alterations in bowel habits, specifically noting a change in stool consistency characterized by thin and unformed stools. There were no instances of bloody stools, and the patient did not exhibit symptoms such as fever, weight loss, or anemia. Subsequently, a colonoscopy revealed a tumor located 20 cm from the anal verge, and tissue biopsy confirmed adenocarcinoma of the sigmoid colon (Figure 3). To assess abdominal infiltration and metastasis, an enhanced abdominal Computed Tomography scan demonstrated thickening of the colon wall, along with thickening of the peritoneum, omentum, and mesentery, accompanied by multiple soft tissue nodules, suggestive of metastasis.

For a comprehensive evaluation of systemic multi-organ tissue metastasis and to guide further treatment strategies, the patient underwent a positron emission tomography scan. Results revealed localized lesions in the transverse and sigmoid colon, as well as multiple soft tissue nodules in the peritoneum and omentum (Figure 4). Following a detailed assessment of tumor metastasis, the hospital organized a multidisciplinary team (MDT) discussion, ultimately determining the treatment plan as XELOX (capecitabine and oxaliplatin) combined with bevacizumab.

After six months, the patient underwent eight cycles of neoadjuvant chemotherapy, and imaging indicated significant tumor reduction, meeting the criteria for tumor debulking surgery. However, a postoperative ultrasound revealed hydrocele in the right spermatic cord and tunica vaginalis. A collaborative procedure by the colorectal and urological surgery teams was performed to eliminate tumor cells. Intraoperatively, multiple miliary and sheet-like metastatic lesions were found at the pelvic floor, internal ring, right liver, spleen, greater omentum, and mesentery. The tunica vaginalis metastasis and the surface of the testis appeared normal. The principal surgeon performed radical resection of the sigmoid colon, excised intra-abdominal metastases, and completely removed the bilateral tunica vaginalis while preserving the testes.

Postoperatively, pathological examination confirmed moderately differentiated adenocarcinoma of the sigmoid colon (Figure 2), no special type, and immunohistochemistry revealed:

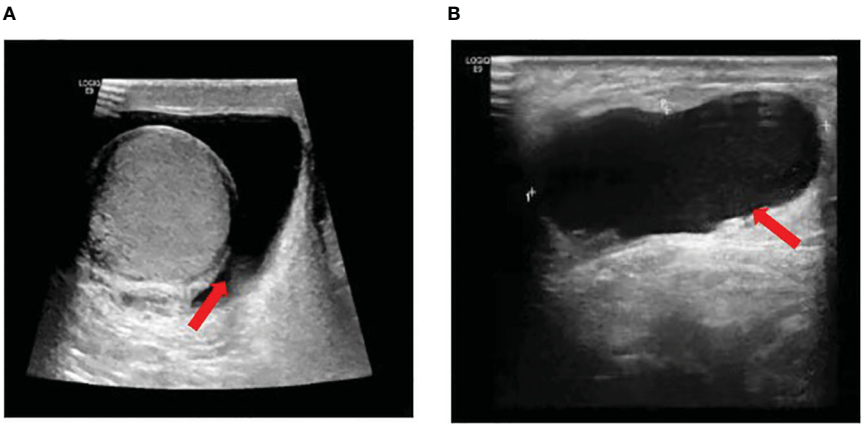

FIGURE 1
(A) Normal size of the right testicle, regular morphology, clear contour, smooth envelope, no apparent focal lesions in the parenchyma, and scattered free fluid hypoechoic areas visible around the testicle. **(B)** Visible patchy free fluid hypoechoic area around the testicle and spermatic cord, measuring approximately 4.31*1.48 cm, with good through-transmission internally.

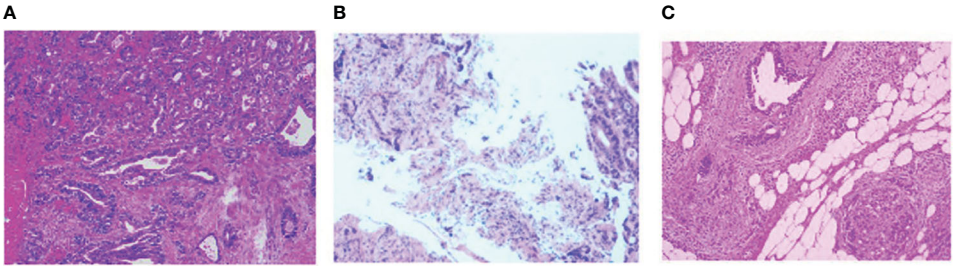

FIGURE 2
(A) Left testicular tunica albuginea fibrous capsule-like tissue with occasional atypical glandular structures in the interstitium, suggestive of a tumor; Right testicular tunica albuginea and appendage tissue reveal atypical glandular structures, indicating a possibility of metastatic adenoma, considering the immunohistochemical results, likely of gastrointestinal origin; **(B)** tissue biopsy confirmed adenocarcinoma of the sigmoid colon; **(C)** Colon adenocarcinoma with differentiation in the transverse colon, post-chemotherapy, measuring approximately 2.1*1cm in size.The Immunohistochemical results is same: CK7-,CK20+,PSA-,MLH1+,MSH2+,MSH6+,PMS2+,c-erbB-2(GC) -,BRAF(-).

P53 (+), ki67 (50%), MLH1 (present), PMS2 (present), MSH2 (present), MSH6 (present). These results were consistent with the previous findings in the testicular tunica vaginalis, confirming that the tunica vaginalis lesion was a metastasis from colon cancer. The patient received postoperative pain management, gastric protection, and other symptomatic treatments before discharge. Currently, one month postoperatively, the patient has commenced postoperative chemotherapy with the regimen of capecitabine and bevacizumab.

Discussion

Differing from pediatric cases where hydrocele is often congenital, in adults, it is typically acquired. The most common form in adults is idiopathic hydrocele (8). Due to the extremely low incidence of testicular and peri-testicular cancers in the Western society, with 3 to 10 new cases per 100,000 males annually (9), hydrocele caused by neoplastic factors is rare. Research indicates that both primary and metastatic tumors can lead to hydrocele (10, 11), with a higher incidence observed in primary tumors. Rapidly developing hydroceles warrant consideration of malignancy possibilities (12), and ultrasound can be employed for initial assessment of testicular and peri-testicular masses. For some small lesions, as in the presented case, ultrasound sensitivity may be insufficient – preoperative ultrasound may not report abnormalities, necessitating further examinations such as Magnetic resonance imaging. The common approach to managing hydrocele is surgical intervention. Currently, there is some controversy regarding the necessity of pathological examination for routine patients (13). However, in the presented case, distinct proliferation was observed in the patient's testicular tunica vaginalis during surgery, supporting the recommendation for routine pathological examination of testicular hydrocele with morphological abnormalities.

Testicular para-testicular tumors can be classified into primary and secondary types. Lipomas originating from the spermatic cord are the most common primary para-testicular tumors. Cystadenomas are the most common among epididymal tumors, followed by leiomyomas. In pediatric patients, embryonal carcinoma and rhabdomyosarcoma can be observed (14). Among primary testicular tunica tumors, the extremely rare malignant mesothelioma of the testicular tunica is noteworthy, with only a few hundred cases reported globally (15). The primary sites of origin for testicular and para-testicular metastatic cancers include the lungs, digestive tract, prostate, and kidneys. According to Charles W and colleagues, the most common primary tumors metastasizing to the testicles include prostate cancer (35%), lung cancer (18%), melanoma (11%), and renal cancer (9%) (16). The metastasis of digestive tract tumors to the testicles is overall rare. Li, Kulkarni, Seo, Liu, and others have reported cases of tumors from

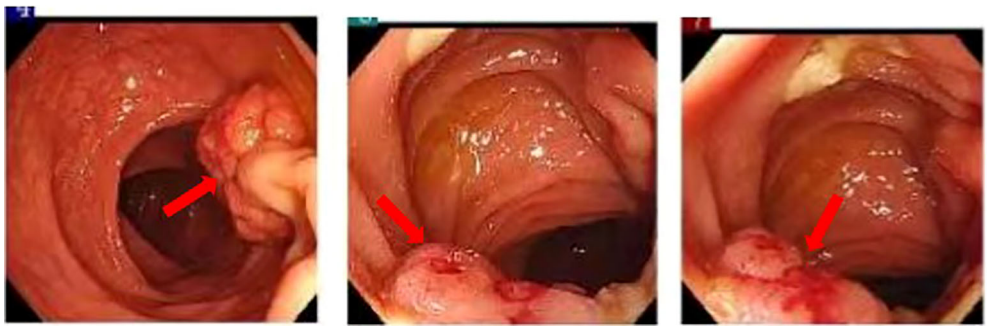

FIGURE 3
A semi-circumferential mass is observed at a distance of 20 cm from the anus, accompanied by localized intestinal wall torsion and slight mucosal stiffness.

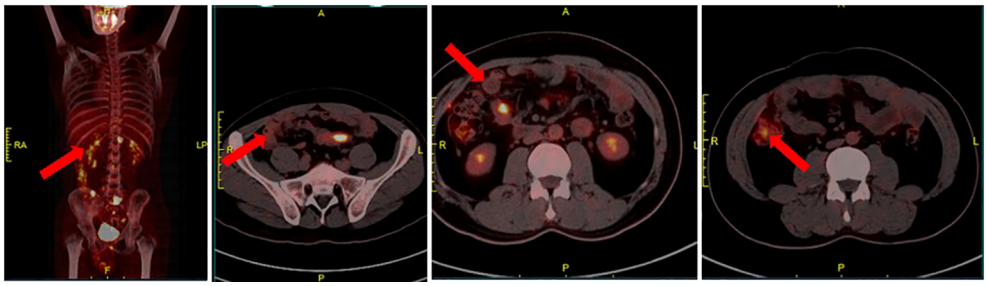

FIGURE 4
Local thickening of the transverse colon and sigmoid colon with concomitant elevated glucose metabolism, raising consideration for cancer; multiple soft tissue nodules with abnormal glucose metabolism in the peritoneal omentum, prompting consideration of metastatic carcinoma.

digestive organs such as the stomach, appendix, pancreas, and colon metastasizing to the testicles or para-testicular tissues (17–19). This often implies extensive peritoneal metastasis and is believed to be related to the anatomical structure of the human body, where the processus vaginalis provides a potential route for metastasis. It has been reported that the incidence of associated tunica fluid in testicular metastatic colon cancer is approximately 30%. Aydin and colleagues reported a case of childhood renal cell carcinoma metastasizing to para-testicular tissues, suspecting tumor spread directly from the abdomen along the processus vaginalis (20). Secondary tumors often present with multifocal lesions, significant growth in the testicular interstitium, and conspicuous involvement of blood vessels. This can be distinguished from primary tumors, and such differentiation holds guiding significance for subsequent treatment (12).

Through a literature search, six reports were identified regarding metastasis of colorectal cancer to the para-testicular tissues (Table 1). Colorectal cancer has the potential to metastasize to the testis, tunica vaginalis, epididymis, spermatic cord, and other sites. Common manifestations include involvement of the testis and surrounding tissues, with mucinous adenocarcinoma, characterized by a high malignant degree, being the predominant pathological type (2–7). In the presented case, intraoperatively, gross examination revealed involvement of the tunica vaginalis without evident signs of testicular metastasis.

TABLE 1 Six cases of metastasis from various types of colorectal tumors to the testes and adjacent tissues.

gender	age	primary tumor	metastasis site
male	NA (old man)	mucinous tumor of the cecum	the tunica vaginalis testis
male	53-year-old	colon adenocarcinoma	the right epididymal tail
male	62-year-old	colon mucinous adenocarcinoma	the spermatic cord
male	56-year-old	colon carcinoma	epididymis
male	65-year-old	colonic mucinous adenocarcinoma	testis, epididymis, spermatic cord
male	75-year-old	colonic mucinous cystadenocarcinoma	the tunica vaginalis testis

In China, the incidence and mortality rates of colorectal cancer are continuously increasing. The statistical results for 2020 indicate 555,000 new cases and 286,000 deaths (1). Colorectal cancer exhibits diverse pathological types, with adenocarcinoma being the most common (21). Other rare and specific types include mucinous adenocarcinoma, signet ring cell carcinoma, and medullary carcinoma, as reported by Liu et al., with two cases being mucinous adenocarcinoma. Histologically, the adenocarcinoma in this case belongs to the moderately differentiated type (G2) (22). Although histologically less malignant than mucinous adenocarcinoma, it still presented rare metastasis to the testicular region, likely due to advanced cancer staging and widespread metastasis. The expression analysis of DNA mismatch repair(MMR) proteins suggests proficient DNA mismatch repair (pMMR), and microsatelliteinstability(MSI) testing indicates microsatellite stability (MSS), indicating no indications for the use of PD-1/PD-L1 immune checkpoint inhibitors (23). The patient did not exhibit mutations in KRAS/NRAS/PIK3CA/BRAF, and there were no indications for the use of anti-EGFR drugs (such as cetuximab). Therefore, the xelox + bevacizumab regimen was adopted.

In the early stages of testicular and paratesticular tumors, apart from symptoms originating from the primary site, there is often no obvious discomfort in the scrotal region. Patients mostly rely on incidental discoveries during ultrasound examinations, with approximately 27% of testicular cancer patients presenting with scrotal swelling and pain (24). In advanced stages, patients typically exhibit scrotal enlargement, and physical examination may reveal hydrocele or scrotal masses. Takahiko Sakuma and colleagues reported a case of colon cancer metastasizing to the testicle, where preoperative ultrasound suggested testicular hydrocele, but pathological examination revealed testicular metastatic cancer. The tumor exhibited cystic changes, mimicking the presentation of testicular hydrocele (25). Therefore, for cases showing signs of hydrocele during physical examination, caution is needed, and relevant investigations should be diligently conducted.

Colorectal cancer can metastasize to the testicles and adjacent tissues through various mainstream pathways. These include: 1. Lymphatic spread from retroperitoneal lymph nodes or lymphatic vessels causing lymphatic obstruction, dilation, dysfunctional lymphatic valves leading to retrograde lymphatic extension, or retrograde venous spread; 2. Direct intraperitoneal dissemination along the inguinal canal, both internally and externally; 3. Hematogenous dissemination following the formation of arterial emboli (26); 4. Retrograde spread along the vas deferens (7). In analyzing the specific case, according to the research by Hassan et al.the short drainage distance of the sigmoid colon from the pre-aortic lymph nodes, where testicular lymph drainage also occurs, makes sigmoid colon tumors more prone to testicular metastasis (27).

However, in this case, the metastatic pathway may involve direct peritoneal dissemination through the Processus vaginalis. Before the second surgery for colon cancer, ultrasound revealed effusion in the spermatic cord and testicles. This is indicative of the presence of an unclosed inguinal canal, and the tumor likely migrated through the Processus vaginalis via the incompletely closed opening in the peritoneum, leading to spermatic cord sheath effusion. Why does the right and left differ,one theoretical explanation for this asymmetric progression could be the earlier descent of the left testicle from the peritoneum, with the later descent of the right testicle potentially allowing the tumor to spread through the residual vaginal membrane (28).

The patient with distant metastasis, exhibits a 5-year survival rate of approximately 15.6% according to SEER CANCER. Literature reports indicate a 3-year survival rate of about 23% (29). Without any intervention, the median survival time for patients with colorectal cancer accompanied by peritoneal metastasis is approximately 6 months (30, 31). For patients undergoing cytoreductive surgery and hyperthermic Intraperitoneal Chemotherapy, the Disease-Free Survival (DFS) is estimated to range between 9.8 and 12.6 months, with a median Overall Survival (mOS) of approximately 38.4 to 40.8 months (32). The therapy significantly prolongs the survival time of patients with relevant conditions. However, according to literature reports, the majority of colorectal cancer (CRC) patients experience recurrence following complete cytoreductive surgery (CRS) with hyperthermic intraperitoneal chemotherapy (HIPEC), with reported recurrence rates of approximately 70% during a 25-month follow-up (33). We still need to explore more effective treatment methods to address late-stage cancer patients.

Conclusion

Although the metastasis of colorectal cancer to the testis is rare, it should not be overlooked in clinical practice. Clinicians should be aware of such uncommon metastases, and when a tumor patient presents with testicular hydrocele, recognize it as a potential manifestation of tumor metastasis.

Data availability statement

The original contributions presented in the study are included in the article/supplementary material. Further inquiries can be directed to the corresponding author.

Ethics statement

In the process of diagnosis and treatment, all examinations and procedures are conducted with the participant's informed consent, duly documented by signing an informed consent form. The participants provided their written informed consent toparticipate in this study. Written informed consent was obtained from the individual(s) for the publication of any potentially identifiable images or data included in this article.

Author contributions

KX: Writing – original draft, Writing – review & editing, Conceptualization, Methodology. YZ: Investigation, Software, Writing – review & editing. MC: Investigation, Software, Writing – review & editing. ZL: Data curation, Supervision, Writing – review & editing. XH: Formal analysis, Funding acquisition, Project administration, Resources, Validation, Visualization, Writing – review & editing.

Funding

The author(s) declare financial support was received for the research, authorship, and/or publication of this article. This project was supported by the National Natural Science Foundation of China under Grant No. 82274258.

Conflict of interest

The authors declare that the research was conducted in the absence of any commercial or financial relationships that could be construed as a potential conflict of interest.

Publisher's note

All claims expressed in this article are solely those of the authors and do not necessarily represent those of their affiliated organizations, or those of the publisher, the editors and the reviewers. Any product that may be evaluated in this article, or claim that may be made by its manufacturer, is not guaranteed or endorsed by the publisher.

References

1. Sung H, Ferlay J, Siegel RL, Laversanne M, Soerjomataram I, Jemal A, et al. Global cancer statistics 2020: globocan estimates of incidence and mortality worldwide for 36 cancers in 185 countries. *CA Cancer J Clin*. (2021) 71(3):209–49. doi: 10.3322/caac.21660

2. Min L, Fan Y, Zhu S, Zhu S. Paratesticular metastasis arising from colonic mucinous adenocarcinoma: A rare case report. *J Int Med Res*. (2022) 50(5). doi: 10.1177/03000605221101332

3. Chung-Yi L, Pang S-T, Chang Y-H, Yu K-J, Lin P-H, Chuang C-K. Paratesticular metastasis from colorectal adenocarcinoma. *Urological Sci*. (2015) 26(1):72–4. doi: 10.1016/j.urols.2015.01.002

4. Wu JM, Zhang A, Dong Y, Lin SH, Meng JC, Fang CT. Colorectal cancer with testicular metastasis: A case report and literature review. *Med (Baltimore)*. (2023) 102 (11):e33214. doi: 10.1097/md.0000000000033214

5. Wald M. Paratesticular colon cancer metastasis in an area of remote trauma. *BMJ Case Rep*. (2020) 13(2). doi: 10.1136/bcr-2019-233106

6. Jang JG, Jeong HY, Kim KS, Park MJ, Lee JS, Kim SS, et al. Metastatic spermatic cord tumor from colorectal cancer. *Ann Coloproctol*. (2015) 31(5):202–4. doi: 10.3393/ac.2015.31.5.202

7. Kanno K, Ohwada S, Nakamura S, Ohya T, Iino Y, Morishita Y, et al. Epididymis metastasis from colon carcinoma: A case report and a review of the Japanese literature. *Jpn J Clin Oncol*. (1994) 24(6):340–4.

8. Cimador M, Castagnetti M, De Grazia E. Management of hydrocele in adolescent patients. *Nat Rev Urol*. (2010) 7(7):379–85. doi: 10.1038/nrurol.2010.80

9. Park JS, Kim J, Elghiaty A, Ham WS. Recent global trends in testicular cancer incidence and mortality. *Med (Baltimore)*. (2018) 97(37):e12390. doi: 10.1097/md.0000000000012390

10. Ota T, Shinohara M, Tanaka M, Date Y, Itakura H, Munakata A, et al. Spermatic cord metastases from gastric cancer with elevation of serum hcg-beta: A case report. *Jpn J Clin Oncol*. (2000) 30(5):239–40. doi: 10.1093/jjco/hyd055

11. Qazi HA, Manikandan R, Foster CS, Fordham MV. Testicular metastasis from gastric carcinoma. *Urology*. (2006) 68(4):890.e7–8. doi: 10.1016/j.urology.2006.04.025

12. Ulbright TM, Young RH. Primary mucinous tumors of the testis and paratestis: A report of nine cases. *Am J Surg Pathol*. (2003) 27(9):1221–8. doi: 10.1097/00000478-200309000-00005

13. Shah VS, Nepple KG, Lee DK. "Routine pathology evaluation of hydrocele and spermatocele specimens is associated with significant costs and no identifiable benefit. *J Urol*. (2014) 192(4):1179–82. doi: 10.1016/j.juro.2014.04.085

14. Akbar SA, Sayyed TA, Jafri SZ, Hasteh F, Neill JS. Multimodality imaging of paratesticular neoplasms and their rare mimics. *Radiographics*. (2003) 23(6):1461–76. doi: 10.1148/rg.236025174

15. Drevinskaite M, Patasius A, Kevlicius L, Mickys U, Smailyte G. Malignant mesothelioma of the tunica vaginalis testis: A rare case and review of literature. *BMC Cancer*. (2020) 20(1):162. doi: 10.1186/s12885-020-6648-3

16. Charles W, Joseph G, Hunis B, Rankin L. Metastatic colon cancer to the testicle presenting as testicular hydrocele. *J Clin Oncol*. (2005) 23(22):5256–7. doi: 10.1200/jco.2005.06.109

17. Kulkarni S, Coup A, Kershaw JB, Buchholz NP. Metastatic appendiceal adenocarcinoma presenting late as epididymo-orchitis: A case report and review of literature. *BMC Urol*. (2004) 4:1. doi: 10.1186/1471-2490-4-1

18. Li B, Cai H, Kang ZC, Wu H, Hou JG, Ma LY. Testicular metastasis from gastric carcinoma: A case report. *World J Gastroenterol*. (2015) 21(21):6764–8. doi: 10.3748/wjg.v21.i21.6764

19. Seo IY, Kim SG, Han WC, Rim JS. Paratesticular mucinous cystadenocarcinoma: metastasis from pancreatic cancer. *Int J Urol*. (2004) 11(12):1147–9. doi: 10.1111/j.1442-2042.2004.00964.x

20. Aydin GB, Ciftçi AO, Yalçin B, Akçören Z, Cağlar M, Senocak ME, et al. Paratesticular metastasis from wilms tumor associated with a hydrocele. *Pediatr Blood Cancer*. (2006) 47(1):97–9. doi: 10.1002/pbc.20494

21. Hugen N, Brown G, Glynne-Jones R, de Wilt JH, Nagtegaal ID. Advances in the care of patients with mucinous colorectal cancer. *Nat Rev Clin Oncol*. (2016) 13(6):361–9. doi: 10.1038/nrclinonc.2015.140

22. Turner RR, Li C, Compton CC. Newer pathologic assessment techniques for colorectal carcinoma. *Clin Cancer Res*. (2007) 13(22):6871s–6s. doi: 10.1158/1078-0432.Ccr-07-1151

23. Cercek A, Lumish M, Sinopoli J, Weiss J, Shia J, Lamendola-Essel M, et al. Pd-1 blockade in mismatch repair-deficient, locally advanced rectal cancer. *N Engl J Med*. (2022) 386(25):2363–76. doi: 10.1056/NEJMoa2201445

24. Patrikidou A, Cazzaniga W, Berney D, Boormans J, de Angst I, Di Nardo D, et al. European association of urology guidelines on testicular cancer: 2023 update. *Eur Urol*. (2023) 84(3):289–301. doi: 10.1016/j.eururo.2023.04.010

25. Sakuma T, Aoki K, Ando M, Inaoka K, Ito T, Yamashita K. Testicular metastasis of colon cancer masquerading a hydrocele of testis. *Urol Case Rep*. (2021) 39:101868. doi: 10.1016/j.eucr.2021.101868

26. Tiong HY, Kew CY, Tan KB, Salto-Tellez M, Leong AF. Metastatic testicular carcinoma from the colon with clinical, immunophenotypical, and molecular characterization: report of a case. *Dis Colon Rectum*. (2005) 48(3):582–5. doi: 10.1007/s10350-004-0808-4

27. Hatoum HA, Abi Saad GS, Otrock ZK, Barada KA, Shamseddine AI. Metastasis of colorectal carcinoma to the testes: clinical presentation and possible pathways. *Int J Clin Oncol*. (2011) 16(3):203–9. doi: 10.1007/s10147-010-0140-z

28. Dutt N, Bates AW, Baithun SI. Secondary neoplasms of the male genital tract with different patterns of involvement in adults and children. *Histopathology*. (2000) 37 (4):323–31. doi: 10.1046/j.1365-2559.2000.00983.x

29. Benitez Majano S, Di Girolamo C, Rachet B, Maringe C, Guren MG, Glimelius B, et al. Surgical treatment and survival from colorectal cancer in Denmark, england, Norway, and Sweden: A population-based study. *Lancet Oncol*. (2019) 20(1):74–87. doi: 10.1016/s1470-2045(18)30646-6

30. Solon JG, O'Neill M, Chang KH, Deady S, Cahill R, Moran B, et al. An 18 year population-based study on site of origin and outcome of patients with peritoneal Malignancy in Ireland. *Eur J Surg Oncol*. (2017) 43(10):1924–31. doi: 10.1016/j.ejso.2017.05.010

31. Tseng J, Bryan DS, Poli E, Sharma M, Polite BN, Turaga KK. Under-Representation of Peritoneal Metastases in Published Clinical Trials of Metastatic Colorectal Cancer. *Lancet Oncol*. (2017) 18(6):711–12. doi: 10.1016/s1470-2045(17)30336-4

32. Nielsen MF, Ravn S, Sørensen MM, Funder JA, Iversen LH. Recurrence and survival following cytoreductive surgery and hyperthermic intraperitoneal chemotherapy for synchronous and metachronous peritoneal metastases of colorectal origin. *Cancers (Basel)*. (2024) 16(3). doi: 10.3390/cancers16030631

33. Eva B, Hebeisen M, Schneider MAndré, Roth L, Pauli C, Frischer-Ordu K, et al. Site of recurrence and survival after surgery for colorectal peritoneal metastasis. *JNCI: J Natl Cancer Institute*. (2021) 113(8):1027–35. doi: 10.1093/jnci/djab001

frontiers | Frontiers in Oncology

TYPE Case Report
PUBLISHED 05 April 2024
DOI 10.3389/fonc.2024.1361333

Check for updates

OPEN ACCESS

EDITED BY
Lidia Castagneto Gissey,
Sapienza University of Rome, Italy

REVIEWED BY
Iuliana Pantelimon,
Carol Davila University of Medicine and Pharmacy, Romania
Teodor Florin Georgescu,
Carol Davila University of Medicine and Pharmacy, Romania

*CORRESPONDENCE
Ha Yeun Oh
elefteria@hanmail.net

RECEIVED 25 December 2023
ACCEPTED 13 March 2024
PUBLISHED 05 April 2024

CITATION
Koh NH and Oh HY (2024) Case report: Unusual breast cancer metastasis manifesting as a scalp lesion in a patient with invasive lobular carcinoma.
Front. Oncol. 14:1361333.
doi: 10.3389/fonc.2024.1361333

COPYRIGHT
© 2024 Koh and Oh. This is an open-access article distributed under the terms of the Creative Commons Attribution License (CC BY). The use, distribution or reproduction in other forums is permitted, provided the original author(s) and the copyright owner(s) are credited and that the original publication in this journal is cited, in accordance with accepted academic practice. No use, distribution or reproduction is permitted which does not comply with these terms.

Case report: Unusual breast cancer metastasis manifesting as a scalp lesion in a patient with invasive lobular carcinoma

Nam Hee Koh and Ha Yeun Oh*

Department of Radiology, Kangwon National University Hospital, Chuncheon, Republic of Korea

Breast cancer is the most prevalent cancer in women globally, often leading to distant metastasis in the lung, liver, or bones. Cutaneous metastasis represents an uncommon pattern in breast cancer, but when observed, it tends to manifest in the thorax and upper abdomen, primarily due to lymph node involvement. Therefore, occurrences of cutaneous metastasis on the scalp and extremities are infrequent. Moreover, invasive lobular carcinoma metastasizing to remote skin is rare among the breast cancer. This report presents a case of cutaneous metastasis of invasive lobular carcinoma to the scalp in a patient treated for breast cancer six years ago, with no signs of local recurrence or metastasis to other organs.

KEYWORDS

distant metastasis, cutaneous metastasis, scalp metastasis, invasive lobular carcinoma of the breast, metastatic breast cancer, scalp nodule

Introduction

Breast cancer is globally recognized as the most common cancer in women, with recent trends indicating an increase in both incidence and mortality rates worldwide (1). With advancements in diagnostic technologies, developed countries have witnessed a decline in breast cancer mortality due to early detection and treatment. Paradoxically, however, statistical evidence suggests a rising incidence of metastatic breast cancer (2).

Metastasis in breast cancer predominantly occurs in specific organs, with rare instances of cutaneous metastasis. Although cutaneous metastasis from breast cancer is uncommon, accounting for approximately 2.5%, it stands out as a relatively proficient entity compared to the less than 1% occurrence in general solid tumors. As a result, breast cancer demonstrates a heightened propensity for cutaneous metastasis, accounting for approximately 33% of all cases among metastatic cancers affecting the skin (3, 4).

Cutaneous metastasis primarily occurs in proximity to the primary tumor site, occasionally leading to misinterpretation as a secondary malignancy related to the recurrence or treatment of the primary lesion. Moreover, when tumors appear on the

scalp or extremities far from the primary lesion, linking them to breast cancer becomes more challenging.

This case report discusses a rare scenario where a scalp nodule, incidentally discovered during the surveillance period after breast cancer treatment, was confirmed and treated as a distant metastatic lesion of breast origin through nuclear imaging and histopathological examination. The findings highlight the importance of vigilance in identifying remote metastases manifesting as a skin lesion in breast cancer survivors and underscore the need for comprehensive monitoring strategies.

Case presentation

A 54-year-old female patient presented to the dermatology clinic due to the enlargement of a scalp nodule in the left parietal area. The lesion, measuring approximately 2 cm and displaying a pinkish hue, appeared as a nodular lesion accompanied by localized alopecia (Figure 1). According to the patient's account, she first noticed the lesion five years ago during chemotherapy for breast cancer, experiencing overall hair loss due to the side effect of the treatment. However, since the lesion was small and did not grow, she did not seek further medical attention at that time.

The patient was diagnosed with invasive lobular carcinoma six years ago, located in the upper outer quadrant of the left breast. At the time of diagnosis, Positron emission tomography with 2-deoxy-2-[fluorine-18]fluoro-D-glucose integrated with computed tomography (^{18}F-FDG PET/CT) showed no evidence of distant metastasis. Following left breast-conserving surgery, the postoperative pathological assessment revealed a pT3N1c classification, indicating the presence of cancer cells spreading to the left axillary lymph nodes. Additionally, the tumor tested positive for estrogen and progesterone receptors, and lymphovascular invasion was observed. Subsequently, she underwent adjuvant chemotherapy with the doxorubicin, cyclophosphamide, and docetaxel regimen for six cycles, followed by oral tamoxifen and radiation therapy targeting the left breast and axilla.

Over the course of six years of regular follow-up examinations, there was no evidence of recurrence or distant metastasis. The patient continued oral tamoxifen therapy. The most recent follow-up examination, four months before the dermatology visit for the scalp nodule, also showed no signs of recurrence or distant metastasis.

Considering the patient's medical history, a punch biopsy was performed to rule out the possibility of cutaneous metastasis. The tissue sample obtained from the punch biopsy exhibited structural features similar to those of previously diagnosed breast cancer tissues. Immunohistochemical staining showed positivity for cytokeratin 7 (CK7), estrogen receptor and partial positivity for gross cystic disease fluid protein 15 (GCDFP-15), a breast cancer-specific marker (Figures 2, 3). In light of these cumulative observations, there arose a suspicion that the scalp lesion might be indicative of metastasis originating from breast cancer.

Subsequent ^{18}F-FDG PET/CT imaging revealed slightly increased FDG uptake in the lesion. No evidence of metastasis to other organs, excluding the scalp, or recurrence at the previously treated primary site was observed (Figure 4).

The patient underwent excision of the scalp lesion, and the final pathology confirmed it as a metastatic lesion. Although adjuvant radiation therapy for scalp lesion and gonadotropin-releasing hormone agonist therapy were recommended, the patient declined, opting only to continue oral anastrozole therapy. Subsequent follow-up examinations did not reveal any signs of recurrence or distant metastasis, including in the breast and scalp.

Discussion

The metastasis of breast cancer is not a random occurrence; it can be explained by the concept of organotropic metastasis, where certain organs are more susceptible to metastasis (5). Commonly known sites for metastasis include bones, liver, brain, lungs, and distant lymph nodes (6). This multifaceted phenomenon results from a combination of factors such as the subtype of the primary tumor,

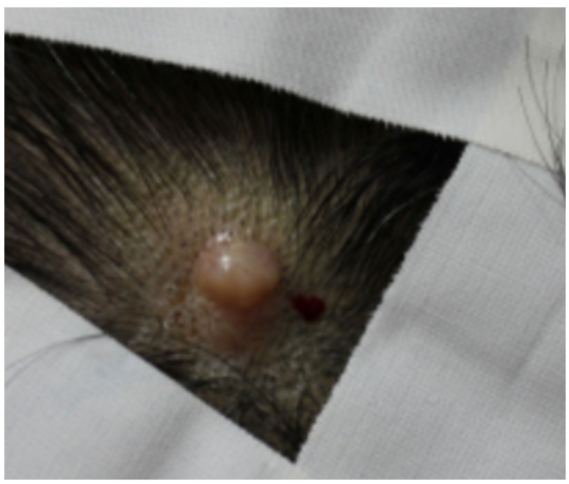

FIGURE 1
Clinical image of the scalp lesion. A pinkish-hued, 2 cm-sized nodular lesion is observed, accompanied by localized alopecia at the left parietal area of the scalp.

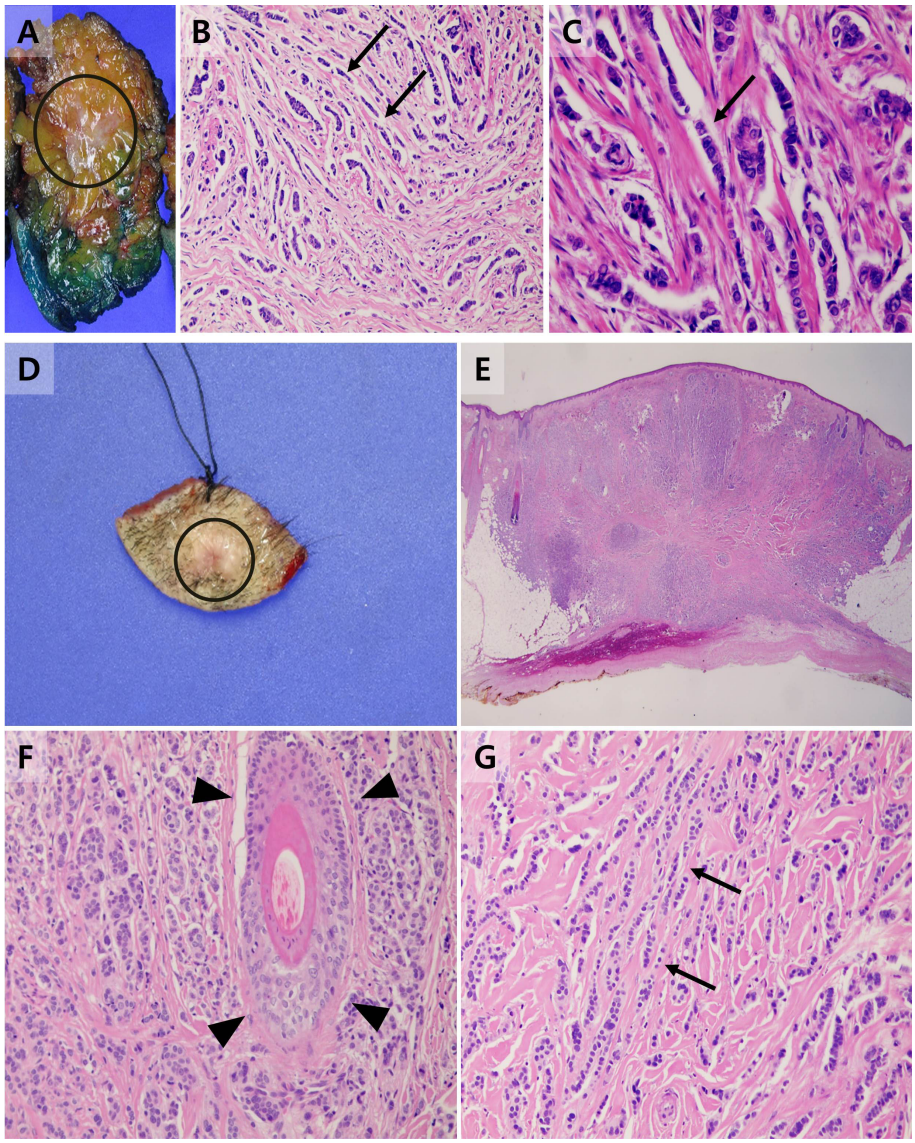

FIGURE 2
Gross specimen and histopathological findings of the primary breast cancer and scalp lesion. **(A)** A gross specimen of the primary breast cancer diagnosed invasive lobular carcinoma with the area involved by the primary tumor annotated as a circle. **(B)** Tumor cells of the primary invasive lobular carcinoma arranged in slender linear strands one to two cells across, exhibiting the so-called Indian file appearance (arrow) (HE x 200). **(C)** On high-power photomicrograph, tumor cells are also arranged in single files, cords, and single cells (arrow) (HE x 400). **(D)** A gross specimen of the scalp lesion with the area involved by the metastasis annotated as a circle. **(E)** On low-power photomicrograph, tumor cells infiltrated the subcutaneous layer of the scalp without evidence of destruction to adjacent structures or skin appendages. (HE x 15) **(F)** Intact skin appendages were observed in high-power photomicrographs (arrowhead) (HE x 200) **(G)** Tumor cells of the scalp tumor showed a similar structural pattern to the primary breast cancer, exhibiting an Indian file appearance (arrow) (HE x 200).

the molecular and genetic characteristics of breast cancer, and the interactions between metastatic organs and cancer cells (7). In this context, it is not surprising that the metastatic patterns differ between invasive ductal carcinoma (IDC) and invasive lobular carcinoma (ILC). As mentioned above, since IDC constitutes the majority of breast cancers, metastases of breast cancer often appear common in the lungs, liver, and bones. However, in the case of ILC, it is known to have a higher prevalence of metastasis to the gastrointestinal tract, gynecologic organs, peritoneal surface, or retroperitoneum due to its distinct pattern of E-cadherin protein expression (8, 9).

Nevertheless, cutaneous metastasis in breast cancer is considered rare in case of both IDC and ILC. According to a study analyzing the metastatic patterns of breast cancer, skin metastasis accounted for 7.1% in IDC and 6.5% in ILC among all metastatic sites, respectively (10). However, it comprises approximately 33% of cutaneous metastatic lesions, underscoring breast cancer's propensity for cutaneous metastasis compared to other malignancies (3, 4).

The majority of breast cancer cutaneous metastases are found in close proximity to the primary tumor, suggesting that metastasis through local lymph node drainage plays a significant role (6).

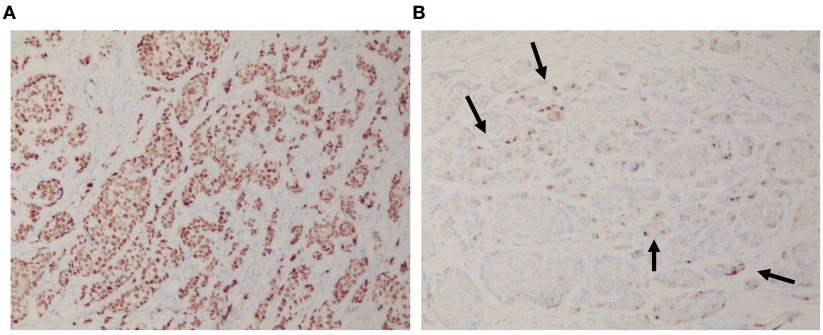

FIGURE 3
Immunohistochemical findings of the scalp lesion. **(A)** The immunohistochemical analysis revealed a positive staining for estrogen receptor, and **(B)** scattered partial positive staining for GCDFP-15.

Consequently, cutaneous metastasis in breast cancer predominantly manifests in the chest wall and upper abdomen (11). Meanwhile, the findings of distant skin metastasis far from the primary lesion (i.e. upper/lower extremities or scalp) still remain questionable. There was no specific paper that precisely explained the mechanism of distant skin metastasis from primary lesions yet. However, by examining the molecular pathology of ILC and the metastatic patterns of both ILC and IDC, a novel insights into the occurrence of cutaneous metastasis distant from the primary lesion could potentially be gained. Some studies reveals that the incidence of cutaneous metastasis is more frequent in ILC than IDC due to the characteristic of loss of E-cadherin (12–14). Among the ILC, certain types exhibit a heightened tendency for metastasis to other organs, believed to be linked to changes in intracellular

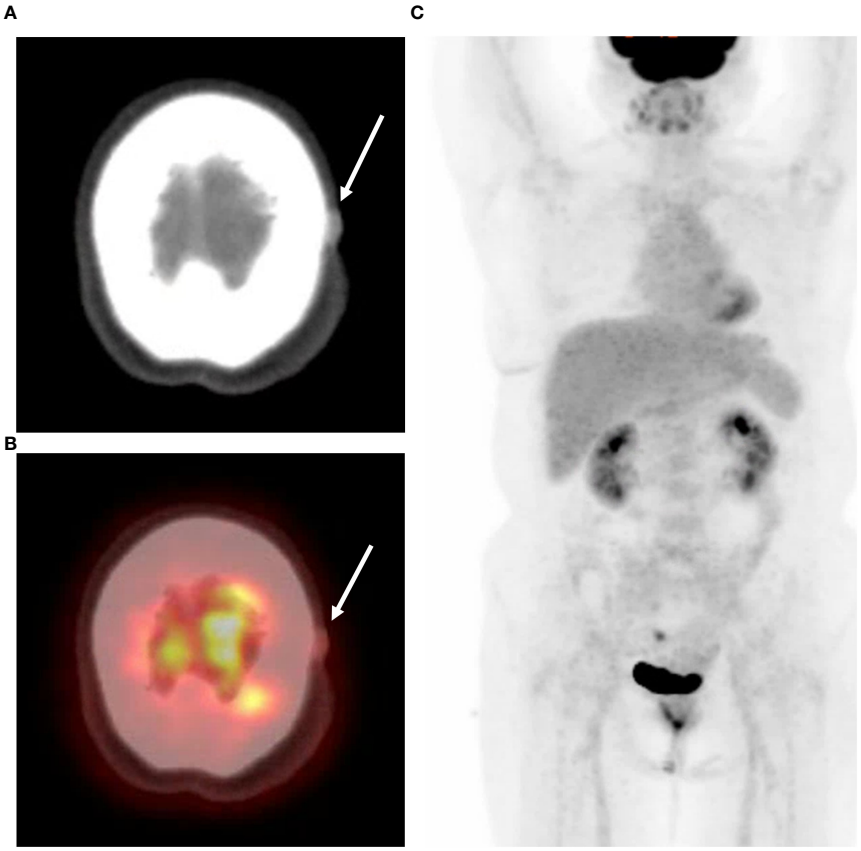

FIGURE 4
PET-CT findings of the patient. **(A)** A 1.5cm sized bulging lesion with soft tissue attenuation, involving subcutaneous layer of scalp along the left parietal area. **(B)** This lesion had a measured SUVmax value of 2, indicating a slight degree of hypermetabolism. **(C)** Maximum intensity projection images of PET-CT showed no evidence of other distant metastasis or recurrence.

protein or hormonal receptor expression, as well as alterations in signaling pathways due to molecular alterations (12).

The patterns of cutaneous metastasis in breast cancer are highly diverse, with normochromic papules or nodules being the predominant forms (15). Particularly when occurring on the scalp, these lesions often present as tumor-associated hair loss, where nodules or hardened plaques lead to irreversible alopecia due to destruction of hair follicles by the primary tumor (16). Lesions of metastatic breast cancer that arise on the scalp occasionally require discrimination from appendage tumors such as eccrine spiradenoma, which are cutaneous appendage-related (17). In such cases, the utility of estrogen receptors is limited, as sweat glands, akin to breast tissue, can express estrogen receptors (18). However, the majority of breast cancers typically show positivity for CK7 and negativity for CK20, making immunostaining with these markers helpful for differentiation (19). Furthermore, GCDFP-15 is known as an immunohistochemical marker frequently used when there is a suspicion that a tumor of unknown primary origin may be of mammary origin, given its specificity for mammary differentiation (20). Of greater significance, the pathological specimen of the scalp lesion exhibited structural features akin to the previously diagnosed breast cancer, with malignant lesions infiltrating surrounding tissues without evident destruction of cutaneous appendages. These findings suggest not so much a primary malignancy originating from cutaneous appendages but rather indicate a metastatic lesion from a past history of breast cancer.

In many cancer types, cutaneous metastasis implies widespread dissemination, making complete resection unfeasible and necessitating palliative and supportive care (21). However, in breast cancer, skin lesions tend to appear regardless of the cancer's stage, occasionally leading to the diagnosis of primary breast cancer through cutaneous metastatic lesions (22–24). Therefore, when diagnosing skin lesions in patients with a history of breast cancer, considering the breast cancer history is imperative. Presently, various types of breast cancers including ILC can be classified beyond the microscopic level to molecular subtypes (12). It is imperative to consider that specific subtypes with a heightened tendency for distant metastasis due to molecular-level mutations may exhibit divergent responses to commonly employed therapeutic agents when formulating a treatment plan. Additionally, recognizing that cutaneous metastasis in breast cancer does not always signify extensive dissemination emphasizes the need for personalized and tailored treatments based on the individual patient's condition.

Data availability statement

The original contributions presented in the study are included in the article/supplementary material. Further inquiries can be directed to the corresponding author.

Ethics statement

The studies involving humans were approved by Institutional Review Board of Kangwon National University Hospital. The studies were conducted in accordance with the local legislation and institutional requirements. Written informed consent for participation was not required from the participants or the participants' legal guardians/next of kin in accordance with the national legislation and institutional requirements. The written informed consent for publication was not obtained due to the retrospective and anonymized nature of the case report. All identifying patient information has been sufficiently anonymized to protect confidentiality. The study adheres to ethical standards, and the retrospective design precluded obtaining individual consents. Additionally, the authors have submitted an exemption request to the institutional review board of their affiliated institution, and the content has been approved. The manuscript strictly follows ethical guidelines and respects patient privacy, ensuring that no identifiable information is disclosed. Written informed consent was obtained from the participant/patient(s) for the publication of this case report.

Author contributions

NK: Writing – original draft. HO: Writing – review & editing.

Funding

The author(s) declare that no financial support was received for the research, authorship, and/or publication of this article.

Acknowledgments

We would like to express our sincere gratitude to Professor Seung Koo Lee from the Department of Pathology at Kangwon National University Hospital for providing valuable assistance in interpreting the pathological findings of the case and for his expertise in the analysis of histopathological images.

Conflict of interest

The authors declare that the research was conducted in the absence of any commercial or financial relationships that could be construed as a potential conflict of interest.

Publisher's note

All claims expressed in this article are solely those of the authors and do not necessarily represent those of their affiliated organizations, or those of the publisher, the editors and the reviewers. Any product that may be evaluated in this article, or claim that may be made by its manufacturer, is not guaranteed or endorsed by the publisher.

References

1. Azamjah N, Soltan-Zadeh Y, Zayeri F. Global trend of breast cancer mortality rate: a 25-year study. *Asian Pac J Cancer Prev*. (2019) 20:2015–20. doi: 10.31557/APJCP.2019.20.7.2015

2. Hendrick RE, Helvie MA, Monticciolo DL. Breast cancer mortality rates have stopped declining in U.S. Women younger than 40 years. *Radiology*. (2021) 299:143–9. doi: 10.1148/radiol.2021203476

3. Hu SC, Chen GS, Wu CS, Chai CY, Chen WT, Lan CC. Rates of cutaneous metastases from different internal Malignancies: experience from a Taiwanese medical center. *J Am Acad Dermatol*. (2009) 60:379–87. doi: 10.1016/j.jaad.2008.10.007

4. Wong CY, Helm MA, Helm TN, Zeitouni N. Patterns of skin metastases: a review of 25 years' experience at a single cancer center. *Int J Dermatol*. (2014) 53:56–60. doi: 10.1111/ijd.2013.53.issue-1

5. Lu X, Kang Y. Organotropism of breast cancer metastasis. *J Mammary Gland Biol Neoplasia*. (2007) 12:153–62. doi: 10.1007/s10911-007-9047-3

6. Yates LR, Knappskog S, Wedge D, Farmery JHR, Gonzalez S, Martincorena I, et al. Genomic evolution of breast cancer metastasis and relapse. *Cancer Cell*. (2017) 32:169–184.e7. doi: 10.1016/j.ccell.2017.07.005

7. Chen W, Hoffmann AD, Liu H, Liu X. Organotropism: new insights into molecular mechanisms of breast cancer metastasis. *NPJ Precis Oncol*. (2018) 2:4. doi: 10.1038/s41698-018-0047-0

8. Borst MJ, Ingold JA. Metastatic patterns of invasive lobular versus invasive ductal carcinoma of the breast. *Surgery*. (1993) 114:637–41. doi: 10.5555/uri:pii:003960609390249D

9. Kowalski PJ, Rubin MA, Kleer CG. E-cadherin expression in primary carcinomas of the breast and its distant metastases. *Breast Cancer Res*. (2003) 5:R217–22. doi: 10.1186/bcr651

10. Mathew A, Rajagopal PS, Villgran V, Sandhu GS, Jankowitz RC, Jacob M, et al. Distinct pattern of metastases in patients with invasive lobular carcinoma of the breast. *Geburtshilfe Frauenheilkd*. (2017) 77:660–6. doi: 10.1055/s-0043-109374

11. Cho J, Park Y, Lee JC, Jung WJ, Lee S. Case series of different onset of skin metastasis according to the breast cancer subtypes. *Cancer Res Treat*. (2014) 46:194–9. doi: 10.4143/crt.2014.46.2.194

12. Batra H, Mouabbi JA, Ding Q, Sahin AA, Raso MG. Lobular carcinoma of the breast: A comprehensive review with translational insights. *Cancers (Basel)*. (2023) 15:5491. doi: 10.3390/cancers15225491

13. Arpino G, Bardou VJ, Clark GM, Elledge RM. Infiltrating lobular carcinoma of the breast: tumor characteristics and clinical outcome. *Breast Cancer Res*. (2004) 6:R149–56. doi: 10.1186/bcr767

14. Korhonen T, Kuukasjärvi T, Huhtala H, Alarmo EL, Holli K, Kallioniemi A, et al. The impact of lobular and ductal breast cancer histology on the metastatic behavior and long term survival of breast cancer patients. *Breast*. (2013) 22:1119–24. doi: 10.1016/j.breast.2013.06.001

15. De Giorgi V, Grazzini M, Alfaioli B, Savarese I, Corciova SA, Guerriero G, et al. Cutaneous manifestations of breast carcinoma. *Dermatol Ther*. (2010) 23:581–9. doi: 10.1111/dth.2010.23.issue-6

16. Scheinfeld N. Review of scalp alopecia due to a clinically unapparent or minimally apparent neoplasm (SACUMAN). *Acta Derm Venereol*. (2006) 86:387–92. doi: 10.2340/00015555-0160

17. Rollins-Raval M, Chivukula M, Tseng GC, Jukic D, Dabbs DJ. An immunohistochemical panel to differentiate metastatic breast carcinoma to skin from primary sweat gland carcinomas with a review of the literature. *Arch Pathol Lab Med*. (2011) 135:975–83. doi: 10.5858/2009-0445-OAR2

18. Bhargava R, Gerald WL, Li AR, Pan Q, Lal P, Ladanyi M, et al. EGFR gene amplification in breast cancer: correlation with epidermal growth factor receptor mRNA and protein expression and HER-2 status and absence of EGFR-activating mutations. *Mod Pathol*. (2005) 18:1027–33. doi: 10.1038/modpathol.3800438

19. Krishna M. Diagnosis of metastatic neoplasms: an immunohistochemical approach. *Arch Pathol Lab Med*. (2010) 134:207–15. doi: 10.5858/134.2.207

20. Darb-Esfahani S, von Minckwitz G, Denkert C, Ataseven B, Högel B, Mehta K, et al. Gross cystic disease fluid protein 15 (GCDFP-15) expression in breast cancer subtypes. *BMC Cancer*. (2014) 14:546. doi: 10.1186/1471-2407-14-546

21. Saeed S, Keehn CA, Morgan MB. Cutaneous metastasis: a clinical, pathological, and immunohistochemical appraisal. *J Cutan Pathol*. (2004) 31:419–30. doi: 10.1111/j.0303-6987.2004.00207.x

22. Costa RLB, Costa-Filho RB, Rosa M, Czerniecki BJ. Occult breast carcinoma presenting as scalp metastasis. *Case Rep Oncol*. (2017) 10:992–7. doi: 10.1159/000484346

23. Alizadeh N, Mirpour H, Azimi S. Scalp metastasis from occult primary breast carcinoma: a case report and review of the literature. *Int J Womens Dermatol*. (2018) 4:230–5. doi: 10.1016/j.ijwd.2018.08.002

24. Abdulraheem AM, Naji D, Al Heyasat AN, Alhasan M, Almasri NM, Odeh R. Breast cancer with scalp metastases: a case report. *J Med Case Rep*. (2023) 17:203. doi: 10.1186/s13256-023-03928-8

frontiers | Frontiers in Oncology

TYPE Case Report
PUBLISHED 10 April 2024
DOI 10.3389/fonc.2024.1355971

Check for updates

OPEN ACCESS

EDITED BY
Ferdinando Agresta,
ULSS2 Marca Trevigiana, Italy

REVIEWED BY
Bixia Tang,
Beijing Cancer Hospital, China
Iuliana Pantelimon,
Carol Davila University of Medicine and Pharmacy, Romania
Teodor Florin Georgescu,
Carol Davila University of Medicine and Pharmacy, Romania

*CORRESPONDENCE
Burcak Karaca
karacaburcak@hotmail.com

RECEIVED 11 January 2024
ACCEPTED 25 March 2024
PUBLISHED 10 April 2024

CITATION
Gunenc D, Ozluk AA, Yıldırım UM, Ascierto PA and Karaca B (2024) Successful application of chemosaturation with percutaneous hepatic perfusion in metastatic uveal melanoma patient progressing after systemic treatment options: a case report.
Front. Oncol. 14:1355971.
doi: 10.3389/fonc.2024.1355971

COPYRIGHT
© 2024 Gunenc, Ozluk, Yıldırım, Ascierto and Karaca. This is an open-access article distributed under the terms of the Creative Commons Attribution License (CC BY). The use, distribution or reproduction in other forums is permitted, provided the original author(s) and the copyright owner(s) are credited and that the original publication in this journal is cited, in accordance with accepted academic practice. No use, distribution or reproduction is permitted which does not comply with these terms.

Successful application of chemosaturation with percutaneous hepatic perfusion in metastatic uveal melanoma patient progressing after systemic treatment options: a case report

Damla Gunenc[1], Ahmet Anil Ozluk[1], Utku Mahir Yıldırım[2], Paolo A. Ascierto[3] and Burcak Karaca[1]*

[1]Department of Medical Oncology, Ege University Faculty of Medicine, Izmir, Türkiye, [2]Department of Interventional Radiology, Izmir University of Economics, Medicalpoint Hospital, Izmir, Türkiye, [3]Melanoma, Cancer Immunotherapy and Development Therapeutics Unit, Istituto Nazionale dei Tumori IRCCS "Fondazione G. Pascale", Naples, Italy

Uveal melanoma (UM) is a rare subtype of melanoma, accounting for less than 5% of all melanoma cases. Metastatic UM differs notably from cutaneous melanoma, exhibiting variations in etiology, prognosis, driver mutations, metastatic patterns, and poor responses to immune checkpoint inhibitors (ICI). Beyond local treatment options, such as resection, radiation therapy, and enucleation, and systemic treatments, such as ICIs, the approval of tebentafusp, a bispecific gp100 peptide-HLA-directed CD3 T-cell engager, marks a breakthrough in treating HLA-A*02:01 metastatic UM. Despite the advancements in treatment options, the long-term survival rates remain inadequate. We report a patient with metastatic UM who previously received ICI and progressed on tebentafusp treatment but subsequently exhibited a remarkable response to local treatment targeting liver metastasis. Such observations highlight the significance of exploring sequential therapeutic strategies for advanced UM, offering potential avenues to enhance treatment efficacy and patient prognosis.

KEYWORDS

uveal melanoma, chemosaturation, immune checkpoint inhibitors, tebentafusp, liver, percutaneous hepatic perfusion

1 Introduction

Uveal melanoma (UM) is a rare form of melanoma originating from melanocytes in the uvea (1). Caucasian population and 50-70 age group are at greater risk for UM, and occurrence before adulthood is uncommon (2). UM poses unique challenges due to its rarity and differences from cutaneous melanoma. Unlike cutaneous melanoma, UM is less associated with UV radiation exposure, characterized by a low mutation burden and a lack of ultraviolet (UV) mutational signatures, especially in posterior UMs (3).

Treatment involves various local therapies, including radiotherapy, phototherapy, and surgical resection, especially in early-stage cases. But, still, approximately half of UM patients progress to metastatic disease, frequently involving the liver due to hematogeneous metastatic behavior different from its cutaneous counterpart, which is usually associated with lymphatic spread.

ICIs revolutionized the prognosis for advanced cutaneous melanoma; however, they have demonstrated disappointing results in UM. Lower somatic mutation burden in UM, reduced immunogenicity, lower presence of neoantigens, and reduced programmed death-ligand 1 (PD-L1) expression, indicating immune evasion by tumor cells, have been proposed as potential reasons. Median progression-free survival (PFS) with ICIs ranges from 3-5.5 months, and median overall survival (OS) ranges from 12.7-19.1 months in phase 2 clinical trials (4, 5). Recently, tebentafusp, a bispecific peptide-HLA-directed T-cell engager, showed promising results with an estimated mOS of 21.7 months for HLA-A*02:01 positive patients with metastatic UM (6). However, the duration of response remains relatively short.

Recent advancements in local therapeutic approaches highlight the significance of hepatic-targeted treatments as a crucial area of research, especially in UM patients where liver metastases are commonly prevalent at the time of patient death, representing a significant challenge in treating metastatic disease. Various endovascular therapies offer promising strategies for addressing primary and metastatic hepatic malignancies, including bland arterial embolization, chemoembolization, radioembolization, and immunoembolization. Among these, chemosaturation with percutaneous hepatic perfusion (CS-PHP) has emerged as a minimally invasive, repeatable targeted hepatic therapy for UM metastases (7).

CS-PHP delivers melphalan directly to the hepatic artery to maximize the local concentration in the liver while minimizing systemic exposure and toxicities. Studies have reported encouraging response rates of up to 83% with improved local tumor control in hepatic metastases of uveal melanoma (8, 9). Furthermore, recent investigations demonstrated superior hepatic PFS rates in patients receiving CS-PHP compared to those treated with the best alternative care, encompassing arterial embolization, systemic chemotherapy, and supportive measures (10, 11).

However, there is a strong need for additional studies exploring therapeutic sequences in UM, especially for challenging cases progressing after limited systemic treatment options, where local treatment options might still offer potential for extended survival rates for these. Herein, we present our case report, aiming to share promising results of CS-HSP observed in a metastatic UM patient with predominantly liver metastases progressing after ICI and tebentafusp therapy.

2 Case report

A 40-year-old male patient was diagnosed with UM in February 2014, presenting with a history of blurry vision for approximately four months. Subsequently, a 12x9x10 mm lesion was detected in his right eye, and enucleation was performed. Optic nerve and sclera invasion were not observed. Whole body scanning showed no signs of distant metastasis.

The patient remained under surveillance without any signs of disease recurrence for seven years. However, in February 2021, two liver lesions measuring 42x30 mm and 12x10 mm were identified in liver segments VI-VII. He was decided to undergo metastasectomy for liver lesions, but unfortunately, surgery was terminated due to widespread millimetric metastases (Supplementary Figure 1). The liver biopsy confirmed UM metastasis. Hepatic angiography was performed to assess the suitability of transarterial radioembolization (TARE), but he was not found to be eligible for local treatment due to low uptake of Tc-99m-macroaggregated albumin (MAA).

He received weekly paclitaxel plus carboplatin chemotherapy. As conventional systemic chemotherapy is usually unsuccessful in metastatic UM, after six weeks of treatment, liver MRI revealed progression in the liver lesions measuring 45x31 mm, 17x7 mm, and a few millimetric metastatic lesions were observed again in the posterior segment level in the right lobe of the liver causing slight indentation in the capsule, leading to a referral to our clinic for further management.

Nivolumab treatment was initiated in May 2021, administering 240 mg doses every two weeks (Q2W) since tebentafusp was not available in our country at that time. After 6th cycle of the nivolumab, bi-phenotypic response was observed. While undergoing ICI treatment, we started discussions with a medical center in Italy for potential inclusion in the tebentafusp Early Access Program (EAP). After confirming HLA*02:01 positivity, the patient was eligible for the tebentafusp EAP.

In December 2021, MRI showed lesion progression in segments VI-VII previously reported 67x36 mm to 100x61mm, and millimetric metastases were found similar in size. The nivolumab treatment was discontinued after 18 cycles due to disease progression, and the patient was referred to Istituto Nazionale Tumori in Naples, Italy, for the tebentafusp EAP in February 2022. He received tebentafusp initially at 20 µg on day 1, 30 µg on day 8, 68 µg on day 15, and then 68 µg intravenously once weekly after that, as recommended in the protocol. He developed hair depigmentation, grade 2 rash, and cutaneous edema (Supplementary Figure 2) without any other severe adverse effects. Following three months of tebentafusp treatment, the most extensive liver lesion slightly decreased in diameter (96x59mm), and after six months of treatment, MRI showed approximately 30% necrosis in the most significant lesion. In the imaging conducted in December 2022, in addition to progression in the target lesion in the liver to 108x56mm, two new lesions were identified in segments 6 and 8. The patient continued weekly

treatment for 50 cycles, and therapy was discontinued due to confirmed progressive disease detected by subsequent imaging 8 weeks later that showed progression of his liver lesions and newly developed 26 mm lesion adjacent to the kidney, along with suspicious millimetric bone metastases in the lumbar and sacral vertebral bodies.

The patient was referred to our medical department for best supportive care. At the first administration to our clinic, the patient was in an excellent performance status (ECOG 0) and greatly desired treatment. He was not suitable for some local treatment options such as surgery and TARE. CS-PHP, being a relatively uncommon practice in our country and performed only in a few specialized centers, had not been utilized in the patient's previous treatment lines. Considering that the liver lesions will determine the survival of this patient, we decided to treat the patient using melphalan-delivered CS-PHP, specifically targeting the liver lesions.

Abdomen MRI before the first CS-PHP showed a 115x66 mm solid metastatic lesion without necrosis, involving liver segments 6-7 and growing towards the inferior vena cava, as well as many scattered metastatic lesions in both lobes of the liver, the largest of which measured 16 mm in diameter and a 26 mm stable soft tissue metastasis adjacent to the left kidney. After his first procedure in April 2023, the most extensive lesion, measuring 115x66 mm, decreased to 83x41 mm, most of the millimetric lesions disappeared; interestingly, the 26 mm lesion adjacent to the left kidney reduced to 18 mm. In June 2023, the second CS-PHP procedure was performed. Further decrease in the size of the most extensive lesion was observed from 83x41 mm to 70x28 mm, with the majority exhibiting necrosis, and 16 mm lesion in segment 8 decreased to 12 mm. After the third application of CS-PHP without any severe adverse effect, the most extensive liver lesion measured stable as 67x34 mm and only two remaining lesions were observed as 6 mm and 3 mm in segment 8 (Figure 1). Diffusion-weighted MR images revealed complete necrosis of liver lesions, and there was no newly developed liver lesion. Control PET/CT showed almost complete metabolic response in liver lesions, multiple stable metastatic bone lesions with the acetabular lesion showing partial metabolic response, and a few newly developed lesions in the humerus and columna vertebralis (Supplementary Figure 3). He has initiated treatment with zoledronic acid for new bone lesions.

The MRI conducted in January 2024 revealed findings suggestive of progression characterized by an increase in the area with high T1 signal intensity, which was previously almost necrotic. Additionally, the lesion previously measured at 12 mm has progressed to 32 mm, and on the left lobe side, new lesions measuring 6 mm, 5 mm, and 4 mm have developed. Our patient showing progression after multiple-line systemic treatments achieved a hepatic PFS of 9 months after the first CS-PHP. After 35 months since the initial detection of metastasis, the patient remains asymptomatic with an ECOG 0 performance status. Due to limited treatment options, a fourth CS-PHP has been scheduled for the newly developed liver lesions.

3 Discussion

Treatment options for metastatic UM include tebentafusp, ICIs, and liver-directed locoregional therapies. Therapies targeting BRAF or KIT are not indicated in UM in the absence of the corresponding mutations. MEK inhibition with trametinib and selumetinib has been tested and shows minimal clinical effect (12, 13). ICIs can still be an option in cases where local ablative options are not feasible, and the patient is HLA A*02:01 negative. Tebentafusp is the first

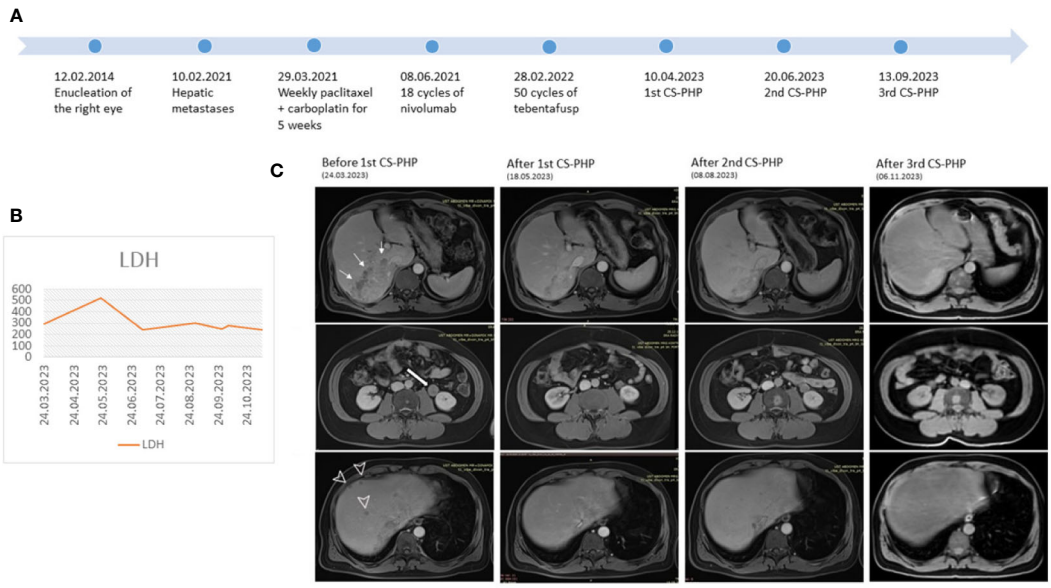

FIGURE 1
(A) Course of the disease **(B)** LDH levels during CS-PHP procedures **(C)** Serial MRI images before and after each CS-PHP procedure showing the biggest lesion in the liver (thin arrows), lesion adjacent to kidney (thick arrow) and scattered liver metastases (arrowhead).

systemic treatment for HLA A*02:01 positive UM ever to show a significant survival benefit in a prospective randomized trial with OS at one year of 73% compared to 59% in the control arm of investigator's choice of therapy with single-agent pembrolizumab, ipilimumab or dacarbazine (6).

Due to the strong hepatotropism of its metastatic pattern, UM patients might usually benefit from liver-directed treatments, and these local interventions can be a valid alternative to systemic therapy, such as hepatic intra-arterial chemotherapy, hepatic embolization, radiofrequency ablation, or stereotactic radiation therapy. Among these liver-directed treatment options, limited clinical efficacy, significant systemic toxicity, and safety concerns have suspended the widespread use of isolated hepatic perfusion for administering high-dose chemotherapy. But, a recent advancement overcame these challenges using isolated hepatic perfusion in a method known as "chemosaturation", utilizing melphalan to deliver highly concentrated chemotherapy directly to the liver. This method provides high concentrated chemotherapy to the hepatic artery through a catheter inserted in the femoral artery. A double-balloon catheter is placed at the atrium–IVC junction and infrahepatic IVC above the renal veins to isolate hepatic venous circulation. Hepatic venous outflow is diverted from the lumen of the double-balloon catheter to extracorporeal circulation. Blood returning from the hepatic veins containing melphalan is passed through special filters that catch 95-96% of melphalan and remove it from hepatic venous blood (14).

In the first phase III trial, 83 UM and 10 cutaneous melanoma patients were randomly assigned to receive either CS-PHP (n = 44) or best alternative care (BAC) (n = 49). In this trial, first-generation filters were used, which are less efficient in removing melphalan than the current second-generation filters. BAC consisted of investigators' choice of treatment, most frequently using temozolamide, and 18.4% of patients received only best supportive care. Hepatic progression-free survival (hPFS) was the primary endpoint of the trial, demonstrating 7 months in CS-PHP arm compared to 1.6 months in BAC arm ($p < 0.0001$). mPFS was 5.4 months for CS-PHP and 1.6 months for BAC ($p < 0.0001$). Median OS did not significantly differ between CS-PHP (10.6 months) and BAC (10.0 months), possibly due to the crossover of 57.1% of BAC patients to CS-PHP after progression. The hepatic overall response was 36.4% for CS-PHP and 2% for BAC (10).

Recently, a multicenter phase III FOCUS study for hepatic dominant UM presented updated results at ASCO 2022 (15). The study was initially started as a randomized trial comparing CS-PHP to BAC. However, it was converted to a single-arm CS-PHP study due to enrollment concerns in the BAC arm. 144 patients were enrolled with 91 PHP and 32 BAC patients receiving treatment. The ORR in the CS-PHP population was 35.2% and 12.5% in the BAC population. While the duration of response (DoR), PFS, and OS data still remain immature, the reported median DoR on CS-PHP was 14 months and not calculable for BAC patients. The median PFS was 9.03 vs. 3.06 months, and OS was 20.53 vs. 14.06 months for CS-PHP and BAC populations, respectively.

In addition to the above-mentioned prospective trials, several retrospective cohorts and case series supported the clinical feasibility and effectiveness of this method. While this innovative approach has demonstrated promising results in patients with metastatic UM (Table 1), further exploration through well-balanced multi-center prospective trials is still needed to enhance clearer generalizability.

When patient selection and treatment goals are appropriately determined, CS-PHP may offer distinct advantages over other local treatment options. The ability of CS-PHP to affect the entire liver makes it a viable option for larger and also non-visible lesions. Additionally, embolization of hepatic artery branches during transarterial chemoembolization (TACE) can lead to ischemic injury, while selective internal radiation therapy (SIRT) poses a risk of radiation injury to healthy liver tissue. Furthermore, CS-PHP may be more suitable for patients with recurrent or refractory disease, allowing for repeat procedures.

In a retrospective study, including 29 patients who underwent TACE using cisplatin, the ORR was 21% and median PFS was 6 months. Adverse events of grade ≥3 included aspartate aminotransferase (AST) elevation in 34.5%, alanine aminotransferase (ALT) elevation in 51.7%, and serum creatinine elevation in 3.4% (22). In the largest prospective study of TACE, 24 patients were evaluated. The ORR was 20%, with a median OS of 5 months. Eight patients experienced grade ≥3 complications (23). In a retrospective study evaluating the efficacy and safety of SIRT in patients with systemic therapy-resistant metastatic uveal melanoma, the ORR remained limited at 17.9%. 2 (7%) of 28 patients receiving SIRT suffered mortality due to hepatic failure within 1 month (24). A single-center study, comparing SIRT and CS-PHP for hepatic metastasized uveal melanoma included 62 patients (SIRT, n=34 vs. CS-PHP, n=28). The disease control rate was 18% for SIRT and 30% for CS-PHP. CS-PHP showed a significant OS benefit as compared with SIRT (median 516 days vs. 300.5 days, $p = 0.006$) (25).

To our knowledge, tebentafusp treatment leads to a high proportion of T-cell infiltration and increased cytokine release in the tumor microenvironment (TME) (26, 27). Some adverse effects related to tebentafusp treatment, such as skin rash or pruritus, are probably a result of the interaction between T cells and gp100-expressing melanocytes (28). Patients who experienced rash within the first week of tebentafusp treatment had significantly better survival rates. Also, several studies showed that inflammatory TME is associated with chemosensitivity (29, 30).

On the other hand, the immunomodulatory effects of chemotherapeutics are currently being investigated, and their clinical use combined with chemotherapy is becoming widespread based on this hypothesis (31). Considering the potentializing effect of either combined or sequential use of these treatments on each other's effectiveness, we emphasize that the response of our patient, who had previously received both ICI and tebentafusp, should be evaluated within this framework. The treatment response in the lesion adjacent to the kidney and some bone lesions that do not receive local treatment may become more explainable in the light of this information.

4 Conclusion

One of the significant issues in UM is high risk for distant recurrence after local treatment, with up to 50% of patients developing distant metastases. In 90% of cases, the liver is the

TABLE 1 CS-PHP cohort studies for metastatic uveal melanoma.

Study	Study Type	Sample Size (n)	ORR (%)	Grade 3-4 Toxicity
Hughes et al. (10)	Phase III	93 (PHP, n = 44 vs. BAC, n = 49) (UM, n = 83; cutaneous melanoma, n = 10)	36.4%; all of PR	85.7% Neutropenia 80% Thrombocytopenia 62.9% Anemia 17.1% Febrile neutropenia 14.3% Bilirubin elevation
Karydis et al. (16)	Retrospective	51	49%; 43.1% PR 5.9% CR	37.5% Non-hematologic 31.3% Neutropenia 31.3% Thrombocytopenia 29.4% Anemia
Artzner et al. (11)	Retrospective	16	60%; all of PR	14% Leukopenia 14% Thrombocytopenia
Brüning et al. (17)	Retrospective	19	53% PR 47% SD	Not specified
Modi et al. (18)	Retrospective	81	60.5%; 51.9% PR 8.6% CR	13.3% Anemia 13.3% Neutropenia 12% Thrombocytopenia 7.2% Coagulopathy
Dewald et al. (19)	Retrospective	66	59%	24.8% Thrombocytopenia 7.6% Hepatic toxicity 4.1% Leukopenia
Meijer et al. (20)	Phase II	35	72%; 69% PR 3% CR	84.8% Lymphocytopenia 75.6% Leukopenia
Tong et al. (21)	Retrospective	101	59.5%; 54.5% PR 5% CR	24% Leukopenia 28.4% Thrombocytopenia 14.2% Hepatic toxicity 7.6% Anemia
Zager et al. (15)	Phase III (FOCUS)	144 (switched to single-arm PHP, n = 91)	35.2%	42.6% Serious TEAE 14.9% Thrombocytopenia 10.9% Neutropenia 4.2% Leukopenia

BAC, best alternative care; CR, complete response; PHP, percutaneous hepatic perfusion; PR, partial response; ORR, Overall response rate; OS, overall survival; TEAE, Treatment emergent adverse events; UM, uveal melanoma.

first site of metastasis (32). Our case underlines that CS-PHP is an effective salvage treatment for liver-dominant metastatic UM even after progression after ICI and tebentafusp treatment. Due to being a rare melanoma and limited treatment options, there is a considerable unmet clinical need of shared experience for combining and sequencing treatments for metastatic UM patients.

Data availability statement

The original contributions presented in the study are included in the article/Supplementary Material. Further inquiries can be directed to the corresponding author.

Ethics statement

Written informed consent was obtained from the patient for the publication of any potentially identifiable images or data included in this article. The study was performed in accordance with the Declaration of Helsinki, Good Clinical Practice and applicable regulatory requirements.

Author contributions

DG: Conceptualization, Writing – original draft, Writing – review & editing. AO: Writing – original draft, Writing – review & editing. UY: Supervision, Writing – original draft, Writing – review & editing. PA: Writing – original draft, Writing – review & editing. BK: Conceptualization, Supervision, Writing – original draft, Writing – review & editing.

Funding

The author(s) declare that no financial support was received for the research, authorship, and/or publication of this article.

Acknowledgments

We would like to thank PA for his great effort regarding access to tebentafusp treatment, all of our colleagues for their care for our

melanoma patients, and our valuable patient for his participation in this study.

Conflict of interest

The authors declare that the research was conducted in the absence of any commercial or financial relationships that could be construed as a potential conflict of interest.

Publisher's note

All claims expressed in this article are solely those of the authors and do not necessarily represent those of their affiliated organizations, or those of the publisher, the editors and the reviewers. Any product that may be evaluated in this article, or claim that may be made by its manufacturer, is not guaranteed or endorsed by the publisher.

Supplementary material

The Supplementary Material for this article can be found online at: https://www.frontiersin.org/articles/10.3389/fonc.2024.1355971/full#supplementary-material

SUPPLEMENTARY FIGURE 1
Widespread millimetric liver metastasis at the time of the diagnosis of metastatic disease.

SUPPLEMENTARY FIGURE 2
Rash and facial edema during tebentafusp treatment.

SUPPLEMENTARY FIGURE 3
Diffusion-weighted MRI images before **(A)** and after **(B)** 3rd CS-PHP procedure. **(C)** PET/CT fusion image showing no FDG uptake in the most extensive liver lesion after the 3rd CS-PHP procedure.

References

1. Jager M, Shields C, Cebulla C, Abdel-Rahman M, Grossniklaus H, Stern M, et al. Uveal melanoma. *Nat Rev Dis Primers*. (2020) 6:24. doi: 10.1038/s41572-020-0158-0

2. Rana'a T, Cassoux N, Desjardins L, Damato B, Konstantinidis L, Coupland SE, et al. The pediatric choroidal and ciliary body melanoma study: a survey by the European Ophthalmic Oncology Group. *Ophthalmology*. (2016) 123:898–907. doi: 10.1016/j.ophtha.2015.12.024

3. Singh AD, Rennie IG, Seregard S, Giblin M, McKenzie J. Sunlight exposure and pathogenesis of uveal melanoma. *Survey Ophthalmol*. (2004) 49:419–28. doi: 10.1016/j.survophthal.2004.04.009

4. Piulats JM, Espinosa E, de la Cruz Merino L, Varela M, Alonso Carrión L, Martín-Algarra S, et al. Nivolumab plus ipilimumab for treatment-naïve metastatic uveal melanoma: an open-label, multicenter, phase II trial by the Spanish multidisciplinary melanoma group (GEM-1402). *J Clin Oncol*. (2021) 39(6):586–98. doi: 10.1200/JCO.20.00550

5. Pelster MS, Gruschkus SK, Bassett R, Gombos DS, Shephard M, Posada L, et al. Nivolumab and ipilimumab in metastatic uveal melanoma: results from a single-arm phase II study. *J Clin Oncol*. (2021) 39:599. doi: 10.1200/JCO.20.00605

6. Nathan P, Hassel JC, Rutkowski P, Baurain J-F, Butler MO, Schlaak M, et al. Overall survival benefit with tebentafusp in metastatic uveal melanoma. *N Engl J Med*. (2021) 385:1196–206. doi: 10.1056/NEJMoa2103485

7. Agarwala SS, Eggermont AM, O'Day S, Zager JS. Metastatic melanoma to the liver: a contemporary and comprehensive review of surgical, systemic, and regional therapeutic options. *Cancer*. (2014) 120:781–9. doi: 10.1002/cncr.28480

8. Vogl TJ, Koch SA, Lotz G, Gebauer B, Willinek W, Engelke C, et al. Percutaneous isolated hepatic perfusion as a treatment for isolated hepatic metastases of uveal melanoma: patient outcome and safety in a multi-centre study. *Cardiovasc interventional Radiol*. (2017) 40:864–72. doi: 10.1007/s00270-017-1588-2

9. Forster MR, Rashid OM, Perez MC, Choi J, Chaudhry T, Zager JS. Chemosaturation with percutaneous hepatic perfusion for unresectable metastatic melanoma or sarcoma to the liver: a single institution experience. *J Surg Oncol*. (2014) 109:434–9. doi: 10.1002/jso.23501

10. Hughes MS, Zager J, Faries M, Alexander HR, Royal RE, Wood B, et al. Results of a randomized controlled multicenter phase III trial of percutaneous hepatic perfusion compared with best available care for patients with melanoma liver metastases. *Ann Surg Oncol*. (2016) 23:1309–19. doi: 10.1245/s10434-015-4968-3

11. Artzner C, Mossakowski O, Hefferman G, Grosse U, Hoffmann R, Forschner A, et al. Chemosaturation with percutaneous hepatic perfusion of melphalan for liver-dominant metastatic uveal melanoma: a single center experience. *Cancer Imaging*. (2019) 19:1–8. doi: 10.1186/s40644-019-0218-4

12. Carvajal RD, Piperno-Neumann S, Kapiteijn E, Chapman PB, Frank S, Joshua AM, et al. Selumetinib in combination with dacarbazine in patients with metastatic uveal melanoma: A phase III, multicentre, randomised trial (SUMIT). *J Clin Oncol*. (2018) 36:1232–9. doi: 10.1200/JCO.2017.74.1090

13. Steeb T, Wessely A, Ruzicka T, Heppt MV, Berking C. How to MEK the best of uveal melanoma: A systematic review on the efficacy and safety of MEK inhibitors in metastatic or unresectable uveal melanoma. *Eur J Cancer*. (2018) 103:41–51. doi: 10.1016/j.ejca.2018.08.005

14. de Leede EM, Burgmans MC, Meijer TS, Martini CH, Tijl FG, Vuyk J, et al. Prospective clinical and pharmacological evaluation of the Delcath system's second-generation (GEN2) hemofiltration system in patients undergoing percutaneous hepatic perfusion with melphalan. *Cardiovasc interventional Radiol*. (2017) 40:1196–205. doi: 10.1007/s00270-017-1630-4

15. Zager JS, Orloff MM, Ferrucci PF, Glazer ES, Ejaz A, Richtig E, et al. FOCUS phase 3 trial results: Percutaneous hepatic perfusion (PHP) with melphalan for patients with ocular melanoma liver metastases (PHP-OCM-301/301A). *Am Soc Clin Oncol*. (2022) 40:9510. doi: 10.1200/JCO.2022.40.16_suppl.9510

16. Karydis I, Gangi A, Wheater MJ, Choi J, Wilson I, Thomas K, et al. Percutaneous hepatic perfusion with melphalan in uveal melanoma: a safe and effective treatment modality in an orphan disease. *J Surg Oncol*. (2018) 117:1170–8. doi: 10.1002/jso.24956

17. Brüning R, Tiede M, Schneider M, Wohlmuth P, Weilert H, Oldhafer K, et al. Unresectable hepatic metastasis of uveal melanoma: hepatic chemosaturation with high-dose melphalan—long-term overall survival negatively correlates with tumor burden. *Radiol Res Pract*. (2020) 2020:5672048. doi: 10.1155/2020/5672048

18. Modi S, Gibson T, Vigneswaran G, Patel S, Wheater M, Karydis I, et al. Chemosaturation with percutaneous hepatic perfusion of melphalan for metastatic uveal melanoma. *Melanoma Res*. (2022) 32:103. doi: 10.1097/CMR.0000000000000806

19. Dewald CL, Warnke M-M, Brüning R, Schneider MA, Wohlmuth P, Hinrichs JB, et al. Percutaneous hepatic perfusion (PHP) with melphalan in liver-dominant metastatic uveal melanoma: the German experience. *Cancers*. (2021) 14:118. doi: 10.3390/cancers14010118

20. Meijer TS, Burgmans MC, de Leede EM, de Geus-Oei L-F, Boekestijn B, Handgraaf HJ, et al. Percutaneous hepatic perfusion with melphalan in patients with unresectable ocular melanoma metastases confined to the liver: a prospective phase II study. *Ann Surg Oncol*. (2021) 28:1130–41. doi: 10.1245/s10434-020-08741-x

21. Tong T, Samim M, Kapiteijn E, Meijer T, Speetjens F, Brüning R, et al. Predictive parameters in patients undergoing percutaneous hepatic perfusion with melphalan for unresectable liver metastases from uveal melanoma: a retrospective pooled analysis. *Cardiovasc Interventional Radiol*. (2022) 45:1304–13. doi: 10.1007/s00270-022-03225-9

22. Shibayama Y, Namikawa K, Sone M, Takahashi A, Tsutsumida A, Sugawara S, et al. Efficacy and toxicity of transarterial chemoembolization therapy using cisplatin and gelatin sponge in patients with liver metastases from uveal melanoma in an Asian population. *Int J Clin Oncol*. (2017) 22:577–84. doi: 10.1007/s10147-017-1095-0

23. Patel K, Sullivan K, Berd D, Mastrangelo MJ, Shields CL, Shields JA, et al. Chemoembolization of the hepatic artery with BCNU for metastatic uveal melanoma: results of a phase II study. *Melanoma Res*. (2005) 15:297–304. doi: 10.1097/00008390-200508000-00011

24. Xing M, Prajapati HJ, Dhanasekaran R, Lawson DH, Kokabi N, Eaton BR, et al. Selective internal yttrium-90 radioembolization therapy (90Y-SIRT) versus best supportive care in patients with unresectable metastatic melanoma to the liver refractory to systemic therapy. *Am J Clin Oncol*. (2017) 40:27–34. doi: 10.1097/COC.0000000000000109

25. Kolb M, Forschner A, Artzner C, Grözinger G, Said I, Dittmann H, et al. Selective internal radiotherapy (SIRT) and chemosaturation percutaneous hepatic

perfusion (CS-PHP) for metastasized uveal melanoma: A retrospective comparative study. *Cancers*. (2023) 15:4942. doi: 10.3390/cancers15204942

26. Butler MO, Stanhope S, Naidoo R, Leach E, Kaur S, Collins L, et al. Tebentafusp induces transient systemic inflammation and modifies the micro-environment to sensitize uveal melanoma tumors to cytotoxic CD8 cells. *Cancer Res*. (2021) 81:517–. doi: 10.1158/1538-7445.AM2021-517

27. Middleton MR, McAlpine C, Woodcock VK, Corrie P, Infante JR, Steven NM, et al. Tebentafusp, a TCR/anti-CD3 bispecific fusion protein targeting gp100, potently activated antitumor immune responses in patients with metastatic melanoma. *Clin Cancer Res*. (2020) 26:5869–78. doi: 10.1158/1078-0432.CCR-20-1247

28. Sacco J, Carvajal R, Butler M, Shoushtari A, Hassel J, Ikeguchi A, et al. 64MO A phase (ph) II, multi-center study of the safety and efficacy of tebentafusp (tebe) (IMCgp100) in patients (pts) with metastatic uveal melanoma (mUM). *Ann Oncol*. (2020) 31:S1442–S3. doi: 10.1016/j.annonc.2020.10.552

29. Loi S, Sirtaine N, Piette F, Salgado R, Viale G, Van Eenoo F, et al. Prognostic and predictive value of tumor-infiltrating lymphocytes in a phase III randomized adjuvant breast cancer trial in node-positive breast cancer comparing the addition of docetaxel to doxorubicin with doxorubicin-based chemotherapy: BIG 02-98. *J Clin Oncol*. (2013) 31:860–7. doi: 10.1200/JCO.2011.41.0902

30. Sistigu A, Yamazaki T, Vacchelli E, Chaba K, Enot DP, Adam J, et al. Cancer cell–autonomous contribution of type I interferon signaling to the efficacy of chemotherapy. *Nat Med*. (2014) 20:1301–9. doi: 10.1038/nm.3708

31. Principe DR, Kamath SD, Korc M, Munshi HG. The immune modifying effects of chemotherapy and advances in chemo-immunotherapy. *Pharmacol Ther*. (2022) 236:108111. doi: 10.1016/j.pharmthera.2022.108111

32. Rodriguez-Vidal C, Fernandez-Diaz D, Fernandez-Marta B, Lago-Baameiro N, Pardo M, Silva P, et al. Treatment of metastatic uveal melanoma: systematic review. *Cancers*. (2020) 12:2557. doi: 10.3390/cancers12092557

frontiers | Frontiers in Oncology

TYPE Case Report
PUBLISHED 17 April 2024
DOI 10.3389/fonc.2024.1368564

Check for updates

OPEN ACCESS

EDITED BY
Dragos Eugen Georgescu,
Carol Davila University of Medicine and Pharmacy, Romania

REVIEWED BY
Alessandro Boscarelli,
Institute for Maternal and Child Health Burlo Garofolo (IRCCS), Italy
Milena Villarroel,
Hospital Luis Calvo Mackenna, Chile

*CORRESPONDENCE
Jian Bian
756640046@qq.com

RECEIVED 10 January 2024
ACCEPTED 01 April 2024
PUBLISHED 17 April 2024

CITATION
Liu Z, Bian J, Yang Y, Wei D and Qi S (2024) Ewing sarcoma of the pancreas: a pediatric case report and narrative literature review.
Front. Oncol. 14:1368564.
doi: 10.3389/fonc.2024.1368564

COPYRIGHT
© 2024 Liu, Bian, Yang, Wei and Qi. This is an open-access article distributed under the terms of the Creative Commons Attribution License (CC BY). The use, distribution or reproduction in other forums is permitted, provided the original author(s) and the copyright owner(s) are credited and that the original publication in this journal is cited, in accordance with accepted academic practice. No use, distribution or reproduction is permitted which does not comply with these terms.

Ewing sarcoma of the pancreas: a pediatric case report and narrative literature review

Zhensheng Liu, Jian Bian*, Yong Yang, Decheng Wei and Shiqin Qi

Department of General Surgery, Anhui Provincial Children's Hospital, Hefei, Anhui, China

Ewing's Sarcoma (ES) is an rare, small round-cell sarcoma that predominantly occurs in children and young adults, with both skeletal and extraskeletal manifestations. However, pancreatic ES, due to its rarity, is infrequently featured in scholarly literature, with only a scant 43 reported instances. Our study describes a case of pancreatic ES in an 8-year-old boy who was found to have an abdominal mass. Following an exhaustive examination, the boy was diagnosed with a neoplasm in the pancreatic head and underwent a complex surgical procedure encompassing pancreatoduodenectomy and partial transverse colectomy. Immunohistochemical assays confirmed the neoplastic cells' positivity for Cluster of Differentiation 99(CD99), Vimentin, and NK2 Homeobox 2(NKX2.2), while genomic testing identified an EWSR1-FLI1(Ewing Sarcoma Breakpoint Region 1–Friend Leukemia Integration 1) gene fusion. This led to a conclusive diagnosis of pancreatic Ewing's Sarcoma. The patient underwent seven cycles of adjuvant chemotherapy, alternating between VDC (Vincristine, Doxorubicin, Cyclophosphamide) and IE (Ifosfamide, Etoposide) tri-weekly, but did not undergo radiotherapy. At present, the patient remains neoplasm-free. Through our case analysis and comprehensive review of the existing literature, we aim to underscore th rarity of pancreatic Ewing's sarcoma and to highlight the efficacy of our individualized therapeutic approach.

KEYWORDS

pancreatic neoplasms, child, Ewing sarcoma, small round cell malignant tumor, pancreaticoduodenectomy

Introduction

Ewing sarcoma is characterized by a unique, small, round-cell sarcoma that exhibits gene fusions, typically involving one element from the FET family of genes, commonly Ewing Sarcoma Breakpoint Region 1 (EWSR1), and an element from the E-twenty-six (ETS) protein family of transcription factors. The most common Ewing sarcoma translocation, which is present in approximately 85% of cases, is t (1, 2)(q24;q12), leading to the EWSR1-FLI1 (Ewing Sarcoma Breakpoint Region 1–Friend Leukemia Integration 1) fusion transcript (3).

The use of terms such as "Askin tumor" and "primitive neuroectodermal tumor (PNET) " is not recommended according to the 2020 World Health Organization's (WHO) classification of undifferentiated small round cell sarcomas of bone and soft tissue to prevent potential confusion or misunderstanding (3). ES generally originates in bones and soft tissues, but there have been occasional reports of these tumors arising in unconventional locations such as the gastrointestinal tract, genitourinary tract, adrenal glands, parotid glands, and lungs (4–6). Apart from the aforementioned organs, such tumors could potentially emerge in the pancreatic region, corresponding to nearly 0.3% of primary pancreatic neoplasia occurrences (6, 7). Grasping the diverse presentation of ES and the various anatomical sites where it could potentially develop is crucial for clinicians to make timely diagnoses and develop appropriate management strategies for cases involving atypical locations (8).

This investigation presents a comprehensive analysis of a rare instance of pancreatic Ewing's sarcoma in an eight-year-old boy, exploring the diagnostic methodologies and therapeutic approaches utilized along his clinical journey. Through this research, we aim to enhance our understanding of rare tumors, improve early diagnosis, and develop more effective management strategies for such complex cases.

Case description

An 8-year-old boy was admitted to the pediatric general surgery department due to a palpable mass in the upper abdominal region, with no prior family history of cancer. Upon physical examination, no obvious enlargement of the superficial lymph nodes was palpated throughout the body. However, in the right upper quadrant of the abdomen, a localized protrusion revealed a firm, non-tender mass upon palpation. This mass, approximately 12cm x 10cm x 8cm in size, exhibited some mobility. Nonetheless, its boundaries with adjacent structures were not clearly defined.

The ultrasound examination revealed a heterogeneous echoic mass in the right upper abdomen, displaying nodular changes in certain parts of the tumor. Blood vessels traversing the mass were visible. The tumor had a close relationship with the head of the pancreas. The Computed Tomography(CT) scan showed a mixed-density mass in the pancreatic head area, primarily solid, with areas of low attenuation within. The mass was lobulated in shape, approximately 11.5cmx10.3cmx9.0cm in size. Upon enhancement, the mass demonstrated heterogeneous enhancement, with the solid component significantly enhanced, interspersed with a few low-attenuation foci, and tortuous small vessels could be seen within the mass (Figures 1A–C). No metastatic lesions were detected in the lungs or brain. The bone marrow smear, liver and kidney function tests, complete blood count, and coagulation parameters showed no abnormalities. The values of the serum tumor markers neuron-specific enolase (NSE), carcinoembryonic antigen(CEA), alpha-fetoprotein(AFP), lactate dehydrogenase (LDH), and carcinoma antigen 199 (CA199) were within normal limits. To further clarify the relationship between the tumor and surrounding blood vessels and organs, we employed a volume rendering technique (VR) for tumor assessment, as seen in Video 1. This technique also enabled individual analysis and assessment of the arteries, veins, and organs surrounding the tumor, facilitating an evaluation of the tumor's resectability (Figures 2A–D).

A pancreaticoduodenectomy and partial transverse colonectomy were successfully performed on the child. Intraoperative findings revealed a large tumor, approximately 12 cm x 10 cm x 11 cm, originating from the head of the pancreas and extending to the right middle lower abdomen. It had invaded about 2/3 of the transverse colon near the hepatic flexure and compressed the superior mesenteric vein (SMV). We excised the suspiciously invaded right wall of the SMV and reconstructed it using a continuous suturing technique with a 5-0 polypropylene surgical suture. No obvious peritoneal metastases were observed. In addition, we also noticed that the posterior edge of the tumor was pushing against the right kidney, and the right renal vein was deformed by the compression of the tumor. The postoperative gross specimen is depicted in Figure 3. All visible tumor within the operative field was excised during the surgical procedure (Figure 4). The tumor was characterized as a small round cell malignancy through an intraoperative frozen section procedure. However, the exact histological type of the tumor remained undetermined.

The pathology report from Fudan University Shanghai Cancer Center confirmed that the tumor, located in the head of the

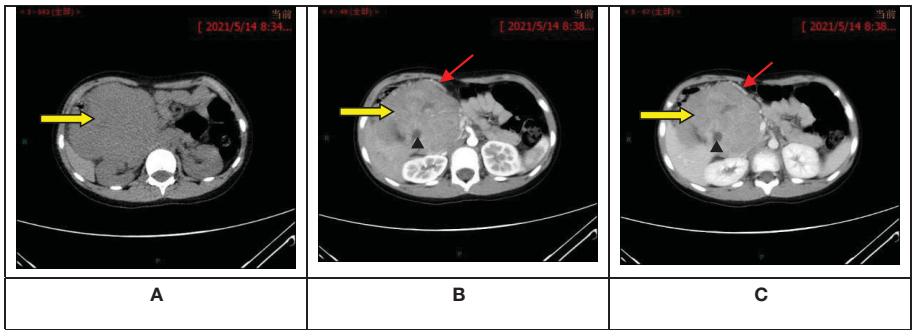

FIGURE 1
Abdominal computed tomography scan + enhancement show a primarily solid, mixed-density mass in the pancreatic head area, with significant enhancement of the solid component, interspersed low-attenuation foci, and visible tortuous small vessels within. **(A)** Pre-contrast phase; **(B)** Artery stage; **(C)** Portal vein stage. ⇨: Tumor; →: Visible tortuous small vessels; ▲: Interspersed low-attenuation foci.

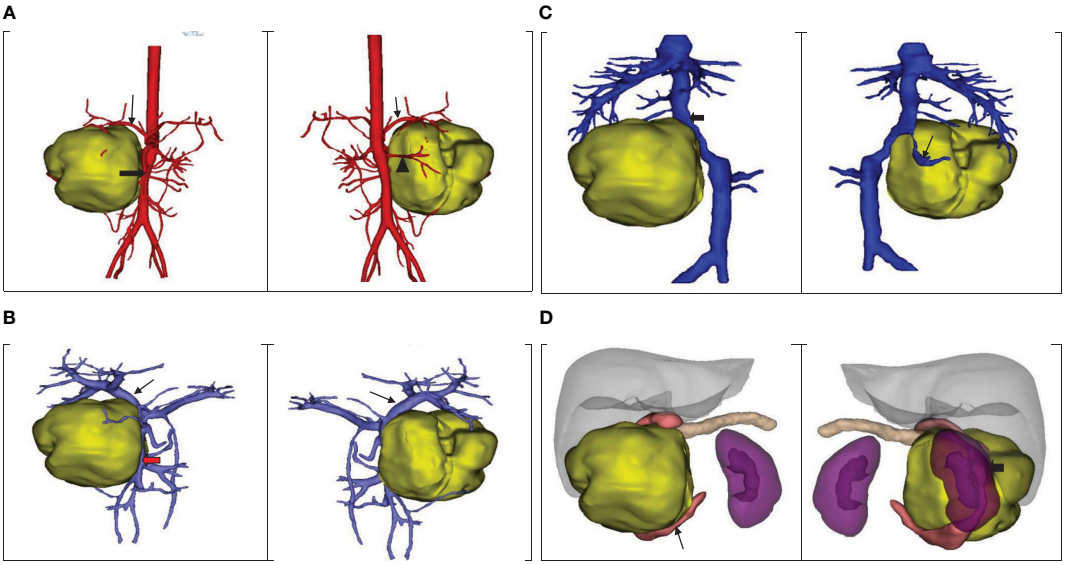

FIGURE 2
(A) The positional relationship between the tumor and the artery. ↓: Celiac trunk; ➡: Superior mesenteric artery; ▲: Right renal artery. **(B)** The positional relationship between the tumor and the portal vein. ↓: Portal vein; ➡:Superior mesenteric vein. **(C)** The tumor's positional relationship with the inferior vena cava and right renal vein.↓: Right renal vein; ➡: Inferior vena cava. **(D)** The positional relationship between the tumor and the adjacent organs. ➡: Duodenum; ➡: Right kidney.

pancreas, was identified as Ewing's sarcoma (Figure 5A) and invaded the full thickness of the small intestine and colon. Additionally, the presence of a vascular tumor thrombus was noted, along with the infiltration of tumor cells into the omental fibro-fatty tissue. The excised right wall of the superior mesenteric vein showed no signs of tumor invasion. No neoplastic activity was observed at the surgical margins of the gastric antrum, small intestine, and colon. The immunohistochemical assay revealed positivity for Vim, CD99(Figure 5B), NKX2.2(Figure 5C), SE (partially), Syn(Figure 5D), CgA (small focus), Ki-67 (approximately 60% in hotspot areas), INI-1, B-catenin (cytomembrane), and CK, negativity for Desmin, Myogenin, MyoD1, CD3, CD20, CD45, EMA, WwT1, Fli-1, and ERG. To further substantiate the diagnosis, we forwarded the specimens to Kang Shengda Medical Laboratory in Wuhan for comprehensive gene testing of pediatric solid tumors. The conducted test identified a breakpoint in the EWSR1 gene at chr22:29684161 and the FLI1 gene at chr11:128676663, resulting in an EWSR1-FLI1 fusion. Consequently, the final diagnosis confirmed that the patient had pancreatic Ewing's sarcoma.

The pediatric patient experienced a smooth postoperative recovery and was transferred to the Hematology-Oncology department on the 15th day after surgery. Comprehensive evaluations, which included bone marrow aspiration and biopsy, postoperative fluorodeoxyglucose (FDG)-PET, cerebrospinal fluid analysis, abdominal enhanced Magnetic Resonance Imaging (MRI), enhanced CT, cranial and full-spine MRI, as well as color sonographic examination of both the urogenital and cardiac systems, and an ultrasound of the superficial lymph nodes, were performed. Collectively, these examinations confirmed the absence of distant metastasis. Subsequently, the patient underwent seven alternating cycles of VDC and IE chemotherapy. Upon reassessment, there were no signs of tumor recurrence, resulting in the cessation of the chemotherapy regimen. Following a period of 2 years and 6 months of regular follow-up

FIGURE 3
Postoperative gross specimen.

FIGURE 4
Gross resection of the visible tumor. ⇨: Portal vein; ➡: Common hepatic artery. ⇨: Superior mesenteric vein. △The pancreatic cut surface after tumor resection.

examinations, the patient consistently demonstrated a sustained state of remission with no recurrence of the tumor.

Informed consent was obtained from the patient's parents for the reporting of this case.

Discussion

Ewing Sarcoma, recognized as the second most common malignant bone tumor in children and young adults, is typically identified in both bone and soft tissue. However, Extraskeletal Ewing Sarcoma, which exhibits a widespread anatomical distribution, can also sporadically appear in visceral organs such as the pancreas (9, 10). The presence of these tumors in the pancreas creates a distinct diagnostic dilemma due to the dominance of pancreatoblastoma, solid-pseudopapillary tumors, adenocarcinomas, and neuroendocrine tumors (11).

After conducting a comprehensive search and review of the literature, we discovered that, to date, there have been 44 reported cases of pancreatic Ewing's sarcoma (1, 2, 5–7, 12–41), as shown in Table 1. This count also includes the case from the current study. It appears that the authors, Achufusi TG and Ahmad M, may have reported the same patient's case from different perspectives (28, 32). Consequently, there would be only 43 reported cases of pancreatic Ewing's sarcoma. Literature reports suggest that patients with pancreatic Ewing's sarcoma typically have no specific clinical manifestations and often seek medical consultation due to upper abdominal pain. It occasionally presents as paraneoplastic syndromes such as precocious puberty, exophthalmos, and diabetes. However, jaundice is not a common manifestation. Upon discovery, the tumor frequently presents with a large size and is in an advanced stage, exhibiting local invasion or metastasis to the surrounding tissues and organs. At times, it is uncovered in

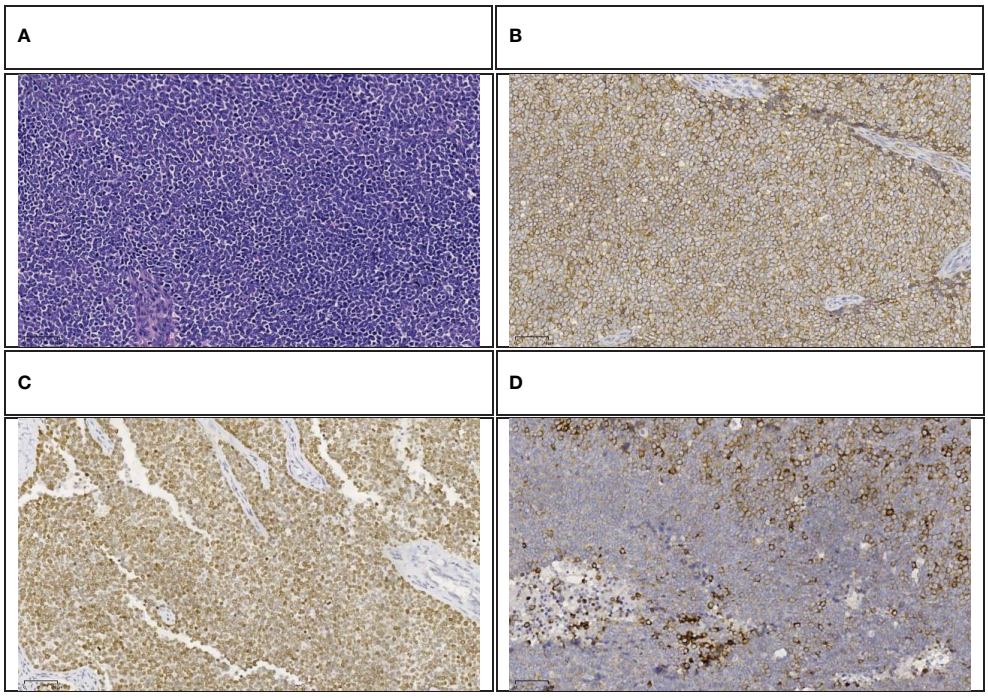

FIGURE 5
(A) Small round-cell malignant tumor (HE,100×). **(B)** Positive immunohistochemical staining for CD99(100×). **(C)** Positive immunohistochemical staining for NKX2.2 (100×). **(D)** Positive immunohistochemical staining for Syn (100×).

TABLE 1 44 cases of Ewing sarcoma in the pancreas: demographics and clinical features.

Publication	Age	Gender	size(cm)	Location	Signs/symptoms	Treatment	Follow-up (months)	Outcome
Danner DB, 1994 (27)	17	M	Ukn	Head	UAQpain	Whipple	33	AWD
Lüttges J, 1997 (41)	13	F	2.2×8×10	Body	Dyspepsia,exophthalmus	operation,CT	2	AWD
Lüttges J, 1997 (41)	31	M	Ukn	Body	UAQpain	Biopsy,CT,operation	Ukn	Ukn
Bülchmann G, 2000 (31)	6	F	6×5×5	Head	UAQpain	Whipple and transverse Colon Resection	6	DOD
O'Sullivan MJ, 2001 (39)	20	M	3.5	Head	Ukn	Whipple	30	AWD
Gemechu T,2002 (20)	17	M	Ukn	Body	Abdominal swelling	Ukn	36	AWD
Movahedi-Lankarani S, 2002 (33)	21	F	Ukn	Head	Abdominal pain	Whipple	0	DOC
Movahedi-Lankarani S, 2002 (33)	25	F	Ukn	Head	Abdominal pain	Biopsy	Ukn	Ukn
Movahedi-Lankarani S, 2002 (33)	25	F	8	Head	Jaundice,abdominal pain	Biopsy	Ukn	Ukn
Movahedi-Lankarani S, 2002 (33)	6	M	3.5	Head	Jaundice,abdominal pain	Whipple,CT	48	DOD
Movahedi-Lankarani S, 2002 (33)	13	M	6	Head	Abdominal pain	Biopsy	43	AWD
Movahedi-Lankarani S, 2002 (33)	20	M	3.5	Head	Jaundice,abdominal pain	Whipple,CT(Ukn)	27	AWD
Movahedi-Lankarani S, 2002 (33)	17	M	9	Head	Jaundice,abdominalpain	Whipple,CT	33	AWD
Shorter NA, 2002 (21)	5	M	Ukn	Head	Jaundice	Whipple,CT	48	DOD
Shorter NA, 2002 (21)	12	M	Ukn	tail	Ukn	DP,CT	72	AWD
Takeuchi M, 2003 (40)	10	F	Ukn	Body	UAQpain	Ukn	3	DOD
Perek S, 2003 (30)	31	M	10×12	Head	UAQpain	Whipple,Recurrent mass resection with right kidney,CT,Metastatic lung wedge resection,CT	50	DOD
Schutte WP, 2006 (24)	2	F	6×4	Body	Precocious puberty	DP,CT	12	AWD
Welsch T, 2006 (18)	33	M	18×18×16	Body and tail	Nausea,vomiting	Partial gastrectomy and DPS,CT,Resection of liver metastases,Autologous stem cell transplantation	12	AWD
Doi H, 2009 (29)	37	M	4.2	Head	Jaundice	FNA,Whipple and a hepatic metastasis resection,CT,RT,ablation	10	AD
Menon BS, 2009 (2)	8	F	10 ×6×10	Body	UAQpain,Precocious Puberty	Bisopy,CT,RT	19	DOC
Jing H, 2011 (13)	24	F	Ukn	Uncinate process	None	tumor resection,RT,CT,Resection of recurrent tumor and the invaded tissue,CT	30	AD
Wakao J, 2011 (14)	3	M	8.2×6.5×10	Head	UAQpain and swelling	Biopsy,CT,Whipple	8	AWD

(Continued)

10.3389/fonc.2024.1368564

TABLE 1 Continued

Publication	Age	Gender	size(cm)	Location	Signs/symptoms	Treatment	Follow-up (months)	Outcome
Maxwell L, 2011 (38)	11	M	9.8×7.8×6.4	Head	Anemia	Biopsy,CT,Whipple	Ukn	Ukn
Tortorelli AP 2012 (19)	18	M	33×27×18	Body and tail	Abdominal pain,exophthalmos	Total gastrectomy with DPS and Transverse Colon Resection;CT	9	AWD
Bose P, 2012 (17)	35	F	3	Body	Gallstone,pancreatitis	DPS and cholecystectomy	16	AWD
Reilly C, 2013 (26)	23	M	5.6 × 5.0 × 3.0	Body	UAQpain,nausea	Laparoscopic DPS	Ukn	Ukn
Jayant K, 2013 (22)	20	F	11 × 9	Body and tail	UAQpain	DPS,CT, RT	24	DOD
Mao Y, 2013 (7)	13	F	15×15×10	Head	UAQpain,diabetes mellitus	Resection of the uncinate process,CT,RT	41	DOD
Dias AR, 2013 (37)	25	F	4×3×2.5	Head	UAQpain	Whipple,CT	8	AWD
Kim JY, 2014 (25)	58	F	Ukn	Body	None	Bisopy,CT	Ukn	Ukn
Changal KH, 2014 (34)	60	M	3×3	Head	Abdominal pain	FNA,Biopsy,CT,Operation	Ukn	Ukn
Teixeira U, 2015 (6)	28	F	13×9×13	Head and body	UAQpain,Jaundice	Whipple	36	AWD
Kumar DN, 2015 (20)	22	M	20×15	Head	Abdominal pain	FNA,Whipple,CT	3	AWD
Nishizawa N, 2015 (12)	22	M	8	Head	UAQpain,nausea,vomiting	FNA,PPPD,CT,RT	12	AWD
Golhar A, 2017 (1)	17	F	5.6×7.4	Head and uncinate	Jaundice,itching	FNA,Whipple;CT,RT	6	AWD
Saif MW, 2017 (16)	38	F	8×10	Body	Abdominal pain	DPS;CT	6	AWD
Komforti MK, 2018 (15)	39	M	8×5.8	Body	Abdominal pain	FNA,Bisopy	1	AD
Yohannan B, 2020 (5)	26	F	10×9×7	Body and tail	left upper quadrant abdominal pain	FNA,CT,"DPS, subtotal gastrectomy, and left colectomy",CT	9	DOD
Ahmad M, 2020 (32)	61	M	18.5×11×20	Head	abdominal pain,nausea	FNA,Pancreatic Tumour Excision, Cholecystectomy and Distal gastrectomy	Ukn	Ukn
Pinheiro RN, 2020 (36)	22	M	14	Head and body	abdominal pain	Resection: Pancreatic Body/Tail, Spleen, Omentum, Gastric Antrum/Body (Roux-en-Y), Hepatic III, Gallbladder;CT;RT	96	AWD
Achufusi TG, 2021 (28)	61	M	Ukn	Head	abdominal pain	FNA,Pancreatic Tumour Excision, Cholecystectomy and Distal gastrectomy	0.33	DOD
Liu Y-C, 2022 (35)	16	M	8.0 × 5.3× 9.3	Tail	left lower quadrant abdominal pain and dysuria	Biopsy,CT,tumor resection and left nephrectomy and left partial adrenalectomy,CT,RT	48	AWD
Present case	8	M	12×11×10	Head	None	Whipple and Partial transverse colectomy,CT	20	AWD

10.3389/fonc.2024.1368564

that the tumor has invaded other organs, causing corresponding symptoms. Therefore, early diagnosis is quite difficult. In this case, the pediatric patient sought medical attention due to an unintentionally found abdominal lump, without experiencing any significant discomfort, corroborating the literature report. Surprisingly, despite the large size of the tumor, jaundice is not commonly observed, a marked contrast to adult pancreatic cancer where obstructive jaundice tends to appear early on. This may be attributed to several factors, which encompass the more uniform distribution of tumors across the gland, their infrequent origin from the ductal epithelium, and the distinct expansive growth pattern of these tumors, which contrasts with the infiltrative pattern often seen in ductal adenocarcinoma of the pancreas (21).

ES is recognized as a locally invasive tumor exhibiting aggressive growth patterns that are simultaneously infiltrative and expansive. These characteristics concur with the findings of numerous studies (42–44). Ewing's sarcoma often presents with ill-defined margins and tends to displace surrounding organs (45). Although lymph node involvement in Ewing's sarcoma cases is relatively infrequent, reported in merely 17.6%, the occurrence of distant metastases is common (46). Radiological findings often show the tumors to be iso-dense with regions of necrosis on pre-contrast CT images. These tumors typically appear iso-intense or hypo-intense on T1-weighted images (T1WI) and display heterogeneous hyper-intensity on T2-weighted images (T2WI) (45). Calcification is a rare phenomenon in Ewing's sarcoma, observed in less than 10% of the cases. Typically, Ewing's sarcoma presents as a large soft tissue mass, often exceeding 5 cm in size. One of the imaging characteristics of pancreatic Ewing's sarcoma could be the absence of the typical double duct sign, indicative of pancreatic head cancer, even when the tumor is large (43, 45, 47).

We used the VR technique to assess the anatomical relationship between the tumor and surrounding blood vessels and organs. The assessment indicated that the tumor was located in the head of the pancreas, causing compression on the right kidney. It also suggested that the superior mesenteric vein was compressed and deformed, but not directly invaded by the tumor. This was confirmed by intraoperative findings that the superior mesenteric vein, despite being noticeably compressed, could be easily separated from the tumor. However, to achieve R0 resection, we excised part of the lateral wall of the superior mesenteric vein that was directly compressed by the tumor. Postoperative pathology confirmed that the removed mesenteric vascular wall was not invaded by the tumor, a characteristic that contrasts with pancreatic cancer which often directly invades surrounding blood vessels. This suggests that surgical resection for pancreatic Ewing's sarcoma should not be readily dismissed merely based on preoperative imaging indicating vascular invasion or intraoperative findings of the tumor compressing or invading surrounding blood vessels. Some studies indicate that FDG PET-CT can potentially detect metastases in bone marrow and could potentially replace invasive procedures like bone marrow aspirates and trephine biopsies (11, 48). Regrettably, this specific examination was not conducted on the patient before the surgery. However, a comprehensive PET-CT scan was performed as part of a systematic evaluation before chemotherapy, which ruled out the presence of distant metastasis, serving to rectify the preoperative evaluation's inadequacies.

The essential diagnostic criteria of ES include small round cell morphology and CD99 membranous expression, whereas the detection of FET-ETS fusion forms the desirable diagnostic criteria (3). Based on these criteria, the diagnosis of Pancreatic Ewing's Sarcoma for the pediatric patient is confirmed. The standard treatment for newly identified Ewing sarcoma integrates multi-agent cytotoxic chemotherapy with local control strategies which include surgery and/or radiotherapy (49). Induction chemotherapy is necessary given the large tumor size and micrometastases (10). The approach to diagnosing and treating extraskeletal Ewing sarcoma (ES) follows the same guidelines as those implemented for bone ES (49). Despite the well-defined therapeutic principles, challenges persist in the diagnostic and therapeutic process for this specific case. For instance, the intraoperative frozen section analysis for this case revealed a small round-cell malignant tumor. The potential diagnoses could involve lymphoma, neuroblastoma, neuroendocrine tumor, poorly differentiated carcinoma, melanoma, or other round-cell sarcomas (5). The exact tumor type remained uncertain during the operation. Moreover, intraoperative exploration indicated that the tumor had no abdominal metastasis and appeared to be potentially resectable. We were then confronted with two choices. The first option entailed solely performing a biopsy, choosing induction chemotherapy based on the final pathological diagnose, and then conducting radical surgery. The primary advantage of the approach is an increased likelihood of achieving R0 resection, potentially eliminating the need for combined colectomy and superior mesenteric vein sidewall resection, and thereby reducing surgical risk and disability rate. However, a tumor biopsy could potentially lead to tumor dissemination, thus advancing the cancer stage and necessitating the child patient to endure the trauma and pain of two surgeries. The second approach involves one-stage radical tumor resection. For the case, this would entail not only performing a traditional pancreatoduodenectomy but also conducting a resection of part of the transverse colon. One major drawback of this approach lies in its high risk and aggressive nature, especially when the specific pathological type remains uncertain. Should postoperative pathology confirm diseases, such as lymphoma, which are treatable with chemotherapy (50), the consequent trauma inflicted on the child would be excessive.

Considering that open biopsy is quite traumatic and may increase the risk of tumor staging and dissemination, preoperative fine needle aspiration (FNA) has become a crucial diagnostic procedure for pediatric solid tumors. Therefore, we have compiled the FNA examination results of these 43 cases of pancreatic Ewing's sarcoma. Table 2 presents the FNA results of the eight patients who underwent preoperative FNA examination. Various studies advocate FNA as the initial diagnostic method for patients with pancreatic mass. The diagnostic step carries utmost significance as it guides the treatment regimen and enhances the likelihood of a favorable outcome (51–53). However, FNA harbors certain limitations. For instance, it may fail to procure sufficient tissue necessary for a comprehensive diagnosis, particularly for tests necessitating larger tissue samples. Additionally, the results obtained from FNA can occasionally be inconclusive or ambiguous, mandating open abdominal biopsy to reach a

TABLE 2 8 cases FNA Examination Results of Ewing sarcoma in the pancreas.

Publication	FNA Examination Results
Achufusi TG,2021 (28)	no evidence of malignancy
Yohannan B, 2020 (5)	extraosseous ES of the pancreas
Komforti MK,2018 (15)	scant cellularity and rare atypical single cells
Golhar A,2017 (1)	a pancreatic neuroendocrine neoplasm was suspected
Nishizawa N, 2015 (12)	PNET was suspected, a definitive diagnosis was difficult because of inadequate samples
Kumar DN, 2015 (20)	undifferentiated small round cell malignant tumor
Changal KH, 2014 (34)	A histopathologic possibility of round cell tumour was made
Doi H, 2009 (29)	a metastatic carcinoma or poorly differentiated endocrine carcinoma was suspected

definitive diagnosis. Of the 43 cases of pancreatic Ewing's sarcoma summarized in this article, eight had FNA examinations. However, only one case was confirmed as pancreatic Ewing's sarcoma through FNA. Two cases were negative, one was misdiagnosed as a pancreatic endocrine tumor, one was diagnosed as a neuroendocrine tumor metastasized to the liver, and one was suspected of pancreatic neuroectodermal tumor, but could not be confirmed. Another two cases were diagnosed as small round cell tumors. Although the diagnosis rate is not high, the value of FNA is expected to increase with advancements in medical technology. In our report, given the unique exophytic growth pattern and the substantial size of the tumor that was palpable under the skin, the pediatric patient should ideally have undergone an FNA examination prior to surgery. This procedure could have potentially facilitated a precise preoperative diagnosis.

Studies have identified specific predictors for improved survival, such as younger age at diagnosis and complete tumor resections. Conversely, factors including age over 14 years, primary tumor volume exceeding 200 cc, and the occurrence of bone marrow or lung metastases have been recognized as major risk factors for a poorer prognosis (54, 55). The pediatric patient has been followed up for two and a half years with no recurrence of the tumor and has exhibited satisfactory growth and development. Favorable prognostic factors for this patient include a younger age at diagnosis, the absence of distant metastases, and complete tumor resection. The large tumor volume, visible tumor thrombus in the vessels, and tumor invasion into the omentum are considered adverse factors. All invaded tissues and organs were completely resected, which explains the decision not to administer postoperative radiation therapy to the patient. Despite the favorable therapeutic outcome in this case, our diagnostic and treatment process had its shortcomings. For example, we did not sufficiently recognize the necessity of preoperative whole-body PET CT scans and tumor FNA procedures. Through the study of this case and related literature, we have deepened our understanding of rare tumors in children. Given the paramount goal of optimizing the patient's survival benefit, it is essential to refer such rare cases of pediatric pancreatic tumors to specialized centers dedicated to pediatric solid tumor treatment.

Conclusion

ES can originate in the pancreas and is highly aggressive. Early and accurate diagnosis is crucial for effective management of these tumors. Aggressive surgical resection, alongside multimodal therapy, can potentially improve prognosis. However, the prognosis for this rare malignancy remains unsatisfactory. Therefore, further case accumulation and investigation are required to improve outcomes.

Data availability statement

The original contributions presented in the study are included in the article/Supplementary Materials, further inquiries can be directed to the corresponding author/s.

Ethics statement

The studies involving humans were approved by Ethics Committee of the Children's Hospital of Anhui Province. The studies were conducted in accordance with the local legislation and institutional requirements. Written informed consent for participation was not required from the participants or the participants' legal guardians/next of kin in accordance with the national legislation and institutional requirements. Written informed consent was obtained from the individual(s) for the publication of any potentially identifiable images or data included in this article.

Author contributions

ZL: Writing – original draft, Writing – review & editing. JB: Conceptualization, Data curation, Supervision, Writing – review & editing. YY: Methodology, Visualization, Writing – review & editing. DW: Data curation, Formal analysis, Writing – review & editing. SQ: Conceptualization, Project administration, Writing – review & editing.

Funding

The author(s) declare that no financial support was received for the research, authorship, and/or publication of this article.

Conflict of interest

The authors declare that the research was conducted in the absence of any commercial or financial relationships that could be construed as a potential conflict of interest.

Publisher's note

All claims expressed in this article are solely those of the authors and do not necessarily represent those of their affiliated organizations, or those of the publisher, the editors and the reviewers. Any product that may be evaluated in this article, or claim that may be made by its manufacturer, is not guaranteed or endorsed by the publisher.

Supplementary material

The Supplementary Material for this article can be found online at: https://www.frontiersin.org/articles/10.3389/fonc.2024.1368564/full#supplementary-material

References

1. Golhar A, Ray S, Haugk B, Singhvi SK. Cytogenetically confirmed primary Ewing's sarcoma of the pancreas. *BMJ Case Rep*. (2017), bcr–2017-219219. doi: 10.1136/bcr-2017-219219

2. Menon BS, Juraida E, Mohamed M, Manaf Z, Zahari Z, Yusuf S, et al. Pancreatic primitive neuroectodermal tumour associated with precocious puberty. *Pediatr Blood Cancer*. (2009) 53:518–9. doi: 10.1002/pbc.22099

3. Organisation mondiale de la santé, Centre international de recherche sur le cancer. *Soft tissue and bone tumours. 5th ed*. Geneva: OMS (2020). Available at: https://zh.zlibrary-east.se/book/16279720/0736bd/soft-tissue-and-bone-tumours-who-classification-of-tumours-medicine.html.

4. Carvajal R, Meyers P. Ewing's sarcoma and primitive neuroectodermal family of tumors. *Hematol Oncol Clin North Am*. (2005) 19:501–25. doi: 10.1016/j.hoc.2005.03.004

5. Yohannan B, Feldman M. A nonpediatric extraosseous ewing sarcoma of the pancreas: differential diagnosis and therapeutic strategies. *Case Rep Oncol Med*. (2020) 2020:1–4. doi: 10.1155/2020/2792750

6. Teixeira U, Goldoni M, Unterleider M, Diedrich J, Balbinot D, Rodrigues P, et al. Primitive neuroectodermal tumor of the pancreas: A case report and review of the literature. *Case Rep Surg*. (2015) 2015:1–4. doi: 10.1155/2015/276869

7. Mao Y, Sang X, Liang N, Yang H, Lu X, Yang Z, et al. Peripheral primitive neuroectodermal tumors arising in the pancreas: the first case report in Asia and a review of the 14 total reported cases in the world. *Hepatobil Surg Nutr*. (2013) 2:10. doi: 10.3978/j.issn.2304-3881.2012.08.01

8. Bernstein M, Kovar H, Paulussen M, Randall RL, Schuck A, Teot LA, et al. Ewing's sarcoma family of tumors: current management. *Oncologist*. (2006) 11:503–19. doi: 10.1634/theoncologist.11-5-503

9. Kumar J, Agrawal S, Agarwal RK, Dayama K. A review of a rare entity in pancreas-extraosseous Ewing's sarcoma. *J Pancreas*. (2016) 17:574–9.

10. Grünewald TGP, Cidre-Aranaz F, Surdez D, Tomazou EM, de Álava E, Kovar H, et al. Ewing sarcoma. *Nat Rev Dis Primers*. (2018) 4:5. doi: 10.1038/s41572-018-0003-x

11. Kilpatrick SE, Reith JD, Rubin B. Ewing sarcoma and the history of similar and possibly related small round cell tumors: from whence have we come and where are we going? *Adv Anat Pathol*. (2018) 25:314–26. doi: 10.1097/PAP.0000000000000203

12. Nishizawa N, Kumamoto Y, Igarashi K, Nishiyama R, Tajima H, Kawamata H, et al. A peripheral primitive neuroectodermal tumor originating from the pancreas: a case report and review of the literature. *Surg Case Rep*. (2015) 1:80. doi: 10.1186/s40792-015-0084-7

13. Jing H, Li F, Chen L, Zhang T, Zhao Y. Detection of recurrent pancreatic primitive neuroectodermal tumor by tc-99m hydrazinonicotinyl-tyr3-octreotide scan. *Clin Nucl Med*. (2011) 36:54–5. doi: 10.1097/RLU.0b013e3181feeffa

14. Wakao J, Ono S, Hosoi H, Tsuda T. Ewing sarcoma family tumor in the pancreatic head incidentally diagnosed by abdominal trauma. *Japan Soc Pediatr Hematology/Oncol*. (2011) 48:7–11.

15. Komforti MK, Sokolovskaya E, D'Agostino CA, Benayed R, Thomas RM. Extra-osseous Ewing sarcoma of the pancreas: case report with radiologic, pathologic, and molecular correlation, and brief review of the literature. *Virchows Arch*. (2018) 473:361–9. doi: 10.1007/s00428-018-2344-y

16. Saif MW, Kaley K. Extraosseous Ewing's sarcoma of the pancreas: an uncommon but treatable disease. *Cureus*. (2017) 9(11):e1882. doi: 10.7759/cureus.1882

17. Bose P, Murugan P, Gillies E, Holter JL. Extraosseous Ewing's sarcoma of the pancreas. *Int J Clin Oncol*. (2012) 17:399–406. doi: 10.1007/s10147-011-0311-6

18. Welsch T. Huge primitive neuroectodermal tumor of the pancreas: Report of a case and review of the literature. *WJG*. (2006) 12:6070. doi: 10.3748/wjg.v12.i37.6070

19. Tortorelli AP, Alfieri S, Sanchez AM, Rosa F, Doglietto GB. Image of the month. PNET of the pancreas. *Arch Surg (Chicago Ill: 1960)*. (2012) 147:1063–4. doi: 10.1001/archsurg.2011.1620a

20. Kumar DN, Sharma DG, Gupta DS, Daga DR, Hussain DI, Khan DSA. Large operable Ewing sarcoma of the pancreas: Report of a case and review of the literature. *SAS J Surg*. (2015) 1:152–6.

21. Shorter NA, Glick RD, Klimstra DS, Brennan MF, LaQuaglia MP. Malignant pancreatic tumors in childhood and adolescence: The Memorial Sloan-Kettering experience, 1967 to present. *J Pediatr Surg*. (2002) 37:887–92. doi: 10.1053/jpsu.2002.32897

22. Jayant K, Agrawal S, Agarwal R, Khoiwal S. Pancreatic Ewings sarcoma- A dreadful tumor. *AJCP*. (2013) 1:24–6. doi: 10.12691/ajcp-1-3-2

23. Gemechu T, Ersumo T. Peripheral primitive neuroectodermal tumor presenting in the retroperitoneum: a case report with immunohistochemical study. *Ethiop Med J*. (2002) 40:69–77.

24. Schutte WP, Knight PJ. Precocious puberty because of a pancreatic neuroectodermal tumor. *J Pediatr Surg*. (2006) 41:1916–8. doi: 10.1016/j.jpedsurg.2006.05.046

25. Kim JY, Song JS, Park H, Byun JH, Song K-B, Kim K, et al. Primary mesenchymal tumors of the pancreas: single-center experience over 16 years. *Pancreas*. (2014) 43:959–68. doi: 10.1097/MPA.0000000000000130

26. Reilly C, Zenoni S, Hasan MK, Varadarajulu S, Tran T-A, de la Fuente SG, et al. Primary pancreatic Ewing's sarcoma with portal vein tumor thrombosis. *J Gastrointest Surg*. (2013) 17:1015–9. doi: 10.1007/s11605-012-2098-9

27. Danner DB, Hruban RH, Pitt HA, Hayashi R, Griffin CA, Perlman EJ. Primitive neuroectodermal tumor arising in the pancreas. *Mod Pathol*. (1994) 7:200–4.

28. Achufusi TG, Sohal R, Zamora E, Harne P, Russo R. Primitive neuroectodermal tumor of the pancreas. *Baylor Univ Med Center Proc*. (2021) 34:144–5. doi: 10.1080/08998280.2020.1826760

29. Doi H, Ichikawa S, Hiraoka A, Ichiryu M, Nakahara H, Ochi H, et al. Primitive neuroectodermal tumor of the pancreas. *Internal Med*. (2009) 48:329–33. doi: 10.2169/internalmedicine.48.1484

30. Perek S, Perek A, Sarman K, Tuzun H, Buyukunal E. Primitive neuroectodermal tumor of the pancreas. *Pancreatology*. (2003) 3:352–6. doi: 10.1159/000071776

31. Bülchmann G, Schuster T, Haas RJ, Joppich I. Primitive Neuroectodermal Tumor of the Pancreas An Extremely Rare Tumor - Case report and review of the literature -. *Klin Padiatr*. (2000) 212:185–8. doi: 10.1055/s-2000-9675

32. Ahmad M, Chowdhury N, Chowdhury NA, Saleem A. S1564 primitive neuroectodermal tumor - an extremely rare cancer of pancreas. *Am J Gastroenterol*. (2020) 115:S794–95. doi: 10.14309/01.ajg.0000708304.25136.41

33. Movahedi-Lankarani S, Hruban RH, Westra WH, Klimstra DS. Primitive neuroectodermal tumors of the pancreas. *Am J Surg Pathol*. (2002) 26:1040–7. doi: 10.1097/00000478-200208000-00009

34. Changal KH, Mir MH, Azaz SA, Qadri SK, Lone AR. Primitive neuroectodermal tumour of pancreas; second case from Asia. *Malays J Med Sci*. (2014) 21:65–9.

35. Liu Y-C, Yeh T-C, Wu P-S, Sheu J-C, Lee H-C, Yeung C-Y, et al. Rare presentation in a rare case of pancreatic extraosseous Ewing's sarcoma: A case report. *Medicine*. (2022) 101:e31752. doi: 10.1097/MD.0000000000031752

36. Pinheiro RN, Cesário FKO dos S, Mondragon JPM, da Silva FDB, Fontoura RP, Netto JD de S, et al. Therapeutic approach of a pancreatic Ewing Sarcoma/PNET: case report and literature review. *Braz J Oncol*. (2020) 16:e-20200020. doi: 10.5935/2526-8732.20200020

37. Dias AR, Arantes T, Sampaio RC, Jureidini R, da Cunha JEM, Cecconello I. Tumor primitivo ectodérmico pancreático: relato de caso. *ABCD arq Bras cir dig*. (2013) 26:159–61. doi: 10.1590/S0102-67202013000200021

38. Maxwell L, Hederman A, Jackson C, Sawaya D, Giles H, Nowicki MJ. Uncommon presentation of rare disorder—Duodenal ulcer secondary to invasive pancreatic primitive neuroectodermal tumor. *J Pediatr Hematology/Oncol*. (2011) 33:543–8. doi: 10.1097/MPH.0b013e31821041af

39. O'Sullivan MJ, Perlman EJ, Furman J, Humphrey PA, Dehner LP, Pfeifer JD. Visceral primitive peripheral neuroectodermal tumors: A clinicopathologic and molecular study. *Hum Pathol*. (2001) 32:1109–15. doi: 10.1053/HUPA.2001.28247

40. Takeuchi M. Primitive neuroectodermal tumor of the pancreas. *Arch Histopathol Differ Diagn*. (2003) 10:23–6.

41. Lüttges J, Pierré E, Zamboni G, Weh G, Lietz H, Kußmann J, et al. Maligne nichtepitheliale Tumoren des Pankreas. *Der Pathologe*. (1997) 18:233–7. doi: 10.1007/s002920050211

42. Ibarburen C, Haberman JJ, Zerhouni EA. Peripheral primitive neuroectodermal tumors. CT and MRI evaluation. *Eur J Radiol*. (1996) 21:225–32. doi: 10.1016/0720-048X(95)00731-5

43. Sallustio G, Pirronti T, Lasorella A, Natale L, Bray A, Marano P. Diagnostic imaging of primitive neuroectodermal tumour of the chest wall (Askin tumour). *Pediatr Radiol*. (1998) 28:697–702. doi: 10.1007/s002470050443

44. Kim MS, Kim B, Park CS, Song SY, Lee EJ, Park NH, et al. Radiologic findings of peripheral primitive neuroectodermal tumor arising in the retroperitoneum. *Am J Roentgenol*. (2006) 186:1125–32. doi: 10.2214/AJR.04.1688

45. Li X, Zhang W, Song T, Sun C, Shen Y. Primitive neuroectodermal tumor arising in the abdominopelvic region: CT features and pathology characteristics. *Abdom Imaging*. (2011) 36:590–5. doi: 10.1007/s00261-010-9655-z

46. Winer-Muram HT, Kauffman WM, Gronemeyer SA, Jennings SG. Primitive neuroectodermal tumors of the chest wall (Askin tumors): CT and MR findings. *Am J Roentgenol*. (1993) 161:265–8. doi: 10.2214/ajr.161.2.8392786

47. Sabaté JM, Franquet T, Parellada JA, Monill JM, Oliva E. Malignant neuroectodermal tumour of the chest wall (Askin tumour): CT and MR findings in eight patients. *Clin Radiol*. (1994) 49:634–8. doi: 10.1016/S0009-9260(05)81882-3

48. Newman EN, Jones RL, Hawkins DS. An evaluation of [F-18]-fluorodeoxy-D-glucose positron emission tomography, bone scan, and bone marrow aspiration/biopsy as staging investigations in Ewing Sarcoma. *Pediatr Blood Cancer*. (2013) 60:1113–7. doi: 10.1002/pbc.24406

49. Strauss SJ, Frezza AM, Abecassis N, Bajpai J, Bauer S, Biagini R, et al. Bone sarcomas: ESMO–EURACAN–GENTURIS–ERN PaedCan Clinical Practice Guideline for diagnosis, treatment and follow-up. *Ann Oncol*. (2021) 32:1520–36. doi: 10.1016/j.annonc.2021.08.1995

50. Facchinelli D, Sina S, Boninsegna E, Borin A, Tisi MC, Piazza F, et al. Primary pancreatic lymphoma: Clinical presentation, diagnosis, treatment, and outcome. *Eur J Haematol*. (2020) 105:468–75. doi: 10.1111/ejh.13468

51. Kridis W, Toumi N, Chaari H, Khanfir A, Ayadi K, Keskes H, et al. A review of ewing sarcoma treatment: is it still a subject of debate? *RRCT*. (2017) 12:19–23. doi: 10.2174/1574887112666170120100147

52. Gaspar N, Hawkins DS, Dirksen U, Lewis IJ, Ferrari S, Le Deley M-C, et al. Ewing sarcoma: current management and future approaches through collaboration. *J Clin Oncol*. (2015) 33:3036–46. doi: 10.1200/JCO.2014.59.5256

53. Miller DL, Roy-Chowdhuri S, Illei P, James A, Hruban RH, Ali SZ. Primary pancreatic Ewing sarcoma: a cytomorphologic and histopathologic study of 13 cases. *J Am Soc Cytopathol*. (2020) 9:502–12. doi: 10.1016/j.jasc.2020.04.013

54. Ahmad R, Mayol BR, Davis M, Rougraff BT. Extraskeletal ewing's sarcoma. *Cancer*. (1999) 85:725–31. doi: 10.1002/(SICI)1097-0142(19990201)85:3<725::AID-CNCR23>3.0.CO;2-2

55. Ladenstein R, Pötschger U, Le Deley MC, Whelan J, Paulussen M, Oberlin O, et al. Primary disseminated multifocal ewing sarcoma: results of the euro-EWING 99 trial. *J Clin Oncol*. (2010) 28:3284–91. doi: 10.1200/JCO.2009.22.9864

frontiers | Frontiers in Oncology

TYPE Case Report
PUBLISHED 23 April 2024
DOI 10.3389/fonc.2024.1350043

Check for updates

OPEN ACCESS

EDITED BY
Ferdinando Agresta,
ULSS2 Marca Trevigiana, Italy

REVIEWED BY
Laura Schmidt,
National Cancer Institute at Frederick (NIH), United States
Yewei Zhang,
Nanjing Medical University, China

*CORRESPONDENCE
Xiaofang Zhang
xf2029@163.com
Zhengkui Sun
sunzhengkui@sohu.com
Tenghua Yu
yutenghua0107@sina.cn

†These authors have contributed equally to this work

RECEIVED 05 December 2023
ACCEPTED 10 April 2024
PUBLISHED 23 April 2024

CITATION
Xu S, Xu J, Yu C, Zeng Y, Tang L, Tang M, Yu T, Sun Z and Zhang X (2024) Case report: Report of a rare encounter: metastasis of renal cell carcinoma to the thyroid. *Front. Oncol.* 14:1350043. doi: 10.3389/fonc.2024.1350043

COPYRIGHT
© 2024 Xu, Xu, Yu, Zeng, Tang, Tang, Yu, Sun and Zhang. This is an open-access article distributed under the terms of the Creative Commons Attribution License (CC BY). The use, distribution or reproduction in other forums is permitted, provided the original author(s) and the copyright owner(s) are credited and that the original publication in this journal is cited, in accordance with accepted academic practice. No use, distribution or reproduction is permitted which does not comply with these terms.

Case report: Report of a rare encounter: metastasis of renal cell carcinoma to the thyroid

Siyi Xu[1,2†], Jiawei Xu[2†], Chengdong Yu[2†], Ying Zeng[2†], Lei Tang[2], Mu Tang[2], Tenghua Yu[2*], Zhengkui Sun[2*] and Xiaofang Zhang[1*]

[1]Department of pathology, Jiangxi Cancer Hospital, Nanchang, China, [2]Jiangxi Medical College, Nanchang University, Nanchang, China

Renal cell carcinoma (RCC) is the most common renal tumor, with lung, bone, and liver being the primary sites of metastasis. Thyroid metastasis, on the other hand, is relatively uncommon. Metastatic tumors in the thyroid gland typically manifest as multiple or isolated nodules, which can be easily overlooked due to the lack of specific clinical and imaging features. However, the identification of thyroid metastasis suggests the presence of systemic metastasis and is indicative of a poor prognosis for patients. In this paper, we present two cases of thyroid metastasis following nephrectomy, with the objective of enhancing understanding among medical community regarding the diagnosis and treatment of thyroid metastasis originating from renal cell carcinoma. By raising awareness about this phenomenon, we emphasize the importance of early detection and diagnosis to improve patient prognoses. The implementation of standardized treatment protocols at the earliest possible stage is also emphasized. Through this research, we aim to contribute to the early identification and management of thyroid metastasis in patients with renal cell carcinoma, ultimately leading to improved outcomes.

KEYWORDS

renal cell carcinoma, thyroid, metastasis, pathology, diagnosis, case report

Case 1

In 2012, a middle-aged gentleman of 48 years presented with the clinical manifestation of hematuria characterized by the presence of blood clots, without an identifiable underlying etiology (Figure 1). Seeking medical attention, he promptly sought care at a local healthcare facility, where a comprehensive abdominal computed tomography (CT) examination revealed findings indicative of a neoplastic growth localized within the right renal structure. Following comprehensive preoperative evaluations, a right nephrectomy was conducted at the hospital. The subsequent postoperative histopathological examination revealed clear cell carcinoma originating from the right kidney. The postoperative patient underwent regular follow-up evaluations at intervals of 3 months. Approximately 1 year

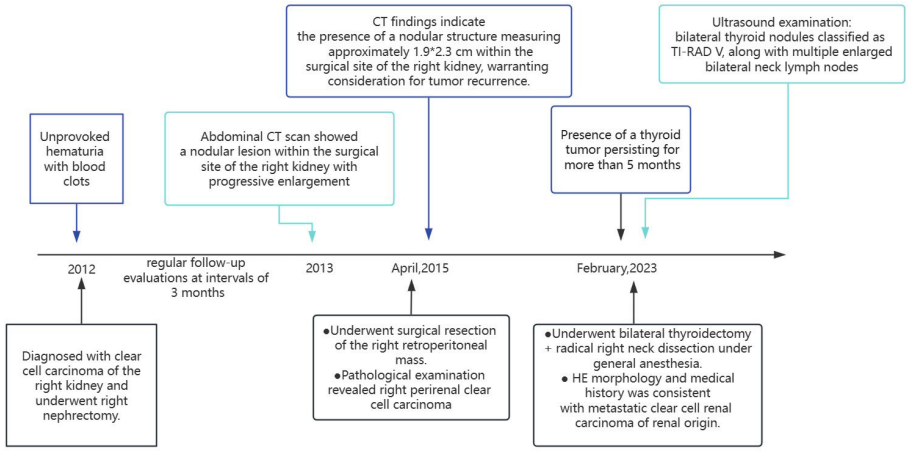

FIGURE 1
Patient medical history timeline of case 1.

post-surgery, a subsequent abdominal CT scan revealed the presence of a nodular lesion within the surgical site of the right kidney, the nature of which remained undetermined. Consequently, ongoing surveillance and close monitoring were advised. Following the initial evaluation, subsequent reviews conducted in March revealed a progressive enlargement of the nodule within the surgical site of the right kidney. Further assessment at the Affiliated Cancer Hospital of Fudan University in April 2015 demonstrated a significant enlargement of the nodule to 24 mm, thereby raising concerns regarding the potential presence of recurrent foci. Our CT findings indicate the presence of a nodular structure measuring approximately 1.9*2.3 cm within the surgical site of the right kidney, warranting consideration for tumor recurrence. On April 24, 2015, the patient underwent surgical resection of the right retroperitoneal mass. The postoperative pathological examination revealed right perirenal clear cell carcinoma, Furman grade 3, characterized by small nuclei, abundant and translucent cytoplasm, lamellar arrangement, and infiltrative growth of tumor cells (immunohistochemistry was not performed at that time). The patient had a favorable postoperative recovery.

In February 2023, the patient underwent an ultrasound examination due to the presence of a thyroid tumor persisting for more than 5 months. The findings revealed bilateral thyroid nodules classified as TI-RAD V, along with multiple enlarged bilateral neck lymph nodes. Physical examination: The neck exhibited symmetrical features and had a soft texture, there was no jugular vein distention, and the trachea was centrally aligned, palpation of the neck revealed a palpable swelling in the right thyroid gland, measuring approximately 3.5 cm. The swelling had a soft consistency and did not elicit any discomfort upon pressure. It exhibited mobility and moved up and down with swallowing. No evident abnormalities were detected in the left thyroid gland. Additionally, there were no palpable enlarged lymph nodes in the bilateral neck, and no tremor or vascular murmur was observed. Ultrasound examination of the thyroid gland and neck (Figure 2): Multiple thyroid nodules were identified, classified as C-TIRADS class 4A, within the right lobe of the thyroid gland, multiple hypoechoic nodules were diffusely distributed, some of which partially merged to form a mass, the largest nodule measured approximately 38*21 mm, displaying an irregular morphology with a well-defined boundary, abundant blood flow signals were detected within. In the left lobe and isthmus, multiple hypoechoic nodules were also identified, the largest nodule in this region measured approximately 21*8 mm, featuring an irregular morphology with a clear boundary and abundant blood flow signals, furthermore, multiple enlarged lymph nodes were detected in the right side of the neck. Chest and abdominal CT scan (Figure 2D): the scan revealed an occupying lesion in the right lobe of the thyroid gland, warranting further ultrasonography, suspiciously enlarged lymph nodes were observed in the right upper mediastinal trachea, multiple nodules were also present in both lungs, indicating the possibility of metastases, postoperative changes were noted in the left kidney. The blood thyrotropin level showed a mild elevation at 4.817 uIU/mL, while the blood levels of FT3, FT4, and cancer markers were all within the normal range. Given the patient's prior history of renal carcinoma and local recurrence, an ultrasound-guided fine-needle aspiration (FNA) of the thyroid mass was performed as part of the preoperative evaluation, to our surprise, the cytologic examination yielded results indicative of follicular carcinoma of the thyroid. The patient underwent bilateral thyroidectomy+ radical right neck dissection under general anesthesia on February 15, 2023. During the intraoperative examination, multiple nodules were identified in the right thyroid gland, with the largest measuring approximately 3*3 cm. The nodules had a firm consistency, and the capsule remained intact. Subsequent postoperative pathological analysis revealed the presence of several gray-white masses in the right lobe of the thyroid gland, which were fused together and measured approximately 5*4*2.5 cm, additionally, gray-yellow medium-sized nodules, approximately 1.6*1.5*0.6 cm in size, were observed in the left lobe and isthmus near the envelope, the tumor tissue exhibited cluster and sheet arrangements of cancer nests, characterized by large, deeply stained nuclei. Furthermore, lymph node metastases

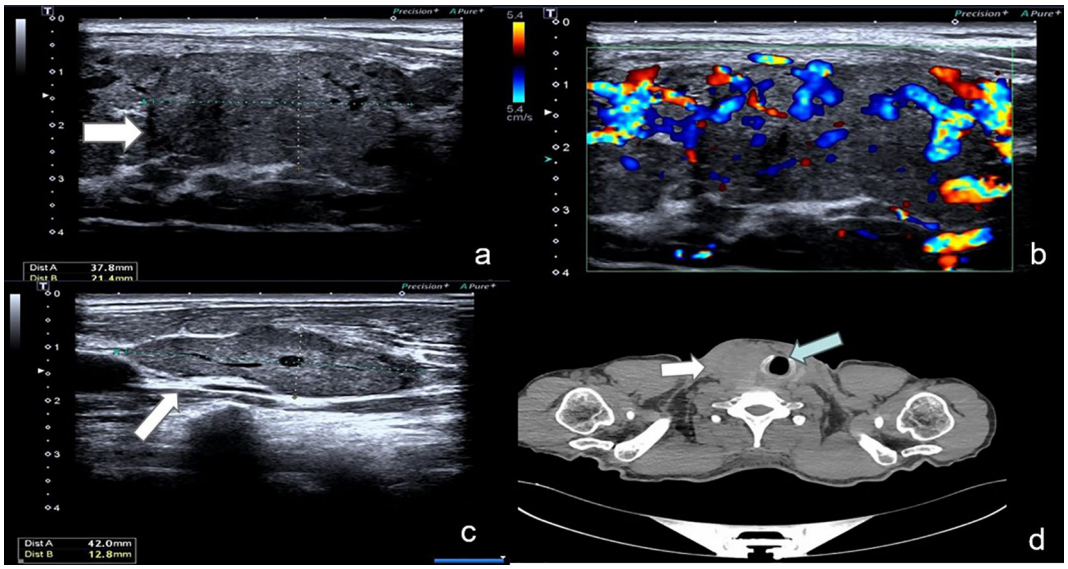

FIGURE 2
Ultrasound and CT of the thyroid gland and neck. **(A, B)** Multiple hypoechoic nodules were identified in the right lobe of the thyroid gland, some of which were partially fused, forming a mass with a maximum dimension of approximately 38*21mm. The nodules exhibited irregular morphology and were associated with abundant blood flow signals. **(C)** Multiple enlarged lymph nodes were detected in the right cervical region, the largest of which was about 42*13mm and contained abundant blood flow signals. **(D)** CT shows that the right lobe of the thyroid gland exhibited enlargement, accompanied by the presence of a slightly hypodense mass measuring approximately 4.3*4.9 cm. The surrounding fat interstitial space appeared blurred, and the lesion showed indistinct demarcation from the adjacent trachea and esophagus, resulting in leftward displacement of the trachea.

were detected in 6 out of 11 lymph nodes examined. Immunohistochemical results (Figure 3): CD10(+), Pax-8(+), CK19(+), CyclinD1(+), Ki-67(+, 15%), TG(-), TPO(-), TTF-1(-), Cal-3(-), CD56(-), CgA(-), Syn(-), TFE3(-), BRAF-V600E(-) the combination of HE morphology and medical history was consistent with metastatic clear cell renal cell carcinoma of renal origin. The patient underwent regular post-operative evaluations at the hospital, revealing no evidence of disease progression up to the present moment.

Case 2

A 62-year-old female was admitted to our institution in 2021 due to the incidental discovery of an anterior neck mass that had been present for 1 year. She reported a history of right nephrectomy for clear cell carcinoma of the right kidney at an external hospital, with satisfactory postoperative recovery and regular follow-up. Approximately one year ago, she noticed a painless lump in the anterior neck measuring approximately 2.0*1.5 cm. She did not experience any associated symptoms such as pain, fever, sweating, dysphagia, or hoarseness, and she did not seek medical attention at that time. There was no family history of kidney tumors or thyroid disease. Physical examination: Multiple palpable swellings were identified in the bilateral thyroid gland and isthmus, the largest swelling measured approximately 2.5 * 2.0 cm and exhibited a smooth surface with medium consistency, no pressure pain was reported, and the boundaries of the swellings remained clear, the swellings moved up and down with swallowing, and no vascular murmurs were detected. Ultrasound of the thyroid and neck (Figure 4): The ultrasound examination revealed the presence of multiple mixed echogenic nodules (TI-RADS III) in the right lobe of the thyroid gland, these nodules exhibited well-defined borders, regular morphology, and prominent blood flow signals within and surrounding them, some of the nodules exhibited punctiform strong echogenic clusters. Thyroid function indices were found to be within normal limits. The patient underwent a right-sided thyroid lobectomy combined with a left-sided thyroid lumpectomy on June 17, 2021. Postoperative pathological findings revealed the presence of a clear cell tumor in the right lobe of the thyroid gland. The cut surface of the right thyroid gland exhibited a grayish-yellow area with dimensions measuring approximately 2.2 * 1.5 * 2 cm. The mass demonstrated a well-defined boundary and was encapsulated. Furthermore, a cancerous thrombus was observed within the choroid. In contrast, the mass identified in the left lobe of the thyroid gland was determined to be a nodular goiter. Immunohistochemistry (Figure 4C–H): TG(mild+), TPO(-), CK19(-), CyclinD1(+), TTF-1(-), Ki-67(+,10%), pan-CK(+), CD10 (+), CD31(-), CD34(-), EMA(-), PAX-8(+), Cal-3(-), CgA(-), P504s (+). The combination of morphological characteristics and immunohistochemical analysis provided evidence consistent with the diagnosis of metastatic clear cell renal carcinoma.

Furthermore, abdominal MRI revealed the presence of multiple blood-rich occupying lesions in the pancreas caput and pancreas cauda, indicating a high probability of neuroendocrine tumors. Given the patient's medical history and the findings from this examination, a consultation with a medical oncologist recommended that the patient be referred to the medical oncology department for further treatment. However, despite these recommendations, the patient and her family declined any

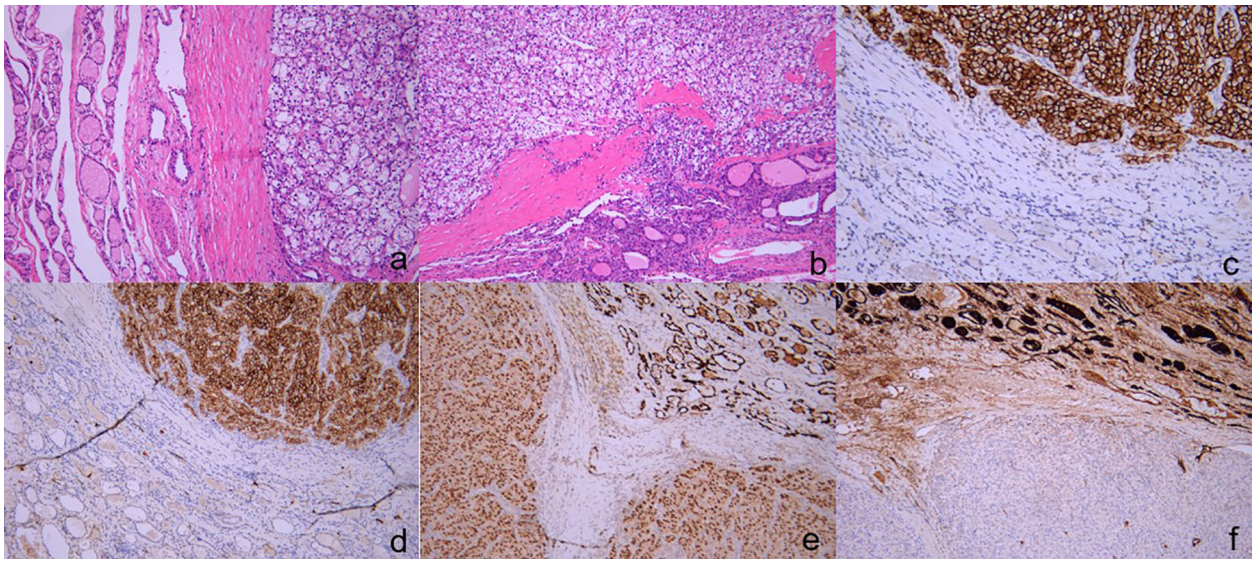

FIGURE 3
The pathology and immunohistochemical staining of thyroid specimens. The tumor tissue demonstrates a distinctive organization in nested clusters and sheets, characterized by the presence of large nuclei with intense staining. ((**A**) H&E, ×200), ((**B**) H&E, ×100). Immunohistochemical staining revealed that the tissue were positive for CA9 ((**C**) ×200)[CD10 ((**D**) ×200)[PAX-8 ((**E**) ×100), negative for TG ((**F**) ×100).

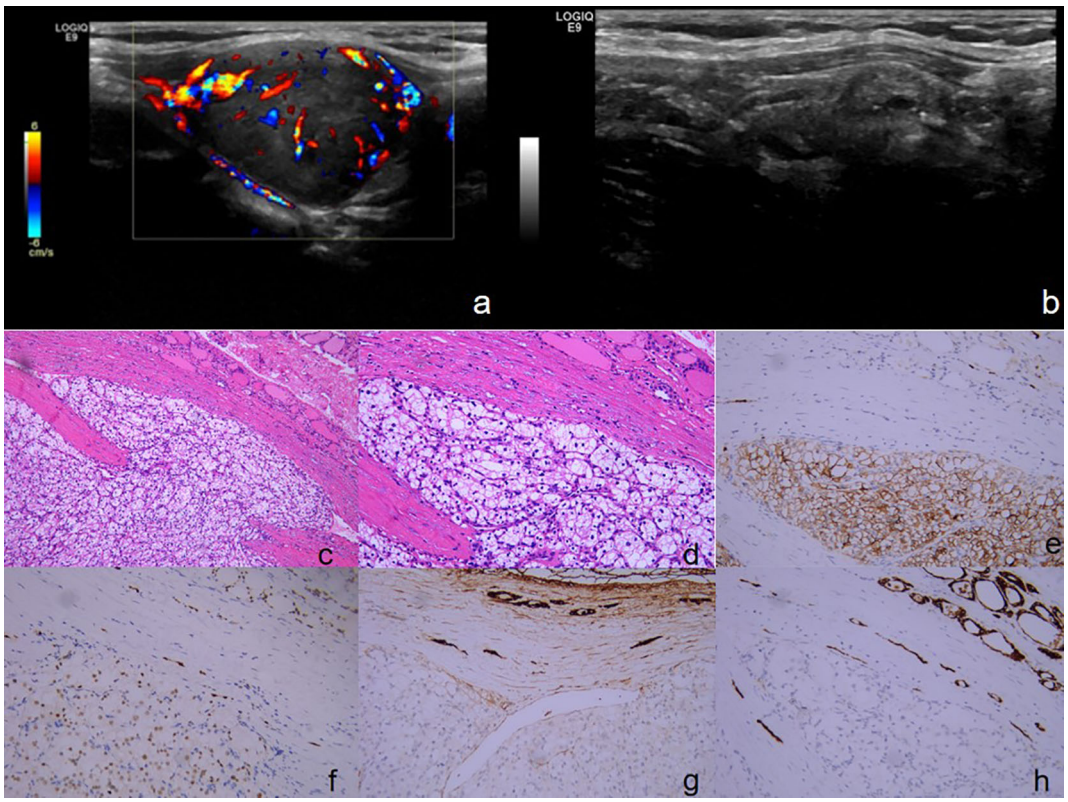

FIGURE 4
(A, B) Ultrasound of the thyroid and neck: **(A)** The largest mixed echogenic nodule in the right lobe of the thyroid gland, measuring about 27*20 mm, with clear borders, regular morphology, and showed abundant blood flow signals both within and around the area. **(B)** Multiple mixed echogenic nodules were observed in the right lobe of the thyroid gland, and some of the nodules exhibited punctate strong echoes. **(C-H)** The pathology and immunohistochemical staining of tyroid specimens. Tumor cells exhibit a growth pattern characterized by the formation of nests composed of cells with translucent cytoplasm, the nuclei of these cells are rounded, displaying varying sizes and prominent staining, with abundant interstitial blood sinuses. ((**C**) H&E, ×100), ((**D**) H&E, ×200). Immunohistochemical staining revealed that the tissue were positive for CD10 ((**E**) ×200) [PAX-8 ((**F**) ×200)[, negative for TG ((**G**) ×200)[TPO ((**H**) ×200).

therapeutic interventions. Following a satisfactory recovery, the patient was discharged from the hospital. Through a subsequent telephone follow-up, it was ascertained that the patient is currently experiencing a favorable recovery trajectory.

Discussion

This article presents a case report of two patients with thyroid metastasis originating from clear cell renal carcinoma. The clinical features, imaging findings, and treatment approaches for thyroid metastasis from renal clear cell carcinoma are discussed and summarized in the context of relevant literature (Table 1). The aim is to provide valuable insights for clinicians in the diagnosis and management of this rare condition.

Renal cell carcinoma (RCC) is a prevalent malignancy in the field of urology, representing approximately 2%-3% of adult malignant tumors. Among the various histological subtypes, clear cell renal carcinoma (ccRCC) is the predominant type, constituting approximately 70%-80% of primary renal tumors (8, 16). The onset of RCC is characterized by its subtle and indolent nature. Astonishingly, approximately 20%-30% of patients present with distant metastases upon the initial diagnosis, while an additional 30% develop heterotopic metastases even after undergoing radical surgery. Regrettably, the prognosis for metastatic kidney cancer remains disheartening, with a meager median survival of merely 2 years (17). The lungs, bones, liver, brain, and contralateral kidneys are the most frequent sites of metastasis for RCC, while other less frequently observed sites of metastasis have also been reported in isolated cases.

Despite the thyroid being an organ with abundant vascularization, the occurrence of metastatic tumors from distant sites to the thyroid is exceedingly uncommon, constituting a mere 1.4%-3% of all malignant thyroid tumors (16). Several scholars postulate that the rarity of metastatic tumors in the thyroid can be attributed to two factors. Firstly, the normal thyroid tissue is highly vascularized but lacks the capacity for cancer cell entrapment. Consequently, cancer cells find it challenging to establish a foothold in this environment. Secondly, the elevated levels of iodine and oxygen within the thyroid gland create an inhospitable milieu for tumor cell proliferation, thereby exerting a certain degree of growth inhibition (18). The median interval for the development of thyroid metastasis in renal clear cell carcinoma has been reported to be 8.7 years. However, the presence of thyroid metastases signifies an advanced stage of the primary tumor. Furthermore, a significant proportion of patients (35-80%) with thyroid involvement also exhibit metastases in multiple organs, which is associated with an unfavorable prognosis (19).

Thyroid metastases from RCC typically manifest as solitary or multiple thyroid masses. The presence and severity of symptoms such as dysphagia, dyspnea, and hoarseness depend on the size and location of the metastatic masses. In the cases presented in this study, both patients exhibited neck masses with localized lesions. However, these masses did not lead to concurrent symptoms such as dyspnea and were non-specific when compared to primary thyroid tumors.

In general, imaging studies alone are insufficient to differentiate between primary and secondary tumors of the thyroid. Debnam et al (20) reported that secondary thyroid tumors, both primary and metastatic, exhibit similar ultrasound characteristics to primary thyroid tumors. They can be classified into nodular and diffuse infiltrative changes, with nodular patterns accounting for approximately 65% of cases. Nodular secondary thyroid tumors often manifest as solid hypoechoic nodules with ill-defined margins, accompanied by hyperechoic foci and detectable blood flow signals. On the other hand, the diffuse infiltrative pattern is nonspecific and cannot be reliably distinguished from thyroiditis or other diffuse thyroid diseases. In patients with a history of ccRCC, long-term follow-up and routine thyroid ultrasound should be performed, and metastasis should be highly suspected if new thyroid nodules are detected (21). Compared to CT, PET-CT exhibits higher sensitivity in tumor diagnosis, making it an advantageous imaging modality for detecting tumor recurrence and metastasis. PET-CT provides whole-body imaging, which is particularly useful for patients with a previous history of malignant tumors. When evaluating the thyroid gland with 18F-PET-CT, the presence of a mass or diffuse uptake or infiltration should raise a high suspicion of thyroid metastasis (22). Furthermore, in the diagnosis of secondary thyroid tumors, a non-functional or "cold" nodule observed on thyroid scintigraphy can provide valuable diagnostic information (23). Given that PET-CT and scintigraphy are not standard procedures at our institution and are associated with considerable costs, both patients opted against undergoing these tests due to financial constraints.

Although fine-needle aspiration (FNA) is commonly employed in the preoperative assessment of thyroid nodules, its diagnostic accuracy for metastatic thyroid tumors, particularly from renal cell carcinoma (RCC), has certain limitations. Studies have reported a false-negative rate of up to 28.7% in the diagnosis of RCC metastases using FNA. This highlights the challenges associated with accurately identifying metastatic thyroid tumors originating from RCC through FNA alone (24). Given the patient's previous history of renal tumor and recurrence in Case 1, a preoperative ultrasound-guided fine needle aspiration (FNA) was performed on the thyroid mass. However, the cytologic results indicated follicular carcinoma of the thyroid, highlighting the limitations and uncertainty of FNA in accurately diagnosing secondary thyroid tumors. Histopathological examination using Hematoxylin and Eosin (HE) staining of postoperative resection specimens provides a basis for distinguishing between primary and secondary thyroid tumors. However, it is worth noting that identifying tumors secondary to clear cell renal carcinoma and breast carcinoma can be challenging due to their tendency to exhibit follicular glandular structures that closely resemble those composed of clear cells, which is a common occurrence in hyperplastic thyroid nodules (25). For cases where differentiation between primary and secondary thyroid tumors is challenging using HE staining alone, additional immunohistochemical staining (IHC) can be employed. IHC not only aids in distinguishing between primary and secondary thyroid tumors but also assists in identifying the origin of secondary tumors. Positive staining for markers such as thyroglobulin (Tg), calcitonin, and thyroid transcription factor (TTF-1) suggests primary thyroid tumors, while negative staining for these thyroid

TABLE 1 Cases of tumor-to-tumor metastasis from RCC to thyroid carcinoma.

Study	Age	Time interval to diagnosis of metastatic disease(year)	FNAB	Localization	Treatment	IHC
C.Gawlik et al (1)	63	1	Accepted, indeterminacy	Isthmus + Unilateral	Left thyroid lobectomy and isthmectomy	PAX-8(+),TTF-1(+)
A.Solmaz et al (2)	64	1.5	Not accepted	Unilateral	total thyroidectomy	CD10(+),Vimentin(+),TTF-1(-)
D.Macedo-Alves et al. (3)	80	9	Accepted, indeterminate	Unilateral	Hemithyroidectomy and isthmectomy	CD10(+),Vimentin(+),TTF-1(-), TG (-),chromogranin(-)
I. Chiardi et al. (4)	76	8	Accepted, suspicious	entire thyroid gland	thyroidectomy	
J. L. Shi et al. (5)	56	5			resection of thyroid metastatic renal cell carcinoma	Rcc (+), AmACR (−),vimentin (+++), CK (−), TPO (−), CK19 (−), galectim-3 (+++) and CD10 (++)
C.P.Ramírez-Plaza et al. (6)	62	Thyroid nodules as the first symptom	Accepted, indeterminate	Bilateral	total thyroidectomy with a prophylactic central compartment dissection	CD10(+),TTF-1(-),TG(-),
C.E.Connolly et al. (7)	84	Thyroid nodules as the first symptom	Not accepted	entire thyroid gland	total thyroidectomy	
F.Badawi et al. (8)	63	14	Accepted, indeterminate	Bilateral	total thyroidectomy	CD10(+), CAIX(+),galectin-3(+), vimentin(+)
M.Yamauchi et al. (9)	59	Thyroid nodules as the first symptom	Accepted, indeterminate	Unilateral	left hemithyroidectomy	CD10(+)
M. Di Furia et al. (10)	53	1	Accepted, indeterminate	Unilateral	total thyroidectomy	RCC(+),CD10(+), Vimentin(+), TTF1 (-), Thyroglobulin(-)
R.N.Hellums et al. (11)	69	10	Accepted, diagnosed	Unilateral	hemithyroidectomy	CA9(+),PAX8(+), TTF-1(+)
F. Wu et al. (12)	55	4	Accepted, indeterminate	Bilateral	total thyroidectomy+ post-operative chemotherapy	RCC(+),CD10(+),PAX-8(+), TTF1(-), Thyroglobulin(-)
M. Kefeli et al. (13)	80	18	Accepted, unreported	Unilateral	left hemithyroidectomy	PAX-8(+),CD10(+),Vimentin(+), TTF1(-),TG(-),GATA-3(-)
C. Manini et al. (14)	42	synchronic	Accepted, indeterminate	Unilateral	total thyroidectomy	PAX-8(+),CD10(+),carbonic anhydrase IX(+)
F. Medas et al. (15)	62	6	Not accepted	Unilateral	total thyroidectomy	CD10(+),TTF1(-),Hector Battifora mesothelial cell monoclonal antibody-1(-),galectin-3(-)

+: weakly positive, ++: moderately positive, +++: strongly positive, -: negative.

markers suggests secondary thyroid tumors. In the case of secondary thyroid tumors originating from renal cell carcinoma (RCC), positive staining for markers such as CD10[PAX-8/PAX-2 [CA9[CK7[vimentin can aid in the diagnosis, while GATA-3, ER, and PR, aiding in the diagnosis of breast cancer-derived tumors (26).

The management of secondary thyroid tumors encompasses various treatment modalities, including surgery, chemotherapy, and radiation therapy. Typically, distant metastases from malignant tumors do not warrant surgical intervention. However, in cases where patients present with isolated metastatic thyroid nodules, surgical treatment may offer the potential for long-term control or even cure. The 5-year overall survival rate in such cases typically ranges from 30% to 50%. Surgical resection of isolated metastatic thyroid nodules has shown promise in achieving favorable outcomes for selected patients (27). It has been posited that total thyroidectomy is recommended for patients lacking concurrent metastases from other anatomical sites, in order to optimize the management of symptoms stemming from neck metastases of RCC and achieve complete excision of metastatic lesions (28). Russell et al. (29) found that significantly improved overall survival rates among patients with secondary thyroid tumors who underwent surgical intervention as opposed to conservative treatment. The greatest surgical benefit was observed in cases of kidney cancer, with a median survival of 6 months for patients receiving conservative treatment compared to 27 months for those who underwent surgery. However, the survival benefit associated with surgery was found to be lower for tumors originating from the lung or

gastrointestinal tract, potentially due to the aggressive nature of these primary tumors. It is important to note that prompt surgical intervention is recommended when thyroid tumor patients experience compression symptoms, as it can effectively enhance their quality of life. For patients with extensive systemic metastases or thyroid metastases that cannot be completely resected, chemotherapy or radiation therapy may be considered as alternative treatment options. Compared with other metastatic tumors, RCC demonstrates limited sensitivity to chemotherapy. Therefore, the cornerstone of current RCC treatment lies in targeted therapy and immunotherapy. Among these, the targeted drug sunitinib has proven to be highly effective in the management of metastatic RCC, and the findings from the CheckMate 9ER study (30) provide compelling evidence that a combination approach involving targeted therapy with cabozantinib and immunotherapy utilizing nivolumab outperforms sunitinib in both efficacy and safety. Additionally, various alternative combination regimens are currently under investigation in clinical trials, offering promising prospects for improved prognoses among patients with metastatic RCC. RCC inherently exhibits resistance to radiotherapy, making postoperative radiotherapy generally an unadvised course of action (31). Neither of the two patients described in this article underwent postoperative adjuvant therapy, continuing treatment with sunitinib targeted therapy or immunotherapy would likely be more beneficial for them.

Both patients featured in this report developed thyroid metastases subsequent to undergoing nephrectomy surgery (Case 1 exhibited metastases nine years after the RCC diagnosis, while the precise timing of metastasis onset in Case 2 remains unknown). Both patients underwent comprehensive preoperative assessments as part of the standard protocol preceding surgery. The treatment approach adopted aligns with the established management principles for thyroid metastases originating from RCC, emphasizing surgical intervention. However, it is noteworthy that postoperative adjuvant therapy was not pursued, representing a potential area for improvement in the treatment protocol. Based on the preoperative evaluation of the cases, neither clinical presentation nor imaging modalities could effectively discriminate between primary thyroid cancer and metastatic thyroid tumors. Despite encountering a considerable number of false negatives, preoperative FNA remains indispensable in the diagnostic process, the diagnosis of metastatic thyroid tumors originating from RCC continues to depend on postoperative morphology and immunohistochemical identification. Given the current progress in Radiomics and Pathomics, we envisage the potential for training artificial intelligence (AI) models to distinguish between primary and metastatic thyroid cancer, as well as metastatic thyroid tumors, preoperatively. However, this endeavor demands a significant repository of image data sourced from imaging and pathology, underscoring the importance of enhanced collaboration among clinical researchers to facilitate data sharing for effective AI model development. In line with the cases presented in this study, the primary treatment modality for patients with thyroid metastases originating from RCC remains surgical intervention. While surgery alone can confer a degree of survival benefit, contemporary therapeutic approaches such as targeted therapy and immunotherapy have demonstrated efficacy. Enhanced outcomes may be achievable by maintaining and intensifying targeted or immunotherapeutic interventions following surgery. Further research endeavors can be directed towards identifying targets for RCC metastasis, thereby enhancing the efficacy of metastasis control strategies in RCC management.

Thyroid metastases originating from renal cell carcinoma (RCC) are infrequent in clinical practice, and the current literature mainly consists of sporadic case reports with a dearth of standardized guidelines for clinical management. Differentiating secondary thyroid tumors from primary thyroid tumors can be challenging as they lack specific clinical manifestations and imaging features. Therefore, a comprehensive evaluation of the patient's clinical presentation, medical history, and imaging findings is crucial for accurate diagnosis. Immunohistochemical staining plays a pivotal role in confirming the diagnosis. Surgical intervention is the primary treatment modality and has shown significant improvements in overall patient survival. However, further research and consensus guidelines are needed to establish a standardized approach for managing thyroid metastases from RCC. This article offers clinical practitioners valuable insights by detailing the diagnostic and treatment experiences of two patients with thyroid metastasis originating from renal cancer. Moreover, it conducts a comprehensive literature review to consolidate and critically assess the deficiencies encountered throughout the diagnostic and treatment procedures. The objective is to provide a substantive reference for healthcare professionals.

Data availability statement

The original contributions presented in the study are included in the article/supplementary material. Further inquiries can be directed to the corresponding authors.

Ethics statement

The studies involving humans were approved by Ethics Committee of Jiangxi Cancer Hospital. The studies were conducted in accordance with the local legislation and institutional requirements. The participants provided their written informed consent to participate in this study. Written informed consent was obtained from the individual(s) for the publication of any potentially identifiable images or data included in this article.

Author contributions

SX: Writing – review & editing, Writing – original draft. JX: Writing – review & editing, Writing – original draft. CY: Writing – review & editing, Writing – original draft. YZ: Writing – review & editing, Writing – original draft. LT: Writing – review & editing, Methodology. MT: Writing – review & editing, Methodology.

TY: Writing – review & editing, Supervision. ZS: Writing – review & editing, Supervision. XZ: Writing – review & editing, Supervision, Methodology.

Funding

The author(s) declare financial support was received for the research, authorship, and/or publication of this article. This work was financially supported by the National Natural Science Foundation of China (82160565, 82260565), the Youths Program of the Natural Science Foundation of Jiangxi Province (20212BAB216063), the Distinguished Young Scholars Fund of Jiangxi Cancer Hospital (2021DYS04). Jiangxi Postgraduate Innovation Fund (YC2022-s206).

Conflict of interest

The authors declare that the research was conducted in the absence of any commercial or financial relationships that could be construed as a potential conflict of interest.

Publisher's note

All claims expressed in this article are solely those of the authors and do not necessarily represent those of their affiliated organizations, or those of the publisher, the editors and the reviewers. Any product that may be evaluated in this article, or claim that may be made by its manufacturer, is not guaranteed or endorsed by the publisher.

References

1. Gawlik C, Lane J, Horattas M. Tumor-to-tumor spread: a case report and literature review of renal cell carcinoma metastasis into thyroid cancer. *World J Surg Oncol*. (2023) 21:362. doi: 10.1186/s12957-023-03220-5

2. Solmaz A, Muhammedoğlu A, Altınay S, Erçetin C, Yavuz E, Gülçiçek OB, et al. Isolated thyroid metastasis from renal cell carcinoma. *Turk J Surg*. (2017) 33(2):110–2. doi: 10.5152/TurkJSurg.

3. Macedo-Alves D, Koch P, Soares V, Gouveia P, Honavar M, Taveira-Gomes A, et al. Thyroid metastasis from renal cell carcinoma-A case report after 9 years. *Int J Surg Case Rep*. (2015) 16:59–63. doi: 10.1016/j.ijscr.2015.09.004

4. Chiardi I, Gaffuri P, Leoncini A, Trimboli P. Thyroid metastasis from renal cell carcinoma presenting as a solid mass with rapid enlargement. *Endocrinol Diabetes Metab Case Rep*. (2024) 2024. doi: 10.1530/EDM-23-0126

5. Shi JL, Zhou JQ, Li JP. Renal clear cell carcinoma with thyroid and parotid metastases: A case report. *Oncol Lett*. (2015) 10:2617–9. doi: 10.3892/ol.2015.3549

6. Ramírez-Plaza CP, Domínguez-López ME, Blanco-Reina F. Thyroid metastasis as initial presentation of clear cell renal carcinoma. *Int J Surg Case Rep*. (2015) 10:101–3. doi: 10.1016/j.ijscr.2015.03.003

7. Connolly CE. Renal cell metastasis to the thyroid gland: An emerging phenomenon. *Int J Surg Case Rep*. (2018) 45:104–6. doi: 10.1016/j.ijscr.2018.03.032

8. Badawi F, Meliti A. Tumor-to-tumor metastasis of renal cell carcinoma to a follicular variant of papillary thyroid carcinoma: A case report and literature review. *Cureus*. (2022) 14(4):e23742. doi: 10.7759/cureus.23742

9. Yamauchi M, Kai K, Shibamiya N, Shimazu R, Monji M, Suzuki K, et al. Didactic surgical experience of thyroid metastasis from renal cell carcinoma: A case report. *World J Clin cases*. (2018) 6:1018–23. doi: 10.12998/wjcc.v6.i15.1018

10. Di Furia M, Penna Della A, Salvatorelli A, Clementi M, Guadagni S. A single thyroid nodule revealing early metastases from clear cell renal carcinoma: case report and review of literature. *Int J Surg Case Rep*. (2017) 34:96–9. doi: 10.1016/j.ijscr.2017.03.020

11. Hellums RN, Kovatch KJ, Friscia ME, Schwartz TR, Pellitteri PK. Metastatic renal cell carcinoma to the thyroid with cervicothoracic venous tumor thrombosis. *Head Neck*. (2023) 45:E31–e35. doi: 10.1002/hed.27391

12. Wu F, Xia C, Hai R, Chen X, Li M, Guo Q, et al. Papillary thyroid carcinoma with clear cell renal cell carcinoma metastasized to the thyroid gland: A case report. *Oncol Lett*. (2023) 26(6):528. doi: 10.3892/ol

13. Kefeli M, Mete O. An unusual solitary thyroid nodule with bloody follicles: metastatic renal cell carcinoma within an infiltrative follicular variant papillary carcinoma. *Endocr Pathol*. (2016) 27:171–4. doi: 10.1007/s12022-016-9425-8

14. Manini C, Provenza C, Andrés L, Imaz I, Guarch R, Nunziata R, et al. Tumor-to-tumor metastases involving clear cell renal cell carcinomas: A diagnostic challenge for pathologists needing clinical correlation. *Clin Pract*. (2023) 13(1):288–96. doi: 10.3390/clinpract13010026

15. Medas F, Calò PG, Lai ML, Tuveri M, Pisano G, Nicolosi A. Renal cell carcinoma metastasis to thyroid tumor: a case report and review of the literature. *J Med Case Rep*. (2013) 7:265.

16. Xu B, Scognamiglio T, Cohen PR, Prasad ML, Hasanovic A, Tuttle RM, et al. Metastatic thyroid carcinoma without identifiable primary tumor within the thyroid gland: a retrospective study of a rare phenomenon. *Hum Pathol*. (2017) 65:133–9. doi: 10.1016/j.humpath.2017.05.013

17. Padala SA, Barsouk A, Thandra KC, Saginala K, Mohammed A, Vakiti A, et al. Epidemiology of renal cell carcinoma. *World J Oncol*. (2020) 11(3):79–87. doi: 10.14740/wjon1279

18. Correia AL. Locally sourced: site-specific immune barriers to metastasis. *Nat Rev Immunol*. (2023) p:1–17. doi: 10.1038/s41577-023-00836-2

19. Tang Q, Wang Z. Metastases to the thyroid gland: what can we do? *Cancers (Basel)*. (2022) 14(12):3017. doi: 10.3390/cancers14123017

20. Debnam JM, Kwon M, Fornage BD, Krishnamurthy S, Clayman GL, Edeiken-Monroe BS, et al. Sonographic evaluation of intrathyroid metastases. *J Ultrasound Med*. (2017) 36(1):69–76. doi: 10.7863/ultra.16.02033

21. Jia HY, Chen J, Zhai ZX, Fan WW, Yuan SJ, Liu Q, et al. Characterization of thyroid metastasis from clear cell renal cell carcinoma on ultrasonography: a report of three cases and literature review. *Eur Thyroid J*. (2023) 12(6):e230121. doi: 10.1530/ETJ-23-0121

22. Millare GG, Kwon M, Edeiken-Monroe BS, Debnam JM. (18)F-PET/CT imaging of metastasis to the thyroid gland: Imaging findings and effect on patient management. *J Solid Tumors*. (2017) 9(2):7–13. doi: 10.5430/jst.v7n2p7

23. Iesalnieks I, Trupka A, Raab M, Glockzin G, Woenckhaus M, Schlitt HJ, et al. Renal cell carcinoma metastases to the thyroid gland-8 cases reported. *Thyroid*. (2007) 17(1):49–52. doi: 10.1089/thy.2006.0176

24. Chung AY, Tran TB, Brumund KT, Weisman RA, Bouvet M. Metastases to the thyroid: a review of the literature from the last decade. *Thyroid*. (2012) 22(3):258–68. doi: 10.1089/thy.2010.0154

25. Straccia P, Mosseri C, Brunelli C, Rossi ED, Lombardi CP, Pontecorvi A, et al. Diagnosis and treatment of metastases to the thyroid gland: a meta-analysis. *Endocr Pathol*. (2017) 28(2):112–20. doi: 10.1007/s12022-017-9475-6

26. Tan PH, Cheng L, Rioux-Leclercq N, Merino MJ, Netto G, Reuter VE, et al. Renal tumors: diagnostic and prognostic biomarkers. *Am J Surg Pathol*. (2013) 37(10):1518–31. doi: 10.1097/PAS.0b013e318299f12e

27. Khaddour K, Marernych N, Ward WL, Liu J, Pappa T. Characteristics of clear cell renal cell carcinoma metastases to the thyroid gland: A systematic review. *World J Clin cases*. (2019) 7(21):3474–85. doi: 10.12998/wjcc.v7.i21.3474

28. Tjahjono R, Phung D, Gurney H, Gupta R, Riffat F, Palme CE. Thyroid gland metastasis from renal cell carcinoma: a case series and literature review. *ANZ J Surg*. (2021) 91(4):708–15. doi: 10.1111/ans.16482

29. Russell JO, Yan K, Burkey B, Scharpf J. Nonthyroid metastasis to the thyroid gland: case series and review with observations by primary pathology. *Otolaryngol Head Neck Surg*. (2016) 155(6):961–8. doi: 10.1177/0194599816655783

30. Cella D, Motzer RJ, Suarez C, Blum SI, Ejzykowicz F, Hamilton M, et al. Patient-reported outcomes with first-line nivolumab plus cabozantinib versus sunitinib in patients with advanced renal cell carcinoma treated in CheckMate 9ER: an open-label, randomised, phase 3 trial. *Lancet Oncol*. (2022) 23(2):292–303. doi: 10.1016/S1470-2045(21)00693-8

31. Navani V, Heng DY. Treatment selection in first-line metastatic renal cell carcinoma—the contemporary treatment paradigm in the age of combination therapy: a review. *JAMA Oncol*. (2022) 8:292–9. doi: 10.1001/jamaoncol.2021.4337

frontiers | Frontiers in Oncology

TYPE Original Research
PUBLISHED 10 May 2024
DOI 10.3389/fonc.2024.1395273

Check for updates

OPEN ACCESS

EDITED BY
Dragos Eugen Georgescu,
Carol Davila University of Medicine and Pharmacy, Romania

REVIEWED BY
Zsuzsanna Lengyel,
University of Pécs, Hungary
Teodor Florin Georgescu,
Carol Davila University of Medicine and Pharmacy, Romania
Iuliana Pantelimon,
Carol Davila University of Medicine and Pharmacy, Romania

*CORRESPONDENCE
Jianqiang Yang
yjq@zjhu.edu.cn

RECEIVED 03 March 2024
ACCEPTED 25 April 2024
PUBLISHED 10 May 2024

CITATION
Chen X, Hao Y, Chou M and Yang J (2024) Epidemiology of the non-head and neck sebaceous carcinoma and implications for distant metastasis screening.
Front. Oncol. 14:1395273.
doi: 10.3389/fonc.2024.1395273

COPYRIGHT
© 2024 Chen, Hao, Chou and Yang. This is an open-access article distributed under the terms of the Creative Commons Attribution License (CC BY). The use, distribution or reproduction in other forums is permitted, provided the original author(s) and the copyright owner(s) are credited and that the original publication in this journal is cited, in accordance with accepted academic practice. No use, distribution or reproduction is permitted which does not comply with these terms.

Epidemiology of the non-head and neck sebaceous carcinoma and implications for distant metastasis screening

Xi Chen, Yangyang Hao, Mengwei Chou and Jianqiang Yang*

Department of Dermatology, The First People's Hospital of Huzhou, Huzhou, Zhejiang, China

Introduction: Extraocular sebaceous carcinoma (SC), particularly those outside the head and neck region, is rare and not well-described.

Purpose: This study aimed to explore the epidemiology and identify the prognostic factors of non-head and neck SC, describe the possible relevant factors of distant metastasis, and provide implications for distant metastasis screening.

Methods: Data from the 17 registries in the Surveillance, Epidemiology, and End Results database were retrospectively collected for patients with SC outside the head and neck from 2000 through 2020. Overall survival (OS) and disease-specific survival (DSS) were the primary endpoints. Survival analysis was conducted through Kaplan–Meier curves, and multivariate analysis was carried out using Cox proportional hazard models.

Results: A total of 1,237 patients with SC outside the head and neck were identified. The mean age at diagnosis of the entire patient cohort was 67.7 years (30 to 90+ years), and the mean tumor size was 2.2 cm (0.1–16 cm). Patients with distant disease experienced the lowest OS (mean, 29.5 months) than those with localized disease and regional disease ($p < 0.0001$). Multivariate analysis revealed that age, tumor size, and stage were independent determinants of OS; age, stage, and primary site were independent determinants of DSS. Tumor grade and lymph node status had less prognostic value for survival. Undifferentiated tumors have a trend toward distant metastasis, especially those at the primary site of the trunk.

Conclusion: The prognosis of the non-head and neck SC is excellent, while the survival of distant disease is very poor. Distant metastasis screening can be considered for undifferentiated tumors, especially those located in the trunk region with large tumor sizes.

KEYWORDS

sebaceous carcinoma, non-head and neck, distant metastasis, SEER, overall survival, disease-specific survival

Introduction

Sebaceous carcinoma (SC) is a rare cutaneous malignancy that arises from the sebaceous gland, one of the adnexal structures of the skin (1). SC most commonly affects the head and neck, especially the periocular region; moreover, it can occur in many other locations of the body, such as the external genitalia, trunk, and extremities (2). Sebaceous carcinoma is generally considered indolent, but there is also the possibility of local infiltration and distant metastasis (3). Guidelines for the management of SC, including screening and identification for distant metastasis, are currently scarce.

Given the low incidence of SC outside the head and neck, most of the records are limited to case reports with short follow-ups. The epidemiology regarding this malignancy is thus scanty. To date, this study presents the largest population-based multivariate analysis to determine prognostic factors for patients diagnosed with SC, specifically outside the head and neck via the Surveillance, Epidemiology, and End Results (SEER) program database. Moreover, this analysis provides important counseling value about distant metastasis screening for non-head and neck SC in clinical practice.

Methods

Patient selection

The SEER database's 17 registries were queried for patients diagnosed with SC outside the head and neck between the years 2000 and 2020. The right to access these data through SEER Stat software was granted by the National Cancer Institute upon submission of a signed SEER data use agreement. This population-based database contains comprehensive data on cancer survival and is updated annually by the National Cancer Institute. It comprises 26% of the population in 17 geographic regions of the USA. Patients diagnosed with SC outside the head and neck were identified using the International Classification of Diseases for Oncology (ICD-O) histologic code 8410/3 (sebaceous carcinoma) and site-specific codes C44.5 (skin of trunk), C44.6 (skin of upper limb and shoulder), C44.7 (skin of lower limb and hip), C51.0 (labium majus), C51.1 (labium minus), C51.9 (vulva, NOS), C60.2 (body of penis), C60.9 (penis, NOS), and C63.2 (scrotum, NOS).

Variables

The following primary data were extracted for analysis: sex, age at diagnosis, race, primary site, tumor size, lymph node involvement (yes/no), tumor grade (well differentiated, moderately differentiated, poorly differentiated, and undifferentiated), stage (localized, regional, and distant), cause of death, survival months, and vital status. Tumor grade was categorized as low (well to moderately differentiated) or high (poorly differentiated or undifferentiated). Race was grouped into three categories, including white, black, and others (American Indian/Alaska Native, Asian, or Pacific Islander). For the purpose of analysis, the continuous variables age and tumor size were transformed into categorical variables. Age was presented as four subgroups (years): ≤ 60, 61–70, 71–80, or > 80, and tumor size was categorized into three subgroups (cm): ≤ 2, 2–4, or > 4. In addition, the anatomic location of C51.0, C51.1, C51.9, C60.2, C60.9, and C63.2 were reclassified as external genitalia. Treatment modality was initially collected but was not reported due to large deficiencies in radiotherapy data.

Statistical analysis

The primary endpoints were defined as the time in months from diagnosis to death from any cause for overall survival (OS) and as the time from diagnosis to a documented death due to SC for disease-specific survival (DSS). Kaplan–Meier survival analysis was conducted to assess the impact of various variables on OS and DSS, and the statistical difference in curves was calculated by log-rank tests. All clinically significant variables or covariates with a log-rank $p < 0.2$ on univariate analysis were chosen for multivariate analysis. Through Cox proportional hazard models, multivariate analysis was performed to identify prognostic factors. All statistical analyses were carried out using SPSS version 26.0. Statistical significance in this study was set at two-sided $p < 0.05$.

Results

Baseline characteristics

A total of 1,237 patients diagnosed with SC outside the head and neck from 2000 through 2020 were identified and included in the analysis. The demographics and clinicopathologic characteristics are listed in Table 1. There was a predominance of men (66.5%) and whites (91.2%). The mean and median ages at diagnosis of the entire patient cohort were 67.7 years and 68 years, ranging from 30 to 90+ years (90+ is regarded as 90 in statistical analysis). Among the patients with known tumor stage and grade, 96.2% had localized disease, and 79.1% presented with low-grade features. Precise tumor sizes were acquired for 548 cases (mean, 2.2 cm), of which 33% have diameters greater than 2 cm with a maximum size of 16 cm. The mean tumor size of patients with distant metastasis was 7 cm (range, 2–15.5 cm). The overall rate of lymph node involvement was 1.2%. In this cohort, the most common primary site was the trunk (65%), followed by the upper limb and shoulder (23.8%), the lower limb and hip (7.6%), and the external genitalia (3.6%).

Survival analysis by sex, race, and age

No statistical significance of survival analysis in OS and DSS was reached with regard to gender and race ($p > 0.05$). This cohort spanned a wide age range, from 30 to 90+, and cases were relatively evenly distributed across the four age subgroups (≤ 60, 61–70, 71–80, > 80). OS decreased as age increased ($p < 0.0001$), and patients over 80 years of age had significantly worse DSS than other age groups ($p < 0.001$) (Figure 1).

TABLE 1 The demographics and clinicopathologic characteristics of patients diagnosed with sebaceous carcinoma outside the head and neck.

Characteristics	*N* (%)
Age (years)	
≤ 60	379 (30.6%)
61–70	329 (26.6%)
71–80	296 (23.9%)
> 80	233 (18.8%)
Sex	
Male	822 (66.5%)
Female	415 (33.5%)
Race	
White	1,073 (91.2%)
Black	48 (4.1%)
Others	56 (4.8%)
Tumor size (cm)	
≤ 2	367 (67.0%)
2–4	114 (20.8%)
>4	67 (12.2%)
Primary site	
Trunk	804 (65.0%)
Upper limb and shoulder	294 (23.8%)
Lower limb and hip	94 (7.6%)
External genitalia	45 (3.6%)
Grade	
Low (well to moderately differentiated)	257 (79.1%)
High (poorly differentiated or undifferentiated)	68 (20.9%)
Summary stage	
Localized	876 (96.2%)
Regional	20 (2.2%)
Distant	15 (1.6%)
Lymph node involvement	
Yes	10 (1.2%)
No	852 (98.8%)

Survival analysis by tumor stage and grade at diagnosis

Survival analysis from Kaplan–Meier curves revealed statistical significance in the tumor stage (Figure 1). In this study, 911 cases with a known SEER stage were available, and only 15 patients had distant disease (1.6%), experiencing the lowest 5-year OS of 21.8% (mean OS, 29.5 months). Of the 15 patients with distant disease, seven had specific tumor grades, and most (six of seven) were characterized by poorly differentiated or undifferentiated histological morphology. Patients with localized disease had statistically better DSS than those with regional disease and distant disease ($p < 0.0001$). In addition, patients with low-grade tumors experienced better survival than those with high-grade tumors, regardless of OS ($p = 0.012$) or DSS ($p < 0.0001$) (Figure 1).

Survival analysis by tumor size, anatomic site, and lymph node status

Smaller tumor size (≤ 2 cm) at presentation was associated with better OS than greater tumor size (2–4 cm and > 4 cm) ($p < 0.0001$). In addition, patients with tumors larger than 4 cm had the worst DSS ($p = 0.02$) (Figure 2). No significant difference in OS was found among anatomic sites ($p = 0.174$), while SC located on the external genitalia had worse DSS than those of other sites ($p = 0.013$) (Figure 2). Notably, patients with lymph node involvement had significantly worse DSS than those without lymph node involvement ($p < 0.0001$). On the contrary, lymph node involvement or not had less prognostic value in OS ($p = 0.089$) (Figure 2).

Multivariate analyses on OS and DSS

Tables 2, 3 show the multivariate analyses of OS and DSS, respectively. Increasing age and tumor size were independent and significant predictors of worse OS ($p < 0.0001$). Moreover, the SEER stage at "distant" increased the risk of overall mortality than those at "localized" (HR, 6.97 [95% CI, 3.71–13.10]). Age at "71–80 years" (HR, 3.02 [95% CI, 1.32–6.93]) and "80+ years" (HR, 4.89 [95% CI, 2.10–11.37]) had worse DSS than those ≤ 60 years. Compared to patients with localized disease, patients with distant disease experienced significantly higher DSS (HR, 23.62 [95% CI, 6.68–83.49]). In addition, the primary site was a statistically significant predictor of DSS, and the SC located on the external genitalia had a 3.3 times greater risk of death than those on the trunk.

Discussion

SC is a kind of cutaneous adnexal carcinoma with low incidence, accounting for less than 1% of all malignant cutaneous neoplasms (4). Although SC most commonly involves the head and neck, especially the periocular area, it can occur anywhere sebaceous glands are located.

The precise etiology of SC is not well elucidated, but several factors have been implicated with an increased risk of development. Some cases are associated with inherited mutations in mismatch repair genes, such as Muir–Torre Syndrome (MTS), a form of Lynch syndrome, with microsatellite instability and cancer

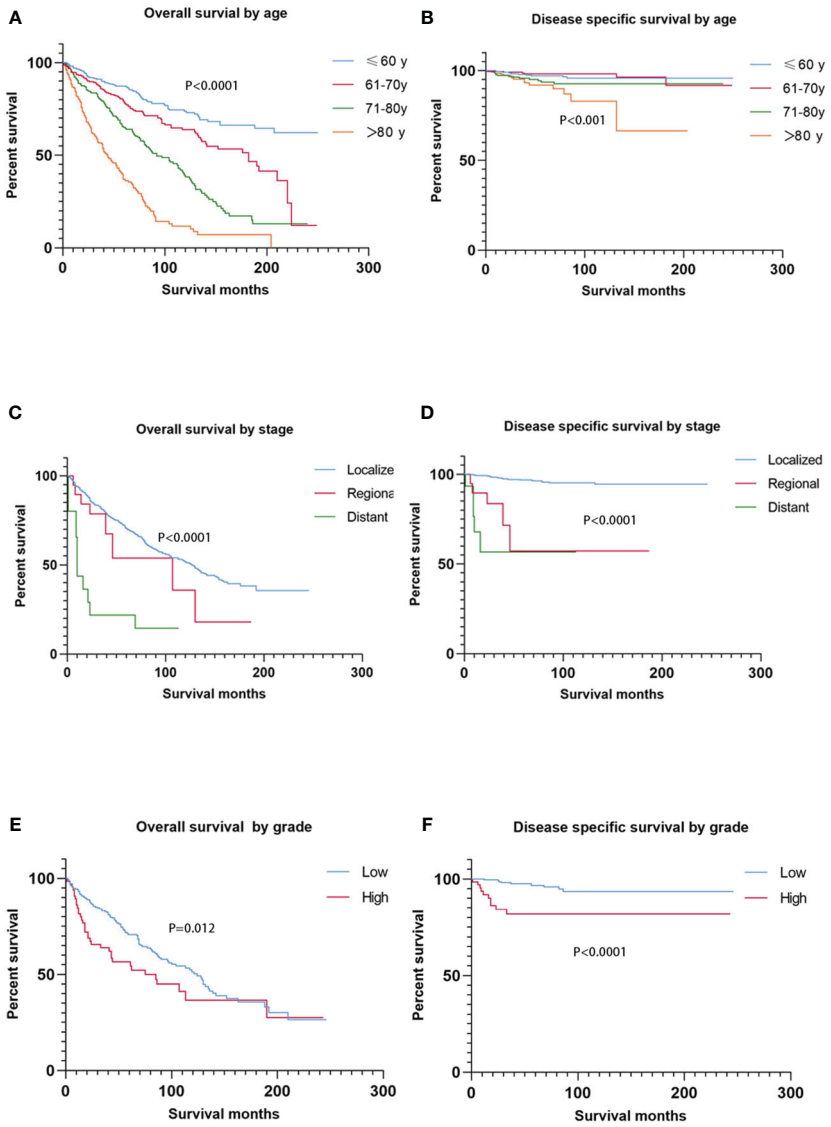

FIGURE 1
Kaplan–Meier estimates of OS and DSS by age, stage, and grade. OS decreased as age increased **(A)**, and patients over 80 years had significantly worse DSS than other age groups **(B)**. Patients with distant disease experienced the lowest OS **(C)**, and patients with localized disease experienced the best DSS **(D)**. Regarding grade, patients with high differentiation had better OS and DSS than those with low differentiation **(E, F)**. OS, overall survival; DSS, disease-specific survival.

tendency (5, 6). In MTS, SC can occur concurrently with other cutaneous malignancies (keratoacanthomas) and internal malignancies (colorectal and genitourinary cancers), and, thus, additional screening workup is indicated (7). SC tends to affect older individuals, and the mean age of non-head and neck SC in this analysis was 67.7 years (8). However, SC may also present in younger patients, and the minimum age was 30 years in this cohort. For these patients, early screening for genetic mutations is important. Additionally, UV-light exposure is considered another risk factor in the development of SC (9). In this study, 96.4% of tumors involved sun-exposed skin of the trunk and extremities, and 91.2% of cases were diagnosed in whites, who were more susceptible to UV-induced damage. Sebaceous carcinoma exhibits a slight male preponderance, which was further confirmed in this analysis, with a male-to-female ratio of 1.98 (5). Moreover, prior radiation therapy and immunosuppression contribute to the development of SC (10–12).

Extraocular SC usually presents as an ulcerated yellowish nodule, resembling nonmelanoma skin cancers such as squamous cell carcinoma and basal cell carcinoma (13). Moreover, extraocular SC can also imitate benign conditions, including molluscum contagiosum, sebaceous cyst, pyogenic granuloma, or keratoacanthoma (14–16). Due to delayed visit and diagnosis and the large extension space for SC outside the head and neck, the tumor size tends to be large, with a mean of 2.2 cm in this analysis. Notably, histopathological examination, immunohistochemistry, and dermoscopic images may help detect SC and distinguish it from other easily confused diseases (17).

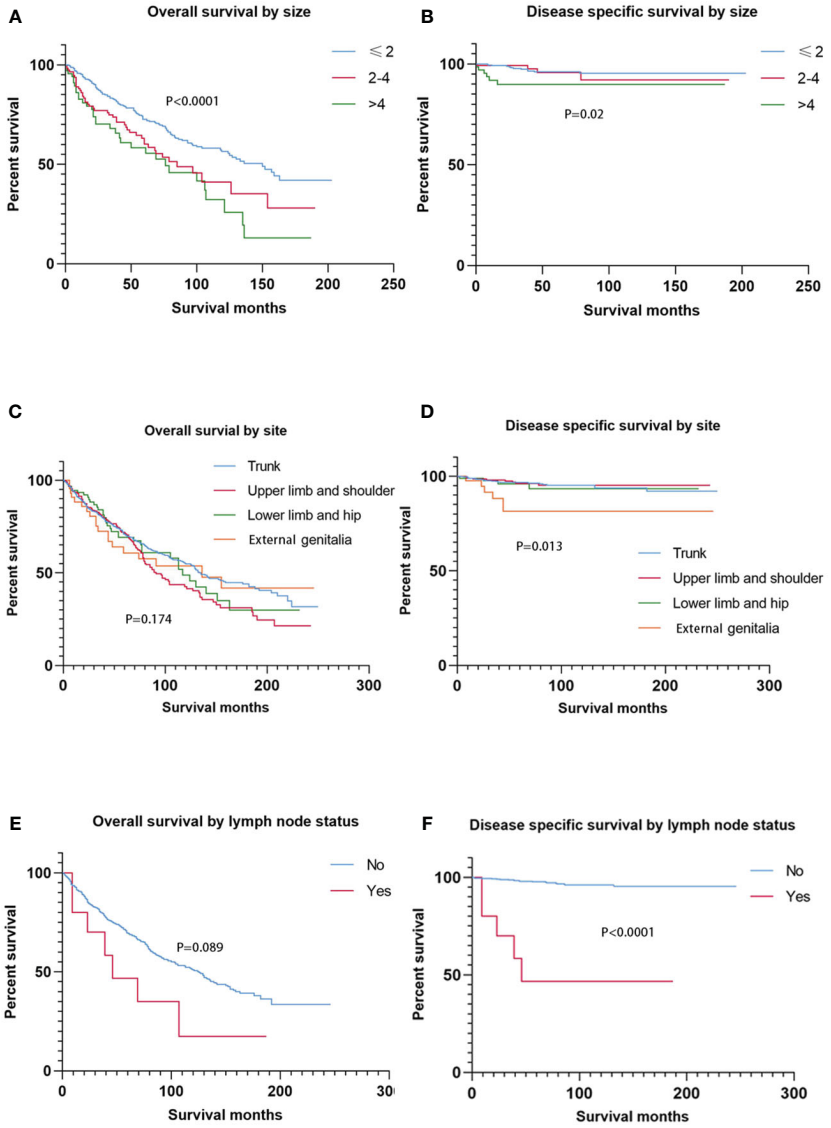

FIGURE 2
Kaplan–Meier estimates of OS and DSS by tumor size, primary site, and node status. Patients with tumors ≤ 2 cm had better OS than those with tumors > 2 cm (2–4 cm and > 4 cm), and patients with tumors > 4 cm had the worst DSS **(A, B)**. The primary site had no prognostic value for OS, while SC located on the external genitalia had worse DSS than those of other sites. There was no significant difference in OS between node-negative cases and node-positive cases, while node-positive cases experienced higher DSS than node-negative cases. OS, overall survival; DSS, disease-specific survival; SC, sebaceous carcinoma.

SC is usually indolent and with low-stage presentation. Nevertheless, there were cases of aggressive behavior and metastasis represented in the literature (18, 19). The metastasis rate was 1.6% in this cohort, and the 5-year OS was worse at 21.8%. Of 288 patients with a specific tumor grade, only eight were undifferentiated (2.8%), developing in the trunk (n = 5) and limbs (n = 2). Among undifferentiated carcinoma, three cases had distant disease, and all occurred in the trunk region. Therefore, there was a high incidence of distant metastasis in undifferentiated diseases (three of eight), especially those located in the trunk (three of five). In addition, patients with distant disease had a relatively large tumor size, a mean of 7 cm, ranging from 2 to 15.5 cm. It was concluded that although there were no distinct guidelines concerning systemic evaluation of SC, patients with undifferentiated disease, especially those in the trunk region, simultaneously with large tumors, may benefit from CT or MRI imaging to detect metastasis.

SC of the external genitalia is extremely rare, taking up 3.7% of the cohort. Multivariate analysis showed that SC on the external genitalia had a poorer outcome than those on the trunk, with a 3.3-fold increased risk of DSS, which indicated that the clinicopathologic behavior of SC on the external genitalia appeared different from other extraorbital sites. Notably, lymph node involvement and tumor grade have not been described as independent prognostic factors for SC outside the head and neck in this analysis.

Our study does have some shortcomings. Several variables, such as surgical modalities, histological types, metastatic sites, infiltration depth, genetic factors, tumor recurrence, and the time interval from

TABLE 2 Multivariate analyses of overall survival for nonhead and neck sebaceous carcinoma.

Characteristics	HR	95% CI	*p*-value
Age			
≤ 60	Reference		
61–70	1.89	1.40–2.55	0.000
71–80	3.76	2.83–5.00	0.000
> 80	8.37	6.27–11.19	0.000
Tumor size (cm)			
≤ 2	Reference		
2–4	1.93	1.37–2.71	0.000
> 4	2.87	1.88–4.39	0.000
Primary site			
Trunk	Reference		
Upper limb and shoulder	1.17	0.95–1.45	0.143
Lower limb and shoulder	0.99	0.69–1.40	0.934
External genitalia	0.95	0.60–1.50	0.816
Summary stage			
Localized	Reference		
Regional	1.16	1.16–0.44	0.763
Distant	6.97	3.71–13.10	0.000
Grade			
Low (well to moderately differentiated)	Reference		
High (poorly differentiated or undifferentiated)	1.10	0.73–1.65	0.647
Lymph node involvement			
No	Reference		
Yes	0.58	0.205–1.65	0.310

TABLE 3 Multivariate analyses of disease-specific survival for nonhead and neck sebaceous carcinoma.

Characteristics	HR	95% CI	*p*-value
Age			
≤ 60	Reference		
61–70	1.37	0.52–3.56	0.524
71–80	3.02	1.32–6.93	0.009
> 80	4.89	2.10–11.37	0.000
Tumor size (cm)			
≤ 2	Reference		
2–4	1.93	0.43–3.82	0.659
> 4	1.07	0.31–3.65	0.913
Primary site			
Trunk	Reference		
Upper limb and shoulder	0.80	0.38–1.71	0.571
Lower limb and hip	1.17	0.40–3.42	0.775
External genitalia	3.32	1.34–8.26	0.010
Summary stage			
Localized	Reference		
Regional	4.29	0.96–19.14	0.056
Distant	23.62	6.68–83.49	0.000
Grade			
Low (well to moderately differentiated)	Reference		
High (poorly differentiated or undifferentiated)	2.35	0.84–6.60	0.104
Lymph node involvement			
No	Reference		
Yes	2.63	0.61–11.28	0.19

onset of symptoms to diagnosis were not attained from the SEER database for further research. In addition, there was a large amount of missing data on the administration of radiation therapy and lymph node metastasis that may introduce a particular bias. Furthermore, the data included in this study were retrospective, and the conclusions drawn from this study still need to be verified by more high-quality clinical studies.

Despite the above limitations, this population-based study represents the first large-scale analysis of non-head and neck SC and provides significant insight into distant metastasis screening.

Conclusion

This study conducted a comprehensive analysis of patients with non-head and neck SC from a well-defined population. Tumors located in these areas may grow to large sizes. In general, non-head and neck SC have a great prognosis, but survival becomes very poor once distant metastasis occurs. Patients with undifferentiated disease, especially those in the trunk region, are suggested to complete screening for distant metastasis.

Data availability statement

The raw data supporting the conclusions of this article will be made available by the authors, without undue reservation.

Ethics statement

Ethical approval was not required for the study involving humans in accordance with the local legislation and institutional requirements. Written informed consent to participate in this study

was not required from the participants or the participants' legal guardians/next of kin in accordance with the national legislation and the institutional requirements.

Author contributions

XC: Writing – original draft, Software, Investigation, Conceptualization. YH: Writing – review & editing. MC: Writing – review & editing. JY: Writing – review & editing, Supervision.

Funding

The author(s) declare that no financial support was received for the research, authorship, and/or publication of this article.

Conflict of interest

The authors declare that the research was conducted in the absence of any commercial or financial relationships that could be construed as a potential conflict of interest.

Publisher's note

All claims expressed in this article are solely those of the authors and do not necessarily represent those of their affiliated organizations, or those of the publisher, the editors and the reviewers. Any product that may be evaluated in this article, or claim that may be made by its manufacturer, is not guaranteed or endorsed by the publisher.

References

1. Goyal A, Marghitu T, Goyal N, Rubin N, Patel K, Goyal K, et al. Surgical management and lymph-node biopsy of rare Malignant cutaneous adnexal carcinomas: a population-based analysis of 7591 patients. *Arch Dermatol Res*. (2021) 313:623–32. doi: 10.1007/s00403–020-02143–5

2. Dasgupta T, Wilson LD, Yu JB. A retrospective review of 1349 cases of sebaceous carcinoma. *Cancer*. (2009) 115:158–65. doi: 10.1002/cncr.23952

3. Martinez SR, Barr KL, Canter RJ. Rare tumors through the looking glass: an examination of Malignant cutaneous adnexal tumors. *Arch Dermatol*. (2011) 147:1058–62. doi: 10.1001/archdermatol.2011.229

4. Ghosh SK, Bandyopadhyay D, Gupta S, Chatterjee G, Ghosh A. Rapidly growing extraocular sebaceous carcinoma occurring during pregnancy: a case report. *Dermatol Online J*. (2008) 14:8. doi: 10.5070/D361R8G620

5. Lazar AJ, Lyle S, Calonje E. Sebaceous neoplasia and Torre-Muir syndrome. *Curr Diagn Pathol*. (2007) 13:301–19. doi: 10.1016/j.cdip.2007.05.001

6. Everett JN, Raymond VM, Dandapani M, Marvin M, Kohlmann W, Chittenden A, et al. Screening for germline mismatch repair mutations following diagnosis of sebaceous neoplasm. *JAMA Dermatol*. (2014) 150:1315–21. doi: 10.1001/jamadermatol.2014.1217

7. Entius MM, Keller JJ, Drillenburg P, Kuypers KC, Giardiello FM, Offerhaus GJ. Microsatellite instability and expression of hMLH-1 and hMSH-2 in sebaceous gland carcinomas as markers for Muir-Torre syndrome. *Clin Cancer Res*. (2000) 6:1784–9.

8. Tripathi R, Chen Z, Li L, Bordeaux JS. Incidence and survival of sebaceous carcinoma in the United States. *J Am Acad Dermatol*. (2016) 75:1210–5. doi: 10.1016/j.jaad.2016.07.046

9. Sargen MR, Mai ZM, Engels EA, Goldstein AM, Tucker MA, Pfeiffer RM, et al. Ambient ultraviolet radiation and sebaceous carcinoma incidence in the United States, 2000–2016. *JNCI Cancer Spectr*. (2020) 4:pkaa020. doi: 10.1093/jncics/pkaa020

10. Lanoy E, Dores GM, Madeleine MM, Toro JR, Fraumeni JF Jr, Engels EA. Epidemiology of nonkeratinocytic skin cancers among persons with AIDS in the United States. *AIDS*. (2009) 23:385–93. doi: 10.1097/QAD.0b013e3283213046

11. Sargen MR, Cahoon EK, Lynch CF, Tucker MA, Goldstein AM, Engels EA. Sebaceous carcinoma incidence and survival among solid organ transplant recipients in the United States, 1987–2017. *JAMA Dermatol*. (2020) 156:1307–14. doi: 10.1001/jamadermatol.2020.3111

12. Kivelä T, Asko-Seljavaara S, Pihkala U, Hovi L, Heikkonen J. Sebaceous carcinoma of the eyelid associated with retinoblastoma. *Ophthalmology*. (2001) 108:1124–8. doi: 10.1016/s0161–6420(01)00555–3

13. Owen JL, Kibbi N, Worley B, Kelm RC, Wang JV, Barker CA, et al. Sebaceous carcinoma: evidence-based clinical practice guidelines. *Lancet Oncol*. (2019) 20:e699–714. doi: 10.1016/S1470–2045(19)30673–4

14. Sindhura M, Santosh T, Kumar JR, Shankaralingappa A, Pannerselvam NK, Balakrishna P. Extra-ocular sebaceous carcinoma - A rare case report. *Indian J Pathol Microbiol*. (2024) 67:169–71. doi: 10.4103/ijpm.ijpm_860_21

15. Pearl K, Zielinski P, Zaragoza BJ. Extra-ocular sebaceous carcinoma unveiled: A case study of dermal challenges in an elderly african american patient. *Cureus*. (2024) 16:e51934. doi: 10.7759/cureus.51934

16. Knackstedt T, Samie FH. Sebaceous carcinoma: A review of the scientific literature. *Curr Treat Options Oncol*. (2017) 18:47. doi: 10.1007/s11864–017-0490–0

17. Dowell-Esquivel C, Lee R, DiCaprio RC 3rd, Nouri K. Sebaceous carcinoma: an updated review of pathogenesis, diagnosis, and treatment options. *Arch Dermatol Res*. (2023) 316:55. doi: 10.1007/s00403–023-02747–7

18. Jaiswal LS, Neupane D, Lagegu N, Khadka S, Sah B, Pradhan A. Sebaceous carcinoma of trunk with bilateral axillary lymph node metastasis: a rare presentation of Malignant adnexal tumor in young adult. *J Surg Case Rep*. (2022) 2022:rjac280. doi: 10.1093/jscr/rjac280

19. Kwon BS, Chung EH, Kim JW. A recurrent case of extraocular sebaceous carcinoma with distant organ metastasis. *Arch Craniofac Surg*. (2021) 22:56–61. doi: 10.7181/acfs.2020.00675

frontiers | Frontiers in Oncology

TYPE Case Report
PUBLISHED 13 May 2024
DOI 10.3389/fonc.2024.1366546

Check for updates

OPEN ACCESS

EDITED BY
Dragos Eugen Georgescu,
Carol Davila University of Medicine and Pharmacy, Romania

REVIEWED BY
Octav Ginghina,
Carol Davila University of Medicine and Pharmacy, Romania
Adelina Silvana Gheorghe,
Carol Davila University of Medicine and Pharmacy, Romania
Iuliana Pantelimon,
Carol Davila University of Medicine and Pharmacy, Romania

*CORRESPONDENCE
Songjie Shen
shensj@pumch.cn

†These authors have contributed equally to this work and share first authorship

RECEIVED 06 January 2024
ACCEPTED 25 April 2024
PUBLISHED 13 May 2024

CITATION
Deng Z, Xia C, Li Y, Luo Y and Shen S (2024) Myofibroblastic sarcoma in breast: a case report and literature review. *Front. Oncol.* 14:1366546. doi: 10.3389/fonc.2024.1366546

COPYRIGHT
© 2024 Deng, Xia, Li, Luo and Shen. This is an open-access article distributed under the terms of the Creative Commons Attribution License (CC BY). The use, distribution or reproduction in other forums is permitted, provided the original author(s) and the copyright owner(s) are credited and that the original publication in this journal is cited, in accordance with accepted academic practice. No use, distribution or reproduction is permitted which does not comply with these terms.

Myofibroblastic sarcoma in breast: a case report and literature review

Zixi Deng[1†], Chuan Xia[2†], Yuechong Li[1], Yongchao Luo[1] and Songjie Shen[1*]

[1]Department of Breast Surgery, Peking Union Medical College Hospital, Peking Union Medical College, Chinese Academy of Medical Sciences, Beijing, China, [2]Department of Pathology, Peking Union Medical College Hospital, Chinese Academy of Medical Sciences and Peking Union Medical College, Beijing, China

Myofibroblastic sarcoma is a malignancy in which myofibroblasts are the main component, with a very low incidence. In this study, we report a case of low-grade myofibroblastic sarcoma (LGMS) in the breast. After the diagnosis of LGMS, the patient received a mastectomy. The patient showed no relapse or progression during the follow-up time of 3 months following the operation. LGMS in the breast is extremely rare, and the limited experience with its diagnosis and treatment brings obstacles to doctors. Therefore, this report summarizes the preoperative diagnosis, treatment, and prognosis of breast LGMS through a literature review.

KEYWORDS

myofibroblastic sarcoma, myofibrosarcoma, breast, myofibroblast, immunohistochemistry

1 Introduction

Myofibroblasts are primarily found in reactive granulation tissue, they are generally secondary components of malignancies, reflecting the response of the host stromal tissue to malignant cells. However, malignancies in which myofibroblasts are the main component are rare (1). Low-grade myofibroblastic sarcoma (LGMS) was first reported by Mentzel et al. in a case series of 18 cases in 1998, and it was classified as a distinct type of soft-tissue tumor by the World Health Organization in 2002 (2, 3). LGMS mainly occurs in the head and neck but can also occur in the bones, trunk, limbs, retroperitoneal, and other parts, LGMS in the breast is extremely rare (4–6). About 20 patients with LGMS of the breast have been previously reported in the literature. In this report, we report a rare case of breast LGMS. The patient underwent a right mastectomy, and no recurrence or metastasis has been found so far.

2 Case presentation

A 54-year-old woman found a palpable, non-tender mass of the right breast, which she first noted on self-examination 9 months earlier. She denied any nipple discharge, itching, skin redness, and swelling of her breast. She underwent a right breast mass excision in July 2019, and the biopsy was fibroadenoma. She had no family history of breast cancer. On physical examination, a 1.5cm nodule was palpable at the 5 o'clock position of the right breast, with the obscured margin and the local skin retraction (Figure 1). There was no evidence of lymphadenopathy. Her laboratory tests are normal, and the tumor marker showed no abnormalities. Ultrasound reported a 1.5 ×0.9×1.0cm hypoechoic irregular mass located in the 5 o'clock position of the breast with a surgical scar on the skin. The aspect ratio of the node was greater than 1, and no clear blood flow signal was seen (Figure 2A). A mammogram confirmed the presence of a mass in the inner lower quadrant of the right breast (Figures 2B, C). Ultrasound-guided core biopsy of the lesion revealed a low-grade malignant spindle cell tumor with necrosis and peripheral lymphocyte infiltration. She underwent a right mastectomy on July 06, 2023. The patient's postoperative recovery was uneventful, and she was discharged home after three days. Examination of the resected specimens revealed 1.8cm gray and white nodules with unclear boundaries. Under hematoxylin-eosin (HE) staining, spindle tumor cells can be seen as arranged in sweeping fascicles (Figures 3A, B). Combined with immunohistochemistry, LGMS was diagnosed, and the surgical margins were negative. Immunohistochemical (IHC) staining showed (Figure 4): CD34 (Vascular+) (Figure 4A), CK5/6 (-) (Figure 4B), CK14 (-) (Figure 4C), Desmin (-) (Figure 4D), Ki-67 (index 30%) (Figure 4E), SMA (partial+) (Figure 4F), AE1/AE3 (-), CD31 (Vascular+), ALK-D5F3 (-), ALK-D5F3 (NC) (-), ALK-D5F3 (PC) (+), β-catenin (-), S-100 (-), STAT6 (-), P63 (scattered +), EGFR (-), GFAP (-). Following mastectomy, the patient received no chemotherapy or radiation therapy. Furthermore, it is noteworthy that the patient maintained a positive attitude and collaborative spirit throughout the entire treatment process. Due to concerns about recurrence, the patient strongly requested a mastectomy, demonstrating resilience and optimism despite the challenging nature of the procedure, which played a pivotal role in the successful management of her condition. Additionally, we utilized physical examinations and imaging studies (ultrasound and mammography) during subsequent follow-up visits to ensure treatment continuity. She exhibits no evidence of metastasis or local recurrence after 3 months of follow-up.

FIGURE 1
A 1.5cm mass at the 5 o'clock position of the right breast, with the boundary unclear and the local skin sunken (shown by arrow).

3 Discussion

We reviewed previous case reports of breast LGMS, and Table 1 shows the relevant studies we reviewed, in which one case focused on the imaging features of breast LGMS (case 15), and the rest of the cases described the histological features, treatment and prognosis. LGMS consists of fibrosarcoma-like spindle tumor cells arranged in sweeping fascicles, sheets, or storiform whorls (21). Tapered or ovoid nuclei with deep staining have small nucleoli surrounding homogenous chromatin and display light to moderate atypia with slightly increased proliferative activity. The tumor cells have small or moderate amounts of eosinophilic cytoplasm with distinct cell boundaries. The peripheral stroma is collagenous and/or has a myxoid background, and necrosis occurs in a minority of cases. The mitotic activity ranged from 8 to 35 per 10 high power field (HPF), but abnormal mitotic figures are rare (22). A superficial biopsy may have a strong resemblance to a myofibroma. However, the histological features of invasive growth of tumor cells are different from those of myofibromatosis and similar diseases such as nodular fasciitis or inflammatory myofibroblastic tumor (IMT) and more similar to the growth pattern of fibromatosis (23).

Widely accepted for diagnosing LGMS, an electron microscope is required to demonstrate specialized ultrastructural organelles, including abundant rough endoplasmic reticulum, fibronexus junctions, and fibronectin fibrils (5). Among them, fibronexus was not found in smooth muscle cells and fibroblasts. It has been regarded as the most specific ultrastructural marker for myofibroblasts, connecting the myofibroblast to the extracellular matrix (1). The cell-to-matrix junction consists of myofilament and fibronectin filament systems converging on a discrete cell-surface plaque. Calponin and caldesmon, the main components of smooth muscle filaments, are regulators of smooth muscle contraction, and they can interact with actin to inhibit the ATPase activity of muscle actomyosin, thereby regulating muscle contraction (24). Some studies have also found that IMT and LGMS cells, following immunohistochemical staining, suggest diffusely positive for actin-associated proteins and fibronectin (25). These proteins were noted to be mainly distributed in the cytoplasm of tumor cells, with a tendency to extend into the extracellular space. Actin-associated proteins generally include α-smooth muscle actin (α-SMA), muscle-specific actin (MSA), and calponin, etc. As

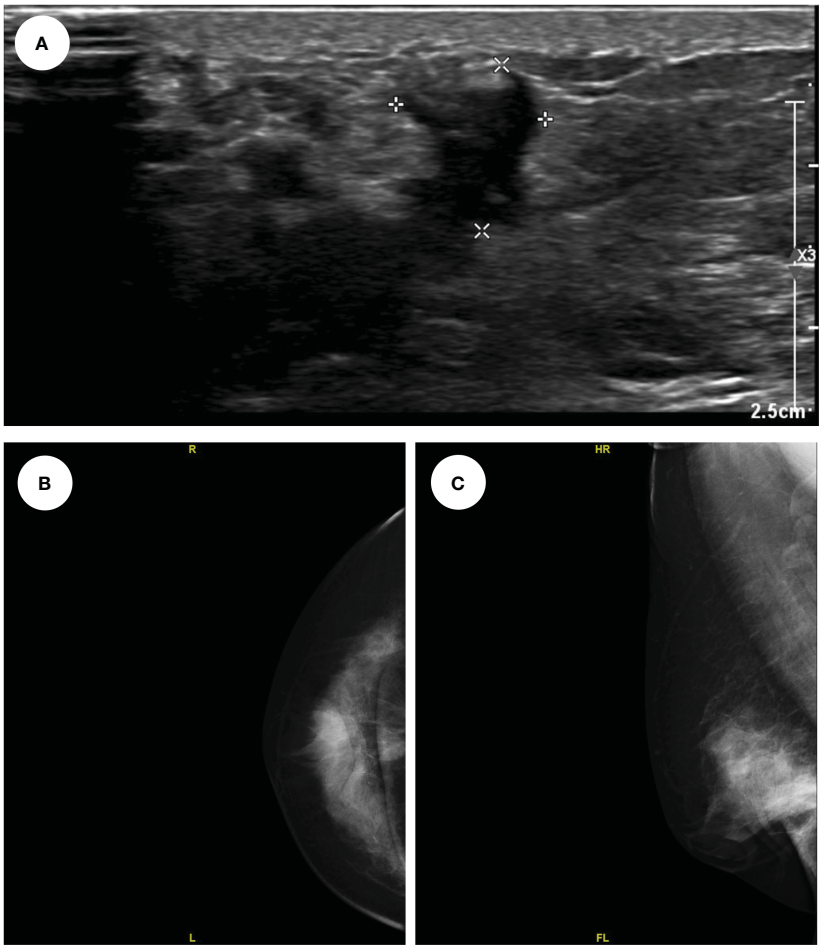

FIGURE 2
The ultrasound showed a 1.5*0.9*1.0cm hypo echoes irregular mass located in the 5 o'clock position of the right breast **(A)**; The mammogram showed a mass in the inner lower quadrant of the right breast (CC, **B**); (MLO, **C**).

mentioned above, actin exists in myofilaments to regulate the contractile function of muscles. Proteins that are stained positive may be able to prove that myofibroblasts contain myofilaments. Fibronectin staining of spindle cells with extracellular extension might be equivalent to fibronectin fibrils known at the ultrastructure of myofibroblasts (25). Therefore, the combined expression of these markers may immunohistochemically reflect the characteristic cell-to-matrix ultrastructural components of myofibroblasts.

In immunohistochemical studies of LGMS, α-SMA and vimentin can be positive in most cases, but desmin can be both positive and negative (21). In this case, α-SMA staining showed positive, vimentin and desmin staining showed negative. Although SMA is regarded as the most specific and frequently expressed marker of myofibroblasts, a small percentage of cases express only SMA or desmin. In addition, calponin can often be positive, and CK/CD34/S-100 is often negative, as in this case. Focal expression of S-100 protein and CD34 has been observed in a minority of cases (23).

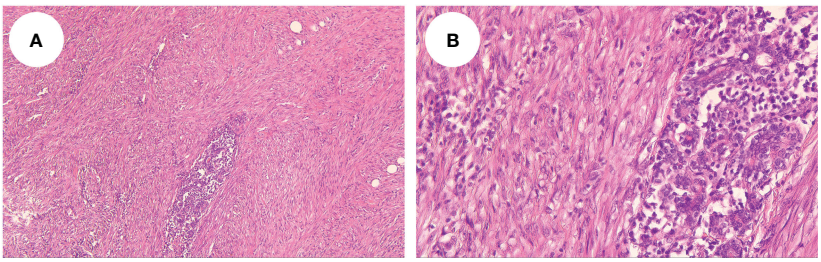

FIGURE 3
Microscopy showed that the spindle tumor cells were arranged in sweeping fascicles (HE, × 10, **A**); (HE, × 40, **B**).

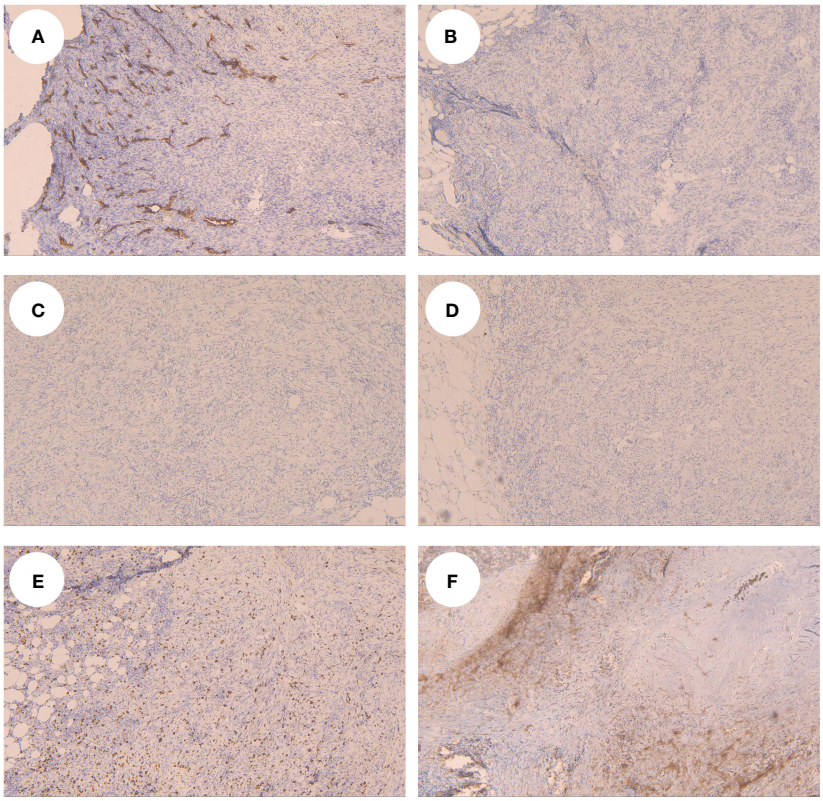

FIGURE 4
Tumor cells showed CD34 positive in the vessel in IHC **(A)**, showed CK5/6 **(B)**, CK14 **(C)** and Desmin **(D)** negative, Ki-67 **(E)** and SMA **(F)** showed partial positive.

TABLE 1 Cases of myofibroblastic sarcomas of the breast.

Case	Background	Age/ Sex	Medical history	Size (cm)	Imaging	Operation	RT/ CT	IHC	Following up (months)
1/(7)	Nm	55/F	1W	2	**Ultrasound**: the neoplasm is found to consist of confluent nodules forming an overall mass	Mastectomy, lymphadenectomy	CT	Vimentin (+), SMA (+), others (−)	Recurrence (1); Pleuropulmonary metastasis and dead (11)
2/(8)	Nm	59/F	Nm	2.3	Nm	Mastectomy, lymphadenectomy	RT	Vimentin (+), SMA (+), S100 (+), CD68 (+), others (-)	Alive (20)
3/(9)	Nm	60/M	1M	2.5	Nm	Mastectomy, lymphadenectomy	No	Vimentin (+), SMA (+), others (-)	Recurrence and alive (120)
4/(5)	Nm	72/F	Nm	3.4	Nm	Local excision	No	SMA (+), MSA (+), desmin (+), others (-)	Recurrence (5); Lung metastasis (12)
5/(22)	Nm	51/F	3M	22	**Ultrasound**: a huge tumor replacing almost the entire breast tissue	Mastectomy	RT and CT	Vimentin (+), SMA (+), others (-)	Alive (24)
6/(1)	Nm	46/M	6M	2.2	**Mammogram**: a lobular mass with partially circumscribed edges in the	Mastectomy	No	Vimentin (+), SMA (+),	Alive (12)

(Continued)

TABLE 1 Continued

Case	Background	Age/ Sex	Medical history	Size (cm)	Imaging	Operation	RT/ CT	IHC	Following up (months)
					upper inner quadrant, measuring 22*21*16 mm			fibronectin (+), others (-)	
7/(10)	Nm	46/F	Nm	4	Nm	Local excision	Nm	Vimentin (+), SMA (+), CD34 (+), others (-)	Recurrence (12)
8/(11)	Nm	81/F	2W	4.2	**Mammogram**: the lesion is identified as a confluent mass lesion measuring 4.2 *3.5*2.5 cm	Mastectomy	RT	Vimentin (+), SMA (+), Bcl-2 (+), others (-)	Pleuropulmonary metastasis and alive (14)
9/(12)	Nm	37/F	Nm	2	**Ultrasound**: solid echo mass. **MRI**: ring enhancement pattern, signal intensity/ time curve: fast initial phase, plateau delayed phase	Mastectomy	No	Vimentin (+), SMA (+), CD34 (+), ALK (+), Ki67 30%, others (-)	Alive (3)
10/(13)	Nm	61/F	1Y	6	**Mammogram**: a lobular mass with high density, obscured margin	Nm	Nm	Vimentin (+), Actin (+), CD34 (+), ALK (+), others (-)	Bone metastasis (Nm)
11/(14)	Nm	57/F	Nm	Nm	Nm	Nm	Nm	SMA (+), others (-)	Pulmonary and brain metastasis, dead (12)
12/(14)	Nm	82/F	Nm	Nm	Nm	Nm	Nm	SMA (+), desmin (+), calponin (+), others (-)	Dead (15)
13/(15)	Arising in fibroadenoma	61/F	8M	5	**Mammogram**: a 3.5-cm-sized well-defined nodular mass with high density at 11 o'clock position of center breast	Local excision	No	Vimentin (+), SMA (+), fibronectin (+), calponin (+), others (-)	Alive (24)
14/(16)	Nm	47/F	6M	3.8	**Ultrasound**: 3.8*2.1cm hypoechoic mass at 3 o'clock position of center breast	Local excision	No	Vimentin (+), SMA (+), CD34 (+), Ki67 30%, others (-)	Alive (3)
15/(6)	Nm	Nm/F	1Y	6.2	**Mammogram**: a lobulated mass, high density, multiple angular and poorly circumscribed margins, a lack of encapsulation	Nm	No	Nm	Bone metastasis (11)
16/(17)	RT associated	49/F	1M	2.8	**Mammogram**: microcalcifications in the upper outer quadrant of the center breast and the upper inner quadrant of the right breast. **Ultrasound**: a hypogenic area of poorly defined limits and several enlarged axillary lymph nodes	Local excision	No	SMA (+), MSA (+), fibronectin (+), CD99 (+), calponin (+), others (-)	Alive (2)
17/(18)	Mastectomy and ALND with CT	53/F	2M	Nm	Nm	No	No	Nm	Lung metastasis (2)

(Continued)

TABLE 1 Continued

Case	Background	Age/ Sex	Medical history	Size (cm)	Imaging	Operation	RT/ CT	IHC	Following up (months)
18/(30)	Nm	62/F	Nm	2	**Mammogram**: 2-cm-sized well-defined nodular mass with high density	Local excision	No	Vimentin (+), SMA (+), Ki67 20%, others (-)	Recurrence (Nm)
19/(19)	BCS with RT and CT	49/F	Nm	3	**Ultrasound**: an oval heterogeneous mass measuring 30 mm in the right retropectoral area	Mastectomy	RT	Vimentin (+), SMA (+), Ki67 43.1%, others (-)	Nm
20/(20)	Nm	56/F	Nm	3	**Ultrasound**: 3*2cm hypoechoic mass at 7 o'clock position of right breast	Local excision	Nm	Vimentin (+), SMA (+), CD34 (+), Ki67 10%, others (-)	Nm
21/ (present case)	Arising in fibroadenoma	54/F	9M	1.5	**Ultrasound**: a 1.5 *0.9*1.0cm hypoechoic irregular mass located in the 5 o'clock position of the breast with a surgical scar on the skin. **Mammogram**: a mass in the inner lower quadrant of the right breast	Mastectomy	No	CD34 (+), SMA (+), Ki67 30%, CD31 (+), ALK-D5F3 (+), P63 (+), others (-)	Alive (3)

Nm, no mentioned; RT, radiotherapy; CT, chemotherapy; IHC, immunohistochemistry; ALND, axillary lymph nodes dissection; BCS, breast conservation surgery; F, female; M, male; Y, year; M, month; W, week.

Furthermore, H-caldesmon is usually expressed positively in leiomyosarcoma but negatively in LGMS, which plays a vital role in the differential diagnosis of the two. Moreover, CK expression is commonly seen in other myofibroblastic proliferations, like the inflammatory myofibroblastic tumor (4).

The mammograms of breast LGMS are generally irregular shapes and high density, with a lack of encapsulation (6). LGMS of the breast are tumors of stromal origin and are etiologically more likely to have hematologic metastases than to have lymphoid metastases compared to epithelial original breast cancers. Therefore, mammograms of advanced-stage breast cancers usually find interstitial edema and opacity of the subcutaneous fat layer (6). On the other hand, there are no signs of interstitial edema and swollen axillary lymph nodes in LGMS. We reviewed cases of breast LGMS, and a few patients underwent computed tomography (CT) and magnetic resonance imaging (MRI), so they could not provide sufficient imaging evidence for diagnosis.

Breast LGMS seems to have a higher incidence of distant metastasis. In the cases we reviewed, almost all patients underwent surgical treatment, with 31.3% of postoperative recurrences and 18.8% of distant metastases. In terms of LGMS at other sites, previous studies have calculated a local recurrence rate of 13.3% to 44.4% (5, 26, 27). In the previous study by Munehisa Kito, 24 patients with LGMS were counted and analyzed statistically (4). Among them, 22 patients underwent surgical treatment, the results showed that the local recurrence rate was 20%, and the incidence of distant metastasis was 4.2%. In a population-based study on LGMS, 49 LGMS patients in the Surveillance, Epidemiology, and End Results Program (SEER) database had survival data with 3-year and 5-year overall survival (OS) of 75.0% and 71.6%, and disease-specific survival (DSS) of 80.0% and 76.3%, respectively. Of these, 93.9% underwent surgery (28). Additionally, a univariate analysis of prognostic outcomes was performed, and the results showed that only tumors larger than 5cm in diameter had a higher local recurrence rate (29). However, this conclusion may not apply to breast LGMS, as shown in Table 1, patients with local recurrence had tumors smaller than 5 cm. Tumor size is not one of the critical factors affecting the long-term prognosis of breast LGMS patients. Therefore, for the prognostic analysis of breast LGMS, more cases and data analysis are still needed.

As for the treatment of LGMS, the benefits of radiotherapy and chemotherapy for patients after surgery are unclear (28). Almost all patients have undergone surgery, and no patients have received radiotherapy or chemotherapy alone. Thus, the therapeutic effect of radiotherapy or chemotherapy cannot be evaluated separately (22, 26, 30). In Y. Xu's study, 96 patients with LGMS were included in the SEER database, of whom 89.6% had received surgery, 29.2% had received radiotherapy, and 10.4% had received chemotherapy (31). According to the results, chemotherapy and radiotherapy had no significant benefit on patients' OS and DSS. Only For unresectable cases, radiotherapy may be a treatment option (4). However, there have been reports of cases of recurrence outside the irradiated area after radiotherapy in LGMS patients, likely related to the pattern of invasive tumor growth. Thus, the choice of radiotherapy may be considered in some cases. In summary, surgery may currently be the primary treatment for LGMS patients, while the prognosis and benefits of radiotherapy and chemotherapy are still unknown. This study comes with its limitations, a three-month follow-up period may not be sufficient to fully ascertain the long-term prognosis of LGMS. Future studies with extended follow-up periods are

imperative to gain a more comprehensive understanding of the recurrence patterns and overall prognosis for patients with LGMS.

4 Conclusions

The diagnosis of LGMS still relies on discovering special ultrastructure under electron microscopy, and the specificity of immunohistochemistry and imaging methods is still insufficient. According to the current literature, surgery is the most important treatment. Notably, LGMS occurring in the breast is a tumor with a high rate of recurrence and a higher incidence of distant metastasis relative to other sites. The currently summarized data on the clinical manifestations, treatment, and prognosis of LGMS mainly come from other sites, and the data of LGMS in the breast need to be further accumulated.

Data availability statement

The original contributions presented in the study are included in the article/supplementary material. Further inquiries can be directed to the corresponding author.

Ethics statement

Ethical approval was not required for the study involving humans in accordance with the local legislation and institutional requirements. Written informed consent to participate in this study was not required from the participants or the participants' legal guardians/next of kin in accordance with the national legislation and the institutional requirements. Written informed consent was obtained from the individual(s), and minor(s)' legal guardian/next of kin, for the publication of any potentially identifiable images or data included in this article.

Author contributions

ZD: Writing – original draft, Methodology, Conceptualization. CX: Writing – original draft, Resources. YLi: Writing – review & editing. YLu: Writing – review & editing. SS: Writing – review & editing, Project administration, Methodology, Conceptualization.

Funding

The author(s) declare financial support was received for the research, authorship, and/or publication of this article. This study was supported by National High Level Hospital Clinical Research Funding (2022-PUMCH-B-038).

Acknowledgments

The authors thank AiMi Academic Services (www.aimieditor.com) for English language editing and review services.

Conflict of interest

The authors declare that the research was conducted in the absence of any commercial or financial relationships that could be construed as a potential conflict of interest.

Publisher's note

All claims expressed in this article are solely those of the authors and do not necessarily represent those of their affiliated organizations, or those of the publisher, the editors and the reviewers. Any product that may be evaluated in this article, or claim that may be made by its manufacturer, is not guaranteed or endorsed by the publisher.

References

1. Morgan PB, Chundru S, Hatch SS, Hawkins HK, Adegboyega PA, Eltorky MA. Uncommon Malignancies: case 1. Low-grade myofibroblastic sarcoma of the breast. *J Clin Oncol.* (2005) 23:6249–51. doi: 10.1200/jco.2005.06.213

2. Fletcher C, Bridge JA, Hogendoorn PCW, Mertens F. *WHO classification of tumours of soft tissue and bone: WHO classification of tumours* Vol. 5. France: World Health Organization (2013).

3. Mentzel T, Dry S, Katenkamp D, Fletcher CD. Low-grade myofibroblastic sarcoma: analysis of 18 cases in the spectrum of myofibroblastic tumors. *Am J Surg Pathol.* (1998) 22:1228–38. doi: 10.1097/00000478-199810000-00008

4. Kito M, Ae K, Okamoto M, Endo M, Ikuta K, Takeuchi A, et al. Clinical outcome of low-grade myofibroblastic sarcoma in Japan: A multicenter study from the Japanese musculoskeletal oncology group. *Cancers (Basel).* (2023) 15(8):2314. doi: 10.3390/cancers15082314

5. Montgomery E, Goldblum JR, Fisher C. Myofibrosarcoma: a clinicopathologic study. *Am J Surg Pathol.* (2001) 25:219–28. doi: 10.1097/00000478-200102000-00010

6. Wang L, Li LX, Chen DQ, Yang L, Li SK, Cheng C. Low-grade Myofibroblastic sarcoma: clinical and imaging findings. *BMC Med Imaging.* (2019) 19:36. doi: 10.1186/s12880-018-0287-z

7. Taccagni G, Rovere E, Masullo M, Christensen L, Eyden B. Myofibrosarcoma of the breast: review of the literature on myofibroblastic tumors and criteria for defining myofibroblastic differentiation. *Am J Surg Pathol.* (1997) 21:489–96. doi: 10.1097/00000478-199704000-00017

8. Gocht A, Bösmüller HC, Bässler R, Tavassoli FA, Moinfar F, Katenkamp D, et al. Breast tumors with myofibroblastic differentiation: clinico-pathological observations in myofibroblastoma and myofibrosarcoma. *Pathol Res Pract.* (1999) 195:1–10. doi: 10.1016/s0344-0338(99)80087-9

9. Gonzalez-Palacios F, Enriquez JL, Miguel P, Vazzquez R, Carcia-Cosio M. Myofibroblastic tumors of the breast: A histologic spectrum with a case of recurrent male breast myofibrosarcoma. *Int J Surg Pathol.* (1999) 7:11–7. doi: 10.1177/106689699900700102

10. Jie W. Clinical and pathological analysis of breast fibroblastic/myofibroblastic tumors. *Chin J Clin Exp Pathol.* (2009) 25:33–6. doi: 10.13315/j.cnki.cjcep.2009.01.015

11. Stark M, Hoffmann A, Xiong Z. Mammary myofibrosarcoma: case report and literature review. *Breast J.* (2011) 17:300–4. doi: 10.1111/tbj.2011.17.issue-3

12. Anfei W, Yi Z, Wugan Z, Ying H, Yanping J, Xiaoyan W. A case of myofibroblastic sarcoma of the breast diagnosed by MRI. *J Clin Radiology.* (2011) 30:1186–7. doi: 10.13437/j.cnki.jcr.2011.08.028

13. Weiwei Z, Yikai X. Imaging findings of low-grade myofibroblastic sarcoma. *Chin J Med Imaging Technology*. (2012) 28:1591–5. doi: 10.13929/j.1003-3289.2012.08.029

14. Shenjere P, Eyden B, Banerjee SS, Chakrabarty B, Shanks JH, Sikand KA, et al. Ultrastructurally confirmed myofibrosarcoma: a series of 10 new cases, with a discussion on diagnostic criteria. *Int J Surg Pathol*. (2013) 21:29–36. doi: 10.1177/1066896912454568

15. Myong NH, Min JW. Low-grade myofibroblastic sarcoma arising in fibroadenoma of the breast-A case report. *Diagn Pathol*. (2016) 11:33. doi: 10.1186/s13000-016-0480-8

16. Ming Z, Xiangru W, Jian Z, Yipeng Y, Yunshu L, Baosan H, et al. A case of low-grade Malignant myofibroblastic sarcoma originating from the breast and review of the literature. *Chin J Breast Disease(Electronic Edition)*. (2017) 11:255–6. doi: CNKI:SUN:ZHRD.0.2017-04-015

17. Val-Bernal JF, Hermana S, Alonso-Bartolomé MP. Myofibroblastic sarcoma of the breast. Report of a case induced by radiotherapys. *Pathol Res Pract*. (2019) 215:152664. doi: 10.1016/j.prp.2019.152664

18. Jiaxin Y, Yin T, Chunfu D, Yiou C. A case of new low-grade Malignant myofibroblastic sarcoma in the postoperative incision of a breast cancer patient. *J Med Theory Pract*. (2019) 32:2360. doi: 10.19381/j.issn.1001-7585.2019.15.015

19. Park SY, Kim HJ, Lee J, Jeong JY, Byun J, Kim WH, et al. A radiation induced low-grade myofibroblastic sarcoma in the retropectoral area after breast conserving surgery: A case report. *J Breast Cancer*. (2023) 26:397–402. doi: 10.4048/jbc.2023.26.e36

20. Zhe L, Meng Z, Jie Y, Chenmao X, Bin L, Yali S. Low-grade myofibroblastic sarcoma of mammary gland: A case report. *J Clin Pathological Res*. (2023) 43:634–8. doi: 10.3978/j.issn.2095-6959.2022

21. Fisher C. Myofibroblastic Malignancies. *Adv Anat Pathol*. (2004) 11:190–201. doi: 10.1097/01.pap.0000131773.16130.aa

22. Lucin K, Mustać E, Jonjić N. Breast sarcoma showing myofibroblastic differentiation. *Virchows Arch*. (2003) 443:222–4. doi: 10.1007/s00428-003-0853-8

23. Cai C, Dehner LP, El-Mofty SK. In myofibroblastic sarcomas of the head and neck, mitotic activity and necrosis define grade: a case study and literature review. *Virchows Arch*. (2013) 463:827–36. doi: 10.1007/s00428-013-1494-1

24. Makuch R, Birukov K, Shirinsky V, Dabrowska R. Functional interrelationship between calponin and caldesmon. *Biochem J*. (1991) 280:33–8. doi: 10.1042/bj2800033

25. Qiu X, Montgomery E, Sun B. Inflammatory myofibroblastic tumor and low-grade myofibroblastic sarcoma: a comparative study of clinicopathologic features and further observations on the immunohistochemical profile of myofibroblasts. *Hum Pathol*. (2008) 39:846–56. doi: 10.1016/j.humpath.2007.10.010

26. Kim JH, Choi W, Cho HS, Lee KS, Park JK, Kim BK. Surgical treatment and long-term outcomes of low-grade myofibroblastic sarcoma: a single-center case series of 15 patients. *World J Surg Oncol*. (2021) 19:339. doi: 10.1186/s12957-021-02454-5

27. Meng GZ, Zhang HY, Bu H, Zhang XL, Pang ZG, Ke Q, et al. Myofibroblastic sarcomas: a clinicopathological study of 20 cases. *Chin Med J (Engl)*. (2007) 120:363–9. doi: 10.1097/00029330-200703010-00003

28. Chan JY, Gooi Z, Wong EW, Ng SK, Tong MC, Vlantis AC. Low-grade myofibroblastic sarcoma: A population-based study. *Laryngoscope*. (2017) 127:116–21. doi: 10.1002/lary.26146

29. Maki RG, Moraco N, Antonescu CR, Hameed M, Pinkhasik A, Singer S, et al. Toward better soft tissue sarcoma staging: building on american joint committee on cancer staging systems versions 6 and 7. *Ann Surg Oncol*. (2013) 20:3377–83. doi: 10.1245/s10434-013-3052-0

30. Scardina L, Franceschini G, Di Leone A, D'Archi S, Santoro A, Mulè A, et al. Low-grade myofibroblastic sarcoma of the breast. *Breast J*. (2020) 26:2077–8. doi: 10.1111/tbj.13956

31. Xu Y, Xu G, Wang X, Mao M, Wu H, Baklaushev VP, et al. Is there a role for chemotherapy and radiation in the treatment of patients with low-grade myofibroblastic sarcoma? *Clin Transl Oncol*. (2021) 23:344–52. doi: 10.1007/s12094-020-02425-4

frontiers | Frontiers in Oncology

TYPE Original Research
PUBLISHED 21 May 2024
DOI 10.3389/fonc.2024.1393707

Check for updates

OPEN ACCESS

EDITED BY
Dragos Eugen Georgescu,
Carol Davila University of Medicine and Pharmacy, Romania

REVIEWED BY
Giuseppe Scibilia,
Gynecology and Obstetrics Department, Italy
Michele Peiretti,
University of Cagliari, Italy
Nicolae Bacalbasa,
Carol Davila University of Medicine and Pharmacy, Romania

*CORRESPONDENCE
Rosanna Mancari
rosanna.mancari@ifo.it

RECEIVED 29 February 2024
ACCEPTED 25 April 2024
PUBLISHED 21 May 2024

CITATION
Mancari R, Yusuf Y, Macuks R, Achimas-Cadariu P, Piek JM, Sperduti I, Corrado G, Vizza E and Zapardiel I (2024) Prognostic factors in uterine adenosarcoma: subanalysis of the SARCUT study. *Front. Oncol.* 14:1393707. doi: 10.3389/fonc.2024.1393707

COPYRIGHT
© 2024 Mancari, Yusuf, Macuks, Achimas-Cadariu, Piek, Sperduti, Corrado, Vizza and Zapardiel. This is an open-access article distributed under the terms of the Creative Commons Attribution License (CC BY). The use, distribution or reproduction in other forums is permitted, provided the original author(s) and the copyright owner(s) are credited and that the original publication in this journal is cited, in accordance with accepted academic practice. No use, distribution or reproduction is permitted which does not comply with these terms.

Prognostic factors in uterine adenosarcoma: subanalysis of the SARCUT study

Rosanna Mancari[1]*, Yildirim Yusuf[2], Ronalds Macuks[3], Patriciu Achimas-Cadariu[4,5], Jurgen Martinus Piek[6], Isabella Sperduti[7], Giacomo Corrado[8], Enrico Vizza[1] and Ignacio Zapardiel[9]

[1]Gynecologic Oncology Unit, IRCCS Regina Elena National Cancer Institute, Rome, Italy, [2]Gynecologic Oncology Department, Tepecik Training and Research Hospital, Izmir, Türkiye, [3]Latvian Oncology Center of Riga Eastern Clinical University Hospital, Riga, Latvia, [4]Gynecologic Oncology Department, Institute of Oncology Prof. Dr. I Chiricuta, Cluj-Napoca, Romania, [5]Gynecologic Oncology Department, University of Medicine and Pharmacy Iuliu Hatieganu, Cluj Napoca, Romania, [6]Gynecologic Oncology Department, Catharina Ziekenhuis Department of Gynecology, Eindhoven, Netherlands, [7]Unit of Biostatistical, IRCCS Regina Elena National Cancer Institute, Rome, Italy, [8]Gynecologic Oncology Unit, Department of Woman, Child and Public Health, Fondazione Policlinico Uni-versitario A. Gemelli IRCCS, Rome, Italy, [9]Gynecologic Oncology Unit, La Paz University Hospital, Madrid, Spain

Objective: The purpose of the study was to analyse the role of prognostic factors on the risk of recurrence and overall survival of patients with uterine adenosarcoma.

Methods: A retrospective international multicentre study involving 46 centres collected 32 cases of uterine adenosarcoma, and these cases were included in the present subanalysis. Clinical and demographic features and tumour characteristics were gathered, as well as information on treatment and relapse. Disease-free and overall survival were analysed.

Results: The 5-year disease-free survival (DFS) was 85.3% and the 5-year overall survival (OS) rate was 89.5%. The risk factors significantly associated with overall survival were age (HR 1.09, 95% CI 1.03–1.15; $p = 0.004$) and FIGO stage II–III (HR 17.75, 95% CI 2.87–109.93; $p = 0.002$). Patients who experienced early relapse (within 12 months) had a tumour size >30 mm and advanced stage. The majority of recurred cases were treated with radiotherapy or surgery and obtained a good response rate.

Conclusion: The most significant prognostic factors in uterine adenosarcoma were age and FIGO stage and, indirectly, tumour size at diagnosis. The use of secondary surgery and/or radiotherapy could help in prolonging the disease-free status of the patients.

KEYWORDS

adenosarcoma, uterine neoplasms, prognosis, disease-free survival, survival rate

1 Introduction

Uterine adenosarcoma is a rare tumour accounting for 5.5%–9% of all uterine sarcomas and 0.2% of all uterine neoplasms (1). Patients with adenosarcoma are usually diagnosed with stage I disease and have a 5-year overall survival (OS) of 60%–80% (1). First described by Clement and Scully in 1974 (2), this neoplasia consists of a malignant stromal component and benign epithelium (3, 4). The stromal component is typically characterised by a low-grade spindle cell sarcoma, while the epithelial components are commonly endometrioid exhibiting frequent metaplasia and occasionally atypia (4).

While the sarcomatous component typically stains for CD10, the epithelial part regularly exhibits estrogen and progesterone receptors (5).

Uterine adenosarcoma (AS) is the intermediate step of the spectrum beginning with benign entities such as adenofibromas and adenomyomatosis and ending in the high end of the spectrum with carcinosarcoma (6).

It usually manifests as a polypoid endometrial tumour, but it can be found in the cervix, ovary or other extrauterine areas.

It has the highest incidence in the fifth and sixth decades, but it may be diagnosed at a younger age (3–8). AS is usually defined as a low-grade sarcoma (3), and it shows wide variability in survival rate, depending on the possible manifestation of some negative prognostic factors, mainly on the presence of the sarcomatous overgrowth (SO)—when more than 25% of the tumour consists of a high-grade sarcomatous component—which is associated with worse prognosis (3). The variant with SO exhibits aggressive behaviour along with frequent recurrences and shorter survival (3).

Additional known prognostic factors include stromal atypia, deep myometrial invasion and vascular space invasion, which are associated with aggressive evolution and lend the disease the name of high-grade adenosarcoma (9). The presence of hormone receptors, CD10 and WT1 expression is generally associated with a good prognosis and contributes to the diagnosis of the so-called low-grade adenosarcoma (10).

The standard treatment of uterine adenosarcoma consists of performing a total hysterectomy, with or without bilateral salpingo-oophorectomy, and the removal of all visible disease (1). Adjuvant treatment is controversial due to a lack of prospective trials. In the same way, the optimal treatment for relapsed uterine adenosarcomas is yet to be clearly defined: radiotherapy, chemotherapy and hormonal therapy may be potential options (11).

Identifying the most relevant prognostic factors is essential in order to improve the outcomes and proper management of patients with this diagnosis.

The aim of this study was to analyse the prognostic factors associated with oncological outcomes in patients diagnosed with uterine adenosarcoma via subanalysis of the patients included in the multicentric international SARCUT study.

2 Materials and methods

The SARCUT (SARComa of the UTerus) study was a retrospective international multicentre study of patients diagnosed with uterine sarcoma. This study involved 46 different European institutions which included 966 patients diagnosed with uterine sarcoma between January 2001 and December 2007, and patients were followed until 2012. For the current subanalysis, we selected patients diagnosed with uterine adenosarcoma, including 32 cases from 18 participating institutions.

The inclusion criteria for the present analysis included a pathological diagnosis of uterine AS, as well as primary surgical treatment performed at the participating centre. The review from the Institutional Review Board (IRB) was first obtained at the coordinating centre (#PI-1382), and for the rest of the participating institutions, approval was obtained according to local regulation requirements. After receiving approval from the IRB, informed consent was not necessary to review the participants' medical records. Uterine AS was classified according to the 2009 International Federation of Gynecology and Obstetrics (FIGO) classification system (12). The baseline clinical and demographic features of the patients and the tumour characteristics of uterine adenosarcoma were collected.

Primary treatment and recurrences were recorded; the terminology for surgical procedures, the sites of recurrence and adjuvant treatment were standardised. Surgical procedures were adapted to address the extension of disease, and complete cytoreduction was achieved when no residual tumour was present after surgery (13). Adjuvant treatment was administered at the institution's discretion based on local protocols.

After primary treatment, follow-up was performed every 3 months on average for the first year, every 6 months until the fifth year and then annually. Patients lacking follow-up information were excluded from the analysis. Imaging techniques involved an ultrasound of the abdomen, alternating with either computed tomography or magnetic resonance imaging, depending on clinical practice and availability at each centre.

Disease-free survival (DFS) was defined as the interval between the end of primary treatment and the appearance of recurrence. Recurrence was defined as the appearance of the tumour after primary treatment, during the follow-up period. We distinguished between pelvic and distant recurrences based on the site of the relapsed disease. Secondary surgery, hormonal therapy, radiotherapy and/or chemotherapy were administered at the institution's discretion in accordance with local protocols. OS was defined as the length of time from the date of diagnosis to the death or last follow-up.

Data collection was conducted via a web-based database. Individual researchers were responsible for the registration of their own cases. This manuscript was prepared in accordance with STROBE guidelines (14).

10.3389/fonc.2024.1393707

2.1 Statistical analysis

Descriptive statistics were used to describe patient characteristics. Continuous variables are presented as median and range. Discrete variables are presented as absolute values and percentages. The chi-square test or Fisher's exact test was used to estimate the association between categorical variables when appropriate.

Overall survival and DFS were calculated by the Kaplan–Meier survival curves from the date of the surgery until relapse or demise. If a patient were alive, survival was then censored at the time of the last visit. DFS was calculated from the date of surgery to the date of relapse or death. If a patient had not relapsed, DFS was censored at the time of the last visit. The log-rank test was used to assess differences between subgroups. Significance was defined at the p <0.05 level. The hazard risk and the confidence limits were estimated for each variable using the Cox univariate model. A multivariate Cox proportional hazard model was also developed using stepwise regression (forward selection) with variables, which were significant in the univariate analyses. The enter limit and remove limit were p = 0.10 and p = 0.15, respectively. The statistical software used was SPSS v.21 (SPSS Inc., Chicago, IL, USA).

3 Results

A total of 32 women with uterine AS were identified. The baseline clinical data and demographics of the study population are illustrated in Table 1.

The median age at diagnosis was 61.5 (range 17–88) years and 22 (68%) patients were postmenopausal at the time of diagnosis. The unique reported symptom was abnormal vaginal bleeding, present in 27 (84.3%) patients, while 5 (15.6%) women were asymptomatic. The tumour was diagnosed after undergoing a routine exam in addition to detecting an enlarged uterus. Twenty-five (78.1%) patients had FIGO stage I, 4 (12.5%) patients presented FIGO stage II and 3 (9.4%) patients had FIGO stage III. Among the three FIGO stage III cases, two of them presented pathological confirmation of nodal metastases, and one patient presented pathologic enlarged nodes at the preoperative CT scan with suspected vascular infiltration; therefore, no surgery was carried out. This last patient received radiotherapy with complete response and remained free of disease for 79 months.

The median tumour size (referred to as the main nodule at diagnosis) was 30 (range 2–170) mm. Lymphovascular space invasion (LVSI) determination was available in only 12 (37.5%) patients and was always reported as negative. Sarcomatous overgrowth was available in only three cases; therefore, we decided not to consider it in the statistical analysis.

Concerning surgical treatment, all patients underwent a total hysterectomy. The surgical route taken was laparoscopy in 4 (12.5%) cases, laparotomy in 27 (84.4%) cases and vaginal in 1 (3.1%) case. Twenty-nine (90.6%) patients also underwent a bilateral salpingo-oophorectomy (BSO). Three (9.4%) patients received additional procedures, such as omentectomy in two cases and appendectomy in one case. Complete cytoreduction was achieved in 31 (96.9%) patients. Seven (21.9%) patients underwent pelvic lymphadenectomy, one of them with an additional para-aortic dissection.

TABLE 1 Baseline characteristics of the patients with uterine adenosarcoma.

Variables	Number of cases (%)
Age, years (median, range)	61.5 (17–88)
Menopause	22 (68)
Smokers	2 (6.2)
Parity, births (median, range)	2 (0–4)
Previous fibroids	1 (3.1)
Previous pelvic radiation	0
Previous use of tamoxifen	1 (3.1)
Symptoms	
Pain	0
Pelvic mass	0
Bleeding	27 (84.4)
None	5 (15.6)
FIGO stage	
I	25 (78.2)
II	4 (12.5)
III	3 (9.3)
IV	0
Margin involvement	1 (3.1)
Tumour size, mm (median, range)	30 (2–170)
Extrauterine involvement	3 (9.3)
Surgical approach	
Laparoscopy	4 (12.5)
Laparotomy	27 (84.4)
Vaginal	1 (3.1)
Surgical procedure	
Hysterectomy	32 (100)
Bilateral salpingo-oophorectomy	29 (90.6)
Omentectomy	2 (6.2)
Pelvic lymphadenectomy	7 (21.8)
Para-aortic lymphadenectomy	1 (3.1)
Appendectomy	1 (3.1)
Involved margin after resection	
No	31 (96.9)
Yes	1 (3.1)
Radiotherapy	13 (40.6)
Chemotherapy	2 (6.2)

Adjuvant treatment was administered in 15 (46.8%) cases, radiotherapy in 13 (40.6%) patients and chemotherapy in 2 (6.2%) patients.

At a median follow-up of 48 months (range 1–140), the 5-year DFS was 85.3% and the 5-year OS was 89.5%. Five (15.6%) patients relapsed, two (6.25%) with pelvic recurrence, two (6.25%) with pelvic and distant disease and one (3.1%) with distant metastasis only. Three (9.4%) of them relapsed within 1 year of follow-up. When comparing the 5-year DFS according to tumour size, we did not find any significant differences between patients with tumours measuring <30 mm vs. ≥30 mm (87.5% vs. 81.9%, respectively; $p = 0.28$) (Figure 1).

The same findings were observed between FIGO stage I vs. II–III (89.9% vs. 71.4%, respectively; $p = 0.25$) (Figure 2).

Both tumour size ≥30 mm and FIGO stage II–III indicated a trend towards worse prognosis compared with the rest of the population with a 5-year DFS of 60% ($p = 0.06$) (Figure 3).

In the multivariate analysis, the only risk factors significantly associated with overall survival were age (HR 1.09, 95% CI 1.03–1.15; $p = 0.004$) and FIGO stage II–III (HR 17.75, 95% CI 2.87–109.93; $p = 0.002$).

When we analysed patients with early relapse (within 12 months), we observed that they had a tumour size >30 mm and at an advanced stage more frequently than others; however, this was deemed not significant.

Relapsed patients were treated with surgery or radiotherapy. Two (6.2%) patients with early relapse survived for 45 months and 17 months after secondary treatment, and the third one was lost to follow-up.

The patient relapsed with only distant metastasis after 66 months and was subsequently treated with secondary surgery and obtained a DFS of 95 months. Only one (3.1%) patient died from AS, and two more patients passed away from other diseases.

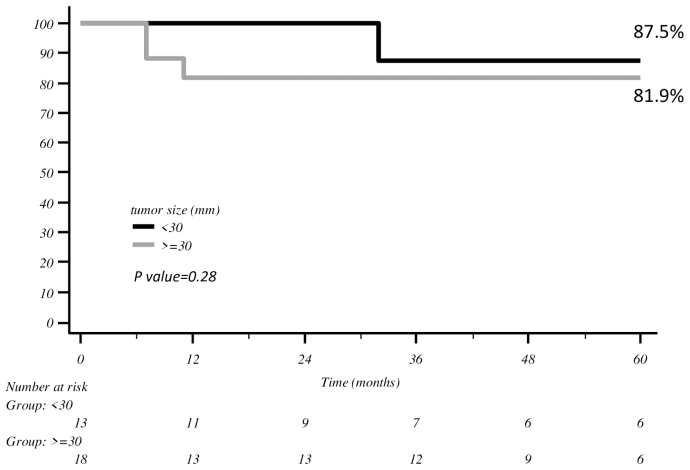

FIGURE 1
DFS with Kaplan–Meier curve according to tumour size.

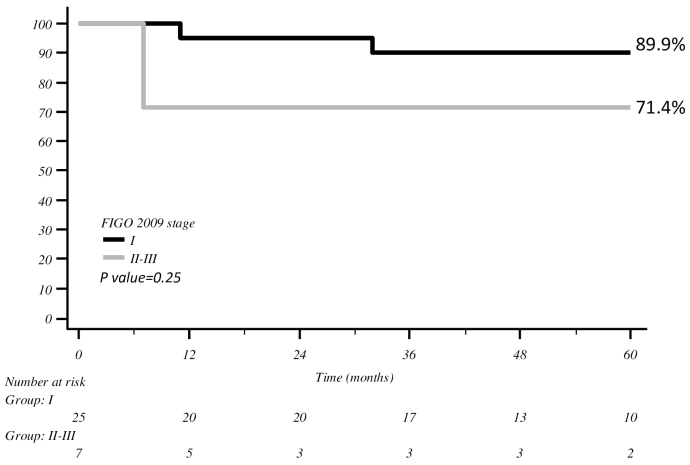

FIGURE 2
DFS with Kaplan–Meier curve according to FIGO stage.

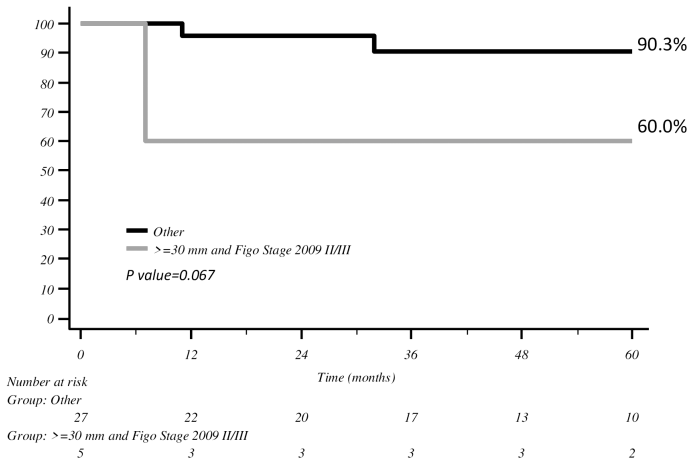

FIGURE 3
DFS with Kaplan–Meier curve according to tumour size >30 mm and FIGO stage II–III.

4 Discussion

This study evaluated the prognostic factors impacting the oncological outcome of patients with uterine adenosarcoma. The most important prognostic factors seemed to be age and FIGO stage at diagnosis. In addition, we observed a long 5-year DFS and OS, where our results were found to be consistent with the most favourable cases reported in the literature.

Carroll found similar results in his publication, where older age and FIGO stage were associated with worse PFS on multivariate analysis, in addition to sarcomatous overgrowth and LVSI (15). In a huge study by Arend, 544 patients with uterine AS were identified and their 5-year survival was 79% for stage I disease and 48% for stage III disease (16), confirming the importance of FIGO stage in the prognosis of these women. Similarly, Zaloudek found that extrauterine spread is one of the most relevant prognostic factors (17), and Ulrich upheld the good prognosis of patients with stage I disease (18).

Carroll (15) examined 74 patients with uterine AS, showing a worse survival with increasing age. Nathenson described a significant worse prognosis in terms of DFS and OS when patients were older than 53 years (19). These data confirm that age is a significant prognostic factor in women with uterine AS like in many other neoplastic diseases.

Despite the good prognosis of the disease, three out of our five patients with relapse recurred within 1 year (early relapse, ER). Therefore, we decided to concentrate on this group and observed that these patients exhibited large tumour size and advanced FIGO stage more frequently than late or non-relapsed patients. Even if we did not find any statistically significant differences, we observed a trend of significant to worse prognosis among patients with both tumour size ≥30 mm and FIGO stage II–III, which partially agrees with the results of the multivariate analysis performed.

The high proportion of pelvic recurrences in the group of ER patients could be related to local factors, such as myometrial invasion and tumour size, although we cannot assess it due to the number of cases. Even though we could not find any significant differences in the multivariate analysis, these data are congruent with the literature, where size is considered a prognostic factor (20) even if its power is weaker than that of sarcomatous overgrowth, myometrial invasion and lymphovascular invasion. Seagle in 2016 affirmed that increasing tumour size was associated with a decline in OS in patients with adenosarcoma (20). In his series, the risk of death was related to an increase in each centimetre in tumour size among patients with uterine AS. Machida found that patients with uterine AS have smaller-sized tumours than those diagnosed with endometrial stromal sarcoma or uterine leiomyosarcoma, both presenting worse prognosis (21). In this setting, the use of adjuvant radiotherapy could be justified to prevent local recurrence (22), but some retrospective trials failed to demonstrate its efficacy since it had no effect on survival for women with uterine AS (16, 21, 23). Moreover, to our knowledge, no prospective trials have been planned due to the rarity of the disease. In another series, adjuvant radiotherapy has been shown to be a negative prognostic factor, but this was probably due to selection bias, in relation to the high percentage of risk factors in that group of women (20).

According to the literature, the most important prognostic factors for uterine AS are age, myometrial invasion, sarcomatous overgrowth, presence of LVSI and node involvement. In addition, tumour size, mitotic index and tumour necrosis could have an impact but cannot be considered independent prognostic factors (6, 22). During the M.D. Anderson Cancer experience, the median tumour size of AS ranged from 60 mm to 200 mm (22); our median tumour size was much lower (30 mm), and this fact could be considered a bias, but it can also justify the better prognosis of our patients.

In the GOG study published in 1992 (6), 31 patients with stage I–II uterine AS were enrolled with a median age of 62 years, similar to our population. In 85% of patients, the diameter of the uterine lesion ranged between 2 cm and 10 cm. This study underlined the importance of SO in worsening the prognosis of patients and the tendency towards the association between older age and worse prognosis, data confirmed by many other studies (22–24). The

population with SO consisted of 17 patients (55%) and was compared to a population without SO: the mean age of the first group was approximately 5 years older than the second, even if it was not statistically significant. Recurrence occurred in 44% of the first group and in 14% of the second one, and 31% of the patients died in the first group vs. only 7% of the second one. Denschlag found that mortality for typical adenosarcoma was 10%–25%, while the mortality rate for adenosarcoma with sarcomatous overgrowth was up to 75% (25).

Several publications illustrated a low rate of nodal metastases among patients with uterine AS, ranging from 3% to 6.5% (6, 15, 16). In a SEER database analysis, 994 cases with uterine AS were identified, and the incidence of lymph node metastasis was 2.9% (21). For this reason, the role of lymphadenectomy in women with uterine AS appears to be limited similar to patients with uterine leiomyosarcoma, and lymphadenectomy is not routinely undertaken (15).

Nevertheless, lymph node involvement may be an indicator of a poorer prognosis; therefore, it is suggested to first try all options to achieve optimal surgical debulking, thus promoting the use of lymphadenectomy when bulky nodal disease is present (22, 25).

Recently, another histologic pattern has been described called the high-grade stromal component (26). It is defined by the presence of severe nuclear pleomorphism and is usually but not exclusively present in the context of sarcomatous overgrowth. We could not analyse the SO nor the high-grade stromal component in our group of patients since these characteristics were not collected nor included in our data.

One of our study's main weaknesses is the paucity of data regarding some prognostic factors, such as myometrial invasion and sarcomatous overgrowth, as well as the low number of cases. Conversely, one of our study's main strengths includes the long period of follow-up and the high number of involved participating centres.

It is worth highlighting the importance of FIGO stage and, indirectly, tumour size at diagnosis, which will impact the prognosis of the disease.

The role of systemic therapies in uterine AS has yet to be well established. Due to a lack of clinical trials for uterine AS, there is no standard role of adjuvant chemotherapy for this disease (1), and patients at low risk of recurrence should be thoroughly observed without undergoing any adjuvant therapy.

Guidozzi described the history of three patients with stage II–III uterine AS, who received neoadjuvant chemotherapy and surgery in two cases and surgery followed by chemotherapy and radiotherapy in the third case, obtaining a long disease-free interval, ranging from 34 months to 56 months of follow-up (27).

Verschraegen published his series and described partial response and stable disease after chemotherapy in approximately 50% of patients in recurrent patients (22). These data could reinforce the significance of systemic therapy, even if the number of patients was small and there were scant data on the other prognostic factors.

It is important to also underline the role of secondary therapies, both radiotherapy and secondary surgery, that allowed our relapsed patients to maintain a disease-free status for a relatively long period of time.

In Carroll's paper, the median survival time from the date of recurrence in women who underwent a secondary cytoreduction for relapse was 16.1 months, compared with 8.4 months in patients who did not undergo secondary surgery (15). In reading the results by Krivak, we can hypothesise a correlation between the site of recurrence and the prognosis of the patient since distant relapses—mainly pulmonary—were associated with shorter survival. This is probably due to the difficulties in cytoreducing some areas more than others, consequently highlighting the importance of secondary surgery (28).

In the literature, doxorubicin-based regimens and gemcitabine/docetaxel chemotherapy have been reported to be useful in recurrent and/or metastatic settings (19, 22, 23), while the role of hormonal therapy has not yet been well established since it is limited to a case series (1).

A recent study analysed 58 patients with recurrent or metastatic uterine AS and 20 with extrauterine AS: most recurrences were abdominal and pelvic and a minor part was distant (29). Relapsed patients were treated mainly with surgery and chemotherapy, alone or in combination. Frequently, chemotherapy regimens were doxorubicin-based or gemcitabine and docetaxel, with a response rate of 40% for the first regimen vs. 25% for the second one. The median OS improved in the group of patients with resection for recurrent lesions. One-third of relapsed patients received hormonal therapy (GnRH agonists, progestins, SERMs and aromatase inhibitors), obtaining a relevant lengthening in OS. Nearly two-thirds of patients with recurrent disease had a high-grade sarcoma, with a median OS of half of the patients with a mixed histology. The Italian Consensus Conference on Management of Uterine Sarcomas in 2020 affirmed that hormonal adjuvant treatment can be offered to patients with uterine AS without sarcomatous overgrowth when hormone receptors are present (11). Expression of estrogen receptors is present in more than two-thirds of patients with this diagnosis, but this positivity is lower in SO in women (10). Carroll described a prolonged response with aromatase inhibitors given initially in an adjuvant setting in a patient with stage IV uterine AS and with a strong staining for estrogen and progesterone receptors, and then for recurrent disease, obtaining a stabilisation of disease and reaching a follow-up of 12.5 years from the diagnosis (15).

5 Conclusions

The most important prognostic factors associated with overall survival in our patients diagnosed with uterine adenosarcoma seem to be age and FIGO stage at diagnosis.

Data availability statement

Dataset are available on request to corresponding author. Requests to access these datasets should be directed to RMan, rosanna.mancari@ifo.it.

Ethics statement

The studies involving humans were approved by the Institutional Review Board (IRB), and approval was first obtained at the coordinating centre: La Paz University Hospital, 28046 Madrid, Spain (#PI-1382). The studies were conducted in accordance with the local legislation and institutional requirements. Written informed consent for participation was not required from the participants or the participants' legal guardians/ next of kin in accordance with the national legislation and institutional requirements.

Author contributions

RMan: Writing – review & editing, Writing – original draft, Validation, Supervision, Methodology, Funding acquisition. YY: Writing – review & editing, Validation, Formal analysis. RMac: Writing – review & editing, Resources, Methodology, Data curation. PA: Writing – review & editing, Visualization, Investigation, Data curation. JP: Writing – review & editing, Validation, Software. IS: Writing – review & editing, Software, Formal analysis, Data curation. GC: Writing – review & editing, Validation, Supervision, Conceptualization. EV: Writing – review & editing, Supervision, Funding acquisition. IZ: Writing – review & editing, Writing – original draft, Supervision, Conceptualization.

Funding

The author(s) declare financial support was received for the research, authorship, and/or publication of this article. This work was financially supported through funding from the institutional "Ricerca Corrente" granted by the Italian Ministry of Health.

Conflict of interest

The authors declare that the research was conducted in the absence of any commercial or financial relationships that could be construed as a potential conflict of interest.

The author(s) declared that they were an editorial board member of Frontiers, at the time of submission. This had no impact on the peer review process and the final decision.

Publisher's note

All claims expressed in this article are solely those of the authors and do not necessarily represent those of their affiliated organizations, or those of the publisher, the editors and the reviewers. Any product that may be evaluated in this article, or claim that may be made by its manufacturer, is not guaranteed or endorsed by the publisher.

References

1. Nathenson MJ, Ravi V, Fleming N, Wang W-L, Conley A. Uterine adenosarcoma: a review. *Curr Oncol Rep*. (2016) 18:68. doi: 10.1007/s11912-016-0552-7

2. Clement PB, Scully RE. Mullerian adenosarcoma of the uterus. A clinicopathologic analysis of ten cases of a distinctive type of Mullerian mixed tumor. *Cancer*. (1974) 34:1138–49. doi: 10.1002/(ISSN)1097-0142

3. Clement PB, Scully RE. Mullerian adenosarcoma of the uterus: a clinicopathologic analysis of 100 cases with a review of the literature. *Hum Pathol*. (1990) 21:363–81. doi: 10.1016/0046-8177(90)90198-E

4. Pinto A, Howitt B. Uterine adenosarcoma. *Arch Pathol Lab Med*. (2016) 140:286–90. doi: 10.5858/arpa.2014-0523-RS

5. Amant F, Steenkiste E, Schurmans K, Verbist L, Abeler VM, Tulunay G, et al. Immunohistochemical expression of CD10 antigen in uterine adenosarcoma. *Int J Gynecol Cancer*. (2004) 14:1118–21. doi: 10.1111/j.1048-891X.2004.14610.x

6. Kaku T, Silverberg SG, Major FJ, Miller A, Fetter B, Brady MF. Adenosarcoma of the uterus: a Gynecologic Oncology Group clinicopathologic study of 31 cases. *Int J Gynecol Pathol*. (1992) 11:75–88. doi: 10.1097/00004347-199204000-00001

7. Fleming NA, Hopkins L, de Nanassy J, Senterman M, Black AY. Mullerian adenosarcoma of the cervix in a 10-year-old girl: case report and review of the literature. *J Pediatr Adolesc Gynecol*. (2009) 22:e45–51. doi: 10.1016/j.jpag.2008.06.001

8. Liu H, Shen Z, Zhou Y. Uterine adenosarcoma with sarcomatous overgrowth: A case report of aggressive disease in a 16-year-old girl and a literature review. *J Pediatr Adolesc Gynecol*. (2018) 31:426–31. doi: 10.1016/j.jpag.2017.12.012

9. Hodgson A, Amemiya Y, Seth A, Djordjevic B, Parra-Herran C. High-grade Müllerian adenosarcoma: genomic and clinicopathologic characterization of a distinct neoplasm with prevalent TP53 pathway alterations and aggressive behavior. *Am J Surg Pathol*. (2017) 41:1513–22. doi: 10.1097/PAS.0000000000000907

10. Amant F, Schurmans K, Steenkiste E, Verbist L, Abeler VM, Tulunay G, et al. Immunohistochemical determination of estrogen and progesterone receptor positivity in uterine adenosarcoma. *Gynecol Oncol*. (2004) 93:680–5. doi: 10.1016/j.ygyno.2004.03.021

11. Ferrandina G, Aristei C, Biondetti PR, Cananzi FCM, Casali P, Ciccarone F, et al. Italian consensus conference on management of uterine sarcomas on behalf of S.I.G.O. (Societa' italiana di Ginecologia E Ostetricia). *Eur J Cancer*. (2020) 139:149–68. doi: 10.1016/j.ejca.2020.08.016

12. Prat J. FIGO staging for uterine sarcomas. *Int J Gynaecol Obstet*. (2009) 104:179. doi: 10.1016/j.ijgo.2008.12.009

13. Zapardiel I, Morrow CP. New terminology for cytoreduction in advanced ovarian cancer. *Lancet Oncol*. (2011) 12:214. doi: 10.1016/S1470-2045(10)70292-8

14. Cuschieri S. The STROBE guidelines. *Saudi J Anaesth*. (2019) 13:S31–4. doi: 10.4103/sja.SJA_543_18

15. Carroll A, Ramirez PT, Westin SN, Soliman PT, Munsell MF, Nick AM, et al. Uterine adenosarcoma: an analysis on management, outcomes, and risk factors for recurrence. *Gynecol Oncol*. (2014) 135:455–61. doi: 10.1016/j.ygyno.2014.10.022

16. Arend R, Bagaria M, Lewin SN, Sun X, Deutsch I, Burke WM, et al. Long-term outcome and natural history of uterine adenosarcomas. *Gynecol Oncol*. (2010) 119:305–8. doi: 10.1016/j.ygyno.2010.07.001

17. Zaloudek CJ, Norris HJ. Adenofibroma and adenosarcoma of the uterus: a clinicopathologic study of 35 cases. *Cancer*. (1981) 48:354–66. doi: 10.1002/(ISSN)1097-0142

18. Ulrich UA, Denschlag D. Uterine adenosarcoma. *Oncol Res Treat*. (2018) 41:693–6. doi: 10.1159/000494067

19. Nathenson MJ, Conley AP. Prognostic factors for uterine adenosarcoma: a review. *Expert Rev Anticancer Ther Expert Rev Anticancer Ther*. (2018) 18:1093–100. doi: 10.1080/14737140.2018.1518136

20. Seagle BL, Kanis M, Strohl AE, Shahabi S. Survival of women with mullerian adenosarcoma: a national cancer data base study. *Gynecol Oncol*. (2016) 143:636e41. doi: 10.1016/j.ygyno.2016.10.013

21. Machida H, Nathenson MJ, Takiuchi T, Adams CL, Garcia-Sayre J, Matsuo K. Significance of lymph node metastasis on survival of women with uterine adenosarcoma. *Gynecol Oncol*. (2017) 144:524–30. doi: 10.1016/j.ygyno.2017.01.012

22. Verschraegen CF, Vasuratna A, Edwards C, R Freedman R, Kudelka AP, Tornos C, et al. Clinicopathologic analysis of mullerian adenosarcoma: the M.D. Anderson Cancer experience. *Oncol Rep*. (1998) 5:939–44. doi: 10.3892/or

23. Tanner EJ, Toussaint T, Leitao MM Jr., Hensley ML, Soslow RA, Gardner GJ, et al. Management of uterine adenosarcomas with and without sarcomatous overgrowth. *Gynecol Oncol*. (2013) 129:140–4. doi: 10.1016/j.ygyno.2012.12.036

24. Clement PB. Mullerian adenosarcomas of the uterus with sarcomatous overgrowth. A clinicopathological analysis of 10 cases. *Am J Surg Pathol*. (1989) 13:28–38. doi: 10.1097/00000478-198901000-00004

25. Denschlag D, Thiel FC, Ackermann S, Harter P, Juhasz-Boess I, Mallmann P, et al. Sarcoma of the uterus. Guideline of the DGGG (S2k-level, AWMF registry no. 015/074, august 2015). *Geburtsh Frauenheilkd*. (2015) 75:1028–42. doi: 10.1055/s-00000020

26. Parra-Herran C, Howitt BE. Uterine mesenchymal tumors: update on classification, staging, and molecular features. *Surg Pathol Clin*. (2019) 12:363–96. doi: 10.1016/j.path.2019.01.004

27. Guidozzi F, Smith T, Koller AB, Reinecke L. Management of uterine Mullerian adenosarcoma with extrauterine metastatic deposits. *GynecolOncol*. (2000) 77:464–6. doi: 10.1006/gyno.2000.5757

28. Krivak TC, Seidman JD, McBroom JW, MacKoul PJ, Aye LM, ScottRose G. Uterine adenosarcoma with sarcomatous overgrowth versus uterine carcinosarcoma: comparison of treatment and survival. *Gynecologic Oncol*. (2001) 83:89–94. doi: 10.1006/gyno.2001.6334

29. Nathenson MJ, Conley AP, Lin H, Fleming N, Ravi V. Treatment of recurrent or metastatic uterine adenosarcoma. *Sarcoma*. (2017) 2017:4680273. doi: 10.1155/2017/4680273

frontiers | Frontiers in Oncology

TYPE Case Report
PUBLISHED 22 May 2024
DOI 10.3389/fonc.2024.1370453

Check for updates

OPEN ACCESS

EDITED BY
Ferdinando Agresta,
ULSS2 Marca Trevigiana, Italy

REVIEWED BY
Teodor Florin Georgescu,
Carol Davila University of Medicine and Pharmacy, Romania
Alicia Bolt,
University of New Mexico, United States

*CORRESPONDENCE
Guilong Guo
guoguilong@sina.com

RECEIVED 14 January 2024
ACCEPTED 26 April 2024
PUBLISHED 22 May 2024

CITATION
Ding J, Gu H, Yang Z, Lu Y and Guo G (2024) Breast metastasis from lung adenocarcinoma: a case report and review of the literature. *Front. Oncol.* 14:1370453. doi: 10.3389/fonc.2024.1370453

COPYRIGHT
© 2024 Ding, Gu, Yang, Lu and Guo. This is an open-access article distributed under the terms of the Creative Commons Attribution License (CC BY). The use, distribution or reproduction in other forums is permitted, provided the original author(s) and the copyright owner(s) are credited and that the original publication in this journal is cited, in accordance with accepted academic practice. No use, distribution or reproduction is permitted which does not comply with these terms.

Breast metastasis from lung adenocarcinoma: a case report and review of the literature

Jialing Ding, Huayan Gu, Zhi Yang, Yiqiao Lu and Guilong Guo*

Department of Breast Surgery, The First Affiliated Hospital of Wenzhou Medical University, Wenzhou, Zhejiang, China

Lung cancer (LC) is one of the most lethal and most prevalent malignant tumors, and lung adenocarcinoma (LUAD) is the most common pathological type of lung cancer. Breast cancer (BC) is the most common cancer worldwide, but metastases to the breast from extramammary neoplasms are rare, especially from the lung. Early diagnosis and differentiation of primary from metastatic breast carcinoma are essential. Here, we present a case of metastases to the breast from lung adenocarcinoma, the treatment options varied according to disease progression.

KEYWORDS

lung cancer, breast metastasis, breast cancer, diagnosis, differentiation

Introduction

Female breast cancer has overtaken lung cancer as the most common diagnosed cancer worldwide (1). According to the statistics of the American Cancer Society (2), lung cancer has occupied the first place of cancer deaths (21% in both sexes), and breast cancer is second only to lung cancer in women. However, metastases to the breast from extramammary neoplasms are not very common (3). Koch et al. conducted a statistical analysis of 463 cases and obtained a proportion of breast metastases incidence from primary cancers rate: melanoma (29.8%), bronchial lung cancer (16.4%), gynecological cancer (12.7%), gastrointestinal cancer (9.9%), leukemia and lymphoma (8.4%), sarcoma (7.3%), and renal cancer (1.5%). Differentiating between primary breast cancer and breast metastases is a challenge, particularly when the metastases are identified as lung adenocarcinoma. At present, the main means include clinical manifestation, imaging characteristics, histological examination, and immunohistochemistry testing (IHC). The choice of combination treatment for primary and metastatic breast cancer is also different depending on the primary focus and pathology. Here, we present a case of metastases to the breast from lung adenocarcinoma and its treatment.

Case report

In February 2019, a 52-year-old woman with no history of smoking attended to our hospital complaining of recurring chest distress. Computed tomography (CT) scan revealed an abnormal mass and pleural effusion in her left lung. Subsequently, she underwent pleuroscopy and biopsy. Based on epidermal growth factor receptor (EGFR) mutational analysis, the specimen retrieved at pleuroscopy was identified as pulmonary adenocarcinoma with a mutation in exon-19 19-Del of the EGFR gene. Then, she received icotinib (125 mg orally three times daily) for therapy. However, 1 year later, the patient developed recurring plural effusion that was confirmed to be malignant plural effusion with T790 positivity, which indicated that she had developed a resistance mutation. Therefore, she changed to receive Osimertinib (AZD-9291) for therapy. In July 2022, as the disease progressed, she began to accept pemetrexed plus carboplatin and bevacizumab for 10 cycles of chemotherapy. Unfortunately, 4 years after the diagnosis of lung cancer, the patient's physical examination revealed breast lesions. Previously, the patient had no breast skin changes and no palpable breast lumps or local pain. The ultrasonic examination detected nodules in the left breast with calcifications (BI-RADS 4 degree), accompanied with bilateral axillary lymph node enlargement and left supraclavicular lymph node enlargement. She underwent minimally invasive mammotome biopsy (Figure 1), and the biopsy specimen revealed estrogen receptor (ER)-negative, progesterone receptor (PR)-negative, and HER2-negative invasive ductal carcinoma. Considering the patient's history of lung cancer, we conducted additional immunohistochemical tests on her and found that TTF-1 and Napsin-A results were positive, which indicated that the lung cancer had metastasized to the breast, so we chose to use albumin-bound paclitaxel plus cisplatin and Sintilimab for therapy. In the subsequent telephone follow-up, the patient was actively receiving lung cancer treatment, but we did not obtain effective breast examination information. The patient had no prior or family history of breast cancer before.

Discussion

Early diagnosis and differentiation of primary and metastatic breast cancer are important for timely treatment. Clinical history, imaging, and pathological findings should be taken into account in differentiating secondary mass from primary breast cancer. Previous studies have shown that the most common features of breast metastases present as palpable, rapidly growing, well-circumscribed, and painless breast masses with predilection to the upper outer quadrant. Unlike primary breast cancer, most metastatic breast cancers, while located on the surface, do not manifest as contractions of the skin or nipples (4). Imaging studies differential diagnosis relies on X-ray, ultrasound, and CT. For the wide range of imaging manifestations of the metastatic lesions, it may be extremely difficult to distinguish them if only based on mammographic findings. The absence of micro-calcifications is considered a characteristic of metastatic lesions to the breast, with the exception of ovarian cancer (5). There are very few studies in the literature on MRI findings for breast metastases.

If the diagnosis is based solely on clinical manifestations and imaging, it is easy to make mistakes. Immunohistochemistry plays a crucial role in diagnosis by using specific markers to distinguish primary breast cancer. According to the World Health Organization (WHO) classification, breast cancer (BC) is classified into many subtypes, as defined by IHC testing of ER, PR, HER2, and Ki67 status (6). Based on both molecular and histological evidence, BC could be categorized into three groups: BC expressing hormone receptor [estrogen receptor (ER+) or progesterone receptor (PR+)], BC expressing human epidermal receptor 2 (HER2+), and triple-negative breast cancer (TNBC) (ER−, PR−, and HER2−). The treatment approaches should be based in the BC molecular characteristics (7). ER, PR, and Her-2 were all negative in metastatic breast cancer, which was easily confused with TNBC. Therefore, for patients with a history of malignant tumors, relevant markers of the primary lesion should be added to the immunohistochemical test. Specific immunohistochemical markers for lung carcinoma include thyroid transcription factor-1 (TTF-1),

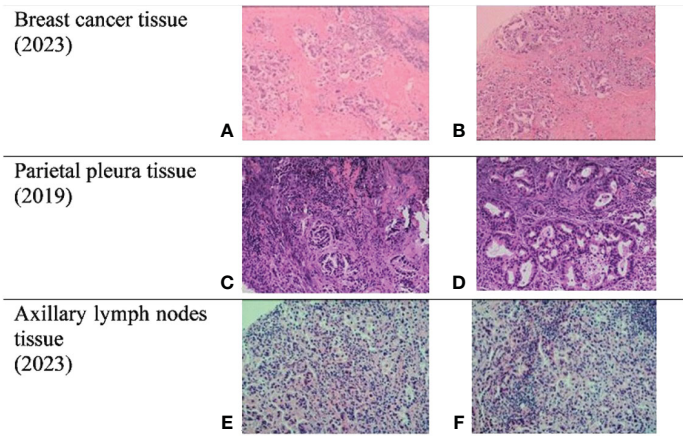

FIGURE 1
Biopsies. **(A, B)** Breast cancer tissue from mammotome biopsy. **(C, D)** Parietal pleura tissue from pleuroscopy biopsy. **(E, F)** Axillary lymph nodes (ALN) tissue from core needle biopsy. ER and PR were both negative in these three tissues, and NapsinA and TTF-1 were both positive in them.

Napsin-A, and CK7. Since no single marker is complete sensitive and false negative results are inevitable, we must use a panel of markers to improve accuracy. The double stain of TTF-1 and Napsin A was proposed for increased sensitivity and specificity for lung cancer. We conducted a comprehensive analysis of the existing literature, including 29 reported cases with detailed immunohistochemical results and our case. (Table 1) TTF-1 was positive in 26 breast biopsies. Only two breast biopsies were negative for TTF-1 and Napsin A, and their lung biopsy markers were also negative, which was consistent. In Takayo Ota' report (25), the patient initially had no detectable immunohistochemical markers specific to lung cancer and was therefore misdiagnosed with a double cancer. However, researchers analyzed her tissues again after her death and again found the same EGFR mutation, which she corrected for metastatic lung adenocarcinoma. In our report, the patient's IHC testing revealed ER–, PR–, and HER2– invasive ductal carcinoma, similar to TNBC. However, TTF-1, NapsinA, and CK7 indexes were all positive, indicating metastatic breast cancer rather than primary

TABLE 1 Breast lesion metastasis from primary lung cancer: literature review 2000–2023.

	Age	Sex	IHC markers of breast biopsy	IHC markers of lung biopsy
Gómez-Caro A (2006) (8)	65	Male	CK4– CK7– TTF-1–	CK4– CK7– TTF-1–
Rimner A(2007) (9)	81	Female	TTF-1+ ER– PR– HER-2–	TTF-1+
Fulciniti F (2007) (10)	59	Female	TTF-1+ ER– PR–	NA
Klingen TA (2009) (11)	79	Female	TTF-1+ CK7+	NA
	70	Male	TTF-1+ CK7+	NA
	54	Female	TTF-1+ CK7+	NA
Maounis N (2010) (12)	73	Female	TTF-1+ SP-A+ GCDFP15– ER– mammaglobin–	TTF-1+ CK 5/6– ER– CA-125- thyroglobulin–
Fukumoto K (2011) (13)	65	Female	TTF-1+ ER– EGFR-19 (E746-A750) mutation	EGFR-19 (E746-A750) +
Ko K (2012) (14)	47	Female	TTF-1+ ER– PR– mammaglobin–	NA
Sato K (2012) (15)	57	Female	TTF1+ CK7+ SP-A+ CK20– GCDFP15– ER– PR– HER-2–	NA
Ji FF (2012) (16)	40	Female	TTF-1+ ER– PR– HER2– GCDFP15– mammaglobin–	NA
	49	Female	TTF-1+ ER– PR– HER2– GCDFP15– mammaglobin–	NA
Sousaris N (2013) (17)	55	Female	TTF-1+ napsin A+ ER– PR– HER-2–	NA
Huang HC (2013) (18)	70	Female	TTF-1+ GCDFP15– ER– PR–	EGFR-21-L858R+
Liam CK (2013) (19)	70	Female	TTF-1+ ALK– ER– PR– HER-2–	TTF-1+ ALK– Exon-20 T790M+
Hachisuka A (2014) (20)	60	Male	TTF-1– Napsin-A– SP-A– ER– PR– GCDFP15–	TTF-1- Napsin-A– SP-A– ER– PR– GCDFP15–
Dansin E, (2015) (21)	52	Female	TTF1+ GATA3– GCDFP15– PAX8– ER– PR-HER2–	Exon-19 19-Del +
Shen YW (2015) (4)	52	Female	TTF-1+ Napsin A+ CK7+ ER– PR– GCDFP15–	TTF-1+ CK7+ Napsin A+ CK20– CK5/6– GCDFP15–
Lin Q (2016) (22)	51	Male	TTF-1+ Chomogranin A+ Synaptophysin+ CD56+ ER– GCDFP15– HER–	TTF-1+ Synaptophysin+ CD56+ EGFR-21-L858R+
Ninan J (2016) (23)	67	Female	TTF-1+ Napsin A+ CK7+ GATA-3– GCDFP15–	NA
Cserni G (2017) (24)	60	Female	TTF-1+ Napsin A+ CK7+ GATA-3– PR– HER2– mammaglobin–	TTF1+ CK7+ p63–
Ota T (2018) (25)	69	Female	ER– PR– HER2– EGFR-21-L858R+	EGFR-21-L858R+
Enrico D (2019) (5)	29	Female	TTF-1+ CK7+ Napsin A+ AE1AE3+ P63– CK20– ER– PR– GATA3– HER2–	TTF-1+ CK7+ AE1AE3+ Napsin A+ P63– CK20–
our (2023)	52	Female	TTF-1+ Napsin A+ CK7+ ER– PR– HER2– Mammaglobin– GATA3– GCDFP15– CK20–	TTF-1+ Napsin-A+ CK7+ CD56– CgA– Syn–

NA, not available (not mentioned in patient's report).

TNBC. Combined with her clinical history, she was finally diagnosed with lung adenocarcinoma and breast metastasis. It is important to note that not everyone with a history of malignant tumors can be diagnosed with metastatic tumors, which can be both cancers at the same time. For example, a woman with a 1-year history of non-small-cell lung cancer came to our hospital with a painless breast mass. Combined with hematoxylin–eosin and immunohistochemical results, the final diagnosis was primary invasive breast cancer with positive ER and PR expression, and radical mastectomy and axillary dissection were performed. The case of metastatic breast cancer described in this report does not require surgery. In addition to surgery therapy, there are also principled differences in drug selection between primary breast cancer and metastatic breast tumor with extramammary cancer. Primary breast cancer is undoubtedly targeted at breast lesions; the treatment of metastatic breast disease is mainly focused on the primary lesion, so the treatment plan for patients with different primary lesions is often different. Targeted therapy and immunotherapy are currently emerging strategies that can target metastatic tumors, but research is still incomplete and their contribution to reducing mortality is not significant (26). It can be concluded that distinguishing metastases breast cancer from primary breast carcinoma is essential because of therapeutic and prognostic significance. Multiple aspects must be combined in diagnosis, especially characteristic immune markers.

Accurate diagnosis and treatment are inseparable. In clinical practice, it is necessary to closely monitor the progress of advanced malignant tumors and make accurate diagnoses in a timely manner to avoid incorrect treatment. In the future, cancer treatment will move towards an era of precision, comprehensiveness, and individualization.

Data availability statement

The raw data supporting the conclusions of this article will be made available by the authors, without undue reservation.

Ethics statement

Written informed consent was obtained from the individual(s) for the publication of any potentially identifiable images or data included in this article.

Author contributions

JD: Conceptualization, Data curation, Formal analysis, Funding acquisition, Investigation, Methodology, Project administration, Resources, Software, Supervision, Validation, Visualization, Writing – original draft, Writing – review & editing. HG: Data curation, Formal analysis, Funding acquisition, Investigation, Methodology, Supervision, Writing – review & editing. ZY: Data curation, Formal analysis, Funding acquisition, Supervision, Validation, Writing – review & editing. YL: Data curation, Investigation, Resources, Software, Validation, Visualization, Writing – review & editing. GG: Conceptualization, Investigation, Methodology, Project administration, Resources, Software, Supervision, Validation, Visualization, Writing – review & editing.

Funding

The author(s) declare that no financial support was received for the research, authorship, and/or publication of this article.

Acknowledgments

The authors thank the patient for her agreement to the publication of the report.

Conflict of interest

The authors declare that the research was conducted in the absence of any commercial or financial relationships that could be construed as a potential conflict of interest.

Publisher's note

All claims expressed in this article are solely those of the authors and do not necessarily represent those of their affiliated organizations, or those of the publisher, the editors and the reviewers. Any product that may be evaluated in this article, or claim that may be made by its manufacturer, is not guaranteed or endorsed by the publisher.

References

1. Hong R, Xu B. Breast cancer: an up-to-date review and future perspectives. *Cancer Commun (Lond)*. (2022) 42:913–36. doi: 10.1002/cac2.12358

2. Siegel RL, Miller KD, Wagle NS, Jemal A. Cancer statistics, 2023. *CA Cancer J Clin*. (2023) 73:17–48. doi: 10.3322/caac.21763

3. Koch A, Richter-Marot A, Wissler MP, Baratte A and Mathelin C. Mammary metastasis of extramammary cancers: current knowledge and diagnostic difficulties. *Gynecol Obstet Fertil*. (2013) 41:653–9. doi: 10.1016/j.gyobfe.2013.09.013

4. Shen YW, Sui YX, Zhang XM, Lv M, Zhang X, Liu PJ, et al. Ipsilateral breast metastasis from a pulmonary adenocarcinoma: a case report and a focused review of the literature. *Int J Clin Exp Pathol*. (2015) 8:9647–54.

5. Enrico D, Saucedo S, Bravo I. Breast metastasis from primary lung adenocarcinoma in a young woman: A case report and literature review. *World J Clin Oncol*. (2019) 10:269–78. doi: 10.5306/wjco.v10.i7.269

6. Dai X, Li T, Bai Z, Yang Y, Liu X, Zhan J, et al. Breast cancer intrinsic subtype classification, clinical use and future trends. *Am J Cancer Res*. (2015) 5:2929–43.

7. Barzaman K, Karami J, Zarei Z, Hosseinzadeh A, Kazemi MH, Moradi-Kalbolandi S, et al. Breast cancer: Biology, biomarkers, and treatments. *Int Immunopharmacol*. (2020) 84:106535. doi: 10.1016/j.intimp.2020.106535

8. Gómez-Caro A, Piñero A, Roca MJ, Torres J, Ferri B, Galindo PJ, et al. Surgical treatment of solitary metastasis in the male breast from non-small cell lung cancer. *Breast J*. (2006) 12:366–7. doi: 10.1111/j.1075-122X.2006.00278.x

9. Rimner A, Rosenzweig KE. Palliative radiation for lung cancer metastases to the breast: two case reports. *J Thorac Oncol*. (2007) 2:1133–5. doi: 10.1097/JTO.0b013e31815ba7ba

10. Fulciniti F, Losito S, Botti G, Di Mattia D, La Mura A, Pisano C, et al. Metastases to the breast: role of fine needle cytology samples. Our experience with nine cases in 2 years. *Ann Oncol*. (2008) 19:682–7. doi: 10.1093/annonc/mdm546

11. Klingen TA, Klaasen H, Aas H, Chen Y, Akslen LA. Secondary breast cancer: a 5-year population-based study with review of the literature. *APMIS*. (2009) 117:762–7. doi: 10.1111/j.1600-0463.2009.02529.x

12. Maounis N, Chorti M, Legaki S, Ellina E, Emmanouilidou A, Demonakou M, et al. Metastasis to the breast from an adenocarcinoma of the lung with extensive micropapillary component: a case report and review of the literature. *Diagn Pathol*. (2010) 5:82. doi: 10.1186/1746-1596-5-82

13. Fukumoto K, Usami N, Okasaka T, Kawaguchi K, Okagawa T, Suzuki H, et al. Late breast metastasis from resected lung cancer diagnosed by epidermal growth factor receptor gene mutation. *Lung Cancer*. (2011) 74:352–3. doi: 10.1016/j.lungcan.2011.08.015

14. Ko K, Ro JY, Hong EK, Lee S. Micropapillary lung cancer with breast metastasis simulating primary breast cancer due to architectural distortion on images. *Korean J Radiol*. (2012) 13:249–53. doi: 10.3348/kjr.2012.13.2.249

15. Sato K, Takeyama Y, Yoshihara M, Kato T, Hashimoto H, Fukui Y, et al. CBDCA + Pemetrexed + Bevacizumab and its maintenance chemotherapy in a case of solitary breast metastasis from a lung adenocarcinoma resistant to gefitinib. *Case Rep Oncol*. (2012) 5:546–53. doi: 10.1159/000343678

16. Ji FF, Gao P, Wang JG, Zhao J, Zhao P. Contralateral breast metastasis from pulmonary adenocarcinoma: two cases report and literature review. *J Thorac Dis*. (2012) 4:384–9. doi: 10.3978/j.issn.2072-1439.2012.02.03

17. Sousaris N, Mendelsohn G, Barr RG. Lung cancer metastatic to breast: case report and review of the literature. *Ultrasound Q*. (2013) 29:205–9. doi: 10.1097/RUQ.0b013e3182a00fc4

18. Huang HC, Hang JF, Wu MH, Chou TY, Chiu CH. Lung adenocarcinoma with ipsilateral breast metastasis: a simple coincidence? *J Thorac Oncol*. (2013) 8:974–9. doi: 10.1097/JTO.0b013e31828f6873

19. Liam CK, Pang YK, Poh ME, Kow KS, Wong CK, Varughese R. Advanced right lung adenocarcinoma with ipsilateral breast metastasis. *Respirol Case Rep*. (2013) 1:20–2. doi: 10.1002/rcr2.14

20. Hachisuka A, Takahashi R, Nakagawa S, Takahashi H, Inoue Y, Akashi M, et al. Lung adenocarcinoma metastasis to the male breast: a case report. *Kurume Med J*. (2014) 61:35–41. doi: 10.2739/kurumemedj.MS63010

21. Dansin E, Carnot A, Servent V, Daussay D, Robin YM, Surmei-Pintilie E, et al. EGFR-mutated breast metastasis of lung adenocarcinoma: a case report. *Case Rep Oncol*. (2015) 8:164–8. doi: 10.1159/000381014

22. Lin Q, Cai GP, Yang KY, Yang L, Chen CS, Li YP. Case report: small cell transformation and metastasis to the breast in a patient with lung adenocarcinoma following maintenance treatment with epidermal growth factor receptor tyrosine kinase inhibitors. *BMC Cancer*. (2016) 16:593. doi: 10.1186/s12885-016-2623-4

23. Ninan J, Naik V, George GM. 'Inflammatory breast cancer' due to metastatic adenocarcinoma of lung. *BMJ Case Rep*. (2016) 2016:bcr2016215857. doi: 10.1136/bcr-2016-215857

24. Cserni G. Solitary breast metastasis from oestrogen receptor-positive pulmonary adenocarcinoma: report of a case with a potential pitfall. *Pol J Pathol*. (2017) 68:168–72. doi: 10.5114/pjp.2017.69694

25. Ota T, Hasegawa Y, Okimura A, Sakashita K, Sunami T, Yukimoto K, et al. Breast metastasis from EGFR-mutated lung adenocarcinoma: A case report and review of the literature. *Clin Case Rep*. (2018) 6:1510–6. doi: 10.1002/ccr3.1636

26. Esposito M, Ganesan S, Kang Y. Emerging strategies for treating metastasis. *Nat Cancer*. (2021) 2:258–70. doi: 10.1038/s43018-021-00181-0

frontiers | Frontiers in Oncology

TYPE Case Report
PUBLISHED 06 June 2024
DOI 10.3389/fonc.2024.1387700

Check for updates

OPEN ACCESS

EDITED BY
Lidia Castagneto Gissey,
Sapienza University of Rome, Italy

REVIEWED BY
Stergios Boussios,
Canterbury Christ Church University, United Kingdom
Teodor Florin Georgescu,
Carol Davila University of Medicine and Pharmacy, Romania
Mario Murguia-Perez,
Mexican Social Security Institute, Mexico

*CORRESPONDENCE
Xiaofeng Yang
yxf73@163.com

†These authors have contributed equally to this work

RECEIVED 18 February 2024
ACCEPTED 17 May 2024
PUBLISHED 06 June 2024

CITATION
Li S, Zhu J, Jiang N, Guo Y, Hou M, Liu X, Yang J and Yang X (2024) Recurrent mucinous carcinoma with sarcomatoid and sarcomatous mural nodules: a case report and literature review.
Front. Oncol. 14:1387700.
doi: 10.3389/fonc.2024.1387700

COPYRIGHT
© 2024 Li, Zhu, Jiang, Guo, Hou, Liu, Yang and Yang. This is an open-access article distributed under the terms of the Creative Commons Attribution License (CC BY). The use, distribution or reproduction in other forums is permitted, provided the original author(s) and the copyright owner(s) are credited and that the original publication in this journal is cited, in accordance with accepted academic practice. No use, distribution or reproduction is permitted which does not comply with these terms.

Recurrent mucinous carcinoma with sarcomatoid and sarcomatous mural nodules: a case report and literature review

Simin Li[1†], Jingyu Zhu[1†], Na Jiang[2], Yanping Guo[1], Meng Hou[1], Xi Liu[2], Jin Yang[3] and Xiaofeng Yang[1*]

[1]Department of Gynecology and Obstetrics, First Affiliated Hospital of Xi 'an Jiaotong University, Xi'an Jiaotong University, Xi'an, Shaanxi, China, [2]Department of Pathology, First Affiliated Hospital of Xi 'an Jiaotong University, Xi'an Jiaotong University, Xi'an, Shaanxi, China, [3]Department of Oncology, First Affiliated Hospital of Xi 'an Jiaotong University, Xi'an Jiaotong University, Xi'an, Shaanxi, China

Ovarian mucinous tumors with sarcomatous mural nodules are rare. Sarcomatous nodules have a bad prognosis. Its diagnosis and treatment are controversial.It is still controversial whether malignant mural nodules represent a dedifferentiated form of mucinous tumors or collisional tumors. This is a case report of a 32-year-old female diagnosed with ovarian mucinous tumor recurred as a mucinous carcinoma combined with sarcomatoid and undifferentiated sarcoma mural nodules after surgery and chemotherapy. The primary lesion did not have a sarcomatous component after comprehensive sampling and repeated review, while the recurrent lesion had a predominantly sarcomatous component. The patient received a second operation and postoperative chemotherapy plus Anlotinib with no progression at 16 months of follow-up. Primary mucinous carcinoma and sarcomatous mural nodules revealed the same K-RAS mutation(c.35G>T, pG12V), TP53 mutation (c.817C>T, p.R273C), MLL2 mutation(c.13450C>T, p.R4484) and NF1 mutation(c.7876A>G, p.S2626G). We present a comprehensive analysis on morphologic characteristics, molecular detection results, clinical management, and prognosis of ovarian mucinous tumors with mural nodules of sarcomatoid and undifferentiated sarcoma. Mutation sharing between primary mucinous carcinoma and recurrent sarcomatous nodules supports monoclonal origin of primary and recurrent tumors, suggesting a tendency for sarcomatous differentiation during the progression of epithelial tumors. Malignant mural nodules represent dedifferentiation in mucinous ovarian tumors rather than collision of two different tumor types. Therefore, it is imperative to conduct comprehensive sampling, rigorous clinical examination, and postoperative follow-up in order to thoroughly evaluate all mural nodules of ovarian mucinous tumors due to their potential for malignancy and sarcomatous differentiation.

KEYWORDS

mucinous ovarian carcinoma, sarcomatous mural nodules, sarcoma-like mural nodule, undifferentiated sarcoma, KRAS, TP53, mutation

Introduction

Ovarian mucinous tumors with mural nodules are a special type of ovarian surface epithelial-stromal tumor. Ovarian mucinous tumors, whether benign, borderline, or malignant, may be associated with a variety of mural nodules, including sarcomatoid mural nodules (SLMNs), sarcoma, and anaplastic carcinoma. Only approximately 12 cases of sarcomatous nodules have been reported in the last 30 years. Reviewing the literature, these nodules range from benign histology, such as sarcomatoid, to malignant histology, including anaplastic carcinoma, carcinosarcoma, and sarcoma (fibrosarcoma, rhabdomyosarcoma, osteosarcoma, and pleomorphic undifferentiated sarcoma) (Table 1). Among these, SLMNs are the most common and have a relatively good prognosis, while sarcomatous nodules are the rarest and are considered to have the worst prognosis (11). To the best of our knowledge, there are no reports of recurrent mucinous carcinoma with mural nodules of ovarian mucinous cystadenocarcinoma. Due to its rarity, most of the knowledge comes from case reports in the literature. Their pathological diagnosis and treatment are still inconclusive due to few reports. The histogenesis of the mural nodule remains unknown.

Using immunohistochemistry and a 1021 gene panel of next-generation gene sequencing for tumors before and after recurrence, we investigated a case of primary ovarian mucinous cystadenocarcinoma and recurrence as mucinous carcinoma with SLMNs and undifferentiated sarcoma. Four common mutations were found in the two groups. This study retrospectively analyzed the clinical manifestation, treatment, prognosis, pathology, immunophenotype and genetic mutations in primary and recurrent tumors to elucidate their classification, origin and treatment. We also summarize similar cases to raise awareness of this disease among clinicians.

Case presentation

A 33-year-old female patient presented with a 10-day history of frequent urination and was subsequently referred to First Affiliated Hospital of Xi 'an Jiaotong University in July 2021. Gynecological examination revealed a well-defined pelvic mass measuring 15 × 15 × 14 cm on the right side. The ultrasound demonstrated a cystic mass measuring 15.2 × 9.6 ×13.7 cm adjacent to the uterus on the left side. Laboratory investigations revealed elevated levels of carcinoembryonic antigen (CEA) at 290 ng/ml, carbohydrate antigen (CA199) exceeding 1000 U/ml, carbohydrate antigen (CA125) at 583 U/ml, and carbohydrate antigen (CA724) surpassing 300 U/ml. Pelvic magnetic resonance imaging (MRI) exhibited a large cystic and solid mass in the left ovary with evidence of minimal intracystic hemorrhage. Computed tomography (CT) scan indicated cystic and solid ovarian neoplasms along with minimal fluid accumulation within the abdomen and pelvis. She underwent appendectomy due to appendicitis in 2004.The patient's family history revealed her mother died of ovarian cancer.

The patient underwent a total abdominal hysterectomy, bilateral salpingo-oophorectomy, and omentectomy at the First Affiliated Hospital of Xi'an Jiaotong University on August 4, 2021. Intraoperatively, a left-sided cystic and solid ovarian mass measuring approximately 18 × 10 × 10 cm with a smooth surface and intact capsule was observed. Intraoperative frozen section pathology revealed a moderately differentiated adenocarcinoma of the left ovary. The final diagnosis was stage Ia ovarian mucinous cystadenocarcinoma according to FIGO classification. Post-surgery, the patient received intraperitoneal infusion chemotherapy with cisplatin and systemic intravenous chemotherapy with paclitaxel and carboplatin.

After completing four courses of chemotherapy, an MRI scan conducted four months post-surgery detected a metastasis in the lower abdomen measuring 5 × 4.8 × 4 cm. A biopsy of the mass confirmed its mucinous nature with sarcomatoid nodules. Pathology consultation at the Cancer Prevention and Treatment Centre of Sun Yat-sen University indicated that mucinous tumors with sarcomatoid nodules and tend to metastatic lesions.

To ascertain the recurrence status and presence of distant metastases, positron emission tomography/computed tomography (PET/CT) was conducted on March 1, 2022. The imaging revealed multiple soft tissue nodules in the splenogastric space, mesenteric space, anterior to the right psoas major muscle at the level of lumbar vertebra 5, pelvis, and left side of the pelvic floor. Some nodules exhibited calcified density and increased glucose metabolism, indicating metastatic involvement. Tumor markers were approximately normal. Considering its rapidly growing biological behavior and pathology findings, a potential recurrence of mucinous tumor with sarcomatous component was considered. The patient underwent two cycles of chemotherapy (doxorubicin and cisplatin) combined with bevacizumab. Subsequent CT scans showed no significant changes. Solid margins were observed along with central necrosis within the pelvic mass (previously exhibiting solid center with calcified spots) (Figure 1). These observations suggest minimal disease progression and limited response to chemotherapy. Therefore, surgical intervention was proposed.

The secondary tumor cell reduction surgery was performed on May 10, 2022. Intraoperatively, a solid mass measuring 16 cm x 11 cm x 9 cm was observed in the pelvic cavity, adhering to the greater omentum, peritoneum, small intestine, and Douglas pouch. Two metastatic lesions measuring approximately 3 cm and 2 cm in diameter were identified in the mesentery of the right paracolic sulci. They exhibited hardness and adherence to both colon and peritoneum. Additionally, two metastatic lesions with an approximate diameter of 2 cm each were found in the splenic flexure. Multiple metastatic foci were observed on the surface of the small intestine's mesentery. Intraoperative frozen section pathology revealed epithelioid malignant tumors with giant cells with necrosis. All macroscopically visible lesions were successfully excised during surgery. Postoperatively, hyperthermic intraperitoneal chemotherapy (HIPEC) was administered along with six cycles of ifosfamide plus doxorubicin chemotherapy regimen. Subsequently, the patient received anlotinib

Abbreviations: SLMNs, sarcomatoid mural nodules; CEA, carcinoembryonic antigen; CA199, carbohydrate antigen 199; CA125, carbohydrate antigen 125; CA724, carbohydrate antigen 724; MRI, magnetic resonance imaging; CT, Computed Tomography; PET/CT, Positron emission tomography/computed tomography; HIPEC, hyperthermic intraperitoneal chemotherapy; VIM, Vimentin; CK, cytokeratin; LOH, Loss of heterozygosity; STS, soft tissue sarcomas.

TABLE 1 Summary of the cases of ovarian mucinous tumors with malignant mural nodules.

	case	age of patients	pathology diagnosis	initial symptom	mural nodule	FIGO stage	therapy	follow-up
Jaime Prat and Robert E. Scully (1979) (1)	2 (Case 1)	61	mucious cystadenoma	abdominal swelling	fibrosarcoma	Unkown	TAH+BSO +appen+RT	36months (hepatic metastases)
Jaime Prat and Robert E. Scully (1979) (1)	2 (Case 2)	49	mucinous cystadenocarcinoma	Progressive abdominal swelling 1month	undifferentiated sarcoma	Unkown	BSO +omen+PALNB	1week (renal failure)
Jan A,Bruijin et al(1987) (2)	1	27	mucinous cystadenocarcinoma	lower abdominal swelling	fibrosarcoma	Ia	USO(left)+omen	Unkown
Takashi Tsujimura and Kiyoshi Kawano (1992) (3)	1	57	mucinous cystadenocarcinoma	lower abdominal mass	Rhabdomyosarcoma	Unkown	TAH+BSO+CHT	NED,3 months
M. A. RAHILLY (1994) (4)	1	69	cystadenocarcinoma	lower abdominal pain	fibrosarcoma	II	TAH+BSO+ appendicectomy +CHT	NED, 12months
Mohamed et al (2014) (5)	1	25	mucious carcinoma	abdominal swelling with ascites	highly malignant sarcoma	Ia	excision of the ovarian mass and complete staged surgery	Unkown
Marie McFarland et al (2015) (6)	2 (Case 1)	34	mucinous carcinoma of intestinal type	persistent vaginal bleeding and abdominal swelling	Osteosarcoma	Ia	TAH+BSO	NED,18months
Marie McFarland et al (2015) (6)	2 (Case 2)	18	borderline mucinous tumor of intestinal type	abdominal swelling	Osteosarcoma	Ic	left oophorectomy +omen	NED,12month
Yan Zhang et al (2017) (7)	2 (Case1)	60	mucinous carcinoma and cystadenoma and borderline malignancy cystadenoma	Lower abdominal pain	sarcomatous	I	BSO+omen	Unkown
Wen Wang et al (2017) (8)	1	42	mucinous borderline tumor		low-grade endometrial stromal sarcoma	II	left salpingo-oophorectomy and adhesiolysis	NED,10months
Ying Shao et al (2020) (9)	3 (Case 2)	41	mucious carcinoma	pelvic mass	sarcoma	IIa	TAH+BSO+omen + PPLND+CHT	18months(lung metastasis); NED,40months
Ling-Hui Chu et al(2021) (10)	1	65	mucious cystadenoma	Progressive abdominal swelling and inadequate uptake	osteosarcoma	Ic	USO(right)	NED,16months

TAH, total abdominal hysterectomy; BSO, bilateral salpingo-oophorectomy; USO, unilateral salpingo-oophorectomy; appen, appendectomy; omen, omentectomy; CHT, chemotherapy; DOD, died of disease; NED, no evidence of disease; RT, radiation therapy; PALNB, para-aortic lymph node biopsy; PPLND, pelvic/para-aortic lymph node dissection.

maintenance therapy. Regular follow-up for a period of sixteen months without any signs of disease progression.

Pathologic results

Primary tumor

Grossly, the left ovarian cystic mass measured 15.5 × 13 × 4 cm and exhibited a grayish red color with a smooth surface. Cross-sections revealed both cystic and solid areas. The multilocular cystic regions contained dark brown and bloody fluid ranging in diameter from 0.5-5 cm. The solid area measured 6 cm × 6 cm and displayed a grayish white section.

Microscopically, the tumor tissue demonstrated an adenoidal arrangement, with some glands exhibiting a back-to-back arrangement. Within the glandular cavity, tumor cells formed complex papillary structures, accompanied by visible fibrovascular axes at the center of each papilla (Figure 2A). These tall columnar tumor cells possessed abundant cytoplasm, primarily mucilaginous.

FIGURE 1
CT scan prior to the second operation. Hepatogastric space, mesenteric space, the largest of multiple soft tissue nodules in front of the right psoas major muscle at the level of the fifth lumbar vertebra, on the left side of the pelvic floor was approximately 13.6*11*9.4 cm in size, which was uneven and partially accompanied by calcified density.

Part of the cytoplasm appeared eosinophilic. The nuclei were rod-shaped or oval with distinct nuclear membranes, prominent nucleoli, and evident nuclear division (Figure 2B).

The final diagnosis indicated highly to moderately differentiated papillary mucinous cystadenocarcinoma of the left ovary without extension to the surface of the left ovary. Subsequently, the patient was referred to the Cancer Prevention and Treatment Centre of Sun Yat-sen University for pathological consultation which confirmed the initial diagnosis: microscopic morphology consistent with well to moderately differentiated papillary mucinous cystadenocarcinoma of the ovary.

Immunohistochemical analysis revealed strong positive expression of CAM52 and Pax-8 in tumor cells. Tumor cells expressed Ki-67 at approximately 60%, while SATB2, H3.3G34 W, WT1,and p63 exhibited negative expression.

Recurrence tumor

Macroscopically, the pelvic nodular mass measured 16 cm x 11 cm x 9 cm and exhibited a grayish-red, grayish-yellow appearance with a rough surface. Upon sectioning, it revealed localized areas of gray-white solid tissue with hemorrhagic, necrotic and crispy areas. Additionally, two nodular masses measuring 1.5-3 cm in diameter were observed in the colonic sulcus. These masses displayed a gray-pink surface and a gray-white section with a firm texture. Furthermore, three mesenteric nodular masses measuring 0.5-1.5 cm in diameter were identified to have similar characteristics of a gray-pink surface, gray-white section, and hard texture.

Microscopically examination revealed the presence of multinucleated tumor giant cells. The tumor cells showed pleomorphic changes arranged in an irregular pattern along with numerous pathological mitotic figures (Figures 2C–F).

The pathological diagnosis indicated the presence of giant cell-rich malignant tumor accompanied by necrosis within the pelvis, as well as malignant tumor infiltration featuring calcification and ossification within the fibrous tissue of the colonic groove and mesenteric nodule. It is considered to be a sarcoma-like mural nodule with local sarcoma formation (undifferentiated sarcoma).

Immunohistochemical analysis demonstrated strong positive expression of vimentin (VIM) and CD68 in tumor cells. Tumor cells expressed P53 and Ki-67 at approximately 60%, while cytokeratin (CK), SMA,Des,CK8/18,CK7,Pax-8,WT-1,CK20,ER,PR,CA125, ALK-1,CK5/6(-),CD10(-),CR(-),EMA(-),D2-40,P16were negative (Figure 3).

DNA sequencing

DNA was extracted separately from tissue sections of primary mucinous ovarian carcinoma and recurrence sarcomatous mural nodules using standard laboratory procedures. Next-generation sequencing (NGS) was performed by Geneplus Ltd (Beijing, China), using custom-designed probes covered approximately 1.1 Mb of genomic sequences of cancer-related genes for DNA capture. The 1021-gene panel sequencing was carried out on a Geneplus 2000 Sequencing System (Beijing, China) with 2×100 bp paired-end reads. The case was annotated for point mutations, small insertions and deletions (indels), copy number alterations, microsatellite instability, and tumor mutational burden. Matched blood samples were sequenced as control. Shared pathogenic KRAS alterations (c.35G>T, p.G12V), TP53 alterations(c.817C>T,p.R273C), MLL2 (c.13450C>T,p.R4484) and NF1(c.7876A>G,p.S2626G) were detected in the mucinous ovarian carcinoma and sarcomatous mural nodules. Besides, mucinous ovarian carcinoma harbored NLRC3 mutation (c.377G>A,p.R126Q). Sarcomatous mural nodules showed APC(c.3625G>A,p.E1209K) mutation and KRAS copy number alterations (NM_033360.2, 2.0 amplification). All mucinous ovarian tumors and mural nodules were microsatellite stable. Tumor mutational burden is 0.96mutations/megabase in mucinous ovarian tumors and 2.25 mutations/megabase in mural nodules.

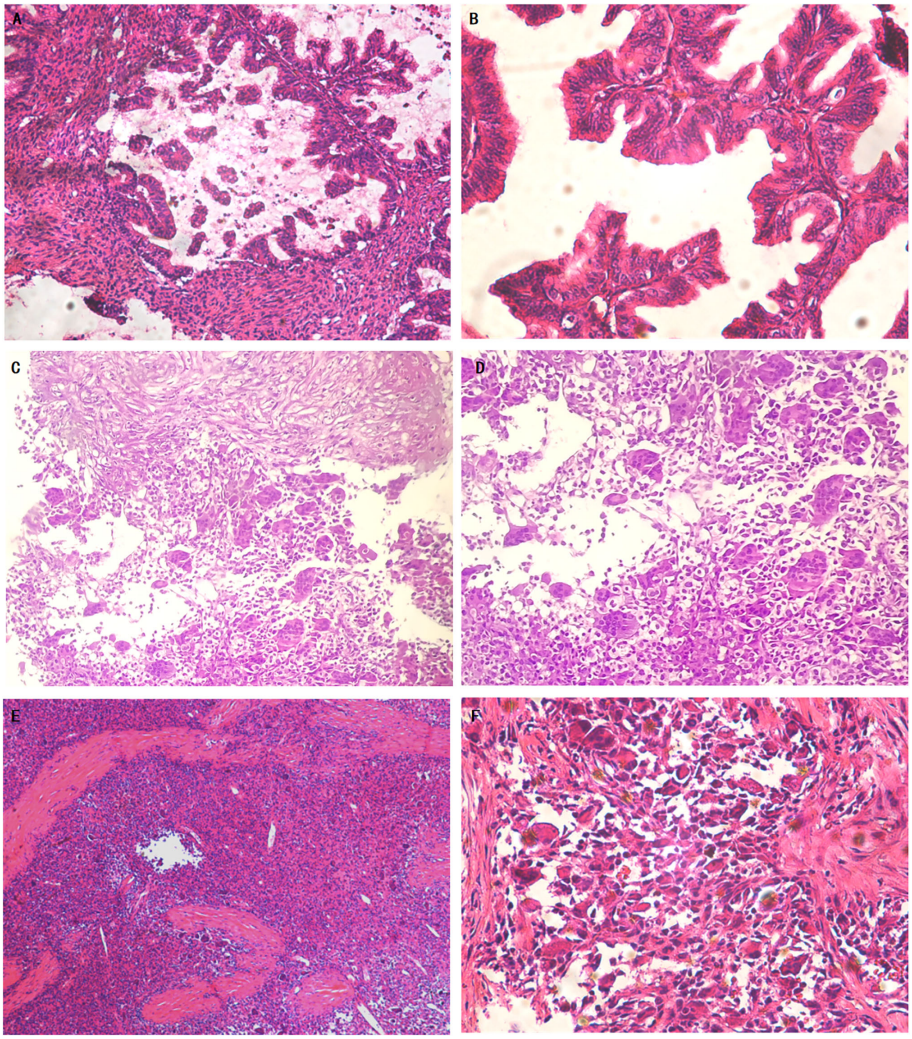

FIGURE 2
Primary mucinous cystadenocarcinoma of the ovary and recurrent mucinous carcinoma with sarcomatoid mural nodule and local undifferentiated sarcoma (Hematoxylin and eosin). Representative microscopic photos demonstrate the well-differentiated to moderately differentiated, invasive mucinous carcinoma **(A)**. On higher power, some of the glands showed back-to-back arrangement. The tumor cells were highly columnar with abundant cytoplasm, most of which was mucilage **(B)**. The pathology of the mass biopsy showed a recurrent mucinous tumor with sarcomatoid nodules. Focal mucinous carcinoma with abundant cytoplasm, most of which was mucinous, is seen in the upper part. In the lower part there are sarcomatoid nodules with multinucleated giant cells **(C)**. On higher power, the sarcomatoid nodules are composed of sarcomatoid multinucleated cells and multinucleated giant cells **(D)**. Sarcomatoid mural nodule with local undifferentiated sarcoma **(E)**. On higher power, multinucleated tumor giant cells were scattered or scaly. The tumor cells showed pleomorphic changes arranged in no fixed direction **(F)**.

Discussion

From 1979 to 2021, there were only 12 cases of ovarian mucinous tumors with sarcomatous mural nodules (Table 1). To our knowledge, this is the first case of SLMNs and undifferentiated sarcoma after treatment of ovarian mucinous cystadenocarcinoma of the ovary with KRAS, TP53, MLL2 and NF1 mutation. We summarize the characteristics of sarcomatous mural nodules and their differentiation from sarcomatoid mural nodules and provide a feasible treatment plan.

Mucinous tumors with mural nodules, such as sarcoma-like mural nodules (SLMNs), sarcomatous mural nodules, or anaplastic carcinoma, usually occur in giant ovarian cystic tumors. Sarcomatous nodules commonly occur in stage I ovarian mucinous tumors in women aged 18 to 65 years. The tumor markers did not increase significantly before the second surgery, which was similar to previously reported tumor markers. In 6 cases with reported tumor markers, serum tumor markers CA125 and CA199 increased slightly or remained normal, and no specific tumor markers of mural nodules were identified.

The prognosis of sarcomatous mural nodules is poor, and the prognosis of sarcoma-like nodules is better. In this case, recurrence and rapid growth were found 4 months after surgery, and the size of the nodule was 16 × 11 × 9 cm at the time of reoperation 8 months later, demonstrating the biological behavior of a sarcoma with rapid growth. Similar to our case, 2 cases of mucinous carcinoma with sarcomatous mural nodules. One patient developed liver metastasis after 36 months, and the other died of renal failure after surgery (1).

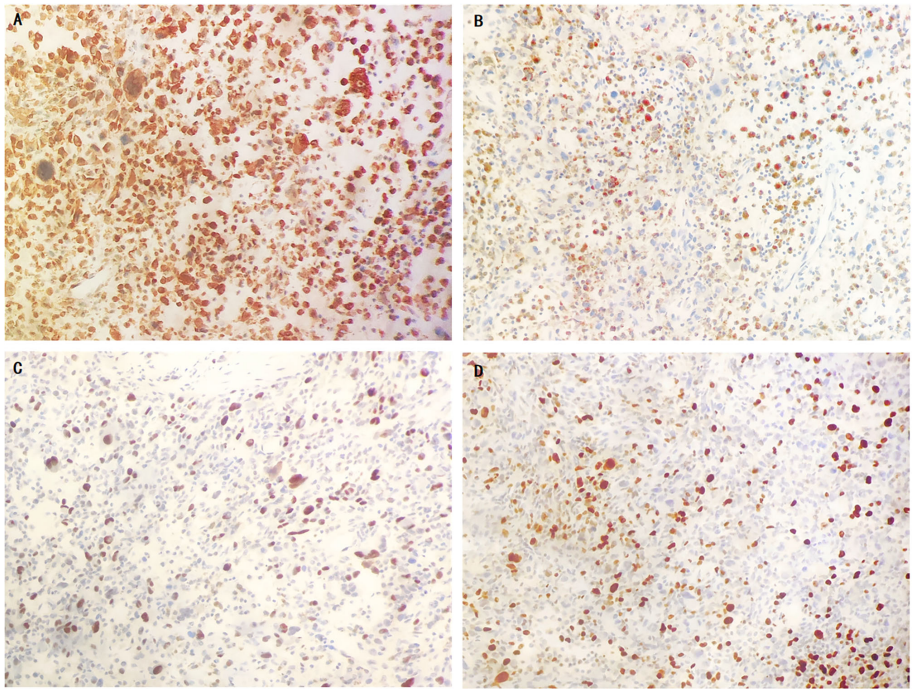

FIGURE 3
The immunohistochemical results of sarcoma component. tumor cells showed diffusely strongly positive for vimentin **(A)**, partially positive for CD68 **(B)**, 60% positive for P53 **(C)** and Ki67 **(D)**.

A stage IIa mucinous carcinoma with sarcomatous mural nodules was reported lung metastasis at 18 months of follow-up (9). In contrast, 7 cases of SLMN reported by J. Prat and R.E. Scully were followed up for 1 to 11 and a half years (mean 7.5 years) with no evidence of recurrence (12). These cases suggest that sarcomatoid mural nodules are not sarcomas and may be a reactive process that does not affect the prognosis of patients (13). However, sarcomas are highly invasive and have a poor prognosis in previous case reports, even in patients with stage Ia ovarian mucinous carcinoma. Stage I primary highly differentiated ovarian mucinous adenocarcinoma has a good prognosis and a high etiology-specific 10-year survival rate (92.7%). In contrast, undifferentiated soft tissue sarcoma has a poor prognosis, with local recurrence rates of 19-31%, metastasis rates of 31-35%, 5-year survival rates of 65-70% and a median survival of approximately 12 months (14, 15). Therefore, the identification of sarcomatous mural nodules is particularly important for the management and prognosis of patients.

Gross morphology and microscopic pathologic diagnosis of mural nodules are essential to identify sarcomatous mural nodules. According to the description of previous cases, sarcomatous nodules are characterized by large volume, obvious hemorrhage and necrosis, indistinct border infiltration, with or without lymphatic vascular invasion, often containing mononuclear or multinucleated malignant tumor cells, giant cells, obvious nuclear atypia and atypical mitosis and inconspicuous inflammatory infiltration (1, 16). The size of the tumor was more than 10 cm, and necrosis in the central area was obvious. In our case, the tumor cells showed polymorphic changes with odd-shaped tumor giant cells and a large number of pathological nuclear divisions. In contrast, SLMNs are predominantly small in size, well demarcated from adjacent mucosal epithelium, and composed of mixed cell groups, including inflammatory cells and osteoclast-like giant cells, which may be prominent around the central hemorrhagic cavity, with significant inflammatory infiltration without vascular infiltration (12, 17). Although morphologic differences have been described, sarcoma and sarcomatoid nodules are not always easy to distinguish morphologically. Both of them have necrosis, obvious nuclear atypia and abundant mitosis (including atypical forms) (13, 17). In this case, atypical vimentin-positive spindle cell and CD68-positive giant cell in the sarcoma component are similar to one case of sarcoma and one case of osteosarcoma nodule (7, 10).Sarcomatoid nodules were sometimes weakly positive for CK (18). Immunohistochemistry of the sarcoma component in this case failed to classify the nodules as any conventional sarcoma because it lacked markers of smooth muscle, skeletal muscle and endothelial differentiation.

On the origin of mucinous cystic tumors of the ovary with mural nodules, SLMNs may be benign reactive changes to intramural bleeding or cyst mucus content, resulting in pseudotumors, such as inflammatory pseudotumors or inflammatory myofibroblastoma elsewhere (17). At present, there are two main theories to explain the origin of sarcomatous mural nodules: (1) The collision theory holds that two tumor types, epithelial cells and mesenchymal cells, collide independently, showing that carcinoma and sarcoma are two independent

tumors with polyclonal characteristics. (2) The transformation theory suggests that the sarcoma component is derived from cancer during tumor evolution or the differentiation of primitive stem cells into one cell type, which in turn differentiates into a second cell type (19). In our case, Gene detection results support the transformation theory, because ovarian mucinous carcinoma and sarcomatous nodules had the same KRAS, TP53, NF1 and MLL2 mutations. Consistent with our case, David B. Chapel found a clonal relationship between mural nodules and ovarian mucinous tumors, with KRAS alterations and TP53 mutations in 10 of 13 cases. There was a codon 12 mutation with different nucleotide substitutions of the K-RAS gene in both ovarian invasive mucinous adenocarcinoma and high-grade sarcomatous mural nodules, suggesting that sarcomatous mural nodules may be a dedifferentiated form of mucinous tumors (20). Increased expression of tumor protein p53, and p53 alongside Wilms tumor 1 (WT1) are associated with reduced overall survival and dismal prognosis of carcinomas and carcinosarcomas (21). In contrast, in another case, loss of heterozygosity (LOH) was present at the D18S51 and FGA loci in the adenocarcinoma component, while LOH was present at the D19S433 locus in the sarcoma component, supporting that sarcoma nodules and mucinous tumors may represent the tumor collision phenomenon (9).

Although recurrence of mucinous ovarian cancer presenting with sarcomatous mural nodules has not been reported, recurrence of epithelial tumors with sarcoma components exists. Seven cases of ovarian cancer recurring as carcinosarcoma have been reported in the past (22). In recent years, these tumors are considered to be metaplastic carcinomas. Frederick found that the composition of metastatic lesions changed over time based on pathology results from 26 women diagnosed with ovarian carcinosarcoma. Two cases of epithelial ovarian cancer relapsed as carcinosarcomas, and the incidence of metastatic lesions dominated by sarcomas was three times higher than that of initial surgery (24% vs 8%, respectively), supporting the potential for phenotypic transformation during ovarian cancer progression (23, 24). In our case, all sections from previous biopsies were re-examined, but no sarcomatous component was detected (25). According to the transformation theory and the hypothesis of Wen Wang (8). We suggest that the subepithelial mesenchymal cells react with intramural bleeding or mucinous contents, resulting in the formation of proliferative nodules and enlargement into the SLMN, mesenchymal cells continue to proliferate and differentiate, and part of the SLMN is transformed into true sarcoma.

It is noteworthy that P53, KRAS was expressed in both primary and recurrent sarcomatous tumors. In other cases, p53 was overexpressed in almost all serous ovarian carcinoma and recurrent carcinoma and sarcoma components (24). The most common genetic alterations in ovarian mucinous tumors are somatic KRAS mutations, with an incidence of 50% to 68% in borderline and malignant tumors (15–17). Some studies believe mural nodules in mucinous ovarian tumors do not associated with KRAS and TP53 genetic abnormalities, as the mutation rates of KRAS and TP53 are equally high in both components (11). Recently, it has been suggested that vimentin expression may be associated with the ability of high-grade epithelial tumors to recur as carcinosarcomas or sarcomas. Breast cancers expressing vimentin proteins may originate from progenitor cells with bilinear (glandular and myoepithelial) differentiation potential (26).

A comprehensive genomic analysis has reported that the NF1 gene is one of the most frequently altered genes in soft tissue sarcomas (STS) (27). Studies have demonstrated that individuals with NF1 mutations are predisposed to developing STS (28). *In vitro* experiments, NF1 promotes the initiation and progression of UPS by inhibiting the PI3K-Akt-mTOR-S6 pathway (28). PI3K pathway is frequently upregulated in epithelial ovarian cancers and plays an important role in cell survival. Chemoresistance and preservation of genomic stability, the inhibition of the PI3K may lead to genomic instability and mitotic catastrophe (29). SIFT (30) and Polvphen-2 (31) predicted a deleterious effect of NF1 mutation in this patient, which may be associated with sarcoma development.

Somatic mutations of MLL1 implicated in the pathogenesis of cancer. High mutation rates have been observed in endometrial carcinoma, esophageal sarcomatoid carcinoma, gastric cancer (32). In colon cancer cells lacking MLL2 expression, the target gene expression spectrum of MLL2 revealed its role in promoting transcription of retinoic acid reactive genes such as ASB2. Additionally, MLL2 regulates other transcription factors including NR3C1 and p53. These findings provide insights into the potential mechanism by which MLL2 contributes to cancer progression (33). Specifically, a MLL2 gene c.13450C>T(p.R4484 nonsense mutation) results in an amino acid substitution at position 4484 of the premature termination codon formation, leading to functional impairment or loss of protein expression through nonsense mediated mRNA degradation. The presence of these inactivating mutations suggests that MLL2 functions as a tumor suppressor altering overall gene expression.

Inactivation of the APC gene plays a crucial role in the development and progression of colorectal cancer, while APC gene alterations are rare in sarcomas. One case of primary osteosarcoma reported an APC gene polymorphism (34). Pathogenic mutations in APC lead to aberrant expression of the APC/Axin/Gsk-3 complex or inhibition of the Wnt pathway, resulting in stabilization and accumulation of β-catenin within epithelial cell cytoplasm (35). This allows for migration into the nucleus where it can form a functional transcription factor with TCF/LEF-1 and activate certain oncogenes such as vimentin (35, 36). In this case, missense mutation detection was found in the sarcoma component but not detected in mucinous carcinoma. Software prediction indicated it is a benign mutation. Therefore we do not believe this change drives occurrence of sarcomas. Firstly, it is unlikely that missense mutations alone are responsible for APC gene inactivation. Secondly, compensatory function by axin (another component of the β-catenin/GSK-3β/APC/axin complex) with tumor suppressor activity has already been confirmed (37).

Studies have shown that maximal cytoreduction improves prognosis in patients with advanced ovarian cancer or

undifferentiated sarcomas (38). In this case, chemotherapy plus bevacizumab was tried after recurrence, and the effect was not satisfactory, so tumor reduction surgery was performed. After surgery, intraperitoneal hyperthermic perfusion chemotherapy was performed for mucinous cancer components. Intravenous chemotherapy with isocyclophosphamide plus doxorubicin for the sarcoma component. Currently she was treated with amlotinib maintenance therapy according to the Chinese Society of Clinical Oncology (CSCO) 2022 guidelines which recommend amlotinib as a second-line treatment for advanced or unresectable class 1A soft tissue sarcoma. A study used amlotinib as maintenance therapy for soft tissue sarcoma after chemotherapy reported complete relief in one case of undifferentiated pleomorphic sarcoma, achieving an overall response rate (ORR) of 14.3% and disease control rate (DCR) of 81.0% (39). No evidence of recurrence has been observed during the 19-month follow-up period. Additionally, pembrolizumab represents another option for advanced soft tissue sarcomas ineligible for chemotherapy. Targeted therapies aimed at inhibiting the K-RAS signaling pathway may theoretically benefit tumor patients with K-RAS mutations. Promising therapeutic targets have emerged from pathways downstream of Ras activation resulting from NF1 mutations (40).

Conclusions

In conclusion, ovarian mucinous cystic tumors with mural nodules are a rare and unique type of ovarian tumor that often occurs in giant ovarian cysts. Patients with sarcoma components tend to relapse rapidly and have a poor prognosis. According to previous reports and the genetic analysis of our case, we believe that the sarcoma component may be formed by the transformation of epithelial components and associated with NF1, MLL2 mutations. In clinical practice, doctors should take care to preserve the integrity of cysts during surgery. Pathologists need to take comprehensive samples of mucinous tumors and carefully evaluate them to avoid misdiagnosis and missed diagnosis.

Data availability statement

The original contributions presented in the study are included in the article/Supplementary Material. Further inquiries can be directed to the corresponding author.

Ethics statement

Written informed consent was obtained from the individual(s) for the publication of any potentially identifiable images or data included in this article.

Author contributions

SL: Data curation, Methodology, Project administration, Validation, Writing – original draft, Writing – review & editing. JZ: Methodology, Writing – review & editing, Software, Visualization. NJ: Data curation, Investigation, Writing – review & editing, Conceptualization, Methodology, Visualization. YG: Writing – review & editing, Data curation, Investigation. MH: Investigation, Methodology, Writing – review & editing. XL: Data curation, Visualization, Writing – review & editing. JY: Investigation, Writing – review & editing. XY: Funding acquisition, Project administration, Writing – review & editing.

Funding

The author(s) declare financial support was received for the research, authorship, and/or publication of this article. Funded by Clinical Research Center, First Affiliated Hospital of Xi ʻan Jiaotong University (grants XJTU1AF2021CRF -025).

Conflict of interest

The authors declare that the research was conducted in the absence of any commercial or financial relationships that could be construed as a potential conflict of interest.

Publisher's note

All claims expressed in this article are solely those of the authors and do not necessarily represent those of their affiliated organizations, or those of the publisher, the editors and the reviewers. Any product that may be evaluated in this article, or claim that may be made by its manufacturer, is not guaranteed or endorsed by the publisher.

Supplementary material

The Supplementary Material for this article can be found online at: https://www.frontiersin.org/articles/10.3389/fonc.2024.1387700/full#supplementary-material

SUPPLEMENTARY FIGURE 1
Timeline with relevant data from the episode of care.

SUPPLEMENTARY FIGURE 2
Heatmap (ChiPlot) shows the comparsion of gene mutation frequency between primary mucinous ovarian carcinoma and recurrence sarcomatous mural nodules. KRAS alterations,TP53 alterations, MLL2 and NF1 were detected in the mucinous ovarian carcinoma and sarcomatous mural nodules. Mucinous ovarian carcinoma harbored NLRC3 mutation. Sarcomatous mural nodules showed APC mutation.

References

1. Prat J, Scully RE. Sarcomas in ovarian mucinous tumors: a report of two cases. *Cancer*. (1979) 44:1327–31. doi: 10.1002/(ISSN)1097-0142

2. Bruijn JA, Smit VT, Que DG, Fleuren GJ. Immunohistology of a sarcomatous mural nodule in an ovarian mucinous cystadenocarcinoma. *Int J Gynecol Pathol*. (1987) 6:287–93. doi: 10.1097/00004347-198709000-00009

3. Tsujimura T, Kawano K. Rhabdomyosarcoma coexistent with ovarian mucinous cystadenocarcinoma: a case report. *Int J Gynecol Pathol*. (1992) 11:58–62. doi: 10.1097/00004347-199201000-00009

4. Rahilly MA, Candlish W, Al-Nafussi A. Fibrosarcoma arising in an ovarian mucinous tumor: a case report. *Int J Gynecol Cancer*. (1994) 4:211–4. doi: 10.1046/j.1525-1438.1994.04030211.x

5. Desouki MM, Khabele D, Crispens MA, Fadare O. Ovarian mucinous tumor with Malignant mural nodules: dedifferentiation or collision? *Int J Gynecol Pathol*. (2015) 34:19–24. doi: 10.1097/pgp.0000000000000105

6. McFarland M, Dina R, Fisher C, McCluggage WG. Osteosarcoma as Malignant mural nodule in ovarian mucinous neoplasms of intestinal type: Report of 2 cases. *Int J Gynecol Pathol*. (2015) 34:369–73. doi: 10.1097/pgp.0000000000000153

7. Zhang Y, Yuan Z, Sun K, Li P. Ultrasonic and pathological characteristics of ovarian mucinous cystic tumors with Malignant mural nodules: Two cases report. *Med (Baltimore)*. (2017) 96:e8636. doi: 10.1097/md.0000000000008636

8. Wang W, Zhuang Y, Zhou F, Huang L. Ovarian mucinous borderline tumor accompanied by LGESS with myxoid change: a case report and literature review. *Eur J Med Res*. (2017) 22:52. doi: 10.1186/s40001-017-0295-4

9. Shao Y, Liu Q, Shi H, Lu B. Ovarian mucinous tumors with mural nodules: immunohistochemical and molecular analysis of 3 cases. *Diagn Pathol*. (2020) 15:35. doi: 10.1186/s13000-020-00956-6

10. Chu LH, Lai HC, Liao YT. Ovarian mucinous cystadenoma with a mural nodule of osteosarcoma: A case report. *Taiwan J Obstet Gynecol*. (2021) 60:136–8. doi: 10.1016/j.tjog.2020.10.002

11. Chapel DB, Lee EK, Da Silva AFL, Teschan N, Feltmate C, Matulonis UA, et al. Mural nodules in mucinous ovarian tumors represent a morphologic spectrum of clonal neoplasms: a morphologic, immunohistochemical, and molecular analysis of 13 cases. *Mod Pathol*. (2021) 34:613–26. doi: 10.1038/s41379-020-0642-9

12. Prat J, Scully RE. Ovarian mucinous tumors with sarcoma-like mural nodules: a report of seven cases. *Cancer*. (1979) 44:1332–44. doi: 10.1002/1097-0142(197910)44:4<1332::AID-CNCR2820440426>3.0.CO;2-#

13. Provenza C, Young RH, Prat J. Anaplastic carcinoma in mucinous ovarian tumors: a clinicopathologic study of 34 cases emphasizing the crucial impact of stage on prognosis, their histologic spectrum, and overlap with sarcomalike mural nodules. *Am J Surg Pathol*. (2008) 32:383–9. doi: 10.1097/PAS.0b013e3181451b93

14. Goldblum JR. An approach to pleomorphic sarcomas: can we subclassify, and does it matter? *Mod Pathol*. (2014) 27 Suppl 1:S39–46. doi: 10.1038/modpathol.2013.174

15. Savina M, Le Cesne A, Blay JY, Ray-Coquard I, Mir O, Toulmonde M, et al. Patterns of care and outcomes of patients with METAstatic soft tissue SARComa in a real-life setting: the METASARC observational study. *BMC Med*. (2017) 15:78. doi: 10.1186/s12916-017-0831-7

16. Prat J, Young RH, Scully RE. Ovarian mucinous tumors with foci of anaplastic carcinoma. *Cancer*. (1982) 50:300–4. doi: 10.1002/(ISSN)1097-0142

17. Bagué S, Rodríguez IM, Prat J. Sarcoma-like mural nodules in mucinous cystic tumors of the ovary revisited: a clinicopathologic analysis of 10 additional cases. *Am J Surg Pathol*. (2002) 26:1467–76. doi: 10.1097/00000478-200211000-00009

18. Matias-Guiu X, Aranda I, Prat J. Immunohistochemical study of sarcoma-like mural nodules in a mucinous cystadenocarcinoma of the ovary. *Virchows Arch A Pathol Anat Histopathol*. (1991) 419:89–92. doi: 10.1007/bf01600221

19. del Carmen MG, Birrer M, Schorge JO. Carcinosarcoma of the ovary: a review of the literature. *Gynecol Oncol*. (2012) 125:271–7. doi: 10.1016/j.ygyno.2011.12.418

20. Desouki MM, Fadare O, Kanbour A, Kanbour-Shakir A. Immunophenotype and K-RAS mutation in mucinous ovarian adenocarcinoma with mural nodule of high-grade sarcoma: case report. *Int J Gynecol Pathol*. (2014) 33:186–90. doi: 10.1097/PGP.0b013e3182830a05

21. Ismail A, Choi S, Boussios S. Frontiers of ovarian carcinosarcoma. *Curr Treat Options Oncol*. (2023) 24:1667–82. doi: 10.1007/s11864-023-01138-4

22. Hale D, Senem DA, Ovgu A, Hakan E, Sennur I, Zerrin C, et al. Serous ovarian carcinoma recurring as Malignant mixed mullerian tumor. *Case Rep Obstet Gynecol*. (2015) 2015:612824. doi: 10.1155/2015/612824

23. Amant F, Vloeberghs V, Woestenborghs H, Moerman P, Vergote I. Transition of epithelial toward mesenchymal differentiation during ovarian carcinosarcoma tumorigenesis. *Gynecol Oncol*. (2003) 90:372–7. doi: 10.1016/s0090-8258(03)00326-3

24. Ferrandina G, Carbone A, Zannoni GF, Martinelli E, Testa AC, Gallotta V, et al. Serous ovarian carcinoma recurring as a heterologous carcinosarcoma. *J Obstet Gynaecol Res*. (2007) 33:95–9. doi: 10.1111/j.1447-0756.2007.00488.x

25. Moritani S, Moriya T, Kushima R, Sugihara H, Harada M, Hattori T. Ovarian carcinoma recurring as carcinosarcoma. *Pathol Int*. (2001) 51:380–4. doi: 10.1046/j.1440-1827.2001.01212.x

26. Korsching E, Packeisen J, Liedtke C, Hungermann D, Wülfing P, van Diest PJ, et al. The origin of vimentin expression in invasive breast cancer: epithelial-mesenchymal transition, myoepithelial histogenesis or histogenesis from progenitor cells with bilinear differentiation potential? *J Pathol*. (2005) 206:451–7. doi: 10.1002/path.1797

27. Lucchesi C, Khalifa E, Laizet Y, Soubeyran I, Mathoulin-Pelissier S, Chomienne C, et al. Targetable alterations in adult patients with soft-tissue sarcomas: Insights for personalized therapy. *JAMA Oncol*. (2018) 4:1398–404. doi: 10.1001/jamaoncol.2018.0723

28. Zhang P, Huang L, Ma P, Niu X. Altered expressions of NF1 and NF1-related microRNAs as biomarkers in the diagnosis of undifferentiated pleomorphic sarcoma. *Front Genet*. (2022) 13:870191. doi: 10.3389/fgene.2022.870191

29. Aliyuda F, Moschetta M, Ghose A, Sofia Rallis K, Sheriff M, Sanchez E, et al. Advances in ovarian cancer treatment beyond PARP inhibitors. *Curr Cancer Drug Targets*. (2023) 23:433–46. doi: 10.2174/1568009623666230209121732

30. Sorting Intolerant From Tolerant (2023). Available online at: https://sift.bii.a-star.edu.sg/ (Accessed 5 September 2023).

31. PolyPhen-2 (Polymorphism Phenotyping v2) (2023). Available online at: http://genetics.bwh.harvard.edu/pph2/ (Accessed 5 September 2023).

32. Klonou A, Chlamydas S, Piperi C. Structure, activity and function of the MLL2 (KMT2B) protein lysine methyltransferase. *Life (Basel)*. (2021) 11:823. doi: 10.3390/life11080823

33. Li Y, Zhao L, Tian X, Peng C, Gong F, Chen Y. Crystal structure of MLL2 complex guides the identification of a methylation site on P53 catalyzed by KMT2 family methyltransferases. *Structure*. (2020) 28:1141–1148.e1144. doi: 10.1016/j.str.2020.07.002

34. Kuhnen C, Herter P, Monse H, Kahmann S, Muehlberger T, Vogt PM, et al. APC and beta-catenin in alveolar soft part sarcoma (ASPS)–immunohistochemical and molecular genetic analysis. *Pathol Res Pract*. (2000) 196:299–304. doi: 10.1016/S0344-0338(00)80059-X

35. Saito T, Oda Y, Sakamoto A, Kawaguchi K, Tanaka K, Matsuda S, et al. APC mutations in synovial sarcoma. *J Pathol*. (2002) 196:445–9. doi: 10.1002/path.1066

36. Miyoshi Y, Iwao K, Nagasawa Y, Aihara T, Sasaki Y, Imaoka S, et al. Activation of the beta-catenin gene in primary hepatocellular carcinomas by somatic alterations involving exon 3. *Cancer Res*. (1998) 58:2524–7.

37. Nakamura T, Hamada F, Ishidate T, Anai K, Kawahara K, Toyoshima K, et al. Axin, an inhibitor of the Wnt signalling pathway, interacts with beta-catenin, GSK-3beta and APC and reduces the beta-catenin level. *Genes Cells*. (1998) 3:395–403. doi: 10.1046/j.1365-2443.1998.00198.x

38. Yalcin I, Meydanli MM, Turan AT, Taskin S, Sari ME, Gungor T, et al. Carcinosarcoma of the ovary compared to ovarian high-grade serous carcinoma: impact of optimal cytoreduction and standard adjuvant treatment. *Int J Clin Oncol*. (2018) 23:329–37. doi: 10.1007/s10147-017-1215-x

39. Zhang RS, Liu J, Deng YT, Wu X, Jiang Y. The real-world clinical outcomes and treatment patterns of patients with unresectable locally advanced or metastatic soft tissue sarcoma treated with anlotinib in the post-ALTER0203 trial era. *Cancer Med*. (2022) 11:2271–83. doi: 10.1002/cam4.4613

40. Walker JA, Upadhyaya M. Emerging therapeutic targets for neurofibromatosis type 1. *Expert Opin Ther Targets*. (2018) 22:419–37. doi: 10.1080/14728222.2018.1465931

frontiers | Frontiers in Oncology

TYPE Case Report
PUBLISHED 07 June 2024
DOI 10.3389/fonc.2024.1353943

Check for updates

OPEN ACCESS

EDITED BY
Lidia Castagneto Gissey,
Sapienza University of Rome, Italy

REVIEWED BY
Joselle Cook,
Mayo Clinic, United States
Paweł Kiczmer,
Medical University of Silesia, Poland

*CORRESPONDENCE
Katarzyna Stawarz
katarzyna.stawarz@coi.pl

RECEIVED 11 December 2023
ACCEPTED 20 May 2024
PUBLISHED 07 June 2024

CITATION
Stawarz K, Galazka A, Gorzelnik A, Durzynska M, Bienkowska-Pluta K and Zwolinski J (2024) Case report: An uncommon presentation of extramedullary plasmacytoma without a concurrent diagnosis of multiple myeloma. *Front. Oncol.* 14:1353943. doi: 10.3389/fonc.2024.1353943

COPYRIGHT
© 2024 Stawarz, Galazka, Gorzelnik, Durzynska, Bienkowska-Pluta and Zwolinski. This is an open-access article distributed under the terms of the Creative Commons Attribution License (CC BY). The use, distribution or reproduction in other forums is permitted, provided the original author(s) and the copyright owner(s) are credited and that the original publication in this journal is cited, in accordance with accepted academic practice. No use, distribution or reproduction is permitted which does not comply with these terms.

Case report: An uncommon presentation of extramedullary plasmacytoma without a concurrent diagnosis of multiple myeloma

Katarzyna Stawarz[1]*, Adam Galazka[1], Anna Gorzelnik[1], Monika Durzynska[2], Karolina Bienkowska-Pluta[1] and Jakub Zwolinski[1]

[1]Head and Neck Cancer Department, Maria Sklodowska-Curie National Research Institute of Oncology, Warsaw, Poland, [2]Department of Pathology, Maria Sklodowska-Curie, National Research Institute of Oncology, Warsaw, Poland

Introduction: Extramedullary plasmacytoma (EMP) is an uncommon solitary tumor originating from neoplastic plasma cells located outside the bone marrow. Despite its rarity, the occurrence of EMP without a concurrent diagnosis of multiple myeloma (MM) is considered extremely rare. Approximately 80–90% of EMP cases are found in the head and neck region, with a higher incidence in men aged between 50 and 60 years. The current treatment modalities include radiotherapy (RT) as a first-line approach, with surgery or chemotherapy regarded as other therapeutic options. While RT proves effective in the majority of EMP cases, there are instances where the tumor remains refractory to radiation. In this case report, we present an unusual scenario of EMP resistant to RT without concurrent signs of multiple myeloma which was successfully treated with surgery followed by systemic therapy.

Case report: A 72-year-old male was admitted to the Head and Neck Cancer Clinic with a 6-month history of swallowing difficulties. He denied experiencing weight loss or pain on swallowing. Basic laboratory tests yielded results within normal limits, except for beta-2 microglobulin. Physical examination revealed an enlarged submandibular lymph node on the right side. Fiberoptic examination identified a soft tissue polypoid mass within the right piriform fossa, slightly protruding into the vocal slit. A CT scan displayed a well-circumscribed 2 cm polypoid, homogeneously enhancing soft tissue mass adjacent to the posterior surface of the epiglottis and the right side of the tongue base. Bone marrow biopsy revealed no abnormalities, and there were no clinical or laboratory signs of multiple myeloma. Based on the tumor biopsy results and imaging studies, a diagnosis of EMP was made. Due to the lack of response to RT, surgical removal of the tumor was pursued, followed by systemic therapy. Ultimately, the patient achieved full recovery with effective disease control.

Conclusion: In conclusion, EMP without concurrent multiple myeloma is an exceedingly rare condition that demands a multidisciplinary approach for both diagnosis and treatment. Moreover, although RT continues to be the primary standard treatment for EMP, in some cases other therapeutic regimens prove to be successful.

KEYWORDS

extramedullary plasmacytoma, multiple myeloma, case report, radiotherapy, surgery

Introduction

Extramedullary plasmacytoma (EMP) is a rare solitary tumor originating from neoplastic plasma cells located outside the bone marrow. It does not involve the bone marrow and can manifest anywhere in the body, with a predilection for soft tissues, particularly in the head and neck region (1, 2). EMP accounts for approximately one-third of solitary plasmacytoma tumors, constituting up to 5% of all plasma cell malignancies (3). The upper respiratory and digestive tracts are the most common sites for EMP, representing 80–90% of cases (4). This slow-growing submucosal malignancy typically presents its initial symptoms related to the mass effect, resulting in the obstruction of local structures and causing dysphagia, odynophagia, or voice problems. Male patients are more frequently affected, with an average age at diagnosis in their fifth to sixth decade of life (5). While EMP is regarded as an uncommon malignancy which can sometimes progresses to multiple myeloma, the occurrence of EMP without multiple myeloma remain exceedingly rare (6). The diagnosis of EMP is established through tumor and bone marrow biopsies, as well as laboratory tests and imaging studies (7). Although radiotherapy (RT) is the currently recommended treatment option due to the tumor's radiosensitivity and excellent disease control, its efficacy may be insufficient in certain cases (8). Moreover, the challenging location of the tumor underscores the importance of individualizing the optimal therapeutic approach. In instances of resistance to RT, surgery and chemotherapy remain viable therapeutic alternatives that have proven effective in some patients (9). In this case scenario we described a patient with the EMP resistant to RT with no signs of multiple myeloma which was successfully treated with surgery and systemic therapy.

Abbreviations: CRAB, (C) calcium elevation, (R) renal insufficiency, (A) anemia, (B) bone abnormalities; CT, computed tomography; EBV, Epstein Barr virus EMP, extramedullary plasmacytoma; Gy, Grey; HR, heart rate; IMRT, intensity-modulated radiation therapy; LBCL, large B-cell lymphoma; MM, multiple myeloma; LDH, lactate dehydrogenase; MRI, magnetic resonance imaging; RR, respiratory rate, RT, radiotherapy; SCC, squamous cell carcinoma.

Case report

A 72-year-old male of Polish origin was admitted to the Head and Neck Cancer Clinic at the National Institute of Oncology in Poland with a 6-month history of swallowing problems. He denied weight loss but admitted occasional swallowing difficulties, with no reported hoarseness or pain on swallowing. His past medical history was notable for hypertension, and there was no family history of neoplastic, genetic, or metabolic disorders. The patient denied cigarette smoking or alcohol use disorder. On presentation, his vital signs were within normal limits (HR: 87, RR: 132/87 mm Hg, temperature: 36.6°C). Physical examination revealed no abnormalities in the mouth or nasal cavities, but an enlarged submandibular lymph node was palpated on the right side of the neck. Indirect laryngoscopy and fiberoptic exams revealed a round 2 cm, smooth polypoid mass protruding from the right piriform fossa, partially occluding the vocal slit during phonation (Figures 1A, B). Laboratory tests showed Hb 13 g/dL, calcium level of 10.5 mg/dL, free kappa chains of 18.30 mg/L, free lambda chains of 15.90 mg/L, with a Kappa/Lambda ratio of 1.15. Additionally, normal serum BUN/creatinine, sodium, potassium, albumin, and LDH levels were detected. The patient underwent a whole body CT scan, and based on the laboratory results, a hematological and oncological consultation was ordered to rule out lymphoma, multiple myeloma, or other hematological malignancies. Further tests included serum quantitative immunoglobulins (IgM: 42.3 mg/dL, IgG: 796 mg/dL, IgA: 245 mg/dL), serum protein electrophoresis, monoclonal protein immunofixation (all normal), and a slightly elevated beta-2-microglobulin level of about 3.33 mg/L. No Bence-Jones protein was detected in the 24-hour urine collection. The CT scan revealed a well-circumscribed polypoid homogeneously enhancing soft tissue mass adjacent to the posterior surface of the epiglottis and the right side of the tongue base, approximately measuring 17x11mm x 23mm. An enlarged lymph node posterior to the right submandibular gland, reaching about 23x20mm, was also noted. Subsequently, the patient underwent an open biopsy procedure of the tumor, along with a bone marrow biopsy. The tumor pathological findings confirmed the diagnosis of EMP (Figures 2A–F). Additionally, since the patient showed no signs of multiple myeloma, and the bone marrow biopsy yielded normal results, the diagnosis of multiple myeloma was excluded. Moreover,

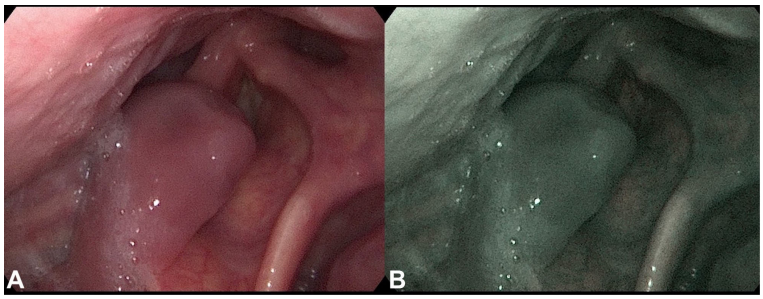

FIGURE 1
Fiberoptic examination of the throat tumor. Fiberoptic exam displaying a polypoid throat protruding from the right piriform fossa, partially occluding the vocal slit during phonation. **(A)** Conventional white-light image. **(B)** NBI (Narrow Band Imaging) image of the same site.

the histopathological findings helped rule out diagnoses such as lymphoma, sarcoma, or squamous cell carcinoma (SCC).Given the histopathological, laboratory, and imaging findings, the patient was scheduled for a re-consultation with a hematologic specialist and radiotherapist to initiate treatment. Subsequently, the patient underwent intensity-modulated radiation therapy (IMRT) with a total dose of 42 Gy over the next 4 weeks, comprising five sessions per week. Nevertheless, the RT turned out to be unsuccessful with no evidence of a tumor decrease on fiberoptic exam upon therapy completion. Due to the unsuccessful response to the radiotherapy, the patient underwent a PET/CT scan and was scheduled for surgical tumor removal. Whole-body PET/CT images displayed an increased FDG uptake in a soft tissue density lesion in the right throat originating from the right piriform fossa, as well as in the right cervical lymph node of IIA group, with no abnormal FDG avid uptake elsewhere suggesting a distant lesion. The maximum standardized uptake value of the tumor was 7.1 (Figures 3A, B). The surgical procedure was conducted under general anesthesia, with the use of a laryngoscope. The tumor was visualized and partially removed using microlaryngeal scissors and bipolar coagulation, as complete resection was not feasible, and only a debulking approach was applied (Figures 4A, B). Post-surgery, the patient underwent a follow-up visit after two weeks, during which a fiberoptic exam revealed a residual tumor mass (Figures 4C, D). Following this, the patient was referred for a hematological and oncological consultation to proceed with a chemotherapeutic regimen of dexamethasone and bortezomib, but due to severe side effects including numerous bleeding episodes, anemia and dizziness, and the absence of a MM diagnosis, chemotherapy was discontinued after one course. The therapeutic regimen comprised subcutaneous injections of bortezomib at a dose of 1.3 mg/m^2 on days 1, 4, 8, and 11 of a 21-day treatment cycle, along with dexamethasone administered at 20 mg on the day of and the day following bortezomib injection. Regular follow-up included fiberoptic exams every 3 months during the first year, MRI every 6 months, and a PET scan once per year. It has been 18 months since the diagnosis of EMP, and the patient remains under observation at the National Institute of Oncology with no signs of multiple myeloma or tumor recurrence detected thus far. Despite initially feeling overwhelmed by the diagnosis and the lack of response to radiotherapy, the patient

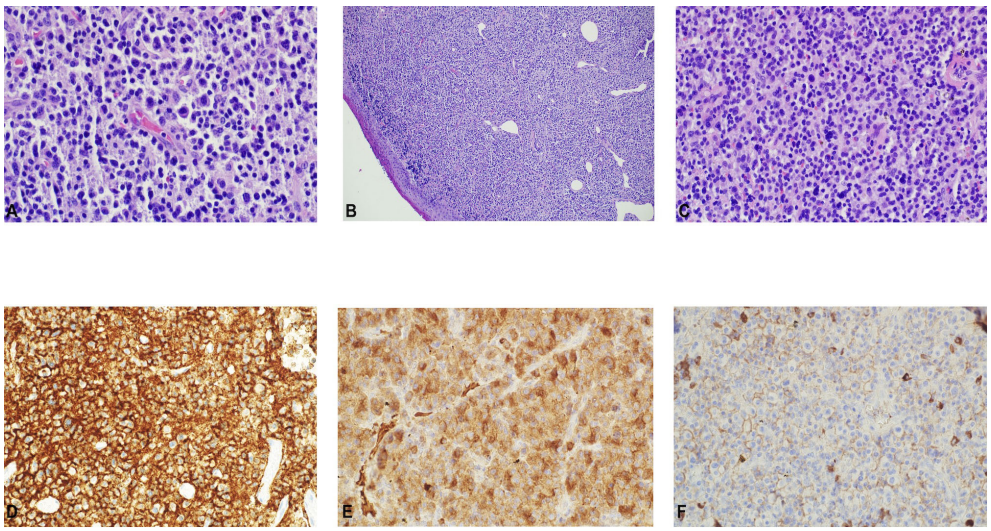

FIGURE 2
Histopathological assessment of the tumor. **(A–C)**. Throat tumor biopsy showing sheets of plasma cells. H&E. (x 400). Immunohistochemistry displaying positivity for **(D)** CD138, **(E)** lamda, and the **(F)** absence of kappa light chain expression.

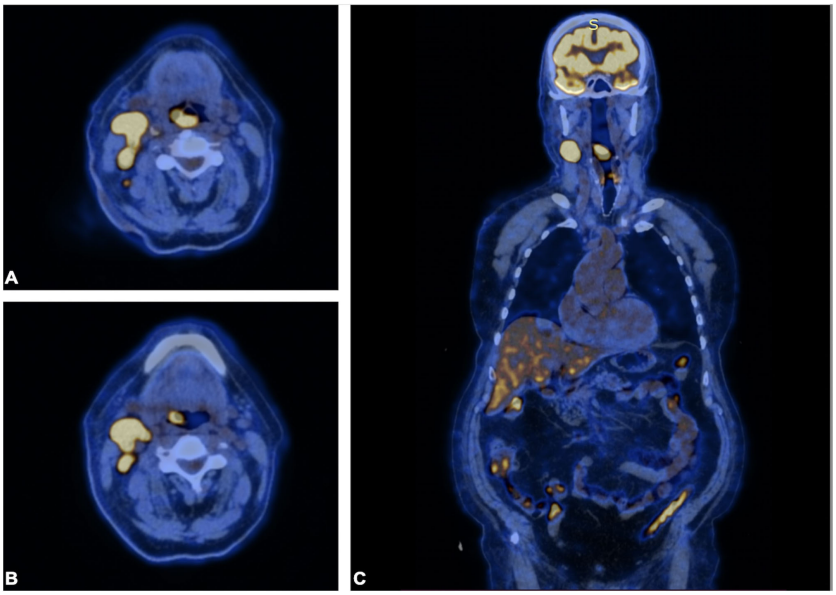

FIGURE 3
PET scan. PET scan showing increased FDG uptake in a **(A, B)** soft tissue density lesion in the right throat originating from the right piriform fossa (horizontal section) and in the **(C)** right cervical lymph node of IIA group (coronal section). Note that no abnormal FDG avid uptake was observed elsewhere, indicating the absence of a distant lesion.

remained calm and optimistic about recovery. Eventually, his convalescence was uneventful, with no tumor recurrence observed after the surgical and chemotherapeutic approach.

Discussion

In this case scenario, we present a rare example of EMP without a concomitant diagnosis of multiple myeloma. EMP is an uncommon malignancy originating from plasma cells and can manifest in soft tissues throughout the body. Typically, EMP is characterized by a slow-growing submucosal tumor within the respiratory and digestive tract, with the head and neck region being the most common location (6, 10). Predominantly observed in nasal cavities, paranasal sinuses, nasopharynx, oropharynx, and larynx, EMP's symptoms are location-dependent and primarily associated with the mass effect, leading to issues such as swallowing difficulties, breathing problems, epistaxis, or nasal obstruction (6, 11). EMP does not affect the bone marrow but can progress to multiple myeloma (MM) (12). Two forms of EMP are recognized: primary and secondary. Primary EMP denotes tumors present without any other plasma cell malignancies, such as multiple myeloma or monoclonal gammopathy. On the other hand, secondary EMP occurs in the presence of other plasma cell dyscrasias, most commonly MM (8). To date, numerous cases of EMP without MM have been reported in the literature, with several cases presenting the tumor in the laryngopharynx location (13–17). Given its rarity, a high index of suspicion is required for an accurate diagnosis, necessitating tumor and bone marrow biopsies to assess the level of monoclonal plasma cells (7). Histopathological examination of the tumor tissue reveals a dense infiltrate of plasmablastic or anaplastic plasma cells, which may be immature or mature (18). However, the similarities in histopathological features and the high pleomorphism of plasma cells may lead to confusion with aggressive lymphoma, rhabdomyosarcoma, or other sarcomas (19). Specifically, EMP should be distinguished from plasmablastic lymphoma, which exhibits overlapping features with myeloma and lymphoma. Plasmablastic lymphoma comprises B-cells, lymphoplasmablastic cells, and monoclonal cells with an immunohistochemical profile that typically includes CD20 expression, but not CD138 and is often associated with Epstein-Barr virus (EBV) infection (20). It is a highly aggressive lymphoma observed in immunocompromised patients, primarily affecting the oral cavity and gastrointestinal tract (17). Conversely, EMP may also be occasionally confused with angiosarcoma. However, angiosarcoma, consisting of atypical endothelial cells that may resemble plasmocytes, typically induces the destruction of surrounding tissues (21). Additionally, an extremely rare anaplastic MM may occasionally mimic EMP. Originating from immature plasma cells and presenting with extramedullary tumors, it leads to bone marrow invasion and osseous lytic lesions, which are not observed in EMP (22). Another condition that can sometimes mimic EMP is SCC, which is the most common malignancy in the head and neck region (23). Despite the similarity in location, EMP typically presents with localized growth, while SCC is more aggressive with a higher potential for metastasis. Additionally, poorly differentiated SCC cells may sometimes test positive for CD138 or plasma cell markers, making it crucial to use a comprehensive panel of antibodies to differentiate between carcinoma and EMP (24). On the other hand, large B-cell

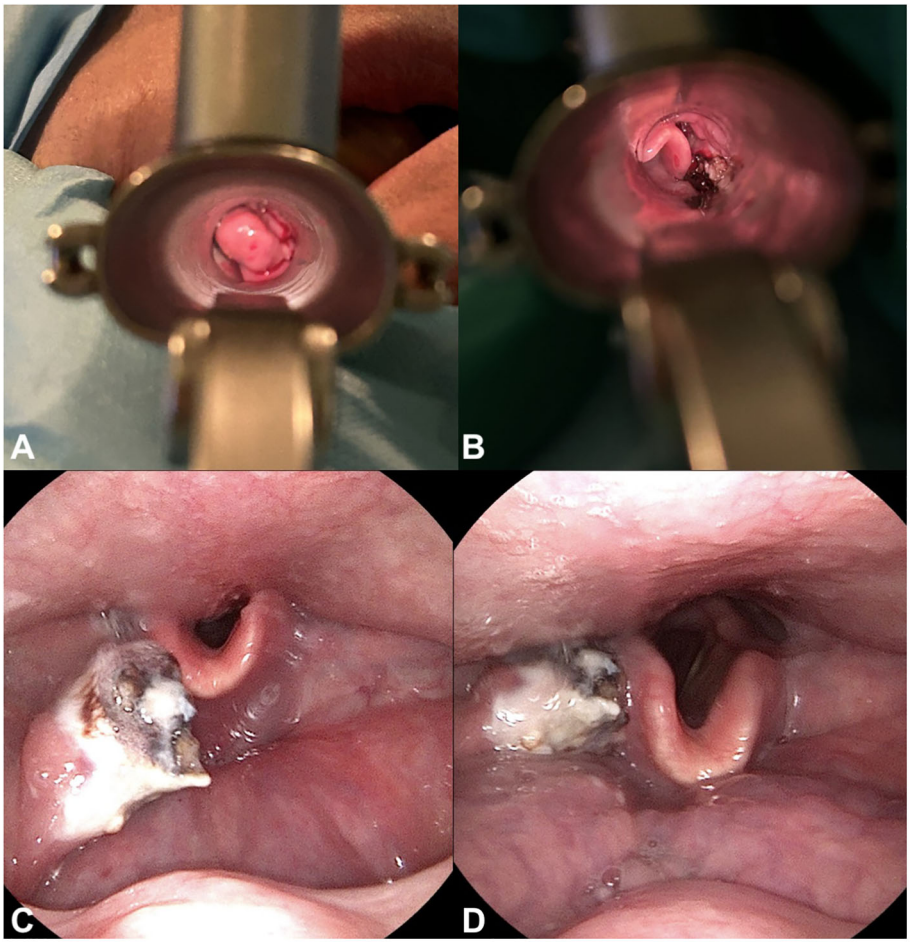

FIGURE 4
Surgical procedure and post-surgical fiberoptic exam. Visualization of the tumor through a laryngoscope, shown **(A)** during the surgical removal of the tumor and **(B)** post-removal. **(C, D).** Fiberoptic examination post-surgery revealing residual tumor tissue.

lymphoma (LBCL) cells, while they may share similar microscopic characteristics with EMP, typically express CD19, CD20, CD79a, and PAX5, but are negative for plasma cell markers such as CD138 and CD38 (25). Additionally, LBCL typically presents as a rapidly growing mass with extranodal involvement in over 50% of cases with stomach or gastrointestinal tract most commonly affected (26).

Furthermore, for adequate locoregional staging of EMP, a CT scan or MRI is essential. However, a PET scan appears to be the preferred imaging study for ruling out MM or other hematologic malignancies. The diagnostic approach should encompass the following evaluation criteria: (i) biopsy of a solitary lesion of bone or soft tissue with evidence of clonal plasma cells, (ii) bone marrow biopsy within normal limits with no clonal plasma cells, (iii) no abnormalities in the skeletal survey displayed on MRI (or CT) of the spine and pelvis (except for the primary solitary lesion), (iv) no evidence of hypercalcemia, anemia, renal insufficiency, or bone lesions (CRAB) caused by a lymphoplasmacytic cell proliferative disorder (27).The rarity of EMP and its prolonged course make it challenging to determine the optimal treatment strategy. In the presented case study a radiotherapeutic regimen was used as a primary approach as it is the preferred first-line treatment of EMP due to the tumor's radiosensitivity (28). This approach is considered feasible, particularly when the location of the EMP presents challenges for surgical intervention, such as proximity to vital and sensory organs. According to the literature, RT is typically administered over a 4-week period with a total dose ranging from 40 to 50 Gy (29). In the majority of EMP cases, radiotherapy is effective, demonstrating excellent disease control and a low risk of recurrence (30). Given the radiosensitive nature of EMP, RTH remains the treatment of choice. However, in cases refractory to radiotherapy, other therapeutic approaches need to be employed. Depending on the tumor location and the proximity of critical structures, radical surgical resection may not be feasible. Therefore, additional treatment modalities are required. In a case report described by Karakullukcu et al., surgical debulking combined with photodynamic therapy was employed to manage residual EMP tumor resulting in a successful outcome (31). Another therapeutic approach presented in the available literature involved bronchoscopic electrocautery snare combined with CO2 cryotherapy, followed by RTH for EMP located in the trachea (32). In the presented case report, a surgical debulking approach was employed because radical resection was not feasible. Consequently, due to the risk of

progression to MM, lack of response to RTH and the residual tumor, the patient underwent a subsequent chemotherapeutic regimen of dexamethasone and bortezomib. Nevertheless, existing literature suggests that the majority of cases of EMP respond well to radiotherapy, and the other treatment options should be implemented in case of radiotherapy resistance. The current publications confirm positive outcomes with surgery and/or systemic therapy, including bortezomib or cyclophosphamide alone or in combination with vincristine and prednisolone (33). In their case report on gastric EMP, Katodritou et al. were the first to present dexamethasone and bortezomib as an effective treatment approach for managing EMP without associated multiple myeloma (34). Similarly, in a case report by Wei et al., pancreatic EMP was successfully treated with a combination of bortezomib and dexamethasone after the tumor failed to respond to the traditional chemotherapy regimen of vincristine, doxorubicin, and dexamethasone (the VAD regimen) (35). Moreover, certain immunomodulatory agents, such as daratumumab, have also been found to be effective in EMP patients (36). However, the potential toxicity of chemotherapy, including risks of myelosuppression, neuropathy, and organ toxicity, are significant drawbacks that can limit its application. Decisions regarding chemotherapy should consider factors like the patient's overall health, existing comorbidities, potential drug interactions, and the severity or progression of the disease. In our patient, poor tolerance to chemotherapy and the absence of signs of MM led to the discontinuation of the chemotherapy regimen after just one course. Moreover, it appears that the resistance to radiotherapy in EMP tumors requires further molecular research to assess the likelihood of the radiotherapy efficacy. As such, this rare case study of EMP without multiple myeloma diagnosis proves the rarity of this malignancy as well as shed some light on its possible resistance to radiotherapy. Although the patient described in this manuscript achieved recovery with no evidence of tumor recurrence, he experienced side effects of initial radiotherapy, including xerostomia and radiation-induced skin reactions. A significant limitation of this case report is the inability to generalize these findings and to establish causality. However, despite these limitations, this case report highlights a rare and unusual case of EMP that is refractory to radiotherapy, underscoring the importance of a personalized medicine approach and raising awareness among healthcare professionals about EMP. Though, the presented case underscores the need for further research on a larger group of patients with EMP to identify the most effective therapeutic approach. This case report underscores the exceptionally rare form of EMP without MM, further compounded by its resistance to radiotherapy, rendering it an even more unique case within the EMP spectrum. A high degree of clinical suspicion is necessary for diagnosing EMP. Namely, counseling patients with EMP demands a considerate and patient-centered approach, considering the rarity of the condition and its potential for progression to MM. While SCC remains the most common malignancy within the head and neck region, the diagnosis of EMP should always be considered in a patient with a tumor in this region. Consequently, there is an imperative for clinicians to maintain a high index of suspicion when assessing EMP patients and determining the most appropriate treatment plan.

Data availability statement

The raw data supporting the conclusions of this article will be made available by the authors, without undue reservation.

Ethics statement

Written informed consent was obtained from the individual(s) for the publication of any potentially identifiable images or data included in this article. Written informed consent was obtained from the participant/patient(s) for the publication of this case report.

Author contributions

KS: Writing – review & editing. AGa: Writing – review & editing, Investigation. AGo: Writing – review & editing, Supervision. MD: Writing – review & editing, Supervision, Investigation. KB-P: Writing – review & editing, Investigation. JZ: Writing – review & editing, Supervision.

Funding

The author(s) declare financial support was received for the research, authorship, and/or publication of this article. The research was funded by Maria Sklodowska-Curie National Research Institute of Oncology, Warsaw, Poland.

Conflict of interest

The authors declare that the research was conducted in the absence of any commercial or financial relationships that could be construed as a potential conflict of interest.

Publisher's note

All claims expressed in this article are solely those of the authors and do not necessarily represent those of their affiliated organizations, or those of the publisher, the editors and the reviewers. Any product that may be evaluated in this article, or claim that may be made by its manufacturer, is not guaranteed or endorsed by the publisher.

Supplementary material

The Supplementary Material for this article can be found online at: https://www.frontiersin.org/articles/10.3389/fonc.2024.1353943/full#supplementary-material

References

1. Alexiou C, Kau RJ, Dietzfelbinger H, Kremer M, Spiess JC, Schratzenstaller B, et al. Extramedullary plasmacytoma: tumor occurrence and therapeutic concepts. *Cancer*. (1999) 85:2305–14. doi: 10.1002/(ISSN)1097-0142

2. Reed V, Shah J, Medeiros LJ, Ha CS, Mazloom A, Weber DM, et al. Solitary plasmacytomas: outcome and prognostic factors after definitive radiation therapy. *Cancer*. (2011) 117:4468–74. doi: 10.1002/cncr.26031

3. Barzenje DA, Kolstad A, Ghanima W, Holte H. Long-term outcome of patients with solitary plasmacytoma treated with radiotherapy: a population-based, single-center study with median follow-up of 13.7 years. *Hematol Oncol*. (2018) 36:217–23. doi: 10.1002/hon.2415

4. Castro EB, Lewis JS, Strong EW. Plasmacytoma of paranasal sinuses and nasal cavity. *Arch Otolaryngol*. (1973) 97:326–9. doi: 10.1001/archotol.1973.00780010336009

5. Merino F, Hernández IP, Aniceto GSánchez, Ballestín C. Extramedullary plasmacytoma in the maxillofacial region: A review of the literature and case report. *Oral Maxillofac Surg cases*. (2018) 4:141–5. doi: 10.1016/j.omsc.2018.07.004

6. Liebross RH, Ha CS, Cox JD, Weber D, Delasalle K, Alexanian R. Clinical course of solitary extramedullary plasmacytoma. *Radiother Oncol*. (1999) 52:245–9. doi: 10.1016/S0167-8140(99)00114-0

7. Caers J, Paiva B, Zamagni E, Leleu X, Bladé J, Kristinsson SY, et al. Diagnosis, treatment, and response assessment in solitary plasmacytoma: updated recommendations from a European Expert Panel. *J Hematol Oncol*. (2018) 11:10. doi: 10.1186/s13045-017-0549-1

8. Holler A, Cicha I, Eckstein M, Haderlein M, Pöttler M, Rappl A, et al. Extramedullary plasmacytoma: tumor occurrence and therapeutic concepts—a follow-up. *Cancer Med*. (2022) 11:4743–55. doi: 10.1002/cam4.4816

9. Pham A, Mahindra A. Solitary plasmacytoma: a review of diagnosis and management. *Curr Hematol Malig Rep*. (2019) 14:63–9. doi: 10.1007/s11899-019-00499-8

10. Granato L, Petitto JW, Prospero JD. Plasmocitoma extramedular do aparelho respiratório Apresentação do caso. *Rev Bras Otorrinolaringol*. (1977) 43:214–23.

11. Majumdar S, Raghavan U, Jones NS. Solitary plasmacytoma and extramedullary plasmacytoma of the paranasal sinuses and soft palate. *J Laryngol Otol*. (2002) 116:962–5. doi: 10.1258/00222150260369561

12. Hughes M, Doig A, Soutar R. Solitary plasmacytoma and multiple myeloma: adhesion molecule and chemokine receptor expression patterns. *Br J Haematol*. (2007) 137:486. doi: 10.1111/j.1365-2141.2007.06599.x

13. Padhi P, El-Behery R. Extramedullary solitary plasmacytoma with anaplastic features of the nasopharynx. *Case Rep Hematol*. (2020) 2020:8845546–4. doi: 10.1155/2020/8845546

14. Raghuram S, Faizal B, Sanjeevan KV, Eapen M, Nair IR, Philip A, et al. Recurrent extramedullary plasmacytomas without multiple myeloma: A case report with review of the literature. *Cancer Treat Res Commun*. (2022) 31(2022):100550. doi: 10.1016/j.ctarc.2022.100550

15. Szczepanek E, Drozd-Sokołowska J, Sokołowski J, Rzepakowska A, Moskwa A, Pachla J, et al. Solitary extramedullary plasmacytoma of the larynx and secondary laryngeal involvement in plasma cell myeloma: single-centre retrospective analysis and systematic literature review. *J Clin Med*. (2022) 11:4390. doi: 10.3390/jcm11154390

16. Mokhtari TE, Sadow PM, Naunheim MR. Extramedullary plasmacytoma of the larynx. *Mayo Clin Proc*. (2024) 99:13–4. doi: 10.1016/j.mayocp.2023.07.001

17. Tanrivermis Sayit A, Elmali M, Gün S. Evaluation of extramedullary plasmacytoma of the larynx with radiologic and histopathological findings. *Radiologia (Engl Ed)*. (2020) 22:S0033–8338(20)30121–1. doi: 10.1016/j.rx.2020.07.006

18. Torne R, Su WP, Winkelmann RK, Smolle J, Kerl H. Clinicopathologic study of cutaneous plasmacytoma. *Int J Dermatol*. (1990) 29:562–6. doi: 10.1111/j.1365-4362.1990.tb03469.x

19. Jacevičiūtė E, Rudžianskienė M, Dambrauskienė R, Vajauskas D, Gerbutavičius R. Anaplastic extramedullary plasmacytoma resistant to novel therapies: a case report. *Oncologie (De Gruyter)*. (2023) 25:327–32. doi: 10.1515/oncologie-2023-0054

20. Zuze T, Painschab MS, Seguin R, Kudowa E, Kaimila B, Kasonkanji E, et al. Plasmablastic lymphoma in Malawi. *Infect Agent Cancer*. (2018) 13:22. doi: 10.1186/s13027-018-0195-4

21. Gaballah AH, Jensen CT, Palmquist S, Pickhardt PJ, Duran A, Broering G, et al. Angiosarcoma: clinical and imaging features from head to toe. *Br J Radiol*. (2017) 90:20170039. doi: 10.1259/bjr.20170039

22. Wu J, Chu E, Chase CC, Choi T, Gasparetto C, Young K, et al. Anaplastic multiple myeloma: case series and literature review. *Asploro J BioMed Clin Case Rep*. (2022) 5:1–11. doi: 10.36502/asjbccr

23. Barsouk A, Aluru JS, Rawla P, Saginala K, Barsouk A. Epidemiology, risk factors, and prevention of head and neck squamous cell carcinoma. *Med Sci (Basel)*. (2023) 11:42. doi: 10.3390/medsci11020042

24. Zuo Z, Tang Y, Bi CF, Zhang WY, Zhao S, Wang XQ, et al. Extraosseous (extramedullary) plasmacytomas: a clinicopathologic and immunophenotypic study of 32 Chinese cases. *Diagn Pathol*. (2011) 6:123. doi: 10.1186/1746–1596-6–12323

25. Fan J, Thanedar S, Ovechko V, Jana B. Diffuse large B-cell lymphoma with aberrant coexpression of CD5 and CD8 T-cell markers. *Case Rep Oncol*. (2024) 17:517–23. doi: 10.1159/000536571

26. Conlan MG, Bast M, Armitage JO, Weisenburger DD. Bone marrow involvement by non-Hodgkin's lymphoma: the clinical significance of morphologic discordance between the lymph node and bone marrow. *Nebraska Lymphoma Study Group J Clin Oncol*. (1990) 8:1163–72. doi: 10.1200/JCO.1990.8.7.1163

27. Rajkumar SV, Dimopoulos MA, Palumbo A, Blade J, Merlini G, Mateos MV, et al. International Myeloma Working Group updated criteria for the diagnosis of multiple myeloma. *Lancet Oncol*. (2014) 15:e538–48. doi: 10.1016/S1470–2045(14)70442–5

28. Kilciksiz S, Celik OK, Pak Y, Demiral AN, Pehlivan M, Orhan O, et al. Clinical and prognostic features of plasmacytomas: a multicenter study of Turkish Oncology Group-Sarcoma Working Party. *Am J Hematol*. (2008) 83:702–7. doi: 10.1002/ajh.21211

29. Wen G, Wang W, Zhang Y, Niu S, Li Q, Li Y. Management of extramedullary plasmacytoma: Role of radiotherapy and prognostic factor analysis in 55 patients. *Chin J Cancer Res*. (2017) 29:438–46. doi: 10.21147/j.issn.1000-9604.2017.05.08

30. Gaube A, Nica SG, Dobrea C, Neicu SA, Moldoveanu VG, Serbanescu M, et al. Radiation response of soft-tissue extramedullary plasmacytoma in multiple myeloma-A case report. *Clin Case Rep*. (2021) 9:e05084. doi: 10.1002/ccr3.5084

31. Karakullukcu B, De Boer JP, Van Veen R, Wegman J, Tan B. Surgical debulking combined with photodynamic therapy to manage residual extramedullary plasmacytoma of the nasopharynx. *Photodiagnosis Photodyn Ther*. (2011) 8:264–6. doi: 10.1016/j.pdpdt.2011.03.340

32. Zhang X, Su L, Ran YG, Qie S, Zhang X, Liu C, et al. Extramedullary plasmacytoma of the trachea: A case report and review of the literature. *Med (Baltimore)*. (2018) 97:e9594. doi: 10.1097/MD.0000000000009594

33. Wiltshaw E. Chemotherapy in the management of extramedullary plasmacytoma. *Cancer Chemother Pharmacol*. (1978) 1:167–75. doi: 10.1007/BF00253117

34. Katodritou E, Kartsios C, Gastari V, Verrou E, Mihou D, Banti A, et al. Successful treatment of extramedullary gastric plasmacytoma with the combination of bortezomib and dexamethasone: first reported case. *Leuk Res*. (2008) 32:339–41. doi: 10.1016/j.leukres.2007.04.016

35. Wei JY, Tong HY, Zhu WF, Liu H, Zhang FJ, Yu WJ, et al. Bortezomib in treatment of extramedullary plasmacytoma of the pancreas. *Hepatobiliary Pancreat Dis Int*. (2009) 8:329–31.

36. Li Y, Sun Z, Qu X. Advances in the treatment of extramedullary disease in multiple myeloma. *Trans Oncol*. (2022) 22:101465. doi: 10.1016/j.tranon.2022.101465

frontiers | Frontiers in Oncology

TYPE Case Report
PUBLISHED 11 June 2024
DOI 10.3389/fonc.2024.1395144

Check for updates

OPEN ACCESS

EDITED BY
Lidia Castagneto Gissey,
Sapienza University of Rome, Italy

REVIEWED BY
Rafael S. Czepielewski,
Augusta University, United States
Rajendra Ghritlaharey,
Gandhi Medical College and Associated Hospitals, India

*CORRESPONDENCE
Zhiming Wang
wzmdoc@163.com
Yanqing Diao
diaoyanqing1981@163.com

RECEIVED 03 March 2024
ACCEPTED 10 May 2024
PUBLISHED 11 June 2024

CITATION
Da B, Zhang J, Zhu F, Wang Z and Diao Y (2024) Extranodal marginal zone lymphoma of mucosa-associated lymphoid tissue of the ileum in an adult presenting with intussusception: a case report and literature review. *Front. Oncol.* 14:1395144. doi: 10.3389/fonc.2024.1395144

COPYRIGHT
© 2024 Da, Zhang, Zhu, Wang and Diao. This is an open-access article distributed under the terms of the Creative Commons Attribution License (CC BY). The use, distribution or reproduction in other forums is permitted, provided the original author(s) and the copyright owner(s) are credited and that the original publication in this journal is cited, in accordance with accepted academic practice. No use, distribution or reproduction is permitted which does not comply with these terms.

Extranodal marginal zone lymphoma of mucosa-associated lymphoid tissue of the ileum in an adult presenting with intussusception: a case report and literature review

Binlin Da, Juanjuan Zhang, Feng Zhu, Zhiming Wang* and Yanqing Diao*

Research Institute of General Surgery, Jinling Hospital, Affiliated Hospital of Medical School, Nanjing University, Nanjing, Jiangsu, China

Extranodal marginal zone lymphoma of mucosa-associated lymphoid tissue (EMZL), also known as MALT lymphoma, is an extranodal multiorgan-invasive proliferative lymphoma composed of small B cells with variable morphology. It most commonly occurs in the digestive tract, with a high prevalence in the stomach, but EMZL originating in the small intestine is rare and lacks specificity in clinical manifestations, which makes it easy to be misdiagnosed. Herein, we report a rare case of small intestinal EMZL presentation as intussusception in a 32-year-old man. A colonoscopy performed at the local hospital revealed a pedicled polyp about 5 cm × 5 cm in size with a rough surface, and hyperemia was seen in the ileocecal region. He was admitted to our hospital for a polypectomy. A contrast-enhanced computed tomographic (CT) scan suggested ileocolic intussusception, which was subsequently confirmed by a colonoscopy in our hospital. Adult intussusception is relatively rare, with 90% of cases having a known causative mechanism and 40% of cases caused by primary or secondary malignancies. Therefore, we performed a laparoscopic-assisted right hemicolectomy for the patient. The resected specimen showed that the terminal ileum was intussuscepted into the ascending colon, and the intussusception was hyperemia and edema. A 2.5 cm × 2.5 cm × 1.5 cm mass was seen at the end of the intussusception. Postoperative pathology revealed that the mass was EMZL, partially transformed into a large B-cell lymphoma. The patient was transferred to the hematology department and completed a PET-CT showing postoperative manifestations of primary intestinal lymphoma, Lugano staging IE2. Although EMZL was an indolent lymphoma and the patient was in the early stages, the rituximab, cyclophosphamide, doxorubicin, vincristine, and prednisone (R-CHOP) regimen was given in view of the histological transformation. The patient is in regular follow-up. This was a rare case of

10.3389/fonc.2024.1395144

small intestinal mass due to EMZL presented as intussusception in adults, which highlighted laparoscopic-assisted enterectomy as a potential therapeutic approach in the multidisciplinary collaborative therapy of small intestine EMZL.

KEYWORDS

extranodal marginal zone B-cell lymphoma of the mucosa-associated lymphoid tissue, MALT lymphoma, Ileocolic intussusception, abdominal pain, case report

1 Introduction

Extranodal marginal zone lymphoma of mucosa-associated lymphoid tissue (EMZL), also known as MALT lymphoma, is a low-grade lymphoma composed of small B cells of different morphology that invade multiple organs (1). It was first proposed in 1983 by P. Isaacson and D. H. Wright (2). EMZL most frequently occurs in the stomach, followed by ocular appendages, lungs, salivary glands, and other positions. The pathogenesis has not been elucidated and is linked to immune system dysregulation caused by prolonged immunological activation from chronic infections or autoimmune illnesses (3). Primary small intestinal EMZL is rare and lacks typical signs and symptoms, with great challenges in diagnosis and treatment. Intussusception is a disease in which part of the proximal bowel and its mesentery are embedded in the adjacent distal bowel. Intussusception is the main cause of acute abdomen in infants but is uncommon in adults. Unlike intussusception in children, 70%–90% of intussusception in adults has a clear etiology, of which about 40% is caused by primary or secondary malignancies, such as lymphoma, leiomyosarcoma, and adenocarcinoma (4, 5). To our knowledge, this is the first case of small intestinal EMZL with intussusception as the initial presentation, partially transforming into large B-cell lymphoma. Herein, we reported it to provide experience for clinical diagnosis and treatment. The presentation of this case adhered to the CARE checklists.

2 Case description

A 32-year-old male patient was admitted to the local hospital for abdominal distension for more than 1 year and abdominal pain for 1 week. A colonoscopy (Figure 1) performed at the local hospital revealed a pedicled polyp about 5 cm × 5 cm in size with a rough surface and hyperemia was seen in the ileocecal region (biopsy). The pathology showed that the ileocecal region had chronic inflammation of the mucosal tissues with polypoid hyperplasia. A week later, the patient was admitted to our hospital for a polypectomy. The patient was previously in good health and had no family history of cancer. On clinical examination, pressing pain was located in the lower right abdomen without rebound pain or muscle tension; no palpable mass was in the abdomen; and no palpable liver or spleen was under the ribs. Blood testing was within normal limits. A chest computed tomographic (CT) examination showed no obvious abnormalities. A colonoscopy (Figure 2) was performed in our hospital for polypectomy, but it revealed a section of the small intestine with congestion and edema on the surface was embedded in the ascending colon. The ileocecal flap was not discernible. The abdominal contrast-enhanced CT scan (Figure 3) showed that the wall of the ileocecal region was blurred, and the mesentery and end of the ileum were collapsed into the ascending colon's lumen, presenting "sausage-like" signs and "concentric circles" along with a few oozing shadows and small lymph nodes surrounding it. Different-sized lymph nodes were

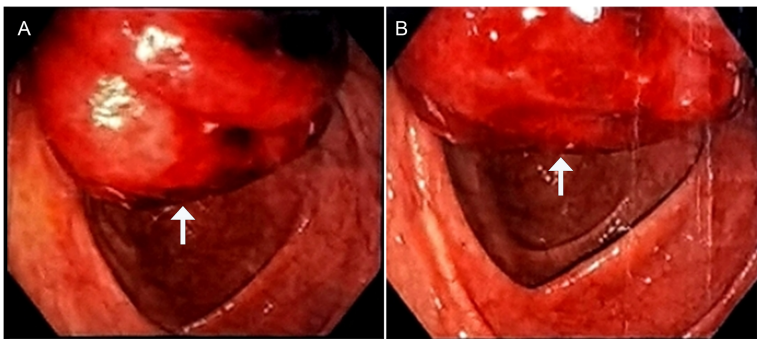

FIGURE 1
A colonoscopy performed at the local hospital reveals that a pedicled polyp with a rough surface and hyperemia was seen in the ileocecal region (the white arrows refer to the pedicled polyp).

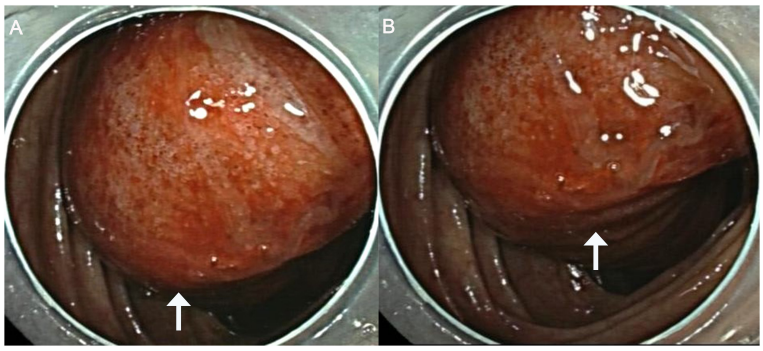

FIGURE 2
Results of the colonoscopy show a section of the terminal ileum with congestion and edema on the surface collapsing into the ascending colon (the white arrows refer to the terminal ileum collapsing into the ascending colon).

observed in the mesenteric region. A small amount of fluid was in the pelvic cavity. Considering that 90% of adults with intussusception involve a pathologic lead point, about 40% of which are malignancies (6), laparoscopic-assisted right hemicolectomy with lymph node dissection was performed. Intraoperative findings were as follows: no lesions in the pelvic and abdominal cavity; terminal ileum imbedded in the ascending colon; mild adhesions in the right lower abdomen; and a small amount of yellowish-clear ascites. The resected specimen showed that the terminal ileum intussuscepted into the ascending colon; intussusception was hyperemia and edema; and a 2.5 cm × 2.5 cm × 1.5 cm mass was seen at the end of the intussusception. Postoperative pathology (Figure 4) showed the right hemicolon resection specimen: B-cell lymphoma of the terminal ileum. Combined with immunohistochemical markers and T and B lineage gene rearrangement tests, it was considered to be lymphoma of small B-cell origin (extranodal marginal zone B-cell lymphoma), partially transformed into large B-cell lymphoma (moderately aggressive). The tumor tissue infiltrated the whole layer of the intestinal wall; there was no tumor tissue involvement in the lateral margins of the intestinal canal at the two ends and the omental tissues; and there was no metastasis of the tumor tissue to periampullary lymph nodes (0 out 17 lymph nodes removed during surgery). The remaining intestinal mucosa showed mild chronic inflammation with localized intussusception. Tumor cells were immunohistochemically shown to be positive for CD20, CD79a, BCL 2, and BCL 6; focal positive for CD23 and CD10; and negative for CD3, CD5, CD43, CD4, CD8, cyclin D1, SOX11, MUM 1, TdT, CD30, or CD15. Ki-67 showed hot spots at about

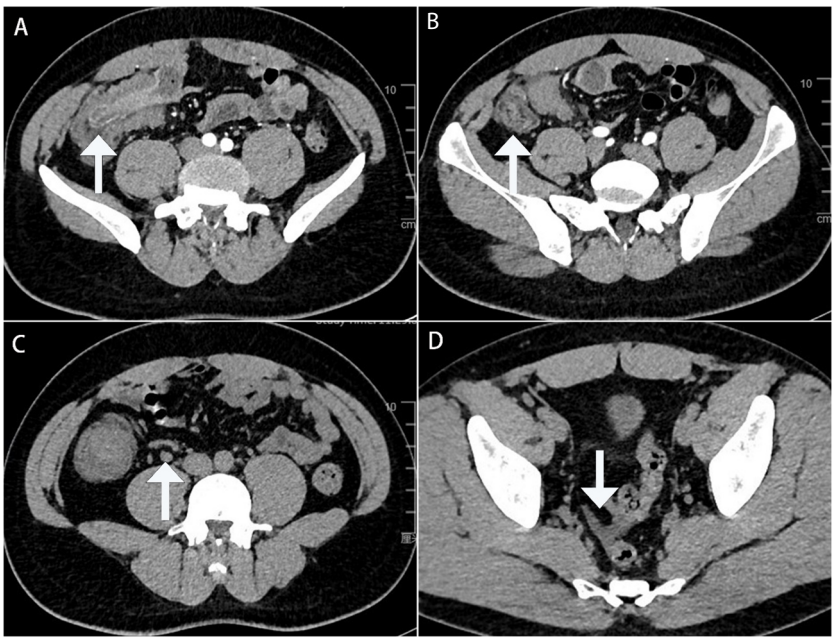

FIGURE 3
Enhanced computed tomography cross-section images show the terminal ileum collapsing into the ascending colon's lumen: **(A)** with the typical "concentric circles" appearance (white arrows); **(B)** with the typical "sausage-like" sign appearance (white arrows); **(C)** with enlarged lymph nodes in the mesenteric region (white arrows); and **(D)** with a small amount of fluid in the pelvic cavity (white arrows).

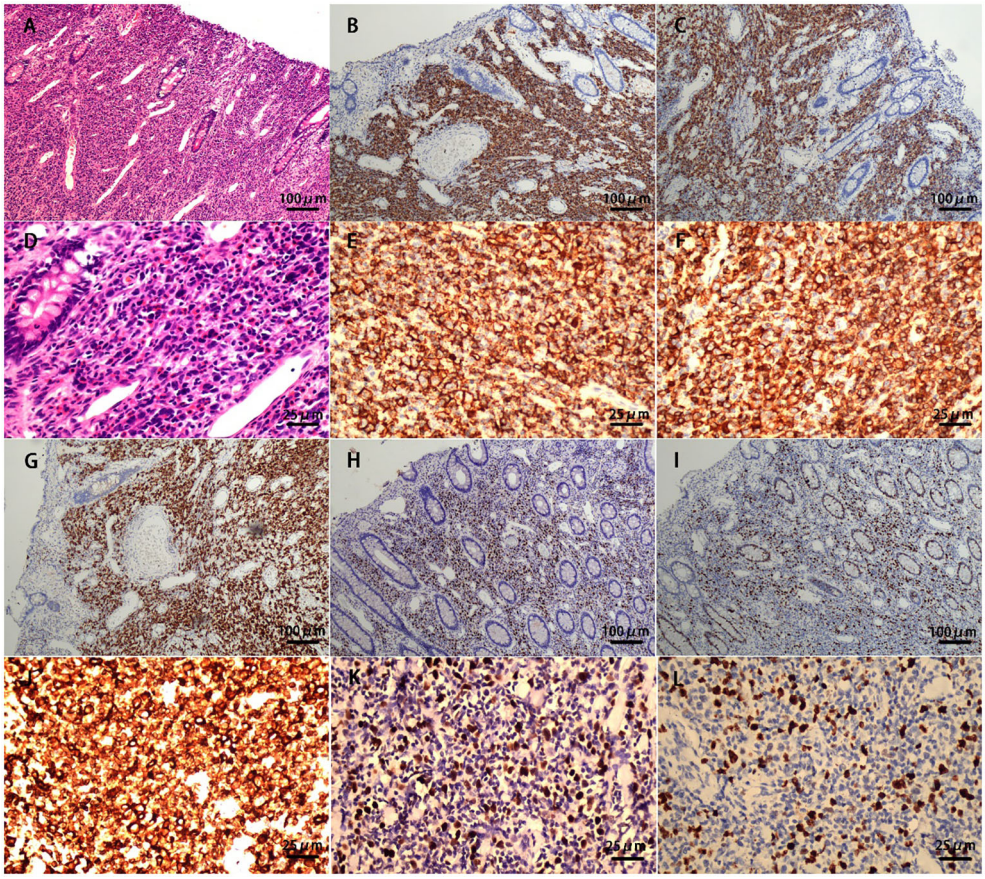

FIGURE 4
Postoperative pathology: **(A)** small bowel with a dense and diffuse lymphocytic infiltrate (HE, ×100); **(B)** atypical cells are diffusely positive for the marker CD20 (IHE CD20, ×100); **(C)** atypical cells are diffusely positive for the marker CD79a (IHE CD79a, ×100); **(D)** small bowel with a dense and diffuse lymphocytic infiltrate (HE, ×400); **(E)** atypical cells are diffusely positive for the marker CD20 (IHE CD20, ×400); **(F)** atypical cells are diffusely positive for the marker CD79a (IHE CD79a, ×400); **(G)** atypical cells are diffusely positive for the marker BCL-2 (IHE BCL-2, ×100); **(H)** atypical cells are diffusely positive for the marker BCL-6 (IHE BCL-6, ×100); **(I)** Ki-67 hot spots at about 40% (+) (IHE Ki-67, ×100); **(J)** atypical cells are diffusely positive for the marker BCL-2 (IHE BCL-2, ×400); **(K)** atypical cells are diffusely positive for the marker BCL-6 (IHE BCL-6, ×400); and **(L)** Ki-67 hot spots at about 40% (+) (IHE Ki-67, ×400).

40% (+). The rest of the findings were as follows: *in situ* hybridization: EBER (-). PCR: B lineage gene rearrangement detection: B and D tubes monoclonal bands detected (+); IGK: monoclonal band detected (+); PCR: T lineage gene rearrangement detection: TCRB: monoclonal band detected (-); TCRD: monoclonal band detected (-); and TCRG: monoclonal band detected (-).

After the operation, he was referred to the hematology department for adjuvant chemotherapy. Whole-body PET-CT was consistent with the postoperative manifestations of the primary intestinal lymphoma, Lugano staging IE2; systemic bone marrow FDG metabolism is mildly increased, suggesting a reactive hyperplasia; mesenteric lymph nodes in the operation area; and FDG metabolism is not abnormally increased. Bone marrow aspiration with lymphocyte immunophenotyping showed no abnormal findings. The results of the genetic examination showed that no mutation in the B-cell lymphoma-related gene locus was found. Although the patient is in the early stages of EMZL, the patient underwent a rituximab, cyclophosphamide, doxorubicin, vincristine, and prednisone (R-CHOP) regimen at a frequency of every 21 days in view of the histological transformation into large B-cell lymphoma. The fourth cycle of treatment has just been completed and was well-tolerated, with the patient experiencing only mild hair loss and numbness in the fingers. At present, the blood routine and liver and kidney functions are basically normal. The patient is in regular follow-up.

3 Discussion

MZL is a group of B-cell malignant neoplastic diseases originating in the follicular marginal zone that can occur in lymph nodes and extra-lymph nodes, accounting for 5%–15% of non-Hodgkin lymphoma (NHL) in western countries (7). It is the second most common subtype of B-cell NHL in Asia [after diffuse large B-cell lymphoma (DLBCL)] and the fourth most common subtype in the USA (after DLBCL, follicular, and Burkitt lymphoma) (8). The 5th edition of the WHO Classification classifies MZL into four types: mucosa-associated lymphoid tissue extranodal marginal zone lymphoma (EMZL), lymph node MZL, primary cutaneous marginal zone lymphoma, and pediatric marginal zone lymphoma in 2022,

TABLE 1 A summary of four cases of intussusception due to EMZL reported in the literature from 1995 to 2024.

Reference	Year	Age	Sex	Complaint	Palpable mass	Diagnostic tools	Location	Surgical procedure	Medical approach	Follow-up
(19)	1995	44	F	AP + anemia	Positive	Col	Terminal ileum	Right hemicolectomy	NS	NS
(20)	2013	35	F	AP	Positive	US	Terminal ileum	Right hemicolectomy	ChT	NS
(21)	2016	83	F	AP + diarrhea	Positive	CT	Terminal ileum	Seg Resection	NS	NS
(22)	2022	78	M	AP + weight loss	Negative	MRI	Ileum	Seg Resection	ChT (R-CHOP)	4 months

AP, abdominal pain; col, colonoscopy; NS, not stated; US, ultrasonography; ChT, chemotherapy; CT, computed tomography; Seg: segmental; and MRI, magnetic resonance imaging.

which is different from the 4th edition of the WHO Classification of Haematolymphoid Tumours: Lymphoid Neoplasms (9). EMZL is an uncommon cause of primary gastrointestinal lymphoma and can involve multiple organs, such as the stomach, ocular appendages, lungs, and salivary glands. Primary small intestinal EMZL is rare and is slightly more common in men (men:women ratio of 1.5:1), and the incidence increased exponentially with age, with a median age at diagnosis of 59 years old (8).

EMZL is associated with chronic antigenic stimulation caused by infectious agents or autoimmune processes and can occur at widely different sites, with gastric EMZL accounting for >30% of cases and other common sites including ocular appendages, salivary glands, and lungs, with varying site-specific etiologies (10). Chronic *Helicobacter pylori* gastritis was reported as a susceptibility factor for gastric EMZL; *Campylobacter jejuni* for small intestinal EMZL; *Achromobacter xylosoxidans* possibly for lung; and *Borrelia burgdorferi* for cutaneous MZLs (11–13). Some studies have also shown that hepatitis C virus (HCV) infection is associated with a portion of B-cell NHL, including EMZL (14, 15). Autoimmune diseases such as Sjogren syndrome and Hashimoto's thyroiditis are associated with an increased risk of salivary gland and thyroid EMZL, respectively. In addition, a family history of EMZL suggests its genetic susceptibility (3).

The clinical presentation of EMZL varies widely, depending on the site of involvement. The symptoms of small intestinal EMZL vary from abdominal pain, chronic bleeding, weight loss, and intestinal obstruction to no symptoms only detected by abdominal CT or endoscopy (16, 17). The patient in this case report presented with chronic abdominal distension and abdominal pain, and then he completed an abdominal CT and colonoscopy considering ileocolic intussusception. Considering that the patient did not present with acute intestinal obstruction, we chose a minimally invasive approach. We know that 90% of adult intussusceptions had underlying etiologies, and 40% of them were malignancies. The principles of oncology surgery must be followed, and appropriate resection of the bowel and lymph node dissection should be performed depending on the location (18), so we chose laparoscopic-assisted right hemicolectomy for this patient because the lesion was in the ileocecum. Postoperative pathology revealed B-cell lymphoma of the terminal ileum. Combined with CD20 (3+), CD79a (3+), and BCL-2 (3+), it is considered EMZL. However, BCL-6 is partially expressed and the hotspot area of Ki-67 is approximately 40%, considering it partially transformed into large B-cell lymphoma. Several studies have shown that patients with aggressive lymphoma have shorter progression-free survival and overall survival (19, 20). Although small intestinal EMZL with intussusception has been previously reported (Table 1) (21–24), histological transformation in this case is very rare. At present, the mechanism related to transformation remains unclear. Continuous exposure to foreign antigens lowers the physiological threshold for triggering proliferation, which may predispose them to histological transformation. Some studies have shown that the transformation into higher-grade lymphoma was associated with high lactate dehydrogenase and multiple lymph node involvement at diagnosis, failure to achieve a complete response after initial treatment (25), multiple mucosal site involvement, CD5 expression, and complex karyotypes (26). However, this patient had none of the risk factors.

If EMZL is suspected, clinicians should obtain the largest biopsy specimen possible, as small specimens may not provide enough tissue. The diagnosis of small intestine EMZL remains difficult because most tumors are not detectable by gastroscopy and colonoscopy. Only balloon enteroscopy can be used to detect lesions and determine the histological type by biopsy. The literature regarding the endoscopic features of small intestinal EMZL is not sufficient. In a meta-analysis of 415 cases of small intestinal lymphoma in the Chinese population, 97 cases of EMZL were identified, of which 48% were described as ulcers and 17% as masses (27). Another review included 53 cases of small intestinal EMZL-reported endoscopy in 23 patients. Endoscopic manifestations of ulcerative and erosive lesions were found in 82.6% of patients (8). Some cases of gastrointestinal tract obstruction or intussusception require emergent surgical intervention, and postoperative pathology can also identify the tumor type (23, 28). Consistent with other published cases (Table 1). The case reported in this study underwent emergency surgery due to intussusception, and postoperative gross specimens showed that the starting point of intussusception was a mass.

Most cases present with local lesions (I–II) at diagnosis of EMZL, and about 25% of cases present with multifocal single-organ involvement or diffuse extranodal involvement (IV), especially in extragastric EMZL (29). Both gastrointestinal and non-gastrointestinal EMZL have good prognoses, with 5-year overall survival (OS) rates above 90% and 10-year OS rates of 75% to 80% (16). An observational study including 321 MZL patients showed that disease progression within 24 months after initial treatment

with MZL was a predictor of reduced OS, compared to patients whose disease did not progress within 24 months (3-year OS, 95%), and patients whose disease progressed within 24 months had a 3-year OS of only 53%, with a hazard ratio of 19.5 (95% confidence interval, 8.4–45) (30). Due to the risk of occult spread, extensive initial staging assessment is required regardless of the site of onset, especially before antibiotic therapy or radiotherapy (31). The EMZL staging of the gastrointestinal tract depends mainly on the 2014 Lugano classification based on CT, MRI, or PET-CT (32). The lymphoma in this case was confined to the small intestine, which infiltrated into the serous membrane without lymph node metastasis or distant metastasis, so for this patient, the stage was IE2 according to the Lugano classification.

The treatment and monitoring of EMZL require multidisciplinary collaboration, including gastroenterologists, hematologists, oncologists, and doctors in other related specialties. All gastric EMZL patients should receive H. pylori eradication therapy, regardless of stage, and most patients can achieve complete remission. Studies showed that with the increase in H. pylori eradication rate, the proportion of H. pylori-negative gastric EMZL began to increase, which accounted for 40% of all gastric EMZL patients (33, 34). The value of anti-infective therapy in other EMZLs is poorly understood. For patients whose lymphoma has not subsided after antibiotic therapy, radiation therapy (RT) and systemic tumor therapy should be used, depending on the stage of the disease. In H. pylori-negative patients, if no signs of lymphoma regression are seen in a repeat endoscopic evaluation 3–6 months after antibiotic treatment, RT should be considered (35). Chemotherapy, immunotherapy, or chemotherapy combined immunotherapy may be used for patients with EMZL with contraindications to radiotherapy, failure of antibiotics, surgery or radiotherapy, histological transformation, and symptomatic systemic disease. Patients whose disease has undergone histological transformation into large B-cell lymphoma should be treated with chemo-immunotherapy as DLBCL (7). Although the disease of the patient in this case report was staged in Lugano IE2, the pathologic findings suggested EMZL of the ileum and partial transformation into DLBCL, which suggested a poor prognosis and a shorter OS. Therefore, this case was treated with R-CHOP chemo-immunotherapy after surgery, the first-line treatment for DLBCL (36). He had completed four cycles of R-CHOP so far, with clinical remission.

4 Conclusion

MZLs are indolent lymphomas with great heterogeneity in etiology, clinical manifestations, diagnosis, and treatment. EMZL is the most common subtype of MZL. The symptoms of small intestinal EMZL include abdominal pain, chronic bleeding, loss of weight, and intestinal obstruction. A few patients present with intussusception. For adult intussusception, although preoperative imaging data do not indicate a tumor, performing resection and lymph node dissection are still needed according to the principle of tumorectomy. After an operation, the next treatment plan is determined according to the pathologic type.

Data availability statement

The original contributions presented in the study are included in the article/supplementary material. Further inquiries can be directed to the corresponding authors.

Ethics statement

This article was a case report and the patient has signed informed consent for publication. The studies were conducted in accordance with the local legislation and institutional requirements. The participants provided their written informed consent to participate in this study. Written informed consent was obtained from the individual(s) for the publication of any potentially identifiable images or data included in this article.

Author contributions

BD: Conceptualization, Writing – original draft. JZ: Writing – review & editing. FZ: Writing – review & editing. ZW: Supervision, Writing – review & editing. YD: Supervision, Writing – review & editing.

Funding

The author(s) declare that no financial support was received for the research, authorship, and/or publication of this article.

Conflict of interest

The authors declare that the research was conducted in the absence of any commercial or financial relationships that could be construed as a potential conflict of interest.

Publisher's note

All claims expressed in this article are solely those of the authors and do not necessarily represent those of their affiliated organizations, or those of the publisher, the editors and the reviewers. Any product that may be evaluated in this article, or claim that may be made by its manufacturer, is not guaranteed or endorsed by the publisher.

References

1. Cerhan JR, Habermann TM. Epidemiology of marginal zone lymphoma. *Ann Lymphoma*. (2021) 5(1). doi: 10.21037/aol

2. Isaacson P, Wright DH. Malignant lymphoma of mucosa-associated lymphoid tissue. A distinctive type of B-cell lymphoma. *Cancer*. (1983) 52:1410–6. doi: 10.1002/(ISSN)1097-0142

3. Rossi D, Bertoni F, Zucca E. Marginal-zone lymphomas. *N Engl J Med*. (2022) 386:568–81. doi: 10.1056/NEJMra2102568

4. Marsicovetere P, Ivatury SJ, White B, Holubar SD. Intestinal intussusception: etiology, diagnosis, and treatment. *Clin Colon Rectal Surg*. (2017) 30:30–9. doi: 10.1055/s-0036-1593429

5. Aydin N, Roth A, Misra S. Surgical versus conservative management of adult intussusception: Case series and review. *Int J Surg Case Rep*. (2016) 20:142–6. doi: 10.1016/j.ijscr.2016.01.019

6. Sun M, Li Z, Shu Z, Wu Q, Liu X. Adult intussusception: a challenge to laparoscopic surgery? *PeerJ*. (2022) 10:e14495. doi: 10.7717/peerj.14495

7. Zucca E, Arcaini L, Buske C, Johnson PW, Ponzoni M, Raderer M, et al. Marginal zone lymphomas: ESMO Clinical Practice Guidelines for diagnosis, treatment and follow-up. *Ann Oncol*. (2020) 31:17–29. doi: 10.1016/j.annonc.2019.10.010

8. Markopoulos K, Bührer E, Banz Y, Dawson H, Engelbrecht S, Essig M, et al. Challenges in the diagnosis of marginal zone lymphoma with symptoms of small intestinal disease: a case report and scoping review of the literature. *J Gastrointest Oncol*. (2022) 13:2583–607. doi: 10.21037/jgo

9. Alaggio R, Amador C, Anagnostopoulos I, Attygalle AD, Araujo IBO, Berti E, et al. The 5th edition of the world health organization classification of haematolymphoid tumours: lymphoid neoplasms. *Leukemia*. (2022) 36:1720–48. doi: 10.1038/s41375-022-01620-2

10. Sriskandarajah P, Dearden CE. Epidemiology and environmental aspects of marginal zone lymphomas. *Best Pract Res Clin Haematol*. (2017) 30:84–91. doi: 10.1016/j.beha.2016.07.002

11. Won JH, Kim SM, Kim JW, Park JH, Kim JY. Clinical features, treatment and outcomes of colorectal mucosa-associated lymphoid tissue (MALT) lymphoma: literature reviews published in English between 1993 and 2017. *Cancer Manag Res*. (2019) 11:8577–87. doi: 10.2147/CMAR

12. Palo S. Biligi DS. A unique presentation of primary intestinal MALT lymphoma as multiple lymphomatous polyposis. *J Clin Diagn Res*. (2016) 10:Ed16–18. doi: 10.7860/JCDR/2016/17861.7607

13. Adam P, Czapiewski P, Colak S, Kosmidis P, Tousseyn T, Sagaert X, et al. Prevalence of Achromobacter xylosoxidans in pulmonary mucosa-associated lymphoid tissue lymphoma in different regions of Europe. *Br J Haematol*. (2014) 164:804–10. doi: 10.1111/bjh.12703

14. Zucca E, Bertoni F. The spectrum of MALT lymphoma at different sites: biological and therapeutic relevance. *Blood*. (2016) 127:2082–92. doi: 10.1182/blood-2015-12-624304

15. Zucca E, Bertoni F, Vannata B, Cavalli F. Emerging role of infectious etiologies in the pathogenesis of marginal zone B-cell lymphomas. *Clin Cancer Res*. (2014) 20:5207–16. doi: 10.1158/1078-0432.CCR-14-0496

16. Raderer M, Kiesewetter B, Ferreri AJ. Clinicopathologic characteristics and treatment of marginal zone lymphoma of mucosa-associated lymphoid tissue (MALT lymphoma). *CA Cancer J Clin*. (2016) 66:153–71. doi: 10.3322/caac.21330

17. Tannoury J, Amiot A, Lemonnier F, Dupuis J, Gagnière C, Belhadj K, et al. Colonic mucosa-associated lymphoid tissue lymphoma: a case series. *Leuk Lymphoma*. (2020) 61:582–7. doi: 10.1080/10428194.2019.1686501

18. Mathis KL. Expert commentary on adult intussusception. *Dis Colon Rectum*. (2021) 64:648–9. doi: 10.1097/DCR.0000000000002043

19. Conconi A, Franceschetti S, Aprile von Hohenstaufen K, Margiotta-Casaluci G, Stathis A, Moccia AA, et al. Histologic transformation in marginal zone lymphomas†. *Ann Oncol*. (2015) 26:2329–35. doi: 10.1093/annonc/mdv368

20. Casulo C, Friedberg J. Transformation of marginal zone lymphoma (and association with other lymphomas). *Best Pract Res Clin Haematol*. (2017) 30:131–8. doi: 10.1016/j.beha.2016.08.029

21. Hierlmeier FX, Kolbinger W, Goldbrunner P, Obermeier B. [MALT lymphoma of the ileum as the cause of an enterocolic invagination]. *Dtsch Med Wochenschr*. (1995) 120:1435–8. doi: 10.1055/s-2008-1055496

22. Jayabackthan L, Murgi SB, Graham S, Kini RG. A rare case of primary lymphoma of the caecum presenting as intussusception. *J Lab Physicians*. (2013) 5:118–20. doi: 10.4103/0974-2727.119864

23. Adams KM, Roe NM. A rare case of MALT lymphoma underlying ileocecal intussusception. *J Am Osteopath Assoc*. (2016) 116:e37–40. doi: 10.7556/jaoa.2016.108

24. Coelho MD, Sequeira C, Freire R, Oliveira AP. Small bowel intussusception from an underlying MALT Lymphoma: A double rarity case report. *Hematol Transfus Cell Ther*. (2024) 46:96–8. doi: 10.1016/j.htct.2022.08.010

25. Alderuccio JP, Zhao W, Desai A, Gallastegui N, Ramdial J, Kimble E, et al. Risk factors for transformation to higher-grade lymphoma and its impact on survival in a large cohort of patients with marginal zone lymphoma from a single institution. *J Clin Oncol*. (2018), Jco1800138. doi: 10.1200/JCO.18.00138

26. Cheah CY, Seymour JF. Marginal zone lymphoma: 2023 update on diagnosis and management. *Am J Hematol*. (2023) 98:1645–57. doi: 10.1002/ajh.27058

27. Chen Y, Chen Y, Chen S, Wu L, Xu L, Lian G, et al. Primary gastrointestinal lymphoma: A retrospective multicenter clinical study of 415 cases in Chinese province of Guangdong and a systematic review containing 5075 Chinese patients. *Med (Baltimore)*. (2015) 94:e2119. doi: 10.1097/MD.0000000000002119

28. Resina Sierra E, Miranda García P, Adrados M, Santander Vaquero C. Pedunculated mucosa-associated lymphoid tissue (MALT) lymphoma causing gastric outlet obstruction. *Rev Esp Enferm Dig*. (2021) 113:842–3. doi: 10.17235/reed.2021.8204/2021

29. Wöhrer S, Kiesewetter B, Fischbach J, Müllauer L, Troch M, Lukas J, et al. Retrospective comparison of the effectiveness of various treatment modalities of extragastric MALT lymphoma: a single-center analysis. *Ann Hematol*. (2014) 93:1287–95. doi: 10.1007/s00277-014-2042-z

30. Luminari S, Merli M, Rattotti S, Tarantino V, Marcheselli L, Cavallo F, et al. Early progression as a predictor of survival in marginal zone lymphomas: an analysis from the FIL-NF10 study. *Blood*. (2019) 134:798–801. doi: 10.1182/blood.2019001088

31. Dreyling M, Thieblemont C, Gallamini A, Arcaini L, Campo E, Hermine O, et al. ESMO Consensus conferences: guidelines on Malignant lymphoma. part 2: marginal zone lymphoma, mantle cell lymphoma, peripheral T-cell lymphoma. *Ann Oncol*. (2013) 24:857–77. doi: 10.1093/annonc/mds643

32. Cheson BD, Fisher RI, Barrington SF, Cavalli F, Schwartz LH, Zucca E, et al. Recommendations for initial evaluation, staging, and response assessment of Hodgkin and non-Hodgkin lymphoma: the Lugano classification. *J Clin Oncol*. (2014) 32:3059–68. doi: 10.1200/JCO.2013.54.8800

33. Ishioka M, Hirasawa T, Mishima Y. Latest trends in the incidence of Helicobacter pylori-uninfected gastric mucosa-associated lymphoid tissue lymphoma at the Cancer Institute Hospital, Japan. *Int J Hematol*. (2021) 113:770–1. doi: 10.1007/s12185-021-03086-x

34. Matysiak-Budnik T, Priadko K, Bossard C, Chapelle N, Ruskoné-Fourmestraux A. Clinical management of patients with gastric MALT lymphoma: A gastroenterologist's point of view. *Cancers (Basel)*. (2023) 15(15):3811. doi: 10.3390/cancers15153811

35. Thieblemont C, Zucca E. Clinical aspects and therapy of gastrointestinal MALT lymphoma. *Best Pract Res Clin Haematol*. (2017) 30:109–17. doi: 10.1016/j.beha.2017.01.002

36. Sehn LH, Salles G. Diffuse large B-cell lymphoma. *N Engl J Med*. (2021) 384:842–58. doi: 10.1056/NEJMra2027612

frontiers | Frontiers in Oncology

TYPE Original Research
PUBLISHED 20 June 2024
DOI 10.3389/fonc.2024.1417761

Check for updates

OPEN ACCESS

EDITED BY
Lidia Castagneto Gissey,
Sapienza University of Rome, Italy

REVIEWED BY
Stergios Boussios,
Canterbury Christ Church University, United Kingdom
Giuseppe Angelico,
Agostino Gemelli University Polyclinic (IRCCS), Italy

*CORRESPONDENCE
Xiupeng Jia
Jiaxiup@163.com
Shusheng Liao
lshsh303@sina.com

†These authors have contributed equally to this work

RECEIVED 15 April 2024
ACCEPTED 05 June 2024
PUBLISHED 20 June 2024

CITATION
Chen M, Zhang S, Jia X, Xu Y, Wei Y and Liao S (2024) Ultrasonographic and clinicopathological features of pelvic yolk sac tumors in women: a single-center retrospective analysis.
Front. Oncol. 14:1417761.
doi: 10.3389/fonc.2024.1417761

COPYRIGHT
© 2024 Chen, Zhang, Jia, Xu, Wei and Liao. This is an open-access article distributed under the terms of the Creative Commons Attribution License (CC BY). The use, distribution or reproduction in other forums is permitted, provided the original author(s) and the copyright owner(s) are credited and that the original publication in this journal is cited, in accordance with accepted academic practice. No use, distribution or reproduction is permitted which does not comply with these terms.

Ultrasonographic and clinicopathological features of pelvic yolk sac tumors in women: a single-center retrospective analysis

Mei Chen[1†], Shengmin Zhang[1†], Xiupeng Jia[2*], Youfeng Xu[1], Yaping Wei[3] and Shusheng Liao[4*]

[1]Department of Ultrasonography, The First Affiliated Hospital of Ningbo University, Ningbo, Zhejiang, China, [2]Department of Histopathology, Ningbo Clinical Pathology Diagnosis Center, Ningbo, Zhejiang, China, [3]Department of Ultrasonography, Ningbo Women and Children's Hospital, Ningbo, Zhejiang, China, [4]Department of Ultrasound, The First Affiliated Hospital of Wenzhou Medical University, Wenzhou, Zhejiang, China

Objectives: Yolk sac tumors (YSTs) are rare and highly malignant ovarian malignancies that have a very poor prognosis. The aim of this study is to delineate the ultrasound and clinicopathological features of female pelvic YSTs to better understand the disease.

Methods: This study was a retrospective analysis of the clinicopathological and ultrasound imaging data from 16 YST patients who received treatment at our hospital between January 2012 and August 2023. Then, the ultrasound imaging characteristics were compared with pathological findings.

Results: Among the 16 patients, various degrees of serum AFP increase were observed, and CA125 levels increased in 58.33% (7 out of 12) of patients. Thirteen patients (81.25%) had tumors located in ovary, two patients (12.5%) had tumors located in the sacrococcygeal region, and one patient (6.25%) had tumors located in the mesentery. Pathologically, nine patients presented with simple yolk sac tumors and seven with mixed germ cell tumors. According to the ultrasound manifestations, YST lesions can be classified into three types. (1) the cystic type, was diagnosed in two patients who presented with a large cystic mass with regular morphology and clear boundary and dense liquid within the cyst; and (2) the cystic-solid mixed type, was diagnosed in 4 patients. On 2D ultrasound, the lesions showed a cystic-solid mixed echo, and color Doppler showed a rich blood flow signal in the solid region and cystic separation. made up of four cases. (3) In ten patients with the solid type, 2D ultrasound showed solid uniform echoes with clear boundaries. The "fissure sign" was observed in the lesion. Color Doppler displayed rich blood flow in the solid part, and PW showed low to moderate resistance index of artery (RI:0.21–0.63). On contrast-enhanced ultrasound (CEUS), rapid and high enhancement in the solid part and cystic separation was observed in 2 patients.

Conclusions: Combining ultrasound features with clinical information and tumor markers provides reliable clues for the diagnosis of YST. The application of two-dimensional ultrasound and CEUS combined with patient tumor marker levels can provide a robust reference for determining the necessity of fertility-preserving surgery and postoperative chemotherapy, which can improve clinical decision-making and patient consultation.

KEYWORDS

ovarian, yolk sac tumor, ultrasound, CEUS, malignant germ cell tumor

Introduction

Primary ovarian tumors are usually classified as epithelial, intercord or germ cell tumors, with germ cell tumors accounting for approximately 15–20% of all ovarian tumors (1). Germ cell tumors are further divided into benign and malignant types, with mature teratoma being the most common benign type and malignant germ cell tumors being the most common undifferentiated carcinoma types. Contrary to epithelial ovarian cancers, germ cell tumors mostly present at an earlier age in women, grow faster and present unilaterally (2). Yolk sac tumor (YST), also known as endodermal sinus tumor, is a rare and highly malignant germ cell tumor that accounts for 1% of all ovarian malignancies (3). Ovarian YSTs predominantly affect children and young women, with onset typically occurring before the age of 30; even some patients are pregnant or postmenopausal period (4, 5). It exhibits rapid growth, invasiveness, and a propensity for metastasis, resulting in a very poor prognosis. Before the 1970s, the three-year survival rate for patients was only 13% (6). However, advancements in diagnostic techniques, surgical methods, and adjuvant therapy, particularly the use of modern treatment regimens such as BEP (bleomycin, etoposide, cisplatin) have significantly improved the 5-year survival rate for patients with YSTs (7, 8). As life expectancy increases, patients, especially younger patients, have heightened expectations for quality of life, including concerns about fertility preservation after surgery. Therefore, early diagnosis through imaging methods is crucial for patients to achieve favorable outcomes. Ultrasonographic diagnosis plays an important role in imaging diagnosis, with contrast-enhanced ultrasound(CEUS), a new technique reflecting tumor microcirculation, holding particular significance in the early diagnosis of tumors (9–11). Due to the low incidence of YSTs, previous reports in the literature mainly consist of individual cases (12). Moreover, ultrasound reports have been limited to two-dimensional gray scale ultrasound (13), and there is a lack of literature on classifying YST basing on ultrasound images. In this study, a retrospective analysis of multimodality ultrasound manifestations of 16 patients with YSTs, combined with clinical data, was conducted to improve the diagnostic accuracy of YSTs.

Abbreviations: AFP, alpha fetoprotein; CEUS, contrast-enhanced ultrasound; CDFI, color Doppler flow imaging; FIGO, international Federation of Gynecology and Obstetrics; YST, yolk sac tumor.

Materials and methods

Study population

This retrospective study was conducted at Ningbo First Hospital and it adhered to the principles outlined in the Declaration of Helsinki. The study was approved by the ethics committee of Ningbo First Hospital (No.2023RS128). Individual consent was obtained from all patients in this retrospective analysis. A computerized search of the pathology records at the hospital was conducted from January 2012 to August 2023. This resulted in the identification of 27 patients with a histological diagnosis of YSTs. Subsequently, a second search was performed on the hospital's imaging archiving and communication system to identify female patients who underwent 2D and/or CEUS examination prior to surgery. Ultimately, 16 patients were identified, 9 of whom were male. All 16 patients had 2D ultrasound examination data, and two of them also had CEUS results.

Ultrasound examination

The equipment and parameters for this study included the GE E8, Toshiba Aplio 500, and Philips IU22 color Doppler ultrasound diagnostic systems. Ultrasound examinations were conducted using a transvaginal probe with a frequency range of 5–9 MHz and a transabdominal probe with a frequency range of 3.5–5.0 MHz. All patients underwent standard two-dimensional and color Doppler ultrasound assessments. The two-dimensional ultrasonography was used to evaluate the lesion location, size, shape, boundaries, internal echo characteristics, and the presence of pleuritic and abdominal effusion. Color Doppler flow imaging (CDFI) was utilized to analyze the blood flow within the lesions.

Additionally, two patients underwent contrast-enhanced ultrasound (CEUS) to investigate the microcirculation patterns

within the lesions. This procedure involved the administration of a contrast agent (SonoVue, Bracco) at a 1.8 ml dose via the median antecubital vein. Throughout the contrast-enhanced phase, continuous observation was made of the enhancement pattern, timing, intensity, and washout of the contrast agent within the lesions.

Statistical methods

Continuous data are presented as mean or median (interquartile spacing (IQR)), and categorical data are presented as frequencies and percentages. The analysis was performed using IBM SPSS 17.0 (IBM, Armonk, NY)

Results

Clinical data of the 16 patients

Sixteen female patients with a pathological diagnosis of YST were enrolled in this study. The clinical characteristics are shown in Table 1. The mean age of the 16 patients was 23.25 ± 20.80 (range: 1 ~72) years, 68.75% were younger than 30 years, while 31.25% were older than 30 years. Additionally, 12.5% (2 out of 16) were menopausal, and 87.5% (14 out of 16) were non-menopausal. The patients were follow-up for a mean duration of 22.5 ± 14.56 months (range: 3–54).Fourteen patients presented with abdominal pain, while two patients were asymptomatic. Serum AFP levels were increased in all (100%, 16 out of 16) patients, with 70% (7 out of 10) of patients showing higher CA 125 levels, 16.66% (2 out of12)of patients showing higher CEA levels, 36.36% (4 out of 11) of patients showing increased CA199 levels, and only 12.5% (1 out of 8) of patients showing higher CA724 levels. The CA153 level in 8 patients, along with the β-hCG level in 11 patients, was within the normal range. Employing the FIGO tumors staging system, this study revealed that 87.5% (14 out of 16) of patients were classified as stage I, 6.25% (1 out of 16) as stage III, and 6.25% (1 out of 16) as stage IV. Thirteen patients (81.25%) had tumors located in the ovary, two patients (12.5%) had tumors located in the sacrococcygeal region, and one patient (6.25%) had tumors located in the mesentery. Among these 16 patients, ten underwent transabdominal ovarian and adnexectomy, three received total and double appendicectomy, and three had only lesion resected. Gross specimen examination revealed a round or oval mass with a yellow color, clear capsule, and visible "cobblestone", similar to irregular liquid dark areas. Some dark areas were brown (Figure 1A).

TABLE 1 Clinical characteristics of 16 patients with ovarian yolk sac tumor.

Parameters		Yolk Sac tumor (n = 16)
Age at surgery [years]		23 (1–72)
0–9		18.75% (3/16)
10–19		31.25% (5/16)
20–30		18.75% (3/16)
>30		31.25% (5/16)
Serum CA125 level [U/mL] Reference range(0–30)	<30	41.66% (5/12)
	>30	58.33% (7/12)
Serum CA-724 level [U/ml] Reference range(0–7)	<7	87.50% (7/8)
	>7	12.50% (1/8)
Serum CA-153 level [U/mL] Reference range(0–25)	<25	100% (8/8)
	>25	0
Serum CA-199 level [U/ml] Reference range(0–25)	<25	63.63% (7/11)
	>25	36.36% (4/11)
AFP level [ng/mL] Reference range(0–25)	<25	0
	>25	100% (16/16)
CEA level [U/mL] Reference range(0–10)	<10	83.33% (10/12)
	>10	16.66% (2/12)
Menstruation	Premenopausal	87.50% (14/16)
	Postmenopausal	12.50% (2/16)
Symptomatology	Asymptomatic	12.50% (2/16)
	Pelvic pain	87.50% (14/16)
Surgery	Transabdominal tylectomy	25.0% (4/16)
	Salpingo-oophorectomy laparotomy	56.25% (9/16)
	Total abdominal hysterectomy	18.75% (3/16)
FIGO by stages	I designated time	81.25% (13/16)
	II designated time	0
	III designated time	12.5% (2/16)
	VI designated time	6.25% (1/16)
pathology	Simplicity	56.25% (9/16)
	Mixed type	43.75% (7/16)

Pathological characteristics of the patients

Histopathological analysis revealed that nine (56.25%) patients had pure YSTs (Figures 2A–C), while seven (43.75%) patients had mixed germ cell tumors (Figures 2D–F). Among the mixed germ cell tumors, 25% (4 out of 16) had different combinations of YSTs and mature teratomas (Figure 2F); 12.5% (2 out of 16) had a combination of 10% YSTs and 90% immature teratomas, and one patient had poorly differentiated carcinoma with yolk sac differentiation. Among patients with serum AFP levels greater than 3000, 71.42% (5 out of 7) had pure yolk sac tumor, while 29.58% (2 out of 7) had a combination of 90% yolk sac tumors and 10% mature teratomas. Regarding immunohistochemical markers in the 16 patients, 93.75% (15 out of 16) of the patients were AFP positive (Figure 1B). One hundred percent (10 out of 10) of patients were CK (pan) positive, and

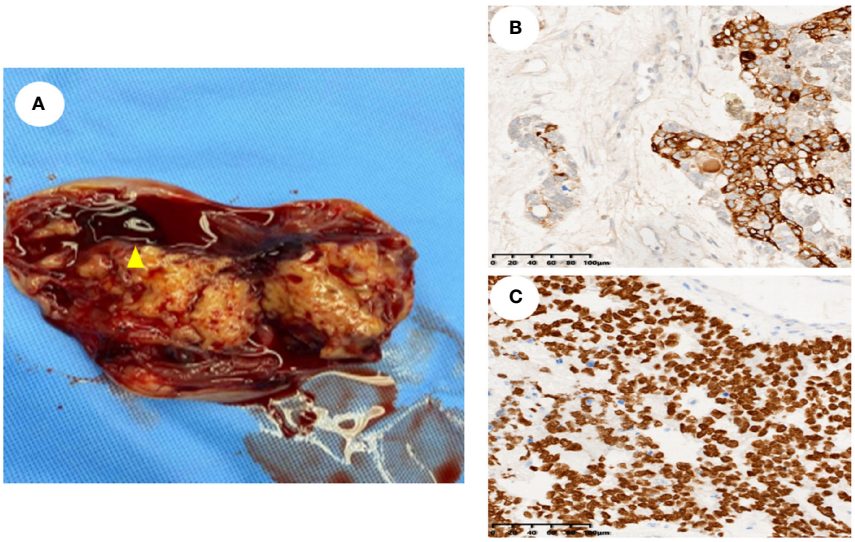

FIGURE 1
General sample and immunohistochemical markers of ovarian yolk sac tumor. **(A)**. A gross specimen of an ovarian yolk sac tumor was an oval mass with a yellow vision, a smooth capsule and visible capsular hemorrhage (triangle); **(B)**. Immunohistochemistry showed high AFP expression in yolk sac tumor cells (SP method, ×200); **(C)**. Immunohistochemistry showed high SALL4 expression in yolk sac tumor cells (SP method, ×200).

100% (13 out of 13) of patients were SALL 4 (+) positive (Figure 1C). One hundred percent (12 out of 12) of patients were positive for GPC 3, 91.66% (11out of 12) of patients were positive for HNF1β and 100% (7 out of 7) of patients were positive for Lin28. The Ki-67 (%) ranged between 25% and 90% in 15 patients. All 12 patients were tested negative for D2–40 and β-HCG, while 90.90% (10 out of 11) of the patients tested negative for NapsinA. The immunohistochemistry results are shown in Table 2.

Ultrasound classification and image characteristics of 16 patients

The ultrasound findings are shown in Table 3. All 16 patients presented with solitary tumors, including seven in the left ovary, six in the right ovary, two in the sacrococcygeal region and one in the mesentery. According to the ultrasound image of the tumor, it was divided into cystic, cystic-solid mixed type and solid type.

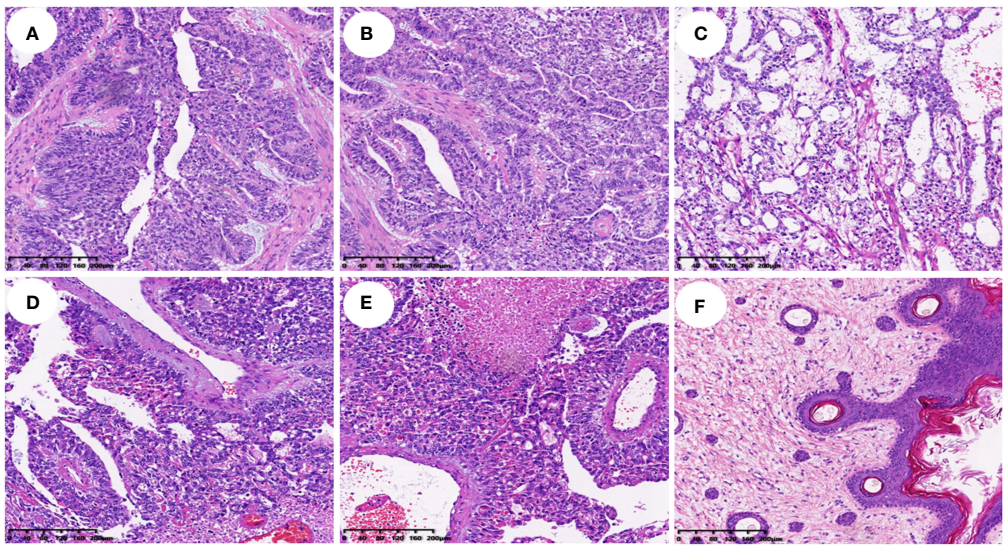

FIGURE 2
Histopathological findings of different types of yolk sac tumor (HE staining, all ×100). **(A–C)**. Histopathological findings of a simple yolk sac tumor; **(D–F)**. Histopathological findings of a mixed germ cell tumor with yolk sac tumor cell component in **(D)**, Schiller-Duval (SD) body in **(E)**, and mature teratoma in **(F)**.

TABLE 2 Two-dimensional and color Doppler ultrasound findings of the 16 patients with YSTs.

Ultrasonic classification		Cystic (n=2)	Cystic-solid Mixed (n=4)	Solid (n=10)
Number		12.50% (2/16)	25% (4/16)	62.50% (10/16)
Position	Left		12.50% (2/16)	31.25% (5/16)
	Right	12.50% (2/16)	12.50% (2/16)	12.50% (2/16)
	Other			18.75% (3/16)
Maximum diameter (cm)		9.6~12.1	10.7~25	6.9~16.9
Shape	Regular	12.50% (2/16)	18.75% (3/16)	38.45% (7/16)
	Irregular	0	6.25% (1/16)	43.75% (3/16)
Border	Clear	12.50% (2/16)	25% (4/16)	50% (8/16)
	Unclear			12.50% (2/16)
Cystic fluid	Clear	6.25% (1/16)		
	Unclear	6.25% (1/16)	25% (4/16)	12.50% (2/16)
	No			50.0% (8/16)
Separated	Yes	6.25% (1/16)	25% (4/16)	12.50% (2/16)
	No	6.25% (1/16)		50.0% (8/16)
Parenchymal echo and blood flow in the sac	Yes	6.25% (1/16)	25% (4/16)	0
	No	6.25% (1/16)	0	62.50% (10/16)
RI				0.21–0.63
Calcification	Yes		0	
	No	12.50% (2/16)	25.0% (4/16)	62.50% (10/16)
Associated with ascites	No		6.25% (1/16)	25.0% (4/16)
	Mild	12.50% (2/16)	12.5% (2/16)	12.5% (2/16)
	Medium			12.50% (2/16)
	Severe		6.25% (1/16)	12.50% (2/16)
Associated with hydrothorax	Yes	6.25% (1/16)		
	No	6.25% (1/16)	25% (4/16)	62.50% (10/16)
Associated with uterine fibroids	Yes	6.25% (1/16)		6.25% (1/16)
	No	6.25% (1/16)	25% (4/16)	56.25% (9/16)
Associated with Endometrial polyp	Yes	6.25% (1/16)		
	No	6.25% (1/16)	25% (4/16)	62.50% (10/16)
Ultrasound diagnosis	Benign	12.50% (2/16)	6.25% (1/16)	
	Uncertain			18.75% (3/16)
	Malignant		18.75% (3/16)	43.75% (7/16)

(1) Two patients had the cystic type (Figure 3A; Figure 4C), with a maximum diameter of 12.1cm, regular morphology and clear boundary. One patient presented with a cyst filled with dense liquid; the other patient presented with a cyst with septation and mural papillary protrusion, and color Doppler imaging revealed punctate blood flow signal in septation and papillary (Figure 3D). Two patients had moderate ascites, and one patient had pleural effusion.

(2) There were four cases of the cystic-solid mixed type (Figure 3B), with a maximum diameter of 25cm, clear boundary and regular morphology, and cystic part was filled with fine light spot echoes. Color Doppler demonstrated a rich blood flow signal in solid part and cystic separation (Figure 3E). One patient had a large amount of ascites, two patients had moderate ascites. One patient was classified as a benign tumor according to ultrasound performance, and three cases as malignant.

TABLE 3 Expression of immune markers in tumor cells of 16 patients with yolk sac tumor.

Immunohistochemical markers	AFP	CK (pan)	SALL4 (+)	GPC3	CK7	HNF1β	CD 30	CD 117	D2–40	HCG-β	Lin28	NapsinA	Ki-67 (%)
Case1	+	+	+	+			–	–	–	–	+		80
Case2	+	+	+	+	–	+	–	–	–	–	+	–	70
Case3	+	+			+	+						+	70
Case4	+		+	+	–	+	–	–	–	–		–	80
Case5	+	+	+	+	–	+	–	+	–	–		–	25
Case6	+	+		+	–	+		+	–	–		–	80
Case7	+		+	+	–	+	–	+	–	–	+	–	80
Case8	+	+++	+				–	+					80
Case9	+		+	+	–	+	+			–	+		80
Case10	+	+	+	+	–	+	–	+	–	–	+	–	60
Case11	–				+	–						–	70
Case12	+		+	+	–	+	–	+	–	–	+	–	90
Case13	+		+	+	–	+	–	+	–	–		–	40
Case14	+	+	+	+	+	+		+	–	–	+	–	60
Case15	+	+	+				–	+	–				
Case16	+	+	+	+			–	+	–	–			60

+, positive; +++, strongly positive; -, negative.

10.3389/fonc.2024.1417761

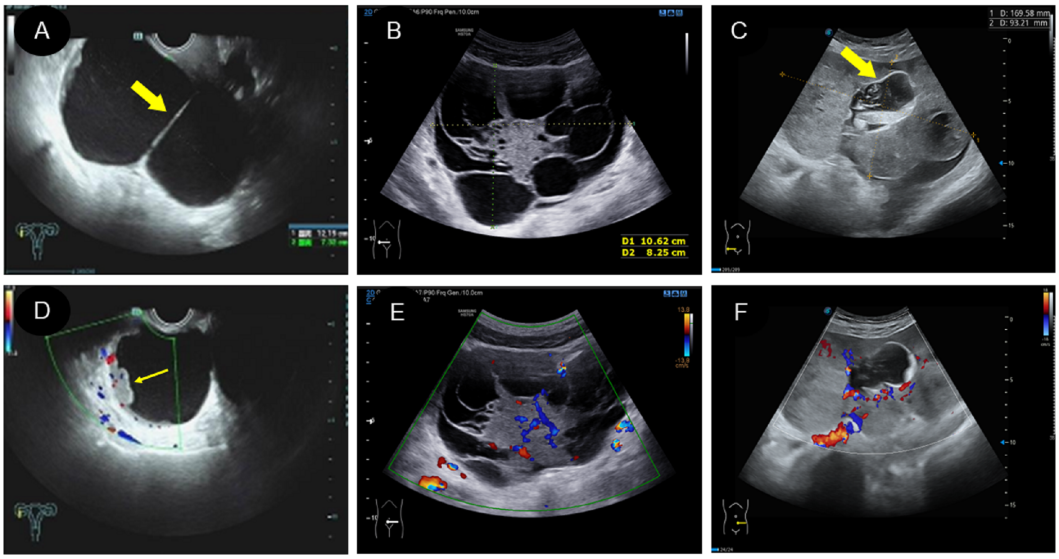

FIGURE 3
Two dimensional and color Doppler ultrasound findings of different types of yolk sac tumors. **(A, D)**. Cystic yolk sac tumor is a large cyst with regular morphology and clear boundary. The cyst is filled with weak echoes, with septation (thick arrow) and mural papillary nodules (thin arrow) visible on the wall. Color Doppler flow imaging (CDFI) showed punctate blood flow signals in the cystic wall and nodules; **(B, E)**. Cystic solid mixed yolk sac tumor also showed regular morphology and a clear boundary. The solid part showed low echoes, while the cystic part displayed large separation of different sizes and uneven thickness, separating the cystic area into many small chambers. CDFI revealed rich blood flow signals in the solid part and separation; **(C, F)**. Solid yolk sac tumor appears as a large solid mass with a more irregular morphology but a clear boundary. It displayed moderate echogenicity, less uniformity, and partially visible small cystic area (thick arrow), CDFI showed rich internal flow signals.

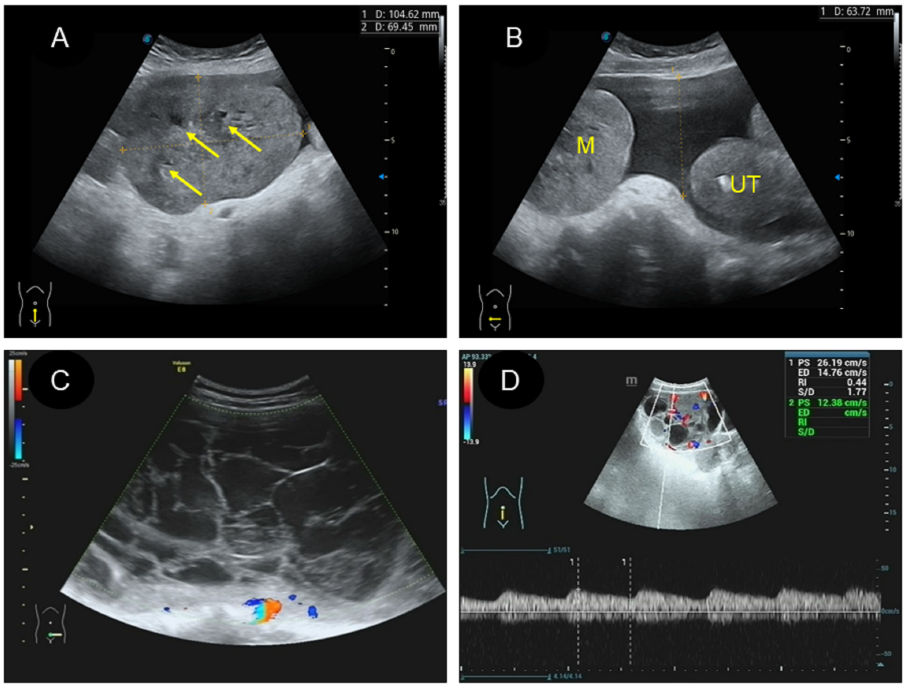

FIGURE 4
Some specific ultrasound findings of different types of yolk sac tumor. **(A)**." Fissure sign " inside the solid yolk sac tumor (thin arrow); **(B)**. A solid yolk sac tumor complicated with a large amount of ascites; **(C)**. A large number of irregular arrangement separation in cystic type of yolk sac tumor, and CDFI showed no blood flow signal in separation; **(D)**. PW showed low resistance of artery in the solid type of yolk sac tumor.

(3) There were 10 patients with the solid type (Figure 3C), with a maximum diameter of 16cm. Among them, three patients had irregular morphology, and two had unclear boundaries. The "fissure sign" was observed in lesions (Figure 4A). Color Doppler showed rich blood flow in the solid region (Figure 3F), and the PW showed a low to moderate resistance index of artery (RI:0.21–0.63) (Figure 4D). Six patients exhibited various degree of ascites (Figure 4B). One patient accompanied with uterine fibroids. No calcification was observed in any of the lesions.

A and D. Cystic yolk sac tumor is a large cyst with regular morphology and clear boundary. The cyst is filled with weak echoes, with septation (thick arrow) and mural papillary nodules (thin arrow) visible on the wall. Color Doppler flow imaging (CDFI) showed punctate blood flow signals in the cystic wall and nodules; B and E. Cystic solid mixed yolk sac tumor also showed regular morphology and a clear boundary. The solid part showed low echoes, while the cystic part displayed large separation of different sizes and uneven thickness, separating the cystic area into many small chambers. CDFI revealed rich blood flow signals in the solid part and separation; C and F. Solid yolk sac tumor appears as a large solid mass with a more irregular morphology but a clear boundary. It displayed moderate echogenicity, less uniformity, and partially visible small cystic area (thick arrow), CDFI showed rich internal flow signals.

CEUS image characteristics in two patients

Two of the 16 patients in this study underwent CEUS. Patient 1 was of cystic-solid mixed type, and after contrast agent injection, the solid and separated parts were rapidly enhanced and quickly subsided (Figures 5A, D; Supplementary Video 1). There was no contrast agent entry into the capsule, and no contrast echo was observed in the pelvic fluid. Patient 2 had a 17-year-old solid lesion with rapid contrast enhancement after contrast agent injection (Figures 5B, E; Supplementary Video 2). One of the cystic separations showed contrast accumulation, and the contrast agent flooded into and accumulated into the sac wall after a burst, leaving a large amount of contrast agent in the cystic cavity (Figures 5C, F). However, there was no contrast agent in the pelvic cavity. The patient stood up after ultrasound examination and then experienced shock. There was an intraoperative opening in the tumor, and a large amount of bloody fluid were observed in the pelvic cavity.

Discussion

Pathologically, our study revealed that yolk sac tumors can present as pure or mixed germ cell tumors. A significantly higher AFP level was the diagnostic biomarker for YSTs. YST can present as cystic, cystic-solid or solid profiles on two-dimension ultrasound, and each type has distinct features. Rich blood flow in the solid part at color Doppler examination is another important ultrasound feature. Exploratively, rapid and high enhancement in the solid part was observed in two YST patients by using CEUS. Therefore, an important strength of this study is that the integration of conventional ultrasound and CEUS methods was introduced to elaborate the characteristics of YSTs. A second strength is that the combination of ultrasound features and biomarkers has been emphasized in the diagnosis of YSTs.

In 1939, Schiller named the characteristic reticuloglomerular-like structure of yolk sac tumors and described the tumors as

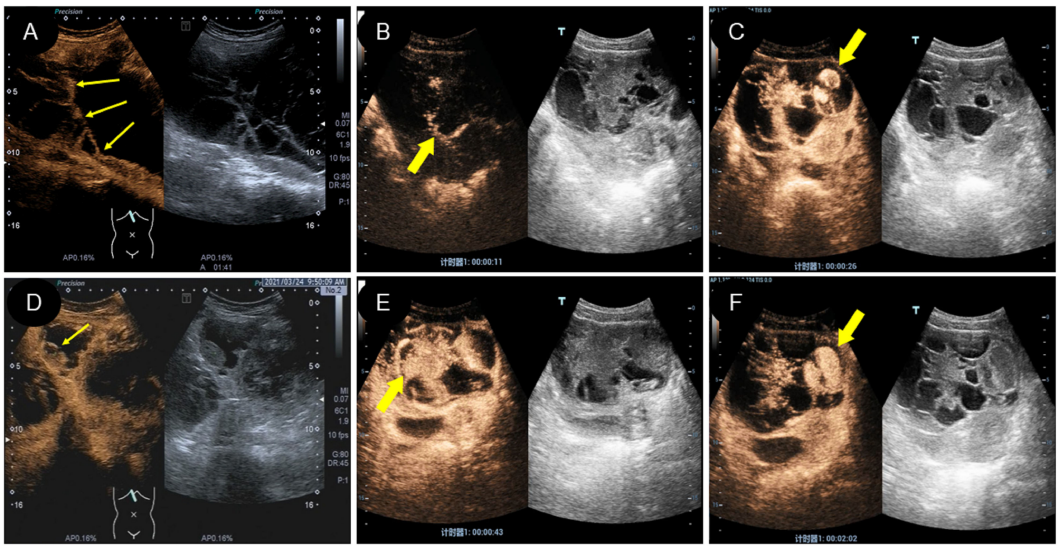

FIGURE 5
Characteristics of CEUS different types of yolk sac tumor. **(A, D)**. A mixed yolk sac tumor showed rapid contrast enhancement and no contrast perfusion in the sac (thin arrow); **(B, E)**. A solid yolk sac tumor showed rapid enhancement of solid and cystic area separation, with large internal vessels in the early stage (thick arrow) and uniform high enhancement after peak (thick arrow); **(C, F)**. In this case of a solid yolk sac tumor, the contrast agent flooded into and accumulated into the sac wall (thick arrow) after a burst, leaving a large number of contrast agent remained in the cystic cavity (thick arrow) after the resolution of the solid part.

originating in the middle kidney (8, 14). In 1959, it was discovered that the endodermal sinus of rat placenta was derived from extraembryonic germ cells (15). Studies by Kojimahara (7) and Nasioudis (16) confirmed that yolk sac tumors typically present unilaterally, are large and present often in the early stages of the disease (17). In this study, 87.5% (14 out of 16) of patients were diagnosed with stage FIGO I tumors, with tumor diameters ranging from 6.5cm to 25.0cm. Interestingly, there have reports of successful pregnancies in patients with YSTs, with some patients continuing pregnancy and experiencing smooth deliveries after surgery, as reported by Alrjoub (18) and Pafilis (19). YSTs are more common in female ovaries or male testis, but they can also manifest along the migration path of testicular tissue or in unusual locations, such as the vulva, mediastinum, sacral tail, mesentery, and even intracranial sites, such as the nasopharynx, sinuses, and pineal body (20). Pathologically, YSTs can present as simple lesions or as a part of mixed germ cell tumors (17, 21). Malignant mixed germinoma are defined by the presence of two or more malignant germ cell components, including yolk sac tumors, embryonal carcinomas, choriocarcinomas or immature teratomas (7, 22). Among these, the combination of asexual cell tumor and yolk sac tumor is the most common (23). Therefore, pathology reports should elaborate on the sizes and percentages of all germ cell components (22).

In this study, 87.50% (14 out of 16) of patients presented with abdominal pain, and 12.50% (2 out of 16) had no obvious symptoms, which is consistent with the findings of the study by Faure et al. (17). This discrepancy in symptoms may be attributed to the size and aggressiveness of the tumor. Asymptomatic patients likely have smaller tumors in the early stages, whereas those experiencing abdominal pain and distension may have larger, rapidly growing tumors that compress surrounding organs. In addition, the aggressive nature of the tumor can lead to thoracic or abdominal metastasis, resulting in pleural fluid or ascites. Among the 16 patients in this study, 11 had various degrees of ascites. All 16 patients underwent surgical procedures, with 56.25% (9 out of 16) presenting with pure YST, and 43.75% (7 out of 16) with mixed germ cell tumors, which is consistent with previous reports (17). Within the mixed germ cell tumors subgroup, 25% (4 out of 16) had different combinations of YSTs and mature teratomas, while 12.5% (2 out of 16) had a 10% YST and 90% immature teratoma combination, along with one case of poorly differentiated carcinoma with yolk sac differentiation. These findings contrast with those of Ulbright (14), who reported that mixed germ cell tumors are common in patients with yolk sac tumor. Post-surgery tumor staging revealed that 81.25% (13 out of 16) of patients had stage FIGO I tumors, which were confined to one side of the ovary, suggesting an early stage despite a larger tumor size. After surgery, patients received BEP chemotherapy, and after a follow-up period of 22.5 ± 14.56 (ranging from 3 to 54 months), none of the patients experienced recurrence or metastasis. Comprehensive treatment has significantly improved the 5-year survival rate for female YST, across FIGO stages I, II, III and IV, and the percentages for each stage are 94.8%, 97.1%, 70.9% and 51.6% respectively (7). Even patients with advanced FIGO stage disease benefited from comprehensive treatment for fertility protection, underscoring its efficacy in prolonging life and improving the quality of life. Therefore, timely detection through imaging methods and laboratory examination forms the cornerstone for achieving favorable prognosis.

Due to their origin from primordial germ cells, nearly all YST patients exhibit positive expression of serum AFP, which is a fundamental diagnostic tool and prognostic indicator for the tumor (24). In this study, all 16 patients demonstrated elevated AFP levels, with 43.75% (7 out of 16) showing levels greater than 3000. Postoperative pathology confirmed that 71.42% (5 out of 7) of patients had pure yolk sac tumors, while 29.58% (2 out of 7) had predominantly yolk sac tumors with a minor component of mature teratoma. The level of AFP correlates closely with the tumor pathology; pure yolk sac tumors show significantly higher AFP levels than mixed germ cell tumors, aiding in preoperative tumor classification and postoperative efficacy and recurrence assessment. Although YST is mostly present at early age of women, but an ovarian mass with elevated serum AFP level in postmenopausal women should suspect the diagnosis of germ cell tumors (5). In this study, 70% (7 out of 10) of patients exhibited various degrees of CA125 elevation, potentially linked to enteroid cells with multiphase differentiation potential (25). However, the specificity of CA125 in yolk sac tumors is less strong. Recent literature has indicated that combination of various serum biomarkers and patient characteristics may provide effective screening modalities for ovarian cancer (26). Currently, CA-125 and HE4 are considered two important biomarkers of gynecological malignancies and are mostly found in epithelial-derived tumors (26). However, these methods are not sufficient for early detection of pelvic masses. Conversely, the serum levels of CEA, CA724, CA153, and β-hCG did not significantly increase in this study.

Regarding the immunohistochemical markers in this cohort, 100% (10 out of 10) were positive for CK (pan), 100% (13 out of 13) were positive for SALL 4 (+), 100% (12 out of 12) were positive for GPC 3 and 100% (7 out of 7) were positive for Lin28.This finding confirms the significance of these markers as strong and specific indicators for YSTs, which is consistent with the findings of previous literature (27). Additionally, 93.75% (15 out of 16) of patients tested positive for AFP, with the exception of Patient 11, who had a serum AFP level of 12.95ng/mL. This patient was identified as having undifferentiated cancer with a small amount of yolk sac differentiation, indicating that a negative AFP result on immunohistochemistry cannot completely exclude the possibility of yolk sac tumor components, possibly due to their limited presence in the tumor. SALL 4 (+) is a more representative immune marker than AFP (28), with all 13 patients in this study testing positive. There are also studies suggesting that HNF1β is a new indicator of YST (29). In this study, 91.66% (11out of12) of patients were tested positive for HNF1β. Furthermore, 80.0% (12 out of15) patients were tested positive for CD117, and in the case of Ki-67 (%), which ranged between 25% and 90%, a positive correlation was observed with the content of yolk sac tumor component, showing its potential as an important immunohistochemical indicator. Conversely, 100% (12 out of 12) tested negative for D2–40 and

HCG- β, and 90.9% (10out of11) tested negative for NapsinA, providing a basis for the differential diagnosis of YST.

This study recorded the clinical data and two-dimensional ultrasound findings of 16 patients with YSTs, attempting to classify and elaborate the characteristics of each subtype, while also documenting the CEUS findings in two patients. The lesions were classified into three types according to ultrasound findings: (1) the cystic type, diagnosed in 2 patients, one of whom showed septation and nodules in the sac. This type is easily confused with cystadenoma of the ovary (13). Although it can appear as a large cyst with intracapsular septa and protrusion, the serum AFP of patients with cystadenoma of the ovary was negative. (2) The cystic-solid mixed type showed a well-defined mass with cystic separation of varying thickness, an irregular morphology of solid part, and rich blood flow, as observed on color Doppler imaging. This ultrasonographic manifestation may be attributed to rapid tumor growth and the imperfect development of capillaries, resulting in internal ischemic necrosis. In this study, one patient was erroneously classified as a benign tumor, while three patients were deemed malignant. It is challenging to identify YST only by ultrasound images, especially those with rich blood flow, and it is difficult to distinguish them from ovarian cystadenocarcinoma (30) and ovarian metastases. Ovarian cystadenocarcinoma usually occurs at an older age, and serum AFP is negative, whereas metastatic tumors have a history of primary malignancy in other organs.

(3) The solid type showed slightly more solid echoes, fine inner texture, and "crack" and "cheese" sign, with a low resistance index. Seven patients were considered possibly malignant, while three patients were difficult to diagnose. The "fissure sign" observed in ultrasound manifestations is attributed to rapid tumor growth, immature development of internal blood vessels, and the band-like ischemic necrosis in the weak areas with limited blood supply. The difficulty in determining the nature of these three tumors may stem from their smooth boundaries and lack of invasive breakthrough envelope growth characteristics. Ascites in these patients result from the large mass compressing surrounding tissues, obstructing lymphatic reflux (13). This type of tumor should be distinguished from various solid ovarian tumors, such as subserous fibroids, broad ligament myoma, granulosa cell tumor. During the ultrasound examination, the echo of the tumor was found in the adnexa area, and normal acoustic images of the ovary were visible. Moreover, CDFI showed that the color blood flow signal extended from the uterine wall to the interior of the tumor, and the lesion may be a uterine subserous myoma or broad ligament myoma. Granulosa cell tumors have elevated level of estrogen and testosterone or androgen (31). In summary, when differentiating YSTs from other benign and malignant ovarian tumors based on ultrasound images is difficult, the patient's age of onset, clinical manifestations and serum AFP can be used as important references for improving diagnosis.

CEUS plays an important role in reflecting the microcirculation within the tumor (32). In this study, two patients underwent CEUS examination. One patient was a 24-year-old female with a solid mixture tumor, exhibiting rapid and high enhancement after the injection of contrast agent. However, there was no contrast agent perfusion in the cystic area. Although the ultrasound images were similar to those of ovarian serous or mucinous tumors (33), these tumors were negative for serum AFP. The other patient, a 17-year-old woman with a solid tumor displayed rapid enhancement of the solid part and separation after contrast agent injection, followed by rapid subsidence. During this process, the contrast agent accumulated in the cystic cavity, with the tumor capsule remaining intact and no contrast agent distributed in the pelvic cavity. However, the patient experienced syncope immediately after the CEUS procedure, which was caused by the rupture of the tumor's anterior and posterior walls and the presence of a large amount of bloody fluid in the pelvic cavity, which was identified after surgery. Retrospective analysis of the ultrasound contrast images revealed no contrast in the pelvic fluid, indicating damage to the cyst wall with contrast influx, despite smooth and intact tumor capsule observed in some patients' general specimen. Real-time contrast-enhanced ultrasound can identify the location and extent of blood vessel damage in the cystic wall (34). With increasing bleeding in the tumor, tension can stimulate the capsule and cause lower abdominal pain. Abrupt increases in abdominal pressure, such as changes in the patient's position or external forces, can lead to rupture of the tumor. Evaluating the distribution of contrast agent helps to assess tumor torsion and local bleeding, guiding clinicians on optimal timing for surgery.

Conclusion

Combining ultrasound features with clinical information and tumor markers provides reliable clues for the diagnosis of yolk sac tumor. CEUS aids clinicians in assessing internal microcirculation and detecting internal bleeding. The integration of two-dimensional ultrasound and CEUS findings with patient tumor marker levels strengthens the decision-making process regarding the necessity of fertility-preserving surgery and postoperative chemotherapy, enhancing clinical outcomes and patient counseling. Due to the limitation of sample size in this study, a multicenter, large sample study is needed to further increase the understanding of this topic.

Data availability statement

The raw data supporting the conclusions of this article will be made available by the authors, without undue reservation.

Ethics statement

The studies involving humans were approved by the ethics committee of Ningbo First Hospital (No.2023RS128). The studies were conducted in accordance with the local legislation and institutional requirements. Written informed consent for participation in this study was provided by the participants' legal guardians/next of kin. Written informed consent was obtained from the individual(s), and minor(s)' legal guardian/next of kin, for the publication of any potentially identifiable images or data included in this article.

Author contributions

MC: Conceptualization, Formal analysis, Funding acquisition, Investigation, Methodology, Resources, Validation, Writing – original draft, Writing – review & editing. SZ: Data curation, Investigation, Methodology, Project administration, Resources, Visualization, Writing – review & editing. XJ: Conceptualization, Methodology, Project administration, Resources, Supervision, Validation, Writing – review & editing. YX: Conceptualization, Methodology, Project administration, Validation, Visualization, Writing – review & editing. YW: Data curation, Project administration, Resources, Visualization, Writing – review & editing. SL: Conceptualization, Investigation, Project administration, Supervision, Visualization, Writing – original draft, Writing – review & editing.

Funding

The author(s) declare financial support was received for the research, authorship, and/or publication of this article. This work was supported by the Medical and Health Science and Technology Project of Zhejiang Province (NO. 2020KY830).

Conflict of interest

The authors declare that the research was conducted in the absence of any commercial or financial relationships that could be construed as a potential conflict of interest.

Publisher's note

All claims expressed in this article are solely those of the authors and do not necessarily represent those of their affiliated organizations, or those of the publisher, the editors and the reviewers. Any product that may be evaluated in this article, or claim that may be made by its manufacturer, is not guaranteed or endorsed by the publisher.

Supplementary material

The Supplementary Material for this article can be found online at: https://www.frontiersin.org/articles/10.3389/fonc.2024.1417761/full#supplementary-material

References

1. Gupta N, Yadav M, Gupta V, Chaudhary D, Patne SCU. Distribution of various histopathological types of ovarian tumors: A study of 212 cases from a tertiary care center of Eastern Uttar Pradesh. *J Lab Phys*. (2019) 11:75–81. doi: 10.4103/JLP.JLP_117_18

2. Saani I, Raj N, Sood R, Ansari S, Mandviwala HA, Sanchez E, et al. Clinical challenges in the management of Malignant ovarian germ cell tumours. *Int J Environ Res Public Health*. (2023) 20:6089. doi: 10.3390/ijerph20126089

3. Dallenbach P, Bonnefoi H, Pelte MF, Vlastos G. Yolk sac tumours of the ovary: an update. *Eur J Surg Oncol*. (2006) 32:1063–75. doi: 10.1016/j.ejso.2006.07.010

4. Boussios S, Moschetta M, Tatsi K, Tsiouris A, Pavlidis N. A review on pregnancy complicated by ovarian epithelial and non-epithelial Malignant tumors: Diagnostic and therapeutic perspectives. *J Adv Res*. (2018) 12:1–9. doi: 10.1016/j.jare.2018.02.006

5. Boussios S, Attygalle A, Hazell S, Moschetta M, Mclachlan J, Okines A, et al. Malignant ovarian germ cell tumors in postmenopausal patients: The royal marsden experience and literature review. *Anticancer Res*. (2015) 35:6713–22.

6. Kurman RJ, Norris HJ. Endodermal sinus tumor of the ovary: a clinical and pathologic analysis of 71 cases. *Cancer*. (1976) 38:2404–19. doi: 10.1002/(ISSN)1097-0142

7. Kojimahara T, Nakahara K, Takano T, Yaegashi N, Nishiyama H, Fujimori K, et al. Yolk sac tumor of the ovary: a retrospective multicenter study of 33 Japanese women by Tohoku Gynecologic Cancer Unit (TGCU). *Tohoku J Exp Med*. (2013) 230:211–7. doi: 10.1620/tjem.230.211

8. Young RH. The yolk sac tumor: reflections on a remarkable neoplasm and two of the many intrigued by it-Gunnar Teilum and Aleksander Talerman-and the bond it formed between them. *Int J Surg Pathol*. (2014) 22:677–87. doi: 10.1177/1066896914558265

9. Zhang Z, Ma C, Luo Y. Diagnostic value of liver contrast-enhanced ultrasound in early hepatocellular carcinoma: a systematic review and meta-analysis. *J Gastrointest Oncol*. (2023) 14:626–35. doi: 10.21037/jgo

10. Wang L, Li M, Dong T, Li Y, Yin C, Nie F. Pancreatic ductal adenocarcinoma: The characteristics of contrast-enhanced ultrasound are correlated with the hypoxic microenvironment. *Diagnostics*. (2023) 13:3270. doi: 10.3390/diagnostics13203270

11. Xie Y, Chen Y, Wang Q, Li B, Shang H, Jing H. Early prediction of response to neoadjuvant chemotherapy using quantitative parameters on automated breast ultrasound combined with contrast-enhanced ultrasound in breast cancer. *Ultrasound Med Biol*. (2023) 49:1638–46. doi: 10.1016/j.ultrasmedbio.2023.03.017

12. Elbaz M, Qadiry RE, Fouraiji K, Jalal H, Elhoudzi J. Yolk sac tumor of vagina: a rare cause of vaginal bleeding in adolescents - a case report. *Pan Afr Med J*. (2020) 37:169. doi: 10.11604/pamj.2020.37.169.20949

13. Anfelter P, Testa A, Chiappa V, Froyman W, Fruscio R, Alcazar JL, et al. Imagng in gynecological disease (17): ultrasound features of Malignant ovarian yolk sac tumors (endodermal sinus tumors). *Ultrasound Obst Gyn*. (2020) 56:276–84. doi: 10.1002/uog.22002

14. Ulbright TM. Germ cell tumors of the gonads: a selective review emphasizing problems in differential diagnosis, newly appreciated, and controversial issues. *Mod Pathol*. (2005) 18 Suppl 2:S61–79. doi: 10.1038/modpathol.3800310

15. Teilum G. Endodermal sinus tumors of the ovary and testis. Comparative morphogenesis of the so-called mesoephroma ovarii (Schiller) and extraembryonic (yolk sac-allantoic) structures of the rat's placenta. *Cancer*. (1959) 12:1092–105. doi: 10.1002/(ISSN)1097-0142

16. Nasioudis D, Chapman-Davis E, Frey MK, Caputo TA, Holcomb K. Management and rognosis of ovarian yolk sac tumors; an analysis of the National Cancer Data Base. *Gynecol Oncol*. (2017) 147:296–301. doi: 10.1016/j.ygyno.2017.08.013

17. Faure Conter C, Xia C, Gershenson D, Hurteau J, Covens A, Pashankar F, et al. Ovarian yolk sac tumors; does age matter? *Int J Gynecol Cancer*. (2018) 28:77–84. doi: 10.1097/IGC.0000000000001149

18. Alrjoub MM, SIndiani A, Alshriedeh O, Amarin Z. Pregnancy and delivery after ovarian yolk sac tumor: A case report. *Am J Case Rep*. (2021) 22:e932091. doi: 10.12659/AJCR.932091

19. Pafilis I, Haidopoulos D, Rodolakis A, Vlachos G, Voulgaris Z, Sotiropoulou M, et al. Management of a pregnancy complicated by yolk sac tumor. *Arch Gynecol Obs tet*. (2009) 280:803–6. doi: 10.1007/s00404-009-0977-4

20. Sebire NJ, Fowler D, Ramsay AD. Sacrococcygeal tumors in infancy and childhood; a retrospective histopathological review of 85 cases. *Fetal Pediatr Pathol*. (2004) 23:295–303. doi: 10.1080/15227950490952424

21. Elgendy A, Mostafa M, Salem MA, Ali A, Khairi A, Shehata S. Surgical resection and outcome of Malignant ovarian germ cell tumors in children-a national multicentric study compared to international results. *Pediatr Surg Int*. (2020) 36:1067–75. doi: 10.1007/s00383-020-04716-x

22. Goyal LD, Kaur S, Kawatra K. Malignant mixed germ cell tumour of ovary–an unusual combination and review of literature. *J Ovarian Res*. (2014) 7:91. doi: 10.1186/PREACCEPT-1404916347126367

23. Gershenson DM. Management of early ovarian cancer: germ cell and sex cord-stromal tumors. *Gynecol Oncol*. (1994) 55:S62–72. doi: 10.1006/gyno.1994.1343

24. Nogales FF, Preda O, Nicolae A. Yolk sac tumours revisited. A review of their many faces and names. *Histopathology*. (2012) 60:1023 – 33. doi: 10.1111/j.1365-2559.2011.03889.x

25. Mizejewski GJ. Alpha-fetoprotein structure and function: relevance to isoforms, epitopes, and conformational variants. *Exp Biol Med*. (2001) 226:377–408. doi: 10.1177/153537020122600503

26. Ghose A, McCann L, Makker S, Mukherjee U, Gullapalli S, Erekkath J, et al. Diagnostic biomarkers in ovarian cancer: advances beyond CA125 and HE4. *Ther Adv Med Oncol*. (2024) 16:1–12. doi: 10.1177/17588359241233225

27. Gao Y, Jiang J, Liu Q. Extragonadal Malignant germ cell tumors: a clinicopathological and immunohistochemical analysis of 48 cases at a single Chinese institution. *Int J Clin Exp Pathol*. (2015) 8:5650–7.

28. Cao D, Guo S, Allan RW, Molberg KH, Peng Y. SALL4 is a novel sensitive and specific marker of ovarian primitive germ cell tumors and is particularly useful in distinguishing yolk sac tumor from clear cell carcinoma. *Am J Surg Pathol*. (2009) 33:894–904. doi: 10.1097/PAS.0b013e318198177d

29. Gallo A, Fankhauser C, Hermanns T, Beyer J, Christiansen A, Moch H. HNF1β is a sensitive and specific novel marker for yolk sac tumor: a tissue microarray analysis of 601 testicular germ cell tumors. *Modern Pathol*. (2020) 33:2354–60. doi: 10.1038/s41379-020-0597-x

30. Li Q, Zou C, Xu Y, Liu S, Yan T. Mucinous cystadenocarcinoma of the ovary in a 14-year-old girl: a case report and literature review. *BMC Womens Health*. (2023) 23:382. doi: 10.1186/s12905-023-02551-5

31. Levitin A, Haller KD, Cohen HL, Zinn DL, O'Connor MT. Endodermal sinus tumor of the ovary: imaging evaluation. *AJR Am J Roentgenol*. (1996) 167:791–3. doi: 10.2214/ajr.167.3.8751702

32. Ishida H, Naganuma H. Letter to the editor on "Strategy for accurate diagnosis by contrast-enhanced ultrasound of focal liver lesions in patients not at high risk for hepatocellular carcinoma". *J Ultras Med*. (2023) 42:2913–4. doi: 10.1002/jum.16325

33. Xie L, Liu X, Li H, Huang L, Chen F, Wang X, et al. The multimodal ultrasound features of ovarian serous surface papillary borderline tumor. *Womens Health Rep (New Rochelle)*. (2022) 3:523–32. doi: 10.1089/whr.2021.0140

34. Wang J, Lv F, Fei X, Cui Q, Wang L, Gao X. Study on the characteristics of contrast-enhanced ultrasound and its utility in assessing the microvessel density in ovarian tumors or tumor-like lesions. *Int J Biol Sci*. (2011) 7:600–6. doi: 10.7150/ijbs.7.600

frontiers | Frontiers in Oncology

TYPE Case Report
PUBLISHED 26 June 2024
DOI 10.3389/fonc.2024.1400257

Check for updates

OPEN ACCESS

EDITED BY
Dragos Eugen Georgescu,
Carol Davila University of Medicine and Pharmacy, Romania

REVIEWED BY
Luiza Serbanescu,
Carol Davila University of Medicine and Pharmacy, Romania
Huan Chen,
Zhuzhou Central Hospital, China
Ramesh Shrestha,
B.P. Koirala Institute of Health Sciences, Nepal

*CORRESPONDENCE
Rutie Yin
yrtt2020@163.com

RECEIVED 13 March 2024
ACCEPTED 03 June 2024
PUBLISHED 26 June 2024

CITATION
Zhang M, Yin R, Song L, Zhong L and Wang R (2024) Primary cervical malignant melanoma that was successfully treated with pembrolizumab: a case report and literature review.
Front. Oncol. 14:1400257.
doi: 10.3389/fonc.2024.1400257

COPYRIGHT
© 2024 Zhang, Yin, Song, Zhong and Wang. This is an open-access article distributed under the terms of the Creative Commons Attribution License (CC BY). The use, distribution or reproduction in other forums is permitted, provided the original author(s) and the copyright owner(s) are credited and that the original publication in this journal is cited, in accordance with accepted academic practice. No use, distribution or reproduction is permitted which does not comply with these terms.

Primary cervical malignant melanoma that was successfully treated with pembrolizumab: a case report and literature review

Mengpei Zhang[1,2], Rutie Yin[1,2]*, Liang Song[1,2], Lan Zhong[1,2] and Ruiyu Wang[1,2]

[1]Department of Obstetrics and Gynecology, West China Second University Hospital of Sichuan University, Chengdu, China, [2]Key Laboratory of Birth Defects and Related Diseases of Women and Children (Sichuan University), Ministry of Education, Chengdu, China

Primary malignant melanoma (MM) arising from the cervix is an exceedingly rare occurrence, and patients diagnosed with this condition often face a dismal clinical prognosis. Here, we present a case study of a postmenopausal woman presenting with vaginal bleeding and a conspicuous 5-centimeter black mass on the cervix. Based on the staging criteria established by the International Federation of Gynecology and Obstetrics, she was diagnosed with stage IIB primary cervical MM. The patient underwent neoadjuvant therapy prior to a radical hysterectomy and a bilateral salpingo-oophorectomy. Subsequently, she completed 18 cycles of pembrolizumab therapy, achieving clinical complete remission. Notably, at the 31-month follow-up, there were no signs of recurrence. This successful treatment outcome serves as a valuable clinical reference for the management of primary cervical MM.

KEYWORDS

primary cervical malignant melanoma, pembrolizumab, case report, cervical cancer, immunotherapy

Introduction

The National Cancer Database (NCDB), spanning the years from 1985 to 1994, revealed that cutaneous melanoma comprises 91.2% of all melanocytomas, with ocular melanoma accounting for 5.2%, mucosal melanoma accounting for 1.3%, and melanomas of unknown origin accounting for 2.2% (1). Cervical melanoma is classified as a mucosal melanoma and accounts for 3%–9% of all mucosal melanomas (2). Cervical melanoma carries a poor prognosis, and there remains no standardized and effective treatment approach. Despite significant advancements in the use of immune checkpoint inhibitors for the treatment of melanoma since 2015, a standardized protocol for managing cervical melanoma remains elusive, with particularly scant data on the application of immune checkpoint inhibitors in this context (3). Herein, we present a case of a patient diagnosed

with stage IIB cervical melanoma. This individual underwent neoadjuvant therapy, followed by a radical hysterectomy and a bilateral salpingo-oophorectomy. Subsequently, the patient completed 18 cycles of pembrolizumab therapy, achieving clinical complete remission. Notably, at the 31-month follow-up, there were no signs of recurrence, providing valuable insights into the potential of immunotherapy in the management of cervical melanoma.

Case report

A 77-year-old postmenopausal woman (para 2) presented to our hospital with a 2-month history of vaginal bleeding. Notably, she had a past history of tuberculosis, which was successfully treated with regular anti-tuberculosis therapy. Additionally, she was diagnosed with hypertension, coronary heart disease, and hypothyroidism over 10 years ago and is currently maintaining a stable condition with regular medication. A comprehensive physical examination revealed no abnormalities, and thorough dermatological, mucosal, and ocular inspections failed to detect any signs of primary melanoma. However, a significant finding was a 5 cm × 4 cm cauliflower-shaped dark brown lesion with a blood clot adhering to the surface of the cervix. Furthermore, a black nodule approximately 1 cm in diameter was observed at the 7 o'clock position on the posterior vaginal wall, located 2 cm from the fornix. Scattered melanin deposits were also visible on the lateral wall of the vagina. Gynecological examination suggested bilateral parametrial tissue invasion, although it did not extend to the lateral pelvic wall. A cervical biopsy revealed a round-cell tumor exhibiting solid growth and abnormal mitotic activity. The tumor cells were round-shaped and atypical, with conspicuous nucleoli indicative of malignant melanoma. Immunohistochemical results strongly suggest a diagnosis of malignant melanoma, based on positivity for HMB45, Melan-A, and S-100 and negativity for epithelial markers including P-CK, EMA, P16, P63, CK5/6, and P40. Vim positivity indicates a possible mesenchymal origin, while a high Ki67 positive rate (80%) suggests a tumor with high proliferative activity and potential for metastasis (Figure 1). However, a comprehensive evaluation, including clinical, histopathological, and radiological data, is necessary for a final diagnosis.

The pelvic CT scan indicates a relatively enlarged cervix with inhomogeneous enhancement. (Figure 2). Positron-emission tomography-computed tomography (PET-CT) also revealed increased fluorine-18-deoxyglucose intake lesions in the cervix without lymph node enlargement or any metastasis involving the skin or other mucosal sites (Figure 3). The patient was clinically diagnosed as stage IIB according to the International Federation of Gynecology and Obstetrics (FIGO 2018) classification system.

Research indicates that dacarbazine demonstrates significant therapeutic effects in 15% to 20% of patients with mucosal melanoma. The combination of temozolomide and cisplatin chemotherapy has been shown to prolong relapse-free survival. Additionally, the combination of dacarbazine, cisplatin, and vinca alkaloids has an effective rate of up to 32% (4). Based on the chemotherapy experience with mucosal melanoma, the recommended primary chemotherapy regimen for cervical melanoma involves monotherapy or combination therapy, primarily using dacarbazine or its oral analog, temozolomide. The patient first received two cycles of neoadjuvant chemotherapy: dimethyl triazemo imidazole, carboxamide 200 mg d1 to d5, and cisplatin 30 mg d1 to d3 for two cycles. After two cycles of chemotherapy, the patient was assessed for no significant reduction in the cervical lesion. The treatment regimen was then switched to pabrolizumab 200 mg for three cycles. After previous treatment, the patient's cervical lesion shrank (Figure 4). The total diameter of the target lesion decreased by approximately 28%, and the patient achieved SD according to the RECIST guideline (version 1.1) (5). After evaluation by the surgical professor, it was pointed out that the patient had a chance for surgery. Therefore, a radical hysterectomy and a bilateral salpingo-oophorectomy were performed. The size of the tumor was 5 cm × 4 cm (Figure 5). The postoperative results revealed a highly cellular neoplasm that was composed of a round-shaped atypical tumor with a conspicuous nucleolus. The immunohistochemical staining of Melan-A, HMB-45, and s-100, S-100 was positive. The NARS, BRAF, and KIT mutations were negative. The tumor invaded the

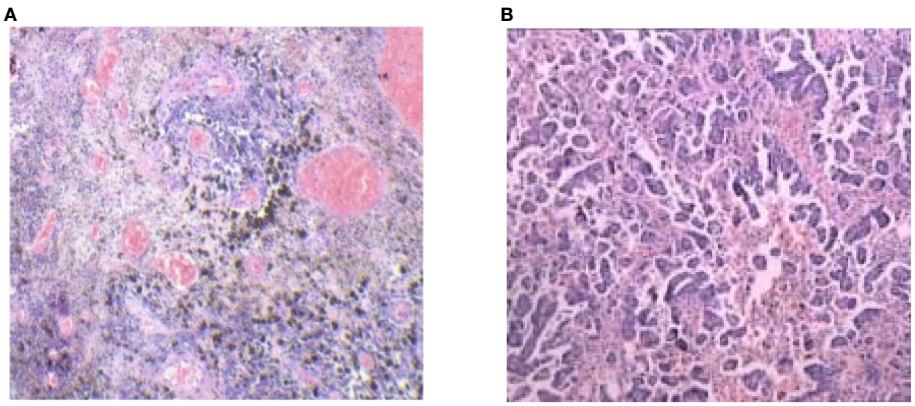

FIGURE 1
Pathologic examination of tumor tissue confirmed typical cervical MM histological features (hematoxylin and eosin stain 100/400).

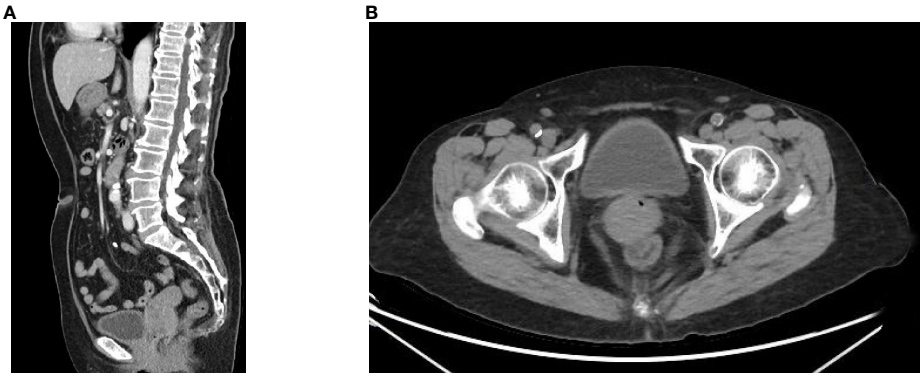

FIGURE 2
The CT scan before treatment revealed an enlarged cervix with inhomogeneous enhancement.

middle 1/3 of the cervical mesenchyme, and the vaginal surgical margin of the specimen was positive. The tumor did not extend to the cervical-uterine junction, surgical resection margins of the pelvic sidewall, parametrial tissues, lymph nodes, or adnexa. After the operation, she underwent intravenous administration of 200 mg of pembrolizumab, administered every 3 weeks for 18 courses. This patient was assessed after the end of treatment and achieved clinical complete remission (Figure 6). She was reviewed every 3 months after treatment, and to this day, no signs of tumor recurrence have been detected. Throughout the time of treatment and follow-up, this patient developed immune-related dermatitis, which improved with the administration of hormonal therapy. This patient has survived for 49 months since the initial treatment and is now generally living a good life.

Discussion

MM primarily occurs on the skin surface, with less than 2% of cases occurring in the female genitalia. Among these cases of MM in the female reproductive tract, the vulva or vagina are particularly common sites (6). However, primary MM of the cervix is extremely rare, and its prognosis is quite poor. Over the years, the incidence rate of primary cervical MM has not shown significant changes. Research suggests that radiation exposure, the influence of estrogen, and immunosuppression during pregnancy may be potential risk factors for this condition (7). Due to the rarity of its manifestations, the scarcity of evidence for optimal treatment strategies, and the absence of follow-up data, accurate survival predictions remain elusive. Regardless of staging and treatment methods, the prognosis

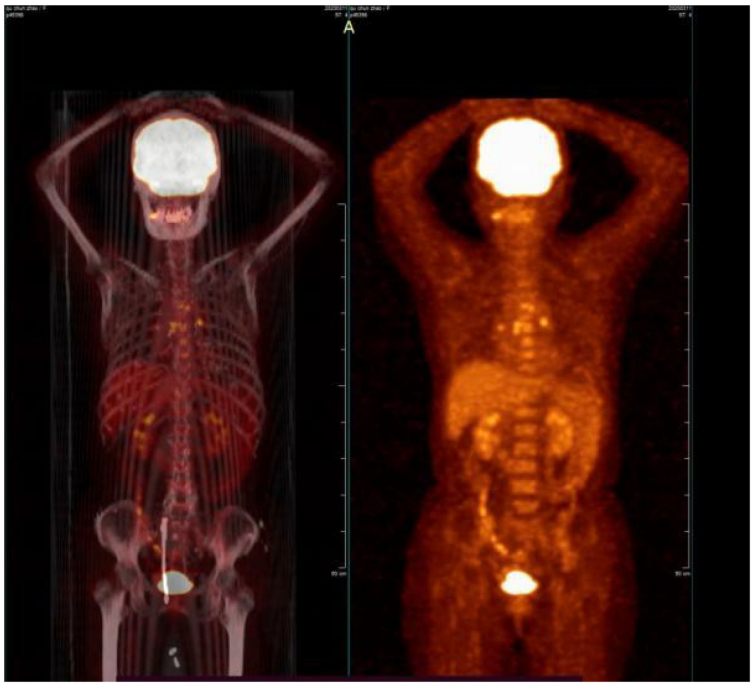

FIGURE 3
PET-CT before treatment showed that the mass was located in the cervix.

FIGURE 4
The pelvic CT scan showed that the cervical lesion had shrunk after neoadjuvant therapy.

is typically poor, with 87.5% of patients reported in the literature succumbing to the disease within 36 months of diagnosis. Reported survival times range from 6 months to 14 years, averaging 22.9 months. Based on a comprehensive review of available literature, the 5-year survival rate for primary cervical melanoma stands at 25% for stage I, 14% for stage II, and 0% for both stages III and IV (8, 9). Currently, there are no clear guidelines for the treatment of primary cervical MM. Aiping et al. first conducted a summary analysis of 149 cases of primary cervical melanoma. They discovered that patients who underwent radical hysterectomy, those with non-metastatic lymph nodes, and those who received lymphadenectomy had significantly improved survival rates. Among patients who underwent radical hysterectomy-based surgery, those who did not receive additional treatments had higher 24-month survival rates, while for those who underwent total hysterectomy, adding other treatments might be beneficial for extending median survival rates (10). Therefore, clinicians primarily rely on surgical standards for cervical squamous cell carcinoma when treating patients with primary cervical malignant melanoma. Decision-making regarding adjuvant therapy before or after surgery often depends on clinical experience (11).

FIGURE 5
Surgical specimen.

The pathogenesis of female genital melanoma is largely unknown and is similar to that of other mucosal melanomas. Similar to other mucosal melanomas, c-KIT, BRAF, and NRAS mutations are frequently detected in female genital melanomas. However, in different studies, the proportion of mutations in each gene varies considerably between lesions in different sites, such as the vulva, vagina, and cervix (12, 13). Hou et al. found that PD-1 and PD-L1 were expressed in 75% and 56% of vulvovaginal melanomas. However, these data are not clear for cervical malignant melanoma (14). The development of vulvar, vaginal, and cervical melanomas may involve different molecular pathways. Therefore, molecularly targeted therapy and immunotherapy in vulvar, vaginal, and cervical malignant melanoma should be studied categorically.

As primary cervical malignant melanoma is extremely rare, there is no standard, agreed-upon treatment. Surgery is the first choice for early, feasible melanoma of the cervix. For these patients, surgery usually entails radical hysterectomy, pelvic lymph node dissection, and partial vagotomy vaginectomy with free surgical margins of at least 2 cm, but total extra-fascial hysterectomy has been reported in the literature in some cases (15, 16). The utilization of chemotherapy alone for the treatment of cervical malignant melanoma is not advocated and is mostly used for neoadjuvant chemotherapy or adjuvant treatment after surgery (16). Dacarbazine is used most widely for advanced-stage or recurrent disease, and about 15%–20% of patients respond to this

FIGURE 6
The pelvic CT scan showed that after the end of treatment, the patient achieved clinical complete remission.

treatment (17). Adjuvant pelvic radiotherapy may be considered for patients at high risk of recurrence, such as those with positive surgical margins, positive parametrium, and positive lymph nodes. Malignant melanoma is not sensitive to radiation, and conventional radiation therapy is ineffective. For patients who are not suitable for radical surgery, external pelvic irradiation ± intracavitary irradiation may be a palliative treatment modality (16). Karasawa et al. treated 23 patients with gynecologic genital tract malignant melanoma, including 14 vaginal MM, 6 vulval MM, and 3 cervical MM, with gynecologic genital tract malignant melanoma with carbon ion radiotherapy (C-ion RT). The 3-year local control and overall survival rates were 49.9% and 53.0%, respectively. The results of this study suggest that C-ion RT may become a non-invasive treatment option for gynecological melanoma (18).

In recent years, immunotherapy has shown encouraging results with a significantly improved prognosis in the treatment of cutaneous malignant melanoma. However, immunotherapy with immune checkpoint inhibitors has been poorly studied in mucosal melanoma, especially in cervical melanoma, with poor long-term clinical outcomes. The vast majority of studies were case reports, and their findings were inconsistent. Indini A. et al. reported in a case series, including seven cases of mucosal MM, that the role of immunotherapy in metastatic melanoma of the lower genital tract showed a response rate of 28% and was proved to have a poor prognosis (19). Reiko Suzuki et al. reported a case with primary MM of the uterine cervix that had a poor response to pembrolizumab and had an OS of 6 months (20). The study reported by Mayuka Anko et al. seems encouraging. They described a recurrent cervical MM case, and a patient with vaginal MM was diagnosed as stage IV with multiple metastases. After initiating nivolumab therapy, both patients were clinically diagnosed as being in remission without tumor progression (21). Until now, only five cases of cervical melanoma patients treated with immune checkpoint inhibitors have been reported. The first four cases showed poor outcomes, but the last case reported tumor reduction. Schiavone B. S. et al. described a patient who received ipilimumab before surgery and pembrolizumab after recurrence but passed away 19 months later (22). Kim M.S. et al. and Reiko Suzuk et al. reported similar cases with pembrolizumab post-surgery, but both patients died within 8 months and 6 months (20, 23). Noguchi T. et al. reported a case where nivolumab was used after recurrence with a limited 13-month survival (15). However, Anko M. et al. provided hope, reporting a patient with a recurrent pelvic tumor who achieved complete tumor disappearance with nivolumab and has been progression-free for 17 months (21). Despite limited cases and mixed outcomes, Anko M. et al.'s findings offer promise for future research and improved treatment options for cervical melanoma patients.

According to literature reports, the median OS benefit from immunotherapy with PD-1 or PD-L1 inhibitors in patients with mucosal melanoma is significantly shorter compared to patients with cutaneous melanoma (18 months vs. 45 months, P=0.003), and significant efficacy is only observed in a subset of patients (24). Therefore, chemotherapy remains the preferred postoperative adjuvant therapy for operable mucosal melanoma patients, while immunotherapy has a relatively lower recommendation level. However, for locally advanced, recurrent, or metastatic mucosal melanoma, immunotherapy may potentially enhance disease remission rates. In the case we reported, although the patient showed insensitivity to the preoperative chemotherapy regimen, immunotherapy appeared to demonstrate effectiveness. Given that the patient had comprehensive commercial health insurance that could adequately cover the high medical costs, she decided to continue immunotherapy postoperatively after thorough communication with the medical team. The final treatment outcome confirmed the effectiveness of our therapeutic approach, and the patient achieved significant clinical benefits. The final outcome demonstrated that our treatment measures were effective. The patient has survived a total of 49 months since initial treatment and has had no tumor recurrence to date. During the course of treatment, the patient repeatedly developed immune-related dermatitis, which improved after hormone therapy. No other severe adverse reactions were observed. And the side effects were within manageable limits, which proved that the use of pembrolizumab may be effective as a pre- and post-surgical adjuvant immunotherapy. It has been reported in the study of Eggermont A et al. that regardless of PD-1 ligand expression level and BRAF mutation status, pembrolizumab has been found to be associated with longer progression-free survival and overall survival in melanoma (25). In this patient, the NARS, BRAF, and KIT mutation genes were negative. This patient could show different molecular features compared to cutaneous MM and other cervical

MM, so the clinic outcome was different. Although our case suggests that pembrolizumab is effective in the adjuvant treatment of primary cervical malignant melanoma, more data and randomized trials on mucosal MM, including cervical MM, are necessary to stratify successful cases.

Conclusion

In summary, cervical primary MM is a rare type of cervical cancer with limited research. Surgical resection is the recommended treatment for early-stage disease. There is no standard treatment for advanced cervical primary MM. Based on this case report, surgery combined with immunotherapy may be a suitable option for locally advanced cervical primary MM.

Data availability statement

The raw data supporting the conclusions of this article will be made available by the authors, without undue reservation.

Ethics statement

Written informed consent was obtained from the minor(s)' legal guardian/next of kin for the publication of any potentially identifiable images or data included in this article.

Author contributions

MZ: Writing – original draft, Formal Analysis, Data curation. RY: Writing – review & editing. LS: Writing – review & editing, Methodology. LZ: Writing – review & editing, Software. RW: Writing – review & editing.

Funding

The author(s) declare that no financial support was received for the research, authorship, and/or publication of this article.

Conflict of interest

The authors declare that the research was conducted in the absence of any commercial or financial relationships that could be construed as a potential conflict of interest.

Publisher's note

All claims expressed in this article are solely those of the authors and do not necessarily represent those of their affiliated organizations, or those of the publisher, the editors and the reviewers. Any product that may be evaluated in this article, or claim that may be made by its manufacturer, is not guaranteed or endorsed by the publisher.

References

1. Chang AE, Karnell LH, Menck HR. The National Cancer Data Base report on cutaneous and noncutaneous melanoma: a summary of 84,836 cases from the past decade. The American College of Surgeons Commission on Cancer and the American Cancer Society. *Cancer*. (1998) 83:1664–78. doi: 10.1002/(ISSN)1097-0142

2. Adelman AS, McLaughlin CC, Wu XC, Chen VW, Groves FD. Urbanisation and incidence of acute lymphocytic leukaemia among United States children aged 0-4. *Br J Cancer*. (2005) 92:2084–8. doi: 10.1038/sj.bjc.6602607

3. Robert C, Long GV, Brady B, Dutriaux C, Maio M, Mortier L, et al. Nivolumab in previously untreated melanoma without BRAF mutation. *N Engl J Med*. (2015) 372:320–30. doi: 10.1056/NEJMoa1412082

4. Campaner AB, Fernandes GL, de Araujo Cardoso F, Veasey JV. Vulvar melanoma: relevant aspects in therapeutic management. *Anais Brasileiros Dermatol*. (2017) 92:398–400. doi: 10.1590/abd1806-4841.20174941

5. Eisenhauer EA, Therasse P, Bogaerts J, Schwartz LH, Sargent D, Ford R, et al. New response evaluation criteria in solid tumours: revised RECIST guideline (version 1.1). *Eur J Cancer*. (2009) 45:228–47. doi: 10.1016/j.ejca.2008.10.026

6. Yuan Y, Fu A, Cai J, Ma Z, Chen Y, Zou X, et al. Primary Malignant melanoma of the cervix: A comprehensive analysis of case reports in the Chinese population. *Cancer Med*. (2023) 12:14052–61. doi: 10.1002/cam4.6054

7. Tranoulis A, Laios A, Munot S, Theophilou G, Pathak D, Nugent D, et al. Multidisciplinary approach in the management of primary Malignant melanoma of the uterine cervix: diagnostic and management challenges. *J Gynecol Surg*. (2018) 34:209–13. doi: 10.1089/gyn.2018.0005

8. Shrestha R, Adhikari P, Rimal SP, Basnet P, Rijal P, Regmi MC. Primary Malignant melanoma of uterine cervix. *Nepal J Obstetrics Gynaecol*. (2020) 15 (1):86–8. doi: 10.3126/njog.v15i1.29352

9. Lee JH, Yun JH, Seo J, Bae G, Lee JW, Kim SW. Primary Malignant melanoma of cervix and vagina. *Obstetrics Gynecol Sci*. (2016) 59:415. doi: 10.5468/ogs.2016.59.5.415

10. Min A, Fu A, Huang M, Wang H, Chen H. Primary Malignant melanoma of the cervix: an integrated analysis of case reports and series. *Front Oncol*. (2022) 12:913964. doi: 10.3389/fonc.2022.913964

11. Colombo N, Carinelli S, Colombo A, Marini C, Rollo D, Sessa C. Cervical cancer: ESMO Clinical Practice Guidelines for diagnosis, treatment and follow-up. *Ann Oncol*. (2017) 28:v72–83. doi: 10.1093/annonc/mdx220

12. Rouzbahman M, Kamel-Reid S, Al HA, Butler M, Dodge J, Laframboise S, et al. Malignant melanoma of vulva and vagina: A histomorphological review and mutation analysis–A single-center study. *J Low Genit Tract Dis*. (2015) 19:350–3. doi: 10.1097/LGT.0000000000000142

13. Omholt K, Grafstrom E, Kanter-Lewensohn L, Hansson J, Ragnarsson-Olding BK. KIT pathway alterations in mucosal melanomas of the vulva and other sites. *Clin Cancer Res*. (2011) 17:3933–42. doi: 10.1158/1078-0432.CCR-10-2917

14. Hou JY, Baptiste C, Hombalegowda RB, Tergas AI, Feldman R, Jones NL, et al. Vulvar and vaginal melanoma: A unique subclass of mucosal melanoma based on a comprehensive molecular analysis of 51 cases compared with 2253 cases of nongynecologic melanoma. *Cancer*. (2017) 123:1333–44. doi: 10.1002/cncr.30473

15. Noguchi T, Ota N, Mabuchi Y, Yagi S, Minami S, Okuhira H, et al. A case of Malignant melanoma of the uterine cervix with disseminated metastases throughout the vaginal wall. *Case Rep Obstet Gynecol*. (2017) 2017:5656340. doi: 10.1155/2017/5656340

16. Piura B. Management of primary melanoma of the female urogenital tract. *Lancet Oncol*. (2008) 9:973–81. doi: 10.1016/S1470-2045(08)70254-7

17. Cetinkaya K, Benzer E, Dervisoglu H. Primary mucosal Malignant melanoma of the cervix: case report and review of the literature. *Tumori*. (2015) 101:e147–50. doi: 10.5301/tj.5000304

18. Karasawa K, Wakatsuki M, Kato S, Kiyohara H, Kamad T. Clinical trial of carbon ion radiotherapy for gynecological melanoma. *J Radiat Res*. (2014) 55:343–50. doi: 10.1093/jrr/rrt120

19. Indini A, Di Guardo L, Cimminiello C, Lorusso D, Raspagliesi F, Del VM. Investigating the role of immunotherapy in advanced/recurrent female genital tract melanoma: a preliminary experience. *J Gynecol Oncol*. (2019) 30:e94. doi: 10.3802/jgo.2019.30.e94

20. Suzuki R, Endo H, Sasaki T, Nakamura T, Yamanaka H, Hosonuma S, et al. Primary Malignant melanoma of uterine cervix treated with pembrolizumab as adjuvant immunotherapy. *Int Cancer Conf J*. (2021) 10:254–8. doi: 10.1007/s13691-021-00477-z

21. Anko M, Nakamura M, Kobayashi Y, Tsuji K, Nakada S, Nakamura Y, et al. Primary Malignant melanoma of the uterine cervix or vagina which were successfully treated with nivolumab. *J Obstetrics Gynaecol Res*. (2020) 46:190–5. doi: 10.1111/jog.14136

22. Schiavone MB, Broach V, Shoushtari AN, Carvajal RD, Alektiar KM, Kollmeier MA, et al. Combined immunotherapy and radiation for treatment of mucosal melanomas of the lower genital tract. *Gynecol Oncol Rep*. (2016) 16:42–6. doi: 10.1016/j.gore.2016.04.001

23. Kim MS, Choi C, Kim T, Lee JW, Lee J, Bae D, et al. Primary Malignant melanoma of the uterine cervix treated with pembrolizumab after radical surgery: a case report and literature review. *Obstetrics Gynecol Sci*. (2018) 61:524. doi: 10.5468/ogs.2018.61.4.524

24. Mao L, Qi Z, Zhang L, Guo J, Si L. Immunotherapy in acral and mucosal melanoma: current status and future directions. *Front Immunol*. (2021) 12. doi: 10.3389/fimmu.2021.680407

25. Eggermont A, Blank CU, Mandala M, Long GV, Atkinson V, Dalle S, et al. Adjuvant pembrolizumab versus placebo in resected stage III melanoma. *N Engl J Med*. (2018) 378:1789–801. doi: 10.1056/NEJMoa1802357

frontiers | Frontiers in Oncology

TYPE Case Report
PUBLISHED 27 June 2024
DOI 10.3389/fonc.2024.1364008

Check for updates

OPEN ACCESS

EDITED BY
Ferdinando Agresta,
ULSS2 Marca Trevigiana, Italy

REVIEWED BY
Nicolae Bacalbasa,
Carol Davila University of Medicine and Pharmacy, Romania
Iuliana Pantelimon,
Carol Davila University of Medicine and Pharmacy, Romania
Teodor Florin Georgescu,
Carol Davila University of Medicine and Pharmacy, Romania

*CORRESPONDENCE
Feng Gao
fenggao@hebmu.edu.cn

RECEIVED 01 January 2024
ACCEPTED 27 May 2024
PUBLISHED 27 June 2024

CITATION
Feng X, Zhang P and Gao F (2024) Primary retroperitoneal müllerian adenocarcinoma: a case report.
Front. Oncol. 14:1364008.
doi: 10.3389/fonc.2024.1364008

COPYRIGHT
© 2024 Feng, Zhang and Gao. This is an open-access article distributed under the terms of the Creative Commons Attribution License (CC BY). The use, distribution or reproduction in other forums is permitted, provided the original author(s) and the copyright owner(s) are credited and that the original publication in this journal is cited, in accordance with accepted academic practice. No use, distribution or reproduction is permitted which does not comply with these terms.

Primary retroperitoneal müllerian adenocarcinoma: a case report

Xiaohui Feng[1], Ping Zhang[2] and Feng Gao[1]*

[1]Department of Pathology, The Third Hospital of Hebei Medical University, Shijiazhuang, China, [2]Department of Radiology, The Third Hospital of Hebei Medical University, Shijiazhuang, China

A 45-year-old woman presented with right hip pain for a month. Imaging results revealed that the left peritoneal mass was accompanied by metastases of the right sciatic branch, lung, and retroperitoneal lymph nodes. A biopsy of the left peritoneal mass was performed. The pathological morphology demonstrated clear cell adenocarcinoma. Immunohistochemical staining revealed a positive expression of keratin7 and PAX8 and a negative expression of keratin20, GCDFP-15, ER, PR, WT1, CDX2, villin, TTF-1, napsin-A, vimentin, calretinin, and GATA3. Finally, the diagnosis of primary retroperitoneal müllerian adenocarcinoma (PRMA) was confirmed. PRMA is a very rare type of primary retroperitoneal tumor. PRMA should be considered for the retroperitoneal mass.

KEYWORDS

müllerian tumor, adenocarcinoma, retroperitoneum, pathology, immunohistochemistry

1 Introduction

In women, the müller tube forms the fallopian tubes, uterine horn, cervix, and the upper part of the vagina. Although most malignant müllerian adenocarcinomas occur in the uterus, ovaries, fallopian tubes, and vagina, they may occur in rare parts, including the retroperitoneum (1, 2).

Primary retroperitoneal müllerian adenocarcinoma (PRMA) is an extremely rare entity, which often presents in elderly menopausal women and is highly aggressive. Several mechanisms of this clinical entity have been suggested, including retroperitoneal ectopic supernumerary ovarian tissue, retroperitoneal mono-dermal teratoma, coelomic metaplasia, the secondary müllerian system, and retroperitoneal endometriosis (3). The purpose of this study is to report a patient of PRMA and analyze the characteristics of imaging and histomorphology of PRMA to improve the understanding of this tumor.

2 Case presentation

This study was conducted under the approval of the Ethics Committee of the Third Hospital of Hebei Medical University, and the protocol was accorded with its standards.

A 45-year-old woman had pain in the right hip for half a month. After admission, the computed tomography (CT) scan incidentally revealed a huge mass in the left retroperitoneum, in addition to the bone destruction of the right ischia. The patient's menstrual cycle was regular, starting at the age of 14. She was pregnant twice and had given birth twice. No malignant tumors were discovered in this patient before. Results of the gynecological ultrasonic examination showed hysteromyoma, and no abnormality was found in bilateral accessories. The intraepithelial lesions or malignant lesions were not noted by liquid-based thin-layer cell detection. The gastroscopy and enteroscopy results were also normal. The serum CEA increased to 8.39 ng/mL (normal range: <5.2), CA 199 was 1,000 U/mL (normal range: <27), CA125 was 58.29 U/mL (normal range: <35), Cyfra21–1 was 13.4 ng/mL (normal range: <3.3), CA50 was >500 IU/mL (normal range: <25), and CA242 was 184.9 IU/mL (normal range: <20). No abnormality was observed in myeloma monitoring (Figure 1).

The CT scan revealed a 58 × 43-mm retroperitoneal cystic mass with solid components that were indistinguishable from the psoas major and left kidney. Contrast-enhanced CT showed delayed enhancement of solid components and no enhancement of cystic components (Figure 2A). Enlarged lymph nodes were scattered in the retroperitoneum. Normality was noted in the liver, gallbladder, pancreas, kidney, pelvis, ureter, and bladder. Multiple small nodules were observed in the lungs, which were highly consistent with pulmonary metastasis (not shown).

A needle biopsy was performed to determine the nature of the retroperitoneal mass. The tumor cells are large and highly atypical, with necrosis in some areas. Most of the cytoplasm was pink, but a small part was transparent. The tissue morphology was glandular and solid and has a cribriform growth pattern. The final pathology result was clear cell adenocarcinoma (Figure 2B). The cells were positive for keratin7 and PAX8, and they were negative for keratin20, GCDFP-15, ER, PR, WT1, CDX2, villin, TTF-1, napsin-A, vimentin, calretinin, and GATA3 (Figures 2C–F). Finally, PRMA was confirmed.

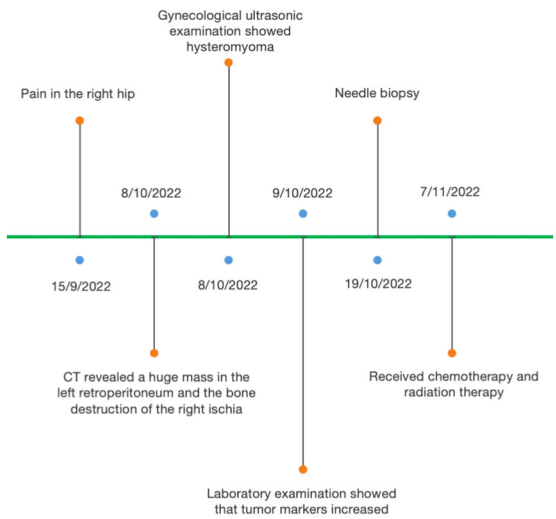

FIGURE 1
Representative timelines of patient's relevant data history.

The patient in this report received six cycles of chemotherapy with carboplatin + paclitaxel, and the tumor bed and the right ischia were irradiated with 45-Gy-intensity modulated volumetric radiotherapy. After the second chemotherapy cycle, the CT scan revealed liver metastasis in this patient. After the fourth chemotherapy cycle, the patient experienced lower back pain and had multiple bone destruction, enlarged pulmonary nodules, and pleural effusion. Adenocarcinoma cells were found in the pleural fluid by pathological examination. Considering the tumor progression of the patient's condition, targeted treatment with sevotinib was administered. The patient was followed up for 12 months and survived with tumors.

3 Discussion

PRMA is an extremely rare entity, which is a diagnosis of exclusion. Primary peritoneal malignant mesothelioma and metastasis of malignant tumors in the urinary system (kidney, bladder) and the female reproductive system (ovaries, fallopian tubes, uterus), digestive system (colon, stomach, pancreas, intestines, gallbladder), and breast and lung must be excluded (4). In this patient, the origin of the breast, digestive system, female reproductive system, and kidney was excluded by medical history, ultrasound, and imaging examination. Pathological histomorphology and immunohistochemistry excluded breast cancer, malignant mesothelioma, and malignant tumors of the digestive system, and female reproductive system.

Patients usually present with specific clinical symptoms, including abdominal distension, pain, and/or palpable masses, but some cases are not specific. The first symptom of our patient was bone pain caused by bone metastasis. The preoperative diagnostic management included ultrasound, CT, and, if necessary, MRI (5). The growth pattern of the tumor was mainly a mixture of solid and cystic components (6). The imaging features were cystic areas with necrosis. In the current case, the characteristics were consistent with the literature.

A variety of different histological subtypes of PRMA, including serous (7), endometrioid (1), clear cell (8), mucinous (4), papillary (2), mixed (serous, mucinous, and endometrioid), and even malignant mixed müllerian tumor (2, 9), has been reported in the literature. The serous, endometrioid, and clear cell histologies were the common types (3). In this report, our PRMA case had poor cell differentiation, and the histopathology was clear cell adenocarcinoma.

The preoperative diagnosis of PRMA is very challenging. Due to the rarity of this tumor, there are no guidelines for the staging, classification, and treatment of PRMA (4). The main treatment methods for PRMA include surgical resection, chemotherapy, and radiation therapy. It is generally recommended that tumor resection should be taken as the main method of treatment in clinical practice, but there is still controversy about the adjuvant treatment of PRMA (2, 3, 7). Patients whose tumors were completely removed had a better prognosis. Due to the strong aggressiveness of this tumor, it is recommended not to break the integrity of the tumor during surgical resection to avoid any peritoneal implantation. Although there is no standard evidence supporting the benefit of adjuvant chemotherapy or radiotherapy

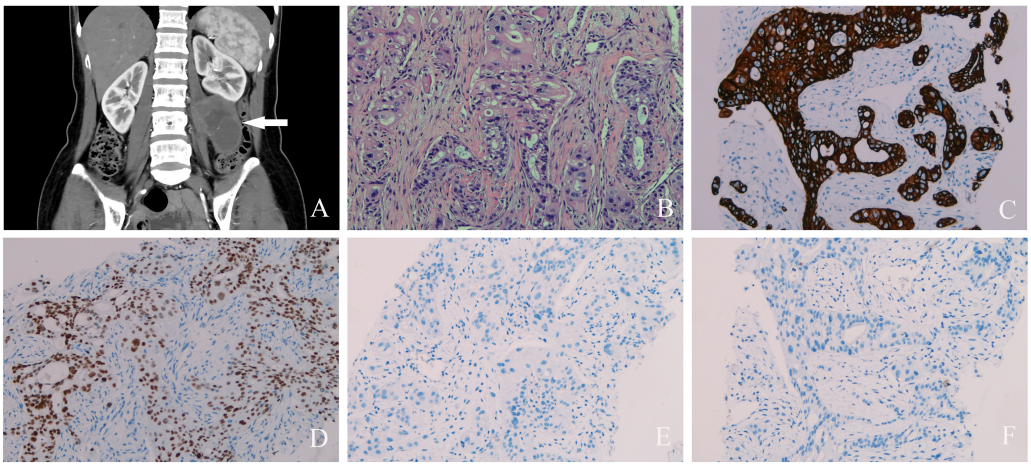

FIGURE 2
(A) Contrast-enhanced computed tomography scan of abdominal pelvic cavity showed a huge cystic and solid mass (white arrow) in the left retroperitoneal space. **(B)** Hematoxylin and eosin staining of primary retroperitoneal müllerian adenocarcinoma (×200). **(C)** Positive keratin7 immunostaining was observed (×200). **(D)** Positive PAX8 immunostaining was observed (×200). **(E)** Negative WT1 immunostaining was observed (×200). **(F)** Negative CDX-2 immunostaining was observed (×200).

because the biological behavior of PRMA resembles that of epithelial-type ovarian carcinoma, platinum-based adjuvant chemotherapy is suggested for these patients. Since metastasis of bone, lung, and lymph nodes has been found in this patient, the tumor was not removed after a puncture biopsy. The patient in this report received palliative chemotherapy with carboplatin + paclitaxel, and external irradiation was selected. After the patient developed the tumor progression, sevotinib was administered.

The differential diagnosis of PRMA should be borne in mind for cases with retroperitoneal mass when the typical adenocarcinoma was noted and the immunohistochemical staining showed positive for keratin7 and PAX8.

Data availability statement

The raw data supporting the conclusions of this article will be made available by the authors, without undue reservation.

Ethics statement

The studies involving humans were approved by the Ethics Committee of the Third Hospital of Hebei Medical University. The studies were conducted in accordance with the local legislation and institutional requirements. The participants provided their written informed consent to participate in this study. Written informed consent was obtained from the individual(s) for the publication of any potentially identifiable images or data included in this article.

Author contributions

XF: Writing – original draft. PZ: Writing – original draft. FG: Writing – review & editing.

Funding

The author(s) declare that no financial support was received for the research, authorship, and/or publication of this article.

Conflict of interest

The authors declare that the research was conducted in the absence of any commercial or financial relationships that could be construed as a potential conflict of interest.

Publisher's note

All claims expressed in this article are solely those of the authors and do not necessarily represent those of their affiliated organizations, or those of the publisher, the editors and the reviewers. Any product that may be evaluated in this article, or claim that may be made by its manufacturer, is not guaranteed or endorsed by the publisher.

References

1. Tanaka K, Kobayashi Y, Shibuya H, Nishigaya Y, Momomura M, Matsumoto H, et al. Primary retroperitoneal Müllerian adenocarcinoma arising from endometriosis. *J Obstet Gynaecol Res*. (2014) 40:1823–7. doi: 10.1111/jog.12377

2. Elnemr A, Yonemura Y, Shinbo M, Nishino E. Primary retroperitoneal mullerian adenocarcinoma. *Rare Tumors*. (2010) 2:e6. doi: 10.4081/rt.2010.e6

3. Vatansever D, Misirlioglu S, Arslan T, Zeren EH, Celik C, Bolukbasi Y, et al. Primary retroperitoneal Müllerian adenocarcinoma: report of two cases treated with radical surgery. *J Obstet Gynaecol Can*. (2021) 43:242–6. doi: 10.1016/j.jogc.2020.08.009

4. Myriokefalitaki E, Luqman I, Potdar N, Brown L, Steward W, Moss EL. Primary retroperitoneal mucinous cystadenocarcinoma (PRMCa): a systematic review of the literature and meta-analysis. *Arch Gynecol Obstet*. (2016) 293:709–20. doi: 10.1007/s00404-015-3975-8

5. Yang DM, Jung DH, Kim H, Kang JH, Kim SH, Kim JH, et al. Retroperitoneal cystic masses: CT, clinical, and pathologic findings and literature review. *Radiographics*. (2004) 24:1353–65. doi: 10.1148/rg.245045017

6. Berretta R, Patrelli TS, Faioli R, Mautone D, Gizzo S, Mezzogiorno A, et al. Secondary müllerian system: an atypical case of tumor originating from vestigial müllerian cells embedded in the peritoneum. *Clin Genitourin Cancer*. (2013) 11:365–9. doi: 10.1016/j.clgc.2013.04.028

7. Arichi N, Yasumoto H, Mitsu Y, Hiraoka T, Honda S, Shiina H, et al. A case of primary retroperitoneal serous adenocarcinoma. *Int J Urol*. (2011) 18:844–6. doi: 10.1111/j.1442-2042.2011.02875.x

8. Brooks JJ, Wheeler JE. Malignancy arising in extragonadal endometriosis. *A Case Rep summary World literature Cancer*. (1977) 40:3065–73. doi: 10.1002/1097-0142(197712)40:6<3065::aid-cncr2820400645>3.0.co;2-3

9. Spinelli C, Strambi S, Tartaglia D, Franco GD, Pucci V, Faviana P, et al. Primary retroperitoneal müllerian adenocarcinoma: a case report and literature review. *Case Rep Oncol*. (2013) 6:616–21. doi: 10.1159/000357424

frontiers | Frontiers in Oncology

TYPE Case Report
PUBLISHED 03 July 2024
DOI 10.3389/fonc.2024.1430531

Check for updates

OPEN ACCESS

EDITED BY
Lidia Castagneto Gissey,
Sapienza University of Rome, Italy

REVIEWED BY
Luigi Della Corte,
University of Naples Federico II, Italy
Andrea Giannini,
Umberto 1 Hospital, Italy

*CORRESPONDENCE
Fei Xiang
150455873@qq.com

RECEIVED 10 May 2024
ACCEPTED 17 June 2024
PUBLISHED 03 July 2024

CITATION
Zhang Z, Lin X, Wang X, He F, Cai W, Min X and Xiang F (2024) Case report: Magnetic resonance imaging findings of patients with diffuse uterine leiomyomatosis. *Front. Oncol.* 14:1430531. doi: 10.3389/fonc.2024.1430531

COPYRIGHT
© 2024 Zhang, Lin, Wang, He, Cai, Min and Xiang. This is an open-access article distributed under the terms of the Creative Commons Attribution License (CC BY). The use, distribution or reproduction in other forums is permitted, provided the original author(s) and the copyright owner(s) are credited and that the original publication in this journal is cited, in accordance with accepted academic practice. No use, distribution or reproduction is permitted which does not comply with these terms.

Case report: Magnetic resonance imaging findings of patients with diffuse uterine leiomyomatosis

Zanhua Zhang[1], Xianhui Lin[2], Xue Wang[3], Fang He[1], Weiwei Cai[1], Xiaoyan Min[1] and Fei Xiang[1]*

[1]Department of ICU, The Second Affiliated Hospital and Yuying Children's Hospital of Wenzhou Medical University, Wenzhou, China, [2]Department of Pathology, The Second Affiliated Hospital and Yuying Children's Hospital of Wenzhou Medical University, Wenzhou, China, [3]Department of Radiology, The Second Affiliated Hospital and Yuying Children's Hospital of Wenzhou Medical University, Wenzhou, China

Background: Diffuse uterine leiomyomatosis (DUL) is a seldom-seen condition, with only a handful of cases of magnetic resonance imaging (MRI) findings documented. In clinical settings, it is often mistaken for multiple uterine leiomyomas due to a lack of adequate recognition of DUL.

Objective: This study shows two instances of DUL, underscoring their MRI findings to improve preoperative diagnostic precision.

Conclusion: For patients exhibiting multiple uterine leiomyomas with masses present in the parametrial and abdominal cavities, consideration should be given to diagnosing DUL with DPL. The discoveries outlined in this paper furnish insights that can assist in directing treatment choices.

KEYWORDS

diffuse uterine leiomyomatosis, magnetic resonance imaging, case report, preoperative diagnosis, differential diagnosis

Introduction

Uterine tumors are categorized as either benign or malignant. The predominant benign type is uterine leiomyoma (ULM), whereas endometrial cancer and uterine sarcoma are the most frequently observed malignant types. Uterine leiomyoma, also termed uterine fibroid, is a non-malignant, steroid-dependent tumor originating from the uterine muscle layer and represents the most prevalent benign tumor within the female reproductive system, occurring in approximately 20%–25% of women (1). This tumor is benign but commonly diagnosed, with ULM generally displaying slow growth rates. However, a rapid increase in size may indicate a potential for malignancy, such as sarcomas. Despite a limited response of the normal uterine muscle layer to estrogen, uterine fibroids demonstrate increased activity of estrogen regulatory genes and receptors and show an enhanced growth response to progesterone (2). It is noteworthy that although uterine

leiomyomas are benign, there exists a risk of encountering an undiagnosed malignant tumor in one in 498 uterine tumors, such as leiomyosarcoma (3). Uterine leiomyoma and leiomyosarcoma share similar clinical and morphological features, making them challenging to differentiate; diagnosis is dependent on histological examination (4). Surgery remains the primary treatment option for ULMs and uterine leiomyosarcomas (ULMSs), thus underscoring the importance of precise preoperative diagnosis. Current diagnostic techniques, including ultrasound, CT, MRI, and CA-125 tests, fail to reliably differentiate between malignant and benign uterine fibroids. Therefore, a novel approach for differential diagnosis of ULM and ULMS is under investigation.

Diffuse uterine leiomyomatosis (DUL), classified as a borderline leiomyoma of the uterus, is distinguished by numerous small smooth muscle nodules that lead to a symmetrical enlargement of the uterus (5). These nodules vary in size, with the largest typically measuring up to 3 cm and most remaining under 1 cm in diameter (6). The smooth muscle cells of these nodules exhibit a uniform, bland, spindled shape with smaller dimensions compared to typical leiomyomas (7). DUL predominantly affects women of reproductive age and is a known cause of infertility (8). In clinical settings, DUL is often misidentified as multiple uterine leiomyomas due to its low recognition (9). Consequently, precise diagnosis of DUL is critical for appropriate treatment guidance. This report highlights two cases of DUL, focusing on the application of MRI to improve preoperative diagnostic accuracy.

Case reports

Patient 1

A 40-year-old unmarried woman with no children was admitted to the hospital, complaining of occasional abdominal bloating, fatigue, a history of uterine leiomyoma surgery 10 years ago, and abnormal menstruation for the past 5 years. Blood tests revealed severe anemia (hemoglobin level of 4.6 g/dL) and elevated serum tumor markers: a CA-125 level of 245.80 U/mL and a CA-199 level of 55.25 U/mL. Transvaginal ultrasound showed a notably enlarged uterus with multiple nodules displaying hypoechoic or uneven echoes. The uterine cavity line and endometrium were not visible, leading to the diagnosis of multiple uterine leiomyomas.

MRI examination before surgery revealed that the uterine volume was significantly increased and that the myometrium showed multiple diffuse nodules and masses, which were isointense on T1-weighted imaging (T1WI) and had a slightly low signal on T2-weighted imaging (T2WI); additionally, some lesions showed heterogeneous signals and slightly high signals on diffusion-weighted imaging (DWI). The enhancement of the lesions was slightly lower than that of the uterine body (Figure 1). The diagnosis was multiple uterine leiomyomas. The right ovary showed a long cystic T1 and long T2 signal, measuring approximately 27 mm × 22 mm, with no obvious appearance on the enhanced scan.

The patient underwent a total abdominal hysterectomy, bilateral salpingectomy, right ovarian cystectomy, pelvic adhesiolysis, and pelvic uterine electrocautery. During the operation, the uterus appeared spherical, resembling that of a fifth-month pregnancy. A fibroid protrusion measuring approximately 6 cm × 6 cm × 7 cm was identified in the lower segment of the posterior uterine wall. Dense adhesions were observed between the anterior wall of the uterus and the bladder, as well as the lateral abdominal wall. Moreover, part of the mesentery was densely adhered to the posterior uterine wall. Multiple purple–blue nodules were noticed on the uterine surface and uterosacral ligaments. Additionally, the right ovary exhibited enlargement with a cyst measuring approximately 3 cm × 2 cm × 2 cm.

Histopathological examination of the hysterectomy specimen confirmed diffuse leiomyomatosis of the uterus and focally abundant cells with active mitotic activity (approximately 5–8/10 HPF). The immunostaining results were as follows: P53 (some positive), progesterone receptor (PR) (+), smooth muscle actin (SMA) (+), CD10 (−), Ki-67 (approximately 5%–10%+), and P16 (some +) (Figure 2).

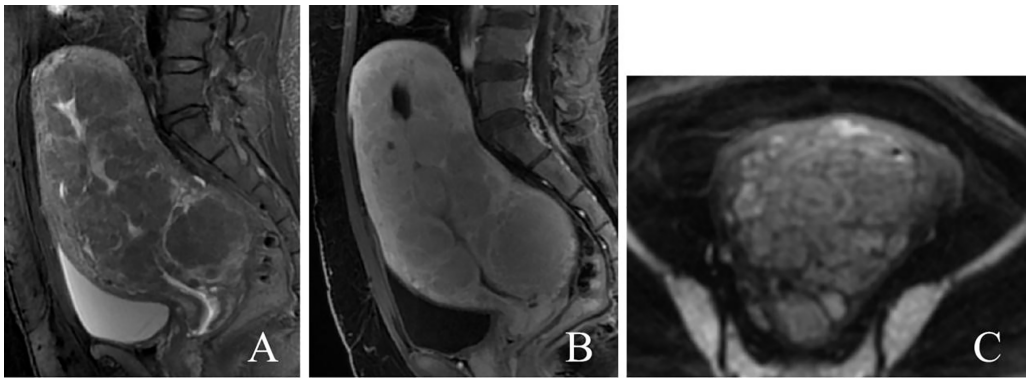

FIGURE 1
A 40-year-old patient with diffuse uterine leiomyomatosis. **(A–C)** Diffuse thickening of the myometrium with multiple masses showing a low signal in sagittal T2WI, mild enhancement in sagittal T1-enhanced image, and a slightly greater signal in DWI. T2WI, T2-weighted imaging; DWI, diffusion-weighted imaging.

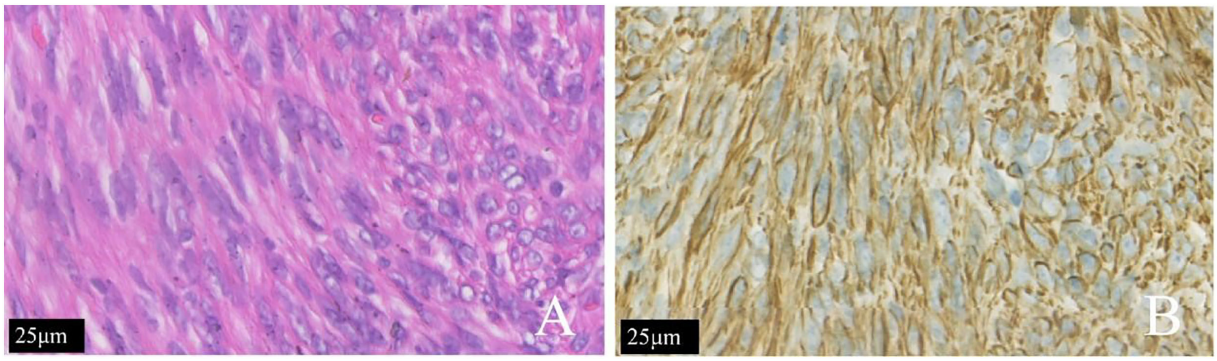

FIGURE 2
The same patient shown in Figure 1. **(A)** The tumor cells of the patient with diffuse uterine leiomyomatosis were long and fusiform. The cytoplasm was rich in red dye and was arranged in bundles or interleaved shapes according to H&E staining. **(B)** The SMA (+) is shown by immunohistochemical staining.

Patient 2

A 46-year-old married female, G2P2, was admitted to the hospital. The patient had a regular menstrual cycle, lasting 25–26 days, with a menstrual period lasting 6 days. There were no complaints of dysmenorrhea or alterations in vaginal discharge. However, 2 months ago, the patient reported a palpable lump in the lower abdomen, accompanied by intermittent lower abdominal swelling and pain. There were no associated symptoms such as fever, abnormal vaginal bleeding, nausea, vomiting, or discomfort such as frequent or urgent urination. The patient had previously undergone natural delivery and ligation. Additionally, 13 years ago, she had undergone open surgery for the removal of uterine fibroids.

Blood samples were collected, and the results were as follows: alpha-fetoprotein (AFP), 2.45 ng/mL; carcinoembryonic antigen (CEA), 0.83 ng/mL; CA-125, 103.20 U/mL; CA-199, 4.85 U/mL; and squamous cell carcinoma (SCC), 1.10 ng/mL.

An abdominal CT plain scan revealed large cystic and solid masses in the abdomen and pelvis, which were closely related to the bilateral adnexa. The volume of the uterus increased, and the bilateral adnexa was not clearly visible. CT enhancement was recommended.

Pelvic MRI revealed numerous cystic and solid masses present in the bilateral adnexal area, as well as in the parametrial and abdominal cavities. The largest mass, measuring 83 mm × 67 mm × 70 mm, was situated within the muscular layer of the anterior uterine wall. These masses displayed slightly hypointense signals on T2WI, isointensity on T1WI, and hyperintensity on DWI. The diagnosis indicated a typical uterine leiomyoma, while multiple lesions in the abdomen and pelvis were identified as metastatic tumors (Figure 3).

The patient underwent total hysterectomy, bilateral adnexectomy, and partial omentum resection while under general anesthesia. Several nodules, approximately 1.5 cm in diameter, were found attached to the greater omentum, positioned anterior to the uterus. These nodules were firm in texture and had smooth surfaces. Additionally, tumor protrusions measuring 10 cm and 12 cm were observed on the left and right sides of the uterine horn, respectively. These protrusions exhibited smooth surfaces, cystic degeneration, and multiple cysts and contained clear fluid. Ranging in size from 1.5 cm to 4 cm, the tumors had clear borders, smooth surfaces, and a non-thick cervix and showed no abnormalities in the appearance of the bilateral adnexa.

Histopathological examination of the uterus, double adnexectomy, and nodules of multiple greater omentum specimens confirmed uterine diffuse leiomyomatosis with disseminated peritoneal leiomyomatosis (DPL), a hypercellular type. The immunostaining results were as follows: P53 (−), Ki-67 (<1% +), SMA (+), caldesmon (+), and CD117 (a few scattered +) (Figure 4).

Discussion

The etiology of DUL remains uncertain, and unified diagnostic criteria have yet to be established. DUL predominantly impacts women of reproductive age (10), with instances reported in individuals as young as 16 years (11). The diagnosis is based on the imaging features observed through preoperative ultrasound or MRI. Patients with DUL show an enlarged uterus filled with numerous, poorly defined, small leiomyomas that replace much of the myometrium (12). In clinical settings, hysterectomy is the definitive treatment. Performing myomectomy on many nodules with unclear margins is challenging, and recurrence rates are high (7, 13). Furthermore, as DUL represents a borderline leiomyoma pattern, it warrants increased attention for its potential malignancy (14) compared to typical leiomyomas. Thus, accurate preoperative diagnosis of DUL is crucial.

Currently, no standard diagnostic approach for DUL exists. MRI facilitates early detection and precise preoperative assessment. Although ultrasound is recommended as the initial imaging technique for pelvic, uterine, or ovarian conditions, MRI is now the preferred and most effective method due to its multiplanar imaging capabilities, superior soft tissue contrast, and utility in pretreatment mapping. Imaging tests show diffuse leiomyomas with indistinct boundaries and merging, whereas typical leiomyomas appear as distinct masses with asymmetric uterine involvement. In two cases of DUL, the initial misdiagnoses included multiple

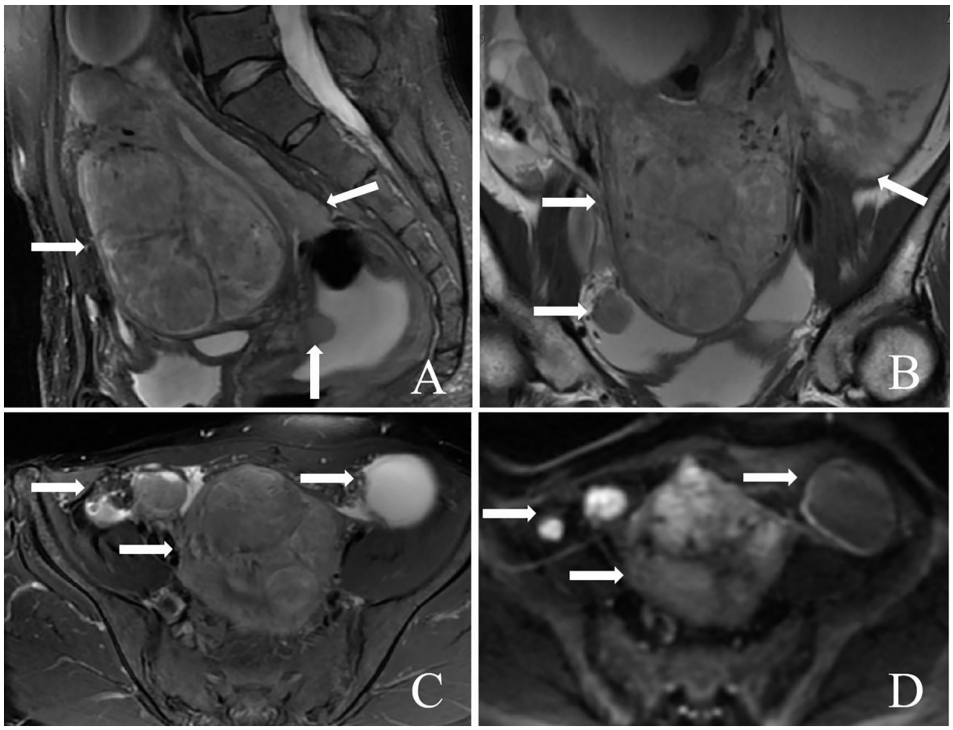

FIGURE 3
A 46-year-old patient with diffuse uterine leiomyomatosis (DUL) with peritoneal disseminated leiomyoma (DPL). **(A–D)** A large mass was observed in the anterior wall of the uterus. In addition, multiple masses were also observed in the posterior wall of the uterus and the abdominal and pelvic cavities beside the peritoneum (arrow). The masses above the myometrium and beside the peritoneum showed low signal intensity on sagittal T2WI, mild signal intensity on sagittal T1WI, and greater signal intensity on DWI. T2WI, T2-weighted imaging; T1WI, T1-weighted imaging; DWI, diffusion-weighted imaging.

ordinary leiomyomas and metastatic tumors. When MRI displays numerous, undefined leiomyomas replacing the majority of the myometrium, a diagnosis of DUL is possible. The second instance involved DUL with peritoneal disseminated leiomyoma, presenting multiple smooth muscles or smooth muscle-like nodules throughout the abdominal cavity, also known as leiomyomatosis peritonealis disseminata (15, 16).

Hysteroscopy, a standard surgical procedure for addressing intrauterine lesions, involves inserting a hysteroscope into the endometrial cavity via the cervical canal. A liquid expansion medium facilitates the observation and treatment of abnormalities within the uterine cavity. In the instances documented herein, both patients underwent total hysterectomy following a comprehensive evaluation of all relevant factors. It has been suggested that hysteroscopy may be a preferable option for patients with fetal DUL, as indicated by a case report of successful repeated pregnancies following “cold loop” hysteroscopic myomectomy (17). Additionally, successful pregnancies have been reported in

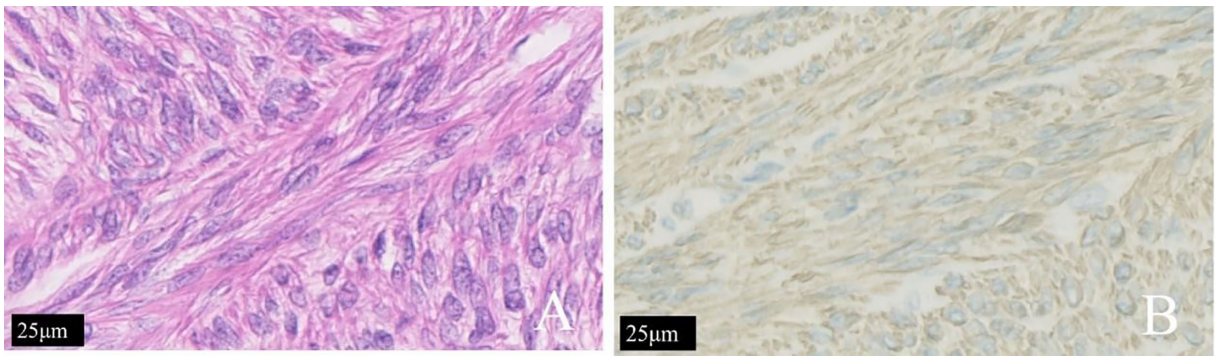

FIGURE 4
The same patient shown in Figure 3. **(A)** The tumor cells of patients with diffuse uterine leiomyomatosis were long and fusiform. The cytoplasm was rich in red dye and was arranged in bundles or interleaved shapes according to H&E staining. **(B)** Immunohistochemical staining for h-caldesmon (+) is shown.

women with DUL after undergoing hysteroscopic management (18). Conversely, recent findings in patients with incomplete spontaneous miscarriage have indicated that hysteroscopic surgery is not associated with higher subsequent delivery rates or greater safety compared to vacuum aspiration in those planning future pregnancies (19). Hence, further clinical data are required before definitive conclusions can be drawn. High-intensity focused ultrasound (HIFU) has been employed in patients with DUL, with studies indicating its safety, efficacy, and reliability. These findings support the use of drug therapy in conjunction with HIFU, yielding promising outcomes after conception (20).

Most cases of DUL with peritoneal disseminated leiomyoma recur following surgical intervention (21). Clinically, it is often initially misdiagnosed as peritoneal malignancy due to prominent imaging features, such as disseminated masses in the abdomen and pelvis. However, the absence of omental fatty infiltration, significant ascites, or solid organ metastases on imaging modalities like CT or MRI aids in distinguishing these DUL cases from malignant conditions (22). Additionally, well-circumscribed nodules are indicative of DUL with peritoneal dissemination. For the second patient documented in this report, the diagnosis was facilitated by the presence of a large uterine leiomyoma in the anterior wall of the uterus, exhibiting low signal intensity on T2WI with some hyperintensity due to hyaline degeneration. These characteristics, along with similar signal features of uterine leiomyoma in peritoneal masses, supported the diagnosis of DUL with peritoneal dissemination. Furthermore, most patients display normal blood levels of tumor markers, although CA-125 may be elevated. The features of well-circumscribed and similar signals of uterine leiomyoma for masses around the peritoneum in the abdomen and pelvis were helpful for the diagnosis of DUL with peritoneal dissemination. Moreover, most patients have normal blood levels of tumor markers, and CA-125 may be elevated. Finally, the results of histopathological examination can help to determine a definitive diagnosis, and the data can be positive for caldesmon, estrogen receptor (ER), PR, CD117, and muscle membrane antigen (SMA) (23).

Given the rare nature of DUL, only a few cases have been reported. Therefore, there are still many unknowns in the field. Moreover, different features might present in different patients. Therefore, more clinical data are needed to identify patient characteristics in MR images.

Conclusion

In conclusion, DUL is a borderline leiomyoma with malignant potential and may be accompanied by peritoneal dissemination. Multiple uterine leiomyomas on MRI were innumerable and poorly defined in the myometrium, and DUL could be diagnosed. In addition, the bilateral adnexal area and the parametrial and abdominal cavities were noted. In this paper, our findings emphasized the importance of MRI in the accurate diagnosis of DUL. Given the rapid progress in artificial intelligence, it is reasonable to believe that algorithms can be developed to read MRI data with high efficiency and accuracy. For patients with multiple uterine leiomyomas with masses in the parametrial and abdominal cavities, a diagnosis of DUL with DPL should be considered. Finally, clinicians should be assisted in guiding treatment decisions.

Data availability statement

The original contributions presented in the study are included in the article/supplementary material. Further inquiries can be directed to the corresponding author.

Ethics statement

Ethical approval was not required for the studies on humans in accordance with the local legislation and institutional requirements because only commercially available established cell lines were used. Written informed consent was obtained from the individual(s) for the publication of any potentially identifiable images or data included in this article.

Author contributions

ZZ: Writing – original draft. XL: Writing – review & editing, Conceptualization. XW: Writing – review & editing, Methodology, Supervision. FH: Writing – review & editing, Investigation. WC: Writing – review & editing, Project administration. XM: Writing – review & editing, Validation. FX: Writing – review & editing, Supervision.

Funding

The author(s) declare financial support was received for the research, authorship, and/or publication of this article. This work was supported by the Zhejiang Provincial Medical and Health Project (No. 2023RC212).

Conflict of interest

The authors declare that the research was conducted in the absence of any commercial or financial relationships that could be construed as a potential conflict of interest.

Publisher's note

All claims expressed in this article are solely those of the authors and do not necessarily represent those of their affiliated organizations, or those of the publisher, the editors and the reviewers. Any product that may be evaluated in this article, or claim that may be made by its manufacturer, is not guaranteed or endorsed by the publisher.

References

1. Della Corte L, Guarino MC, Vitale SG, Angioni S, Mercorio A, Bifulco G, et al. C-section technique vs minilaparotomy after minimally invasive uterine surgery: a retrospective cohort study. *Arch Gynecol Obstet*. (2024) 309:219–26. doi: 10.1007/s00404-023-07239-7

2. Lippman SA, Warner M, Samuels S, Olive D, Vercellini P, Eskenazi B. Uterine fibroids and gynecologic pain symptoms in a population-based study. *Fertil Steril*. (2003) 80:1488–94. doi: 10.1016/S0015-0282(03)02207-6

3. Mas A, Simón C. Molecular differential diagnosis of uterine leiomyomas and leiomyosarcomas. *Biol Reprod*. (2019) 101:1115–23. doi: 10.1093/biolre/ioy195

4. Siedhoff MT, Doll KM, Clarke-Pearson DL, Rutstein SE. Laparoscopic hysterectomy with morcellation vs abdominal hysterectomy for presumed fibroids: an updated decision analysis following the 2014 Food and Drug Administration safety communications. *Am J Obstet Gynecol*. (2017) 216:259.e251–259.e256. doi: 10.1016/j.ajog.2016.11.1039

5. Suminaga Y, Taki M, Okamoto H, Kawamura Y, Sagae Y, Sunada M, et al. A case of a patient with adhesive small bowel obstruction in pregnancy after extensive myomectomy for diffuse uterine leiomyomatosis. *Case Rep Obstet Gynecol*. (2022) 2022:3601945. doi: 10.1155/2022/3601945

6. Rosica G, Santilli G, Bucari D, Amici B, Bulletti F, Patacchiola F, et al. A case of disseminated peritoneal leiomyomatosis and diffuse uterine leiomyomatosis. *Clin Exp Obstet Gynecol*. (2011) 38:84–7. doi: 10.1111/j.1524-4741.2010.01035.x

7. Konishi I. Diffuse leiomyomatosis: complete myomectomy for innumerable small nodules to achieve fertility sparing and childbearing. *Surg J (N Y)*. (2020) 6:S50–s57. doi: 10.1055/s-0039-1693709

8. Lapan B, Solomon L. Diffuse leiomyomatosis of the uterus precluding myomectomy. *Obstet Gynecol*. (1979) 53:82s–4s.

9. Silva CA, Rosa F, Rito M, Cunha TM. Diffuse leiomyomatosis: A rare cause of a diffusely enlarged uterus. *Radiol Case Rep*. (2022) 17:1536–9. doi: 10.1016/j.radcr.2022.02.029

10. Purohit R, Sharma JG, Singh S. A case of diffuse uterine leiomyomatosis who had two successful pregnancies after medical management. *Fertil Steril*. (2011) 95:2434.e2435–2436. doi: 10.1016/j.fertnstert.2011.04.004

11. Pai D, Coletti MC, Elkins M, Ladino-Torres M, Caoili E. Diffuse uterine leiomyomatosis in a child. *Pediatr Radiol*. (2012) 42:124–8. doi: 10.1007/s00247-011-2114-3

12. Fedele L, Bianchi S, Zanconato G, Carinelli S, Berlanda N. Conservative treatment of diffuse uterine leiomyomatosis. *Fertil Steril*. (2004) 82:450–3. doi: 10.1016/j.fertnstert.2004.01.029

13. Dai YX, Feng FZ, Leng JH, Shi HH, Cheng NH, Wan XR, et al. [Imaging features and clinical analysis of diffuse uterine leiomyomatosis cases]. *Zhonghua Yi Xue Za Zhi*. (2020) 100:2263–7. doi: 10.3760/cma.j.cn112137-20200307-00634

14. Otsubo Y, Nishida M, Arai Y, Ichikawa R, Sakanaka M. Diffuse uterine leiomyomatosis in patient with successful pregnancy following new surgical management. *Arch Gynecol Obstet*. (2014) 290:815–8. doi: 10.1007/s00404-014-3309-2

15. Willson JR, Peale AR. Multiple peritoneal leiomyomas associated with a granulosa-cell tumor of the ovary. *Am J Obstet Gynecol*. (1952) 64:204–8. doi: 10.1016/S0002-9378(16)38757-9

16. Thang NM, Thien DH, Huyen Anh NT, Cuong TD. Leiomyomatosis peritonealis dissemianata five years after laparoscopic uterine myomectomy: A case report. *Ann Med Surg (Lond)*. (2021) 66:102377. doi: 10.1016/j.amsu.2021.102377

17. Mazzon I, Favilli A, Grasso M, Morricone D, Di Renzo GC, Gerli S. Is 'cold loop' hysteroscopic myomectomy a better option for reproduction in women with diffuse uterine leiomyomatosis? A case report of successful repeated pregnancies. *J Obstet Gynaecol Res*. (2015) 41:474–7. doi: 10.1111/jog.12548

18. Zhao H, Yang B, Li H, Xu Y, Feng L. Successful pregnancies in women with diffuse uterine leiomyomatosis after hysteroscopic management using the hysteroscopy endo operative system. *J Minim Invasive Gynecol*. (2019) 26:960–7. doi: 10.1016/j.jmig.2018.10.003

19. Huchon C, Drioueche H, Koskas M, Agostini A, Bauville E, Bourdel N, et al. Operative hysteroscopy vs vacuum aspiration for incomplete spontaneous abortion: A randomized clinical trial. *Jama*. (2023) 329:1197–205. doi: 10.1001/jama.2023.3415

20. Gong C, Lin Z, Deng Y, Yang B, Zhang L. Successful pregnancies in women with diffuse uterine leiomyomatosis after high-intensity focused ultrasound ablation: report of three cases. *Int J Hyperthermia*. (2023) 40:2234674. doi: 10.1080/02656736.2023.2234674

21. Żyła MM, Dzieniecka M, Kostrzewa M, Stetkiewicz T, Wilamowska A, Księżakowska-Łakoma K, et al. Leiomyomatosis peritonealis disseminata of unusual course with Malignant transformation: case report. *Acta Obstet Gynecol Scand*. (2015) 94:220–3. doi: 10.1111/aogs.12549

22. Belmarez JA, Latifi HR, Zhang W, Matthews CM. Simultaneously occurring disseminated peritoneal leiomyomatosis and multiple extrauterine adenomyomas following hysterectomy. *Proc (Bayl Univ Med Cent)*. (2019) 32:126–8. doi: 10.1080/08998280.2018.1520555

23. Chen X, Liu H, Shi H, Fan Q, Sun D, Lang J. Leiomyomatosis peritonealis disseminata following laparoscopic surgery with uncontained morcellation: 13 cases from one institution. *Front Surg*. (2021) 8:788749. doi: 10.3389/fsurg.2021.788749

frontiers | Frontiers in Oncology

TYPE Original Research
PUBLISHED 04 July 2024
DOI 10.3389/fonc.2024.1406872

Check for updates

OPEN ACCESS

EDITED BY
Dragos Eugen Georgescu,
Carol Davila University of Medicine and Pharmacy, Romania

REVIEWED BY
Jessica Crystal,
University of Miami, United States
Teodor Florin Georgescu,
Carol Davila University of Medicine and Pharmacy, Romania
Bixia Tang,
Beijing Cancer Hospital, China

*CORRESPONDENCE
Danielle H. Tran
dtran85@uw.edu
Evidio Domingo-Musibay
musib024@umn.edu

RECEIVED 25 March 2024
ACCEPTED 27 May 2024
PUBLISHED 04 July 2024

CITATION
Tran DH, Shanley R, Giubellino A, Tang PH, Koozekanani DD, Yuan J, Dusenbery K and Domingo-Musibay E (2024) Radiation and systemic immunotherapy for metastatic uveal melanoma: a clinical retrospective review. *Front. Oncol.* 14:1406872. doi: 10.3389/fonc.2024.1406872

COPYRIGHT
© 2024 Tran, Shanley, Giubellino, Tang, Koozekanani, Yuan, Dusenbery and Domingo-Musibay. This is an open-access article distributed under the terms of the Creative Commons Attribution License (CC BY). The use, distribution or reproduction in other forums is permitted, provided the original author(s) and the copyright owner(s) are credited and that the original publication in this journal is cited, in accordance with accepted academic practice. No use, distribution or reproduction is permitted which does not comply with these terms.

Radiation and systemic immunotherapy for metastatic uveal melanoma: a clinical retrospective review

Danielle H. Tran[1,2*], Ryan Shanley[3], Alessio Giubellino[4], Peter H. Tang[5,6], Dara D. Koozekanani[6], Jianling Yuan[7], Kathryn Dusenbery[7] and Evidio Domingo-Musibay[8,9*]

[1]University of Minnesota Medical School, Minneapolis, MN, United States, [2]Department of Medicine, University of Washington, Seattle, WA, United States, [3]Biostatistics Core, University of Minnesota Masonic Cancer Center, Minneapolis, MN, United States, [4]Department of Laboratory Medicine and Pathology, University of Minnesota, Minneapolis, MN, United States, [5]Department of Ophthalmology, Storm Eye Institute, Medical University of South Carolina, Charleston, SC, United States, [6]Department of Ophthalmology & Visual Neurosciences, University of Minnesota, Minneapolis, MN, United States, [7]Department of Radiation Oncology, University of Minnesota, Minneapolis, MN, United States, [8]Department of Medicine, Division of Hematology and Oncology, University of Minnesota, Minneapolis, MN, United States, [9]Department of Medical Oncology, Allina Health Cancer Institute, Minneapolis, MN, United States

Introduction: Metastatic uveal melanoma (mUM) is a difficult to treat disease. The liver is the primary site of metastasis in most patients, though uveal melanoma spreads widely in advanced disease. The only FDA approved immunotherapy medication for metastatic uveal melanoma is the HLA-A02:01 restricted bispecific T cell engager drug, Tebentafusp. Checkpoint inhibitor strategies and combination approaches have been tried with some limited success. We describe our experience treating patients at the University of Minnesota.

Methods: Patients were included if they had biopsy-confirmed mUM. Twenty-five (25) patients meeting the criteria were identified. Medical records were reviewed and data extracted for patient baseline characteristics and response to treatments.

Results: Median time to metastasis from the time of local therapy to the eye was 14.2 months (IQR; 9.3-22.0), and first site of metastasis was liver in 92% of patients. Two patients (8%) did not receive systemic therapy or radiation therapy for metastatic disease. Twenty-three (92%) patients received systemic therapy, 13 patients (52%) received ipilimumab-nivolumab as the first-line, while 4 patients (16%) received pembrolizumab. Landmark survival analysis by receipt of systemic therapy and radiation therapy treatments within 6 months of biopsy confirmed diagnosis is shown. Twenty patients (80%) received systemic therapy within 6 months of mUM diagnosis. Thirteen patients (52%) received liver directed radiation therapy within 6 months of mUM diagnosis.

Discussion: Within our cohort, there was no overall survival benefit for patients receiving treatment of metastatic disease within 6 months of mUM diagnosis,

versus those electing later or no treatment at all. There was remarkable clinical activity of ipilimumab and nivolumab in a subset of patients with mUM, in agreement with prior studies, and metastatic PD-L1 positive tumors were associated with a prolonged survival.

KEYWORDS

metastatic uveal melanoma, immunotherapy, radiation therapy (radiotherapy), retrospective study, ipilimumab, nivolumab, PD-L1

Introduction

Uveal melanoma (UM) is the most common primary intraocular tumor found in adults and arises within the uveal tract of the eye (1). Melanocytes within the iris, ciliary body, and choroid can give rise to malignancy with a propensity for invasion and metastasis. Primary UM can be treated with enucleation or with various strategies involving radiotherapy, including plaque brachytherapy, gamma-knife stereotactic radiosurgery (GK-SRS), and proton beam therapy. While adjuvant therapy for high-risk UM has been tried with some additional benefit (2), early metastasis is common, and overall survival remains poor (3). Nearly half of UM ultimately metastasize, with the most common extraocular sites being the liver (95%), lungs (24%), bone (16%), and skin and soft tissue (11%) (4).

Due to the high rate of liver metastasis, targeted therapy to this organ is common. The selection of optimal therapeutic modality generally depends on the location and extent of metastasis. Liver-directed therapies include image-guided ablation (thermal ablation, radiofrequency ablation, or cryoablation), radioembolization [also known as selective internal radiation therapy (SIRT)], immunoembolization (IE), and transarterial chemoembolization (TACE). Benefits have also been seen with isolated hepatic perfusion and hepatic artery infusion (5). In select cases of oligometastatic disease, resection of metastatic nodules and/or stereotactic radiation therapy (SBRT) can also be considered.

The use of systemic chemotherapy (dacarbazine, fotemustine, temozolomide, cisplatin, or a combination thereof) for metastatic disease has yielded disappointing results (6). Response rates to chemotherapy were generally less than 10%, and neither single nor multiagent chemotherapy extended overall survival (OS) in patients with metastatic disease. In the last decade, immunotherapy using immune checkpoint blockade with inhibitors for programmed death 1 (PD-1) and cytotoxic T-lymphocyte-associated antigen (CTLA-4) has shown promise. While efficacy of checkpoint inhibition has radically changed the approach to treatment of cutaneous melanoma and many other solid tumors, its efficacy in metastatic UM has been less dramatic.

In a retrospective analysis, 56 patients with metastatic UM refractory to prior lines of therapy were treated with anti-PD1 or anti-PDL1 therapy. Thirty-eight patients (68%) received pembrolizumab, 16 (29%) received nivolumab, and 2 (4%) received atezolizumab. Objective responses were seen in two patients for an overall response rate of 3.6% (7). In an analysis across 14 academic medical centers, the combination of nivolumab with ipilimumab yielded an overall response rate of 11.6%, median OS of 15 months, and median progression-free survival (PFS) of 2.7 months. Overall efficacy remains considerably lower than that seen for metastatic cutaneous melanoma (8). Similarly, in a recent prospective phase II study, patients received ipilimumab 3 mg/kg with nivolumab 1 mg/kg for four cycles, followed by nivolumab maintenance therapy for up to 2 years. The primary outcome of the study was overall response rate as determined by the Response Evaluation Criteria in Solid Tumors (RECIST) 1.1 criteria. Of 33 patients evaluated for efficacy, the overall response rate was 18%, including one confirmed complete response and five confirmed partial responses (9).

More recently, tebentafusp, a bispecific T-cell engager that redirects T cells to target glycoprotein 100-positive melanoma cells, has been approved for use in metastatic UM. Tebentafusp has been shown to produce longer OS than control therapy (either single-agent pembrolizumab, ipilimumab, or dacarbazine) with OS at 1 year of 73% in the tebentafusp group and 59% in the control group (10). Notably, the treatment is limited to patients that are HLA-A*02:01 positive and requires weekly IV infusions and initial blood pressure support and monitoring. There remains a critical unmet need for additional efficacious therapies in this patient population.

Here, we describe our recent experience in treating patients with metastatic UM at the University of Minnesota. Patients during this time period received several different treatments, including SBRT, Y90 radioembolization, chemotherapy, high-dose IL-2, dual- or single-agent checkpoint inhibitors, and cellular therapy. We report clinical data, response to radiation and systemic treatments, survival, and treatment-related adverse events in evaluable subjects.

Materials and methods

Patients and treatment

We conducted a single-center retrospective study of patients with metastatic UM treated at the University of Minnesota between 2016 and 2022. Patients were included if they had biopsy-confirmed

metastatic UM. Twenty-five patients meeting the criteria were identified. Medical records were reviewed, and data were extracted for patient baseline characteristics and response to therapy.

PD-L1 immunohistochemistry

Biopsied metastatic lesions were assessed for expression of PD-L1 on the surface of the tumor cells at the University of Minnesota Central Pathology Laboratory or an external laboratory by means of immunohistochemical testing of formalin-fixed, paraffin-embedded tumor specimens using a monoclonal antihuman PD-L1 antibody. PD-L1 positivity was defined as having at least 1% of tumor cells showing PD-L1 staining of any intensity on the cell surface in 100 cells being evaluated. Seven patients in our study did not have PD-L1 results available.

Adverse events and assessments

Toxicity data were abstracted from clinical notes. Toxicity events were categorized. Imaging assessments were performed every 3 months using cross-sectional computed tomography (CT), combined positron emission tomography and CT (PET-CT), and magnetic resonance imaging (MRI) modalities. Response was evaluated by the treating oncologist and reported as the best overall response (BOR) using RECIST v1.1 criteria (11).

Statistical analysis

Survival was estimated using the Kaplan–Meier method and groups compared by log-rank test. Log-log confidence intervals are reported. OS of metastatic UM was measured from the date of biopsy-confirmed diagnosis of metastatic disease to the date of death or last known follow-up. Time to metastasis (TTM) was calculated from the date of local therapy to the eye to the date of biopsy-confirmed diagnosis of metastatic disease.

We used landmark analysis for overall survival through receipt of systemic therapy and radiation therapy. Six months after metastatic disease diagnosis was selected as the landmark time. Patients who experienced an event or were censored before the landmark were excluded from the analysis. For the analysis of OS by PD-L1 status, the full cohort was used, and the time of origin remained as the date of metastatic disease diagnosis. Statistical calculations were performed using R software, version 4.2.

Results

Patient characteristics

We identified 25 patients with metastatic UM treated in our medical center with confirmed biopsy. Table 1 summarizes the baseline characteristics of the full cohort of patients. The median age at diagnosis of metastasis was 68.9 years old. All patients were Caucasian, and 13 patients (52%) were male. Median time to metastasis was 14.2 months (IQR; 9.3–22.0), and initial organ of spread was the liver in 92% of the patients. PD-L1 status was known for 18 patients; 4 were PD-L1+ and 14 were PD-L1-. PD-L1 status was not known for seven patients.

TABLE 1 Baseline patient characteristics, n = 25.

Characteristic	N=25
Age at mUM diagnosis, n (%)	
<60 years	9 (36)
≥60 years	16 (64)
Median (IQR), years	68.9 (52.2 - 77.6)
Sex, n (%)	
Male	13 (52)
Female	12 (48)
Primary Treatment, n (%)	
Plaque brachytherapy	12 (48)
Gamma knife radiosurgery	2 (8)
Proton beam Radiotherapy	3 (12)
Enucleation	6 (24)
Orbital exenteration	2 (8)
Adjuvant therapy, n (%)	
Sunitinib	2 (8)
Nivolumab	2 (8)
Time to metastasis (TTM)	
Median, months	14.2
IQR	9.3 - 22.0
Liver involvement at mUM diagnosis	
Positive	23 (92)
Negative	2 (8)
PD-L1 expression of metastasis	
Positive	4 (16)
Negative	14 (56)
Unknown	7 (28)

mUM, metastatic uveal melanoma; IQR, interquartile range.

Treatment

Two patients (2/25) did not receive systemic therapy or radiation therapy for metastatic disease. First-line treatment regimens are summarized in Table 2. Of the 23 patients that received systemic therapy, 13 patients (57%) received ipilimumab–nivolumab as a first-line, while 4 patients (17%) received pembrolizumab. Three patients received first-line sequential high dose IL-2 (6 weeks) and

TABLE 2 First-line metastatic disease treatment regimen.

Treatments	No (%)
Ipilimumab/Nivolumab	13 (57)
HD IL-2 plus Ipilimumab/ Nivolumab[a,b]	3 (13)
Pembrolizumab	4 (17)
Haploidentical NK cells[b]	1 (4)
Carboplatin/Paclitaxel	2 (9)
Treatment within 6 months[c]	21 (91)

[a]sequentially administered HD IL-2 and Ipilimumab/Nivolumab.
[b]treatment on clinical trial protocol.
[c]receipt of first-line systemic therapy within 6 months of metastatic disease diagnosis.

ipilimumab–nivolumab (13%), and 2 patients received first-line carboplatin–paclitaxel (9%). Nearly all patients (21/23, 95%) received ipilimumab and nivolumab at some point during their treatment. Of the patients receiving treatment, 13 (57%) received palliative intent radiation therapy within 6 months of metastasis diagnosis (Table 3).

Treatment responses

Median OS for the entire patient cohort was 24 months. Figure 1 depicts the OS as measured from time of pathologic diagnosis of metastatic disease for all 25 patients. Figure 2 depicts the landmark analysis of OS, stratified by systemic therapy treatment initiation within 6 months of metastasis diagnosis. Overall survival for the 20 treated patients was 48% at 24 months after diagnosis (95% CI: 23, 69) versus 75% (95% CI: 13, 96) for the 4 patients not treated before 6 months (p = 0.57). Two patients who began treatment after 6 months were included in the non-treated group for the landmark analysis. One patient who received systemic therapy but died within 6 months of diagnosis was not included in the landmark analysis.

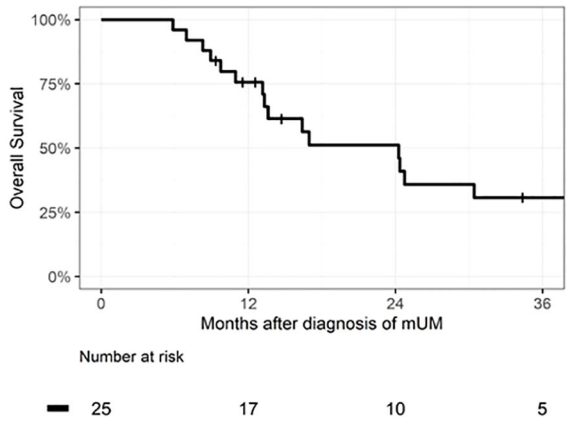

FIGURE 1
Kaplan–Meier curve of overall survival of the full cohort of patients diagnosed with metastatic uveal melanoma (mUM), n = 25 patients. Median survival time was 24 months (IQR 13–48).

Patients receiving systemic immunotherapy were also included in the best overall response analysis to check-point blockade. In Figure 3, BOR for ipilimumab/nivolumab as first-line treatment was 15% versus 0% for pembrolizumab. There were two complete responses (CR) and three stable diseases (SD) with the combination of ipilimumab/nivolumab, while only one patient treated with pembrolizumab maintained stable disease.

A total of 20 patients received radiation therapy for disease palliation, described in Table 3. Fourteen patients received liver-directed therapy (either SBRT or Y-90 radioemoblization), with one patient initially receiving SBRT to the liver followed by Y90 radioembolization at a later time. Two patients received GK SRS

TABLE 3 Radiation treatment for metastatic disease.

Treatments	No (%)
CNS	
GK SRS	2 (10)
Pulmonary	
SBRT	1 (5)
Liver	
SBRT	5 (25)
Y-90 Radioembolization	10 (50)
Bone	
Palliative EBRT	3(15)
RT within 6 months[a]	
Yes	13 (65)
No	7 (35)

SBRT, stereotactic body radiotherapy; EBRT, external beam radiation therapy; GK SRS, gamma knife stereotactic radiosurgery; RT, radiation therapy. [a]receipt of radiation therapy within 6 months of metastatic disease diagnosis.

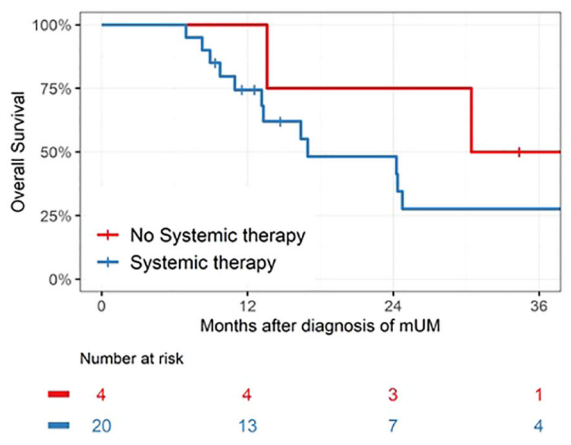

FIGURE 2
Landmark analysis of patients receiving systemic therapy within 6 months of mUM diagnosis. Median survival was 17 months (IQR 11 –50, n = 20) for the Systemic Therapy group versus 39 months (IQR 22–48, n = 4) for the No Systemic Therapy group, p = 0.57.

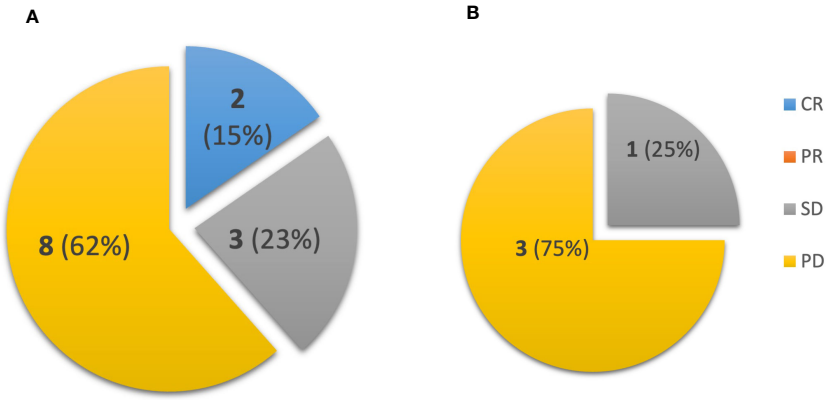

FIGURE 3
Patients were evaluated for Best Overall Response (BOR) with **(A)** first-line ipilimumab/nivolumab (n = 13), compared with **(B)** first-line pembrolizumab (n = 4). CR, complete response; PR, partial response; SD, stable disease; PD, progressive disease.

for brain metastases, three patients received palliative dose radiation therapy for bone metastases, and one patient received SBRT for lung metastasis.

A total of 13 patients received radiation therapy for metastases within 6 months of metastasis diagnosis: four received SBRT to dominant hepatic masses, eight received Y90-radioembolization to the liver (generally as two separate treatments), and one received palliative radiation to a painful bony vertebral metastasis. For the purpose of the landmark analysis, patients who initiated radiotherapy within 6 months were included in the Radiation Therapy group (n = 13). Patients who did not initiate radiotherapy within 6 months (n = 11) were counted in the No Radiation Therapy group, which included six patients who later initiated radiotherapy. There was no survival benefit seen with radiotherapy initiated within 6 months of diagnosis. OS at 24 months was 37% (95% CI: 11, 65) for the Radiation Therapy group versus 70% (95% CI: 33, 89) for the No Radiation Therapy group (p = 0.02; Figure 4).

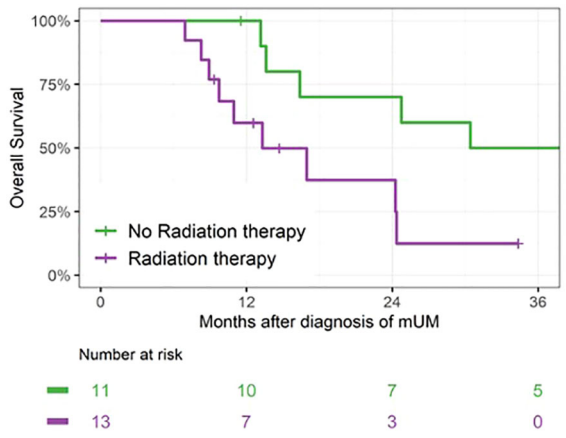

FIGURE 4
Landmark analysis of patients receiving radiation therapy within 6 months of mUM diagnosis. For patients in the Radiation Therapy group, median survival was 13 months (IQR 10–24, n = 13) versus 39 months (IQR 16–56, n = 11) for patients in the No Radiation Therapy group, p = 0.02.

We also assessed the potential impact of PD-L1 expression on survival. The median survival for PD- L1-negative cases (14/25, 56%) was 17 months and for PD-L1+ cases (4/25, 16%), it was 56 months (p = 0.04; Figure 5). All PD-L1+ patients received systemic therapy. None of the PD-L1+ received radiotherapy within 6 months.

Immune-related adverse events

Of the 23 patients who opted to receive systemic therapy, 16 reported immune-related adverse events (irAEs) during treatment with either pembrolizumab, ipilimumab/nivolumab, or maintenance nivolumab (Table 4). The median number of reported irAEs were 2 per patient (range: 0–6). The severity of irAEs correlated with response. The median reported irAEs of the PD- L1-positive patients (n = 4) was 3.5 (range: 2–6), while those of the PD- L1-negative patients (n = 13) was 1 (range: 0–5), and of the unknown PD-L1 status patients (n = 3) was 2 (range: 0–2).

Discussion

In this study of 25 patients with metastatic UM, median overall survival of the entire patient cohort was 24 months. This fares well with historical accounts of median survival of 6–10 months (12, 13). Although patient numbers are small, median OS was not statistically improved in patients receiving systemic therapy within 6 months of diagnosis of metastatic disease. Similarly, no apparent survival benefit was seen with (early) radiation therapy within 6 months of diagnosis. In fact, there was a statistically significant difference in survival favoring no radiation, though later radiation therapy administration in six patients and inclusion of all four PD- L1-positive patients in the No Radiation Therapy group may have skewed results. Nonetheless, our results suggest that early systemic and radiation therapy treatments may

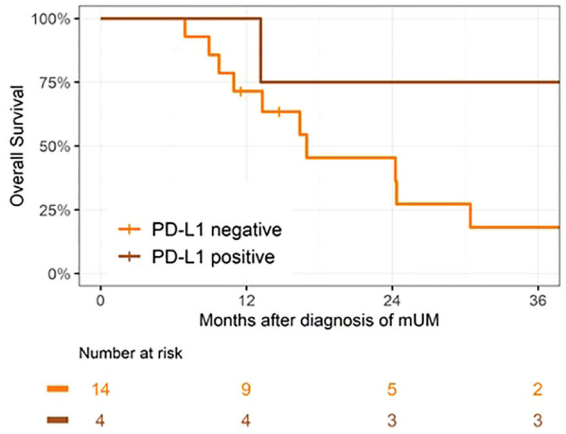

FIGURE 5
Kaplan–Meier curves of overall survival by PD-L1 status. p = 0.04.

not seemingly confer significant survival benefit for most patients. The data appear to agree with results of the meta-analysis by Rantala et al. suggesting there is no evidence for longer median OS for patients with metastatic UM by any treatment modality (3).

We did, however, note objective responses with immunotherapy and radiotherapy treatments. Systemic immunotherapy responses were highest with ipilimumab/nivolumab. BOR to ipilimumab/nivolumab as a first-line treatment was 15% versus 0% for pembrolizumab. The BOR to ipilimumab/nivolumab, irrespective of treatment line, was 24%. Our analysis showed a statistically significant difference in survival when patients were stratified by PD-L1 status. While only a small number of patients expressed PD-L1 on their tumors, survival appears improved in this small group of patients treated with checkpoint inhibition.

PD-L1 expression on metastatic UM biopsies was associated with a higher likelihood of complete responses to first-line ipilimumab/nivolumab supporting the notion that PD-L1 expression may help predict response to dual checkpoint blockade. Of the four PD- L1-positive patients in this study, there were two CRs, one PR, and one PD with ipilimumab/nivolumab. On the other hand, in the PD-L1-negative majority of patients, there were no CRs and only two PRs seen. The PD- L1-positive responses are consistent with our current understanding that high PD-L1 expression in the tumor cell population correlates positively with response to anti-PD-1 antibodies (14, 15). Unfortunately, only about 10% of primary UM tumors and just 5% of metastatic UM cells at distant sites express PD-L1 in the microenvironment (16).

PD1 checkpoint blockade in metastatic UM is less efficacious than in cutaneous melanoma likely due to differences in biology, including differences in PD-L1 and immune checkpoint molecule expression, and low mutational burden compared to cutaneous melanoma (14). However, patients with low or negative PD-L1 expression may still respond to immunotherapy, and treatment based solely on PD-L1 expression may exclude potential patient responders. For example, there is a reported case of a complete response after treatment with pembrolizumab in a patient with UM with metastases to the liver, lung, and bones (17). Another

TABLE 4 Reported Immune-related Adverse Events (irAEs) during immunotherapy treatment, n=23.

Adverse Event (all grades)	Number of events (%)
Gastrointestinal	
Diarrhea/Colitis	8 (35)
Hepatitis	4 (17)
Pancreatitis	1 (4)
Dermatologic	
Pruritus	4 (17)
Dermatitis	3 (13)
Vitiligo	1 (4)
Hematologic	
Neutropenia	1 (4)
Endocrine	
DM type I	1 (4)
Hypothyroidism	6 (26)
Hypophysitis	3 (13)
Hypogonadism	1 (4)
Adrenal insufficiency (secondary)	2 (9)
Renal	
AKI	2(9)
Pulmonary	
Pneumonitis	3 (13)
MSK/Rheum	
Arthritis	2 (9)
Myalgia	1 (4)
Ocular	
Uveitis	1 (4)

metastatic UM patient received ipilimumab plus pembrolizumab and maintained stable disease for 10 months and experienced a prolonged survival for 2 years, twice the median survival length (18). Instructively, the tumors of these two patients had a high mutational burden, and both harbored germline mutations of methyl-CpG-binding domain protein (MBD4) found in approximately 2% of UM patients (17, 18). Their exceptional response may be explained by prior studies showing that immunotherapy may be more effective in tumors with a high mutational burden and that these tumors are more likely to be recognized by CTLs due to a higher expression of recognizable neoantigens (14, 19, 20). However, UM is a tumor with a relatively low mutational burden, with an average of 0.5 per Mb sequence (21). Therefore, the probability of recognizable neoantigens is generally low in UM, likely contributing to the disappointing overall response to checkpoint inhibition compared with UV radiation-associated cutaneous melanomas. Intriguingly, one of

our best overall responders had a low tumor mutational burden (TMB) of 2 Muts/Mb.

We also note that one patient initially negative for PD-L1 expression, after two cycles of high dose IL-2, had an increase in tumor cell PD-L1 expression. More than 7 months after the diagnosis of metastasis, biopsy of the patient's liver tumor after IL-2 therapy demonstrated PD-L1 expression >5%. She was subsequently treated with two cycles of combination ipilimumab plus nivolumab and had a partial response (PR) to treatment, though complicated by severe autoimmune colitis. The patient was treated with high-dose corticosteroids, infliximab, and mycophenolate, but ultimately transitioned to hospice and received no additional cancer-directed therapy.

Our findings also suggested higher median irAEs among PD-L1-positive patients versus PD- L1-negative patients. This is consistent with the literature that supports the notion of irAEs to reflect the response to immunotherapy. In a retrospective analysis of 148 melanoma patients treated with nivolumab monotherapy, cutaneous irAEs were associated with an improved survival (22). Another meta-analysis of 48 clinical trials investigated the incidence rates of irAEs and their correlations with objective response rate (ORR) in patients with advanced solid tumors treated with nivolumab or nivolumab plus ipilimumab (23). The authors found that the ORR of nivolumab positively correlated with the incidence rate of the skin, gastrointestinal, and endocrine irAEs, but not hepatic, pulmonary, and renal irAEs. Similarly, the ORR of nivolumab plus ipilimumab was positively correlated with the incidence rate of the skin and gastrointestinal irAEs, but not endocrine, hepatic, pulmonary, and renal irAEs (23). There were higher rates of irAEs in complete responders compared to patients who did not achieve a complete response. In our patient population, patients receiving systemic treatment (n = 20) reported a range of 1 to 6 irAEs per patient. PD- L1-positive patients (n = 4) had a higher median number of 3.5 irAEs compared to the PD- L1-negative patients (n = 13) with a median of 1 irAE per patient.

Beyond PD1, alternative checkpoints may contribute to the susceptibility of metastatic UM to immune checkpoint inhibition strategies. T-cell immunoglobulin and ITIM domain (TIGIT) inhibition is being investigated in clinical trials (24, 25). Chauviin et al. originally found an upregulation of TIGIT and a co-expression of PD-1 in patients with melanoma (26). Stalhammer et al. discovered that metastatic primary UM has a higher number of TIGIT-positive cells/mm^2 than non-metastatic UM (27). Several monoclonal antibodies have been synthesized to target TIGIT, with clinical trials on TIGIT inhibition in several cancer types underway, but further investigation for activity against metastatic UM is needed (28, 29). On the other hand, lymphocyte activation gene 3 (LAG-3) inhibition has been focused on recently as an immune checkpoint in solid tumors, including both cutaneous and UM (30–32). Opdualag (combination of relatlimab and nivolumab) has become the first FDA-approved immunotherapy to target LAG-3, with relatlimab blocking the activity of LAG-3. The RELATIVITY-047 trial compared the combination of nivolumab and relatlimab versus nivolumab alone, and showed that inhibition of two immune checkpoints (LAG-3 and PD-1) provided greater progression-free survival compared to PD-1 inhibition alone (10.1 vs. 4.6 months) in patients with advanced cutaneous melanoma (33). Ongoing trials with Opdualag in metastatic UM are currently underway (NCT04552223 and NCT05077280).

There are key limitations of this study, which are inherent to its retrospective nature, including a small number of patients and selection bias of a single-center series. There was also variability in data reporting due to patients receiving some of their care at other institutions. It was also not possible to correlate PD-L1 expression and response to radiotherapy as there were no PD- L1-positive patients treated with radiotherapy. PD-L1-positive skewing of the No Radiation Therapy group may have contributed to a measured survival difference favoring this cohort, and larger numbers of patients balanced for PD-L1 expression are needed for further verification. Adverse events were based on patient charts and descriptions, and therefore likely underreported patient-subjective adverse events (e.g., fatigue, myalgias, pruritus). Furthermore, mild toxicities and symptoms occurring between clinical visits may not have been reported.

There is an unmet need for efficacious treatment of metastatic UM. Therapeutic options are limited, and it is crucial to understand the impact of immunotherapy in combination strategies involving checkpoint inhibitors, chemotherapy, cytokines, and radiation therapy approaches.

Conclusion

UM is a distinct subset of melanoma with decreased response to checkpoint inhibition versus cutaneous melanoma. Due to the rarity of the diagnosis and poor outcomes, there is a need for studies aimed at understanding the response to systemic and local treatments for metastatic disease. Our study showed no significant difference in survival for patients electing early treatment of their disease. There was remarkable clinical activity of ipilimumab and nivolumab in a subset of patients with UM, in agreement with prior studies. In our cohort, there were two complete responses to ipilimumab–nivolumab. Our data suggests that PD- L1-positive tumors may respond better to checkpoint blockade, and these tumors were associated with a prolonged survival. However, larger datasets are necessary to characterize the biomarkers of response to checkpoint blockade and identify molecular signatures of responders and non-responders in UM. Our data supports anti-PD-1/anti-CTLA-4 therapy as a viable treatment approach for metastatic UM patients particularly in those with PD- L1-positive tumors.

Data availability statement

The raw data supporting the conclusions of this article will be made available by the authors, without undue reservation.

Ethics statement

The studies involving humans were approved by University of Minnesota Institutional Review Board. The studies were conducted

in accordance with the local legislation and institutional requirements. Written informed consent for participation was not required from the participants or the participants' legal guardians/next of kin in accordance with the national legislation and institutional requirements.

Author contributions

DT: Writing – review & editing, Writing – original draft, Methodology, Investigation, Formal analysis, Data curation, Conceptualization. RS: Writing – review & editing, Writing – original draft, Software, Methodology, Formal analysis, Data curation. AG: Writing – review & editing, Writing – original draft, Methodology, Data curation. PT: Writing – review & editing, Writing – original draft, Formal analysis, Data curation. DK: Writing – review & editing, Writing – original draft. JY: Writing – review & editing, Writing – original draft, Data curation. KD: Writing – review & editing, Writing – original draft. ED-M: Writing – review & editing, Writing – original draft, Supervision, Software, Resources, Project administration, Methodology, Investigation, Formal analysis, Data curation, Conceptualization.

Funding

The author(s) declare financial support was received for the research, authorship, and/or publication of this article. Research reported in this publication was supported by NIH grant P30CA077598 utilizing the Biostatistics and Bioinformatics Core shared resource of the Masonic Cancer Center, University of Minnesota and by the National Center for Advancing Translational Sciences of the National Institutes of Health Award Number UM1TR004405.

Conflict of interest

The authors declare that the research was conducted in the absence of any commercial or financial relationships that could be construed as a potential conflict of interest.

The author(s) declared that they were an editorial board member of Frontiers, at the time of submission. This had no impact on the peer review process and the final decision.

Publisher's note

All claims expressed in this article are solely those of the authors and do not necessarily represent those of their affiliated organizations, or those of the publisher, the editors and the reviewers. Any product that may be evaluated in this article, or claim that may be made by its manufacturer, is not guaranteed or endorsed by the publisher.

Author disclaimer

The content is solely the responsibility of the authors and does not necessarily represent the official views of the National Institutes of Health.

References

1. Kaliki S, Shields CL. Uveal melanoma: relatively rare but deadly cancer. *Eye (Lond)*. (2017) 31:241–57. doi: 10.1038/eye.2016.275

2. Valsecchi ME, Orloff M, Sato R, Chervoneva I, Shields CL, Shields JA, et al. Adjuvant sunitinib in high-risk patients with uveal melanoma: comparison with institutional controls. *Ophthalmology*. (2018) 125:210–7. doi: 10.1016/j.ophtha.2017.08.017

3. Rantala ES, Hernberg M, Kivelä TT. Overall survival after treatment for metastatic uveal melanoma: a systematic review and meta-analysis. *Melanoma Res*. (2019) 29:561–8. doi: 10.1097/CMR.0000000000000575

4. Collaborative Ocular Melanoma Study Group. Assessment of metastatic disease status at death in 435 patients with large choroidal melanoma in the Collaborative Ocular Melanoma Study (COMS): COMS report no. 15. *Arch Ophthalmol*. (2001) 119:670–6. doi: 10.1001/archopht.119.5.670

5. Rowcroft A, Loveday BPT, Thomson BNJ, Banting S, Knowles B. Systematic review of liver directed therapy for uveal melanoma hepatic metastases. *HPB (Oxford)*. (2020) 22:497–505. doi: 10.1016/j.hpb.2019.11.002

6. Pereira PR, Odashiro AN, Lim LA, Miyamoto C, Blanco PL, Odashiro M, et al. Current and emerging treatment options for uveal melanoma. *Clin Ophthalmol*. (2013) 7:1669–82. doi: 10.2147/OPTH.S28863

7. Algazi AP, Tsai KK, Shoushtari AN, Munhoz RR, Eroglu Z, Piulats JM, et al. Clinical outcomes in metastatic uveal melanoma treated with PD-1 and PD-L1 antibodies. *Cancer*. (2016) 122:3344–53. doi: 10.1002/cncr.30258

8. Najjar YG, Navrazhina K, Ding F, Bhatia R, Tsai K, Abbate K, et al. Ipilimumab plus nivolumab for patients with metastatic uveal melanoma: a multicenter, retrospective study [published correction appears in J Immunother Cancer. *J Immunother Cancer*. (2020) 8:e000331. doi: 10.1136/jitc-2019-000331. 2020.

9. Pelster MS, Gruschkus SK, Bassett R, Gombos DS, Shephard M, Posada L, et al. Nivolumab and ipilimumab in metastatic uveal melanoma: results from a single-arm phase II study. *J Clin Oncol*. (2021) 39:599–607. doi: 10.1200/JCO.20.00605

10. Nathan P, Hassel JC, Rutkowski P, Baurain JF, Butler MO, Schlaak M, et al. Overall survival benefit with tebentafusp in metastatic uveal melanoma. *N Engl J Med*. (2021) 385:1196–206. doi: 10.1056/NEJMoa2103485

11. Eisenhauer EA, Therasse P, Bogaerts J, Schwartz LH, Sargent D, Ford R, et al. New response evaluation criteria in solid tumours: revised RECIST guideline (version 1.1). *Eur J Cancer*. (2009) 45:228–47. doi: 10.1016/j.ejca.2008.10.026

12. Damato B, Eleuteri A, Taktak AF, Coupland SE. Estimating prognosis for survival after treatment of choroidal melanoma. *Prog Retin Eye Res*. (2011) 30:285–95. doi: 10.1016/j.preteyeres.2011.05.003

13. Krantz BA, Dave N, Komatsubara KM, Marr BP, Carvajal RD. Uveal melanoma: epidemiology, etiology, and treatment of primary disease. *Clin Ophthalmol*. (2017) 11:279–89. doi: 10.2147/OPTH.S89591

14. Yarchoan M, Hopkins A, Jaffee EM. Tumor mutational burden and response rate to PD-1 inhibition. *N Engl J Med*. (2017) 377:2500–1. doi: 10.1056/NEJMc1713444

15. Shen X, Zhao B. Efficacy of PD-1 or PD-L1 inhibitors and PD-L1 expression status in cancer: meta-analysis. *BMJ*. (2018) 362:k3529. doi: 10.1136/bmj.k3529

16. Wessely A, Steeb T, Erdmann M, Heinzerling L, Vera J, Schlaak M, et al. The role of immune checkpoint blockade in uveal melanoma. *Int J Mol Sci*. (2020) 21:879. doi: 10.3390/ijms21030879

17. Rodrigues M, Mobuchon L, Houy A, Fievet A, Gardrat S, Barnhill RL, et al. Outlier response to anti-PD1 in uveal melanoma reveals germline MBD4 mutations in hypermutated tumors. *Nat Commun*. (2018) 9:1866. doi: 10.1038/s41467-018-04322-5

18. Johansson PA, Stark A, Palmer JM, Bigby K, Brooks K, Rolfe O, et al. Prolonged stable disease in a uveal melanoma patient with germline MBD4 nonsense mutation treated with pembrolizumab and ipilimumab [published correction appears in Immunogenetics. 2019 Jul;71(7):511]. *Immunogenetics*. (2019) 71:433–6. doi: 10.1007/s00251-019-01108-x

19. Rizvi NA, Hellmann MD, Snyder A, et al. Cancer immunology. Mutational landscape determines sensitivity to PD-1 blockade in non-small cell lung cancer. . *Science*. (2015) 348:124–8. doi: 10.1126/science.aaa1348

20. Schumacher TN, Schreiber RD. Neoantigens in cancer immunotherapy. *Science*. (2015) 348:69–74. doi: 10.1126/science.aaa4971

21. Johansson P, Aoude LG, Wadt K, Glasson WJ, Warrier SK, Hewitt AW, et al. Deep sequencing of uveal melanoma identifies a recurrent mutation in PLCB4. *Oncotarget*. (2016) 7:4624–31. doi: 10.18632/oncotarget.6614

22. Freeman-Keller M, Kim Y, Cronin H, Richards A, Gibney G, Weber JS. Nivolumab in resected and unresectable metastatic melanoma: characteristics of immune-related adverse events and association with outcomes. *Clin Cancer Res*. (2016) 22:886–94. doi: 10.1158/1078-0432.CCR-15-1136

23. Xing P, Zhang F, Wang G, Xu Y, Li C, Wang S, et al. Incidence rates of immune-related adverse events and their correlation with response in advanced solid tumours treated with NIVO or NIVO+IPI: a systematic review and meta-analysis [published correction appears in J Immunother Cancer. *J Immunother Cancer*. (2019) 7:341. doi: 10.1186/s40425-019-0779-6. 2020.

24. Rousseau A, Parisi C, Barlesi F. Anti-TIGIT therapies for solid tumors: a systematic review. *ESMO Open*. (2023) 8:101184. doi: 10.1016/j.esmoop.2023.101184

25. Banta KL, Xu X, Chitre AS, Au-Yeung A, Takahashi C, O'Gorman WE, et al. Mechanistic convergence of the TIGIT and PD-1 inhibitory pathways necessitates co-blockade to optimize anti-tumor $CD8^+$ T cell responses. *Immunity*. (2022) 55:512–526.e9. doi: 10.1016/j.immuni.2022.02.005

26. Chauvin JM, Pagliano O, Fourcade J, Sun Z, Wang H, Sander C, et al. TIGIT and PD-1 impair tumor antigen-specific $CD8^+$ T cells in melanoma patients. *J Clin Invest*. (2015) 125:2046–58. doi: 10.1172/JCI80445

27. Stålhammar G, Seregard S, Grossniklaus HE. Expression of immune checkpoint receptors Indoleamine 2,3-dioxygenase and T cell Ig and ITIM domain in metastatic versus nonmetastatic choroidal melanoma. *Cancer Med*. (2019) 8:2784–92. doi: 10.1002/cam4.2167

28. Masaoutis C, Kokkali S, Theocharis S. Immunotherapy in uveal melanoma: novel strategies and opportunities for personalized treatment. *Expert Opin Investig Drugs*. (2021) 30:555–69. doi: 10.1080/13543784.2021.1898587

29. Kim TW, Bedard PL, LoRusso P, Gordon MS, Bendell J, Oh D, et al. Anti-TIGIT antibody tiragolumab alone or with atezolizumab in patients with advanced solid tumors: A phase 1a/1b nonrandomized controlled trial. *JAMA Oncol*. (2023) 9:1574–82. doi: 10.1001/jamaoncol.2023.3867

30. Triebel F, Jitsukawa S, Baixeras E, Roman-Roman S, Genevee C, Viegas-Pequignot E, et al. LAG-3, a novel lymphocyte activation gene closely related to CD4. *J Exp Med*. (1990) 171:1393–405. doi: 10.1084/jem.171.5.1393

31. Souri Z, Wierenga APA, Kroes WGM, van der Velden PA, Verdijk RM, Eikmans M, et al. *LAG3* and its ligands show increased expression in high-risk uveal melanoma. *Cancers (Basel)*. (2021) 13:4445. doi: 10.3390/cancers13174445

32. Woo SR, Turnis ME, Goldberg MV, Bankoti J, Selby M, Nirschl CJ, et al. Immune inhibitory molecules LAG-3 and PD-1 synergistically regulate T-cell function to promote tumoral immune escape. *Cancer Res*. (2012) 72:917–27. doi: 10.1158/0008-5472.CAN-11-1620

33. Tawbi HA, SChadendorf D, Lipson EJ, Ascierto PA, Matamala L, Gutierrez EC, et al. Relatlimab and nivolumab versus nivolumab in untreated advanced melanoma. *N Engl J Med*. (2022) 386:24–34. doi: 10.1056/NEJMoa2109970

frontiers | Frontiers in Oncology

TYPE Original Research
PUBLISHED 11 July 2024
DOI 10.3389/fonc.2024.1430742

Check for updates

OPEN ACCESS

EDITED BY
Dragos Eugen Georgescu,
Carol Davila University of Medicine and Pharmacy, Romania

REVIEWED BY
Mario Murguia-Perez,
Mexican Social Security Institute, Mexico
Teodor Florin Georgescu,
Carol Davila University of Medicine and Pharmacy, Romania
Nicolae Bacalbasa,
Carol Davila University of Medicine and Pharmacy, Romania

*CORRESPONDENCE
Qingli Li
liqingli73@163.com
Rutie Yin
yinrutie@scu.edu.cn

RECEIVED 10 May 2024
ACCEPTED 24 June 2024
PUBLISHED 11 July 2024

CITATION
Zeng J, Jiang W, Li K, Zhang M, Chen J, Duan Y, Li Q and Yin R (2024) Clinical and pathological characteristics of cervical clear cell carcinoma in patients not exposed to diethylstilbestrol: a comprehensive analysis of 49 cases.
Front. Oncol. 14:1430742.
doi: 10.3389/fonc.2024.1430742

COPYRIGHT
© 2024 Zeng, Jiang, Li, Zhang, Chen, Duan, Li and Yin. This is an open-access article distributed under the terms of the Creative Commons Attribution License (CC BY). The use, distribution or reproduction in other forums is permitted, provided the original author(s) and the copyright owner(s) are credited and that the original publication in this journal is cited, in accordance with accepted academic practice. No use, distribution or reproduction is permitted which does not comply with these terms.

Clinical and pathological characteristics of cervical clear cell carcinoma in patients not exposed to diethylstilbestrol: a comprehensive analysis of 49 cases

Jing Zeng[1,2], Wei Jiang[2,3], Kemin Li[1,2], Mengpei Zhang[1,2], Jinghong Chen[1], Yuanqiong Duan[1], Qingli Li[1,2]* and Rutie Yin[1,2]*

[1]Department of Obstetrics and Gynecology, West China Second University Hospital, Sichuan University, Chengdu, China, [2]Key Laboratory of Birth Defects and Related Diseases of Women and Children, West China Second University Hospital, Sichuan University, Chengdu, China, [3]Department of Pathology, West China Second University Hospital, Sichuan University, Chengdu, China

Purpose: This study aimed to investigate the clinical and pathological characteristics, treatment strategies, and prognosis of cervical clear cell carcinoma (CCCC) in patients not exposed to diethylstilbestrol *in utero*

Methods: The patients diagnosed with CCCC at West China Second University Hospital of Sichuan University between January 2011 and Jun 2023 were enrolled for this retrospective study. The clinical characteristics and information on treatment and follow-up were collected. The Kaplan–Meier method and Cox regression analysis were performed to identify the relative variables for predicting progression-free survival (PFS) and overall survival (OS).

Results: Of the 49 patients included, the Federation International of Gynecology and Obstetrics (FIGO) (2018) stage distribution was 37 (75.5%) stage I, 6 (12.2%) stage II, and 6 (12.2%) stage III. The median follow-up interval was 24.1 months. Six (12.2%) patients had a recurrence, and five (10.2%) patients died. The 5-year PFS rate was 86.8%, and the 5-year OS rate was 88.2%. No recurrence or death was detected in two patients who successfully completed fertility-preserving treatment and seven patients who underwent surgery to preserve ovaries. Two patients became pregnant, giving birth to two babies. The univariate analysis showed that FIGO stage, Pelvic lymph node (PLN) metastasis, lymph vascular space invasion, and depth of stromal invasion ($P < 0.05$) were significantly associated with PFS and OS. However, no significant prognostic factors were identified in the multivariate analysis.

Conclusion: Ovary-preserving treatment and fertility-preserving surgery are safe and feasible in early-stage CCCC. Surveillance other than adjuvant treatment may be a better choice for early-stage CCCC without any pathological risk factors. More targeted therapies and immunotherapy should be pursued in future studies.

KEYWORDS

adjuvant chemotherapy, adjuvant radiotherapy, cervical clear cell adenocarcinoma, fertility preservation, prognosis

Introduction

The etiology of cervical cancer is firmly linked to high-risk human papillomavirus (HPV) infection; however, only 60%–100% of cervical adenocarcinomas (ADCs) are associated with high-risk HPV (hrHPV) infection (1–3). In 2020, the World Health Organization (WHO) reclassified cervical ADCs into HPV-associated (HPVA) adenocarcinomas and HPV-independent (HPVI) ADCs according to their etiologic link to HPV infection, as well as morphology (4, 5). HPVI ADCs include gastric, clear cell, endometrioid, miscellaneous, and not otherwise specified types (4), which have type-specific pathogenesis, clinicopathological characteristics, and prognosis.

Cervical clear cell carcinoma (CCCC) is a rare subtype of ADC, accounting for only 4%–9% of cervical ADC (6). In 1971, Herbst reported a significant correlation between CCCC and *in utero* exposure to diethylstilbestrol (DES) (7). The clinical characteristics and prognosis of DES-associated CCCC received extensive attention, and the long-term survival data were reported (8). However, CCCC has still been reported in some patients with no exposure to DES in recent years. The clinicopathological characteristics and prognostic factors of CCCC without documentation of DES exposure are still lacking. Currently, gynecologic oncologists use the therapy and treatment principle referring to that of cervical squamous cell carcinoma and usual-type cervical ADC.

Therefore, our study summarized the clinicopathological characteristics and prognostic factors of 49 patients with CCCC in the gynecologic cancer center in Southwest China from January 2011 to June 2023. Meanwhile, the survival and obstetrical outcomes of ovarian and fertility preservation in young patients were analyzed and reported. The findings of this study might contribute to clinical decision-making and serve as a useful supplement to existing knowledge of this rare disease.

Materials and methods

Study population and pathological review

We identified 52 consecutive patients diagnosed with CCCC in West China Second University Hospital of Sichuan University between January 2011 and Jun 2023. Two senior pathologists reviewed the specimens from each patient, and three patients were excluded due to spread of clear cell ADC of the endometrium. All cases were diagnosed according to the WHO 2020 guidelines derived from the international endocervical ADC criteria and classification system (4, 5). The histological features of CCCC include three architectural patterns: solid, papillary, and tubulocystic structures, characterized by cuboidal, flattened, hobnail-shaped cells with abundant clear, glycogen-rich cytoplasm (Figure 1). The immunohistochemical markers are listed in Table 1.

The data on demographics, clinical features, surgeries, pathologies, and adjuvant treatments were retrieved from individual medical records of the patients using the electronic medical record system. The stage of each patient was revised using the FIGO staging system of cervical cancer (2018) for consistency in statistical analysis (9). The follow-up information was obtained from the outpatient medical record system or via telephone call. Progression-free survival (PFS) was defined as the time of diagnosis until the date of clinically confirmed recurrence or death from any cause. Overall survival (OS) was calculated from the date of diagnosis to the date of death from any cause or the last follow-up date.

Statistical analysis

The Kaplan–Meier method was used to estimate the hazard ratios related to PFS and OS. A multiple regression analysis was performed using the Cox proportional-hazards model to identify the relative importance of variables as factors for predicting PFS and OS. All statistical analyses were two sided, and statistical significance was considered when P was <0.05. The data were tabulated using Microsoft Excel software and analyzed using SPSS 20.0 software (IBM Inc., IL, USA).

Ethics approval

This study was approved by the Ethics Committee of the West China Second University Hospital of Sichuan University. All procedures were performed following the guidelines and regulations of this ethics board. Informed consent was not required because of the retrospective nature of the study.

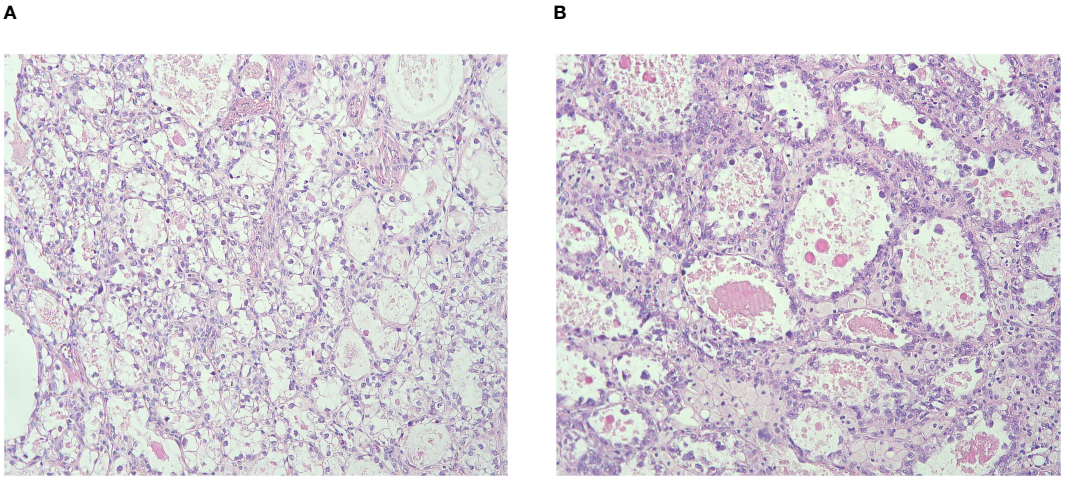

FIGURE 1
(A) Tumor cells presenting with abundant clear, glycogen-rich cytoplasm; **(B)** Tubulocystic structure with cuboidal, flattened, hobnail-shaped cells.

Results

Clinical features of CCCC

Forty-nine patients with CCCC were retrospectively analyzed. The median age at diagnosis was 48 years (range, 10–71 years). Further, 19 patients were aged less than or equal to 45 years (38.8%), and 30 patients were older than 45 years (61.2%). Seven patients were diagnosed before the age of 30 years. The age distribution is depicted in Figure 2. *In utero* DES exposure was documented in none of the patients. Thirty-six (73.5%) patients had the presenting symptoms of vaginal bleeding and four (8.2%) of vaginal discharge. Nine (18.3%) patients had no clinical symptoms, eight (16.3%) were diagnosed during a health check-up, and one (2.0%) was accidentally detected after a hysterectomy due to uterine myoma.

TABLE 1 Immunohistochemical Markers of cervical clear cell adenocarcinoma.

Immunohistochemical markers	Percentage of positivity(%)
Napsin A	26/35(74.3)
HNF1β	26/27(96.3)
PAX8	36/36(100.0)
WT1	3/19(15.8)
ER	12/38(31.6)
PR	3/27(8.1)
P53,wide type	28/32(87.5)
Ki-67(>40%)	28/42(66.7)
CK7	30/30(100.0)
CK20	1/20(5.0)
CEA	2/13(15.4)
P16	33/40(82.5)

A total of 17 patients underwent cytological screening, and 27 HPV screening. Also, 6 (35.3%) of the 17 patients tested negative using the thinprep cytology test (TCT). Of the 11 (64.7%) patients with positive results, 2 (11.8%) had atypical squamous cells of undermined significance, 1 (5.9%) had a low-grade squamous intraepithelial lesion, 2 (11.8%) had a high-grade squamous intraepithelial lesion, 3 (17.6%) had atypical glandular cells, and 3 (17.6%) had ADC. Further, 19 (70.4%) patients tested negative using the HPV test. Among the remaining eight (39.6%) HPV-positive patients, the number of HPV16-positive patients was four (14.8%). Three (11.1%) patients had other high-risk HPV types, including HPV33, HPV51, and HPV52, and one (3.7%) patient had a low-risk HPV61 infection.

All patients underwent surgery. Forty-six patients underwent radical hysterectomy and pelvic lymphadenectomy. Among these, 41 patients underwent bilateral salpingo-oophorectomy, and 29 underwent para-aortic lymphadenectomy. Extrafacial hysterectomy was performed on one patient with a primary diagnosis of uterine myoma whose TCT and HPV screening was negative. Two patients underwent trachelectomy and pelvic lymphadenectomy. Further, 32 patients underwent laparotomy, and the remaining 17 patients underwent laparoscopy. The FIGO (2018) stage of the 49 patients was as follows: 18 (36.7%) stage IB1, 11 (22.4%) stage IB2, 8 (16.3%) stage IB3, 4 (8.2%) stage IIA1, 2 (4.1%) stage IIA2, 5 (10.2%) stage IIIC1P, and 1 (2.0%) stage IIIC2P. Lymph node metastasis was present in 6 (12.2%), absent in 41 (83.7%), and not reported in 2 (4.1%) patients. Vaginal cuff involvement was detected in 2 (4.1%) and deep cervical stromal invasion (more than one half) in 18 (36.7%) patients. Lymphovascular space invasion was present in 5 (10.2%) and absent in 44 (89.8%). Ovarian metastasis was present in two (2.0%) patients. None of the patients presented with parametrium or surgical margin involvement.

Among the 23 patients with risk factors (PLN metastasis, vaginal cuff involvement, tumor size more than 4 cm, lymph vascular space invasion, depth of stromal invasion, or metastasis to ovaries or fallopian tubes), 5 received adjuvant pelvic radiotherapy, 2 received consolidation chemotherapy, 13 received radiotherapy and

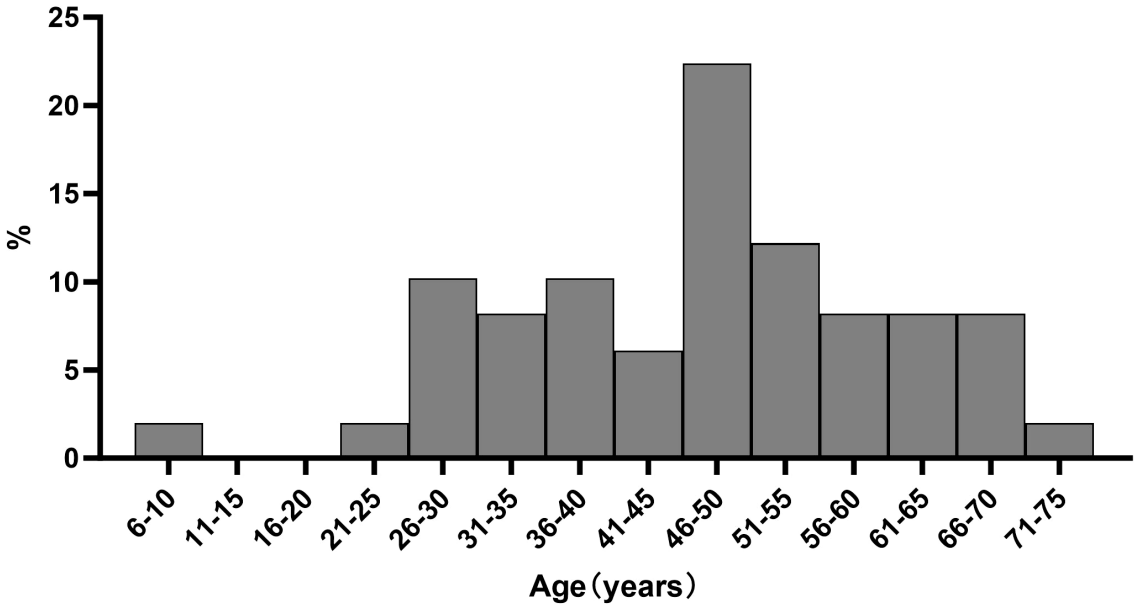

FIGURE 2
Age distribution of patients with cervical clear cell adenocarcinoma.

chemotherapy, and 3 did not receive adjuvant therapy. Of 26 patients with no risk factors, 2 received adjuvant radiotherapy, 7 received consolidation chemotherapy, 7 received radiotherapy and chemotherapy, and 7 did not receive adjuvant therapy. Three patients (6.1%) had no data regarding adjuvant treatment. The external-beam radiotherapy (EBRT) dose was approximately 45–50 Gy with daily fractionation of 1.8–2.0 Gy. The brachytherapy fractionation schemes 6 Gy × 2 fractions dosed at 5 mm were used as a boost to EBRT in patients with positive vaginal mucosal surgical margins. Consolidation chemotherapy consisted of platinum-based regimens, including paclitaxel with cisplatin or paclitaxel with carboplatin for two to six cycles (Table 2).

Survival and obstetrical outcomes with fertility or ovarian function preservation

The median follow-up interval was 24.1 months (range, 2.5–140 months). Six (12.2%) patients had recurrence. Sites of recurrence included lung (one patient), vaginal cuff (one patient), and multisite involvement (one patient); the information on site was not available for three patients. The 5-year PFS rate was 86.8%. The patient with lung metastases received chemotherapy, whereas the other five (10.2%) patients died of the disease. The 5-year OS rate was 88.2%. The survival curves are shown in Figure 3.

No recurrence or death was reported in two patients who successfully completed fertility-preserving treatment and seven patients who underwent ovary-preserving surgery. Two patients became pregnant, giving birth to two babies. Both patients conceived by *in vitro* fertilization–embryo transfer. One patient delivered at full term, and the other delivered at $26 + {}^{3}$ weeks due to the premature rupture of membranes.

Prognostic factors for CCCC

The univariate Cox regression analysis comparing clinicopathological parameters demonstrated that OS was influenced by FIGO stage ($P = 0.001$), PLN metastasis ($P = 0.002$), lymph vascular space invasion ($P = 0.026$), depth of stromal invasion ($P = 0.025$), and tumor size ($P = 0.018$). In contrast, PFS was influenced by FIGO stage ($P = 0.000$), PLN metastasis ($P = 0.000$), lymph vascular space invasion ($P = 0.000$), and depth of stromal invasion ($P = 0.008$). However, the multivariate analysis revealed no significant prognostic factors (Table 3).

Discussion

Since 1971, Herbst et al. conducted a series of studies on clear cell carcinomas of the vagina and cervix in patients exposed to DES *in utero* (10). One of his studies reported that the risk of developing CCCC in a woman with no exposure to DES from birth through the age of 34 years was approximately 1 case per 1000 women (11). The use of DES during pregnancy was officially banned by the US Food and Drug Administration. The study also showed that the youngest patient exposed to DES who developed clear cell ADC was 7 years old at the time of diagnosis, whereas the oldest patient was 34 years (12). Further, 91% of DES-exposed women were diagnosed when they were between the ages of 15 and 27 years; the median age at diagnosis was 19 years (7). CCCC in patients not exposed to DES had bimodal age distributions, with the first peak among women aged 17–37 years (mean age 26 years) and the second among women aged 44–88 years (mean age 71 years) (6). Although the youngest patient in our study was only 10 years old, seven patients were less than 30 years old. However, the age distribution was not

TABLE 2 Clinicopathological characteristics of cervical clear cell adenocarcinoma.

Clinicopathological characteristics	CCCCs,n(%)
Age, median(range),y	48(10-71)
Age(y)	
≤45	19(38.8)
>45	30(61.2)
Presenting symptoms	
Vaginal bleeding	36(73.5)
Vaginal discharge	4(8.2)
Physical examination finding	8(16.3)
Accidental Found after BSO	1(2.0)
FIGO stage*	
I	37(75.5)
II	6(12.2)
III	6(12.2)
PLN metastasis	
No	41(83.7)
Yes	6(12.2)
NA	2(4.1)
Vaginal cuff involvement	
No	47(95.9)
Yes	2(4.1)
Tumor size,cm	
≤2	25(51.0)
>2, ≤4	13(26.5)
>4	11(22.4)
Lymph vascular space invasion	
No	44(89.8)
Yes	5(10.2)
Depth of stromal invasion	
Less than one half	31(63.3)
More than one half	18(36.7)
Metastasis in ovaries/fallopian tubes	
No	40(81.6)
Yes	2(2)
NA	7(14.3)
Surgery to preserve fertility	
No	47(95.9)
Yes	2(4.1)
Surgery to preserve ovaries	
No	42(85.7)
Yes	7(14.3)
surgical approaches	
Laparotomy	32(65.3)
Laparoscopy	17(36.7)
Adjuvant treatment	
No	10(20.4)
Single radiotherapy	7(14.3)
Single chemotherapy	9(18.4)
Radiotherapy and Chemotherapy	20(40.8)
NA	3(6.1)
Recurrences	
Yes	6(12.2)
No	43(87.8)
Recurrence site	
Lung	1(2.0)
Vaginal cuff	1(2.0)
Multisite involvement	1(2.0)
NA	3(6.1)
Death	
Yes	5(10.2)
No	44(89.8)

CCCC, cervical clear cell adenocarcinoma; BSO, Bilateral salpingo-oophorectomy; PLN, Pelvic lymph node; NA, not available.
*We use FIGO staging system: cervical carcinoma (FIGO 2018).

bimodal. CCCC occurred in all age groups, which was consistent with the findings of Seki et al. (13).

Although the WHO classification system (2020) reclassified CCCC as HPVI ADC, the association between CCCC and HPV remains controversial. Some studies found that the HPV infection rate in CCCC ranged from 0% to 33.3% (2, 14–16). The HPV infection rate in our study was 39.6%, which was slightly higher than the rate reported previously. Previous studies also reported that up to one third of patients with CCCC were P16 positive (4, 17). Therefore, the pathogenesis of CCCC in patients with no exposure to DES needs further exploration. The hit-and-run theory could explain the absence of the viral genome in HPVI ADCs. It proposed that once a viral infection caused sufficient cellular alteration, tumor maintenance no longer required the expression of viral proteins or viral infection, and thus the virus might be lost during cancer progression (18). The other reasons for undetected HPV infection were the presence of viral genotypes not included in the molecular tests and the failure in the detection of the diagnostic method employed. The

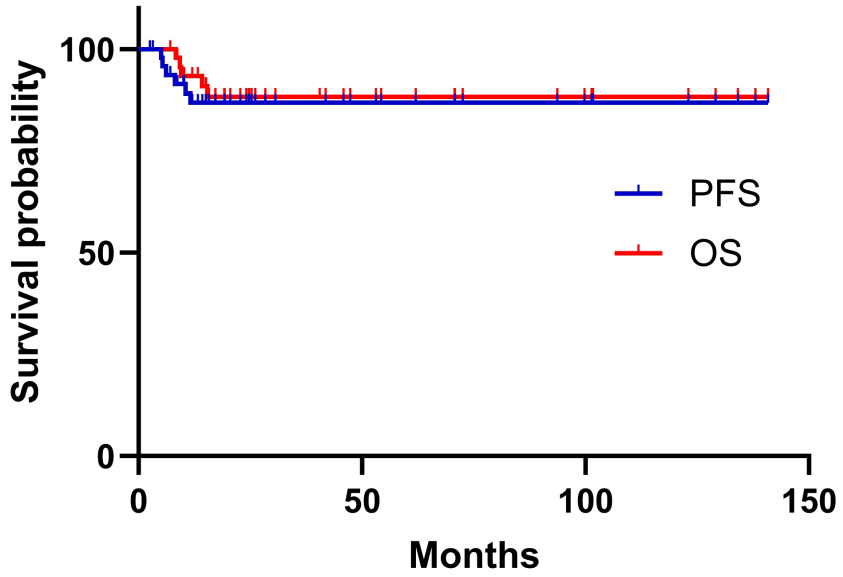

FIGURE 3
Kaplan-Meier survival curve for PFS and OS in 49 patients with CCCC.

occurrence of CCCC might also be related to *P53* gene mutation, Bcl-2 overexpression, instability of microsatellite repeats, and cervical endometriosis (19–21).

With the introduction and implementation of cervical cancer screening methods by the 1960s, the incidence of cervical cancer has decreased by 70% in the United States. At present, all countries in the world have established cervical cancer screening systems in line with their conditions. Also, HPV vaccination is gradually being rolled out in all countries, although the screening and early diagnosis of CCCC are still challenging. Pirog et al. provided comprehensive data on HPV genotype distribution in patients with different histological subtypes of tumors. They demonstrated that HPV testing and vaccination did not prevent CCCC (2). Previous studies reported an abnormal Pap smear of 18%–66.7% in patients with CCCC (22, 23). Our study revealed 64.7% abnormal TCT findings. The discrepancy in cervical cytology results was not only due to different pathologists but also related to the different cytologic techniques used. TCT was more effective in detecting cervical lesions than traditional smears. Tournaire et al. published CCCC screening recommendations for young women exposed to DES in France (24). The methods suggested the association of cytology and hrHPV testing with cervical and vaginal sampling. The screening timing was recommended as annual or not exceeding a 3-year interval, continuing after 65 years and after a hysterectomy. Effective screening methods for CCCC in patients without exposure to DES are still lacking. Therefore, timely cervical biopsy and endocervical curettage are essential in patients with positive cytology and hrHPV.

Thomas et al. conducted an outcome analysis of patients with CCCC after exposure to DES at three major gynecologic cancer centers between 1982 and 2004. The result showed that stage I or IIA CCCC was amenable to surgical resection and displayed an excellent 3-year OS of 91% (22). Hanselaar et al. reported similar survival rates for patients with early-stage CCCC (6). Therefore, some gynecologic oncologists continue to explore the use of fertility-preserving surgery for early-stage CCCC. However, cold-knife conization or radical trachelectomy has been recommended by the National Comprehensive Cancer Network guidelines for early-stage cervical cancer considering only the histological characteristics of squamous cell carcinoma, ADC, or adenosquamous carcinoma. Liu et al. reported six patients with stage IA-IB CCCC who successfully completed fertility-preserving treatment (16). No recurrence or death was reported in all patients, and two patients became pregnant with a live birth rate of 100%. In our study, two patients undergoing fertility-preserving surgery had stage IB CCCC with no other high-risk factors and remained disease free after 71 and 62 months, respectively. The pregnancy rate was 100%, and the live birth rate was 100%. It is safe and feasible for patients with early-stage CCCC to receive fertility-preserving treatment. Pelvic magnetic resonance imaging should be used to carefully evaluate the tumor size and the degree and extent of cervical canal invasion and also to exclude distant metastasis. Therefore, for patients with early-stage CCCC, a multidisciplinary team with cooperation is needed for comprehensive evaluation. Also, patients need to be informed that fertility-preserving surgery is not the standard treatment.

The use of ovary-preserving surgery for patients with non-squamous cell cervical carcinoma remains controversial. Many studies have reported an ovarian metastasis rate of 4.2%–16.3% in patients with non-squamous cell carcinoma (23, 25–27), which is 2.4%–4.3% in patients with CCCC (28, 29). In our study, the ovarian metastasis rate was 4.1%, which was similar to that in the aforementioned studies. No recurrence or death was reported in seven patients who underwent ovary-preserving surgery. In this study, the ovary-preserving treatment appeared safe and feasible in patients with early-stage CCCC. However, considering the limited sample size and the retrospective nature of our study, ovary-preserving surgery should still be cautiously selected for patients with CCCC.

10.3389/fonc.2024.1430742

TABLE 3 Univariate and multivariate survival analysis of associated clinicopathological characteristics with PFS in 49 cases.

Variables	Categories	PFS			OS		
		Univariate P Value	Multivariate P Value	Multivariate HR(95%CI)	Univariate P Value	Multivariate P Value	Multivariate HR(95%CI)
Age(y)	≤45	0.288			0.469		
	>45						
FIGO stage*	Stage I and II	0.000	0.106	0.81-8.78	0.001	0.133	0.75-8.40
	Stage III						
PLN metastasis	No	0.000			0.002		
	Yes						
Vaginal cuff involvement	No	0.131			0.633		
	Yes						
Tumor size, cm	≤2	0.077			0.018		
	>2						
Lymph vascular space invasion	No	0.000	0.746	0.16-13.50	0.026	0.868	0.07-9.09
	Yes						
Depth of stromal invasion	<1/2	0.008	0.252	0.36-46.70	0.025	0.249	0.37-48.08
	>1/2						
Metastasis in ovaries/ fallopian tubes	No	0.559			0.583		
	Yes						
Surgery to preserve ovaries	No	0.340			0.392		
	Yes						
surgical approaches	Laparotomy	0.342			0.500		
	Laparoscopy						
Adjuvant treatment	No	0.941			0.835		
	Yes						

*FIGO stage: stage by The International Federation of Gynecology and Obstetrics.

The 5-year OS rate was 88.2% in our study, which was higher than previously reported survival rates of 40%–78% (4, 16, 22, 28–30). This was mainly because a high percentage of the study population comprised patients with early-stage CCCC who underwent surgery, and the other six patients with stage III CCCC had lymph node metastasis after surgery re-staged according to the 2018 FIGO staging. Previous studies reported that advanced stage and lymphatic involvement were associated with worse prognosis (16, 22, 28, 29). Thomas et al. found that patients with stage I or IIA CCCC had a better 3-year OS compared with patients with stage III or IV CCCC (91% vs 22%, $P < 0.001$), and the presence of positive lymph nodes had a negative impact on 5-year PFS (31% vs 92%, $P = 0.001$) and 5-year OS (80% vs 100%, $P = 0.02$) in patients with stages I and IIA CCCC (22). In our study, the univariate analysis showed that advanced stage (III), PLN metastasis, LVSI, and depth of stromal invasion were significantly associated with PFS and OS; however, the multivariate analysis revealed no significant prognostic factors. We also found that 26 patients in our population had no risk factors, 16 of which received adjuvant radiotherapy and/or chemotherapy and only 7 did not receive adjuvant therapy. However, adjuvant treatment did not affect survival outcomes in early-stage CCCC without any pathological risk factors. Surveillance other than adjuvant treatment might be a better choice for these patients.

In our study, six patients relapsed, of which 4 had stage III CCCC. Five patients received radiotherapy and chemotherapy, whereas one patient had no data regarding adjuvant treatment. Therefore, even adjuvant therapy did not seem to improve the prognosis of patients with high-risk prognostic factors. Five patients died, and only one patient who was alive underwent whole-exome sequencing, revealing suspected pathogenic mutations of AT-rich

interaction domain 1A gene (*ARID1A*) and ataxia telangiectasia mutated (*ATM*) genes. She was treated with the mammalian target of rapamycin complex 1/2 (mTORC1/2) dual inhibitor ATG-008 combined with toripalimab after participating in one clinical trial, achieving a PFS of 9 months. Zorn et al. compared endometrial, ovarian, and renal clear cell carcinomas and reported that clear cell carcinomas had a remarkable similarity in gene expression profiles (31). This finding indicated the possibility of treating clear cell carcinomas in the same way, that is, some molecular events were the same irrespective of the organ of origin. Ueno et al. demonstrated increased epidermal growth factor receptor (EGFR) or human epidermal growth factor receptor-2 (HER2) expression or activation of protein kinase B (Akt) or mTOR in 13 patients with CCCC (15), indicating that the inhibitors of tyrosine kinases or the Akt–mTOR pathway might be suitable treatment regimens for CCCC. Therefore, we look forward to the clinical research data of targeted therapy and immune checkpoint inhibitors in CCCC.

Limitations

Our study had certain limitations. First, the retrospective nature of the study led to inevitable missing data and bias. Second, the sample size of the study was small due to the low incidence of CCCC, and hence some subgroup analyses could not be performed. We hope to provide more evidence and data to improve the diagnosis and treatment of this rare disease by conducting international multicenter prospective studies in the future.

Conclusions

CCCC is an HPVI-related cancer, and hence traditional screening methods are ineffective. Therefore, timely cervical biopsy and endocervical curettage are extremely important. Ovary- and fertility-preserving surgeries are safe and feasible due to the good prognosis of early-stage CCCC; however, we still recommend careful selection of treatment modalities because of the limited data on this issue. Chemotherapy and/or radiotherapy does not affect the survival of patients with early-stage cervical cancer. Therefore, more studies on targeted therapy and immunotherapy for CCCC should be conducted in the future.

Data availability statement

The raw data supporting the conclusions of this article will be made available by the authors, without undue reservation.

Ethics statement

The studies involving humans were approved by Medical Ethics Committee of West China Second University Hospital, Sichuan University. The studies were conducted in accordance with the local legislation and institutional requirements. The ethics committee/institutional review board waived the requirement of written informed consent for participation from the participants or the participants' legal guardians/next of kin because of the retrospective nature of the study. And the human samples used in this study were acquired from electronic medical record system. Written informed consent for participation was not required from the participants or the participants' legal guardians/next of kin in accordance with the national legislation and institutional requirements.

Author contributions

JZ: Conceptualization, Data curation, Formal analysis, Funding acquisition, Investigation, Methodology, Project administration, Resources, Software, Writing – original draft, Writing – review & editing. WJ: Data curation, Resources, Visualization, Writing – original draft. KL: Data curation, Methodology, Writing – original draft. MZ: Data curation, Writing – original draft. JC: Data curation, Writing – original draft. YD: Data curation, Writing – original draft. QL: Conceptualization, Supervision, Validation, Writing – review & editing. RY: Conceptualization, Funding acquisition, Supervision, Validation, Writing – review & editing.

Funding

The author(s) declare financial support was received for the research, authorship, and/or publication of this article. This study was supported by the Foundation of horizontal subject (grant no. 22H1536), the Key Project of Sichuan Provincial Department of Science and Technology (grant no. 2019YFS0532), and the Scientific Research Project of Cadre Health Care in Sichuan Province (grant no. 2023-1702).

Conflict of interest

The authors declare that the research was conducted in the absence of any commercial or financial relationships that could be construed as a potential conflict of interest.

Publisher's note

All claims expressed in this article are solely those of the authors and do not necessarily represent those of their affiliated organizations, or those of the publisher, the editors and the reviewers. Any product that may be evaluated in this article, or claim that may be made by its manufacturer, is not guaranteed or endorsed by the publisher.

References

1. Arbyn M, Weiderpass E, Bruni L, de Sanjosé S, Saraiya M, Ferlay J, et al. Estimates of incidence and mortality of cervical cancer in 2018: a worldwide analysis. *Lancet Glob Health*. (2022) 10:e41. doi: 10.1016/S2214–109X(21)00554–4

2. Lee JE, Chung Y, Rhee S, Kim TH. Untold story of human cervical cancers: HPV-negative cervical cancer. *BMB Rep*. (2022) 55:429–38. doi: 10.5483/BMBRep.2022.55.9.042

3. Molijn A, Jenkins D, Chen W, Zhang X, Pirog E, Enqi W, et al. The complex relationship between human papillomavirus and cervical adenocarcinoma. *Int J Cancer*. (2016) 138:409–16. doi: 10.1002/ijc.29722

4. Stolnicu S, Barsan I, Hoang L, Patel P, Terinte C, Pesci A, et al. International endocervical adenocarcinoma criteria and classification (IECC): A new pathogenetic classification for invasive adenocarcinomas of the endocervix. *Am J Surg Pathol*. (2018) 42:214–26. doi: 10.1097/PAS.0000000000000986

5. WHO Classification of Tumors Editorial Board. *WHO Classification of Tumors of Female Reproductive Organs. 5th ed*. Lyon: IARC (2020). [Chapter 8], Tumours of the uterine cervix: adenocarcinomas.

6. Hanselaar A, van Loosbroek M, Schuurbiers O, Helmerhorst T, Bulten J, Bernhelm J. Clear cell adenocarcinoma of the vagina and cervix. An update of the central Netherlands registry showing twin age incidence peaks. *Cancer*. (1997) 79:2229–36. doi: 10.1002/(sici)1097–0142(19970601)79:11<2229::aid-cncr22>3.0.co;2-x

7. Herbst AL. Behavior of estrogen-associated female genital tract cancer and its relation to neoplasia following intrauterine exposure to diethylstilbestrol (DES). *Gynecol Oncol*. (2000) 76:147–56. doi: 10.1006/gyno.1999.5471

8. Huo D, Anderson D, Herbst AL. Follow-up of patients with clear-cell adenocarcinoma of the vagina and cervix. *N Engl J Med*. (2018) 378:1746–8. doi: 10.1056/NEJMc1800097

9. Bhatla N, Aoki D, Sharma DN, Sankaranarayanan R. Cancer of the cervix uteri. *Int J Gynaecol Obstet*. (2018) 143 Suppl 2:22–36. doi: 10.1002/ijgo.12611

10. Scully RE, Robboy SJ, Herbst AL. Vaginal and cervical abnormalities, including clear-cell adenocarcinoma, related to prenatal exposure to stilbestrol. *Ann Clin Lab Sci*. (1974) 4:222–33.

11. Melnick S, Cole P, Anderson D, Herbst A. Rates and risks of diethylstilbestrol-related clear-cell adenocarcinoma of the vagina and cervix. *update. N Engl J Med*. (1987) 316:514–6. doi: 10.1056/NEJM198702263160905

12. Herbst AL, Anderson D. Clear cell adenocarcinoma of the vagina and cervix secondary to intrauterine exposure to diethylstilbestrol. *Semin Surg Oncol*. (1990) 6:343–6. doi: 10.1002/ssu.2980060609

13. Seki H, Takada T, Sodemoto T, Hoshino H, Saitoh K, Uekusa T. A young woman with clear cell adenocarcinoma of the uterine cervix. *Int J Clin Oncol*. (2003) 8:399–404. doi: 10.1007/s10147–003-0358–0

14. Lei J, Andrae B, Ploner A, Lagheden C, Eklund C, Nordqvist Kleppe S, et al. Cervical screening and risk of adenosquamous and rare histological types of invasive cervical carcinoma: population based nested case-control study. *BMJ*. (2019) 365:l1207. doi: 10.1136/bmj.l1207

15. Ueno S, Sudo T, Oka N, Wakahashi S, Yamaguchi S, Fujiwara K, et al. Absence of human papillomavirus infection and activation of PI3K-AKT pathway in cervical clear cell carcinoma. *Int J Gynecol Cancer*. (2013) 23:1084–91. doi: 10.1097/IGC.0b013e3182981bdc

16. Liu Y, Shi X, Yang J, Zhou H, Peng P, Cao D. Clinical features and prognostic factors of cervical clear cell adenocarcinoma: A retrospective analysis of 74 cases from a tertiary hospital. *Technol Cancer Res Treat*. (2023) 22:15330338221149297. doi: 10.1177/15330338221149297

17. Smith HO, Tiffany MF, Qualls CR, Key CR. The rising incidence of adenocarcinoma relative to squamous cell carcinoma of the uterine cervix in the United States–a 24-year population-based study. *Gynecol Oncol*. (2000) 78:97–105. doi: 10.1006/gyno.2000.5826

18. Fernandes A, Viveros-Carreño D, Hoegl J, Ávila M, Pareja R. Human papillomavirus-independent cervical cancer. *Int J Gynecol Cancer*. (2022) 32:1–7. doi: 10.1136/ijgc-2021–003014

19. Waggoner SE, Anderson SM, Luce MC, Takahashi H, Boyd J. p53 protein expression and gene analysis in clear cell adenocarcinoma of the vagina and cervix. *Gynecol Oncol*. (1996) 60:339–44. doi: 10.1006/gyno.1996.0052

20. Bocaneti F, Altamura G, Corteggio A, Velescu E, Borzacchiello G. Expression of bcl-2 and p53 in bovine cutaneous fibropapillomas. *Infect Agent Cancer*. (2015) 10:2. doi: 10.1186/1750–9378-10–2

21. Hashiguchi M, Kai K, Nishiyama S, Nakao Y, Yokoyama M, Aishima S. Clear cell carcinoma of the uterine cervix presented as a submucosal tumor arising in a background of cervical endometriosis. *Int J Gynecol Pathol*. (2018) 37:88–92. doi: 10.1097/PGP.0000000000000386

22. Thomas MB, Wright JD, Leiser AL, Chi DS, Mutch DG, Podratz KC, et al. Clear cell carcinoma of the cervix: a multi-institutional review in the post-DES era. *Gynecol Oncol*. (2008) 109:335–9. doi: 10.1016/j.ygyno.2008.02.007

23. Shimada M, Kigawa J, Nishimura R, Yamaguchi S, Kuzuya K, Nakanishi T, et al. Ovarian metastasis in carcinoma of the uterine cervix. *Gynecol Oncol*. (2006) 101:234–7. doi: 10.1016/j.ygyno.2005.10.004

24. Tournaire M, Devouche E, Lafaye N, Levadou A. Screening for cancers of the cervix and vagina for women exposed to diethylstilbestrol (DES) in utero. *J Gynecol Obstet Hum Reprod*. (2021) 50:102042. doi: 10.1016/j.jogoh.2020.102042

25. Bao Y, Zhang H, Huang W, Luo X, Yao L, Feng G, et al. Novel predictors for identifying cervical minimal deviation adenocarcinoma patients with poor prognosis: a long-term observational study in a tertiary centre. *Arch Gynecol Obstet*. (2024) 309:1483–90. doi: 10.1007/s00404–023-07207–1

26. Yamamoto R, Okamoto K, Yukiharu T, Kaneuchi M, Negishi H, Sakuragi N, et al. A study of risk factors for ovarian metastases in stage Ib-IIIb cervical carcinoma and analysis of ovarian function after a transposition. *Gynecol Oncol*. (2001) 82:312–6. doi: 10.1006/gyno.2001.6277

27. Zhou L, Sun CT, Lin L, Xie Y, Huang Y, Li Q, et al. Independent risk factors for ovarian metastases in stage IA-IIB cervical carcinoma. *Acta Obstet Gynecol Scand*. (2019) 98:18–23. doi: 10.1111/aogs.13442

28. Yang L, Zheng A, Zhang X, Fang X, Sun W, Chen Y. Clear cell carcinoma of the uterine cervix: A clinical and pathological analysis of 47 patients without intrauterine diethylstilbestrol exposure. *Int J Gynecol Cancer*. (2017) 27:1009–14. doi: 10.1097/IGC.0000000000000992

29. Wang T, Lu Z, Zhang X, Hua K. Factors associated with patient survival in clear cell adenocarcinoma of the cervix: A single-center experience in China. *Int J Gen Med*. (2022) 15:4625–34. doi: 10.2147/IJGM.S358094

30. Reich O, Tamussino K, Lahousen M, Pickel H, Haas J, Winter R. Clear cell carcinoma of the uterine cervix: pathology and prognosis in surgically treated stage IB-IIB disease in women not exposed in *utero* to diethylstilbestrol. *Gynecol Oncol*. (2000) 76:331–5. doi: 10.1006/gyno.1999.5700

31. Zorn KK, Bonome T, Gangi L, Chandramouli GV, Awtrey CS, Gardner GJ, et al. Gene expression profiles of serous, endometrioid, and clear cell subtypes of ovarian and endometrial cancer. *Clin Cancer Res*. (2005) 11:6422–30. doi: 10.1158/1078–0432.CCR-05–0508

frontiers | Frontiers in Oncology

TYPE Case Report
PUBLISHED 18 July 2024
DOI 10.3389/fonc.2024.1427341

Check for updates

OPEN ACCESS

EDITED BY
Dragos Eugen Georgescu,
Carol Davila University of Medicine and Pharmacy, Romania

REVIEWED BY
Mahboubeh Nabavinia,
The Research Institute at Nationwide Children's Hospital, United States
Jorge Aparicio,
Hospital Universitario y Politécnico La Fe, Spain

*CORRESPONDENCE
Jian M. Tang
ldyy_tangjm@lzu.edu.cn

RECEIVED 03 May 2024
ACCEPTED 02 July 2024
PUBLISHED 18 July 2024

CITATION
Bai X, Liu XH, Liang HW, Li YS, Shan BF and Tang JM (2024) Testicular choriocarcinoma with pelvic and pulmonary metastases: a case report. *Front. Oncol.* 14:1427341. doi: 10.3389/fonc.2024.1427341

COPYRIGHT
© 2024 Bai, Liu, Liang, Li, Shan and Tang. This is an open-access article distributed under the terms of the Creative Commons Attribution License (CC BY). The use, distribution or reproduction in other forums is permitted, provided the original author(s) and the copyright owner(s) are credited and that the original publication in this journal is cited, in accordance with accepted academic practice. No use, distribution or reproduction is permitted which does not comply with these terms.

Testicular choriocarcinoma with pelvic and pulmonary metastases: a case report

Xin Bai[1], Xiao H. Liu[1], Hai W. Liang[1], Yi S. Li[1], Biao F. Shan[1] and Jian M. Tang[2*]

[1]The First Clinical Medical College, Lanzhou University, Lanzhou, Gansu, China, [2]Department of Radiation Oncology, The First Hospital of Lanzhou University, Lanzhou University, Lanzhou, Gansu, China

Testicular tumors represent a common form of solid tumor in young men, with choriocarcinoma of the testis being a rare, non-granulomatous germ cell tumor. It accounts for less than 0.3% of all testicular germ cell tumors. Pelvic and pulmonary metastases originating from testicular choriocarcinoma are exceptionally uncommon in men. This study describes a case of a 27-year-old male diagnosed with testicular choriocarcinoma, presenting initially with nausea, vomiting, and abdominal pain. Furthermore, this review encompasses cases of testiclar choriocarcinoma in individuals aged 30 years and below, both in China and internationally, over the past 20 years.

KEYWORDS

testicular choriocarcinoma, pelvic metastases, lung metastases, genital examination, retroperitoneal mass

Introduction

Choriocarcinoma, a malignant trophoblastic tumor, secretes human chorionic gonadotropin (β-HCG). Although the majority of choriocarcinomas develop in women following either normal or abnormal pregnancies, their occurrence in non-pregnant individuals is exceptionally rare (1). Testicular choriocarcinoma, in particular, is extremely uncommon, comprising less than 0.3% of all testicular germ cell tumors. Typically occurring as part of mixed germ cell tumors, pure choriocarcinoma is especially rare. Previous meta-analyses have determined the most common sites of metastasis to be the lungs, vagina, brain, liver, and kidneys, listed in descending order. Other less frequently involved sites include the pancreas, small and large intestines, bone marrow, and abdominal wall (2). This article examines a complex case of choriocarcinoma metastasizing to the lungs, retroperitoneum, and pelvis, presenting as abdominal pain and nausea.

Clinical history and pathology

On 9 January 2023, a 25-year-old man reported pain in the abdomen and left lower back, accompanied by nausea and vomiting. No fever, chills, diarrhea, or blood in the stool were reported. Initially, the patient disregarded these symptoms. On 16 January, he sought treatment at another hospital where an ultrasound examination revealed solid lesions in the retroperitoneal area, likely neoplastic, causing compression of the left upper ureter, dilatation of the left ureter with pyelonephritis, salt crystals in the renal urethra, and no abnormalities in the right kidney. Suspecting ectopic pheochromocytoma, retrograde angiography and stenting of the left ureter were performed under local anesthesia on 16 January 2023, subsequently, the patient was discharged.

Subsequently, on 31 January, the patient experienced intermittent worsening of pain with nausea and vomiting, which intensified with eating and drinking. A subsequent CT scan of the entire abdomen at that medical facility revealed an irregular mass in the left retroperitoneum invading the ureter, abdominal segments, and abdominal aorta. On 3 February 2023, resection of the left retroperitoneal mass was conducted under general anesthesia. Postoperative evaluation identified a left retroperitoneal germ cell malignancy, and immunohistochemical analysis confirmed choriocarcinomac (Figure 1). Further ultrasound evaluation of the reproductive system detected a solid mass within the left testis, most likely a homologous germ cell tumor. Recommendations included further sequencing and follow-up treatment. Upon discharge, the physician advised a follow-up in three weeks, which would include removal of the intratesticular mass and 3-4 cycles of postoperative chemotherapy with a BEP (bleomycin, etoposide, and cisplatin) regimen.

On 22 February 2023, the patient reported increased abdominal pain. A subsequent CT scan displayed a soft tissue mass at the previous surgery site, indicating tumor recurrence. This recurrence affected multiple sites, including the nearby abdominal aorta, inferior vena cava, upper left ureter, left psoas muscle, and neighboring bowel. Consequently, the left kidney and upper ureter were observed to be dilated and exhibited hydrops. Additionally, the left ureter showed signs of stenting, with a curvature at the end. Further, some mildly enlarged mesenteric root lymph nodes were noted, along with suspicious small nodules in the mesenteric vessel wall in the pelvic region, necessitating regular monitoring. The patient developed hydronephrosis, leading the urology department to recommend replacing the ureteral stent. As the existing stent was deformed and could not accommodate the guidewire, a left nephrostomy and drainage were performed in 2023. Despite receiving symptomatic supportive treatment, the patient's condition had not significantly improved by 29 February 2024 when he was admitted to our hospital.

The patient was admitted to the hospital with the following metrics: height of 176 cm, weight of 60 kg, body surface area of 1.76 cm^2, NRS score of 0, and a KPS score of 70. The general condition of the patient was characterized by normal growth, malnutrition, and facial pain, however, gait, posture, and mental state were normal, and cooperation during the examination was observed.

Past medical history indicated that the patient had been healthy, with no prior surgical interventions or trauma, no history of hepatitis or tuberculosis, no infectious diseases, no known exposures, no vaccinations, no drug allergies, and no blood transfusions. In terms of personal history, the patient was single, had not resided in infectious areas, and had abstained from smoking, alcohol, and substance abuse, with no exposure to industrial toxins, dust, or radiation, and no travel history. No genetic diseases were reported in the family history.

Laboratory results revealed an erythrocyte count of 2.88×10^{12}/L (outside the reference range of 130-175), and a hemoglobin level of 86g/L (below the reference range of 130-175g/L). The β-HCG level was over 10,000mIU/ml (exceeding the reference range of 0-2.60 mIU/ml), and the LDH stood at 518U/L (above the reference range of 120-250U/L), indicating elevated levels. Other noted abnormalities included increased levels of ferritin, total and direct bilirubin, alkaline phosphatase, aspartate aminotransferase, alanine aminotransferase, and glutamyl aminotransferase. Both fecal and urinary occult blood tests yielded positive results. On March 1, 2023, an abdominal CT scan was performed on the patient, revealing irregular mixed-density masses in the retroperitoneum and left abdominal cavity, measuring 66 mm × 82 mm and 46 mm × 44 mm, respectively. These masses surrounded the abdominal aorta, extends below the bifurcation, and affected the left psoas major muscle and ureter definition. Heterogeneous enhancement in the mass with migrating vascular shadows was observed, along with multiple lymph nodes in the left abdominal cavity and a nodular omentum. Additionally, multiple

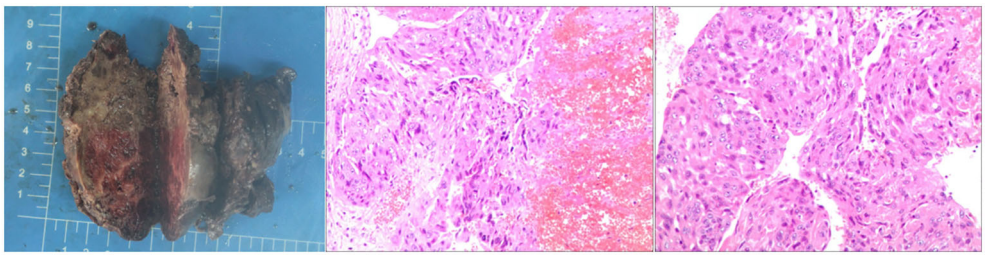

FIGURE 1
The post-op specimen measures 9x8x4.5 cm and shows grey-red to grey-brown inelastic tissue. Cross-section displays grey-red and grey-white areas with necrotic and hardened regions. Diagnosed as a malignant germ cell tumor (left retroperitoneal), consistent with choriocarcinoma of epithelial origin per immunohistochemical staining.

intensifying nodules were noted in the right hepatic lobe during the arterial phase, with isodensity in the portal and delayed phases. No fluid was present in the abdominal cavity, but enlargement of retroperitoneal lymph nodes and multiple nodules in both lungs were suspected to be metastatic (Figure 2).

The patient's initial condition was poor, characterized by abdominal and back pain. Following the administration of hepatoprotective and antiemetic medications, symptoms of pain were alleviated. However, at 20:10 on 1 March, the patient suffered a sudden altered state of consciousness, displaying dilated pupils at 5 mm and diminished light responsiveness. Within two minutes, both consciousness and pupil size reduced to 3 mm, with a fading light reflex absent any obvious pathology signs. Through anti-infective and supportive therapies, continuous cardiac monitoring, and consultations with multiple specialists, the patient's condition gradually stabilized. To investigate the cause of the abdominal pain, a CT scan of the whole abdomen on 2 March revealed (Figure 3): 1) a new hyperdense shadow in the abdominal cavity indicative of potential hemorrhage, necessitating clinical correlation; 2) a notably increased number of lung nodules compared to previous scans, and 3) a fresh abdominopelvic effusion. A diagnostic laparotomy was performed, yielding non-clotting blood that confirmed a ruptured retroperitoneal mass with associated bleeding. Treatment included a red blood cell transfusion and continued supportive care. The medical team informed the family of the severe risks including shock and respiratory failure due to tumor rupture and hemorrhage. They opted against transfer to the ICU or extubation. After consultations with interventional and general surgeons, immediate intervention was deemed risky and ineffective. The risks of surgical hemostasis included potential respiratory and circulatory failure during the procedure. The family remained undecided upon learning of these risks and the ongoing need for treatment, leading to a decision to continue with symptomatic supportive care. on 3 March, the family declined surgery, fluids, endotracheal intubation for potential respiratory or circulatory failure, mechanical ventilation, and all resuscitative efforts, requesting solely pain management and signed a "refusal of treatment" notice. Thus, interventions were confined to managing pain. At 20; 44 on 6 March, the patient ceased to breathe spontaneously, aortic pulsation was absent, pupils were dilated and unresponsive, and the ECG registered as flat; he was pronounced clinically dead.

Discussion

Imaging features of testicular choriocarcinoma are insufficiently distinct to differentiate it from other germ cell tumors. Diagnosis is challenging and typically relies on pathological confirmation during surgical resection. Treatment response monitoring is conducted through serum levels of beta-human chorionic gonadotropin (beta-HCG). According to the International Germ Cell Carcinoma Collaborative Group, beta-HCG levels exceeding 50,000 IU/L are indicative of a poor prognosis. While testicular cancer generally has high cure rates, with five-year survival rates reaching 95 percent, choriocarcinoma responds poorly to chemotherapy. Patients often exhibit severe symptoms and demonstrate a poor response to standard chemotherapy regimens, including three to four cycles of BEP (bleomycin, etoposide, and cisplatin). In cases of recurrence, salvage chemotherapy with vincristine and ifosfamide may decrease tumor burden, but some patients may require palliative care (3). As fewer patients are included in Table 1 compared to the statistical analysis, it is clear that survival rates are significantly lower for patients treated solely with surgery, while combining surgery with other therapies markedly improves survival duration (13, 14).

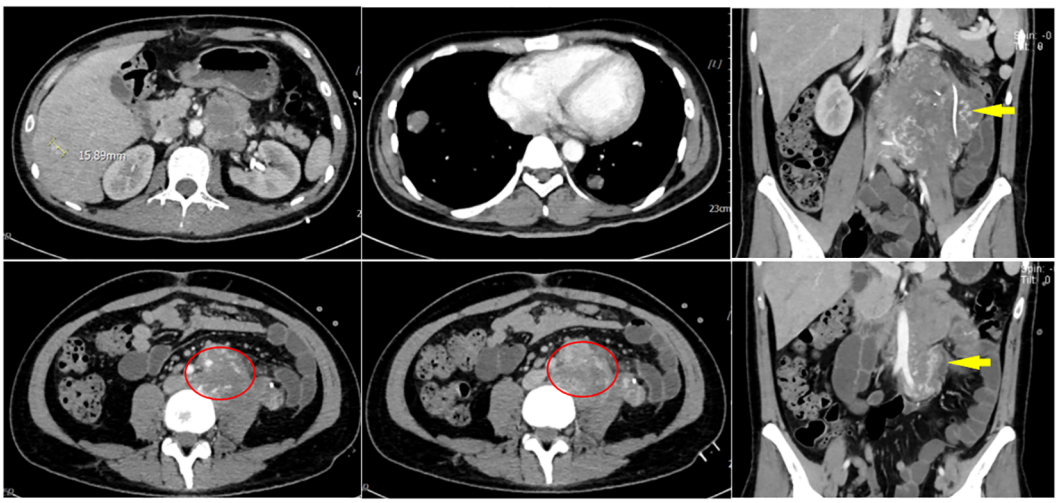

FIGURE 2
On March 1, 2023, an abdominal CT scan revealed irregular mixed-density masses in the retroperitoneum and left abdominal cavity, measuring 66 mm × 82 mm and 46 mm × 44 mm, respectively. These masses surrounded the abdominal aorta, extended below the bifurcation, and affected the left psoas major muscle and ureter definition. Heterogeneous enhancement in the mass with migrating vascular shadows was observed, along with multiple lymph nodes in the left abdominal cavity and a nodular omentum. Additionally, multiple intensifying nodules were noted in the right hepatic lobe during the arterial phase, with isodensity in the portal and delayed phases. No fluid was present in the abdominal cavity, but enlargement of retroperitoneal lymph nodes and multiple nodules in both lungs were suspected to be metastatic.

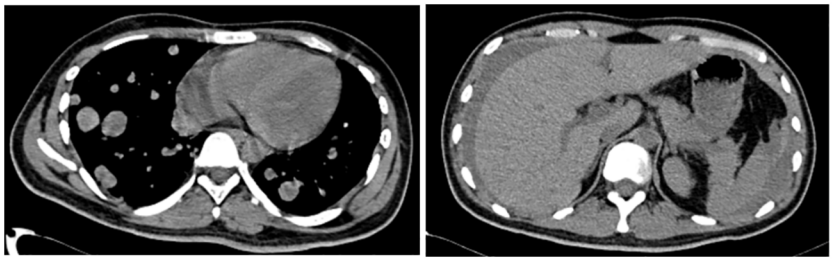

FIGURE 3
A full abdominal CT scan on 2 March revealed: 1) a new hyperdense shadow in the abdominal cavity indicative of potential hemorrhage, necessitating clinical correlation; 2) a notably increased number of lung nodules compared to previous scans, and 3) a fresh abdominopelvic effusion.

TABLE 1 Clinical data of gastrointestinal bleeding caused by metastatic testicular choriocarcinoma.

Case	Year	Age	First symptoms	Primary site of metastasis	Treatment	Ending
1 (4)	2009	24	Painless lump in left testicle	Lungs, brain, liver, intestines	Surgical+chemotherapy+Radiotherapy	live
2 (5)	2009	17	Testicular lumps	Lungs, liver, duodenum	Surgical+chemotherapy	live
3 (6)	2011	25	Dyspnoea, black stools, weight loss	Lungs, scrotum, skin	Surgical	Death
4 (7)	2012	24	Black stools, palpitations	lungs	Surgical+chemotherapy+Radiotherapy	Death
5 (8)	2012	24	tachycardia	Lungs, kidneys, scrotum, stomach	Surgical+chemotherapy	live
6 (5)	2015	18	Black stools, drowsiness, dizziness	Brain, lungs, lymph nodes, stomach	Surgical+chemotherapy	live
7 (9)	2019	30	Shortness of breath, chest pain	Lungs, duodenum, stomach	Symptomatic supportive therapy	live
8 (3)	2020	17	shock	Brain, duodenum, scrotum	Surgical+chemotherapy	live
9 (10)	2022	28	dark stool	Lungs, liver, jejunum	Surgical+chemotherapy	live
10 (11)	2022	20	Dyspnoea, black stools	lungs	chemotherapy	live
11 (12)	2023	27	Enlargement of the right scrotum	Lungs, Bones	Surgical+chemotherapy	live

Death refers to death during hospitalization.

In this article, the initial out-of-hospital evaluation neglected to assess the reproductive system or conduct HCG testing, leading to diagnostic delays. Testicular choriocarcinoma progresses rapidly, yet the outpatient facility mistook it for a pheochromocytoma without adequately examining the retroperitoneal mass. This oversight delayed treatment and excluded ultrasonography of the reproductive system and HCG monitoring. Conversely, immediate initiation of cisplatin-based chemotherapy, bypassing pre-surgery retroperitoneal examination, could improve patient survival. Tumor rupture and bleeding were primary causes of mortality, where radiotherapy could assist in controlling bleeding.

This case highlights the critical need for comprehensive history taking, systematic examination, and thorough laboratory testing in patients presenting with abdominal pain and nausea. Early and accurate diagnosis of testicular choriocarcinoma is crucial, as delayed detection increases mortality rates, prolongs hospital stays, and raises healthcare expenses. Therefore, an initial assessment of the reproductive system is essential. Preventing tumor rupture and hemorrhage, and enhancing the overall condition of the patient, are crucial for effective anti-tumor treatment. Early identification, prompt intervention, and precise diagnosis are essential for improving patient outcomes.

Examination of the reproductive system should be integrated into the systematic evaluation of patients, irrespective of apparent clinical correlation, to ensure a comprehensive approach. Early and prompt diagnosis and treatment of testicular choriocarcinoma are vital for enhancing patient survival rates. While the approach in this case was not without flaws, it serves as a critical reminder of the importance of early detection and intervention in cancer care.

Data availability statement

The original contributions presented in the study are included in the article/supplementary material. Further inquiries can be directed to the corresponding author.

Ethics statement

The studies involving humans were approved by Ethics Committee of the First Hospital of Lanzhou University. The studies were conducted in accordance with the local legislation and institutional requirements. Written informed consent for

participation in this study was provided by the participants' legal guardians/next of kin. Written informed consent was obtained from the individual(s) for the publication of any potentially identifiable images or data included in this article.

Author contributions

XB: Conceptualization, Data curation, Formal analysis, Funding acquisition, Investigation, Methodology, Project administration, Resources, Software, Supervision, Validation, Visualization, Writing – original draft, Writing – review & editing. XL: Conceptualization, Data curation, Investigation, Software, Writing – review & editing. HL: Conceptualization, Data curation, Investigation, Methodology, Writing – original draft. YL: Conceptualization, Data curation, Investigation, Methodology, Writing – original draft. BS: Formal Analysis, Investigation, Methodology, Validation, Writing – review & editing. JT: Conceptualization, Data curation, Formal analysis, Funding acquisition, Investigation, Methodology, Project administration, Resources, Software, Supervision, Validation, Visualization, Writing – review & editing, Writing – original draft.

Funding

The author(s) declare that no financial support was received for the research, authorship, and/or publication of this article.

Conflict of interest

The authors declare that the research was conducted in the absence of any commercial or financial relationships that could be construed as a potential conflict of interest.

Publisher's note

All claims expressed in this article are solely those of the authors and do not necessarily represent those of their affiliated organizations, or those of the publisher, the editors and the reviewers. Any product that may be evaluated in this article, or claim that may be made by its manufacturer, is not guaranteed or endorsed by the publisher.

References

1. Richie JP. Detection and treatment of testicular cancer. *CA Cancer J Clin*. (1993) 43:151–75. doi: 10.3322/canjclin.43.3.151

2. Deligdisch L, Waxman J. Metastatic gestational trophoblastic neoplasm. A study of two cases in unusual clinical settings and review of the literature. *Gynecol Oncol*. (1984) 19:323–8. doi: 10.1016/0090-8258(84)90199-9

3. Zeighami S, Naghdi Sede N, Khajeh F, Ariafar A, Soltani M, Jahanabadi Z, et al. Genital exam, a missed piece of the puzzle in medical diagnosis, can be lifesaving in men: A lesson from a case of a state of shock due to duodenal metastasis of testicular choriocarcinoma. *Qatar Med J*. (2020) 2020:31. doi: 10.5339/qmj.2020.31

4. Cicin I, Ozyilmaz F, Karagol H, Yalcin F, Uzunoglu S, Kaplan M. Massive upper gastrointestinal bleeding from pure metastatic choriocarcinoma in patient with mixed germ cell tumor with subclinical intestinal metastasis. *Urology*. (2009) 73:443.e15–443.e17. doi: 10.1016/j.urology.2008.02.044

5. Bain AJ, Owens DJ, Savides TJ. Image of the month. Upper gastrointestinal bleeding caused by metastatic testicular choriocarcinoma. *Clin Gastroenterol Hepatol*. (2010) 8:A22. doi: 10.1016/j.cgh.2009.05.005

6. Fosado Gayosso M, Pérez Hernández JL, Bernal Sahagún F, Acevedo García C, Aguilar Ayala EL, Pérez Espinosa J. Upper gastrointestinal bleeding as an initial manifestation of metastasis, secondary to a choriocarcinoma in a patient suffering from testicular mixed cell tumour. *Rev Esp Enferm Dig*. (2011) 103:46–7. doi: 10.4321/s1130-01082011000100013

7. Fu S, Avezbakiyev B, Zhi W, Kodali S, Rizvon K, Alaverdian A, et al. Germ cell cancer presenting as gastrointestinal bleeding and developing brain metastases: case report and review of the literature. *Future Oncol*. (2012) 8:1487–93. doi: 10.2217/fon.12.133

8. Vardaros M, Subhani M, Rizvon K, Gotlieb V, Mustacchia P, Freedman L, et al. A case of gastrointestinal bleeding due to duodenal metastasis from a testicular choriocarcinoma. *J Gastrointest Cancer*. (2013) 44:234–7. doi: 10.1007/s12029-012-9433-y

9. Chaar A, Mouabbi JA, Alrajjal A, Barawi M. Metastatic testicular choriocarcinoma: an unusual cause of upper gastrointestinal bleed. *Cureus*. (2019) 11:e5243. doi: 10.7759/cureus.5243

10. Zhang B, Yan Y-Y, Gu Y-Q, Teng F, Lin X, Zhou X-L, et al. Inhibition of TRIM32 by ibr-7 treatment sensitizes pancreatic cancer cells to gemcitabine via mTOR/p70S6K pathway. *J Cell Mol Med*. (2022) 26:515–26. doi: 10.1111/jcmm.17109

11. Yang XY, Bégin LR, Tamaz R. A 20-year-old-man with new onset of melena. *Gastroenterology*. (2022) 162:e14–5. doi: 10.1053/j.gastro.2021.05.065

12. Zhang X, Yang F, Ma X, Zhao H. The primary choriocarcinoma of testis with systemic metastasis in a patient with cryptorchidism. *Asian J Surg*. (2023) 46:5289–90. doi: 10.1016/j.asjsur.2023.07.070

13. Zerbib P, Prieur E, Khoury-Helou A, Catala P, Pruvot FR, Chambon JP. [Hemorrhagic digestive metastases from testicular choriocarcinoma]. *Ann Chir*. (2002) 127:300–1. doi: 10.1016/S0003-3944(02)00743-5

14. Zhang P, Wang Y, Xiong L. Gastrointestinal bleeding caused by metastatic testicular choriocarcinoma: a case report and literature review. *World J Surg Oncol*. (2022) 20:205. doi: 10.1186/s12957-022-02670-7

frontiers | Frontiers in Oncology

TYPE Review
PUBLISHED 29 July 2024
DOI 10.3389/fonc.2024.1413793

Check for updates

OPEN ACCESS

EDITED BY
Nikhil I. Khushalani,
Moffitt Cancer Center, United States

REVIEWED BY
Ilze Strumfa,
Riga Stradiņš University, Latvia
Emily Avitan-Hersh,
Rambam Health Care Campus, Israel

*CORRESPONDENCE
Paul W. Harms
paulharm@med.umich.edu

†These authors have contributed equally to this work

RECEIVED 07 April 2024
ACCEPTED 08 July 2024
PUBLISHED 29 July 2024

CITATION
Pedersen EA, Verhaegen ME, Joseph MK, Harms KL and Harms PW (2024) Merkel cell carcinoma: updates in tumor biology, emerging therapies, and preclinical models. *Front. Oncol.* 14:1413793. doi: 10.3389/fonc.2024.1413793

COPYRIGHT
© 2024 Pedersen, Verhaegen, Joseph, Harms and Harms. This is an open-access article distributed under the terms of the Creative Commons Attribution License (CC BY). The use, distribution or reproduction in other forums is permitted, provided the original author(s) and the copyright owner(s) are credited and that the original publication in this journal is cited, in accordance with accepted academic practice. No use, distribution or reproduction is permitted which does not comply with these terms.

Merkel cell carcinoma: updates in tumor biology, emerging therapies, and preclinical models

Elisabeth A. Pedersen[1†], Monique E. Verhaegen[1†], Mallory K. Joseph[1], Kelly L. Harms[1] and Paul W. Harms[1,2*]

[1]Department of Dermatology, University of Michigan, Ann Arbor, MI, United States, [2]Department of Pathology, University of Michigan, Ann Arbor, MI, United States

Merkel cell carcinoma (MCC) is an aggressive cutaneous neuroendocrine carcinoma thought to arise via either viral (Merkel cell polyomavirus) or ultraviolet-associated pathways. Surgery and radiotherapy have historically been mainstays of management, and immunotherapy has improved outcomes for advanced disease. However, there remains a lack of effective therapy for those patients who fail to respond to these established approaches, underscoring a critical need to better understand MCC biology for more effective prognosis and treatment. Here, we review the fundamental aspects of MCC biology and the recent advances which have had profound impact on management. The first genetically-engineered mouse models for MCC tumorigenesis provide opportunities to understand the potential MCC cell of origin and may prove useful for preclinical investigation of novel therapeutics. The MCC cell of origin debate has also been advanced by recent observations of MCC arising in association with a clonally related hair follicle tumor or squamous cell carcinoma *in situ*. These studies also suggested a role for epigenetics in the origin of MCC, highlighting a potential utility for this therapeutic avenue in MCC. These and other therapeutic targets form the basis for a wealth of ongoing clinical trials to improve MCC management. Here, we review these recent advances in the context of the existing literature and implications for future investigations.

KEYWORDS

neuroendocrine carcinoma (NEC), immunotherapy, mouse model, Merkel cell carcinoma (MCC), epigenetics, viral tumorigenesis, UV signature, clinical trial

1 Introduction

Merkel cell carcinoma (MCC) is a poorly differentiated primary cutaneous neuroendocrine carcinoma. It is among the most aggressive cutaneous solid tumors, with significant rates of disease-associated morbidity and mortality. MCC is now known to consist of two molecular subclasses: Merkel cell polyomavirus-associated and UV-associated, which are denoted as virus-positive MCC (VP-MCC) and virus-negative MCC

(VN-MCC) throughout this review. Recently, immunotherapy has dramatically improved prognosis in advanced disease, but is not universally effective. Thus, there is continued need for better molecular understanding, prognostication, and therapeutic options for MCC.

In this review, we discuss the current state of MCC treatment and how it relates to the cellular and molecular pathogenesis of MCC. We also review the emerging therapeutic strategies and the related need for improved preclinical models of MCC.

2 Clinical management of MCC

2.1 Clinical presentation and diagnosis

MCC arises most frequently in fair-skinned patients, with 89.9% of MCC cases identified in White, 5.7% in Hispanic, 2.3% in Asian American or Pacific Islander, and 1.5% in Black patients (1). The greatest incidence of MCC has been noted in Australia (1.6 cases per 100,000 individuals) (2), and is in line with the observed greater MCC incidence with geographic proximity to the equator (3). In 2013, the incidence in the United States was approximately 0.7 per 100,000, which was a 95% increase since 2000 (4). MCC is more common in males compared to females (3:2, respectively) (4–6), and the median age of diagnosis is >75 years, with very rare incidence in patients < 40 years (5). For MCC, the incidence continues to rise with each additional decade of life, whereas in most other malignancies, the incidence peaks at a mid-/later decade of life and then declines with further age (2). The incidence of MCC is greater in patients with impaired immune functioning such as organ transplantation, hematologic malignancy, immunosuppressive medications, and other causes of decreased immunity (3).

MCC most often arises as a red-to-violaceous papule or nodule on sun-exposed skin. It may also arise as a subcutaneous nodule with no overlying skin changes. Tumors often grow rapidly over the course of 2-3 months. MCC has a high propensity for metastasis; up to 35% of patients will have either regional lymph node or distant metastases (7) at the time of diagnosis. Frequent sites of metastatic involvement are adjacent skin (satellite or in-transit metastases); regional lymph nodes; and distant sites including bone, visceral organs (liver, lungs), distant skin, and distant lymph nodes.

MCC is a poorly-differentiated neuroendocrine carcinoma with round cell morphology (Figure 1) (2, 7–9). In most cases, the tumor is centered in the dermis, possibly with extension into the subcutis (Figure 1A) (7). In a minority of cases, there is pagetoid scatter in the overlying epidermis. Purely intraepidermal cases are exceptionally rare. There can be squamous metaplasia, eccrine differentiation, or rarely sarcomatoid change. A minority of VN-MCC is accompanied by SCCIS in the overlying epidermis, or less frequently invasive SCC (7, 10). Rarely, VP-MCC can be associated with other tumor types including trichoblastoma or poroma (11, 12).

MCC, like other poorly-differentiated tumors, can be challenging to distinguish from histopathologic mimics. The differential diagnosis for MCC depends on site of presentation and tumor morphology (7, 9). Extracutaneous small cell carcinoma metastatic to the skin is morphologically identical to MCC. Other small round cell tumors, such as lymphoma, small cell melanoma, or Ewing sarcoma, might also enter the differential diagnosis (7, 9). For MCC with more prominent pleomorphism, other poorly differentiated cutaneous carcinomas might also be considered (7).

Several other neuroendocrine tumors arise in the skin or subcutis and must be distinguished from MCC. Endocrine mucin-producing sweat gland carcinoma, and the related neuroendocrine subtype of mucinous carcinoma, are adenocarcinomas of the eyelid that may resemble MCC but lack round cell morphology (13). Primary cutaneous neuroendocrine tumors (carcinoids) display morphologic features of neuroendocrine tumors but are histologically lower grade than MCC (14). Recently, another category of primary cutaneous neuroendocrine carcinoma, termed sweat gland carcinoma with neuroendocrine differentiation (SCAND), has been proposed; however, these tumors also lack the round cell morphology of MCC (15).

Immunohistochemistry is critical for confirming the diagnosis of MCC and excluding histopathologic mimics (7–9). It should be noted that no single marker is completely sensitive for MCC, thus diagnosis often requires multiple immunohistochemical stains, expert evaluation, and clinical correlation to confirm the diagnosis. Commonly used markers include CK20 expression in a paranuclear dot pattern (Figure 1C), which is distinctive for MCC, but may not always be present (7). Neuroendocrine markers such as chromogranin A or synaptophysin are typically expressed (Figure 1D). Paranuclear dot labeling for neurofilament is also highly characteristic (Figure 1E) (7, 16, 17). Thyroid transcription factor 1 (TTF-1) and cytokeratin 7 are typically negative. Detection of MCPyV by immunohistochemistry or RNA *in-situ* hybridization supports a diagnosis of MCC (Figure 1F) (7, 10, 18). INSM1 is a highly sensitive marker for MCC, although specificity is limited relative to other neuroendocrine carcinomas (19–21). SATB2 has more limited sensitivity, but provides added specificity in that strong diffuse expression favors MCC over metastatic small cell carcinoma (22–24). SOX2 expression is highly sensitive for MCC (92%), and is highly specific for MCC compared to other cutaneous carcinomas, as well as 70% specific for MCC compared to other neuroendocrine carcinomas (25, 26). ATOH1 is expressed in MCC, however there is mixed data regarding the specificity of this marker for excluding other non-MCC neuroendocrine carcinomas (23, 27–30). VN-MCC has a higher rate of immunophenotypic aberrancy such as CK20 negativity (7, 31–33).

Morphology alone is usually sufficient to distinguish MCC from malignancies other than small cell carcinomas. However, several pitfalls merit mention. Neuroendocrine marker expression can be seen in some cases of other cutaneous carcinoma including basal cell carcinoma. Brisk obscuring inflammation, and/or expression of certain lymphoid markers (TdT, PAX5, SOX11, immunoglobulins) in a subset of MCC (7, 34, 35), can raise confusion with a lymphoid process. S100 expression has been described for MCC (7), and conversely can be lacking in small cell melanoma (36), potentially raising diagnostic difficulty. However, nuclear SOX10 expression is exceedingly rare in MCC, and other melanocytic markers will be negative, thus allowing reliable distinction from small cell

10.3389/fonc.2024.1413793

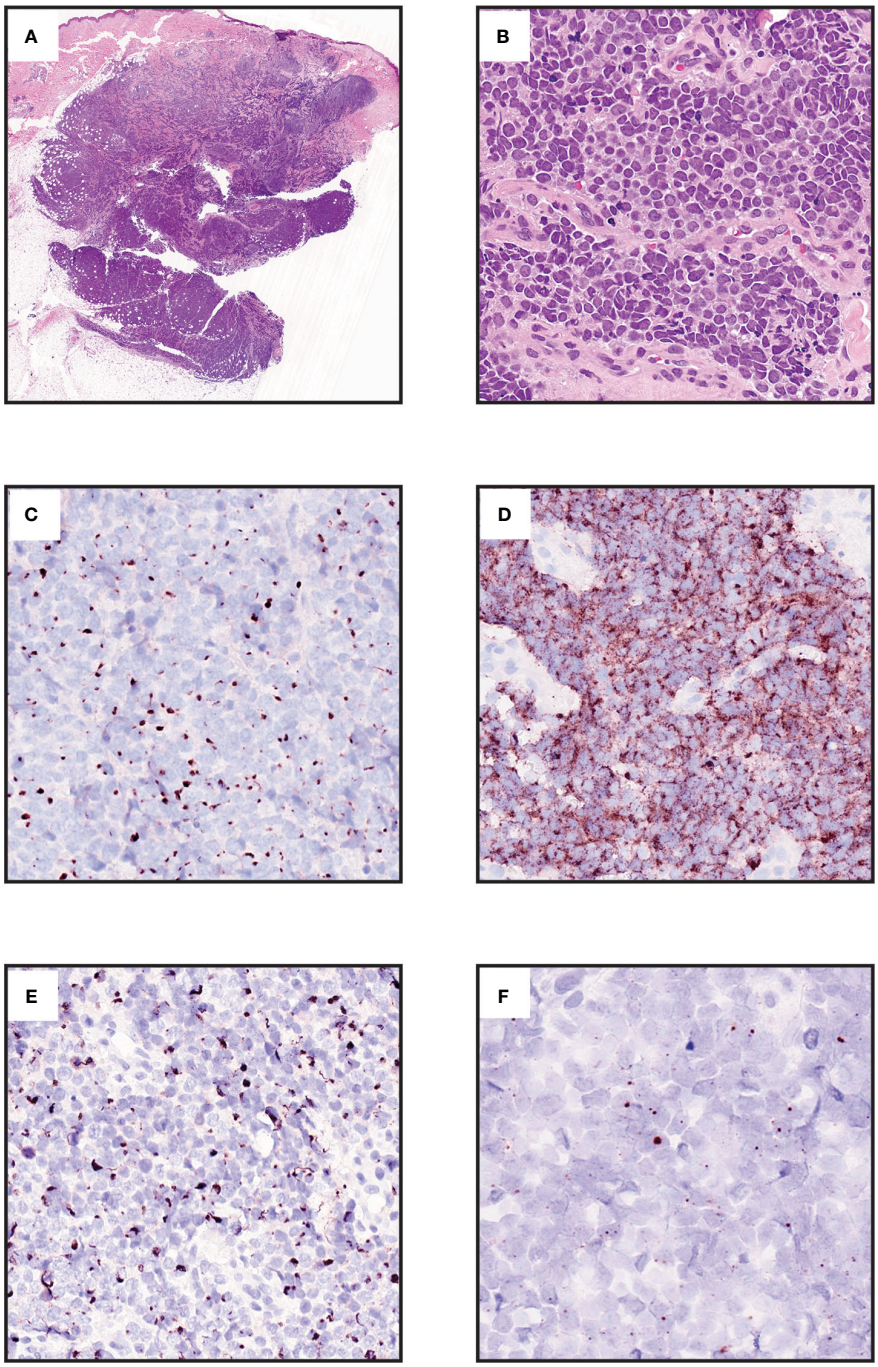

FIGURE 1
Morphologic and immunophenotypic features of Merkel cell carcinoma. **(A)** Expansile blue cell tumor occupying dermis with extension into subcutis (hematoxylin and eosin [H&E], 0.7x. **(B)** Small round cell tumor with neuroendocrine chromatin, mitotic activity, and crush artifact (H&E, 40x). **(C)** Cytokeratin 20 displays distinctive paranuclear dot labelling. (Chromogen DAB, counterstain hematoxylin, 40x). **(D)** Neuroendocrine marker Chromogranin A is immunohistochemically expressed in most cases (Chromogen DAB, counterstain hematoxylin, 40x). **(E)** Neurofilament immunohistochemistry displays paranuclear dot labelling and provides a more specific marker than cytokeratin 20 for MCC (Chromogen DAB, counterstain hematoxylin, 40x). **(F)** RNA *in situ* hybridization for the MCPyV T-antigen transcript in a virus-positive MCC (Chromogen DAB, counterstain hematoxylin, 80x).

melanoma (7, 37–40). MCC can express CD99 similar to small round cell sarcomas such as Ewing sarcoma, but will lack *EWSR1* rearrangements (2, 7, 41).

In challenging cases such as neuroendocrine carcinomas presenting in the parotid, or carcinomas of unknown primary, analyses demonstrating MCPyV or UV-signature mutations can also be useful for distinguishing MCC from extracutaneous neuroendocrine carcinomas (2, 7, 23, 42–45). Of note, the potential for primary parotid neuroendocrine carcinomas to be MCPyV-positive has been debated (44, 46–48), and thus currently

clinicopathologic correlation remains essential for classifying MCPyV-positive neuroendocrine carcinomas in the parotid.

2.2 Prognosis

The AJCC 8th edition defines staging guidelines for MCC based upon tumor size and the presence/pattern of metastatic spread (5). In addition, it is well established that advanced age, male sex, immunosuppression, and patients with a known primary lesion with clinically evident nodal metastases are associated with a higher risk of recurrence (49, 50). Additional prognostic factors are a subject of ongoing research. Many potential biomarkers for predicting MCC outcome have been proposed (2, 7, 51). Although data from smaller studies is mixed, several large studies have found that the viral status of MCC is prognostic: specifically, the presence of MCPyV is a favorable prognostic finding, with improved disease-specific and progression-free survival in VP-MCC compared to VN-MCC (2, 7, 10, 52–54). Tumor expression of p63 has been proposed to be predictive of outcomes (7, 55–58), however the clinical utility of this marker has been questioned (58). Many studies have found that immune infiltration patterns or marker expression can be informative of outcome for MCC tumors (2, 7, 10, 59, 60), especially CD8+ T-cells (7, 61–63). The predictive value of immune markers might vary based upon tumor MCPyV status (10), which was often not considered in such studies. Notably, the great majority of these studies were based upon outcomes data collected prior to the approval of immunotherapy for MCC, and thus reappraisal of these findings in the immunotherapy era will be essential.

2.3 Treatment

Clinical trials and the results of single- and multi-institution cohort studies provide the best evidence to support current practices for MCC treatment. Given the rarity of MCC, high-powered randomized controlled trials to identify optimal treatment approaches have not been feasible. The National Comprehensive Cancer Network (NCCN) Guidelines for MCC provides an annually updated evidence-based, and consensus-driven algorithmic approach for management of all stages of MCC (64). In addition, the European consensus-based interdisciplinary guideline was published in 2022 (65). Importantly, for patients with any stage of MCC, a multidisciplinary team is recommended as management requires the involvement of multiple specialties. Please refer to the NCCN and European Consensus guidelines for the most comprehensive and up-to-date algorithms for management (64, 65).

Initial evaluation and work-up of a patient newly diagnosed with MCC includes a thorough history with special attention directed towards immunosuppression. Immunosuppression is a known adverse prognostic factor, and it is recommended that immunosuppressive regimens are reduced by the prescribing physician when medically feasible. The initial physical exam should focus on identifying clinical staging parameters including the clinical size of the primary tumor, clinical in-transit metastases, and clinically detectable regional lymph node metastases. For patients without clinical lymph node metastases, baseline imaging with PET-CT is often recommended, as it has been shown to find additional asymptomatic sites of disease and impact staging (66). Suspected metastases should be confirmed by biopsy. Subsequent management is based upon stage of disease (64).

Surgical treatment with or without radiotherapy is the current standard of care. Due to the lack of randomized controlled trials, the optimal surgical margin is not well defined. The current NCCN recommendation is for excision with 1-2 cm margins, with Mohs micrographic excision (excision done by stages with frozen section evaluation of margins) designated as useful in certain circumstances (64). The risk of occult metastasis is high in patients presenting without clinically detected regional lymph node metastasis, and sentinel lymph node biopsy (SLNB) is recommended at the time of surgical removal of the primary tumor. Studies have demonstrated SLNB positivity rates as high as 26 - 45% (67–69) in institution based-cohorts. Observation is recommended for patients with a negative SLNB result, with evidence supporting a low risk of regional recurrence after a negative SLNB (70). For management of SLNB-positive disease, current guidelines recommend further treatment including lymph node dissection or radiation therapy (64), which have both demonstrated association with low rates of regional recurrence (71, 72).

MCC is highly sensitive to radiation therapy, and adjuvant radiation is recommended in cases of positive surgical margins (versus re-excision) and in the presence of adverse risk factors, such as primary tumors > 1 cm in size, immunosuppression, head/neck site, or lymphovascular invasion. For patients who are not surgical candidates, the recommendation is for multidisciplinary discussion and consideration of definitive radiation therapy or systemic therapy (64).

For patients with clinically detected lymph node metastases prior to surgery, a lymph node biopsy via fine needle aspiration or core needle biopsy is recommended to confirm the presence of metastatic MCC. For treatment of biopsy-confirmed clinically detectable lymph node metastases, current NCCN guidelines recommend clinical trial, or combination of lymph node dissection and radiation therapy. In addition, neoadjuvant therapy (e.g. treatment prior to surgery) with immunotherapy is emerging as a potential option for treatment.

Reports of immune-mediated spontaneous regression in some cases of MCC suggested the potential for therapeutic harnessing of antitumor immunity for advanced disease (2). Immunotherapy, also known as immune checkpoint inhibitor therapy, has become widely used in management of metastatic MCC and preferred over traditional chemotherapy due to improved responses and more favorable side effect profiles. Three immune checkpoint inhibitors are currently FDA-approved for the management of metastatic or advanced MCC. Avelumab, a monoclonal antibody targeted against programmed cell death ligand 1 (anti-PD-L1) was FDA-approved in 2017 for metastatic MCC. The JAVELIN Merkel 200 trial part A showed a 32% objective response rate to second-line avelumab (73); long-term follow up demonstrated a median overall survival (OS) of

12.6 months and a 5-year OS of 26% (74). Results of JAVELIN Merkel 200 part B showed a 62% objective response rate (ORR) to first-line avelumab (75). More recently, a retrospective review of patients with advanced MCC initiated on avelumab reported durable response rates as high as 73% (76). Pembrolizumab and retifanlimab, monoclonal antibody therapies targeting programmed cell death protein -1 (PD-1), were FDA-approved in 2018 and 2023, respectively, for recurrent, locally advanced and metastatic MCC (77). In the Keynote-017 trial, pembrolizumab demonstrated 56% overall response rate (ORR) (78); long-term follow-up demonstrated a 24-month overall survival rate of 68.7% (79). The PODIUM-201 trial demonstrated a 46.2% ORR, and 62% of patients had a response of ≥ 12 months (80). Nivolumab, an anti-PD-1 antibody, is also showing promise in the treatment of MCC, with numerous ongoing studies evaluating the efficacy of single and multi-agent therapy (2, 81).

Emerging neoadjuvant studies have shown promising results and are being recommended more frequently. The Checkmate 358 trial demonstrated that half of patients with clinically detectable lymph node metastases who received neoadjuvant nivolumab responded with tumor reductions of > 30% (82). NCCN guidelines currently recommend multidisciplinary discussion for consideration of neoadjuvant immunotherapy (64).

Overall, evidence across studies suggests that immunotherapy can achieve durable response in a significant proportion of patients with advanced MCC, especially when used as first-line therapy (83). However, patient factors including advanced age often seen in MCC patients and morbidity from treatment may alter treatment course or deem immunotherapy a less favorable option. Additional investigations with longer follow-up times in larger cohorts will be essential for more definitive assessment of durable response rates across different patient groups.

Management of metastatic MCC has historically included chemotherapy with etoposide and carboplatin/cisplatin-based regimens; however, the response to chemotherapy is not durable and most patients experience relapse. In a retrospective study of patients with metastatic MCC, first-line chemotherapy had a response rate was 55%, but also had a median progression free survival of 94 days (84). For second-line chemotherapy, the response rate was 23% with a median progression free survival of 61 days. Given initial response rates, chemotherapy may be useful in certain circumstances, such as for those who cannot undergo immune checkpoint inhibition due to immunocompromised status or the presence of a comorbid autoimmune condition (2, 85). It may also serve as a palliative therapy to slow the rate of rapidly growing symptomatic tumors or metastases.

As immunotherapy is not universally effective in MCC, predicting treatment response could be helpful to avoid the risk of immunotherapy toxicity in patients who will not benefit from therapy, and to consider alternative treatments if those become available. However, predictors of MCC response to immunotherapy have been elusive. Responses have not correlated with tumor PD-L1 expression (73, 78, 82, 86, 87), MCPyV status (73, 82, 86–89), tumor mutational burden (82, 86, 87), or UV mutation signatures (87). A retrospective study showed that single nucleotide variants of *ARID2* and *NTRK1* were associated with a better response to immunotherapy (87). More sophisticated approaches may be informative, such as characterizing immune populations (especially T-cells) (88, 90–95) or measuring spatial associations of cell populations in the tumor microenvironment (88, 96). However, to date none of these approaches have reached routine clinical use for decisions on immunotherapy eligibility.

After definitive treatment with surgery, radiation, and/or systemic therapy, close surveillance is typically recommended. Due to the significant risk of recurrence, current management for MCC includes imaging (such as by CT) every 3-6 months for several years following diagnosis (64). Alternative and emerging methods for disease surveillance include circulating burden of antibodies against MCPyV T-antigens (64, 77, 97, 98), and circulating tumor DNA (77, 99).

3 Molecular and cellular pathogenesis of MCC

3.1 Overview of molecular alterations in MCC

The above average prevalence of MCC in immune-compromised transplant and HIV patients (100) alluded to a possible viral etiology. This possibility was confirmed when analysis of MCC tumors via digital transcriptome subtraction methodology identified viral transcripts from a previously unknown human polyomavirus, which the authors thus named the Merkel cell polyomavirus (MCPyV) (101). The initial finding that only about 80% of tumors had integrated viral sequences suggested that a fraction of MCCs arise by a distinct mechanism. Following additional studies, two often histologically indistinguishable molecular subclasses have now been defined: MCPyV associated (virus-positive MCC; VP) and UV-associated (virus-negative MCC; VN) tumors (2, 43, 45, 102).

3.2 The Merkel cell polyomavirus and viral-associated MCC

The MCPyV belongs to the *Polyomaviridae* (PyV) family of small non-enveloped, circular, double-stranded DNA viruses, of which to date, 15 have been isolated from human samples with 13 identified as genuine human viruses (103). Several polyomaviruses are associated with cutaneous infections (trichodysplasia spinulosa polyomavirus, human polyomavirus 6, and human polyomavirus 7) and other human diseases (JC Polyomavirus, BK polyomavirus). However, MCPyV is the sole family member classified as a Group 2A carcinogen (probably carcinogenic to humans) by the International Agency for Research on Cancer (104). Polyomaviruses are widely prevalent in the human population, and MCPyV can be detected in the skin of most healthy individuals and at low levels in a wide variety of tissues. Serological studies indicate primary infection occurs most

likely in early childhood and seroprevalence in adults is typically 60–80% (105).

During the MCPyV infectious cycle, the MCPyV helicase (C-terminal domain of LTAg) mediates replication of viral DNA by recruiting the host cell machinery. The viral DNA of MCPyV can be repeatedly and rapidly amplified during a single cell cycle, referred to as unlicensed replication (106). The host cell factors that contribute to MCPyV replication are poorly understood. In healthy populations, antiviral responses induced by MCPyV, such as IFN production, may inhibit early transcription and restrict propagation, whereas skin injury or UV irradiation may induce growth factors promoting viral propagation, thus providing a way to support persistent MCPyV infection (107, 108). Degradation of LTAg by ubiquitin ligases, which may be abrogated by cellular stresses, is another proposed mechanism for latency and reactivation of MCPyV (109–112), although this mechanism has been debated (113).

Despite a lifelong history of MCPyV exposure and infection in most individuals, development of MCC tumors remains remarkably rare. Productive viral infection is associated with host cell death (114), precluding the possibility of cell transformation during the normal viral life cycle. Two critical events are thus hypothesized to precede MCPyV-driven transformation: accidental integration of the viral genome into the host genome, and loss of viral replicative capacity due to LTAg mutations which yield a non-replicative truncated LTAg (tLTAg) (101, 115). The clonal pattern of viral integration suggests infection and integration occurs before tumor expansion, providing evidence for MCPyV being causal for tumorigenesis (101).

3.3 MCPyV T antigens

Like other polyomaviruses, the MCPyV genome consists of an early region (ER) coding for regulatory proteins involved in replication and transcription, a late region (LR) coding for structural proteins, and a non-coding control region (NCCR) containing the origin of DNA replication, regulatory elements, and transcription promoters (116). Four spliced transcripts are produced by the ER that code for four proteins: the large T antigen (LTAg) and the alternative splicing product 57kT; the small T antigen (sTAg); and alternate frame of the LTAg open reading frame (ALTO, as analogous to middle T antigen or MT) (Table 1) (101, 129, 131). The LR encodes two capsid proteins (VP1 and VP2) required for viral assembly, and a microRNA targeting the TAg transcripts (132–134).

Evidence suggests that tLTAg and sTAg both contribute to the oncogenic potential of MCPyV (117, 118, 135–140). Expression of these oncoproteins is required for VP-MCC cell growth and survival (141, 142). Interestingly, while LTAgs from most other polyomaviruses such as SV40 typically demonstrate transforming ability (143), the MCPyV tLTAg is not sufficient to drive transformation alone *in vitro* (135) or *in vivo* (118), but rather cooperates with sTAg to drive transformation (137).

TABLE 1 MCPyV T antigen gene products, domains, and functions.

MCPyV T antigens	Key structural components	Associations and Functions
sTAg (ST) Small T Antigen	N-terminal DnaJ domain LTAg stabilization domain (LSD) PP2A binding domain	LSD is required for oncogenesis *in vitro* and *in vivo*. Regulates protein stability of oncoproteins including LTAg (109, 117–119). LSD domain inhibits E3 ubiquitin ligases (109). Acts in complex with MYCL and EP400 (120). The role of the PP2A binding domain is currently unclear and possibly dispensable (117, 118, 121).
LTAg (LT) Large T antigen	N-terminal DnaJ domain MCPyV-unique region (MUR): *LXCXE retinoblastoma-associated protein (RB1) binding domain* *Nuclear localization signal (NLS)* *Origin binding domain (OBD)* *C-terminal helicase/ATPase domain*	LXCXE binding motif drive proliferation via inactivation of RB and subsequent activation of E2F cell cycle genes (2, 115, 122). Forced LTAg expression promotes reprogramming toward a Merkel cell-like lineage via induction of ATOH1 and SOX2 (123–125). LTAg expression is dependent upon and regulates neuroendocrine phenotypes (126).
tLTAg (tLT) Truncated Large T antigen	In MCPyV integrated within MCC cells, the LTAg gene is affected by a truncating mutation or deletion. *DnaJ domain and the LXCXE binding motif are retained* *OBD and helicase domain are eliminated* The exact mutation or deletion event resulting in truncation is highly variable among individual tumors.	LXCXE (Rb binding domain) contributes to virus-driven cellular proliferation (2, 122). Deletion of the OBD and helicase domain render the MCPyV non-replicative (2, 115, 127, 128).
ALTO Alternate frame of the LTAg open reading frame	Translated from an internal start site in the second exon of LTAg Possesses a distinct C-terminus Similarity to middle T antigen	ALTO likely has structural and functional similarities to the murine polyomavirus MT (129). May target Src family kinases, leading to activation of the NF-κB inflammatory signaling pathway, possibly impacting viral replication (130).

The LTAg contains several functional domains, most notably the LXCXE retinoblastoma-associated protein (RB1) binding domain, and C-terminal region responsible for mediating viral replication [reviewed in (144)]. In MCPyV integrated within MCC cells, the LTAg gene is affected by a truncating mutation or deletion to generate tLTAg, eliminating the C-terminus and rendering the virus non-replicative (101, 115, 145) while sparing the LXCXE binding motif (2, 146), which plays a critical role in LTAg-driven proliferation via inactivation of RB and subsequent activation of E2F cell cycle genes (2).

In contrast to sTAgs of other polyomaviruses, the MCPyV sTAg displays transformation capability in culture (135) and *in vivo* (117, 118, 139). Several potential mechanisms for this activity have been investigated, including promoting activity of the mTOR pathway (135), regulation of protein stability via a unique LTAg stabilization domain (LSD) of sTAg proposed to inhibit E3 ubiquitin ligases and stabilize oncoproteins including LTAg (109, 117–119), cell surface localization of proteins involved in tumor cell recognition and tumor microenvironment regulation such as CD47 (147), and interacting with protein phosphatases and the NF-kB essential modulator (NEMO) to achieve inhibition of NF-kB signaling, a potential mechanism for repressing inflammatory signaling (148).

One of the most recently described roles for sTAg may have an even more profound influence on cellular functions. MCPyV sTAg can complex with the MYC homolog, L-MYC and its binding partner MAX, which in turn recruit the chromatin remodeling complex EP400 (120). The sTAg-MYCL-EP400 complex transcriptionally activates hundreds of downstream targets involved in ribosomal biogenesis, splicing, glycolysis, and other metabolic functions. This complex also increases levels of the mouse double minute 2 homolog (*MDM2*) E3 ubiquitin-protein ligase, which binds p53 and promotes its ubiquitination and proteasomal degradation, as well as CK1α, an activator of MDM4 (120, 149). Thus, although VP-MCC typically harbor wild-type *TP53* (43), p53 is indirectly inactivated by MCPyV sTAg via this mechanism. Additional activated targets of the sTAg-MYCL-EP400 complex include LSD1, RCOR2 and INSM1, which form part of a transcriptional repressor complex that opposes the ncBAF complex involved in differentiation, and the ATOH1 transcription factor which governs Merkel cell fate (150). The sTAg complex has also been shown to upregulate genes involved in cell motility, and downregulate genes involved with cell adhesion properties, revealing possible sTAg roles in invasion and metastasis (120, 140, 151–153).

Analogous to other sTAgs, the MCPyV sTAg contains a PP2A binding domain. However, the role of the PP2A binding domain in sTAg-mediated transformation is currently unclear and possibly dispensable (117, 118, 121).

To date, the functional role of MCPyV ALTO has not been well recognized, but emerging evidence now suggests that ALTO has structural and functional similarities to the murine polyomavirus MT, targeting Src family kinases, leading to activation of the NF- κB inflammatory signaling pathway, and possibly impacting viral replication (130).

While not yet functionally understood, significant levels of intrinsic protein structure disorder have recently been described in sTAg, LTAg, ALTO, 57kT, and VP1, characterized by the lack of a consistent three-dimensional structure (154). These disordered structures may present MCPyV viral proteins with unique functional properties including exceptional binding promiscuity and interactions with unexpected partners (154). This feature might contribute to the high diversity of functions that have been attributed to MCPyV T antigens.

3.4 UV-associated virus negative MCC

Initial focused sequencing studies on MCC identified recurrent mutations including *TP53* and *RB1* in a subset of tumors but did not correlate these findings with MCPyV or global mutation changes (54, 155–159). However, later studies that broadly examined the MCC mutational landscape in the context of MCPyV immediately identified two molecular subclasses with significant differences in mutational burden (43, 45, 102). Virus-negative tumors displayed a high UV-signature mutational burden with recurrent inactivation of tumor suppressor genes *TP53* and *RB1*, while virus-positive tumors had an extremely low mutational burden (43, 45, 102). VN-MCC can present with a mutational burden of 40 mutations per megabase, which is higher than any cancer sequenced by The Cancer Genome Atlas and more than 100-fold higher than VP-MCC (43, 102). Metastatic VN-MCC tumors exhibit additional genomic complexity (160). In contrast, VP-MCC typically have relatively normal diploid genomes with few somatic mutations (43, 45, 102), and those present are often subclonal, suggesting they occurred after tumor initiating events (161). Mutations in UV-associated VN-MCC often result in inactivation of genes involved in several signaling pathways, including NOTCH (*NOTCH1, NOTCH2*), DNA damage repair (*KMT2A*, *KMT2C KMT2D*, *ASXL1*, *ARID1A*, *ARID1B*, *SMARCA4)* and chromatin-modifying pathways (*ATM*, *MSH2*, *BRCA1*, *BRCA2*, and *BCOR) (*10, 43, 45, 86, 102, 146*)*.

Oncogene activation events tend to be detected with greater frequency in VN-MCC than VP-MCC and are overall heterogeneous (10, 86). The most highly recurrent oncogene activation events include *MYCL* amplification and *PIK3CA* activating point mutation. Other hotspot activating mutations reported in MCC include *TERT* promoter, *KNSTRN*, *RAC1*, *HRAS, KRAS, NRAS*, *AKT1*, *CTNNB1, IDH1, IDH2* and *EZH2*, among others (2, 42, 43, 45, 86, 102, 157, 162, 163).

At the transcriptional level, VN-MCC shows distinct patterns of gene expression from VP-MCC (10, 164–168), including upregulation of genes involved in the epithelial-to-mesenchymal transition and developmental processes, and downregulation of genes involved in neuroendocrine and epidermal differentiation, which may contribute to its more aggressive nature (165, 167).

3.5 Epigenetic changes in MCC

Epigenetic modifications encompass a spectrum of reversible covalent modifications, especially to histone proteins and DNA, that exert powerful effects on chromatin accessibility and hence

gene expression (169, 170). Alterations in epigenetic patterning can contribute to the hallmarks of cancer, and are frequently observed in malignancies (169–171).

A consistent model for the contribution of epigenetic dysregulation to MCC tumor biology has remained elusive. Although many sequencing studies have identified mutations involving chromatin modifier genes in MCC, the genes involved are heterogeneous with no highly recurrent mutational driver of epigenetic dysregulation (10, 42, 43, 45, 86, 102, 161, 172, 173). Until recently there have been relatively few studies establishing patterns and significance of epigenetic alterations in MCC. However, recent studies have provided new insights into the biological importance of the tumor epigenome in MCC.

Methylation of DNA occurs on cytosine residues and is a major regulator of gene expression. Methylation of promoter CpG islands and adjacent shores is associated with silencing, whereas methylation of gene body sites is associated with increased expression (174–176). Patterns of DNA methylation can yield insights into tumor classification and cell of origin (177). DNA methylation is perturbed in tumorigenesis, including global methylation changes and specific silencing of tumor suppressor genes (171). DNA hypomethylation agents have been approved as antitumor therapy for some myeloid neoplasms and are under investigation as therapeutics for solid tumors (178, 179), underscoring the mechanistic importance of altered DNA methylation in tumor biology.

Until recently, studies into epigenetic patterning in MCC have been limited to specific genes. Promoter hypermethylation has been described for tumor suppressor genes including *CDKN2A, RASSF1, RB1, DUSP2*, and *MGMT* (180–184), although protein expression studies have not shown that these genes are consistently silenced in MCC tumors (53, 164, 182, 184, 185). Hypomethylation of the *PTCH1* tumor suppressor has been described in MCC, but this did not consistently correlate with gene expression (186). Thus, the biological significance of these methylation events has remained unclear. The cell surface protein PD-1 (encoded by *PDCD1*), long known to be associated with immune exhaustion when expressed on T-cells, has recently been proposed to also be a tumor suppressor expressed on some tumor cells (187). *PDCD1* promoter hypermethylation has been described in MCC, in which context it may correlate with reduced immune response and worse prognosis (188).

Recent studies have provided greater detail on patterns of DNA methylation in MCC (189–192). Based on global genomic patterns, MCC assorts into a distinct cluster from other tumor types, with closest similarity to small cell lung carcinoma, and relative similarity to squamous cell carcinoma (189). Comparison to other tumor types by a score-based approach also demonstrated the epithelial and neuroendocrine-type patterning of DNA methylation in MCC (190). VP-MCC displays distinctive genome-wide DNA methylation patterns as compared to VN-MCC, although the magnitude and significance of such differences is unclear (189–191). In particular, VP-MCC displays globally decreased methylation compared to VN-MCC, as indicated by direct measurement of genomic methylation, and by expression of the hypomethylation marker long interspersed nuclear element-1 (189, 193). The mechanism for DNA methylation dysregulation in MCC remains unclear, as DNA methyltransferase genes (DNMTs) are not consistently overexpressed or mutated in MCC (43, 45, 102, 189). Nonetheless, promoter methylation might provide a mechanistic explanation for expression patterns of many diagnostic and prognostic markers in MCC (189, 191). There is also evidence that DNA methylation patterns change with MCC progression (191). DNA methylation may also coordinate or promote other epigenetic changes in MCC such as histone methylation and acetylation (189, 191). In support of a biological role for DNA methylation in MCC biology, treatment with the DNA hypomethylating agent decitabine is associated with antiproliferative effects in VN-MCC and cell death in VP-MCC (189).

In addition to this proposed role in cell proliferation and survival, DNA methylation also appears to be a mechanism of immune evasion for MCC (189). HLA presentation of "non-self" antigens, either viral antigens for VP-MCC or UV-mutational neoantigens for VN-MCC (2), represents a potentially powerful trigger for antitumor immunity against MCC. HLA presentation can be downregulated by direct silencing of HLA genes and/or by repressing expression of the antigen presenting machinery responsible for mediating cell-surface localization and antigen presentation by HLA. In MCC, promoter hypermethylation is observed for HLA and antigen presenting machinery genes (189). This is likely functionally significant, as treatment by a hypomethylating agent resulted in de-repression and restored membrane localization of HLA (189). Therefore, hypomethylating agents might increase the antigenicity of MCC to promote antitumor immunity.

The reversal of DNA methylation is achieved via an intermediate step in which TET enzymes convert 5-methylcytosine to 5-hydroxymethylcytosine (5-hmc). The dysregulation of TET activity plays a significant role in driving some hematopoietic neoplasms (194). Inactivating mutations of *TET2*, and activating mutations of *IDH1/IDH2* that inhibit TET activity, can occur in MCC but are uncommon relative to other potential drivers (10, 42, 86). Global loss of 5-hmc has been reported in aggressive cases of MCC (195), although the mechanism for TET dysregulation in such cases remains unclear.

Histone modifications, especially methylation, phosphorylation, and acetylation, can play roles in either promoting or silencing gene expression (170, 196). Histone acetylation on lysine residues promotes chromatin relaxation to facilitate gene expression, and is regulated by histone acetyltransferases (HATs) and histone deacetylases (HDACs). Histone methylation (either mono-, di-, or tri-methylation) on lysine and arginine residues represents a complex multistep regulatory process that generally promotes closed chromatin and transcriptional repression (170). However, some histone methylation marks such as H3K4 trimethylation are associated with active transcription. Histone methylation is regulated by histone methyltransferases (including SET domain proteins such as the MLL family) and demethylases such as LSD1. Analogous to DNA methylation, histone modification can be a mechanism for tumor suppressor silencing or oncogene overexpression, and thus histone modifiers such as histone deacetylases represent therapeutic targets in tumors (170).

The Polycomb repressor complex 2 (PRC2) silences genes via repressive trimethylation of Histone 3 lysine 27 (H3K27Me3) (197). Dysregulated activity of PRC2, especially the catalytic subunit EZH2, has been implicated in many malignancies (197). EZH2 inhibitors display antitumor activity in epithelioid sarcoma and follicular lymphoma (198, 199). The role of PRC2 activity in MCC may be more complex. During embryogenesis, PRC2 acts to oppose normal Merkel cell development via silencing of the master Merkel cell fate regulator SOX2 (200). Global H3K27Me3 loss can be observed in many MCC consistent with loss of PRC2 activity (173, 201–204). H3K27Me3 loss occurs in tandem with the transition from a squamous progenitor population into MCC in at least some cases (173), suggesting similar roles for PRC2 in antagonizing both normal Merkel cell development and the emergence of MCC.

Given this evidence that PRC2 opposes Merkel cell formation, it is perhaps surprising that the PRC2 catalytic subunit EZH2 has been shown to be expressed in some MCC tumors (205–208), in which context it has been correlated with worse prognosis (206, 207). Activating EZH2 mutations, however, are rare in MCC (10, 42, 43, 86). EZH2 expression can be promoted by E2F transcription factors (209), suggesting a mechanism by which this gene might be upregulated in Rb-deficient tumors such as MCC. Thus far, there is conflicting data on the potential efficacy and mechanism of EZH2 inhibitors in MCC, with 2 reports finding that inhibition of the EZH2 methyltransferase activity had cytotoxic effects on VP-MCC cells and/or xenografts (208, 210), whereas another study found that protein degraders of EZH2 impaired VP-MCC cell line viability independently of the methyltransferase function (211). The antitumor effect of EZH2 inhibition on MCC might be mediated by reversing EZH2-mediated repression of inner ear differentiation genes including *SIX1* (210). Further investigations are needed to better clarify the complex roles for PRC2 and the EZH2 subunit in MCC tumor biology.

The Myc oncoprotein exerts broad effects on transcription patterns in tumors via multiple mechanisms, including epigenetic modification. In keeping with a role for Myc family dysregulation in MCC, *MYCL* (and to a lesser extent *MYC*) can be amplified in a subset of MCC tumors (10, 212). More recently, evidence has shown that MCPyV small T antigen also acts in complex with MYCL and EP400 to promote LSD1 expression. In turn, LSD1 regulates methylation of H3K4 and H3K9 (associated with transcriptional activation and repression, respectively), resulting in gene expression changes that promote tumor proliferation and survival (150, 213). Importantly, Myc overexpression in MCC has been linked to the activating epigenetic mark H3K27Ac in the *MYC* promoter region (214). This represents a potential therapeutic vulnerability, as the H3K27Ac is bound by BRD4, which can be targeted by BET inhibitors to result in antitumor effects in MCC (214–216); however, the Myc-dependency of this effect has been debated (215).

Other histone methylation marks that may be altered in MCC include H3K9 methylation via PRDM8 (217), and induction of histone changes by sTAg (including H3K4Me2, H4K20me2, and the DNA damage associated phosphorylation of H2AX) (218).

Alongside DNA methylation, histone modifications also appear to be an epigenetic mechanism for immune evasion by MCC. Silencing of antigen-presenting machinery in MCC via histone deacetylation results in loss of surface HLA expression, promoting immune evasion (219). Thus, HDAC inhibitors can restore HLA expression and promote immunogenicity of MCC (189, 219–221). H3K9 deacetylation has been associated with silencing of MHC class I chain-related protein, thus removing an activating signal for NK cell targeting of tumor cells (222). Histone methylation may also play a role in HLA silencing in MCC. Specifically, HLA silencing correlates with loss of global H3K27Me3 in MCC, both in fully developed tumors (208, 223), and during the transition of precursor squamous cells into MCC (173); this silencing can be reversed by EZH2 inhibition (223).

Of small regulatory RNAs, evidence thus far supports roles for microRNAs in MCC tumor biology (224). MCCs display distinct patterns of microRNA expression relative to normal tissues and other skin tumor types (225). In addition, microRNA expression patterns may differ between VP-MCC and VN-MCC (226, 227), possibly due in part to microRNA regulation by MCPyV T-antigen(s) (228). A highly expressed microRNA in a subset of MCC is miR-375 (226, 229). Studies have found that miR-375 may contribute to tumor biology in MCC via intracellular and intercellular mechanisms, although reports are mixed regarding the significance and mechanism of this effect (123, 228, 230–234). In addition to these cellular microRNAs, MCPyV encodes a microRNA, MCV-mir-M1-5p, that may suppress LTAg expression and contribute to viral latency and episomal persistence (134, 228, 235, 236).

3.6 Cell of origin of MCC

MCC was originally named “trabecular carcinoma”, but further investigation soon revealed a high degree of similarity with normal Merkel cells (MCs), prompting a name change to Merkel cell carcinoma (237, 238), and also suggesting these tumors were derived from their namesake. However, multiple lines of evidence now suggest that MCs are not the cell of origin for MCC, including tissue localization, post-mitotic and terminal differentiation status of MCs, differential expression of multiple markers including keratins, as well as the failure of mouse modeling using MC specific drivers (239). Considerable debate about the MCC cell of origin persists, with proposed cells of origin including epithelial, dermal, and lymphoid cell populations (Figure 2) (34, 240, 241).

Furthermore, current genomic data suggests VP- and VN-MCC arise from distinct progenitor populations since VN tumors carry a high UV-signature mutational burden (43, 45, 102), which is characteristic of tumors originating in the epidermis. In contrast, VP tumors harbor few UV-mutations, suggesting they are not derived from sun-damaged epidermal cells, and possibly reside at deeper locations (Figure 2). This is in keeping with the nascent tumors arising in mice with epidermal-driven expression of TAgs and ATOH1, which appeared spatially restricted to the outer root sheath of the hair follicle, near the bulge compartment (242). The lack of UV-mutations, and the dermal location characteristic of MCC, could also be explained by a non-epithelial cell of origin. Interestingly, dermal fibroblasts have a similar mutational burden as VP-MCCs (239, 243) and thus far are the only host cell that has

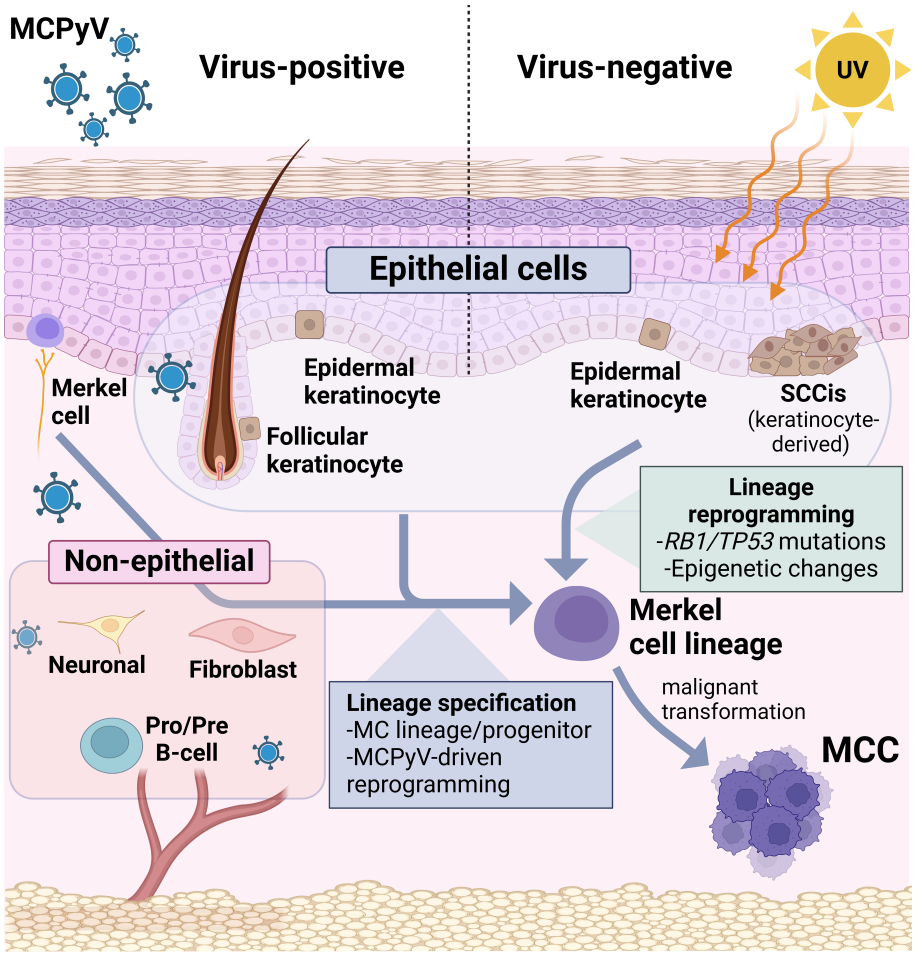

FIGURE 2
Candidates for MCC cell of origin. (Left) Proposed candidates for VP-MCC include many diverse cell types, especially UV-shielded dermal populations such as follicular epithelial cells and precursors, and non-epithelial lineages including neuronal, fibroblast, and pre-pro B-cells. By contrast, direct observations from human tumors strongly suggest epidermal keratinocytes to be the precursors for VN-MCC. In either scenario, lineage reprogramming (with an as-yet unknown trigger) would be required for a shift to the Merkel cell phenotype in addition to malignant transformation.

been shown to support the MCPyV viral life cycle by *in vitro* assays (241). Another non-epithelial candidate cell type with dermal localization is the B-cell lineage, proposed mainly due to MCC expression of early B-cell lineage markers and immunoglobulins (34, 244). Neuronal cells are another possible candidate, since TAg knockdown in VP-MCC cells converts them to a differentiated neuronal phenotype (124).

Although lymphoid or mesenchymal populations have been proposed for the VP-MCC cell of origin, currently, most mouse modeling studies support epithelial populations for this role, since MCPyV TAgs were shown to drive transformation or tumor development in mice from epidermal drivers (117, 118, 138, 242). While murine MCCs only developed upon exogenous ATOH1 expression driving an epidermal-neuroendocrine fate switch, this lineage was also maintained following transient ATOH1 activation (118). This suggests that MCCs may therefore arise from epithelial cells with transitory ATOH1 expression if a neuroendocrine cell fate feed forward loop is established (200, 245, 246). These findings support the concept that commitment to the MC lineage may be a fundamental characteristic of the MCC cell of origin.

Recent data showing mutational overlap between a trichoblastoma and a VP-MCC in a rare combined tumor implies that viral integration in a follicular epithelial cell triggered MCC development (11). Although rare, this case demonstrates the potential for follicular epithelial cells to give rise to human VP-MCC tumors. This aligns with reports of MCPyV protein expression in human follicular epithelial cells, consistent with infection of that cell population by wild-type MCPyV in human skin (247). Furthermore, the appearance of nascent tumors spatially restricted to the hair follicle outer root sheath, in mice with epidermal-driven expression of TAgs and ATOH1, also supports these cells as a potential cell of origin (242).

VN-MCC can display squamous differentiation, or coexist with invasive squamous cell carcinoma or SCCIS (7, 10). Squamous and neuroendocrine areas of differentiation in combined tumors share mutations and copy number abnormalities (159, 172); however, it is

not clear to what extent this similarity reflects squamous metaplasia and/or bidirectional tumor differentiation, rather than evidence for MCC arising within a squamous precursor. Recent studies more specifically comparing SCCIS associated with VN-MCC found that both components share key driver mutations in *TP53* and *RB1* (173, 248, 249) and copy number variations (173, 250). Together, these findings suggest that SCCIS is clonally related to the underlying MCC and thus may be a progenitor lesion. However, these studies did not identify a mutational event responsible for the transition from SCCIS to MCC, rather uncovering a shift associated with epigenetic changes (173, 248).

Comprehensive analysis of DNA-methylation patterns in classical VP- and VN-MCC cell lines suggests an epithelial origin for both MCC subtypes (189, 190). Taken together, these findings provide strong support for an epithelial origin for MCC, and further suggest that VP-MCC and VN-MCC might arise from distinct follicular epithelial and epidermal progenitors, respectively.

4 Emerging and investigational therapies for Merkel cell carcinoma

Immune therapy has improved the prognosis of advanced and metastatic MCC, but is not universally effective or tolerated. Thus, there is continued need for additional therapeutic options that are effective either alone or that work in combination with immunotherapy. Furthermore, the potential benefit of adjuvant or neoadjuvant immunotherapy in MCC must be defined. Here, we review the current status of therapeutic strategies that are being studied in the clinical setting, based upon the fundamental observations of MCC tumor biology described above.

4.1 Adjuvant immunotherapy

Adjuvant immunotherapy trials are underway to determine the efficacy of immunotherapy to prevent disease relapse in treated patients. The ADMEC-O trial (NCT02196961) is evaluating adjuvant nivolumab in treated stage I-IV MCC patients (251). Interim analysis showed a 9% risk reduction at 1 year and 10% at 2 years (252). The STAMP (Surgically Treated Adjuvant Merkel Cell Carcinoma with Pembrolizumab) trial (NCT03712605) is evaluating pembrolizumab as adjuvant therapy in patients with resected stage I-IIIB MCC versus current standard-of-care observation (253). Adjuvant avelumab is being studied in stage III MCC patients in the ADAM (Adjuvant Avelumab in Merkel) trial (NCT03271372) (251). Clinical trial NCT03798639 is studying the effect of nivolumab and radiation or nivolumab and ipilimumab for patients with resected stage IIIA or IIIB MCC (251).

4.2 Neoadjuvant immunotherapy

Neoadjuvant therapy trials are underway for MCC. The Checkmate-358 trial (NCT02488759) evaluated neoadjuvant nivolumab in stage IIA-IV MCC (82). Additional trials are ongoing to evaluate the efficacy of the neoadjuvant approach with immunotherapies including pembrolizumab (NCT05496036), pembrolizumab with lenvatinib (NCT04869137), cemiplimab (NCT04975152), and retifanlimab with cisplatin (NCT05594290) (77). Neoadjuvant intratumoral injection with L19IL2/L19TNF (NCT05329792) and PH-762, an RNAi targeting PD-1 (NCT06014086) is also under evaluation (251).

4.3 Combination immunotherapy

Combination therapy with nivolumab and the CTLA-4 inhibitor ipilimumab is under evaluation as first-line therapy and in checkpoint inhibitor-refractory disease. A randomized, open label phase 2 trial (NCT03071406) evaluated the combination of ipilimumab and nivolumab with or without stereotactic body radiation therapy (SBRT) as first line or following PD-1/PD-L1 monotherapy (254). This study found ORR in both the first-line and second-line treatment groups. A retrospective study of 14 patients from the German-based multi-center prospective skin cancer registry ADOREG demonstrated a response to combined ipilimumab and nivolumab in Avelumab-refractory patients, demonstrating a progression-free survival rate of 42.9% at 12 months and 26.8% at 24 months (255). Conversely, a retrospective study of 13 patients refractory of checkpoint inhibitor inhibition found only a limited benefit from treatment with combination of ipilimumab and nivolumab (256). Another retrospective study, of patients who received rescue therapy following unsuccessful anti-PD1 therapy, observed objective responses in 4/13 patients treated with anti-CTLA4 in combination with immunotherapy, although some responses were not durable (257). The Checkmate-358 trial (NCT02488759) evaluated ipilimumab in combination with nivolumab for metastatic MCC (251); the results have not been published.

4.4 Other immune-based approaches

Given the high immunogenicity of MCC, continued investigations into immune-based approaches other than PD-1/PD-L1 inhibition have substantial promise for identifying effective new therapies. Therapeutic vaccines are an active avenue of investigation for cancer therapy, including MCC (77). In melanoma, a trial evaluating the role of a vaccine against telomerase in combination with pembrolizumab was shown to have preliminary positive results (258). For MCC, vaccines might potentially target either MCPyV epitopes for VP-MCC, or patient-specific tumor neoantigens for VN-MCC (259). Mouse modeling experiments with DNA vaccines based upon LTAg, sTAg, and VP1 peptides have shown promising results (260–263). A phase I DNA vaccine trial utilizing a modified MCPyV LTAg is underway in MCPyV-positive MCC patients (NCT05422781), with results pending (251).

Talimogene laherparepvec (T-VEC) is an injectable engineered oncolytic virus that has been shown to induce an immunologic anti-tumor response in melanoma (264). The efficacy of T-VEC injection

is currently in clinical trials as a single agent in locally advanced MCC (NCT03458117), with or without radiotherapy in metastatic lesions of MCC (NCT02819843), and with nivolumab in refractory disease (NCT02978625) (251).

CD47 is a cell surface ligand that opposes antitumor immunity by preventing immune-mediated phagocytosis. *In vitro* expression of CD47 has been shown to be influenced by the sTAg of MCPyV (147). Anti-CD47 therapy has been investigated in a clinical trial for CTCL which also included MCC (NCT02890368) (147).

Other immune-based therapeutic strategies under investigation for MCC include natural killer cell immunotherapy, stimulating tumor MHC expression (via approaches including interferons or epigenetic modifiers), and adoptive T-cell transfer including chimeric antigen receptor (CAR) T-cells (251, 259).

4.5 Epigenetic therapy

Epigenetic modulation can normalize cell cycle and apoptosis regulation, thus facilitating removal of aberrant cells. Histone deacetylases (HDACs) are a class of enzymes that play an important role in gene expression. Abnormal regulation and expression of HDACs has been identified in several malignancies. Domatinostat is a HDAC class I inhibitor that has shown anti-tumor effects and upregulation of MHC class 1 molecules in MCC cells (221). Domatinostat in combination with Avelumab is currently being evaluated in the MERKLIN 2 trial for patients with advanced MCC who have progressed on anti-checkpoint inhibitor therapy (NCT04393753) (251). The Bromodomains and Extra-terminal Domains (BET) family of proteins also play a role in gene expression. Both a BET inhibitor and BET degrader, JQ1, and BETd-246, respectively, have demonstrated *in vitro* anti-tumor effect in MCC cell lines (215, 216). Similarly, the hypomethylating agent decitabine has shown anti-tumor effects in MCC cell lines and xenograft tumors (189). Finally, as noted above, activity of the histone demethylase LSD1 (KDM1A) may represent a therapeutic vulnerability for MCC (150, 213). These promising early results underscore the need for further investigation of epigenetic modifiers as therapeutics for MCC.

4.6 Targeted therapies in clinical trials

As the underlying mechanisms of MCC tumor biology are more precisely characterized, distinct therapeutic targets will emerge. These might be useful as single agents, in combination with immunotherapy, or for immunotherapy-refractory disease. There have been many trials of investigational agents in both humans and preclinical mouse models based upon biomarker expression patterns and therapeutic performance in other tumor types, as summarized in Table 2 (89, 149, 197, 205–208, 210, 211, 223, 259, 265–274, 277–279, 283–285, 288–294, 304).

5 Preclinical mouse models of MCC

Accurate and reliable preclinical models are invaluable for testing new therapeutic strategies prior to testing in humans. While a better understanding of the molecular pathogenesis of MCC has led to improve *in vitro* and *in vivo* models since the discovery of the MCPyV [reviewed in (305)], multiple questions remain that could be addressed by mouse models. Types of murine models used in cancer research include cell line xenografts (CLX), patient-derived xenografts (PDX), syngeneic models, and genetically engineered mouse models (GEMMs)(Figure 3). Each provides different opportunities or poses specific challenges for investigating tumor initiation, progression, and metastases as well as possible prevention and therapeutic strategies. Successful

TABLE 2 Emerging targets in clinical and preclinical studies.

Target	Rationale	Evidence	*Refs*
MDM2/4 inhibitors	VP-MCC typically harbor wild-type p53 that is functionally inactivated via small T antigen-activation of MDM2. Inhibition of MDM2 and MDM4 removes this suppression of p53.	MDM2/4 inhibitors show reduced growth in mouse MCC models. KRT-232 or Navtemadlin, an oral inhibitor of MDM2, is in clinical trial for immunotherapy-naïve or in combination with Avelumab for checkpoint inhibitor-refractory MCC (NCT03787602).	(149) (265),
EZH2 inhibitors	EZH2 is a histone methyltransferase that has been shown to be overexpressed in MCC and can play a role in tumorigenesis by epigenetic gene silencing. However, the loss of H3K27Me3 in VN-MCC raises questions regarding the role of EZH2, and thus the potential efficacy of EZH2 inhibitors, in that subset of MCC.	Tazemetostat shows reduced growth of MCC in xenografts.	(197, 205–208, 211, 223, 259)
Tyrosine kinase inhibitors (TKIs)	Due to the role of angiogenesis in tumorigenesis, TKIs targeting vascular endothelial growth factor receptor (VEGFR) and related kinases have been investigated as potential therapies for MCC. The tyrosine kinase c-kit is frequently expressed in MCC. However, MCC lacks highly recurrent tyrosine kinase amplification or mutation events that would otherwise provide a rationale for targeted tyrosine kinase inhibitor	Apatinib showed clinical benefit in a case report of one patient with recurrent MCC. Imatinib provided benefit in two case reports. Pazopanib showing temporary benefit in a case report of a patient with MCC. 5 of 24 patients with metastatic MCC demonstrated a clinical response to either pazopanib or cabozantinib (case series).	(266–276)

(Continued)

TABLE 2 Continued

Target	Rationale	Evidence	Refs
	(TKI) therapy. molecular studies have not demonstrated a significant rate of activating mutations of the *KIT* gene, the tyrosine kinase c-kit is frequently expressed in MCC.	A clinical trial of the multi-kinase inhibitor cabozantinib in advanced MCC (NCT02036476) was halted to due toxicities and lack of response. A recent trial including kinase inhibitors as salvage therapy in patients who failed first-line immunotherapy failed to show response. In a phase II trial, patients showed progression of disease on imatinib.	
Anti-apoptosis inhibitors	Pro-survival molecules including Bcl-2 family of proteins and inhibitor of apoptosis proteins (IAP) contributes to tumor biology by prevention of apoptosis. It has been shown that inhibition of these proteins facilitate apoptosis in MCC cells.	Navitoclax, a Bcl-2 family inhibitor showed *in vitro* efficacy in combination with a PI3K kinase inhibitor. Alpelisib induces apoptosis *in vitro* and in mouse models. The novel bcl-2 antisense agent (G3139, Genasense) showed decreased growth in a mouse model. However, a phase II trial of Genasense failed to show efficacy.	(277–282)
Epigenetic modifiers	Histone deacetylase inhibition, histone demethylase inhibition, and hypomethylating agents are an active area of development for many cancers. MCC harbors numerous epigenetic changes as detailed in the text. The sTAg activates the lysine-specific histone demethylase (LSD1) and is required for tumorigenesis.	Multiple LSD1 inhibitors inhibit MCC growth *in vitro* and in xenograft models. The hypomethylating agent decitabine inhibited virus-positive MCC cells *in vitro* and in xenograft models. Histone deacetylase inhibition combined with PD-1/PD-L1 blockade did not show clinical benefit in a series of four patients.	(189, 213, 219, 222)
Antibody-drug conjugates	Antibody-drug conjugates are emerging as a method of treatment for malignancies, including MCC. CD56 is a glycoprotein expressed on neuroendocrine tumors, and has been shown to be expressed on MCC tumors. DLL3 has also been proposed as a target for antibody-drug conjugates.	A conjugate that combines a CD56-targeting antibody to the cytotoxic drug, monomethyl auristatin E inhibits growth in mouse xenograft models of MCC. A Phase I clinical trial using a different (subsequently discontinued) CD56-targeting conjugate reported responses in a minority of patients with MCC.	(283–287)
Somatostatin analogs	Somatostatin analogs have demonstrated efficacy in the treatment of neuroendocrine tumors. Somatostatin receptors are expressed in MCC. Somatostatin analogs are an active area of investigation, especially those paired with radionuclides.	Somatostatin analogs have shown clinical benefit in some MCC patients, although the rates of response to somatostatin analogs as monotherapy has been low.	(288–290)
JAK inhibitors	Janus kinases (JAK) are the intracellular non-receptor tyrosine kinases of the JAK-STAT pathway. A World Health Organization (WHO) international database query identified a disproportionate increase in MCC diagnoses among patients taking the JAK inhibitors ruxolitinib, tofactinib, and baricitinib.	Case reports have validated increased MCC diagnoses in patients treated with JAK inhibitors. However, case reports have also described a robust tumor response upon addition of nivolumab despite continuation of ruxolitinib. Thus, it is currently unclear whether ruxolitinib is antagonistic or synergistic to anti-PD1 therapy.	(291–294)
Ras inhibitors	Ras signaling downstream of receptor tyrosine kinase activity may be amenable to treatment.	Farnesylthiosalicylic acid was associated with reduced growth in MCC xenografts.	(295)
Bromodomain inhibitors	BET family members Brd2, Brd3, and Brd4 are expressed in MCC and upregulate MYC. BET protein inhibitors are being actively developed for several cancers	JQ1 inhibits BET proteins and blocked MCC xenograft growth.	(214–216, 296)
HSP70 inhibitors	LTAgs require heat shock protein 70 (HSP70) family members to exert their transforming activity.	The HSP70 modulator MAL3-101 inhibits tumor growth *in vitro* and in MCC xenograft models.	(297)
PI3K/Akt/ mTOR inhibitors	Activation of the phosphatidylinositide-3-kinase (PI3K)/ AKT/mTOR pathway is frequently detected in MCC	MLN0128 suppress mTOR signaling and blocked MCC xenograft growth. Copanlisib inhibits PI3K signaling *in vitro* and in a MCC xenograft model.	(157, 162, 296, 298)
ABCB5 inhibition	ATP–binding cassette member B5 (ABCB5) mediates chemoresistance. ABCB5 expression was detected in MCC cell lines and tumors at levels significantly higher than those in normal skin. Carboplatin- and etoposide-resistant MCC cell lines exhibited increased expression of ABCB5.	ABCB5 blockade inhibits growth in MCC xenograft models.	(299)
Serine/ threonine kinase inhibitors	Aurora kinase A is being investigated as a target in many cancers. Glycogen synthase kinase (GSK3) may be required for viral T antigen function.	AK-01/LY3295668 (Aurora kinase A inhibitor) and CHIR99021 (GSK3 inhibitor) block MCC growth *in vitro* and in xenograft models.	(300, 301)

(Continued)

TABLE 2 Continued

Target	Rationale	Evidence	Refs
MUC1-C inhibitor	MUC1-C is broadly expressed in MCCs and regulates common sets of signaling pathways related to RNA synthesis, processing, and transport.	GO-203 inhibits MUC1-C and blocks tumor growth *in vitro* and in MCC xenograft model.	(302)
Pyrvinium pamoate	The FDA-approved antihelminthic drug that was identified in a computational drug screen. It was shown to inhibit Wnt signaling, activate p53-mediated apoptosis, and disrupt mitochondrial function.	Pyrvinium pamoate inhibited tumor growth in a MCC xenograft model.	(303)

development of these models is critical to advance understanding of both viral and UV-driven MCC tumors.

5.1 Transplantable MCC mouse models

Establishment of cancer cell lines from human tumors has traditionally allowed for the development of CLX models in immunocompromised mice, which have classically been powerful tools for drug efficacy and toxicity studies, including in MCC (150, 189, 213, 215, 216, 219, 222, 265, 275, 277, 280–282, 284, 295–303).

While the rarity of MCC may in part be responsible for the lack of PDX models to date, several recent studies now provide compelling preclinical data for the use of targeted monotherapies or potential combinatorial regimens in select MCC patients. The PI3K/mTOR/AKT pathway is commonly activated in MCC, and use of the PI3K inhibitor copanlisib, specifically targeting PI3K-α and PI3K-δ isoforms, showed antitumor effects in multiple MCC PDX models compared to other PI3K inhibitors (298). CDK4/6 inhibition with palbociclib increases PD-L1 expression, and when combined with HIF2alpha inhibition results in growth inhibition using both CDX models and a PDX-derived cell line (306). Additionally, PDX models have proven valuable for assessing MDM2 inhibition via the small molecule inhibitor, milademetan, in MCCs with wild-type p53 (265).

Though classically used for therapeutic strategizing, CLX and PDX models have additionally provided opportunities for establishing and characterizing MCC cell lines (277, 307–309). They have been valuable for observing the appearance of circulating MCC tumor cells and metastasis formation (310), determining the requirement of TAg expression in MCC cells (136), as well as for studying vaccine development (260, 261), vasculogenic mimicry as a novel MCC biomarker (311), and circulating microRNA miR-375 as a surrogate biomarker (230). Xenograft models have also helped establish the role of cancer-associated fibroblasts in promoting MCC progression (312).

5.2 Genetically engineered mouse models of MCPyV tumorigenesis

Undoubtedly, transplantable mouse models can be powerful in specific settings. However, a GEMM that develops spontaneous MCC tumors recapitulating the human cancer will provide the best insight into tumor development and reveal possibilities for prevention and treatment. The clonal integration of MCPyV sequences expressing TAgs in MCC supports this virus as the driver of tumorigenesis. However, despite multiple attempts to capitalize on MCPyV TAg expression in mice over the years (117, 118, 138, 139, 242, 313, 314), generation of a faithful, accessible MCC GEMM has been complicated and hindered by the unknown cell of origin.

The *in vitro* transforming potential of sTAg (135) was subsequently corroborated in transgenic mice expressing sTAg (117). Although this study did not yield MCC tumors, it was the first evidence in a mouse model that sTAg expression is sufficient for epithelial transformation. Using a Keratin 5 (K5) promoter to drive expression of wild-type or mutant sTAgs in epidermis, this model revealed that the transformation phenotype was dependent on the sTAg LSD-binding domain. These sTAg transforming studies, initially performed in a preterm embryo model, were validated in an adult model that rapidly developed epidermal hyperplasia and advanced skin lesions with histological changes that collectively recapitulated human squamous cell carcinoma *in situ* (SCCIS), also known as Bowen's disease (117).

That same year, two additional studies implicated the TAgs in cancer formation (138, 139). Use of an epithelial tissue-specific conditional mouse model further demonstrated that a K14-driven MCPyV early region expressing TAgs has tumorigenic activity *in vivo*. These mice also developed epidermal hyperplasia, with some advancing to cutaneous papillomas (138). Another mouse model generated to conditionally express sTAg from the ROSA26 locus revealed ubiquitous sTAg was lethal at high levels, while lower expression could induce a hyperplastic skin phenotype (139). Expression of ubiquitous sTAg in the context of a homozygous p53 deletion in this model generated poorly differentiated malignancies in spleen and liver, however, MCC development was not observed.

Taken together, these initial mouse models demonstrated the capability of sTAg to drive undifferentiated malignancy, epidermal hyperplasia, and epidermal dysplasia, but did not culminate in a neuroendocrine tumor. The lack of MCC development suggests the TAgs might not have been targeted to the appropriate cell population or required the contribution of additional factors. An early theory of MCC origin (no longer considered likely) posited that these represent malignant transformation of Merkel cells (MCs), due to their shared structural and immunohistochemical characteristics (239). However, sTAg-targeted to embryonic or adult Merkel cells showed no sustained proliferative capacity and no transforming potential, even in the p53 null setting (139, 239).

This is consistent with most MCs being post-mitotic or terminally differentiated, and thus unlikely to generate a neoplastic proliferation (315).

Merkel cells themselves have been shown to be derived from an epidermal progenitor in an ATOH1 dependent manner (316, 317), and epidermal expression of ATOH1 in embryonic and adult mice drives formation of ectopic Merkel cells (245). MCC tumors express ATOH1 (27, 28, 30), suggesting that these tumors might arise from epidermal progenitors in a process that recapitulates the differentiation pathway of normal Merkel cells. This insight led to a key advance in MCC mouse modeling. When keratinocytes were reprogrammed to the MC lineage by ATOH1, sTAg expression was sufficient to initiate small blue cell tumors resembling human intraepidermal MCC in late-stage mouse embryos (118). These MCC-like tumors expressed MC markers and K8 and K20 in a clumped or dot-like pattern typically detected in MCC tumor cells (7, 318).

This finding was followed up by a study designed to ascertain whether TAg-expressing epidermal cells reprogrammed to the MC lineage via ATOH1 would develop murine MCC tumors in adult mice (242). These conditional mice expressing sTAg, tLTAg and ATOH1 in *Krt5*-expressing cells and their progeny, yielded microscopic collections of proliferating MCC-like cells, but no gross tumors.

An important modification of this mouse model was additional targeted deletion of *Trp53* (Figure 3). This change, which ensured the loss of p53 activity known to be critical in human MCC tumors, was the final step to yield macroscopic skin tumors with classic MCC histology including a monomorphous small blue cell phenotype, finely stippled chromatin, prominent mitoses, and nuclear molding. Furthermore, they mimicked human MCC tumors at the marker expression level, and cross-species transcriptomic analysis revealed close similarity to human tumors. Thus, this model which relies on epidermal expression of MCPyV TAgs, ectopic expression of ATOH1 to drive epidermal reprogramming, and loss of p53, is the first GEMM to successfully develop murine MCC (242).

5.3 Unmet needs in translational mouse models

Despite the initial promise raised by CLX and PDX studies, targeted approaches for MCC have performed poorly in clinical trials (267, 270, 274, 279, 289), and there is currently no approved targeted therapy for advanced MCC. Since CLX models do not necessarily accurately recapitulate the phenotypic and molecular heterogeneity of MCC tumors, use of PDX models utilizing patient tumor material may be more representative and better predictors of clinical responses to anticancer agents (319–321). Importantly, both CLX and PDX models require immune depleted mice, thus they are not informative for immunotherapy strategies. Preclinical immunotherapy studies are best tested in a mouse model where an intact immune system is present.

For these reasons, "humanized" mouse models, consisting of immune deficient mice with various human immune cell engraftments, used in conjunction with CLXs or PDXs have become fundamentally important in onco-immunology studies (322, 323). Use of a humanized mouse model has suggested the potential application for T-cell-mediated immunotherapy directed against MCPyV TAgs (324). Although not yet extensively used for MCC studies, such humanized mice may provide a powerful platform for testing responsiveness to novel immunotherapies or combination regimens, as well as better predicting clinical responses.

Another alternative strategy is to develop syngeneic models utilizing immune-competent animals. Syngeneic mouse models utilize immune-competent mice that develop tumors derived from murine cancer cells that have been engrafted from genetically identical congenic mouse strains. Syngeneic models are typically considered the workhorse for investigating immunotherapies and studying the immune surveillance of cancer development (322, 325, 326). Since the only current FDA-approved MCC therapies target the PD-1/PD-L1 (programmed cell death protein 1/PD1 ligand) immune checkpoint pathway, which benefits ~50% of MCC patients (73, 75, 76, 78, 327), a syngeneic model would be a tremendous benefit and provide a much-needed immunotherapy pre-clinical model. However, currently there are no syngeneic MCC mouse models available.

To date, MCC viral-driven mouse modeling has focused on expression of individual or TAg combinations, however the role of each has not been fully dissected. sTAg in the absence of LTAg was shown to be the primary oncogenic driver in several mouse models (117, 118, 139). The precise contribution of tLTAg in the latest murine MCC model (242) is currently unknown. A recent study utilizing the previously developed *K14*-driven transgenic mouse expressing both sTAg and tLTAg (138) indicates the resulting epithelial phenotypes are dependent upon the LTAg-pRb interaction (313). The functional role of TAgs was additionally investigated in a multi-stage chemically-induced mouse model of skin carcinogenesis, revealing that expression of TAgs in stratified epithelia synergize with the tumor-inducing agent dimethylbenz(a) anthracene (DMBA), but not the tumor promoter 12-*O*-tetradecanoylphorbol-13-acetate (TPA), suggesting TAgs operate predominantly as tumor promoters (314). Exactly how the MCPyV TAgs contribute to MCC tumorigenesis remains an open question, and poorly understood or disparate functions of TAgs *in vivo* may be a consequence of experimental design and modeling strategies which do not truly recapitulate human MCCs.

The unexpected requirement for the loss of p53 to drive full blown virus-positive murine tumors remains perplexing (242). While *TP53* mutations are common in UV-driven MCCs, they are rare in viral-driven MCC (10, 43, 45, 102) conceivably because sTAg upregulates MDM2 and the MDM4 activator CK1α to repress p53, thus abrogating the need for mutational inactivation (149). Interestingly, the requirement for the loss of p53 in sTAg-induced transformation was seen previously in mouse embryonic fibroblasts and in mice, and it was hypothesized that sTAg induces mitotic catastrophe and p53 activation leading to apoptosis (139). The presence of activated p53 and apoptotic cells in microscopic lesions of adult mice expressing sTAg, tLTAg and ATOH1 potentially supports this theory (242). However, the differential requirement for the loss of *Trp53* in human and mouse TAg-driven tumors may

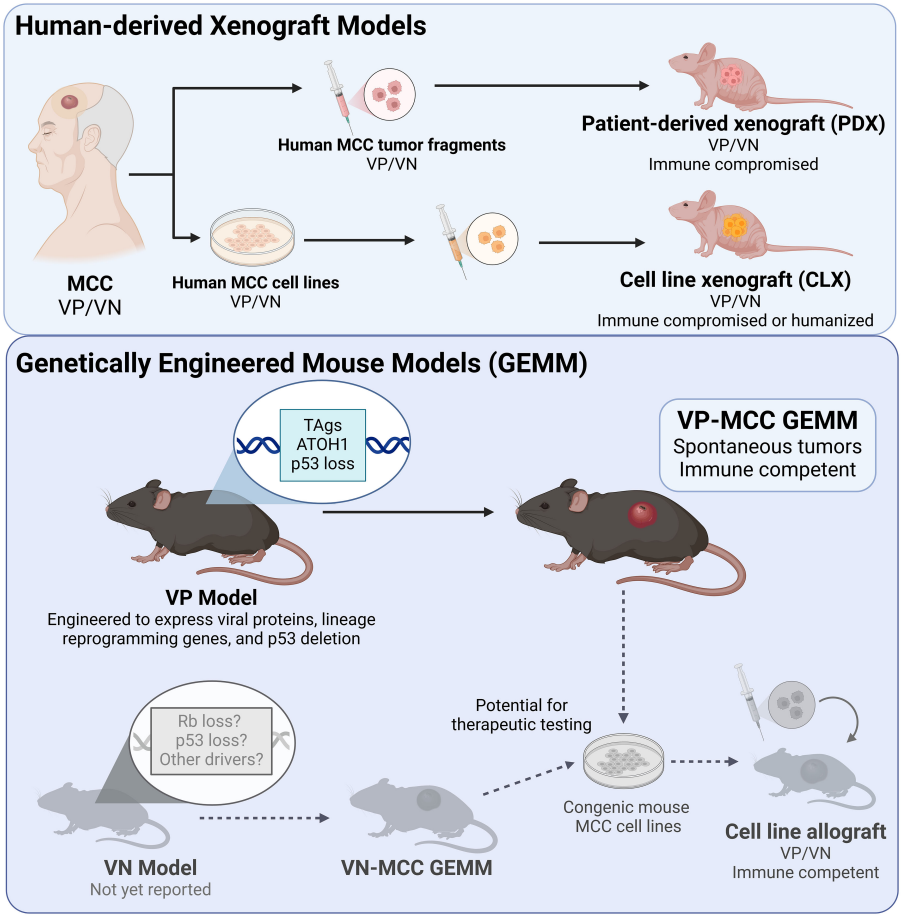

FIGURE 3
Mouse models of MCC. (Top panel) Mouse models of MCC utilizing xenografts of human MCC include patient-derived xenograft models in immune compromised mice, and cell line xenografts in immune compromised or humanized mice. Of these, only humanized mice allow for assessment of antitumor immune response. (Bottom panel) Generation of a murine virus positive (VP) MCC tumor required genetically engineered mice expressing MCC oncoproteins (TAgs) accompanied by ATOH1 for neuroendocrine reprogramming, and inactivation of p53. The resulting tumors can be studied in immune competent mice, allowing for studies of antitumor immunity (such as for immunotherapy). There is currently no virus negative (VN) MCC mouse model, however such a model would presumably require inactivation of the *Trp53* and *RB1* tumor suppressor genes similar to human VN-MCC tumors. Generation of congenic mouse cell lines from VP and VN GEMMs would allow pre-clinical therapeutic studies in an immune competent syngeneic model. Examples in gray have not yet been reported.

be a result of divergence in p53-regulated targets between the species (328). Regardless of mechanism, abrogating p53 activity in viral-driven MCC appears to be critical.

The development of murine MCCs established a fundamental role for the TAgs in viral-driven MCC tumorigenesis. However this model is dependent on the shift of TAg-expressing epidermal cells into a Merkel cell fate via ectopic ATOH1 expression (242). While this highlights the novelty of manipulating cell fate to generate tumors of unknown origin, it does not accurately reflect MCC development in humans. Although expression of MCPyV TAgs in Sox9-positive epidermal cells has recently been shown to drive hyperproliferative lesions and reprogram cells to express neuroendocrine markers, full blown MCC tumors were not observed (125). Determining whether other types of skin cells can be ATOH1-reprogrammed to yield MCCs, or whether different candidate cells of origin are competent to form MCCs without exogenous ATOH1 or p53 deficiency, remains an active area of research.

Effectively modeling VN-MCC in mice remains challenging. Although transplantable VN-MCC mouse models have been successfully generated and utilized (277), there are currently no GEMMs reported in the peer-reviewed literature for this tumor subtype. While the frequent inactivation of *TP53* and *RB1* genes in human VN-MCC tumors indicates this will likely be a prerequisite for development of a VN-MCC GEMM, additional drivers or pathway perturbations that might be required are unclear. Furthermore, the unknown cell of origin and speculation, that VP- and VN-MCCs arise from distinct progenitor populations (2, 173, 239, 248), suggest this mouse model may be particularly challenging to develop.

6 Summary/conclusion

The pathogenesis of MCC has remained poorly understood. Recent studies have fundamentally advanced our understanding

regarding potential cells of origin for MCC, the role of epigenetic modifications in tumor biology, and potential therapeutic options. Remaining challenges include more conclusive evidence for MCC origins, mouse models for VN-MCC, syngeneic mouse models suitable for immunotherapy research, and effective therapies for patients who fail to respond to, or tolerate, immunotherapy.

Author contributions

EP: Conceptualization, Supervision, Visualization, Writing – original draft, Writing – review & editing. MV: Conceptualization, Data curation, Methodology, Project administration, Visualization, Writing – original draft, Writing – review & editing. MJ: Writing – original draft, Writing – review & editing. KH: Writing – original draft, Writing – review & editing. PH: Conceptualization, Project administration, Resources, Supervision, Visualization, Writing – original draft, Writing – review & editing.

Funding

The author(s) declare financial support was received for the research, authorship, and/or publication of this article. PH receives support from the National Institute of Arthritis and Musculoskeletal and Skin Diseases P30 AR075043. MV receives support from the National Cancer Institute R01 CA241947.

Acknowledgments

Figures 2 and 3 were created with Biorender.com.

Conflict of interest

The authors declare that the research was conducted in the absence of any commercial or financial relationships that could be construed as a potential conflict of interest.

Publisher's note

All claims expressed in this article are solely those of the authors and do not necessarily represent those of their affiliated organizations, or those of the publisher, the editors and the reviewers. Any product that may be evaluated in this article, or claim that may be made by its manufacturer, is not guaranteed or endorsed by the publisher.

References

1. Mohsin N, Martin MR, Reed DJ, Vilasi SM, Miao L, Hill NT, et al. Differences in merkel cell carcinoma presentation and outcomes among racial and ethnic groups. *JAMA Dermatol.* (2023) 159:536–40. doi: 10.1001/jamadermatol.2023.0061

2. Harms PW, Harms KL, Moore PS, DeCaprio JA, Nghiem P, Wong MKK, et al. The biology and treatment of Merkel cell carcinoma: current understanding and research priorities. *Nat Rev Clin Oncol.* (2018) 15:763–76. doi: 10.1038/s41571-018-0103-2

3. SChadendorf D, Lebbé C, Zur Hausen A, Avril MF, Hariharan S, Bharmal M, et al. Merkel cell carcinoma: Epidemiology, prognosis, therapy and unmet medical needs. *Eur J Cancer.* (2017) 71:53–69. doi: 10.1016/j.ejca.2016.10.022

4. Paulson KG, Park SY, Vandeven NA, Lachance K, Thomas H, Chapuis AG, et al. Merkel cell carcinoma: Current US incidence and projected increases based on changing demographics. *J Am Acad Dermatol.* (2018) 78:457–463.e2. doi: 10.1016/j.jaad.2017.10.028

5. Harms KL, Healy MA, Nghiem P, Sober AJ, Johnson TM, Bichakjian CK, et al. Analysis of prognostic factors from 9387 merkel cell carcinoma cases forms the basis for the new 8th edition AJCC staging system. *Ann Surg Oncol.* (2016) 23:3564–71. doi: 10.1245/s10434-016-5266-4

6. Silling S, Kreuter A, Gambichler T, Meyer T, Stockfleth E, Wieland U. Epidemiology of merkel cell polyomavirus infection and merkel cell carcinoma. *Cancers.* (2022) 14(24):6176. doi: 10.3390/cancers14246176

7. Tetzlaff MT, Harms PW. Danger is only skin deep: aggressive epidermal carcinomas. An overview of the diagnosis, demographics, molecular-genetics, staging, prognostic biomarkers, and therapeutic advances in Merkel cell carcinoma. *Modern Pathol.* (2020) 33:42–55. doi: 10.1038/s41379-019-0394-6

8. Harms PW. Update on merkel cell carcinoma. *Clin Lab Med.* (2017) 37:485–501. doi: 10.1016/j.cll.2017.05.004

9. Pulitzer M. Merkel cell carcinoma. *Surg Pathol Clin.* (2017) 10:399–408. doi: 10.1016/j.path.2017.01.013

10. Harms KL, Zhao L, Johnson B, Wang X, Carskadon S, Palanisamy N, et al. Virus-positive merkel cell carcinoma is an independent prognostic group with distinct predictive biomarkers. *Clin Cancer res: an Off J Am Assoc Cancer Res.* (2021) 27:2494–504. doi: 10.1158/1078-0432.CCR-20-0864

11. Kervarrec T, Aljundi M, Appenzeller S, Samimi M, Maubec E, Cribier B, et al. Polyomavirus-positive merkel cell carcinoma derived from a trichoblastoma suggests an epithelial origin of this merkel cell carcinoma. *J Invest Dermatol.* (2020) 140:976–85. doi: 10.1016/j.jid.2019.09.026

12. Kervarrec T, Appenzeller S, Tallet A, Jullie ML, Sohier P, Guillonneau F, et al. Detection of wildtype Merkel cell polyomavirus genomic sequence and VP1 transcription in a subset of Merkel cell carcinoma. *Histopathology.* (2024) 84:356–68. doi: 10.1111/his.15068

13. Au RTM, Bundele MM. Endocrine mucin-producing sweat gland carcinoma and associated primary cutaneous mucinous carcinoma: Review of the literature. *J cutaneous Pathol.* (2021) 48:1156–65. doi: 10.1111/cup.13983

14. Jedrych J, Pulitzer M. Primary carcinoid tumor of the skin: a literature review. *Int J Surg Pathol.* (2014) 22:129–35. doi: 10.1177/1066896913516672

15. Goto K, Kukita Y, Honma K, Ohike N, Komori T, Ishida Y, et al. Sweat-gland carcinoma with neuroendocrine differentiation (SCAND): a clinicopathologic study of 13 cases with genetic analysis. *Modern Pathol.* (2022) 35:33–43. doi: 10.1038/s41379-021-00921-8

16. McCalmont TH. Paranuclear dots of neurofilament reliably identify Merkel cell carcinoma. *J cutaneous Pathol.* (2010) 37:821–3. doi: 10.1111/j.1600-0560.2010.01567_1.x

17. Stanoszek LM, Chan MP, Palanisamy N, Carskadon S, Siddiqui J, Patel RM, et al. Neurofilament is superior to cytokeratin 20 in supporting cutaneous origin for neuroendocrine carcinoma. *Histopathology.* (2019) 74:504–13. doi: 10.1111/his.13758

18. Wang L, Harms PW, Palanisamy N, Carskadon S, Cao X, Siddiqui J, et al. Age and gender associations of virus positivity in merkel cell carcinoma characterized using a novel RNA *in situ* hybridization assay. *Clin Cancer Res.* (2017) 23:5622–30. doi: 10.1158/1078-0432.CCR-17-0299

19. Rush PS, Rosenbaum JN, Roy M, Baus RM, Bennett DD, Lloyd RV. Insulinoma-associated 1: A novel nuclear marker in Merkel cell carcinoma (cutaneous neuroendocrine carcinoma). *J cutaneous Pathol.* (2018) 45:129–35. doi: 10.1111/cup.13079

20. Leblebici C, Yeni B, Savli TC, Aydin O, Gunes P, Cinel L, et al. A new immunohistochemical marker, insulinoma-associated protein 1 (INSM1), for Merkel cell carcinoma: Evaluation of 24 cases. *Ann Diagn Pathol.* (2019) 40:53–8. doi: 10.1016/j.anndiagpath.2019.04.002

21. Lilo MT, Chen Y, LeBlanc RE. INSM1 is more sensitive and interpretable than conventional immunohistochemical stains used to diagnose merkel cell carcinoma. *Am J Surg Pathol.* (2018) 42:1541–8. doi: 10.1097/PAS.0000000000001136

22. Fukuhara M, Agnarsdottir M, Edqvist PH, Coter A, Ponten F. SATB2 is expressed in Merkel cell carcinoma. *Arch Dermatol Res.* (2016) 308:449–54. doi: 10.1007/s00403-016-1655-6

23. Kervarrec T, Tallet A, Miquelestorena-Standley E, Houben R, Schrama D, Gambichler T, et al. Diagnostic accuracy of a panel of immunohistochemical and molecular markers to distinguish Merkel cell carcinoma from other neuroendocrine carcinomas. *Modern Pathol*. (2019) 32:499–510. doi: 10.1038/s41379-018-0155-y

24. Bellizzi AM. SATB2 in neuroendocrine neoplasms: strong expression is restricted to well-differentiated tumours of lower gastrointestinal tract origin and is most frequent in Merkel cell carcinoma among poorly differentiated carcinomas. *Histopathology*. (2020) 76:251–64. doi: 10.1111/his.13943

25. Laga AC, Lai CY, Zhan Q, Huang SJ, Velazquez EF, Yang Q, et al. Expression of the embryonic stem cell transcription factor SOX2 in human skin: relevance to melanocyte and merkel cell biology. *Am J Pathol*. (2010) 176:903–13. doi: 10.2353/ajpath.2010.090495

26. Thanguturi S, Tallet A, Miquelestorena-Standley E, Coco C, Le Corre Y, Hainaut-Wierzbicka E, et al. Investigation of the RB1-SOX2 axis constitutes a tool for viral status determination and diagnosis in Merkel cell carcinoma. *Virchows Arch*. (2022) 480:1239–54. doi: 10.1007/s00428-022-03315-6

27. Heiskala K, Arola J, Heiskala M, Andersson LC. Expression of Reg IV and Hath1 in neuroendocrine neoplasms. *Histol histopathol*. (2010) 25:63–72. doi: 10.14670/HH-25.63

28. Gambichler T, Mohtezebsade S, Wieland U, Silling S, Hoh AK, Dreissigacker M, et al. Prognostic relevance of high atonal homolog-1 expression in Merkel cell carcinoma. *J Cancer Res Clin Oncol*. (2017) 143:43–9. doi: 10.1007/s00432-016-2257-6

29. Vilasi SM, Nguyen J, Wang CJ, Miao L, Daily K, Eid M, et al. ATOH1, TFAP2B, and CEACAM6 as immunohistochemical markers to distinguish merkel cell carcinoma and small cell lung cancer. *Cancers*. (2024) 16(4):788. doi: 10.3390/cancers16040788

30. Leonard JH, Cook AL, Van Gele M, Boyle GM, Inglis KJ, Speleman F, et al. Proneural and proneuroendocrine transcription factor expression in cutaneous mechanoreceptor (Merkel) cells and Merkel cell carcinoma. *Int J Cancer J Int du Cancer*. (2002) 101:103–10. doi: 10.1002/ijc.10554

31. Miner AG, Patel RM, Wilson DA, Procop GW, Minca EC, Fullen DR, et al. Cytokeratin 20-negative Merkel cell carcinoma is infrequently associated with the Merkel cell polyomavirus. *Modern Pathol*. (2014) 28(4):498–504. doi: 10.1038/modpathol.2014.148

32. Pasternak S, Carter MD, Ly TY, Doucette S, Walsh NM. Immunohistochemical profiles of different subsets of Merkel cell carcinoma. *Hum Pathol*. (2018) 82:232–8. doi: 10.1016/j.humpath.2018.07.022

33. Kervarrec T, Tallet A, Miquelestorena-Standley E, et al. Morphologic and immunophenotypical features distinguishing Merkel cell polyomavirus-positive and negative Merkel cell carcinoma. *Modern Pathol*. (2019) 32:1605–16. doi: 10.1038/s41379-019-0288-7

34. Zur Hausen A, Rennspiess D, Winnepenninckx V, Speel EJ, Kurz AK. Early B-cell differentiation in Merkel cell carcinomas: clues to cellular ancestry. *Cancer Res*. (2013) 73:4982–7. doi: 10.1158/0008-5472.CAN-13-0616

35. Murakami I, Takata K, Matsushita M, Nonaka D, Iwasaki T, Kuwamoto S, et al. Immunoglobulin expressions are only associated with MCPyV-positive Merkel cell carcinomas but not with MCPyV-negative ones: comparison of prognosis. *Am J Surg Pathol*. (2014) 38:1627–35. doi: 10.1097/PAS.0000000000000279

36. Kirkham N. Small cell melanoma. *Histopathology*. (2002) 40:196–8. doi: 10.1046/j.1365-2559.2002.01317.x

37. Wong AS, du Plessis JJ, Jackett LA. Merkel cell carcinoma: an unusual case with SOX10 nuclear staining. *Pathology*. (2023) 55:718–21. doi: 10.1016/j.pathol.2022.12.352

38. Jackson CR, Linos K. SOX10 dot-like paranuclear positivity in merkel cell carcinoma: report of 2 cases. *Am J dermatopathol*. (2019) 41:694–5. doi: 10.1097/DAD.0000000000001230

39. Miettinen M, McCue PA, Sarlomo-Rikala M, Biernat W, Czapiewski P, Kopczynski J, et al. Sox10–a marker for not only schwannian and melanocytic neoplasms but also myoepithelial cell tumors of soft tissue: a systematic analysis of 5134 tumors. *Am J Surg Pathol*. (2015) 39:826–35. doi: 10.1097/PAS.0000000000000398

40. Nonaka D, Chiriboga L, Rubin BP. Sox10: a pan-schwannian and melanocytic marker. *Am J Surg Pathol*. (2008) 32:1291–8. doi: 10.1097/PAS.0b013e3181658c14

41. Fernandez-Flores A, Suarez-Penaranda JM, Alonso S. Study of EWS/FLI-1 rearrangement in 18 cases of CK20+/CM2B4+ Merkel cell carcinoma using FISH and correlation to the differential diagnosis of Ewing sarcoma/peripheral neuroectodermal tumor. *Appl immunohistochem Mol morphol*. (2013) 21:379–85. doi: 10.1097/PAI.0b013e318273a9e0

42. Harms PW, Collie AM, Hovelson DH, Cani AK, Verhaegen ME, Patel RM, et al. Next generation sequencing of Cytokeratin 20-negative Merkel cell carcinoma reveals ultraviolet-signature mutations and recurrent TP53 and RB1 inactivation. (2016) 29 (3):240–8. doi: 10.1038/modpathol.2015.154

43. Harms PW, Vats P, Verhaegen ME, Robinson DR, Wu YM, Dhanasekaran SM, et al. The distinctive mutational spectra of polyomavirus-negative merkel cell carcinoma. *Cancer Res*. (2015) 75:3720–7. doi: 10.1158/0008-5472.CAN-15-0702

44. Sun L, Cliften PF, Duncavage EJ, Lewis JS Jr., Chernock RD. UV signature mutations reclassify salivary high-grade neuroendocrine carcinomas as occult metastatic cutaneous merkel cell carcinomas. *Am J Surg Pathol*. (2019) 43:682–7. doi: 10.1097/PAS.0000000000001231

45. Wong SQ, Waldeck K, Vergara IA, Schroder J, Madore J, Wilmott JS, et al. UV-associated mutations underlie the etiology of MCV-negative merkel cell carcinomas. *Cancer Res*. (2015) 75:5228–34. doi: 10.1158/0008-5472.CAN-15-1877

46. Fisher CA, Harms PW, McHugh JB, Edwards PC, Siddiqui J, Palanisamy N, et al. Small cell carcinoma in the parotid harboring Merkel cell polyomavirus. *Oral surgery Oral med Oral Pathol Oral Radiol*. (2014) 118:703–12. doi: 10.1016/j.oooo.2014.09.012

47. Chernock RD, Duncavage EJ, Gnepp DR, El-Mofty SK, Lewis JS Jr. Absence of Merkel cell polyomavirus in primary parotid high-grade neuroendocrine carcinomas regardless of cytokeratin 20 immunophenotype. *Am J Surg Pathol*. (2011) 35:1806–11. doi: 10.1097/PAS.0b013e318236a9b0

48. de Biase D, Ragazzi M, Asioli S, Eusebi V. Extracutaneous Merkel cell carcinomas harbor polyomavirus DNA. *Hum Pathol*. (2012) 43:980–5. doi: 10.1016/j.humpath.2011.08.014

49. McEvoy AM, Lachance K, Hippe DS, Cahill K, Moshiri Y, Lewis CW, et al. Recurrence and mortality risk of merkel cell carcinoma by cancer stage and time from diagnosis. *JAMA Dermatol*. (2022) 158:382–9. doi: 10.1001/jamadermatol.2021.6096

50. McEvoy AM, Hippe DS, Lachance K, Park S, Cahill K, Redman M, et al. Merkel cell carcinoma recurrence risk estimation is improved by integrating factors beyond cancer stage: A multivariable model and web-based calculator. *J Am Acad Dermatol*. (2024) 90:569–76. doi: 10.1016/j.jaad.2023.11.020

51. Hoang MP, Donizy P, Wu CL, Kopczynski J, Pieniazek M, Miller DM, et al. TdT expression is a marker of better survival in merkel cell carcinoma, and expression of B-cell markers is associated with merkel cell polyomavirus. *Am J Clin Pathol*. (2020) 154:38–47. doi: 10.1093/ajcp/aqaa017

52. Moshiri AS, Doumani R, Yelistratova L, Blom A, Lachance K, Shinohara MM, et al. Polyomavirus-negative merkel cell carcinoma: A more aggressive subtype based on analysis of 282 cases using multimodal tumor virus detection. *J Invest Dermatol*. (2016) 137(4):819–27. doi: 10.1016/j.jid.2016.10.028

53. Sihto H, Kukko H, Koljonen V, Sankila R, Bohling T, Joensuu H. Merkel cell polyomavirus infection, large T antigen, retinoblastoma protein and outcome in Merkel cell carcinoma. *Clin Cancer Res*. (2011) 17:4806–13. doi: 10.1158/1078-0432.CCR-10-3363

54. Higaki-Mori H, Kuwamoto S, Iwasaki T, Kato M, Murakami I, Nagata K, et al. Association of Merkel cell polyomavirus infection with clinicopathological differences in Merkel cell carcinoma. *Hum Pathol*. (2012) 43:2282–91. doi: 10.1016/j.humpath.2012.04.002

55. Portilla N, Alzate JP, Sierra FA, Parra-Medina R. A Systematic review and Meta-Analysis of the survival and clinicopathological features of p63 expression in Merkel cell carcinoma. *Australas J Dermatol*. (2020) 61:e276–82. doi: 10.1111/ajd.13211

56. Hall BJ, Pincus LB, Yu SS, Oh DH, Wilson AR, McCalmont TH. Immunohistochemical prognostication of Merkel cell carcinoma: p63 expression but not polyomavirus status correlates with outcome. *J cutaneous Pathol*. (2012) 39:911–7. doi: 10.1111/j.1600-0560.2012.01964.x

57. Asioli S, Righi A, Volante M, Eusebi V, Bussolati G. p63 expression as a new prognostic marker in Merkel cell carcinoma. *Cancer*. (2007) 110:640–7. doi: 10.1002/cncr.22828

58. Stetsenko GY, Malekirad J, Paulson KG, et al. p63 expression in Merkel cell carcinoma predicts poorer survival yet may have limited clinical utility. *Am J Clin Pathol*. (2013) 140:838–44. doi: 10.1309/AJCPE4PK6CTBNQJY

59. Feldmeyer L, Hudgens CW, Ray-Lyons G, Nagarajan P, Aung PP, Curry JL, et al. Density, distribution, and composition of immune infiltrates correlate with survival in merkel cell carcinoma. *Clin Cancer Res*. (2016) 22(22):5553–63. doi: 10.1158/1078-0432.CCR-16-0392

60. Sihto H, Bohling T, Kavola H, Koljonen V, Salmi M, Jalkanen S, et al. Tumor infiltrating immune cells and outcome of Merkel cell carcinoma: a population-based study. *Clin Cancer Res*. (2012) 18:2872–81. doi: 10.1158/1078-0432.CCR-11-3020

61. Paulson KG, Iyer JG, Simonson WT, Blom A, Thibodeau RM, Schmidt M, et al. CD8+ lymphocyte intratumoral infiltration as a stage-independent predictor of Merkel cell carcinoma survival: a population-based study. *Am J Clin Pathol*. (2014) 142:452–8. doi: 10.1309/AJCPIKDZM39CRPNC

62. Paulson KG, Iyer JG, Tegeder AR, Thibodeau R, Schelter J, Koba S, et al. Transcriptome-wide studies of merkel cell carcinoma and validation of intratumoral CD8+ lymphocyte invasion as an independent predictor of survival. *J Clin Oncol*. (2011) 29:1539–46. doi: 10.1200/JCO.2010.30.6308

63. Donizy P, Wu CL, Kopczynski J, Pieniazek M, Biecek P, Rys J, et al. Prognostic role of tumoral PD-L1 and IDO1 expression, and intratumoral CD8+ and foxP3+ Lymphocyte infiltrates in 132 primary cutaneous merkel cell carcinomas. *Int J Mol Sci*. (2021) 22(11):5489. doi: 10.3390/ijms22115489

64. Schmults CD, Blitzblau R, Aasi SZ, Alam M, Amini A, Bibee K, et al. NCCN guidelines(R) insights: merkel cell carcinoma, version 1.2024. *J Natl Compr Canc Netw*. (2024) 22(1D):e240002. doi: 10.6004/jnccn.2024.0002

65. Gauci ML, Aristei C, Becker JC, Blom A, Bataille V, Dreno B, et al. Diagnosis and treatment of Merkel cell carcinoma: European consensus-based interdisciplinary guideline - Update 2022. *Eur J Cancer*. (2022) 171:203–31. doi: 10.1016/j.ejca.2022.03.043

66. Singh N, Alexander NA, Lachance K, Lewis CW, McEvoy A, Akaike G, et al. Clinical benefit of baseline imaging in Merkel cell carcinoma: Analysis of 584 patients. *J Am Acad Dermatol*. (2021) 84:330–9. doi: 10.1016/j.jaad.2020.07.065

67. Sims JR, Grotz TE, Pockaj BA, Joseph RW, Foote RL, Otley CC, et al. Sentinel lymph node biopsy in Merkel cell carcinoma: The Mayo Clinic experience of 150 patients. *Surg Oncol*. (2018) 27:11–7. doi: 10.1016/j.suronc.2017.10.005

68. Gupta SG, Wang LC, Penas PF, Gellenthin M, Lee SJ, Nghiem P. Sentinel lymph node biopsy for evaluation and treatment of patients with Merkel cell carcinoma: The Dana-Farber experience and meta-analysis of the literature. *Arch Dermatol*. (2006) 142:685–90. doi: 10.1001/archderm.142.6.685

69. Schwartz JL, Griffith KA, Lowe L, Wong SL, McLean SA, Fullen DR, et al. Features predicting sentinel lymph node positivity in Merkel cell carcinoma. *J Clin Oncol*. (2011) 29:1036–41. doi: 10.1200/JCO.2010.33.4136

70. Grotz TE, Joseph RW, Pockaj BA, Foote RL, Otley CC, Bagaria SP, et al. Negative sentinel lymph node biopsy in merkel cell carcinoma is associated with a low risk of same-nodal-basin recurrences. *Ann Surg Oncol*. (2015) 22:4060–6. doi: 10.1245/s10434-015-4421-7

71. Lee JS, Durham AB, Bichakjian CK, Harms PW, Hayman JA, McLean SA, et al. Completion lymph node dissection or radiation therapy for sentinel node metastasis in merkel cell carcinoma. *Ann Surg Oncol*. (2019) 26:386–94. doi: 10.1245/s10434-018-7072-7

72. Perez MC, Oliver DE, Weitman ES, Boulware D, Messina JL, Torres-Roca J, et al. Management of sentinel lymph node metastasis in merkel cell carcinoma: completion lymphadenectomy, radiation, or both? *Ann Surg Oncol*. (2019) 26:379–85. doi: 10.1245/s10434-018-6810-1

73. Kaufman HL, Russell J, Hamid O, Bhatia S, Terheyden P, D'Angelo SP, et al. Avelumab in patients with chemotherapy-refractory metastatic Merkel cell carcinoma: a multicentre, single-group, open-label, phase 2 trial. *Lancet Oncol*. (2016) 17:1374–85. doi: 10.1016/S1470-2045(16)30364-3

74. D'Angelo SP, Bhatia S, Brohl AS, Hamid O, Mehnert JM, Terheyden P, et al. Avelumab in patients with previously treated metastatic Merkel cell carcinoma (JAVELIN Merkel 200): updated overall survival data after >5 years of follow-up. *ESMO Open*. (2021) 6:100290. doi: 10.1016/j.esmoop.2021.100290

75. D'Angelo SP, Russell J, Lebbe C, Chmielowski B, Gambichler T, Grob JJ, et al. Efficacy and safety of first-line avelumab treatment in patients with stage IV metastatic merkel cell carcinoma: A preplanned interim analysis of a clinical trial. *JAMA Oncol*. (2018) 4:e180077. doi: 10.1001/jamaoncol.2018.0077

76. Bhatia S, Nghiem P, Veeranki SP, Vanegas A, Lachance K, Tachiki L, et al. Real-world clinical outcomes with avelumab in patients with Merkel cell carcinoma treated in the USA: a multicenter chart review study. *J Immunother Cancer*. (2022) 10. doi: 10.1136/jitc-2022-004904

77. Singh N, McClure EM, Akaike T, Park SY, Huynh ET, Goff PH, et al. The evolving treatment landscape of merkel cell carcinoma. *Curr Treat Options Oncol*. (2023) 24:1231–58. doi: 10.1007/s11864-023-01118-8

78. Nghiem PT, Bhatia S, Lipson EJ, Kudchadkar RR, Miller NJ, Annamalai L, et al. PD-1 blockade with pembrolizumab in advanced merkel-cell carcinoma. *N Engl J Med*. (2016) 374:2542–52. doi: 10.1056/NEJMoa1603702

79. Nghiem P, Bhatia S, Lipson EJ, Sharfman WH, Kudchadkar RR, Brohl AS, et al. Durable tumor regression and overall survival in patients with advanced merkel cell carcinoma receiving pembrolizumab as first-line therapy. *J Clin Oncol*. (2019) 37:693–702. doi: 10.1200/JCO.18.01896

80. In brief: Retifanlimab (Zynyz) for Merkel cell carcinoma. *Med Lett Drugs Ther*. (2023) 65:e73–4. doi: 10.58347/tml.2023.1674h

81. Uchi H. Merkel cell carcinoma: an update and immunotherapy. *Front Oncol*. (2018) 8:48. doi: 10.3389/fonc.2018.00048

82. Topalian SL, Bhatia S, Amin A, Kudchadkar RR, Sharfman WH, Lebbe C, et al. Neoadjuvant nivolumab for patients with resectable merkel cell carcinoma in the checkMate 358 trial. *J Clin Oncol*. (2020) 38:2476–87. doi: 10.1200/JCO.20.00201

83. Angeles CV, Sabel MS. Immunotherapy for Merkel cell carcinoma. *J Surg Oncol*. (2021) 123:775–81. doi: 10.1002/jso.26319

84. Iyer JG, Blom A, Doumani R, Lewis C, Tarabadkar ES, Anderson A. Response rates and durability of chemotherapy among 62 patients with metastatic Merkel cell carcinoma. *Cancer Med*. (2016) 5:2294–301. doi: 10.1002/cam4.815

85. Nghiem P, Kaufman HL, Bharmal M, Mahnke L, Phatak H, Becker JC. Systematic literature review of efficacy, safety and tolerability outcomes of chemotherapy regimens in patients with metastatic Merkel cell carcinoma. *Future Oncol*. (2017) 13:1263–79. doi: 10.2217/fon-2017-0072

86. Knepper TC, Montesion M, Russell JS, Sokol ES, Frampton GM, Miller VA, et al. The genomic landscape of merkel cell carcinoma and clinicogenomic biomarkers of response to immune checkpoint inhibitor therapy. *Clin Cancer Res*. (2019) 25:5961–71. doi: 10.1158/1078-0432.CCR-18-4159

87. Kacew AJ, Dharaneeswaran H, Starrett GJ, Thakuria M, LeBoeuf NR, Silk AW, et al. Predictors of immunotherapy benefit in Merkel cell carcinoma. *Oncotarget*. (2020) 11:4401–10. doi: 10.18632/oncotarget.v11i47

88. Spassova I, Ugurel S, Kubat L, Zimmer L, Terheyden P, Mohr A, et al. Clinical and molecular characteristics associated with response to therapeutic PD-1/PD-L1 inhibition in advanced Merkel cell carcinoma. *J Immunother Cancer*. (2022) 10(1): e003198. doi: 10.1136/jitc-2021-003198

89. Nghiem P, Bhatia S, Lipson EJ, Sharfman WH, Kudchadkar RR, Brohl AS, et al. Three-year survival, correlates and salvage therapies in patients receiving first-line pembrolizumab for advanced Merkel cell carcinoma. *J Immunother Cancer*. (2021) 9 (4):e002478. doi: 10.1136/jitc-2021-002478

90. Pulliam T, Jani S, Jing L, Ryu H, Jojic A, Shasha C, et al. Circulating cancer-specific CD8 T cell frequency is associated with response to PD-1 blockade in Merkel cell carcinoma. *Cell Rep Med*. (2024) 5:101412. doi: 10.1016/j.xcrm.2024.101412

91. Ryu H, Bi TM, Pulliam TH, Sarkar K, Church CD, Kumar N, et al. Merkel cell polyomavirus-specific and CD39(+)CLA(+) CD8 T cells as blood-based predictive biomarkers for PD-1 blockade in Merkel cell carcinoma. *Cell Rep Med*. (2024) 5:101390. doi: 10.1016/j.xcrm.2023.101390

92. Church C, Pulliam T, Longino N, Park SY, Smythe KS, Makarov V, et al. Transcriptional and functional analyses of neoantigen-specific CD4 T cells during a profound response to anti-PD-L1 in metastatic Merkel cell carcinoma. *J Immunother Cancer*. (2022) 10(9):e005328. doi: 10.1136/jitc-2022-005328

93. Spassova I, Ugurel S, Terheyden P, Sucker A, Hassel JC, Ritter C, et al. Predominance of central memory T cells with high T-cell receptor repertoire diversity is associated with response to PD-1/PD-L1 inhibition in merkel cell carcinoma. *Clin Cancer Res*. (2020) 26:2257–67. doi: 10.1158/1078-0432.CCR-19-2244

94. Tao Q, Du JX, Zhang S, Lin W, Luo Y, Liu Y, et al. Longitudinal multi-functional analysis identified responses of T cells, B cells, and monocytes as hallmarks of immunotherapy tolerance in patients with merkel cell carcinoma. *PloS One*. (2023) 18:e0293922. doi: 10.1371/journal.pone.0293922

95. Tabachnick-Cherny S, Pulliam T, Rodriguez HJ, Fan X, Hippe DS, Jones DC, et al. Characterization of immunosuppressive myeloid cells in Merkel cell carcinoma: correlation with resistance to PD-1 pathway blockade. *Clin Cancer Res*. (2023) 30 (6):1189–99. doi: 10.1158/1078-0432.CCR-23-1957

96. Giraldo NA, Nguyen P, Engle EL, Kaunitz GJ, Cottrell TR, Berry S, et al. Multidimensional, quantitative assessment of PD-1/PD-L1 expression in patients with Merkel cell carcinoma and association with response to pembrolizumab. *J Immunother Cancer*. (2018) 6:99. doi: 10.1186/s40425-018-0404-0

97. Samimi M, Molet L, Fleury M, Laude H, Carlotti A, Gardair C, et al. Prognostic value of antibodies to Merkel cell polyomavirus T antigens and VP1 protein in patients with Merkel cell carcinoma. *Br J Dermatol*. (2016) 174:813–22. doi: 10.1111/bjd.2016.174.issue-4

98. Paulson KG, Lewis CW, Redman MW, Simonson WT, Lisberg A, Ritter D, et al. Viral oncoprotein antibodies as a marker for recurrence of Merkel cell carcinoma: A prospective validation study. *Cancer*. (2017) 123:1464–74. doi: 10.1002/cncr.30475

99. Akaike T, Hippe DS, So N, Maloney N, Gunnell L, Hall E, et al. Circulating tumor DNA reflects tumor burden and detects early recurrence in patients with Merkel cell carcinoma. presented at: International Society of Investigative Dermatology. Tokyo, Japan *J Invest Dermatol*. (2023) 143(5):S265. doi: 10.26226/m.64199a16337ccc00143861ee

100. Engels EA, Frisch M, Goedert JJ, Biggar RJ, Miller RW. Merkel cell carcinoma and HIV infection. *Lancet*. (2002) 359:497–8. doi: 10.1016/S0140-6736(02)07668-7

101. Feng H, Shuda M, Chang Y, Moore PS. Clonal integration of a polyomavirus in human Merkel cell carcinoma. *Science*. (2008) 319:1096–100. doi: 10.1126/science.1152586

102. Goh G, Walradt T, Markarov V, Blom A, Riaz N, Doumani R, et al. Mutational landscape of MCPyV-positive and MCPyV-negative Merkel cell carcinomas with implications for immunotherapy. *Oncotarget*. (2016) 7:3403–15. doi: 10.18632/oncotarget.v7i3

103. Moens U, Prezioso C, Pietropaolo V. Genetic diversity of the noncoding control region of the novel human polyomaviruses. *Viruses*. (2020) 12(12):1406. doi: 10.3390/v12121406

104. Becker JC, Stang A, DeCaprio JA, Cerroni L, Lebbe C, Veness M, et al. Merkel cell carcinoma. *Nat Rev Dis Primers*. (2017) 3:17077. doi: 10.1038/nrdp.2017.77

105. Yang JF, You J. Merkel cell polyomavirus and associated Merkel cell carcinoma. *Tumour Virus Res*. (2022) 13:200232. doi: 10.1016/j.tvr.2021.200232

106. Wan L, Toland S, Robinson-McCarthy LR, Lee N, Schaich MA, Hengel SR, et al. Unlicensed origin DNA melting by MCV and SV40 polyomavirus LT proteins is independent of ATP-dependent helicase activity. *Proc Natl Acad Sci USA*. (2023) 120: e2308010120. doi: 10.1073/pnas.2308010120

107. Wang R, Yang JF, Senay TE, Liu W, You J. Characterization of the impact of merkel cell polyomavirus-induced interferon signaling on viral infection. *J Virol*. (2023) 97:e0190722. doi: 10.1128/jvi.01907-22

108. Krump NA, Wang R, Liu W, Yang JF, Ma T, You J. Merkel cell polyomavirus infection induces an antiviral innate immune response in human dermal fibroblasts. *J Virol*. (2021) 95:e0221120. doi: 10.1128/JVI.02211-20

109. Kwun HJ, Shuda M, Feng H, Camacho CJ, Moore PS, Chang Y. Merkel cell polyomavirus small T antigen controls viral replication and oncoprotein expression by targeting the cellular ubiquitin ligase SCFFbw7. *Cell Host Microbe*. (2013) 14:125–35. doi: 10.1016/j.chom.2013.06.008

110. Pham AM, Ortiz LE, Lukacher AE, Kwun HJ. Merkel cell polyomavirus large T antigen induces cellular senescence for host growth arrest and viral genome persistence through its unique domain. *Cells*. (2023) 12(3):380. doi: 10.3390/cells12030380

111. Ortiz LE, Pham AM, Kwun HJ. Identification of the merkel cell polyomavirus large tumor antigen ubiquitin conjugation residue. *Int J Mol Sci*. (2021) 22(13):7169. doi: 10.3390/ijms22137169

112. Kwun HJ, Chang Y, Moore PS. Protein-mediated viral latency is a novel mechanism for Merkel cell polyomavirus persistence. *Proc Natl Acad Sci USA*. (2017) 114:E4040–7. doi: 10.1073/pnas.1703879114

113. Dye KN, Welcker M, Clurman BE, Roman A, Galloway DA. Merkel cell polyomavirus Tumor antigens expressed in Merkel cell carcinoma function independently of the ubiquitin ligases Fbw7 and beta-TrCP. *PloS Pathog*. (2019) 15: e1007543. doi: 10.1371/journal.ppat.1007543

114. Kwun HJ, Wendzicki JA, Shuda Y, Moore PS, Chang Y. Merkel cell polyomavirus small T antigen induces genome instability by E3 ubiquitin ligase targeting. *Oncogene*. (2017) 36:6838. doi: 10.1038/onc.2017.389

115. Shuda M, Feng H, Kwun HJ, Rosen ST, Gjoerup O, Moore PS, et al. T antigen mutations are a human tumor-specific signature for Merkel cell polyomavirus. *Proc Natl Acad Sci USA*. (2008) 105:16272–7. doi: 10.1073/pnas.0806526105

116. Moens U, Van Ghelue M, Johannessen M. Oncogenic potentials of the human polyomavirus regulatory proteins. *Cell Mol Life Sci*. (2007) 64:1656–78. doi: 10.1007/s00018-007-7020-3

117. Verhaegen ME, Mangelberger D, Harms PW, Vozheiko TD, Weick JW, Wilbert DM, et al. Merkel cell polyomavirus small T antigen is oncogenic in transgenic mice. *J Invest Dermatol*. (2015) 135:1415–24. doi: 10.1038/jid.2014.446

118. Verhaegen ME, Mangelberger D, Harms PW, Eberl M, Wilbert DM, Meireles J, et al. Merkel cell polyomavirus small T antigen initiates merkel cell carcinoma-like tumor development in mice. *Cancer Res*. (2017) 77:3151–7. doi: 10.1158/0008-5472.CAN-17-0035

119. Shuda M, Velasquez C, Cheng E, Cordek DG, Kwun HJ, Chang Y, et al. CDK1 substitutes for mTOR kinase to activate mitotic cap-dependent protein translation. *Proc Natl Acad Sci USA*. (2015) 112:5875–82. doi: 10.1073/pnas.1505787112

120. Cheng J, Park DE, Berrios C, White EA, Arora R, Yoon R, et al. Merkel cell polyomavirus recruits MYCL to the EP400 complex to promote oncogenesis. *PloS Pathog*. (2017) 13:e1006668. doi: 10.1371/journal.ppat.1006668

121. Kwun HJ, Shuda M, Camacho CJ, Gamper AM, Thant M, Chang Y, et al. Restricted protein phosphatase 2A targeting by Merkel cell polyomavirus small T antigen. *J Virol*. (2015) 89:4191–200. doi: 10.1128/JVI.00157-15

122. Richards KF, Guastafierro A, Shuda M, Toptan T, Moore PS, Chang Y. Merkel cell polyomavirus T antigens promote cell proliferation and inflammatory cytokine gene expression. *J Gen Virol*. (2015) 96:3532–44. doi: 10.1099/jgv.0.000287

123. Fan K, Gravemeyer J, Ritter C, Rasheed K, Gambichler T, Moens U, et al. MCPyV large T antigen-induced atonal homolog 1 is a lineage-dependency oncogene in merkel cell carcinoma. *J Invest Dermatol*. (2020) 140:56–65 e3. doi: 10.1016/j.jid.2019.06.135

124. Harold A, Amako Y, Hachisuka J, Bai Y, Li MY, Kubat L, et al. Conversion of Sox2-dependent Merkel cell carcinoma to a differentiated neuron-like phenotype by T antigen inhibition. *Proc Natl Acad Sci USA*. (2019) 116:20104–14. doi: 10.1073/pnas.1907154116

125. Weber M, Nguyen MB, Li MY, Flora P, Shuda M, Ezhkova E. Merkel cell polyomavirus T antigen-mediated reprogramming in adult merkel cell progenitors. *J Invest Dermatol*. (2023) 143:2163–2176 e6. doi: 10.1016/j.jid.2023.04.031

126. Frost TC, Gartin AK, Liu M, Cheng J, Dharaneeswaran H, Keskin DB, et al. YAP1 and WWTR1 expression inversely correlates with neuroendocrine markers in Merkel cell carcinoma. *J Clin Invest*. (2023) 133(5):e157171. doi: 10.1172/JCI157171

127. Kwun HJ, Guastafierro A, Shuda M, Meinke G, Bohm A, Moore PS, et al. The minimum replication origin of merkel cell polyomavirus has a unique large T-antigen loading architecture and requires small T-antigen expression for optimal replication. *J Virol*. (2009) 83:12118–28. doi: 10.1128/JVI.01336-09

128. Li J, Wang X, Diaz J, Tsang SH, Buck CB, You J. Merkel cell polyomavirus large T antigen disrupts host genomic integrity and inhibits cellular proliferation. *J Virol*. (2013) 87:9173–88. doi: 10.1128/JVI.01216-13

129. Carter JJ, Daugherty MD, Qi X, Bheda-Malge A, Wipf GC, Robinson K, et al. Identification of an overprinting gene in Merkel cell polyomavirus provides evolutionary insight into the birth of viral genes. *Proc Natl Acad Sci USA*. (2013) 110:12744–9. doi: 10.1073/pnas.1303526110

130. Peng WY, Abere B, Shi H, Toland S, Smithgall TE, Moore PS, et al. Membrane-bound Merkel cell polyomavirus middle T protein constitutively activates PLCgamma1 signaling through Src-family kinases. *Proc Natl Acad Sci USA*. (2023) 120:e2316467120. doi: 10.1073/pnas.2316467120

131. Gjoerup O, Chang Y. Update on human polyomaviruses and cancer. *Adv Cancer Res*. (2010) 106:1–51. doi: 10.1016/S0065-230X(10)06001-X

132. Neu U, Hengel H, Blaum BS, Schowalter RM, Macejak D, Gilbert M, et al. Structures of Merkel cell polyomavirus VP1 complexes define a sialic acid binding site required for infection. *PloS pathogens*. (2012) 8:e1002738. doi: 10.1371/journal.ppat.1002738

133. Schowalter RM, Buck CB. The Merkel cell polyomavirus minor capsid protein. *PloS pathogens*. (2013) 9:e1003558. doi: 10.1371/journal.ppat.1003558

134. Lee S, Paulson KG, Murchison EP, Afanasiev OK, Alkan C, Leonard JH, et al. Identification and validation of a novel mature microRNA encoded by the Merkel cell polyomavirus in human Merkel cell carcinomas. *J Clin Virol*. (2011) 52:272–5. doi: 10.1016/j.jcv.2011.08.012

135. Shuda M, Kwun HJ, Feng H, Chang Y, Moore PS. Human Merkel cell polyomavirus small T antigen is an oncoprotein targeting the 4E-BP1 translation regulator. *J Clin Invest*. (2011) 121:3623–34. doi: 10.1172/JCI46323

136. Houben R, Adam C, Baeurle A, Hesbacher S, Grimm J, Angermeyer S, et al. An intact retinoblastoma protein-binding site in Merkel cell polyomavirus large T antigen is required for promoting growth of Merkel cell carcinoma cells. *Int J Cancer J Int du Cancer*. (2012) 130:847–56. doi: 10.1002/ijc.26076

137. Cheng J, Rozenblatt-Rosen O, Paulson KG, Nghiem P, DeCaprio JA. Merkel cell polyomavirus large T antigen has growth-promoting and inhibitory activities. *J Virol*. (2013) 87:6118–26. doi: 10.1128/JVI.00385-13

138. Spurgeon ME, Cheng J, Bronson RT, Lambert PF, DeCaprio JA. Tumorigenic activity of merkel cell polyomavirus T antigens expressed in the stratified epithelium of mice. *Cancer Res*. (2015) 75:1068–79. doi: 10.1158/0008-5472.CAN-14-2425

139. Shuda M, Guastafierro A, Geng X, Shuda Y, Ostrowski SM, Lukianov S, et al. Merkel cell polyomavirus small T antigen induces cancer and embryonic merkel cell proliferation in a transgenic mouse model. *PloS One*. (2015) 10:e014232: doi: 10.1371/journal.pone.0142329

140. Nwogu N, Ortiz LE, Kwun HJ. Surface charge of Merkel cell polyomavirus small T antigen determines cell transformation through allosteric FBW7 WD40 domain targeting. *Oncogenesis*. (2020) 9:53. doi: 10.1038/s41389-020-0235-y

141. Houben R, Shuda M, Weinkam R, Schrama D, Feng H, Chang Y, et al. Merkel cell polyomavirus-infected Merkel cell carcinoma cells require expression of viral T antigens. *J Virol*. (2010) 84:7064–72. doi: 10.1128/JVI.02400-09

142. Shuda M, Chang Y, Moore PS. Merkel cell polyomavirus-positive Merkel cell carcinoma requires viral small T-antigen for cell proliferation. *J Invest Dermatol*. (2014) 134:1479–81. doi: 10.1038/jid.2013.483

143. Khalili K, Sariyer IK, Safak M. Small tumor antigen of polyomaviruses: role in viral life cycle and cell transformation. *J Cell Physiol*. (2008) 215:309–19. doi: 10.1002/jcp.21326

144. Ahmed MM, Cushman CH, DeCaprio JA. Merkel cell polyomavirus: oncogenesis in a stable genome. *Viruses*. (2021) 14(1):58. doi: 10.3390/v14010058

145. Houben R, Angermeyer S, Haferkamp S, Aue A, Goebeler M, Schrama D, et al. Characterization of functional domains in the Merkel cell polyoma virus Large T antigen. *Int J Cancer J Int du Cancer*. (2015) 136:E290–300. doi: 10.1002/ijc.29200

146. Starrett GJ, Thakuria M, Chen T, Marcelus C, Cheng J, Nomburg J, et al. Clinical and molecular characterization of virus-positive and virus-negative Merkel cell carcinoma. *Genome Med Mar 18*. (2020) 12:30. doi: 10.1186/s13073-020-00727-4

147. Schlemeyer T, Ohnezeit D, Virdi S, Korner C, Weisselberg S, Starzonek S, et al. Merkel cell carcinoma and immune evasion: merkel cell polyomavirus small T-antigen –Induced surface changes can be reverted by therapeutic intervention. *J Invest Dermatol*. (2022) 142:3071–3081.e13. doi: 10.1016/j.jid.2022.04.029

148. Griffiths DA, Abdul-Sada H, Knight LM, Jackson BR, Richards K, Prescott EL, et al. Merkel cell polyomavirus small T antigen targets the NEMO adaptor protein to disrupt inflammatory signaling. *J Virol*. (2013) 87:13853–67. doi: 10.1128/JVI.02159-13

149. Park DE, Cheng J, Berrios C, Montero J, Cortes-Cros M, Ferretti S, et al. Dual inhibition of MDM2 and MDM4 in virus-positive Merkel cell carcinoma enhances the p53 response. *Proc Natl Acad Sci USA*. (2019) 116:1027–32. doi: 10.1073/pnas.1818798116

150. Park DE, Cheng J, McGrath JP, Lim MY, Cushman C, Swanson SK, et al. Merkel cell polyomavirus activates LSD1-mediated blockade of non-canonical BAF to regulate transformation and tumorigenesis. *Nat Cell Biol*. (2020) 22:603–15. doi: 10.1038/s41556-020-0503-2

151. Knight LM, Stakaityte G, Wood JJ, Abdul-Sada H, Griffiths DA, Howell GJ, et al. Merkel cell polyomavirus small T antigen mediates microtubule destabilization to promote cell motility and migration. *J Virol*. (2015) 89:35–47. doi: 10.1128/JVI.02317-14

152. Stakaityte G, Nwogu N, Dobson SJ, Knight LM, Wasson CW, Salguero FJ, et al. Merkel cell polyomavirus small T antigen drives cell motility via rho-GTPase-induced filopodium formation. *J Virol*. (2018) 92. doi: 10.1128/JVI.00940-17

153. Nwogu N, Boyne JR, Dobson SJ, Poterlowicz K, Blair GE, Macdonald A, et al. Cellular sheddases are induced by Merkel cell polyomavirus small tumour antigen to mediate cell dissociation and invasiveness. *PloS Pathog*. (2018) 14:e1007276. doi: 10.1371/journal.ppat.1007276

154. Lanclos N, Radulovic P, Bland J, Oganisyan V, Radefeld K, Uversky VN. Implications of intrinsic disorder and functional proteomics in the merkel cell polyomavirus life cycle. *J Cell Biochem*. (2023). doi: 10.1002/jcb.30485

155. Cimino PJ, Robirds DH, Tripp SR, Pfeifer JD, Abel HJ, Duncavage EJ. Retinoblastoma gene mutations detected by whole exome sequencing of Merkel cell carcinoma. *Modern Pathol*. (2014) 27(8):1073–87. doi: 10.1038/modpathol.2013.235

156. Van Gele M, Kaghad M, Leonard JH, Van Roy N, Naeyaert JM, Geerts ML, et al. Mutation analysis of P73 and TP53 in Merkel cell carcinoma. *Br J Cancer*. (2000) 82:823–6. doi: 10.1054/bjoc.1999.1006

157. Nardi V, Song Y, Santamaria-Barria JA, Cosper AK, Lam Q, Faber AC, et al. Activation of PI3K signaling in Merkel cell carcinoma. *Clin Cancer Res*. (2012) 18:1227–36. doi: 10.1158/1078-0432.CCR-11-2308

158. Popp S, Waltering S, Herbst C, Moll I, Boukamp P. UV-B-type mutations and chromosomal imbalances indicate common pathways for the development of Merkel and skin squamous cell carcinomas. *Int J Cancer J Int du Cancer*. (002) 99:352–60. doi: 10.1002/ijc.10321

159. Pulitzer MP, Brannon AR, Berger MF, Louis P, Scott SN, Jungbluth AA, et al. Cutaneous squamous and neuroendocrine carcinoma: genetically and immunohistochemically different from Merkel cell carcinoma. *Modern Pathol*. (2015) 28(8):1023–32. doi: 10.1038/modpathol.2015.60

160. Robb TJ, Ward Z, Houseman P, Woodhouse B, Patel R, Fitzgerald S, et al. Chromosomal aberrations accumulate during metastasis of virus-negative merkel cell carcinoma. *J Invest Dermatol*. (2023) 143:1168–1177 e2. doi: 10.1016/j.jid.2023.01.015

161. Harms KL, Lazo de la Vega L, Hovelson DH, Rahrig S, Cani AK, Liu CJ, et al. Molecular profiling of multiple primary merkel cell carcinoma to distinguish genetically distinct tumors from clonally related metastases. *JAMA Dermatol*. (2017) 153:505–12. doi: 10.1001/jamadermatol.2017.0507

162. Hafner C, Houben R, Baeurle A, Ritter C, Schrama D, Landthaler M, et al. Activation of the PI3K/AKT pathway in Merkel cell carcinoma. *PloS One*. (2012) 7: e31255. doi: 10.1371/journal.pone.0031255

163. Veija T, Sarhadi VK, Koljonen V, Bohling T, Knuutila S. Hotspot mutations in polyomavirus positive and negative Merkel cell carcinomas. *Cancer Genet*. (2016) 209:30–5. doi: 10.1016/j.cancergen.2015.11.006

164. Harms PW, Patel RM, Verhaegen ME, Giordano TJ, Nash KT, Johnson CN, et al. Distinct gene expression profiles of viral- and nonviral-associated merkel cell carcinoma revealed by transcriptome analysis. *J Invest Dermatol*. (2013) 133:936–45. doi: 10.1038/jid.2012.445

165. Karpinski P, Rosales I, Laczmanski L, Kowalik A, Wenson S, Hoang MP. Expression of genes associated with epithelial-mesenchymal transition in merkel cell polyomavirus-negative merkel cell carcinoma. *Lab Invest*. (2023) 103:100177. doi: 10.1016/j.labinv.2023.100177

166. Starrett GJ, Marcelus C, Cantalupo PG, Katz JP, Cheng J, Akagi K, et al. Merkel cell polyomavirus exhibits dominant control of the tumor genome and transcriptome in virus-associated merkel cell carcinoma. *mBio*. (2017) 8(1):e02079-16. doi: 10.1128/mBio.02079-16

167. Sundqvist BZ, Kilpinen SK, Bohling TO, Koljonen VSK, Sihto HJ. Transcriptomic analyses reveal three distinct molecular subgroups of Merkel cell carcinoma with differing prognoses. *Int J Cancer J Int du Cancer*. (2023) 152:2099–108. doi: 10.1002/ijc.34425

168. Torre-Castro J, Rodriguez M, Alonso-Alonso R, Mendoza Cembranos MD, Diaz-Alejo JF, Rebollo-Gonzalez M, et al. LT and SOX9 expression are associated with gene sets that distinguish Merkel cell polyomavirus-positive and -negative Merkel cell carcinoma. *Br J Dermatol*. (2024) 190(6):876–84. doi: 10.1093/bjd/ljae033

169. Jones PA, Baylin SB. The epigenomics of cancer. *Cell*. (2007) 128:683–92. doi: 10.1016/j.cell.2007.01.029

170. Flavahan WA, Gaskell E, Bernstein BE. Epigenetic plasticity and the hallmarks of cancer. *Science*. (2017) 357(6348):eaal2380. doi: 10.1126/science.aal2380

171. Stirzaker C, Taberlay PC, Statham AL, Clark SJ. Mining cancer methylomes: prospects and challenges. *Trends Genet*. (2014) 30:75–84. doi: 10.1016/j.tig.2013.11.004

172. Carter MD, Gaston D, Huang WY, Greer WL, Pasternak S, Ly TY, et al. Genetic profiles of different subsets of Merkel cell carcinoma show links between combined and pure MCPyV-negative tumors. *Hum Pathol*. (2018) 71:117–25. doi: 10.1016/j.humpath.2017.10.014

173. Harms PW, Verhaegen ME, Hu K, Hrycaj SM, Chan MP, Liu CJ, et al. Genomic evidence suggests that cutaneous neuroendocrine carcinomas can arise from squamous dysplastic precursors. *Modern Pathol*. (2022) 35:506–14. doi: 10.1038/s41379-021-00928-1

174. Lao VV, Grady WM. Epigenetics and colorectal cancer. *Nat Rev Gastroenterol Hepatol*. (2011) 8:686–700. doi: 10.1038/nrgastro.2011.173

175. Irizarry RA, Ladd-Acosta C, Wen B, Wu Z, Montano C, Onyango P, et al. The human colon cancer methylome shows similar hypo- and hypermethylation at conserved tissue-specific CpG island shores. *Nat Genet*. (2009) 41:178–86. doi: 10.1038/ng.298

176. Weber M, Hellmann I, Stadler MB, Ramos L, Paabo S, Rebhan M, et al. Distribution, silencing potential and evolutionary impact of promoter DNA methylation in the human genome. *Nat Genet*. (2007) 39:457–66. doi: 10.1038/ng1990

177. Mancarella D, Plass C. Epigenetic signatures in cancer: proper controls, current challenges and the potential for clinical translation. *Genome Med*. (2021) 13:23. doi: 10.1186/s13073-021-00837-7

178. Nunes SP, Henrique R, Jeronimo C, Paramio JM. DNA methylation as a therapeutic target for bladder cancer. *Cells*. (2020) 9(8):1850. doi: 10.3390/cells9081850

179. Baylin SB, Jones PA. Epigenetic determinants of cancer. *Cold Spring Harb Perspect Biol*. (2016) 8(9):a019505. doi: 10.1101/cshperspect.a019505

180. Haag T, Richter AM, Schneider MB, Jimenez AP, Dammann RH. The dual specificity phosphatase 2 gene is hypermethylated in human cancer and regulated by epigenetic mechanisms. *BMC Cancer*. (2016) 16:49. doi: 10.1186/s12885-016-2087-6

181. Richter AM, Haag T, Walesch S, Herrmann-Trost P, Marsch WC, Kutzner H, et al. Aberrant promoter hypermethylation of RASSF family members in merkel cell carcinoma. *Cancers*. (2013) 5:1566–76. doi: 10.3390/cancers5041566

182. Improta G, Ritter C, Pettinato A, Vasta V, Schrama D, Fraggetta F, et al. MGMT promoter methylation status in Merkel cell carcinoma: *in vitro* versus *in vivo*. *J Cancer Res Clin Oncol*. (2017) 143:1489–97. doi: 10.1007/s00432-017-2413-7

183. Lassacher A, Heitzer E, Kerl H, Wolf P. p14ARF hypermethylation is common but INK4a-ARF locus or p53 mutations are rare in Merkel cell carcinoma. *J Invest Dermatol*. (2008) 128:1788–96. doi: 10.1038/sj.jid.5701256

184. Sahi H, Savola S, Sihto H, Koljonen V, Bohling T, Knuutila S. RB1 gene in Merkel cell carcinoma: hypermethylation in all tumors and concurrent heterozygous deletions in the polyomavirus-negative subgroup. *APMIS: Acta pathologica microbiologica immunologica Scandinavica*. (2014) 122:1157–66. doi: 10.1111/apm.2014.122.issue-12

185. Talsma CE, Wang M, Andea AA, Fullen DR, Harms PW, Chan MP. Expression of p16 in Merkel cell carcinoma. *J cutaneous Pathol*. (2021) 48:455–7. doi: 10.1111/cup.13790

186. Gambichler T, Dreissigacker M, Kasakovski D, Skrygan M, Wieland U, Silling S, et al. Patched 1 expression in Merkel cell carcinoma. *J Dermatol*. (2021) 48:64–74. doi: 10.1111/1346-8138.15611

187. Wang X, Yang X, Zhang C, Wang Y, Cheng T, Duan L, et al. Tumor cell-intrinsic PD-1 receptor is a tumor suppressor and mediates resistance to PD-1 blockade therapy. *Proc Natl Acad Sci USA*. (2020) 117:6640–50. doi: 10.1073/pnas.1921445117

188. Ricci C, Morandi L, Righi A, Gibertoni D, Maletta F, Ambrosi F, et al. PD-1 (PDCD1) promoter methylation in Merkel cell carcinoma: prognostic relevance and relationship with clinico-pathological parameters. *Modern Pathol*. (2019) 32:1359–72. doi: 10.1038/s41379-019-0261-5

189. Harms PW, Verhaegen ME, Vo JN, Tien JC, Pratt D, Su F, et al. Viral status predicts patterns of genome methylation and decitabine response in merkel cell carcinoma. *J Invest Dermatol*. (2021) 142(3 Pt A):641–52. doi: 10.1016/j.jid.2021.07.173

190. Gravemeyer J, Spassova I, Verhaegen ME, Dlugosz AA, Hoffmann D, Lange A, et al. DNA-methylation patterns imply a common cellular origin of virus- and UV-associated Merkel cell carcinoma. *Oncogene*. (2022) 41:37–45. doi: 10.1038/s41388-021-02064-1

191. Gujar H, Mehta A, Li HT, Tsai YC, Qiu X, Weisenberger DJ, et al. Characterizing DNA methylation signatures and their potential functional roles in Merkel cell carcinoma. *Genome Med*. (2021) 13:130. doi: 10.1186/s13073-021-00946-3

192. Chteinberg E, Vogt J, Kolarova J, Bormann F, van den Oord J, Speel EJ, et al. The curious case of Merkel cell carcinoma: epigenetic youth and lack of pluripotency. *Epigenetics*. (2020) 15:1319–24. doi: 10.1080/15592294.2020.1773096

193. Kuriyama Y, Shimizu A, Kim J, Yasuda M, Motegi SI. The differential expression of long interspersed nuclear elements-1 as a marker for hypomethylation in Merkel cell carcinoma. *Clin Exp Dermatol*. (2022) 47:1726–8. doi: 10.1111/ced.15265

194. Li W, Xu L. Epigenetic function of TET family, 5-methylcytosine, and 5-hydroxymethylcytosine in hematologic Malignancies. *Oncol Res Treat*. (2019) 42:309–18. doi: 10.1159/000498947

195. Gambichler T, Schmitt K, Ruddel I, Dreibigacker M, Stockfleth E, Becker JC. Decreased 5-hydroxymethylcytosine immunoreactivity in primary Merkel cell carcinoma is a strong predictor for disease-specific death. *Br J Dermatol*. (2019) 181:389–90. doi: 10.1111/bjd.17705

196. Mazziotta C, Lanzillotti C, Gafa R, Touze A, Durand MA, Martini F, et al. The role of histone post-translational modifications in merkel cell carcinoma. *Front Oncol*. (2022) 12:832047. doi: 10.3389/fonc.2022.832047

197. Kim KH, Roberts CW. Targeting EZH2 in cancer. *Nat Med*. (2016) 22:128–34. doi: 10.1038/nm.4036

198. Morschhauser F, Tilly H, Chaidos A, McKay P, Phillips T, Assouline S, et al. Tazemetostat for patients with relapsed or refractory follicular lymphoma: an open-label, single-arm, multicentre, phase 2 trial. *Lancet Oncol*. (2020) 21:1433–42. doi: 10.1016/S1470-2045(20)30441-1

199. Gounder M, Schoffski P, Jones RL, Agulnik M, Cote GM, Villalobos VM, et al. Tazemetostat in advanced epithelioid sarcoma with loss of INI1/SMARCB1: an international, open-label, phase 2 basket study. *Lancet Oncol*. (2020) 21:1423–32. doi: 10.1016/S1470-2045(20)30451-4

200. Bardot ES, Valdes VJ, Zhang J, Perdigoto CN, Nicolis S, Hearn SA, et al. Polycomb subunits Ezh1 and Ezh2 regulate the Merkel cell differentiation program in skin stem cells. *EMBO J*. (2013) 32:1990–2000. doi: 10.1038/emboj.2013.110

201. Busam KJ, Pulitzer MP, Coit DC, Arcila M, Leng D, Jungbluth AA, et al. Reduced H3K27me3 expression in Merkel cell polyoma virus-positive tumors. *Modern Pathol*. (2017) 30:877–83. doi: 10.1038/modpathol.2017.8

202. Marchione DM, Lisby A, Viaene AN, Santi M, Nasrallah M, Wang LP, et al. Histone H3K27 dimethyl loss is highly specific for Malignant peripheral nerve sheath tumor and distinguishes true PRC2 loss from isolated H3K27 trimethyl loss. *Modern Pathol*. (2019) 32:1434–46. doi: 10.1038/s41379-019-0287-8

203. Matsushita M, Iwasaki T, Wardhani LO, Kuwamoto S, Nonaka D, Nagata K, et al. Decreased H3K27me3 expression is associated with merkel cell polyomavirus-negative merkel cell carcinoma, especially combined with cutaneous squamous cell carcinoma. *Anticancer Res*. (2019) 39:5573–9. doi: 10.21873/anticanres.13751

204. Krajisnik A, Rezaee N, Crystal J, Duncan ER, Balzer BL, Frishberg DP, et al. The intricate relationship between H3K27 trimethylation and merkel cell polyomavirus status in merkel cell carcinoma. *Am J dermatopathol*. (2023) 45:783–5. doi: 10.1097/DAD.0000000000002541

205. Veija T, Koljonen V, Bohling T, Kero M, Knuutila S, Sarhadi VK. Aberrant expression of ALK and EZH2 in Merkel cell carcinoma. *BMC Cancer*. (2017) 17:236. doi: 10.1186/s12885-017-3233-5

206. Harms KL, Chubb H, Zhao L, Fullen DR, Bichakjian CK, Johnson TM, et al. Increased expression of EZH2 in Merkel cell carcinoma is associated with disease progression and poorer prognosis. *Hum Pathol*. (2017) 67:78–84. doi: 10.1016/j.humpath.2017.07.009

207. Acikalin A, Bagir E, Paydas S. Prognostic and predictive value of EZH2 expression and the tumor immune microenvironment in Merkel cell carcinoma. *Pol J Pathol*. (2021) 72:140–7. doi: 10.5114/pjp.2021.109516

208. Durand MA, Drouin A, Mouchard A, Durand L, Esnault C, Berthon P, et al. Distinct regulation of EZH2 and its repressive H3K27me3 mark in polyomavirus-positive and -negative merkel cell carcinoma. *J Invest Dermatol*. (2023) 143:1937–1946 e7. doi: 10.1016/j.jid.2023.02.038

209. Bracken AP, Pasini D, Capra M, Prosperini E, Colli E, Helin K. EZH2 is downstream of the pRB-E2F pathway, essential for proliferation and amplified in cancer. *EMBO J*. (2003) 22:5323–35. doi: 10.1093/emboj/cdg542

210. Gartin AK, Frost TC, Cushman CH, Leeper BA, Gokhale PC, DeCaprio JA. Merkel cell carcinoma sensitivity to EZH2 inhibition is mediated by SIX1 derepression. *J Invest Dermatol*. (2022) 142:2783–2792.e15. doi: 10.1016/j.jid.2022.03.008

211. Khattri M, Amako Y, Gibbs JR, Collura JL, Arora R, Harold A, et al. Methyltransferase-independent function of enhancer of zeste homologue 2 maintains tumorigenicity induced by human oncogenic papillomavirus and polyomavirus. *Tumour Virus Res*. (2023) 16:200264. doi: 10.1016/j.tvr.2023.200264

212. Paulson KG, Lemos BD, Feng B, Jaimes N, Penas PF, Bi X, et al. Array-CGH reveals recurrent genomic changes in Merkel cell carcinoma including amplification of L-Myc. *J Invest Dermatol*. (2009) 129:1547–55. doi: 10.1038/jid.2008.365

213. Leiendecker L, Jung PS, Krecioch I, Neumann T, Schleiffer A, Mechtler K, et al. LSD1 inhibition induces differentiation and cell death in Merkel cell carcinoma. *EMBO Mol Med*. (2020) 12:e12525. doi: 10.15252/emmm.202012525

214. Sengupta D, Kannan A, Kern M, Moreno MA, Vural E, Stack B Jr, et al. Disruption of BRD4 at H3K27Ac-enriched enhancer region correlates with decreased c-Myc expression in Merkel cell carcinoma. *Epigenetics*. (2015) 10:460–6. doi: 10.1080/15592294.2015.1034416

215. Choi JE, Verhaegen ME, Yazdani S, Malik R, Harms PW, Mangelberger D, et al. Characterizing the therapeutic potential of a potent BET degrader in merkel cell carcinoma. *Neoplasia*. (2019) 21:322–30. doi: 10.1016/j.neo.2019.01.003

216. Shao Q, Kannan A, Lin Z, Stack BC Jr., Suen JY, Gao L. BET protein inhibitor JQ1 attenuates Myc-amplified MCC tumor growth *in vivo*. *Cancer Res*. (2014) 74:7090–102. doi: 10.1158/0008-5472.CAN-14-0305

217. Orouji E, Peitsch WK, Orouji A, Houben R, Utikal J. Unique role of histone methyltransferase PRDM8 in the tumorigenesis of virus-negative merkel cell carcinoma. *Cancers*. (2020) 12(4):1057. doi: 10.3390/cancers12041057

218. Wu JH, Narayanan D, Limmer AL, Simonette RA, Rady PL, Tyring SK. Merkel cell polyomavirus small T antigen induces DNA damage response. *Intervirology*. (2019) 62:96–100. doi: 10.1159/000501419

219. Ritter C, Fan K, Paschen A, Reker Hardrup S, Ferrone S, Nghiem P, et al. Epigenetic priming restores the HLA class-I antigen processing machinery expression in Merkel cell carcinoma. *Sci Rep*. (2017) 7:2290. doi: 10.1038/s41598-017-02608-0

220. Ugurel S, Spassova I, Wohlfarth J, Drusio C, Cherouny A, Melior A, et al. MHC class-I downregulation in PD-1/PD-L1 inhibitor refractory Merkel cell carcinoma and its potential reversal by histone deacetylase inhibition: a case series. *Cancer Immunol Immunother*. (2019) 68:983–90. doi: 10.1007/s00262-019-02341-9

221. Song L, Bretz AC, Gravemeyer J, Spassova I, Muminova S, Gambichler T, et al. The HDAC inhibitor domatinostat promotes cell-cycle arrest, induces apoptosis, and increases immunogenicity of merkel cell carcinoma cells. *J Invest Dermatol*. (2021) 141:903–912 e4. doi: 10.1016/j.jid.2020.08.023

222. Ritter C, Fan K, Paulson KG, Nghiem P, Schrama D, Becker JC. Reversal of epigenetic silencing of MHC class I chain-related protein A and B improves immune recognition of Merkel cell carcinoma. *Sci Rep*. (2016) 6:21678. doi: 10.1038/srep21678

223. Durand MA, Drouin A, Bachiri K, Durand L, Berthon P, Houben R, et al. Enhancer of zeste homolog 2 inhibition induces HLA class I re-expression in merkel cell carcinoma. *J Invest Dermatol*. (2023) 144(6):1398–401.e1. doi: 10.1016/j.jid.2023.10.036

224. Mazziotta C, Cervellera CF, Lanzillotti C, Touze A, Gaboriaud P, Tognon M, et al. MicroRNA dysregulations in Merkel cell carcinoma: Molecular mechanisms and clinical applications. *J Med Virol*. (2023) 95:e2837: doi: 10.1002/jmv.28375

225. Ning MS, Kim AS, Prasad N, Levy SE, Zhang H, Andl T. Characterization of the merkel cell carcinoma miRNome. *J skin cancer*. (2014) 2014:289548. doi: 10.1155/2014/289548

226. Xie H, Lee L, Caramuta S, Hoog A, Browaldh N, Bjornhagen V, et al. MicroRNA expression patterns related to merkel cell polyomavirus infection in human merkel cell carcinoma. *J Invest Dermatol*. (2014) 134:507–17. doi: 10.1038/jid.2013.355

227. Veija T, Sahi H, Koljonen V, Bohling T, Knuutila S, Mosakhani N. miRNA-34a underexpressed in Merkel cell polyomavirus-negative Merkel cell carcinoma. *Virchows Arch*. (2015) 466:289–95. doi: 10.1007/s00428-014-1700-9

228. Kumar S, Xie H, Shi H, Gao J, Juhlin CC, Bjornhagen V, et al. Merkel cell polyomavirus oncoproteins induce microRNAs that suppress multiple autophagy genes. *Int J Cancer J Int du Cancer*. (2020) 146:1652–66. doi: 10.1002/ijc.32503

229. Renwick N, Cekan P, Masry PA, McGeary SE, Miller JB, Hafner M, et al. Multicolor microRNA FISH effectively differentiates tumor types. *J Clin Invest*. (2013) 123:2694–702. doi: 10.1172/JCI68760

230. Fan K, Ritter C, Nghiem P, Blom A, Verhaegen ME, Dlugosz A, et al. Circulating cell-free miR-375 as surrogate marker of tumor burden in merkel cell carcinoma. *Clin Cancer Res*. (2018) 24:5873–82. doi: 10.1158/1078-0432.CCR-18-1184

231. Kumar S, Xie H, Scicluna P, Lee L, Bjornhagen V, Hoog A, et al. MiR-375 regulation of LDHB plays distinct roles in polyomavirus-positive and -negative merkel cell carcinoma. *Cancers*. (2018) 10(11):443. doi: 10.3390/cancers10110443

232. Abraham KJ, Zhang X, Vidal R, Pare GC, Feilotter HE, Tron VA. Roles for miR-375 in Neuroendocrine Differentiation and Tumor Suppression via Notch Pathway Suppression in Merkel Cell Carcinoma. *Am J Pathol*. (2016) 186:1025–35. doi: 10.1016/j.ajpath.2015.11.020

233. Fan K, Spassova I, Gravemeyer J, Ritter C, Horny K, Lange A, et al. Merkel cell carcinoma-derived exosome-shuttle miR-375 induces fibroblast polarization by inhibition of RBPJ and p53. *Oncogene*. (2021) 40:980–96. doi: 10.1038/s41388-020-01576-6

234. Fan K, Zebisch A, Horny K, Schrama D, Becker JC. Highly Expressed miR-375 is not an Intracellular Oncogene in Merkel Cell Polyomavirus-Associated Merkel Cell Carcinoma. *Cancers*. (2020) 12(3):529. doi: 10.3390/cancers12030529

235. Seo GJ, Chen CJ, Sullivan CS. Merkel cell polyomavirus encodes a microRNA with the ability to autoregulate viral gene expression. *Virol Jan 20*. (2009) 383:183–7. doi: 10.1016/j.virol.2008.11.001

236. Theiss JM, Gunther T, Alawi M, Neumann F, Tessmer U, Fischer N, et al. A comprehensive analysis of replicating merkel cell polyomavirus genomes delineates the viral transcription program and suggests a role for mcv-miR-M1 in episomal persistence. *PloS Pathog*. (2015) 11:e1004974. doi: 10.1371/journal.ppat.1004974

237. Toker C. Trabecular carcinoma of the skin. A question of title. *Am J dermatopathol*. (1982) 4:497–500. doi: 10.1097/00000372-198212000-00003

238. Rywlin AM. Malignant Merkel-cell tumor is a more accurate description than trabecular carcinoma. *Am J dermatopathol*. (1982) 4:513–5. doi: 10.1097/00000372-198212000-00007

239. Sunshine JC, Jahchan NS, Sage J, Choi J. Are there multiple cells of origin of Merkel cell carcinoma? *Oncogene*. (2018) 37:1409–16. doi: 10.1038/s41388-017-0073-3

240. Tilling T, Moll I. Which are the cells of origin in merkel cell carcinoma? *J skin cancer*. (2012) 2012:680410. doi: 10.1155/2012/680410

241. Liu W, Yang R, Payne AS, Schowalter RM, Spurgeon ME, Lambert PF, et al. Identifying the target cells and mechanisms of merkel cell polyomavirus infection. *Cell Host Microbe*. (2016) 19:775–87. doi: 10.1016/j.chom.2016.04.024

242. Verhaegen ME, Harms PW, Van Goor JJ, Arche J, Patrick MT, Wilbert D, et al. Direct cellular reprogramming enables development of viral T antigen-driven Merkel cell carcinoma in mice. *J Clin Invest*. (2022) 132(7):e152069. doi: 10.1172/JCI152069

243. Milholland B, Dong X, Zhang L, Hao X, Suh Y, Vijg J. Differences between germline and somatic mutation rates in humans and mice. *Nat Commun*. (2017) 8:15183. doi: 10.1038/ncomms15183

244. Sauer CM, Haugg AM, Chteinberg E, Rennspiess D, Winnepenninckx V, Speel EJ, et al. Reviewing the current evidence supporting early B-cells as the cellular origin of Merkel cell carcinoma. *Crit Rev Oncol Hematol*. (2017) 116:99–105. doi: 10.1016/j.critrevonc.2017.05.009

245. Ostrowski SM, Wright MC, Bolock AM, Geng X, Maricich SM. Ectopic Atoh1 expression drives Merkel cell production in embryonic, postnatal and adult mouse epidermis. *Development*. (2015) 142:2533–44. doi: 10.1242/dev.123141

246. Helms AW, Abney AL, Ben-Arie N, Zoghbi HY, Johnson JE. Autoregulation and multiple enhancers control Math1 expression in the developing nervous system. *Development*. (2000) 127:1185–96. doi: 10.1242/dev.127.6.1185

247. Nemeth K, Gorog A, Mezey E, Pinter D, Kuroli E, Harsing J, et al. Cover Image: Detection of hair follicle-associated Merkel cell polyomavirus in an immunocompromised host with follicular spicules and alopecia. *Br J Dermatol*. (2016) 175:1409. doi: 10.1111/bjd.15039

248. Kervarrec T, Appenzeller S, Samimi M, Sarma B, Sarosi EM, Berthon P, et al. Merkel cell polyomavirusNegative merkel cell carcinoma originating from in situ squamous cell carcinoma: A keratinocytic tumor with neuroendocrine differentiation. *J Invest Dermatol*. (2022) 142:516–27. doi: 10.1016/j.jid.2021.07.175

249. DeCoste RC, Walsh NM, Gaston D, Ly TY, Pasternak S, Cutler S, et al. RB1-deficient squamous cell carcinoma: the proposed source of combined Merkel cell carcinoma. *Modern Pathol*. (2022). doi: 10.1038/s41379-022-01151-2

250. Pacaud M, Kervarrec T, Masliah-Planchon J, Tallet A, Collin C, Guyetant S, et al. Merkel cell carcinoma from renal transplant recipients are mostly MCPyV-negative and are frequently associated with squamous cell carcinomas or precursors. *J Eur Acad Dermatol Venereol*. (2023). doi: 10.1111/jdv.19076

251. (2023). clinicaltrials.gov (Accessed December 30, 2023).

252. Becker JC, Ugurel S, Leiter U, Meier F, Gutzmer R, Haferkamp S, et al. Adjuvant immunotherapy with nivolumab versus observation in completely resected Merkel cell carcinoma (ADMEC-O): disease-free survival results from a randomised, open-label, phase 2 trial. *Lancet*. (2023) 402:798–808. doi: 10.1016/S0140-6736(23)00769-9

253. Teke ME, Rossi AJ, Hernandez JM, Gastman B. Pembrolizumab compared with standard-of-care observation in treating patients with completely resected stage I-III merkel cell cancer (STAMP). *Ann Surg Oncol*. (2022) 6:3379–80. doi: 10.1245/s10434-022-11498-0

254. Kim S, Wuthrick E, Blakaj D, Eroglu Z, Verschraegen C, Thapa R, et al. Combined nivolumab and ipilimumab with or without stereotactic body radiation therapy for advanced Merkel cell carcinoma: a randomised, open label, phase 2 trial. *Lancet*. (2022) 400:1008–19. doi: 10.1016/S0140-6736(22)01659-2

255. Glutsch V, Schummer P, Kneitz H, Gesierich A, Goebeler M, Klein D, et al. Ipilimumab plus nivolumab in avelumab-refractory Merkel cell carcinoma: a multicenter study of the prospective skin cancer registry ADOREG. *J Immunother Cancer*. (2022) 10(11):e005930. doi: 10.1136/jitc-2022-005930

256. Shalhout SZ, Emerick KS, Kaufman HL, Silk AW, Thakuria M, Miller DM. A retrospective study of ipilimumab plus nivolumab in anti-PD-L1/PD-1 refractory merkel cell carcinoma. *J Immunother*. (2022) 45:299–302. doi: 10.1097/CJI.0000000000000432

257. LoPiccolo J, Schollenberger MD, Dakhil S, Rosner S, Ali O, Sharfman WH, et al. Rescue therapy for patients with anti-PD-1-refractory Merkel cell carcinoma: a multicenter, retrospective case series. *J Immunother Cancer*. (2019) 7:170. doi: 10.1186/s40425-019-0661-6

258. Ellingsen EB, O'Day S, Mezheyeuski A, Gromadka A, Clancy T, Kristedja TS, et al. Clinical activity of combined telomerase vaccination and pembrolizumab in advanced melanoma: results from a phase I trial. *Clin Cancer Res*. (2023) 29:3026–36. doi: 10.1158/1078-0432.CCR-23-0416

259. Celikdemir B, Houben R, Kervarrec T, Samimi M, Schrama D. Current and preclinical treatment options for Merkel cell carcinoma. *Expert Opin Biol Ther*. (2023) 23:1015–34. doi: 10.1080/14712598.2023.2257603

260. Gomez B, He L, Tsai YC, Wu TC, Viscidi RP, Hung CF. Creation of a Merkel cell polyomavirus small T antigen-expressing murine tumor model and a DNA vaccine targeting small T antigen. *Cell Biosci*. (2013) 3:29. doi: 10.1186/2045-3701-3-29

261. Zeng Q, Gomez BP, Viscidi RP, Peng S, He L, Ma B, et al. Development of a DNA vaccine targeting Merkel cell polyomavirus. *Vaccine*. (2012) 30:1322–9. doi: 10.1016/j.vaccine.2011.12.072

262. Gomez BP, Wang C, Viscidi RP, Peng S, He L, Wu TC, et al. Strategy for eliciting antigen-specific CD8+ T cell-mediated immune response against a cryptic CTL epitope of merkel cell polyomavirus large T antigen. *Cell Biosci*. (2012) 2:36. doi: 10.1186/2045-3701-2-36

263. Xu D, Jiang S, He Y, Jin X, Zhao G, Wang B. Development of a therapeutic vaccine targeting Merkel cell polyomavirus capsid protein VP1 against Merkel cell carcinoma. *NPJ Vaccines*. (2021) 6:119. doi: 10.1038/s41541-021-00382-9

264. Shalhout SZ, Miller DM, Emerick KS, Kaufman HL. Therapy with oncolytic viruses: progress and challenges. *Nat Rev Clin Oncol*. (2023) 20:160–77. doi: 10.1038/s41571-022-00719-w

265. Ananthapadmanabhan V, Frost TC, Soroko KM, Knott A, Magliozzi BJ, Gokhale PC, et al. Milademetan is a highly potent MDM2 inhibitor in Merkel cell carcinoma. *JCI Insight*. (2022) 7(13):e160513. doi: 10.1172/jci.insight.160513

266. Feng Y, Song X, Jia R. Case report: favorable response to the tyrosine kinase inhibitor apatinib in recurrent merkel cell carcinoma. *Front Oncol*. (2021) 11:625360. doi: 10.3389/fonc.2021.625360

267. Davids MS, Charlton A, Ng SS, Chong ML, Laubscher K, Dar M, et al. Response to a novel multitargeted tyrosine kinase inhibitor pazopanib in metastatic Merkel cell carcinoma. *J Clin Oncol*. (2009) 27:e97–100. doi: 10.1200/JCO.2009.21.8149

268. Tarabadkar ES, Thomas H, Blom A, Parvathaneni U, Olencki T, Nghiem P, et al. Clinical benefit from tyrosine kinase inhibitors in metastatic merkel cell carcinoma: A case series of 5 patients. *Am J Case Rep*. (2018) 19:505–11. doi: 10.12659/AJCR.908649

269. Maroto P, Porta C, Capdevila J, Apolo AB, Viteri S, Rodriguez-Antona C, et al. Cabozantinib for the treatment of solid tumors: a systematic review. *Ther Adv Med Oncol*. (2022) 14:17588359221107112. doi: 10.1177/17588359221107112

270. Rabinowits G, Lezcano C, Catalano PJ, McHugh P, Becker H, Reilly MM, et al. Cabozantinib in patients with advanced merkel cell carcinoma. *Oncologist*. (2018) 23:814–21. doi: 10.1634/theoncologist.2017-0552

271. Su LD, Fullen DR, Lowe L, Uherova P, Schnitzer B, Valdez R. CD117 (KIT receptor) expression in Merkel cell carcinoma. *Am J dermatopathol*. (2002) 24:289–93. doi: 10.1097/00000372-200208000-00001

272. Frenard C, Peuvrel L, Brocard A, Saint-Jean M, Moreau A, Dreno B, et al. Dramatic response of an inoperable Merkel cell carcinoma with imatinib. *JAAD Case Rep*. (2016) 1:16–8. doi: 10.1016/j.jdcr.2015.10.007

273. Loader DE, Feldmann R, Baumgartner M, Breier F, Schrama D, Becker JC, et al. Clinical remission of Merkel cell carcinoma after treatment with imatinib. *J Am Acad Dermatol*. (2013) 69:e181–3. doi: 10.1016/j.jaad.2013.03.042

274. Samlowski WE, Moon J, Tuthill RJ, Heinrich MC, Balzer-Haas NS, Merl SA, et al. A phase II trial of imatinib mesylate in merkel cell carcinoma (neuroendocrine carcinoma of the skin): A Southwest Oncology Group study (S0331). *Am J Clin Oncol*. (2010) 33:495–9. doi: 10.1097/COC.0b013e3181b9cf04

275. Knepper TC, Panchaud RA, Muradova E, Cohen L, DeCaprio JA, Khushalani NI, et al. An analysis of the use of targeted therapies in patients with advanced Merkel cell carcinoma and an evaluation of genomic correlates of response. *Cancer Med*. (2021) 10:5889–96. doi: 10.1002/cam4.4138

276. Swick BL, Ravdel L, Fitzpatrick JE, Robinson WA. Merkel cell carcinoma: evaluation of KIT (CD117) expression and failure to demonstrate activating mutations in the C-KIT proto-oncogene - implications for treatment with imatinib mesylate. *J cutaneous Pathol*. (2007) 34:324–9. doi: 10.1111/j.1600-0560.2006.00613.x

277. Verhaegen ME, Mangelberger D, Weick JW, Vozheiko TD, Harms PW, Nash KT, et al. Merkel cell carcinoma dependence on bcl-2 family members for survival. *J Invest Dermatol*. (2014). doi: 10.1038/jid.2014.138

278. Chteinberg E, Wetzels S, Gerritsen W, Temmerman L, van den Oord J, Biessen E, et al. Navitoclax combined with Alpelisib effectively inhibits Merkel cell carcinoma cell growth in *vitro*. *Ther Adv Med Oncol*. (2020) 12:1758835920975621. doi: 10.1177/1758835920975621

279. Shah MH, Varker KA, Collamore M, Zwiebel JA, Coit D, Kelsen D, et al. G3139 (Genasense) in patients with advanced merkel cell carcinoma. *Am J Clin Oncol*. (2009) 32:174–9. doi: 10.1097/COC.0b013e31817eebf8

280. Schlagbauer-Wadl H, Klosner G, Heere-Ress E, Waltering S, Moll I, Wolff K, et al. Bcl-2 antisense oligonucleotides (G3139) inhibit Merkel cell carcinoma growth in SCID mice. *J Invest Dermatol*. (2000) 114:725–30. doi: 10.1046/j.1523-1747.2000.00937.x

281. Arora R, Shuda M, Guastafierro A, Feng H, Toptan T, Tolstov Y, et al. Survivin is a therapeutic target in Merkel cell carcinoma. *Sci Trans Med*. (2012) 4:133ra56. doi: 10.1126/scitranslmed.3003713

282. Dresang LR, Guastafierro A, Arora R, Normolle D, Chang Y, Moore PS. Response of Merkel cell polyomavirus-positive merkel cell carcinoma xenografts to a survivin inhibitor. *PloS One*. (2013) 8:e80543. doi: 10.1371/journal.pone.0080543

283. Leiendecker L, Jung PS, Obenauf AC. Targeting CD56 with an antibody-drug conjugate in Merkel cell carcinoma. *Br J Dermatol*. (2022) 186:209–10. doi: 10.1111/bjd.20894

284. Esnault C, Leblond V, Martin C, Desgranges A, Baltus CB, Aubrey N, et al. Adcitmer(®), a new CD56-targeting monomethyl auristatin E-conjugated antibody, is a potential therapeutic approach in Merkel cell carcinoma. *Br J Dermatol*. (2022) 186:295–306. doi: 10.1111/bjd.20770

285. Shah MH, Lorigan P, O'Brien ME, Fossella FV, Moore KN, Bhatia S, et al. Phase I study of IMGN901, a CD56-targeting antibody-drug conjugate, in patients with CD56-positive solid tumors. *Invest New Drugs*. (2016) 34:290–9. doi: 10.1007/s10637-016-0336-9

286. McNiff JM, Cowper SE, Lazova R, Subtil A, Glusac EJ. CD56 staining in Merkel cell carcinoma and natural killer-cell lymphoma: magic bullet, diagnostic pitfall, or both? *J cutaneous Pathol*. (2005) 32:541–5. doi: 10.1111/j.0303-6987.2005.00378.x

287. Kurokawa M, Nabeshima K, Akiyama Y, Maeda S, Nishida T, Nakayama F, et al. CD56: a useful marker for diagnosing Merkel cell carcinoma. *J Dermatol Sci*. (2003) 31:219–24. doi: 10.1016/S0923-1811(03)00029-X

288. Stueven AK, Kayser A, Wetz C, Amthauer H, Wree A, Tacke F, et al. Somatostatin analogues in the treatment of neuroendocrine tumors: past, present and future. *Int J Mol Sci*. (2019) 20(12):3049. doi: 10.3390/ijms20123049

289. Akaike T, Qazi J, Anderson A, Behnia FS, Shinohara MM, Akaike G, et al. High somatostatin receptor expression and efficacy of somatostatin analogues in patients with metastatic Merkel cell carcinoma. *Br J Dermatol*. (2021) 184:319–27. doi: 10.1111/bjd.19150

290. Askari E, Moghadam SZ, Wild D, Delpassand E, Baldari S, Nilica B, et al. Peptide receptor radionuclide therapy in merkel cell carcinoma: A comprehensive review. *J Nucl Med Technol*. (2023) 51:22–5. doi: 10.2967/jnmt.122.264904

291. Jalles C, Lepelley M, Mouret S, Charles J, Leccia MT, Trabelsi S. Skin cancers under Janus kinase inhibitors: A World Health Organization drug safety database analysis. *Therapie*. (2022) 77(6):649–56. doi: 10.1016/j.therap.2022.04.005

292. Rastrelli M, Ferrazzi B, Tropea S, Costa A, Finotto S, Marino D, et al. Aggressive merkel cell carcinoma after janus kinase inhibitor ruxolitinib for polycythemia vera. *In vivo*. (2019) 33(5):1667–9. doi: 10.21873/invivo.11653

293. Wallis LS, Rakita U, Grushchak S, Asadbeigi SN, Yazdan P, Liu W, et al. Merkel cell carcinoma associated with tofacitinib therapy. *JAAD Case Rep*. (2021) 14:94–6. doi: 10.1016/j.jdcr.2021.06.011

294. Debureaux PE, Arrondeau J, Bouscary D, Goldwasser F. Nivolumab combined with ruxolitinib: antagonism or synergy? *Ann Oncol*. (2018) 29:1334–5. doi: 10.1093/annonc/mdy077

295. Jansen B, Heere-Ress E, Schlagbauer-Wadl H, Halaschek-Wiener J, Waltering S, Moll I, et al. Farnesylthiosalicylic acid inhibits the growth of human Merkel cell carcinoma in SCID mice. *J Mol Med (Berl)*. (1999) 77:792–7. doi: 10.1007/s001099900052

296. Kannan A, Lin Z, Shao Q, Zhao S, Fang B, Moreno MA, et al. Dual mTOR inhibitor MLN0128 suppresses Merkel cell carcinoma (MCC) xenograft tumor growth. *Oncotarget*. (2016) 7:6576–92. doi: 10.18632/oncotarget.v7i6

297. Adam C, Baeurle A, Brodsky JL, Wipf P, Schrama D, Becker JC, et al. The HSP70 modulator MAL3-101 inhibits Merkel cell carcinoma. *PloS One*. (2014) 9:e92041. doi: 10.1371/journal.pone.0092041

298. Fang B, Kannan A, Zhao S, Nguyen QH, Ejadi S, Yamamoto M, et al. Inhibition of PI3K by copanlisib exerts potent antitumor effects on Merkel cell carcinoma cell lines and mouse xenografts. *Sci Rep*. (2020) 10:8867. doi: 10.1038/s41598-020-65637-2

299. Kleffel S, Lee N, Lezcano C, Wilson BJ, Sobolewski K, Saab KR, et al. ABCB5-targeted chemoresistance reversal inhibits merkel cell carcinoma growth. *J Invest Dermatol*. (2016) 136:838–46. doi: 10.1016/j.jid.2015.12.038

300. Das BK, Kannan A, Nguyen Q, Gogoi J, Zhao H, Gao L. Selective inhibition of aurora kinase A by AK-01/LY3295668 attenuates MCC tumor growth by inducing MCC cell cycle arrest and apoptosis. *Cancers*. (2021) 13(15):3708. doi: 10.3390/cancers13153708

301. Houben R, Hesbacher S, Sarma B, Schulte C, Sarosi EM, Popp S, et al. Inhibition of T-antigen expression promoting glycogen synthase kinase 3 impairs merkel cell carcinoma cell growth. *Cancer Lett*. (2022) 524:259–67. doi: 10.1016/j.canlet.2021.10.031

302. Morimoto Y, Fushimi A, Yamashita N, Hagiwara M, Bhattacharya A, Cheng J, et al. Addiction of Merkel cell carcinoma to MUC1-C identifies a potential new target for treatment. *Oncogene*. (2022) 41:3511–23. doi: 10.1038/s41388-022-02361-3

303. Yang J, Lim JT, Victor P, Chen C, Khwaja H, Schnellmann RG, et al. Integrative analysis reveals therapeutic potential of pyrvinium pamoate in Merkel cell carcinoma. *bioRxiv*. (2023). doi: 10.1101/2023.11.01.565218

304. Xie H, Kaye FJ, Isse K, Sun Y, Ramoth J, French DM, et al. Delta-like protein 3 expression and targeting in merkel cell carcinoma. *Oncologist*. (2020) 25:810–7. doi: 10.1634/theoncologist.2019-0877

305. Loke ASW, Lambert PF, Spurgeon ME. Current *in vitro* and *in vivo* models to study MCPyV-associated MCC. *Viruses*. (2022) 14(10):2204. doi: 10.3390/v14102204

306. Lee JH, Lee JD, Paulson K, Voillet V, Berndt A, Church C, et al. Enhancing immunogenic responses through CDK4/6 and HIF2alpha inhibition in Merkel cell carcinoma. *Heliyon*. (2024) 10:e23521. doi: 10.1016/j.heliyon.2023.e23521

307. Leonard JH, Bell JR, Kearsley JH. Characterization of cell lines established from Merkel-cell ("small-cell") carcinoma of the skin. *Int J Cancer J Int du Cancer*. (1993) 55:803–10. doi: 10.1002/ijc.2910550519

308. Krasagakis K, Almond-Roesler B, Geilen C, Fimmel S, Krengel S, Chatzaki E, et al. Growth and characterization of a cell line from a human primary neuroendocrine carcinoma of the skin (Merkel cell carcinoma) in culture and as xenograft. *J Cell Physiol*. (2001) 187:386–91. doi: 10.1002/jcp.1086

309. Guastafierro A, Feng H, Thant M, Kirkwood JM, Chang Y, Moore PS, et al. Characterization of an early passage Merkel cell polyomavirus-positive Merkel cell carcinoma cell line, MS-1, and its growth in NOD scid gamma mice. *J Virol Methods*. (2013) 187:6–14. doi: 10.1016/j.jviromet.2012.10.001

310. Knips J, Czech-Sioli M, Spohn M, Heiland M, Moll I, Grundhoff A, et al. Spontaneous lung metastasis formation of human Merkel cell carcinoma cell lines transplanted into scid mice. *Int J Cancer J Int du Cancer*. (2017) 141:160–71. doi: 10.1002/ijc.30723

311. Lezcano C, Kleffel S, Lee N, Larson AR, Zhan Q, DoRosario A, et al. Merkel cell carcinoma expresses vasculogenic mimicry: demonstration in patients and experimental manipulation in xenografts. *Lab Invest*. (2014) 94:1092–102. doi: 10.1038/labinvest.2014.99

312. Albertini S, Martuscelli L, Borgogna C, Virdi S, Indenbirken D, Lo Cigno I, et al. Cancer-associated fibroblasts exert proangiogenic activity in merkel cell carcinoma. *J Invest Dermatol*. (2023) 143:965–976 e15. doi: 10.1016/j.jid.2022.12.006

313. Spurgeon ME, Cheng J, Ward-Shaw E, Dick FA, DeCaprio JA, Lambert PF. Merkel cell polyomavirus large T antigen binding to pRb promotes skin hyperplasia and tumor development. *PloS Pathog*. (2022) 18:e1010551. doi: 10.1371/journal.ppat.1010551

314. Spurgeon ME, Liem A, Buehler D, Cheng J, DeCaprio JA, Lambert PF. The merkel cell polyomavirus T antigens function as tumor promoters in murine skin. *Cancers*. (2021) 13(2):222. doi: 10.3390/cancers13020222

315. Wright MC, Reed-Geaghan EG, Bolock AM, Fujiyama T, Hoshino M, Maricich SM. Unipotent, Atoh1+ progenitors maintain the Merkel cell population in embryonic and adult mice. *J Cell Biol*. (2015) 208:367–79. doi: 10.1083/jcb.201407101

316. Morrison KM, Miesegaes GR, Lumpkin EA, Maricich SM. Mammalian Merkel cells are descended from the epidermal lineage. *Dev Biol*. (2009) 336:76–83. doi: 10.1016/j.ydbio.2009.09.032

317. Van Keymeulen A, Mascre G, Youseff KK, Harel I, Michaux C, De Geest N, et al. Epidermal progenitors give rise to Merkel cells during embryonic development and adult homeostasis. *J Cell Biol*. (2009) 187:91–100. doi: 10.1083/jcb.200907080

318. Moll R, Lowe A, Laufer J, Franke WW. Cytokeratin 20 in human carcinomas. A new histodiagnostic marker detected by monoclonal antibodies. *Am J Pathol*. (1992) 140:427–47.

319. Gillet JP, Calcagno AM, Varma S, Marino M, Green LJ, Vora MI, et al. Redefining the relevance of established cancer cell lines to the study of mechanisms of clinical anti-cancer drug resistance. *Proc Natl Acad Sci USA*. (2011) 108:18708–13. doi: 10.1073/pnas.1111840108

320. Mak IW, Evaniew N, Ghert M. Lost in translation: animal models and clinical trials in cancer treatment. *Am J Transl Res*. (2014) 6:114–8.

321. Gao H, Korn JM, Ferretti S, Monahan JE, Wang Y, Singh M, et al. High-throughput screening using patient-derived tumor xenografts to predict clinical trial drug response. *Nat Med*. (2015) 21:1318–25. doi: 10.1038/nm.3954

322. Zitvogel L, Pitt JM, Daillere R, Smyth MJ, Kroemer G. Mouse models in oncoimmunology. *Nat Rev Cancer*. (2016) 16:759–73. doi: 10.1038/nrc.2016.91

323. Cogels MM, Rouas R, Ghanem GE, Martinive P, Awada A, Van Gestel D, et al. Humanized mice as a valuable pre-clinical model for cancer immunotherapy research. *Front Oncol*. (2021) 11:784947. doi: 10.3389/fonc.2021.784947

324. Gavvovidis I, Leisegang M, Willimsky G, Miller N, Nghiem P, Blankenstein T. Targeting merkel cell carcinoma by engineered T cells specific to T-antigens of merkel cell polyomavirus. *Clin Cancer Res*. (2018) 24:3644–55. doi: 10.1158/1078-0432.CCR-17-2661

325. Ostrand-Rosenberg S. Animal models of tumor immunity, immunotherapy and cancer vaccines. *Curr Opin Immunol*. (2004) 16:143–50. doi: 10.1016/j.coi.2004.01.003

326. Dranoff G. Experimental mouse tumour models: what can be learnt about human cancer immunology? *Nat Rev Immunol*. (2011) 12:61–6. doi: 10.1038/nri3129

327. Colunga A, Pulliam T, Nghiem P. Merkel cell carcinoma in the age of immunotherapy: facts and hopes. *Clin Cancer Res*. (2018) 24:2035–43. doi: 10.1158/1078-0432.CCR-17-0439

328. Fischer M. Mice are not humans: the case of p53. *Trends Cancer*. (2021) 7:12–4. doi: 10.1016/j.trecan.2020.08.007

frontiers | Frontiers in Medicine

TYPE Case Report
PUBLISHED 31 July 2024
DOI 10.3389/fmed.2024.1386089

Check for updates

OPEN ACCESS

EDITED BY
Shuai Ren,
Affiliated Hospital of Nanjing University of Chinese Medicine, China

REVIEWED BY
Xingli Xu,
Qilu Hospital of Shandong University, China
Zhiguo Zou,
Shanghai Jiao Tong University, China

*CORRESPONDENCE
Juan S. Izquierdo-Condoy
✉ juan1izquierdo11@gmail.com

RECEIVED 14 February 2024
ACCEPTED 10 July 2024
PUBLISHED 31 July 2024

CITATION
Nati-Castillo HA, Quintero JM, Molina OA, Arias-Intriago M, Melgar Muñoz FP and Izquierdo-Condoy JS (2024) Unusual adult-onset cardiac rhabdomyomas in tuberous sclerosis complex: a case report. *Front. Med.* 11:1386089. doi: 10.3389/fmed.2024.1386089

COPYRIGHT
© 2024 Nati-Castillo, Quintero, Molina, Arias-Intriago, Melgar Muñoz and Izquierdo-Condoy. This is an open-access article distributed under the terms of the Creative Commons Attribution License (CC BY). The use, distribution or reproduction in other forums is permitted, provided the original author(s) and the copyright owner(s) are credited and that the original publication in this journal is cited, in accordance with accepted academic practice. No use, distribution or reproduction is permitted which does not comply with these terms.

Unusual adult-onset cardiac rhabdomyomas in tuberous sclerosis complex: a case report

H. A. Nati-Castillo[1], Juan Manuel Quintero[2], Oswaldo Aguilar Molina[3], Marlon Arias-Intriago[4], Fernando P. Melgar Muñoz[4] and Juan S. Izquierdo-Condoy[4]*

[1]Interinstitutional Internal Medicine Group (GIMI 1), Department of Internal Medicine, Universidad Libre, Cali, Colombia, [2]Department of Internal Medicine, Universidad del Valle, Cali, Colombia, [3]Department of Cardiology, Hospital Universitario del Valle, Cali, Colombia, [4]One Health Research Group, Universidad de las Américas, Quito, Ecuador

Background: Tuberous sclerosis complex is a genetic neurocutaneous autosomal dominant syndrome, characterized by the development of multiple benign tumors (hamartomas) affecting various systems. Heart-benign tumors that result from the complex are called cardiac rhabdomyomas. Unlike hamartomas that occur in other organs, cardiac rhabdomyomas are most prevalent in infants and very young children with tuberous sclerosis complex. We present a case of a young adult with tuberous sclerosis who had an unusually late diagnosis of cardiac rhabdomyomas.

Case report: A 22-year-old male patient of Afro-descendant, diagnosed with tuberous sclerosis complex in childhood, presented with refractory epilepsy and was treated only with lacosamide. The patient came to medical consultation due to a recent history of episodic, persistent chest pain in the sternal region, associated with physical effort. Echocardiography revealed a non-dilated left ventricle, with several rounded masses of high echogenicity without pedicles at the apical level, the largest measuring 14 × 11 mm, consistent with cardiac rhabdomyomas.

Conclusion: Cardiac rhabdomyomas rarely develop in adulthood for individuals with tuberous sclerosis. These late-onset cases can exhibit various symptoms, from simple to complex presentations. Regular clinical checkups are essential for adults with tuberous sclerosis complex.

KEYWORDS

chest pain, cardiac rhabdomyoma, tuberous sclerosis, echocardiography, adult onset

1 Introduction

Tuberous sclerosis complex is a rare genetic neurocutaneous autosomal dominant syndrome in humans, caused by mutations in TSC1 or TSC2 gene. It is characterized by the growth of benign tumors (hamartomas) in multiple locations, including organs such as the skin, brain, kidneys, heart, and lungs. Heart benign tumors resulting from tuberous sclerosis complex are called cardiac rhabdomyomas, composed of normal heart tissue (rhabdo) that grows in a disorganized mass (myoma) (1, 2). Unlike hamartomas that occur in other organs, cardiac rhabdomyomas are most prevalent in infants and very young

children with tuberous sclerosis complex. In fact, these are the only lesions that regress over time in tuberous sclerosis, in some cases disappearing entirely (3, 4). In rare cases, large or several cardiac rhabdomyomas that grow on or near the heart valves can disrupt heart rhythm or blood flow, causing angina symptoms and possibly death (5).

Clinically, up to 64% of patients present the syndrome asymptomatically, and a smaller percentage (approximately 35%) present symptoms expressed by arrhythmias and Wolff–Parkinson–White syndrome. The estimated mortality associated with cardiac rhabdomyomas due to cardiac complications has been estimated to be close to 2% in cohorts of patients (5–8). Abnormalities within the echocardiogram have been reported in up to 39%, with focal areas of intramyocardial hyperechogenicity being the most prevalent (9).

We present a case of tuberous sclerosis complex accompanied by cardiac rhabdomyomas with symptomatic expression in adulthood.

2 Case presentation

A 22-year-old male patient of Afro-descendant, diagnosed with tuberous sclerosis complex in childhood, presented with refractory epilepsy and was treated only with 100 mg lacosamide every 12 h. He has an opioid allergy (tramadol). His family history includes a father with obesity and type 2 diabetes mellitus, a mother with high blood pressure, and a maternal grandfather with prostate cancer. He has no family history of tuberous sclerosis. Previous interventions identified unspecified epilepsy on electroencephalogram 8 years ago (2015), with no past surgical interventions.

The patient sought medical consultation for a 1-year history of episodic, persistent chest pain in the sternal region, lasting 1 to 5 min and exclusively associated with physical effort. There is no relief with any specific factor.

On physical examination, the examination of the left eye fundus revealed slightly elevated yellowish-white xanthochromic lesions at the end of the upper temporal arch, suggestive of and compatible with retinal hamartomas. The abdominal cavity showed no alterations. A cardiac examination revealed a systolic murmur in the mitral and aortic focus, grade III/IV. The respiratory system showed no abnormalities. The skin and integumentary system exhibited multiple elevated lesions without inflammatory changes, which were not painful and compatible with angiofibromas located on the face and head (Figure 1).

Given the patient's condition, the initial electrocardiogram showed no alterations. Consequently, diagnostic studies, including a brain MRI a few weeks later, were performed. The MRI revealed small bilateral subependymal lesions, the largest measuring 1.6 × 1.6 cm on the lateral wall of the occipital extension of the right lateral ventricle. Additionally, approximately 4 months later, renal ultrasound and echocardiogram were performed. The renal ultrasound showed bilateral renal involvement with multiple rounded masses of variable size (ranging between 12.5 mm and 4 mm) at the parenchymal level, characteristic of angiomyolipomas (Figure 2). Echocardiography revealed a non-dilated left ventricle with several rounded masses of high echogenicity without pedicles at the apical level, the largest measuring 14 × 11 mm. These masses were retractile, with mobility toward the ventricular wall, consistent with cardiac rhabdomyomas (Figure 3). No contractility disorders were observed, and the ejection fraction was 60% (Simpson's biplane method). The atria, valves, and the right ventricle showed no abnormalities.

At the diagnosis of a cardiac rhabdomyoma in the left ventricle, the patient received symptomatic management for the chest precordial pain using neuromodulators (Pregabalin). Cardiological surveillance was initiated, which, after 4 months (March 2024) of management, has shown improvement in pain without other significant symptoms.

3 Discussion

Tuberous sclerosis or Bourneville's disease of autosomal dominant genetic origin is a very rare syndrome (5–7/10,000 live births) (10). The spectrum of clinical manifestations of the syndrome includes neurological manifestations, such as autism spectrum disorders, cortical tuberomas, epilepsy, and intellectual disability, with the latter being the most common (11, 12). Main cutaneous manifestations include facial angiofibromas (formerly sebaceous adenomas), periungual fibromas, ash-leaf spots, and hypochromic macules (up to 80%). Cutaneous clinical manifestations are essential for reliably approximating the clinical diagnosis of the disease (11).

Cardiac manifestations encompass cardiac rhabdomyomas, which are benign tumors considered the most common since perinatal diagnosis (60%). They can be detected ultrasonographically even in the prenatal period (between 20 and 30 weeks), with the most common location being in the ventricles (70%) (13). These tumors usually behave asymptomatically; however, they can interfere with valvular function, alter the ventricular inflow or outflow tract, generate anomalies in the cardiac conduction system, or occlude the adequate irrigation of the coronary system. This can lead to myocardial ischemic events, triggering heart failure and arrhythmias in up to 43.3% (13, 14).

In this case, although the patient shares characteristics similar to those reported in the literature, such as the clinical diagnosis of tuberous sclerosis based on common manifestations, including neurological (epilepsy), cutaneous (angiofibromas), and ocular (hamartomas) during childhood, a distinctive aspect of this report is that the key clinical manifestation for discovering cardiac rhabdomyomas occurred in young adulthood (21 years). This manifestation presented as chest pain of prolonged duration (1 year), which, along with findings from the initial examination and the patient's history, led to a transthoracic echocardiographic study. This study revealed multiple lesions, leading to the diagnosis of cardiac rhabdomyomas, without evidence of damage to cardiac conduction, highlighting a very unusual presentation. It is important to note that the nature of the case reflects the patient's environment with limited resources, living in a rural area with difficult access to healthcare, which contributed to the prolonged progression and delay in obtaining a definitive diagnosis.

This case is of interest because, according to the recent review by Frudit et al. (13), it could be the second to date of a young adult with tuberous sclerosis that had a late diagnosis of cardiac rhabdomyomas, characterized only by chest pain. The only previous report was by Enbergs et al. (15) in 1996 on a 23-year-old patient accompanied by ventricular tachycardia.

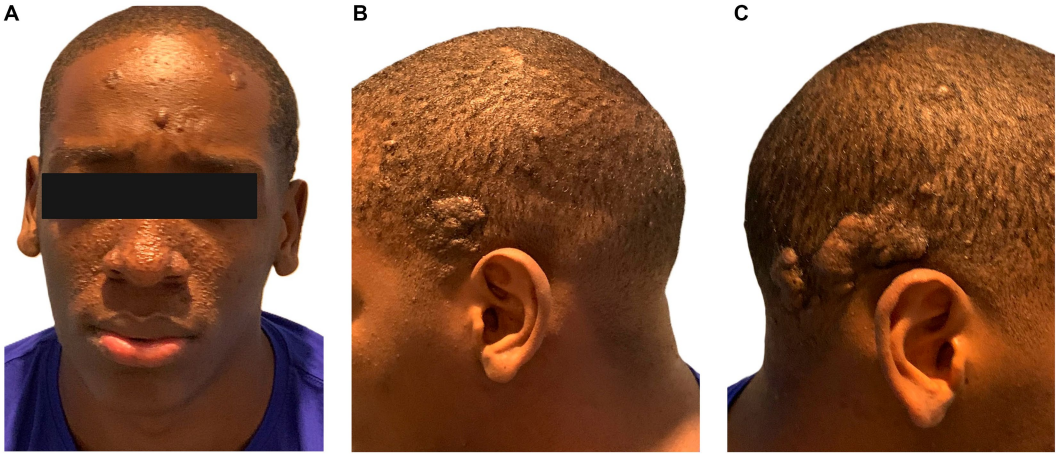

FIGURE 1
Phenotype of a 22-year-old male patient with tuberous sclerosis. **(A)** Phototype V, at frontal-level euchromatic nodules, soft smooth surface about angiofibroma. In the middle facial third, papules smaller than 5 mm in diameter, smooth euchromatic and violaceous surface, regular distribution on nasal dorsum and bilateral malar region in relation with angiofibromas. **(B)** Hairy skin left temporo-occipital region: exophytic tumor, well-defined irregular borders, smooth surface with convolutions, not ulcerated, size 4 cm by 3 cm. **(C)** Hairy skin right temporo-occipital region: exophytic tumors, well defined, irregular borders, smooth surface with convolutions, not ulcerated, size 5 cm by 3 cm and 2.5 cm by 1.5 cm, respectively.

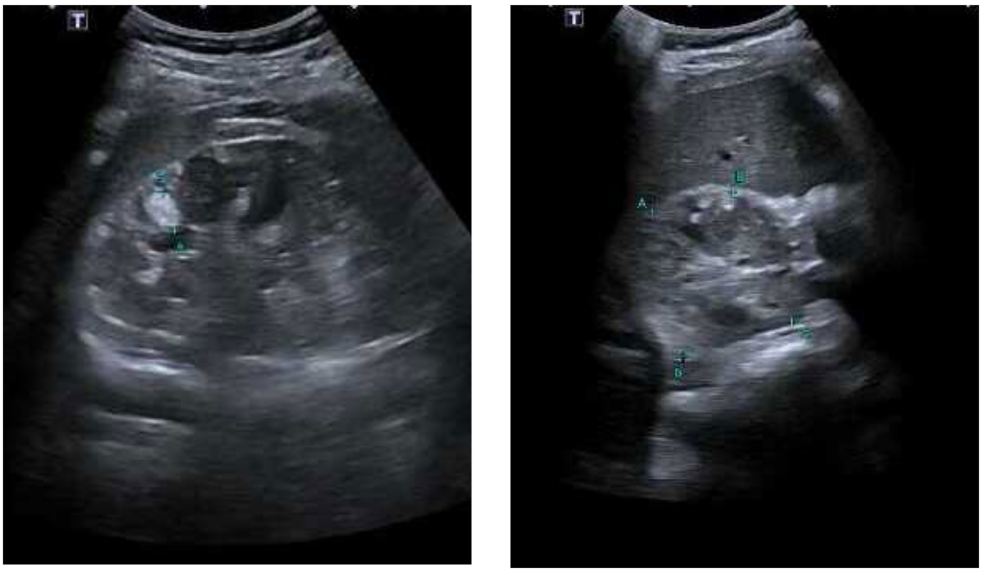

FIGURE 2
Bilateral renal ultrasound. Parenchyma displays multiple small rounded echogenic images distributed throughout, with sizes ranging between 12.5 mm, 10 mm, 7 mm, 5 mm, and 4 mm.

Although a relationship between ethnicity and the syndrome or its accompanying features has not been established, apparently, presentation in individuals of African descent is rare (16, 17). This case broadens the phenotypic picture of tuberous sclerosis associated with cardiac rhabdomyomas by presenting in an individual of African descent ethnicity. It proposes considering ethnicity as a variable to study in future patients' reports with tuberous sclerosis complex with rare features.

Despite not all patients with tuberous sclerosis presenting with cardiac rhabdomyomas, this case highlights the importance of active cardiac screening for these patients during the disease, given the potential complications even in adulthood. In this context, the standard of choice is cardiac echocardiography with a complete Doppler study, which shows well-circumscribed, nodular, multiple masses in the myocardium, which usually project into the ventricular chamber (14). Their diagnosis can be difficult if they present atypical locations such as the atria or present as solitary tumors (5). Additionally, the clinician may opt for cardiac MRI, which, although not widely available in developing settings like this case, can provide a more accurate description of the masses when

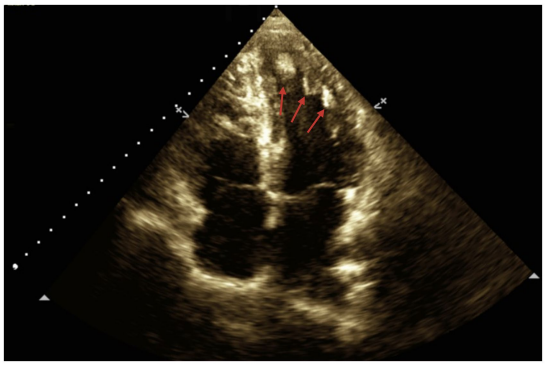

FIGURE 3
Two-dimensional echocardiography of the patient, showing an apical four-chamber view. The red arrows indicate several homogeneous masses with well-defined borders, retractile and without pedicles, affecting the entire interventricular septum and apical region. The largest mass, located closer to the interventricular septum, measures approximately 14 mm × 11 mm.

the echocardiographic diagnosis is unclear and as a useful adjunct when surgical resolution is planned (14). The follow-up of this entity is usually based on growth monitoring with echocardiography and electrocardiograms every 3 to 5 years to assess possible conduction disorders and risks of disease progression such as heart failure (18).

4 Conclusion

The late onset of cardiac rhabdomyomas in adulthood among patients with tuberous sclerosis is particularly rare and may manifest symptomatically with a variety of presentations, ranging from simple to complex. Regular clinical inspections should be conducted for individuals with tuberous sclerosis complex, even in adulthood, to monitor the emergence of benign cardiac masses.

Data availability statement

The original contributions presented in the study are included in the article/supplementary material, further inquiries can be directed to the corresponding author.

Ethics statement

Written informed consent was obtained directly from the patient. Written informed consent was obtained from the participant/patient(s) for the publication of this case report.

Author contributions

HN-C: Conceptualization, Data curation, Formal analysis, Investigation, Methodology, Project administration, Resources, Validation, Visualization, Writing – original draft. JQ: Conceptualization, Data curation, Investigation, Methodology, Resources, Validation, Visualization, Writing – original draft. OM: Conceptualization, Data curation, Investigation, Methodology, Resources, Validation, Visualization, Writing – original draft. MA-I: Formal analysis, Investigation, Methodology, Resources, Software, Visualization, Writing – original draft. FM: Formal analysis, Investigation, Methodology, Resources, Software, Visualization, Writing – review & editing. JI-C: Data curation, Funding acquisition, Investigation, Methodology, Project administration, Software, Supervision, Validation, Visualization, Writing – original draft, Writing – review & editing.

Funding

The author(s) declare that no financial support was received for the research, authorship, and/or publication of this article.

Conflict of interest

The authors declare that the research was conducted in the absence of any commercial or financial relationships that could be construed as a potential conflict of interest.

Publisher's note

All claims expressed in this article are solely those of the authors and do not necessarily represent those of their affiliated organizations, or those of the publisher, the editors and the reviewers. Any product that may be evaluated in this article, or claim that may be made by its manufacturer, is not guaranteed or endorsed by the publisher.

References

1. Habib SL. Tuberous sclerosis complex and DNA repair. *Adv Exp Med Biol.* (2010) 685:84–94. doi: 10.1007/978-1-4419-6448-9_8

2. Portocarrero LKL, Quental KN, Samorano LP, Oliveira ZNP, Rivitti-Machado MCM. Tuberous sclerosis complex: review based on new diagnostic criteria. *An Bras Dermatol.* (2018) 93:323–31. doi: 10.1590/abd1806-4841.20186972

3. Sciacca P, Giacchi V, Mattia C, Greco F, Smilari P, Betta P, et al. Rhabdomyomas and tuberous sclerosis complex: our experience in 33 cases. *BMC Cardiovasc Disord.* (2014) 14:66. doi: 10.1186/1471-2261-14-66

4. Dimario FJ Jr, Diana D, Leopold H, Chameides L. Evolution of cardiac rhabdomyoma in tuberous sclerosis complex. *Clin Pediatr.* (1996) 35:615–9. doi: 10.1177/000992289603501202

5. Benyounes N, Fohlen M, Devys J-M, Delalande O, Moures J-M, Cohen A. Cardiac rhabdomyomas in tuberous sclerosis patients: a case report and review of the literature. *Arch Cardiovasc Dis.* (2012) 105:442–5. doi: 10.1016/j.acvd.2012.01.009

6. Madueme P, Hinton R. Tuberous sclerosis and cardiac rhabdomyomas: a case report and review of the literature. *Congenit Heart Dis.* (2011) 6:183–7. doi: 10.1111/j.1747-0803.2011.00502.x

7. Valero E, Miñana G, Chorro FJ. Afección cardiaca en la esclerosis tuberosa. *Rev Esp Cardiol.* (2013) 66:402. doi: 10.1016/j.recesp.2011.06.012

8. Lince R, López G, de Mesa C, Arteaga A, Montoya JH, Vásquez LM. Rabdomioma cardiaco como manifestación de esclerosis tuberosa: Presentación de dos casos y revisión de la literatura. *Rev Colom Cardiol.* (2009) 16:224–8.

9. Adriaensen MEAPM, Cramer MJM, Brouha MEE, Schaefer-Prokop CM, Prokop M, Doevendans PAFM, et al. Echocardiographic screening results in patients with tuberous sclerosis complex. *Tex Heart Inst J.* (2010) 37:280–3.

10. Grajkowska W, Kotulska K, Jurkiewicz E, Matyja E. Brain lesions in tuberous sclerosis complex. Review. *Folia Neuropathol.* (2010) 48:139–49.

11. Crino PB, Nathanson KL, Henske EP. The tuberous sclerosis complex. *N Engl J Med*. (2006) 355:1345–56. doi: 10.1056/NEJMra055323

12. Northrup H, Aronow ME, Bebin EM, Bissler J, Darling TN, de Vries PJ, et al. Updated international tuberous sclerosis complex diagnostic criteria and surveillance and management recommendations. *Pediatr Neurol*. (2021) 123:50–66. doi: 10.1016/j.pediatrneurol.2021.07.011

13. Frudit P, Vitturi BK, Navarro FC, Rondelli I, Pozzan G. Multiple cardiac rhabdomyomas in tuberous sclerosis complex: case report and review of the literature. *Autops Case Rep*. (2019) 9:e2019125. doi: 10.4322/acr.2019.125

14. Hinton RB, Prakash A, Romp RL, Krueger DA, Knilans TK. Cardiovascular manifestations of tuberous sclerosis complex and summary of the revised diagnostic criteria and surveillance and management recommendations from the International Tuberous Sclerosis Consensus Group. *J Am Heart Assoc*. (2014) 3:e001493. doi: 10.1161/JAHA.114.001493

15. Enbergs A, Borggrefe M, Kurlemann G, Fahrenkamp A, Scheld HH, Jehle J, et al. Ventricular tachycardia caused by cardiac rhabdomyoma in a young adult with tuberous sclerosis. *Am Heart J*. (1996) 132:1263–5. doi: 10.1016/S0002-8703(96)90470-6

16. Au KS, Williams AT, Roach ES, Batchelor L, Sparagana SP, Delgado MR, et al. Genotype/phenotype correlation in 325 individuals referred for a diagnosis of tuberous sclerosis complex in the United States. *Genet Med*. (2007) 9:88–100. doi: 10.1097/GIM.0b013e31803068c7

17. Pounders AJ, Rushing GV, Mahida S, Nonyane BAS, Thomas EA, Tameez RS, et al. Racial differences in the dermatological manifestations of tuberous sclerosis complex and the potential effects on diagnosis and care. *Ther Adv Rare Dis*. (2022) 3:26330040221140125. doi: 10.1177/26330040221140125

18. Ghosh S, Milunski MR. Cardiac rhabdomyoma in adult. *Cureus*. (2021) 13:e14565. doi: 10.7759/cureus.14565

frontiers | Frontiers in Oncology

TYPE Case Report
PUBLISHED 06 August 2024
DOI 10.3389/fonc.2024.1398055

Check for updates

OPEN ACCESS

EDITED BY
Ferdinando Agresta,
ULSS2 Marca Trevigiana, Italy

REVIEWED BY
Nicoletta Cordani,
University of Milano-Bicocca, Italy
Yudong Li,
Capital Medical University, China

*CORRESPONDENCE
Marta Laganà
marta.lagana@unibs.it

RECEIVED 15 March 2024
ACCEPTED 19 July 2024
PUBLISHED 06 August 2024

CITATION
Fassi E, Amoroso V, Cosentini D, Ferrari V, Laganà M, Berruti A and di Mauro P (2024) Regorafenib-related erythrocytosis in metastatic extra-gastrointestinal stromal tumor: a case report.
Front. Oncol. 14:1398055.
doi: 10.3389/fonc.2024.1398055

COPYRIGHT
© 2024 Fassi, Amoroso, Cosentini, Ferrari, Laganà, Berruti and di Mauro. This is an open-access article distributed under the terms of the Creative Commons Attribution License (CC BY). The use, distribution or reproduction in other forums is permitted, provided the original author(s) and the copyright owner(s) are credited and that the original publication in this journal is cited, in accordance with accepted academic practice. No use, distribution or reproduction is permitted which does not comply with these terms.

Regorafenib-related erythrocytosis in metastatic extra-gastrointestinal stromal tumor: a case report

Elena Fassi, Vito Amoroso, Deborah Cosentini, Vittorio Ferrari, Marta Laganà*, Alfredo Berruti and Pierluigi di Mauro

Medical Oncology Unit, Department of Medical and Surgical Specialties, Radiological Sciences, and Public Health, University of Brescia. ASST Spedali Civili, Brescia, Italy

Introduction: Regorafenib is an oral multi-targeted tyrosine kinase inhibitor (TKI) indicated for the treatment of various tumor types, including metastatic gastrointestinal stromal tumors (GIST), as a third-line systemic therapy. Erythrocytosis, which is characterized by an increase in erythrocyte count, hemoglobin, and hematocrit levels, has been described as a side effect of some antiangiogenic TKIs but has never been associated with regorafenib administration.

Case presentation: An extra-GIST was diagnosed in a 58-year-old woman after she underwent surgery to remove a pelvic mass. Three years later, systemic therapy with imatinib was started due to pelvic disease recurrence. However, after six months, due to disease progression, we prescribed sunitinib, which the patient received for four years. Regorafenib was initiated in June 2019, and after six months, we noted an increase in the erythrocytes' count and hemoglobin (Hb) levels. Given that the patient had clinical benefit and hematocrit was within normal range, we only monitored the blood cell count and continued to give regorafenib at the same dose. The drug was then stopped for over six weeks due to hospitalization for severe acute respiratory syndrome coronavirus 2 (SARS-CoV-2) infection, and Hb levels returned to normal. Therefore, we decided to restart regorafenib at a lower dose. However, Hb levels rose again in conjunction with increased hematocrit, resulting in the need for multiple phlebotomies. We attempted to restart regorafenib every other day, but it was unsuccessful, so we stopped it permanently in May 2023, and all values returned to normal.

Conclusion: Regorafenib may cause secondary erythrocytosis that could not be dose-related, as this case report suggests. Secondary erythrocytosis might be a marker of TKI efficacy, given the patient's prolonged clinical benefit during regorafenib treatment (48 months). In patients receiving regorafenib, monitoring blood count as well as any symptoms associated with erythrocytosis may be suggested.

KEYWORDS

erythrocytosis, regorafenib, polycythemia, EGIST, TKIs

1 Introduction

Gastrointestinal stromal tumors (GISTs) are the most common mesenchymal tumors of the gastrointestinal tract (1, 2). They probably arise from interstitial Cajal (ICC) cells, which regulate gastrointestinal motility and, in most cases, have oncogenic gain-of-function mutations in KIT or PDGFRA genes (3). Extra-gastrointestinal stromal tumors (EGISTs) are a rare subtype that originate outside the gastrointestinal tract, mainly from the mesentery, omentum, or peritoneum (4). Their incidence is estimated to be between 5% and 10% of all GISTs (5). Given the rarity of EGISTs, recommended treatment approaches are not different compared to GISTs. In particular, surgery is the first treatment choice for localized disease, while systemic therapy with specific tyrosine kinase inhibitors (TKIs) is indicated in metastatic or unresectable disease (6). Patients with metastatic disease characterized by KIT mutations receive imatinib as first-line therapy. In the case of disease progression, the standard second-line treatment for GIST is sunitinib, while regorafenib is approved as the third-line (2, 6).

Regorafenib is an oral multi-targeted TKI, whose targets are involved in the regulation of tumor angiogenesis (VEGFR1–3 and TEK), oncogenesis (KIT, RET, RAF1, BRAF, and and $BRAF^{V600E}$), and maintenance of the tumor microenvironment (PDGFRA, PDGFRB and FGFR) (7). Fatigue, diarrhea, hand-foot skin reaction, and hypertension are the most commonly reported adverse events with this drug (8–10).

Erythrocytosis is defined as an increase in erythrocyte count, hemoglobin (Hb), and hematocrit (Hct) levels beyond the sex-specific normal range (11). Primary erythrocytosis is secondary to myeloproliferative diseases such as polycythemia vera (PV), while secondary erythrocytosis is associated with elevated serum erythropoietin (EPO) levels (11). This increase could be determined by hypoxia, solid tumors that produce EPO, congenital causes (e.g., erythropoietin receptor mutations or increased Hb-oxygen affinity), or drugs (12). Specific World Health Organization (WHO) criteria should be satisfied for diagnosing PV (13), while clinical and laboratory testing is necessary to diagnose secondary erythrocytosis. In particular, patients should undergo a drug history and a complete cardio-pulmonary evaluation to identify any signs of hypoxia, carbon monoxide exposure, or obstructive sleep apnea. Additionally, abdominal imaging examination may identify erythropoietin-producing tumors (11).

Here, we report a case of regorafenib-related secondary erythrocytosis in a patient treated for metastatic EGIST.

2 Case presentation

In 2011, a 58-year-old patient underwent surgical removal of a pelvic mass (16x10x15cm) and hysterectomy with bilateral salpingo-oophorectomy. The histological examination revealed a morphologically biphasic mesenchymal neoplasm with spindle and epithelioid cells; the mitotic index was less than 5/50 high-power field (HPF) and the Ki-67 labelling index was 5%. The tumor cells tested positive for CD117, P16, and SMA but negative for CD34 (Table 1). Based on the morphological features and the knowledge that CD34 is negative in 50% of EGIST cases (14, 15), a low-to-moderate EGIST was diagnosed. The assessment of KIT and PDGFRA mutations was not performed because it was not required at the time of the first diagnosis. Preoperative staging with CT scan did not show other lesions. According to the pathological stage (pT4N0M0) and high risk of recurrence based on Miettinen's criteria (16), the treating physician could have recommended adjuvant therapy with imatinib; however, the patient only started a clinical and imaging-based follow-up program.

Three years later, a gynecologic ultrasound examination revealed three pelvic non-cystic lesions (38x40x33mm, 78x42x54mm, and 27x17mm), which were confirmed as malignant relapse with an abdominal computed tomography. Then, the patient was referred to our Institution and started first-line treatment with imatinib 400 mg/day, which was associated with recurrent neutropenia of grade 2 (G2). After six months of therapy, peritoneal disease progression was documented after a radiological evaluation; therefore, second-line treatment with sunitinib continuous daily dosing of 25 mg was prescribed at a lower dose because of previous neutropenia secondary to imatinib. The treatment was well tolerated except for recurrent G2 neutropenia, after which the sunitinib dose was reduced to 12,5 mg/day. After four years of sunitinib therapy, further peritoneal disease progression was noted, and regorafenib 160 mg/day (once daily

TABLE 1 Immunohistochemical analysis performed on primary tuomor at baseline.

	Positive	Negative
CD117	x	
SMA	x	
P16	x	
DOG1	x	
CD34		x
CAM 5,2		x
CK34betaE12		x
Cromogranin		x
HMB45		x
Inibin		x
Calretinin		x
S100		x
Melan A		x
Desmin		x
CD21		x
CD23		x
ER		x
EMA		x

for 3 weeks followed by 1 week off-therapy) was prescribed as a third-line treatment in June 2019 (Figure 1). Six months after starting regorafenib, an increase in Hb level to 16.7 g/dl (normal range, 12-16 g/dl), which correspond to G1 according to CTCAE v 5.0, and in erythrocyte count to $5.65x10^6$/μL (normal range, 4.0-$5.2x10^6$/μL) was detected during routine blood examinations. In the following months, the Hb level continued to slightly rise to 17.6 g/dl (G1) without symptoms onset or significant increase in Hct values: considering the clinical benefit the same dose of regorafenib was maintained. However, following the patient's hospitalization due to severe acute respiratory syndrome coronavirus 2 (SARS-CoV-2) infection in June 2022, regorafenib was discontinued for over six weeks and the Hb levels decreased to normal values (13.6 g/dl at hospital discharge). Considering the patient's ongoing clinical frailty after hospitalization and previous oncological treatments, as well as the prolonged disease stability, regorafenib was resumed at a lower dose (40 mg/day). Despite dose reduction, Hb levels rapidly increased to a maximum value of 19.5 g/dl (G2), with 60% of Hct value (normal range 41-54%) in January 2023. EPO level was 21.4 mU/ml (normal range 2.59-18.50 mU/ml). The patient remained asymptomatic. After immediately stopping regorafenib and hematologic consultation, the patient underwent phlebotomies, resulting in normalized Hb and Hct levels after two sessions. We attempted to restart the TKI therapy at the same dose, but a third phlebotomy session was necessary after one week, as the Hb level rose to 17.4 g/dl (G1) and the Hct was 54.3%. Regorafenib was restarted at 40 mg every other days as a final attempt; however, the patient required another phlebotomy after two weeks, so we ultimately stopped TKI therapy in May 2023 (time to treatment failure after regorafenib initiation: 48 months). Afterwards, the Hb and Hct levels finally returned to normal values. (Figure 2).

The patient remained asymptomatic, and the diagnostic testrequested by the hematologist demonstrated no JAK V617F mutation, thereby excluding the possibility of primary erythrocytosis.

The patient did not take any other concomitant medications throughout the entire period.

CT re-evaluation revealed pelvic disease stability. Since the patient had a good performance status, we tried a re-challenge treatment with imatinib 200mg/day in August 2023. Unfortunately, in December 2023, the patient developed a systemic infection that led her to death. The patient's overall survival from the first diagnosis was 151 months (12 years and seven months).

3 Discussion

To our knowledge, we described the first case of regorafenib-related erythrocytosis in a patient diagnosed with metastatic EGIST who achieved a prolonged clinical benefit with third-line regorafenib therapy. We assessed the probability that erythrocytosis was a regorafenib-related side effect using the Naranjo scale (17, 18), obtaining a score of 6, corresponding to a probable correlation. Furthermore, no other EGIST cases with erythrocytosis are described in the literature. Nevertheless, in a preclinical study, mice with a particular loss-of-function mutation in KIT developed polycythemia vera in addition to GIST, suggesting a function of KIT in early erythropoiesis (19).

In patients with different tumor types, elevated Hb levels have been documented in association with multiple TKIs, including sunitinib (20), sorafenib (21), axitinib (22), and pazopanib (23).

While the exact mechanism of TKI-related erythropoiesis is still unknown, different hypotheses have been proposed. In a preclinical study, Tam et al. showed that endogenous VEGF plays a role in the down-regulation of vertebrate erythropoiesis (24). They also demonstrated that complete inhibition of VEGF can induce erythrocytosis and hepatic EPO synthesis (24). Van Der Veldt et al. hypothesized that sunitinib-related erythrocytosis may be secondary to vasoconstriction caused by VEGFR-2 inhibition that leads to intravascular fluid leakage. The decrease in plasma volume results in a relative increase in Hb, Hct, and erythrocytes (20). Alexandrescu et al. proposed that erythrocytosis could result from sensitization to the effects of EPO and is a rebound to VEGF inhibition-induced hypoxia after observing reversible erythrocytosis in patients treated with sunitinib or sorafenib for different tumor types (renal cell carcinoma [RCC], melanoma, and hepatocellular carcinoma) (21). Wang et al. reported a case series of six metastatic RCC patients treated with various anti-VEGF drugs (but not regorafenib) who developed polycythemia (25). They concluded that polycythemia was secondary to the release of EPO by

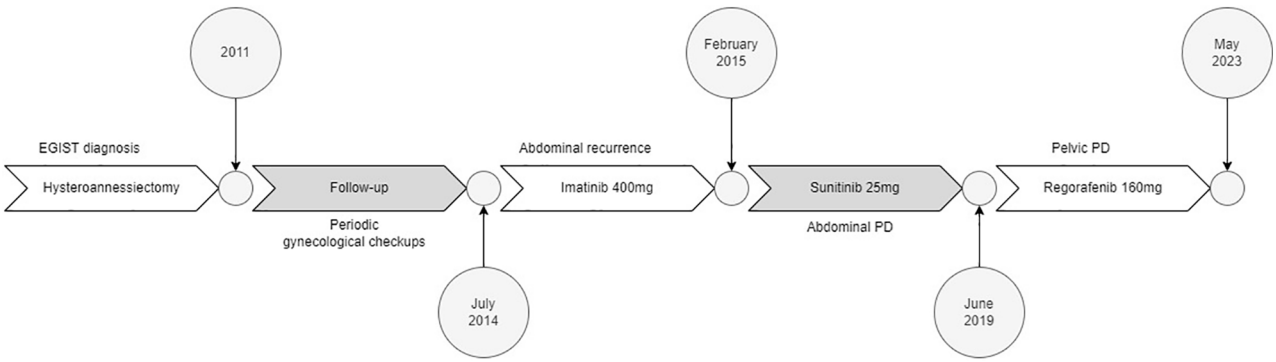

FIGURE 1
Drugs' timeline.

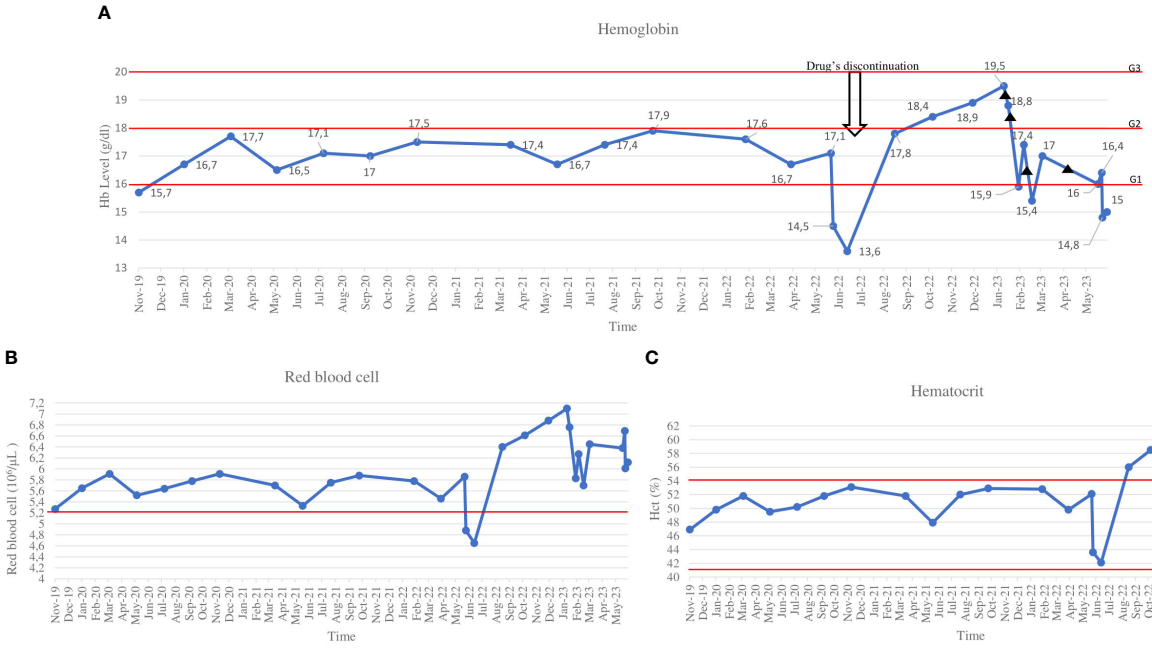

FIGURE 2
Hemoglobin **(A)**, red blood cells **(B)** and hematocrit **(C)** trend. ▲ phlebotomy.

malignant clones in response to anti-VEGF therapy, considering that RCC cells can synthesize EPO (26). Tripathi et al. conducted a retrospective analysis of 71 patients with advanced clear-cell RCC treated with different anti-VEGFR TKIs. They found Hb elevation in 83% of them, with a median time to increase of 2.4 weeks (27). However, higher Hb levels were associated with poor prognosis in this study. They assumed that hypoxia caused by anti-VEGF drugs led to the activation of other pro-angiogenic pathways that resulted in treatment resistance (27).

Similarly to other anti-VEGFR TKIs, we hypothesized that regorafenib could induce secondary erythrocytosis, even if the mechanism is unclear. Our patient continued to develop erythrocytosis even after we attempted to restart the drug at a reduced dose, suggesting that this adverse effect was not dose-related. In addition, considering that Hb levels increased six months after regorafenib initiation, we cannot exclude a potential sensitization effect.

Furthermore, in our patient, the clinical benefit was significantly prolonged with regorafenib therapy compared to what was reported in clinical trials (47 months vs 4.8 months) (9), despite EGISTs are characterized by a lower survival in comparison to other GISTs. Secondary erythrocytosis may result from VEGFR inhibition (25). Hence, the development of erythrocytosis could be a potential marker of regorafenib efficacy based on the prolonged response highlighted in this case. However, these observations are only hypothesis-generating and should be validated by further empirical research. Therefore, close monitoring of Hb, Hct, and erythrocytes levels, as well as any symptoms associated with erythrocytosis may be suggested in patients treated with regorafenib and exploring the potential association between the occurrence of erythrocytosis and the clinical outcome might be warranted.

Data availability statement

The original contributions presented in the study are included in the article/supplementary material. Further inquiries can be directed to the corresponding author.

Ethics statement

Written informed consent was obtained from the individual(s) for the publication of any potentially identifiable images or data included in this article.

Author contributions

EF: Writing – original draft, Writing – review & editing, Conceptualization. VA: Methodology, Supervision, Writing – review & editing. DC: Writing – review & editing. VF: Supervision, Writing – review & editing, Conceptualization. ML: Writing – review & editing. AB: Supervision, Writing – review & editing, Conceptualization. PdM: Supervision, Writing – original draft, Writing – review & editing, Conceptualization.

Funding

The author(s) declare that no financial support was received for the research, authorship, and/or publication of this article.

Conflict of interest

The authors declare that the research was conducted in the absence of any commercial or financial relationships that could be construed as a potential conflict of interest. The authors declared that they were an editorial board member of Frontiers, at the time of submission. This had no impact on the peer review process and the final decision.

Publisher's note

All claims expressed in this article are solely those of the authors and do not necessarily represent those of their affiliated organizations, or those of the publisher, the editors and the reviewers. Any product that may be evaluated in this article, or claim that may be made by its manufacturer, is not guaranteed or endorsed by the publisher.

References

1. Ma GL, Murphy JD, Martinez ME, Sicklick JK. Epidemiology of gastrointestinal stromal tumors in the era of histology codes: results of a population-based study. *Cancer Epidemiol biomark Prev Publ Am Assoc Cancer Res Cosponsored Am Soc Prev Oncol*. (2015) 24:298–302. doi: 10.1158/1055-9965.EPI-14-1002

2. Sharma AK, Kim TS, Bauer S, Sicklick JK. Gastrointestinal stromal tumor: new insights for a multimodal approach. *Surg Oncol Clin N Am*. (2022) 31:431–46. doi: 10.1016/j.soc.2022.03.007

3. Yamamoto H, Oda Y, Kawaguchi KI, Nakamura N, Takahira T, Tamiya S, et al. c-kit and PDGFRA mutations in extragastrointestinal stromal tumor (gastrointestinal stromal tumor of the soft tissue). *Am J Surg Pathol*. (2004) 28:479–88. doi: 10.1097/00000478-200404000-00007

4. Fagkrezos D, Touloumis Z, Giannila M, Penlidis C, Papaparaskeva K, Triantopoulou C. Extra-gastrointestinal stromal tumor of the omentum: a rare case report and review of the literature. *Rare Tumors*. (2012) 4:e44. doi: 10.4081/rt.2012.e44

5. El Charif MH, Amro S, Boulos F, Khalife M, Shamseddine A, Assi H, et al. Extra-gastrointestinal stromal tumors (EGISTs): A case report for a mischief entity. *Med (Baltimore)*. (2023) 102:e33394. doi: 10.1097/MD.0000000000033394

6. Casali PG, Blay JY, Abecassis N, Bajpai J, Bauer S, Biagini R, et al. Gastrointestinal stromal tumours: ESMO–EURACAN–GENTURIS Clinical Practice Guidelines for diagnosis, treatment and follow-up. *Ann Oncol*. (2022) 33:20–33. doi: 10.1016/j.annonc.2021.09.005

7. Wilhelm SM, Dumas J, Adnane L, Lynch M, Carter CA, Schütz G, et al. Regorafenib (BAY 73-4506): a new oral multikinase inhibitor of angiogenic, stromal and oncogenic receptor tyrosine kinases with potent preclinical antitumor activity. *Int J Cancer*. (2011) 129:245–55. doi: 10.1002/ijc.25864

8. Grothey A, Cutsem EV, Sobrero A, Siena S, Falcone A, Ychou M, et al. Regorafenib monotherapy for previously treated metastatic colorectal cancer (CORRECT): an international, multicentre, randomised, placebo-controlled, phase 3 trial. *Lancet*. (2013) 381:303–12. doi: 10.1016/S0140-6736(12)61900-X

9. Demetri GD, Reichardt P, Kang YK, Blay JY, Rutkowski P, Gelderblom H, et al. Efficacy and safety of regorafenib for advanced gastrointestinal stromal tumours after failure of imatinib and sunitinib (GRID): an international, multicentre, randomised, placebo-controlled, phase 3 trial. *Lancet*. (2013) 381:295–302. doi: 10.1016/S0140-6736(12)61857-1

10. Bruix J, Qin S, Merle P, Granito A, Huang YH, Bodoky G, et al. Regorafenib for patients with hepatocellular carcinoma who progressed on sorafenib treatment (RESORCE): a randomised, double-blind, placebo-controlled, phase 3 trial. *Lancet*. (2017) 389:56–66. doi: 10.1016/S0140-6736(16)32453-9

11. Mithoowani S, Laureano M, Crowther MA, Hillis CM. Investigation and management of erythrocytosis. *CMAJ*. (2020) 192:E913–8. doi: 10.1503/cmaj.191587

12. McMullin MF, Harrison CN, Ali S, Cargo C, Chen F, Ewing J, et al. A guideline for the diagnosis and management of polycythaemia vera. *A Br Soc Haematol Guideline Br J Haematol*. (2019) 184:176–91. doi: 10.1111/bjh.15648

13. Arber DA, Orazi A, Hasserjian R, Thiele J, Borowitz MJ, Le Beau MM, et al. The 2016 revision to the World Health Organization classification of myeloid neoplasms and acute leukemia. Blood. 2016;127(20):2391-2405. *Blood*. (2016) 128:462–3. doi: 10.1182/blood-2016-06-721662

14. Miettinen M, Monihan JM, Sarlomo-Rikala M, Kovatich AJ, Carr NJ, Emory TS, et al. Gastrointestinal stromal tumors/smooth muscle tumors (GISTs) primary in the omentum and mesentery: clinicopathologic and immunohistochemical study of 26 cases. *Am J Surg Pathol*. (1999) 23:1109–18. doi: 10.1097/00000478-199909000-00015

15. Lin J, Liao W, Wang J, Li W, Tang X, Li H, et al. Primary extra-gastrointestinal stromal tumor of retroperitoneum: Clinicopathologic characteristics and prognosis of six cases. *Front Oncol*. (2023) 13:1033598. doi: 10.3389/fonc.2023.1033598

16. Agaimy A. Gastrointestinal stromal tumors (GIST) from risk stratification systems to the new TNM proposal: more questions than answers? A review emphasizing the need for a standardized GIST reporting. *Int J Clin Exp Pathol*. (2010) 3:461–71.

17. Naranjo CA, Busto U, Sellers EM, Sandor P, Ruiz I, Roberts EA, et al. A method for estimating the probability of adverse drug reactions. *Clin Pharmacol Ther*. (1981) 30:239–45. doi: 10.1038/clpt.1981.154

18. Rawat BPS, Jagannatha A, Liu F, Yu H. Inferring ADR causality by predicting the Naranjo Score from Clinical Notes. *AMIA Annu Symp Proc*. (2021) 2020:1041–9.

19. Bosbach B, Deshpande S, Rossi F, Shieh JH, Sommer G, de StanChina E, et al. Imatinib resistance and microcytic erythrocytosis in a KitV558Δ;T669I/+ gatekeeper-mutant mouse model of gastrointestinal stromal tumor. *Proc Natl Acad Sci USA*. (2012) 109:E2276–2283. doi: 10.1073/pnas.1115240109

20. Van Der Veldt AAM, Boven E, Vroling L, Broxterman HJ, Van Den Eertwegh AJM, Haanen JG. Sunitinib-induced hemoglobin changes are related to the dosing schedule. *J Clin Oncol*. (2009) 27:1339–40. doi: 10.1200/JCO.2008.20.6151

21. Alexandrescu DT, McClure R, Farzanmehr H, Dasanu CA. Secondary erythrocytosis produced by the tyrosine kinase inhibitors sunitinib and sorafenib. *J Clin Oncol*. (2008) 26:4047–8. doi: 10.1200/JCO.2008.18.3525

22. Dulgar O, Cil I, Zirtiloglu A, Tural D. Long-lasting response with polycythemia to third-line axitinib treatment in metastatic renal cell carcinoma: Very rare case presentation. *J Oncol Pharm Pract Off Publ Int Soc Oncol Pharm Pract*. (2019) 25:1512–5. doi: 10.1177/1078155218790342

23. Fanelli M, Caputo F, Cerma K, Gelsomino F, Bari A, Dominici M, et al. Pazopanib-related secondary polycythemia in metastatic myxofibrosarcoma: A case report and review of the literature. *J Oncol Pharm Pract*. (2021) 27:766–70. doi: 10.1177/1078155220950440

24. Tam BY, Wei K, Rudge JS, Hoffman J, Holash J, Park SK, et alVEGF modulates erythropoiesis through regulation of adult hepatic erythropoietin synthesis. (2006) 12 (7):793-800. doi: 10.1038/nm1428

25. Wang W, Cheng J, Mallon C, Al-Marrawi MY, Holder S, Joshi M, et al. Symptomatic secondary polycythemia induced by anti-VEGF therapy for the treatment of metastatic renal cell carcinoma: A case series and review. *Clin Genitourin Cancer*. (2015) 13:e391–395. doi: 10.1016/j.clgc.2015.07.003

26. Sherwood JB, Shouval D. Continuous production of erythropoietin by an established human renal carcinoma cell line: development of the cell line. *Proc Natl Acad Sci USA*. (1986) 83:165–9. doi: 10.1073/pnas.83.1.165

27. Tripathi A, Jacobus S, Feldman H, Choueiri TK, Harshman LC. Prognostic significance of increases in hemoglobin in renal cell carcinoma patients during treatment with VEGF-directed therapy. *Clin Genitourin Cancer*. (2017) 15:396–402. doi: 10.1016/j.clgc.2016.12.009

frontiers | Frontiers in Oncology

TYPE Case Report
PUBLISHED 12 August 2024
DOI 10.3389/fonc.2024.1434720

Check for updates

OPEN ACCESS

EDITED BY
Lidia Castagneto Gissey,
Sapienza University of Rome, Italy

REVIEWED BY
Teodor Florin Georgescu,
Carol Davila University of Medicine and Pharmacy, Romania
Roberto Altamirano,
University of Chile, Chile
Mario Murguia-Perez,
Mexican Social Security Institute, Mexico

*CORRESPONDENCE
Qing Liu
2305470816@qq.com

†These authors have contributed equally to this work

RECEIVED 18 May 2024
ACCEPTED 24 July 2024
PUBLISHED 12 August 2024

CITATION
Sun J, Jiao X, Wu Z, Yao T, Tuo S, Wang Y, Chen R, He J, Qian J, Xu S and Liu Q (2024) Intraperitoneal spread in uterine sarcoma following unprotected laparoscopic transvaginal uterine morcellation: a case report and literature review. *Front. Oncol.* 14:1434720. doi: 10.3389/fonc.2024.1434720

COPYRIGHT
© 2024 Sun, Jiao, Wu, Yao, Tuo, Wang, Chen, He, Qian, Xu and Liu. This is an open-access article distributed under the terms of the Creative Commons Attribution License (CC BY). The use, distribution or reproduction in other forums is permitted, provided the original author(s) and the copyright owner(s) are credited and that the original publication in this journal is cited, in accordance with accepted academic practice. No use, distribution or reproduction is permitted which does not comply with these terms.

Intraperitoneal spread in uterine sarcoma following unprotected laparoscopic transvaginal uterine morcellation: a case report and literature review

Jianhao Sun[1,2†], Xinjuan Jiao[3†], Zhenzhen Wu[1†], Tingting Yao[1], Shumei Tuo[1], Yueyuan Wang[1], Ruirong Chen[1], Jing He[1], Jifang Qian[1], Shengfang Xu[1] and Qing Liu[1*]

[1]Gansu Provincial Maternity and Child-care Hospital, Lanzhou, Gansu, China, [2]Clinical Medical College, Yangzhou University, Yangzhou, Jiangsu, China, [3]Qingyang Second People's Hospital, Qingyang, Gansu, China

Clinically and through auxiliary examinations, distinguishing uterine leiomyoma from early-stage uterine sarcoma presents significant challenges. A 48-year-old patient underwent a laparoscopic hysterectomy for uterine leiomyoma, during which a large uterus was excised through the vagina and extracted. Four months post-operation, the patient developed abdominal distension, indicative of extensive pelvic-abdominal dissemination of uterine sarcoma. We hypothesize that unprotected fibroid fragmentation increases the risk of uterine sarcoma spread, thereby worsening the prognosis. Our literature review aims to thoroughly understand the risks associated with unprotected transvaginal laparoscopic tumor division.

KEYWORDS

uterine sarcomas, morcellation, laparoscopy, undifferentiated sarcomas, tumor spread

1 Introduction

With advancements in laparoscopic techniques, an increasing number of patients with uterine fibroids are opting for laparoscopic surgery. In 2014, the U.S. Food and Drug Administration (FDA) issued a warning against the use of power morcellation in laparoscopic uterine fibroid surgeries. Specifically, they discouraged removing the uterus or uterine fibroids via laparoscopic power morcellation, particularly in patients with suspected or confirmed uterine malignancy (1). Uterine sarcoma, a rare malignant tumor, comprises approximately 1% of female reproductive tract malignancies and 3% to 7% of uterine malignancies. With an incidence rate of 0.36 per 100,000, it is most prevalent among women aged 45 to 55. It is highly malignant, prone to recurrence, distant metastasis, and associated with a poor

prognosis (2, 3). According to the World Health Organization (WHO) classification of tumors, uterine sarcoma is derived from mesenchymal tissue and primarily includes uterine leiomyosarcoma (LMS), endometrial stromal sarcoma (ESS), and undifferentiated uterine sarcoma (UUS) (4). Previous studies reported that between 0.29% and 0.63% of patients initially diagnosed with leiomyoma and treated with laparoscopic surgery were found to have uterine sarcoma upon postoperative pathological examination (5–7). Previously, case reports of tumor spread due to morcellation primarily focused on laparoscopic myomectomy or subtotal hysterectomy (8, 9), with rare documentation of cases involving morcellation through vaginal extraction. In this report, we discuss a case of extensive pelvic and abdominal sarcoma dissemination following laparoscopic transvaginal uterine fragmentation, along with a review of related literature. The patient provided written informed consent for the publication of her information anonymously.

2 Case presentation

In December 2021, a 48-year-old woman was admitted to our center for a pelvic mass initially identified seven years earlier by transabdominal ultrasonography, which suggested a leiomyoma. Over the last three years, her menstrual cycles have lengthened, and her flow has increased. She has experienced abdominal pain and noticeable abdominal enlargement over the past five months. Following her hospitalization, a comprehensive preoperative evaluation was conducted. All serum tumor markers, including carbohydrate antigen 12-5 (CA12-5), CA19-9, alpha-fetoprotein (AFP), human epididymis protein 4 (HE4), and carcinoembryonic antigen (CEA), were within normal limits. However, her serum lactate dehydrogenase (LDH) level was elevated to 289U/L. Ultrasonography identified a heterogeneously echogenic mass in the anterior wall of the uterus measuring 12.6x12.0x8.4cm with a regular outline and clear boundaries, consistent with a uterine fibroid. It also revealed endometrial thickening to 15mm. MRI imaging displayed two quasi-circular masses within the uterine muscle wall; the larger was located in the anterior wall, measuring approximately 9.9x12.0x12.6cm, with 80% protruding into the subserosal area. The MRI suggested degeneration of the leiomyomas, possibly indicating a cellular leiomyoma (Figure 1). An endometrial biopsy was performed, which indicated a secretory-responsive endometrium.

On December 14, 2021, we performed a total laparoscopic hysterectomy and bilateral salpingectomy on a patient. During surgery, the uterus resembled that of a five-month pregnancy in size and was irregularly shaped with multiple fibroids, the largest being 12 cm in diameter on the anterior wall. The uterus was removed transvaginally without protective measures. The general picture is as follows (Figure 2). Microscopic examination post-surgery revealed the mass to be a leiomyoma, with most areas infarcted and some showing bizarre nuclei and rare mitotic figures (0-1/10 HPF) (Figure 3). The patient was advised of the need for close follow-up. A month post-operation, transabdominal ultrasonography showed no abnormalities. However, four months later, she developed abdominal distension. Repeat ultrasonography identified several heterogeneous masses of varying sizes in the right pelvic and abdominal regions, the largest measuring 12.5x11.8x7.8 cm. Further MRI revealed multiple abnormal signal shadows involving the vaginal stump, right lower quadrant, omentum, mesentery, intestinal space, pelvic cavity, and areas near the common iliac vessel bifurcation and rectum. A lesion in the right lower quadrant had penetrated the right transversus abdominis muscle, reaching the subcutaneous fat (Figure 4). Serum CA12-5 and LDH levels were elevated to 46.4 U/mL and 340 U/L, respectively, while other markers remained normal. Physical examination revealed significant abdominal distention with a large, palpable mass extending three fingers above the umbilicus and showing limited mobility. A firm, cystic mass approximately 5 cm in diameter was palpable at the vaginal stump, although the vaginal mucosa was intact.

On April 29, 2022, we performed an exploratory laparotomy, including resections of pelvic, abdominal, and mesenteric tumors, and a palliative resection of the right colon tumor. During surgery, we identified a 20 cm tumor in the abdominal cavity, covered by the greater omentum and prone to bleeding, with complex, primarily mucous internal tissue. The tumor encased parts of the ascending and transverse colon, as well as the ileum, and extended through the right peritoneum to the right rectus abdominis muscle. Additional tumors up to 3 cm in diameter were found on the small intestine and

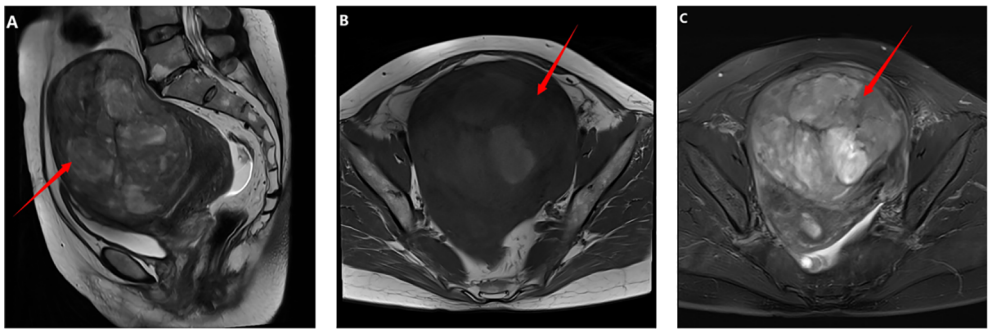

FIGURE 1
Imaging findings before the first operation: **(A–C)** Pelvic MRI revealed a tumor measuring approximately 9.9x12.0x12.6 cm in the anterior wall of the uterus. On T1-weighted images, the tumor was isointense with areas of hyperintensity. T2-weighted and fat-suppressed images showed hypointensity with areas of hyperintensity.

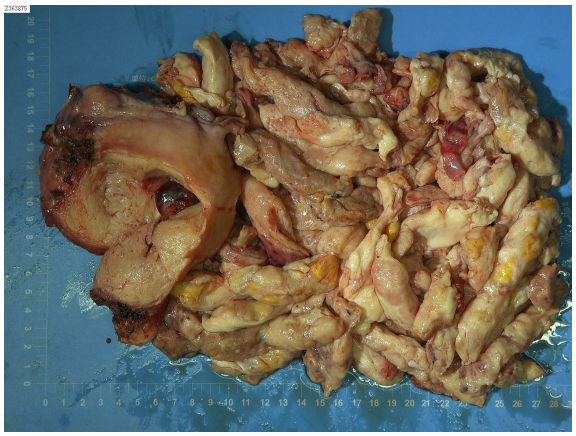

FIGURE 2
General view after the first operation. The fragmented uterus measured 15x9x4 cm. Between the muscle layers, two grayish-white nodular masses ranging from 1.5 to 3 cm in diameter were identified. These masses had tough, vortex-like textures upon sectioning. Additionally, a cluster of cylindrical tissue, grayish-white to grayish-red in color and measuring 20x20x2 cm, was discovered. This tissue was slightly tough in consistency, with a similar grayish-white to grayish-red appearance on sectioning.

descending colon, and larger tumors up to 7 cm were present in the pelvis. Enlarged retroperitoneal lymph nodes were noted, the largest measuring 4 cm. The bilateral ovaries were not visible. We advised the patient's family of the challenging intraoperative conditions and the impossibility of complete cytoreductive surgery, recommending a palliative approach instead. They consented to this plan. Microscopic analysis confirmed undifferentiated sarcomas in the abdominal and pelvic masses, with tumor involvement noted in the right colon, part of the ileum, mesentery and its lymph nodes, omentum, and appendix (Figure 5). Postoperatively, the patient experienced pleural effusion, right hydronephrosis, and poor incision healing.

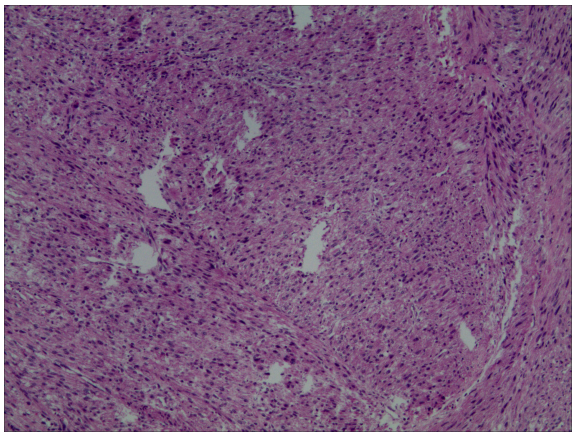

FIGURE 3
Light microscopic examination of the tumor post-first resection (H&E stain, 10x10) revealed spindle-shaped cells arranged in fascicles. These cells exhibited indistinct boundaries, mild nuclear atypia, and slightly coarse chromatin. Additionally, bizarre nuclei were scattered, and mitotic figures ranged from 0 to 1 per 10 high power fields. Infarction was observed in some tumor cells.

After symptomatic treatment, her condition improved. Considering her overall status, we recommended follow-up chemotherapy. However, the patient chose to discontinue treatment for personal reasons and was discharged, resulting in unsuccessful follow-up.

3 Discussion

Morcellation, a surgical technique, involves dividing tissue into smaller fragments to facilitate removal through tiny incisions or with laparoscopic tools, thereby reducing the size of the uterus or myomas. Historically, gynecologists employed manual morcellation via the vagina to extract an enlarged uterus (10). Power morcellation, introduced in 1993, shaves or cuts tissue to facilitate tissue extraction (11). Studies have shown that both power morcellation and manual segmentation increase the risk of recurrence (12, 13). Anupama et al. (14) and Della Badia et al. (15) research demonstrated that the inappropriate use of fibroids in patients with uterine sarcoma can promote tumor metastasis and even result in patient mortality. Small visible and microscopic tissue fragments may scatter throughout the abdomen following morcellation. As a consequence, tumor tissue may disseminate to the peritoneum as a result of this process (16). The meta-analysis comprised 24 studies involving 384 patients, investigating the prognosis of patients with uterine leiomyosarcoma across various morcellation methods. The findings indicated that patients undergoing electric morcellation exhibited the poorest prognosis, with a 5-year survival rate of 30%, whereas those without morcellation demonstrated the most favorable prognosis, boasting a 5-year survival rate of 60%. Patients subjected to cold knife morcellation (e.g., electrocautery or scissors) exhibited an intermediate prognosis, achieving a 5-year survival rate of 59% (17). The laparoscopic removal of uterine fibroids has garnered attention following the issuance of a safety communication warning by the FDA in 2014 (1). In 2017, the European Society of Gynecological Oncology Statement (ESGO) and the US FDA 2020 recommended employing closed shredding bags. These bags aim to facilitate minimally invasive techniques while preventing tissue dissemination in the abdominal cavity (17, 18). These measures are effective in preventing the dissemination of tumor tissue.

The previously described case involved the removal of a tumor that was initially fragmented into small pieces using a scalpel within the vagina. Following the initial operation, the tumor rapidly developed extensive pelvic and abdominal metastases, prompting an analysis of potential causes. Firstly, the malignancy risk associated with the uterine tumor was not thoroughly evaluated before the initial operation. Secondly, the dissemination of lesions resulted from the fragmentation of the uterus without protective measures. Thirdly, the initial pathological diagnosis of uterine sarcoma was imprecise, exacerbated by the impact of morcellation on pathological assessment. The lack of further treatment post-operation significantly affected the prognosis. Therefore, adherence to the tumor-free principle in vaginal tumor excision is crucial. While the vagina serves as an optimal natural passage for uterine extraction, difficulties arise in extracting large uteri from narrow vaginas, necessitating techniques such as segmentation, cutting, and splitting. Previous studies indicate that even intravaginal shredding with a protective bag fails to prevent tumor spread due to potential bag leakage during vaginal morcellation

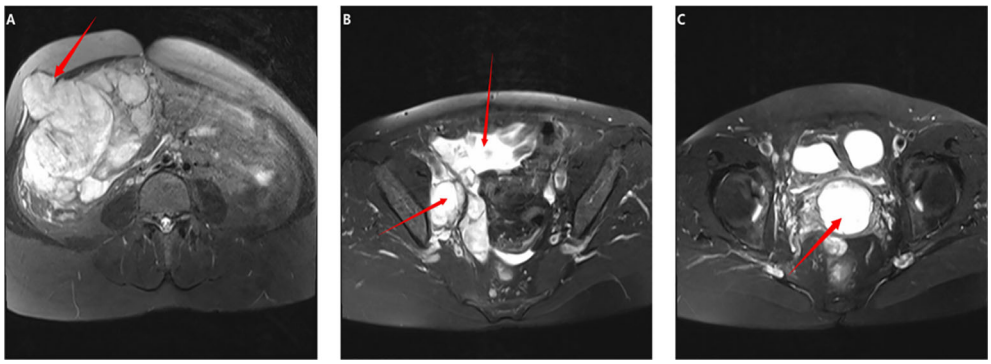

FIGURE 4
Imaging findings prior to the second surgery: **(A–C)** Whole abdomen MRI: **(A, B)** Multiple space-occupying lesions were identified in the right lower abdomen and pelvic cavity. The largest lesion, located in the lower abdomen, measured 11.6x10.6x8.4 cm and locally protruded into the right abdominal wall, involving the right rectus abdominis muscle. It exhibited isointense and hypointense signals on T1-weighted images and a slightly hyperintense signal on T2-weighted images. **(C)** A mass measuring approximately 3.6x4.2x4.2 cm was observed at the vaginal stump, displaying a hypointense signal on T1-weighted and a slightly hyperintense signal on T2-weighted images.

(19). Thus, our attention should be directed towards the shredding technique itself, regardless of the method of extraction.

Measures should be implemented to maximize the benefits of morcellation while minimizing the risk of tumor dissemination associated with it. Specific patient screening for suitability for morcellated surgery is imperative. However, there is currently no reliable preoperative diagnostic method for uterine sarcoma (17). This presents a considerable challenge for gynecologists. Patients undergoing laparoscopic hysterectomy (myomectomy) require thorough evaluation regarding the malignancy risk of uterine tumors prior to surgery. As specialists, we must focus on identifying clinical risk factors for uterine sarcoma. These factors include the following (5): Patients were predominantly perimenopausal and postmenopausal women, with uterine sarcoma typically diagnosed between the ages of 50 and 60, while cases under 40 were relatively uncommon. The patient presented with abnormal uterine bleeding, indicative of rapid fibroid growth, particularly notable in postmenopausal women not undergoing hormone replacement therapy. Additionally, the patient had a

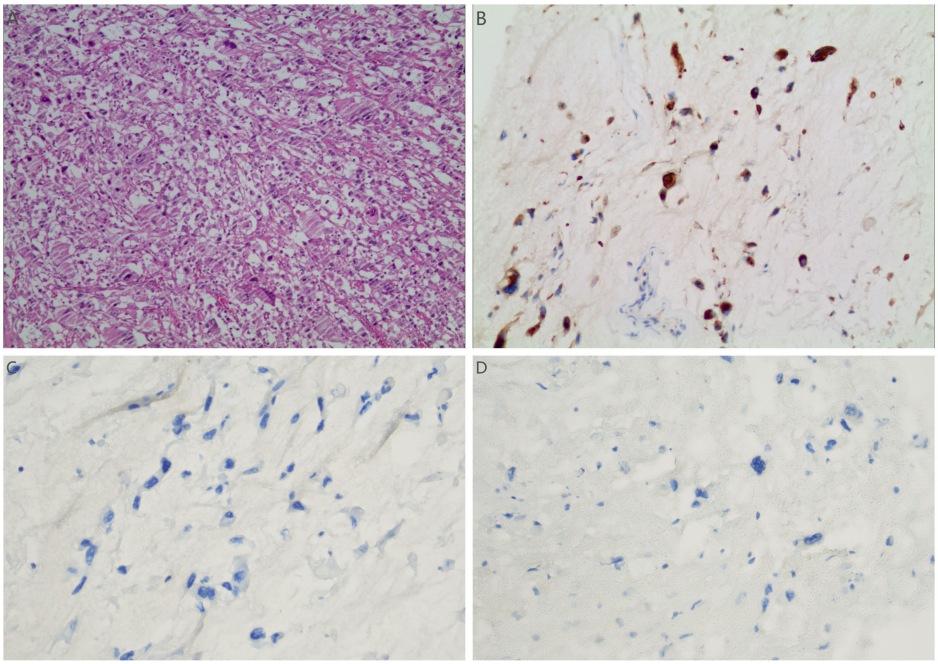

FIGURE 5
(A) Light microscopic examination of the tumor post-second resection (H&E stain, 10x10) showed pleomorphic cells with indistinct boundaries. The cytoplasm varied from eosinophilic to clear. There was severe nuclear atypia, prominent nucleoli, and conspicuous mitotic figures. The immunohistochemical results of sarcoma component: **(B–D)** tumor cells showed positive for Vimentin **(B)**, negative for SMA **(C)** and Desmin **(D)**.

medical history of tamoxifen use and pelvic radiation therapy, as well as a childhood history of retinoblastoma and hereditary leiomyomatosis and renal cell carcinoma (HLRCC). Furthermore, further imaging examinations, cervical cancer screenings, and endometrial tissue sampling are necessary to identify malignancies (17). MRI can assess tumor invasion into the uterine muscles and surrounding structures, as well as lymph node metastasis, which are typical manifestations of uterine sarcoma on MRI (20–22). MRI imaging of uterine sarcoma typically reveals a large solid mass with an indistinct boundary and heterogeneous signal intensity. Uterine sarcomas exhibit abnormally high signals on T2-weighted imaging (T2WI), whereas uterine fibroids often display low signals. Additionally, uterine sarcomas may demonstrate unclear borders and infiltrative growth patterns. A slightly elevated signal on T1-weighted imaging (T1WI) suggests intra-mass hemorrhage and necrosis. During dynamic contrast-enhanced MRI (DCE-MRI), the mass exhibits early enhancement, while the necrotic areas remain unenhanced. Diffusion-weighted imaging (DWI) typically reveals restricted diffusion within the sarcoma due to dense tumor cellularity, resulting in decreased apparent diffusion coefficient (ADC) values. Nonetheless, there are overlapping MRI features between uterine sarcoma and atypical uterine fibroids (23), therefore, it is crucial to integrate detailed clinical information with T1WI, T2WI, DWI, and DCE-MRI for preoperative diagnosis to avoid missing patients with potential uterine sarcoma. While patients with uterine sarcoma do not exhibit specific tumor markers, elevated serum levels of LDH and CA12-5, as demonstrated in some studies, hold diagnostic significance for uterine sarcoma (24, 25). Despite thorough preoperative evaluation, it is essential to thoroughly discuss all available treatment options, along with their respective benefits and drawbacks, with patients considering laparoscopic hysterectomy. Provide patients with information on diverse surgical approaches for managing uterine fibroids, empowering them to make informed decisions.

Undoubtedly, intraoperative tumor-free technique remains pivotal for preventive measures. Emphasizing the closed morcellation bag's role as a safety measure in laparoscopic hysterectomy (myoma) is crucial, representing an integral component of morcellation. However, during total laparoscopic hysterectomy, where an enlarged uterus is extracted from the vagina, there has been limited advocacy for protective sleeves. Under such circumstances, morcellation could theoretically lead to the dissemination of undetected malignant cells (17). Based on this case, it is imperative to adhere to the tumor-free principle, irrespective of whether tumor removal occurs from the abdomen, vagina, or elsewhere. Recognizing this concern, some studies suggest placing the uterus in a specimen bag before vaginal extraction if tissue fragmentation is required post laparoscopic hysterectomy (26). Recent studies have introduced a novel technique for vaginal morcellation within a closed environment. This approach offers both vaginal protection and retraction while securely containing the specimen to prevent loss during morcellation, thereby minimizing the risk of unforeseen malignancy (27).

Morcellation disrupts the structural integrity of tissue specimens, posing specific challenges for intraoperative pathological diagnosis and surgical pathological staging (28). Research indicates that morcellation frequently disrupts the junctional region between endometrial stromal or smooth muscle tumors and the surrounding myometrium. However, histological examination of this junctional region is crucial for the classification of atypical stromal tumors (29). Following uterine morcellation, accurately assessing the size of the uterine tumor and the depth of myometrial infiltration by epithelial or stromal lesions becomes challenging. This may have contributed to the incomplete or even missed pathological diagnosis during the initial operation of this case.

4 Conclusions

In conclusion, while morcellation can benefit patients, it can also lead to complications. To prevent similar tragedies, whether removing morcellated tumor tissue from the vagina or the abdomen, the concept of maintaining a tumor-free environment should be further emphasized and the application of tumor-free technology should be strengthened.

Data availability statement

The original contributions presented in the study are included in the article/supplementary material. Further inquiries can be directed to the corresponding author.

Ethics statement

Written informed consent was obtained from the individual(s) for the publication of any potentially identifiable images or data included in this article.

Author contributions

JS: Conceptualization, Writing – original draft. XJ: Investigation, Writing – original draft. ZW: Data curation, Writing – original draft. TY: Writing – review & editing. ST: Writing – review & editing. YW: Writing – review & editing. RC: Writing – review & editing. JH: Writing – review & editing. JQ: Writing – review & editing. SX: Writing – review & editing. QL: Funding acquisition, Supervision, Writing – review & editing.

Funding

The author(s) declare financial support was received for the research, authorship, and/or publication of this article. This work was supported in part by the Top-notch Leading Talents Project in Gansu Province, the Natural Science Foundation of Gansu Province (No. 22JR5RA718), and the Lanzhou Science and Technology Planning Project (2022-5-88).

Conflict of interest

The authors declare that the research was conducted in the absence of any commercial or financial relationships that could be construed as a potential conflict of interest.

Publisher's note

All claims expressed in this article are solely those of the authors and do not necessarily represent those of their affiliated organizations, or those of the publisher, the editors and the reviewers. Any product that may be evaluated in this article, or claim that may be made by its manufacturer, is not guaranteed or endorsed by the publisher.

References

1. Hampton T. Use of morcellation to remove fibroids scrutinized at FDA hearings. *JAMA*. (2014) 312:588. doi: 10.1001/jama.2014.10041

2. Major FJ, Blessing JA, Silverberg SG, Morrow CP, Creasman WT, Currie JL, et al. Prognostic factors in early-stage uterine sarcoma. *A Gynecologic Oncol Group study. Cancer*. (1993) 71:1702–9. doi: 10.1002/cncr.2820710440

3. Mbatani N, Olawaiye AB, Prat J. Uterine sarcomas. *Int J Gynaecol Obstet*. (2018) 143 Suppl 2:51–8. doi: 10.1002/ijgo.12613

4. McCluggage WG, Singh N, Gilks CB. Key changes to the World Health Organization (WHO) classification of female genital tumours introduced in the 5th edition (2020). *Histopathology*. (2022) 80:762–78. doi: 10.1111/his.14609

5. Sizzi O, Manganaro L, Rossetti A, Saldari M, Florio G, Loddo A, et al. Assessing the risk of laparoscopic morcellation of occult uterine sarcomas during hysterectomy and myomectomy: Literature review and the ISGE recommendations. *Eur J Obstet Gynecol Reprod Biol*. (2018) 220:30–8. doi: 10.1016/j.ejogrb.2017.10.030

6. Zhang J, Li T, Zhang J, Zhu L, Lang J, Leng J. Clinical characteristics and prognosis of unexpected uterine sarcoma after hysterectomy for presumed myoma with and without transvaginal scalpel morcellation. *Int J Gynecol Cancer*. (2016) 26:456–63. doi: 10.1097/IGC.0000000000000638

7. Holzmann C, Kuepker W, Rommel B, Helmke B, Bullerdiek J. Reasons to reconsider risk associated with power morcellation of uterine fibroids. *In Vivo*. (2020) 34:1–9. doi: 10.21873/invivo.11739

8. Stefanko DP, Eskander R, Aisagbonhi O. Disseminated endometriosis and low-grade endometrioid stromal sarcoma in a patient with a history of uterine morcellation for adenomyosis. *Case Rep obstetrics gynecology*. (2020) 2020:7201930. doi: 10.1155/2020/7201930

9. Vimercati A, Santarsiero CM, Esposito A, Putino C, Malvasi A, Damiani GR, et al. An extremely rare case of disseminated peritoneal leiomyomatosis with a pelvic leiomyosarcoma and omental metastasis after laparoscopic morcellation: Systematic review of the literature. *Diagnostics (Basel Switzerland)*. (2022) 12. doi: 10.3390/diagnostics12123219

10. Pratt JH, Gunnlaugsson GH. Vaginal hysterectomy by morcellation. *Mayo Clin Proc*. (1970) 45:374–87.

11. Steiner RA, Wight E, Tadir Y, Haller U. Electrical cutting device for laparoscopic removal of tissue from the abdominal cavity. *Obstet Gynecol*. (1993) 81:471–4.

12. Fulvio B, Luca B, Paola C, Elisa P, Niccolò G, Mario P, et al. Low-grade uterine endometrial stromal sarcoma: Prognostic analysis of clinico-pathological characteristics, surgical management, and adjuvant treatments. Experience from two referral centers. *Front Oncol*. (2022) 12:883344–4. doi: 10.3389/fonc.2022.883344

13. Pedra Nobre S, Hensley ML, So M, Zhou QC, Iasonos A, Leitao MM Jr, et al. The impact of tumor fragmentation in patients with stage I uterine leiomyosarcoma on patterns of recurrence and oncologic outcome. *Gynecologic Oncol*. (2020) 160(1):99–105. doi: 10.1016/j.ygyno.2020.10.020

14. Anupama R, Ahmad SZ, Kuriakose S, Vijaykumar DK, Pavithran K, Seethalekshmy NV. Disseminated peritoneal leiomyosarcomas after laparoscopic "myomectomy" and morcellation. *J Minim Invasive Gynecol*. (2011) 18:386–9. doi: 10.1016/j.jmig.2011.01.014

15. Della Badia C, Karini H. Endometrial stromal sarcoma diagnosed after uterine morcellation in laparoscopic supracervical hysterectomy. *J Minim Invasive Gynecol*. (2010) 17:791–3. doi: 10.1016/j.jmig.2010.07.001

16. Stine JE, Clarke-Pearson DL, Gehrig PA. Uterine morcellation at the time of hysterectomy: techniques, risks, and recommendations. *Obstet Gynecol Surv*. (2014) 69:415–25. doi: 10.1097/OGX.0000000000000088

17. American College of O and Gynecologists' Committee on Gynecologic P. Uterine morcellation for presumed leiomyomas: ACOG committee opinion, number 822. *Obstet Gynecol*. (2021) 137:e63–74. doi: 10.1097/AOG.0000000000004291

18. Halaska MJ, Haidopoulos D, Guyon F, Morice P, Zapardiel I, Kesic V, et al. European society of gynecological oncology statement on fibroid and uterine morcellation. *Int J Gynecol Cancer*. (2017) 27:189–92. doi: 10.1097/IGC.0000000000000911

19. Solima E, Scagnellli G, Austoni V, Natale A, Bertulessi C, Busacca M, et al. Vaginal uterine morcellation within a specimen containment system: A study of bag integrity. *J Minim Invasive Gynecol*. (2015) 22:S86. doi: 10.1016/j.jmig.2015.08.231

20. Suzuki A, Aoki M, Miyagawa C, Murakami K, Takaya H, Kotani Y, et al. Differential diagnosis of uterine leiomyoma and uterine sarcoma using magnetic resonance images: A literature review. *Healthcare (Basel)*. (2019) 7. doi: 10.3390/healthcare7040158

21. Barral M, Place V, Dautry R, Bendavid S, Cornelis F, Foucher R, et al. Magnetic resonance imaging features of uterine sarcoma and mimickers. *Abdom Radiol (NY)*. (2017) 42:1762–72. doi: 10.1007/s00261-017-1076-9

22. Santos P, Cunha TM. Uterine sarcomas: clinical presentation and MRI features. *Diagn Interv Radiol*. (2015) 21:4–9. doi: 10.5152/dir.2014.14053

23. Malek M, Rahmani M, Seyyed Ebrahimi SM, Tabibian E, Alidoosti A, Rahimifar P, et al. Investigating the diagnostic value of quantitative parameters based on T2-weighted and contrast-enhanced MRI with psoas muscle and outer myometrium as internal references for differentiating uterine sarcomas from leiomyomas at 3T MRI. *Cancer Imaging*. (2019) 19:20. doi: 10.1186/s40644-019-0206-8

24. Skorstad M, Kent A, Lieng M. Preoperative evaluation in women with uterine leiomyosarcoma. A nationwide cohort study. *Acta Obstet Gynecol Scand*. (2016) 95:1228–34. doi: 10.1111/aogs.13008

25. Goto A, Takeuchi S, Sugimura K, Maruo T. Usefulness of Gd-DTPA contrast-enhanced dynamic MRI and serum determination of LDH and its isozymes in the differential diagnosis of leiomyosarcoma from degenerated leiomyoma of the uterus. *Int J Gynecol Cancer*. (2002) 12:354–61. doi: 10.1046/j.1525-1438.2002.01086.x

26. Siedhoff MT, Cohen SL. Tissue extraction techniques for leiomyomas and uteri during minimally invasive surgery. *Obstet Gynecol*. (2017) 130:1251–60. doi: 10.1097/AOG.0000000000002334

27. Kliethermes C, Walsh T, Guan Z, Guan X. Vaginal tissue extraction made easy. *J Minim Invasive Gynecol*. (2017) 24:726. doi: 10.1016/j.jmig.2017.02.005

28. Worldwide AAMIG. AAGL practice report: Morcellation during uterine tissue extraction. *J Minim Invasive Gynecol*. (2014) 21:517–30. doi: 10.1016/j.jmig.2014.05.010

29. Han AKW, Hong K, Kim M, Kim MK, Kim ML, Jung YW, et al. Unexpected uterine smooth muscle tumor of uncertain Malignant potential and sarcoma: A single center cohort study in South Korea. *Taiwan J Obstet Gynecol*. (2020) 59:275–81. doi: 10.1016/j.tjog.2020.01.017

frontiers | Frontiers in Oncology

TYPE Case Report
PUBLISHED 16 August 2024
DOI 10.3389/fonc.2024.1436854

Check for updates

OPEN ACCESS

EDITED BY
Ferdinando Agresta,
ULSS2 Marca Trevigiana, Italy

REVIEWED BY
Mario Murguia-Perez,
Mexican Social Security Institute, Mexico
Teodor Florin Georgescu,
Carol Davila University of Medicine and Pharmacy, Romania

*CORRESPONDENCE
Haijian Huang
huanghaijian2008@sina.com

RECEIVED 22 May 2024
ACCEPTED 25 July 2024
PUBLISHED 16 August 2024

CITATION
Li J, Huang H, Zeng Q, Chen X and Chen L (2024) Case report: Ovarian mucinous tumor with a mural nodule of liposarcoma: a rare case.
Front. Oncol. 14:1436854.
doi: 10.3389/fonc.2024.1436854

COPYRIGHT
© 2024 Li, Huang, Zeng, Chen and Chen. This is an open-access article distributed under the terms of the Creative Commons Attribution License (CC BY). The use, distribution or reproduction in other forums is permitted, provided the original author(s) and the copyright owner(s) are credited and that the original publication in this journal is cited, in accordance with accepted academic practice. No use, distribution or reproduction is permitted which does not comply with these terms.

Case report: Ovarian mucinous tumor with a mural nodule of liposarcoma: a rare case

Jiezhen Li[1], Haijian Huang[1]*, Qiang Zeng[2], Xin Chen[1] and Lingfeng Chen[1]

[1]Provincial Clinical Medical College of Fujian Medical University, Department of Pathology, Fujian Provincial Hospital, Fuzhou, China, [2]First Affiliated Hospital of Fujian Medical University, Department of Pathology, Fuzhou, China

Background: Ovarian mucinous tumor with a mural nodule is a rare and special type of ovarian surface epithelial–stromal tumor. Mural nodules are morphologically classified into three types: sarcoma-like, anaplastic carcinomatous, and true sarcomatous nodules. Ovarian mucinous tumors with true sarcomatous mural nodules are rare and challenging to diagnose, with only 10 cases reported worldwide. Currently, liposarcoma mural nodules remain unreported.

Case presentation: A 91-year-old woman was hospitalized for postmenopausal vaginal bleeding for 3 weeks. Imaging revealed a large cystic mass (20.0 cm × 17.7 cm × 12.8 cm) on the right ovary. The mass was multilocular cystic, with a mural nodule (1.4 cm × 1.2 cm × 1.0 cm) in the focal cyst wall. Based on histological morphology, immunohistochemical staining, and MDM2/CDK4 fluorescence *in situ* hybridization testing, the diagnosis was ovarian mucinous cystadenoma with a mural nodule of well-differentiated liposarcoma. To the best of our knowledge, this has never been reported before. High-throughput sequencing identified *KRAS* mutations in the ovarian mucinous cystadenoma. However, the liposarcoma mural nodule did not exhibit *KRAS* mutations but displayed copy number amplifications of *CDK4* and *DDR2*, as well as a frameshift mutation in exon 13 of *ASXL1* (p. A627Gfs*8).

Conclusions: This case broadens the morphological spectrum of mural nodules in ovarian mucinous tumors, deepening our knowledge of this rare morphology. Meanwhile, through high-throughput sequencing, we found no overlapping genetic evidence between the liposarcoma mural nodule and associated ovarian mucinous cystadenoma.

KEYWORDS

ovarian mucinous tumor, mural nodule, liposarcoma, pathological feature, high-throughput sequencing

Abbreviations: FIGO, International Federation of Gynecology and Obstetrics (Fédération Internationale de Gynécologie et d'Obstétrique); FISH, fluorescence *in situ* hybridization; ROMA, risk of ovarian malignancy algorithm; MDM2, murine double minute 2; CDK4, cyclin-dependent kinase 4.

Background

Mural nodules are single- or multiple-boundary masses arising in the cyst wall. Ovarian mucinous tumors with mural nodules are rare, with an incidence rate of 2 to 5 per million (1). Mural nodules are divided into three histological types based on morphology: sarcoma-like, anaplastic carcinomatous, and true sarcomatous nodules (2–5). Sarcoma-like mural nodules are generally considered benign reactive lesions, whereas anaplastic carcinomatous and true sarcomatous nodules are regarded as invasive malignant tumors (5). Currently, reports of ovarian mucinous tumors with mural nodules of leiomyoma are limited (6, 7). Given the significantly different prognoses associated with various mural nodule types, making an accurate pathological diagnosis of mural nodules is crucial. However, mural nodules are often small and attached to the cyst wall, making them difficult to detect on preoperative imaging examinations. Insufficient sampling by pathologists postoperatively can easily lead to missed diagnoses. Therefore, for ovarian mucinous tumors, pathologists must carefully observe gross specimens, perform adequate sampling, and provide precise diagnoses to optimize patient outcomes.

Currently, only 10 cases of ovarian mucinous tumors with true sarcomatous mural nodules have been reported (Table 1), including 3 cases of osteosarcoma mural nodules (9, 10), 3 of fibrosarcoma mural nodules (12–14), 2 of undifferentiated sarcoma mural nodules (8, 14), 1 of rhabdomyosarcoma mural nodule (15), and 1 of high-grade sarcoma mural nodule (11). However, no cases of liposarcoma mural nodules have been reported to date.

Herein, we describe the case of a 91-year-old woman diagnosed with ovarian mucinous cystadenoma with a well-differentiated liposarcoma mural nodule, based on histological morphology, immunohistochemical examination, and MDM2/CDK4 fluorescence *in situ* hybridization (FISH) testing. To the best of our knowledge, this study is the first to report such a case. We compared our case with other cases of true sarcomatous mural nodules to elaborate on the clinicopathological features of this entity, explore the diagnostic and treatment strategies for this rare tumor, and provide reference and insights for future clinical practice.

Case presentation

A 91-year-old woman was hospitalized due to postmenopausal vaginal bleeding for 3 weeks. Tumor marker assessment revealed a human epididymal protein 4 level of 123.30 pmol/L, risk of ovarian malignancy algorithm (ROMA) premenopausal value of 41.52%, and ROMA postmenopausal value of 31.88%. The preoperative serum levels of CA-125, CEA, CA19-9, and AFP were normal. Abdominal computed tomography revealed a large cystic mass (approximately 20.0 cm × 17.7 cm × 12.8 cm) in the pelvic cavity, with clear margins and a few septations inside the cyst. This large cyst was closely related to the right adnexa. The patient underwent total hysterectomy and bilateral salpingo-oophorectomy under general anesthesia. During surgery, a large cystic mass was detected in the right adnexal region, with a diameter of approximately 20 cm. The cyst was oval-shaped, with a smooth surface and rich blood supply, containing septations. Additionally, its pedicle was connected to the right ovary. No abnormalities were visually observed in the right fallopian tube, uterus, and left adnexa, and no abnormalities were noted in the stomach, small intestine, ileocecal region, colon, rectum, and greater omentum intraoperatively.

In pathological examination, we first conducted gross examination. We observed a smooth-surfaced, yellowish-brown cystic mass in the right ovary, measuring 20.0 cm × 17.7 cm × 12.8 cm. This mass was composed of multilocular cysts filled with viscous yellowish-brown fluid or transparent mucinous material. Upon careful dissection, we found a mural nodule within the cyst wall in a local region, measuring 1.4 cm × 1.2 cm × 1.0 cm and protruding into the cyst cavity with a clear boundary. The mural nodule had a solid, grayish-white cut surface with a moderate texture. The remaining cyst wall was smooth, without papillary protrusions, and its septum thickness was uneven, ranging from 0.2 to 0.4 cm. Next, (2) microscopic examination was conducted. The ovarian cyst wall was found to be lined with a single layer of gastrointestinal-type mucinous columnar epithelium (Figure 1A), showing no papillary hyperplasia. The mucinous epithelial cells exhibited no atypia, with nuclei located at the basal portion and the cytoplasm rich in mucus (Figure 1B). A mural nodule was observed beneath the mucinous epithelium. This nodule was composed of short spindle cells, pleomorphic cells, and a few adipocytes (Figure 1C). Under low magnification, the spindle tumor cells were indistinguishable from the surrounding tissue and were arranged in sheets or bundles (Figure 1C). A few adipocytes were scattered between the spindle cells; they showed good differentiation and varied in size (Figure 1D). Under high magnification, the spindle cell nuclei clearly exhibited atypia, with abundant and eosinophilic cytoplasms (Figure 1E). Scattered tumor giant cells were also observed (Figure 1F). Furthermore, some regions demonstrated signs of tumor invasive growth, including large blood vessel invasion (Figure 1G) and perineural growth (Figure 1H). The nuclei of adipocytes showed mild atypia under high magnification, with a few visible lipoblasts (Figures 1I, J). No definite neoplastic necrosis was observed, and the mitotic figures were approximately 3/10 HPF (high-power fields). In the tumor, interstitial collagen markedly degenerated, accompanied by extensive lymphocytic and plasmacytic infiltration; in some regions, lymphoid follicles formation was noted (Figure 1A). In immunophenotyping, the mucinous epithelium expressed cytokeratin (Figure 2A) but not vimentin (Figure 2B). Conversely, the mural nodule tumor cells did not express cytokeratin (Figure 2A) but exhibited diffuse strong positive expression of vimentin (Figure 2B). Additionally, the tumor cells in the mural nodule showed a strong positive expression of MDM2 (Figure 2C), CDK4 (Figure 2D), P16 (Figure 2E), MUC4, and SMA (Figure 2F), with a Ki-67 proliferation index of 30%. Regarding the FISH test, the mural nodule region showed amplification signals of *CDK4* (Figure 3A) and *MDM2* (Figure 3B) genes. Combining the histological morphology, immunohistochemistry, and MDM2/CDK4 FISH test results, we diagnosed the patient with ovarian mucinous cystadenoma with a mural nodule of well-differentiated liposarcoma, International Federation of Gynecology and Obstetrics (FIGO) stage IA. High-throughput sequencing was

TABLE 1 Summary of cases of ovarian mucinous cystic tumor with sarcomatous mural nodules.

References	Yang (2019) (9)	Chu (2021) (8)	McFarland (2015) (10)		Desouki (2014) (11)	Rahilly (1994) (12)	Bruijn (1987) (13)	Prat (1979) (14)		Tsujimura (1992) (15)	Present report
Number of cases	1	1	2		1	1	1	2		1	1
Age (years)	60	65	34	18	25	69	27	61	49	57	91
Tumor location	Right	Right	Left	Left	Right	Left	Left	Right	Left	Left	Right
Tumor size (cm)	9.4	25	29	11	44	12	17	16	14.5	15	20
Nodule size (cm)	1.6–3.8	5	2	–	3–11	–	4	10	7	15	1.4
Presenting symptoms	Lower abdominal discomfort and abdominal distension	Abdominal swelling	Persistent vaginal bleeding and abdominal swelling	Abdominal swelling	Abdominal enlargement and slight distension	Lower abdominal pain	Lower abdominal swelling	Abdominal swelling	Abdominal swelling	Lower abdominal tumor	Vaginal bleeding
Histologic type of primary mucinous ovarian tumor	Borderline cystadenoma with intraepithelial carcinoma	Mucinous cystadenoma	Cystadenocarcinoma	Borderline cystadenoma	Cystadenocarcinoma	Cystadenocarcinoma	Cystadenocarcinoma	Cystadenoma	Cystadenocarcinoma	Cystadenocarcinoma	Cystadenoma
Histologic type of mural nodule	Pleomorphic undifferentiated sarcoma	Osteosarcoma	Osteosarcoma	Osteosarcoma	High-grade sarcoma	Fibrosarcoma	Fibrosarcoma	Fibrosarcoma	Undifferentiated sarcoma	Rhabdomyosarcoma	Well-differentiated liposarcoma
FIGO staging	IC	IC	IA	IC	IA	IIB	IA	IA	IIIA	IA	IA
Treatment	BSO + Omen + ChT	UO	TAH + BSO + Omen	UO	UO	TAH + BSO + appen	USO + Omen	TAH + BSO + appen + RT	TAH + BSO + Omen	TAH + BSO + ChT	TAH + BSO
Follow-up	NED, 36 months	NED, 5 months	NED, 18 months	NED, 12 months	–	–	–	Died of hepatic metastases, 18 months	Died of renal failure, 1 week	NED, 3 months	NED, 25 months

-, unknown; appen, appendectomy; BSO, bilateral salpingo-oophorectomy; ChT, chemotherapy; FIGO, International Federation of Gynecology and Obstetrics; NED, no evidence of disease; Omen, omentectomy; RT, radiation therapy; TAH, total abdominal hysterectomy; UO, unilateral oophorectomy; USO, unilateral salpingo-oophorectomy.

10.3389/fonc.2024.1436854

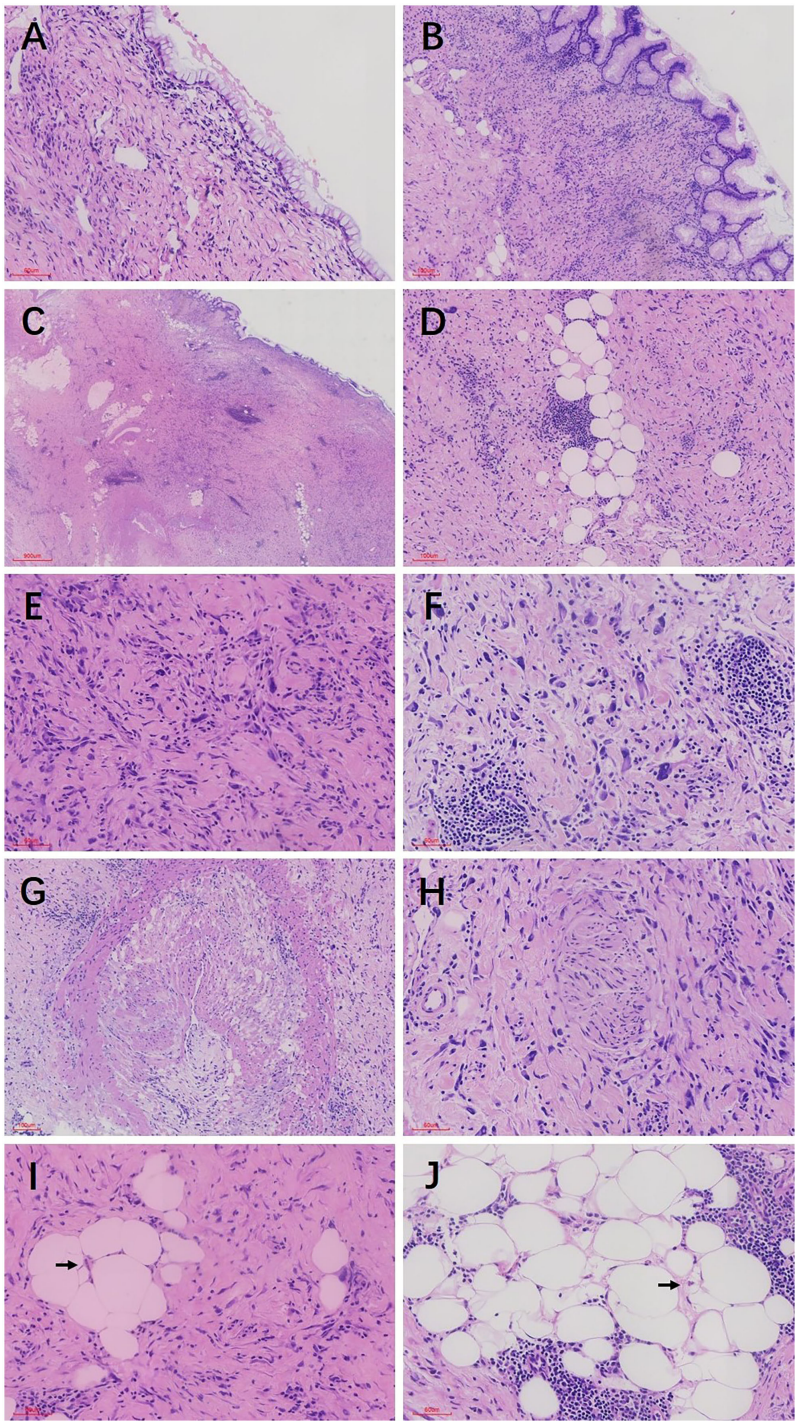

FIGURE 1
(A) The ovarian cyst wall was lined with a single layer of mucinous columnar epithelium, with no significant cellular atypia observed. **(B)** The mucous epithelial cells exhibit a benign morphology, with nuclei located at the basal portion and the cytoplasm rich in mucus **(C)** Mural nodules were present beneath the mucinous epithelium, with unclear boundaries between the nodules and the surrounding tissues. **(D)** The mural nodules consisted of spindle cells, pleomorphic cells, and a few adipocytes. The adipocytes showed good differentiation and varied in size. **(E)** Under high magnification, the spindle cell nuclei exhibited significant atypia, with abundant and eosinophilic cytoplasm, and the tumor stroma demonstrated prominent hyaline degeneration. **(F)** Scattered giant tumor cells were visible. Lymphocyte and plasma cell infiltration and lymphoid follicle formation were noted in the stroma. **(G)** Tumor cells invaded large blood vessels. **(H)** Tumor cells grew around nerves. **(I)** Under high magnification, fat cell nuclei showed mild atypia, with a few visible lipoblasts. **(J)** Adipocytes showed good differentiation and varied in size. Localized nuclei exhibited mild atypia, and lipoblasts were visible. The black arrows in both **I**, **J** indicate lipoblasts.

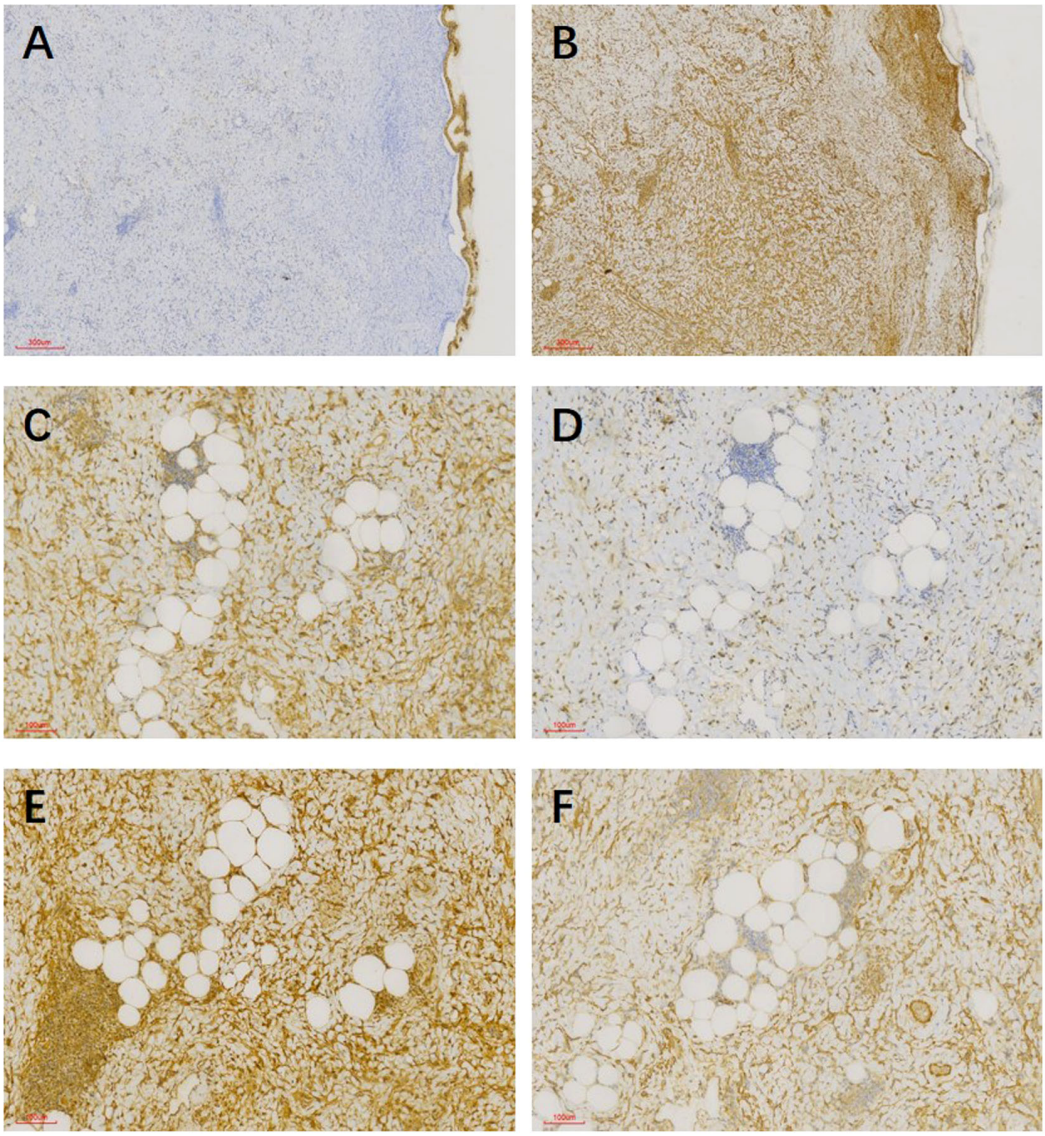

FIGURE 2
(A) Mucinous epithelium expressed cytokeratin, whereas tumor cells in mural nodules did not. **(B)** Mural nodules showed a diffuse strong positive expression of vimentin, whereas mucinous epithelium did not. **(C)** Spindle cells and adipocytes in mural nodules exhibited a strong positive expression of CDK4. **(D)** Spindle cells and adipocytes in mural nodules expressed MDM2. **(E)** Spindle cells and adipocytes in mural nodules exhibited a strong positive expression of P16. **(F)** Spindle cells in mural nodules expressed SMA.

performed separately on the two tumor components. The ovarian mucinous cystadenoma demonstrated the p. G12R, c.34G>C mutation in exon 2 of the *KRAS* gene. Meanwhile, no *KRAS* mutation was observed in the mural nodule of liposarcoma, but rather, amplifications in the copy numbers of *CDK4* and *DDR2*, as well as a frameshift mutation in exon 13 of *ASXL1* (p. A627Gfs*8), were detected.

Regarding treatment and follow-up, the patient did not receive adjuvant therapy postoperatively and was followed-up regularly (the last follow-up was 25 months after surgery). Gynecological ultrasound and tumor marker assessment did not indicate any evidence of recurrence or metastasis.

Discussion and conclusions

Ovarian mucinous tumor with true sarcomatous mural nodules is an extremely rare tumor entity, with only 10 cases reported currently (8–15). Owing to its rarity and significant variability in prognosis, both diagnosis and treatment are highly challenging. This case report describes in detail the clinicopathological features and diagnostic and therapeutic process of ovarian mucinous cystadenoma with a liposarcoma mural nodule. We aim to explore the pathological diagnosis and treatment strategies for this tumor type and improve the understanding of clinicians and pathologists regarding this tumor.

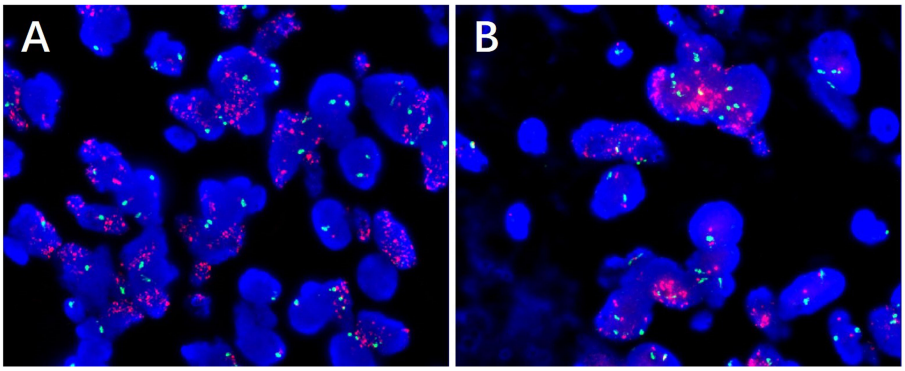

FIGURE 3
FISH testing revealed *CDK4* **(A)** and *MDM2* **(B)** amplification in mural nodules.

Table 1 summarizes cases of ovarian mucinous tumors with true sarcomatous mural nodules (8–15). The onset age range is wide, occurring in women aged 18–91 years (mean age: 51 years). Our patient represents the oldest reported case. Initial clinical manifestations are diverse, primarily presenting as lower abdominal pain or discomfort. In the present case, the clinical presentation was postmenopausal vaginal bleeding. Mucinous ovarian tumors often have a large diameter, ranging from 9.4 to 44.0 cm (mean diameter: 19.4 cm). The mural nodule diameter ranges from 1.4 to 15 cm. The incidence ratio between the left and right ovaries is 6:5. In our patient, the tumor emerged in the right ovary, with a mural nodule diameter of only 1.4 cm, the smallest among all cases. If macroscopic examination is not performed carefully and sampling is inadequate, misdiagnosis is highly likely. According to the FIGO staging system, 6 cases were classified as stage IA, 3 as stage IC, 1 as stage IIB, and 1 as stage IIIA.

Mural nodules can occur in any mucinous ovarian tumors (benign, borderline, or malignant), typically classified into sarcoma-like, anaplastic carcinomatous, and true sarcomatous nodules (2–5). These three mural nodule types are morphologically indistinguishable. The most common are sarcoma-like nodules, which are often multiple and well demarcated from the surrounding mucinous tumor; they generally protrude into the lumen of the mucinous cyst. Microscopically, they are composed of epithelial-like or spindle cells, often mixed with osteoclast-like or ameloblastic giant cells and inflammatory cells (5). Moreover, anaplastic carcinomatous nodules are often poorly defined, large, and infiltrative lesions, with or without lymphovascular invasion. They are usually composed of polygonal cells with high-grade nuclear features; however, the inflammatory infiltration is less prominent (16–18). True sarcomatous mural nodules have wide-ranging morphological spectra. In osteosarcoma mural nodules, atypical spindle-shaped or epithelioid osteoblastic cells can be observed, accompanied with abundant osteoid matrix formation, even lace-like osteoid matrix (9, 10).

Furthermore, fibrosarcoma mural nodules exhibit pleomorphic spindle cells arranged in bundles or fishbone patterns, concurrent with extensive tumor necrosis and mitotic images (12–14). Rhabdomyosarcoma mural nodules demonstrate the typical morphology of rhabdomyoblasts as well as pleomorphic tumor cells, which possess abundant eosinophilic cytoplasm (15).

In the current case, spindle and pleomorphic cells were observed beneath the mucinous epithelium, exhibiting a sheet-like infiltrative growth pattern. Interspersed among the spindle cells are small clusters of adipocytes. Without careful examination, misdiagnosis or overlooking the possibility of liposarcoma is highly possible. Under high magnification, the adipocytes were well differentiated, varying in size, with lipoblasts noted in focal areas. Immunohistochemical staining revealed diffuse strong positivity for CDK4, MDM2, and P16, supporting liposarcoma diagnosis. Further FISH analysis revealed *MDM2* and *CDK4* amplification, thereby confirming the diagnosis of mural nodules in highly differentiated liposarcoma.

Currently, the pathogenesis of ovarian mucinous tumors with mural nodules remains unclear. Mesbah et al. (16) found clonal evidence, including frequent mutations in *KRAS, IDH1, TP53, PTEN*, and *PIK3CA*, in anaplastic carcinomatous nodules and the corresponding ovarian mucinous tumors. Recently, a large-scale series study reported by Chapel et al. (5) showed clonal genetic evidence between various mural nodules and related ovarian mucinous tumors. They suggested no clear and reproducible genetic differences between sarcoma-like, anaplastic carcinomatous, and true sarcomatous mural nodules defined by conventional morphology. Different mural nodule types represent a continuous growth spectrum of ovarian mucinous tumors rather than merely three biologically discrete entities. However, none of the 13 mural nodules reported by Chapel et al. was purely sarcomatous. True sarcomatous mural nodules representing as a dedifferentiated component or a collision of two tumors remains poorly investigated. Desouki et al. (11) reported a case of ovarian mucinous carcinoma with high-grade sarcomatous mural nodules. The mucinous tumor components showed the same *KRAS* mutation as the sarcomatous tumor components, and the sarcomatous mural nodules may represent a form of mucinous tumor dedifferentiation. Whether similar genetic alterations occur when mural nodules exhibit heterologous differentiation (osteosarcoma, rhabdomyosarcoma, and liposarcoma) remains unknown. Currently, the 3 reported cases of osteosarcoma mural nodules (9, 10) and 1 case of rhabdomyosarcoma mural nodule (15) have not undergone relevant molecular testing. Through separate high-throughput sequencing of two distinct tumor components, we found no overlapping genetic evidence between the liposarcoma mural

nodule and associated ovarian mucinous cystadenoma. Our study suggests that when the mural nodule of a true sarcoma exhibits heterologous differentiation, it likely represents a collision of two different tumors rather than a form of dedifferentiation of the mucinous tumor.

Considering that ovarian mucinous tumors with true sarcomatous mural nodules are extremely rare, its clinical understanding and comprehension remain insufficient, and unified standards for its treatment strategies remain unavailable. According to the 10 case reports, the primary treatment for ovarian mucinous tumors with true sarcomatous mural nodules is surgical resection (8–15). The surgical approach depends on the tumor stage, extent of involvement, and the need to preserve fertility, with some patients receiving radiotherapy or chemotherapy postoperatively (8, 14, 15). Among the cases of true sarcomatous mural nodules with follow-up records, only two patients died, as reported by Prat et al. (14). One had a fibrosarcoma mural nodule and died of liver metastasis, and the other had an undifferentiated sarcoma mural nodule and died of renal failure. Provenza et al. (19) analyzed the prognosis of 21 cases of ovarian mucinous tumors with anaplastic carcinomatous mural nodules and found that the only significant factor affecting patient prognosis was FIGO staging; the size and histological type of mural nodules, as well as the type of mucinous component and vascular invasion, did not statistically correlate with prognosis. In the present case, adjuvant therapy was not provided after surgical resection, and regular follow-up for 25 months has not revealed evidence of recurrence or metastasis.

In summary, we have reported a rare case of ovarian mucinous tumor with liposarcoma mural nodule, expanding the morphological spectrum of mural nodules. Additionally, through high-throughput sequencing, we found no overlapping genetic evidence between the liposarcoma mural nodule and associated ovarian mucinous cystadenoma.

Data availability statement

The original contributions presented in the study are included in the article/supplementary material. Further inquiries can be directed to the corresponding author.

Ethics statement

The studies involving humans were approved by the Institutional Ethics Committee of Fujian Provincial Hospital. The studies were conducted in accordance with the local legislation and institutional requirements. The human samples used in this study were acquired from Pathology Department of Fujian Provincial Hospital. Written informed consent for participation was not required from the participants or the participants' legal guardians/next of kin in accordance with the national legislation and institutional requirements. Written informed consent was obtained from the individual(s) for the publication of any potentially identifiable images or data included in this article.

Author contributions

JL: Writing – original draft, Writing – review & editing, Conceptualization. HH: Resources, Writing – original draft, Writing – review & editing. QZ: Data curation, Investigation, Methodology, Writing – review & editing. XC: Methodology, Resources, Supervision, Writing – review & editing. LC: Data curation, Methodology, Validation, Writing – review & editing.

Funding

The author(s) declare financial support was received for the research, authorship, and/or publication of this article. The author(s) declare financial support was received for the research, authorship, and/or publication of this article. This research was supported by Qihang Fund General Project of Fujian Medical University (2022QH1301).

Conflict of interest

The authors declare that the research was conducted in the absence of any commercial or financial relationships that could be construed as a potential conflict of interest.

Publisher's note

All claims expressed in this article are solely those of the authors and do not necessarily represent those of their affiliated organizations, or those of the publisher, the editors and the reviewers. Any product that may be evaluated in this article, or claim that may be made by its manufacturer, is not guaranteed or endorsed by the publisher.

References

1. Yamazaki H, Matsuzawa A, Shoda T, Iguchi H, Kyushima N. Ovarian mucinous cystic tumor of borderline Malignancy with a mural nodule of anaplastic spindle cell carcinoma: a case report. *J Ovarian Res*. (2013) 6:86. doi: 10.1186/1757-2215-6-86

2. Nichols GE, Mills SE, Ulbright TM, Czernobilsky B, Roth LM. Spindle cell mural nodules in cystic ovarian mucinous tumors. A clinicopathologic and immunohistochemical study of five cases. *Am J Surg Pathol*. (1991) 15:1055–62. doi: 10.1097/00000478-199111000-00004

3. Bagué S, Rodríguez IM, Prat J. Sarcoma-like mural nodules in mucinous cystic tumors of the ovary revisited: a clinicopathologic analysis of 10 additional cases. *Am J Surg Pathol*. (2002) 26:1467–76. doi: 10.1097/00000478-200211000-00009

4. Shao Y, Liu Q, Shi H, Lu B. Ovarian mucinous tumors with mural nodules: immunohistochemical and molecular analysis of 3 cases. *Diagn Pathol*. (2020) 15:35. doi: 10.1186/s13000-020-00956-6

5. Chapel DB, Lee EK, Da Silva AFL, Teschan N, Feltmate C, Matulonis UA, et al. Mural nodules in mucinous ovarian tumors represent a morphologic spectrum of clonal neoplasms: a morphologic, immunohistochemical, and molecular analysis of 13 cases. *Mod Pathol*. (2021) 34:613–26. doi: 10.1038/s41379-020-0642-9

6. Mathew M, Gonsalves H, Al-Azawi S, Saparamadu PA. Asymptomatic ovarian mucinous cystadenoma with a solid mural leiomyoma: case report and brief review. *Sultan Qaboos Univ Med J*. (2013) 13:127–31. doi: 10.12816/0003206

7. Hameed A, Ying AJ, Keyhani-Rofagha S, Dl X, Copeland LJ. Ovarian mucinous cystadenoma associated with mural leiomyomatous nodule and massive ovarian edema. *Gynecol Oncol*. (1997) 67:226–9. doi: 10.1006/gyno.1997.4867

8. Yang S, Wang L, Sun K. Ovarian mucinous cystic tumor associated with sarcomatous mural nodule and benign Brenner tumor: a case report and literature review. *Med (Baltim)*. (2019) 98:e14066. doi: 10.1097/MD.0000000000014066

9. Chu LH, Lai HC, Liao YT. Ovarian mucinous cystadenoma with a mural nodule of osteosarcoma: a case report. *Taiwan J Obstet Gynecol*. (2021) 60:136–8. doi: 10.1016/j.tjog.2020.10.002

10. McFarland M, Dina R, Fisher C, McCluggage WG. Osteosarcoma as Malignant mural nodule in ovarian mucinous neoplasms of intestinal type: report of 2 cases. *Int J Gynecol Pathol*. (2015) 34:369–73. doi: 10.1097/PGP.0000000000000153

11. Desouki MM, Fadare O, Kanbour A, Kanbour-Shakir A. Immunophenotype and K-RAS mutation in mucinous ovarian adenocarcinoma with mural nodule of high-grade sarcoma: case report. *Int J Gynecol Pathol*. (2014) 33:186–90. doi: 10.1097/PGP.0b013e3182830a05

12. Rahilly MA, Candlish W, Al-Nafussi A. Fibrosarcoma arising in an ovarian mucinous tumor: a case report. *Int J Gynecol Cancer*. (1994) 4:211–4. doi: 10.1046/j.1525-1438.1994.04030211.x

13. Bruijn JA, Smit VT, Que DG, Fleuren GJ. Immunohistology of a sarcomatous mural nodule in an ovarian mucinous cystadenocarcinoma. *Int J Gynecol Pathol*. (1987) 6:287–93. doi: 10.1097/00004347-198709000-00009

14. Prat J, Scully RE. Ovarian mucinous tumors with sarcoma-like mural nodules: a report of seven cases. *Cancer*. (1979) 44:1332–44. doi: 10.1002/1097-0142(197910)44:4<1332::AID-CNCR2820440426>3.0.CO;2-#

15. Tsujimura T, Kawano K. Rhabdomyosarcoma coexistent with ovarian mucinous cystadenocarcinoma: a case report. *Int J Gynecol Pathol*. (1992) 11:58–62. doi: 10.1097/00004347-199201000-00009

16. Mesbah Ardakani N, Giardina T, Amanuel B, Stewart CJ. Molecular profiling reveals a clonal relationship between ovarian mucinous tumors and corresponding mural carcinomatous nodules. *Am J Surg Pathol*. (2017) 41:1261–6. doi: 10.1097/PAS.0000000000000875

17. Huang M, Lv Q, Xie J. Ovarian mucinous borderline tumor with anaplastic carcinomatous nodules in adolescents. *J Ovarian Res*. (2022) 15:83. doi: 10.1186/s13048-022-01010-3

18. Zou X, Huang H, Zhang Q, Ma Z, Chen Y, Wu W, et al. Mucinous ovarian tumors with anaplastic mural nodules: case report. *Front Med (Lausanne)*. (2021) 8:753904. doi: 10.3389/fmed.2021.753904

19. Provenza C, Young RH, Prat J. Anaplastic carcinoma in mucinous ovarian tumors: a clinicopathologic study of 34 cases emphasizing the crucial impact of stage on prognosis, their histologic spectrum, and overlap with sarcomalike mural nodules. *Am J Surg Pathol*. (2008) 32:383–89. doi: 10.1097/PAS.0b013e3181451b93

frontiers | Frontiers in Oncology

TYPE Original Research
PUBLISHED 22 August 2024
DOI 10.3389/fonc.2024.1427154

Check for updates

OPEN ACCESS

EDITED BY
Sharon R. Pine,
University of Colorado Anschutz Medical Campus, United States

REVIEWED BY
Stergios Boussios,
Canterbury Christ Church University, United Kingdom
Natale Calomino,
University of Siena, Italy

*CORRESPONDENCE
Jingxin Ding
dingjingxin1465@fckyy.org.cn
Xiang Tao
taoxiang1696@fckyy.org.cn

†These authors have contributed equally to this work and share first authorship

RECEIVED 03 May 2024
ACCEPTED 31 July 2024
PUBLISHED 22 August 2024

CITATION
Liang F, Shi Y, Chen Y, Tao X and Ding J (2024) Clinicopathological and molecular features of tubo-ovarian carcinosarcomas: a series of 51 cases.
Front. Oncol. 14:1427154.
doi: 10.3389/fonc.2024.1427154

COPYRIGHT
© 2024 Liang, Shi, Chen, Tao and Ding. This is an open-access article distributed under the terms of the Creative Commons Attribution License (CC BY). The use, distribution or reproduction in other forums is permitted, provided the original author(s) and the copyright owner(s) are credited and that the original publication in this journal is cited, in accordance with accepted academic practice. No use, distribution or reproduction is permitted which does not comply with these terms.

Clinicopathological and molecular features of tubo-ovarian carcinosarcomas: a series of 51 cases

Fan Liang[1†], Yue Shi[1†], Yiqing Chen[1,2], Xiang Tao[2*] and Jingxin Ding[1*]

[1]Department of Gynecology Oncology, Obstetrics and Gynecology Hospital of Fudan University, Shanghai, China, [2]Department of Pathology, Obstetrics and Gynecology Hospital of Fudan University, Shanghai, China

Objective: Tubo-ovarian carcinosarcomas are rare, extremely aggressive malignant tumors that contain both carcinomatous and sarcomatous components. Due to the disease's rarity, developing an effective treatment strategy for ovarian carcinosarcomas has been challenging. A study was conducted to investigate the clinicopathologic and molecular features of this rare disease.

Methods: We enrolled all patients diagnosed with tubo-ovarian carcinosarcomas from January 2007 to December 2022. The clinical and pathological data were gathered from medical records. Kaplan–Meier curves were plotted to calculate OS and PFS. The Log-rank test and Cox regression model were utilized to explore the relationship between clinicopathological parameters and survival. Patients with cancer tissues available had sequencing with a 242-gene panel done to investigate the mutational landscape and signature of the disease.

Results: In total, 65% of the patients were diagnosed with advanced-stage cancer. The median PFS and OS of this cohort were 27 and 40 months, respectively, and there was no significant difference in survival between the homologous and heterologous components of sarcoma. Unexpectedly, staging did not have effects on prognosis. All patients had surgical attempts, and suboptimal debulking status was correlated with poorer PFS and OS. MSI was identified in 0% with low Tumor mutation burden (TMB) indicating a poor response to immunotherapy. Low HER2 expression is controversial, according to previous reports, and gives us limited choices with this rare and aggressive disease. We surprisingly found the homologous recombination deficiency (HRD)-positive status was identified in 64% of OCS, which is significantly higher than UCS and other types of epithelial ovarian cancer. The fact that all patients in our cohort who received olaparib as maintenance therapy had survived over 30 months and two had no evidence of recurrence at the latest

follow-up might further validate the role of poly (ADP-ribose) polymerase inhibitors (PARPi) in the management of OCS.

Conclusion: OCS patients seemed to respond to carboplatin/paclitaxel with optimal PFS and OS. Cytoreduction with no residuals proved to be the sole independent prognostic factor. WES should be done to assess the prognosis and assist with the targeted therapy, especially the HRD test, which might help select potential patients who benefit from PARPi.

KEYWORDS

ovarian carcinosarcomas (OCS), uterine carcinosarcoma (UCS), mutational landscape, homologous recombination deficiency (HRD) score, poly (ADP-ribose) polymerase inhibitors (PARPi)

Introduction

Ovarian carcinosarcomas (OCS), also referred to as mixed malignant Müllerian tumors, are biphasic neoplasms composed of both carcinomatous and sarcomatous components. Despite accounting for 1% to 4% of ovarian malignancies, OCS are extremely aggressive and have a dismal prognosis (1). Tubal carcinosarcomas and ovarian carcinosarcomas have been analyzed and studied together due to their clinicopathologic similarities (2). Most tubo-ovarian carcinosarcomas patients were diagnosed at an advanced stage. According to statistics from the SEER Program, patients with OCS had a worse prognosis than those diagnosed with high-grade serous ovarian cancer (3).

There are usually three main hypotheses for the development of carcinosarcoma. The most widely accepted theory is the conversion hypothesis, for which the sarcomatous component could develop from its carcinomatous counterpart. The combination hypothesis states that both carcinomatous and sarcomatous elements could originate from a single progenitor cell. The last and least plausible hypothesis is the collision theory, which considers that the two components evolve independently of each other (1, 4).

Regarding the sarcomatous component, CS could be divided into homologous and heterologous subtypes (5). Homologous sarcoma could be fibrosarcoma, leiomyosarcoma, or endometrial stromal sarcoma, which is always derived from intrinsic ovarian tissue. Heterologous sarcoma usually includes bone tissue, cartilage, or striated muscles, not anything from intrinsic ovarian tissue. However, the carcinomatous component always consisted of the mono-epithelial element, and high-grade serous carcinoma is most commonly seen. Clear cell, endometrioid, squamous cell, and undifferentiated cancer may also be identified. The carcinomatous element could be composed of two or three components for less than 10% of patients (6).

Despite maximum debulking surgery followed by platinum-based chemotherapy as a conventional therapeutic option, the majority of the patients experienced recurrence within a year and survived for around 2 years (7). Compared with epithelial ovarian cancer (EOC), OCS seemed to recur earlier with a shorter survival time. New therapeutic agents are urgently required because OCS shows highly aggressive behavior and poor prognosis (3, 8).

An investigation into the mutational landscape of this rare tumor could guide us to potentially effective targeted immunotherapy.

Human epidermal growth factor receptor 2 (HER2) could enhance kinase-mediated activation of downstream signal pathways, leading to cellular hyperproliferation and malignant transformation, and its significance in the pathogenesis and subsequent target therapy in breast cancer has been consolidated. Previous studies have shown that 18%–58% of carcinosarcoma also presented with *HER2* overexpression and could potentially benefit from *HER2* target therapy (9). The estimated *HER2*/neu overexpression ranges between 25% and 56% in carcinomatous components compared to low to negligible expression in the sarcomatous element (10). One study showed HER2 overexpression in nine out of 16 cases, with gene amplification by fluorescence *in situ* hybridization (FISH) demonstrated just in one case (11). Another study revealed HER2 overexpression in nine of 28 cases, with gene amplification by FISH seen in four cases (12). *HER2* protein overexpression and gene amplification were detected in 25% (two of eight) of the primary CS cell lines (13). However, after further stratification, only one out of 13 OCS cases (7.7%) was found with positive *HER2* expression, which is significantly lower than in uterine carcinosarcoma (UCS) (12/65,18.5%), and our study seemed to hold a pessimistic result of *HER2* expression in OCS as, elaborated in the Discussion.

Mutations in BReast CAncer gene 1 (*BRCA1*), *BRCA2*, and other homologous recombination deficiency (HRD) genes may sensitize carcinosarcomas in the female genital tract to poly (ADP-ribose) polymerase inhibitors (PARPi), and the high frequency of MMR defects suggested that these tumors may also respond to immunotherapy (14). However, current studies only focused on the detection of *BRCA1/2* and other homologous recombination genes related; no investigation on the prognosis and response of PARPi based on HRD score has been reported so far.

Due to the rarity of OCS, molecular analyses have usually been done on UCS and OCS as a pool, but we gradually found these two displayed remarkably different molecular features and biological behavior (15). Molecular studies with decent sample sizes on OCS are needed to serve as more evidence for clinical management. Therefore, 51 cases of OCS diagnosed at a single institution from 2007 to 2022 were collected, analyzed, and sequenced if accessible to comprehensively present the clinicopathologic features, treatment, prognosis, and molecular characteristics of this rare disease.

Materials and methods

Study population

We identified patients diagnosed with OCS between January 2007 and December 2022 at our institution. All cases enrolled here were thoroughly presented and discussed on our Tumor Board, which is a weekly multidisciplinary team (MDT) meeting held in our department (Gynecology Oncology) to discuss all cancer cases of each week, and the diagnoses and management were then decided for these patients. The MDT records in Chinese were documented under each patient, which is accessible in the electronic system. We conducted a retrospective review of age, surgical extension (R0: no gross tumor, R1: residual tumor of ≤ 1 cm; suboptimal debulking surgery: residual tumor of > 1 cm), and stage as defined by the International Federation of Gynecology and Obstetrics (FIGO) in 2008 (16), perioperative chemotherapy, progression-free survival (PFS), and overall survival (OS). Pathological diagnoses of all cases were confirmed by an expert gynecological pathologist (X.T.). This study was conducted according to the Declaration of Helsinki and approved by the institutional review board of the Obstetrics and Gynecology Hospital of Fudan University (No. 2022-94). Recruited patients provided written informed consent documented.

Statistical analysis

Survival curves were made according to the Kaplan–Meier method (17). Comparisons between survival curves were made with the log-rank statistic. The Cox regression model was employed to explore the relationship between clinicopathological parameters and survival. $p < 0.05$ was considered statistically significant. All analyses were performed with the use of IBM SPSS version 24 (SPSS Inc., Chicago, IL, USA).

Immunohistochemical findings

The Programmed death-ligand 1 (PD-L1) IHC staining assay was performed as previously described (18). The expression of PD-L1 was assessed by IHC analysis of FFPE tumor samples using anti-PD-L1 antibodies (clone 22C3; Cat No. M3653; Dako North America, Carpinteria, CA, USA). The PD-L1 combined positive score (CPS), which is the percentage of tumor cells and surrounding immune cells showing partial or complete membrane staining, was determined and classified as negative, low positive, or high positive (CPS of < 1%, 1%–49%, and ≥ 50%, respectively) (19). The data of HER2 expression were adopted in this study. For HER2 expression, the IHC score was evaluated according to the 2016 ASCO/CAP criteria for gastric cancer (20, 21). IHC was performed using a standard FDA-approved IVD kit, the Pathway HER2 (Clone 4B5), on the BenchMark XT automated system.

(Ventana Medical Systems Inc., Tucson, AZ, USA) according to the manufacturer's protocol. HER2 IHC score 0 is defined as HER2-null, score 1+ is defined as HER2-low, and HER2 IHC score 2+ or score 3+ is defined as HER2-high (22). Currently, no internationally accepted criteria for evaluating HER2 expression is specifically known in UCS or OCS.

Molecular findings

Illumina next-generation sequencing (NGS) was adopted, which covered all exons, including 262 genes (listed in the Supplementary Material). MSI status, TMB, and HRD score were calculated based on the NGS data. Mutational signatures were extracted using base substitutions and additionally included information on the sequence context of each mutation. Furthermore, there are six classes of base substitutions: C > A, C > G, C > T, T > A, T > C, and T > G (all substitutions are referred to by the pyrimidine of the mutated Watson–Crick base pair), and information on the bases immediately 5′ and 3′ to each mutated base is incorporated in this analysis. In published studies (PNAS), applying this approach to multiple human cancer types revealed over 30 distinct validated mutational signatures. Importantly, signature 3 was strongly associated with HRD+ status within the ovarian, breast, and prostate cancer types.

Results

In total, 51 women diagnosed with tubo-ovarian carcinosarcomas at our institution between January 2007 and December 2022 were enrolled in this study. The clinicopathologic characteristics of the cohort are summarized in Table 1. Four patients were found to have concurrent malignancies, including two cases of synchronous uterine carcinosarcoma, one case of cervical adenosquamous carcinoma, and another one with serous adenocarcinoma of the endometrium. The median age of onset was 59 years old, and 76.5% were postmenopausal. The average size of the tumor was 8.7 cm, with 72.5% presented as bilateral masses. The homologous subtype was identified in 28 cases (55%), and the carcinomatous element, consisting of serous carcinoma, was identified in 42 women (82.3%). Endometroid carcinoma and clear-cell carcinoma were both observed in one patient (2%), respectively. In the "mixed" carcinoma cases, four patients were diagnosed with squamous cell carcinoma, while one patient had poorly differentiated carcinoma. Heterologous differentiation was present in 23 cases (45%), chondrosarcoma in 15 patients (29.4%), rhabdomyosarcoma in four patients (7.8%), and mixed sarcoma type in four cases (7.8%).

TABLE 1 Demographic information of the study series.

Characteristics	Value
Median age at diagnosis (year)	59 (33–76)
Menopause status	
Yes	39 (76.5%)
No	12 (23.5%)
Tumor size (range) (cm)	8.7 (2.5–20)
Laterality	
Bilateral	37 (72.5%)
Unilateral	14 (27.5%)
Epithelial histology (*n*; %)	
Serous	42 (82.3%)
Endometrioid	1 (2%)
Clear-cell carcinoma	1 (2%)
> 1 carcinoma type	7 (13.7%)
Mesenchymal histology (*n*; %)	
Homologous	28 (55%)
Heterologous	23 (45%)
Chondrosarcoma	15 (29.4%)
Rhabdomyosarcoma	4 (7.8%)
> 1 sarcoma type	4 (7.8%)
Stage (FIGO)	
I	10 (19.6%)
II	8 (15.7%)
III	26 (51%)
IV	7 (13.7%)
Recurrence status	
No recurrence	19 (37.3%)
Recurrence	32 (62.7%)
Platinum sensitivity	
Platinum sensitive	17 (53.1%)
Platinum resistant	6 (18.8%)
Platinum refractory	9 (28.1%)
Median OS (range) (month)	40 (17.9–62.0)
Median PFS (range) (month)	27 (8.96–45.0)

Intraoperative frozen examinations were performed in 46 cases (90.2%), all of which were suggestive of ovarian malignancy and 10 of which were straightly reported as carcinosarcoma. A total of 64.7% of the patients in the cohort had advanced cancers: 10 patients in stage I (19.6%), eight in stage II, 26 in stage III, and seven in stage IV (13.7%). Of all patients, 32 (62.7%) experienced recurrence during the study period. There were 17 platinum-sensitive, nine platinum-refractory, and six platinum-resistant patients among those who received adjuvant chemotherapy. Figure 1 depicts the overall survival of the group. The median OS was 40 months (95% CI: 17.9–62.0 months), with the median PFS at 27 months (95% CI: 8.97–45.0 months). The 3- and 5-year OS were 38% and 19.6%, respectively.

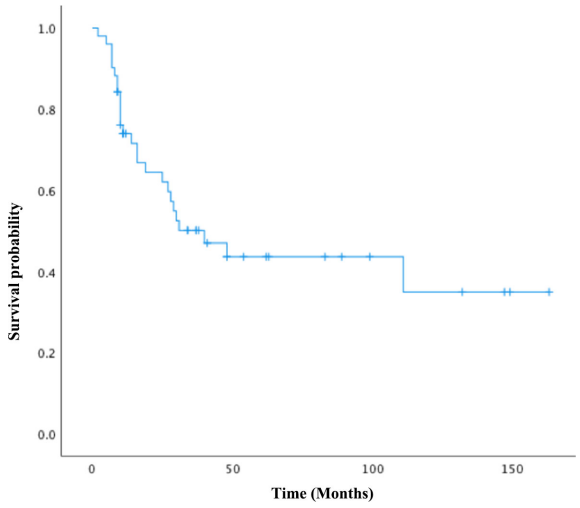

FIGURE 1
Overall survival for all patients.

The adjunctive therapeutic regimens are demonstrated in Table 2. All patients had surgical attempts, of whom 42 (82.4%) achieved optimal debulking status, with R0 (no gross tumor) in 31 cases and R1 (residual tumor of ≤ 1 cm) in 11 cases, and nine patients (17.6%) underwent suboptimal debulking surgery (residual tumor of > 1 cm). In our cohort, 48 patients (94.1%) underwent adjuvant chemotherapy, with 40 (78.4%) receiving carboplatin/paclitaxel as the first chemotherapy, two (3.9%) receiving ifosfamide/paclitaxel, three (5.9%) receiving ifosfamide/carboplatin, two (3.9%) receiving ifosfamide/adriamycin/paclitaxel (IAP), one receiving a vincristine/adriamycin/dacarbazine (VAD) regimen, and three patients refusing chemotherapy, all of whom were at advanced-stage with poor performance status. Five patients received neoadjuvant chemotherapy with carboplatin/paclitaxel (one to three cycles), and among them, four patients (80%) received optimal cytoreductive surgery (*R*0 = 2, *R*1 = 2), with one having suboptimal cytoreductive surgery.

In our study, four advanced-stage patients received bevacizumab treatment, of whom three received bevacizumab in combination with platinum-based therapy in initial treatment and one received bevacizumab in combination with liposomal doxorubicin for platinum-resistant recurrence as second-line chemotherapy. One patient at stage IV participated in a clinical trial of hPV19 (a novel humanized antivascular endothelial growth factor [VEGF] monoclonal antibody) injection for three cycles after platinum-resistant recurrence and discontinued when disease progression was indicated by CT image, and the patient passed away with OS at10 months.

TABLE 2 Therapeutic modalities of the 51 cases.

Characteristics	Value
Debulking surgery	
Optimal cytoreduction	42 (82.4%)
R0	31
R1	11
Suboptimal cytoreduction	9 (17.6%)
Adjuvant chemotherapy	
Carboplatin/paclitaxel	40 (78.4%)
Ifosfamide/paclitaxel	2 (3.9%)
Ifosfamide/carboplatin	3 (5.9%)
Ifosfamide/adriamycin/paclitaxel	2 (3.9%)
Vincristine/adriamycin/dacarbazine	1 (2%)
None	3 (5.9%)
Neoadjuvant chemotherapy	5
Targeted therapy	
Bevacizumab (anti-VEGF mAb)	4
hPV19 (anti-VEGF mAb)	1
Anlotinib (tyrosine kinase inhibitor)	1
Olaparib/niraparib (PARP inhibitor)	4
Trastuzumab (anti-HER2/neu)	1
Radiation	4

TABLE 3 Univariate analysis of the prognosis of 51 cases of tubo-ovarian carcinosarcomas.

Variables	*n*	*p*-value
Menopause status		
Yes	39	0.91
No	12	
Laterality		
Bilateral	37	0.18
Unilateral	14	
Mesenchymal histology		
Homologous	28	0.57
Heterologous	23	
Stage (FIGO)		
I–II	18	0.26
III–IV	33	
Debulking surgery		
Optimal cytoreduction	42	0.01*
Suboptimal cytoreduction	9	
Adjuvant chemotherapy		
Carboplatin/paclitaxel	40	0.036*
Ifosfamide-containing regimens	7	

*$p < 0.05$.

A stage IV tubal carcinosarcoma patient, who was suggested recurrence 14 months after surgery by PET-CT of a presacral mass of 7 cm in diameter, received stereotactic body radiation therapy (gamma knife treatment) and oral anlotinib (tyrosine kinase inhibitor [TKI]) treatment for 5 months as metastasis was indicated by PET-CT evaluation. One patient at stage III with HER2 overexpression was given trastuzumab in combination with platinum-based chemotherapy as initial treatment; however, liver metastasis was indicated by PET-CT follow-up with a PFS as short as 10 months. A total of four patients received PARPi in the cohort, among whom there were three cases with olaparib and one with niraparib. A stage III patient with BRCA1 mutation received olaparib maintenance therapy after optimal debulking surgery (R0) and ifosfamide/carboplatin chemotherapy. She had a survival time of 34 months with no evidence of recurrence at the last follow-up. Olaparib maintenance therapy was also employed in HRD-positive OCS patients without the BRCA1/2 mutation after optimal debulking surgery (R0) and carboplatin/paclitaxel chemotherapy, and they were all free of relapse so far. The previously mentioned patient with a presacral mass of 7 cm in diameter, who relapsed after stereotactic body radiation therapy and TKI treatment, then received secondary cytoreduction surgery followed by platinum-based chemotherapy and was maintained on olaparib for 1 year until recurrence was indicated by PET-CT. She was subsequently put back on the TC regimen and had already survived for 37 months at the latest follow-up. The three patients who received olaparib as maintenance therapy had all survived over 30 months, and two of them (66.67%) had no evidence of recurrence so far, which seems remarkably better than other target therapies, while a larger sample size is needed to consolidate the conclusion. Niraparib was used as maintenance therapy in a stage IV platinum-sensitive, recurrent OCS patient without BRCA mutations and an unknown HRD status. PARPi was discontinued when liver capsule metastasis was indicated by PET-CT scan 3 months later. Subsequently, the patient received four cycles of nab-paclitaxel every-3-week (q3w) regimen before switching to the regimen of adriamycin liposome in combination with bevacizumab, the patient died with an overall survival of 25 months.

Radiation therapy (RT) was applied to only four patients (7.8%). One patient had optimally debulking surgery followed by carboplatin/paclitaxel chemotherapy and was diagnosed with a recurrence in the peritoneum and left clavicular lymph node 14 months later; 4,500 centigray (cGy) RT was delivered to the pelvis and 6,000 cGy to the left clavicular region. The patient with an isolated recurrence of a presacral mass of 7 cm in diameter 14 months after surgery received stereotactic body radiation therapy (gamma knife therapy). The other two cases were complicated by synchronous serous adenocarcinoma of the endometrium and invasive adenosquamous carcinoma of the cervix, respectively, and were

TABLE 4 Multivariate analysis of Cox proportional risk model for prognosis of tubo-ovarian carcinosarcomas.

Variable in the equation						
	B	S.E.	*df*	Sig.	95.0% CI for EXP (*B*)	
					Lower	Upper
Debulking surgery	− 1.289	0.489	1	0.008	0.106	0.719

Variable(s) entered in step 1: adjuvant chemotherapy regimen, debulking surgery.

indicated for postoperative concurrent radiochemotherapy (CCRT).

For univariate survival analysis (Table 3), staging of the disease might have no significant impact on OS (p = 0.26) (Figure 2). No difference was seen in PFS and OS based on histopathological subtype (p = 0.37; p = 0.57) (Figures 3A, B). Survival did not correlate statistically according to laterality (p = 0.18) or menopausal state (p = 0.91). However, suboptimal debulking surgery was associated with significantly worse PFS and OS (p < 0.05) (Figures 4A, B). In the subsequent multivariate analysis (Table 4), the Cox regression model revealed that residual disease was an independent prognostic factor (p = 0.008). Patients who had carboplatin/paclitaxel as first-line chemotherapy exhibited significantly prolonged PFS and OS when compared to those treated with ifosfamide-containing regimens (p = 0.008; p = 0.036) (Figures 5A, B).

Molecular findings

Tissues for the NGS test were acquired for 11 cases (11/51, 21.57%), and 242 genes associated with gynecological tumor (listed in the Supplementary Material), TMB, MSI, HRD score, and PD-L1 expression were comprehensively tested for the cohort. Analyses of the genetic characteristics of the somatic mutation of OCS were highly consistent with the genetic landscape results recently reported. We found alterations in multiple driver genes affecting the *ERBB2/PI3K/AKT/mTOR* pathway, the cell cycle, chromatin and remodeling pathway, and, importantly, the HRD pathways.

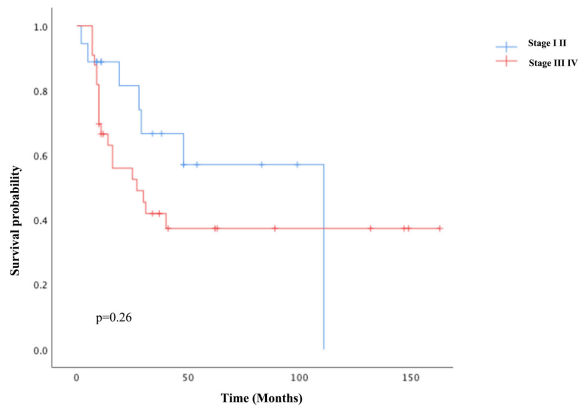

FIGURE 2
Kaplan–Meier curve of overall survival based on the stage of the disease.

Mutations in *TP53*, a common onco-suppressor gene, were identified in six out of 11, as demonstrated in Figure 6. Over half of the entire tumors had mutations in one or more of the *phosphatidylinositol 3-kinase* (*PI3K*) pathway genes: *PIK3CA* (five of 11, 45.5%), *ERBB2* (two of 11, 18.18%), or *PIK3R1* (two of 11, 18.18%), which were also frequently found in UCS. Moreover, a known recurrent mutation in *CHD4* (DNA helicase) was found in 27.27% (three of 11) of cases. Recurrent PPP2R1A mutations in uterine cancer act through a dominant-negative mechanism to promote malignant cell growth, We found one case of OCS also harboring it as a driver mutation. *FBXW7*, a known tumor suppressor gene previously identified in uterine serous carcinoma, was detected in two cases. Additionally, an HRD gene, *BRIP1* mutation, was found in one case.

Surprisingly, no phosphatase and tensin homolog deleted on chromosome 10 (*PTEN*) or Kristen rat sarcoma (*KRAS*) mutation appeared in this cohort. The most common mutation pattern was missense mutation (64%), followed by truncation (28%) and deletion. All cases proved to be MSS with a low TMB of less than 1.5 muts/Mb (median at 1.13 muts/Mb).

Genetic signatures of these 11 OCS cases were generated, and all cases demonstrated a dominant aging-related signature (signature 1A), as shown in Figure 7. HRD was calculated, and seven cases (seven of 11, 63.64%) were considered positive, taking a cutoff score of 42, which was consistent with the minor genetic signature, HRD-related signature (signature 3), distributed all over the cohort. No MSI or other signatures were detected in our cohort.

Discussion

OCS represents a rare and aggressive gynecologic malignancy, and similar to serous ovarian cancer, patients usually presented with advanced-stage disease and were given platinum-based chemotherapy as first-line therapy (23), while patients were found to be older and have larger lesions than serous ovarian cancer (7), and also earlier recurrence and shorter survival time were seen in OCS than other pathological types of EOC.

Owing to the rarity of OCS, the prognostic risk factors have not been comprehensively elucidated. Nonetheless, several factors are known to increase the risk of OCS, including advanced age, nulliparity, decreased lactation rates, reduced use of oral contraceptives, BRCA gene mutations, and the use of assisted reproductive technologies. Poor prognostic indicators include late-stage diagnosis, older age, lymph node metastasis, suboptimal surgical cytoreduction, the presence of heterologous features in histopathology, and elevated expression of VEGF, tumor protein p53, and Wilms tumor 1 (WT1) (24). In our study, the median PFS and OS were 27 and 40 months, respectively, with 64.7% of patients presenting with advanced-stage disease, which is consistent with the cohorts reported. Optimal debulking surgery might be considered an indicator of a better prognosis (25). Our findings revealed that patients who had optimal debulking exhibited significantly better PFS and OS than those who underwent suboptimal cytoreduction. Establishing an effective adjuvant therapy for OCS has been challenging due to limited clinical evidence. In addition to

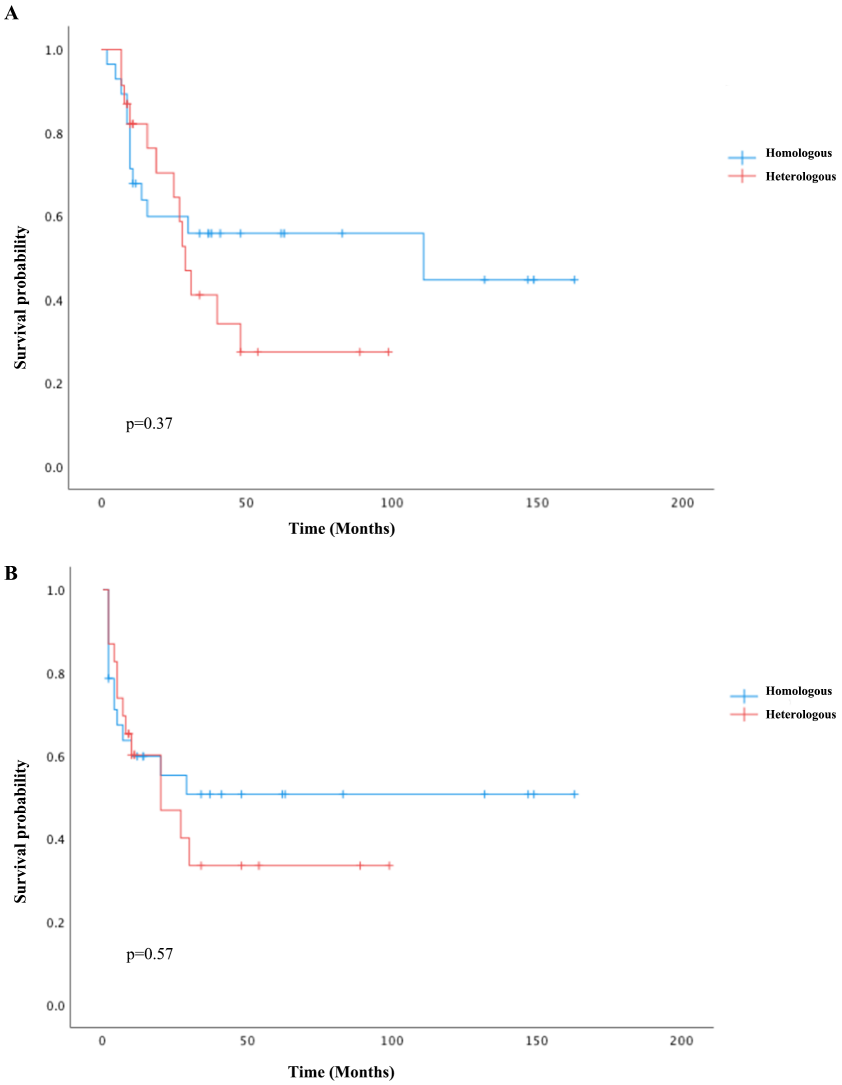

FIGURE 3
Kaplan–Meier curves comparing PFS **(A)** and OS **(B)** between the homologous and heterologous groups.

optional cytoreduction, the clinical management of OCS patients largely relies on data extrapolated from other EOC or sarcomatous malignancies. It is also noteworthy that the PI3K pathway, frequently upregulated in EOC, is crucial for cell survival, chemoresistance, and the maintenance of genomic stability. Targeting the PI3K pathway in OCS may induce genomic instability and mitotic catastrophe by reducing the activity of the spindle assembly checkpoint protein Aurora kinase B, thereby increasing the occurrence of lagging chromosomes during prometaphase (26).

Given the efficacy of both cisplatin and ifosfamide, various investigations evaluated the survival benefits of platinum-taxane chemotherapy to ifosfamide-based regimens; nonetheless, the findings were inconsistent (27–29). In a phase III trial for gynecologic carcinosarcomas in 2019 (GOG-0261, NCT00954174), carboplatin/paclitaxel therapy outperformed ifosfamide/paclitaxel therapy in terms of PFS, especially in advanced-stage disease. NCCN Guidelines 2020 updated their recommendations for carboplatin/paclitaxel from an ifosfamide-based regimen based on this clinical trial (30). Our study further validated this result, as patients who underwent carboplatin/paclitaxel chemotherapy (78.4% of the cohort) had significantly prolonged PFS and OS when compared to the ifosfamide-containing regimen. About three-quarters of the patients were postmenopausal in our cohort, and there was no survival difference regarding menopausal status. It has been previously demonstrated in a study that patients with early-stage disease had greater survival benefits (31), while staging seemed insignificant for their prognosis (p = 0.26). The prognostic significance of the heterologous element in sarcoma has been controversial. Some prior studies supported the idea that homologous subtypes might benefit survival (32, 33), while our study showed no difference in survival regarding this categorization in sarcoma histology.

Unlike UCS, RT was seldom used in the treatment of early-stage OCS patients (34). RT was considered beneficial only in the management of isolated pelvic recurrences for OCS (1). In this

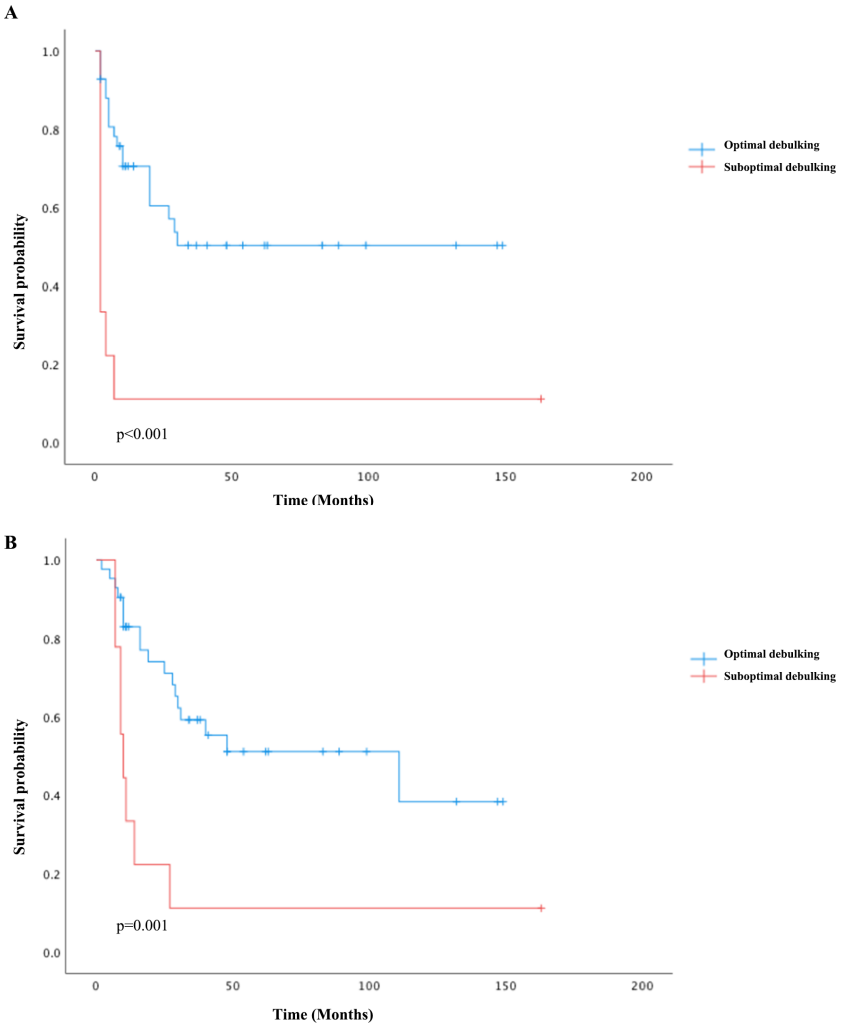

FIGURE 4
Kaplan–Meier survival curves plotted for PFS **(A)** and OS **(B)** according to debulking status: optimal debulking compared to suboptimal debulking status.

case, only four (7.8%) patients received RT in our study, and the potential impact on prognosis could not be generated due to the limited number.

Comprehensive genetic landscape studies of ovarian and uterine CS have recently unequivocally demonstrated that the carcinomatous and sarcomatous elements of these rare but highly aggressive tumors derive from a common precursor having mutations typical of carcinomas (35). Consistent with this view, *TP53* mutation was identified as a dominant driver mutation in OCS (54.5%), with the highest mutation frequency, while still significantly lower than that in UCS (62%–91%) and serous ovarian carcinoma (36, 37).

Although the role of *TP53* as a dominant driver mutation in OCS has been established, the mutation frequency in our cohort seemed higher than in the previous study, at about 30% (15). Mutations in *PIK3CA* and *ARID1A* were more seen in OCS with an endometrioid epithelial component, and *TP53*, *CHD4*, and *FBXW7* mutations were more frequently found in CS with a serous high-grade epithelial component, which is in accordance with previous studies in UCS. However, a larger sample size is definitely needed to validate this conclusion (38, 39). Interestingly, mutations in *KRAS* and *PTEN* were not detected in our OCS cohort, which were mutations commonly found in UCS.

As *HER2* positivity was recommended to be defined as 2+ and 3 + scores on protein expression for gynecologic carcinosarcomas, only two patients (two of 11, 18.2%) met the criteria, which is significantly lower than what was reported in UCS while remarkably higher than that in serous ovarian carcinoma (9).

The diverse genetic patterns among OCS, UCS, and serous ovarian carcinosarcoma were also displayed in their genetic signature features. Mutational signatures have recently provided major insight into the biological processes shaping the tumor genome and can potentially inform therapeutic modalities in multiple tumor types (40). Our cohort demonstrated all cases with a dominant aging-related signature (signature-1), plus seven cases (63.64%) also showing HRD-related signatures (signature-3), which were consistent with their HRD scores. Although no *BRCA* mutation was detected, HRR genes such as *BRIP1* mutation were

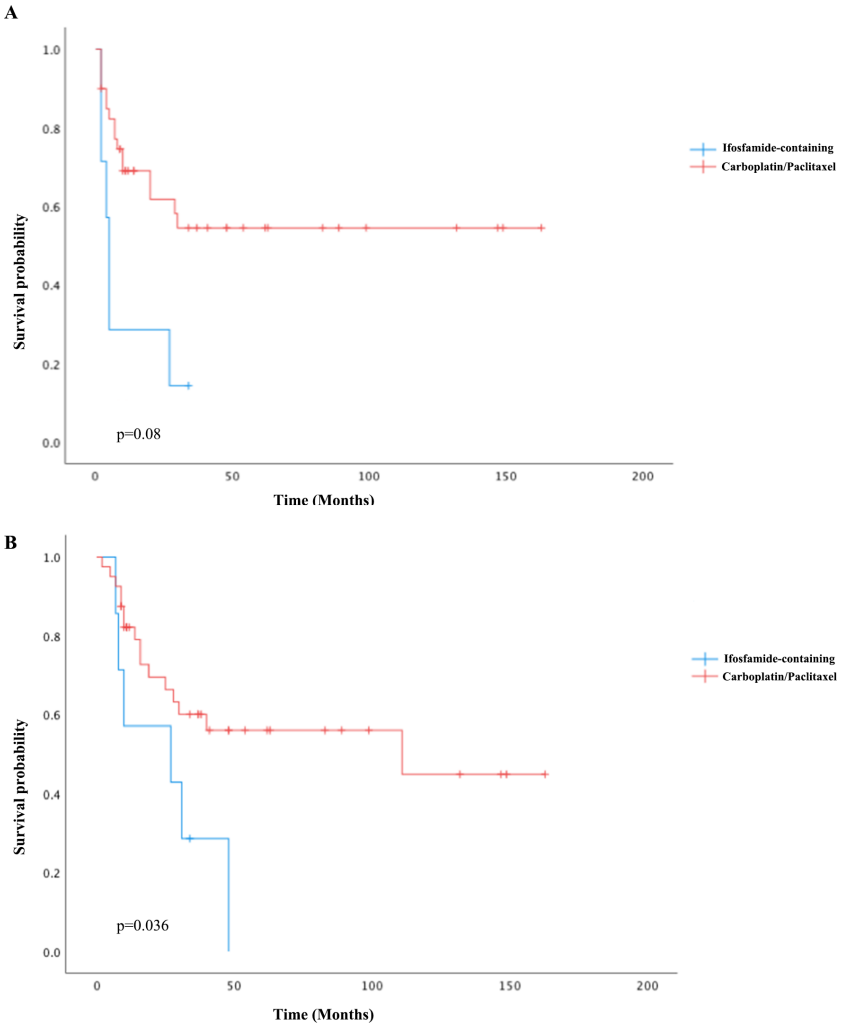

FIGURE 5
Kaplan–Meier curves of PFS **(A)** and OS **(B)** comparing carboplatin/paclitaxel to ifosfamide-containing regimens as first-line chemotherapy.

revealed, and a high incidence of *TP53* mutation could greatly contribute to the genetic scarring and HRD status. This positivity is even higher than the HRD status in serous ovarian carcinoma at 50% (41). HRD patterns in OCS were seldomly analyzed, and our results concluded for the first time that WES-extracted mutational signature consistent with HRD score is significantly more commonly found in OCS (63.64%) when compared to UCS (15%–25%). Aging was identified in 100% of OCS in our cohort, which was close to 86% reported in UCS. In general, OCS presented its tumor signature in line with ovarian cancer, mainly as signature 1 (aging) mixed with signature 3 (HRD).

With these diverse features taken together, it should be noticed that although OCS and UCS may look histologically similar, they significantly differ in their molecular features. Our results may support a differential biological behavior between OCS and UCS, more like serous ovarian cancer, which indicated higher sensitivity to platinum-based chemotherapy and PARP inhibitor than UCS. Importantly, potentially broader use of PARPi might result in improved prognosis in OCS. Pennington et al. (30) also found that four of 12 OCS patients demonstrated loss-of-function mutations in HRR genes, suggesting that PARP inhibitors might be beneficial in this circumstance.

Four out of seven HRD+ patients in our cohort received olaparib as maintenance therapy; all had a survival time of more than 30 months, and two of them had no evidence of recurrence at the latest follow-up. MSS with a low tumor mutation burden was found in all cases, which also differed from the 13%–22% of UCS patients who presented as MSI. This could be explained by the fact that about 85%–90% of UCS had endometrioid histology, which much less happened in OCS. The median TMB of 1.13 muts/Mb is similar to the TMB for ovarian cancer reported (38). Osamu et al. utilized TCGA endometrial molecular stratification system in 92 UCS and 17 OCS samples. OCS comprises mostly CNH tumors with low TMB, while UCS is more heterogeneous in genomic aberration subtypes, and a better prognosis with high TMB was seen, especially in *POLE* and MSI-H groups (42). As in serous ovarian cancer (43, 44), therapy targeting the EGF family and VEGF may be effective in the treatment of OCS. Zorzou et al. (45) reported in their study that four (44%) of nine OCS patients expressed VEGF, a biomarker associated with poorer prognosis in various cancers, and antiangiogenic agents like

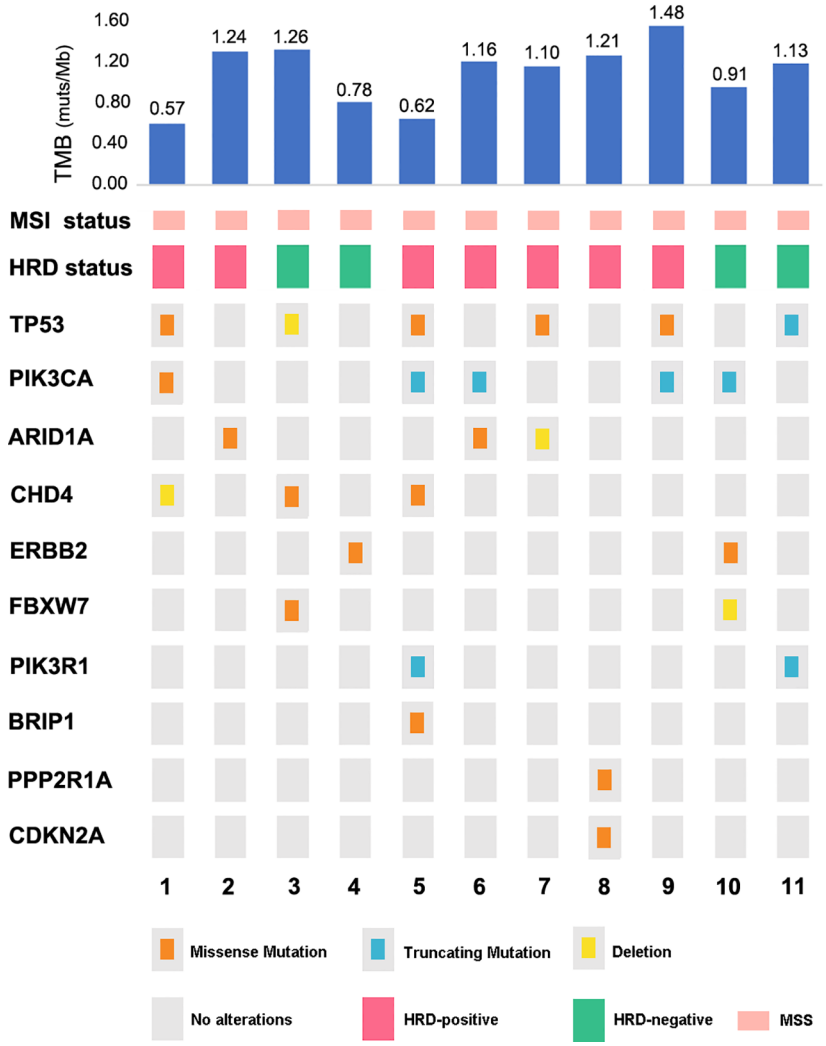

FIGURE 6
The mutational landscape across 11 OCS cases.

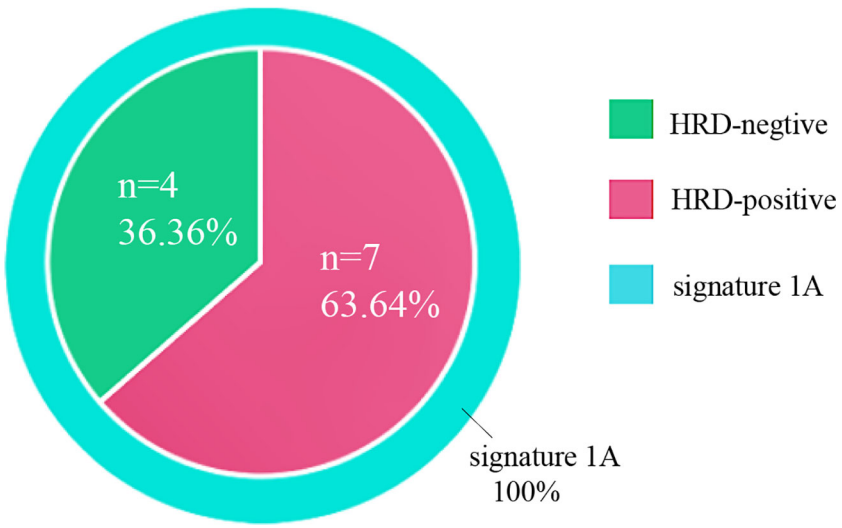

FIGURE 7
Mutational signatures of 11 ovarian carcinosarcomas. Mutational signatures of homologous recombination DNA repair defects and aging are color-coded according to the legend.

bevacizumab could be considered potentially useful (46, 47). hPV19 mAb, a novel humanized monoclonal antibody against VEGF by binding to VEGF-R1 and VEGF-R2, was used in one case in our cohort while the disease progressed under the medication. A prospective clinical study with a larger sample size is needed to validate the VEGF inhibitor's use in the treatment of OCS. Anlotinib, a novel small-molecule tyrosine kinase inhibitor (TKI), targets multiple tyrosine kinases, including vascular endothelial growth factor receptor (VEGFR), fibroblast growth factor receptor (FGFR), platelet-derived growth factor receptors (PDGFR), and c-kit. Cui et al. (48) demonstrated that anlotinib exhibited moderate improvements in PFS and OS in platinum-resistant and platinum-refractory ovarian cancer. It suggested that anlotinib might be an alternative therapeutic option for platinum-resistant or platinum-refractory ovarian malignancies. One patient in our cohort used anlotinib, and the therapeutic effect of TKI in OCS needs further study.

In our study, the patient with *HER2* overexpression who received trastuzumab in combination with platinum-based chemotherapy was found to have liver metastasis with a PFS of 10 months. Further studies are warranted to explore whether HER2-positive OCS patients may benefit from trastuzumab treatment. Trastuzumab emtansine (T-DM1) was proved to be highly efficient in HER2-positive OCS cells in a mouse model (13). In a phase I clinical study (NCT02277717), a novel HER2-targeting ADC (SYD985) has exhibited promising benefits in locally advanced and metastatic tumor cells, indicating that further investigation in OCS patients is warranted. While in our cohort, only two cases displayed OCS *HER2* overexpression, the utilization of HER2 inhibitors could be limited due to the low rate.

The role of immune checkpoint inhibition in carcinosarcoma remains obscure. Although the expression of PD-L1 has been evaluated in a wide range of cancers, there is limited information available in tubo-ovarian carcinosarcomas. In a study of OCS, PD-L1 overexpression was found in 53% of carcinomatous components and 47% of sarcomatous components (49), which was inversely correlated with survival. Of our cohort, 54.5% showed positive PD-L1 expression (CPS ≥1), while no one was put on an immune checkpoint inhibitor as a clinical trial for OCS with PD-1 was unavailable.

Given the high positivity of HRD and PD-L1 expression, a synergistic effect of PARP inhibitors and anti-PD1 therapy could be anticipated to be effective. Additionally, BRCA deficiency has been shown to trigger a STING-dependent innate immune response, leading to the production of type I interferons and proinflammatory cytokines. Moreover, studies have indicated that PARP inhibition can deactivate GSK3 and upregulate PD-L1 in a dose-dependent manner, subsequently suppressing T-cell activation and enhancing cancer cell apoptosis, which might make this combination of target therapies potentially efficient in OCS patients (50). The ROCSAN trial (NCT03651206), which began in 2020, will investigate the effectiveness of niraparib (PARPi) and dostarlimab (PD-1 inhibitor) in gynecological CS, and the data are keenly awaited.

It is hard to draw a conclusion about the potential impact of PARPi in the management of OCS due to the limited number of cases receiving target therapy in our study. However, our results add to the existing understanding and clinical evidence for treating this rare malignancy. Further studies with collaborative, prospective multi-institutional trials are needed to help elaborate the molecular features and therapeutic strategy for patients with this rare and aggressive disease.

Data availability statement

The datasets presented in this study can be found in online repositories. The names of the repository/repositories and accession number(s) can be found in the article/Supplementary Material.

Ethics statement

The studies involving humans were approved by the institutional review board of the Obstetrics and Gynecology Hospital of Fudan University (No. 2022-94). The studies were conducted in accordance with the local legislation and institutional requirements. The participants provided their written informed consent to participate in this study. Written informed consent was obtained from the individual(s) for the publication of any potentially identifiable images or data included in this article.

Author contributions

FL: Visualization, Methodology, Investigation, Writing – review & editing, Writing – original draft, Software, Conceptualization. YS: Data curation, Writing – original draft, Software, Writing – review & editing, Conceptualization. YC: Writing – review & editing, Visualization. XT: Writing – review & editing, Supervision, Methodology, Conceptualization. JD: Supervision, Resources, Funding acquisition, Conceptualization, Writing – review & editing.

Funding

The author(s) declare financial support was received for the research, authorship, and/or publication of this article. This study was supported by the Shanghai Nature Science Foundation (Grant number: 21ZR1410400).

Conflict of interest

The authors declare that the research was conducted in the absence of any commercial or financial relationships that could be construed as a potential conflict of interest.

Publisher's note

All claims expressed in this article are solely those of the authors and do not necessarily represent those of their affiliated organizations, or those of the publisher, the editors and the reviewers. Any product that may be evaluated in this article, or claim that may be made by its manufacturer, is not guaranteed or endorsed by the publisher.

Supplementary material

The Supplementary Material for this article can be found online at: https://www.frontiersin.org/articles/10.3389/fonc.2024.1427154/full#supplementary-material

References

1. del Carmen MG, Birrer M, Schorge JO. Carcinosarcoma of the ovary: a review of the literature. *Gynecol Oncol.* (2012) 125:271–7. doi: 10.1016/j.ygyno.2011.12.418

2. Trento M, Munari G, Carraro V, Lanza C, Salmaso R, Pizzi S, et al. Mutational and immunophenotypic profiling of a series of 8 tubo-ovarian carcinosarcomas revealed a monoclonal origin of the disease. *Int J Gynecol Pathol.* (2020) 39:305–12. doi: 10.1097/PGP.0000000000000645

3. Rauh-Hain JA, Diver E, Clemmer JT, Bradford L, Clark R, Growdon W, et al. Carcinosarcoma of the ovary compared to papillary serous ovarian carcinoma: a SEER analysis. *Gynecol Oncol.* (2013) 131:46–51. doi: 10.1016/j.ygyno.2013.07.097

4. Rauh-Hain JA, Gonzalez R, Bregar AJ, Clemmer J, Hernández-Blanquisett A, Clark RM, et al. Patterns of care, predictors and outcomes of chemotherapy for ovarian carcinosarcoma: A National Cancer Database analysis. *Gynecol Oncol.* (2016) 142:38–43. doi: 10.1016/j.ygyno.2016.04.025

5. Harris MA, Delap LM, Sengupta PS, Wilkinson PM, Welch RS, Swindell R, et al. Carcinosarcoma of the ovary. *Br J Cancer.* (2003) 88:654–7. doi: 10.1038/sj.bjc.6600770

6. Kunkel J, Peng Y, Tao Y, Krigman H, Cao D. Presence of a sarcomatous component outside the ovary is an adverse prognostic factor for primary ovarian Malignant mixed mesodermal/mullerian tumors: a clinicopathologic study of 47 cases. *Am J Surg Pathol.* (2012) 36:831–7. doi: 10.1097/PAS.0b013e31824ee500

7. Barnholtz-Sloan JS, Morris R, Malone JM Jr, Munkarah AR. Survival of women diagnosed with Malignant, mixed mullerian tumors of the ovary (OMMMT). *Gynecol Oncol.* (2004) 93:506–12. doi: 10.1016/j.ygyno.2004.02.016

8. Fader AN, Java J, Tenney M, Ricci S, Gunderson CC, Temkin SM, et al. Impact of histology and surgical approach on survival among women with early-stage, high-grade uterine cancer: An NRG Oncology/Gynecologic Oncology Group ancillary analysis. *Gynecol Oncol.* (2016) 143:460–5. doi: 10.1016/j.ygyno.2016.10.016

9. Rottmann D, Snir OL, Wu X, Wong S, Hui P, Santin AD, et al. HER2 testing of gynecologic carcinosarcomas: tumor stratification for potential targeted therapy. *Mod Pathol.* (2020) 33:118–27. doi: 10.1038/s41379-019-0358-x

10. Menderes G, Bonazzoli E, Bellone S, Black J, Predolini F, Pettinella F, et al. SYD985, a novel duocarmycin-based HER2-targeting antibody-drug conjugate, shows antitumor activity in uterine and ovarian carcinosarcoma with HER2/neu expression. *Clin Cancer Res.* (2017) 23:5836–45. doi: 10.1158/1078-0432.CCR-16-2862

11. Sawada M, Tsuda H, Kimura M, Okamoto S, Kita T, Kasamatsu T, et al. Different expression patterns of KIT, EGFR, and HER-2 (c-erbB-2) oncoproteins between epithelial and mesenchymal components in uterine carcinosarcoma. *Cancer Sci.* (2003) 94:986–91. doi: 10.1111/j.1349-7006.2003.tb01389.x

12. Raspollini MR, Susini T, Amunni G, Paglierani M, Taddei A, Marchionni M, et al. COX-2, c-KIT and HER-2/neu expression in uterine carcino sarcomas: prognostic factors or potential markers for targeted therapies? *Gynecologic Oncol.* (2005) 96:159–67. doi: 10.1016/j.ygyno.2004.09.050

13. Nicoletti R, Lopez S, Bellone S, Cocco E, Schwab CL, Black JD, et al. T-DM1, a novel antibody-drug conjugate, is highly effective against uterine and ovarian carcinosarcomas overexpressing HER2. *Clin Exp Metastasis.* (2015) 32:29–38. doi: 10.1007/s10585-014-9688-8

14. Jones S, Stransky N, McCord CL, Cerami E, Lagowski J, Kelly D, et al. Genomic analyses of gynaecologic carcinosarcomas reveal frequent mutations in chromatin remodelling genes. *Nat Commun.* (2014) 5. doi: 10.1038/ncomms6006

15. Brunetti M, Agostini A, Staurseth J, Davidson B, Heim S, Micci F. Molecular characterization of carcinosarcomas arising in the uterus and ovaries. *Oncotarget.* (2019) 10:3614–24. doi: 10.18632/oncotarget.v10i38

16. Pecorelli S. Revised FIGO staging for carcinoma of the vulva, cervix, and endometrium. *Int J Gynaecol Obstet.* (2009) 105:103–4. doi: 10.1016/j.ijgo.2009.02.012

17. Kaplan EL, Meier P. Nonparametric estimation from incomplete observations. *Journal of the American Statistical Association* (1958) 53:457–81. doi: 10.1080/01621459.1958.10501452

18. Xu X, Yang Y, Liu X, Cao N, Zhang P, Zhao S, et al. NFE2L2/KEAP1 mutations correlate with higher tumor mutational burden value/PD-L1 expression and potentiate improved clinical outcome with immunotherapy. *Oncologist.* (2020) 25:e955–63. doi: 10.1634/theoncologist.2019-0885

19. Ulas EB, Hashemi SMS, Houda I, Kaynak A, Veltman JD, Fransen MF, et al. Predictive value of combined positive score and tumor proportion score for immunotherapy response in advanced NSCLC. *JTO Clin Res Rep.* (2023) 4:100532. doi: 10.1016/j.jtocrr.2023.100532

20. Bartley AN, Washington MK, Colasacco C, Ventura CB, Ismaila N, Benson AB 3rd, et al. HER2 testing and clinical decision making in gastroesophageal adenocarcinoma: guideline from the college of American pathologists, American society for clinical pathology, and the American society of clinical oncology. *J Clin Oncol.* (2017) 35:446–64. doi: 10.1200/JCO.2016.69.4836

21. Yoshida H, Nishikawa T, Matsumoto K, Mori M, Hirashima Y, Takehara K, et al. Histopathological features of HER2 overexpression in uterine carcinosarcoma: proposal for requirements in HER2 testing for targeted therapy. *Virchows Arch.* (2021) 478:1161–71. doi: 10.1007/s00428-021-03017-5

22. Nishikawa T, Hasegawa K, Matsumoto K, Mori M, Hirashima Y, Takehara K, et al. Trastuzumab deruxtecan for human epidermal growth factor receptor 2-expressing advanced or recurrent uterine carcinosarcoma (NCCH1615): the STATICE trial. *J Clin Oncol.* (2023) 41:2789–99. doi: 10.1200/JCO.22.02558

23. Rutledge TL, Gold MA, McMeekin DS, Huh WK, Powell MA, Lewin SN, et al. Carcinosarcoma of the ovary-a case series. *Gynecol Oncol.* (2006) 100:128–32. doi: 10.1016/j.ygyno.2005.07.119

24. Ismail A, Choi S, Boussios S. Frontiers of ovarian carcinosarcoma. *Curr Treat Options Oncol.* (2023) 24:1667–82. doi: 10.1007/s11864-023-01138-4

25. Rauh-Hain JA, Growdon WB, Rodriguez N, Goodman AK, Boruta DM 2nd, Schorge JO, et al. Carcinosarcoma of the ovary: A case-control study. *Gynecologic Oncol.* (2011) 121:477–81. doi: 10.1016/j.ygyno.2011.02.023

26. Aliyuda F, Moschetta M, Ghose A, Rallis KS, Sheriff M, Sanchez E, et al. Advances in ovarian cancer treatment beyond PARP inhibitors. *Curr Cancer Drug Targets.* (2023) 23:433–46. doi: 10.2174/1568009623666230209121732

27. Cicin I, Özatlı T, Türkmen E, Özturk T, Özçelik M, Çabuk D, et al. Predictive and prognostic factors in ovarian and uterine carcinosarcomas. *Balkan Med J.* (2016) 33:517–24. doi: 10.5152/balkanmedj.

28. Yalcin I, Meydanli MM, Turan AT, Taskin S, Sari ME, Gungor T, et al. Carcinosarcoma of the ovary compared to ovarian high-grade serous carcinoma: impact of optimal cytoreduction and standard adjuvant treatment. *Int J Clin Oncol.* (2018) 23:329–37. doi: 10.1007/s10147-017-1215-x

29. Brackmann M, Stasenko M, Uppal S, Erba J, Reynolds RK, McLean K. Comparison of first-line chemotherapy regimens for ovarian carcinosarcoma: a single institution case series and review of the literature. *BMC Cancer.* (2018) 18:172. doi: 10.1186/s12885-018-4082-6

30. Gomez-Raposo C, López-Gómez M, Sereno M, Zambrana F, Casado E. Complete response with pegylated liposomal doxorubicin as a second-line therapy in metastatic ovarian carcinosarcoma: Significance of assessment of the response by FDG-PET. *Gynecol Oncol Case Rep.* (2012) 2:67–8. doi: 10.1016/j.gynor.2012.02.004

31. Muller M, Dupre P-F, Lucas B, Simon H, Malhaire J-P, Guillemet C, et al. [Carcinosarcoma of the ovary]. *J Gynecol Obstet Biol Reprod (Paris).* (2007) 36:399–402. doi: 10.1016/j.jgyn.2007.03.001

32. Loizzi V, Cormio G, Camporeale A, Falagario M, De Mitri P, Scardigno D, et al. Carcinosarcoma of the ovary: analysis of 13 cases and review of the literature. *Oncology*. (2011) 80:102–6. doi: 10.1159/000328794

33. Mok JE, Kim YM, Jung MH, Kim KR, Kim DY, Kim JH, et al. Malignant mixed mullerian tumors of the ovary: experience with cytoreductive surgery and platinum-based combination chemotherapy. *Int J Gynecol Cancer*. (2006) 16:101–5. doi: 10.1136/ijgc-00009577-200601000-00017

34. Berton-Rigaud D, Devouassoux-Shisheboran M, Ledermann JA, Leitao MM, Powell MA, Poveda A, et al. Gynecologic cancer interGroup (GCIG) consensus review for uterine and ovarian carcinosarcoma. *Int J Gynecological Cancer*. (2014) 24:S55–60. doi: 10.1097/IGC.0000000000000228

35. Zhao S, Bellone S, Lopez S, Thakral D, Schwab C, English DP, et al. Mutational landscape of uterine and ovarian carcinosarcomas implicates histone genes in epithelial-mesenchymal transition. *Proc Natl Acad Sci United States America*. (2016) 113:12238–43. doi: 10.1073/pnas.1614120113

36. Borrego SN, Lengyel E, Kurnit KC. Molecular characterizations of gynecologic carcinosarcomas: A focus on the immune microenvironment. *Cancers*. (2022) 14. doi: 10.3390/cancers14184465

37. Lu XF, Zhang L, Zhao H, Chen C, Wang Y, Liu S, et al. Molecular classification and subtype-specific drug sensitivity research of uterine carcinosarcoma under multi-omics framework. *Cancer Biol Ther*. (2019) 20:227–35. doi: 10.1080/15384047.2018.1523853

38. Mermel CH, Schumacher SE, Hill B, Meyerson ML, Beroukhim R, Getz G. GISTIC2.0 facilitates sensitive and confident localization of the targets of focal somatic copy-number alteration in human cancers. *Genome Biol*. (2011) 12:R41. doi: 10.1186/gb-2011-12-4-r41

39. Li C, Bonazzoli E, Bellone S, Choi J, Dong W, Menderes G, et al. Mutational landscape of primary, metastatic, and recurrent ovarian cancer reveals c-MYC gains as potential target for BET inhibitors. *Proc Natl Acad Sci U.S.A*. (2019) 116:619–24. doi: 10.1073/pnas.1814027116

40. Alexandrov LB, Nik-Zainal S, Wedge DC, Aparicio SAJR, Behjati S, Biankin AV, et al. Signatures of mutational processes in human cancer. *Nature*. (2013) 500:415–21. doi: 10.1038/nature12477

41. Gonzalez-Martin A, Pothuri B, Vergote I, Christensen RD, Graybill W, Mirza MR, et al. Niraparib in patients with newly diagnosed advanced ovarian cancer. *N Engl J Med*. (2019) 381:2391–402. doi: 10.1056/NEJMoa1910962

42. Gotoh O, Sugiyama Y, Takazawa Y, Kato K, Tanaka N, Omatsu K, et al. Clinically relevant molecular subtypes and genomic alteration-independent differentiation in gynecologic carcinosarcoma. *Nat Commun*. (2019) 10:4965. doi: 10.1038/s41467-019-12985-x

43. Perren TJ, Swart AM, Pfisterer J, Ledermann JA, Pujade-Lauraine E, Kristensen G, et al. A phase 3 trial of bevacizumab in ovarian cancer. *N Engl J Med*. (2011) 365:2484–96. doi: 10.1056/NEJMoa1103799

44. Burger RA, Brady MF, Bookman MA, Fleming GF, Monk BJ, Huang H, et al. Incorporation of bevacizumab in the primary treatment of ovarian cancer. *N Engl J Med*. (2011) 365:2473–83. doi: 10.1056/NEJMoa1104390

45. Zorzou MP, Markaki S, Rodolakis A, Kastritis E, Bozas G, Dimopoulos MA, et al. Clinicopathological features of ovarian carcinosarcomas: a single institution experience. *Gynecol Oncol*. (2005) 96:136–42. doi: 10.1016/j.ygyno.2004.09.051

46. Nayha V, Stenback F. Angiogenesis and expression of angiogenic agents in uterine and ovarian carcinosarcomas. *Apmis*. (2008) 116:107–17. doi: 10.1111/j.1600-0463.2008.00757.x

47. Basu P, Mukhopadhyay A, Konishi I. Targeted therapy for gynecologic cancers: Toward the era of precision medicine. *Int J Gynecology Obstetrics*. (2018) 143:131–6. doi: 10.1002/ijgo.12620

48. Cui Q, Hu Y, Ma D, Liu H. A retrospective observational study of anlotinib in patients with platinum-resistant or platinum-refractory epithelial ovarian cancer. *Drug Des Devel Ther*. (2021) 15:339–47. doi: 10.2147/DDDT.S286529

49. Zhu J, Wen H, Ju X, Bi R, Zuo W, Wu X. Clinical significance of programmed death ligand1 and intra-tumoral CD8+ T lymphocytes in ovarian carcinosarcoma. *PloS One*. (2017) 12:e0170879. doi: 10.1371/journal.pone.0170879

50. Ghose A, McCann L, Makker S, Mukherjee U, Gullapalli SVN, Erekkath J, et al. Diagnostic biomarkers in ovarian cancer: advances beyond CA125 and HE4. *Ther Adv Med Oncol*. (2024) 16:17588359241233225. doi: 10.1177/17588359241233225

frontiers | Frontiers in Oncology

TYPE Opinion
PUBLISHED 23 August 2024
DOI 10.3389/fonc.2024.1443334

Check for updates

OPEN ACCESS

EDITED BY
Ferdinando Agresta,
ULSS2 Marca Trevigiana, Italy

REVIEWED BY
Mario Murguia-Perez,
Mexican Social Security Institute, Mexico
Nicolae Bacalbasa,
Carol Davila University of Medicine and Pharmacy, Romania

*CORRESPONDENCE
Lisa Feinstein
lisafeinstein@bellsouth.net

RECEIVED 03 June 2024
ACCEPTED 09 August 2024
PUBLISHED 23 August 2024

CITATION
Feinstein L (2024) Letter to the editor regarding "Giant mucinous cystadenocarcinoma of ovary in a young woman: a case report and review of literature" Volume 14 2024.
Front. Oncol. 14:1443334.
doi: 10.3389/fonc.2024.1443334

COPYRIGHT
© 2024 Feinstein. This is an open-access article distributed under the terms of the Creative Commons Attribution License (CC BY). The use, distribution or reproduction in other forums is permitted, provided the original author(s) and the copyright owner(s) are credited and that the original publication in this journal is cited, in accordance with accepted academic practice. No use, distribution or reproduction is permitted which does not comply with these terms.

Letter to the editor regarding "Giant mucinous cystadenocarcinoma of ovary in a young woman: a case report and review of literature" Volume 14 2024

Lisa Feinstein*

Camelot Animal Hospital, Davie, FL, United States

KEYWORDS

ovarian cancer, ovarian mucinous adenocarcinoma, ovarian borderline malignancy, ovarian cystadenoma, ovarian cystadenocarcinoma, MAC

Our 19-year-old daughter Kate died on 23 May 2024 of stage 4 primary ovarian mucinous cystadenocarcinoma 1 year after diagnosis. She first felt abdominal pain while on vacation in Maine in August 2021. CT scan and ultrasound showed a large fluid filled cyst on her right ovary (without concerning solid parts or septation). On her 17th birthday, she had a laparoscopic cystectomy for an 18-cm right ovarian cyst. The pathology for this was (and verified later) mucinous cystadenoma (August 2021). The cyst recurred and was confirmed on ultrasound in late 2022, and she had a laparoscopic right ovarian cystectomy for another 18-cm cyst in mid-March 2023. The pathology report at this time revealed predominantly mucinous cystadenoma, but there was focal borderline tumor and a small amount of mucinous cystadenocarcinoma. By May 2023, when the gynecological oncologist staged her, mucinous carcinoma was in her peritoneal washing and infracolic omentum, making her stage 3. Her cancer antigens were normal until November 2023, when she developed massive ascites and her CA125 went just above 50, soon after finishing six rounds of FOLFOX chemotherapy. When she was administered hyperthermic intraperitoneal chemotherapy cytoreduction at MD Anderson in December 2023, mucinous carcinoma was noted throughout her abdomen/intestinal tract, giving her a Peritoneal Cancer Index score of 39. How does a gynecologist suspect mucinous cancer and know to remove the entire adnexa in a very young woman with normal CA125 and benign imaging? Mucinous cystadenocarcinoma is rare and does not always elevate cancer antigens, as in my daughter's case. My daughter may have been saved if her entire ovary was removed without spillage at the first or second surgery. However, most gynecologists I spoke to would have just done a cystectomy the first and even the second time as she was an asymptomatic, healthy 18-year old, and her cyst was read as benign at the first surgery. You have one chance with primary ovarian mucinous cancer and that is removing the adnexa without spillage at the first surgery, but, unfortunately, my daughter Kate did not have that.

If primary ovarian mucinous cancer is diagnosed beyond stage 1, the prognosis is grim. Removing an ovary unnecessarily is a small sacrifice I would gladly have made if I knew cancer was a possibility and we may have been saving her life. How can gynecologists prevent this tragedy in other young women?

Author contributions

LF: Writing – original draft, Writing – review & editing.

Funding

The author(s) declare that no financial support was received for the research, authorship, and/or publication of this article.

Conflict of interest

The author declares that the research was conducted in the absence of any commercial or financial relationships that could be construed as a potential conflict of interest.

Publisher's note

All claims expressed in this article are solely those of the authors and do not necessarily represent those of their affiliated organizations, or those of the publisher, the editors and the reviewers. Any product that may be evaluated in this article, or claim that may be made by its manufacturer, is not guaranteed or endorsed by the publisher.

frontiers | Frontiers in Oncology

TYPE Case Report
PUBLISHED 26 August 2024
DOI 10.3389/fonc.2024.1415816

Check for updates

OPEN ACCESS

EDITED BY
Ferdinando Agresta,
ULSS2 Marca Trevigiana, Italy

REVIEWED BY
Teodor Florin Georgescu,
Carol Davila University of Medicine and Pharmacy, Romania
Nicolae Bacalbasa,
Carol Davila University of Medicine and Pharmacy, Romania

*CORRESPONDENCE
Yuan-Qing Lin
linyq@hxxy.edu.cn
Dan Luo
835101345@qq.com
Shu-Xia Xu
710221408@qq.com

†These authors have contributed equally to this work and share first authorship

‡These authors have contributed equally to this work and share senior authorship

RECEIVED 11 April 2024
ACCEPTED 05 August 2024
PUBLISHED 26 August 2024

CITATION
Zhang H-B, Lin L-H, Lin Q-P, Lin Y-Q, Luo D and Xu S-X (2024) Case report: Clinicopathological characteristic of two cases of primary endometrial squamous cell carcinoma and review of the literature. *Front. Oncol.* 14:1415816. doi: 10.3389/fonc.2024.1415816

COPYRIGHT
© 2024 Zhang, Lin, Lin, Lin, Luo and Xu. This is an open-access article distributed under the terms of the Creative Commons Attribution License (CC BY). The use, distribution or reproduction in other forums is permitted, provided the original author(s) and the copyright owner(s) are credited and that the original publication in this journal is cited, in accordance with accepted academic practice. No use, distribution or reproduction is permitted which does not comply with these terms.

Case report: Clinicopathological characteristic of two cases of primary endometrial squamous cell carcinoma and review of the literature

Hui-Bin Zhang[1†], Li-Hua Lin[2†], Qiu-Ping Lin[3†], Yuan-Qing Lin[4*‡], Dan Luo[1*‡] and Shu-Xia Xu[1*‡]

[1]Department of Pathology, Fujian Maternity and Child Health Hospital, College of Clinical Medicine for Obstetrics & Gynecology and Pediatrics, Fujian Medical University, Fuzhou, Fujian, China, [2]Department of Health Care Section, Fujian Maternity and Child Health Hospital, College of Clinical Medicine for Obstetrics & Gynecology and Pediatrics, Fujian Medical University, Fuzhou, Fujian, China, [3]Department of Traditional Chinese Medical Science, Fujian Maternity and Child Health Hospital, College of Clinical Medicine for Obstetrics & Gynecology and Pediatrics, Fujian Medical University, Fuzhou, Fujian, China, [4]College of Environment and Public Health, Xiamen Huaxia University, Xiamen, Fujian, China

Primary endometrial squamous cell carcinoma (PESCC) is a rare malignant tumor. To investigate the clinical and pathological features of PESCC, two cases of PESCC in Fujian Maternal and Child Health Hospital were retrospectively studied and the literatures were reviewed. Both of the two cases were menopausal women aged 57–62 years, clinically presenting with "vaginal discharge". Case 1 was a non-keratinising squamous cell carcinoma with high-risk HPV infection. Tumor infiltrated in deep myometrium with multifocal intravascular thrombus and macro metastases to one pelvic lymph node (1/15) and abdominal aortic lymph node (1/1). Lung metastasis occurred 36 months after the surgery. After surgical resection and without postoperative supplemental therapy, the patient remained tumor-free for 110 months to date. Case 2 had a history of breast cancer for 5 years and long-term intake of aromatase inhibitor drugs without HPV infection. It was a keratinized squamous cell carcinoma. Tumor also infiltrated in deep myometrium with multifocal intravascular thrombus and one pelvic lymph node metastasis (1/18), However, no metastasis was seen elsewhere. To date, the patient survived for 16 months without tumor after surgery. Both of the two cases expressed squamous epithelial markers P40, P63, and CK5/6, but neither expressed PAX8 or PR. Case 1 had diffuse expression of P16, wild-type P53, and ER-negative. Case 2 had negative P16, mutant P53, and focal positive ER. PESCC is often associated with HPV infection and low estrogen levels. However, studies in the literatures have found that P16 expression is not always consistent with HPV infection, indicating that PESCC cannot be easily classified as HPV-associated or non-dependent like cervical cancer. There are two main patterns of P16 and P53 expression, P16-positive/P53 wild-type and P16-negative/P53-mutant, but no positive expression of both has been seen so far. It is worth noting that we reported the second case

of PESCC with a history of breast cancer, where the patient had been taking the oral aromatase inhibitor drug (exemestane) for a long period of time to reduce the estrogen level, indicating the low estrogen level may be also a key factor in the pathogenesis of PESCC.

KEYWORDS

primary, endometrial squamous cell carcinoma, pathology, pathogenesis, clinicopathological feature

Introduction

The endometrium is a glandular epithelial tissue and the majority of malignant tumors arising from it are adenocarcinomas. Primary endometrial squamous cell carcinoma (PESCC) is a rare entity, with an incidence accounting for less than 0.5% of all endometrial malignancies (1). The 2020 World Health Organization Classification of Female Genital Tumors provide comprehensive introductions for the most tumor types. However, the description of PESCC is extremely brief, which shows that there is still a lack of knowledge about PESCC.

Here, we present an in-depth research of the clinicopathological features of two cases of PESCC as well as a review of previously published cases. The aim of this paper is to provide practitioners with actionable knowledge to enhance their understanding of this rare malignancy.

Materials and methods

The database of the Department of Pathology at Fujian Maternal and Child Health Hospital was searched from 2011 to 2023 using the keywords "squamous cell carcinoma", "endometrium", and "whole uterus". Cases were further screened according to the following criteria: 1. The absence of endometrial adenocarcinomas or epithelial neoplasms; 2. The exclusion of primary squamous cell carcinoma of the uterine cervix.

After rigorous screening, only 2 cases met 100% of the diagnostic criteria for PESCC. The clinical data for the two cases of PESCC were complete, including patients' demographic information, clinical manifestations, surgical methods, and postoperative patient follow-up data (Table 1).

Surgical specimens were fixed in 10% neutral buffered formalin solution for an appropriate duration, dehydrated in a graded series of alcohols, and then embedded in paraffin wax. Sections were cut at a thickness of 4 μm and stained with hematoxylin and eosin (HE). Immunohistochemical staining was performed using the EnVision method with a panel of primary antibodies including P16, P53, P40, P63, CK5/6, ER, PR, CKH, CKL, PAX8, and Ki-67. The primary antibodies were purchased from Fuzhou Maixin Company. The antibody kits were also purchased from the same source. All immunohistochemistry was performed with positive controls, and the results were reliable. Some of the important immunohistochemical interpretation criteria were as follows: P53 staining was considered positive/mutant when there was diffuse strong nuclear staining (greater than 80% of the tumor) or all negative or diffuse cytoplasmic with weak nuclear staining; wild-type P53 was considered when there was unequal strong and weak nuclear staining. P16 staining was considered positive when there was diffuse block-like staining of P16 nuclei; negative when there was patchy or no staining. ER/PR tumor cells were interpreted as negative when the nuclear staining was less than 1%, focally positive when the staining was between 1% and 10%, and positive when the staining was greater than 10%.

Case description

We confirmed the two cases of PESCC with onset age of 57 to 62 years, the mean age was 59.5 years, menopause for 8–10 years. The clinical symptoms were all of vaginal discharge; the vaginal colorultrasound suggested intrauterine effusion; on gross examination, a large mass formed in the uterine body without involving the cervix. Two cases of PESCC had different clinicopathological features (Table 2): Case 1 was a non-keratinized type SCC with high-risk HPV infection, whereas case 2 was keratinized type SCC without HPV infection. Both of the two cases were expressed squamous epithelial-derived markers such as P63, P40 and CK5/6. However, the expression of P16 and P53 on the two cases were quite opposite. Although both PESCC cases showed strong invasion features and higher clinical stage, they appeared to have a good prognostic outcome: Case 1 presented pelvic lymph node and abdominal aortic lymph node metastasis at diagnosis, lung metastasis occurred on 36 months after surgery, and then the lung mass was surgically removed in another hospital, follow-up 110 months, and the patient survival without tumor; case 2 also had pelvic lymph node metastasis, and was followed up 16 months, the patient survival without tumor. Pathologic features are summarized in detail on a case-by-case basis as follows:

TABLE 1 Clinical features of two primary endometrial squamous cell carcinoma.

NO.	Age (years)	Menopausal status	Clinical symptom	Serum SCC value (normal value<1.5ng/mL)	HPV	Treatments	Stage (FIGO)	Follow-up (mo)
1	62	Postmenopausal 10 years	Vaginal drainage for more than 1 year	8.3↑	+16 +42 +83	Thyst/bso/ lnd/chemo	IIIC2	110 NED
2	57	Postmenopausal 8 years	Vaginal discharge for 1 month	10.23↑	–	Rhyst/bso/ lnd/chemo	IIIC1	16 NED

Thyst, total hysterectomy; Rhyst, radical hysterectomy; bso, bilateral salpingo-ovariectomy; lnd, lymph node dissection; chemo, chemotherapy; NED, no evidence of disease (alive).
↑, higher than 1.5 ng/mL.

Case 1

A 62-year-old postmenopausal woman was admitted to our hospital in March 2015 with a complaint of vaginal discharge for over a year. Pelvic ultrasound revealed fluid in the uterine cavity, and the level of squamous carcinoma-associated antigen (SCC) was elevated to 8.3 ng/mL, which is higher than the normal range of 0.00–1.5 ng/mL. HPV DNA testing was positive for high-risk types 16, 42, and 83. Subsequently, a preoperative hysteroscopy with curettage was performed, and no cervical lesions were identified. The endometrial curetting showed squamous cell carcinoma. Then, the patient underwent radical hysterectomy, bilateral salpingo-oophorectomy, and pelvic lymph node dissection. During the surgery, a greyish-yellow nodule of about 0.5 cm was found adjacent to the abdominal aorta, and frozen section examination revealed metastatic squamous cell carcinoma.

On gross examination, the endometrium displayed thickening with an ichthyosis-like appearance and deep invasion (near the plasma layer). Sampling of all cervical tubes did not reveal any intraepithelial lesions. Microscopically, the endometrial mass showed typical non-keratinizing squamous cell carcinoma with tumor cells distributed in nests resembling high-grade intraepithelial lesions involving glands (Figure 1A) and some areas appeared basal cell carcinoma-like with central necrosis (Figure 1B). Lymphovascular invasion was seen in the mesenchyme. A total of 15 lymph nodes were palpated in the pelvic lymph nodes, and a single metastasis was identified in the left obturator lymph node. Immunohistochemically, the tumor cells were diffusely positive for P63/P40/CK5/6 and P16 (Figure 1C), wild-type P53 (Figure 1D); negative for ER/PR/Pax8 (Figure 1E); and Ki67 index of about 90%. After the surgery, the patient received platinum-based chemotherapy and was followed regularly. At postoperative 36 months, lung metastasis was detected and surgically resected at another hospital, telephone follow-up revealed that the patient had not undergone any additional postoperative treatment. The patient is currently being followed up for 110 months with regular follow-up appointments but has not shown any evidence of disease recurrence to date.

Case 2

A 57-year-old postmenopausal woman was referred to our hospital in March 2023 for a complaint of vaginal discharge for 1 month. She had a history of oral exemestane therapy for breast cancer for 5 years. Pelvic magnetic resonance imaging (MRI) suggested a mass in the uterine cavity measuring approximately 35×42×63 mm. The serum squamous cell carcinoma-associated antigen (SCC) level was elevated to 10.23ng/mL, while CA125, CA199, and CEA values were within the normal range. HPV E6/E7 mRNA detection was negative for high-risk human papillomavirus.

Curettage of the endometrium and endocervix revealed keratinized squamous cells with moderate anisotropy. The patient then underwent radical hysterectomy, bilateral salpingo-oophorectomy, pelvic lymph node, and para-abdominal aortic lymph node dissection. Macroscopically, a bulging mass measuring 40×35×25 mm involved primarily the endometrium (Figure 2A), with tumor invasion into the deeper half of the myometrium and lymphovascular space.

Microscopically, the tumor cells showed typical morphological features of keratinized squamous cell carcinoma with abundant eosinophilic cytoplasm and keratin pearls (Figure 2B), and the cervix was free of disease. A total of 18 lymph nodes were palpated in the pelvic lymph nodes and a single metastasis was identified. Immunohistochemical analysis demonstrated strong positive staining for P63/P40/CK5/6, negative staining for P16/PR, focal

TABLE 2 Pathological characteristics of two primary endometrial squamous cell carcinoma.

NO.	Pathological type	Depth of Invasion	LVI	Metastasis	IHC					
					P16	P53	ER	PR	Pax8	KI-67
1	Non-keratinized type SCC	>50% Myoinvasion	Present	Pelvic lymph nodes(1/15); abdominal aortic lymph node (1/1); Lung	+	Wild-type	–	–	–	90%+
2	Keratinized type SCC	>50% Myoinvasion	Present	Pelvic lymph nodes(1/18)	–	Mutant	<10%+	–	–	50%+

LVI, lymphovascular invasion; IHC, immunohistochemistry; ER, estrogen receptor; PR, progesterone receptor.

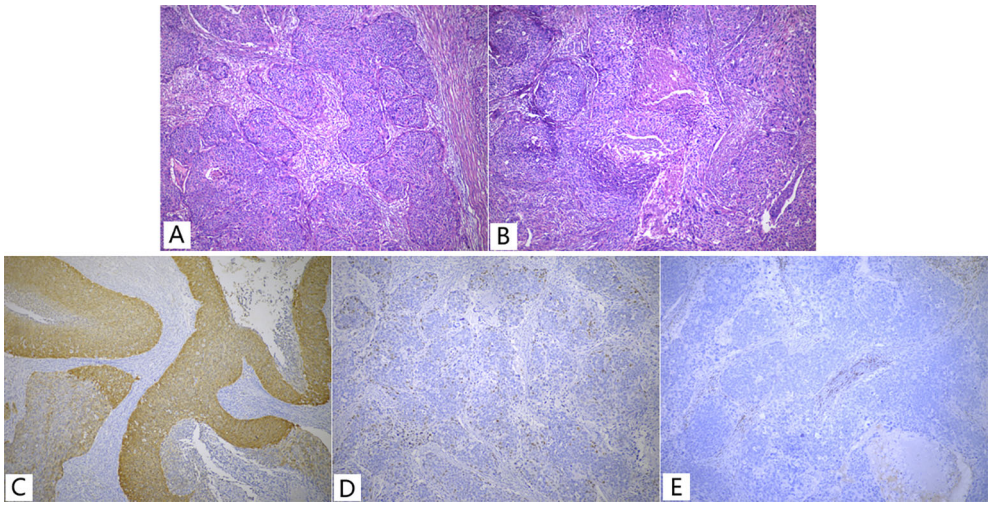

FIGURE 1
Non-keratinized type SCC **(A, B)** and Immunohistochemistry **(C-E)** of Case 1. **(A)** Showed typical features of non-keratinized squamous cell carcinoma; **(B)** Basal cell carcinoma-like with central necrosis; **(C)** P16 showed diffuse strong positive, a little faded; **(D)** P53, wild-type expression pattern; **(E)** PR, negative,<1%.

positive staining for ER, nearly 100% strong positive staining for P53, and Ki-67 index of about 50% (Figures 2C-E).

The patient received chemotherapy with paclitaxel and carboplatin after surgery and has been free of disease for 16 months.

Discussion

Most malignancies occurring in the endometrium are adenocarcinomas, and PESCC is an extremely rare malignancy. Due to the diagnostic criteria for PESCC is stringent and it belongs to an exclusion diagnosis, from 2011 year to 2023 year (as of August 31) in the Department of Pathology, Fujian Maternal and Child Health Hospital, a total number of 1999 of cases of endometrial cancer were reported, including only 2 cases of PESCC were revealed. It accounted for about one in thousand.

The earliest and traditional diagnostic criterion, still in use today, was proposed by Fluhmann (2) in 1928 and requires fulfillment of all three of the following criteria: 1) the absence of endometrial adenocarcinomas or epithelial neoplasms; 2) the absence of endometrial squamous cell carcinoma in association with the squamous epithelium of the uterine cervix; and 3) the absence of primary squamous cell carcinoma of the uterine cervix. However, some pathologists recognize that the diagnostic criteria for PESCC should not be restricted to excluding involvement of the cervical canal because tumors are always invasive. Mark et al. (3)

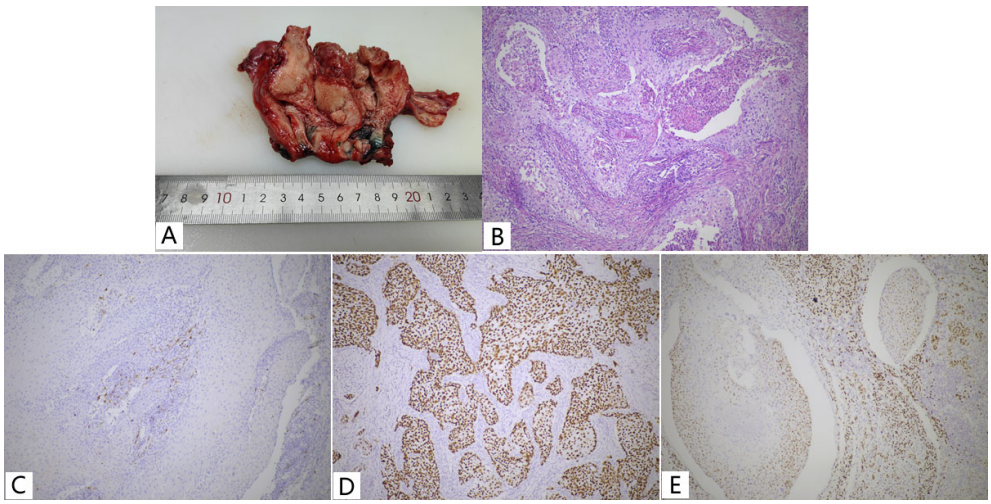

FIGURE 2
Keratinized type SCC **(A, B)** and Immunohistochemistry **(C-E)** of Case 2. **(A)** A prominent mass in the uterine body; **(B)** Pure keratinized squamous cell carcinoma with large amounts of neutrophils aggregated. **(C)** P16, negative; **(D)** P53, Aberrant/mutation-type expression pattern; **(E)** ER, focally positive, between 1% -10%.

reported four cases of endometrial squamous cell carcinoma involving the cervical canal that were confirmed to be PESCC by modern adjuvant techniques such as immunohistochemistry, HPV *in-situ* hybridization, and molecular testing. This suggests that the diagnostic criteria for PESCC can be appropriately relaxed to allow for the presence of involvement of the cervical canal, but this also increases the difficulty of diagnosis because there are not rare cases of squamous cell carcinoma of the cervix involving the endometrium. Therefore, to achieve a more accurate diagnosis, it is necessary to fully understand the clinicopathological features of PESCC.

PESCC patients are mostly seen in perimenopausal or postmenopausal women (4), with an average age of onset of approximately 67 years, and very rarely observed in women of childbearing age (5, 6). The clinical manifestations of PESCC are similar to those of endometrioid carcinoma, with the most common presentation being vaginal bleeding, followed by uterine pus and vaginal discharge, and some patients are found to have uterine fibroids occupying the uterus on further physical examination (7–10). The pathogenesis of PESCC is still unclear, but it is generally believed that the endometrium is stimulated by various factors leading to the squamous development of endometrial precursor cells, which ultimately leads to carcinoma. These causative factors include uterine pus accumulation, uterine fibroids, chronic endometritis, and pelvic radiation, etc. (4–7). A small number of cases of PESCC have been reported to occur as a secondary effect of hormonal therapy or radiotherapy treatment for breast, colorectal and ovarian cancers (8–11). One of the breast cancer patients was on long-term tamoxifen use, which is similar to our reported case 2 patient with a history of breast cancer and long-term use of an estrogen antagonist drug (exemestane). This indicates that low estrogen levels may also be a contributing factor in the development of PESCC.

It is well established that the majority of cervical squamous cell carcinomas are associated with HPV infection. However, the relationship between HPV infection and PESCC remains a topic of debate. Currently, the World Health Organization (WHO) recognizes an association between HPV infection and PESCC. Kataoka et al. (12) were the first to demonstrate that one case of PESCC was positive for HPV type 31 by PCR, and they proposed that HPV infection might be related to the development of PESCC. Subsequently, Darré et al. (5) and Zhang et al. (13) also reported two cases of HPV-associated PESCC. However, many cases of PESCC to date have not been associated with HPV infection, and most of these cases have undergone immunohistochemistry or molecular testing. Most cases of PESCC were found to have abnormal expression or mutation of the oncogene P53 by immunohistochemistry or molecular testing, suggesting that mutation of the oncogene P53 is associated with the development of PESCC (3, 6, 14).

The microscopic appearance and morphological characteristics of PESCC are generally like those of squamous cell carcinoma of the uterine cervix, being predominantly keratinized or non-keratinized types with the two types being able to coexist, and a small proportion being papillomavillous or uroepithelial cells (15, 16).

Immunohistochemistry demonstrates that PESCC expresses squamous differentiation markers such as P40, P63, and CK5/6, and generally lacks Müllerian-derived markers such as PAX8, ER, PR, but ER may be focally expressed in a small number of cases (3), and only one case of PAX8 positivity has been reported so far (17). In addition, there are two patterns of P16 and P53 expression in PESCC: one being positive for P16 with wild-type P53 expression and the other one is negative for P16 with abnormal expression of P53. A small proportion of PESCC are negative for both P16 and P53 markers, indicating the activation of other pathogenic molecular pathways involved in the development of PESCC. Reviewing the literature, there are no cases of positive expression of both P16 and P53 markers, suggestive of a potential mutual exclusivity in the expression of the two in PESCC; however, more data are required to verify this phenomenon, which could aid in distinguishing plasmacytoid carcinomas with extensive squamous differentiation. Additionally, Horn et al. (18) only detected HPV in one out of four cases of P16-positive PESCC, indicating that p16-positive PESCC may not always be HPV-associated and that classification based on HPV status may not be appropriate for PESCC. Molecular alterations in PESCC involve TP53, CDKN2A, pRB-CyclinD1-CDK4/6-p16, PTENT, and PIK3CA (3, 19), and only one case of PESCC has been molecularly typed as MSI-H (20).

PESCC requires differential diagnosis from multiple tumors. The first differential diagnosis is endometrial adenocarcinoma with extensive squamous metaplasia or adenosquamous carcinoma, which is the most common malignancy of the endometrium, often associated with squamous metaplasia and mucinous metaplasia. When endometrial adenocarcinoma is associated with extensive squamous metaplasia, the squamous component may completely cover the glandular component, leading to misdiagnosis as squamous cell carcinoma. However, immunohistochemistry cannot help distinguish between the two, so comprehensive sampling of the endometrium is necessary to determine the presence of endometrial glandular epithelial lesions in the diagnosis of primary squamous cell carcinoma of the endometrium. Even a small amount of glandular epithelial lesion suggests that the tumor may be more common endometrial cancer with squamous metaplasia rather than squamous cell carcinoma of the endometrium. The second differential diagnosis is cervical squamous cell carcinoma involving the endometrium. According to Fluhmann's (2) criteria, when squamous cell carcinoma involves both the cervix and endometrium, it is classified as cervical with endometrial involvement. However, occasionally, PESCC may involve the cervix. All reported cases of this type of PESCC are non-HPV-related and often associated with abnormal P53 expression and negative P16 staining (3), unlike primary cervical squamous cell carcinoma, which is mostly HPV-related, P16-positive, and shows wild-type P53 expression. The final differential diagnosis is from squamous differentiation in papillary serous carcinoma: squamous differentiation is rare in papillary serous carcinoma. Santoro et al. (21) reported a case of endometrial papillary serous carcinoma with extensive squamous differentiation mimicking primary endometrial squamous cell carcinoma. This case presented with features of complete squamous differentiation, expressing squamous markers such as P40, P63, and CK5/6, but not Müllerian-derived markers such as PAX8, ER, PR, etc. P53 was aberrantly expressed and P16 was limited to basal expression. The diagnosis was consistent with primary squamous cell carcinoma, but morphological and immunohistochemical features of papillary serous carcinoma were

seen in the sentinel lymph node. For this rare and atypical case, only comprehensive sampling can reduce unnecessary misdiagnosis.

Due to the rarity of PESCC cases, there is no consensus on the treatment of this disease. Early on, Goodman et al. (4) proposed total hysterectomy with double adnexectomy as the optimal therapy for PESCC. Subsequently, Kennedy et al. (22) reported the first case of PESCC treated with postoperative adjuvant chemotherapy using cisplatin, leading to the development of a treatment pattern based on surgery with postoperative combined radiotherapy and/or chemotherapy. However, there is no recommendation for the optimal combination of modalities. Song et al. (20) analyzed the survival data of 31 cases of PESCC and recommended that surgery remain the main treatment modality for PESCC, with lymph node clearance being advocated. For stage I patients, appropriate radiotherapy could be given after surgery, while for stage III and IV patients, combined radiotherapy and chemotherapy should be given. Molecular typing is recommended because some patients may benefit from immunotherapy such as PD-L1.

Some studies have indicated that PESCC has a poorer prognosis than endometrioid carcinoma (4). Furthermore, the prognosis correlates with pathological staging. A five-year survival analysis conducted by Varras and Kioses revealed that the prognosis for patients diagnosed with early-stage PESCC was significantly more favorable than that of patients diagnosed with late-stage disease (23). The most common causes of death were tumor recurrence and metastasis, with pelvic metastasis being the most prevalent, followed by lung, brain and bone metastases (4, 23). Nevertheless, data from Dalrymple et al. (9) on four patients with PESCC followed up for up to 10 years indicated that the prognosis of even advanced PESCC with distant metastases was not as poor as previously thought. Our case 1, which involved metastases to the lungs, was monitored for over nine years with a favorable prognosis. However, due to the limited number of cases, this does not provide a representative overview of the overall prognosis. PESCC can be comorbid with other types of tumors, as evidenced by a case of PESCC combined with early tubal adenocarcinoma reported by Caulkins et al. (24) and a case of PESCC combined with neuroendocrine tumors reported by Varras and Kioses (23). Similarly, the diagnosis of PESCC necessitates the exclusion of metastasis of SCC from other sites. A case has been reported of vulvar cancer metastasizing to the endometrium of the uterus without involvement of the cervix (25). The presence of these combined higher-grade tumors may contribute to the poor prognosis observed in some cases of PESCC.

Conclusion

The clinical features of the two cases of PESCC we reported here were consistent with those reported in the literature. One case being accompanied by high-risk HPV infection, suggesting that there is a correlation between the occurrence of PESCC and HPV infection. However, a review of the literature showed that the expression of P16 did not coincide with HPV infection, indicating that PESCC is not suitable for simple classification based on HPV-associated or non-dependent cervical cancer classification. PESCC expressed the squamous epithelial markers such as P40, P63 and CK5/6, most of which did not express the mullerian origin markers PAX 8, PR and ER. There were mainly two patterns of P16 and P53 expression, i.e., P16-positive/P53 wild-type and P16-negative/P53-mutant. Only a small number of them were negative for both, but none of them was found to be positive, which suggested that P16 and P53 may be mutually exclusive and more data were needed to verify this. In addition, it is worth mentioning that we reported the second case of PESCC with a history of breast cancer who had been taking the aromatase inhibitor drug "exemestane" for a long time to reduce the estrogen level, indicating a low estrogen level may be also a risk factor for the pathogenesis of PESCC.

Data availability statement

The original contributions presented in the study are included in the article/supplementary material. Further inquiries can be directed to the corresponding authors.

Ethics statement

The studies involving humans were approved by Ethics Committee of Fujian Maternity and Child Health Hospital. The studies were conducted in accordance with the local legislation and institutional requirements. The human samples used in this study were acquired from a by- product of routine care or industry. Written informed consent for participation was not required from the participants or the participants' legal guardians/next of kin in accordance with the national legislation and institutional requirements. The manuscript presents research on animals that do not require ethical approval for their study. Written informed consent was obtained from the individual(s) for the publication of any potentially identifiable images or data included in this article.

Author contributions

H-BZ: Writing – original draft, Methodology, Investigation. L-HL: Writing – original draft, Methodology. S-XX: Writing – original draft, Methodology. Y-QL: Writing – review & editing, Supervision, Project administration. Q-PL: Writing – review & editing, Supervision, Project administration. DL: Writing – review & editing, Supervision, Project administration.

Funding

The author(s) declare that no financial support was received for the research, authorship, and/or publication of this article.

Conflict of interest

The authors declare that the research was conducted in the absence of any commercial or financial relationships that could be construed as a potential conflict of interest.

Publisher's note

All claims expressed in this article are solely those of the authors and do not necessarily represent those of their affiliated organizations, or those of the publisher, the editors and the reviewers. Any product that may be evaluated in this article, or claim that may be made by its manufacturer, is not guaranteed or endorsed by the publisher.

References

1. WHO. *Classification of Tumours Editorial Board. Female Genital Tumours. 5th ed*. Lyon: IARC (2020) p. 264–5.

2. Fluhmann CF. Comparative studies of squamous metaplasia of the cervix uteri and endometrium. *Am J Obstet Gynecol*. (1954) 68:1447–63. doi: 10.1016/0002-9378(54)90296-3

3. Hopkins MR, Palsgrove DN, Ronnett BM, Vang R, Lin J, Murdock TA. Molecular analysis of HPV-independent primary endometrial squamous cell carcinoma reveals TP53 and CDKN2A comutations: A clinicopathologic analysis with re-evaluation of diagnostic criteria. *Am J Surg Pathol*. (2022) 46:1611–22. doi: 10.1097/PAS.0000000000001970

4. Goodman A, Zukerberg LR, Rice LW, Fuller AF, Young RH, Scully RE. Squamous cell carcinoma of the endometrium: a report of eight cases and a review of the literature. *Gynecol Oncol*. (1996) 61:54–60. doi: 10.1006/gyno.1996.0096

5. Darré T, Aboubakari AS, Sonhaye L, Douaguibe B, Bassowa A, Napo-Koura G. Primary squamous cell carcinoma of the endometrium associated with human papilloma virus in a young woman: a case report. *J Med Case Rep*. (2019) 13:167. doi: 10.1186/s13256-019-2098-4

6. Wu Q, Chu Z, Han H, Bai S, Wu W, Li X, et al. Primary squamous cell carcinoma of the endometrium in a woman of reproductive age: a rare case report. *J Int Med Res*. (2018) 46:3417–21. doi: 10.1177/0300060518776579

7. Jain M, Kashyap A, Biswas R. Primary endometrial squamous cell carcinoma *in-situ* with extensive icthyosis uteri: A rare case report. *J Clin Diagn Res*. (2017) 11:ED13–4. doi: 10.7860/JCDR/2017/29967.10384

8. Sorosky JI, Kaminski PF, Kreider J, Podczaski ES, Olt GJ, Zaino R. Endometrial squamous cell carcinoma following whole pelvic radiation therapy: response to carboplatin. *Gynecol Oncol*. (1995) 57:426–9. doi: 10.1006/gyno.1995.1167

9. Dalrymple JC, Russell P. Primary endometrial squamous cell carcinoma with long-term survival. *Aust Nz J Obstet Gyn*. (1993) 33:330–2. doi: 10.1111/j.1479-828x.1993.tb02102.x

10. Abeler V, Kjørstad KE. Endometrial squamous cell carcinoma: report of three cases and review of the literature. *Gynecol Oncol*. (1990) 36:321–6. doi: 10.1016/0090-8258(90)90134-7

11. Simon A, Kopolovic J, Beyth Y. Primary squamous cell carcinoma of the endometrium. *Gynecol Oncol*. (1988) 31:454–61. doi: 10.1016/s0090-8258(88)80031-3

12. Kataoka A, Nishida T, Sugiyama T, Hori K, Honda S, Yakushiji M. Squamous cell carcinoma of the endometrium with human papillomavirus type 31 and without tumor suppressor gene p53 mutation. *Gynecol Oncol*. (1997) 65:180–4. doi: 10.1006/gyno.1996.4597

13. Zhang C, Zhang H, Yang L, Wang Y, Li X, Guo J, et al. Primary squamous cell carcinoma of the endometrium in a woman of perimenopausal age: A case report. *Med (Baltimore)*. (2018) 97:e13418. doi: 10.1097/MD.0000000000013418

14. Lee SJ, Choi HJ. Primary endometrial squamous cell carcinoma: a case report and review of relevant literature on korean women. *Korean J Pathol*. (2012) 46:395–8. doi: 10.4132/KoreanJPathol.2012.46.4.395

15. Ma L, Xu F, Guo X, Zhang Y. Primary papillary squamous-cell carcinoma of the endometrium: A rare case report. *Asian J Surg*. (2023) 46:2250–1. doi: 10.1016/j.asjsur.2022.12.002

16. Ribeiro-Silva A. Immunohistochemical features of a papillary squamous cell carcinoma of the endometrium with transitional cell differentiation. *Diagn Pathol*. (2007) 2:26. doi: 10.1186/1746-1596-2-26

17. Fanni D, Peiretti M, Mais V, Massa E, Gerosa C, Ledda F, et al. PAX8 Positivity, Abnormal p53 Expression, and p16 Negativity in a Primary Endometrial Squamous Cell Carcinoma: A Case Report and Review of the Literature. *Int J Gynecol Pathol*. (2022) 41:431–5. doi: 10.1097/PGP.0000000000000820

18. Horn LC, Richter CE, Einenkel J, Tannapfel A, Liebert UG, Leo C. p16, p14, p53, cyclin D1, and steroid hormone receptor expression and human papillomaviruses analysis in primary squamous cell carcinoma of the endometrium. *Ann Diagn Pathol*. (2006) 10:193–6. doi: 10.1016/j.anndiagpath.2005.09.001

19. Bures N, Nelson G, Duan Q, Magliocco A, Demetrick D, Duggan MA. Primary squamous cell carcinoma of the endometrium: clinicopathologic and molecular characteristics. *Int J Gynecol Pathol*. (2013) 32:566–75. doi: 10.1097/PGP.0b013e31828cb0be

20. Song L, Wu Q, Bai S, Xu R, Wang X, Yang Y. Treatment of primary squamous cell carcinoma of the endometrium and review of previous literature: A case report. *Med (Baltimore)*. (2023) 102:e33667. doi: 10.1097/MD.0000000000033667

21. Santoro A, Travaglino A, Arciuolo D, Fulgione C, Pasquini S, Minucci A, et al. Endometrial serous carcinoma with extensive squamous differentiation mimicking primary endometrial squamous cell carcinoma: Clinicopathological and molecular analysis of a case with literature review. *Pathol Res Pract*. (2022) 240:154209. doi: 10.1016/j.prp.2022.154209

22. Kennedy AS, DeMars LR, Flannagan LM, Varia MA. Primary squamous cell carcinoma of the endometrium: a first report of adjuvant chemoradiation. *Gynecol Oncol*. (1995) 59:117–23. doi: 10.1006/gyno.1995.1277

23. Varras M, Kioses E. Five-year survival of a patient with primary endometrial squamous cell carcinoma: a case report and review of the literature. *Eur J GynaecoL Oncol*. (2002) 23:327–9.

24. Caulkins M, Riccuiti J, Stevens R, Desouki M, Lele S. Primary endometrial squamous cell carcinoma with synchronous early stage Fallopian adenocarcinoma: A case report and review of diagnostic and treatment considerations. *Gynecol Oncol Rep*. (2022) 44:101–6. doi: 10.1016/j.gore.2022.101106

25. Stern JB, Kwon TH. Vulvar carcinoma with metastases to the uterus. *Gynecol Oncol*. (1981) 11:246–51. doi: 10.1016/s0090-8258(81)80017-0

frontiers | Frontiers in Oncology

TYPE Case Report
PUBLISHED 29 August 2024
DOI 10.3389/fonc.2024.1430745

Check for updates

OPEN ACCESS

EDITED BY
Ferdinando Agresta,
ULSS2 Marca Trevigiana, Italy

REVIEWED BY
Arturo Bonometti,
Humanitas University, Italy
Zimu Gong,
Houston Methodist Hospital, United States

*CORRESPONDENCE
Alessandra Carella
a.carella@inrca.it

RECEIVED 10 May 2024
ACCEPTED 02 August 2024
PUBLISHED 29 August 2024

CITATION
Carella A, Spannella F, Morè S, Grifoni R, Settanni CR, Mandolesi A, Filosa A, Goteri G, Boccoli G and Fava G (2024) A rare case of solitary plasmacytoma mimicking submucosal lesion of ascending colon: a case report and literature review. *Front. Oncol.* 14:1430745. doi: 10.3389/fonc.2024.1430745

COPYRIGHT
© 2024 Carella, Spannella, Morè, Grifoni, Settanni, Mandolesi, Filosa, Goteri, Boccoli and Fava. This is an open-access article distributed under the terms of the Creative Commons Attribution License (CC BY). The use, distribution or reproduction in other forums is permitted, provided the original author(s) and the copyright owner(s) are credited and that the original publication in this journal is cited, in accordance with accepted academic practice. No use, distribution or reproduction is permitted which does not comply with these terms.

A rare case of solitary plasmacytoma mimicking submucosal lesion of ascending colon: a case report and literature review

Alessandra Carella[1]*, Francesco Spannella[2,3], Sonia Morè[3,4], Riccardo Grifoni[5], Carlo Romano Settanni[1], Alessandra Mandolesi[6], Alessandra Filosa[6], Gaia Goteri[6], Gianfranco Boccoli[5] and Giammarco Fava[1]

[1]Unit of Gastroenterology and Digestive Endoscopy, Scientific Institute for Research, Hospitalization and Healthcare (IRCCS) Italian National Research Centres on Aging (INRCA), Ancona, Italy, [2]Internal Medicine and Geriatrics, Scientific Institute for Research, Hospitalization and Healthcare (IRCCS) Italian National Research Centres on Aging (INRCA), Ancona, Italy, [3]Department of Clinical and Molecular Sciences, University "Politecnica Delle Marche", Ancona, Italy, [4]Hematology Clinic, Azienda Ospedaliero Universitaria delle Marche, Ancona, Italy, [5]Department of General Surgery, Scientific Institute for Research, Hospitalization and Healthcare (IRCCS) Italian National Research Centres on Aging (INRCA), Ancona, Italy, [6]Anatomic Pathology, Department of Biomedical Sciences and Public Health, University "Politecnica delle Marche", Ancona, Italy

Solitary primary extraosseous plasmacytoma is a rare disease in the gastrointestinal tract, recently classified as an "exceptional" tumor of the colon site. The real incidence (one case/population/year) is unknown but reasonably less than 1/10,000,000 cases/year with very few descriptions in the literature. The rare cases described in the literature are often diagnosed after surgery for perforation and with predominant localization of the left colon. The main endoscopic presentation mimics colon carcinoma with ulcerated mass and obstructing lumen. In this paper, we report a rare case of isolated mass mimicking a submucosal lesion of the ascending colon diagnosed in an older female patient by colonoscopy. The patient was almost asymptomatic; she reported only a history of hematochezia without anemia. This mass was successfully treated by surgery and followed by hematological investigations, including bone marrow biopsy, specific laboratory tests, and CT/PET scan, which confirmed primary isolated plasmacytoma of the colon.

KEYWORDS

plasmacytoma, gastrointestinal tumors, submucosal lesion, colonoscopy, digestive endoscopy

1 Introduction

Solitary primary extraosseous plasmacytoma is a rare disease in the gastrointestinal (GI) tract, recently classified as an "exceptional" tumor of the colon site (1, 2). The rare cases described in the literature are often diagnosed after surgery for perforation and with predominant localization of the left colon (2, 3). The main endoscopic presentation mimics colon carcinoma with ulcerated mass and obstructing lumen (4–6). In this paper, we describe a rare case of isolated submucosal mass of the ascending colon that resulted in solitary plasmacytoma in an older patient and which was successfully treated by surgery.

2 Case description

An 82-year-old Caucasian woman with a history of hematochezia by 1 month was admitted to our unit for a colonoscopy to be performed. She was asymptomatic, and the general physical examination was normal: her abdomen was soft, with no palpable masses, and not painful. The patient did not report weight loss. In her history, there was hypertension and dyslipidemia, a history of gastric ulcer, previous appendectomy, tonsillectomy, and knee prosthesis placement. She had no family history of colorectal cancer. We performed a full colonoscopy up to the cecum. In the ascending colon, near the ileocecal valve, we observed a nodular mass of about 4 cm mimicking a submucosal lesion covered by normal mucosa with two superficially ulcerated areas (Figures 1A, B). A colic gastrointestinal stromal tumor (GIST) was suspected, and multiple biopsies were performed mainly in the ulcerated parts. Histological examination showed a colonic mucosa infiltrated by cells with morphology and immunophenotype of the plasma cell (CD79a+, MUM1+, CD 138+, CD 20-, Bcl1-) with monotypic chain expression (IgA-k). Deposit of amyloid substance in the submucosa is observed.

At subsequent investigations, the abdominal computed tomography (CT) scan showed the known parietal tumor in the ascending colon without lymphadenomegaly or other pertinent abdominal alterations (Figures 2A, B).

The laboratory tests confirmed a good general condition without clear alterations of inflammatory biomarkers or anemia; the tumor markers and hepatic and renal function were normal. A right hemicolectomy was performed without adverse events (Figures 3A, B). The histopathological examination and immunohistochemistry study confirmed the previous result about plasma cell neoplasm (Figure 4). In particular, macroscopically, a 4.5-cm parietal nodule covered with ulcerated mucosa was identified in the ascendent colon. Microscopically, a neoplasm infiltrates the colon wall and perivisceral adipose tissue; the neoplasm is formed by cells with morphology and immunophenotype of a mature plasma cell (CD79a+, CD138+, MUM1+, CD20-, and Bcl1-) with monotypic expression of K light chains and IgA heavy chains. Deposit of amyloid substance is observed. The pericolic lymph nodes are reactive, without localization of the neoplasm (the details of the complete report are shown in the Supplementary Materials). The postoperative course was without complications, and the patient had good general condition at hospital discharge.

After surgery, hematologists performed a PET-CT scan to differentially diagnose solitary plasmacytoma vs. multiple myeloma, but it was negative for other systemic localizations of the disease and documented a complete remission of the unique GI localization. Laboratory serum urinary evaluation was negative, with serum monoclonal component not detected and negative serum immunofixation, urinary monoclonal component non-detected and negative urine immunofixation, and normal free light chain values with a normal ratio. A complete summary of the laboratory tests performed is shown in Supplementary Table S1. Bone marrow biopsy defined 40% cellularity without monoclonal plasma cells nor amyloid deposits (details of the complete report are shown in Supplementary Materials).

The last follow-up hematological visit was 21 months after surgery. Serum–urinary laboratory findings confirmed a hematological complete remission. The clinical conditions were

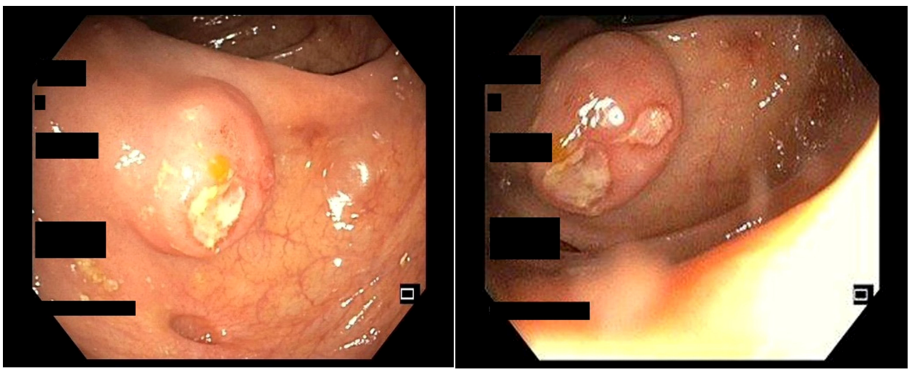

FIGURE 1
Colonoscopic view of a submucosal lesion in the ascending colon with two superficially ulcerated areas.

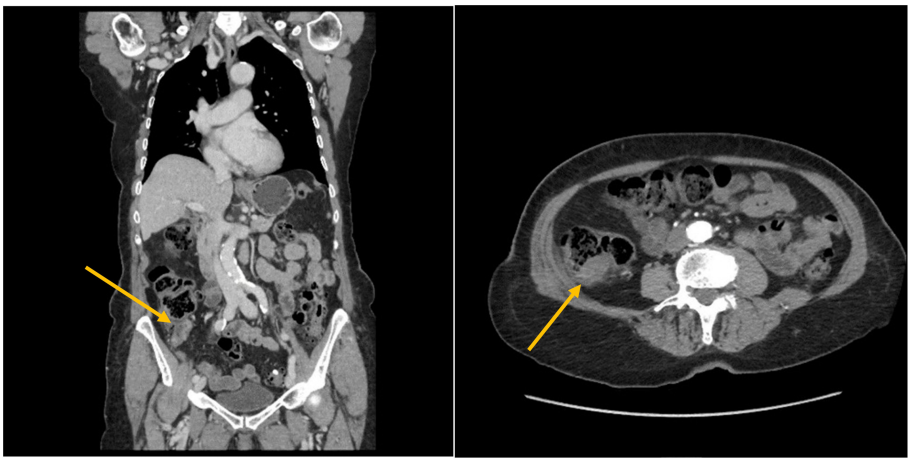

FIGURE 2
Abdominal CT scan view of a parietal tumor in the ascending colon without lymphadenomegaly or other pertinent abdominal alterations.

good, without new hemorrhagic manifestations nor abdominal pain, defining an organ complete remission.

3 Discussion

Plasma cell neoplasms are a group of mature B-cell disorders. Like other hematological cancers, they are currently classified according to two different classifications, the 5th edition WHO and International Consensus Classification (ICC). According to the WHO classification, plasmacytoma is classified within the plasma cell neoplasms, together with plasma cell myeloma and plasma cell neoplasms with the associated paraneoplastic syndrome (7). According to ICC, plasma cell neoplasms are classified in non-IgM monoclonal gammopathy of undetermined significance (MGUS), multiple myeloma (plasma cell myeloma), solitary plasmacytoma of bone and extraosseous plasmacytoma, and the latter diagnoses in our case (8). Plasmacytoma, or its synonym extraosseous plasmacytoma in ICC classification, is a rare disease and accounts for <5% of plasma cell neoplasms. It is most often located in the head and neck region, mainly in the nasopharynx or upper respiratory tract in about 80% of cases; <10% occur in the GI tract (9). A recent review of literature on rare malignant tumors of the colon and rectum classified the plasmacytoma in the group of "exceptional" tumors of the colon and rectum (<1% of colorectal cancers) (2). The real incidence (one case/population/year) is unknown but reasonably less than 1/10,000,000 with very few descriptions in literature (2, 10). There are no markers able to differentiate plasma cells according to their

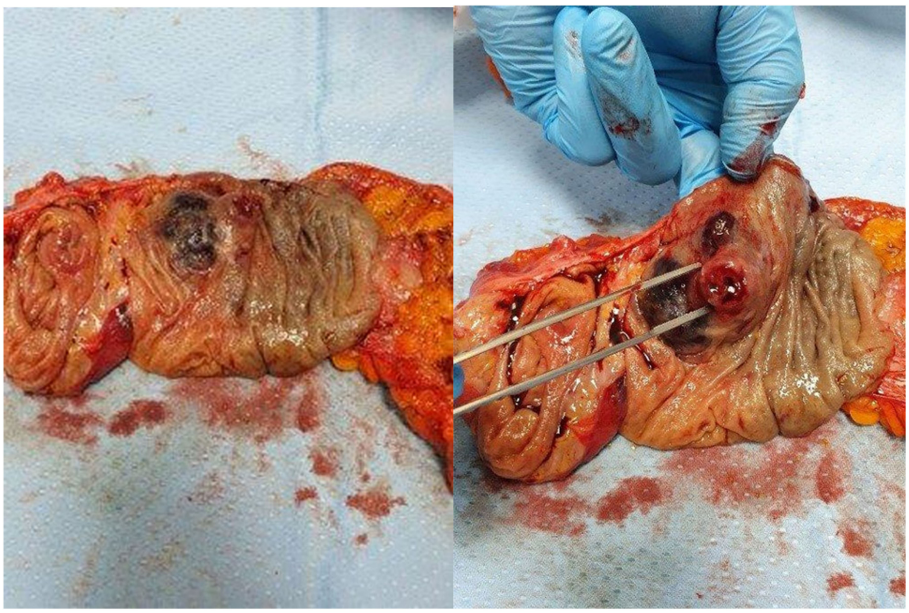

FIGURE 3
View of right hemicolectomy.

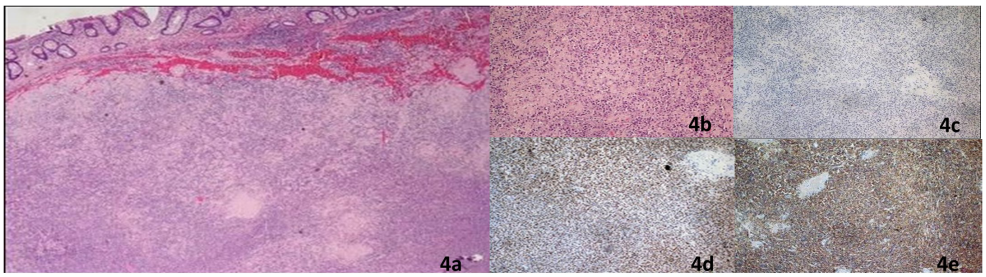

FIGURE 4
Histopathology of the surgical specimen: diffusely parietal infiltration by plasma cells with amyloid deposits **(A, B)** at immunohistochemistry, the plasma cells were CD20 negatives **(C)** and MUM1 positives **(D)** with a monotypic expression of IgA chains **(E)**.

origin. Therefore, plasmacytoma of the GI tract should be distinguished from systemic myeloma involving the GI tract through serological and imaging examinations associated with bone marrow biopsy. Recently, a rare case of plasma cell myeloma with ileal involvement with symptoms of GI obstruction and the presence of monoclonal IgA-k component has been described, as in our case (11). In our patient, PET-CT scan, laboratory tests, and bone marrow biopsy tested negative. Colon biopsies often reveal undifferentiated cells. Typical histological examination shows kappa light chain+, CD38+, CD3-, CD 20-, and CD 43- plasmacytoid cells (12). Kitamura et al. reported well-documented cases of plasmacytoma of the colon (in 2018) with a description of 30 from 1,928 cases, stratified on location, age, and clinical feature (3). Clinical presentation was variable and often reported with abdominal pain, intestinal bleeding, and diarrhea. Some cases were diagnosed by surgery after perforation (rectum and cecum) (3, 13). A case with multiple colonic strictures was also reported (12). Similar to our case, Kitamura et al. reported only two other cases of isolated mass in the ascending colon [Wing et al., 1975 (14); Doki et al., 2008 (15)] and in those cases diagnosed for pain and treated with hemicolectomy; in general, only five of well-documented cases of plasmacytoma were involved in over 80 patients (3). Overall, the localization of the left colon is described in the literature as predominant (2, 3). On endoscopic presentation, colonoscopy has not been described in these cases; it was not often completely performed for strictures. The mass presentation mainly mimicked colon carcinoma with ulcerated mass and obstructing lumen (2, 4–6). It may also mimic inflammatory bowel disease, and plasmacytoma may also coexist with Crohn's disease (4, 12). In our case, the mass mimics a sub-mucosal lesion covered by normal mucosa with two superficially ulcerated areas. Presentation as a submucosal mass is even rarer (16, 17). Kodani et al. described a minute submucosal tumor (<10 mm) at the sigmoid colon that was successfully removed using endoscopic mucosal resection (16). Similarly, in another very recent case report, a polypoid submucosal lesion was found to be an isolated plasmacytoma in a 57-year-old asymptomatic man during screening colonoscopy (18). Previous cases of isolated colonic plasmacytoma and their main characteristics are summarized in Supplementary Table S2. The clinical and radiologic presentations are not specific. Because primary isolated plasmacytoma in the colon is very rare, the clinical course, treatment guidelines, and prognosis remain unclear. The available evidence supports a good prognosis with a 5-year survival of about 90% in localized disease and no lymph node involvement (19). Endoscopic treatments such as submucosal resection or polypectomy have proven to be sufficient in selected cases (16, 20). In our case, with localized disease and no lymph node involvement, surgical treatment appears curative.

4 Conclusion

Primary colonic plasmacytoma is a rare clinical entity. We described a rare case of plasmacytoma of the ascending colon mimicking the submucosal lesion. In our case, the prognosis was good and surgical treatment appears curative. Although these cases are rare, gastroenterologists, radiologists, hematologists, and pathologists should be aware of this entity.

Data availability statement

The raw data supporting the conclusions of this article will be made available by the authors, without undue reservation.

Ethics statement

The studies were conducted in accordance with the local legislation and institutional requirements. The participants provided their written informed consent to participate in this study. Written informed consent was obtained from the individual(s) for the publication of any potentially identifiable images or data included in this article.

Author contributions

AC: Writing – original draft, Writing – review & editing. FS: Writing – original draft, Writing – review & editing. SM: Writing – review & editing. RG: Writing – review & editing. CS: Writing – review & editing. AM: Writing – review & editing. AF: Writing – review & editing. GG: Writing – review & editing. GB: Writing – review & editing. GF: Writing – review & editing.

Funding

The author(s) declare financial support was received for the research, authorship, and/or publication of this article. This work was partly supported by the Italian Health Ministry (Ricerca Corrente to IRCCS INRCA).

Conflict of interest

The authors declare that the research was conducted in the absence of any commercial or financial relationships that could be construed as a potential conflict of interest.

The author(s) declared that they were an editorial board member of Frontiers, at the time of submission. This had no impact on the peer review process and the final decision.

Publisher's note

All claims expressed in this article are solely those of the authors and do not necessarily represent those of their affiliated organizations, or those of the publisher, the editors and the reviewers. Any product that may be evaluated in this article, or claim that may be made by its manufacturer, is not guaranteed or endorsed by the publisher.

Supplementary material

The Supplementary Material for this article can be found online at: https://www.frontiersin.org/articles/10.3389/fonc.2024.1430745/full#supplementary-material

References

1. Caers J, Paiva B, Zamagni E, Leleu X, Bladé J, Kristinsson SY, et al. Diagnosis, treatment, and response assessment in solitary plasmacytoma: updated recommendations from a European Expert Panel. *J Hematol Oncol*. (2018) 11:10. doi: 10.1186/s13045-017-0549-1

2. Ottaiano A, Santorsola M, Perri F, Pace U, Marra B, Correra M, et al. Clinical and molecular characteristics of rare Malignant tumors of colon and rectum. *Biol (Basel)*. (2022) 11(2):267. doi: 10.3390/biology11020267

3. Kitamura F, Doi K, Ishiodori H, Ohchi T, Baba H. Primary extramedullary plasmacytoma of the sigmoid colon with perforation: a case report. *Surg Case Rep*. (2018) 4:28. doi: 10.1186/s40792-018-0437-0

4. Ligato S, El-Naggar A, Cleary KR, Manning J. Extramedullary plasmacytoma mimicking primary colonic carcinoma in a patient with Crohn's disease. *Case Rep literature review. Arch Pathol Lab Med*. (1996) 120:279–82.

5. Zhu Z, Cao H, Chen L. Incomplete colonic obstruction caused by extramedullary plasmacytoma. *Clin Gastroenterol Hepatol Off Clin Pract J Am Gastroenterol Assoc*. (2017) 15:e69–70. doi: 10.1016/j.cgh.2016.08.043

6. Zhang D, Cao D, Shen D, Mulmi Shrestha S, Yin Y. Extramedullary plasmacytoma occuring in ileocecum: A case report and literature review. *Med (Baltimore)*. (2017) 96:e9313. doi: 10.1097/MD.0000000000009313

7. Alaggio R, Amador C, Anagnostopoulos I, Attygalle AD, Araujo IB de O, Berti E, et al. The 5th edition of the world health organization classification of haematolymphoid tumours: Lymphoid neoplasms. *Leukemia*. (2022) 36:1720–48. doi: 10.1038/s41375-022-01620-2

8. Campo E, Jaffe ES, Cook JR, Quintanilla-Martinez L, Swerdlow SH, Anderson KC, et al. The international consensus classification of mature lymphoid neoplasms: a report from the clinical advisory committee. *Blood*. (2022) 140:1229–53. doi: 10.1182/blood.2022015851

9. Alexiou C, Kau RJ, Dietzfelbinger H, Kremer M, Spiess JC, Schratzenstaller B, et al. Extramedullary plasmacytoma: tumor occurrence and therapeutic concepts. *Cancer*. (1999) 85:2305–14. doi: 10.1002/(ISSN)1097-0142

10. Parnell K, Ahmed M, Smalligan RD, Nadesan S. Extramedullary plasmacytoma mimicking colon carcinoma: an unusual presentation and review of the literature. *BMJ Case Rep*. (2015) 2015:bcr2015210973. doi: 10.1136/bcr-2015-210973

11. Bonometti A, Aronico N, Santacroce G, Fraticelli S, Lucioni M, Cartia CS, et al. Case Report: A rare case of small bowel obstruction secondary to plasma cell myeloma. *Front Oncol*. (2022) 12:934566. doi: 10.3389/fonc.2022.934566

12. Lee S-H, Ahn B-K, Baek S-U, Chang H-K. Primary isolated extramedullary plasmacytoma in the colon. *Gastroenterol Res*. (2013) 6:152–5. doi: 10.4021/gr552w

13. Gabriel EM, Savu M. Discovery of a rare ileocecal plasmacytoma. *J Surg Case Rep*. (2014) 2014(3):rju016. doi: 10.1093/jscr/rju016

14. Wing EJ, Perchick J, Hubbard J. Solitary obstructing plasmacytoma of the colon. *JAMA*. (1975) 233:1298–9. doi: 10.1001/jama.1975.03260120060025

15. Doki T, Takeuchi O, Kaiho T, Tsuchiya S, Matsuzaki O, Miyazaki M. Primary isolated extramedullary plasmacytoma of the colon. *Int J Colorectal Dis*. (2008) 23:719–20. doi: 10.1007/s00384-008-0439-7

16. Kodani T, Osada T, Terai T, Ohkusa T, Shibuya T, Sakamoto N, et al. Successful endoscopic mucosal resection of a solitary extramedullary plasmacytoma in the sigmoid colon. *Endoscopy*. (2011) 43 Suppl 2:E298–9. doi: 10.1055/s-0030-1256451

17. Bhangoo RS, McCullough AE, Yang M. Obstructive rectosigmoid colon solitary extramedullary plasmacytoma. *Dig liver Dis Off J Ital Soc Gastroenterol Ital Assoc Study Liver*. (2021) 53:496–7. doi: 10.1016/j.dld.2020.12.008

18. Nassif C, Crabtree M, Pullarkat ST. Isolated asymptomatic colonic plasmacytoma presenting as a polyp at screening colonoscopy. *ACG Case Rep J*. (2023) 10:e01069. doi: 10.14309/crj.0000000000001069

19. Han YJ, Park SJ, Park MI, Moon W, Kim SE, Ku KH, et al. Solitary extramedullary plasmacytoma in the gastrointestinal tract: report of two cases and review of literature. *Korean J Gastroenterol*. (2014) 63:316–20. doi: 10.4166/kjg.2014.63.5.316

20. Nakagawa Y, Nagai T, Okawara H, Nakashima H, Hisamatsu A, Syutou M, et al. Minute primary extramedullary plasmacytomas of the large intestine. *Endoscopy*. (2011) 43(Suppl 2):E105–6. doi: 10.1055/s-0030-1256138

frontiers | Frontiers in Oncology

TYPE Case Report
PUBLISHED 06 September 2024
DOI 10.3389/fonc.2024.1437728

Check for updates

OPEN ACCESS

EDITED BY
Robert Fruscio,
University of Milano Bicocca, Italy

REVIEWED BY
Giuseppe Scibilia,
Ospedale Cannizzaro, Italy
Stergios Boussios,
Canterbury Christ Church University,
United Kingdom

*CORRESPONDENCE
Yankui Wang
qdwangyk@163.com

RECEIVED 24 May 2024
ACCEPTED 08 August 2024
PUBLISHED 06 September 2024

CITATION
Wang Q, Zuo J, Liu C, Zhou H, Wang W and Wang Y (2024) Giant ovarian yolk sac tumor during late pregnancy: a case report and literature review.
Front. Oncol. 14:1437728.
doi: 10.3389/fonc.2024.1437728

COPYRIGHT
© 2024 Wang, Zuo, Liu, Zhou, Wang and Wang. This is an open-access article distributed under the terms of the Creative Commons Attribution License (CC BY). The use, distribution or reproduction in other forums is permitted, provided the original author(s) and the copyright owner(s) are credited and that the original publication in this journal is cited, in accordance with accepted academic practice. No use, distribution or reproduction is permitted which does not comply with these terms.

Giant ovarian yolk sac tumor during late pregnancy: a case report and literature review

Qin Wang[1], Jianxin Zuo[1], Chong Liu[2], Huansheng Zhou[2], Wenjie Wang[3] and Yankui Wang[3]*

[1]Medical College, Qingdao University, Qingdao, China, [2]Department of Obstetrical, The Affiliated Hospital of Qingdao University, Qingdao, China, [3]Department of Gynecology, The Affiliated Hospital of Qingdao University, Qingdao, China

The manifestation of a giant ovarian yolk sac tumor during late pregnancy is relatively rare. A yolk sac tumor is a highly malignant germ cell tumor that originates from primitive germ cells. It is characterized by yolk sac differentiation *in vitro*. The frequency of prenatal examinations should be appropriately increased for ovarian tumors discovered during pregnancy. Furthermore, regular follow-up ultrasound should be performed, and tumor markers should be dynamically detected. If needed, imaging examinations such as computed tomography and magnetic resonance imaging should be combined to comprehensively investigate disease progression. If the tumor diameter and tumor marker levels rapidly increase during pregnancy, the possibility of malignancy increases. Therefore, exploratory laparotomy should be immediately performed to further improve subsequent treatment modalities, early diagnosis, early treatment, and prognosis. Herein, we report the case of a 28-year-old pregnant woman whose pregnancy was terminated at 29 weeks and 5 days. She complained of lower abdominal pain for 2 days. A pelvic mass was detected for 1 week, accompanied by increased levels of tumor markers such as serum alpha-fetoprotein, cancer antigen 125, carbohydrate antigen 724, and human epididymis protein 4. Imaging revealed the presence of a pelvic mass. At 32 weeks and 3 days of pregnancy, a cesarean section was performed, with a transverse incision in the lower uterine segment. Furthermore, pelvic adhesiolysis, omentectomy, right adnexectomy, right pelvic lymph node dissection, and pelvic metastasis peritonectomy were performed. The postoperative pathological diagnosis was yolk sac tumors of the ovary (stage IIB). Postoperatively, a five-cycle chemotherapy regimen comprising bleomycin, etoposide, and cisplatin was administered. During postoperative follow-up, the patient's general condition was noted to be good, with the newborn and pregnant women ultimately achieving good outcomes. We reviewed the relevant literature to increase clinical doctors' understanding of ovarian malignancy during pregnancy, guide treatment selection, and facilitate early intervention for associated diseases.

KEYWORDS

late pregnancy, pregnancy with giant ovarian tumors, ovarian cancer, yolk sac tumor, malignancy during pregnancy

1 Case description

The patient Yi was a 28-year-old woman with a regular menstrual cycle. Her last menstrual period was May 2, 2023. After 28 weeks and 5 days of gestation, an ultrasound at an external hospital revealed the presence of a cystic solid mass in the right posterior pelvic cavity of the uterus. The mass was approximately 14.7 × 10 × 8.6 cm in size. The solid ultrasound characteristics were primarily observed, with relatively uniform low echo and blood flow signals visible inside. The cystic part exhibited multiple liquid dark areas of varying sizes. The largest size range of these areas was approximately 5 × 1.9 cm, with good internal translucency. The liquid dark areas were observed in the abdominal cavity, peri liver, and right abdomen. The deepest depth of the liquid was approximately 4.4 cm in the right abdomen, with good internal translucency. Preoperatively, the blood cancer antigen 125 (CA125) level was 260.9 U/mL. Untreated. Two days before admission, the patient experienced lower abdominal pain. She was admitted to our hospital on November 26, 2023. Ultrasound revealed the presence of a cystic solid mass sized 18.8 × 10.8 × 9.2 cm in the right posterior part of the uterus. The mass had a regular shape and clear boundaries. The edge of the mass exhibited rich blood flow signals (Figures 1, 2). Pelvic magnetic resonance imaging (MRI) revealed the presence of a cystic solid mass in the right posterior part of the uterus, presenting as an equal-length T1 mixed with long and short T2 signal shadows. Diffusion-weighted imaging (DWI) revealed mixed signals, with a size of approximately 95 mm × 148 mm, and a close association with the uterus and adnexa. The tumor markers levels were as follows: CA125: 471.9 U/mL, human epididymis protein 4: 62.6 pmol/L, and alpha-fetoprotein (AFP): 41790 ng/mL. The blood routine findings were as follows: white blood cell (WBC): 16.11 × 10^9/L and hemoglobin (Hb): 123 g/L. Blood biochemistry findings were as follows: albumin: 37.8 g/L. At admission, the patient (G1P0) was initially diagnosed with threatened preterm labor, pregnancy complicated with a pelvic tumor, and pregnancy diabetes. Magnesium sulfate was administered to nourish the fetal brain nerves, and dexamethasone was administered to promote fetal lung maturation. Subsequent blood routine examination revealed the following: WBC: 17.43 × 10^9/L, Hb: 96 g/L, CRP: 50.27 mg/L, PCT: 0.223ng/mL, and albumin: 25.9 g/L. The patient received symptomatic treatment such as "piperacillin sodium tazobactam" anti-infection and albumin infusion.

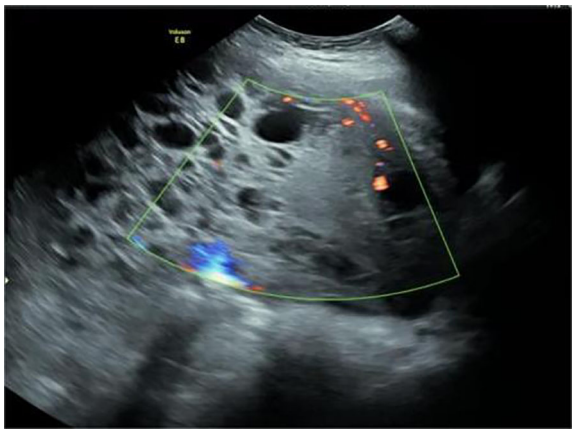

FIGURE 2
Uneven thickness separation and solid mass were observed in the cystic solid mass. Point stripe blood flow signals were observed in the separated and solid components.

At 32 weeks of gestation, a follow-up ultrasound revealed a significant increase in tumor size compared with the previous observation, with an increase in AFP levels. After multidisciplinary consultation, we decided to terminate the pregnancy and administered meropenem as an anti-infective treatment. On December 15, 2023, a transverse incision cesarean section was performed in the lower segment of the uterus. A male infant was delivered, with an Apgar score of 8 points at 1 min and a weight of 1960 g. The infant was transferred to the neonatology department. During the operation, we observed the enlargement of the right ovary, with a size of approximately 25 × 15 × 15 cm. The ovary was extremely fragile

FIGURE 1
A solid cystic mass was detected in the right posterior lower part of the uterus. It was 18.43 × 8.47 × 10.53 cm in size. More compartments were observed in the cystic components, showing a "grid" shape.

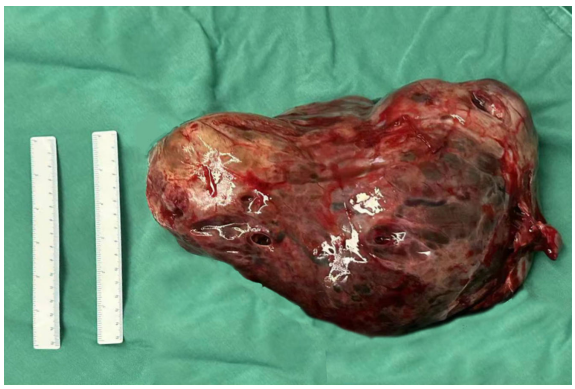

FIGURE 3
The tumor was completely excised. It was approximately 25 × 15 × 15 cm in size.

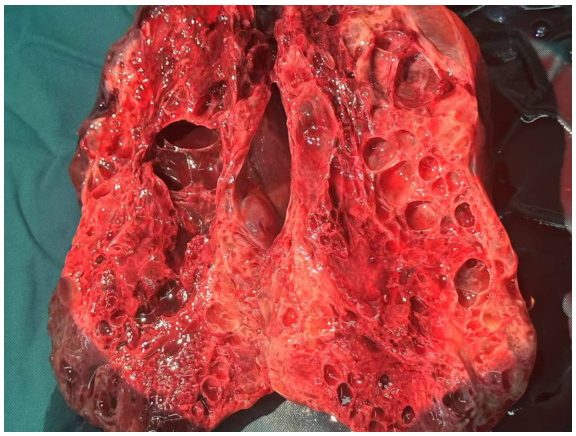

FIGURE 4
Internal view of the dissected tumor.

but without an evident capsule. Figures 3, 4 illustrate the gross specimen. No remarkable anomalies were observed in the appearance of the right fallopian tube, and the right adnexa adhered to the lower segment of the posterior uterine wall, bilateral posterior lobes of the broad ligament, anterior rectum, and uterine rectal depression peritoneum. The right posterior lobe of the broad ligament peritoneum was noted to be thickened. After blunt separation and adhesion, extensive bleeding was observed on the wound. The appearance of the left attachment was not abnormal; however, and no evident metastatic nodules were observed in the omentum, liver, spleen, diaphragm, and abdominal intestinal tract. The lymph nodes adjacent to the abdominal aorta and pelvic cavity were not palpable and enlarged. Right adnexectomy was performed, and frozen section analysis during the operation resulted in the diagnosis of a yolk sac tumor. The patient's family was communicated, and they requested staged surgery to preserve fertility. Accordingly, we decided to perform omentectomy, right pelvic lymph node dissection, and pelvic metastasis peritonectomy. Postoperative paraffin pathology revealed the following: (right) a malignant ovarian tumor with extensive bleeding and necrosis, combined with morphological and immunohistochemical analysis results, consistent with a yolk sac tumor (size 17.5 × 16 × 7 cm). However, no tumor was observed in the tubal tissue. Immunohistochemical analysis revealed the following: SALL4 (+), OCT4 (weak+), AFP (+), GPC3 (+), CD30 (−), Pax-8 (−), NapsinA (−), ER (−), PR (−), WT-1 (−), p53 (+, approximately 20%), Vimentin (−), CKpan (+), EMA (-), Ki-67 (+, approximately 60%). Ascites smear and examination revealed the absence of malignant tumor cells in the lymph nodes.

The patient was discharged from the hospital on day 9 postoperatively. On the day of discharge, AFP levels were 3650 ng/mL. On day 19 postoperatively, a chemotherapy regimen comprising bleomycin + etoposide + cisplatin (BEP) was administered. After the patient completed five chemotherapy cycles, her condition was generally good, with a significant decrease in tumor markers and reaching the normal range. The tumor marker levels on April 2, 2024 were as follows: AFP: 6.48 ng/mL and CA125: 9.5 U/mL. Tables 1, 2 present the fluctuation curves of the tumor markers.

2 Discussion

2.1 Clinical manifestations and pathological features

Ovarian yolk sac tumor (OYST), also called ovarian endoembryonic sinus tumor, is a type of ovarian germ cell malignant tumor (MOGCT) derived from primordium germ cells. MOGCT currently lacks specific clinical predictors. Classic serum tumor markers include AFP, β-HCG, anti-Miller tube hormone (AMH), CA125, and CA199, but most of which are interfered by pregnancy status. The clinical prognosis of ovarian germ cell malignancy (MOGCT) is poor, and the adverse factors include age >45 years, pathological stage > I, incomplete surgical resection and yolk sac tumor (YST) histology (1). This tumor type is characterized by yolk sac differentiation *in vitro* and accounts for approximately 5% of ovarian malignancies. OYST may occur in children and women of childbearing age, with a poor prognosis (2, 3). The tumor tissue is mostly an oval nodular or a lobulated mass, with an envelope, soft substances, cystic solids, and grayish-yellow to colorful sections and accompanied by bleeding and necrosis.

The pathological manifestation is the differentiation of various endoderms and their derivatives. The reticular/microcapsule type is the most common pathological manifestation observed under a microscope. The endoderm sinus type (Schiller–Duval corpuscles) and glandular type (endometrioid type) are some other pathological morphologies (4). Tumor-specific Schiller–Duval bodies with diagnostic significance are observed in the papillary region, which is characterized by papillary structure formation by tumor cells around the axis of the fiber vessels in the cystic cavity (5, 6) (Figures 5, 6). AFP is 100% expressed in pure OYST. Furthermore, it can be expressed in mixed tumors with yolk sac tumor components (2, 7). Glypican-3, which sensitivity is 3 times higher than AFP for OYST, but less specific. And other immunohistochemical markers that are also typically positive in OYST include SALL4、Lin28、CDX2、NANOG、PLAP、CD30、HepPar1、CD117、OCT3/4 and so on. Furthermore, SALL4 is useful in distinguishing OYST from ovarian clear cell adenocarcinoma (2, 8). In the present case, characteristic Schiller–Duval bodies were observed during pathological examination, as indicated by an arrow in Figure 6.

TABLE 1 Fluctuation curves of AFP.

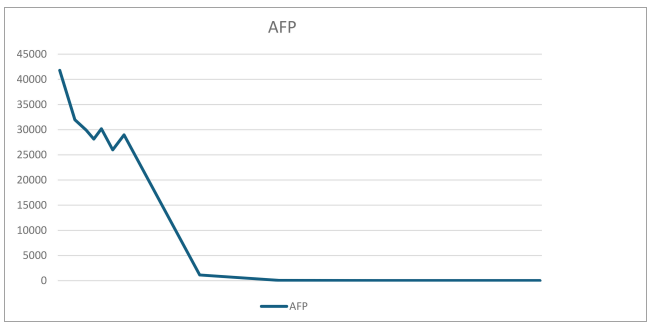

TABLE 2 Fluctuation curves of CA125.

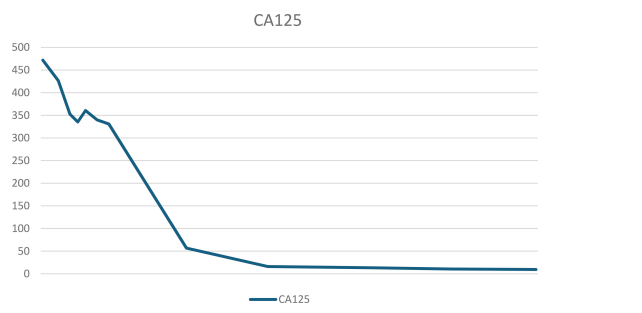

Most patients with OYST present with chronic pelvic and abdominal pain as the primary initial symptom. MOGCT rapidly grows, and most patients have corresponding clinical symptoms in the early disease stage. Approximately 70% of patients with MGOCT present with abdominal pain and abdominal mass as the primary symptoms, followed by abdominal distension (15%), fever (10%), and abnormal vaginal bleeding (5%–10%), with some patients exhibiting irregular menstruation (4). Acute abdominal manifestations such as intracystic hemorrhage, torsion, and rupture are observed in 10% of patients with OYST. Furthermore, approximately 10% of patients with OYST present with an asymptomatic pelvic mass, with irregular vaginal bleeding and infertility also being important symptoms (4). However, owing to the particularity of pregnancy, lower abdominal pain is the primary clinical symptom of pregnancy complicated with OYST, and some symptoms are masked by the pregnancy status, making pregnancy complicated with OYST diagnosis more challenging. In the present case, abdominal pain was the initial symptom, and the pelvic mass diameter rapidly increased without evident directional characteristics.

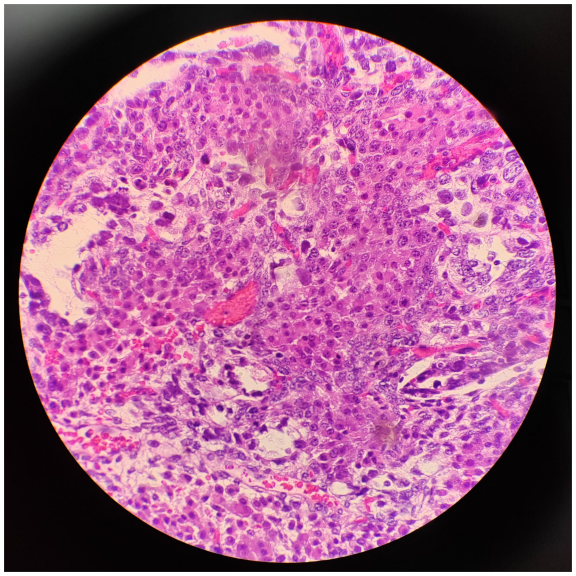

FIGURE 5
Hematoxylin and eosin staining of the yolk sac tumor. Solid areas present within the tumor in this patient, ×40.

2.2 Auxiliary examination

No specific tumor markers are available for OYST during pregnancy and pregnancy interferes with most relevant tumor markers. Fetal antigens such as AFP, beta-human chorionic gonadotropin (β-HCG), and CA125 are detected during pregnancy. Furthermore, the levels of various tumor markers physiologically increase during pregnancy and fluctuate with changes in gestational age. Therefore, the diagnostic value of commonly used tumor markers is limited during pregnancy. Some researchers have proposed that continuous monitoring during pregnancy may facilitate differential diagnosis (9). The AFP levels in our patient were significantly higher than the acceptable range during pregnancy, with the highest level of 41790 ng/mL. Furthermore, during dynamic monitoring, the tumor markers were maintained at high levels in our patient.

Ultrasound examination is a common method for evaluating OYST during pregnancy. The internal echoes of OYST exhibit various manifestations, including solid, cystic, or mixed cystic and solid, particularly the last one. When the tumor is extremely large, cystic changes with varying degrees of hemorrhage and necrosis may occur, with the potential differentiation of other tissue components in the lesion. In general, the solid part of OYST exhibits rich blood flow signals, with medium and low blood flow resistance (10). However, with an increase in the gestational age, the uterus gradually enlarges, with ultrasound evaluation gradually becoming difficult. MRI can be more helpful for determining tumor nature, identifying the degree of the malignant tendency of the tumor, and evaluating the relationship between the tumor and surrounding tissues to help and make treatment decisions. MRI plain scan revealed that the lesions were primarily isointense and low signal on T1WI but isointense and high mixed signal on T2WI. The cystic necrosis area exhibited longer T1 and T2 signals. Furthermore, contrast-enhanced MRI revealed uneven mass enhancement, tortuous blood vessels, no enhancement in the cystic necrosis area, and an expanded enhancement range in the delayed phase, with gradual enhancement (11, 12). However, some studies have revealed that the MRI contrast agent can penetrate the placenta and be excreted by the fetal kidneys into the amniotic fluid, which can easily affect the imaging interpretation (13). Moreover, animal experiments have verified that contrast media can increase the incidence of skeletal malformations in offspring; therefore, caution should be exercised when performing enhanced MRI during pregnancy (9). In this case, B-ultrasound revealed the presence of a predominantly solid cystic mass with a clear boundary, uneven septa, and solid mass within. Furthermore, dotted and strip-like blood flow signals were observed in the septa and solid parts. Lastly, pelvic MRI revealed equal-length T1 mixed long and short T2 signal shadows, and DWI revealed mixed signals, which were closely associated with the uterus and adnexa.

2.3 Treatment and prognosis

In general, the incidence of pregnancy complicated with ovarian tumors is low, and pregnancy complicated with ovarian malignant tumors is even more rare. 90% of ovarian cancers are of an epithelial

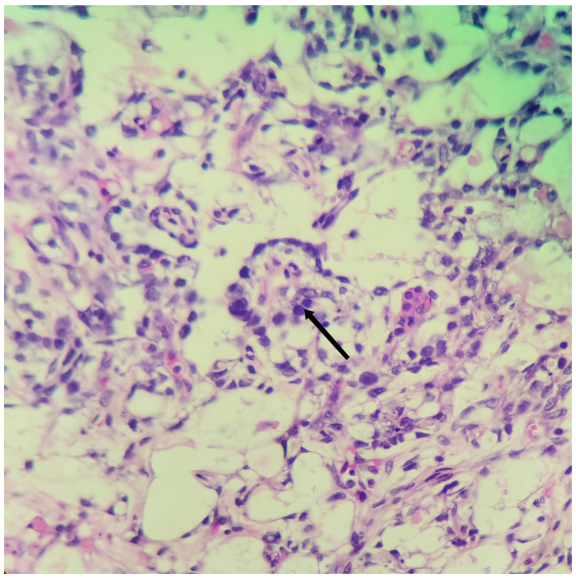

FIGURE 6
Hematoxylin and eosin staining of the yolk sac tumor. Black arrows indicate the Schiller–Duval) corpuscles in this tumor, ×200.

cell type and comprise multiple histologic types, with various specific molecular changes, clinical behaviors, and treatment outcomes. The remaining 10% are non-epithelial ovarian cancers, which include mainly germ cell tumors, sex cord-stromal tumors, and some extremely rare tumors such as small cell carcinomas. Germ cell tumors are the most common ovarian neoplasms in women until 30 years of age and most of the patients are diagnosed with early-stage disease (60–70%) (14). Some researchers have reported that pregnant women have abundant blood supply in the pelvis; increased blood estrogen, progesterone, and β-HCG levels; and an altered immune system in the body. This promotes the proliferation of malignant tumor cells, which may infiltrate and metastasize, affecting the prognosis (15).

Owing to the particularity of pregnancy, comprehensively considering many factors during the clinical treatment of such diseases is essential. The pathological type, stage, fertility requirements, and expectations of this pregnancy as well as fetal factors should be considered to achieve a win–win situation. For patients with high suspicion of malignancy during early pregnancy, standard ovarian cancer treatment should be recommended after pregnancy termination (16). During early pregnancy, the ovarian corpus luteum plays a role in completing hormone secretion and maintaining the pregnancy. If surgery is performed in the early pregnancy stage, the risk of abortion will be significantly increased owing to damage to ovarian function. Patients with strong fertility requirements can be closely monitored until the second trimester of pregnancy for surgery (16). For those in the third trimester, pregnancy can be actively terminated and standardized surgery can be performed after completing fetal lung maturation promotion. Surgery is the primary treatment modality for OYST. Previously, the surgical principles of OYST referred to the surgical principles of ovarian epithelial tumors (2), and radical surgery was performed, i.e., laparotomy with total abdominal hysterectomy, bilateral salpingo-oophorectomy, pelvic lymphadenectomy, para-aortic lymphadenectomy, and ascites exfoliative cell examination. Because most patients with OYST have fertility requirements, the surgical modality that preserves reproductive function has become the basic treatment principle (17). Regardless of the tumor stage, the uterus and at least one ovary or a part of the ovarian tissue can be preserved (2, 17). Therefore, the surgical principle of OYST during pregnancy is similar to that during non-pregnancy. Tewari et al. (18) reported six cases of OYST during pregnancy, of which five cases underwent unilateral salpingo-oophorectomy during 10–26 weeks of pregnancy, whereas 1 of them received three cycles of the BEP chemotherapy regimen owing to metastatic dysgerminoma. All patients delivered their infants after 35 weeks, with no evident anomalies in the five newborns. The sixth patient, who was diagnosed with mixed germ cell tumor stage IIIC, opted for pregnancy termination at 18 weeks of gestation and immediately started adjuvant systemic chemotherapy. After 14 weeks of pregnancy, the placenta can secrete enough hormones to maintain pregnancy and decrease the risk of abortion, with enough free space for surgery in the pelvic cavity. At present, most researchers recommend 16–18 weeks of pregnancy as the best operation time (16). If emergency symptoms such as severe abdominal pain are present and tumor torsion or rupture is suspected, emergency surgery should be performed regardless of the gestational age. Most OYSTs are the cystic solid type inside, with most exhibiting different degrees of cystic changes such as hemorrhage and necrosis. Furthermore, most OYSTs have a large diameter, with a median diameter of approximately 20 cm (2). In addition, the capsule is fragile, prone to rupture, and difficult to remove after resection, restricting the application value of laparoscopy in this disease. In the present case, we detected a large pelvic mass in the third trimester of pregnancy. The tumor had a large diameter and rapidly grew. After completing fetal lung maturation promotion, a cesarean section was performed in the third trimester of pregnancy to terminate the pregnancy, followed by standardized surgery so that the newborn and pregnant women could achieve maximum benefits.

The current guidelines for the diagnosis and treatment of ovarian malignant tumors recommend postoperative chemotherapy for MOGCT, except for stage I dysgerminoma and stage I G1 immature teratoma (4). Furthermore, the current guidelines for OYST recommend BEP as the first-line chemotherapy regimen for MOGCT (17). Tumor marker monitoring should be given attention during chemotherapy. Furthermore, two cycles of consolidation chemotherapy should be administered after the tumor markers are within the normal range. At present, no definite conclusion is available regarding the effect of chemotherapy drugs on pregnancy and the fetus during chemotherapy for pregnancy complicated with OYST. Furthermore, large sample research data are lacking. Jorine de Haan et al. (19) collected 1170 cases of pregnancy complicated with malignant tumors and investigated the outcomes of pregnant patients, i.e., obstetric and neonatal outcomes. They reported the low risk of fetal malformations caused by chemotherapy in the second and third trimester of pregnancy; however, infants who received prenatal chemotherapy may exhibit an increased risk of

complications compared with those who did not receive chemotherapy. For example, the incidence of low-birth-weight infant and neonatal intensive care unit admission increased. The 5–10-week gestation period is important for fetal organ differentiation, during which exposure to cytotoxic drugs increases the risk of teratogenesis (20). To prevent damage to fetal liver and kidney function and myelosuppression of the mother and newborn by chemotherapy drugs, chemotherapy should be stopped after 35 weeks of gestation and 3 weeks before delivery (9, 21). The gestational age of our patient was approximately 30 weeks when the tumor was detected, and the disease continued to progress during the observation. Considering that the gestational age had reached 32 weeks and the possibility of malignancy was high, we decided to terminate the pregnancy and performed a cesarean section to deliver a boy with a 1-min Apgar score of 8 and weight of 1960 g.

In summary, pregnancy complicated with OYST is a rare condition, and pregnancy status may obscure its specific clinical features; therefore, making a clear diagnosis is challenging. Furthermore, owing to physiological fluctuations in tumor marker levels during pregnancy, tumor markers have limited diagnostic value, warranting the dynamic and continuous monitoring of the changes in tumor markers and relying on auxiliary examinations such as ultrasound, CT, and MRI to aid diagnosis. OYST should be considered when pregnant women present with a large pelvic mass with abdominal pain, and ultrasound reveals predominantly cystic and solid echo with rich blood flow signals. If the tumor diameter continues to increase during pregnancy, clinicians should be vigilant and highly suspect malignancy. After assessing the gestational age and fetal condition, early intervention should be performed to achieve early detection, diagnosis, and treatment and improve prognosis.

Data availability statement

The datasets presented in this study can be found in online repositories. The names of the repository/repositories and accession number(s) can be found in the article/supplementary material.

Ethics statement

The studies involving humans were approved by Gynaecology Department of The Affiliated Hospital of Qingdao University, Qingdao Shandong. The studies were conducted in accordance with the local legislation and institutional requirements. The participants provided their written informed consent to participate in this study. Written informed consent was obtained from the individual(s) for the publication of any potentially identifiable images or data included in this article.

Author contributions

QW: Data curation, Investigation, Writing – original draft, Writing – review & editing. JZ: Conceptualization, Writing – review & editing. CL: Supervision, Writing – review & editing. HZ: Supervision, Writing – review & editing. WW: Supervision, Writing – review & editing. YW: Conceptualization, Writing – review & editing.

Funding

The author(s) declare that no financial support was received for the research, authorship, and/or publication of this article.

Conflict of interest

The authors declare that the research was conducted in the absence of any commercial or financial relationships that could be construed as a potential conflict of interest.

Publisher's note

All claims expressed in this article are solely those of the authors and do not necessarily represent those of their affiliated organizations, or those of the publisher, the editors and the reviewers. Any product that may be evaluated in this article, or claim that may be made by its manufacturer, is not guaranteed or endorsed by the publisher.

References

1. Saani I, Raj N, Sood R, Ansari S, Mandviwala HA, Sanchez E, et al. Clinical challenges in the management of Malignant ovarian germ cell tumours. *Int J Environ Res Public Health*. (2023) 20:3. doi: 10.3390/ijerph20126089

2. Xiangdong SHE, Guantai NI. *Progress of Research on Ovarian Yolk Sac Tumour*. Department of Obstetrics and Gynecology, The First Affiliated Hospital ofWannan Medical College, Wuhu 241000, Anhui Province, China.

3. Ramalingam P. Germ cell tumors of the ovary: A review. *Semin Diagn Pathol*. (2023) 40(1):22–36. doi: 10.1053/j.semdp.2022.07.004

4. Liang X, Ye Y, Huang J, Fan J, Zhang S, Wang Y, et al. *Chinese expert consensus on the diagnosis and treatment of ovarian germ cell tumor* (*2022* Edition).

5. Xu L, Wang W, He Y, Wang M, Huang Q, Liu J, et al. Clinicopathological analysis of 46 cases of ovarian yolk sac tumor [J]. *Journal of Sichuan University (Medical Science Edition)* (2018) 49(04):680–2. doi: 10.13464/j.scuxbyxb.2018.04.041

6. Young RH, Wong A, Stall JN. Yolk sac tumor of the ovary: A report of 150 cases and review of the literature. *Am J Surg Pathol*. (2022) 46(6):309–25. doi: 10.1097/PAS.0000000000001793

7. Utami TW, Feharsal Y, Nuranna L, Purwoto G, Siregar TP, Hellyanti T, et al. Histopathological and biomarker complete response after neoadjuvant chemotherapy of advanced stage yolk sac tumor of the ovary: A case report and literature review. *Int J Surg Case Rep*. (2023) 112:1–2. doi: 10.1016/j.ijscr.2023.108915

8. Cheung A, Shah S, Parker J, Soor P, Limbu A, Sheriff M, et al. Non-epithelial ovarian cancers: how much do we really know? *Int J Environ Res Public Health*. (2022) 19:2–3. doi: 10.3390/ijerph19031106

9. Wang Y, Sheng X, Zhang S, Lu Q. Expert Consensus on Diagnosis and treatment of ovarian tumors in pregnancy. *Chinese Journal of Applied Gynecology and Obstetrics* (2020) 36(05):432–40. doi: 10.19538/j.fk2020050113

10. Ye X, Xu R, Huang C, Yan L. Ultrasonographic features and clinical pathological characteristics in yolk sac tumors of ovary. (Department of Ultrasound, the First Affiliated Hospital of Fujian Medical University, Fuzhou 350005, China). doi: 10.13929/j.1003-3289.201701049

11. Liu H, Shi J, Wang Y, Liu J, Kim K, Li B, et al. *Ovarian Yolk Sac Tumor: CT, MRI Findings and Their Pathological Bases, et al.* Department of Medical lmaging, Afliated Hospital of Zunyi Medical College, Zunyi, Jiangxi Prvinee 563003, P.R. China. doi: 10.13437/j.cnki.jcr.2014.09.025

12. Rogers D, Menias C, Shaaban A. Malignant germ cell tumors of the ovary clinical and imaging features. *Radiol Clinics North America*. (2023) 61(4):579–94. doi: 10.1016/j.rcl.2023.02.004

13. Prola-Netto J, Woods M, Roberts VHJ, Sullivan EL, Miller CA, Frias AE, et al. Gadolinium chelate safety in pregnancy: barely detectable gadolinium levels in the juvenile nonhuman primate after in utero exposure. *Radiology*. (2018) 286:122–8. doi: 10.1148/radiol.2017162534

14. Aliyuda F, Moschetta M, Ghose A, Sofia Rallis K, Sheriff M, Sanchez E, et al. Advances in ovarian cancer treatment beyond PARP inhibitors. *Curr Cancer Drug Targets*. (2023) 23(6):433–46. doi: 10.2174/1568009623666230209121732

15. Peters I, Testa AC, Arciuolo D, Amant F, Fagotti A. Low-grade serous ovarian cancer in pregnancy. *Int J Gynecol Cancer*. (2022) 32(6):804–8. doi: 10.1136/ijgc-2022-003577

16. Hu W, Ding X, Yin X. Progress of diagnosis and treatment of ovarian cancer in pregnancy [J]. *Chinese Journal of Medicine* (2019) 55(01):14–8. (in Chinese).

17. Lu H, Ye D, Wu B, Xu M, Huo C, Lin Z, et al. Interpretation of the 2023NCCN Clinical Practice Guidelines for Ovarian Cancer including fallopian tube Cancer and Primary peritoneal Cancer (1st Edition) [J]. *Chinese Journal of Applied Gynecology and Obstetrics* (2019) 39(01):58–67. doi: 10.19538/j.fk2023010116

18. Tewari K, Cappuccini F, Disaia PJ, Berman ML, Manetta A, Kohler MF, et al. Malignant germ cell tumors of the ovary [J]. *Obstet Gynecol*. (2000) 95(1):128–33. doi: 10.1097/00006250-200001000-00024

19. De La Motte Rouge T, Pautier P, Duvillard P, Rey A, Morice P, Haie-Meder C, et al. Oncological management and obstetric and neonatal outcomes for women diagnosed with cancer during pregnancy: a 20-year international cohort study of 1170 patients. *Lancet Oncol*. (2018) 19(3):337–46. doi: 10.1016/S1470-2045(18)30059-7

20. Boussios S, Moschetta M, Tatsi K, Tsiouris AK, Pavlidis N. A review on pregnancy complicated by ovarian epithelial and non-epithelial Malignant tumors: Diagnostic and therapeutic perspectives [J]. *J Advanced Res*. (2018) 12:1–9. doi: 10.1016/j.jare.2018.02.006

21. Pokoradi AJ, Agrawal A. Yolk sac tumour of the ovary in pregnancy treated with surgery and chemotherapy: A case report. *J Obstetrics Gynaecol Canada*. (2021) 43 (10):1177–9. doi: 10.1016/j.jogc.2021.04.013

frontiers | Frontiers in Oncology

TYPE Original Research
PUBLISHED 13 September 2024
DOI 10.3389/fonc.2024.1450382

Check for updates

OPEN ACCESS

EDITED BY
Dragos Eugen Georgescu,
Carol Davila University of Medicine and Pharmacy, Romania

REVIEWED BY
Xiaobin Gu,
First Affiliated Hospital of Zhengzhou University, China
Kai Kang,
Capital Medical University, China

*CORRESPONDENCE
Zhu Yang
yangzhu@hospital.cqmu.edu.cn

†These authors have contributed equally to this work

RECEIVED 17 June 2024
ACCEPTED 26 August 2024
PUBLISHED 13 September 2024

CITATION
Zhang S, Li Q, Ouyang X, Tang Y, Cui J and Yang Z (2024) Radiotherapy can improve overall survival in patients with lymph-node positive, high-grade neuroendocrine cervical cancer: construction of two prognostic nomograms to predict treatment outcome. *Front. Oncol.* 14:1450382. doi: 10.3389/fonc.2024.1450382

COPYRIGHT
© 2024 Zhang, Li, Ouyang, Tang, Cui and Yang. This is an open-access article distributed under the terms of the Creative Commons Attribution License (CC BY). The use, distribution or reproduction in other forums is permitted, provided the original author(s) and the copyright owner(s) are credited and that the original publication in this journal is cited, in accordance with accepted academic practice. No use, distribution or reproduction is permitted which does not comply with these terms.

Radiotherapy can improve overall survival in patients with lymph-node positive, high-grade neuroendocrine cervical cancer: construction of two prognostic nomograms to predict treatment outcome

Siying Zhang[1†], Qinke Li[1†], Xiping Ouyang[2], Ya Tang[1], Ji Cui[1] and Zhu Yang[1*]

[1]Department of Gynecology and Obstetrics, the Second Affiliated Hospital of Chongqing Medical University, Chongqing, China, [2]Department of Gynecology and Obstetrics, the First Affiliated Hospital of Chongqing Medical University, Chongqing, China

Background: To explore the beneficial subgroups after radiotherapy in high-grade neuroendocrine cervical cancer (HGNECC) and construct two survival prognosis models to quantify the efficacy of radiotherapy assessment.

Methods: In this retrospective study, we included 592 eligible samples from the Surveillance, Epidemiology, and End Results (SEER) database and 56 patients with lymph-node positive HGNECC from Chongqing Medical University. Cox regression analysis was used to identify independent survival prognosis risk factors for HGNECC patients. Propensity score matching (PSM) was employed as it balances the baseline differences among grouping methods. Kaplan–Meier (K-M) curves were used to analyze survival differences among different groups. Two survival prediction nomograms were constructed separately (using the "rms" package in R software) based on whether radiotherapy was administered. The stability and accuracy of these models were assessed using receiver operating characteristic (ROC) curves and calibration curves in both the training and validation datasets. $P<0.05$ was considered to indicate statistically significant differences.

Results: Age, Federation of Gynecology and Obstetrics (FIGO)-stage, and treatment methods (surgery vs. chemotherapy) were independent risk factors that affected survival prognosis ($P<0.05$). Radiotherapy showed adverse effects on survival in patients with early tumor staging, lymph-node negative status, and absence of distant metastasis (all $P<0.05$). The lymph-node positive group had a beneficial response to radiotherapy ($P<0.05$), and patients with metastasis in the radiotherapy group showed a survival protection trend ($P=0.069$).

Conclusion: In HGNECC, patients with lymph-node positive status can benefit from radiotherapy in terms of survival outcomes. We constructed two survival prediction models based on whether radiotherapy was administered, thereby offering a more scientifically guided approach to clinical treatment planning by quantifying the radiotherapy efficacy.

KEYWORDS

high-grade neuroendocrine cervical cancer, survival prognosis, SEER database, radiotherapy, nomogram

1 Introduction

Neuroendocrine cervical cancer (NECC) is a rare malignant tumor originating from the cervix, and accounts for approximately 1–1.5% of all cervical malignancies (1). Saavedra et al. first described NECC in 1972 and then categorized it into four main types in 1976 (2). The current WHO classification further categorizes NECC into low-grade with relatively favorable prognosis (carcinoid and atypical carcinoid) and high-grade with worse prognosis (small-cell neuroendocrine carcinoma and large cell neuroendocrine carcinoma, accounting for 80% and 12%, respectively) (1). Given its rarity, the knowledge and treatment of NECC mainly rely on case reports or small sample studies. To our knowledge, there is still no established guideline for managing NECC, which presents a significant challenge in understanding and treating this tumor.

Currently, the treatment approach for NECC is similar to that of cervical adenocarcinoma (AC) or squamous cell carcinoma (SCC). Radical hysterectomy followed by adjuvant radiotherapy or chemotherapy remains the main treatment approach in early-stage NECC. In advanced-stage NECC, a combination of radiotherapy, chemotherapy, and personalized comprehensive treatment is preferred (3). AC/SCC predominantly spreads locally, with a lower incidence of distant metastasis. Radiotherapy, as a key adjuvant treatment, plays a crucial role in suppressing local recurrence, metastasis, thereby enhancing both progression-free survival (PFS), overall-survival (OS), and contributing to favorable long-term survival outcomes. In contrast, NECC has a lower 5-year survival rate of approximately 36% and a median survival period ranging from 22 to 25 months. For the more aggressive small cell neuroendocrine carcinoma of the cervix, the 5-year survival rate is typically less than 2 years (4).

Because NECC is characterized by its highly metastatic nature, surgery in the early stage and adjuvant chemotherapy in all stages are all universally accepted as effective treatment options, regardless of its subtype (5–8).However the efficacy of radiotherapy remains uncertain (6, 8–11). Some studies suggest that combined radiotherapy does not significantly improve survival outcomes but certain subgroups may benefit from this approach. Factors such as age, staging, and lymph node status may influence radiotherapy effectiveness (12–16). Owing to the complexity of individual variables and limited sample sizes, no study has yet comprehensively described the treatment effects of radiotherapy on NECC or quantified the association between prognostic risk factors affecting radiotherapy benefits and survival outcomes. NECC primarily affects young-to-middle-aged women, emphasizing quality of life and survival benefits (17). Hence, further exploration using high-quality, large-sample data are needed for tailored treatment strategies in NECC patients. Our study aims to explore factors affecting radiotherapy outcomes, construct survival prediction models for both radiotherapy and non-radiotherapy groups, and validate these models using clinical data. Successful development of these models will help identify patients who can benefit from radiotherapy, tailor treatment plans, and improve the OS rates.

2 Materials and methods

2.1 Data resource

This was a retrospective clinical cohort study, some of the data were obtained through the SEER*Stat software (V8.3.6) from the SEER public database (https://seer.cancer.gov/). The SEER database, established by the National Cancer Institute in 1973, collects comprehensive cancer data from various regions and subpopulations across the United States. It currently includes data from 18 registration centers, covering a wide range of tumor types. Meanwhile, another Patient data collected from the First and the Second Affiliated Hospital of Chongqing Medical University for the past decade (January 2010 to December 2020).

2.2 Patients selection

This study screened patient data from the Surveillance, Epidemiology, and End Results (SEER) database. Data of all patients in 18 registration centers in U.S from 1988 to 2019 were retrieved, initially including 1342 cases of confirmed cervical

neuroendocrine carcinoma. The patients selection process is as follows: (1) the primary sites selected were C53.0-Endocervix, C53.1-Exocervix, C53.8-Overlapping lesion of cervix uteri, and C53.9-Cervix uteri; (2) according to the International Classification of Diseases for Oncology, 3rd Edition (ICD-O-3), the initial codes proposed for inclusion were 8013/3 (large cell neuroendocrine carcinoma), 8041/3 (small cell neuroendocrine carcinoma), 8045/3 (mixed small cell carcinoma).

Additionally, 66 cases from Chongqing Medical University's affiliated hospitals (2010-2020) were collected. All included patient data were confirmed by the pathology department of our hospital, with a clear pathological diagnosis of cervical neuroendocrine tumors. Both groups have complete follow-up and known survival status.

The exclusion criteria were secondary tumors, duplicate data, and insufficient records. Notably, owing to the limited sample size of low-grade NECCs (<30 cases), patients classified histologically as "other" were excluded. This study focused only on high-grade neuroendocrine carcinomas (HGNECC). The data screening process is shown in Figure 1.

2.3 Variables definition

This study examines patient baseline characteristics and survival status, ensuring data availability in both the SEER database and our hospital's records. Baseline data include demographic factors: Patient ID, Year of diagnosis, Age at diagnosis; Tumor features; Historical stage (AJCC 7th edition), Grade, Primary site, TNM staging, FIGO staging; Treatment details: Surgery, Radiotherapy, Chemotherapy; Follow-up: Survival time, Survival status. Overall Survival (OS) is defined as the time from NECC diagnosis to the last follow-up, with causes of death not limited to NECC.

2.4 Statistical analysis

Continuous variables are described as mean±standard deviation (SD) or median with interquartile range (IQR) values, depending on whether their distribution was normal or non-normal. Categorical variables are shown as numbers and percentages for each group. We used Cox proportional hazards regression analysis to identify factors affecting survival prognosis. Considering variations in the effectiveness of radiotherapy, we analyzed subgroup survival differences across different grouping methods. Propensity score matching (PSM) was employed to balance baseline data among the various groups. Kaplan–Meier (KM) survival curves were plotted to compare survival outcomes. Participants were divided into radiotherapy and non-radiotherapy groups, and two nomogram models were constructed using the "rms" package in R. Receiver operating characteristic (ROC) and calibration curves were used to visually assess the predictive performance of the models. All statistical analyses were performed using R software (version 3.6.3). $P<0.05$ was considered to indicate statistically significant differences.

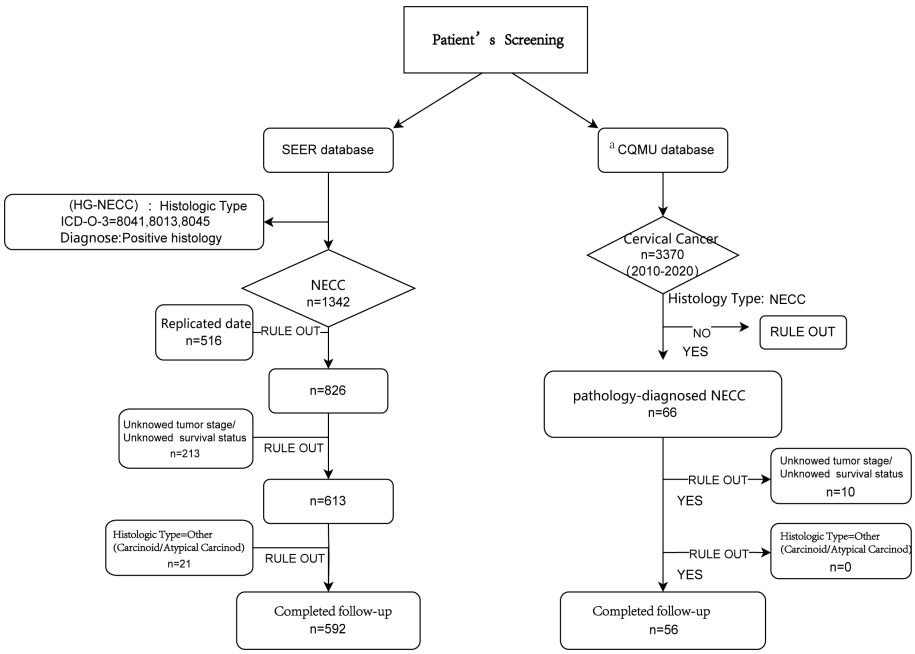

FIGURE 1
The flowchart of enrolled patients screening. [a]CQMU, Chongqing Medical University. Here refers to the First and Second Affiliated Hospitals specifically.

10.3389/fonc.2024.1450382

TABLE 1 Baseline data of all HGNECC patients.

	SEER (N=591)	CQMU* (N=56)
Survival time		
Mean (SD)	49.4 (75.2)	37.7 (25.5)
Median [Min, Max]	16.0 [0, 383]	35.2 [11.2, 120]
Survival Status		
Alive	184 (31.1%)	23 (41.1%)
Death	407 (68.9%)	33 (58.9%)
Age		
<40	194 (32.8%)	16 (28.6%)
40-60	240 (40.6%)	37 (66.1%)
>60	157 (26.6%)	3 (5.4%)
Primary Site		
Cervix uteri	503 (85.1%)	38 (67.9%)
Endo-cervix/Other	88 (14.9%)	18 (32.1%)
Histologic Type		
Large	64 (10.8%)	29 (51.8%)
Small	527 (89.2%)	27 (48.2%)
Grade		
Moderately/well differentiated	6 (1.0%)	0 (0.0%)
Poorly/Un- differentiated	340 (57.5%)	6 (10.7%)
Unknown	245 (41.5%)	50 (89.3%)
FIGO Stage		
I	156 (26.4%)	23 (41.1%)
II	45 (7.6%)	18 (32.1%)
III	163 (27.6%)	12 (21.4%)
IV	227 (38.4%)	3 (5.4%)
T		
T1	237 (40.1%)	23 (41.1%)
T2	130 (22.0%)	18 (32.1%)
T3	126 (21.3%)	11 (19.6%)
T4	30 (5.1%)	4 (7.1%)
TX/Unknown	68 (11.5%)	0 (0%)
N		
N0	269 (45.5%)	43 (76.8%)
N1	259 (43.8%)	13 (23.2%)
NX	63 (10.7%)	0 (0%)
M		
M0	373 (63.1%)	55 (98.2%)
M1	218 (36.9%)	1 (1.8%)
Surgery		
No	309 (52.3%)	5 (8.9%)
Yes	282 (47.7%)	51 (91.1%)
Chemotherapy		
No/Unknown	140 (23.7%)	1 (1.8%)
Yes	451 (76.3%)	55 (98.2%)
Radiation		
No	427 (72.3%)	36 (64.3%)
Yes	164 (27.7%)	20 (35.7%)

*Chongqing Medical University. Here refers to the First and Second Affiliated Hospitals specifically.

SD, standard deviation; OS, overall survival; HGNECC, high-grade neuroendocrine cervical cancer.

3 Results

3.1 Clinical characteristics

Analysis of baseline data (Table 1) from both the SEER database (591 cases) and our hospital database (56 cases) revealed the following: 1) The prognosis for patients in both databases was not optimistic, especially in our hospital database (mean OS: 37.7 months, median survival time: 35.2 months). Over 50% patients had a status of death in the two databases (69.9% vs. 58.9%); 2) age<60 years was the main affected group (73.4% vs. 94.7%), and small cell neuroendocrine carcinoma was the predominant pathological type in HGNECC (89.2% vs. 48.2%); and 3) the majority of patients in both databases underwent surgery and chemotherapy, with a smaller proportion opting for radiotherapy (27.7% vs 35.7%).

3.2 Risk factors for overall survival of HGNECC patients

Due to both T-stage and Federation of Gynecology and Obstetrics (FIGO)-stage being included in the baseline data of all patients from the SEER database, there may be potential overmatching in subsequent Cox analysis and PSM. As for another indicator of grade, 50% patients are classified as poorly differentiated, while the grade of the remaining 50% is unknown. Moreover, obtaining T stage and grade information from our database is challenging. Thus, we plan to exclude T-stage and tumor grade in the subsequent analysis. Cox regression analysis of another 10 subjects from the SEER database (591 cases) identified risk factors affecting OS (Table 2). Among them, age, FIGO-stage,

treatment strategies (surgery vs. chemotherapy) emerged as independent risk factors affecting long-term survival (P<0.05). Surgical group showed a 50% reduction in the risk of death compared to non-surgical group (HR=0.488, P<0.05), while chemotherapy led to a 53% decrease in the mortality risk (HR=0.47, P<0.05). Although initial analysis indicated a 43% lower mortality risk with radiotherapy, further multi-variable Cox analysis revealed a 25% increase in mortality risk compared to non-radiotherapy treatment (HR=1.25, P=0.135), suggesting the potential adverse effect of HGNECC on OS rate.

TABLE 2 Cox hazards regression analysis of OS in patients (HGNECC) from SEER database.

Characteristics	Univariable model				Multivariable model			
	HR	HR.95L	HR.95H	P-value	HR	HR.95L	HR.95H	P-value
Age	2.12	1.696	2.65	<0.001				
<40	1	–	–	–				
40-60	1.668	1.306	2.131	<0.001	1.262	0.975	1.633	0.077
>60	**3.239**	**2.503**	4.192	<0.001	**2.105**	**1.587**	**2.79**	**<0.001**
Primary Site								
Cervix uteri	1	–	–	–				
Endo-cervix/Other	0.793	0.600	1.050	0.103				
Histologic Type								
Large								
Small	0.796	0.586	1.083	0.147				
FIGO_Stage								
I	1	–	–	–				
II	**1.722**	**1.111**	**2.670**	**0.015**	1.061	0.666	1.688	0.804
III	**2.304**	**1.709**	**3.106**	**<0.001**	**1.922**	**1.300**	**2.840**	**0.001**
IV	**5.475**	**4.129**	**7.258**	**<0.001**	**3.007**	**1.534**	**5.895**	**0.001**
N								
N0	1	–	–	–				
N1	**1.988**	**1.606**	**2.461**	**<0.001**	1.234	0.918	1.659	0.163
NX	**3.208**	**2.355**	**4.371**	**<0.001**	1.196	0.837	1.709	0.326
M								
M0	1	–	–	–				
M1	**3.321**	**2.711**	**4.068**	**<0.001**	1.273	0.716	2.266	0.411
Surgery								
No	1	–	–	–				
Yes	**0.38**	**0.31**	**0.465**	**<0.001**	**0.516**	**0.396**	**0.673**	**<0.001**
Chemotherapy								
No	1	–	–	–				
Yes	**0.59**	**0.48**	**0.741**	**<0.001**	**0.470**	**0.372**	**0.594**	**<0.001**
Radiotherapy								
No	1	–	–	–				
Yes	0.567	0.452	0.711	**<0.001**	1.255	0.936	1.683	0.128

HR, hazard ratio; OS, overall survival; CI, confidence interval.
The bold values denote statistical significance at P < 0.05 level.

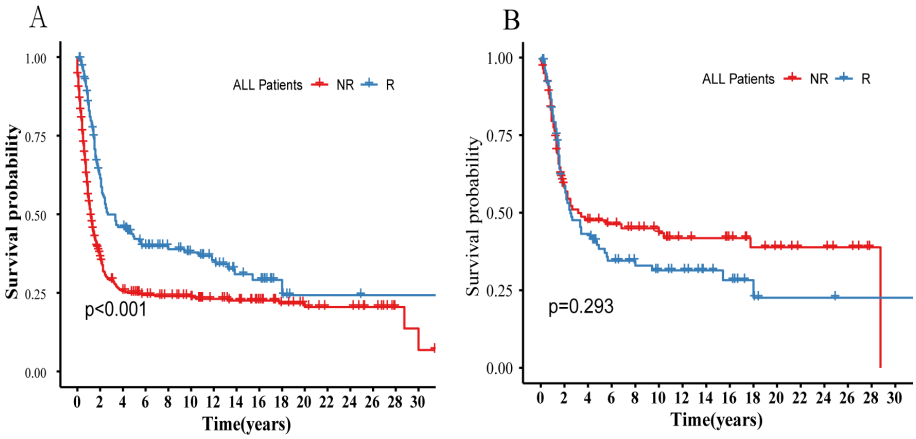

FIGURE 2
Compares the survival differences between the R and NR groups before and after PSM in all patients in the SEER database. **(A)** Survival probability before PSM. **(B)** Survival probability after PSM. R, Radiotherapy; NR, Non radiation therapy.

3.3 Discussing the efficacy of radiotherapy in HGNECC patients

To better understand the benefit of radiotherapy, all subjects from the SEER database were grouped based on whether radiotherapy was administered. Balancing baseline data with PSM (Supplementary Table S1), KM curves then depicted survival differences between groups before and after PSM (Figures 2A, B). The results obtained align with the findings from the Cox regression analysis regarding the benefits of prior radiotherapy (Table 2). Despite no clear advantage in OS with radiotherapy after PSM (P>0.05), both Unix-variables Cox analysis and inter-group comparisons before PSM demonstrated significant survival benefits in the R-group (P<0.05). This suggests potential influencing factors affecting the benefit of radiotherapy. We analyzed all observed indicators included in the study, and subsequent analysis explored some specific indicators related to radiotherapy efficacy, grouping subjects by various criteria, and analyzing survival differences between the radiotherapy (R) and non-radiotherapy (NR) groups.

3.3.1 Analysis of radiotherapy efficacy in different stages

We categorized patients into early-stage (stage I–II) and advanced-stage (stage III–IV) groups based on the FIGO-stage (Figures 3A–D). PSM was used to balance the baseline data (Supplementary Table S2). The KM curves depict survival differences between the R and NR groups. The addition of radiotherapy in early-stage patients had a statistically significant adverse-effect on survival prognosis (Figures 3A, B, P=0.014). Conversely, no significant survival differences were noted in advanced-stage patients (P>0.05, Figures 3C, D).

3.3.2 Analysis of radiotherapy efficacy in different lymph-node status

We categorized patients from the SEER database into two groups (Figures 3E–H) based on lymph node status: N0 (negative) and N1 (positive). PSM was used to balance the baseline data (Supplementary Table S3). KM depicts survival differences between the R and NR groups. After PSM, radiotherapy had a statistically significant adverse effect on survival prognosis in the N0 group (P=0.015, Figures 3E, F), while it showed a clear survival protective effect in the N1 group (P=0.045, Figures 3G, H).

3.3.3 Analysis of radiotherapy efficacy based on the presence and absence of distant metastasis

We categorized patients from the SEER database into two groups (Figures 3I–L): M0 (no distant metastasis) and M1 (distant metastasis). PSM was used to balance the baseline data (Supplementary Table S4). The KM curves depict survival differences between subgroups. After PSM, it was observed that radiotherapy was a clear risk factor in the M0 group (P=0.002, Figures 3I, J). Although radiotherapy did not reach statistical significance, it demonstrated a certain protective trend in the M1 group (P=0.069, Figures 3K, L).

3.3.4 Analysis of radiotherapy efficacy based on histological differences

We categorized patients from the SEER database into two groups (Figures 3M–P): LCNEC and SCNEC. We balanced the baseline data using PSM (Supplementary Table S5). KM curves depict survival differences between subgroups. Radiotherapy was identified as a clear prognostic risk factor in SCNEC, which has poorer differentiation and higher malignancy than LCNEC (P=0.031, (Figures 3M–P).

Our analysis indicates that NECC tends to respond poorly as the malignancy progresses, and the local control benefits of radiotherapy diminish. We also observed the patients with SCNEC had worse OS than LCNEC after radiotherapy (P=0.031, Figures 3O, P). Additionally, in early-stage and lymph node-negative groups, those who did not receive radiotherapy showed significantly better OS (Figures 3B, F). However, there are patients who can benefit from radiotherapy: those with lymph-node positive status exhibited a clear

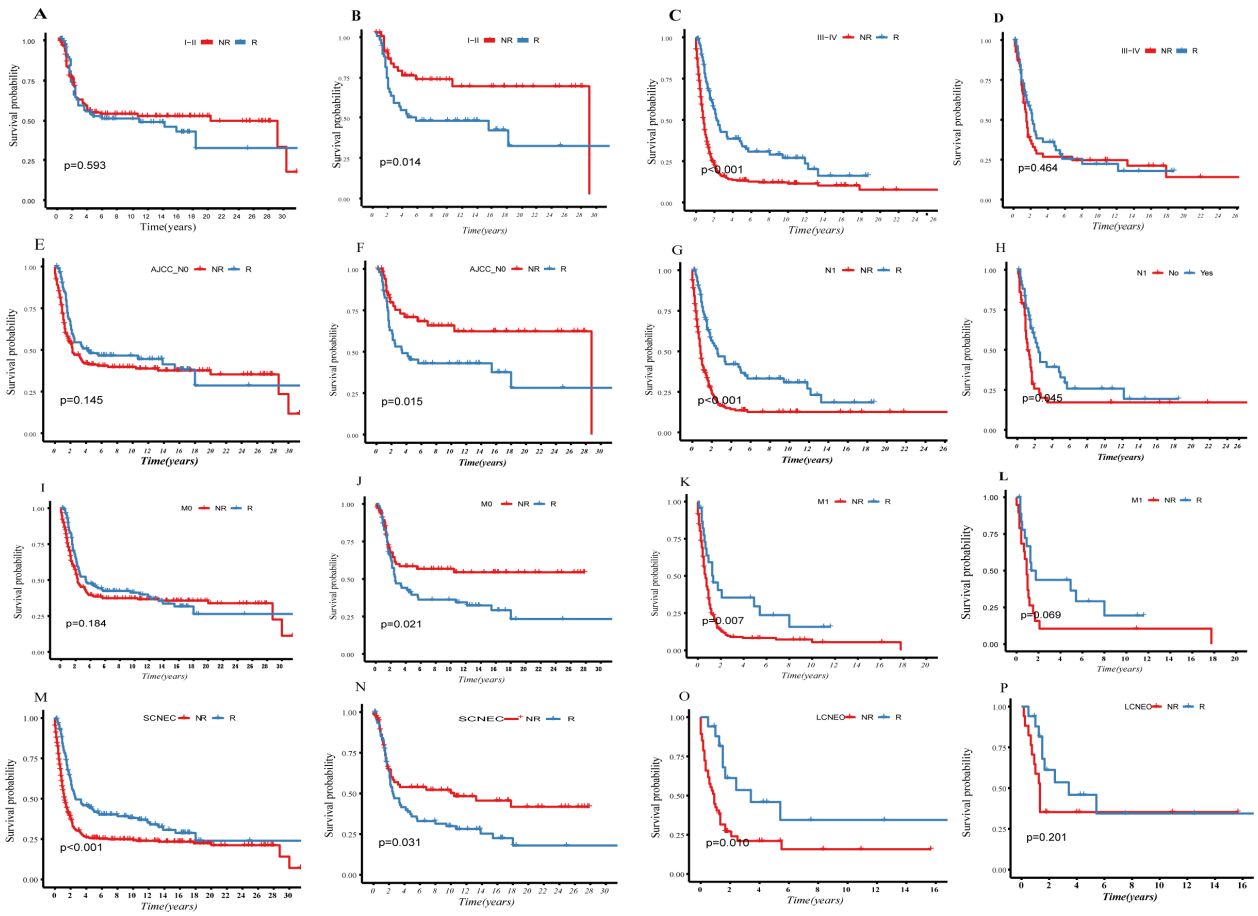

FIGURE 3
Compare the survival difference before and after PSM between the R- and NR-group in different indicators: **(A–D)**, grouping according to FIGO staging; **(E–H)**, grouping according to lymph nodes status; **(I–L)**, grouping according to whether distant metastasis; **(M–P)**, grouping according to histological difference.

survival advantage in the R-group (Figure 3H). Although our study did not show clear benefits in the M1 group, there was a protective trend in the R-group (Figures 3K, L).

3.4 Constructing survival prediction models based on radiotherapy efficacy

Because of the complexity of individual cases, determining whether to add radiation therapy can be challenging when both favorable and unfavorable factors are present. The nomogram, integrating multiple prognostic factors, offers a personalized assessment tool. Based on multi-variable Cox regression analysis, the nomogram combines independent prognostic indicators to calculate their respective weights in predicting survival outcomes.

Following this principle, we divided the SEER database population into two groups: the R and NR groups. Cox regression analysis was used to identify the factors influencing survival outcome in each group independently: We constructed nomograms for both groups, validating both models with data from the SEER database (internal validation group) and our hospital's system (external validation group). Through objective scoring, we quantified the population benefiting from radiation therapy.

3.4.1 Construction and validation of nomogram for NR-group

We began by constructing the predictive model for the NR group. There were 427 samples without radiation therapy in the SEER database. Splitting them in a 7:3 ratio, the computer randomly divided them into a training group (299 patients) and an internal validation group (128 patients). Additionally, we considered 36 non-radiotherapy patients from our institution's database as the external validation group (Supplementary Table S6).

Based on the training group of 199 samples, we conducted Cox regression analysis (Table 3). Multi-variable Cox analysis showed that age, histological type, FIGO stage, treatment regimen, and lymph node status were independent risk factors affecting the survival prognosis in NR group (P<0.05). Based on the results, we developed a nomogram model for predicting the 1, 3, and 5-year survival of the NR group and showed the distribution of risk scores for all patients (Figure 4A). ROC curves were used to assess the model's discriminative ability, and calibration curves were used to

10.3389/fonc.2024.1450382

TABLE 3 COX regression analysis of patients without radiotherapy (the training group).

Cox univariate analysis					Cox multivariate analysis				
	HR	HR.95L	HR.95H	P value		HR	HR.95L	HR.95H	P value
Age					Age				
<40	1.000	–	–	–	<40	1.000	–	–	–
40-60	2.218	1.517	3.243	<0.001	40-60	1.168	0.797	1.712	0.426
>60	3.839	2.618	5.629	<0.001	>60	1.820	1.212	2.732	0.004
Primary Site									
Cervix uteri	1.000	–	–	–					
Endocervix/Other	0.944	0.613	1.456	0.796					
Histologic Type					Histologic Type				
Large	1.000	–	–	–	Large	1.000	–	–	–
Small	0.742	0.495	1.113	0.149	Small	0.574	0.369	0.893	0.014
FIGO_Stage					FIGO_Stage				
I	1.000	–	–	–	I	1.000	–	–	–
II	3.141	1.568	6.292	0.001	II	1.046	0.508	2.154	0.904
III	4.116	2.482	6.825	<0.001	III	2.199	1.213	3.985	0.009
IV	8.050	5.001	12.957	<0.001	IV	2.775	1.147	6.714	0.024
AJCC_N					AJCC_N				
N0	1.000	–	–	–	N0	1.000	–	–	–
N1	2.214	1.636	2.996	<0.001	N1	1.500	1.015	2.216	0.042
NX	3.153	2.107	4.719	<0.001	NX	1.196	0.741	1.929	0.463
AJCC_M					AJCC_M				
M0	1.000	–	–	–	M0	1.000	–	–	–
M1	3.311	2.496	4.392	<0.001	M1	1.558	0.743	3.267	0.241
Therapy									
No	1.000	–	–	–	No	1.000	–	–	–
Surgery +Chemotherapy	0.175	0.113	0.272	<0.001	Surgery +Chemotherapy	0.185	0.108	0.319	<0.001
Surgery	0.217	0.126	0.371	<0.001	Surgery	0.395	0.267	0.584	<0.001
Chemotherapy	0.409	0.295	0.566	<0.001	Chemotherapy	0.407	0.214	0.775	0.006

NR, non radiotherapy; R, radiotherapy.

evaluate the consistency between the predicted survival rate and the actual survival rate of the population. Due to the limited number of analyzable samples, including insufficient data for 5-year survival, some groups lack 5-year survival data, we only conducted accuracy assessment for 1 and 3-year survival predictions in this study.

The predictive results for the 1- and 3-year survival in the training group and internal/external validation groups were assessed using ROC curves (Figures 4C–E). The model shows prediction accuracy by using the AUC values: In the training group, the AUC values were 0.865 and 0.852, respectively (Figure 4C); in the internal validation group, the AUC values were 0.828 and 0.833, respectively (Figure 4D). Meanwhile, Figure 4E illustrates the analysis of predicting the 1- and 3-year survival accuracy in the external validation group, with AUC values of 0.841 and 0.726, respectively.

Regarding the calibration curve, the X-axis denotes the predicted probability, while the Y-axis represents the actual probability, ranging from 0 to 1. Perfect alignment with the reference line (diagonal line) indicates accurate predictions, while deviation above or below indicates overestimation or underestimation of risk, respectively. Calibration curves for the 1- and 3-year predictive models in the training, internal validation,

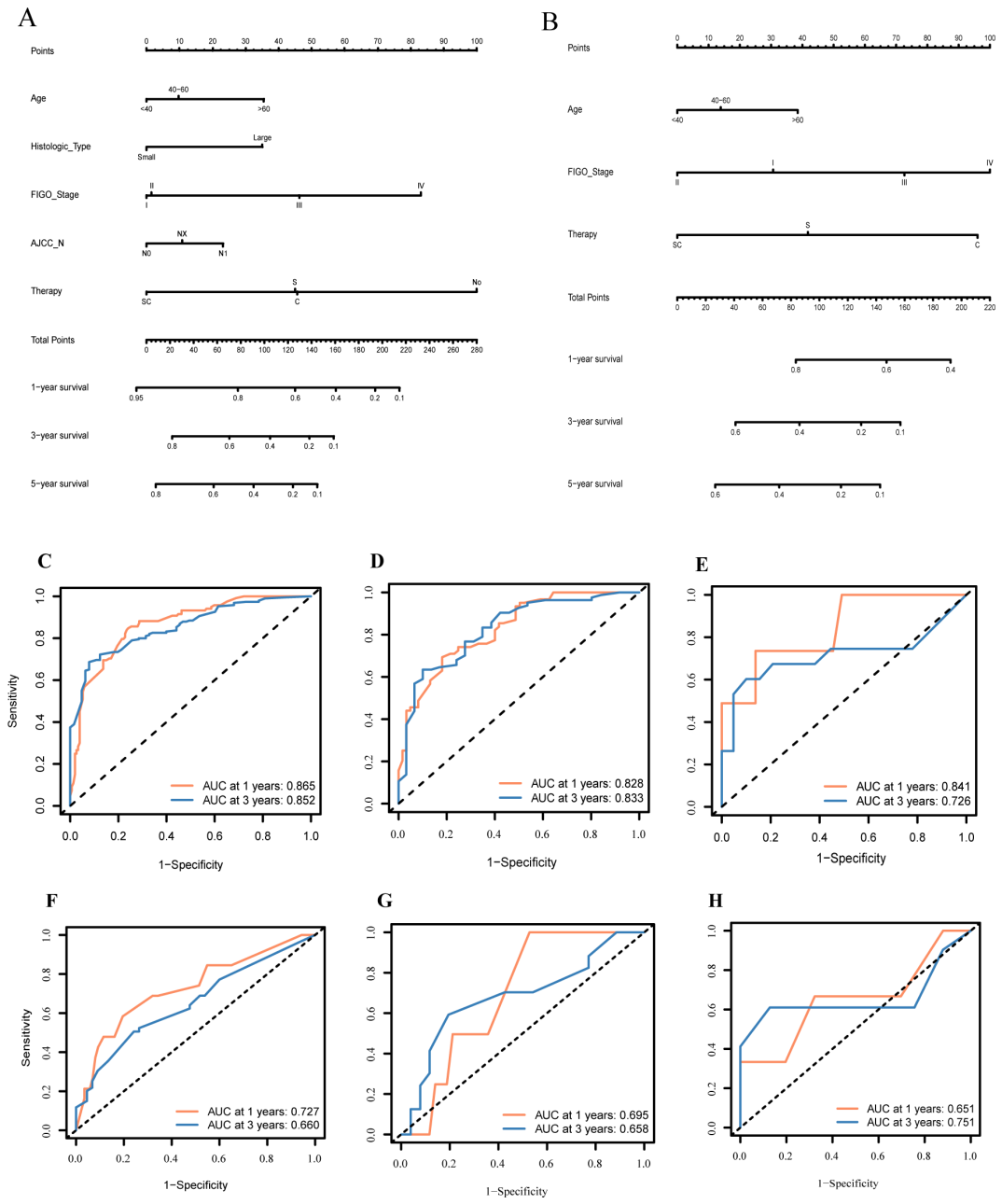

FIGURE 4
Constructing and validating the two nomograms based on therapeutic differences: **(A)** nomogram of patients without radiotherapy; **(B)** nomogram of patients with radiotherapy; **(C–H)** Receiver operating characteristic curve (ROC) of predictive models for 1- and 3- years in NR-group and R-group individually.

and external validation groups are depicted (Supplementary Figure S1). Notably, all curves fluctuate around the 45-degree dashed line, indicating well-calibrated models.

3.4.2 Construction and validation of nomogram for R-group

Similarly, there were 184 samples in the R group from the SEER database. The sample was randomly divided in a 7:3 ratio by the computer into a training group (115 patients) and an internal validation group (49 patients). Additionally, we considered all 20 patients with radiotherapy from our institution's database as an external validation group (Supplementary Table S7). Based on the training group of 115 samples, we conducted Cox regression analysis (Table 4). The results of Cox analysis indicated that FIGO stage and treatment regimen were significant factors affecting survival prognosis in the radiotherapy group. The risk of death increased with age, and higher tumor stages were associated with greater mortality risk ($P<0.05$). Surgery and chemotherapy were found to be protective factors.

Based on the results of the Cox analysis, we constructed a prognostic nomogram for 1-, 3-, and 5-year survival (Figure 4B). The analysis included variables such as age, FIGO stage, and

TABLE 4 COX regression analysis of patients with radiotherapy (the training group).

	COX univariate analysis					COX multivariate analysis			
	HR	HR.95L	HR.95H	P-value		HR	HR.95L	HR.95H	P-value
Age					**Age**				
<40	1.000	–	–	–	<40	1.000	–	–	–
40-60	1.261	0.762	2.083	0.368	40-60	1.197	0.798	2.044	0.509
>60	1.743	0.919	3.307	0.089	>60	1.649	0.798	3.406	0.177
Primary Site									
Cervix uteri	1.000	–	–	–					
Endo-cervix/Other	1.020	0.601	1.715	0.955					
Histologic Type					**Histologic Type**				
Large	1.000	–	–	–	Large	1.000	–	–	–
Small	0.889	0.425	1.856	0.754	Small	0.866	0.390	1.922	0.723
FIGO_Stage					**FIGO_Stage**				
I	1.000	–	–	–	I	1.000	–	–	–
II	0.758	0.265	2.166	0.604	II	0.684	0.228	2.057	0.500
III	1.623	0.960	2.743	0.071	III	3.820	0.797	18.333	0.094
IV	3.064	1.565	5.999	0.001	IV	3.681	1.047	12.950	0.042
AJCC_N					**AJCC_N**				
N0	1.000	–	–	–	N0	1.000	–	–	–
N1	1.689	1.046	2.729	0.032	N1	0.448	0.103	1.948	0.284
NX	2.553	0.991	6.580	0.052	NX	0.790	0.175	3.580	0.760
AJCC_M									
M0	1.000	–	–	–					
M1	1.927	1.072	3.464	0.028					
Therapy					**Therapy**				
Surgery +Chemotherapy	1.000	–	–	–		1.000	–	–	–
Surgery	1.728	0.942	3.168	0.077	Surgery	1.718	0.868	3.402	0.124
Chemotherapy 5.470		2.282	13.111	<0.001	Chemotherapy	4.443	1.539	12.828	0.006

treatment regimen. Using R software, we generated risk charts for 1-, 3- and 5-year survival of the NECC-R group patients, as well as scatter plots showing the distribution of risk scores for all patients.

We validated the 1- and 3-year prediction results of the training group, internal validation group, and external validation group by using ROC curves (Figures 4F–H). Across all models (based on all clinical and pathological factors), the Cox model's AUCs for the 1- and 3-year OS in the training group was 0.727 and 0.660, respectively (Figure 4F). For the internal validation group, the COX model's AUCs for the 1- and 3-year OS was 0.695 and 0.658, respectively (Figure 4G). As for the external validation group, the AUC value was 0.651 and 0.751, respectively (Figure 4H).

Furthermore, we assessed the calibration of the 1- and 3-year survival prediction models for the three groups using calibration curves (Supplementary Figure S2). The curves for predicting the 1- and 3-year survival rates of all three groups fluctuated around the 45-degree line, indicating good calibration performance of the models.

Here, we will demonstrate the application process of the model through two supplementary examples (see in Supplementary Materials).

4 Discussion

In recent years, as the incidence of NECC continues to rise, research on this disease has also increased. To our knowledge, this is not the first study to examine the clinical characteristics and prognosis of NECC using the SEER database (18–20), That said, however, our study's focus was on investigating the effectiveness of radiotherapy in treating NECC. We aimed to provide more

scientifically based clinical guidance for future treatment decisions by quantifying the benefits of radiotherapy and categorizing patients into subgroups based on their radiotherapy status. We believe that this approach is innovative.

In our analysis, we found that the disease tends to affect patients at a younger age and is highly aggressive, with early occurrences of local and distant metastases leading to poor OS. Effective treatments to improve OS rates include surgery and chemotherapy (P<0.05). Cox analysis did not show clear survival benefits from adding radiotherapy. Moreover, the subgroup analysis based on radiotherapy status, after PSM, also did not reveal any significant survival differences between the R and NR groups. However, the radiotherapy group showed a relatively unfavorable survival trend overall (Figure 2), similar to findings from previous studies on neuroendocrine carcinoma of the cervix (7, 8, 17, 21, 22). Analyzing the reason, this may be because of the tumor's aggressive nature and early metastasis, which make chemotherapy more beneficial as a systemic treatment (5, 7, 8, 23). Radiation therapy primarily targets local tumor tissues and may not effectively control distant metastases. Additionally, the combined toxic side effects of chemo-radiotherapy could outweigh its benefits for local tumor lesions, leading to shorter survival, as seen in previous studies (6, 8–10).

In our analysis, we found that radiotherapy showed statistically significant survival benefits in NECC patients in the Unix-variable Cox analysis (Table 2) and before PSM (Figure 2) (P<0.05). This suggests that certain factors in our analysis may maximize the effectiveness of radiotherapy. Radiotherapy can delay the progression and distant metastasis of lesions locally, surpassing the toxic side effects of treatment itself through combined chemo-radiotherapy, thereby prolonging patients' PFS and OS. Recent studies on radiotherapy response in NECC patients have provided insights. Roy et al. (12) studied 25 NECC patients treated with combined chemo-radiotherapy and observed improved OS, with a median survival time of 53.8 months and a 5-year OS rate of 48%. Unfortunately, this study did not further analyze the characteristics of patients who benefited from radiotherapy. Xie et al. (13) analyzed 48 NECC patients' post-surgery and found that the tumor's histological type influenced radiotherapy efficacy. They noted better survival outcomes in neuroendocrine tumors with mixed glandular tissue. Additionally, while early studies mainly focused on adverse effects of radiotherapy in early-stage NECC, recent findings suggest potential benefits in middle and late-stage patients (15, 16).

Our study aimed to identify factors influencing the effectiveness of radiotherapy in patients with HGNECC. The histological type of NECC showed poor response to radiotherapy, especially in SCNEC, which exhibited worse OS outcomes with radiotherapy (P=0.031, Figure 3). In early-stage, lymph node-negative, and non-metastatic NECC, patients who did not receive radiotherapy had significantly better OS than those who did. However, in patients with lymph node metastasis (N1), radiotherapy showed clear benefits, significantly improving OS compared to those without radiotherapy (P=0.045). Radiotherapy exhibited excellent local control in patients with N1, reducing the size of the primary lesion to some extent and delaying further invasion of local lymph nodes into distant areas, thereby prolonging PFS and OS. For patients with distant metastasis (M1), while there was a trend of survival benefit with radiotherapy, it didn't reach statistical significance in our study (P = 0.064). However, in a recent research (24):radiotherapy was identified as the only independent prognostic risk factor in the M1 group. There was a statistically significant benefit for OS in the group combined with radiotherapy (with median survival times of 44.6 months and 80.9 months, respectively, p = 0.004). This study suggests that even in the presence of distant metastasis, aggressive local treatment should be considered. These findings underscore the importance of considering individual patient characteristics when determining the role of radiotherapy in HGNECC.

Our study explored factors affecting radiotherapy's effectiveness, confirming and expanding upon previous findings from smaller studies. However, individual patient responses to radiotherapy are influenced by multiple factors, making it challenging to determine treatment solely based on one factor. To address this, we further investigated by grouping patients based on receipt of radiotherapy to create survival prognosis models. To our knowledge, this is the first study to create subgroup nomograms based on treatment differences. Our analyses showed that factors like age, cancer type, disease stage, and treatment method significantly influenced survival in patients not receiving radiotherapy. Similarly, for those receiving radiotherapy, age, disease stage, and treatment method played significant roles. However, given the sample size and data limitations, the accuracy of models in the radiotherapy group was somewhat lower than in the non-radiotherapy group.

4.1 Strengths and significance

1. Our study, based on the extensive SEER database, provides more robust and generalizable findings compared to previous small-scale studies on NECC 2. We address the ongoing debate surrounding radiotherapy in the treatment of NECC, offering valuable insights and guidance for clinical decision-making 3.Despite not being the first SEER-based study on NECC, our research stands out by focusing on the efficacy of RT, offering innovative directions for future treatment strategies.

4.2 Limitations and future recommendations

1. We know that, for cervical cancer, external irradiation and internal radiation are both used. Although our study discussed the benefits of radiotherapy in patients with HGNECC, there as only "yes, no, or unknown" on radiotherapy information based on the SEER database. Our hospital database only includes 20 cases of radiotherapy patients. Due to the small amount of analyzable data and the limitations imposed by recall bias from patients, the detailed radiotherapy regimens in this study cannot be specifically shown. Therefore, we will further investigate the efficacy of radiotherapy in patients and explore detailed radiotherapy regimens by making more accurate prospective studies. 2. Missing data on crucial factors like postoperative pathology and specific treatment regimens limit the accuracy of our analyses, suggesting the need for more comprehensive data collection methods. 3. We

primarily focuse on survival outcomes, overlooking aspects like recurrence and treatment-related adverse events. 4. Future research should delve deeper into these areas; for a more comprehensive assessment of RT efficacy, additional comparison indicators and validation from other hospital databases are recommended.

4.3 Conclusion

In HGNECC, radiotherapy can result in survival benefits for patients with positive lymph nodes. Patients with distant metastases should also be considered for appropriate. We have established two specific nomograms to predict treatment outcomes, helping doctors plan personalized treatments.

Data availability statement

The datasets presented in this study can be found in online repositories. The names of the repository/repositories and accession number(s) can be found in the article/Supplementary Material.

Ethics statement

Ethical approval was not required for the study involving humans in accordance with the local legislation and institutional requirements. Written informed consent to participate in this study was not required from the participants or the participants' legal guardians/next of kin in accordance with the national legislation and the institutional requirements.

Author contributions

SZ: Data curation, Validation, Writing – original draft, Writing – review & editing, Software. QL: Data curation, Formal analysis, Methodology, Software, Writing – review & editing, Validation. XO: Data curation, Formal analysis, Writing – review & editing. YT: Data curation, Writing – review & editing. JC: Writing – review & editing. ZY: Funding acquisition, Investigation, Project administration, Supervision, Writing – review & editing.

Funding

The author(s) declare financial support was received for the research, authorship, and/or publication of this article. Chongqing Talents Program of the Chongqing Municipal People's Government funded this research (Grant No.: cstc2022ycjh-bgzxm0062).

Conflict of interest

The authors declare that the research was conducted in the absence of any commercial or financial relationships that could be construed as a potential conflict of interest.

Publisher's note

All claims expressed in this article are solely those of the authors and do not necessarily represent those of their affiliated organizations, or those of the publisher, the editors and the reviewers. Any product that may be evaluated in this article, or claim that may be made by its manufacturer, is not guaranteed or endorsed by the publisher.

Supplementary material

The Supplementary Material for this article can be found online at: https://www.frontiersin.org/articles/10.3389/fonc.2024.1450382/full#supplementary-material

References

1. Lu Z, Chen J. Introduction of WHO classification of tumours of female reproductive organs, fourth edition. *Zhonghua Bing Li Xue Za Zhi*. (2014) 43 (10):649–50. doi: 10.3760/CMA.J.ISSN.0529-5807.2014.10.00

2. Albores-Saavedra J, Larraza O, Poucell S, Rodríguez Martínez HA. Carcinoid of the uterine cervix: additional observations on a new tumor entity. *Cancer*. (1976) 38:2328–42. doi: 10.1002/(ISSN)1097-0142

3. Koh WJ, Abu-Rustum NR, Bean S, Bradley K, Campos SM, Cho KR, et al. Cervical cancer, version 3.2019, NCCN clinical practice guidelines in oncology. *J Natl Compr Canc Netw*. (2019) 17:64–84. doi: 10.6004/jnccn.2019.0001

4. Salvo G, Gonzalez Martin A, Gonzales NR, Frumovitz M. Updates and management algorithm for neuroendocrine tumors of the uterine cervix. *Int J Gynecol Cancer*. (2019) 29:986–95. doi: 10.1136/ijgc-2019-000504

5. Lee SW, Lim KT, Bae DS, Park SY, Kim YT, Kim KR, et al. A multicenter study of the importance of systemic chemotherapy for patients with small-cell neuroendocrine carcinoma of the uterine cervix. *Gynecol Obstet Invest*. (2015) 79:172–8. doi: 10.1159/000367920

6. Ishikawa M, Kasamatsu T, Tsuda H, Fukunaga M, Sakamoto A, Kaku T, et al. Prognostic factors and optimal therapy for stages I-II neuroendocrine carcinomas of the uterine cervix: A multi-center retrospective study. *Gynecol Oncol*. (2018) 148:139–46. doi: 10.1016/j.ygyno.2017.10.027

7. Tempfer CB, Tischoff I, Dogan A, Hilal Z, Schultheis B, Kern P, et al. Neuroendocrine carcinoma of the cervix: a systematic review of the literature. *BMC Cancer*. (2018) 18:530. doi: 10.1186/s12885-018-4447-x

8. Chen Y, Chen J, Lin X, Zheng J, Li S, Zheng X. A prognostic nomogram for predicting overall survival in patients with small-cell carcinoma of the uterine cervix: A SEER population-based study. *Technol Cancer Res Treat*. (2022) 21. doi: 10.1177/15330338221110673

9. Zhou J, Yang HY, Wu SG, He ZY, Lin HX, Sun JY, et al. The local treatment modalities in FIGO stage I-II small-cell carcinoma of the cervix are determined by disease stage and lymph node status. *Cancer Med*. (2016) 5:1108–15. doi: 10.1002/cam4.687

10. Xu F, Ma J, Yi H, Hu H, Fan L, Wu P, et al. Clinicopathological aspects of small cell neuroendocrine carcinoma of the uterine cervix: a multicenter retrospective study and meta-analysis. *Cell Physiol Biochem*. (2018) 50:1113–22. doi: 10.1159/000494538

11. Zhang X, Lv Z, Lou H. The clinicopathological features and treatment modalities associated with survival of neuroendocrine cervical carcinoma in a Chinese population. *BMC Cancer. 7*. (2019) 19(1):22. doi: 10.1186/s12885-018-5147-2

12. Roy S, Ko JJ, Bahl G. Small cell carcinoma of cervix: A population-based study evaluating standardized provincial treatment protocols. *Gynecol Oncol Rep*. (2019) 27:54–9. doi: 10.1016/j.gore.2019.01.003

13. Xie S, Song L, Yang F, Tang C, Yang S, He J, et al. Enhanced efficacy of adjuvant chemotherapy and radiotherapy in selected cases of surgically resected neuroendocrine carcinoma of the uterine cervix: A retrospective cohort study. *Med (Baltimore)*. (2017) 96:e6361. doi: 10.1097/MD.0000000000006361

14. Robin TP, Amini A, Schefter TE, Behbakht K, Fisher CM. Brachytherapy should not be omitted when treating locally advanced neuroendocrine cervical cancer with definitive chemoradiation therapy. *Brachytherapy*. (2016) 15:845–50. doi: 10.1016/j.brachy.2016.08.007

15. Lin AJ, Hassanzadeh C, Markovina S, Schwarz J, Grigsby P. Brachytherapy and survival in small cell cancer of the cervix and uterus. *Brachytherapy*. (2019) 18:163–70. doi: 10.1016/j.brachy.2018.11.006

16. Lin LM, Lin Q, Liu J, Chu KX, Huang YX, Zhang ZK, et al. Prognostic factors and treatment comparison in small cell neuroendocrine carcinoma of the uterine cervix based on population analyses. *Cancer Med*. (2020) 9:6524–32. doi: 10.1002/cam4.3326

17. Margolis B, Tergas AI, Chen L, Hou JY, Burke WM, Hu JC, et al. Natural history and outcome of neuroendocrine carcinoma of the cervix. *Gynecologic Oncol*. (2016) 141:247–54. doi: 10.1016/j.ygyno.2016.02.008

18. Jia M, Pi J, Zou J, Feng M, Chen H, Lin C, et al. A nomogram model based on neuroendocrine markers for predicting the prognosis of neuroendocrine carcinoma of cervix. *J Clin Med*. (2023) 12:1227. doi: 10.3390/jcm12031227

19. Liu J, Lyu Y, He Y, Ge J, Zou W, Liu S, et al. Competing risk nomogram and risk classification system for evaluating overall and cancer-specific survival in neuroendocrine carcinoma of the cervix: a population-based retrospective study. *J Endocrinol Invest*. (2024) 47(6):1545–57. doi: 10.1007/s40618-023-02261-7

20. Yu C, Wu X, Zhang S, Zhang L, Zhang H, Yang H, et al. Prognostic model for survival in patients with neuroendocrine carcinomas of the cervix: SEER database analysis and a single-center retrospective study. *PloS One*. (2024) 19:e0296446. doi: 10.1371/journal.pone.0296446

21. Park HK. Neuroendocrine carcinomas of the uterine cervix, endometrium, and ovary show higher tendencies for bone, brain, and liver organotrophic metastases. *Curr Oncol*. (2022) 29:7461–9. doi: 10.3390/curroncol29100587

22. Chan JK, Loizzi V, Burger RA, Rutgers J, Monk BJ. Prognostic factors in neuroendocrine small cell cervical carcinoma: a multivariate analysis. *Cancer*. (2003) 97:568–74. doi: 10.1002/cncr.11086

23. Ishikawa M, Kasamatsu T, Tsuda H, Fukunaga M, Sakamoto A, Kaku T, et al. A multi-center retrospective study of neuroendocrine tumors of the uterine cervix: Prognosis according to the new 2018 staging system, comparing outcomes for different chemotherapeutic regimens and histopathological subtypes. *Gynecol Oncol*. (2019) 155:444–51. doi: 10.1016/j.ygyno.2019.09.018

24. Dong M, Gu X, Ma T, Mi Y, Shi Y, Fan R. The role of radiotherapy in neuroendocrine cervical cancer: SEER-based study. *Sci Prog*. (2021) 104:368504211009336. doi: 10.1177/00368504211009336

frontiers | Frontiers in Oncology

TYPE Case Report
PUBLISHED 16 September 2024
DOI 10.3389/fonc.2024.1458817

Check for updates

OPEN ACCESS

EDITED BY
Dragos Eugen Georgescu,
Carol Davila University of Medicine and Pharmacy, Romania

REVIEWED BY
Angelo Finelli,
ULSS2 Marca Trevigiana, Italy
José Luis Sánchez Iglesias,
Gynecology Oncology, Spain

*CORRESPONDENCE
Yanhui Lou
louyh@qdu.edu.cn

RECEIVED 03 July 2024
ACCEPTED 26 August 2024
PUBLISHED 16 September 2024

CITATION
Ji S, Yu X, Xia Y, Yin Y, Ge T, Cheng L, Tian C and Lou Y (2024) Case report: Report of a case of female adnexal malignant tumor of Wolffian origin.
Front. Oncol. 14:1458817.
doi: 10.3389/fonc.2024.1458817

COPYRIGHT
© 2024 Ji, Yu, Xia, Yin, Ge, Cheng, Tian and Lou. This is an open-access article distributed under the terms of the Creative Commons Attribution License (CC BY). The use, distribution or reproduction in other forums is permitted, provided the original author(s) and the copyright owner(s) are credited and that the original publication in this journal is cited, in accordance with accepted academic practice. No use, distribution or reproduction is permitted which does not comply with these terms.

Case report: Report of a case of female adnexal malignant tumor of Wolffian origin

Shujun Ji, Xiao Yu, Yufang Xia, Yifan Yin, Tingting Ge, Lihua Cheng, Cui Tian and Yanhui Lou*

Department of Obstetrics & Gynecology, The Affiliated Hospital of Qingdao University, Qingdao, China

A 33-year-old young woman with a rare female appendage tumor of suspected Wolffian origin was initially diagnosed with a benign lesion after the resection of a tubal lesion due to the benign cytomorphology of the tumor tissue. However, 1 year after surgery, she was diagnosed with stage IV fallopian tube cancer due to a recurrence, which presented with substantial ascites and invasion of multiple organs, including the bilateral ovaries, intestines, pelvic peritoneum, greater omentum, and appendix. After tumor cytoreduction, the patient responded well to treatment, which included a regimen of platinum-based drugs combined with docetaxel, aromatase inhibitors such as letrozole, antihormonal therapy, and targeted therapy with bevacizumab.

KEYWORDS

female adnexal tumors, Wolffian tumors, tubal malignancies, targeted therapy, immunotherapy

Case presentation

On Lunar 4, 2021, a 33-year-old patient, presented to our hospital with a pelvic mass discovered half a month earlier. Tumor markers tests revealed normal levels for CA125 (42.9 U/mL), on April 29, 2021, a laparoscopic debulking of the left tubal mesosalpinx tumor was performed. During the operation, a cystic solid mass measuring approximately 8 × 6 cm was identified in the left tubal lining and completely excised. The postoperative pathology findings revealed (left fallopian tube mesentery) the following: solid sheets or microcystic structures, glandular arrangement, mild cellular heterogeneity, occasional nuclear schizophrenia, focal tumor growth around blood vessels, consistent cell morphology and size, and visible nuclear grooves. The provisional diagnosis suggested gonadal-mesenchymal tumors, with a consideration of adult-type granulosa cell tumors, measuring 3 × 2 × 0.8 cm. Immunohistochemistry results showed the following findings: ER (estrogen receptor, ++, 60%), PR (progesterone receptor, ++, 60%), CKpan (+), Ki-67

(+, 20%), Calretinin (+), CD10 (partially +), and CD10 (partial +), Vimentin (+), β-Catenin (membrane +), Inhibinα (+). Due to the mild cell morphology and insignificant tumor heterogeneity observed under the microscope, the diagnosis was difficult. Following pathology consultations with the University of Pittsburgh Medical Center (UPMC) and the People's Hospital of Peking University, a female adnexal tumor (Wolffian tumor) of mesonephric origin was considered. This diagnosis was based on the patient's young age and nulliparous status, and the absence of heterogeneity in the morphology of the tumor cells under the microscope. The tumor was completely excised during the operation, and the patient was advised to undergo regular postoperative reviews and follow-up appointments. The patient had no abnormality in the whole abdomen enhanced computed tomography (CT) in March after surgery and positron emission tomography (PET)-CT in June after surgery.

One year after surgery, due to sudden abdominal distension, the patient underwent a whole abdomen CT, which revealed multiple malignant tumors in the pelvis, indicating extensive metastasis to retroperitoneal lymph nodes, peritoneum, and greater omentum. A chest CT revealed enlarged lymph nodes in the right cardiophrenic angle area, with potential metastasis; the tumor was considered to be recurrent with malignant changes. Tumor marker levels were elevated CA125(453.9 U/mL). On May 10, 2022, an open laparotomy was performed. During the operation, approximately 4000 mL of reddish ascites was seen in the pelvis. The size of the uterine corpus was normal with scattered granular nodules on the surface. An exophytic granular mass approximately 12 cm in diameter was seen in the right adnexal area, and an 8 cm diameter mass in the left adnexal area, with histological structures that were difficult to recognize and no typical tubal-ovarian tissues detected. Furthermore, a 6 cm diameter granular mass was detected in the uterine rectal sulcus. The peritoneum of the uterine rectal recess and the bladder and uterus exhibited nodular thickening. The greater omentum was markedly thickened with granular nodules scattered across its surface. The omentum of the splenic region was markedly thickened, and 2 cm metastatic nodules were seen at the lower level of the spleen. The appendix was markedly thickened, with granular nodules visible on its surface. Furthermore, granular nodules were observed throughout the pelvic and abdominal peritoneum, at the diaphragmatic apex, in the hepatic and renal crypts, along the hepatic ligament, the perihepatic peritoneum, the perisplenic peritoneum, the small bowel, the colon, and mesenteric membrane, ranging 0.2-3 cm in diameter. Granular nodules, most of which were loosely attached to the metastatic site, and enlarged lymph nodes of approximately 5 × 4 cm in size were found on the left side of the abdominal aorta and below the renal vessels, which were fixed, and no obvious enlargement of the pelvic lymph nodes was detected as shown in Figure 1. During intraoperative cryopathology, neoplastic lesions were identified both in the left and right adnexa. These lesions exhibited morphology similar to the previously diagnosed left tubal mesenchymal tumors but with increased heterogeneity and prominent nuclear fission. The opinion was malignant, and female adnexal tumors of mesonephric (Wolffian duct) origin or gonadal-mesenchymal tumors (with malignant biological behavior) were considered. Since the patient was infertile, after explaining her condition to her family, she underwent tumor cytoreductive surgery (R1). This included bilateral adnexectomy, total extrafascial hysterectomy, lymph node dissection (pelvic, para-abdominal aorta, presacral), resection of pelvic metastases, omentectomy, appendectomy, and hyperthermic perfusion chemotherapy for cancer. The postoperative pathological examination revealed the following findings: (1) (Bilateral) ovarian neoplastic lesions with microscopic tumor cells arranged in sieve-like, reticulum-like, solid sheets or tubules, with heterogeneous cells, prominent nuclei, and easily visible nuclear schizophrenic images, suggesting a diagnosis of Wolffian duct tumors. (2) Tumor infiltration was identified in intestinal surface nodules, pelvic masses, pelvic peritoneum, appendix, and greater omentum. (3) Lymph node metastases were detected below the renal artery and in the para-aortic region (2 out of 2 lymph nodes). Immunohistochemistry results revealed the following: CKpan (+), Vimentin (partially +), ER (++, about 30%), PR (++, about 15%), Calretinin (+), Inhibin α (a small amount of +), CD10 (+), β-Catenin (membrane +), and Ki-67 (+, 40%) as shown in Figure 2. The final diagnosis was a malignant tumor of the fallopian tube (stage IV).

Diagnostic process

Following postoperative genetic testing, the results indicated 11 somatic cell variants, of which 9 were identified as clinically significant variants. These variants include CHEK1, NF2, ATM, STK11, ZNF217, BCL2L1, TP53, JAK1, and POLD1. The treatment options may involve chemotherapeutic drugs such as cyclophosphamide, fluorouracil, and platinum compounds. Targeted drugs such as temsirolimus (D), olaparib (C), antivascular agents such as bevacizumab, and endocrine therapies such as anastrozole and letrozole are considered effective. On June 1, 2022, the patient underwent 3 cycles of intravenous "albumin paclitaxel + carboplatin" and the second course of "bevacizumab" antiangiogenic therapy was initiated. After 3 cycles of chemotherapy, the tumor markers exhibited a continuous decline and the size of metastatic lesions improved (PR). However, due to intolerable side effects, the treatment plan was adjusted to include "dormethrin + cyclophosphamide + bevacizumab," and after 3 cycles of chemotherapy, the levels of CA125, NSE, and SCC slowly increased. A whole-abdomen enhanced CT scan revealed new tumor metastases in the perihepatic peritoneum, the bilateral internal mammary arterial routes, and the angle of the heart and diaphragm. These findings indicate disease progression (PD), prompting evaluation of the treatment effectiveness. Due to disease progression and the patient's positive status for ER and PR, the treatment regimen was changed in October 2022. The patient received 5 courses of intravenous chemotherapy consisting of "docetaxel + nedaplatin + bevacizumab" combined with antihormonal therapy using "anastrozole." The review showed that the tumor size was similar to that of the previous one (SD) with no evident tumor size progression. However, due to severe side effects of chemotherapy that the patient could not tolerate, the treatment was transitioned to 5 courses of antivascular treatment with "bevacizumab" starting in March 2023. However, the tumor

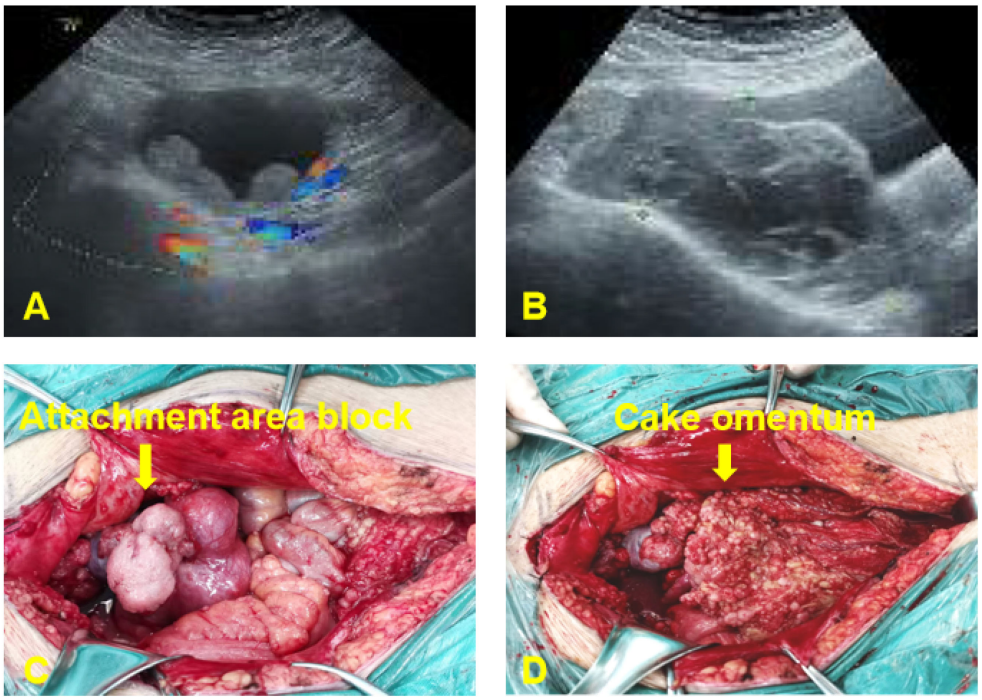

FIGURE 1
Preoperative ultrasound examination and intraoperative investigation of the patient. **(A)** Lunar 4, 2021: A 7.0*7.6 cm cystic mass was found in the upper left part of the uterus, with a thick cyst wall and multiple slightly hyperechoic protrusions. **(B)** May 10, 2022: A 12.8x10.1x5.8 cm solid cystic mass with a detached and multilocular cystic portion was present in the right adnexal region. The mass crosses the anterior aspect of the uterus and involves the left ovary. **(C)** Exophytic granular masses in the adnexal region bilaterally. **(D)** Granular metastatic nodules in the greater omentum.

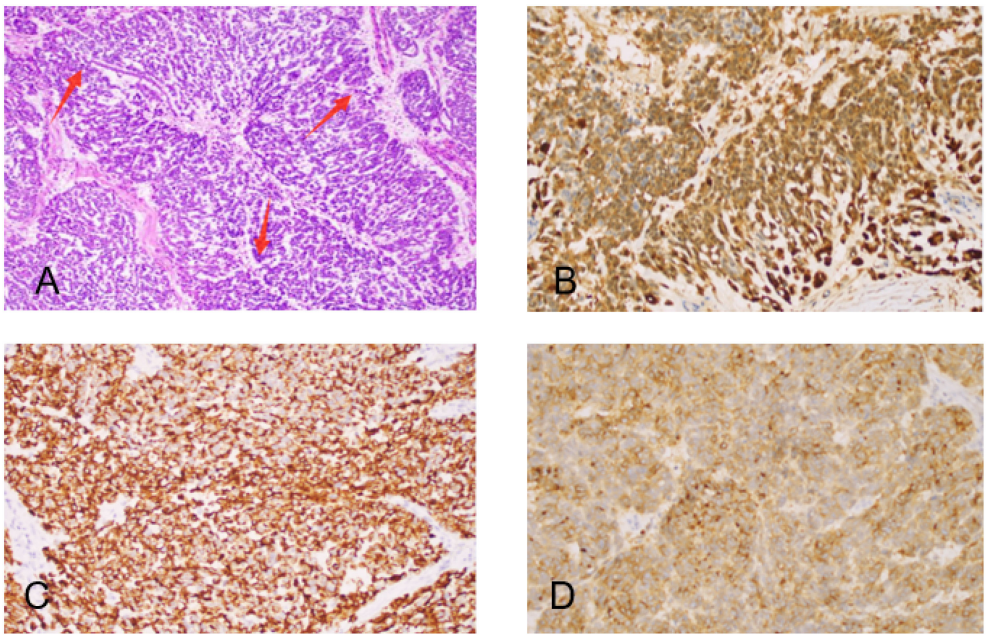

FIGURE 2
Hematoxylin-eosin staining and Immunohistochemical staining (both 400+). **(A)** High magnification micrograph showing medium-sized oval tumor cells with eosinophilic cytoplasm, atypical nuclei, prominent nucleoli, pronounced nuclear grooves, and increased mitotic activity (red arrowheads). **(B)** Calretinin positivity. **(C)** focal CK positivity. **(D)** CD10+ positivity.

markers continued to rise, and new lesion progression (PD) was observed during the maintenance treatment phase as shown in Figure 3.

In June 2023, the patient was admitted to the emergency room with chest pain, and a chest CT scan revealed pleural effusion, pleural metastasis, and peritoneal metastasis. Furthermore, the original metastatic foci in the pelvic and abdominal cavities had increased in size compared to previous assessments, indicating further tumor progression. After discontinuing anastrozole endocrine treatment, the patient underwent chemotherapy again in June 2023, given the use of platinum-containing drugs within the last 3 months, the patient was given 3 courses of treatment of gemcitabine on days 1 and 8 in combination with bevacizumab. However, subsequent evaluations indicated continued progression of the metastatic lesions (PD). On September 4, 2023, the treatment of "gemcitabine d1, d8 + oxaliplatin" was replaced, alongside oral lenvatinib at 8 mg once daily. After completing 4 cycles of this treatment, a CT scan indicated a partial reduction in metastatic lesions compared to previous assessments, and the tumor markers gradually declined, indicating a PR status to the treatment. However, the patient discontinued chemotherapy due to the side effects associated with the treatment. Considering the poor response to anastrozole, the patient's treatment was adjusted on November 20, 2023, to oral maintenance therapy of lenvatinib 12 mg qd combined with letrozole 2.5 mg qd, and the patient has been treated with this regimen for 7 months, with the metastatic lesions progressively reduced, and the tumor markers, such as CA125, have continued to decrease to normal levels, with remarkable therapeutic effects as shown in Figure 4. The patient has now survived for 36 months since the onset of the disease and remains in continuous remission. He is advised to have regular reviews and follow-ups.

Discussion

Wolffian tumor (WAT) is a rare gynecological tumor characterized by the simultaneous presence of various epithelial cells (1), occurring in the remnant tissue of the rich mesonephric ducts (2), mostly in the broad ligament, tubal mesentery, fallopian tubes, ovaries, and peritoneum (3), with malignant possibilities. This tumor generally expresses CK, calretinin, inhibin, CD10, and vimentin (4). However, the expression of ER and PR can vary from strong positive to negative. Due to the rarity of this tumor, there is no specific immunohistochemical staining to diagnose this tumor. Currently, the recommended treatment approach involves total hysterectomy along with double adnexal resection (5), which should be followed up closely for a long period in the clinic.

There are only one hundred cases of Wolffian tumors reported in the literature so far, and there is no uniform standard for clinical treatment. The patient in this case was young, and close observation was taken after the initial operation according to the pathology and the willingness to treat, but the tumor showed malignant biological behavior and recurrence. Based on genetic testing results and evaluation of clinical and test indicators, we found that the combination of platinum-based drugs with other chemotherapeutic drugs (6), such as albumin paclitaxel combined with carboplatin, docetaxel combined with oxaliplatin, etc., have shown favorable therapeutic effects. The antiangiogenic drug bevacizumab was integrated into the initial treatment regimen (a total of 18 courses of treatment). The therapeutic effects were greatly affected by adjustments made to the chemotherapy regimen during the combined application of these agents. The change in chemotherapy regimen affected the treatment outcomes in this case. Initially, the patient experienced disease progression shortly after switching to

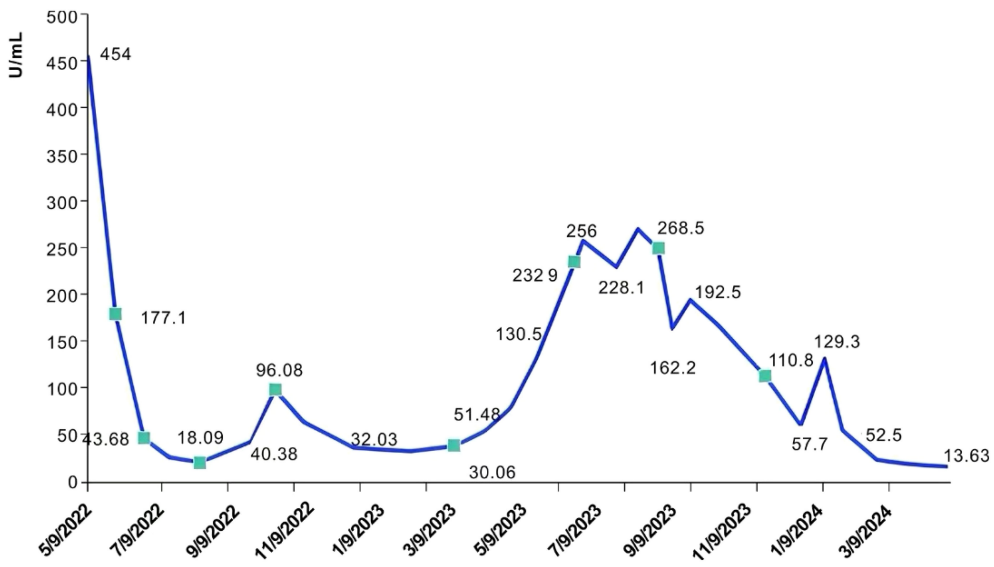

FIGURE 3
Curve of CA125 with treatment regimen. Tumor cell reduction (R1) was performed in May 2022, with the preoperative tumor marker value as the baseline. The treatment regimen included: (1) 1 course of treatment with "albuminpaclitaxel + carboplatin" followed by 2 courses of treatment with "albuminpaclitaxel + carboplatin + bevacizumab"; (2) 3 courses of "Domene + cyclophosphamide + bevacizumab"; (3) 5 courses of "Docetaxel + Nedaplatin + bevacizumab"; (4) 5 courses of "bevacizumab" maintenance treatment; (5) 3 courses of "gemcitabine + bevacizumab"; (6) 4 courses of Gemcitabine + oxaliplatin + Renvastinib; and (7) 4 months treatment with "Letrozole + lenvatinib".

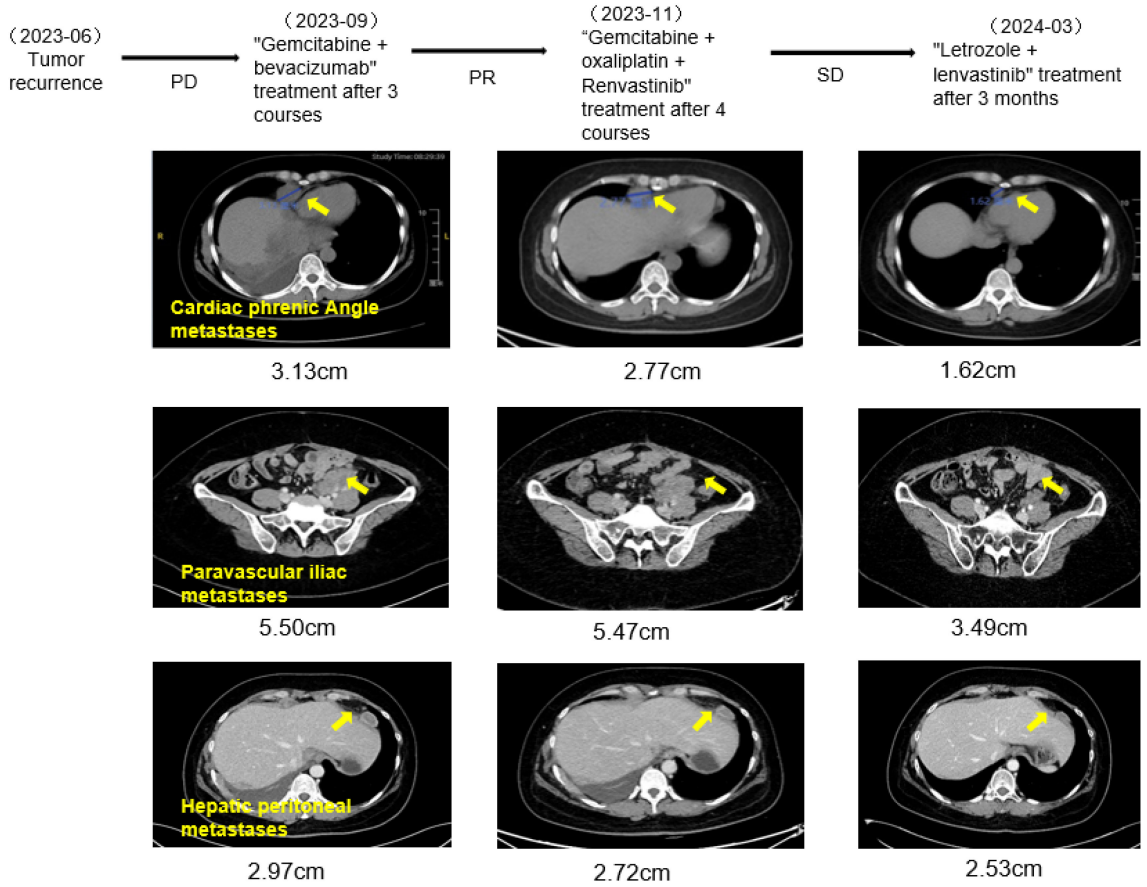

FIGURE 4
CT examination of the patient (the trend of lesion change with the change of treatment regimen).

single-agent maintenance therapy with bevacizumab. Subsequent attempts to combine different chemotherapy agents did not yield satisfactory clinical results. Lenvatinib is a tyrosine kinase inhibitor with dual target inhibition properties (7–10), acting on vascular endothelial growth factor (VEGF), fibroblast growth factor (FGF), rearranged during transfection (RET), and other pathways. It can not only inhibit tumor angiogenesis but also regulate the tumor immune microenvironment to enhance the antitumor immune response (11). After the patient's disease progressed, the combination of lenvatinib with chemotherapy led to significant remission, and the patient's condition was ideally controlled. The patient is still in remission while receiving maintenance therapy with letrozole. It has been shown that endocrine therapy is indicated for patients with recurrent gynecologic tumors that express estrogen receptor (ER^+) (12). In this case, the patient initially received a regimen combining anastrozole (13) with chemotherapy after experiencing progression on initial therapy. However, due to continued disease progression, this treatment was discontinued. Currently, the patient is receiving a maintenance regimen consisting of letrozole in combination with lenvatinib, which is clinically effective with no new signs of disease progression observed. This response was unexpected and we look forward to a more durable clinical benefit for the patient.

Therefore, for advanced or recurrent Wolffian tumors, a combination of platinum-based chemotherapy combined with antivascular drugs and endocrine therapy appears promising in providing patients with a longer survival benefit. However, further follow-up and collection of additional clinical data are essential to validate the long-term efficacy. Physicians should strive to achieve the best therapeutic outcomes by delaying tumor progression and extending patient survival.

Data availability statement

The raw data supporting the conclusions of this article will be made available by the authors, without undue reservation.

Ethics statement

The studies involving humans were approved by The Ethics Committee of the Affiliated Hospital of Qingdao University approved this study, ethics no. QYFY WZLL 28912. The studies were conducted in accordance with the local legislation and institutional requirements. The participants provided their written informed consent to participate in this study. Written informed consent was obtained from the individual(s) for the publication of any potentially identifiable images or data included in this article.

Author contributions

SJ: Conceptualization, Methodology, Investigation, Formal analysis, Writing – original draft. XY: Data Curation, Writing – original draft. YX: Data Curation, Writing – original draft. YY: Formal analysis, Writing – review & editing. TG: Writing – original draft. LC: Methodology, Investigation, Writing – review & editing. CT: Investigation, Resources, Writing – review & editing. YL: Conceptualization, Resources, Writing – review & editing.

Funding

The author(s) declare that no financial support was received for the research, authorship, and/or publication of this article.

Conflict of interest

The authors declare that the research was conducted in the absence of any commercial or financial relationships that could be construed as a potential conflict of interest.

Publisher's note

All claims expressed in this article are solely those of the authors and do not necessarily represent those of their affiliated organizations, or those of the publisher, the editors and the reviewers. Any product that may be evaluated in this article, or claim that may be made by its manufacturer, is not guaranteed or endorsed by the publisher.

References

1. Gardner GH, Greene RR, Peckham B. Tumors of the broad ligament. *Am J Obstet Gynecol.* (1957) 73:536–54. doi: 10.1016/S0002-9378(16)37427-0

2. Kariminejad MH, Scully RE. Female adnexal tumor of probable Wolffian origin. A distinctive pathologic entity. *Cancer.* (1973) 31:671–7. doi: 10.1002/(ISSN)1097-0142

3. Heatley MK. Is female adnexal tumour of probable wolffian origin a benign lesion? *A Systematic Rev English Literature Pathol.* (2009) 41:645–8. doi: 10.3109/00313020903273084

4. Devouassoux-Shisheboran M, Silver SA, Tavassoli FA. Wolffian adnexal tumor, so-called female adnexal tumor of probable Wolffian origin (FATWO): immunohistochemical evidence in support of a Wolffian origin. *Hum Pathol.* (1999) 30:856–63. doi: 10.1016/S0046-8177(99)90148-X

5. Montagut C, Mármol M, Rey V, Ordi J, Pahissa J, Rovirosa A, et al. Activity of chemotherapy with carboplatin plus paclitaxel in a recurrent mesonephric adenocarcinoma of the uterine corpus. *Gynecol Oncol.* (2003) 90:458–61. doi: 10.1016/S0090-8258(03)00228-2

6. Deshimaru R, Fukunaga T, Sato T, Morinaga S, Takahashi M. A case of metastatic female adnexal tumor of probable Wolffian origin. *Gynecol Oncol Rep.* (2014) 10:22–4. doi: 10.1016/j.gore.2014.07.001

7. Rosen C, Reardon E, Shyu S, Terhune J, Saats P, Ioffe O, et al. Wolffian tumor (female adnexal tumor of Wolffian origin) presenting as a pelvic side wall mass: Report of a case. *SAGE Open Med Case Rep.* (2019) 7:3–5. doi: 10.1177/2050313X19839534

8. Liu L, Fang Q, Xing Y. Female adnexal tumor of probable Wolffian origin arising from mesosalpinx: A case report and review. *J Obstet Gynaecol Res.* (2018) 44:1859–63. doi: 10.1111/jog.13704

9. Wakayama A, Matsumoto H, Aoyama H, Saio M, Kumagai A, Ooyama T, et al. Recurrent female adnexal tumor of probable Wolffian origin treated with debulking surgery, imatinib and paclitaxel/carboplatin combination chemotherapy: A case report. *Oncol Lett.* (2017) 13:3403–8. doi: 10.3892/ol.2017.5874

10. Syriac S, Durie N, Kesterson J, Lele S, Mhawech-Fauceglia P. Female adnexal tumor of probable Wolffian origin (FATWO) with recurrence 3 years postsurgery. *Int J Gynecol Pathol.* (2011) 30:231–5. doi: 10.1097/PGP.0b013e3182005340

11. Xu J, Shen J, Gu S, Zhang Y, Wu L, Wu J, et al. Camrelizumab in combination with apatinib in patients with advanced hepatocellular carcinoma (RESCUE): A nonrandomized, open-label, phase II trial. *Clin Cancer Res.* (2021) 27:1003–11. doi: 10.1158/1078-0432.CCR-20-2571

12. George A, McLachlan J, Tunariu N, Della Pepa C, Migali C, Gore M, et al. The role of hormonal therapy in patients with relapsed high-grade ovarian carcinoma: a retrospective series of tamoxifen and letrozole. *BMC Cancer.* (2017) 17:456. doi: 10.1186/s12885-017-3440-0

13. Kok PS, Beale P, O'Connell RL, Grant P, Bonaventura T, Scurry J, et al. PARAGON (ANZGOG-0903): a phase 2 study of anastrozole in asymptomatic patients with estrogen and progesterone receptor-positive recurrent ovarian cancer and CA125 progression. *J Gynecol Oncol.* (2019) 30:e86. doi: 10.3802/jgo.2019.30.e86

frontiers | Frontiers in Oncology

TYPE Case Report
PUBLISHED 20 September 2024
DOI 10.3389/fonc.2024.1465130

Check for updates

OPEN ACCESS

EDITED BY
Lidia Castagneto Gissey,
Sapienza University of Rome, Italy

REVIEWED BY
Bilgin Kadri Aribas,
Bülent Ecevit University, Türkiye
Helmut Schöllnast,
Medical University of Graz, Austria

*CORRESPONDENCE
Luigi Formisano
luigi.formisano1@unina.it

RECEIVED 15 July 2024
ACCEPTED 03 September 2024
PUBLISHED 20 September 2024

CITATION
Flauto F, Servetto A, Bianco R and Formisano L (2024) Malignant granular cell tumor of chest wall: a case report. *Front. Oncol.* 14:1465130. doi: 10.3389/fonc.2024.1465130

COPYRIGHT
© 2024 Flauto, Servetto, Bianco and Formisano. This is an open-access article distributed under the terms of the Creative Commons Attribution License (CC BY). The use, distribution or reproduction in other forums is permitted, provided the original author(s) and the copyright owner(s) are credited and that the original publication in this journal is cited, in accordance with accepted academic practice. No use, distribution or reproduction is permitted which does not comply with these terms.

Malignant granular cell tumor of chest wall: a case report

Fabiano Flauto, Alberto Servetto, Roberto Bianco and Luigi Formisano*

Department of Clinical Medicine and Surgery, University of Naples Federico II, Naples, Italy

Background: Granular Cell Tumors (GCTs), also known as Abrikossoff tumors, are rare neoplasms that typically originate from Schwann cells. These tumors most commonly occur in the head and neck region, particularly the tongue. While GCTs are generally benign, less than 2% of cases exhibit aggressive biological features such as rapid growth, high recurrence rates, and metastasis. In this report, we present a rare case of a Malignant Granular Cell Tumor (MGCT) of the chest wall, which posed significant challenges in both characterization and management.

Case Presentation: A fifty-year-old man underwent an ultrasound examination for a nodular mass on his right chest wall. The ultrasound revealed a firm, hard mass measuring 2 cm x 2 cm with an uncertain diagnosis. A fine-needle aspiration biopsy (FNAB) guided by ultrasound was performed, resulting in a diagnosis of Abrikossoff tumor. The patient subsequently underwent radical excision of the mass, which confirmed the initial diagnosis. Nine months after surgery, a new mass with similar characteristics was detected during a physical examination. The patient underwent a second surgery, but this time the histopathological examination was negative for neoplastic cells. However, another mass appeared at the same site as the previous surgical excision. A CT scan and MRI of the right chest wall confirmed the presence of a 2 cm x 2 cm nodular mass. The patient then underwent a deeper excision. Histomorphological and immunohistochemical assessments confirmed the recurrence of MGCT.

Conclusion: This case highlights the malignant potential of GCTs. The numerous local recurrences necessitated three surgeries and additional procedures. The aggressive nature of this pathology underscores the complexity of managing these tumors, which are poorly understood and lack proven post-operative strategies for controlling local and distant disease.

KEYWORDS

rare tumor, skin tumor, granular cell tumor (Abrikosov tumor), recurrent granular cell tumor, multidiscipliary team

10.3389/fonc.2024.1465130

Introduction

Granular Cell Tumors (GCTs) are rare, generally benign neoplasms of neural origin, most likely arising from Schwann cells (1). GCTs constitute approximately 0.5% of all soft tissue tumors and most commonly occur in adults aged 30 to 50, with a slight predominance in females. Although GCTs can develop in any part of the body, they are most frequently found in the head and neck region, particularly the tongue, which is the most common single site. Diagnosis of GCTs is primarily based on histopathological examination following a biopsy. The mainstay of treatment for GCTs is surgical excision with clear margins to prevent recurrence, and complete excision is generally curative for benign GCTs (2). Malignant GCTs, accounting for less than 2% of all GCTs, require more aggressive treatment, including wider surgical resection and may benefit from adjuvant radiotherapy or chemotherapy (3). This article aims to present an uncommon case of a chest wall MGCT and its complex, multidisciplinary management. We report this case in accordance with the CARE reporting checklist.

Case presentation

A fifty-year-old man, who smoked fifteen cigarettes a day and had no significant medical history, presented with a firm, nodular mass on his right chest wall, in the submammary region. During the physical examination, a well-defined, hard-ligneous nodular area approximately 2 cm in diameter was detected on the right chest wall, inferior and lateral to the nipple-areola complex.

There was no ulceration or pigmentation of the overlying skin. There was no palpable peripheral lymphadenopathy. The patient had no systemic complaint. Routine hematological and biochemical investigations were normal.

An ultrasonographic evaluation of the right chest wall (Figure 1) revealed a hypoechogenic nodular mass with irregular margins, expanding in the subcutaneous plane and above fascial planes, measuring approximately 2 cm x 2 cm, with no signal on Color-Doppler analysis. No direct invasion was seen in the muscle or overlying skin. The differential diagnosis was very difficult, given the clinical features of the nodular mass.

In August 2022, an ultrasound-guided needle biopsy of the right chest wall, targeting the lower external quadrant of the breast, was performed, yielding a 1 cm tissue sample. The histopathologic diagnosis confirmed GCT. Immunohistochemical analysis revealed positivity for S100 and TFE3, and negativity for cytokeratins AE1/AE3, CD163, desmin, and MART1, with a Ki-67 proliferative index of 2%. These features were suggestive of GCT.

In October 2022, the patient underwent surgical excision. A 4 cm x 1.5 cm x 1.5 cm skin lozenge and a 3 cm x 2.5 cm fibro-yellowish nodular tissue were removed. The latter contained a nodular formation with a maximum diameter of 2 cm. Pathological examination showed fibroadipose and striated muscle tissue with neoplastic proliferation, exhibiting expansive and focally infiltrative margins. The lesion consisted of polygonal cells with eosinophilic cytoplasm and intracytoplasmic granules, organized in laminae. No necrosis or atypical mitoses were observed. The skin overlying the lesion was free from significant histopathological changes. Immunohistochemical analysis revealed positivity for S100 and CD68, and negativity for Cytokeratin PAN, with a Ki-67 index of 10%. The diagnosis was consistent with GCT with neoplastic infiltration of surgical margins (Figure 2).

In November 2022, a secondary surgical procedure was performed to enlarge the excision margins around the right breast region. The excised specimen measured 6 cm x 1 cm x 0.5 cm, including a central surgical scar of 4 cm. Pathological examination revealed dermal scar fibrosis with no residual neoplastic tissue.

Considering the unusual behavior of this neoplasm and the uncertainty of its histology, we requested a revision of the tissue samples from a center with high expertise in GCT and soft tissue neoplasms. This analysis suggested a diagnosis of MGCT. Given the aggressive biology of the tumor, the patient was monitored closely

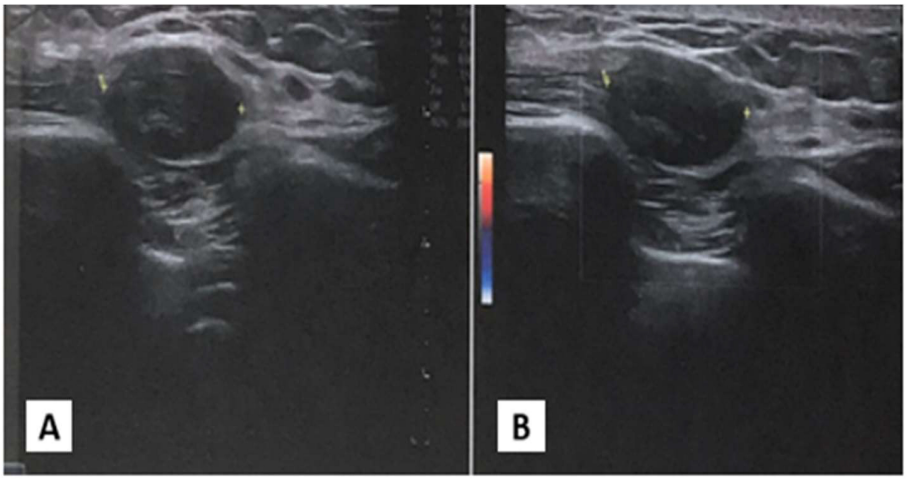

FIGURE 1
Ultrasonography of chest wall. **(A)** Ipoechoic soprafascial nodular mass with 2 cm x 2xm of diameter. **(B)** Absence of signal to Color Doppler examination.

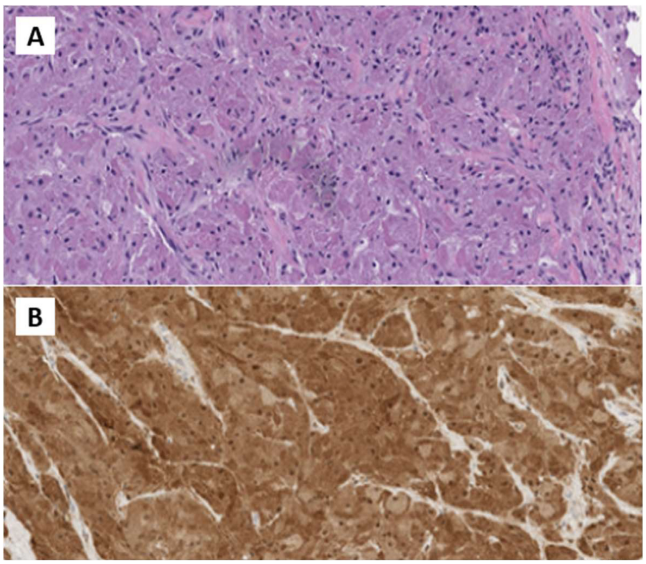

FIGURE 2
(A) H&E Medium power microphotographs demonstrating sheets or nests of large, polygonal tumor cells with abundant slightly basophilic and granular cytoplasm and vesicular nuclei infiltrating among skeletal muscle fibers. **(B)** Immunostained microphotograph showing that the tumor granular cells were positive for S-100 prote.

with physical examinations and ultrasonographic monitoring of the percutaneous and scar region.

In August 2023, nine months post-surgery, a new nodule was detected at the previous surgical scar on the right chest wall. The nodule was firm, non-mobile, and consistent with previous findings. Chest wall ultrasonography revealed a hypoechogenic, subcutaneous, suprafascial nodular formation approximately 18 mm in diameter, suggestive of recurrent neoplastic disease.

In September 2023, an excision of an 8 cm x 2.5 cm skin lozenge from the right submammary site was performed, centered on the surgical scar. Pathological examination revealed skin with dermal scar fibrosis, without any residual neoplastic tissue.

In January 2024, a new nodule was identified at the previous surgical site, resembling prior findings. Ultrasound showed a hypoechogenic, subcutaneous, suprafascial nodular formation approximately 25 mm in diameter, indicative of likely recurrent neoplastic process. A CT scan with contrast (Figure 3) on the same day revealed a 20 mm nodular formation in the QIE of the right breast, in the context of subcutaneous fat, showing inhomogeneous enhancement and adherence to the intercostal muscles and the anterior margin of the right fifth rib, consistent with the known solid lesion from previous assessments.

The patient also underwent an MRI (Figure 4) of the right breast and chest wall with a paramagnetic contrast agent. The MRI revealed an irregular nodular formation, approximately 2.8 cm x 1.4 cm, in the right anterolateral subcutaneous region at the height of the fifth rib at the anterior inferior margin of the pectoralis major. The mass had an inhomogeneous signal, predominantly internal fluid, with intense peripheral enhancement and a soft tissue infiltrating appearance.

In April 2024, a major surgical intervention was performed under total anesthesia. The surgery removed a skin lozenge close to the right chest wall, measuring 6 cm x 2 cm and 5 cm thick. Histopathological examination revealed a nodular lesion with circumscribed margins of 2 cm x 1.3 cm, located in the hypodermal section of the operative specimen. The lesion bordered the deep margin and was largely contained within the other margins of the surgical excision. Microscopically, the morphological picture showed a nodular hypodermal neoplasm consisting of epitheliomorphic cells with characteristic clear cytoplasm, displaying a vaguely nodular solid growth pattern and an infiltrative attitude toward the muscle tissue. There was very little fibrous intercellular component. Immunohistochemical analysis showed positivity for S100, CD68, Inhibin, MITF, TFE3 and negativity for MELANA and CALRETININ. The Ki-67 proliferative index was between 5% and 7%. Histomorphology and immunohistochemical assessment confirmed the recurrence of GCT.

The short-term recurrence indicated aggressive biological behavior of the neoplasm. Genetic analyses using next-generation sequencing (NGS) technology did not reveal any relevant mutations sui for diagnostic characterization or therapeutic strategies.

Despite the major surgery, the patient did not experience significant post-operative complications and achieved a complete recovery. Additionally, there were no functional or aesthetic impairments. In June 2024, the patient underwent a skin and pericardial subcutaneous ultrasound with monitoring of axillary, laterocervical, submandibular, supraclavicular, and inguinal lymph node stations. The examination did not reveal any suspicious elements for disease recurrence.

Following multidisciplinary discussion, there was no indication for adjuvant radiotherapy treatment. The patient was then a candidate for close follow-up with physical esaem and ultrasonography of the scar and pericatricial region, abdomen, and axillary, supraclavicular, laterocervical, and inguinal lymph node stations.

10.3389/fonc.2024.1465130

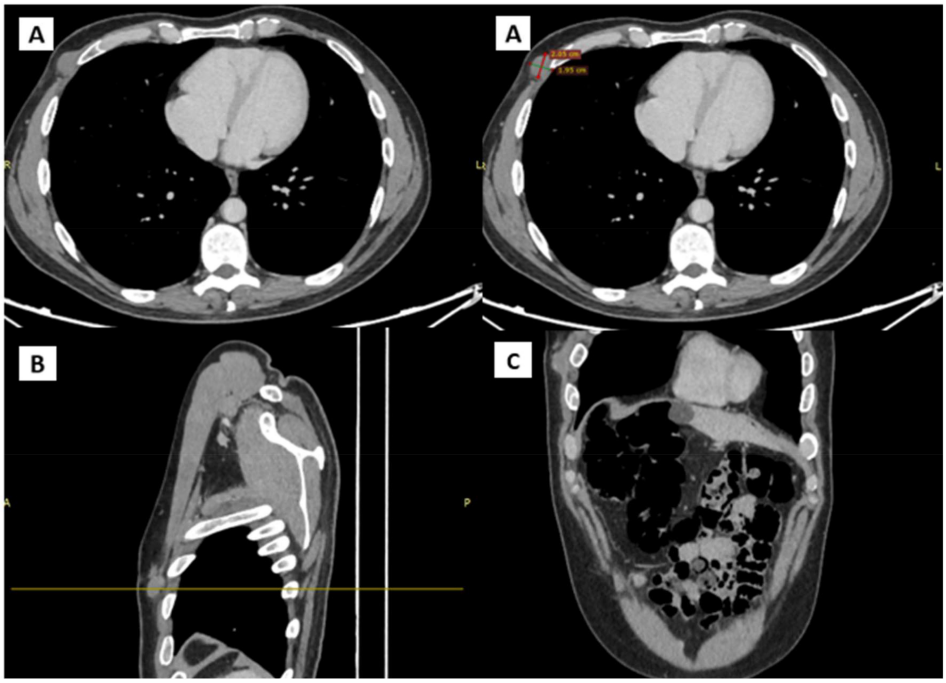

FIGURE 3
CT scans showing the presence and anatomical relation of the heteroplastic mass. **(A)** Transverse plane **(B)** Sagittal plane **(C)** Coronal plane.

Discussion

Granular Cell Tumors (GCTs) are rare neoplasms first described by the Russian pathologist Alexei Abrikossoff in 1926. Typically benign, GCTs constitute a small percentage of all soft tissue tumors, and their exact cause remains a topic of debate. The most widely accepted hypothesis is that GCTs originate from Schwann cells or their precursors, supported by the strong and consistent positivity for S-100 protein, a marker for neural crest-derived cells. GCTs primarily affect adults, with a higher prevalence in females, typically diagnosed between the second and sixth decades of life. The male-to-female ratio ranges from 1:1.8 to 1:2.4, indicating a significant female predilection.

GCTs account for approximately 0.5% of all soft tissue tumors, with only about 1-2% being malignant. They most commonly occur in the head and neck region, particularly the tongue, which accounts for about 40% of cases. Other common locations include the breast (15%), respiratory tract (10%), and esophagus (2%).

The clinical presentation of GCTs varies depending on the tumor location. Most GCTs are asymptomatic and discovered

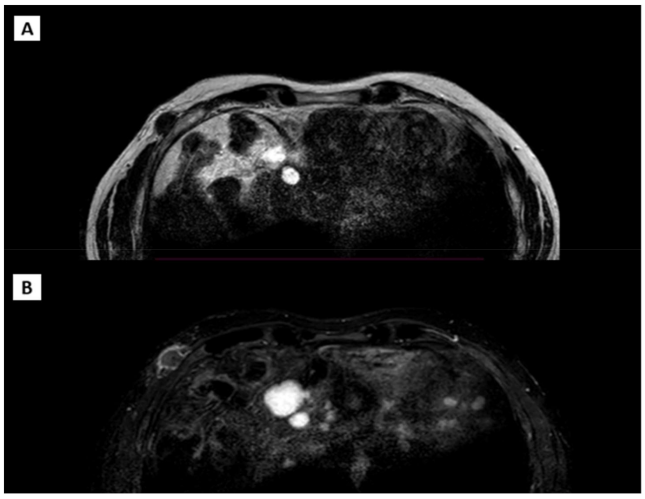

FIGURE 4
(A) T1 weighted acquisition. **(B)** T2 weighted acquisition.

incidentally. When symptoms occur, they may include a painless nodule or mass, discomfort, or functional impairment depending on the anatomical site involved (4). In rare cases, particularly in the gastrointestinal tract, GCTs can cause more serious symptoms like obstruction or bleeding. Diagnosis of GCTs is primarily based on histopathological examination following a biopsy. Imaging studies such as ultrasound, MRI, or CT scans can aid in assessing the tumor size, location, and extent, but are not definitive for diagnosis. Fine-needle aspiration (FNA) can sometimes be used, but its utility is limited due to the granular cell's distinctive features being less apparent in cytological preparations.

The cytological features of GCTs can sometimes make differentiation from other tumors challenging. The cells are generally round to polygonal with abundant, finely granular, eosinophilic cytoplasm (5). The nuclei are round to oval, eccentrically placed, with fine chromatin and occasionally small, inconspicuous nucleoli. These cells typically have indistinct cell membranes and a granular background due to the accumulation of lysosomes and autophagosomes. Under electron microscopy, these granules can be observed along with replicated basal lamina. Immunoistochemically, both benign and malignant tumor cells typically stain positively for S-100, CD68, neuron-specific enolase, CD57, inhibin, calretinin, TFE3, SOX10, and nestin (6, 7).

Malignant GCTs are rare and tend to present as rapidly growing tumors, often larger than 5 cm. The diagnosis of malignant GCTs is based on specific histopathological criteria. According to studies by Fanburg-Smith et al. (5), a tumor is classified as malignant if it exhibits three or more of the following six features: 1) necrosis, 2) presence of spindle cells, 3) mitosis rate of more than 2 per 10 high-power fields, 4) presence of a vesicular nucleus with a large nucleolus, 5) high nucleus-to-cytoplasm (N) ratio, and 6) pleomorphism. If two of these features are present, the tumor is labeled as "atypical GCT."

Whole-exome and targeted sequencing have identified recurrent inactivating mutations in ATP6AP1, ATP6AP2, and ATP6V0C in up to 72% of GCTs (8, 9). These mutations in Schwann cells, when replicated *in vitro*, not only triggered oncogenesis through increased phosphorylation of PDGFR-B, SFK, and STAT-5 but also led to impaired vesicle acidification, disrupted endocytosis, and the accumulation of intracytoplasmic granules. It's also hypothesized that the nuclear localization and activation of MITF/TFE3, caused by V-ATPase dysfunction, might contribute to GCT development, as TFE3 gene fusions and the nuclear presence of resulting fusion proteins are seen in various sarcomas. These mutations, found in less than 0.1% of other cancers, are considered diagnostic of GCTs (8–10). The disruption of ATP6AP1, ATP6AP2, and ATPV0C impairs the V-ATPase (H+ ATPase) complex, reducing lysosomal activity. This disruption not only aligns with the typical cytoplasmic characteristics but also explains the tumor's positive immunohistochemical staining for TFE3 and wild-type MITF, as lysosomal inhibition activates the transcription factors MITF, TFE3, and TFEB (8, 9).

Mutations in genes associated with the TGFβ and MAPK pathways have also been reported. Loss-of-function mutations in TGFBR1, TGFBR2, and LTBP2 can allow cells to evade the inhibitory effects of TGF-β, leading to increased cell proliferation. Additionally, a loss-of-function mutation in MAP3K15 has been identified, which is thought to promote tumor cell survival by preventing apoptosis. Both the TGFβ and MAPK pathways are crucial in regulating the cell cycle, tumor formation, and metastasis in many cancers. While these pathways typically have opposing roles TGFβ inhibits cell proliferation, whereas MAPK promotes it in the context of malignant transformation, they appear to support each other, with TGFβ shifting from a tumor suppressor to a promoter of metastasis (11).

The PIK3CA gene encodes the catalytic subunit of phosphatidylinositol-3 kinase (PI3K), which is activated by various tyrosine kinase receptors, including EGFR, ERBB2 (HER2), RET, MET, and VEGFR. PI3K then initiates downstream AKT/mTOR signaling, which promotes cell survival, proliferation, growth, and motility. In malignant GCTs, alterations in key oncogenes such as TP53 and PIK3CA have been observed, whereas these genes remain unaltered in benign GCTs (10).

GCTs also express markers such as CD63, LC3 (a specific marker of autophagy), and the antigen-presenting cell marker HLA-DR. Strong immunoreactivity for HLA-DR and CD68 suggests that GCTs may exhibit an antigen-presenting cell (APC) phenotype. HLA-DR is typically expressed by APCs (like monocytes, macrophages, and dendritic cells), B lymphocytes, and activated T lymphocytes. The significance of these findings is still debated. It's possible that, in addition to CD68, HLA-DR immunoreactivity might be reactive and play a role in antigen presentation during the innate immune response in GCTs. Alternatively, HLA-DR expression could be a positive prognostic marker for survival, or it might indicate epithelial–mesenchymal transformation, suggesting tissue dedifferentiation rather than involvement in tumor antigen presentation (12).

Understanding these molecular alterations is crucial for advancing research and developing systemic therapies.

The mainstay of treatment for GCTs is surgical excision with clear margins to prevent recurrence. Complete excision is generally curative for benign GCTs. Malignant GCTs, which are exceedingly rare, require more aggressive treatment, including wider surgical resection, and may benefit from adjuvant radiotherapy or chemotherapy. The prognosis for benign GCTs is excellent, with a very low recurrence rate when adequately excised. Malignant GCTs, however, have a poorer prognosis, with higher rates of recurrence and metastasis (13).

For recurrent cases, additional surgery may be necessary. Close follow-up is essential to monitor for recurrence, particularly in cases where the initial excision was incomplete. Radiation therapy is generally not used for benign GCTs due to their indolent nature. However, it may be considered for malignant GCTs, especially when surgical margins are positive, or the tumor is unresectable. The use of adjuvant radiotherapy (dose not specified) after local excision of a large (5 cm) GCT has also been reported, with no evidence of recurrence or metastasis at 5 years (14). However, further investigation will be needed in order to better define the role of radiotherapy in the management of GCT.

The efficacy of classic cytotoxic chemotherapy in clinically malignant GCTs seems very limited, based on the published evidence, with few cases reported in the literature achieving a

notorious dimensional response (15, 16). In literature are described sporadic cases of response to gemcitabine plus paclitaxel (6) and carboplatin plus etoposide (16, 17). Metastatic GCTs are relatively chemo-resistant; however, there is growing evidence of the benefit of using pazopanib and other targeted therapies in this histology (18).

Alterations in the MAPK (10, 11), PI3K (10), TGFβ (10, 11) pathways, and the description of VATPase (8, 9) variants are considered promising therapeutic targets that may provide novelties in the near future.

This case underscores the malignant potential and aggressive biological behavior of GCTs. The patient required multiple surgical interventions due to recurrent disease. Despite the generally benign nature of most GCTs, this case of MGCT demonstrated a propensity for rapid recurrence and infiltrative growth, posing significant challenges in management. The aggressive course of this MGCT highlights the necessity for vigilant long-term follow-up and comprehensive management strategies, including the potential use of advanced imaging techniques and possibly adjuvant therapies, even though they are not conventionally applied in benign cases. Genetic analyses, although not revealing actionable mutations in this instance, may become increasingly relevant as our understanding of the molecular underpinnings of GCTs evolves.

Conclusion and patient perspective

In conclusion, this case exemplifies the complexity of diagnosing and treating MGCTs, emphasizing the need for a multidisciplinary approach and the consideration of more aggressive therapeutic strategies to manage such rare but potentially life-threatening neoplasms. Continued research and clinical awareness are essential to improve outcomes for patients with MGCT. Considering the numerous recurrences and the biological aggressiveness of the tumor, the patient was a candidate for restricted follow-up with physical examination and ultrasound of the lymph node stations and scar area. The patient was followed up at a reference center for this type of pathology and due to the complexity and rarity of the diagnosis, two histological revisions were performed. Due to the numerous surgeries received, the patient had to change employment due to reduced mobility of the right upper limb resulting from the surgery. The patient will continue close clinical and instrumental follow-up.

Data availability statement

The raw data supporting the conclusions of this article will be made available by the authors, without undue reservation.

Ethics statement

Written informed consent was obtained from the individual(s) for the publication of any potentially identifiable images or data included in this article.

Author contributions

FF: Conceptualization, Supervision, Writing – original draft, Writing – review & editing. AS: Supervision, Validation, Writing – review & editing. RB: Supervision, Validation, Writing – review & editing. LF: Supervision, Validation, Visualization, Writing – review & editing.

Funding

The author(s) declare that no financial support was received for the research, authorship, and/or publication of this article.

Conflict of interest

The authors declare that the research was conducted in the absence of any commercial or financial relationships that could be construed as a potential conflict of interest.

Publisher's note

All claims expressed in this article are solely those of the authors and do not necessarily represent those of their affiliated organizations, or those of the publisher, the editors and the reviewers. Any product that may be evaluated in this article, or claim that may be made by its manufacturer, is not guaranteed or endorsed by the publisher.

References

1. Kallen ME, Hornick JL. The 2020 WHO classification: what's new in soft tissue tumor pathology? *Am J Surg Pathol*. (2021) 45:e1–e23. doi: 10.1097/PAS.0000000000001552

2. Sunkara T, Nagaraj SV, Gaduputi V. Granular cell tumor of rectum: A very rare entity. *Case Rep Gastrointest Med*. (2017) 2017:3795482. doi: 10.1155/2017/3795482

3. Wang J, Zhu XZ, Zhang RY. Malignant granular cell tumor: a clinicopathologic analysis of 10 cases with review of literature. *Zhonghua Bing Li Xue Za Zhi*. (2004) 33:497–502.

4. Amphlett A. An update on cutaneous granular cell tumors for dermatologists and dermatopathologists. *Clin Exp Dermatol*. (2022) 47:1916–22. doi: 10.1111/ced.15309

5. Fanburg-Smith JC, Meis-Kindblom JM, Fante R, Kindblom LG. Malignant granular cell tumor of soft tissue: diagnostic criteria and clinicopathologic correlation. *Am J Surg Pathol*. (1998) 22:779–94. doi: 10.1097/00000478-199807000-00001

6. MaChado I, Cruz J, Lavernia J, Llombart-Bosch A. Solitary, multiple, benign, atypical, or Malignant: the "Granular Cell Tumor" puzzle. *Virchows Arch*. (2016) 468:527–38. doi: 10.1007/s00428-015-1877-6

7. Rekhi B, Jambhekar NA. Morphologic spectrum, immunohistochemical analysis, and clinical features of a series of granular cell tumors of soft tissues: a study from a tertiary referral cancer center. *Ann Diagn Pathol*. (2010) 14:162–7. doi: 10.1016/j.anndiagpath.2010.01.005

8. Sekimizu M, Yoshida A, Mitani S, Asano N, Hirata M, Kubo T, et al. Frequent mutations of genes encoding vacuolar H^+ -ATPase components in granular cell tumors. *Genes Chromosomes Cancer*. (2019) 58:373–80. doi: 10.1002/gcc.22727

9. Pareja F, Brandes AH, Basili T, Selenica P, Geyer FC, Fan D, et al. Loss-of-function mutations in ATP6AP1 and ATP6AP2 in granular cell tumors. *Nat Commun*. (2018) 9:3533. doi: 10.1038/s41467-018-05886-y

10. Corso G, Di Nubila B, Ciccia A, De Camilli E, Vicini E, Trentin C, et al. Granular cell tumor of the breast: Molecular pathology and clinical management. *Breast J*. (2018) 24:778–82. doi: 10.1111/tbj.13036

11. Dehner CA, Moon T, Lyu Y, Zhang X, Zhou Z, Yang K, et al. Mutations involving TGFB and MAPK may be associated with Malignancy in granular cell tumors. *Genes Chromosomes Cancer*. (2023) 62:301–7. doi: 10.1002/gcc.23123

12. Rogala B, Khan ZA, Jackson-Boeters L, Darling MR. Investigation of the molecular profile of granular cell tumors and schwannomas of the oral cavity. *Dent J (Basel)*. (2022) 10:38. doi: 10.3390/dj10030038

13. Lack EE, Worsham GF, Callihan MD, Crawford BE, Klappenbach S, Rowden G, et al. Granular cell tumor: a clinicopathologic study of 110 patients. *J Surg Oncol*. (1980) 13:301–16. doi: 10.1002/jso.2930130405

14. Khansur T, Balducci L, Tavassoli M. Granular cell tumor. Clinical spectrum of the benign and Malignant entity. *Cancer*. (1987) 60:220–2. doi: 10.1002/(ISSN)1097-0142

15. Imanishi J, Yazawa Y, Saito T, Shimizu M, Kawashima H, Ae K, et al. Atypical and Malignant granular cell tumors in Japan: a Japanese Musculoskeletal Oncology Group (JMOG) study. *Int J Clin Oncol*. (2016) 21:808–16. doi: 10.1007/s10147-016-0949-1

16. Mobarki M, Dumollard JM, Dal Col P, Camy F, Peoc'h M, Karpathiou G. Granular cell tumor a study of 42 cases and systemic review of the literature. *Pathol Res Pract*. (2020) 216:152865. doi: 10.1016/j.prp.2020.152865

17. Lauro S, Trasatti L, Bria E, Gelibter A, Larosa G, Vecchione A. Malignant bronchial Abrikossoff's tumor and small cell lung cancer: a case report and review. *Anticancer Res*. (2001) 21:563–5.

18. Torrado C, Camaño M, Hindi N, Ortega J, Sevillano AR, Civantos G, et al. Antiangiogenics in Malignant granular cell tumors: review of the literature. *Cancers (Basel)*. (2023) 15:5187. doi: 10.3390/cancers15215187

frontiers | Frontiers in Oncology

TYPE Brief Research Report
PUBLISHED 20 September 2024
DOI 10.3389/fonc.2024.1461092

Check for updates

OPEN ACCESS

EDITED BY
Dragos Eugen Georgescu,
Carol Davila University of Medicine and Pharmacy, Romania

REVIEWED BY
José Estevão-Costa,
University of Porto, Portugal
Kenji Nakano,
Cancer Institute Hospital of Japanese Foundation for Cancer Research, Japan

*CORRESPONDENCE
Yali Chen
Yalichen182@163.com

RECEIVED 07 July 2024
ACCEPTED 26 August 2024
PUBLISHED 20 September 2024

CITATION
Bai L, Han L, Zheng A and Chen Y (2024) Uterine inflammatory myofibroblastic tumor: a retrospective analysis.
Front. Oncol. 14:1461092.
doi: 10.3389/fonc.2024.1461092

COPYRIGHT
© 2024 Bai, Han, Zheng and Chen. This is an open-access article distributed under the terms of the Creative Commons Attribution License (CC BY). The use, distribution or reproduction in other forums is permitted, provided the original author(s) and the copyright owner(s) are credited and that the original publication in this journal is cited, in accordance with accepted academic practice. No use, distribution or reproduction is permitted which does not comply with these terms.

Uterine inflammatory myofibroblastic tumor: a retrospective analysis

Liping Bai[1,2], Ling Han[1,2], Ai Zheng[1,2] and Yali Chen[1,2]*

[1]Department of Obstetrics and Gynecology, West China Second University Hospital, Sichuan University, Chengdu, China, [2]Key Laboratory of Birth defects and Related Diseases of Women and Children (Sichuan University), Ministry of Education, Chengdu, China

Objective: Uterine inflammatory myofibroblastic tumor (UIMT) is a rare tumor of the female reproductive tract with uncertain malignant potential. Previous case series reports have limited our understanding of its diagnosis and treatment. Therefore, we conducted a retrospective analysis of patient files at West China Second University Hospital, Sichuan University to contribute valuable clinical insights to future treatment strategies for this disease.

Method: We comprehensively reviewed patient files of individuals diagnosed with UIMT from January 1st, 2013 to May 1st, 2023.

Results: We included twenty-seven cases of uterine inflammatory myofibroblastic tumor in our study. Of these, 51.85% (14 cases) were diagnosed with abnormal uterine bleeding, 2 cases had dysmenorrhea, and 12 were unexpectedly diagnosed with suspected uterine fibroids. Ten cases performed total hysterectomy, and 17 cases underwent lesion resection. The positive rate of anaplastic lymphoma kinase (ALK) immunohistochemistry reached 96.3%. After a median of 8 months follow-up time, all patients were disease-free and had survived.

Conclusion: Uterine inflammatory myofibroblastic tumor is easily misdiagnosed, making its diagnosis challenging. Histological features, immunohistochemical results, and molecular confirmation using fluorescence *in situ* hybridization (FISH) or Next-generation sequencing should be used to confirm the diagnosis. Positive ALK immunohistochemistry, ALK rearrangement, ALK fusion are helpful in diagnosis and ALK inhibitor therapy. Total hysterectomy is often performed for women who do not require fertility, while lesion resection and close follow-up may be considered for those who require fertility preservation.

KEYWORDS

inflammatory myofibroblastic tumor, anaplastic lymphoma kinase, uterine leiomyoma, diagnosis, uterus, retrospective analysis

Introduction

Inflammatory myofibroblastic tumor (IMT), a rare condition characterized by the presence of fibroblastic spindle cells with varying degrees of myxoid stroma and lymphoplasmacytic inflammation (1). Although initially discovered in the lungs, IMT can occur in various anatomical locations, including the female reproductive organs, particularly the uterus. In the uterus, IMT is responsible for only 0.1% of "leiomyomas", but its incidence rises to 10% in pregnant women and 14% in uterine smooth muscle tumors of uncertain malignant potential(STUMP) (2). Most cases of uterine inflammatory myofibroblastic tumor (UIMT) are benign, but the tumor can spread to surrounding tissues or recur after surgery. IMT often involves ALK gene rearrangements and has a low risk of metastasis. It is classified as a tumor of intermediate malignant potential, with recurrence and metastasis rates of approximately 25% and 2%, respectively (3).

Diagnosing IMT can be challenging due to its similarity to other conditions such as leiomyomas, leiomyosarcomas, endometrial stromal tumors, fibroleiomyomatosis, and ligamentous fibroma. The clinical overlap in morphology often leads to misdiagnosis, potentially resulting in a higher incidence than originally estimated. However, advancements in diagnostic tools, such as ALK immunohistochemical testing, have improved the ability to differentiate between STUMP and leiomyosarcoma. In fact, ALK immunohistochemistry, FISH, and RNA sequencing have proven to be highly specific in diagnosing UIMT, enabling its diagnosis with any positive result. Some ALK-negative cases can have other gene abnormalities, including RET, ROS1, or NTRK3 fusion, as well as PDGFRB 3' fusion (4), THBS1, IGFBP5, DES, SEC31, TPM3, and TIMP3. DES-ALK, THBS1, FN1, DCTN1, and PPP1CB (5, 6). Additionally, certain fusion genes, such as TIMP3-ALK and THBS1-ALK, have been found to be highly enriched in pregnancy-related UIMT (7). However, the current diagnosis still relies on histological examination combined with immunohistochemistry, with ALK protein expression and ALK gene rearrangement serving as strong evidence for IMT diagnosis.

Currently, there is a lack of guidelines for the diagnosis and treatment of UIMT. Due to the rarity of the disease, previous literature has primarily consisted of individual case reports. Further research is needed to develop diagnostic and treatment methods for UIMT. The objective of this article is to conduct a retrospective analysis of UIMT patients in our hospital and contribute valuable clinical insights to future treatment strategies for this disease.

Materials and methods

Study population and data sources

This retrospective, observational, single-center study was conducted at West China Second University Hospital, Sichuan University, Chengdu, China, after receiving ethical approval from the hospital's Ethics Committee. Written informed consent was obtained from all 27 patients who were diagnosed with uterine inflammatory myofibroblastic tumor and underwent surgery at the hospital between January 1, 2013, and May 11, 2023.

The study retrospectively examined patients' clinical and pathological information. The pathological specimen was independently reviewed by two pathologists from West China Second University Hospital. Basic patient information, including age, symptoms, tumor characteristics (such as location and size), surgical procedures, comorbidities, adjuvant therapy, recurrence and metastasis rates, follow-up duration, and pregnancy status, was collected. Pathological features, including ALK immunohistochemistry, ALK fluorescence *in situ* hybridization, FH, CD10, caldesmon, desmin, Ki67, border, growth pattern, cell type, nuclear atypia, mitotic index, necrosis, lymphovascular invasion, type and extent of inflammatory infiltrates, as well as primary or metastatic status, were also collected. Oncological outcomes were assessed by following up with patients through outpatient visits and phone calls. Currently, all patients are disease-free, and no recurrence or metastasis has been reported.

Statistical analysis

For continuous normally distributed variables, mean ± standard deviation was used, and the t-test was used for analysis. The Levene's test assessed variance homogeneity. For non-normally distributed continuous variables, medians (range) were used and analyzed using the Wilcoxon-Mann-Whitney U test. Pearson's $\chi 2$ test or Fisher's exact test was used for categorical variables. The likelihood ratio test was used to compare groups of categorical variables. SPSS version 25.0 (IBM Corp, Armonk, NY, USA) was used for statistical analysis. A two-sided p-value <0.05 was considered statistically significant. Descriptive analysis was used for non-continuous variables, and when the p-value was <0.05, the median and interquartile range were used.

Results

Clinical features

The study included 27 patients who were pathologically diagnosed with uterine inflammatory myofibroblastic tumor (UIMT). The patients' basic characteristics are presented in Tables 1–3. UIMTs have been documented in patients aged 21 to 64 years, with a median age of 42 years, and the tumors varied in size from 3 to 8 cm, with a median diameter of 5 cm. Abnormal uterine bleeding was the most common symptom, occurring in 51.85% of cases. Two cases had dysmenorrhea, and 12 cases were incidentally diagnosed due to suspected uterine fibroids. Notably, patient 19 had both dysmenorrhea and abnormal uterine bleeding, patient 13 was unexpectedly diagnosed during a cesarean section, and patient 23 during the removal of an ovarian cyst. The majority (21) of cases were located within the intramuscular layers of the uterus, while 3 were subserosal and 3 were submucosal. All cases of IMT occurred in the uterine body without any extrauterine lesions.

TABLE 1 Clinical characteristics of uterine IMT.

Case	Age	Symptoms	Location	Tumor size (cm)	Surgical procedure	Adjuvant therapy	Recurrence/ metastasis	Follow up time (months)	pregnancy	status
1	46	AUB	IUC	5	HYS	No	No	4	No	NED
2	50	AUB	IUC	6	HYS	No	No	3	No	NED
3	64	PLM	IUC	6	HYS	No	No	7	No	NED
4	57	AUB	IUC	6	HYS	No	No	7	No	NED
5	46	AUB	IUC	5	HYS +BSO+PLA	chemotherapy	No	4	No	NED
6	50	PLM	IUC	6	HYS	No	No	10	No	NED
7	49	PLM	IUC	5.5	HYS	No	No	3	No	NED
8	43	AUB	SMUC	7	HYS	No	No	8	No	NED
9	43	PLM	IUC	4	MYO	No	No	4	No	NED
10	44	DYS	SMUC	5	MYO	No	No	50	No	NED
11	33	AUB	SMUC	4	MYO	No	No	2	No	NED
12	34	PLM	IUC	6	MYO	No	No	6	No	NED
13	32	Other symptoms*	IUC	3	MYO	No	No	6	No	NED
14	46	AUB	IUC	8	MYO	No	No	7	No	NED
15	32	PLM	IUC	5	MYO	No	No	7	No	NED
16	32	PLM	SSUC	6	MYO	No	No	11	No	NED
17	30	PLM	IUC	6	MYO	No	No	17	No	NED
18	39	AUB	IUC	5	MYO	No	No	29	No	NED
19	45	DYS+ AUB	IUC	3	MYO	No	No	20	No	NED
20	27	PLM	IUC	4	MYO	No	No	9	No	NED
21	32	AUB	IUC	3	HYS	No	No	19	No	NED
22	42	AUB	IUC	3.8	HYS	No	No	31	No	NED
23	29	Other symptoms#	SSUC	3	MYO	No	No	9	No	NED
24	30	AUB	IUC	3.8	MYO	No	No	45	Yes	NED
25	30	PLM	IUC	5	MYO	No	No	15	No	NED
26	46	AUB	IUC	6	MYO	No	No	6	No	NED
27	21	AUB	SMUC	4	MYO	No	No	18	No	NED

AUB, abnormal uterine bleeding; NED, no evidence of disease; IUC, intramural of uterus corpus; SMUC, Submucosa of uterus corpus; SSUC, Subserosal of uterus corpus; BSO, Bilateral salpingo-oophorectomy; HYS, hysterectomy; MYO, myomectomy; PLA, pelvic lymphadenectomy; PLM, presumed leiomyoma; DYS, dysmenorrhea.
Other symptoms*: Detected during cesarean section.
Other symptoms#: Detected during oophorocystectomy.

Pathological and molecular results

Macroscopically, most tumors were tan, pink, or white with no apparent capsule, and the sectioned surface of the tumor could have soft consistency, with a whorling appearance, hemorrhage, necrosis, myxoid features, and cyst formation (Figure 1). Tumor cells often comprised plump fusiform cells dispersed in a myxoid extracellular matrix with inflammatory infiltrates of varying amounts, while less commonly, the tumor cells may be epithelioid cell-like (Figure 2). 10 cases showed patchy infiltration, while 17 cases showed diffuse infiltration, and only 1 case exhibited lymphovascular space invasion (LVSI). Twenty-six cases tested positive for ALK immunohistochemistry, with only one case showing a negative result for ALK immunohistochemistry but a positive result for ALK FISH analysis. ALK FISH analysis was carried out on eighteen cases; sixteen cases showed positive results, two tested negative, and 9 cases did not undergo FISH testing.

TABLE 2 The pathological features of the patient.

case	ALK IHC	ALK FISH	caldesmon	FH	CD10	DESMIN	Ki67	border	growth pattern	nuclear atypia	mitotic index(per 10 HPFs)	necrosis	LVSI	type and extent of inflammatory infiltrate
1	P	N	P	P	N		5	well-circumscribed	hyalinized	mild	5%	No	No	patch
2	P	ND	P	P	N		<5	well-circumscribed	hyalinized	mild	10%	No	No	patch
3	N	P		P	P		1	well-circumscribed	myxoid	mild	10%	No	No	patch
4	P	P	P	P	N	P	<3	well-circumscribed	compact fascicular	mild	3%	No	No	patch
5	P	ND	P		P	P	40	infiltrative	myxoid	moderate	40	No	yes	diffuse
6	P	P	P	P	N		3	well-circumscribed	hyalinized	moderate	3%	No	No	diffuse
7	P	ND	P	P	N		<5	well-circumscribed	hyalinized	moderate	5%	No	No	patch
8	P	P	N	P	P	P	20	infiltrative	myxoid	moderate	20	yes	No	diffuse
9	P	P	P	P	N		<5	well-circumscribed	hyalinized	mild	5%	No	No	patch
10	P	ND	N		N	P	30	well-circumscribed	hyalinized	moderate	30%	No	No	diffuse
11	P	P		P	N		5-10	well-circumscribed	compact fascicular	moderate	10%	No	No	diffuse
12	P	P		P	N		5-10	well-circumscribed	compact fascicular	moderate	10%	No	No	diffuse
13	P	ND	P	P	P	P	3	well-circumscribed	compact fascicular	moderate	3%	No	No	patch
14	P	N	P	P	P		5	well-circumscribed	myxoid	moderate	3%	No	No	diffuse
15	P	P		P	N		1	well-circumscribed	hyalinized	mild	1%	No	No	patch
16	P	P		P	N		3-5	well-circumscribed	hyalinized	mild	5%	No	No	patch
17	P	P	P	P	N		<5	well-circumscribed	hyalinized	moderate	5%	No	No	diffuse

(Continued)

10.3389/fonc.2024.1461092

TABLE 2 Continued

case	ALK IHC	ALK FISH	caldesmon	FH	CD10	DESMIN	Ki67	border	growth pattern	nuclear atypia	mitotic index(per 10 HPFs)	necrosis	LVSI	type and extent of inflammatory infiltrate
18	P	ND	P		N		<1	well-circumscribed	hyalinized	moderate	1%	No	No	diffuse
19	P	P	P	P	N		5	well-circumscribed	myxoid	moderate	5%	No	No	diffuse
20	P	P	P	P	P	P	<3	well-circumscribed	compact fascicular	moderate	3%	No	No	diffuse
21	P	P	P	P	N		5-10	well-circumscribed	myxoid	moderate	10%	No	No	diffuse
22	P	ND	P		N	P	5	well-circumscribed	myxoid	moderate	5%	No	No	diffuse
23	P	P	P	P	N		<5	well-circumscribed	compact fascicular	mild	5%	No	No	patch
24	P	ND	P		N		3-5	well-circumscribed	hyalinized	moderate	5%	No	No	diffuse
25	P	P	P	P	P		<5	well-circumscribed	hyalinized	moderate	5%	No	No	diffuse
26	P	ND		P	N		<5	well-circumscribed	hyalinized	mild	5%	No	No	diffuse
27	P	P	P	P	N		5-10	well-circumscribed	myxoid	mild	10%	No	No	diffuse

LVSI, Lymph vascular space invasion; P, positive; N, negative; ND, not done.
In the cell type detection, except for case No. 23, where the majority was spindled and focal was epithelioid, all the other cases were spindled.

10.3389/fonc.2024.1461092

TABLE 3 Clinical and pathological characteristics of the patients.

Parameter	
Age(years)	
Range	21-64
Median	42
Mean	39.7 ± 9.9
Location	
Corpus	27
Cervix	0
Symptom	
AUB	14(51.85%)
dysmenorrhea	2(7.41%)
Incidental finding	12(44.44%)
Size	
Range	3-8
Median	5
Mean ± SD	5 ± 1.35
Surgical procedure	
Tumor resection	17(62.96%)
HYS	10(37.04%)
Follow up months	
Range	2-50
Median	8
Mean ± SD	13 ± 12.2
Pregnancy	
Yes	1(5.88%)
No	16(94.12%)
Borders	
well-circumscribed	25(92.59%)
infiltrative	2(7.41%)
ALK IHC	
Positive	26(96.30%)
Negative	1(3.7%)
ALK FISH	
Rearragement	16(59.26%)
Normal	2(7.41%)
Not done	9(33.33%)
Mitoses	
<5/10 HPF	7(25.93%)
≥5/10 HPF	20(74.07)
Atypia	
No/Mild	10(37.04%)
Moderate/Severe	17(62.96%)
Necrosis	
Yes	1(3.7%)
No	26(96.3)
Inflammation	
Diffuse	17(62.96%)
Patch	10(37.04%)
LVSI	
Yes	1(3.7%)
No	26(96.3%)

Treatment outcomes

Of the 27 patients, 10 underwent total hysterectomy, and 17 had lesion removal. Patient 5 underwent total hysterectomy, bilateral salpingectomy, and pelvic lymph node dissection, followed by adjuvant chemotherapy due to infiltrative growth, while patient 24 opted for fertility preservation and had a successful natural pregnancy after surgery, culminating in a term cesarean section. During the follow-up period, which ranged from 2 to 50 months, all patients remained disease-free. Additionally, the study found no significant difference in prognosis between tumor excision and hysterectomy, suggesting that alternative treatment options may be effective in managing UIMT.

Discussion

Our recent analysis of clinicopathological data at our hospital has provided new insights into the nature of uterine inflammatory myofibroblastic tumor (UIMT). The exact cause of IMT remains elusive, but it is believed that potential triggers may include traumatic injuries, bacterial or EB viral infections, chromosomal abnormalities, abnormal repair processes, severe surgeries, and inflammation spreading (8). According to the latest 2020 WHO definition, IMT is a distinctive and rare tumor characterized by a combination of spindle-shaped myofibroblast cells, fibroblast cells, plasma cells, eosinophils, lymphocytes, and other inflammatory cells, with minimal potential for metastasis (9).

Distinguishing UIMT from uterine leiomyoma based on morphology alone can be challenging due to the atypical clinical features commonly seen in UIMT. Recent research has shown that 0.3% of unselected leiomyomas were reclassified as IMTs based on positive anaplastic lymphoma kinase (ALK) immunohistochemistry (IHC) (4), even though routine ALK screening for the diagnosis of

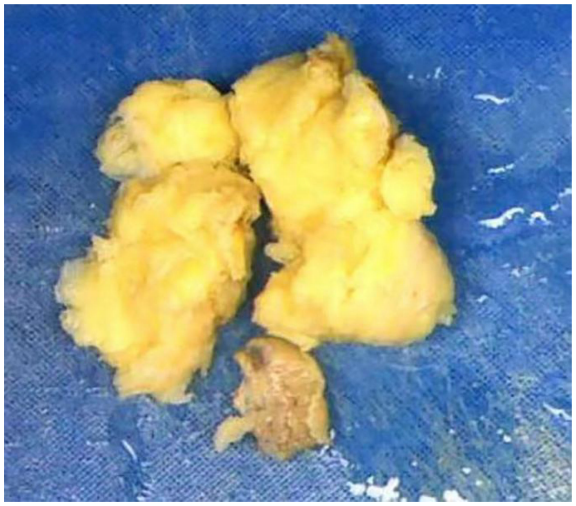

FIGURE 1
Uterine inflammatory myofibroblastic tumor. Macroscopically, most tumors were tan, pink, or white. The sectioned surface of the tumor can be of soft consistency, with a whorling appearance, hemorrhage, necrosis.

leiomyomas is not currently recommended. Our own study found that the median age of UIMT patients was 42 years, in line with previous reports by Karpathiou G. and Shukla PS (2, 10)., who observed a wide age range from 6 to 73 years, with a median age of 39 years. Abnormal uterine (51.85%) and the incidental discovery of uterine fibroids were the most common patient complaints. It is worth noting that many patients were asymptomatic, leading to a high rate of clinical underdiagnosis of UIMT. In other reports, IMT in other parts of the body, such as abdominal IMT, is more common in children and adolescents (11, 12). And the clinical manifestations of these IMTs are nonspecific and broad spectrum, ranging from asymptomatic to severe systemic symptoms (11, 12).

UIMTs are often mistaken for uterine leiomyomas, but they exhibit different texture and morphology, characterized by a softer, gelatinous consistency, and clear or irregular borders. They can be classified histologically into myxoid/vascular type, dense spindle cell type, or hypocellular fibrous type, with varying amounts of chronic inflammatory cells. They express ALK as well as smooth muscle markers (SMA, Desmin, Caldesmon), CD10, and others (6). ALK demonstrates high sensitivity and specificity in diagnosing IMT, with ALK gene rearrangement occurring at the 2p23 locus (13).

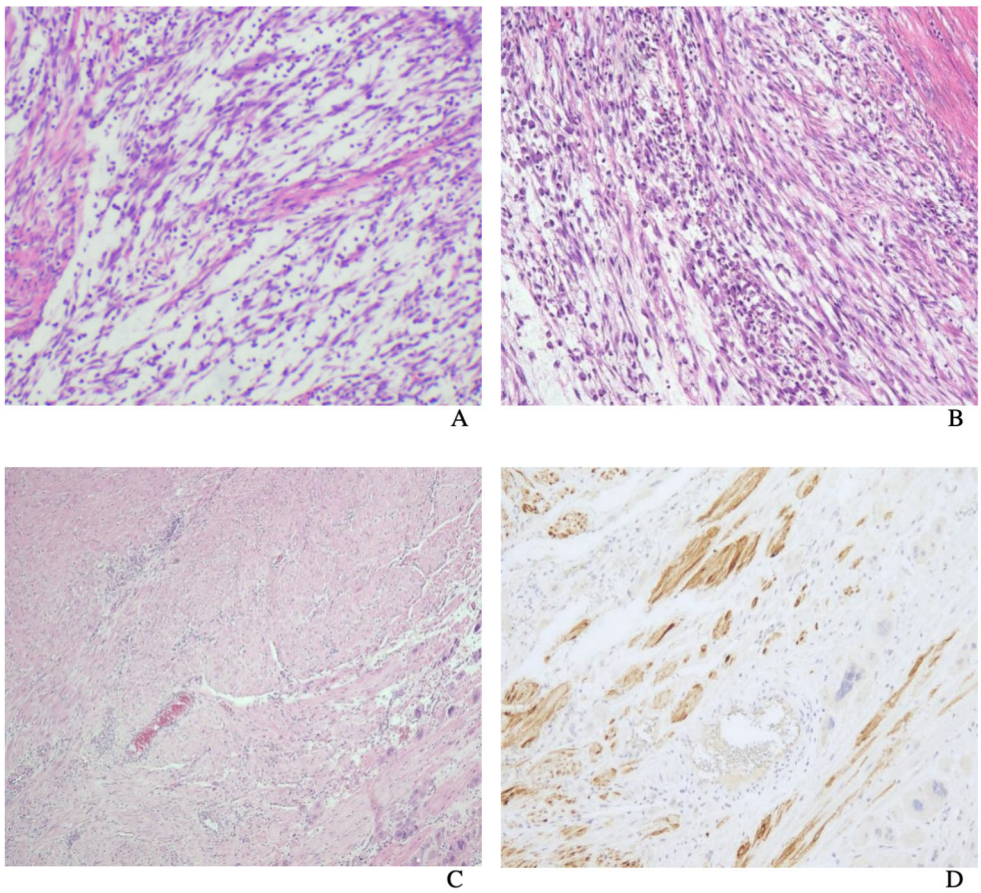

FIGURE 2
Uterine inflammatory myofibroblastic tumor. The tumor cells are usually fusiform cells dispersed in a myxoid extracellular matrix with varying degrees of inflammatory infiltrates **(A)**. Tumor cells are composed of spindle and epithelioid cells admixed with lymphocytes **(B)**. Uterine inflammatory myofibroblastic tumor. H&E **(C)** shows the appearance of tumor cells mimicked that of a smooth muscle tumor (smooth muscle-like) and ALK immunostain **(D)**.

Previous studies have reported ALK positivity rates of 87.5-100% (4), and in our study, the ALK IHC positivity rate reached 96.3%. Various ALK fusion partners have been identified in the literature on IMT (CARS, TPM4, TPM3 EML4, RANBP2, IGFBP4, ATIC, CLTC, etc.), while ALK-negative cases may show ROS1 and PDFGRB alterations, and a small proportion has ETV6-NTRK3 fusion (14). TIMP3 and THBS1 genes are more commonly identified fusion partners in pregnancy-related IMTs (15). Therefore, if ALK is negative, further RNA sequencing is needed to assist in the diagnosis. Nevertheless, it is crucial to note that ALK positivity is a key factor in diagnosing IMT. It is worth mentioning that no ALK fusion genes have been detected in uterine leiomyomas thus far. The current essential diagnostic criteria for IMT include the presence of spindle cell arrangement, infiltration of lymphocytes and plasma cells, expression of SMA, and frequent expression of ALK or ROS1. Notably, IMTs associated with pregnancy exhibit morphological features such as varying amounts of myxoid stroma and lymphoplasmacytic infiltrates (7).

The primary treatment for women diagnosed with noninvasive UIMT who do not require fertility preservation is total hysterectomy, while those who require fertility preservation may consider lesion resection with close follow-up. This approach is in line with previous studies. Prior to 2014, all reported cases of uterine IMT in the literature had a benign clinical course without evidence of recurrence or metastasis after surgery (1). However, research on UIMT invasiveness has been limited to the past decade. However, in patients with other IMT sites that have been reported, they still have a low recurrence rate after conservative surgery and treatment (11, 12)?.

In our case series, the invasive UIMT had a diameter of 5 cm, infiltrative borders, positive lymphovascular space invasion (LVSI), and 40 mitoses in 10 high-power fields. Malignant IMTs have been reported to have a lesion size ≥10.5 cm, severe nuclear atypia, ≥18 mitoses in 10 high-power fields, and features of lymphovascular invasion (5, 6). Studies on the invasiveness of IMT have found that myxoid dominance transitions to dense/spindle dominance in cases of multiple recurrences (16). Bennett's study found that the dense/spindle type was associated with recurrence (5), while other studies have found that myxoid dominance is associated with a higher risk (1). The latest classification by the World Health Organization includes characteristics such as tumor diameter >7 cm, moderate to severe cytological atypia, increased mitotic index, necrosis, and lymphovascular infiltration. However, there are also reports of cases of metastasis and recurrence without these features.

Treatment for recurrent or invasive IMT usually involves a combination of chemotherapy, targeted therapy, or surgery. Tumors with larger diameters, typical nuclear atypia, lymphovascular infiltration, high mitotic count, and tumor necrosis are associated with poor outcomes (4). Understanding the genetics of IMT can facilitate targeted therapies. Approximately 10% of uterine IMTs are ALK-negative, and FISH or RNA sequencing is helpful for diagnosis (15). Confirmed ALK positivity has both diagnostic and therapeutic implications. ALK inhibitors, such as crizotinib, have shown effectiveness in treating recurrent and/or refractory invasive diseases (4, 17). Pregnancy appears to have a certain correlation with IMT, and targeted therapy using tyrosine kinase inhibitors may represent a new treatment option (17, 18).

Recent studies have indicated that minimally invasive procedures such as laparoscopy and hysteroscopy are preferred for treating UIMT, while careful monitoring and continued follow-up are effective strategies for women seeking to preserve fertility (17). However, UIMTs are rare tumors, and the understanding mostly comes from case reports with short follow-up periods, which can lead to selection bias in retrospective analyses.

Conclusion

Uterine inflammatory myofibroblastic tumor (UIMT) is a rare tumor that can be challenging to diagnose and treat. Total hysterectomy is often performed for women who do not require fertility, while lesion resection and close follow-up may be considered for those who require fertility preservation. ALK protein expression and gene rearrangements are used for diagnostic confirmation. Tumors with larger size, nuclear atypia, lymphovascular invasion, high mitotic count, and necrosis are associated with poorer outcomes. Improved understanding of the genetics and invasiveness of IMT is necessary for developing effective treatment strategies.

Data availability statement

The original contributions presented in the study are included in the article/supplementary material. Further inquiries can be directed to the corresponding author.

Ethics statement

The studies involving humans were approved by The Medical Research Ethics Committee of West China Second University Hospital, Sichuan University belongs to Sichuan University, China. The studies were conducted in accordance with the local legislation and institutional requirements. The participants provided their written informed consent to participate in this study. Written informed consent was obtained from the individual(s) for the publication of any potentially identifiable images or data included in this article.

Author contributions

LB: Data curation, Formal analysis, Investigation, Methodology, Project administration, Resources, Writing – original draft, Writing – review & editing. LH: Conceptualization, Investigation, Project administration, Supervision, Validation, Visualization, Writing –

original draft, Writing – review & editing. AZ: Data curation, Formal analysis, Resources, Supervision, Writing – original draft, Writing – review & editing. YC: Conceptualization, Data curation, Formal analysis, Funding acquisition, Investigation, Methodology, Project administration, Resources, Software, Supervision, Validation, Visualization, Writing – original draft, Writing – review & editing.

Funding

The author(s) declare that no financial support was received for the research, authorship, and/or publication of this article.

Conflict of interest

The authors declare that the research was conducted in the absence of any commercial or financial relationships that could be construed as a potential conflict of interest.

Publisher's note

All claims expressed in this article are solely those of the authors and do not necessarily represent those of their affiliated organizations, or those of the publisher, the editors and the reviewers. Any product that may be evaluated in this article, or claim that may be made by its manufacturer, is not guaranteed or endorsed by the publisher.

References

1. Parra-Herran C QC, Howitt BE, Dal Cin P, Quade BJ, Nucci MR. Inflammatory myofibroblastic tumor of the uterus: clinical and pathologic review of 10 cases including a subset with aggressive clinical course. *Am J Surg Pathol*. (2015) 39:157–68. doi: 10.1097/PAS.0000000000000330

2. Karpathiou G, Devouassoux-Shisheboran M, Stolnicu S, Chauleur C, Péoc'h M. Uterine inflammatory myofibroblastic tumor. *Pathol Res Pract*. (2023) 242. doi: 10.1016/j.prp.2023.154335

3. Etlinger P, Kuthi L, Kovács T. Inflammatory myofibroblastic tumors in the uterus: childhood-case report and review of the literature. *Front Pediatr*. (2020) 8. doi: 10.3389/fped.2020.00036

4. Kuisma H JV, Pasanen A, Heikinheimo O, Karhu A, Välimäki N, Aaltonen L, et al. Histopathologic and molecular characterization of uterine leiomyoma–like inflammatory myofibroblastic tumor comparison to molecular subtypes of uterine leiomyoma. *Am J Surg Pathol*. (2022) 46(8):1126–36. doi: 10.1097/PAS.0000000000001904

5. Bennett JA, Nardi V, Rouzbahman M, Morales-Oyarvide V, Nielsen GP, Oliva E. Inflammatory myofibroblastic tumor of the uterus: a clinicopathological, immunohistochemical, and molecular analysis of 13 cases highlighting their broad morphologic spectrum. *Modern Pathol*. (2017) 30:1489–503. doi: 10.1038/modpathol.2017.69

6. Devins KM, Samore W, Nielsen GP, Deshpande V, Oliva E. Leiomyoma-like morphology in metastatic uterine inflammatory myofibroblastic tumors. *Modern Pathol*. (2023) 36. doi: 10.1016/j.modpat.2023.100143

7. Devereaux KA FM, Hartinger S, Jones C, Kunder CA, Longacre TA. Pregnancy-associated inflammatory myofibroblastic tumors of the uterus are clinically distinct and highly enriched for TIMP3-ALK and THBS1-ALK fusions. *Am J Surg Pathol*. (2020) 44:970–81. doi: 10.1097/PAS.0000000000001481

8. Gleason BC, Hornick JL. Inflammatory myofibroblastic tumors: where are we now? *J Clin Pathol*. (2008) 61(4):428–37. doi: 10.1136/jcp.2007.049387

9. Kallen ME, Hornick JL. The 2020 WHO classification: what's new in soft tissue tumor pathology? *Am J Surg Pathol*. (2021) 45(1):e1–e23. doi: 10.1097/PAS.0000000000001552

10. Shukla PS, Mittal K. Inflammatory myofibroblastic tumor in female genital tract. *Arch Pathol Lab Med*. (2018) 143:122–9. doi: 10.5858/arpa.2017-0575-RA

11. Estêvão-Costa J, Correia-Pinto J, Rodrigues FC, Carvalho JL, Campos M, Dias JA, et al. Gastric inflammatory myofibroblastic proliferation in children. *Pediatr Surg Int*. (1998) 13:95–9. doi: 10.1007/s003830050257

12. Fragoso AC, Eloy C, Estevão-Costa J, Campos M, Farinha N, Lopes JM. Abdominal inflammatory myofibroblastic tumor a clinicopathologic study with reappraisal of biologic behavior. *J Pediatr Surg*. (2011) 46:2076–82. doi: 10.1016/j.jpedsurg.2011.07.009

13. Ng ZY, Khaing CT, Aggarwal I. Inflammatory myofibroblastic tumor: an under recognized differential of uterine mesenchymal tumors. *Int J Gynecol Cancer*. (2022) 32:212–3. doi: 10.1136/ijgc-2021-003247

14. Zhang L, Luan L, Shen L, Xue R, Huang J, Su J, et al. Uterine inflammatory myofibroblastic tumor harboring novel NUDCD3-ROS1 and NRP2-ALK fusions: clinicopathologic features of 4 cases and literature review. *Virchows Archiv*. (2023) 482:567–80. doi: 10.1007/s00428-022-03457-7

15. Sim A, Devouassoux-Shisheboran M, Benmoulay-Rigollot C, Picot T, Péoc'h M, Karpathiou G. Uterine inflammatory myofibroblastic tumor with THBS1-INSR fusion. *Pathol Res Pract*. (2023) 246. doi: 10.1016/j.prp.2023.154500

16. Collins K RP, Euscher ED, Llanos AR, Garcia A, Malpica A. Uterine inflammatory myofibroblastic neoplasms with aggressive behavior, including an epithelioid inflammatory myofibroblastic sarcoma: a clinicopathologic study of 9 cases. *Am J Surg Pathol*. (2022) 46:105–17. doi: 10.1097/PAS.0000000000001756

17. Mandato VD, Valli R, Mastrofilippo V, Bisagni A, Aguzzoli L, La Sala GB. Uterine inflammatory myofibroblastic tumor. *Medicine*. (2017) 96. doi: 10.1097/MD.0000000000008974

18. Horwood G, Busca A, Singh S. Fertility-preserving management of an inflammatory myofibroblastic tumor: A case report and review of the literature. *Case Rep Women's Health*. (2023) 37. doi: 10.1016/j.crwh.2023.e00481

frontiers | Frontiers in Oncology

TYPE Case Report
PUBLISHED 25 September 2024
DOI 10.3389/fonc.2024.1428152

Check for updates

OPEN ACCESS

EDITED BY
Dragos Eugen Georgescu,
Carol Davila University of Medicine and Pharmacy, Romania

REVIEWED BY
Corrado Spatola,
University of Catania, Italy
Mithalesh Kumar Singh,
University of Texas Southwestern Medical Center, United States

*CORRESPONDENCE
Gil Bar-Sela
gil_ba@clalit.org.il

RECEIVED 05 May 2024
ACCEPTED 26 August 2024
PUBLISHED 25 September 2024

CITATION
Attrash M, Badran O, Shapira Y and Bar-Sela G (2024) Case report: Conjunctival melanoma treated with relatlimab and nivolumab showing remarkable response. *Front. Oncol.* 14:1428152. doi: 10.3389/fonc.2024.1428152

COPYRIGHT
© 2024 Attrash, Badran, Shapira and Bar-Sela. This is an open-access article distributed under the terms of the Creative Commons Attribution License (CC BY). The use, distribution or reproduction in other forums is permitted, provided the original author(s) and the copyright owner(s) are credited and that the original publication in this journal is cited, in accordance with accepted academic practice. No use, distribution or reproduction is permitted which does not comply with these terms.

Case report: Conjunctival melanoma treated with relatlimab and nivolumab showing remarkable response

Mirona Attrash[1], Omar Badran[1], Yinon Shapira[2,3] and Gil Bar-Sela[1,2]*

[1]Department of Oncology, Emek Medical Center, Afula, Israel, [2]Faculty of Medicine, Technion, Haifa, Israel, [3]Department of Ophthalmology, Carmel Medical Center, Haifa, Israel

Conjunctival melanoma, an uncommon form of ocular melanoma, shares some molecular characteristics with cutaneous melanoma and some with mucosal melanoma. Treatment of cases where it becomes advanced or metastatic raises unique treatment challenges. Nivolumab/relatlimab (Opdualag) recently received FDA approval for metastatic melanoma based on the phase 2/3 RELATIVITY-047 trial, which showed better median progression-free survival (PFS) in the first-line setting without new safety signals. The efficacy of this drug in conjunctival melanoma has not been reported yet.

Case presentation: An 87-year-old woman with a history of mild dementia was admitted to the oncology department with a large, exophytic tumor protruding from her left eye, diagnosed as conjunctival melanoma two years previously. This tumor was secreting a whitish fluid and obstructing her vision. Immunotherapy with Opdualag was started, with a near clinical complete response after the 1st cycle. The patient was treated with only four cycles due to worsening of her dementia.

Conclusion: Nivolumab/relatlimab (Opdualag) is a promising treatment alternative in conjunctival melanoma when surgery is not viable.

KEYWORDS

conjunctival melanoma, nivolumab/relatlimab, Opdualag, immunotherapy, cognitive health

1 Introduction

Conjunctival melanoma, an uncommon form of ocular melanoma, represents a challenging clinical scenario due to its aggressive nature and the potential for local invasion and metastasis (1). This malignancy, while sharing some molecular characteristics with cutaneous melanoma, poses unique treatment dilemmas, especially

in cases where it becomes advanced or metastatic (2). The mainstay of treatment for early-stage disease is surgical excision, often complemented by adjuvant therapies. However, for advanced or metastatic conjunctival melanoma, systemic treatment options, including immunotherapy, have been explored with interest, reflecting practices in cutaneous melanoma management (3). in limited disease the treatment is still the surgery but due to tendency of recurring, radiation therapy is being an important part as adjuvant therapy (4).

The rationale for using immunotherapy, particularly checkpoint inhibitors targeting PD-1/PD-L1 and CTLA-4, stems from their success in treating cutaneous melanoma. These treatments have revolutionized the management of advanced melanoma, offering hope for similar efficacy in ocular melanomas, including conjunctival melanoma. Notably, pembrolizumab and the combination of nivolumab (a PD-1 inhibitor) and ipilimumab (a CTLA-4 inhibitor), known for its enhanced response rates in cutaneous melanoma, has sparked interest in its potential applicability for conjunctival melanoma (5).

Combining two immunotherapy treatments, such as anti-PDL-1 and anti-LAG3 (nivolumab with relatlimab), showed superior PFS over single-agent immunotherapy as a first line in unresectable melanoma patients (6). In our case, the patient had an impressive fungating mass protruding out of her orbit; to spare her orbital exenteration, a significant and disfiguring surgery, we decided to give the patient Opdualag (nivolumab with relatlimab) to induce a rapid response with minimal adverse effects.

Strength of the study: our study had several strengths like showing the positive effect of combined immunotherapy in this rare disease with remarkable results, on the other hand, with such shrinkage maybe Opdualag will be considered as an option for first line treatment in unresectable advanced conjunctival melanoma. Limitations of the study: there is limited data about this topic, and it is self-reported data.

2 Case presentation

An 87-year-old woman with a history of mild dementia presented to the ophthalmology department in August 2021 with noticeable changes in the anatomy and color of her left conjunctiva. A biopsy confirmed the diagnosis of invasive conjunctival melanoma. Given the patient's age and the potential morbidity associated with surgical intervention, the decision of the patient and her family was not to pursue surgery.

Consequently, she did not receive any follow-up care until May 2023, when she was admitted with a large, exophytic, fungating tumor protruding from her left orbit. This tumor was obstructing her left vision and causing left eye pain and resultant insomnia (Figure 1A). MRI of the orbits showed a large, irregular, heterogeneously enhancing mass on the left eye's anterior surface. The left globe was slightly irregular but overall preserved, with no evidence of posterior orbital extension (Figure 1B).

Comprehensive total body computer tomography (TBCT) performed at this time showed signs of chronic cerebral vascular incidents, a 2 cm meningioma near the left para-sellar area, slightly enlarged lymph nodes on both sides of the neck, perihilar lymph nodes, and two ground-glass opacity nodules in the right upper lung lobe. Crucially, there was no evidence of metastatic disease.

Given the extent of the tumor, the patient's discomfort, and the effect on her quality of life, exenteration was presented as a palliative option. However, considering the patient's age and cognitive condition, and after counseling with the patient's family, a multidisciplinary team decided against surgical intervention. Instead, it was decided to initiate treatment with a combination of nivolumab/relatlimab, known for its higher response rate than single-agent immunotherapy and lower side effects than other immunotherapy combinations.

Treatment commenced in June 2023 at HaEmek Medical Center, Israel. Remarkably, the tumor mass disappeared just one month after the first dose, demonstrating a dramatic clinical response (Figure 2A).

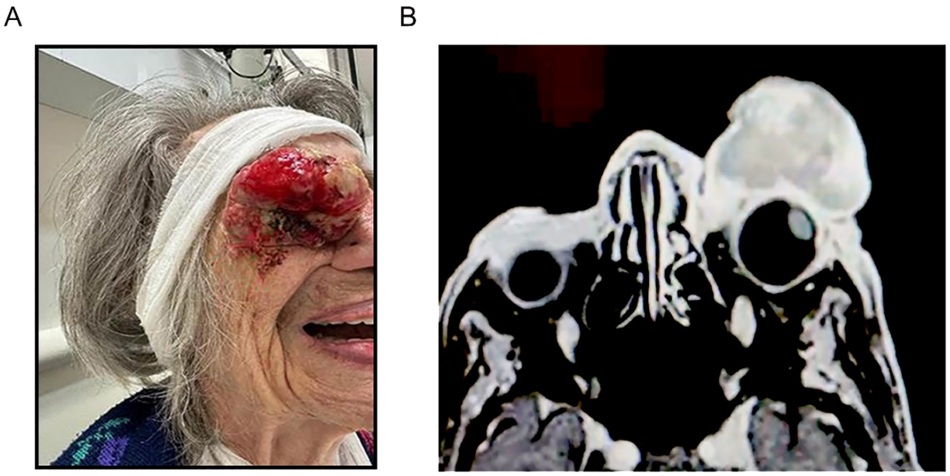

FIGURE 1
(A) The patient, before receiving treatment, showed a large, exophytic, fungating tumor protruding from her left orbit, known as a conjunctival melanoma. **(B)** Axial MRI T1 weighted with fat suppression showing the tumor.

However, the patient's cognitive state worsened significantly after the third treatment dose. Corticosteroid therapy with Prednisone was initiated to manage her symptoms. After tapering off the corticosteroids and administering the fourth dose of nivolumab/relatlimab, further treatment was halted due to further worsening of her cognitive state. Upon completing the treatment cycles, a reevaluation revealed clinically a tiny residual tumor. However, in line with the patient's wishes and considering her general condition, it was decided that it was preferable to avoid surgery. (Figure 2B). The patient continued living in her home without further treatment.

3 Discussion

In the context of our elderly patient, who also suffered from dementia, the decision to initiate immunotherapy underscores the need for careful consideration of both the potential benefits and the risks, particularly given the limited literature on immunotherapy outcomes in patients with pre-existing cognitive impairment. The case highlights the necessity of individualized treatment planning and the importance of ongoing research to understand better the implications of immunotherapy in this unique patient population. Nonetheless, after careful consideration with the patient's family, this treatment spared the patient a large, complex, and disfiguring surgery, the only other palliative alternative to trial with immunotherapy.

The rationale behind combination therapy revolves around the synergistic potential of dual checkpoint inhibition to enhance the anti-tumor immune response. The Opdualag combination, targeting both the PD-1 and LAG-3 pathways, has been investigated for its efficacy in melanoma, showing promising results. Studies in cutaneous melanoma have demonstrated that such combinations can lead to higher response rates compared to single-agent immunotherapy, albeit with an increased risk of immune-related adverse events (irAEs).

The literature on the efficacy of immunotherapy, particularly combination therapy, is sparse but growing in the case of conjunctival melanoma. The decision to employ Opdualag was influenced by its effectiveness in cutaneous melanoma, hypothesizing that its benefits could extend to conjunctival melanoma, a malignancy with limited treatment options once it progresses beyond local therapies.

In the RELATIVITY 047 trial, 714 patients received immunotherapy for unresectable cutaneous melanoma; 359 received nivolumab alone as a single agent, and 355 received combined therapy with Opdualag. The median progression-free survival with Opdualag was 10.1 months, whereas with nivolumab alone, it was 4.6 months, with a 10.3 percentage point difference in the objective response rate. Grade 3-4 adverse events occurred in 18.9% of the Opdualag group and 9.7% of the nivolumab group. The response rate and progression-free survival were significantly higher in the Opdualag group than in single-agent nivolumab. Our patient received Opdualag based on this data.

However, immunotherapy treatments can lead to neurological side effects, especially peripheral complications, which, although rare, can be fatal. The study by Sara Mancone et al. showed that 5 of 55 patients who received immunotherapy treatment developed neurological irAEs grade 3-4. There was no relevant data regarding irAEs and dementia. It is not well known if dementia is a direct side effect of immunotherapy or if there is a regression in the patient's daily activities due to weakness secondary to irAE (7). Therefore, combination therapy in patients with dementia presents additional challenges. In the case of our patient, the progression of dementia following the initiation of immunotherapy raises important questions regarding the safety and tolerability of these agents in individuals with pre-existing cognitive impairment.

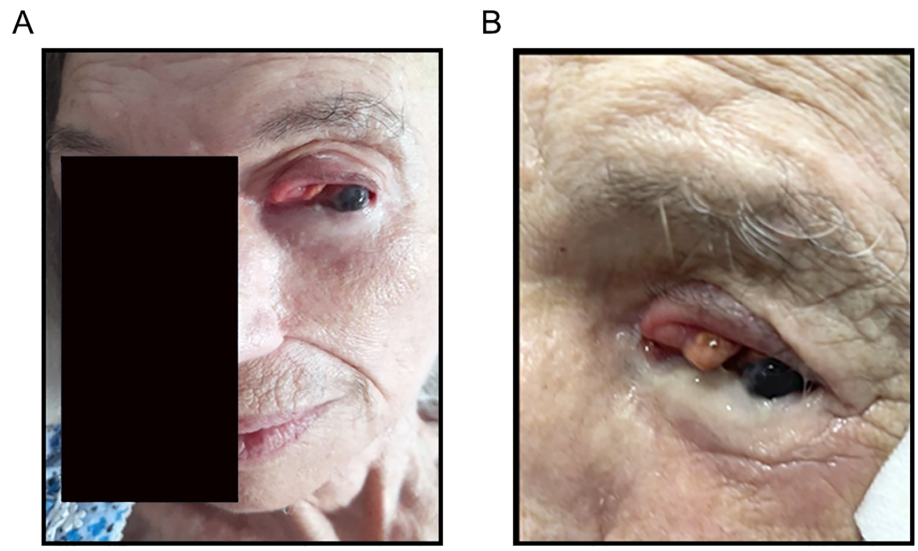

FIGURE 2
(A) Withdrawal of most of the tumor after receiving one course of Opdualag. **(B)** Near complete remission of conjunctival melanoma after receiving the third treatment of Opdualag.

The worsening of dementia in this context was probably related to the patient's general health and was not a direct immune-related side effect. The literature on immunotherapy in patients with pre-existing neurological disorders is limited, highlighting a critical area for further research. Understanding the interactions between immunotherapy and neurological conditions is essential to optimize treatment strategies and manage potential complications effectively.

Regarding alternative treatments, radiation therapy, including brachytherapy, photon-beam, and proton therapy, is often considered an alternative or adjunct to surgical treatment in conjunctival melanoma. These treatments can be particularly beneficial in preserving the eye and maintaining better cosmetic and functional outcomes than extensive surgery (8).

Additionally, combining radiotherapy with immunotherapy is a promising idea. Hypofractionated radiotherapy, such as SABR, has shown improvements in local control and induced an abscopal effect, where localized treatment also reduces distant metastases. A study by Lo Greco demonstrated that combining high-dose radiotherapy with the immune checkpoint inhibitor cemiplimab improved efficacy in advanced cutaneous squamous cell carcinoma (4). However, this combination has not been tested in conjunctival melanoma and thus was not considered for integration in this context.

4 Conclusions

To our knowledge, the current case is the first reported patient with conjunctival melanoma treated with nivolumab/relatlimab (Opdualag). The case showed this immunotherapy combination's high efficacy in treating a complex conjunctival melanoma case, sparing primary surgical intervention critical in elderly patients with additional health considerations. The possible correlation between immunotherapy and the worsening of dementia should be studied in real-world data reports.

Data availability statement

The original contributions presented in the study are included in the article/supplementary material. Further inquiries can be directed to the corresponding author.

Ethics statement

Written informed consent was obtained from the individual(s) for the publication of any potentially identifiable images or data included in this article.

Author contributions

MA: Writing – original draft, Writing – review & editing. OB: Writing – original draft, Writing – review & editing. YS: Writing – original draft, Writing – review & editing. GB: Conceptualization, Writing – original draft, Writing – review & editing.

Funding

The author(s) declare that no financial support was received for the research, authorship, and/or publication of this article.

Conflict of interest

The authors declare that the research was conducted without commercial or financial relationships that could create a conflict of interest.

The author(s) declared that they were an editorial board member of Frontiers, at the time of submission. This had no impact on the peer review process and the final decision.

Publisher's note

All claims expressed in this article are solely those of the authors and do not necessarily represent those of their affiliated organizations, or those of the publisher, the editors and the reviewers. Any product that may be evaluated in this article, or claim that may be made by its manufacturer, is not guaranteed or endorsed by the publisher.

References

1. Alsalem AN, Scarffe LA, Briemberg HR, Aaroe AE, Harrison RA. Neurologic complications of cancer immunotherapy. *Curr Oncol.* (2023) 30:5876–97. doi: 10.3390/curroncol30060440

2. Boutros A, Croce E, Ferrari M, Gili R, Massaro G, Marconcini R, et al. The treatment of advanced melanoma: Current approaches and new challenges. *Crit Rev Oncol Hematol.* (2024) 196:104276. doi: 10.1016/j.critrevonc.2024.104276

3. Knight A, Karapetyan L, Kirkwood JM. Immunotherapy in melanoma: recent advances and future directions. *Cancers*. (2023) 15:1106. doi: 10.3390/cancers15041106

4. Spatola C, Liardo RLE, Milazzotto R, Raffaele L, Salamone V, Basile A, et al. Radiotherapy of conjunctival melanoma: role and challenges of brachytherapy, photon-beam and protontherapy. *Appl Sci*. (2020) 10:9071. doi: 10.3390/app10249071

5. Kreidieh FY, Tawbi HA. The introduction of LAG-3 checkpoint blockade in melanoma: immunotherapy landscape beyond PD-1 and CTLA-4 inhibition. *Ther Adv Med Oncol.* (2023) 15:17588359231186027. doi: 10.1177/17588359231186027

6. Long GV, Stephen Hodi F, Lipson EJ, SChadendorf D, Ascierto PA, Matamala L, et al. Overall survival and response with nivolumab and relatlimab in advanced melanoma. *NEJM Evid.* (2023) 2. doi: 10.1056/EVIDoa2200239

7. McCombe JA, Sechi E, Zekeridou A. Chapter 28 - Neurologic manifestations of autoimmunity with immune checkpoint inhibitors, in: *Handbook of Clinical Neurology* (2024). Elsevier. Available online at: https://www.sciencedirect.com/science/article/pii/B9780128239124000244 (Accessed 2024 Apr 30). Paraneoplastic Neurologic Disorders.

8. lo Greco MC, Marano G, Milazzotto R, Liardo RLE, Finocchiaro I, la Rocca M, et al. The immunomodulatory potential of concurrent high-dose radiotherapy and immune checkpoint inhibitor cemiplimab in advanced cutaneous squamous cell carcinoma: initial results. *J Personalized Med*. (2024) 14:581. doi: 10.3390/jpm14060581

frontiers | Frontiers in Oncology

TYPE Case Report
PUBLISHED 27 September 2024
DOI 10.3389/fonc.2024.1410291

Check for updates

OPEN ACCESS

EDITED BY
Sophia George,
University of Miami, United States

REVIEWED BY
Jinghui Sun,
Medical University of South Carolina, United States
Mohammed Alradhi,
Qingdao Binhai University, China

*CORRESPONDENCE
Qingli Li
liqingli73@163.com
Ping Wang
wangping_886@126.com

†These authors have contributed equally to this work and share first authorship

‡These authors have contributed equally to this work

RECEIVED 31 March 2024
ACCEPTED 06 September 2024
PUBLISHED 27 September 2024

CITATION
Wang Y, Li M, Yang K, Li Q and Wang P (2024) Urachal adenocarcinoma with cervical invasion misdiagnosed as primary cervical adenocarcinoma: a case report and literature review. *Front. Oncol.* 14:1410291. doi: 10.3389/fonc.2024.1410291

COPYRIGHT
© 2024 Wang, Li, Yang, Li and Wang. This is an open-access article distributed under the terms of the Creative Commons Attribution License (CC BY). The use, distribution or reproduction in other forums is permitted, provided the original author(s) and the copyright owner(s) are credited and that the original publication in this journal is cited, in accordance with accepted academic practice. No use, distribution or reproduction is permitted which does not comply with these terms.

Urachal adenocarcinoma with cervical invasion misdiagnosed as primary cervical adenocarcinoma: a case report and literature review

Yiran Wang[1,2†], Maomao Li[1,2†], Kaixuan Yang[3], Qingli Li[1,2*‡] and Ping Wang[1,2*‡]

[1]Department of Gynecology and Obstetrics, West China Second University Hospital, Sichuan University, Chengdu, Sichuan, China, [2]Key Laboratory of Birth Defects and Related Diseases of Women and Children (Sichuan University), Ministry of Education, Chengdu, Sichuan, China, [3]Department of Pathology, West China Second University Hospital, Sichuan University, Chengdu, Sichuan, China

Background: Urachal carcinoma (UrC) is a rare malignancy with no known specific early symptoms. It is often diagnosed at advanced stages and is associated with poor prognosis.

Case presentation: This study presents a rare case of urachal adenocarcinoma (UrAC) invading the bladder and vagina in a female patient. Initially, the patient was misdiagnosed as having a primary cervical adenocarcinoma 2.5 years prior. Subsequently, anterior pelvic exenteration and bilateral ureterocutaneostomies were performed. Twenty months after the first surgery, the patient was diagnosed with rectal metastasis and received gemcitabine chemotherapy. After achieving a stable disease state, the patient underwent laparoscopic ultralow rectal anterior resection, ultralow anastomosis of the sigmoid colon and rectum, prophylactic transverse colostomy, and right common iliac and external iliac lymph node dissection. The patient then received a cycle of postoperative chemotherapy with oxaliplatin and capecitabine; however, treatment was stopped due to adverse reactions. The patient continues to receive regular follow-ups, and her general condition is good.

Conclusions: UrC is rare, and preoperative differential diagnosis is difficult. This is the first report of UrC being misdiagnosed as cervical cancer. The presented case highlights the importance of accurate histopathological examination and comprehensive analysis. Anterior pelvic exenteration was also identified as a potentially effective treatment strategy for patients with local pelvic recurrence of UrC, although further investigation is required.

KEYWORDS

urachal carcinoma, cervical cancer, histopathological examination, anterior pelvic exenteration, case report

1 Introduction

Urachal carcinoma (UrC) is a rare non-urothelial malignancy that accounts for less than 1% of all bladder cancers (1). Adenocarcinoma is the most common type of UrC (2), which generally occurs along the midline from the apex vesicae to the umbilicus and within the Retzius space (3). The most common symptom at diagnosis is hematuria (58–82%); however, approximately 8% of patients are asymptomatic (4, 5). Most patients with UrC present at advanced stages and have poor prognosis, which is partly because of the lack of specific and early symptoms (5–7). The reported 5-year overall survival (OS) rate for UrC ranges between 27% and 61% (1, 2, 4, 8, 9). No standard evidence-based diagnostic or treatment guidelines have been established for UrC owing to its rarity. Here we report a rare case of urachal adenocarcinoma (UrAC) with cervical invasion that was initially misdiagnosed as primary cervical adenocarcinoma.

2 Case description

In July 2020, a 63-year-old woman was admitted to the Department of Gynecology in our hospital with a bladder mass that was detected during a follow-up examination after treatment for cervical adenocarcinoma.

The patient was diagnosed with International Federation of Gynecology and Obstetrics (FIGO) stage IIIB cervical adenocarcinoma in November 2017 at a local hospital after attending because of irregular vaginal bleeding. She had a history of hypertension, and her blood pressure was well controlled. The patient was treated with concurrent chemoradiotherapy, including vaginal brachytherapy, and the last treatment was in February 2018. Then the patient underwent regular follow-ups, and no recurrence or metastasis was observed until 27 months after treatment. During a periodic examination in June 2020, magnetic resonance imaging (MRI) identified a 2.4 × 1.7 cm space-occupying lesion in the posterior wall of the bladder. The probability that the mass was a malignant tumor was considered high. Physical examination showed that the anterior vaginal wall was hard and thickened, and an irregular mass with a diameter of approximately 3 cm was discovered by palpating. The vaginal vault disappeared, and the cervix was difficult to expose. The patient was asymptomatic. Transvaginal biopsy suggested adenocarcinoma of the posterior urethral wall without tumor involvement in the cervix. A subsequent positron emission tomography-computed tomography (PET-CT) scan of the entire body revealed a high possibility of disease recurrence in the uterine cervix, posterior bladder wall, and bilateral ureteral orifices. No distant metastases were noted on the PET-CT scan. Colonoscopy and gastroscopy did not show any signs of tumors. Therefore, the primary diagnosis was considered to be the recurrence and metastasis of cervical cancer.

Pathologists at our hospital reassessed the pathological sections that had previously been obtained by another hospital when the patient was admitted. The cervical and vaginal biopsy in 2017 indicated poorly differentiated adenocarcinoma with a vascular cancer embolus, but the squamous epithelium was normal (Figures 1A, B). The immunohistochemical (IHC) test revealed ER(-), PR(-), P16(-), CA125(-), CK7(+), CK20(-), SATB2(-), CDX-2(local+), CEA(+), P53(-), Napsin-A(-), CA199(+), MUC6(-), MUC2(-), and Ki67(+20–60%) (Figures 2A–L). Therefore, metastatic mucinous cancer was considered; however, the primary tumor remained unclear. Transvaginal biopsy performed in June 2020 confirmed adenocarcinoma of the posterior urethral wall, which was considered highly likely to be a mucinous adenocarcinoma (Figure 1C).

A case discussion was conducted by the gynecological oncologists to evaluate the possibility of surgical resection and prepare for anterior pelvic exenteration after communicating with the patient. During laparoscopic exploration in July 2020, a contractural lesion and tight adhesion between the posterior wall of the bladder and the anterior wall of the uterus were found, with the upper 3/4 of the vaginal wall being qualitatively hard. A laparoscopic radical hysterectomy with bilateral adnexectomy, pelvic lymphadenectomy, cystectomy, and vaginal and urethral resection were performed. The organs were removed through the vulva before vulvalplasty. Subsequently, bilateral ureterocutaneostomy was performed using two mono-J catheters as ureteral stents, and a pelvic drainage tube was inserted. The entire operation lasted 320 min, with an estimated blood loss of 300 mL, and no intraoperative complications were identified.

The final pathological analysis indicated that the lesion was a poorly differentiated mucinous metastatic adenocarcinoma that extensively infiltrated the muscular layer and outer layer of almost the entire bladder wall and the upper 3/4 of the vaginal wall interstitium. The cancer invaded some skeletal muscles outside the vaginal wall and some nerves and blood vessels in the bladder wall (Figures 1D–F). The bladder mucosa was normal, and no residual cancer was detected in the uterine cervix. No metastatic lymph nodes were observed, and the resected margins were negative. The IHC examination of bladder tumor cells showed CK7(+), CAM5.2(+), CA199(+), CD10(+), GATA3(local+), Ki67 (+70%), and Ber-ep4(+) staining, while IHC staining was negative for ER, PR, P16, CA125, CK20, SATB2, CDX-2, Pax-8, MUC2, MUC5, Vim, P53, S-100, SMA, D2-40, Calretinin, and MC (Figures 3A–L). The IHC examination of vaginal tumor cells revealed CK7(+), CDX-2(+), CEA(+), CA199(+), GATA3(+), TTF-1(local+), MUC5(+), Villin(+), and Ki67(+70%), whereas IHC staining was negative for ER, PR, P53, P16, CA125, CK20, HNF1-β, Napsin-A, and MUC6. Based on the morphology, distribution characteristics of the tumors, and IHC results, the pathologists concluded that the primary cancer arose from UrAC. The clinical cancer stage was IIID UrC, according to the staging system proposed by Sheldon (10).

Regular follow-ups were conducted after surgery, and the patient underwent a tension-free hernioplasty for a pelvic floor

Abbreviations: CT, computerized tomography; ECAs, endocervical adenocarcinomas; HPVA, HPV-associated; IECC, International Endocervical Adenocarcinoma Criteria and Classification; IHC, immunohistochemistry; MRI, magnetic resonance imaging; NHPVA, non-HPV-associated; NOS, not otherwise specified; PET-CT, positron emission tomography-computed tomography; UrAC, urachal adenocarcinoma; UrC, Urachal carcinoma.

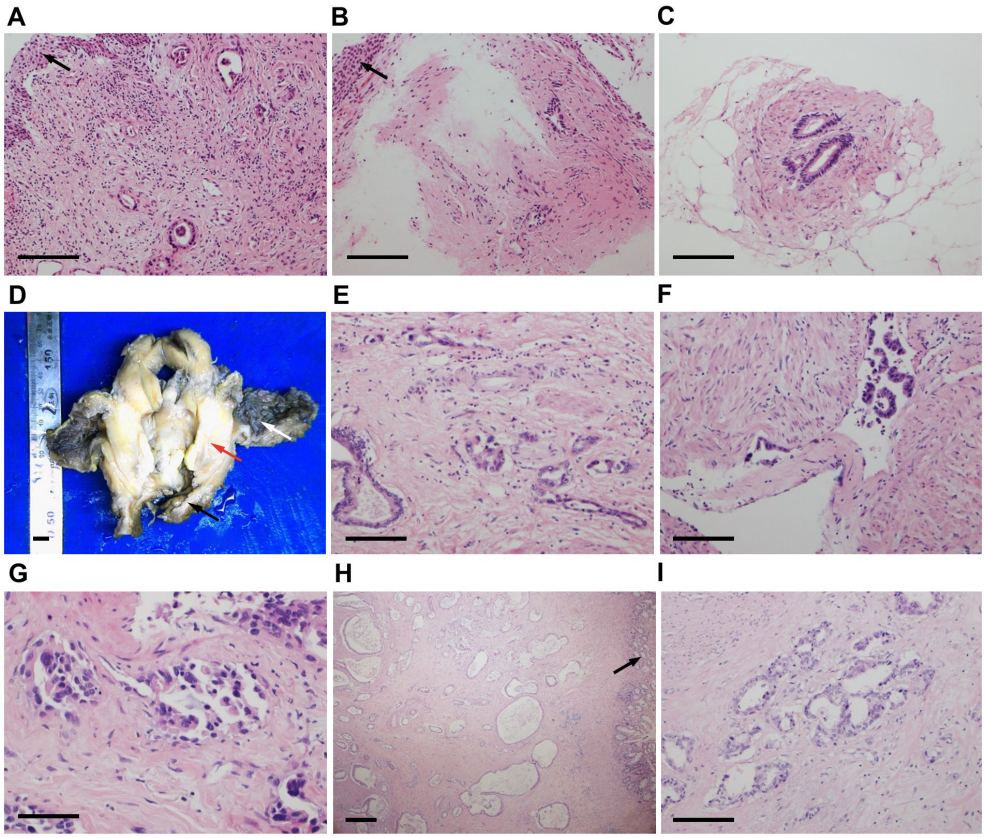

FIGURE 1
Hematoxylin and eosin (HE) staining of cervical (**A**, ×200), vaginal (**B**, ×200) and urethral (**C**, ×200) biopsy tissues. Squamous epithelium was normal (black arrows). **(D)** Surgical specimens of the bladder, uterus (red arrow), and vagina (black arrow). The bladder mucosa was normal (white arrow). HE staining of the bladder tumor (**E**, ×200) with a vascular cancer embolus (**F**, ×200). **(G)** HE staining of the puncture tissue in the thickened area of the rectum (×400). **(H, I)** HE staining of the surgical rectum specimen (**H**, ×40; I, ×200). The rectal mucosa was normal (black arrow). Similar tumor cells have been observed in cervical, vaginal, urethral, bladder, and rectal tumors, where cells are arranged in a single layer with glandular tube-like structures. Scale bars: **(A–C, E, F, I)** 400 μm. **(D)** 1 cm. **(G)** 200 μm. **(H)** 1 mm.

incisional hernia in January 2021. Follow-up MRI scans were performed within 1.5 years of the anterior pelvic exenteration and showed no signs of cancer recurrence or metastasis. In March 2022, another MRI scan revealed a thickening of the middle and lower rectal walls, with an enhanced nodule on the left wall of the middle rectum. A PET-CT scan showed a high probability of metastasis to the left posterior mesentery of the middle rectum and right common iliac lymph nodes. An ultrasound-guided rectal puncture was performed, and the pathology report revealed a mucinous adenocarcinoma in the smooth muscle tissue (Figure 1G). IHC results revealed CK7(+), CK20(-), CDX-2 (local+), SATB2(-), PAX-8(-), P16(-), HPVRNAscope(-), WT1(-), P53(wild-type), Ki67(+10%), CEA(+), PAX-2(-), ER(-), and PR(-). The immunophenotype was not aligned with HPV-associated cervical adenocarcinoma metastasis but was consistent with the metastasis of urachal mucinous adenocarcinoma.

The patient then began tumor immunotherapy with sintilimab but stopped because of severe edema in both lower extremities. From May to August 2022, the patient received four cycles of gemcitabine chemotherapy. In September 2022, after achieving a stable disease state, the patient underwent laparoscopic ultralow rectal anterior resection, ultralow anastomosis of the sigmoid colon and rectum, prophylactic transverse colostomy, and right common iliac and external iliac lymph node dissection. The postoperative pathological report indicated a highly to moderately differentiated adenocarcinoma involving the submucosa, muscular layer, and adventitia of the rectum, while the rectal mucosa was normal (Figures 1H, I). Based on the microscopic tumor growth pattern and the patient's clinical history, the tumor was considered metastatic. The resected margins were negative, and no metastatic lymph nodes were observed.

After surgery, the patient received chemotherapy with oxaliplatin and capecitabine tablets in October 2022. However, the patient developed severe lower extremity edema and allergic reactions and refused to continue the chemotherapy. At the time of submission, the patient was continuing with regular follow-ups, and her general condition was good. The treatment timeline for the current case is shown in Figure 4.

3 Discussion

Bladder cancer is a common cancer globally, with over 600,000 new cases annually (11). Urothelial carcinoma is the most

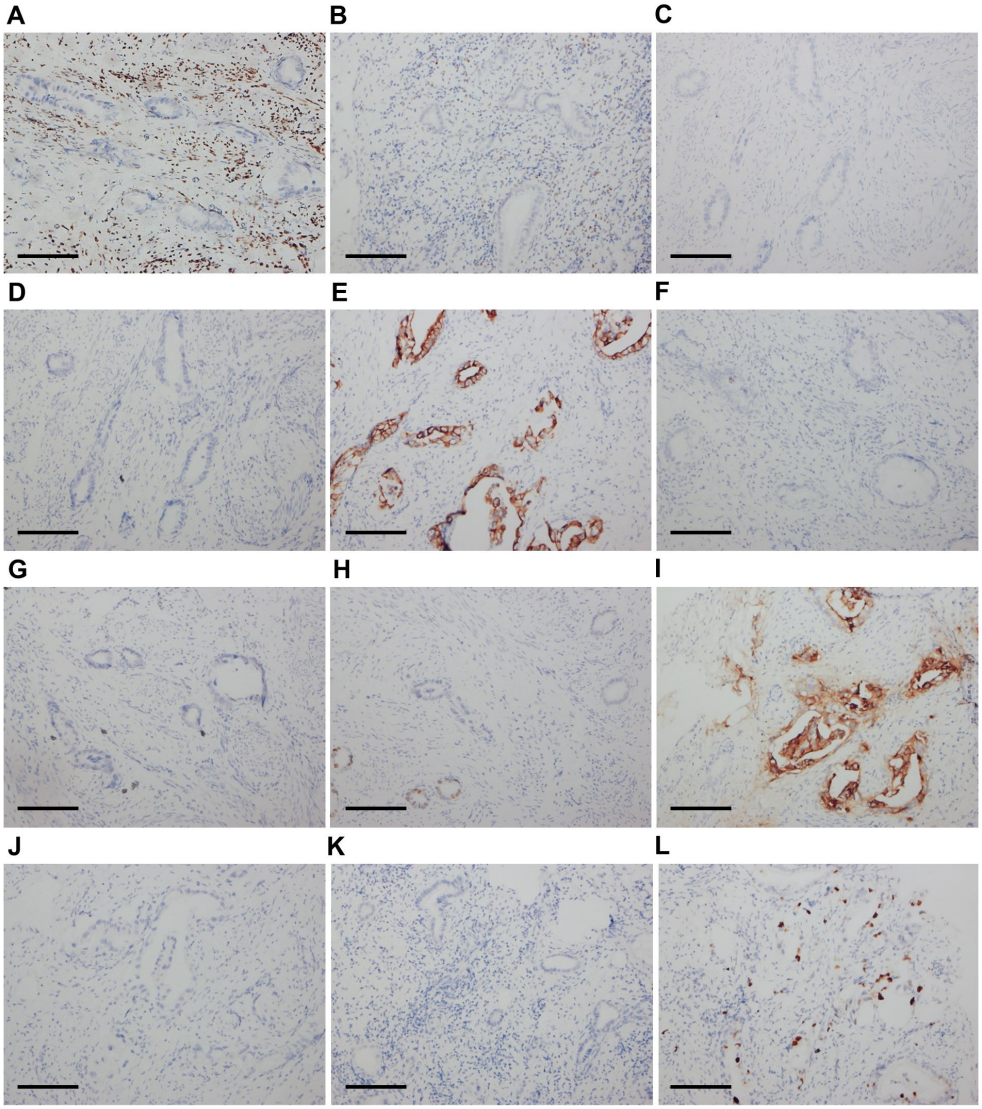

FIGURE 2
Immunohistochemical results of cervical tumor cells (×200). The cells were negative for ER **(A)**, PR **(B)**, P16 **(C)**, and CA125 **(D)**. The cells were diffusely positive for CK7 **(E)**. The cells were negative for CK20 **(F)** and SATB2 **(G)**. The cells were locally positive for CDX-2 **(H)** and diffusely positive for CEA **(I)**. The cells were negative for MUC6 **(J)** and MUC2 **(K)**. The Ki67 score was 20-60% **(L)**. Scale bars: **(A–L)** 400 μm.

commonpathological type, whereas bladder carcinomas with adenocarcinomatous features are rare and comprise 0.5–2% of cases, including primary adenocarcinoma in the bladder, UrAC, and Müllerian-type tumors (12–14). In a population-based study, including 1525 patients with primary adenocarcinoma of the bladder, UrACs accounted for approximately 10% of cases (2).

The urachus canal connects the fetal bladder and allantois. In early infancy, the urachus obliterates into a fibromuscular cord stretching between the bladder dome and umbilicus, known as the median umbilical ligament (1, 3). However, urachal remnants persist in approximately one-third of the population and carry a risk of developing various lesions (3).

In 1930, Begg published the first extensive description of UrC (15). The case reported here differs from previously reported cases of UrC because the patient had a history of cervical cancer diagnosed 2.5 years prior. When reassessing the pathological sections of the cervical and vaginal biopsies, metastatic mucinous adenocarcinoma was considered instead of primary cervical cancer. Cervical invasion or metastasis from non-gynecological cancers is relatively rare and difficult to diagnose (16). However, it is important to differentiate non-primary cervical carcinomas from primary cervical carcinomas because treatments and prognoses differ depending on the origin (17). According to the International Endocervical Adenocarcinoma Criteria and Classification (IECC), endocervical adenocarcinomas (ECAs) are classified as either HPV-associated (HPVA) or non-HPV-associated (NHPVA) (18). Mucinous ECAs comprise HPVA and NHPVA tumor subtypes (18). The former, including intestinal, signet ring cell, mucinous not otherwise specified (NOS), and invasive stratified mucin-producing carcinoma types, are usually

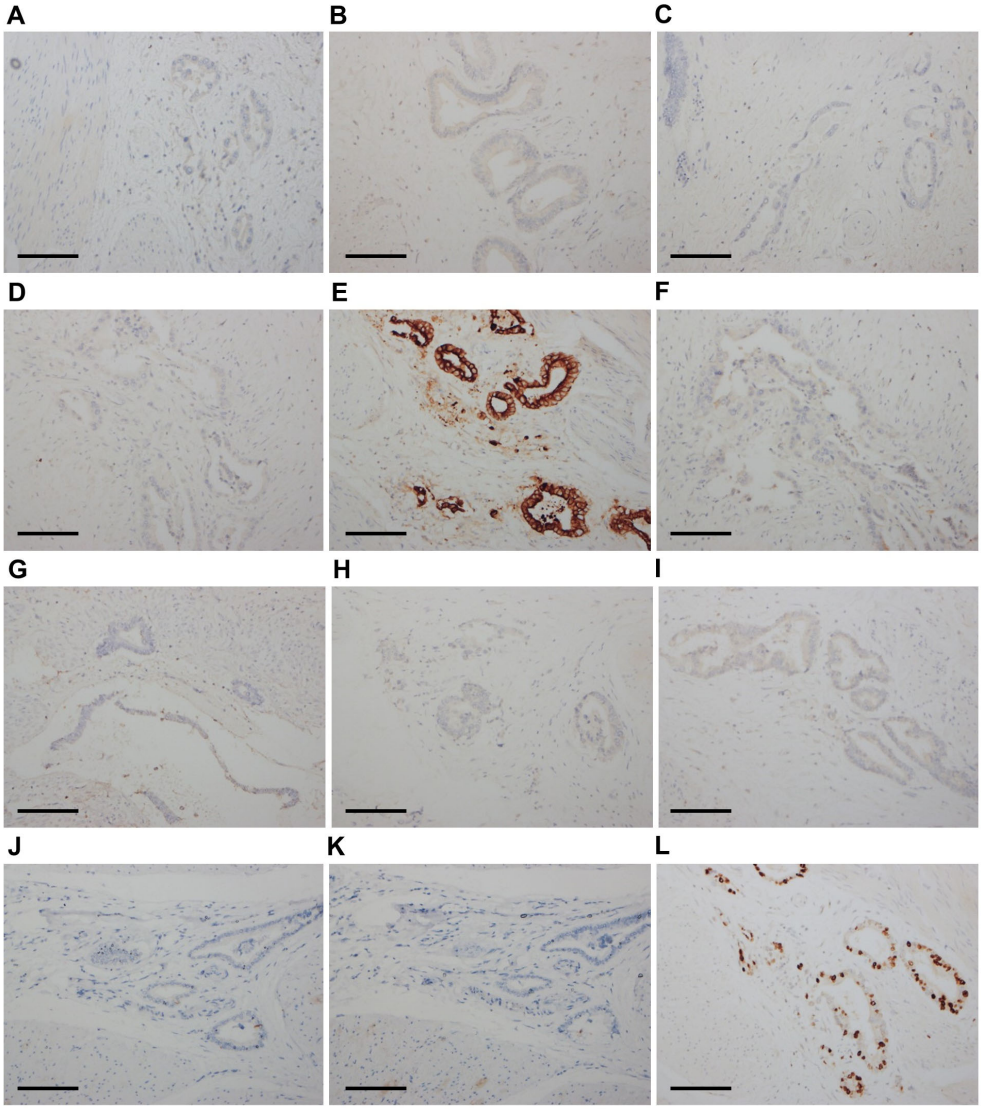

FIGURE 3
Immunohistochemical results of bladder tumor cells (×200). The cells were negative for ER **(A)**, PR **(B)**, P16 **(C)**, and CA125 **(D)**. The cells were diffusely positive for CK7 **(E)**. The cells were negative for CK20 **(F)**, SATB2 **(G)**, CDX-2 **(H)**, Pax-8 **(I)**, MUC2 **(J)**, and MUC5 **(K)**. The Ki67 score was 70% **(L)**. Scale bars: **(A–L)** 400 μm.

HPV-positive (18). NHPVA mucinous ECAs refer to gastric-type adenocarcinomas (18), which usually stain positive for CK7, CEA, CA125, MUC6, CA199, and HNF1-β (19). The pathological results of the tumor specimens in this study showed that the mucinous adenocarcinoma was P16-negative, and *in-situ* hybridization with the RNAscope probe showed that it was HPV-negative. Thus, a differential diagnosis to exclude NHPVA cervical adenocarcinoma, particularly gastric-type carcinoma, was considered in this case. Consequently, the described case was reviewed and discussed by oncologists and pathologists. Similar tumor cells have been observed in cervical, vaginal, urethral, rectal, and bladder tumors arranged in a single layer with glandular tube-like structures. The nuclei were mildly to moderately atypical, with occasional mitotic figures. The squamous epithelium was normal in the cervical and vaginal biopsy tissues collected in 2017, and the mucosae of the bladder and rectum sampled in the surgeries were also normal. The IHC examination of tumor cells revealed CK7(+), CEA(+), and CA199(+), whereas IHC staining was negative for ER, PR, P53, P16, CA125, CK20, HNF1-β, and MUC6. The patient was initially diagnosed with stage IIIB cervical cancer six years prior to this report; however, the tumor was always confined to the pelvis, and the patient's general condition was good during treatment. These findings are consistent with the pathomorphological, immunohistochemical, and clinical characteristics of UrAC rather than those of primary cervical adenocarcinoma. After discussion, the patient was diagnosed with primary advanced UrAC. We determined that the patient had been misdiagnosed as having primary cervical adenocarcinoma in 2017, and the correct diagnosis would have been urachal mucinous adenocarcinoma with cervical invasion.

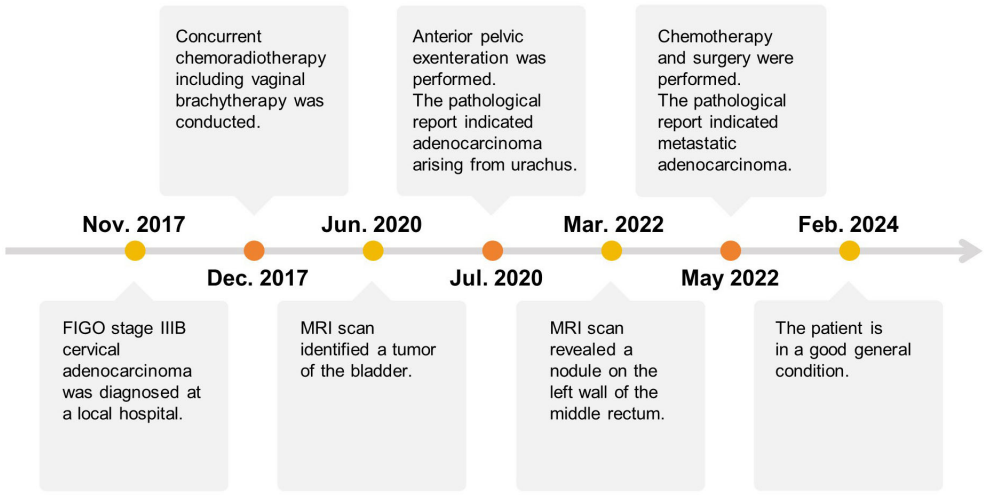

FIGURE 4
The treatment timeline of the patient.

UrC is a rare malignancy, and there is still no consensus on diagnostic criteria and standard treatment (1). Several diagnostic criteria for UrCs were proposed in 1954 (20, 21). In 2016, Paner et al. modified the UrAC criteria to include the following characteristics: (a) tumor located in the dome/anterior wall of the bladder; (b) epicenter of carcinoma in the bladder wall; (c) absence of a urothelial bladder tumor; (d) absence of widespread atypical intestinal metaplasia, cystitis/glandularis beyond the dome/anterior wall; and (e) absence of primary adenocarcinoma of a different origin that has spread secondarily to the bladder (3). However, some researchers consider these criteria overly restrictive. For example, Arlene et al. emphasized that urethral cancers occur anywhere along the urachal ligament. Although it occurs in most cases, bladder involvement is not medatory at the time of diagnosis (22). Further, urachal remnants are observed not only at the bladder dome but also on the anterior or posterior wall along the midline in surgical series (23). In our case, the cancer invaded almost the entire bladder wall at admission to our hospital, meeting the diagnostic criteria for UrC on postoperative pathology.

Diagnosing UrC before surgery is challenging. Abdominal ultrasound can detect the masses in the bladder wall. Computerized tomography (CT) scans and MRIs can evaluate local invasions, lymph nodes, or distant metastases (4, 24). Cystoscopy aids in tumor localization and biopsies of the mass (4, 24). Szarvas et al. (24) found that urinary cytology presented as positive in only 29% of cases. Siefker-Radtke et al. (25) explored the potential role of serum markers in a cohort of 42 UrC and reported an increase in CEA (59%), CA19-9 (60%), and CA125 (44%). Meeks et al. (26) assessed the preoperatively available methods for the diagnosis of UrC, such as biopsy by transurethral resection, imaging, cytology, and exploration under anesthesia. Biopsy had the highest specificity (1) and positive predictive value (1), with a sensitivity and negative predictive value of 0.93 and 0.5, respectively. Combining imaging and biopsy did not offer a high negative predictive value (0.60). Therefore, reliable preoperative UrC diagnosis methods are currently lacking (26).

In our case, when the cervical mass was initially detected, an MRI did not reveal any suspicious tumor lesions beyond those in the cervix and vagina. However, due to limited MRI sensitivity and biopsy specimen content, ruling out urachal mucinous adenocarcinoma with cervical invasion was difficult. We feel that oncologists and pathologists should consider non-primary cervical carcinoma, especially when cervical biopsy tissue is limited. A thorough workup for differential diagnosis is necessary for patients with uncommon presentations or pathological findings for cervical adenocarcinoma. In addition, a comprehensive analysis is crucial, as imaging and histopathological findings may not be definitive.

Adenocarcinoma is the most common type of UrC and shares similarities with adenocarcinomas of other origins, particularly colorectal adenocarcinomas (4, 27). Usually, IHC is crucial for differential diagnosis; however, in some cases, it cannot provide an accurate diagnosis because of overlapping tumor features. In UrAC, CK20 is positive in approximately 97% of cases, while CK7 is positive in 51% (27). CDX2 and MUC5AC are often detected at high rates in UrACs (90% and 92%, respectively), and nuclear staining with β-catenin is found to be positive in 14% of cases (27). According to Bayrak et al., the CK7-/CK20+ immunophenotype is a specific and sensitive marker of colorectal origin. The CK7+/CK20- phenotype was expressed in only 1.7% (2 of 118) of colorectal adenocarcinomas (28). Diffused CK7 and β-catenin can help differentiate the enteric subtype of UrAC from colonic adenocarcinoma, with the former being nuclear β-catenin(-) and CK7 (+/-), while the latter being diffuse nuclear β-catenin(+) and CK7(-) (3, 27, 29). In our case, the CK7+/CK20- phenotype and intact normal colorectal mucosa did not support primary colorectal adenocarcinoma.

The occurrence and development of bladder urothelial carcinoma are reported to be associated with DNA-level molecular alterations (30, 31). Additionally, the most frequently mutated genes in ordinary bladder cancer are KMT2C, ATM,

FAT1, CREBBP, ERBB2, SPTAN1, and KMT2A (30, 31). However, several molecular analyses in previous studies have shown that the mutation pattern of UrC is more similar to colorectal than to urothelial carcinoma (4, 32, 33). Mutational hotspots of selected genes were tested in 22 UrC samples, and KRAS mutations in 6 of the 22 (27%) UrC cases were found, followed by BRAF (18%) and NRAS (5%). No mutations in the PIK3CA and EGFR genes were observed (32). In a research study on 17 patients with UrC by Lee et al., they found that six genes in functionally important domains had recurrent mutations: COL5A1, APC, LRP1B, SMAD4, KIF26B, and TP53. In addition, the fibroblast growth factor receptor (FGFR) gene family was amplified in six patients, while the epidermal growth factor receptor (EGFR) family was amplified in four (33). These findings also suggest that potential treatments for urachal cancer should target these gene families; for example, anti-EGFR agents and FGFR inhibitors (33).

Surgery is the recommended therapy for localized cases of UrC. Excision of the urachus, the umbilicus, partial/radical cystectomy, and bilateral pelvic lymphadenectomy are standard procedures and thus routinely performed (34). Research indicates that survival outcomes do not significantly differ between patients treated with either partial cystectomy or radical cystectomy procedures (35, 36). However, UrAC often recurs (20–54%) post-surgery, and the median time to recurrence after resection of the primary tumor is reported to be approximately 29–32.7 months (4, 25, 37). Chemotherapy, with cisplatin and 5-FU, is the most commonly used regimen for treating metastatic disease (4). A meta-analysis showed that cisplatin-5-FU combination therapy might be the most effective treatment as it shows a high (43%) response rate and a low (14%) progression rate (24). The similarity of urachal cancer to colorectal adenocarcinoma has led some researchers to propose several schemes that are reasonable for small sample sizes, such as mFOLFOX6 (a modified combination of 5-fluorouracil, leucovorin, and oxaliplatin), cetuximab, and irinotecan (38–40). For example, Yanagihara et al. stated that mFOLFOX6 appears to be effective for the treatment of metastatic urachal cancer, with one of the five patients (20%) achieving a clinically complete response and another one achieving a partial response (40). Collazo-Lorduy et al. (38) reported a patient with metastatic urachal cancer who was EGFR amplified and had wild-type KRAS. The patient was treated with cetuximab, an anti-EGFR monoclonal antibody, and achieved a partial response for more than eight months (38). However, multicenter collaborations are required to validate these drug treatments for this rare malignancy.

Pelvic exenteration is an ultra-radical surgery that involves complete en bloc resection of malignant lesions and pelvic viscera, divided into anterior, posterior, and total pelvic exenterations (41). It is the only curative option for many locally advanced and recurrent pelvic malignancies after patients have previously undergone chemotherapy, radiotherapy, or surgery (42). In our case, anterior pelvic exenteration was performed before a clear diagnosis. The procedure seems to be effective against the local pelvic recurrence of UrC. However, as only one case was evaluated, further investigations, including prospective data, are needed to validate the efficacy of the procedure.

4 Conclusions

UrC is a rare malignancy that is diagnostically and therapeutically challenging for oncologists, and accurate histopathological examinations and comprehensive analyses are essential to avoid misdiagnoses. In this report, anterior pelvic exenteration was identified as a potentially effective treatment for a patient with a local pelvic recurrence of UrC. However, further study of existing treatment methods is required to establish a standard treatment strategy. To the best of our knowledge, this is the first report of a patient with UrAC misdiagnosed as primary cervical cancer, and we hope to provide further reference material to improve the diagnosis and treatment of this disease.

Data availability statement

The original contributions presented in the study are included in the article/supplementary material. Further inquiries can be directed to the corresponding authors.

Ethics statement

This study was approved by the medical ethics committee of West China Second Hospital of Sichuan University (No.2023(359)). Written informed consent was obtained from the individual(s) for the publication of any potentially identifiable images or data included in this article.

Author contributions

YW: Data curation, Formal analysis, Investigation, Writing – original draft, Visualization. ML: Data curation, Formal analysis, Investigation, Writing – original draft, Visualization. KY: Methodology, Visualization, Writing – review & editing. QL: Conceptualization, Project administration, Supervision, Writing – review & editing. PW: Conceptualization, Project administration, Supervision, Writing – review & editing.

Funding

The author(s) declare that financial support was received for the research, authorship, and/or publication of this article. This study was supported by the National Key Research and Development Program of China (No. 2021YFC2009100).

Acknowledgments

We thank all authors for their contributions.

Conflict of interest

The authors declare that the research was conducted in the absence of any commercial or financial relationships that could be construed as a potential conflict of interest.

Publisher's note

All claims expressed in this article are solely those of the authors and do not necessarily represent those of their affiliated organizations, or those of the publisher, the editors and the reviewers. Any product that may be evaluated in this article, or claim that may be made by its manufacturer, is not guaranteed or endorsed by the publisher.

References

1. Bruins HM, Visser O, Ploeg M, Hulsbergen-van de Kaa CA, Kiemeney LALM, Witjes JA. The clinical epidemiology of urachal carcinoma: results of a large, population based study. *J Urol*. (2012) 188:1102–7. doi: 10.1016/j.juro.2012.06.020

2. Wright JL, Porter MP, Li CI, Lange PH, Lin DW. Differences in survival among patients with urachal and nonurachal adenocarcinomas of the bladder. *Cancer*. (2006) 107:721–8. doi: 10.1002/cncr.22059

3. Paner GP, Lopez-Beltran A, Sirohi D, Amin MB. Updates in the pathologic diagnosis and classification of epithelial neoplasms of urachal origin. *Adv Anat Pathol*. (2016) 23:71–83. doi: 10.1097/PAP.0000000000000110

4. Claps M, Stellato M, Zattarin E, Mennitto A, Sepe P, Guadalupi V, et al. Current understanding of urachal adenocarcinoma and management strategy. *Curr Oncol Rep*. (2020) 22:9. doi: 10.1007/s11912-020-0878-z

5. Dhillon J, Liang Y, Kamat AM, Siefker-Radtke A, Dinney CP, Czerniak B, et al. Urachal carcinoma: a pathologic and clinical study of 46 cases. *Hum Pathol*. (2015) 46:1808–14. doi: 10.1016/j.humpath.2015.07.021

6. Guerin M, Miran C, Colomba E, Cabart M, Herrmann T, Pericart S, et al. Urachal carcinoma: a large retrospective multicentric study from the French Genito-Urinary Tumor Group. *Front Oncol*. (2023) 13:1110003. doi: 10.3389/fonc.2023.1110003

7. Mennitto A, Vernieri C, Procopio G. Urachal carcinoma: towards a precision medicine. *Transl Cancer Res*. (2016) 5:S1307-10. doi: 10.21037/tcr.2016.12.28

8. Grignon DJ, Ro JY, Ayala AG, Johnson DE, Ordóñez NG. Primary adenocarcinoma of the urinary bladder. A clinicopathologic analysis of 72 cases. *Cancer*. (1991) 67:2165–72. doi: 10.1002/1097-0142(19910415)67:8<2165::aid-cncr2820670827>3.0.co;2-m

9. Wang T, Lv Z, Feng H, Li J, Cui B, Yang Y, et al. Survival of patients with urAC and primary BAC and urothelial carcinoma with glandular differentiation. *Front Oncol*. (2022) 12:860133. doi: 10.3389/fonc.2022.860133

10. Sheldon CA, Clayman RV, Gonzalez R, Williams RD, Fraley EE. Malignant urachal lesions. *J Urol*. (1984) 131:1–8. doi: 10.1016/s0022-5347(17)50167-6

11. Bray F, Laversanne M, Sung H, Ferlay J, Siegel RL, Soerjomataram I, et al. Global cancer statistics 2022: GLOBOCAN estimates of incidence and mortality worldwide for 36 cancers in 185 countries. *CA Cancer J Clin*. (2024) 74:229–63. doi: 10.3322/caac.21834

12. Alradhi M, Safi M, Tao S, Al-danakh A, Almoiliqy M, Baldi S, et al. Surgery improves survival in bladder signet-ring cell carcinoma-a population-based study. *Ther Adv Urol*. (2022) 14:17562872221079473. doi: 10.1177/17562872221079473

13. Zaghloul MS, Nouh A, Nazmy M, Ramzy S, Zaghloul AS, Sedira MA, et al. Long-term results of primary adenocarcinoma of the urinary bladder: A report on 192 patients. *Urol Oncol Semin Orig Investig*. (2006) 24:13–20. doi: 10.1016/j.urolonc.2005.05.027

14. Park S, Reuter VE, Hansel DE. Non-urothelial carcinomas of the bladder. *Histopathology*. (2019) 74:97–111. doi: 10.1111/his.13719

15. Begg RC. The urachus: its anatomy, histology and development. *J Anat*. (1930) 64:170–83.

16. Clement PB. Miscellaneous primary tumors and metastatic tumors of the uterine cervix. *Semin Diagn Pathol*. (1990) 7:228–48.

17. Martínez-Román S, Frumovitz M, Deavers MT, Ramirez PT. Metastatic carcinoma of the gallbladder mimicking an advanced cervical carcinoma. *Gynecol Oncol*. (2005) 97:942–5. doi: 10.1016/j.ygyno.2005.01.054

18. Stolnicu S, Barsan I, Hoang L, Patel P, Terinte C, Pesci A, et al. International endocervical adenocarcinoma criteria and classification (IECC): A new pathogenetic classification for invasive adenocarcinomas of the endocervix. *Am J Surg Pathol*. (2018) 42:214–26. doi: 10.1097/PAS.0000000000000986

19. Carleton C, Hoang L, Sah S, Kiyokawa T, Karamurzin YS, Talia KL, et al. A detailed immunohistochemical analysis of a large series of cervical and vaginal gastric-type adenocarcinomas. *Am J Surg Pathol*. (2016) 40:636–44. doi: 10.1097/PAS.0000000000000578

20. Wheeler JD, Hill WT. Adenocarcinoma involving the urinary bladder. *Cancer*. (1954) 7:119–35. doi: 10.1002/1097-0142(195401)7:1<119::aid-cncr2820070113>3.0.co;2-8

21. Mostofi FK, Thomson RV, Dean AL. Mucous adenocarcinoma of the urinary bladder. *Cancer*. (1955) 8:741–58. doi: 10.1002/1097-0142(1955)8:4<741::aid-cncr2820080417>3.0.co;2-c

22. Siefker-Radtke A. Urachal carcinoma: surgical and chemotherapeutic options. *Expert Rev Anticancer Ther*. (2006) 6:1715–21. doi: 10.1586/14737140.6.12.1715

23. Schubert GE, Pavkovic MB, Bethke-Bedürftig BA. Tubular urachal remnants in adult bladders. *J Urol*. (1982) 127:40–2. doi: 10.1016/S0022-5347(17)53595-8

24. Szarvas T, Módos O, Niedworok C, Reis H, Szendröi A, Szász MA, et al. Clinical, prognostic, and therapeutic aspects of urachal carcinoma-A comprehensive review with meta-analysis of 1,010 cases. *Urol Oncol*. (2016) 34:388–98. doi: 10.1016/j.urolonc.2016.04.012

25. Siefker-Radtke AO, Gee J, Shen Y, Wen S, Daliani D, Millikan RE, et al. Multimodality management of urachal carcinoma: the M. D. Anderson Cancer Center experience. *J Urol*. (2003) 169:1295–8. doi: 10.1097/01.ju.0000054646.49381.01

26. Meeks JJ, Herr HW, Bernstein M, Al-Ahmadie HA, Dalbagni G. Preoperative accuracy of diagnostic evaluation of the urachal mass. *J Urol*. (2013) 189:1260–2. doi: 10.1016/j.juro.2012.10.043

27. Reis H, Krafft U, Niedworok C, Módos O, Herold T, Behrendt M, et al. Biomarkers in urachal cancer and adenocarcinomas in the bladder: A comprehensive review supplemented by own data. *Dis Markers*. (2018) 2018:7308168. doi: 10.1155/2018/7308168

28. Bayrak R, Haltas H, Yenidunya S. The value of CDX2 and cytokeratins 7 and 20 expression in differentiating colorectal adenocarcinomas from extraintestinal gastrointestinal adenocarcinomas: cytokeratin 7-/20+ phenotype is more specific than CDX2 antibody. *Diagn Pathol*. (2012) 7:9. doi: 10.1186/1746-1596-7-9

29. Paner GP, McKenney JK, Barkan GA, Yao JL, Frankel WL, Sebo TJ, et al. Immunohistochemical analysis in a morphologic spectrum of urachal epithelial neoplasms: diagnostic implications and pitfalls. *Am J Surg Pathol*. (2011) 35:787–98. doi: 10.1097/PAS.0b013e3182189c11

30. Alradhi M, Wen S, Safi M, Al-danakh A, Wang H, Shopit A, et al. Molecular genetic and clinical characteristic analysis of primary signet ring cell carcinoma of urinary bladder identified by a novel OR2L5 mutation. *Cancer Med*. (2023) 12:3931–51. doi: 10.1002/cam4.5121

31. Robertson AG, Kim J, Al-Ahmadie H, Bellmunt J, Guo G, Cherniack AD, et al. Comprehensive molecular characterization of muscle-invasive bladder cancer. *Cell*. (2018) 174:1033. doi: 10.1016/j.cell.2018.07.036

32. Módos O, Reis H, Niedworok C, Rübben H, Szendröi A, Szász MA, et al. Mutations of KRAS, NRAS, BRAF, EGFR, and PIK3CA genes in urachal carcinoma: Occurence and prognostic significance. *Oncotarget*. (2016) 7:39293–301. doi: 10.18632/oncotarget.9828

33. Lee S, Lee J, Sim SH, Lee Y, Moon KC, Lee C, et al. Comprehensive somatic genome alterations of urachal carcinoma. *J Med Genet*. (2017) 54:572–8. doi: 10.1136/jmedgenet-2016-104390

34. Tiutiucă RC, Năstase Puşcaşu AI, Ţarcă E, Stoenescu N, Cojocaru E, Trandafir LM, et al. Urachal carcinoma, an unusual possibility of hematuria; case report and literature review. *Diagnostics*. (2022) 12:1892. doi: 10.3390/diagnostics12081892

35. Ashley RA, Inman BA, Sebo TJ, Leibovich BC, Blute ML, Kwon ED, et al. Urachal carcinoma: clinicopathologic features and long-term outcomes of an aggressive Malignancy. *Cancer*. (2006) 107:712–20. doi: 10.1002/cncr.22060

36. Milhoua PM, Knoll A, Bleustein CB, Ghavamian R. Laparoscopic partial cystectomy for treatment of adenocarcinoma of the urachus. *Urology*. (2006) 67:423.e15–7. doi: 10.1016/j.urology.2005.08.044

37. Duan F, Zhai W, Zhang B, Guo S. Urachal carcinoma: Impact of recurrence pattern and lymphadenectomy on long-term outcomes. *Cancer Med*. (2020) 9:4166–74. doi: 10.1002/cam4.3059

38. Collazo-Lorduy A, Castillo-Martin M, Wang L, Patel V, Iyer G, Jordan E, et al. Urachal carcinoma shares genomic alterations with colorectal carcinoma and may respond to epidermal growth factor inhibition. *Eur Urol*. (2016) 70:771–5. doi: 10.1016/j.eururo.2016.04.037

39. Kume H, Tomita K, Takahashi S, Fukutani K. Irinotecan as a new agent for urachal cancer. *Urol Int*. (2006) 76:281–2. doi: 10.1159/000091635

40. Yanagihara Y, Tanji N, Miura N, Shirato A, Nishimura K, Fukumoto T, et al. Modified FOLFOX6 chemotherapy in patients with metastatic urachal cancer. *Chemotherapy*. (2013) 59:402–6. doi: 10.1159/000362400

41. Jäger L, Nilsson PJ, Rådestad AF. Pelvic exenteration for recurrent gynecologic Malignancy: a study of 28 consecutive patients at a single institution. *Int J Gynecol Cancer*. (2013) 23:755–62. doi: 10.1097/IGC.0b013e318287a874

42. Peacock O, Waters PS, Kong JC, Warrier SK, Wakeman C, Eglinton T, et al. Complications after extended radical resections for locally advanced and recurrent pelvic Malignancies: A 25-year experience. *Ann Surg Oncol*. (2020) 27:409–14. doi: 10.1245/s10434-019-07816-8

frontiers | Frontiers in Oncology

TYPE Case Report
PUBLISHED 01 October 2024
DOI 10.3389/fonc.2024.1449870

Check for updates

OPEN ACCESS

EDITED BY
Sophia George,
University of Miami, United States

REVIEWED BY
Junlin Liao,
The University of Iowa, United States
Shuhei Yoshida,
Hiroshima University, Japan

*CORRESPONDENCE
Tao Ye
349581341@qq.com

RECEIVED 16 June 2024
ACCEPTED 04 September 2024
PUBLISHED 01 October 2024

CITATION
Lei H, Sun J, Wang Y and Ye T (2024) Recurrent giant cystic lymphangioma of peritoneum: a case report and literature review.
Front. Oncol. 14:1449870.
doi: 10.3389/fonc.2024.1449870

COPYRIGHT
© 2024 Lei, Sun, Wang and Ye. This is an open-access article distributed under the terms of the Creative Commons Attribution License (CC BY). The use, distribution or reproduction in other forums is permitted, provided the original author(s) and the copyright owner(s) are credited and that the original publication in this journal is cited, in accordance with accepted academic practice. No use, distribution or reproduction is permitted which does not comply with these terms.

Recurrent giant cystic lymphangioma of peritoneum: a case report and literature review

Hongyan Lei, Jinxin Sun, Yongzhou Wang and Tao Ye*

Department of Gynecology, The Affiliated Traditional Chinese Medicine Hospital, Southwest Medical University, Luzhou, China

Cystic lymphangioma (CL) is a rare benign tumor of the lymphatic system, most commonly found in the neck, head, and armpits. The incidence of lymphangiomas in the abdominal cavity is less than 5%, and the incidence of retroperitoneal tumors is even lower. We report here a case of recurrent giant CL that recurred 20 years after the first complete surgical resection. Pelvic MRI at 6 months follow-up after the second complete surgical resection indicated a recurrence of the tumor. The main purpose of this article is to explore the treatment and follow-up strategies for recurrent lymphangioma.

KEYWORDS

cystic lymphangioma, surgical resection, case report, recurrence, treatment

Introduction

CL is a cyst formed by congenital lymphatic malformation, which can occur in anywhere in the body (1). It originates from lymphatic endothelial cells and is believed to be due to the dilation or abnormal development of lymphatic vessels (2). CL is more common in the neck or armpit, accounting for only 5% of lesions in the abdominal lymphatic vessels, and retroperitoneal lymphangioma is even rarer (3). It can occur at any age, but is more common in children (4). Histologically, it consists of an enlarged cystic space containing a proteinaceous fluid with thin septa lined by endothelial cells[(5). Preoperative diagnosis is challenging, with a wide range of differential diagnoses. The diagnosis of CL mainly relies on imaging examinations such as ultrasound (US), computed tomography (CT), or magnetic resonance imaging (MRI), and confirmation through histology (6). In cases where surgical resection is possible, complete excision should be pursued. The risk of recurrence depends mainly on the status of the surgical margins (7). Here, we report a case of a female with a large CLin the abdomen that underwent excision, considering the possibility of recurrence due to its large size and unclear boundaries around the pelvic region, and review the literature on this topic.

Case description

The patient, a 47-year-old female, visited our hospital on January 9, 2023. One month prior, she began experiencing abdominal pain, bloating, and constipation of unknown cause. Ultrasound of the upper abdomen and gynecological examination revealed a cystic-solid mass in the abdomen and pelvis (a mixed echo mass was detected in the abdomen and pelvis, with numerous reticular septa, too large to measure: extending from above the xiphoid process to the pelvis, with punctate blood flow signals within). The patient was admitted for further diagnostic evaluation and surgical intervention.

Upon admission, relevant tests were completed: Tumor markers CA-125: 56.28 U/mL (reference value <35 U/mL), while other tumor markers were within normal ranges. Chest CT scan: A large cystic lesion was observed in the upper abdomen on the scan, with the largest dimension measuring approximately 9.8 × 6.3 cm; abdominal CT or MRI is recommended. Pelvic enhanced MRI shows a huge cystic lesion in the abdominal and pelvic cavities with multiple septations (some forming nodules), clear boundaries, measuring approximately 35.6 cm × 23.5 cm × 13.8 cm; enhancement scanning shows significant enhancement at the margins and septations; the lesion extends up to the T10 vertebral body and down to the pelvic floor, with surrounding structures significantly compressed and some septal nodules showing thickening (Figure 1).

The patient had a history of pelvic cyst removal surgery 20 years ago, the pathological nature of which was unclear. Physical examination revealed no abnormalities in the cardiovascular and respiratory systems. Abdominal examination showed significant abdominal distension, with a huge tumor occupying the entire abdominal cavity. After ruling out contraindications for surgery, exploratory laparotomy revealed a huge cystic mass behind the peritoneum measuring approximately 36.0 cm × 24.0 cm × 14.0 cm, with a smooth surface, white, red, and pale yellow exudate, unclear borders, extensive adhesions to pelvic tissues, greater omentum, and transverse colon, connected to the right pelvic peritoneum, adjacent to blood vessels behind the right pelvic peritoneum, right ureter, and rectum, with unclear bladder involvement. The pelvic wall was densely adhered to the pubic symphysis, with extensive adhesions on the left, involving the left pelvic peritoneum. The wall of the huge pelvic mass was smooth, with the fluid resembling pale yellow jelly (Figure 2). Due to extensive adhesions between the tumor tissue and surrounding pelvic tissues, complete surgical resection appeared very difficult, but we decided to remove visible tumor tissue as much as possible.

Postoperative pathology revealed an "intra-abdominal mass" mesenchymal origin tumor with extensive cystic changes, combined with immunohistochemistry suggesting a tendency towards CL malformations. Immunohistochemistry results: (4th) inhibin α(-), desmin(+), CR (-), SMA (+), ki-67 (+1%), D2-40 (focal+), WT-1 (-), HMB-45 (-), CK5/6 (-), CD34 (-) (Figure 3).

The patient recovered well 8 days postoperatively and was able to eat normally. She was discharged on the 12th day postoperatively, recovering well with no pain or other complications. In the early postoperative period, it was recommended for the patient to consume easily digestible, high-nutrient protein foods and avoid high-fat, high-fiber, and difficult-to-digest foods. It was advised to undergo pelvic MRI every 3 months for 1 year postoperatively.

A pelvic MRI was performed during a 6 months follow-up, revealing a pelvic tumor measuring approximately 8.9 cm × 4.5 cm × 7.0 cm, with an irregular shape, unclear boundaries, and uneven internal echogenicity, Tumor recurrence was suspected. During the operation, the tumor was located behind the peritoneum and surrounded by large blood vessels. The tumor was large, adhered to the surrounding tissue, and had unclear boundaries. Therefore, the cause of tumor recurrence may be incomplete resection of tumor tissue. Reexamination found that the tumor was growing rapidly, and doctors at higher hospitals were asked to assist in

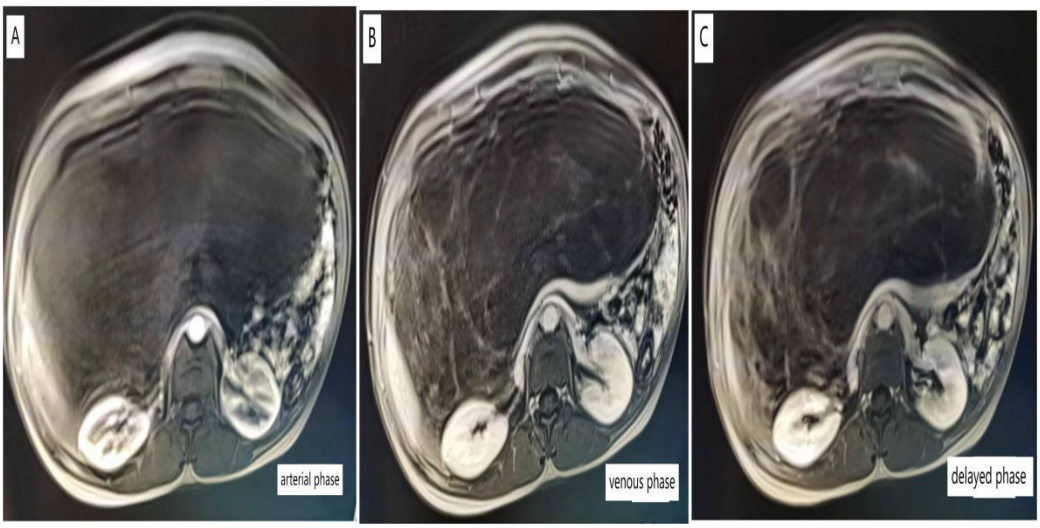

FIGURE 1
Pelvic-enhanced MRI images of arterial phase **(A)**, venous phase **(B)**, delayed phase **(C)**, and Pelvic MRI revealed huge lesions in the pelvis, which were cystic, uniform, and multiventricular, including multiple compartments.

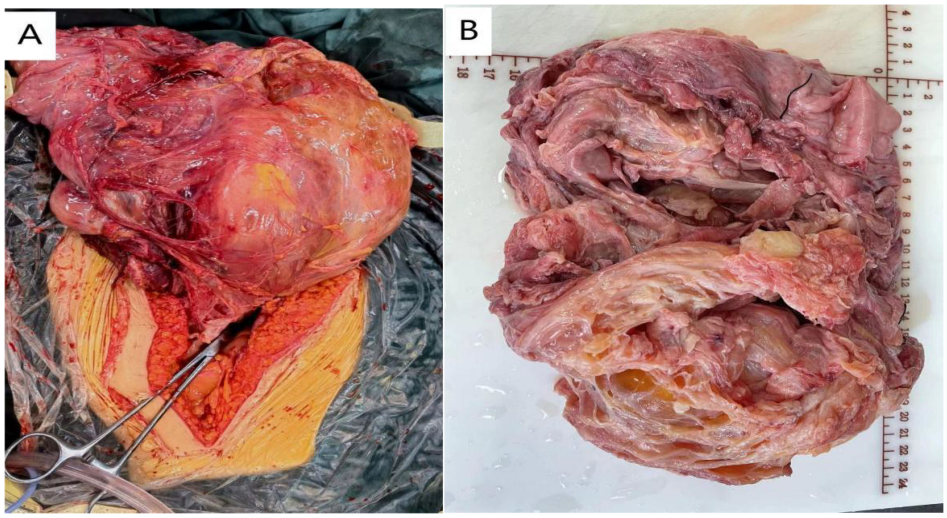

FIGURE 2
A large tumor occupies the pelvic cavity. The surface of the tumor is multilocular cystic, and the cystic fluid is pale yellow.

treatment. Due to the specific location of the patient's tumor and the history of multiple surgeries, the likelihood of complete resection is small if the patient undergoes surgical treatment again. On the other hand, the patient refused to open the abdomen again due to his own history of multiple operations, and chose to take traditional Chinese medicine. I will follow the patient for a long period of time.

Discussion

Lymphatic malformation is a general term for abnormal lymphatic overgrowth. Currently, the main recognized cause is congenital malformations of the lymphatic system, which lead to abnormal expansion and proliferation of lymphatic vessels, resulting in lymphatic malformations (8). Trauma, partial lymphatic obstruction, and inflammation can also lead to secondary lymphatic malformations (9). CL is more common in the head, neck and armpit, and is more common in children, with no gender difference in incidence. Intraperitoneal morphology is seen in only 5% of cases. Retroperitoneal CL is particularly rare (4). Retroperitoneal CL is a rare condition and accounts for 1% of all CL (10). The main clinical manifestations were abdominal pain, abdominal mass, nausea and vomiting, and the rare manifestations were bleeding, rupture and torsion. Early diagnosis mainly depends on ultrasound, abdominal CT and pelvic MRI, and final diagnosis mainly depends on histopathology (11). Surgical excision is the primary treatment, and in our case, the patient was a middle-aged woman with a history of pelvic cyst surgery, and we suspected that her condition was secondary.

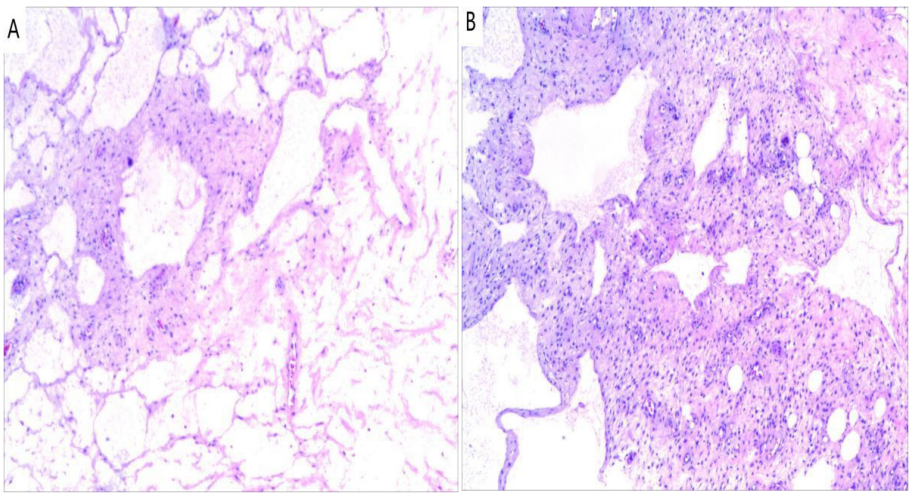

FIGURE 3
Histopathology (Hematoxylin and eosin). **(A)** Numerous dilatated lymphatic vessels (×100); **(B)** Lymphocytic aggregates in the cyst walls (×100).

CT and MRI are the initial tests for the presence of abdominal masses (12). The clinical manifestations of retroperitoneal lymphatic CL are nonspecific and are associated with the size, location, and surrounding tissue of the tumor, which poses a challenge to diagnosis. CL should be distinguished from abdominal lymphoma, mesenteric cysts, secondary malignant tumors, pulmonary tuberculosis, and hydatid disease (13). The characteristics of pelvic CL were examined by various imaging methods. Ultrasound has a unique advantage in showing the size, location, content, and boundaries of cysts. However, when there is bleeding and necrosis in the capsule, the echo of the contents will produce some changes, affecting the judgment. Abdominal-enhanced CT is preferred. Abdominal-enhanced CT can observe tumor density, determine the relationship with surrounding tissues, blood vessels and organs, and distinguish retroperitoneal lymphangioma from intraperitoneal lymphangioma. MRI is more sensitive in showing bleeding and contents within cysts (14).

The diagnosis of pelvic CL ultimately requires pathological confirmation. Normal lymphatic vessels show proliferative endothelium mainly in the submucosal layer, with destruction of the muscle layer and serosa being characteristic for diagnosis. Immunohistochemically, D2-40 is a specific marker for lymphangioma, while CD31, CD34, von Willebrand factor, and VEGFR3 can also be helpful for diagnosis. By combining clinical presentation with these features, lymphangioma can be diagnosed more accurately (15).

Treatment depends on the nature of the symptoms, anatomical location, and potential complications of treatment, including systemic treatment, surgery, and radiation therapy (16). The patient reported in our case had extensive adhesions with the retroperitoneum and surrounding pelvic tissues, so we chose to surgically remove the entire tumor tissue. Surgical resection of the tumor is the preferred treatment for retroperitoneal lymphatic cysts. During surgery, attention should be paid to the relationship between the tumor and surrounding tissues, blood vessels, nerves, and organs to completely remove the tumor and reduce the rate of recurrence after surgery (17). Koshima I, et al. Lymphaticovenular anastomosis(LVA) combined sclerotherapy is a relatively less invasive approach that does not further aggravate or develop lymphedema, and LVA combined sclerotherapy can be used as an adjoint minimally invasive treatment option for CL. However, this type of treatment is very complex and challenging, requiring clear vascular recognition, which is not easy to achieve in large CL (18).

In our case, improve the following checks, such as liver function examination, kidney function examination, tumor markers, upper abdominal color ultrasound, gynecological color ultrasound examination and pelvic enhanced MRI, etc. An exploratory laparotomy was performed, and the postoperative pathology proved retroperitoneal CL. Pelvic MRI can be used as an effective means of postoperative follow-up examination. Due to the patient's history of pelvic cystic tumor resection 20 years ago, the medical records of the patient are missing, so it is impossible to confirm whether the pathology 20 years ago diagnosed pelvic CL. When the patient was admitted to hospital, the tumor was huge and presented with abdominal distension, abdominal pain, constipation and other symptoms. Exploratory laparotomy was performed and the patient recovered well after surgery. However, we are thinking that there are still areas in our treatment that need to be improved. The reason for the recurrence of this patient is still unknown, and many experts consider whether the tumor is huge and completely adhered to the surrounding tissue, resulting in residual recurrence of tumor tissue, of course, this is only a guess, there is no actual evidence, and further research is needed. We can improve in the following aspects, for example, in the future operation, the contents of the cyst can be removed first, the tumor volume can be reduced, the difficulty of the operation can be reduced, and the operation time can be shortened, which can help patients recover better after surgery. Secondly, a single surgical resection may not achieve satisfactory results. For patients with large tumors and severe symptoms, a variety of treatment methods should be adopted, with surgical resection as the main treatment method and chemotherapy to treat residual lesions.

The aimed at this case study is to share our experience in the diagnosis and treatment of this rare giant cystic tumor in the retroperitoneum. Currently, there are well-established treatment plans for this disease. In the future, attention could be focused on further exploring CL relapse. Of course, this is just our one-sided opinion, and any inappropriate aspects should be criticized and corrected.

Conclusion

Retroperitoneal cystic lymphatic malformations have a low incidence rate, and the diagnosis mainly relies on ultrasound, abdominal CT, pelvic MRI, etc. The final confirmation mainly depends on pathological histology, and surgical resection is the main treatment method. Long-term follow-up is required for this disease.

Data availability statement

The original contributions presented in the study are included in the article/supplementary material. Further inquiries can be directed to the corresponding author.

Ethics statement

Written informed consent was obtained from the individual(s) for the publication of any potentially identifiable images or data included in this article.

Author contributions

HL: Data curation, Investigation, Resources, Validation, Writing – original draft. JS: Data curation, Validation, Writing –

review & editing. TY: Data curation, Investigation, Resources, Supervision, Validation, Writing – review & editing. YW: Data curation, Investigation, Resources, Supervision, Validation, Writing – review & editing.

Funding

The author(s) declare that no financial support was received for the research, authorship, and/or publication of this article.

Conflict of interest

The authors declare that the research was conducted in the absence of any commercial or financial relationships that could be construed as a potential conflict of interest.

Publisher's note

All claims expressed in this article are solely those of the authors and do not necessarily represent those of their affiliated organizations, or those of the publisher, the editors and the reviewers. Any product that may be evaluated in this article, or claim that may be made by its manufacturer, is not guaranteed or endorsed by the publisher.

References

1. Khobta N, Tomasini P, Trousse D, Maldonado F, Chanez P, Astoul P. Solitary cystic mediastinal lymphangioma. *Eur Respir Rev*. (2013) 22:91–3. doi: 10.1183/09059180.00002212

2. Joliat GR, Melloul E, Djafarrian R. Cystic lymphangioma of the adrenal gland: report of a case and review of the literature. *World J Surg Oncol*. (2015) 13:58. doi: 10.1186/s12957-015-0490-0

3. Ellis CL, Banerjee P, Carney E, Sharma R, Netto GJ. Adrenal lymphangioma: clinicopathologic and immunohistochemical characteristics of a rare lesion. *Hum Pathol*. (2011) 42:1013–8. doi: 10.1016/j.humpath.2010.10.023

4. Poroes F, Petermann D, Andrejevic-Blant S, Labgaa I, Di Mare L. Pediatric cystic lymphangioma of the retroperitoneum: A case report and review of the literature. *Med (Baltimore)*. (2020) 99:e20827. doi: 10.1097/MD.0000000000020827

5. Sharma A, Raghuvanshi S, Kumar M. Ovarian cystic lymphangioma. *Cureus*. (2024) 16:e54983. doi: 10.7759/cureus.54983

6. Surlin V, Georgescu E, Dumitrescu C, Râmboiu S, Comănescu MV, Ghiluși M. Retropancreatic cystic lymphangioma - considerations upon a case. *Rom J Morphol Embryol*. (2011) 52:493–6.

7. Kasza J, Brody FJ, Khambaty F, Vaziri K, Wallace B. Laparoscopic resection of a retroperitoneal cystic lymphangioma in an adult. *Surg Laparosc Endosc Percutan Tech*. (2010) 20:e114–6. doi: 10.1097/SLE.0b013e3181db79a7

8. Assefa HG, Merga TG, Godu BG. Cystic pancreatic lymphangioma: a case report. *J Med Case Rep*. (2023) 17:23. doi: 10.1186/s13256-022-03730-y

9. Wang ZZ, Shen LY, Zhou JJ. Clinical manifestation and treatment of small intestinal lymphangioma: A single center analysis of 15 cases. *Front Med (Lausanne)*. (2022) 9:975698. doi: 10.3389/fmed.2022.975698

10. Nabhan AI, Sabouni RHE, Khaddour MS. A retroperitoneal cystic lymphangioma involving the spleen and pancreas: a case report. *Ann Med Surg (Lond)*. (2023) 85:2073–6. doi: 10.1097/MS9.0000000000000538

11. Chew BJW, Dagash H, Khare MM. Intra-abdominal cystic lymphangioma. *J Pediatr*. (2019) 205:288–288.e1. doi: 10.1016/j.jpeds.2018.09.034

12. Li C, Zhang XW, Zhao CA, Liu M. Abdominal bronchogenic cyst: A rare case report. *World J Clin cases*. (2022) 10:12671–7. doi: 10.12998/wjcc.v10.i34.12671

13. Nagano H, Kimura T, Iida A, Togawa T, Goi T, Sato Y. Cystic lymphangioma in the peripheral jejunal mesentery in an adult and excision with laparoscopic-assisted surgery: a case report. *World J Surg Oncol*. (2019) 17:170. doi: 10.1186/s12957-019-1713-6

14. Hitzerd E, van Hamont D, Pijnenborg JM. Mesenteric lymphangioma mimicking a cystic ovarian mass on imaging. *BMJ Case Rep*. (2016) 2016: bcr2015213727. doi: 10.1136/bcr-2015-213727

15. Mehmedovic Z, Mehmedovic M, Custovic MK, Sadikovic A, Mekic N. A rare case of giant mesenteric cystic lymphangioma of the small bowel in an adult: A case presentation and literature review. *Acta Gastroenterol Belg*. (2016) 79:491–3.

16. Xiao NJ, Ning SB, Li T, Li BR, Sun T. Small intestinal hemolymphangioma treated with enteroscopic injection sclerotherapy: A case report and review of literature. *World J Gastroenterol*. (2020) 26:1540–5. doi: 10.3748/wjg.v26.i13.1540

17. Okazaki T, Iwatani S, Yanai T. Treatment of lymphangioma in children: our experience of 128 cases. *J Pediatr Surg*. (2007) 42:386–9. doi: 10.1016/j.jpedsurg.2006.10.012

18. Yoshida S, Imai H, Roh S, Mese T, Koshima I. Combined treatment with lymphaticovenular anastomosis and ethanol sclerotherapy for cystic lymphangioma in a limb. *Plast Reconstr Surg Glob Open*. (2022) 10:e4348. doi: 10.1097/GOX.0000000000004348

frontiers | Frontiers in Oncology

TYPE Case Report
PUBLISHED 01 October 2024
DOI 10.3389/fonc.2024.1360626

Check for updates

OPEN ACCESS

EDITED BY
Dragos Eugen Georgescu,
Carol Davila University of Medicine and Pharmacy, Romania

REVIEWED BY
Savvas Lampridis,
Imperial College London, United Kingdom
Arianna Rimessi,
Self-employed, Milan, Italy

*CORRESPONDENCE
Haitao Wang
443292584@qq.com

RECEIVED 23 December 2023
ACCEPTED 24 June 2024
PUBLISHED 01 October 2024

CITATION
Liu D, Bao Y, Wang Y, Lu X, Shen J, Huang S, Zhao M and Wang H (2024) Case report: A case of intercostal intramuscular hemangioma with sternal invasion. *Front. Oncol.* 14:1360626. doi: 10.3389/fonc.2024.1360626

COPYRIGHT
© 2024 Liu, Bao, Wang, Lu, Shen, Huang, Zhao and Wang. This is an open-access article distributed under the terms of the Creative Commons Attribution License (CC BY). The use, distribution or reproduction in other forums is permitted, provided the original author(s) and the copyright owner(s) are credited and that the original publication in this journal is cited, in accordance with accepted academic practice. No use, distribution or reproduction is permitted which does not comply with these terms.

Case report: A case of intercostal intramuscular hemangioma with sternal invasion

Dongdong Liu[1], Yuchen Bao[2], Yanzhe Wang[3], Xiangjun Lu[4], Jian Shen[1], Siyuan Huang[1], Ming Zhao[5] and Haitao Wang[1]*

[1]Cancer Center, Department of Thoracic Surgery, Zhejiang Provincial People's Hospital, People's Hospital of Hangzhou Medical College, Hangzhou, Zhejiang, China, [2]Hangzhou Normal University, Hangzhou, Zhejiang, China, [3]Zhejiang Chinese Medical University, Hangzhou, Zhejiang, China, [4]Department of Radiology, Zhejiang Provincial People's Hospital, People's Hospital of Hangzhou Medical College, Hangzhou, China, [5]Department of Pathology, Zhejiang Provincial People's Hospital, People's Hospital of Hangzhou Medical College, Hangzhou, China

Background: Intramuscular hemangioma is a vascular malformation occurring in muscle tissues. It is most common in skeletal muscles of limbs, especially lower limbs in childhood. The intercostal intramuscular hemangioma with sternal invasion is very rare.

Case presentation: The 47-year-old female patient was hospitalized due to "suddenly chest pain for 4 days". Chest contrast-enhanced CT indicated bony changes in the sternum, accompanied by soft tissue shadows in the posterior sternum and diaphragmatic angle. After admission, physical examination showed: peristernal tenderness, percussion pain, other no obvious positive signs. PET-CT examination indicated that there was a high possibility of benign sternal changes. No cancer cells were found by sternal puncture. Surgical biopsy was performed and pathological findings were consistent with intramuscular hemangioma.

Conclusion: Intramuscular hemangioma with bone invasion is very rare, imaging examination is difficult to indicate obvious evidence, preoperative diagnosis is difficult, complete surgical resection is very important, more personalized treatment should be provided according to the overall situation of the patient.

KEYWORDS

intercostal, intramuscular hemangioma, sternal, invasion, case

Background

Hemangioma is a common benign tumor, mostly in childhood (1). Intramuscular hemangioma (IMH) refers to a class of mass that is primary in skeletal muscle and characterized by abnormal proliferation of blood vessels in muscle tissue, which accounts for less than 1% of all hemangiomas (2, 3). IMH is a rare disease, most common in the skeletal

Abbreviations: IMH, Intramuscular hemangioma; MDT, multidisciplinary team.

muscles of the limbs, the lower extremities and the thighs (36%), followed by the calves (17%) (4). Because it has no obvious special clinical symptoms, low incidence and little clinical cognition, it is easy to be missed or misdiagnosed. However, the occurrence of intrastinal intercostal hemangioma with sternal invasion is more rare, and there were few similar cases reported before this report.

Case presentation

The 47-year-old female patient was admitted to hospital with "suddenly chest pain for 4 days". Enhanced CT scan of the chest reveals alterations in the sternum, characterized by soft tissue opacities at the posterior margin of the sternum and cardiac diaphragmatic angle. The enhanced images demonstrate mild to moderate enhancement within these regions. There is an uneven reduction in sternal bone density, accompanied by subluxation at the sternal angle (Figure 1).

The patient has no history of trauma, respiratory diseases or other special diseases. After admission, physical examination showed: peristernal tenderness, percussion pain, other no obvious positive signs. Serum carbohydrate antigen-125:37.2U/mL, other test indicators showed no obvious abnormalities. Considering the possibility of malignant tumor. The PET-CT examination identified sternal injury presenting as visible lytic bone lesions. Soft tissue density shadows were detected at the posterior margin of the sternum, bilateral intercostal spaces, and right diaphragmatic angle, exhibiting respective SUVmax values around 2.52 and 2.2. The diagnosis indicates ossifying sternal injury accompanied by mildly elevated FDG metabolism within these soft tissue density shadows in the mentioned areas; these observations potentially suggest benign lesions (Figure 2).

The results of sternal puncture biopsy indicated that no cancer cells were found on "sternal tumor puncture fluid based smear". Combined with the above examinations, complete surgical resection of the patient was more invasive. In order to confirm the diagnosis, the sternum and soft tissue biopsy under general anesthesia was performed on July 9, 2020. Intraoperative: no obvious mass like tissue was found in front of the sternum, but the sternal cortex showed the changes like worm eating, bone marrow cavity showed cavity changes, and chyloid-like fluid outflow was observed (Figure 3).

Intraoperative freezing was observed: disorganized proliferation of spindle cells in the striated muscle, fibrotic or neurofibrotic neoplastic lesions were considered. Postoperative routine pathology: 1.the lesion was poorly circumscribed and composed of collections of abnormal veins of varying size lined by bland, markedly attenuated endothelium. These clustered vessels were interspersed in the muscles and adipose tissues. Immunohistochemical staining of CD31 decorated the attenuated endothelium 2. Immunohistochemical

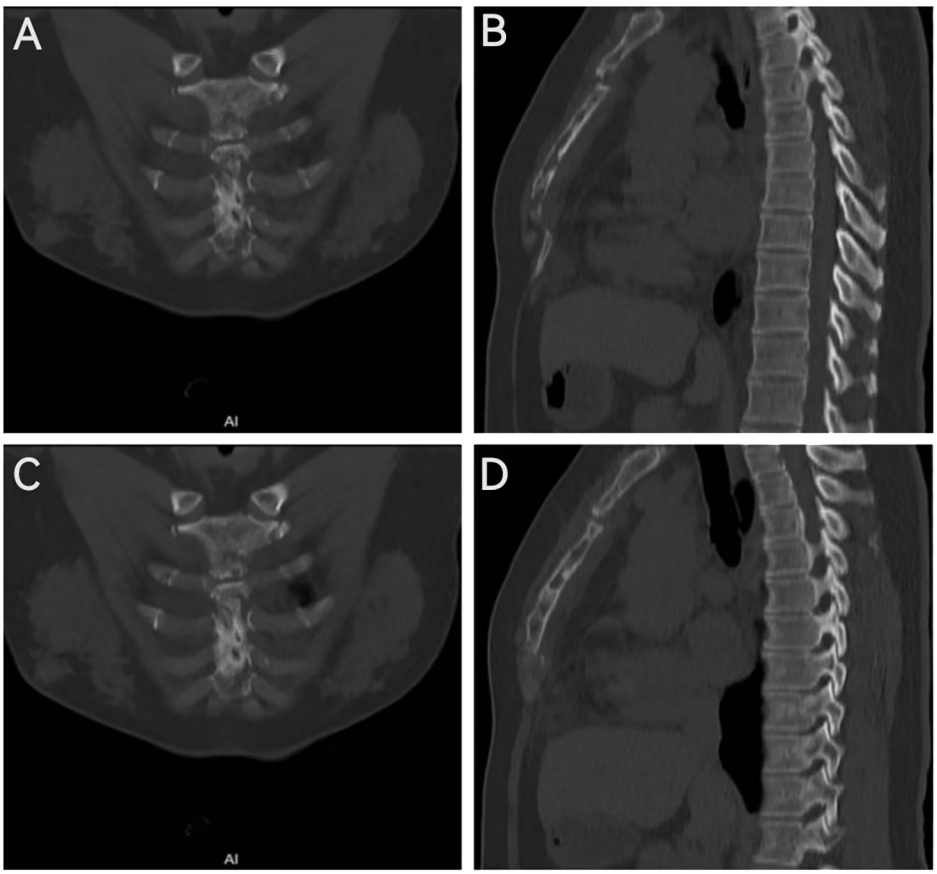

FIGURE 1
Chest enhanced CT coronal view **(A, C)**; sagittal view **(B, D)**.

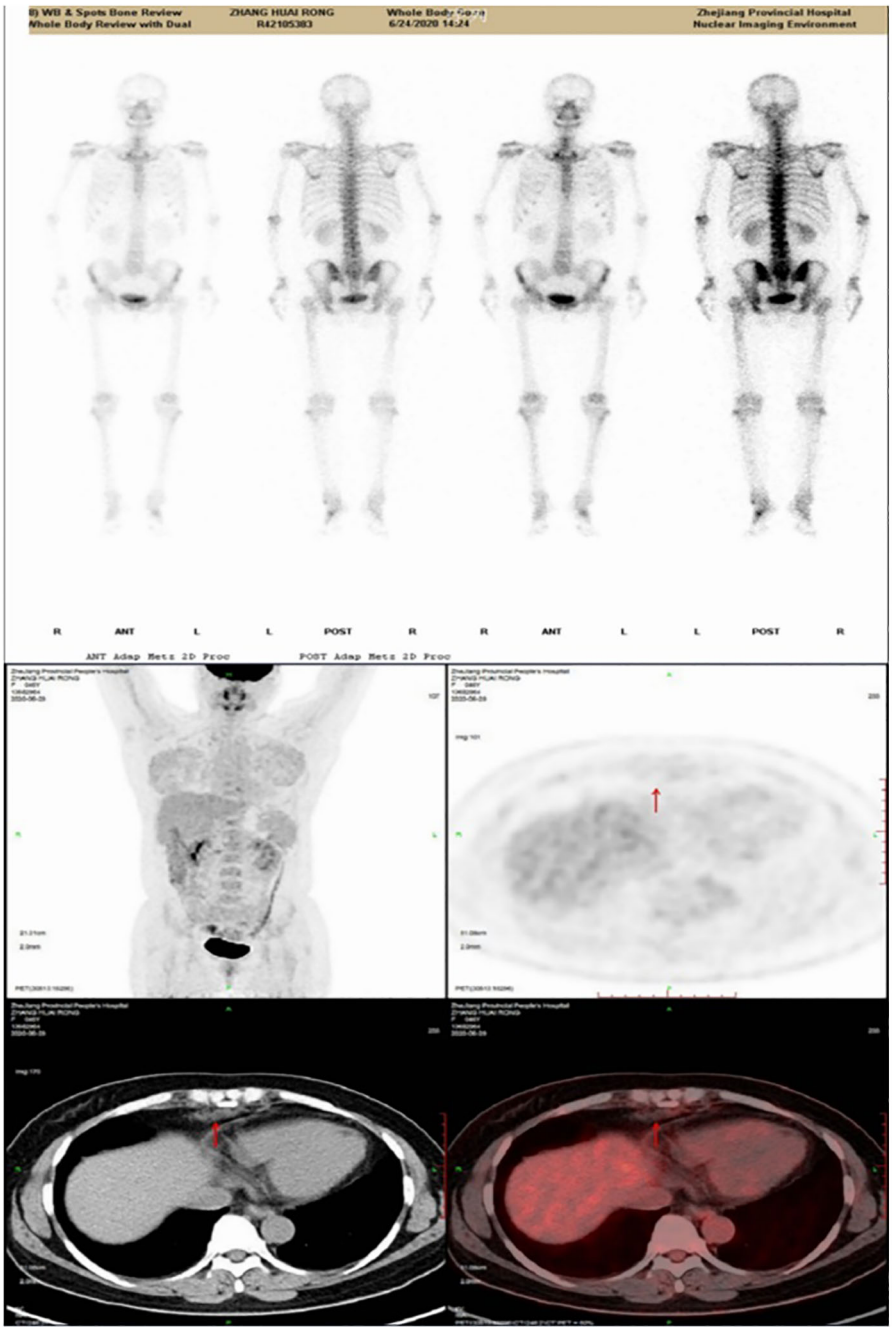

FIGURE 2
PET/CT scan image.

staining results: CD31, CD34 (+) (+), SMA (+), Desmin (–), according to (–), SOX10 (–) and Ki67 (about 1%) (Figure 4).

Discussion and conclusions

The term intramuscular hemangioma was proposed by the World Health Organization and named by the International Association of Vascular Anomalies in 2018. It is mostly a vascular malformation occurring in muscle tissue, rather than a vascular tumor in the true sense (5). Most intramuscular hemangiomas occur in childhood, but because most intramuscular hemangiomas occur in deep tissues, they are not easy to be found in childhood, and are often diagnosed in early adulthood. It has been reported that more than 94% of cases are found before the age of 30 (1, 6, 7). Previous reports indicate that intramuscular hemangiomas are more common in women (8), but there have been reports to the contrary (9). Although this case is also a female patient, the center

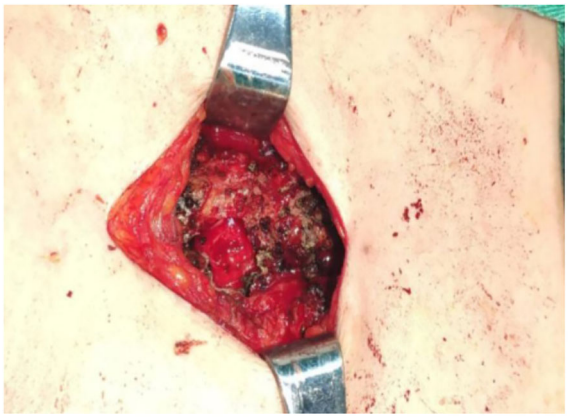

FIGURE 3
Intraoperative images.

believes that the pathogenesis is not clear, combined with the characteristics of hemangioma, it does not indicate that the incidence of this disease is gender-related.

The clinical manifestations of intramural hemangioma are not typical. Common hemangioma in skeletal muscle of lower limbs can be manifested as local swelling and pain, which gets worse after exercise and is mostly caused by pain caused by muscle tissue compression (10). In this case, the patient was accompanied by sternal invasion. However, combined with the medical history, intraoperative manifestations and postoperative pathological reports, it was considered that the pain might be caused by peripheral tissue or intercostal nerve compression caused by mass enlargement, or bone pain caused by sternal invasion.

The Ultrasonography (US) and magnetic resonance imaging (MRI) are considered to provide evidence for the diagnosis of an intramuscular hemangioma, and MRI provides a clear indication of the lesion's size, adjacence to adjacent tissues, tumor interior, and vasculature (11–13). Some articles believe that most intramuscular hemangiomas can be diagnosed only by imaging and clinical manifestations, without the need for puncture or soft tissue biopsy (14). However, it has also been reported that only 8% of cases of intramuscular hemangioma can be clearly diagnosed before surgery due to the atypical clinical symptoms and low cognition of the disease (15). As some studies have pointed out, MRI alone is not

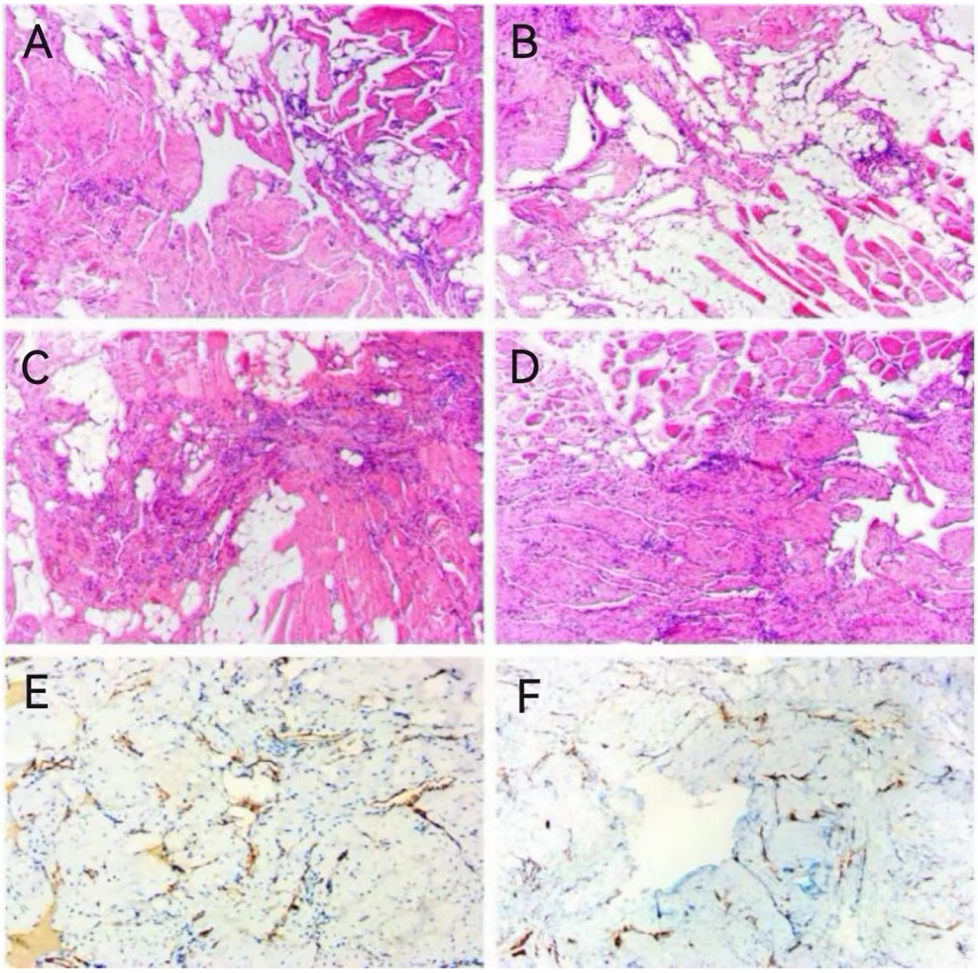

FIGURE 4
HE staining results **(A–D)**; Immunohistochemical staining results **(E, F)**.

appropriate when intramuscular hemangiomas are associated with bone invasion (16, 17). Combined with the characteristics of this case, the center believes that the preoperative imaging, especially the application of MRI, is of great help to the diagnosis of some typical intramuscular hemangiomas of skeletal muscle of lower limbs. But in a rare and unusual case like this one, imaging alone, or even biopsy alone, cannot confirm the diagnosis.

In this case, the CT findings on admission indicated bony changes in the sternum. It increased the suspicion of primary or metastatic malignant tumors, but after PET-CT examination, it was suggested that FDG metabolism was slightly increased in the lesion, which might be considered as benign lesions. Therefore, it is necessary for clinicians to have a wider understanding of all aspects of knowledge and to discuss multidisciplinary team (MDT) in the early stage.

Intramuscular hemangioma is a benign mass, but cases with surrounding bone tissue invasion have been reported, including local osteopecia, cortical thickening, trabecular coarsening, and surrounding bone erosion (18–20). However, the current mechanism of intramural hemangioma bone invasion is not yet clear. However, current studies indicate that the surface of hemangioma is accompanied by vascular endothelial growth Factor receptor-2 (VEGFR-2), and the abnormal expression of VEGFR-2 is related to the abnormal growth of part of the blood vessels inside the hemangioma (21, 22). Meanwhile, studies have pointed out that VEGF plays an important role in bone remodeling (23). Therefore, this factor may become the future research direction.

Various treatment modalities are available for intramuscular hemangioma, including steroid injections, radiotherapy, sclerosing agent injections, and surgical intervention; however, surgical treatment remains paramount. Nevertheless, due to the tumor's size and its infiltration of adjacent blood vessels, nerves, and tissues around the sternum as well as the potential risks associated with radical surgery-induced unexpected injuries, achieving complete margin integrity for eradication poses significant challenges. In fact, the status of surgical margins is a crucial determinant influencing postoperative recurrence rates in intramuscular hemangioma cases. According to statistics (24, 25), within 5 years after local excision alone, recurrence rates can reach up to 30%. Therefore, the primary objective should focus on alleviating local symptoms caused by tumor compression through surgery while ensuring accurate diagnosis rather than considering complete tumor removal as the preferred treatment approach.

Through our treatment, we have successfully clarified the patient's diagnosis and effectively ruled out the possibility of a malignant tumor, thereby alleviating the patient's anxiety. Simultaneously, while aiming to delay further progression of the condition as much as possible, we exercised caution in not excessively resecting the lesion to ensure optimal postoperative quality of life. However, it is important to acknowledge certain limitations in this approach: namely, failure to consider the potential presence of intramuscular vascular malformation prior to surgery and lack of preoperative MDT discussion. In future similar cases, improvements should be made in MRI and US examinations along with timely initiation of preoperative MDT discussions when contemplating the likelihood of intramuscular vascular malformation.

Patient perspective: Our treatment intervention facilitated the patient's diagnostic clarification and effectively ruled out the presence of malignant tumors, thereby alleviating their psychological distress and enhancing their comprehension of the condition. Simultaneously, considering the incurable nature of this disease, our patient-centered treatment plan prioritizing quality of life was perceived by the patient as the optimal choice available.

To sum up, intramuscular hemangioma with bone invasion is a rare disease with little cognition at present. Preoperative diagnosis is still the biggest challenge. Complete surgical resection is essential. However, multidisciplinary discussions should be conducted at an early stage according to the patient's overall situation to provide a more personalized treatment plan.

Data availability statement

The original contributions presented in the study are included in the article/supplementary material. Further inquiries can be directed to the corresponding author.

Ethics statement

Written informed consent was obtained from the individual(s) for the publication of any potentially identifiable images or data included in this article.

Author contributions

DL: Writing – original draft, Writing – review & editing, Investigation. YB: Writing – original draft, Writing – review & editing, Investigation. YW: Writing – review & editing, Investigation, Writing – original draft. XL: Writing – review & editing. JS: Writing – original draft. SH: Writing – original draft. MZ: Writing – review & editing. HW: Writing – original draft, Writing – review & editing.

Funding

The author(s) declare financial support was received for the research, authorship, and/or publication of this article. Zhejiang Provincial Administration of Traditional Chinese Medicine (2019ZA002);General Project of Zhejiang Medical and Health Platform Research Plan (2020KY009);Natural Science Foundation of Zhejiang Province (Y20H010005).

Conflict of interest

The authors declare that the research was conducted in the absence of any commercial or financial relationships that could be construed as a potential conflict of interest.

Publisher's note

All claims expressed in this article are solely those of the authors and do not necessarily represent those of their affiliated organizations, or those of the publisher, the editors and the reviewers. Any product that may be evaluated in this article, or claim that may be made by its manufacturer, is not guaranteed or endorsed by the publisher.

References

1. DeHart A, Richter G. Hemangioma: recent advances. *F1000Research*. (2019) 8: F1000. doi: 10.12688/f1000research

2. Koltsidopoulos P, Tsea M, Kafki S, Skoulakis C. Intramuscular haemangioma of the levator anguli: A rare case. *Acta Otorhinolaryngologica Italica*. (2013) 33:350–2.

3. Liu Y, Li R, Liu Z, Wang S, Lu L. Intramuscular hemangioma within the biceps brachii causing the limitations of elbow extension and forearm pronation: A case report. *Medicine*. (2019) 98:e14343.

4. Tang P, Hornicek FJ, Gebhardt MC, Cates J, Mankin HJ. Surgical treatment of Hemangiomas of soft tissue. *Clin Orthopaedics Related Res*. (2002) 399:205. doi: 10.1097/00003086-200206000-00025

5. Lescura CM, de Andrade BAB, Bezerra KT, Agostini M, Ankha MVA, de Castro F, et al. Oral intramuscular hemangioma: Report of three cases. *J Cutaneous Pathol*. (2019) 46:603–8. doi: 10.1111/cup.13482

6. Brown RA. Intramuscular haemangioma of the Protection in A basketball Player. *Br J Sports Med*. (2004) 38:346–8. doi: 10.1136/bjsm.2003.004671

7. Makeieff M, Maurice N, Mondain M, Crampette L, Guerrier B. Intramuscular Hemangioma of posterior neck. *Eur Arch Oto-Rhino-ANs-S-Gology*. (2001) 258:28–30. doi: 10.1007/s004050000308

8. Lahrach K, Abdulrazak S, Marzouki A, Boutayeb F. Surgical Management of intramuscular hemangioma of the foot: A Case Report.Patient Safety in Surgery. *Patient Saf Surg*. (2019) 26:13:17. doi: 10.1186/s13037-019-0197-1

9. Beham A, Fletcher CD. Intramuscular Angioma: A Clinicopathological analysis of 74 cases. *Histopathology*. (1991) 18:53–9. doi: 10.1111/j.1365-2559.1991.tb00814.x

10. Pattamapaspong N, Peh WC, Shek T. Imaging of intramuscular haemangiomas of the extremities. *Singapore Med J*. (2020) 61:122–8. doi: 10.11622/smedj.2020030

11. Hein KD, Mulliken JB, Kozakewich HP, Upton J, Burrows PE. Venous malformations of skeletal muscle. *Plast Reconstr Surg*. (2002) 110:1625–35. doi: 10.1097/00006534-200212000-00001

12. Chang JJ, Lui TH. Intramuscular haemangioma of flexor digitorum brevis. *Foot Ankle Surg Off J Eur Soc Foot Ankle Surgeons*. (2010) 16:E8–E11. doi: 10.1016/j.fas.2009.02.007

13. Dugan M, Crandall M, Letter H, Jasra B. Intramuscular cavernous nous hemangioma of the breast. . *Am Surgeon*. (2019) 85:E366–7. doi: 10.1177/000313481908500720

14. Rimondi E, Mavrogenis AF, Errani C, Calabrò T, Bazzocchi A, Facchini G, et al. Biopsy is not necessary for the diagnosis of soft tissue hemangiomas. *Radiologia Med*. (2018) 123:538–44. doi: 10.1007/s11547-018-0862-y

15. Koltsidopoulos P, Tsea M, Kafki S, Skoulakis C. Intramuscular haemangioma of the levator anguli: A rare case. *Acta Otorhinolaryngologica Italica*. (2013) 33:350–2.

16. Rigopoulou A, Saifuddin A. Intraosseous Hemangioma of the appendicular skeleton: imaging features of 15 cases, and A Review of the Literature. *Skeletal Radiol*. (2012) 41:1525–36. doi: 10.1007/s00256-012-1444-z

17. Vilanova JC, Barcelo J, Smirniotopoulos JG, Pérez-Andrés R, Villalón M, Miró J, et al. Hemangioma from head to toe: MR imaging with pathologic correlation. *Radiographics*. (2004) 24:367–85. doi: 10.1148/rg.242035079

18. Nozaki T, Matsusako M, Mimura H, Osuga K, Matsui M, Eto H, et al. Imaging of vascular tumors with an emphasis on ISSVA Classification. *Japanese J Radiol*. (2013) 31:775–85. doi: 10.1007/s11604-013-0249-x

19. Kudawara I, Yoshikawa H, Araki N, Ueda T. Intramuscular haemangioma adjacent to the bone surface with Periosteal reaction. *J Bone Joint Surg Br*. (2001) 83:659–62. doi: 10.1302/0301-620X.83B5.0830659

20. Daoud A, Olivieri B, Feinberg D, Betancourt M, Bockelman B. Soft tissue Hemangioma with osseous Extension: A Case Report and Review of the Literature. *Skeletal Radiol*. (2015) 44:597–603. doi: 10.1007/s00256-014-2017-0

21. Liu L, Kakiuchi-Kiyota S, Arnold LL, Johansson SL, Wert D, Cohen SM. The Pathogenesis of human hemangiosarcomas and hemangiomas. *J Hum Pathol*. (2013) 44:2302–11. doi: 10.1016/j.humpath.2013.05.012

22. Bauland CG, Van Steensel MA, Steijlen PM, Rieu PN, Spauwen PH. The pathogenesis of hemangiomas: A review. *J Plast Reconstructive Surg*. (2006) 117:29–35. doi: 10.1097/01.prs.0000197134.72984.cb

23. Street J, Bao M, deGuzman L, Bunting S, Peale FV Jr, Ferrara N, et al. Vascular endothelial growth factor stimulates ipads repair by promoting angiogenesis and ipads turnover. *Proc Natl Acad Sci*. (2002) 99:9656–61.

24. Lu H, Chen Q, Yang H, Shen H. Aggressive Intramuscular amushemangiomas in the upper Extremity. *Medicine*. (2017) 96:E5939.

25. Bella GP, Manivel JC, Thompson RC Jr, Clohisy DR, Cheng EY. Intramuscular hemangioma: tattoo risk related to surgical navigation. *Clin Orthop Relat Res*. (2007) 459:186–91. doi: 10.1097/BLO.0b013e318063c61b

frontiers | Frontiers in Oncology

TYPE Case Report
PUBLISHED 10 October 2024
DOI 10.3389/fonc.2024.1482768

Check for updates

OPEN ACCESS

EDITED BY
Dragos Eugen Georgescu,
Carol Davila University of Medicine and Pharmacy, Romania

REVIEWED BY
Martina Arcieri,
Ospedale Santa Maria della Misericordia di Udine, Italy
Olugbenga Akindele Silas,
University of Jos, Nigeria

*CORRESPONDENCE
Xuemei Qing
qingxuemei1988@outlook.com

RECEIVED 18 August 2024
ACCEPTED 19 September 2024
PUBLISHED 10 October 2024

CITATION
Qing X, Xie M, Guo H, Zhang L, Ye J, Zhang Y and Ma Y (2024) Mullerian adenosarcoma accidentally detected and coexisting with cervical carcinoma *in situ*: a rare case report. *Front. Oncol.* 14:1482768. doi: 10.3389/fonc.2024.1482768

COPYRIGHT
© 2024 Qing, Xie, Guo, Zhang, Ye, Zhang and Ma. This is an open-access article distributed under the terms of the Creative Commons Attribution License (CC BY). The use, distribution or reproduction in other forums is permitted, provided the original author(s) and the copyright owner(s) are credited and that the original publication in this journal is cited, in accordance with accepted academic practice. No use, distribution or reproduction is permitted which does not comply with these terms.

Mullerian adenosarcoma accidentally detected and coexisting with cervical carcinoma *in situ*: a rare case report

Xuemei Qing [1,2*], Min Xie [1,3], Hongying Guo [1], Liying Zhang [1], Jiatian Ye [3], Yong Zhang [2,4] and Ying Ma [4,5]

[1]Department of Obstetrics and Gynecology, People's Hospital of Qingbaijiang District, Chengdu, Sichuan, China, [2]Department of Obstetrics and Gynecology, Southwest Medical University, Luzhou, Sichuan, China, [3]Department of Obstetrics and Gynecology, West China Second University Hospital, Sichuan University, Chengdu, Sichuan, China, [4]Department of Obstetrics and Gynecology, Mianyang Central Hospital, Mianyang, Sichuan, China, [5]Department of Obstetrics and Gynecology, Chengdu Medical College, Chengdu, Sichuan, China

Mullerian adenosarcoma is rare, usually found in the uterine corpus and rarely in the cervix. Adenosarcoma that grows diffusely in the uterine cavity and the cervical canal is even rarer without symptoms. Herein, we report a rare case of multiple primary malignant neoplasms of Mullerian adenosarcoma accidentally detected and coexisting with cervical carcinoma *in situ*. Fortunately, the tumor was in the early stage and the Mullerian adenosarcoma was treated together with the cervical carcinoma *in situ* by hysterectomy + bilateral adnexectomy. Histopathology and immunohistochemistry results confirmed this diagnosis, further confirmed by a pathology consultation at the University Hospital. The patient recovered well from the surgical treatment and was discharged with regular follow-up. The patient did not undergo pelvis–abdomen CT and diagnostic curettage preoperatively, and no malignancy was detected by cryo-pathology intraoperatively, which may be related to the rarity of the disease and the relative lack of awareness and experience of our clinicians and pathologists for this tumor. We hope that this rare case can provide some lessons for gynecologists and pathologists.

KEYWORDS

Mullerian adenosarcoma, cervical carcinoma in situ, multiple primary malignant neoplasms, rare, case report

Introduction

Mullerian adenosarcoma (MA), also known as uterine adenosarcoma, is a rare mixed tumor consisting of benign epithelial and malignant mesenchymal components, which occurs predominantly in the uterus (approximately 81%) and rarely in the cervix (approximately 2%) (1). It varies in clinical symptoms and may be asymptomatic. Cervical intraepithelial neoplasia (CIN) III with glandular involvement, equivalent to cervical carcinoma *in situ* (CCIS), often caused by persistent high-risk human papillomavirus (HPV) infection, manifests primarily as vaginal bleeding following coitus but some may also be asymptomatic. Multiple primary malignant neoplasms (MPMN) are even rarer, but with the increase in human life expectancy and the advancement of medical technology, the rate of early cancer detection has increased and the reports about MPMN also increased (2, 3). Now, we report a rare case of asymptomatic CCIS coexisting with MA as an MPMN.

Case presentation

The patient, a 56-year-old woman, G_0P_0, menopause for 8 years, was admitted to our hospital for "Abnormal cervical cancer screening results detected for more than 3 months". Past medical history and family history were not specific; she had a middle school education, had freelance work, and drank in moderation for 40+ years. She denied postmenopausal vaginal bleeding and discharge, without abdominal pain, or bloating. More than 3 months ago, she had a health checkup with positive HPV-58 and an abnormal Thin-prep cytologic test about atypical squamous cells. Eleven days before admission, a cervical biopsy was carried out, and the results showed that "Cervix 6 point" and "Cervix 12 point" had foci of high-grade squamous intraepithelial neoplasia (CIN III) with glandular involvement, considered CCIS, and surgery was recommended.

Physical examination showed the following: temperature, 36.3°C; pulse rate, 68 times/min; respiratory rate, 20 times/min; blood pressure, 100/62 mmHg; weight, 62.5 kg; height, 151 cm. There were no positive signs in the general examination. However, gynecological examination showed cervical atrophy with post-biopsy changes, visible heterogeneous vessels, and uterine atrophy slightly, with no masses and pressure pain detected in the bilateral adnexal area. Pathologic results of cervical biopsy were as follows: High-grade squamous intraepithelial neoplasia (CIN III) with glandular involvement was seen in both "Cervix 6 point" and "Cervix 12 point". Preliminary diagnosis showed CIN III with glandular involvement and high-risk HPV infection. She underwent a series of preoperative ancillary examinations, in which a transvaginal ultrasound (Figures 1A-H) showed that the cervix was thickened with an anteroposterior diameter of 4.3 cm and multiple cystic echoes, the largest one being approximately 2.2 cm x 1.4 cm without blood flow signal, and punctate blood signals throughout the cervix was detected with an RI of 0.66. The anteroposterior diameter of the uterus was 4.3 cm with a longitudinal diameter of 6.1 cm and a transverse diameter of 5.1 cm. The endometrium is poorly visualized without a blood flow signal but with the arterioles in the surrounding area, no mass in the bilateral adnexal area, and no free echogenicity in the pelvis. Other results showed no abnormalities, including chest computed tomography (CT), which was required before elective laparoscopic surgery at our hospital.

Then, because of obvious atrophy of the cervix after years of menopause, because cervical conization proved to be difficult, and because there was no desire to preserve her uterus, a trans-umbilical single-port laparoscopic hysterectomy + bilateral adnexectomy was performed. Intraoperative observation: the uterus anterior was slightly larger than normal, spherical, with no tumor on the corpus surface, but one mass approximately 3 cm x 4 cm in size was seen at the junction of the lower part of the posterior wall and the cervix, with a smooth surface, and the bilateral adnexa had no abnormality in appearance. The gross view of the isolated uterus specimen profile (Figure 2A): No neoplasm was seen on the surface of the external cervix, the cervix was significantly thickened with a diameter of approximately 5 cm, with multiple cystic cavities containing mucus, located mainly in the posterior wall, and the muscular wall of the uterus was not uniform, with many small gray-white papillomatous nodules, diffused in the uterine cavity. The results of cryo-pathology showed the following: chronic cervical and endocervical inflammation with retention cysts, small foci of CIN III with glandular involvement, and multiple grayish-white polypoid protrusions in the uterine cavity, which tended to be adenomyoma-like polyps. Thus, with no malignant lesions seen, the operation was over.

The pathological results showed the following: "Uterus" (Figures 2B-H) (1): Endometrial glandular dilatation, dense peri-endometrial glandular–mesenchymal stroma with polypoid changes, considered a mixed epithelial–mesenchymal tumor of the uterine corpus, low-grade uterine adenosarcoma, but extensive sampling and immunohistochemistry were required (2); chronic cervical and endocervical inflammation with trapping cyst formation, with small foci of epithelium showing CIN III involving glands, another small focal peri-epithelial mesenchymal hyperplasia of the cervical canal adenohypophysis was seen enthusiastically, and it was considered a mixed epithelial–mesenchymal tumor of the uterine corpus involving the cervix. "Bilateral adnexa": bilateral ovarian leucoplast and both fallopian tubes chronic inflammation, with interstitial vascularization and congestion. The results of immunohistochemistry (IHC) (Figures 3A-H) showed the following: Wax Block No. 17: endometrial gland peritubular dense mesenchymal stroma showed ER (+), PR (+), CD10 (+/−), SMA (−), Desmin (−), P53 (−), and Ki-67 (+; hot spot area of approximately 5%); Wax Block Nos. 10, 11, 12, 14, and 20: peritubular dense mesenchymal stroma were all CD10 (+). The

Abbreviations: MA, Mullerian adenosarcoma; CIN, Cervical intraepithelial neoplasia; CCIS, Cervical carcinoma *in situ;* HPV, Human papillomavirus; MPMN Multiple primary malignant neoplasms; CT, Computed tomography; IHC, Immunohistochemistry; MRI, Magnetic resonance imaging; SO, Sarcoma overgrowth.

10.3389/fonc.2024.1482768

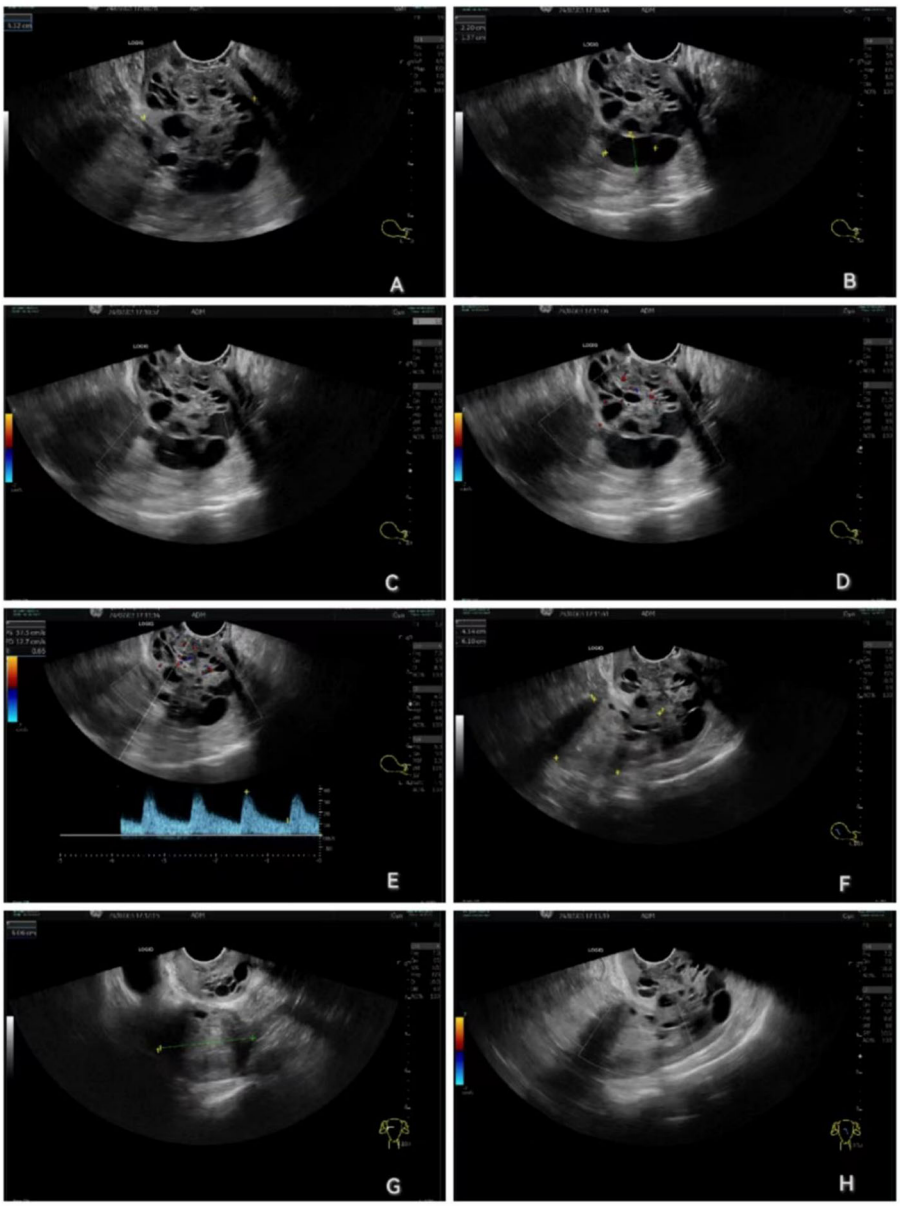

FIGURE 1
Transvaginal ultrasound images. **(A)** The cervix was thickened with an anteroposterior diameter of 4.3 cm and multiple cystic echoes. **(B)** The largest cystic echo of the cervix was approximately 2.2 cm x 1.4 cm. **(C)** Maximum cystic echoes of the cervix show no blood flow signal. **(D)** Punctate blood signals throughout the cervix. **(E)** RI: 0.66. **(F)** The anteroposterior diameter of the uterus was 4.3 cm with a longitudinal diameter of 6.1 cm. **(G)** The transverse diameter of the uterus was 5.1 cm. **(H)** The endometrium is poorly visualized without a blood flow signal but with the arterioles in the surrounding area.

combination of hematoxylin–eosin staining morphology and IHC findings supported a uterine mixed epithelial–mesenchymal tumor predisposing to low-grade uterine adenosarcoma involving the muscle wall and cervix. Differential diagnoses include (1) adenomyoma-like polyps with adenomyosis (2), mixed endometrial–cervical polyps with adenomyosis, and (3) low-grade endometrial mesenchymal sarcoma with gland differentiation. A pathology consultation at a higher hospital was recommended. Then, the consultation results of West China Second Hospital of Sichuan University (pathology no. JCS202403489) showed the following: <Uterine cavity protruding> uterine adenosarcoma, sarcoma component is low-grade endometrial mesenchymal sarcoma, the tumor grows downward and involves the cervix, and adenomyosis foci can be found in the attached muscle wall; <cervix> CIN II and glandular involvement were also seen. IHC: sarcoma component: Ck-P (−), EMA (−), Vim (+), Des (+), Caldesmon (−), CD10 (++), ER (++), PR (−), and Ki-67 positivity <1%.

On the fifth postoperative day, she recovered well and was discharged. About 1 month later, she came for a follow-up with no abnormality of the pelvic–abdominal CT (Figure 4). She will continue to be followed up regularly.

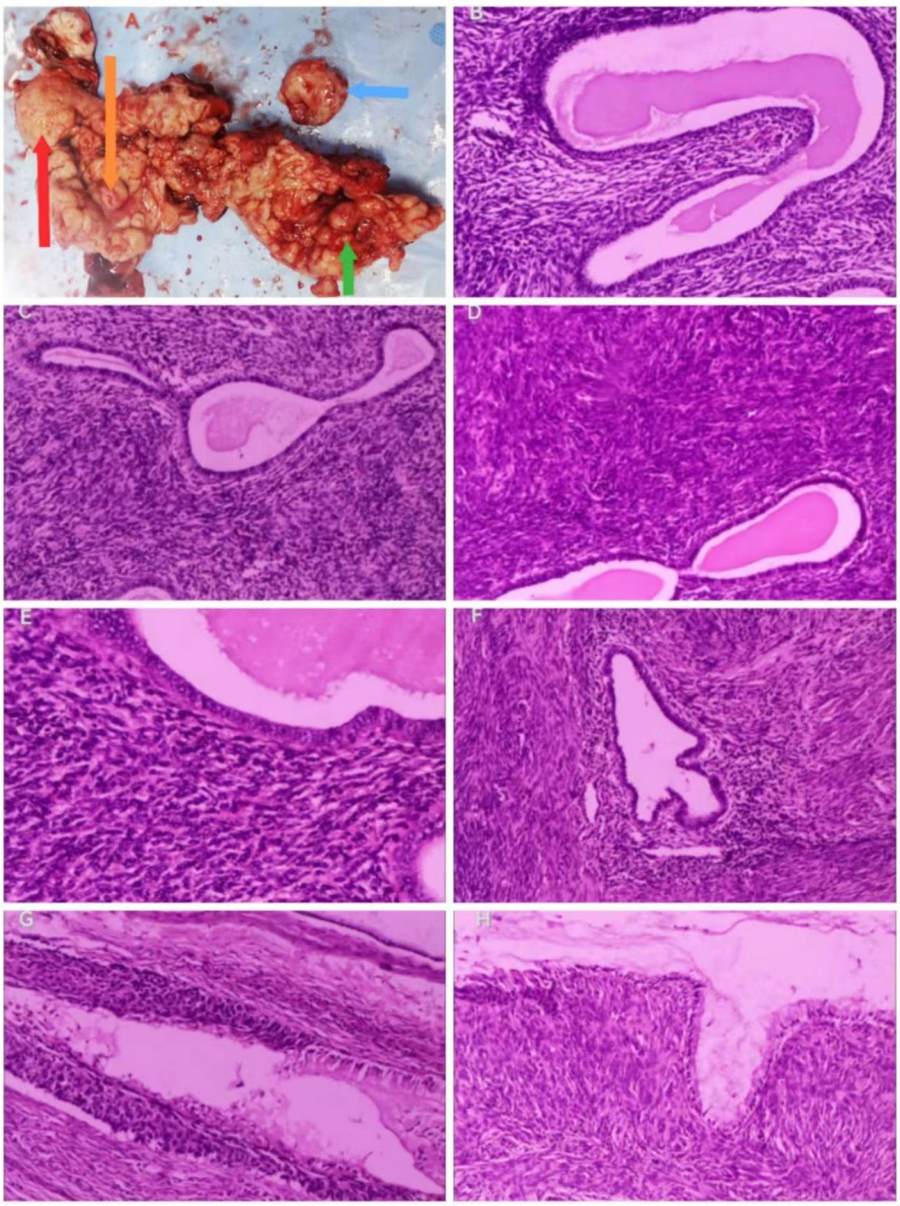

FIGURE 2
Gross view of the specimen and histopathologic results (hematoxylin–eosin staining). Gross view of the specimen. **(A)** The arrows point to red: adenomyosis, orange: uterine adenosarcoma, green: cervical adenosarcoma, and blue: the largest cystic echogenic mass of the cervix). Histopathologic results. **(B)** Irregular endothelial glands, 100x. **(C)** (100x), **(D)** (100x), and **(E)** (200x): Dense mesenchyme surrounding endothelial glands. **(F)** Adenomyosis, 100x. **(G)** CIN III with glandular involvement, 100x. **(H)** Dense mesenchyme around the cervical glands, 100x.

Discussion

MPMNs refer to the simultaneous or sequential appearance of two or more histologically unrelated primary malignant lesions in the same body, which may originate from the same organ, paired organs, different parts of the same system, or organs of different systems, accounting for 0.52%–11.7% of all malignant tumors. MPMN originating in the female reproductive system is relatively rare, accounting for 1%–2% of gynecologic malignant tumors. The pathogenesis is still unclear and may be related to genetic factors, host susceptibility, immune deficiencies, hormonal factors, unhealthy lifestyles, and oncogenic side effects from previous cancer treatments and even environmental exposure (2). It can be divided into synchronous MPMN with occurrence time intervals <6 months and heterochrony MPMN with intervals >6 months, accounting for approximately 90% of cases (4). This patient was diagnosed with CCIS and MA within 1 month of each other, with different primary sites and pathologic types, consistent with synchronous MPMN, which is a rare type. High-risk HPV infection led to her CCIS, and early diagnosis was achieved by combined cervical lesion screening; thus, the treatment was performed promptly. However, one study has shown that HPV is not associated with MA (5).

MA is rare and usually lacks specificity, commonly in postmenopausal women (mean age of 58 years), but it can

10.3389/fonc.2024.1482768

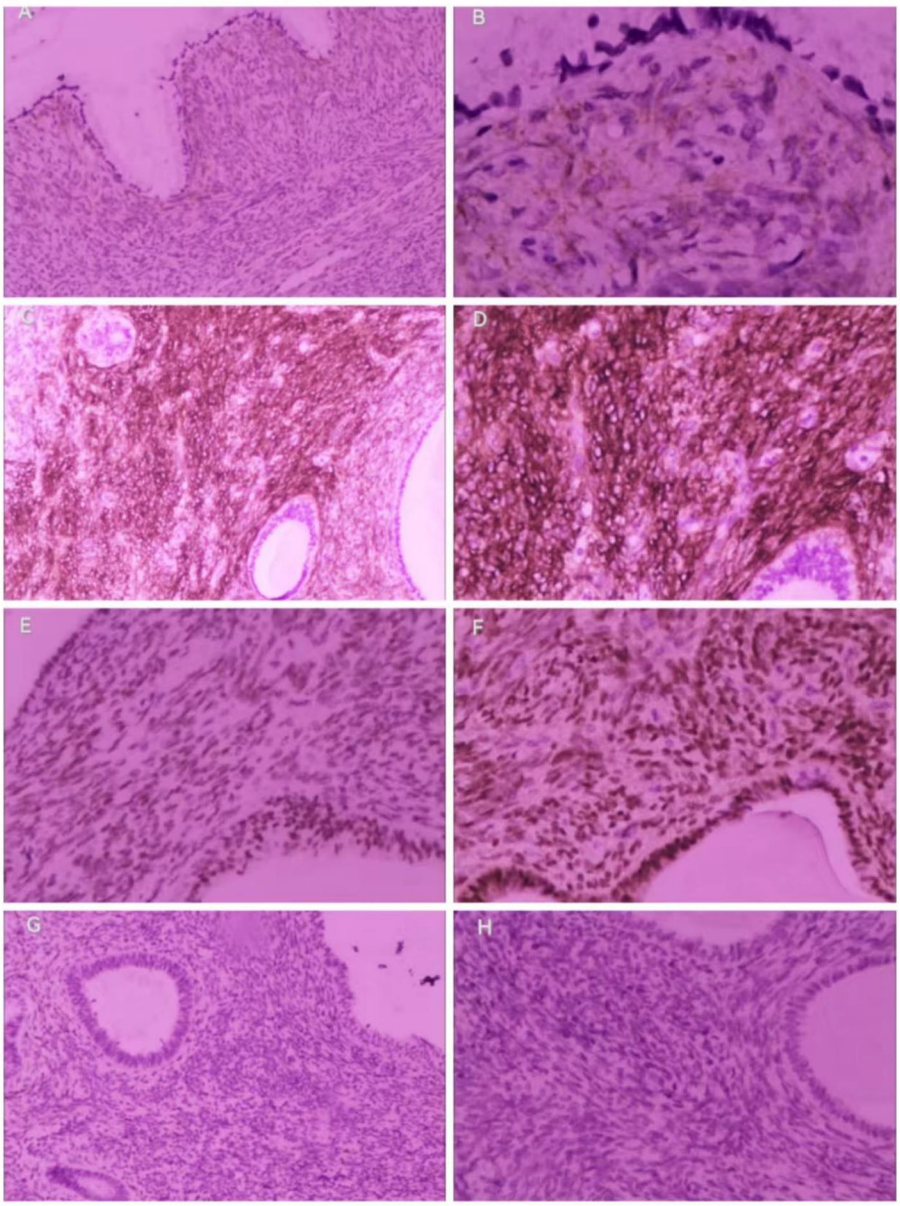

FIGURE 3
IHC of the adenosarcoma. Dense mesenchyme surrounding cervical glands: CD10 (+), **(A)**: 100x; **(B)** (400x). Dense mesenchyme surrounding endometrial glands: CD10 (+), **(C):** 100x; **(D)** (:200x); **(E)** ER (+), 200x;**(F)** PR (+), 200x; **(G)** Desmin (–), 100x; **(H)** SMA (–), 100x.

develop before menopause or even during adolescence (30%). The most common symptom is abnormal vaginal bleeding, and some may present with increased vaginal discharge or pelvic pain. Typically, the tumor grows in the uterine cavity of an exophytic polyp form, which may be located in the lower part of the uterine cavity, and rarely in the cervical or extra-uterine area. Gynecologic color Doppler ultrasound is the most used imaging modality, with a limited differential diagnostic value. In contrast, magnetic resonance imaging (MRI) can provide more details: the tumor is mass-shaped, with clear and sharp borders, intra-tumor heterogeneity, multiple microscopic vesicle shadows, rich blood supply, and even shadows of flow vessels, and the degree of enhancement of the tumor increases with increasing tumor diameter, with higher diffusion-weighted imaging signals and lower apparent diffusion coefficient values. In addition, diffusion-weighted imaging is useful for tumor localization and characterization. Although diagnostic curettage or endometrial biopsy may help diagnose some MA, the sensitivity is poor. It is difficult to differentiate the benign or malignant nature of the tumor preoperatively, by either ultrasound, CT, or MRI, and the diagnosis relies on pathophysiologic examination.

For MA incidentally found after hysterectomy, chest/abdominal/pelvic CT or abdominal/pelvic MRI and chest CT should be performed for the presence of metastatic lesions (6). This patient was diagnosed with CIN III with glandular involvement, and because of obvious atrophy of the cervix,

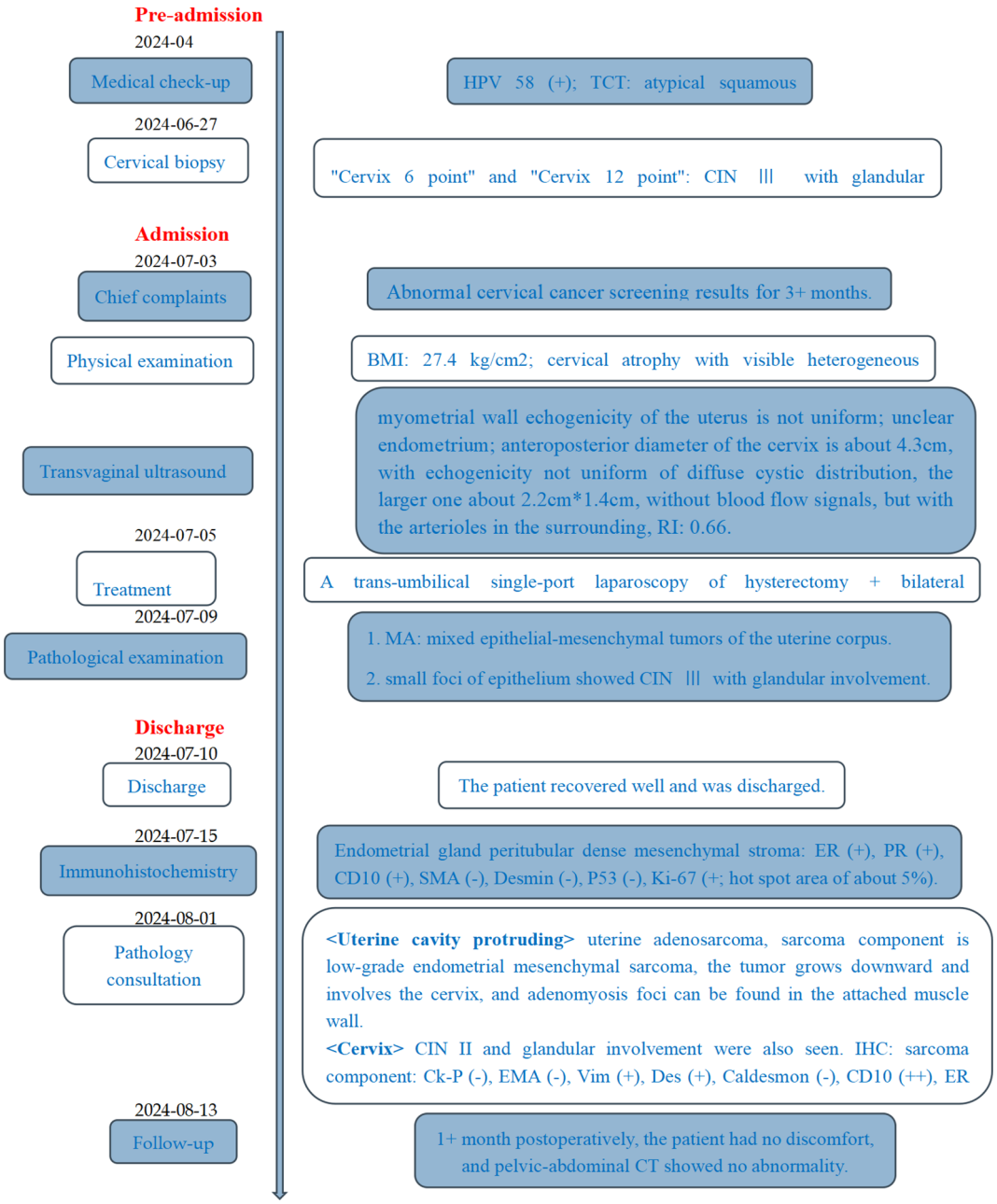

FIGURE 4
Timeline. HPV, human papillomavirus; TCT, thin-prep cytologic test; CIN, cervical intraepithelial neoplasia; BMI, body mass index; RI, resistance index; MA, Mullerian adenosarcoma.

because cervical conization proved to be difficult, and because there was no desire to preserve her uterus, hysterectomy + bilateral adnexectomy was performed (7), with cryo-pathology intraoperatively, but without preoperative pelvic/abdominal CT or MRI. Early-stage cervical cancer is usually asymptomatic, emphasizing the importance of screening diagnosis based on histology. Diagnostic suspicion in initial cases is based on a suspicious or positive Pap test report, followed by a colposcopy, which allows a biopsy to be performed. If insufficient to determine invasiveness, a cervical conization may be required. The tumor marker squamous cell carcinoma antigen has not been evaluated in all international guidelines except the Italian AIOM guidelines. The latest evidence supports the surgical treatment of patients with early-stage cervical cancer in stages not more than IA1, where both cervical conization and extra-fascial hysterectomy can be performed without lymphadenectomy (8). A systematic review of 18 studies demonstrated the importance of a multidisciplinary approach to cervical cancer patients, tailoring the best treatment plan for them, informing them about possible postoperative vaginal changes and menopausal symptoms, and providing them with the best possible psychological support, as well as encouraging a balanced diet and physical activity (9).

In addition, transvaginal ultrasound showed that her endometrium was poorly visualized, which was mistaken for possible endometrial adhesions due to low estrogen levels, and the cervix was enlarged with an anteroposterior diameter of approximately 4.3 cm with multiple cystic echoes, which was mistaken for cervical natriuretic cysts; thus, diagnostic curettage or endocervical curettage was not performed. However, intraoperative dissection with the isolated uterus revealed the presence of diffuse exophytic papillae in the uterine cavity and cervical canal, which aroused the interest of all operators, whether it is an endometrial malignancy with infiltration of the cervix or a cervical invasive carcinoma spreading to the endometrium. However, the pathology report negated both of the above hypotheses. It revealed a rare uterine adenosarcoma (both uterus and cervix involved) with no infiltrative component of CCIS, as determined by our gynecologic pathologist through extensive sampling, careful microscopic examination, and a combination of IHC, literature review, and departmental discussion. The patient's uterine adenosarcoma was stage I, and hysterectomy + bilateral adnexectomy was the standard procedure, without additional surgery, radiotherapy, chemotherapy, or tumor endocrine therapy (i.e., tumor hormone therapy, which refers to the method of controlling and treating tumors by altering the balance of the body's endocrine environment, mainly including anti-estrogen and anti-progesterone treatment).

MA has a very low incidence, a rare biphasic tumor with unclear pathogenesis and etiology, which may be associated with several high-risk factors, such as overload or imbalance of estrogen, and use of oral contraceptives or tamoxifen for a long period; high body mass index; and history of pelvic radiation therapy (1). The patient has none of the above high-risk factors, except for a high body mass index of 27.4 kg/cm^2, close to obesity, which causes various metabolic diseases and is also an important risk factor for endometrial cancer. It is worthwhile for clinicians to pay enough attention, especially perimenopausal and postmenopausal women. In addition, the patient's ultrasound suggested that the myometrial wall echogenicity is not uniform, which was also confirmed intraoperatively. Whether the tumor infiltrated the myometrial wall microscopically or a manifestation of adenomyosis posed a difficult problem for our pathologists to distinguish it from adenomyoma-like polyp with adenomyosis, mixed endometrial–cervical polyp with adenomyosis, or low-grade endometrial mesenchymal sarcoma with gland differentiation. Furthermore, the report from the gynecologic pathologist at the university hospital confirmed that "adenomyosis foci were detected in the attached muscle wall". Thus, it is reasonable to wonder whether the presence of adenomyosis is one of the risk factors for MA, or whether MA is a malignant transformation of adenomyosis, which is based on evidence (10, 11). Additionally, a recent report shows that endometriosis may be a factor in the development of MA (12).

The diagnosis of MA relies on histopathology, with the following features: a mixed tumor composed of benign neoplastic glandular and sarcomatous mesenchymal components that are lobulated and may be seen as fissured or dilated glands lined by benign endometrial epithelium, with cuff-like neoplastic mesenchymal cells surrounding the glands, which are abundant and show varying degrees of anisotropy, and the nuclear schizophrenic phenomenon is generally rare or absent. The malignant mesenchymal component is usually low grade and consists of spindle-shaped and/or rounded cells, the former often arranged in whorls, the latter loosely arranged, with the mesenchymal cells clustered around the gland and sparsely cuffed away from the gland, forming the so-called germinal layer. The sarcoma component is homogeneous, showing either endometrial mesenchymal or smooth muscle differentiation, when the overall prognosis of the tumor is better than that of other sarcomas of the uterus. When the growth of the mesenchymal sarcoma component significantly exceeds the gland component, meaning that the pure sarcoma component accounts for more than 25% of the tumor volume and that the cellular abnormality increases, presenting high-grade sarcoma manifestations or the appearance of rhabdomyosarcoma and other heterogeneous differentiation, it is called adenosarcoma with sarcomatous overgrowth (SO), with high invasiveness and poor prognosis (13). IHC is not mandatory, but low-grade adenosarcomas are usually positive for CD10 and hormone receptors, and their mesenchymal components resemble endometrial mesenchymal sarcomas immunohistochemically. p53 shows aberrant expression in the overgrown sarcoma component, and its mesenchymal components resemble high-grade uterine sarcomas with a high Ki-67 index. Desmin, myogenin, and MyoD1 help identify rhabdomyosarcoma components (14). In this patient, immunohistochemistry, as well as consultation with the pathologist at the university hospital, showed that the adenosarcoma originated in the uterine cavity, the adenosarcoma in the cervical canal was due to a downward invasion of the uterine lesion, the lesion was low grade, and no sarcoma overgrowth was seen as demonstrated in the pathology report (p53-negative, low positivity for Ki-67, etc.).

With the development of molecular pathology, several genetic tests have been applied to MA. Their molecular characteristics lack features such as specific gene mutations or chromosomal variants; some are seen with *8q13* amplification and *MYBL1* copy number increase associated with SO, and few are seen with *NCOA2/3* gene fusion. It has been shown that the genomic and clinicopathologic features of high-grade MA include generalized *TP53* pathway alteration and aggressive behavior (15). A recent study showed that in 29 MA cases among 40 commonly mutated genes detected by whole-genome sequencing and verified by next-generation sequencing, *KMT2C* and *BCOR* were common with and without SO, whereas *MAGEC1* and *KDM6B* were strongly associated with SO, and that the frequent gene mutation rate of approximately 33% of MA with SO was higher than that without SO (11%) (16).

Surgery is the mainstay of treatment, supplemented by endocrine therapy, chemotherapy, and radiotherapy. Systematic pelvic and para-aortic lymph node dissection is not routinely performed, but exploration is needed, and enlarged or suspicious lymph nodes should be removed. If the lesion is confined to the uterus (1): hysterectomy + bilateral adnexectomy; (2) inoperable: external pelvic radiation ± brachytherapy and/or systemic treatment. If extrauterine: (1) hysterectomy + bilateral adnexectomy + resection of metastatic foci, including metastatic lymph nodes; (2) inoperable: extra-pelvic irradiation ± brachytherapy and/or systemic treatment.

The complete removal of the uterine tumor is emphasized, and tumor fractionation in the peritoneal cavity is contraindicated. The supplemented therapy depends on the disease stage after surgery: (1) Adenosarcoma without sarcoma overgrowth: stage I can be observed or estrogen blockade; stages II–IV_A with anti-estrogen therapy and/or radiotherapy; stage IV_B with anti-estrogen therapy and/or palliative radiotherapy; (2) adenosarcoma with sarcoma overgrowth: stage I can be observed, and stage II–IV needs chemotherapy (6). Clinically, corrections based on clinicopathologic prognostic factors are often required, and a review by the gynecologic pathologist is strongly recommended. Relevant risk factors include hysterectomy, completeness of tumor specimen, tumor size, histologic type, number of nuclear schizonts, presence of vascular infiltration, myometrial invasion, and histologic grade. In addition, the location and number of extrauterine metastases should be recorded in detail, and the number and location of lymph nodes involved should be clarified.

MA is of low malignant potential and has a relatively good prognosis, but still, 25% of patients die. Poor prognostic factors include sarcoma overgrowth, deep mesenchymal infiltration, high-grade component, high heterogeneous component, and lympho-vascular infiltration, of which the first two are associated with the worst prognosis (14). Local recurrence and distant metastases occur in approximately 5%. Regular follow-up is important, including general and gynecological examinations, imaging tests, and health education.

Conclusions

MA is rare, and even rarer coexisting with CCIS as an MPMN. The patient did not undergo pelvis–abdomen CT and diagnostic curettage preoperatively, and the cryo-pathology failed to detect the MA, which may be related to the rarity of the disease and the lack of experience of our clinicians and pathologists. Fortunately, it is stage I and the hysterectomy + bilateral adnexectomy surgical procedure was suitable, without additional surgery or other supplemented therapy. Raising awareness for MA and MPMN to reduce misdiagnosis and underdiagnosis is profoundly important for the diagnosis and treatment.

Data availability statement

The datasets presented in this study can be found in online repositories. The names of the repository/repositories and accession number(s) can be found in the article/supplementary material.

Ethics statement

Ethics committee approval was unnecessary due to the nature of the study. Written informed consent was obtained from the individual(s) for the publication of any potentially identifiable images or data included in this article. Written informed consent was obtained from the participant/patient(s) for the publication of this case report.

Author contributions

XQ: Conceptualization, Data curation, Supervision, Validation, Writing – original draft, Writing – review & editing. MX: Data curation, Writing – review & editing. HG: Conceptualization, Writing – review & editing. LZ: Validation, Writing – review & editing. JY: Validation, Writing – review & editing. YZ: Supervision, Writing – review & editing. YM: Supervision, Writing – review & editing.

Funding

The author(s) declare that no financial support was received for the research, authorship, and/or publication of this article.

Acknowledgments

We thank the pathologists of West China Second Hospital for consultation support and our colleagues in the Department of Pathology for help with pathological analysis.

Conflict of interest

The authors declare that the research was conducted without any commercial or financial relationships that could be construed as a potential conflict of interest.

Publisher's note

All claims expressed in this article are solely those of the authors and do not necessarily represent those of their affiliated organizations, or those of the publisher, the editors and the reviewers. Any product that may be evaluated in this article, or claim that may be made by its manufacturer, is not guaranteed or endorsed by the publisher.

References

1. Dai WN, Wang PF, Yao G, Peng YH. Diagnosis and treatment progress of cervical adenosarcoma. *Oncol Res Clinical*. (2019) 31:570–3. doi: 10.3760/cma.j.issn.1006-9801.2019.08.016

2. Copur MS, Manapuram S. Multiple primary tumors over a lifetime. *Oncol (Williston Park)*. (2019) 33(7):629384.

3. He Y, Wang Y, Ji C, Liu Y, Wu YM. Clinical analysis of 23 cases with simultaneous double primary gynecological Malignant tumors. *Zhonghua Fu Chan Ke Za Zhi*. (2022) 57:352–60. doi: 10.3760/cma.j.cn112141-20220214-00086

4. del Carmen MG, Birrer M, Schorge JO. Carcinosarcoma of the ovary: A review of the literature. *Gynecologic Oncol*. (2012) 125:271–7. doi: 10.1016/j.ygyno.2011.12.418

5. Mumba E, Ali H, Turton D, Cooper K, Grayson W. Human papillomaviruses do not play an aetiological role in Müllerian adenosarcomas of the uterine cervix. *J Clin Pathology*. (2008) 61:1041–4. doi: 10.1136/jcp.2008.056614

6. Gynecologic Oncology Committee of the Chinese Anti-Cancer Association. Guidelines for diagnosis and treatment of uterine sarcoma (2021 edition). *Chin J Cancer*. (2021) 31:513–9. doi: 10.19401/j.cnki.1007-3639.2021.06.09

7. Zhang J, Wang DB. Chinese expert consensus on elective application of hysterectomy in the treatment of cervical high-grade squamous intraepithelial lesion (2022 edition). *Chin J Pract Gynecology Obstetrics*. (2022) 38:1108–10. doi: 10.3760/cma.j.issn.1006-9801.2019.08.016

8. Restaino S, Pellecchia G, Arcieri M, Bogani G, Taliento C, Greco P, et al. Management for cervical cancer patients: A comparison of the guidelines from the international scientific societies (ESGO-NCCN-ASCO-AIOM-FIGO-BGCS-SEOM-ESMO-JSGO). *Cancers*. (2024) 16(14):2541. doi: 10.3390/cancers16142541

9. Cianci S, Tarascio M, Arcieri M, La Verde M, Martinelli C, Capozzi VA, et al. Treatment sexual function and quality of life of patients affected by cervical cancer: A systematic review. *Post Medicina*. (2023) 59(4):704. doi: 10.3390/medicina59040704

10. Lee S-J, Park JY. A rare case of intramural müllerian adenosarcoma arising from adenomyosis of the uterus. *J Pathol Trans Med*. (2017) 51:433–40. doi: 10.4132/jptm.2017.06.11

11. Talia KL, Naaman Y, McCluggage WG. Uterine adenosarcoma originating in adenomyosis: report of an extremely rare phenomenon and review of published literature. *Int J Gynecol Pathol*. (2021) 40:342–8. doi: 10.1097/PGP.0000000000000709

12. Bruguier H, Maalouf N, Smyth SL, Damato S, Reddy P, Soleymani majd H. Rare Mullerian adenosarcoma of the uterine cervix arising on a background of endometriosis: A diagnostic challenge with risk of Malignant transformation—A case report and review of the current literature. *Clin Case Rep*. (2024) 12(6):e9075. doi: 10.1002/ccr3.9075

13. Togami S, Kawamura T, Fukuda M, Yanazume S, Kamio M, Kobayashi H. Clinical management of uterine cervical mullerian adenosarcoma: A clinicopathological study of six cases and review of the literature. *Taiwanese J Obstetrics Gynecology*. (2018) 57:479–82. doi: 10.1016/j.tjog.2018.04.032

14. Croce S, Devouassoux-Shisheboran M, Pautier P, Ray-Coquard I, Treilleux I, Neuville A, et al. Uterine sarcomas and rare uterine mesenchymal tumors with Malignant potential. Diagnostic guidelines of the French Sarcoma Group and the Rare Gynecological Tumors Group. *Gynecol Oncol*. (2022) 167:373–89. doi: 10.1016/j.ygyno.2022.07.031

15. Hodgson A, Amemiya Y, Seth A, Djordjevic B, Parra-Herran C. High-grade müllerian adenosarcoma: genomic and clinicopathologic characterization of a distinct neoplasm with prevalent TP53 pathway alterations and aggressive behavior. *Am J Surg Pathol*. (2017) 41:1513–22. doi: 10.1097/PAS.0000000000000907

16. Ban Y, Fischer JV, Maniar KP, Guo H, Zeng C, Li Y, et al. Whole-genome sequencing and target validation analysis of müllerian adenosarcoma: A tumor with complex but specific genetic alterations. *Front Oncol*. (2020) 10. doi: 10.3389/fonc.2020.00538

frontiers | Frontiers in Oncology

TYPE Original Research
PUBLISHED 17 October 2024
DOI 10.3389/fonc.2024.1399079

Check for updates

OPEN ACCESS

EDITED BY
Dragos Eugen Georgescu,
Carol Davila University of Medicine and Pharmacy, Romania

REVIEWED BY
Adina Emilia Croitoru,
Fundeni Clinical Institute, Romania
Traian Dumitrascu,
Carol Davila University of Medicine and Pharmacy, Romania

*CORRESPONDENCE
Yanping Hu
yphu92@163.com

RECEIVED 11 March 2024
ACCEPTED 19 September 2024
PUBLISHED 17 October 2024

CITATION
Li N, Hu Y, Wu L and An J (2024) Clinicopathological correlations in 38 cases of gastroenteropancreatic high-grade neuroendocrine neoplasms.
Front. Oncol. 14:1399079.
doi: 10.3389/fonc.2024.1399079

COPYRIGHT
© 2024 Li, Hu, Wu and An. This is an open-access article distributed under the terms of the Creative Commons Attribution License (CC BY). The use, distribution or reproduction in other forums is permitted, provided the original author(s) and the copyright owner(s) are credited and that the original publication in this journal is cited, in accordance with accepted academic practice. No use, distribution or reproduction is permitted which does not comply with these terms.

Clinicopathological correlations in 38 cases of gastroenteropancreatic high-grade neuroendocrine neoplasms

Na Li, Yanping Hu*, Linguo Wu and Jianduo An

Department of Pathology, Beijing Luhe Hospital, Capital Medical University, Beijing, China

Objective: Diagnosis and treatment of gastroenteropancreatic high-grade neuroendocrine neoplasms (GEP-HG-NENs), particularly G3 well-differentiated neuroendocrine tumours (NETs) and poorly differentiated neuroendocrine carcinomas (NECs) relies on histopathological morphology, immunohistochemistry, and molecular biological markers, which are lacking especially in cases with ambiguous histomorphology. In this study to contribute to the development of more targeted treatment strategies, we examined various immunohistochemical and molecular biological markers and their association with clinicopathological features in GEP-HG-NENs.

Methods: We included 38 patients with GEP-HG-NENs in this study, with their retrospective follow-up data. The expression of tumour protein p53 (TP53), RB transcriptional corepressor 1 (RB1), somatostatin receptor 2 (SSTR2), clusterin (CLU), and marker of proliferation Ki-67 (MKI67) was immunohistochemically analysed. KRAS proto-oncogene, GTPase (*KRAS*) and B-Raf proto-oncogene, serine/threonine kinase (*BRAF*) *V600E* expression was evaluated using quantitative real-time polymerase chain reaction (qRT-PCR). The relationships between immunohistochemical and molecular biological markers and clinicopathological characteristics were examined using a Cox risk regression model, receiver operating characteristic (ROC) curve, and Kaplan–Meier survival analyses.

Results: SSTR2, RB, TP53, and CLU expression differed between NET G3 and NECs, with variations among the NET G3 and small- and large-cell NEC (SCNEC and LCNEC, respectively) groups ($p < 0.05$). The median MKI67 proliferative index was approximately 40% and 70% in G3 NETs and NECs, respectively. The NET G3 group exhibited a median survival of 25 months, indicating a relatively better prognosis than that of the NECs group (median survival, 11 months). Both Kaplan–Meier survival analysis and the Cox risk regression model indicated a statistical correlation among treatment methods, CLU expression, and prognosis ($p < 0.05$). The *BRAF V600E* mutation rate was 32.4% in G3 NETs and SCNEC, demonstrating a significant difference between both types ($p = 0.0086$). Furthermore, ROC curve analysis highlighted the diagnostic significance of the positive expression of the immunohistochemical markers CLU, SSTR2, and RB in identifying NET G3.

Conclusion: To guide more suitable treatment strategies, it is essential to develop and apply valuable and more targeted immunohistochemical and molecular pathological markers for a comprehensive analysis.

KEYWORDS

gastroenteropancreatic high-grade neuroendocrine neoplasms, NET G3, Ki-67, *BRAF V600E*, clinicopathological features, prognostic analysis

1 Introduction

Gastroenteropancreatic neuroendocrine neoplasms (GEP-NENs) encompass various tumours originating from neuroendocrine cells within mucosal glands of the gastroenteropancreatic system. A new category called "highly proliferative neuroendocrine tumours" has been introduced for cases showing good morphological differentiation but a high MKI67 proliferation index, as supported by previous clinical and pathological findings (1). The 2019 World Health Organization (WHO) Classification of Tumours of the Digestive System categorises these tumours into well-differentiated neuroendocrine tumours (NETs) and poorly differentiated neuroendocrine carcinomas (NECs) according to their distinct morphology (1).

The NETs category has three subcategories: low-, intermediate-, and high-grade (NET G1, G2, and G3, respectively). The fifth edition of the WHO classification further refined the classification of NENs based on their proliferative activity into high-grade (HG)-NENs, which included NET G3 and NECs (>20 mitoses/2 mm^2 or MKI67 proliferation index >20%). Recent research suggests that relying solely on MKI67 proliferation index >20% may not provide a comprehensive prognostic assessment of NET G3 or NECs. A previous study reported significant differences in biological behaviour, treatment options, and survival rates between HG-NENs with an MKI67 proliferation index of 20–55% compared to those with an MKI67 index of ≥55% (2).

Although the definition of HG-NENs is clear, G3 NETs and NECs have distinct pathomorphological and molecular characteristics, and differ in epidemiology, treatment, and prognosis (3). This is indicative of the pathological heterogeneity of HG-NENs and differences in their biological behaviour (4). In addition, in the initial stages of clinical discovery, certain HG-NENs cases are associated with metastasis or infiltration; however, deep infiltration and liver and lung metastases may have been present at the time of diagnosis. Additionally, the degeneration in the biological behaviour of NECs is substantially worse than that of NET G3 (5). Distinguishing between NET G3 and NECs is often challenging because of their similar pathological appearances, which further contributes to difficulties in their clinical diagnosis and treatment. Furthermore, multivariate analysis of the disease clinicopathology has associated advanced age, specific type of HG-NENs, higher tumour proliferative activity, and the presence of distant metastases with poor clinical prognosis (6).

Immunohistochemistry can be used to detect specific polypeptide hormones and bioactive amines secreted by tumour cells, which aids in the diagnosis and grading of HG-NENs. The fifth edition of the WHO grading system for GEP-NENs defines HG-NENs as having an MKI67 proliferation index <20%. However, distinguishing between G3 NETs and NECs requires additional evaluation of the level of cell differentiation. Some studies suggest an MKI67 proliferation index of 55% as the threshold, indicating differences in behaviour, treatment, and prognosis among NET G3 subgroups (2). Antibodies against somatostatin receptor 2A (SSTR2A), TP53, RB, cyclin dependent kinase inhibitor 2A (CDKN2A [P16]), and BCL2 apoptosis regulator (BCL2) are commonly used to assess the genetic status of sporadic pancreatic NETs and NECs, with a higher prevalence of TP53 mutations and RB protein inactivation in NECs (7–9). SSTR2A expression is higher in well-differentiated NETs than it is in poorly differentiated NECs. Clusterin (CLU) expression is notably high in LG-NENs (10), but further research is needed to determine whether these indicators show distinct patterns in gastroenteropancreatic NETs.

Recent advancements in molecular pathology have provided further insight into the distinct molecular pathogenesis of HG-NENs. Genome-wide studies have revealed that pancreatic NETs exhibit molecular alterations in several key pathways, including DNA damage repair, chromatin remodelling, telomere alterations, and the phosphatidylinositol-4,5-bisphosphate 3 kinase (PI3K)/mechanistic target of rapamycin kinase (MTOR) signalling pathway (11, 12). Similarly, mutated genes such as *TP53*, phosphatase and tensin homolog (*PTEN*), cyclin dependent kinase inhibitor 2A (*CDKN2A*), F-box and WD repeat domain containing 7 (*FBXW7*), and AKT serine/threonine kinase 1 (*AKT1*) have been detected in rectal NETs (13, 14).

In contrast, NECs follow a different molecular pathway characterised by mutations in genes such as *TP53*, *RB1*, KRAS proto-oncogene, GTPase (*KRAS*), B-Raf proto-oncogene, serine/threonine kinase (*BRAF*), APC regulator of WNT signalling pathway (*APC*). *TP53* mutations are rare in NETs, and *RB1* gene mutation is absent in NETs (15). Some studies suggest that *TP53* mutations are limited to certain G3 NETs (16). Most research in this field relies on high-throughput sequencing technology, which

requires high-quality specimens from tumour core regions for accurate sequencing. Obtaining fresh tumour and whole blood samples for molecular analysis can be challenging, emphasising the need for innovative molecular and immune labelling methods for formalin-fixed paraffin-embedded samples.

In clinical practice, there is a notable difference in the choice of treatment regimen between NET G3 and NECs. The standard first-line chemotherapy regimen for NECs typically involves a combination of platinum and etoposide. For NET G3, guidelines typically advise the use of treatment strategies comparable to those recommended for NET G2. However, further large-scale studies are needed to identify the most suitable therapeutic options (11). Therefore, the current study aimed to explore a targeted HG-NEN mutation model in conjunction with lineage alterations at the primary tumour site to identify NECs and NET G3, with the goal of guiding the development of more rational and standardised treatment approaches.

2 Materials and methods

2.1 Case selection

This study included a total of 38 cases of patients with GEP-HG-NENs who underwent biopsy, puncture, or surgery or who received consultation at Beijing Luhe Hospital Affiliated to Capital Medical University, from January 1, 2004, to May 1, 2022. Three senior pathologists performed the diagnostic evaluation based on the criteria outlined in the 5th edition of the 2019 WHO Classification of Tumours of the Digestive System. Where discrepancies in pathological grading occurred, a consensus was reached through consultation and discussion among the three pathologists. The clinicopathological characteristics of all cases were summarised and analysed.

The need for informed consent was waived owing to the retrospective nature of this study, which only involved an analysis of previously collected data and utilised anonymised data obtained from existing records. Nonetheless, strict confidentiality and adherence to ethical guidelines regarding patient privacy were ensured.

2.2 Immunohistochemistry and quantitative real-time polymerase chain reaction

Immunohistochemical staining and analysis were conducted on paraffin-embedded samples from 38 HG-NEN cases. The primary antibodies used in this study were chromogranin A (CHGA), synaptophysin (SYP), CD56, death domain associated protein (DAXX), ATRX chromatin remodeler (ATRX), TP53, RB, insulin-related protein 1 (INSM1), SSTR2, recombinant human CLU, and MKI67. The cell membrane or cytoplasmic markers were positively stained for SYP, CHGA, CD56, and CLU, whereas nuclear staining was observed for DAXX, ATRX, TP53, RB, INSM1, and MKI67. The SSTR2 expression was interpretated and scored using the following scale, based on the HER2 criteria for gastric cancer, as recommended by the Chinese consensus on the pathological diagnosis of gastrointestinal and pancreatic neuroendocrine neoplasms in 2020 (17): 0, no discoloration; 1+, weak membrane staining in at least 10% of tumour cells; 2+, weak to moderately intense membrane staining in at least 10% of tumour cells; and 3+, strong membrane staining in at least 10% of tumour cells. Because *TP53* expression in GEP-HG-NENs lacks a standardised evaluation method, in this study, mutations were identified based on moderate–intensity positivity (>30%) or no staining (18, 19). The scoring criteria for the remaining immunohistochemical markers were as follows: >10%, negative; 10% to 25%, 1+; 25% to 50%, 2+; <50%, 3+. *KRAS* and *BRAF V600E* mutations were screened in 34 cases of GEP-HG-NENs, including 1 and 3 cases of NET G3 and SCNEC 4, respectively that predated 2012 and were excluded because of specimen size and storage period considerations.

2.3 Statistical analysis

Data were analysed using descriptive statistics, and differences in frequencies were assessed using the chi-squared (χ^2) test or Fisher's exact test. Logistic regression was used to assess categorical variables in both the multivariate and univariate analyses. Overall survival was assessed from the date of diagnosis to the date of death or last follow-up. Survival curves were drawn using the Kaplan–Meier method, and differences between groups were assessed using the log-rank test. Univariate and multivariate Cox proportional hazards regression analyses were conducted to assess the prognostic significance of various clinical and histopathological characteristics. Data analysis was performed using SPSS software version 26.0 (IBM Corp., Armonk, NY, USA). All tests were two-sided, and statistical significance was defined as $p < 0.05$.

3 Results

3.1 Clinicopathological features

A total of 181 patients with GEP-NENs were treated at our hospital from January 1, 2004, to May 1, 2022. Overall, 38 cases (21.0%) were confirmed to be HG-NENs. Among these, 9 and 29 cases were diagnosed as NET G3 (23.7%) and NECs (76.3%), respectively, including 11 and 18 LCNEC (37.9% of NECs) and SCNEC (62.1% of NECs) cases, respectively (Figure 1A). Of the 38 patients with HG-NENs, 22 (57.9%) and 16 (42.1%) were male and female (age range: 49–86 years, average age: 66 years). Specifically, nine NET G3 cases involved seven male and two female patients, with an average age of 72.5 years.

Among 29 cases of NECs, 11 were LCNEC cases (involving five and six male and female patients, respectively; median age: 69 years) with a median age of 69 years, whereas 18 were SCNEC cases (involving nine male and female patients each; average age: 67.5 years). The specimen types collected were needle biopsy and surgical resection specimens in 31 cases (81.6%) and specimens in 7 cases (18.4%). Tumours originated in different locations—specifically, in the stomach, colorectum, oesophagus, pancreas and ampulla, and gallbladder in 13 (34.2%), 10 (26.3%), 7 (18.4%), 3 (7.9%), and 2 (5.2%) cases, respectively, and in the duodenum, ileum, and liver in 1

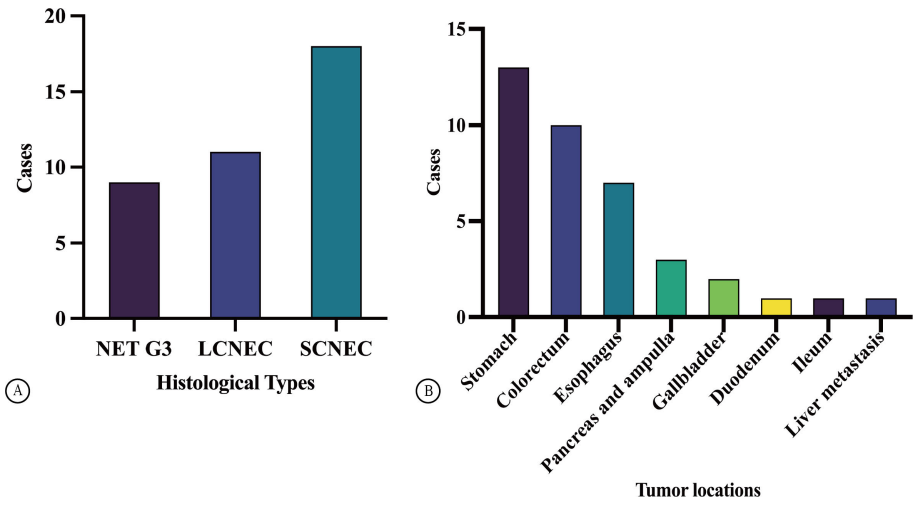

FIGURE 1
Case distribution of GEP HG NENs **(A)**. The distribution of tumor locations in GEP HG NENs **(B)**.

case each (2.6% each, Figure 1B). There was a higher proportion of male than female patients with HG-NENs (male-to-female ratio, 1.4:1); among the 9 and 29 cases of NET G3 and NECS, the male-to-female ratio was 3.5:1 and 0.9:1, respectively. Most tumours were located in the stomach (13/38), followed by the colorectum and oesophagus. Interestingly, four cases (44.4%) of stomach-originating HG-NENs were classified as NET G3.

Nerve invasion was observed in three cases (42.9%) among all those involving patients who had surgically resected specimens, which consisted of one and two cases of LCNEC and SCNEC, respectively. In addition, intravascular tumour thrombus and SCNEC were observed in three (42.9%) and five (71.4%), cases, respectively, whereas surrounding lymph node metastasis occurred in two LCNEC cases and three SCNEC cases. The most common distant metastatic sites were the liver, lungs, and peritoneum during the follow-up period (Table 1). No significant correlation ($p > 0.05$) was found between the patients' sex, age, smoking history, drinking history, MKI67 index, and histological type.

3.2 Pathological features

NET G3 appeared uniform in size with a round or oval shape and exhibited mild-to-moderate atypia. The cytoplasm appeared fine or finely granular, basophilic or dichromatic, whereas the nuclear chromatin was coarse and resembled pepper–salt-like granules. Mitosis was rare, and focal necrosis resembled a comedo (Figure 2A). In contrast, the NECs demonstrated diffuse lamellar growth, irregular tumour cell arrangement, lack of organ structure, significant cellular atypia, prominent mitotic activity, and extensive areas of necrosis. LCNEC had a relatively abundant cytoplasm, obvious nuclear atypia, and large prominent nucleoli (Figure 2B). In contrast, SCNEC exhibited sparse cytoplasm, high nucleus-to-cytoplasm ratio, and hyperchromatic naked nuclei with inconspicuous nucleoli (Figure 2C).

TABLE 1 Metastasis between different histological types.

Metastatic sites	NET G3 (%)	LCNEC (%)	SCNEC (%)
liver	2 (22.2)	4 (36.4)	6 (33.3)
lungs	1 (11.1)	0 (0)	3 (16.7)
peritoneal metastasis	1 (11.1)	1 (9.1)	0 (0)

3.3 Analysis of immunohistochemical results

The immunohistochemical analysis indicated that 47.4% of HG-NENs expressed SSTR2 at a level above 1+ based on the HER2 criteria for gastric cancer (Table 2). Furthermore, eight of the nine NET G3 cases expressed SSTR2, mainly at scores of 2+ and 3+. Additionally, weakly positive SSTR2 expression was detected in four and six LCNEC and SCNEC cases, respectively, in areas with better histological differentiation than others. Moreover, a statistically significant difference in SSTR2 positivity was observed between NECs and NET G3 ($p = 0.012$) (Figures 2D–F).

We found that the total positivity rate for *INSM1* expression was 86.8% (33/38), with 77.8% (7/9) and 89.7% (26/29) in the NET G3 and NEC groups, respectively (Figures 2G–I). CLU was expressed in 50.0% (19/38) of the cases, with 100% and 34.5% positivity in the NET G3 and NEC groups, respectively (Figures 2J–L). *TP53* mutation was present in 81.6% (31/38) of cases, with mutation rates of 44.4% (4/9) and 82.8% (24/29) in the NET G3 and NEC groups, respectively (Figures 2M–O). RB expression was loss in 11.1% (1/9) and 55.2% (16/29) of the cells in the NET G3 and NEC groups, respectively (Figures 2P–R). Specifically, the expression rates of SYP, CHGA, and CD56 were 92.1%, 57.9%, and 60.5%, respectively.

The MKI67 proliferative index varied greatly between the NET G3 and NECs groups, with a median of approximately 40% and 70% and range of 25%–70% and 50%–90%, respectively. The

10.3389/fonc.2024.1399079

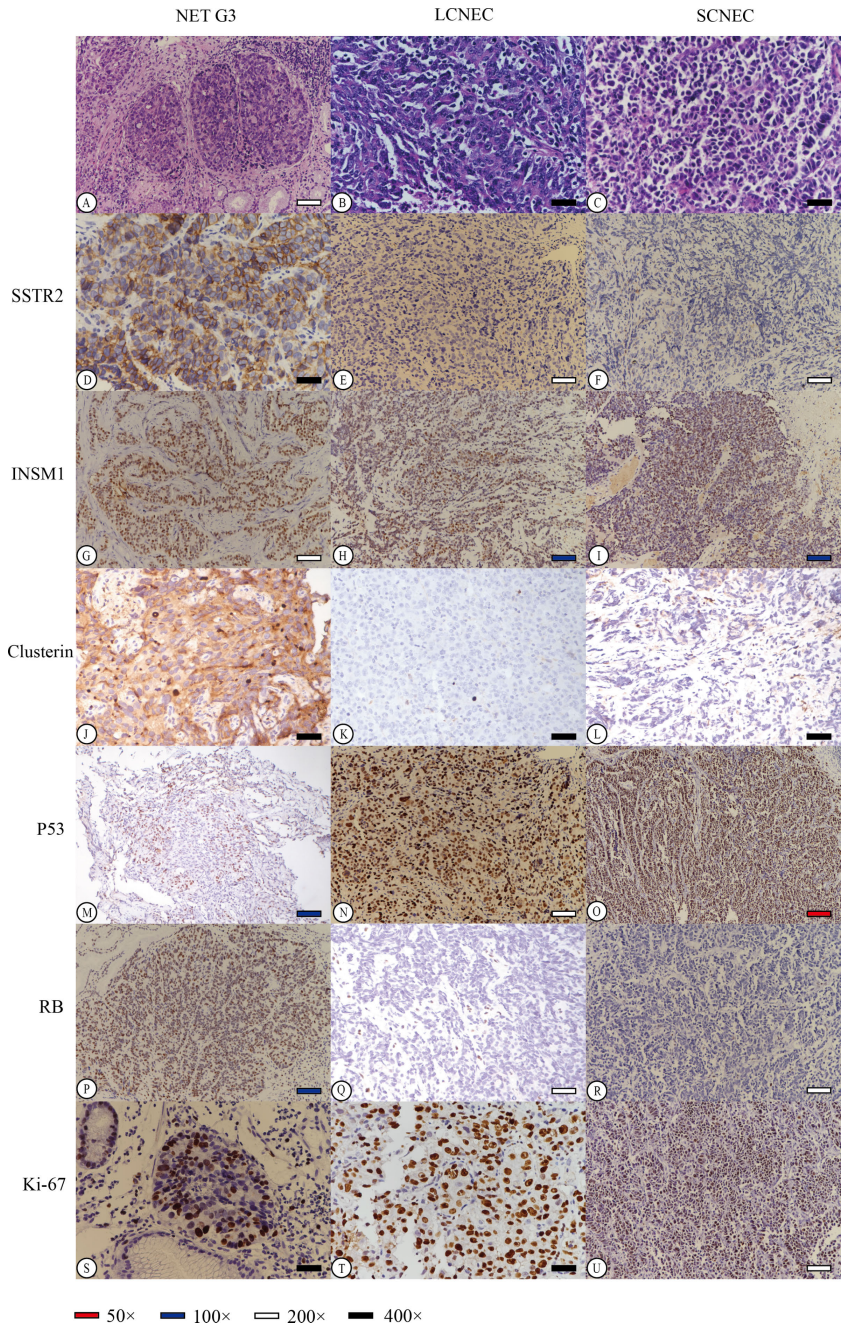

FIGURE 2
Hematoxylin-Eosin (HE) staining of different neuroendocrine tumor subtypes revealed distinct characteristics. NET G3 **(A)** displayed well-differentiated tumor cells with uniform morphology and slightly eosinophilic cytoplasm. LCNEC **(B)** exhibited fine cytoplasm and prominent hyperchromatic large nucleoli, while SCNEC **(C)** showed sparse cytoplasm, inconspicuous cell nucleus, and active caryomitosis. We carefully selected representative stained regions from various histological subtypes to effectively demonstrate the staining patterns of each immunohistochemical marker (D-U). Diffuse strong membrane staining of SSTR2 was observed in NET G3, with a score of 4 **(D)**. Conversely, in LCNEC and SCNEC, tumor cells showed no expression of SSTR2, resulting in a score of 0 **(E, F)**. Furthermore, all tumor cells tested positive for INSM1 in NET G3, LCNEC, or SCNEC **(G–I)**. Clusterin staining in tumor cells of NET G3 exhibited strong positive staining in both the cell membrane and cytoplasm, with a score of 3+ **(J)**. However, LCNEC and SCNEC showed negative expression of clusterin in tumor cells, with a score of 0 **(K, L)**. Additionally, P53 expression in tumor cells of NET G3 was wild-type **(M)**, while LCNEC and SCNEC displayed mutant p53 expression (missense mutation) **(N, O)**. RB protein expression was positive in NET G3, scoring 3+ **(P)**, but was lost in tumor cells of LCNEC and SCNEC, scoring 0 **(Q, R)**. The Ki-67 index in tumor cells was approximately 35% in NET G3 **(S)**, 85% in LCNEC **(T)**, and 90% in SCNEC **(U)**.

correlation analysis showed that an MKI67 index between 20% and 55% was more likely to indicate NET G3. A 55% cutoff value was used for the MKI67 index; 11 cases fell between 20% and 55%, whereas 27 cases were at ≥55%, including 26 cases of NECs (Figures 2S–U). *DAXX* and *ATRX* gene expression was positive in 60.5% (23/38) and 84.2% (32/38) of the cases, respectively. SSTR2, RB, TP53, CLU, and *MKI67* expression levels were significantly different between the NET G3 and NEC groups of HG-NENs ($p <$

0.05, Table 2), while other indicators did not show statistically significant differences.

3.4 qRT-PCR of *KRAS* and *BRAF V600E*

Among the 34 HG-NEN cases, 11 (32.4%) harboured the *BRAF V600E* mutation. This included five cases of NET G3 (62.5%) and six cases of NECs (23.1%), which consisted of one and five cases of SCNEC (6.7%) and LCNEC (45.5%), respectively. A significant difference in *BRAF V600E* mutation was observed between NET G3 and SCNEC ($p = 0.0086$) (Figure 3A). Mutation rates varied across primary sites: 60.0% in the colon (3/5), 20.0% in the rectum (1/5), 41.7% in the stomach (5/12), and 33.3% in the oesophagus (2/6). *KRAS* mutations were observed in 8 of the 34 HG-NEN cases (23.5%). This included one case of NET G3 (12.5%) and seven of

TABLE 2 Correlation analysis between various immunohistochemical indexes and histological types.

	NET G3(%)	LCNEC(%)	SCNEC(%)	P value (<0.05)	NET G3(%)	NEC(%)	P value (<0.05)
SSTR2							
0	1 (11.1)	7 (63.6)	12 (66.7)	0.090	1 (11.1)	19 (65.5)	0.012*
1+	2 (22.2)	1 (9.1)	3 (16.7)		2 (22.2)	4 (13.8)	
2+	3 (33.3)	2 (18.2)	2 (11.1)		3 (33.3)	4 (13.8)	
3+	3 (33.3)	1 (9.1)	1 (5.6)		3 (33.3)	2 (6.9)	
Rb							
0	1 (11.1)	3 (27.4)	12 (66.7)	0.001*	1 (11.1)	15 (51.7)	0.110
1+	3 (33.3)	0 (0)	5 (27.8)		3 (33.3)	5 (17.2)	
2+	4 (44.4)	6 (54.4)	1 (5.6)		4 (44.4)	7 (24.1)	
3+	1 (11.1)	2 (18.2)	0 (0)		1 (11.1)	2 (6.9)	
P53							
Wild-type form	5 (55.6)	1 (9.1)	4 (22.2)	0.076	5 (55.6)	5 (17.2)	0.036*
Mutation	4 (44.4)	10 (90.9)	14 (77.8)		4 (44.4)	24 (82.8)	
Ki-67 index							
<55	8 (88.9)	2 (18.2)	1 (5.6)	0.000026*	7 (87.5)	3 (14.3.2)	0.000028*
≥55	1 (11.1)	9 (81.8)	17 (94.4)		1 (12.5)	18 (85.7)	
ATRX							
0	1 (11.1)	2 (18.2)	3 (16.7)	0.484	1 (11.1)	5 (17.2)	0.219
1+	3 (33.3)	1 (9.1)	2 (11.1)		3 (33.3)	3 (10.3)	
2+	3 (33.3)	1 (9.1)	5 (27.8)		3 (33.3)	6 (20.7)	
3+	2 (22.2)	7 (63.6)	8 (44.4)		2 (22.2)	15 (51.7)	
Clusterin							
0	0 (0)	7 (63.6)	12 (66.7)	0.001*	0 (0)	19 (65.5)	0.0001*
1+	1 (11.2)	2 (18.2)	2 (11.1)		1 (11.2)	4 (13.8)	
2+	4 (44.4)	1 (9.1)	4 (22.2)		4 (44.4)	5 (17.2)	
3+	4 (44.4)	1 (9.1)	0 (0)		4 (44.4)	1 (3.4)	
DAXX							
0	5 (55.6)	4 (36.4)	6 (33.3)	0.918	5 (55.6)	10 (34.5)	0.634
1+	3 (33.3)	4 (36.4)	5 (27.8)		3 (33.3)	9 (31.1)	
2+	1 (11.1)	2 (18.2)	5 (27.8)		1 (11.1)	7 (24.1)	
3+	0 (0)	1 (9.1)	2 (11.1)		0 (0)	3 (10.3)	

*: $p < 0.05$, indicating a statistically significant difference.

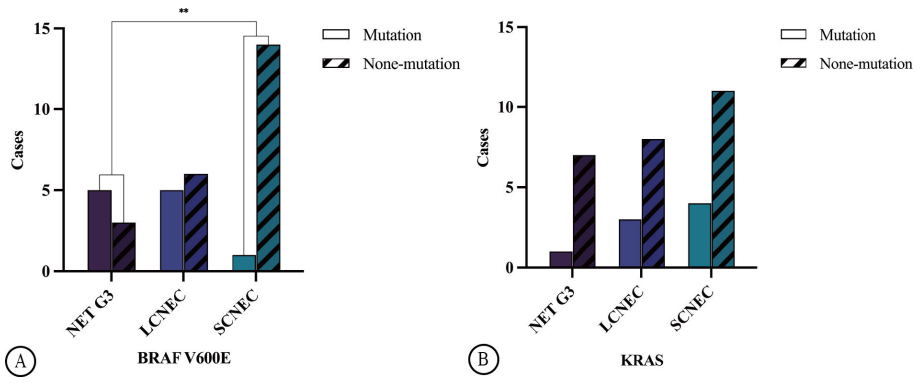

FIGURE 3
Illustrates the distribution of BRAF V600E mutation in GEP HG-NENs. A statistically significant disparity (**p=0.0086) was observed between NET G3 and SCNEC **(A)**. The distribution of KRAS mutation in GEP HG-NENs is also shown in the figure **(B)**.

NECs (26.9%), which comprised three and four cases of LCNEC (27.3%) and SCNEC (26.7%), respectively (Figure 3B).

There was no significant difference in *KRAS* mutation frequency between the different histological types (p = 0.763), while the mutation rate varied across primary sites, with 40.0% and 25% in the colorectum (4/10) and stomach (3/12), respectively. No *KRAS* mutations were detected in the primary oesophageal cancer cases. Loss of RB protein expression was identified in 16 cases, with one case involving NET G3 while the remaining 15 involved NECs and consisted of 3 and 12 cases of LCNEC and SCNEC, respectively. Statistically significant differences were observed in RB protein expression among the NET G3, LCNEC, and SCNEC groups (p = 0.001). Further comparison revealed that SCNEC showed higher susceptibility to the loss of RB protein expression than NET G3 and LCNEC did.

3.5 Prognostic analysis

Complete follow-up data was obtained for 35 of the 38 patients with HG-NENs, whereas two and one patient with NECs and NET G3, respectively, were lost to follow-up. The median follow-up time was 12 (range: 3–86) months. The median survival time (MST) for the NET G3 and NEC groups was 25 (range: 5–80, average: 32) and 11 (range: 3–86, average 16) months, respectively. There were 23 deaths (60.5%), consisting of 7, 11, and 5 in the LCNEC (63.6%), SCNEC (61.1%), and NET G3 (55.6%) groups, respectively. Organ failure due to liver and lung metastases or multiple systemic metastases or a combination of these was the primary cause of death (Table 1).

The Kaplan–Meier survival curve for CLU (p = 0.0081, Figure 4A) and TP53 (p = 0.041, Figure 4B) indicated statistically significant differences between the two different groups. Univariate and multivariate Cox regression analyses showed that the expression of the immunohistochemical index CLU (p = 0.014, Figure 5 and Table 3) significantly affected the patients' survival time and outcomes.

In this study, an MKI67 proliferation index of 55% was used as the cutoff for analysing different factors. The survival analysis did not show a statistically significant difference (p = 0.201, Figure 4C). Other factors such as sex, age, and history of smoking and drinking did not show a statistically significant correlation with survival time (all p > 0.05; Figures 4D–G). The receiver operating characteristic (ROC) curve analysis indicated that the positive expression of the immunohistochemical markers CLU, SSTR2, and RB has significant implications for diagnosing NET G3 (Figure 4H).

4 Discussion

In this study we investigated various immunohistochemical and molecular biological markers and their association with clinicopathological features in GEP-HG-NENs. The fifth edition of the WHO Classification of Tumours of the Digestive System places greater focus on precisely categorising NET G3 and NECs according to the varying levels of differentiation seen in pathological tissue morphology. However, this approach may result in discrepancies among pathologists. Grossly, NET G3 tumours typically present as a solid nodule with a raised or polyp-like appearance, while some show ulceration, medium-hard texture, and greyish-white or greyish-yellow surface. It exhibits outwardly expanding growth with a distinct demarcation.

In contrast, NECs often display an irregular ulcer or cauliflower-like bulge, are frequently accompanied by haemorrhage or necrosis, and have a brittle texture. When these tumours occur in the colorectum, they tend to grow around the circumference, leading to luminal narrowing. Some cystic lesions may have poorly defined borders with the surrounding tissues. Microscopically, NET G3 resembles a well-differentiated NENs shows organ-like structures or growth in trabecular, ribbon-, and gland-like patterns. Certain cells form pseudo-rosettes. In our study, the slides were reviewed by a minimum of three senior pathologists and reclassified according to the most recent classification criteria.

We found a higher prevalence of HG-NENs in male patients than in female patients, with most tumours being located in the stomach, followed by the colorectum and oesophagus. Interestingly, the classification of all four stomach-originating HG-NEN cases as

10.3389/fonc.2024.1399079

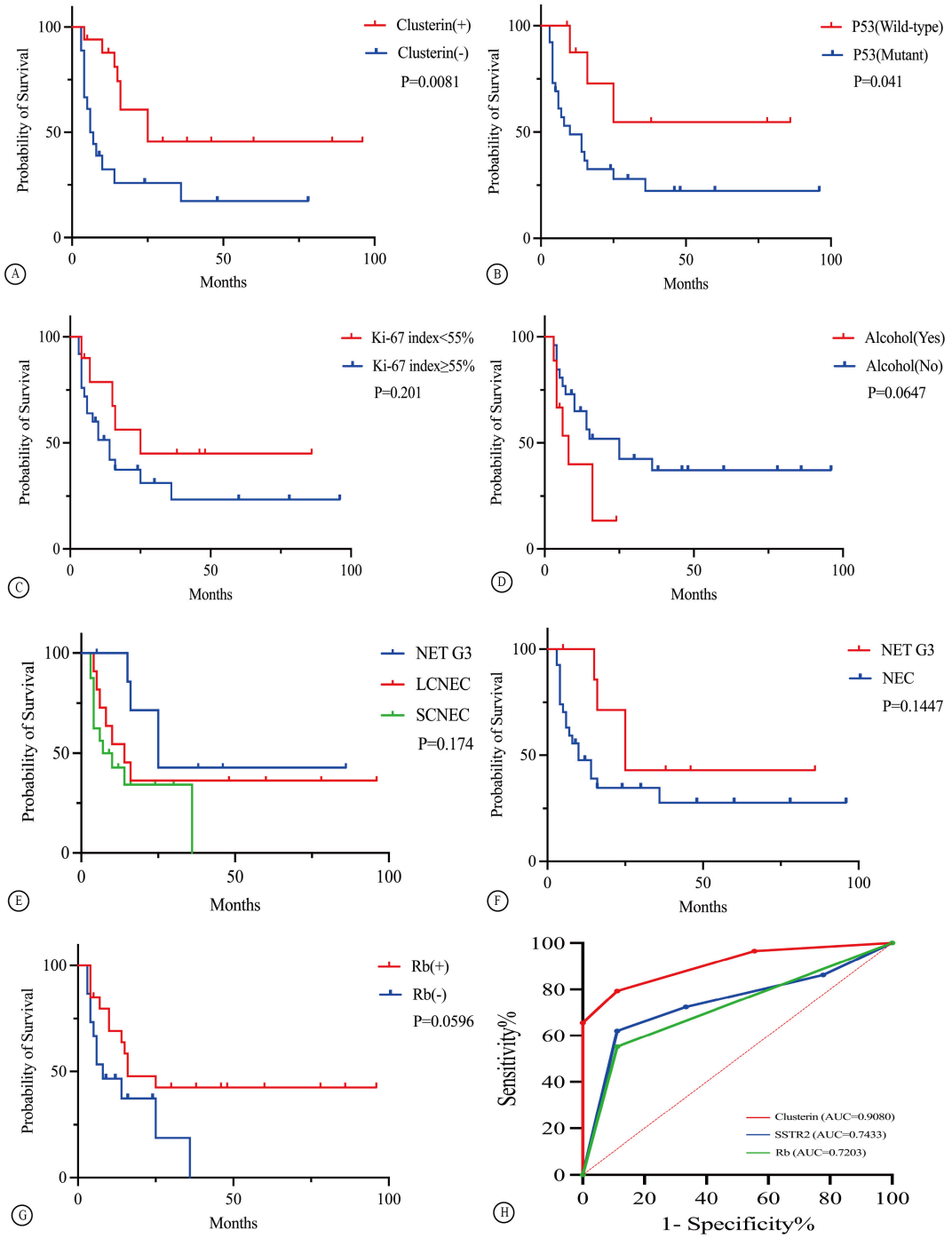

FIGURE 4
Overall survival of patients with GEP HG-NENs of various clinical and histopathological characteristics **(A–G)**. The ROC curves for the Rb, Clusterin, and SSTR2 markers **(H)**.

NET G3 differed slightly from those previously reported, suggesting that NET G3 primarily occurs in the pancreas (11). This discrepancy may be attributed to the adoption of new classification standards and the variations in specimen types across different research institutions. Busico et al. (2) further classified HG-NENs into three subgroups (namely, NET G3, NECs <55%, and NECs ≥55%) and reported notable variations in survival rates across these subgroups. However, in our study, the Cox regression analysis indicated that patient survival duration was not significantly correlated with an MKI67 proliferative index of 55%.

In this study, we also found that GEP-HG-NENs were positive for immunohistochemical markers with varying degrees of diagnostic significance. The histological types were further classified into NET G3, LCNEC, and SCNEC, with distinct differences observed in immunohistochemical indicators such as SSTR2, TP53, RB, and CLU. The SSTR2 expression in gastric cancer

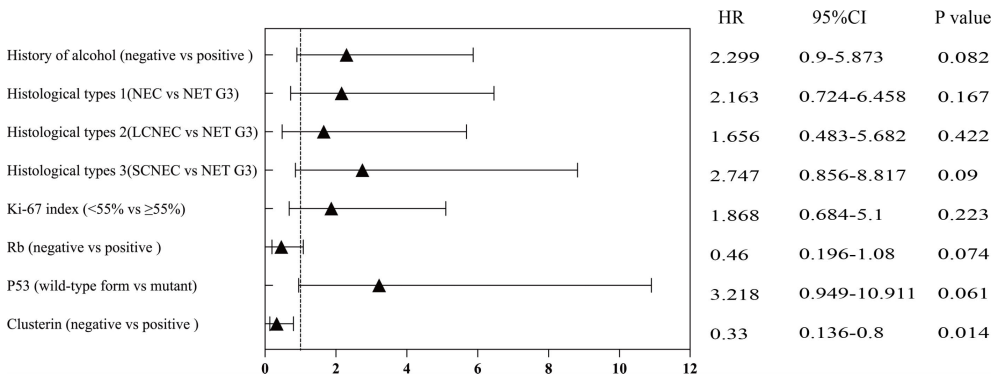

FIGURE 5
Univariate analysis (based on selected variables) of overall survival in various subgroups.

was interpreted based on the HER2 interpretation criteria outlined in the 2020 Chinese consensus on the pathological diagnosis of gastrointestinal and pancreatic neuroendocrine neoplasms. In our previous study, Fisher's test revealed a statistically significant difference among NET G3, LCNEC, and SCNEC when SSTR2 expression was negative; however, after including nine new cases, no significant difference was observed among the three groups (20).

In this study, the RB, ATRX, DAXX, and CLU levels were interpreted based on the SSTR2 interpretation standard. Previous studies reported high CLU expression in LG-NENs (10), which is similar to our present finding in which the NET G3 group exhibited a significantly higher CLU expression and ≥2+ frequency rate than the NEC group did. Notably, tumours originating from the midgut were not included in the cases studied, suggesting that the CLU expression level was potentially lower in NET G3 from the midgut than in those originating elsewhere (21). Strong CLU expression has been hypothesised to be probably more indicative of NET G3 in cases where cell morphology shows a deceptive divergence.

Cox regression analysis indicated that patients with positive CLU had a 0.33-fold lower risk of mortality than those with negative

TABLE 3 Univariate and multivariable analysis (based on selected variables) of overall survival.

	HR	95%CI	*p*-value
Univariate analysis			
History of alcohol (negative vs positive)	2.299	0.9-5.873	0.082
Histological types 1(NEC vs NET G3)	2.163	0.724-6.458	0.167
Histological types 2(LCNEC vs NET G3)	1.656	0.483-5.682	0.422
Histological types 3(SCNEC vs NET G3)	2.747	0.856-8.817	0.09
Ki-67 index (<55% vs ≥55%)	1.868	0.684-5.1	0.223
Rb (negative vs positive)	0.46	0.196-1.08	0.074
P53 (wild-type form vs mutant)	3.218	0.949-10.911	0.061
Clusterin (negative vs positive)	0.33	0.136-0.8	0.014*
Multivariate analysis			
Clusterin (negative vs positive)	0.33	0.136-0.8	0.014*

*: $p < 0.05$, indicating a statistically significant difference.

expression do. Consequently, the use of the immunohistochemical marker CLU as a prognostic indicator of survival in patients with GEP-HG-NENs has significant clinical implications. Furthermore, the potential use of the CLU inhibitor custirsen (OGX-111) in GEP-HG-NENs has been proposed to improve the survival prognosis of GEP-HG-NENs (22–24). We found that the prevalence of *TP53* mutation was significantly higher in NECs than it was in NET G3. However, there were no significant difference in P53 mutation between LCNEC and SCNEC.

Among the four cases of *TP53* mutation in NET G3, two were located in the oesophagus and one each in the colorectum and gastric body. These patients showed metastases to the liver or lungs during the later stages of disease progression. This suggests that the *TP53* mutation may be associated with the aggressive behaviour of HG-NENs, which aligns with previous findings (25). Previous studies have proposed that combined immunohistochemical staining of SSTR2, TP53, and RB could facilitate in distinguishing HG-NENs that are morphologically challenging to differentiate (8).

Theoretically, high and robust SSTR2 expression in combination with wild-type TP53 and RB protein expression, is more indicative of NET G3 than it is of NECs, whereas the opposite expression pattern tends to indicate NECs. Our study revealed a high level of SSTR2 expression in the NET G3 group and a higher prevalence of *TP53* missense mutation in the NEC group than in the NET G3, which is consistent with previous research findings (19). Nevertheless, a substantial amount of clinical sample data would be necessary to determine the correlation between these target immunohistochemical markers and their prognostic significance in GEP-HG-NENs.

Recent studies have reported that approximately 20.8% and 9.9% of patients with colorectal NECs and GEP-NENs, respectively, harbour the *BRAF V600E* mutation (26, 27). Targeting the *BRAF* oncogene may serve as a promising therapeutic approach for individuals with *BRAF*-mutated colorectal NECs. In our study, the *BRAF V600E* mutation was identified in 32.4% of the HG-NEN cases. Interestingly, the colon exhibited the highest BRAF mutation rate among the various primary tumour sites, which is consistent with previous research findings (26).

Significant differences were observed between NET G3 and SCNEC in our study, and the mutation rate of NET G3 was higher

than that of NECs, which contradicts the existing literature reports (27). This discrepancy could be due to the small sample size and variations in the qRT-PCR detection results from the different primary tumour sites. Therefore, further experimental validation using a larger sample size is warranted. The implications of *BRAF* mutation detection vary across different histological types and primary tumour sites, which highlights the need for a comprehensive investigation with a larger sample size to clarify the correlation between these factors.

A recent study found *KRAS* mutations in 31% and 25% of NECs from the colon and rectum, respectively, and identified *KRAS* mutations in three cases of primary gastric NECs but not in NET G3 (26). In our study of 34 HG-NEN cases, although *KRAS* gene mutations were identified NET G3 and NEC cases, no significant differences were observed among different histological types. The rate of *KRAS* mutations in the colorectum was notably higher than that in the stomach and other sites, which is consistent with previous findings (28).

Among the eight cases of NET G3, *KRAS* mutation was detected in one, which involved a 61-year-old male patient with a history of smoking and drinking. The patient presented with upper gastrointestinal bleeding and elevated blood alpha fetoprotein (AFP) and CEA cell adhesion molecule (CEA) levels and survived for only 16 months. These findings may be useful in developing clinical treatment strategies, suggesting that a *KRAS* mutation in NET G3 may lead to poor survival outcomes and rapid disease progression. Detecting *KRAS* mutations is essential for guiding treatment, but further analyses of larger sample sizes are needed to confirm its correlation with specific types of GEP-HG-NENs.

Nevertheless, the current study has certain limitations. Owing to the rarity of GEP-HG-NENs, the number of patients included in this study was relatively small, and the retrospective study spanned 18 years. Although statistical errors were minimised and patient survival was assessed using Fisher's exact test and the Kaplan–Meier method, which are suitable for a small sample size, these factors may still limit the statistical power and generalisability to larger populations. The extended time frame of the collected cases introduced some heterogeneity within the patient cohort, making it more challenging to draw definitive conclusions. This heterogeneity included variations in the tumour type, clinical staging, and treatment approaches. Additionally, further validation of *KRAS* and *BRAF V600E* mutations in these tumours requires larger-scale sequencing data. In future research, we plan to collect more clinical samples to arrive at more precise conclusions.

5 Conclusion

The recent update on the GEP-HG-NEN standard highlights significant differences in pathogenesis, pathological diagnosis, clinical treatment, and prognosis between NET G3 and NECs. Therefore, clinical pathologists essentially must have a comprehensive understanding of the histological and cytological morphological characteristics of tumours to accurately classify HG-NENs. The use of valuable immunohistochemical and molecular pathological indicators in combination with the MKI67 proliferation index is essential for comprehensive analysis when indicated. Our research findings can aid clinical pathologists in distinguishing NET G3 from NECs; however, there are still some limitations. We will persist in gathering relevant cases to broaden the sample size and achieve more dependable results. Enhancing the comprehension of GEP-HG-NENs will facilitate not only the development of standardised and rational treatment plans in clinical practice but also the implementation of appropriate prognostic management.

Data availability statement

The original contributions presented in the study are included in the article/supplementary material. Further inquiries can be directed to the corresponding author.

Ethics statement

The studies involving humans were approved by IRB of Beijing Luhe Hospital, Capital Medical University. The studies were conducted in accordance with the local legislation and institutional requirements. The participants provided their written informed consent to participate in this study. Written informed consent was obtained from the individual(s) for the publication of any potentially identifiable images or data included in this article.

Author contributions

NL: Conceptualization, Data curation, Formal analysis, Investigation, Methodology, Validation, Writing – original draft. YH: Conceptualization, Project administration, Writing – review & editing. LW: Formal analysis, Investigation, Methodology, Writing – review & editing. JA: Investigation, Writing – review & editing.

Funding

The author(s) declare financial support was received for the research, authorship, and/or publication of this article. Beijing Tongzhou District Science and Technology Committee Project Fund (KJ2024CX027).

Conflict of interest

The authors declare that the research was conducted in the absence of any commercial or financial relationships that could be construed as a potential conflict of interest.

Publisher's note

All claims expressed in this article are solely those of the authors and do not necessarily represent those of their affiliated organizations, or those of the publisher, the editors and the reviewers. Any product that may be evaluated in this article, or claim that may be made by its manufacturer, is not guaranteed or endorsed by the publisher.

References

1. Nagtegaal ID, Odze RD, Klimstra D, Paradis V, Rugge M, Schirmacher P, et al. The 2019 WHO classification of tumours of the digestive system. *Histopathology*. (2020) 76:182–8. doi: 10.1111/his.13975

2. Busico A, Maisonneuve P, Prinzi N, Pusceddu S, Centonze G, Garzone G, et al. Gastroenteropancreatic high-grade neuroendocrine neoplasms: histology and molecular analysis, two sides of the same coin. *Neuroendocrinology*. (2020) 110:616–29. doi: 10.1159/000503722

3. Dasari A, Mehta K, Byers LA, Sorbye H, Yao JC. Comparative study of lung and extrapulmonary poorly differentiated neuroendocrine carcinomas: a SEER database analysis of 162,983 cases. *Cancer*. (2018) 124:807–15. doi: 10.1002/cncr.31124

4. Dasari A, Shen C, Halperin D, Zhao B, Zhou S, Xu Y, et al. Trends in the incidence, prevalence, and survival outcomes in patients with neuroendocrine tumors in the United States. *JAMA Oncol*. (2017) 3:1335–42. doi: 10.1001/jamaoncol.2017.0589

5. Heetfeld M, Chougnet CN, Olsen IH, Rinke A, Borbath I, Crespo G, et al. Characteristics and treatment of patients with G3 gastroenteropancreatic neuroendocrine neoplasms. *Endocr Relat Cancer*. (2015) 22:657–64. doi: 10.1530/ERC-15-0119

6. Wang ZJ, An K, Li R, Shen W, Bao MD, Tao JH, et al. Analysis of 72 patients with colorectal high-grade neuroendocrine neoplasms from three Chinese hospitals. *World J Gastroenterol*. (2019) 25:5197–209. doi: 10.3748/wjg.v25.i34.5197

7. Huang D, Tan C, Weng WW, Ni SJ, Wang L, Sheng WQ. Clinicopathological features and outcome of gastroenteropancreatic high-grade (WHO G3) neuroendocrine tumors: a study of 60 cases. *Zhonghua Bing Li Xue Za Zhi*. (2020) 49:12–6. doi: 10.3760/cma.j.issn.0529-5807.2020.01.003

8. Konukiewitz B, Schlitter AM, Jesinghaus M, Pfister D, Steiger K, Segler A, et al. Somatostatin receptor expression related to TP53 and RB1 alterations in pancreatic and extrapancreatic neuroendocrine neoplasms with a Ki67-index above 20. *Mod Pathol*. (2017) 30:587–98. doi: 10.1038/modpathol.2016.217

9. Yachida S, Vakiani E, White CM, Zhong Y, Saunders T, Morgan R, et al. Small cell and large cell neuroendocrine carcinomas of the pancreas are genetically similar and distinct from well-differentiated pancreatic neuroendocrine tumors. *Am J Surg Pathol*. (2012) 36:173–84. doi: 10.1097/PAS.0b013e3182417d36

10. Bellizzi AM. Immunohistochemistry in the diagnosis and classification of neuroendocrine neoplasms: what can brown do for you. *Hum Pathol*. (2020) 96:8–33. doi: 10.1016/j.humpath.2019.12.002

11. Pellat A, Coriat R. Well differentiated grade 3 neuroendocrine tumors of the digestive tract: a narrative review. *J Clin Med*. (2020) 9:1677. doi: 10.3390/jcm9061677

12. Scarpa A, Chang DK, Nones K, Corbo V, Patch AM, Bailey P, et al. Whole-genome landscape of pancreatic neuroendocrine tumours. *Nature*. (2017) 543:65–71. doi: 10.1038/nature21063

13. Park HY, Kwon MJ, Kang HS, Kim YJ, Kim NY, Kim MJ, et al. Targeted next-generation sequencing of well-differentiated rectal, gastric, and appendiceal neuroendocrine tumors to identify potential targets. *Hum Pathol*. (2019) 87:83–94. doi: 10.1016/j.humpath.2019.02.007

14. Uccella S, La Rosa S. Looking into digestive mixed neuroendocrine - nonneuroendocrine neoplasms: subtypes, prognosis, and predictive factors. *Histopathology*. (2020) 77:700–17. doi: 10.1111/his.14178

15. Mafficini A, Scarpa A. Genetics and epigenetics of gastroenteropancreatic neuroendocrine neoplasms. *Endocr Rev*. (2019) 40:506–36. doi: 10.1210/er.2018-00160

16. Konukiewitz B, Jesinghaus M, Steiger K, Schlitter AM, Kasajima A, Sipos B, et al. Pancreatic neuroendocrine carcinomas reveal a closer relationship to ductal adenocarcinomas than to neuroendocrine tumors G3. *Hum Pathol*. (2018) 77:70–9. doi: 10.1016/j.humpath.2018.03.018

17. Division of Digestive Diseases, Chinese Society of Pathology and 2020 Chinese Consensus on the Pathological Diagnosis of Gastrointestinal and Pancreatic Neuroendocrine Neoplasms Experts Group. Chinese consensus on the pathological diagnosis of gastrointestinal and pancreatic neuroendocrine neoplasms (2020). *Zhonghua Bing Li Xue Za Zhi*. (2021) 50:14–20. doi: 10.3760/cma.j.cn112151-20200805-00623

18. Nielsen K, Binderup T, Langer SW, Kjaer A, Knigge P, Grøndahl V, et al. P53, Somatostatin receptor 2a and chromogranin A immunostaining as prognostic markers in high grade gastroenteropancreatic neuroendocrine neoplasms. *BMC Cancer*. (2020) 20:27. doi: 10.1186/s12885-019-6498-z

19. Ali AS, Grönberg M, Federspiel B, Scoazec JY, Hjortland GO, Grønbæk H, et al. Expression of p53 protein in high-grade gastroenteropancreatic neuroendocrine carcinoma. *PloS One*. (2017) 12:e0187667. doi: 10.1371/journal.pone.0187667

20. Li N, Wu LG, Hu YP. Gastroenteropancreatic high grade neuroendocrine neoplasms: a clinicopathological analysis of 29 cases. *Zhonghua Bing Li Xue Za Zhi*. (2022) 51:1036–8. doi: 10.3760/cma.j.cn112151-20220315-00184

21. Czeczok TW, Stashek KM, Maxwell JE, O'Dorisio TM, Howe JR, Hornick JL, et al. Clusterin in neuroendocrine epithelial neoplasms: absence of expression in a well-differentiated tumor suggests a jejunoileal origin. *Appl Immunohistochem Mol Morphol*. (2018) 26:94–100. doi: 10.1097/PAI.0000000000000563

22. Koltai T. Clusterin: a key player in cancer chemoresistance and its inhibition. *Onco Targets Ther*. (2014) 7:447–56. doi: 10.2147/OTT.S58622

23. Al-Asaaed S, Winquist E. Custirsen (OGX-011): clusterin inhibitor in metastatic prostate cancer. *Curr Oncol Rep*. (2013) 15:113–8. doi: 10.1007/s11912-012-0285-1

24. Xiu P, Dong XF, Li XP, Li J. Clusterin: review of research progress and looking ahead to direction in hepatocellular carcinoma. *World J Gastroenterol*. (2015) 21:8262–70. doi: 10.3748/wjg.v21.i27.8262

25. Vijayvergia N, Boland PM, Handorf E, Gustafson KS, Gong Y, Cooper HS, et al. Molecular profiling of neuroendocrine Malignancies to identify prognostic and therapeutic markers: a Fox Chase Cancer Center Pilot Study. *Br J Cancer*. (2016) 115:564–70. doi: 10.1038/bjc.2016.229

26. Chen L, Liu M, Zhang Y, Guo Y, Chen MH, Chen J. Genetic characteristics of colorectal neuroendocrine carcinoma: more similar to colorectal adenocarcinoma. *Clin Colorectal Cancer*. (2021) 20:177–185.e13. doi: 10.1016/j.clcc.2020.09.001

27. Dizdar L, Werner TA, Drusenheimer JC, Möhlendick B, Raba K, Boeck I, et al. BRAFV600E mutation: a promising target in colorectal neuroendocrine carcinoma. *Int J Cancer*. (2019) 144:1379–90. doi: 10.1002/ijc.31828

28. Venizelos A, Elvebakken H, Perren A, Nikolaienko O, Deng W, Lothe IMB, et al. The molecular characteristics of high-grade gastroenteropancreatic neuroendocrine neoplasms. *Endocr Relat Cancer*. (2021) 29:1–14. doi: 10.1530/ERC-21-0152

frontiers | Frontiers in Oncology

TYPE Case Report
PUBLISHED 21 October 2024
DOI 10.3389/fonc.2024.1382415

Check for updates

OPEN ACCESS

EDITED BY
Lidia Castagneto Gissey,
Sapienza University of Rome, Italy

REVIEWED BY
Qiqi Xie,
Indiana University Bloomington, United States
Yue Guo,
Regeneron Pharmaceuticals, Inc.,
United States
Teodor Florin Georgescu,
Carol Davila University of Medicine and Pharmacy, Romania

*CORRESPONDENCE
Yongqiang Yao
dlyyq0411@163.com

†These authors have contributed equally to this work

RECEIVED 03 April 2024
ACCEPTED 30 September 2024
PUBLISHED 21 October 2024

CITATION
Yu J, Yao T, Zhang M, Li B and Yao Y (2024) Case report: Advanced breast cancer with scalp metastases: a report of two cases. *Front. Oncol.* 14:1382415. doi: 10.3389/fonc.2024.1382415

COPYRIGHT
© 2024 Yu, Yao, Zhang, Li and Yao. This is an open-access article distributed under the terms of the Creative Commons Attribution License (CC BY). The use, distribution or reproduction in other forums is permitted, provided the original author(s) and the copyright owner(s) are credited and that the original publication in this journal is cited, in accordance with accepted academic practice. No use, distribution or reproduction is permitted which does not comply with these terms.

Case report: Advanced breast cancer with scalp metastases: a report of two cases

Jiaxuan Yu[1†], Tianze Yao[2†], Min Zhang[3], Bingxin Li[3] and Yongqiang Yao[3*]

[1]Health Management Center, Affiliated Zhongshan Hospital of Dalian University, Dalian, China, [2]Department of Clinical Medicine, Jinzhou Medical University, Jinzhou, China, [3]Department of Breast and Thyroid Surgery, Affiliated Zhongshan Hospital of Dalian University, Dalian, China

Background: Breast cancer, identified as the most prevalent cancer worldwide, presents considerable difficulties in advanced stages, especially when involving metastatic spread. Scalp metastasis from breast cancer represents a rare and insufficiently explored occurrence. This paper seeks to illuminate this uncommon manifestation by presenting two cases of scalp metastatic breast cancer in Chinese women.

Case report: Case 1: A 45-year-old Chinese woman with a history of invasive ductal carcinoma presented with a scalp lesion indicative of recurrence. Concurrently, she was diagnosed with bone metastases and recurrence at the original site. Despite undergoing various treatments, including chemotherapy and hormonal therapy, her condition worsened, ultimately leading to her passing. Case 2: A 40-year-old Chinese woman was initially diagnosed with bilateral breast invasive mucinous carcinoma presenting with bilateral breast masses and a scalp lesion. She also had multiple bone metastases. Following chemotherapy and hormonal therapy, her disease stabilized.

Conclusion: These cases of scalp metastatic breast cancer underscore the complexities involved in managing advanced stages of the disease, especially with rare metastatic manifestations. They highlight the importance of comprehensive diagnostic methods, encompassing full-body skin evaluations, and draw attention to the socioeconomic challenges faced in cancer treatment. These findings point to the necessity for more targeted research on uncommon metastatic forms in breast cancer aiming to enhance patient outcomes and refine management approaches.

KEYWORDS

breast cancer, end-stage breast cancer, metastasis, metastatic breast cancer, cutaneous metastasis

Introduction

Breast cancer is a significant concern in women's health, with a considerable impact on individuals and healthcare systems globally. The World Health Organization (WHO) has reported that it is the world's most prevalent cancer given that there were 7.8 million women alive with a breast cancer diagnosis as of the end of 2020 (1). Though the death rates from breast cancer have been steadily decreasing since 1989, it is still the second leading cause of cancer death in women (2). Based on the Surveillance, Epidemiology, and End Results (SEER) database, the overall 5-year relative survival rate in patients with localized and regional diseases was 99% and 86%, respectively. However, those with distant metastases had a lower rate of 30% (3). Thus, addressing the unmet need for patients with distal metastatic diseases remains a significant topic.

The most common distal locations for metastatic breast cancer are the bones, lungs, brain, and liver (3–5). Cutaneous metastases from internal carcinoma are rare; reportedly, approximately 23.9% of them originate from breast cancer (6, 7). The exact prevalence of skin metastases among breast cancer patients remains unknown, but it is frequently associated with poorer outcomes (8). Scalp metastatic breast cancer is an even rarer presentation of skin involvement; there have only been limited case reports (9–11), and its clinical characteristics and prognostic value have not been thoroughly investigated. Here, we aimed to contribute to adding evidence to this subset of patients by reporting two cases of scalp metastatic breast cancer.

Case report

Case 1

A 45-year-old Chinese female presented with an enlarging left parietal skin lesion in December 2019. She denied any other symptoms and notable masses. She had no pertinent medical, surgical, or family history. She also did not have any specific breast cancer risk factors. Before the onset of scalp lesions, she had a complicated medical history of left recurrent invasive ductal carcinoma (IDC). It was initially diagnosed in 2016 with a size of 1.3 × 1.3 × 1.3 cm. Pathology showed Ki-67 of 20%, positive estrogen receptors (ER), progesterone receptors (PR), and negative ErbB2 receptors (formerly known as HER-2). She underwent left lumpectomy with axillary lymph node dissection, followed by adjuvant chemotherapy (docetaxel, epirubicin, and cyclophosphamide) and localized radiation therapy. She had been on toremifene maintenance. In 2018, a 2.0 × 1.0 × 1.5-cm focus was noticed underneath the previous surgical scar, and it was confirmed to be recurrent IDC by core needle biopsy. The bone scan revealed possible metastases in multiple areas, and whole-body magnetic resonance imaging (MRI) did not find other suspicious lesions. She then underwent bilateral oophorectomies for ovarian suppression and switched to maintenance anastrozole and zoledronic acid.

Upon the recent scalp presentation, the physical exam showed a 2.5 × 2.0 × 0.5-cm flat hard, well-demarcated erythematous lesion without ulcerations (Figure 1A). Left breast ultrasound revealed multiple nodular masses with calcifications [breast imaging report and data system (BI-RADS) category 6], and head computed tomography (CT) showed a 1.3-cm hyperdense patchy lesion (Figures 2A, B). Dermatology was consulted, and a biopsy was obtained. The final pathology reported skin metastatic breast cancer with Ki-67 of 20%, positive ER, PR, and negative ErbB2 (Supplementary Figures 1A–D). The patient was eventually diagnosed with Stage IV (rpT1cN1M1) recurrent IDC.

The patient and family initially refused further chemotherapy as well as CDK 4/6 inhibitors, exemestane, and everolimus. She was switched to single-agent fulvestrant and continued zoledronic acid. In November 2020, she had a noticeable enlargement of the previous scalp lesion and a new one on the left occipital region (Figure 1B) accompanied by intermittent pain. In addition to worsening bony involvement and left breast recurrent foci, multiple lymph nodes in the right axillary and left supraclavicular region were seen. The new scalp lesion was biopsied, and the pathology showed metastatic breast cancer with Ki-67 of 40%, positive ER, PR, and low ErbB2. After completing eight cycles of

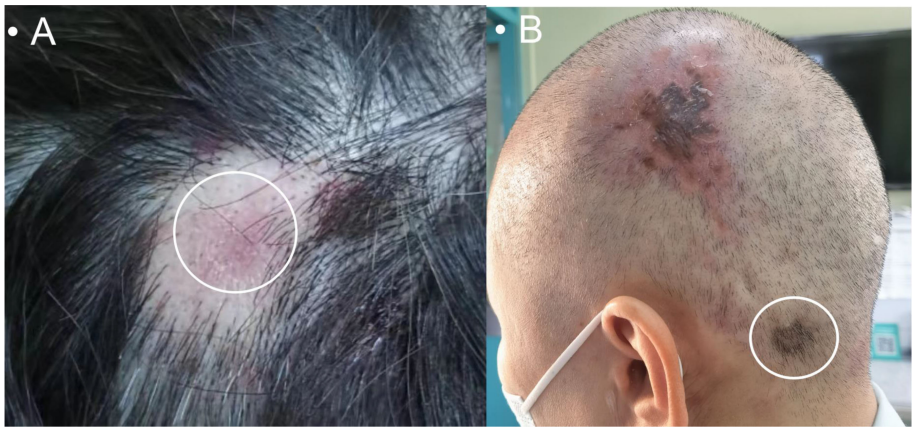

FIGURE 1
A 2.5 × 2.0 × 0.5-cm flat hard, well-demarcated erythematous lesion without ulcerations on the top of the scalp **(A)**; a new lesion on the left occipital region **(B)**.

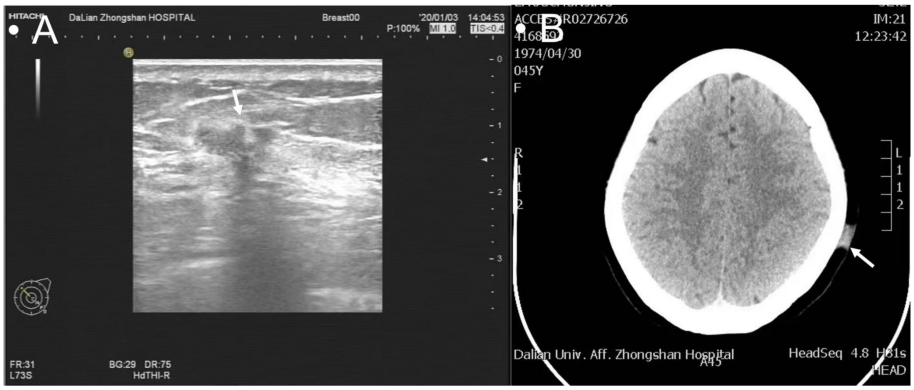

FIGURE 2
Multiple nodular masses with calcifications on ultrasound classified as BI-RADS 6 **(A)**; a 1.3-cm hyperdense patchy lesion on CT scan **(B)**.

salvage chemotherapy (paclitaxel and capecitabine), the skin lesion improved; however, the metastatic bone diseases, left recurrent foci, and lymph nodes did not show any response. We recommended multidisciplinary team (MDT) consults for further management, but she and her family refused due to financial reasons. In early 2022, the patient passed away due to multiorgan failure and cachexia.

Case 2

This case involved a 40-year-old Chinese woman with bilateral breast masses and occipital scalp lesions. In July 2020, she underwent evaluation for palpable masses in both breasts presenting with no nipple discharge or skin changes. She reported no other symptoms. Her past surgical history included a partial hip replacement and a left salpingo-oophorectomy. She did not have any pertinent medical or family history. She had no specific risk factors related to breast cancer. Physical examination revealed several lumps: a 2.0 × 2.0-cm firm, non-mobile mass with poorly defined borders in the right breast's outer lower quadrant; a 3.5 × 2.5-cm mass with similar characteristics in the left upper medial region; a 2.5 × 1.5-cm enlarged node in the right axillary region; no significant enlarged lymph nodes on the left; and a 2.0 × 0.5-cm non-mobile nodule in the occipital scalp region (Figure 3A). A diagnostic mammogram showed multiple nodules with calcifications in both breasts (BI-RADS 4a-b). Breast ultrasound identified several hyper- and hypoechoic masses with calcifications, the largest being 2.7 × 2.5 × 2.7 cm in the right breast (BI-RADS 4c) and 3.7 × 2.0 × 3.9 cm in the left breast (BI-RADS 4b). A full-body CT scan revealed enlarged right axillary lymph nodes, compression fractures in the 12th thoracic spine, and a hyper-dense area in the 1st lumbar spine, suspicious for metastases. She underwent an ultrasound-guided vacuum-assisted excision of the right breast mass. She also had right axillary lymph nodes and occipital scalp nodules (Figures 3B, C). The pathology reports were consistent across all samples indicating invasive mucinous carcinoma with positive hormonal receptors (ER and PR), low Ki-67, and negative ErbB2 (Supplementary Figures 2A–D). She was ultimately diagnosed with right Stage IV (pT3N1M1) breast mucinous carcinoma and left Stage IV (pT2N0M1) breast mucinous carcinoma.

Systemic therapy was started promptly, and the patient received six cycles of docetaxel, epirubicin, and cyclophosphamide. She was then on goserelin for ovarian suppression and zoledronic acid for metastatic bone diseases. In December 2020, the patient underwent a right salpingo-oophorectomy and had been on maintenance anastrozole. After completing the chemotherapy, ultrasound revealed slightly decreased sizes of breast masses, while all other follow-up imagines remained stable. We recommended CDK 4/6 inhibitors with aromatase inhibitors or single-agent fulvestrant, but the patient and her family refused. She remained on anastrozole and

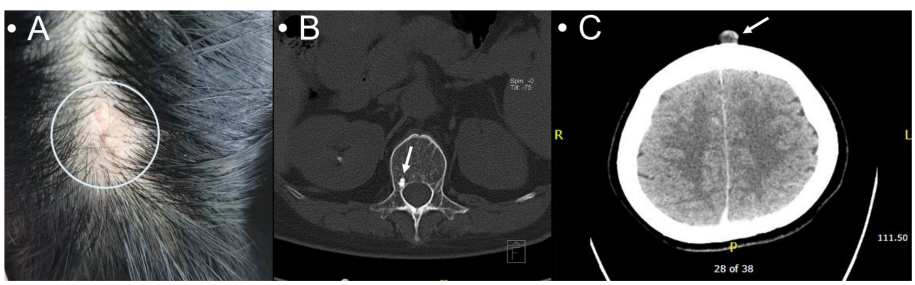

FIGURE 3
A 2.0 × 0.5-cm non-mobile non-erythematous elevated poorly demarcated nodule in the occipital scalp **(A)**; hyperdensity in the 1st lumbar spine suspicious for metastases **(B)**; a cutaneous occipital scalp nodule on the CT scan **(C)**.

zoledronic acid and followed up regularly at a local hospital. She contacted in December 2023 and reported a stable condition.

We have included a detailed timeline of relevant events, including surgery time and a chemoradiation treatment course (Figure 4).

Discussion

In both cases, the patients had aggressive hormonal receptor-positive (ER and PR) ErbB2-negative breast cancers with nodal involvement and distant metastases. One patient presented with invasive ductal carcinoma, while the other had mucinous carcinoma. Physical examinations revealed palpable nodules in all scalp lesions. Differential diagnoses encompass inflammatory diseases, lipoma, benign cutaneous tumors, primary cutaneous malignancies, and metastatic diseases from other origins. Skin biopsies were performed on both patients underscoring the significance of comprehensive skin exams in advanced-stage breast cancer cases. Notably, both patients exhibited symptomatic bone metastases and skin involvement suggesting a poorer prognosis. However, further data and studies are necessary for definitive conclusions. Financial constraints led both patients to decline positron emission tomography/computed tomography (PET/CT) for extended cancer assessment and recommended treatments highlighting the socioeconomic barriers facing patients with advanced cancers in developing countries. The outcomes differed between the two patients, with one deceased and the other with stable disease. The reasons for these divergent outcomes could be multifactorial, potentially linked to the cancer subtype.

Scalp metastases originating from non-cutaneous primary malignancies, such as lung, ovarian, gastric, or renal cell carcinoma (12–15), are a relatively rare phenomenon. There is limited comprehensive data available regarding its exact prevalence and prognosis. While the exact prevalence remains unclear due to the scarcity of comprehensive studies, it is generally considered uncommon. For instance, a study by Brownstein and Helwig reported that scalp metastases account for approximately 4% of all cutaneous metastases (16). The clinical characteristics and prognosis of scalp metastases in these cases can vary widely depending on the primary cancer type, stage at the time of diagnosis, and individual patient factors. Gupta's team reported scalp lesions as an initial presentation of an aggressive lung adenocarcinoma in a patient who had no response to chemoradiation therapy (17). Ryu and his team reported that a scalp metastasis case originated from a primary gastric adenocarcinoma (3). After upgrading the tumor stage and systemic therapy, the patient underwent palliative surgery and unfortunately passed away a year after diagnosis. Though no extensive cohort studies have investigated this, scalp involvement appears more frequently in advanced stages and recurrent diseases indicating the linkage to a poorer outcome.

Like other primary origins, scalp metastasis from invasive breast cancer is also a rare presentation; there have been only case reports of this complication (9–11, 18, 19). Costa's team reported a scalp

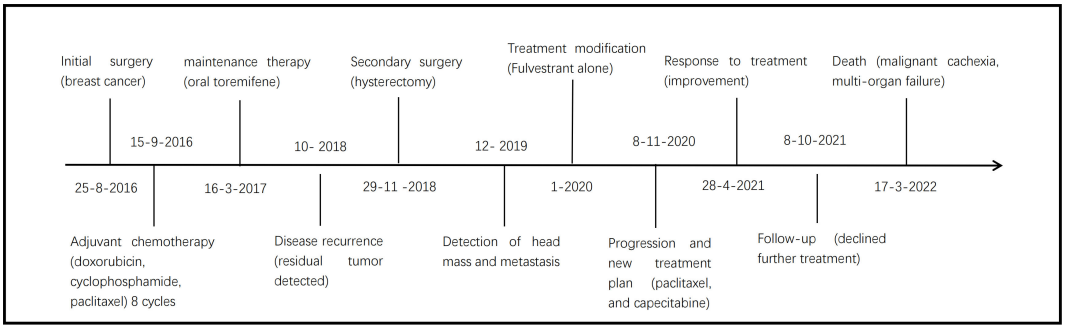

Case 1 timeline illustrates the course of treatment and disease progression from the time a patient completes surgery for breast cancer to death.

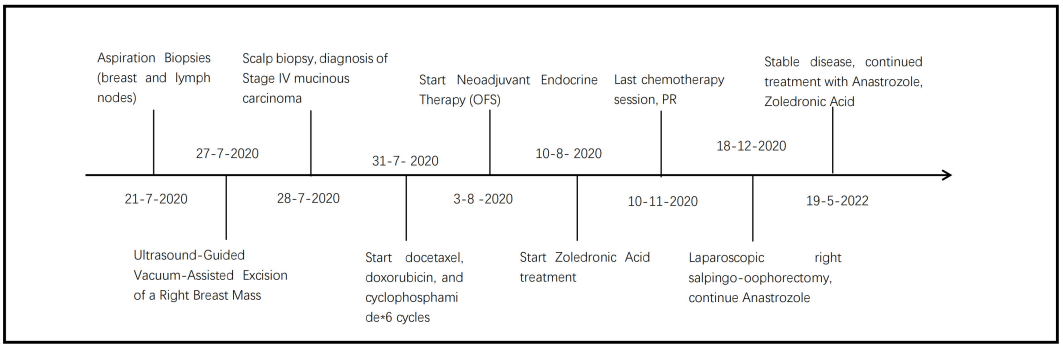

Case 2 timeline illustrates the course of treatment from the patient's completion of the discovery of breast cancer to Stable disease.

FIGURE 4
Summary of timelines of both patients.

metastatic case in a 66-year-old female; however, imaging modalities, including diagnostic mammogram and PET/CT, did not show any pertinent breast axillary abnormalities (19). Alizadeh et al. also reported a similar case in a 44-year-old female with metastatic breast carcinoma. However, no concrete disease foci were identified on MRI, CT, or ultrasound (10). Besides the presentation in possible occult breast cancer cases, Ciazynska et al. reported a case of occipital scalp lesion in a 47-year-old female, with the scalp nodule being the initial presentation of left breast cancer confirmed by CT and pathology (20). Both of our cases had definite evidence of primary breast foci, and the major difference compared to others was that the scalp findings were signs of recurrence and concurrent findings instead of the initial presentation. Abdelhafeez et al. also reported scalp lesions as a sign of recurrence of breast cancer (21). These all highlight that scalp metastatic breast cancer has various presentations along the disease course. Thus, a full-body skin examination by a dermatologist is crucial when evaluating a suspicious new skin lesion in advanced breast cancer patients. Performing a dermoscopy exam and skin biopsy can help establish a definitive diagnosis, and sometimes, it can assist with tumor staging. Given limited data, no standard treatment options have been proposed. However, in the case of metastatic disease, systemic treatment might be a more optimal choice. The value of local surgical and topical treatment remains unknown.

Prognosis and outcomes for patients with scalp metastases from breast cancer are often contingent upon disease extent, treatment response, and the presence of concurrent metastases in other organs. A case similar to ours, reported by Abdulraheem and colleagues, described a patient with recurrent ER-positive breast cancer and multiple distant metastases (11). Despite undergoing extensive chemoradiation therapy, the patient experienced poor outcomes. Conversely, the case published by Abdelhafeez's team showed 1 year of disease-free survival following chemoradiation therapy and secondary hormonal treatment. There is a clear need for further research and more extensive studies to gain a more precise understanding of the prevalence and prognosis of scalp metastatic cancer in breast cancer patients. This would enable more informed clinical decision making and enhance management strategies.

Conclusion

The cases presented here, involving scalp metastatic breast cancer in two Chinese women, underscore a rare yet significant facet of breast cancer progression. These instances, marked by late-stage, hormone receptor-positive, and ErbB2-negative cancers, highlight the intricacies and challenges associated with treating advanced breast cancer that manifests with unusual metastatic presentations. Furthermore, these cases reflect the profound influence of socioeconomic factors on treatment choices and outcomes shedding light on the frequently overlooked obstacles in managing advanced cancer cases. There is a pressing need for more inclusive and comprehensive research, mainly focused on understanding and managing the rare metastatic forms of breast cancer, to enhance prognosis and patient care.

Data availability statement

The original contributions presented in the study are included in the article/Supplementary Material. Further inquiries can be directed to the corresponding author.

Ethics statement

The studies involving humans were approved by Ethics Committee of Affiliated Zhongshan Hospital Dalian University. The studies were conducted in accordance with the local legislation and institutional requirements. The participants provided their written informed consent to participate in this study. Written informed consent was obtained from the individual(s) for the publication of any potentially identifiable images or data included in this article.

Author contributions

JY: Data curation, Methodology, Supervision, Validation, Writing – original draft, Writing – review & editing. TY: Data curation, Writing – original draft. MZ: Formal Analysis, Software, Writing – review & editing. BL: Investigation, Visualization, Writing – review & editing. YY: Conceptualization, Funding acquisition, Project administration, Resources, Writing – review & editing.

Funding

The author(s) declare that financial support was received for the research, authorship, and/or publication of this article. This study was supported by the Basic Scientific Research Project of Liaoning Education Department in 2022 (Grant number: LJKMZ2022184).

Conflict of interest

The authors declare that the research was conducted in the absence of any commercial or financial relationships that could be construed as a potential conflict of interest.

Publisher's note

All claims expressed in this article are solely those of the authors and do not necessarily represent those of their affiliated organizations, or those of the publisher, the editors and the

reviewers. Any product that may be evaluated in this article, or claim that may be made by its manufacturer, is not guaranteed or endorsed by the publisher.

Supplementary material

The Supplementary Material for this article can be found online at: https://www.frontiersin.org/articles/10.3389/fonc.2024.1382415/full#supplementary-material

SUPPLEMENTARY FIGURE 1
Scalp skin biopsy with hematoxylin and eosin staining showing invasive ductal carcinoma **(A)**; estrogen receptor-positive with moderate nuclear staining intensity **(B)**; progesterone receptor positive with strong nuclear staining intensity **(C)**; ErbB2 receptor negative **(D)** (×400).

SUPPLEMENTARY FIGURE 2
Scalp skin biopsy with hematoxylin and eosin staining showing invasive mucinous carcinoma **(A)**; estrogen receptor positive with strong nuclear staining intensity **(B)**; progesterone receptor positive with strong nuclear staining intensity **(C)**; ErbB2 receptor negative **(D)** (×100).

References

1. World Health Organization. *Breast Cancer* . Available online at: https://www.who.int/news-room/fact-sheets/detail/breast-cancer (Accessed 2023/11/09).

2. American Cancer Society. *Key Statistics for Breast Cancer* . Available online at: https://www.cancer.org/cancer/types/breast-cancer/about/how-common-is-breast-cancer.html:~:text=(Only%20lung%20cancer%20kills%20more,decline%20of%2043%25%20through%202020 (Accessed 2023/11/09).

3. *Cancer Facts & Figures 2023*. Atlanta: American Cancer Society, Inc (2022). Available online at: https://www.cancer.org/research/cancer-facts-statistics/all-cancer-facts-figures/2023-cancer-facts-figures.html.

4. Inoue M, Nakagomi H, Nakada H, Furuya K, Ikegame K, Watanabe H, et al. Specific sites of metastases in invasive lobular carcinoma: a retrospective cohort study of metastatic breast cancer. *Breast Cancer*. (2017) 24:667–72. doi: 10.1007/s12282-017-0753-4

5. Chen M-T, Sun H-F, Zhao Y, Fu W-Y, Yang L-P, Gao S-P, et al. Comparison of patterns and prognosis among distant metastatic breast cancer patients by age groups: a SEER population-based analysis. *Sci Rep*. (2017) 7:9254. doi: 10.1038/s41598-017-10166-8

6. Lookingbill DP, Spangler N, Helm KF. Cutaneous metastases in patients with metastatic carcinoma: a retrospective study of 4020 patients. *J Am Acad Dermatol*. (1993) 29:228–36. doi: 10.1016/0190-9622(93)70173-q

7. Krathen RA, Orengo IF, Rosen T. Cutaneous metastasis: a meta-analysis of data. *South Med J*. (2003) 96:164–7. doi: 10.1097/01.Smj.0000053676.73249.E5

8. González-Martínez S, Pizarro D, Pérez-Mies B, Caniego-Casas T, Curigliano G, Cortés J, et al. Clinical, pathological, and molecular features of breast carcinoma cutaneous metastasis. *Cancers*. (2021) 13:5416. doi: 10.3390/cancers13215416

9. Lemieux J, Desbiens C, Hogue JC. Breast cancer scalp metastasis as first metastatic site after scalp cooling: two cases of occurrence after 7- and 9-year follow-up. *Breast Cancer Res Treat*. (2011) 128:563–6. doi: 10.1007/s10549-011-1453-y

10. Alizadeh N, Mirpour H, Azimi SZ. Scalp metastasis from occult primary breast carcinoma: A case report and review of the literature. *Int J Womens Dermatol*. (2018) 4:230–5. doi: 10.1016/j.ijwd.2018.08.002

11. Abdulraheem AM, Naji D, Al Heyasat AN, Alhasan M, Almasri NM, Odeh R. Breast cancer with scalp metastases: a case report. *J Med Case Rep*. (2023) 17:203. doi: 10.1186/s13256-023-03928-8

12. Salemis NS, Veloudis G, Spiliopoulos K, Nakos G, Vrizidis N, Gourgiotis S. Scalp metastasis as the first sign of small-cell lung cancer: management and literature review. *Int Surg*. (2014) 99:325–9. doi: 10.9738/intsurg-d-13-00070.1

13. Ryu HR, Lee DW, Choi HJ, Kim JH, Ahn H. Scalp metastasis of advanced gastric cancer. *Arch Craniofac Surg*. (2021) 22:157–60. doi: 10.7181/acfs.2021.00129

14. Errami M, Margulis V, Huerta S. Renal cell carcinoma metastatic to the scalp. *Rare Tumors*. (2016) 8:6400. doi: 10.4081/rt.2016.6400

15. Coco D, Leanza S. Cutaneous metastasis in ovarian cancer: case report and literature review. *Maedica (Bucur)*. (2020) 15:552–5. doi: 10.26574/maedica.2020.15.4.552

16. Brownstein MH, Helwig EB. Patterns of cutaneous metastasis. *Arch Dermatol*. (1972) 105:862–8. doi: 10.1001/archderm.1972.01620090034008

17. Gupta V, Bhutani N, Marwah N, Sen R. Scalp metastasis as an initial presentation of lung adenocarcinoma: A case report and literature review. *Int J Surg Case Rep*. (2017) 41:327–31. doi: 10.1016/j.ijscr.2017.10.060

18. Liu Y-F, Liu L-Y, Xia S-L, Li T, Li J. An unusual case of scalp metastasis from breast cancer. *World Neurosurg*. (2020) 137:261–5. doi: 10.1016/j.wneu.2020.01.230

19. Costa Ricardo LB, Costa-Filho Rubens B, Rosa M, Czerniecki Brian J. Occult breast carcinoma presenting as scalp metastasis. *Case Rep Oncol*. (2017) 10:992–7. doi: 10.1159/000484346

20. Ciążyńska M, Płużańska-Srebrzyńska K, Narbutt J, Kolano P, Stasikowska-Kanicka O, Lesiak A. Scalp metastases as the first sign of a breast carcinoma. *Postepy Dermatol Alergol*. (2021) 38:530–2. doi: 10.5114/ada.2021.107942

21. Abdelhafeez AAM, Ibrahim W, Elsherief W. Solitary scalp metastatic lesion as a sign of breast cancer recurrence—a case report. *Memo - Magazine Eur Med Oncol*. (2019) 12:185–8. doi: 10.1007/s12254-019-0471-z

frontiers | Frontiers in Oncology

TYPE Case Report
PUBLISHED 28 October 2024
DOI 10.3389/fonc.2024.1481251

Check for updates

OPEN ACCESS

EDITED BY
Ferdinando Agresta,
ULSS2 Marca Trevigiana, Italy

REVIEWED BY
Anna-Lea Amylidi,
University Hospital of Ioannina, Greece
Marcin Oplawski,
Andrzej Frycz Modrzewski Krakow University, Poland

*CORRESPONDENCE
Zhiyu Lin
1228861969@qq.com

RECEIVED 15 August 2024
ACCEPTED 07 October 2024
PUBLISHED 28 October 2024

CITATION
Zan N, Zhang X, Yu D, Liu J, Lin Z and Zhu Y (2024) Case report: Long-term progression-free survival in advanced ovarian cancer treated with apatinib in first-line maintenance treatment.
Front. Oncol. 14:1481251.
doi: 10.3389/fonc.2024.1481251

COPYRIGHT
© 2024 Zan, Zhang, Yu, Liu, Lin and Zhu. This is an open-access article distributed under the terms of the Creative Commons Attribution License (CC BY). The use, distribution or reproduction in other forums is permitted, provided the original author(s) and the copyright owner(s) are credited and that the original publication in this journal is cited, in accordance with accepted academic practice. No use, distribution or reproduction is permitted which does not comply with these terms.

Case report: Long-term progression-free survival in advanced ovarian cancer treated with apatinib in first-line maintenance treatment

Ning Zan[1], Xuan Zhang[1], Danfei Yu[1], Juan Liu[1], Zhiyu Lin[1]* and Yanlin Zhu[2]

[1]Department of Oncology And Hematology, People's Hospital of Leshan, Leshan, China, [2]Pulmonary and Critical Care Medicine, People's Hospital of Leshan, Leshan, China

Ovarian cancer is one of the most common gynecological malignancies. The current first-line treatment strategies for advanced ovarian cancer include surgery, chemotherapy, and maintenance therapy. Bevacizumab and poly (ADP-ribose) polymerase inhibitors (PARPi) are primary maintenance treatments for advanced ovarian cancer. Previously, many patients declined these therapies before medicare coverage because of high costs. Bevacizumab and apatinib are anti-tumor angiogenic agents. In this case study, we describe a patient with advanced ovarian cancer who underwent neoadjuvant chemotherapy, interval debulking surgery, and adjuvant chemotherapy. She declined bevacizumab and PARPi maintenance therapy owing to the prohibitive expenses. The patient was administered off-label apatinib and achieved a progression-free survival of 54 months. Thus, apatinib may offer substantial therapeutic value as a first-line maintenance therapy in advanced ovarian cancer.

KEYWORDS

ovarian cancer, maintain therapy, angiogenic, apatinib, gynecology, case report

1 Introduction

Ovarian cancer is a serious threat to women's health. Even though its incidence is lower than that of gynecological cancers of the cervix and uterus. It is the second most common gynecological cancer with the highest mortality rate (1). Most patients are diagnosed at an advanced stage owing to a lack of symptoms and other reasons (2). Therefore, patients with ovarian cancer have a poor prognosis. Prior to the introduction of targeted therapies, the standard treatment for ovarian cancer primarily involved surgery accompanied by platinum-based chemotherapy. The integration of poly (ADP-ribose) polymerase

inhibitors (PARPi) and bevacizumab as first-line maintenance therapies has revolutionized the treatment paradigm of ovarian cancer, significantly prolonging the progression-free survival (PFS) and overall survival (OS) in patients with advanced stages of the disease (3–5). Despite their benefits, many patients declined the use of PARPi and bevacizumab owing to their high costs, which were not being covered by the national health insurance. Both apatinib and bevacizumab serve as anti-tumor angiogenic agents, with apatinib being efficacious as either part of combination regimens or as a monotherapy in treating recurrent ovarian cancer (6, 7). Further, apatinib costs lesser than bevacizumab and PARPi. However, the use of apatinib as first-line maintenance therapy in ovarian cancer has not been reported to date. This report documents a case of prolonged PFS achieved in a patient with stage IVb ovarian cancer using apatinib as a first-line maintenance therapy.

2 Case description

In November 2018, a 44-year-old female was admitted to a local hospital for abdominal pain. The medication she received during this period is not known. Symptomatic treatment provided no obvious relief. Previously, the patient had undergone a hysterectomy for uterine fibroids at the age of 39 years. She had no family history of cancer. In January 2019, computed tomography (CT) scans revealed no normal uterine and ovarian tissues. Multiple masses were observed on both sides of the pelvis, with the largest cross-section measuring approximately 7.6×6.2 cm (Figure 1A). Multiple masses were observed in the peritoneum and omentum. Moreover, multiple metastatic lesions were observed in the liver and lungs (Figures 1B, C). Enlargement of the abdominal, retroperitoneal, and cardiophrenic angle lymph nodes was suggestive of metastasis. The level of carbohydrate antigen 125 (CA125) was elevated at 486.0 U/ml. On January 30, 2019, the patient underwent a laparoscopic biopsy of the peritoneal lesions. Histopathological and immunohistochemical analyses confirmed high-grade serous adenocarcinoma of ovarian origin. Immunohistochemical staining results were as follows: CK7(+++), Vim(-), P53(++), P16(+++), WT-1(+++), CA125(+++), CA199(-), CK5/6(-), P63(-), CK7(+), CK20(-), Villin(-), ER (partially +), PR (-), PAX-8 (partially +), Ki67 (+; approximately 60%). The patient was diagnosed with stage IVb high-grade serous adenocarcinoma of the ovary. On February 1, 2019, the patient commenced treatment with paclitaxel (175 mg/m2, intravenously, day 1) and carboplatin (AUC 5, intravenously, day 1), administered every three weeks for a total of three cycles. On April 2, 2019, a CT scan revealed a significant reduction in all lesions (Figures 1D–F). However, achieving satisfactory tumor resection based on the Suidan score remains challenging. The patient continued with the original

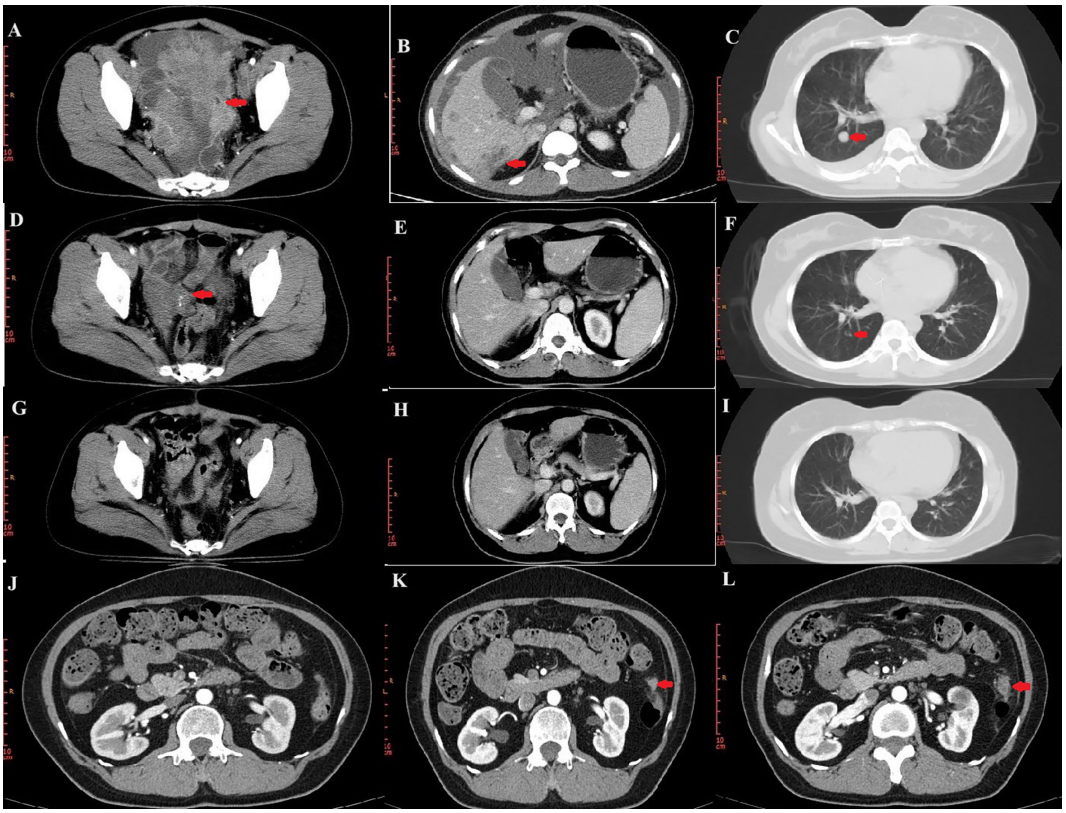

FIGURE 1
CT images during treatment. **(A–C)** CT image of the lesion at initial treatment. Pelvic lesions **(A)**. Liver lesions **(B)**. Lung lesions **(C)**. **(D–F)** CT images after three cycles of chemotherapy. **(G–I)** CT images at the end of chemotherapy. **(J)** No tumor recurrence on CT on April 19, 2023. **(K, L)** Lesions of peritoneum on CT.

chemotherapy regimen for two cycles before undergoing interval debulking surgery (IDS) on May 31, 2019. This procedure included the resection of bilateral ovarian tissues, fallopian tubes, peritoneum, omentum, appendix, and enlarged lymph nodes. Histopathological and immunohistochemical analyses confirmed a high-grade serous adenocarcinoma of the right ovary. The left ovarian inclusion cyst was calcified and contained foam cell aggregations. Notably, peritoneal and omental tissues exhibited fibrous hyperplasia with numerous foam cell aggregates. No tumor cells were present in the fallopian tubes, appendix, or lymph nodes bilaterally. The immunohistochemical staining yielded positive results for Vim (nucleus+), CA125(+), CK7(+), P53(+), P16(+), ER(+), and Ki67 (approximately 25%), with negative results for PR(-) and CK20(-). Postoperatively, the patient declined bevacizumab because of its high cost and instead completed three more cycles of the initial chemotherapy regimen. Subsequently, a CT scan on September 10, 2019, revealed the resolution of tumor metastases in the abdomen, pelvis, lungs, and liver (Figures 1G–I). The patient declined genetic testing and PARPi maintenance therapy owing to the high costs. She consented to receive off-label apatinib (750 mg, oral, QD) starting in October 2019. Subsequently, she developed palmar-plantar erythrodysesthesia syndrome (Common Terminology Criteria for Adverse Events [CTCAE] grade 3) and requested a dose adjustment. After the daily dose was reduced to 500 mg, her symptoms improved. The patient remained stable with regular follow-ups, and a CT scan on April 19, 2023, showed no signs of tumor recurrence (Figure 1J). Computed tomography (CT) revealed new lesions on the left side of the peritoneum and omentum in April 2024 (Figures 1K, L). The patient underwent laparoscopic tumor resection for peritoneal and omental diseases on May 10, 2024. Histopathological and immunohistochemical analyses indicated a high-grade serous adenocarcinoma of the female reproductive system. Immunohistochemical staining results were as follows: CK(AE1/AE3)(+), Syn(-), Pax-8(+), S100(-), SALL4(-), Ki67(+; about 80%). Recurrence of ovarian cancer was determined based on patient history and pathology findings. The patient achieved a PFS of 54 months following first-line maintenance therapy with apatinib. The timeline of the patient's treatment is shown in Figure 2.

3 Discussion

Advanced ovarian cancer has a poor prognosis. In recent years, bevacizumab and PARPi have been shown to improve the prognosis of patients with advanced ovarian cancer (3–5). Tumor growth requires blood vessels to provide oxygen and nutrients. Furthermore, the vascular endothelial growth factor (VEGF) plays an important role in the process of angiogenesis (8). Notably, VEGF expression is higher in ovarian tumor tissues than in normal and benign ovarian tissues (9). There are two different clinical treatment strategies for VEGF. Bevacizumab, an anti-VEGF monoclonal antibody, inhibits the proangiogenic effect of VEGF. Another clinical treatment strategy targeting VEGF is inhibiting the function of the VEGF receptor (VEGFR), using apatinib for example. VEGF, especially VEGF-A, has been identified as a key factor in tumor angiogenesis. Bevacizumab inhibits the binding of VEGF-A to VEGFR tyrosine kinases (VEGFR1-3), inhibits tumor vascular growth, promotes tumor vascular normalization, and causes tumor cell death (10). Moreover, VEGFR2 is the main signaling pathway of VEGFR in vascular endothelial cells (11). Apatinib is a small oral VEGFR-2 tyrosine kinase inhibitor molecule that inhibits tumor angiogenesis by blocking downstream signaling (7).

Apatinib, alone or in combination with chemotherapy, has shown favorable antitumor effects and manageable safety in patients with platinum-resistant or platinum-refractory ovarian cancer (12, 13). Furthermore, it improves the overall survival (OS) in patients receiving third-line treatment for gastric cancer or gastroesophageal junction carcinoma (14). Apatinib plus camrelizumab has a survival benefit as a first-line therapy for unresectable hepatocellular carcinoma (15). Notably, patients with advanced ovarian cancer also benefit from first-line maintenance therapy with bevacizumab (4, 16). However, there have been no clinical studies on apatinib as a first-line maintenance therapy for ovarian cancer.

Till date, no studies have compared the efficacy of apatinib versus bevacizumab in ovarian cancer maintenance therapy. However, animal studies have shown that apatinib has stronger antitumor activity than bevacizumab in transgenic zebrafish embryo and human lung cancer xenotransplantation models (17).

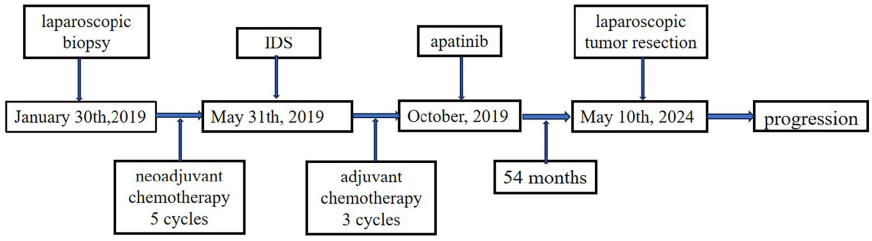

FIGURE 2
Timeline of the patient's treatment. PARPi, Poly (ADP-ribose) polymerase inhibitors; PFS, Progression-free survival; OS, Overall survival; CT, Computed tomography; CA125, Carbohydrate antigen 125; AUC, Area under the curve; IDS, Interval debulking surgery; CTCAE, Common Terminology Criteria for Adverse Events; VEGF, Vascular endothelial growth factor; VEGFR, VEGF receptor.

In advanced gastric cancer, apatinib is more effective than bevacizumab (18). The study of real-world drug treatment models of novel targeted drugs showed that the total drug costs and per capita drug cost of bevacizumab or PARPi were higher than those of apatinib in Chinese patients with gynecological cancer from 2017 to 2021 (19). The price of bevacizumab was significantly higher than apatinib before the national health insurance coverage and the price of bevacizumab is still higher than apatinib after the national health insurance coverage in China (20).

In the current case, advanced ovarian cancer was suspected at the initial diagnosis. The patient received neoadjuvant chemotherapy, interval debulking surgery, and adjuvant chemotherapy. The patient declined bevacizumab and PARPi maintenance therapy owing to their high costs. Consequently, the patient opted for the less costly off-label apatinib maintenance therapy. The patient attained a long-term PFS of up to 54 months. This outcome holds potential therapeutic value for first-line maintenance in advanced ovarian cancer. However, some patients may experience adverse events. Since this is a single case, which is a limitation of this study, it is not known whether this treatment model will be applicable to other patients with advanced ovarian. Further studies and clinical trials are necessary to verify the effectiveness of this strategy.

Data availability statement

The original contributions presented in the study are included in the article/supplementary material. Further inquiries can be directed to the corresponding author.

Ethics statement

Written informed consent was obtained from the individual(s) for the publication of any potentially identifiable images or data included in this article.

Author contributions

NZ: Writing – original draft. XZ: Writing – original draft. DY: Writing – original draft. JL: Writing – original draft. ZL: Writing – review & editing. YZ: Writing – original draft.

Funding

The author(s) declare that no financial support was received for the research, authorship, and/or publication of this article.

Acknowledgments

The authors are grateful to the patient for agreeing to share the information. We would like to thank Editage (www.editage.cn) for English language editing.

Conflict of interest

The authors declare that the research was conducted in the absence of any commercial or financial relationships that could be construed as a potential conflict of interest.

Publisher's note

All claims expressed in this article are solely those of the authors and do not necessarily represent those of their affiliated organizations, or those of the publisher, the editors and the reviewers. Any product that may be evaluated in this article, or claim that may be made by its manufacturer, is not guaranteed or endorsed by the publisher.

References

1. Bray F, Laversanne M, Sung H, Ferlay J, Siegel RL, Soerjomataram I, et al. Global cancer statistics 2022: GLOBOCAN estimates of incidence and mortality worldwide for 36 cancers in 185 countries. *CA Cancer J Clin*. (2024) 74:229–63. doi: 10.3322/caac.21834

2. Seibaek L, Petersen LK, Blaakaer J, Hounsgaard L. Symptom interpretation and health care seeking in ovarian cancer. *BMC Womens Health*. (2011) 11:31. doi: 10.1186/1472-6874-11-31

3. Li N, Zhu J, Yin R, Wang J, Pan L, Kong B, et al. Treatment with niraparib maintenance therapy in patients with newly diagnosed advanced ovarian cancer: A phase 3 randomized clinical trial. *JAMA Oncol*. (2023) 9:1230–7. doi: 10.1001/jamaoncol.2023.2283

4. You B, Purdy C, Copeland LJ, Swisher EM, Bookman MA, Fleming G, et al. Identification of patients with ovarian cancer experiencing the highest benefit from bevacizumab in the first-line setting on the basis of their tumor-intrinsic chemosensitivity (KELIM): the GOG-0218 validation study. *J Clin Oncol*. (2022) 40:3965–74. doi: 10.1200/JCO.22.01207

5. DiSilvestro P, Banerjee S, Colombo N, Scambia G, Kim BG, Oaknin A, et al. Overall survival with maintenance olaparib at a 7-year follow-up in patients with newly diagnosed advanced ovarian cancer and a BRCA mutation: the SOLO1/GOG 3004 trial. *J Clin Oncol*. (2023) 41:609–17. doi: 10.1200/JCO.22.01549

6. Wang T, Tang J, Yang H, Yin R, Zhang J, Zhou Q, et al. Effect of apatinib plus pegylated liposomal doxorubicin vs pegylated liposomal doxorubicin alone on platinum-resistant recurrent ovarian cancer: the APPROVE randomized clinical trial. *JAMA Oncol*. (2022) 8:1169–76. doi: 10.1001/jamaoncol.2022.2253

7. Wang Z, Huang Y, Long L, Zhou L, Huang Y, Gan L, et al. Apatinib treatment efficiently delays biochemical-only recurrent ovarian cancer progression. *J Ovarian Res*. (2021) 14:91. doi: 10.1186/s13048-021-00843-8

8. Hicklin DJ, Ellis LM. Role of the vascular endothelial growth factor pathway in tumor growth and angiogenesis. *J Clin Oncol*. (2005) 23:1011–27. doi: 10.1200/JCO.2005.06.081

9. Wang H, Huang X, Zhang J, Shao N, Chen LO, Ma D, et al. The expression of VEGF and Dll4/Notch pathway molecules in ovarian cancer. *Clin Chim Acta*. (2014) 436:243–8. doi: 10.1016/j.cca.2014.06.005

10. Garcia J, Hurwitz HI, Sandler AB, Miles D, Coleman RL, Deurloo R, et al. Bevacizumab (Avastin®) in cancer treatment: A review of 15 years of clinical experience and future outlook. *Cancer Treat Rev*. (2020) 86:102017. doi: 10.1016/j.ctrv.2020.102017

11. Simons M, Gordon E, Claesson-Welsh L. Mechanisms and regulation of endothelial VEGF receptor signalling. *Nat Rev Mol Cell Biol*. (2016) 17:611–25. doi: 10.1038/nrm.2016.87

12. Lan CY, Wang Y, Xiong Y, Li JD, Shen JX, Li YF, et al. Apatinib combined with oral etoposide in patients with platinum-resistant or platinum-refractory ovarian cancer (AEROC): a phase 2, single-arm, prospective study. *Lancet Oncol*. (2018) 19:1239–46. doi: 10.1016/S1470-2045(18)30349-8

13. Miao M, Deng G, Luo S, Zhou J, Chen L, Yang J, et al. A phase II study of apatinib in patients with recurrent epithelial ovarian cancer. *Gynecol Oncol*. (2018) 148:286–90. doi: 10.1016/j.ygyno.2017.12.013

14. Zhang C, Xiang Y, Wang J, Yan D. Comparison of the efficacy and safety of third-line treatments for advanced gastric cancer: A systematic review and network meta-analysis. *Front Oncol*. (2023) 13:1118820. doi: 10.3389/fonc.2023.1118820

15. Qin S, Chan SL, Gu S, Bai Y, Ren Z, Lin X, et al. Camrelizumab plus rivoceranib versus sorafenib as first-line therapy for unresectable hepatocellular carcinoma (CARES-310): a randomised, open-label, international phase 3 study. *Lancet*. (2023) 402:1133–46. doi: 10.1016/s0140-6736(23)00961-3

16. Oza AM, Cook AD, Pfisterer J, Embleton A, Ledermann JA, Pujade-Lauraine E, et al. Standard chemotherapy with or without bevacizumab for women with newly diagnosed ovarian cancer (ICON7): overall survival results of a phase 3 randomised trial. *Lancet Oncol*. (2015) 16:928–36. doi: 10.1016/S1470-2045(15)00086-8

17. Jin Y, Wei L, Jiang Q, Song X, Teng C, Fan C, et al. Comparison of efficacy and toxicity of bevacizumab, endostar and apatinib in transgenic and human lung cancer xenograftzebrafish model. *Sci Rep*. (2018) 8:15837. doi: 10.1038/s41598-018-34030-5

18. Zhao TT, Xu H, Xu HM, Wang ZN, Xu YY, Song YX, et al. The efficacy and safety of targeted therapy with or without chemotherapy in advanced gastric cancer treatment: a network meta-analysis of well-designed randomized controlled trials. *Gastric Cancer*. (2018) 21:361–71. doi: 10.1007/s10120-018-0813-2

19. Li C, Jin J, Tang J. Real-world drug treatment models of novel targeted drugs in Chinese patients with gynecological cancer from 2017 to 2021: A cross-sectional analysis. *Heliyon*. (2024) 10:e31371. doi: 10.1016/j.heliyon.2024.e31371

20. Fang W, Xu X, Zhu Y, Dai H, Shang L, Li X. Impact of the national health insurance coverage policy on the utilisation and accessibility of innovative anti-cancer medicines in China: an interrupted time-series study. *Front Public Health*. (2021) 9:714127. doi: 10.3389/fpubh.2021.714127

frontiers | Frontiers in Oncology

TYPE Case Report
PUBLISHED 28 October 2024
DOI 10.3389/fonc.2024.1472061

Check for updates

OPEN ACCESS

EDITED BY
Dragos Eugen Georgescu,
Carol Davila University of Medicine and Pharmacy, Romania

REVIEWED BY
Guglielmo Stabile,
Institute for Maternal and Child Health Burlo Garofolo (IRCCS), Italy
Andrea Giannini,
Umberto 1 Hospital, Italy

*CORRESPONDENCE
Le Luo
499291610@qq.com

RECEIVED 28 July 2024
ACCEPTED 02 October 2024
PUBLISHED 28 October 2024

CITATION
Li J and Luo L (2024) Ultrasound findings of ovarian intravenous leiomyomatosis: a case report.
Front. Oncol. 14:1472061.
doi: 10.3389/fonc.2024.1472061

COPYRIGHT
© 2024 Li and Luo. This is an open-access article distributed under the terms of the Creative Commons Attribution License (CC BY). The use, distribution or reproduction in other forums is permitted, provided the original author(s) and the copyright owner(s) are credited and that the original publication in this journal is cited, in accordance with accepted academic practice. No use, distribution or reproduction is permitted which does not comply with these terms.

Ultrasound findings of ovarian intravenous leiomyomatosis: a case report

Jin Li[1] and Le Luo[2*]

[1]Department of Ultrasound, Deyang People's Hospital, Deyang, Sichuan, China, [2]Medical Records Statistics Division, Deyang People's Hospital, Deyang, Sichuan, China

Intravenous leiomyomatosis (IVL), an abnormal growth pattern of uterine leiomyomas, is a rare tumor characterized by masses of smooth muscle cells appearing histologically benign and proliferating within the blood vessels but not invading the tissue. Currently, there have been limited reports of early cases of IVL, and the imaging characteristics of IVL remain uncertain, resulting in frequent misdiagnosis prior to surgery. The present study utilized a case of early IVL detected through conventional ultrasound and subsequently confirmed *via* contrast-enhanced ultrasound (CEUS) to further investigate ultrasound's diagnostic efficacy for early IVL detection. Here, a case of a 49-year-old woman was reported who presented with uterine leiomyoma and an echogenic mass in the left adnexal region on physical examination. Subsequent transvaginal CEUS examination revealed a left ovarian venous leiomyoma. The patient underwent resection of tumors in the uterus, bilateral ovaries, and left ovarian vein under general anesthesia. A venous plexus was identified above the left broad ligament close to the left ovary, and a myoma-like growth was detected in the posterior uterine wall during the operational procedure. Reports on pathology and immunohistochemistry verified leiomyomatosis with fatty metaplasia in the left broad ligament and uterine wall vein. The prognosis of patients with IVL is determined based on the appropriate surgical methods and the timely diagnosis of the condition. In this case, conventional ultrasound aided in the early identification of IVL, which was later verified by a CEUS examination, resulting in a successful surgical treatment. This example highlights the importance of ultrasound technology in diagnosing this uncommon condition and presents a new method for preoperative detection of IVL.

KEYWORDS

intravenous leiomyomatosis, contrast-enhanced ultrasound, ovarian vein, ultrasound examination, case report

Introduction

Intravenous leiomyomatosis (IVL) is a rare malignancy characterized by aberrant growth patterns of uterine leiomyomas. Although IVL appears benign during histological examination, it can display aggressive malignant characteristics by spreading beyond the pelvic vein, inferior vena cava, adrenal vein, and renal vein to affect the right ventricular compartment and major pulmonary artery in some instances. This can lead to symptoms such as cardiac murmurs, syncope, and even sudden death (1). Frequent misdiagnosis or delayed diagnosis before surgery, which can result in incorrect medical treatment, is often observed due to the rarity of this condition. Accurate preoperative diagnosis of IVL necessitates comprehensive imaging examination, with computed tomography (CT) or magnetic resonance imaging (MRI) commonly employed due to multifocal lesions involving various locations, including the iliac vein and heart. However, there remains untapped potential for transvaginal and contrast-enhanced ultrasound (CEUS) in the early detection of this disease, which warrants further exploration. Herein, a case has been presented where conventional ultrasound identified intravenous low echo within the ovary that was subsequently evaluated using CEUS, revealing a leiomyoma. This leiomyoma was ultimately confirmed *via* surgical intervention and histopathological analysis as an early-stage IVL case.

Case presentation

Over 10 months ago, the patient, a 49-year-old female, was developed an irregular menstrual cycle without an apparent cause, which lasted for about 1-2 months, with a menstrual period of 7 days, accompanied by increased menstrual volume, blood clots, no abdominal pain and distension, no frequent urination, and no diarrhea and constipation. Over 5 months ago, the patient received a regular ultrasound examination at our hospital as part of a physical examination (Figures 1A–C), revealing leiomyoma of the uterus's posterior wall with a size of about 40.2 mm × 45.0 mm, with a clear boundary, and a regular shape. An enhanced echo was observed in the left adnexal region, measuring approximately 51.0 mm × 29.5 mmm, with an unclear boundary, particularly concerning the left lateral wall of the uterus. Color Doppler flow imaging (CDFI) detected a meandering flow signal. Pulse wave (PW) measurement and venous flow spectrum were also observed. These findings suggest the presence of a left adnexal ovarian venous leiomyoma. After this, a CEUS examination was recommended for the patient. CEUS examination (Figures 1D–F) showed a leiomyoma in the posterior wall of the uterus, and a solid space-occupying lesion in the left ovarian vein course region considered a left ovarian vein leiomyoma. The patient underwent a transvaginal ultrasound examination (Figures 1G–I) in our hospital more than 20 days ago. The examination revealed an isoechoic mass located on the posterior wall of the uterus. The mass measures approximately 45.5 mm × 39.9 mm × 44.2 mm in size and showed a clear boundary and regular shape. The CDFI revealed blood flow signals, indicating the presence of a leiomyoma on the posterior wall of the uterus. An elongated, isoechoic structure was identified in the left adnexal region, measuring 53.0 mm × 14.0 mm. The convoluted blood flow signal was observed using CDFI, and the spectrum of venous blood flow was analyzed using PW, indicating the presence of a left ovarian venous leiomyoma. The echocardiography of the heart and ultrasonography of the major arteries in the abdomen revealed no anomalies. The Contrast-enhanced CT scan of the chest and abdomen (Figures 1J–L) revealed an enlarged uterus with a 46.2 mm × 43.7 mm isodense mass in the posterior wall. The mass exhibited a relatively low but uniform enhancement, consistent with a diagnosis of uterine leiomyoma. An isodense mass of about 39.6 mm × 29.4 mm was found in the left lateral wall of the uterus, which was slightly enhanced, and the boundary with the left adnexa was not clear. No abnormalities were seen in the iliac vein, inferior vena cava, renal vein, or heart. Summarizing the above analysis, ovarian venous leiomyomas and uterine fibroids were the final diagnoses of the patient.

The patient underwent resection of tumors in the uterus, bilateral ovaries, and left ovarian vein under general anesthesia. The patient was positioned in lithotomy, and following adequate anesthetic, standard disinfection and draping were performed. An artificial pneumoperitoneum was then established, and laparoscopic surgery was conducted: A leiomyoma-like mass (50.0 mm × 40.0 mm) was observed in the posterior wall, some of which was convex to the serosa layer. A venous plexus (20.0 mm × 30.0 mm) was seen above the left broad ligament near the left ovary, among which a venous tumor was identified. The postoperative cesarean section revealed that the cervix was hypertrophic and had a uniform texture. A fibroid mass of approximately 40.0 mm in diameter was located between the posterior wall of the uterus, exhibiting a whorl-like appearance on the cut surface. The tumor's sliced surface had a purple-blue coloration. The gross pathological examination (Figures 2A, B) revealed that the size of the uterine body was 94.0 mm × 92.0 mm × 61.0 mm. Gray-white nodules measuring 44.0 mm × 32.0 mm × 42.0 mm appeared between the muscle walls. The cut surface was gray-white, solid, and tough, with purple-blue bleeding spots between the muscle walls. The left broad ligament included two nonplastic tissues, measuring approximately 31.0 mm × 21.0 mm × 9.0 mm and 19.0 mm × 14.0 mm × 8.0 mm, which were gray-red and gray-brown in color. The cut surface of these tissues seemed soft and gray-brown. Pathological analysis verified the presence of a spindle cell tumor (Figures 2C, D).

Immunohistochemical identification of tumors in the uterus and left broad ligament: Spindle cells were CK (–), CR (–), D2-40 (–), Desmin (+), Caldesmon (+), CD34 (vascular +), CD31 (vascular +), and Ki-67 (+,<5%). When combined with the morphology and immunophenotype of hematoxylin and eosin staining, IVL with fatty metaplasia was observed in the uterine wall and the left broad ligament (Figures 2E, F). Throughout the 6-month follow-up, no abnormalities were found in the iliac vessels, great abdominal vessels, or heart.

Discussion

IVL is a unique and rare tumor that appears histologically benign but has malignant biological behavior. Ordulu et al (2)

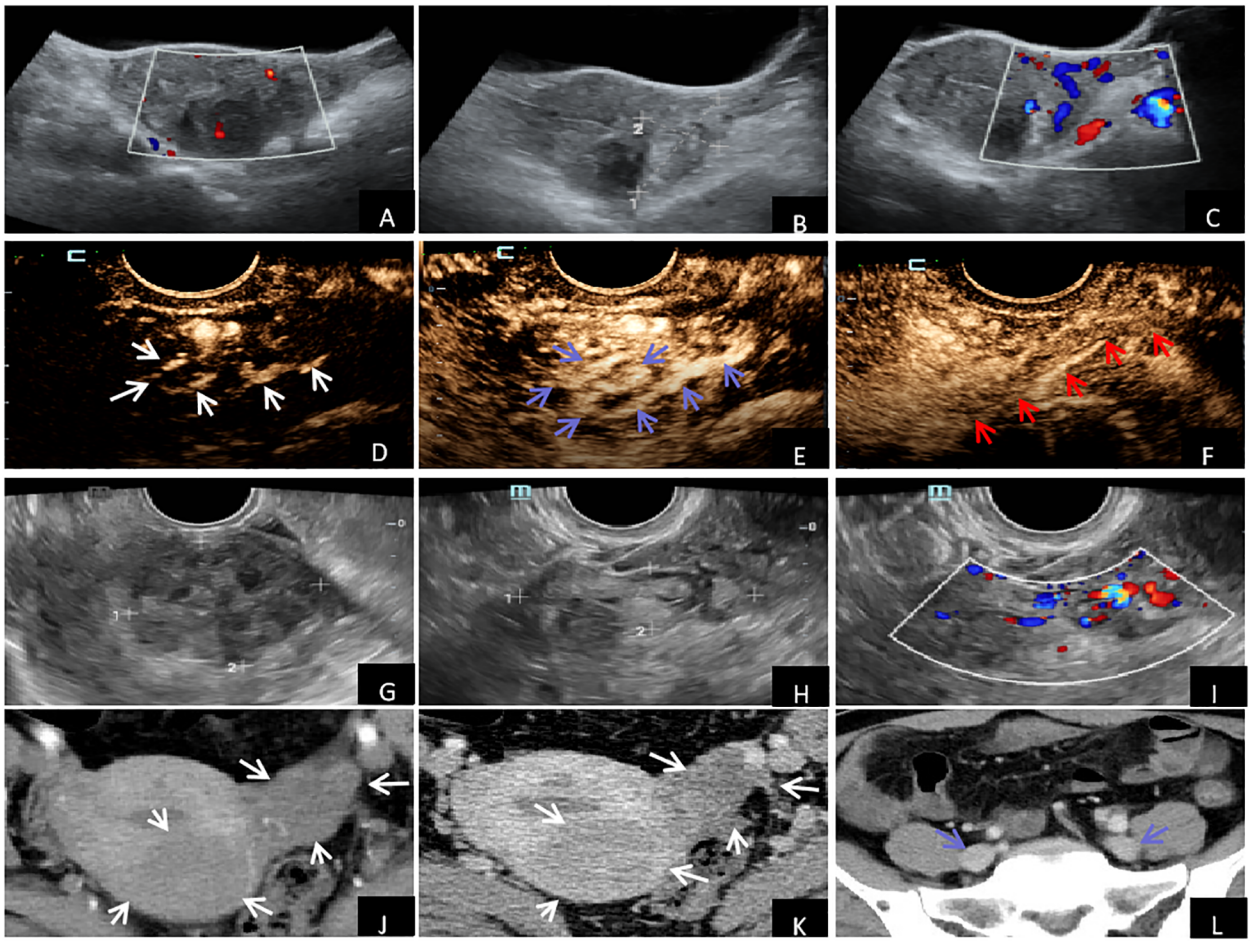

FIGURE 1
Imaging examination: **(A–C)** Conventional ultrasound examination showed uterine fibroids in the posterior wall, enhanced gyrus mass in the left adnexal area, and tortuous flow signals detected by CDFI. **(D–F)** CEUS showed synchronous and rapid hyperenhancement in the early stage of the arterial mass with enhanced echo in the left adnexal area (white arrow). During the peak stage, the interior enhancement exhibited irregularities resembling the shape of an earthworm (blue arrow). During the venous phase, the lesion exhibited reduced enhancement (hypoenhancement), whereas the outside vessel wall displayed uniform and intensified enhancement (hyperenhancement) (red arrow). **(G–I)** Vaginal ultrasound showed leiomyoma in the posterior wall of the uterus, with cord-like isoecho in the left adnexal area and tortuosity of blood flow signals detected by CDFI. Contrast-enhanced CT of the chest and abdomen of **(J–L)** showed uterine enlargement and leiomyomas in the uterus's posterior and left lateral walls (white arrows). There were no anomalies observed in the iliac vein (blue arrow).

mentioned that IVL is an atypical intermediary stage between benign and malignant uterine smooth muscle tumors; however, no cases of malignancy have been documented. The cause of IVL is still unclear. Research has indicated a correlation between IVL and elevated levels of estrogen in patients. This condition predominantly affects women who have not yet reached menopause, particularly those with a reproductive history and uterine fibroids (3). There are two views on the mechanism of histological origin of IVL (4, 5). One suggests that it arises from the smooth muscle tissue of the vascular wall. In contrast, the other indicates that it develops from the uterine leiomyoma or myometrium and can aggressively infiltrate nearby venous vessels and spread to distant areas. The patients have been confirmed to have myometrium intravenous vascular leiomyoma and left ovarian intravenous leiomyoma by pathological and immunohistochemical analysis. This suggests that the IVL originated from the uterine fibroids, supporting the second perspective. Some studies have confirmed that phosphoproteome is involved in the inhibition of leiomyoma cell apoptosis and cell proliferation, emphasizing the role of phosphoproteome in leiomyoma growth, which may open up new ideas for the drug treatment of uterine leiomyoma and venous leiomyoma (6).

Early detection and correct diagnosis of IVL are essential for the choice of surgical methods and the prognosis of patients. However, IVL itself has no specific clinical manifestations and is easily ignored because it is often complicated due to the presence of uterine fibroids (3). Early IVL extension occurs within the muscular layer of small blood vessels. It is challenging to detect through imaging examinations. However, in some cases, the tumor may spread to the inferior vena cava and right atrium, or it may be observed during pelvic surgery when a worm-shaped tumor involving the broad ligament is found (7). Correct preoperative diagnosis depends on a large amount of information, especially comprehensive imaging examination. Some scholars tend to

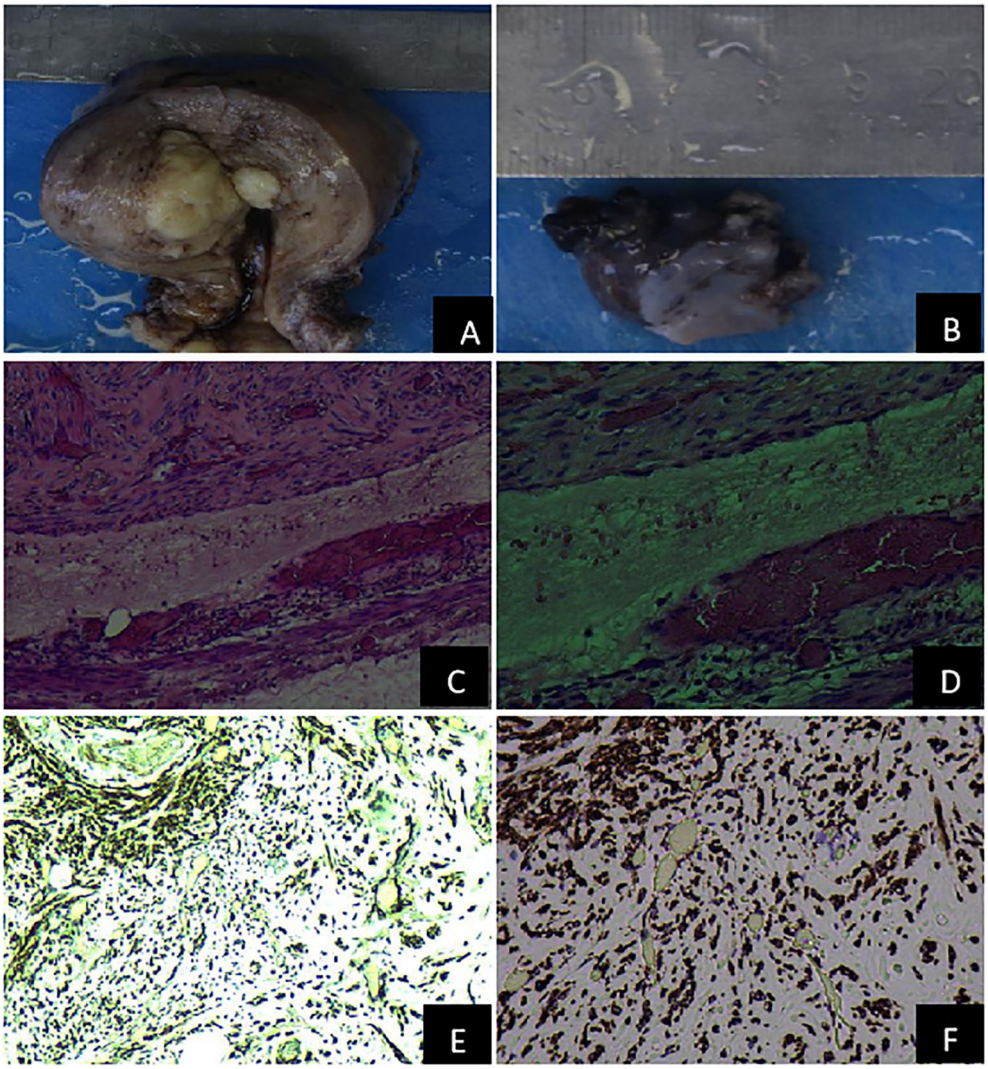

FIGURE 2
Pathological features of the uterus and the left adnexal mass. **(A)** Gross specimen of the uterus; **(B)** Gross specimen of the left adnexa; **(C)** The pathological examination of venous leiomyoma (H&E 100×); **(D)** The pathological assessment of venous leiomyoma (H&E 200×); **(E)** The immunohistochemical detection of intravenous leiomyoma (Desmin 100×); **(F)** The Immunohistochemical identification of intravenous leiomyomas (Desmin 200×).

recommend advanced chest and abdominal CT, gynecological ultrasound, and MRI as better monitoring methods according to different clinical conditions (8), but it is difficult to differentiate ovarian malignant tumors by imaging diagnosis alone. It is especially difficult to differentiate from uterine sarcoma, which usually lacks specific imaging features and is diagnosed as a presumed benign leiomyoma after hysterectomy or myomectomy. In fact, distinguishing between these diagnoses requires surgical exploration and pathological analysis of resected specimens, which undoubtedly increases the difficulty of leiomyoma treatment and standardized management (9).

IVL was found in the left ovarian vein in the present case. Doppler flow imaging revealed tortuous venous blood flow signals and conventional ultrasound detected an enhanced echogenic mass in the left adnexal area that was not separated from the left lateral wall of the uterus. A transvaginal ultrasound revealed a long tube with isoecho in the left adnexal region, some of which appeared tortuous into clusters. Doppler flow imaging demonstrated tortuous blood flow signals and evaluated the spectrum of venous blood flow. The ultrasound findings mentioned above were in accordance with the information documented in the literature (5). Hence, it is crucial to carefully observe this phenomenon while utilizing traditional ultrasound for physical or screening examinations. This will help distinguish it from ovarian malignant tumors and enhance the early detection rate of IVL. While conventional ultrasonography effectively identifies the site of pelvic veins, it typically struggles to detect minor lesions. Additionally, the limited sensitivity of color Doppler ultrasound prevents the display of lesions in blood perfusion during diagnosis. CEUS provides good visualization of tiny blood vessels and tissue perfusion, compensating for conventional ultrasound's limitations. IVL CEUS has distinct characteristic manifestations. During the arterial phase, the

lesions exhibited fast enhancement, marked by worm-like hyperenhancement. The edge of the lesions displayed a linear and heterogeneous hypoenhancement, with the flowing movement of microbubbles from the edge into the interior. During the venous phase, the lesions decreased in size gradually, exhibiting heterogeneous hypoenhancement. The peripheral wall of the blood vessels displayed homogeneous hyperenhancement, and a marginally thin linear hypoenhancement was observed parallel to the hyperenhancement of the vessel wall. These features are consistent with literature reports (10). Hence, it is crucial to carefully observe this phenomenon during ultrasonographic examination to distinguish it from ovarian malignant tumors and enhance the rate of early IVL diagnosis. In addition, pelvic varicose vein is a gynecological condition that ultrasound can detect. It appears as elongated tubular structures with a worm-like appearance and hypoechogenicity. Blood flow can be observed, except in cases where there is thrombosis. CEUS without the use of contrast agents and IVL can be employed to confirm the presence of thrombosis. Ultrasonography, when compared to enhanced CT and MRI (11, 12), may be helpful for the preoperative diagnosis of IVL. Still, they require longer duration and are associated with the risk of contrast agent allergy, thus limiting their early detection value. Ultrasonic imaging technology is a reliable and safe way of noninvasive radiography and has become the preferred option for screening and diagnosing gynecological diseases. Therefore, improving the understanding of IVL ultrasound imaging is crucial for detecting IVL lesions at an early stage (12, 13). Using CEUS, along with its various features, such as enhancement time, mode, level, and morphology, can significantly improve the comprehension and diagnostic accuracy of IVL (10, 14). This has crucial clinical implications for early intervention and prognosis of IVL.

Ma et al (15) suggested employing echocardiography and CT scanning to evaluate the advancement of intravascular tumors in IVL, provide insight into the preoperative progress of IVL, and aid in developing treatment strategies. Stage I: Disease limited to the pelvic region; Stage II: Lesions present in the iliac vein or inferior vena cava; Stage III: The tumor has invaded the right atrium or ventricle; Stage IV: Cancer has spread to the pulmonary artery. The primary intervention for IVL is surgery; however, there has been ongoing debate on the optimal surgical approach. Depending on the patient's health, there are two options for surgery: one-stage surgery and two-stage surgery. In severe instances, multidisciplinary collaboration is necessary (15, 16). Given that IVL is a hormone-dependent tumor because of its positive expression of estrogen and progesterone receptors, total hysterectomy (TH) with bilateral oophorectomy (TH-BSO) were previously recommended as the primary surgical approach (17). Moreover, some scholars have shown that compared with transabdominal tumor resection, laparoscopic tumor resection has a variety of benefits, including reducing blood loss, shortening hospital stays, reducing postoperative analgesia needs, and the incidence of complications is not significantly increased (18). Therefore, laparoscopic surgery can be considered as the best treatment for early IVL. However, it depends on the early detection of IVL and making the correct diagnosis. During a regular physical examination, a mixed echoic mass was noticed in the left adnexa of the patient, in the present case study. Based on this finding, it was determined that the mass was an ovarian venous leiomyoma using CEUS. Following a 6-month observation, there was no notable alteration in the lesion. Subsequently, the patient had TH-BSO, and it was determined that the lesion was an ovarian venous leiomyoma. This case shows that transvaginal ultrasound and CEUS technology have great potential in the early detection of this disease, which is consistent with some other researchers who believe that CEUS has higher diagnostic accuracy (14). This significant finding offers novel imaging concepts for the preoperative diagnosis of IVL and warrants further investigation. Simultaneously, sonographers and gynecologists must enhance their understanding of the clinical significance of IVL and ultrasound technology. They should remain attentive in their clinical practice to improve the rate of early diagnosis for IVL.

This case resolved the deadlock on the challenging nature of making a definitive preoperative diagnosis of early IVL based on clinical symptoms and imaging analysis. It introduced a novel imaging approach for diagnosing early IVL. Nevertheless, this case has few limitations since it is subject to the inherent constraints of case reporting. Initially, a comprehensive analysis of imaging pictures of this uncommon ailment, clinical manifestations, and pathological characteristics was not conducted systematically. Furthermore, the patient was monitored briefly, and the outcome in the long run remained uncertain.

Conclusions

IVL is an uncommon and distinctive tumor, histologically benign but exhibiting malignant biological behavior. Early identification and precise assessment of IVL are essential for choosing suitable surgical methods and evaluating patient prognosis. In this case, conventional ultrasound facilitated early detection of IVL, subsequently confirmed through CEUS examination, leading to a successful surgical intervention. This case highlights the diagnostic significance of ultrasound technology in this uncommon condition and presents a new method for preoperative diagnosis of IVL.

Data availability statement

The original contributions presented in the study are included in the article/supplementary material. Further inquiries can be directed to the corresponding author.

Ethics statement

Written informed consent was obtained from the individual(s) for the publication of any potentially identifiable images or data included in this article.

Author contributions

LL: Data curation, Formal analysis, Resources, Supervision, Validation, Writing – review & editing. JL: Methodology, Resources, Supervision, Validation, Writing – original draft, Writing – review & editing.

Funding

The author(s) declare financial support was received for the research, authorship, and/or publication of this article. Funding for this work was provided by Sichuan Medical Association Orthopaedics (Shang Antong) Scientific Research Special Project (Project No.: 2023SAT18).

Conflict of interest

The authors declare that the research was conducted in the absence of any commercial or financial relationships that could be construed as a potential conflict of interest.

Publisher's note

All claims expressed in this article are solely those of the authors and do not necessarily represent those of their affiliated organizations, or those of the publisher, the editors and the reviewers. Any product that may be evaluated in this article, or claim that may be made by its manufacturer, is not guaranteed or endorsed by the publisher.

References

1. Liu HY, Xu JG, Zhang CX. The optimal diagnosis and treatment of intravenous leimyomatosis. *Cardiovasc J Afr*. (2023) 34:44–7. doi: 10.5830/CVJA-2022-002

2. Ordulu Z, Nucci MR, Dal Cin P, Hollowell ML, Otis CN, Hornick JL, et al. Intravenous leiomyomatosis: an unusual intermediate between benign and Malignant uterine smooth muscle tumors. *Mod Pathol*. (2016) 29:500–10. doi: 10.1038/modpathol.2016.36

3. Peng J, Zhong F, Zhu Y, Zhang M, Zhang M, Lu C, et al. Clinical analysis of uterine intravenous leiomyomatosis: A retrospective study of 260 cases. *J Obstet Gynaecol Res*. (2021) 47:4357–64. doi: 10.1111/jog.15013

4. Lu B, Liu Q, Tang L, Ma Y, Shi H. Intravenous leiomyomatosis: molecular analysis of 17 cases. *Pathology*. (2020) 52:213–7. doi: 10.1016/j.pathol.2019.10.009

5. Tang L, Lu B. Intravenous leiomyomatosis of the uterus: A clinicopathologic analysis of 13 cases with an emphasis on histogenesis. *Pathol Res Pract*. (2018) 214:871–5. doi: 10.1016/j.prp.2018.04.011

6. Ura B, Monasta L, Arrigoni G, Battisti I, Licastro D, Di Lorenzo G, et al. Phosphoproteins involved in the inhibition of apoptosis and in cell survival in the leiomyoma. *J Clin Med*. (2019) 8:691. doi: 10.3390/jcm8050691

7. Kuklik E, Drelich-Zbroja A, Kuczyńska M, Szmygin M, Grzycka-Kowalczyk L, Jargiełło T. Intravenous leiomyomatosis as an unusual cause of the misdiagnosis of deep vein thrombosis. *Pol Arch Intern Med*. (2021) 131:75–7. doi: 10.20452/pamw.15654

8. Su Q, Zhang X, Zhang H, Liu Y, Dong Z, Li G, et al. Intravenous leiomyomatosis of the uterus: A retrospective single-center study in 14 cases. *BioMed Res Int*. (2020) 2020:9758302. doi: 10.1155/2020/9758302

9. Giannini A, Golia D'Augè T, Bogani G, Laganà AS, Chiantera V, Vizza E, et al. Uterine sarcomas: A critical review of the literature. *Eur J Obstet Gynecol Reprod Biol*. (2023) 287:166–70. doi: 10.1016/j.ejogrb.2023.06.016

10. Ma H, Niu Y, Yang Z, Zheng M. Echocardiographic characteristics and contrast-enhanced imaging of intravenous leiomyomatosis with intracardiac extension. *J Ultrasound Med*. (2022) 41:1101–8. doi: 10.1002/jum.15799

11. Sun R, Guan H, Li H, Bai Y, Wang F, Li C. Computed tomography evaluation of extensive intravenous angioleiomyoma: a case report. *BMC Med Imaging*. (2020) 20:13. doi: 10.1186/s12880-020-0417-2

12. Wang H, Nie P, Chen B, Hou F, Dong C, He F, et al. Contrast-enhanced CT findings of intravenous leiomyomatosis. *Clin Radiol*. (2018) 73:503.e1–6. doi: 10.1016/j.crad.2017.12.016

13. Jalaguier-Coudray A, Allain-Nicolai A, Thomassin-Piana J, Villard-Mahjoub R, Delarbre B, Rua S, et al. Radio-surgical and pathologic correlations of pelvic intravenous leiomyomatosis. *Abdom Radiol (NY)*. (2017) 42:2927–32. doi: 10.1007/s00261-017-1225-1

14. Ge Z, Wang Y, Wang Y, Li W, Yang X, Li J, et al. Diagnostic experience of intravenous leiomyomatosis with emphasis on conventional ultrasonography imaging: a single-center study. *Front Oncol*. (2023). doi: 10.3389/fonc.2023.1203591

15. Ma G, Miao Q, Liu X, Zhang C, Liu J, Zheng Y, et al. Different surgical strategies of patients with intravenous leiomyomatosis. *Med (Baltimore)*. (2016) 95:e4902. doi: 10.1097/MD.0000000000004902

16. Tan Y, Han J, Wang Z, Yan J, Dong L, Liu R. Different clinical diagnosis end up in the same pathological diagnosis of intravascular leiomyomatosis: Two case reports. *Med (Baltimore)*. (2024) 103:e36887. doi: 10.1097/MD.0000000000036887

17. Li B, Chen X, Chu YD, Li RY, Li WD, Ni YM. Intracardiac leiomyomatosis: a comprehensive analysis of 194 cases. *Interact Cardiovasc Thorac Surg*. (2013) 17:132–8. doi: 10.1093/icvts/ivt117

18. Giannini A, Cuccu I, D'Auge TG, De Angelis E, Laganà AS, Chiantera V, et al. The great debate: Surgical outcomes of laparoscopic versus laparotomic myomectomy. A meta-analysis to critically evaluate current evidence and look over the horizon. *Eur J Obstet Gynecol Reprod Biol*. (2024) 297:50–8. doi: 10.1016/j.ejogrb.2024.03.045

frontiers | Frontiers in Oncology

TYPE Case Report
PUBLISHED 29 October 2024
DOI 10.3389/fonc.2024.1380717

Check for updates

OPEN ACCESS

EDITED BY
Ferdinando Agresta,
ULSS2 Marca Trevigiana, Italy

REVIEWED BY
Antonella Marrocco,
National Institute for Insurance against Accidents at Work (INAIL), Italy
Pedro Guerra-Canchari,
National University of San Marcos, Peru

*CORRESPONDENCE
Liang Bu
thoracicsurgeon@vip.sina.com

RECEIVED 02 February 2024
ACCEPTED 24 September 2024
PUBLISHED 29 October 2024

CITATION
Huang L, Chen C, Sun Q, Yu Z, Wang X, Wang X, Yang S, Jin L and Bu L (2024) Primary hepatoid adenocarcinoma of the lung in patient with silicosis: a case report and literature review. *Front. Oncol.* 14:1380717. doi: 10.3389/fonc.2024.1380717

COPYRIGHT
© 2024 Huang, Chen, Sun, Yu, Wang, Wang, Yang, Jin and Bu. This is an open-access article distributed under the terms of the Creative Commons Attribution License (CC BY). The use, distribution or reproduction in other forums is permitted, provided the original author(s) and the copyright owner(s) are credited and that the original publication in this journal is cited, in accordance with accepted academic practice. No use, distribution or reproduction is permitted which does not comply with these terms.

Primary hepatoid adenocarcinoma of the lung in patient with silicosis: a case report and literature review

Lipeng Huang, Chaoyang Chen, Qingyu Sun, Zhichen Yu, Xiaoyan Wang, Xinle Wang, Shuoqi Yang, Luming Jin and Liang Bu*

Department of Thoracic Surgery, Xiang'an Hospital of Xiamen University, Xiamen, Fujian, China

Introduction: Hepatoid adenocarcinoma of the lung (HAL) is a special type of adenocarcinoma originating from the lung with adenoid- and hepatocyte-like differentiation. HAL is rare in clinical practice. Here, we present the case of a patient with HAL.

Case presentation: A 59-year-old man was admitted to the hospital 4 days because of lung mas observed. Chest computed tomography (CT) revealed a lobulated mass shadow in the right lower lobe, approximately 3.5 × 3.3 cm in size. CT-guided percutaneous biopsy of the right lower lung was performed. The pathological results indicated a moderately to poorly differentiated adenocarcinoma. The patient underwent thoracoscopic right middle and lower lobectomy and systematic lymph node dissection. The postoperative pathology was primary HAL, with the staging of T2bN2M0 (stage III A). Recurrence-free survival and overall survival were 6 and 19 months, respectively Preoperatively, the level of alpha-fetoprotein was negative; however, after recurrence, it increased to 87.8.

Conclusion: Pulmonary hepatoid adenocarcinoma is a rare subtype of malignant lung tumor, combined silicosis is more rare. Early surgical intervention can benefit patients in the early stages of the disease, whereas chemotherapy remains the main systemic treatment modality for postoperative and advanced stages. With the increasing popularity of genetic testing, it is important to focus on improving genetic examination.

KEYWORDS

hepatoid adenocarcinoma, lung malignancy, silicosis, lung metastasis, genetic testing

Introduction

Hepatoid adenocarcinoma (HAC) is a rare α-fetoprotein (AFP)-producing tumor with morphological similarities to hepatocellular carcinoma, characterized by eosinophilic cytoplasm, central nuclei, and tumor cells proliferating in a trabecular pattern, expressing AFP, HepPar1, HEA125, and MOC31 (1). In approximately 5% of HAC cases, the lung is the primary site of disease (1). HAC can metastasize to the brain, liver, adrenal glands, lymph nodes, and bones, with several cases reported. For patients with unresectable HAC, the prognosis is generally poor, with an overall survival of 6 to 11 months. This study reports a rare case of primary HAL complicated with silicosis and discusses the associated literature, including genetic information and comparisons with other case. A total of 94 cases of primary pulmonary hepatoid adenocarcinoma reported in July 2021 were collected from the literature. Another scholar collected 78 cases from the Surveillance, Epidemiology, and End Results (SEER) database for analysis and reporting.

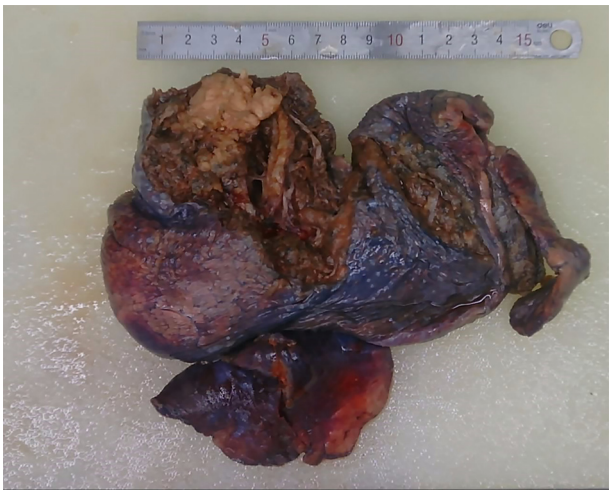

FIGURE 1
Specimen after surgery.

Case presentation

A 59-year-old man was admitted to the hospital because of "cough 4 days." Chest computed tomography (CT) revealed a lobulated mass in the lower lobe of the right lung, approximately 3.5 × 3.3 cm in size. The mass had multiple burrs with rough edges, local bronchial truncation, CT value of approximately 48–58 HU on plain scan, and inhomogeneity after enhancement. The CT values were 90, 79, and 60 HU in the arterial, venous, and delayed phases, respectively. The patient had silicosis 20 years and smoking 30 years. CT-guided percutaneous biopsy of the right lower lung was performed before the operation. The pathological resulted adenocarcinoma. The immunohistochemical results of the tumor tissue were as follows: CK7 (partial +), TTF-1 (−), Ki-67 (about 30% +), napsin A (−), P504S (−), hepatocyte (partial +), Arg-1 (−), CK19 (+), CK20 (−), CDX-2 (+), p63 (−), Smur100 (−), GATA3 (small focus +), CK (+), CgA (−), Syn (−), and vimentin (−). According to the results of positron emission tomography–computed tomography (PET–CT), electronic gastroscope gastroscopy, electronic colonoscopy, and color Doppler ultrasonography of the hepatobiliary, pancreas, and spleen, we excluded the neoplastic lesions of other organs and considered the primary tumor of the lung. There were surgical indications and no obvious contraindications. The patient was treated with thoracoscopic right middle and lower lobectomy and systematic lymph node dissection. The postoperative specimens were sent for pathological examination.

1. Gross specimen description: The lung lobe size was 16 × 10 × 3.5 cm; anastomotic nail length, 8 cm; bronchus broken end length, 1.2 cm; and tube diameter, 1.3 cm (Figure 1). The distance of the tumor from the pleura was 0.3 cm. The tumor that size 4.5 × 3 × 1.5 cm was from bronchial stump 3.5 cm, and no capsule, unclear boundary, gray–white section, and had medium texture.

2. Clinicopathology: The tumor cells showed eosinophilic cytoplasm, obvious nuclear atypia, pathological mitosis, necrosis, nesting, ethmoidal and tubular papilla (Figure 2). The diagnosis was as follows: hepatoid adenocarcinoma, tumor thrombus in the vessel, no cancer infiltration in the visceral pleura and bronchial incisal margin, and vitreous nodules in the parabronchial nodules. In addition, the group 7 lymph node was metastatic and the group 10 lymph node was normal. The level 2, 4, 8, 9, and 11 lymph nodes were found to have fibrous fat and necrotic vitreous tissue.

Tumor was not found on performing electronic colonoscopy and enteroscopy, and PET–CT examination before the operation did not show hypermetabolic shadow in the thyroid, liver, gallbladder, pancreas, stomach, or prostate. Hepatoid adenocarcinomas in the other organs were excluded and metastasized to the lung, which was diagnosed as primary HAL, with the clinical staging of pT2N2M0 (stage IIIA).

3. Immunohistochemical results: CK7 (+), CK20 (focal focus +), villin (+), napsin A (spot focus +), TTF-1 (−), CDX-2 (partial +), CD56 (−), PSA (−), CEA (+), Ki-67 (about 40% +), hepatocyte (partial +), GPC-3 (partial +), Arg-1 (−), D2-40 (−), and CD30 (−).

4. Gene test results: gene: *STK11*, mutation: exon1 c. 232A > T p. K78 *, abundance: 28.10%; gene: *TP53*, variation: exon5 c.395A > T p.K132M, abundance: 30.45%; gene: *FANCI*, variation: exon21 c.2058G > T p.Q686H, abundance: 22.78%; gene: *FLT4*, variation: exon17 c.2413C > A p.H805N, abundance: 28.75%. Gene: *NOTCH1*, variation: exon9 c.1543_1548del p.E515_C516del, abundance: 27.68%; tumor microsatellite instability (MSI): microsatellite stable (MSS); tumor mutation load (TMB): 8.6667 mutations/mb.

5. Follow-up results: The patient underwent thoracoscopic right middle and lower lobectomy and systematic lymph node dissection on October 15, 2019. He refused postoperative adjuvant treatment. Owing to cervical lymph node enlargement, the patient underwent cervical lymphadenectomy, and primary HAL recurrence accompanied by lymph node metastasis was confirmed on April 2, 2021. At the same time, the patient had symptoms of hemoptysis and signs of varicose veins in the neck, chest wall, and abdominal wall (Figure 3). Chest CT revealed a mass (11 × 8 × 10 cm in size) in the right hilum of the lung, enlargement of multiple mediastinal lymph nodes, and tumor invasion in the superior vena cava and right atrium (Figure 4). These findings were considered to indicate tumor

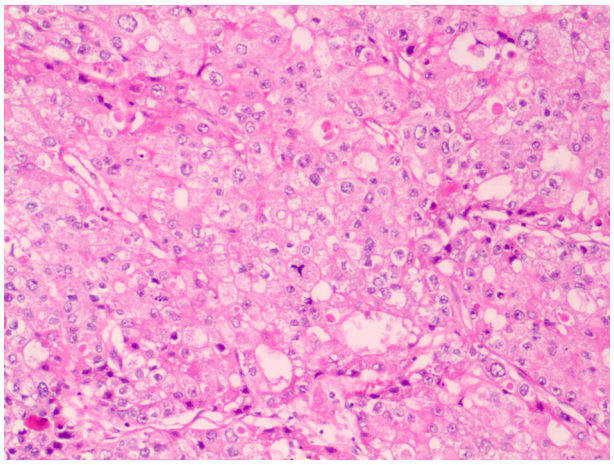

FIGURE 2
Pathological hematoxylin and eosin (HE) staining.

recurrence. However, no metastasis was observed in the liver, brain, bone, kidney, adrenal glands, or other organs. The alpha-fetoprotein (AFP) was 3.42 before the operation and 87.85 during the reexamination on March 12, 2021. The patient continued to refuse systemic antitumor therapy and eventually died on May 15, 2021.

Discussion

Hepatoid adenocarcinoma is a special type of adenocarcinoma that occurs outside the liver at sites whose morphology is similar to that of hepatocytes. The most common sites include the stomach (63%), ovary (10%), lung (5%), gallbladder (4%), pancreas (4%), and uterus (4%) (15). Primary HAL is relatively rare. It was first proposed by Ishikura in 1990 (16). Also, the history of silicosis has not yet been reported. In this study, we have reported a case of primary HAL complicated with silicosis. The disease characterization is likely to improve the awareness on HAL.

FIGURE 3
Secondary superficial venous varices in the patient after superior vena cava obstruction.

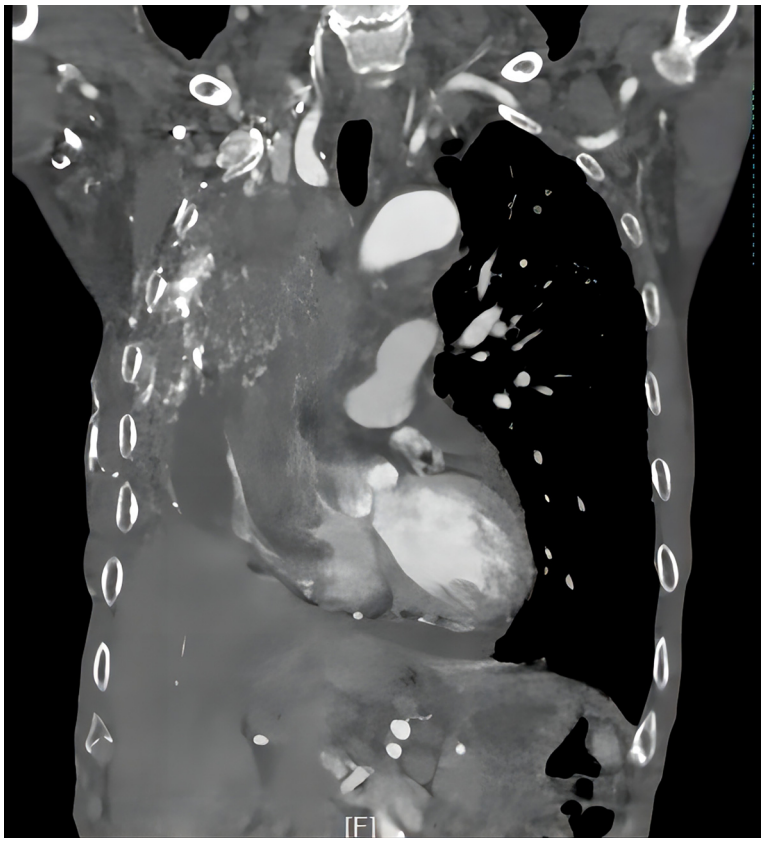

FIGURE 4
Tumor recurrence and invasion of the superior vena cava and right atrium.

1. Clinical case characteristics: The patient was admitted to the hospital for 4 days because of cough. Upon reviewing previous case reports, the clinical manifestations of HAL were found to be similar to those of common lung cancer, the symptoms of which include cough and expectoration, blood in the sputum, hemoptysis, and dyspnea. HAL may also be asymptomatic, depending on the location of the lesion and the stage of the disease. In this patient, the positive symptom was cough. Most patients with HAL have a history of smoking, and this patient also had smoking 30 years. In addition, he had a history of silicosis, which has not been reported in previous studies. Although the World Cancer Organization has identified quartz dust as a human carcinogen (17), there is no evidence to prove the correlation between silicosis and pulmonary hepatoid adenocarcinoma. The patient was found to have silicotic nodules in both lungs, which rendered our diagnosis and preoperative staging very difficult. We determined whether the nodules exhibited calcification on imaging and enhanced CT scan and also the F-fluorodeoxyglucose uptake value SUV_{max} on PET–CT. Based on the SUV_{av}, the nodules were determined to be benign rather than tumor in the lung. The postoperative pathology confirmed the accuracy of our preoperative evaluation.
2. Pathological characteristics: According to the diagnostic criteria of pulmonary hepatoid adenocarcinoma proposed by Haninger et al. in 2013 (1), the tumor component could be simple hepatoid adenocarcinoma or hepatoid adenocarcinoma with typical acinar or papillary adenocarcinoma, signet ring cell, or neuroendocrine carcinoma (2); the AFP and other hepatocyte differentiation markers are not necessary, and (3) adenocarcinoma with the same morphological features as hepatocellular carcinoma but not producing AFP is called AFP-negative pulmonary hepatoid adenocarcinoma. This patients tumor was 4.5 × 3 × 1.5 cm in size, had ill-defined boundaries, no capsule, and gray–white section with medium texture. Microscopically, the tumors were arranged in nests, cribriforms, and tubular papillae. The pathology met the diagnostic criteria for hepatoid adenocarcinoma. The immunohistochemical characteristics were as follows: CK5/6 (1/5), CK7 (3/5), CK19 (4/5), CK20 (1/5), HEA125 (5/5), MOC31 (5/5), CEA (3/5), and napsin A (1/5). AFP is a sensitive marker for hepatocellular carcinoma but is not expressed in some pulmonary hepatoid adenocarcinomas. The results of tumor immunohistochemistry in this patient were as follows: CK7 (+), CK20 (focal +), villin (+), napsin A (spot +), TTF-1 (−), CDX-2 (partial +), CD56 (−), PSA (−), CEA (+), Ki-67 (approximately 40%+), hepatocyte (partial+), GPC-3 (partial+), Arg-1 (−), D2-40 (−), and CD30 (−). The preoperative serology of AFP was negative but became positive after reexamination on March 12, 2021.

3. With the continuous in-depth research on targeted therapy and immunotherapy, the detection of tumor genes has become an important basis for treatment. Thus, we sequenced tumor-related genes in the pathological tissue of this patient, and the abnormally mutated genes detected were *STK11, TP53, FANCI, FLT4*, and *NOTCH1*. The tumor was of the MSS type, and the tumor mutational burden (TMB) was 8.6667 mutations/mb. The immunotherapy-related PD-1/PD-L1 gene was not expressed. Although we failed to detect clinical targeted therapy or immunotherapy-related mutation sites in this case, we further analyzed and explained the detected mutated genes in combination with previous studies. *STK11* is a tumor suppressor gene that encodes serine–threonine kinase 11 (LKB1) (18).According to the COSMIC database, the rate of STK11 gene mutation in lung adenocarcinoma samples was 7.6% (246/3235). In the present case, the mutation was nonsense mutation in exon 1 of the STK11 gene, which caused the original codon encoding lysine to become a stop codon. This mutation was predicted to induce protein function inactivation. Gene mutations were also observed in the cases reported by Sunhui et al. and accounted for 11% (2/17) of the cases reported in the literature (Table 1).

The tumor suppressor gene *TP53* was the most frequently mutated gene in pulmonary hepatoid adenocarcinoma, accounting for 29.4% (5/17). The COSMIC database reported that the mutation rate of the *TP53* gene in lung adenocarcinoma samples was 31.46% (973/3093). In the present case, the mutation was a missense mutation in exon 5 of the *TP53* gene, which was predicted to induce inactivation of the encoded protein.

FANCI encodes a FANC protein involved in DNA replication and DNA damage response, and certain deletion mutants are associated with increased risk of various cancers (19, 20). The COSMIC database reported that the mutation rate of the *FANCI* gene in lung adenocarcinoma samples was 0.8% (9/1124). The mutation was identified as a missense mutation in exon 21 of the *FANCI* gene. Nevertheless, the effect of this mutation on protein function has not yet been documented. The proto-oncogene *FLT4* encodes FMS-like tyrosine kinase-4, also known as vascular endothelial growth factor receptor 3 (Vegfr-3). Vascular endothelial growth factor C (Vegf-C) signaling via Flt-4 promotes lung adenocarcinoma invasion and metastasis of cancer cells (21). The COSMIC database reported that the mutation rate of the *FLT4* gene in lung adenocarcinoma samples was 2.84% (39/1375). The mutation was identified as a missense mutation in exon 17 of the *FLT4* gene. However, the effect of this mutation on protein function has not yet been reported.

NOTCH1 regulates cell differentiation, growth, proliferation, survival, and metabolism from embryonic development to adulthood (22). *NOTCH1* amplification or high protein expression is correlated with the tumor stage, grade, size, metastasis, and venous invasion (23, 24). The COSMIC database reported that the mutation rate of the *NOTCH1* gene in lung adenocarcinoma samples was 2.21% (44/1987). The mutation was identified as noncoding deletion mutation in exon 9 of the *NOTCH1* gene. At present, the effect of this mutation on the protein function is unknown, but the tumor has a strong ability for venous invasion, which appears to be related to this gene mutation. Immunotherapy was FDA-approved for the treatment of microsatellite instability-high or deficient mismatch repair solid tumors that have progressed during initial therapy or have no replacement therapy. The TMB detected in this case was 8.6667 mutation/mb, which is a low level, thereby suggesting that the effect is not ideal.

Another unusual phenomenon was that approximately 50% of conventional lung adenocarcinoma cases had somatic mutations in genes encoding proteins of the EGFR signaling pathway, such as K-RAS, EGFR, HER2, HER4, BRAF, and pik3ca (25). However, only one case reported by ChenHF et al. was positive for EGFR mutation; the rest were negative (16/17), the proportion of which was far lower than that of lung adenocarcinoma.

Based on the results of genetic testing, we did not find any sensitive genes for lung targeted therapy and immunotherapy, thus suggesting that this case may not be sensitive to the aforementioned therapies.

By reviewing previous case reports, we found that surgical resection was the main treatment for stage I–III pulmonary hepatoid adenocarcinoma, and platinum-based dual systemic antitumor therapy was the main treatment for stage IV. The patient in this case underwent thoracoscopic right middle and lower pulmonary resection and systematic lymph node dissection following complete preoperative examination. He was found to have cervical lymphadenopathy 6 months after the surgery and thus underwent superclavian lymph node resection. The patient was diagnosed with metastatic poorly differentiated carcinoma after the surgery, which indicated recurrence of pulmonary hepatoid adenocarcinoma with lymph node metastasis. Liang Zhenzhen et al. (26) searched the SEER database and identified 78 cases of HAL in the United States from 2001 to 2016 for statistical analysis. Only six patients received surgical treatment, which was less than that reported in the literature.

4. Prognosis and follow-up: According to literature reports, the 1-, 2-, and 5-year overall survival (OS) rates of 68 patients were 29.38%, 14.39%, and 5.88%, respectively, and the median survival time was 5 months (26). In another research, the 1-, 3-, and 5-year OS rates of 94 patients were 37%, 30%, and 15% for men and 63%, 63%, and 38% for women, respectively (27). Because most of the cases were reported at present, the statistical difference was large. The 1-year OS rates of patients who underwent surgery- and chemotherapy-based treatment strategies were 53% and 30%, respectively (27). The patient in this study only underwent surgical treatment. The postoperative stage was T2bN2M0 (stage III A), and the recurrence-free survival was 6 months. Six months after the operation, the patient underwent cervical lymphadenectomy owing to cervical lymphadenopathy, and the OS was 19 months. CheYQ et al. reported that their case showed extensive venous invasion. It was controlled by radiotherapy and chemotherapy, but then progressed and spread (28), which was very similar to this case. After recurrence in this patient,

TABLE 1 Previously reported cases on hepatoid adenocarcinoma of the lung (HAL) containing genetic information.

No.	Author	Year	Sex	Age	Smoking	Staging	Treatment	Gene	Immunohistochemistry	Metastasis	Prognosis (month)
1	Haninger (1)	2014	M	65	+	pT2aN0M1b(IVA)	Surgery+Chemotherapy	EGFR(−)	N/A	N/A	10
2	GavrancicT (2)	2015	M	64	−	CT2aN2M1(IV)	Chemotherapy+Targeted therapy	EGFR(−)	AFP(+),HepPar-1(+),CK7(+),Napsin-A (+),TTF-1(+),CK5(−),CK6(−),CK20(−).	Spinal, rib,lymphnode	11
3	Grossman Kate (3)	2016	M	54	+	cT3N0M1b(IVA)	Chemotherapy	ALK(−),EGFR(−),K-ras(−)	AHepPar-1(+),CK7(+),CAM5.2(CK8/18)(+),CEA(+),AFP(−),CK20(−),P63(−),CDX2(−),PSA(−),S-100(−),CgA(−),TTF-1(−)	Brain	3
4	BasseV (4)	2018	M	43	+	cTxN3M1c(IVB)	Chemotherapy+Immunitytherapy	EGFR(−),KRAS(−),ALK(−),ROS1(−),a loss of expression of mutL homolog 1 and PMS1 homolog 2	CK7(+),CK19(+),CK20(+),HepPar-1(+),CEA(+),TTF-1(+);PD-L1(−)	Brain, bone, adrenalglands	N/A
5	Barbara CD (5)	2019	M	63	N/A	N/A	Chemotherapy+Immunity therapy	EGFR(−),ALK(−)	N/A	Skin	7
6	Chen HF (6)	2019	M	53	−	pT3N0M0(IIB)	Surgery+Chemotherapy +Targeted therapy	EGFR p.L747_P753delinsS; EGFR exon 20 T790M mutation	ATTF-1(+),HepPar-1(+),AFP(+),CK(+),napsin A(−),CK5/6(−),P63(−),CD56(−),Syn(−)	N/A	36
7	EI Khoury A (7)	2019	M	50	+	cT4N2M1b(IVA)	Chemotherapy	EGFR(−),ALK(−),BRAFw/t.ROS-1(−),PDL1≥50%	CK7(+),HepPar-1(+),TTF1(−),CK5/6(−)	N/A	14
8	Kuan K (8)	2019	M	47	+	cT4N0M0(IIIA)	Surgery	EGFR(−),ALK(−),PDL1(high)	CK7(+),EMA(+),CEA(+),HepPar-1(+),TTF-1(−),napsin A(−),CK20(−),AFP(−)	N/A	N/A
9	Li J (9)	2019	M	71	−	cT3N3M1b(IVA)	Radiotherapy	EGFR,ALK,ROS1, PDL1,BRAF,HER2, KRAS,MET, RETWildtype;FAT1-Mutated, Copynumber loss; MSI;TMB-1.69mutations/mb	CK(+),SALL-4(+),CK18(+),CK8(+),CK7(+),AFP(+),HepPar-1(+),STAT-6(+),CD117(+),CK20(−),P63(−),P40(−),CK5/6(−),Syn(−),CD56(−),CgA(−),Vim(−),calretinin(−),TTF-1(−),napsin A(−),CD34(−),D240(−),ALK(−),PD-L1(−)	Bone	5.5
10	Wang C (10)	2019	M	70	+	cT3N2M0(IIIB)	Chemotherapy+Immunity therapy	TP53 mutation	HepPar-1(+),CK(+),EA(+),CDX-2(+),AFP(−),TTF-1(−),NapsinA(−),P63(−),P40(−),CD56(−),Syn(−)	N/A	9
11	WangXP (11)	2019	M	48	+	cT4N3M1a(IVA)	Chemotherapy	EGFR(−),ALK(−),ROS1(−),KRAS(−),BRAF(−)	AFP(+),HepPar-1(+),Arg-1(+),P40(−),CK5/6(−),P63(−),TTF1(−),ALK(−),CgA(−),Syn(−),CD56(−),PGP9.5(−),napsin A(−)	bone	12

(Continued)

10.3389/fonc.2024.1380717

TABLE 1 Continued

No.	Author	Year	Sex	Age	Smoking	Staging	Treatment	Gene	Immunohistochemistry	Metastasis	Prognosis (month)
12	Chen LL (12)	2020	F	65	–	pT4NxM1b(IVA)	Chemotherapy +Targetedtherapy+Immunitytherapy	ALK(−),EGFR(−), KRAS hotspot G12V (c.35G>T)mutation	ASALL4(+),AFP(+),GPC3(+),CK7(+), villin(+),TTF(−),napsin A(−),HepPar-1(−)	N/A	52
13	Wang W (13)	2020	M	41	–	N/A	Radiotherapy	EGFR and KRAS(−)	CK(+),CK7(+),PAS-AB(+),vimentin (+),hepatocyte(+),napsin A(−),TTF-1 (−),Ki-67(60%),CD56(−),CD31(−), desmin(−),ERG(−),HMB-45v,melan A (−),MiTF(−),S-100(−),SMA(−), STAT6(−)	N/A	12
14	Sunhui (14)	2021	M	66	+	N/A	Surgery	TP53 SMARCA4CDK8 EPHA5	CKpan(+);CK18(+);CK7(−);CK20(−); TTF1(−);napsin A(−);CGA(−);Syn(−); hepatocyte(−);AFP(+);glypican-3(+); SALL-4(+);SMARCA4(+)	N/A	46
15	Sunhui (14)	2021	M	64	–	N/A	Surgery	TP53 CDKN2A STK11 INPP4B	CKpan(+);CK18(+);CK7(+);CK20 (−) TTF1(−);napsin A(−);CGA(v);Syn(−); hepatocyte(+);AFP(−);glypican-3(−); SALL-4(+);SMARCA4(+)	N/A	26
16	Sunhui (14)	2021	M	64	–	N/A	Surgery	TP53 SMARCA4 CDK8 EPHA5	CKpan(+);CK18(+);CK7(+);CK20(−); TTF1(−);napsin A(+);CGA(−);Syn (−); hepatocyte(+);AFP(+);glypican-3 (−);SALL-4(+);SMARCA4(−)	N/A	23
17	Present case		M	59	+	pT2N2M0(IIIA)	Surgery	STK11,TP53,FANCI, FLT4,NOTCH1	CK7(+),CK20(+),villin(+),napsin A(+), TTF-1(−),CDX-2(+),CD56(−),PSA(−), CEA(+), Ki-67(40%+),hepatocyte(+), GPC-3(+),Arg-1(−), D2-40(−), CD30(−)	lymphnode	19

10.3389/fonc.2024.1380717

the tumor mainly invaded the lymph nodes and veins. In addition, it invaded the brachiocephalic and innominate veins as well as superior vena cava and extended down to the right atrium, occupying the right. A large amount of space in the atrium and severe signs of superior vena cava stenosis, manifested by jugular venous distention and extensive superficial trunk varicose veins. The patient eventually died 19 months after the operation. We considered two main causes of death: one was advanced tumor cachexia and the other was that the tumor invaded the right atrium and continued to progress and led to thrombosis, thus resulting in further mechanical obstruction.

In summary, pulmonary hepatoid adenocarcinoma is a rare subtype of malignant lung tumor, with few reported cases and no large-scale clinical trials; thus, to date, there are no standardized diagnosis and treatment plan. Early surgical intervention can benefit patients in the early stages of the disease, whereas chemotherapy remains the main systemic treatment modality for postoperative and advanced stages. With the increasing popularity of genetic testing, it is important to focus on improving genetic examination. If specific tumor-driving genes are identified through genetic testing, corresponding targeted therapies can be considered. Furthermore, it is expected that more genetic mutations of pulmonary hepatoid adenocarcinoma can be analyzed to provide an evidence for guiding chemotherapy, targeted therapy, and immunotherapy.

Data availability statement

The raw data supporting the conclusions of this article will be made available by the authors, without undue reservation.

Ethics statement

The studies involving humans were approved by Ethics Committee of Xiang'an Hospital, Xiamen University. The studies were conducted in accordance with the local legislation and institutional requirements. The participants provided their written informed consent to participate in this study. Written informed consent was obtained from the individual(s) for the publication of any potentially identifiable images or data included in this article.

Author contributions

LH: Writing – original draft. CC: Writing – review & editing. QS: Writing – review & editing. ZY: Writing – review & editing. XYW: Writing – review & editing. XLW: Writing – review & editing. SY: Writing – review & editing. LJ: Writing – review & editing. LB: Writing – review & editing.

Funding

The author(s) declare that no financial support was received for the research, authorship, and/or publication of this article.

Conflict of interest

The authors declare that the research was conducted in the absence of any commercial or financial relationships that could be construed as a potential conflict of interest.

Publisher's note

All claims expressed in this article are solely those of the authors and do not necessarily represent those of their affiliated organizations, or those of the publisher, the editors and the reviewers. Any product that may be evaluated in this article, or claim that may be made by its manufacturer, is not guaranteed or endorsed by the publisher.

References

1. Haninger DM, Kloecker GH, Bousamra Ii M, Nowacki MR, Slone SP. Hepatoid adenocarcinoma of the lung: report of five cases and review of the literature. *Mod Pathol.* (2014) 27:535–42. doi: 10.1038/modpathol.2013.170

2. Gavrancic T, Park YH. A novel approach using sorafenib in alpha fetoprotein-producing hepatoid adenocarcinoma of the lung. *J Natl Compr Canc Netw.* (2015) 13:387–91. doi: 10.6004/jnccn.2015.0054

3. Grossman K, Beasley MB, Braman SS. Hepatoid adenocarcinoma of the lung: review of a rare form of lung cancer. *Respir Med.* (2016) 119:175–9. doi: 10.1016/j.rmed.2016.09.003

4. Basse V, Schick U, Guéguen P, Le Maréchal C, Quintin-Roué I, Descourt R, et al. A mismatch repair-deficient hepatoid adenocarcinoma of the lung responding to Anti-PD-L1 durvalumab therapy despite no PD-L1 expression. *J Thorac Oncol.* (2018) 13:e120–2. doi: 10.1016/j.jtho.2018.03.004

5. Barbara CD, Felix GDR, Javier VB, Jose AF, Alberto JM. Review and case report: hepatoid adenocarcinoma of the lung treated with nivolumab metastatizing to the skin. *Eur J Clin Pharmacol.* (2019) 21:149–54.

6. Chen HF, Wang WX, Li XL, Xu CW, Du KQ, Zhu YC, et al. Hepatoid adenocarcinoma of the lung with EGFR mutation and the response to tyrosine kinase inhibitors. *J Thorac Oncol.* (2019) 14:e217–46. doi: 10.1016/j.jtho.2019.04.032

7. Khoury A EI, Khoury M EI, De Luca R. Immunotherapeutic approach to a case of advanced hepatoid adenocarcinoma of the lung. *MEMO.* (2019) 12:272–7.

8. Kuan K, Khader SN, El Hussein S. Hepatoid adenocarcinoma of the lung. *Diagn Cytopathol.* (2019) 47:831–3. doi: 10.1002/dc.24195

9. Li J, Qi H, Xu B, Zhao J, Gao H, Ma X, et al. Genomic profiles of a patient of pulmonary hepatoid adenocarcinoma with high AFP level: a case report. *Front Oncol.* (2019) 9:1360. doi: 10.3389/fonc.2019.01360

10. Wang C, Xu G, Wu G, Chen Z, Sun Z, Zheng P, et al. Hepatoid adenocarcinoma of the lung metastasizing to the gingiva. *Onco Targets Ther.* (2019) 12:8765–8.

11. Wang XP, Liu SS, Yang YX, Li XB, Yang J and Du H. Clinicopathologic characteristics of primary hepatoid adenocarcinoma of the lung. *Guangzhou Med.* (2019) 50:61–5.

12. Chen LL, Han X, Gao YJ, Zhao Q, Wang YS, Jiang Y, et al. Anti-PD-1 therapy achieved disease control after multiline chemotherapy in unresectable KRAS-positive hepatoid lung adenocarcinoma: a case report and literature review. *Onco Targets Ther*. (2020) 13:4359–64.

13. Wang W, Li G. Radiotherapy of pulmonary hepatoid adenocarcinoma with intrahepatic hemangioma: A case report. *Onco Targets Ther*. (2020) 13:11947–55.

14. Sun H, Li X, Zhang J, Liu Y. Clinicopathological features and genomicprofiles of hepatoid adenocarcinoma of the lung: report of four cases. *PatholRes Pract*. (2022) 229:153652. doi: 10.1016/j.prp.2021.153652

15. Metzgeroth G, Ströbel P, Baumbusch T, Reiter A, Hastka J. Hepatoid adenocarcinoma - review of the literature illustrated by a rare case originating in the peritoneal cavity. *Onkologie*. (2010) 33:263–9. doi: 10.1159/000305717

16. Ishikura H, Kanda M, Ito M, Nosaka K, Mizuno K. Hepatoid adenocarcinoma: a distinctive histological subtype of alpha-fetoprotein-producing lung carcinoma. *Virchows Arch A Pathol Anat Histopathol*. (1990) 417:73–180. doi: 10.1007/bf01600112

17. International Agency for Research on Cancer. *Silica, someili-cates, coal dust and para-aramid fibrils*. Geneva: IARC Monogreval Carcinog risks Hum. World Health Organization (1997). p. 475.

18. Shaw RJ, Bardeesy N, Manning BD, Lopez L, Kosmatka M, DePinho RA, et al. The LKB1 tumor suppressor negatively regulates mTOR signaling. *Cancer Cell*. (2004) 6:91–9. doi: 10.1016/j.ccr.2004.06.007

19. Naim V, Rosselli F. The FANC pathway and mitosis: a replication legacy. *Cell Cycle*. (2009) 8:2907–11. doi: 10.4161/cc.8.18.9538

20. Parmar K, D'Andrea A, Niedernhofer LJ. Mouse models of Fanconi anemia. *Mutat Res*. (2009) 668:133–40. doi: 10.1016/j.mrfmmm.2009.03.015

21. Su JL, Yang PC, Shih JY, Yang CY, Wei LH, Hsieh CY, et al. The VEGF-C/Flt-4 axis promotes invasion and metastasis of cancer cells. *Cancer Cell*. (2006) 9:209–23. doi: 10.1016/j.ccr.2006.02.018

22. Ntziachristos P, Lim JS, Sage J, Aifantis I. From fly wings to targeted cancer therapies: a centennial for notch signaling. *Cancer Cell*. (2014) 25:318–34. doi: 10.1016/j.ccr.2014.02.018

23. Zhou L, Zhang N, Song W, You N, Li Q, Sun W, et al. The significance of Notch1 compared with Notch3 in high metastasis and poor overall survival in hepatocellular carcinoma. *PloS One*. (2013) 8:e57382. doi: 10.1371/journal.pone.0057382

24. Zhu H, Zhou X, Redfield S, He Z, Lewin J, Miele L. Elevated expression of notch1 is associated with metastasis of human Malignancies. *Int J Surg Pathol*. (2013) 21:449–54. doi: 10.1177/1066896913496146

25. Ding L, Getz G, Wheeler DA, Mardis ER, McLellan MD, Cibulskis K, et al. Somatic mutations affect key pathways in lung adenocarcinoma. *Nature*. (2008) 455:1069–75.

26. Liang Z, Shen S, Li X. Clinical characteristics and prognostic factors of hepatoid adenocarcinoma of lung. *Henan Med Res*. (2020) 29:6372–5.

27. Mao JX, Liu C, Zhao YY, Ding GS, Ma JQ, Teng F, et al. Merged hepatopulmonary features in hepatoid adenocarcinoma of the lung: a systematic review. *Am J Transl Res*. (2021) 13:898–922.

28. Che YQ, Wang S, Luo Y, Wang JB, Wang LH. Hepatoid adenocarcinoma of the lung: presenting mediastinal metastasis without transfer to the liver. *Oncol Lett*. (2014) 8:105–10. doi: 10.3892/ol.2014.2064

frontiers | Frontiers in Oncology

TYPE Original Research
PUBLISHED 30 October 2024
DOI 10.3389/fonc.2024.1449936

Check for updates

OPEN ACCESS

EDITED BY
Ferdinando Agresta,
ULSS2 Marca Trevigiana, Italy

REVIEWED BY
Nektarios Koufopoulos,
University General Hospital Attikon, Greece
Giuseppe Angelico,
Agostino Gemelli University Polyclinic (IRCCS), Italy

*CORRESPONDENCE
Ruiqi Duan
duanxiaoyi2016@163.com

RECEIVED 16 June 2024
ACCEPTED 10 October 2024
PUBLISHED 30 October 2024

CITATION
Yu X, Duan R, Yang B, Huang L, Hou M and Qie M (2024) Perivascular epithelioid cell tumor of the uterus and pelvic cavity. *Front. Oncol.* 14:1449936. doi: 10.3389/fonc.2024.1449936

COPYRIGHT
© 2024 Yu, Duan, Yang, Huang, Hou and Qie. This is an open-access article distributed under the terms of the Creative Commons Attribution License (CC BY). The use, distribution or reproduction in other forums is permitted, provided the original author(s) and the copyright owner(s) are credited and that the original publication in this journal is cited, in accordance with accepted academic practice. No use, distribution or reproduction is permitted which does not comply with these terms.

Perivascular epithelioid cell tumor of the uterus and pelvic cavity

Xiuzhang Yu[1,2], Ruiqi Duan[1,2]*, Bowen Yang[1,2], Liyan Huang[3], Minmin Hou[1,2] and Mingrong Qie[1,2]

[1]Department of Obstetrics and Gynecology, West China Second University Hospital, Sichuan University, Chengdu, China, [2]Key Laboratory of Birth Defects and Related Diseases of Women and Children (Sichuan University), Ministry of Education, Chengdu, China, [3]Department of Pathology, West China Second University Hospital, Sichuan University, Chengdu, China

Background: Primary perivascular epithelioid cell tumors (PEComas) of the female reproductive tract have been primarily reported as case reports owing to their clinical rarity. Limited incidence rates and clinical case data hinder a comprehensive understanding of the risks and invasiveness of this disease. We discuss herein the diagnosis, treatment, and prognosis of this disease to enhance comprehension and therapeutic strategies.

Methods: We conducted a clinical analysis of patients with PEComa treated at the Gynecology Department of The West China Second University Hospital of Sichuan University between May 2018 and January 2024. Diagnosis and treatment were evaluated based on pertinent literature.

Results: Overall, eight patients (seven patients with tumors in the uterus and one patient with tumors in the pelvic cavity) were evaluated. One patient with PEComa of unknown malignant potential and two patients with malignant PEComa underwent hysterectomy and bilateral adnexectomy with or without adjuvant therapy and did not develop recurrence. Meanwhile, three patients who underwent lesion resection only exhibited radiological evidence of new lesions. Furthermore, postoperative imaging identified new pulmonary nodules in three patients.

Conclusion: Although the current criteria are generally effective in assessing the tumor invasiveness of PEComa, emphasizing the significance of complete lesion resection remains crucial. Inadequate treatment significantly increases the risks of recurrence and metastasis. Additionally, the prevalence of pulmonary metastases may have been underestimated. Refining risk stratification to prevent overtreatment of low-grade malignancies or overlooking highly aggressive tumors is an important area for further study.

KEYWORDS

perivascular epithelioid cell tumor, female reproductive system, surgical intervention, invasiveness, pulmonary metastasis

1 Introduction

Perivascular epithelioid cell tumor (PEComa) is an uncommon neoplasm encompassing angiomyolipoma, clear cell "sugar" tumor of the lung and extrapulmonary tissue, lymphangioleiomyomatosis, and nonspecific perivascular epithelioid cell tumor. These tumors are characterized by the World Health Organization as "mesenchymal neoplasms consisting of histologically and immunohistochemically distinct perivascular epithelioid cells." Nonspecific PEComa refers to a PEComa affecting various sites such as the uterus, vulva, rectum, thigh, pancreas, abdominal wall serous membrane, or heart. It occurs most frequently in the uterus, mostly in the uterine body, but a few cases in the cervix have also been reported. Owing to its clinical rarity, primary uterine or pelvic PEComa is mainly reported in the literature as case reports. This study discussed the diagnosis and treatment of this condition based on pertinent literature to enhance comprehension and therapeutic strategies. We performed a clinical analysis of patients with PEComa (seven patients with tumors in the uterus and one patient with a tumor in the pelvic cavity) treated at the Gynecology Department of the Gynecology Department of The West China Second University Hospital of Sichuan University between May 2018 and January 2024.

2 Materials and methods

2.1 Patient selection and pathologic examination

Patients diagnosed with uterine or pelvic PEComa who were admitted and treated at The West China Second University Hospital of Sichuan University between May 2018 and January 2024 were evaluated. Patients with missing data on clinical diagnosis or treatment were excluded. The diagnosis of PEComa was pathologically confirmed.

This study was approved by the institutional review board of the West China Second University Hospital and was conducted according to the tenets of the Declaration of Helsinki. Informed consent was obtained from all the patients.

2.2 Data collection and follow-up

General data, clinical manifestations, auxiliary examinations, pathological features, treatment modalities, and patient prognoses were reviewed and analyzed. The patients were followed up via telephone interviews until January 6, 2024.

3 Results

3.1 Patient characteristics

A 33-year-old female with a cervical PEComa visited our hospital for outpatient treatment. She underwent hysterectomy, bilateral adnexectomy, greater omentum resection, and pelvic lymph node dissection at an external hospital. However, this patient was excluded from this study owing to insufficient clinical follow-up data. A total of eight patients aged between 33 and 52 years were included. One patient experienced amenorrhea due to tuberculosis, while three patients were menopausal. Except for the patient with amenorrhea, all patients had a history of fertility. Five patients previously underwent uterine surgery, including myomectomy, cesarean section, and total hysterectomy (TH). Two patients also had breast nodules, and one patient had a history of breast cancer surgery and chemoradiotherapy. Initial symptoms included postmenopausal vaginal bleeding in one patient, vaginal discharge in two patients, pelvic masses in one patient, and abnormal uterine bleeding characterized by increased menstruation and irregular vaginal bleeding in four patients. The patient characteristics are presented in Table 1.

3.2 Clinicopathological features

Most of the lesions were located in the uterine body (6/8), including the submucosa (n=4), intermuscular wall (n=1), subserous membrane (n=1), submucosa in the lower segment of the uterine body and the junction of the cervical body (n=1), and the pelvic cavity (n=1 patient who had post-TH). The maximum tumor diameter range was1.6–7 cm. Among the eight patients, five patients had PEComa, one patient had PEComa of uncertain malignant potential (UMP), and two patients had malignant PEComa. The intraoperative frozen pathological examination results are presented in Table 2. Only one patient was diagnosed with PEComa intraoperatively. This patient initially underwent hysteroscopic lesion resection, with pathology indicating PEComa. A subsequent surgery was performed involving laparoscopic total hysterectomy and bilateral adnexectomy. Intraoperative frozen section analysis also suggested PEComa. The final postoperative pathology revealed PEComa of UMP.

All patients underwent immunohistochemical analysis of melanocytes and myogenic differentiation markers. Genetic testing for transcription factor E3 (TFE3) conducted in one patient showed no significant findings (Table 3). Pathological images are shown in Figures 1–4.

3.3 Diagnosis, treatment and prognosis

The follow-up period ranged from 9 months to 68 months, and all patients survived. None of the patients exhibited significant tuberous sclerosis symptoms. Among the five patients with PEComa, two patients underwent TH with bilateral adnexectomy. No signs of recurrence were observed in any patient during follow-up. A 46-year-old female was initially diagnosed with uterine fibroids and underwent a single-port laparoscopic myomectomy. An intraoperative frozen-section examination revealed a mesenchymal tumor. TH was not performed at the patient's family member's request to preserve the uterus. Recent B-mode ultrasonography at another hospital revealed a 2.3 cm×2.1 cm mass

TABLE 1 Clinical features of the patients.

Cases	Age	Meno-pausal	Fertility history	Medical and surgical history	Clinical presentation	Preoperative imaging examination
1	46	no	G4P1	cesarean section, cholecystectomy, breast nodules, hypothyroidism	increased menstruation	ultrasound: suspected uterine fibroids
2	48	no	G3P1	cesarean section; thyroid and breast nodules	irregular vaginal bleeding	CT: Mildly enhanced patchy soft tissue shadow in the uterus, with an unclear boundary between the soft tissue and the uterine wall muscle layer
3	51	yes	G2P2	TH for "multiple uterine fibroids"	the pelvic masses	ultrasound: suspected angioleiomyoma CT: multiple variable-sized nodules in both lungs
4	52	yes	G4P1	diabetes	vaginal discharge	ultrasound: rich blood flow signals detected in the mass
5	33	no	G0P0 (amenorrhea after contracting tuberculosis)	tuberculosis	vaginal discharge, uterine cavity occupancy	ultrasound: malignant lesions? CT: several small nodules in the right subpleural and interlobar regions
6	51	yes	G2P1	Myomectomy; surgery, chemoradiotherapy and targeted therapy for breast cancer	postmenopausal vaginal bleeding	MRI (a)
7	50	no	G3P2	Myomectomy	increased menstruation	ultrasound: submucosal myoma?
8	40	no	G4P1	ectopic pregnancy tubal resection surgery, cholecystectomy, diabetes	irregular vaginal bleeding	ultrasound: heterogeneous slightly strong echo

a. a nodular lesion measuring 1.5×0.7x1.6 cm in the anterior wall of the lower uterine segment. The T2WI signal exhibited high intensity, slightly lower than that of the endometrium, while the T1WI signal showed slightly higher intensity with restricted diffusion. The lesion involved more than half of the anterior wall muscle layer, demonstrating pronounced enhancement during early dynamic scans and mild enhancement in delayed scans.

occupying the uterine cavity. However, the patient opted not to undergo further treatment for personal reasons. A 33-year-old female underwent curettage and was diagnosed with PEComa. The patient opted for hysteroscopic lesion resection. Postoperative B-wave ultrasonography did not reveal any specific lesions. However, computed tomography (CT) during follow-up revealed an increase in the size of the subpleural nodules in the right lung to varying degrees. Additionally, multiple new nodular lesions were detected in both lungs, suggesting lung metastasis with possible involvement of the mediastinal and right hilar lymph nodes. Repeat B-ultrasound revealed a uterine mass measuring 5 cm, but the patient declined further treatment. One patient had previously undergone TH due to uterine fibroids. This visit was prompted by the discovery of a pelvic lobulated masses with individual lobes measuring 7 cm and 4 cm. The patient opted for bilateral oophorectomy and resection of the pelvic masses. Postoperative pathology confirmed the presence of PEComa. Whether the tumor was primarily peritoneal or related to the previous uterine fibroids remained unclear. During follow-up, B-mode ultrasound detected a 3.6×1.2×1.7 cm3 hypoechoic lesion in the left pelvic cavity. CT scans also revealed multiple nodules of varying sizes in both lungs, suggesting possible metastasis. The patient declined further treatment due to personal reasons.

One patient diagnosed with a PEComa of UMP underwent TH and bilateral adnexectomy. No signs of recurrence were observed on imaging. Two patients diagnosed with malignant PEComas underwent TH and bilateral adnexectomy without pelvic lymph node dissection. One patient underwent six cycles of epirubicin + ifosfamide chemotherapy. The other patient underwent 28 sessions of radiotherapy, one cycle of ifosfamide + adriamycin chemotherapy, and three cycles of paclitaxel + ifosfamide chemotherapy for possible lymph node metastasis, as evidenced by postoperative CT findings of lymph node enlargement in the right obturator region. No significant signs of recurrence on imaging were observed during follow-up (Table 4).

4 Discussion

Current research on the etiology of PEComa primarily focuses on the following (1–3): (1) mutations in tuberous sclerosis complex genes, primarily involving loss of function of the tuberous sclerosis complex 1/tuberous sclerosis complex 2 complex and resulting in increased activation of the mammalian target of rapamycin (mTOR) complex 1 and dysregulation of cell growth signals; (2) rearrangement of the TFE3 gene that may lead to carcinogenic

TABLE 2 Clinicopathological findings of the patients.

Cases	Tumor site	Diameter of lesion (cm)	Intraoperative frozen section pathological examination	Final pathological diagnosis	Other pathological diagnosis
1	subserosal	3	a mesenchymal tumor? an epithelioid smooth muscle tumor or a perivascular epithelioid cell tumor?	PEComa	leiomyoma
2	submucosal	Unknown	/	PEComa	adenomyosis of the uterus, simple endometrial hyperplasia, and complex endometrial hyperplasia
3	the pelvic cavity	7 + 4 (lobulated)	hyperplastic fibrovascular tissue with widespread infiltration of inflammatory cells	PEComa	/
4	intermuscular	1.8	/	PEComa	adenomyosis, leiomyoma
5	submucosal	5	extensive necrotic tissue with focal calcification and suspected granulomas, suggesting tuberculosis	PEComa	tuberculous changes (necrosis and granulomatous inflammation)
6	submucosal (in the lower segment of the uterine body and the junction of the cervical body)	1.6	PEComa (a)	PEComa of UMP	None
7	submucosal	5.3	the tumor predominantly exhibits epithelioid morphology, with visible mitotic figures (accurately counting the number of mitotic figures in frozen sections is difficult). Focal nuclear atypia is observed. Epithelioid leiomyoma is primarily considered, at least as epithelioid leiomyoma of uncertain malignant potential. Other tumors, such as PEComa and endometrial stromal tumors, also need to be excluded	malignant PEComa	multiple leiomyomas and adenomyosis
8	submucosal	4	/	malignant PEComa	leiomyoma

a. The patient initially underwent hysteroscopic lesion resection, with pathology indicating PEComa. A subsequent surgery was performed involving laparoscopic total hysterectomy and bilateral adnexectomy. Intraoperative frozen section analysis also suggested PEComa. The final postoperative pathology revealed PEComa of UMP.

activation by acquiring a strongly expressed promoter; and (3) rearrangement of the RAD51 paralog B gene or other rare gene fusions may play a role. Only one of the eight patients included in this study tested negative for TFE3. The etiology of PEComas remains unclear and requires further research.

PEComa of the female reproductive tract accounts for more than 25% of all PEComa cases, with uterine PEComa being the most prevalent, followed by PEComa affecting the cervix, vagina, broad ligament, round ligament, ovary, and vulva. PEComa can also occur in the pelvis after total or subtotal hysterectomy (4). Recurrence predominantly occurs in the lung, liver, abdomen, vagina, and lymph nodes (5, 6). Uterine PEComa can manifest across a broad age range, spanning from 6 years to 79 years, with a median age of 49 years at onset (5, 6). The clinical manifestations of PEComas lack specificity, and they commonly present as abnormal uterine bleeding, abdominal pain, and compression symptoms. In addition, some patients remain asymptomatic, with imaging revealing only a lower abdominal mass (7). Most tumors are located within the muscle layer. They typically manifest as solitary masses but occasionally occur as multiple masses that are either localized or invasive lesions, with an average diameter of 6.5 cm (range: 0.2–25.0 cm) (5). Some tumors may present with bleeding or necrosis, leading to potential misdiagnosis as uterine fibroids or uterine leiomyosarcoma. The eight patients in this study, aged 33–52 years, exhibited clinical symptoms including abnormal uterine bleeding, vaginal discharge, and pelvic masses. These symptoms are largely consistent with those in previous studies.

PEComa of the female reproductive tract lacks typical imaging manifestations, and it is difficult to make a diagnosis of PEComa before surgery based on imaging features; PEComa is easily misdiagnosed as uterine myoma or sarcoma. Most documented cases of uterine PEComas exhibit heterogeneous echogenicity and prominent central vascularity on ultrasound scans (8). All the patients included in this study underwent ultrasonography, and abundant blood flow signals within and around the masses were common findings, thereby providing valuable diagnostic indications. CT imaging in Patient 2 revealed mild enhancement of the soft tissue, although it was not distinctive. Magnetic resonance imaging provided superior visualization of the internal structure of the lesion, with significant enhancement observed on contrast uptake, offering valuable guidance. In Patient 6, magnetic resonance imaging revealed a nodular lesion measuring 1.5×0.7×1.6 cm in the anterior wall of the lower uterine segment. There was high signal intensity on T2WI, slightly lower than that in the endometrium.

10.3389/fonc.2024.1449936

TABLE 3 Immunohistochemical results of the patients.

Cases	HMB45	Melan-A	TFE3	S-100	Desmin	caldesmon	SMA	CD34	WT-1	Calponin	VIM	Calretinin	CyclinD1	ER	PR	ki67	Genes
1	–	+	/	–	+	–	/	blood vessel +	/	+	/	/	/	partial cells +	partial cells +	/	
2	/	+	/	–	+++	–	/	/	/	/	/	+	scattered cells+	+++	+++	4-5%	
3	++	+	/	/	+++	+++	++	–	/	+++	+++	/	/	++	++	2-3%	No meaningful TFE3 detected
4	focal +	+++	/	–	–	focal +	focal +	/	/	/	+++	/	/	–	–	3%	
5	+	focal +	/	–	/	–	–	/	/	/	partial cells +	/	/	–	+	20% (curettage), <10% (hysteroscopy)	
6	+++	focal +	/	–	–	–	–	/	/	/	/	/	+++	–	++	10%	
7	a few scattered cells +	+	+++	–	+++	focal +	weak +	–	+++	+++	/	focal +	scattered cells +	+++	+++	20%	
8	–	+	/	–	+	–	–	–	/	–	+	–	–	+	+	20%	

+ weak positive, ++ moderate positive, +++ strong positive, / not detected, - negative.

Meanwhile, the T1WI signal showed a slightly higher intensity with restricted diffusion. The lesion involved more than half of the anterior wall muscle layer and showed pronounced enhancement on early dynamic scans and mild enhancement on delayed scans. However, prior research has revealed significant disparities in magnetic resonance image characteristics (6). PEComas have the potential to metastasize to the lungs. CT imaging in this study revealed pulmonary nodules in multiple patients, including those with "benign" PEComa. Surgical intervention was even required in one patient, emphasizing the necessity of vigilance. However, this study did not acquire pathological evidence of pulmonary nodules, indicating the need for further observations in future studies.

PEComas are composed of epithelioid and spindle cells. A crucial morphological characteristic for diagnosing PEComas is the presence of delicate vascular channels surrounding tumor cells and nests, which are atypical for smooth muscle tumors (9). Microscopically, PEComa tumors exhibit rich vascularity with thin vessel walls. Tumor cells are arranged in lamellar or nest-like patterns around blood vessels, displaying polymorphic shapes such as polygonal, oval, circular, and spindle shapes. The cells have well-defined borders; abundant and delicate cytoplasm with granular, eosinophilic, oval, or round nuclei; visible nucleoli; and heterogeneous mitotic images. Other characteristics of smooth muscle tumors include perinuclear vacuoles and a diffuse eosinophilic cytoplasm. Immunohistochemically, the perivascular epithelioid cells express melanocyte and myogenic differentiation markers (10). The important melanin markers include human melanoma black 45 (HMB45), melan-A, melanocyte-inducing transcription factor, and cathepsin K. In uterine PEComa, PNL2 exhibits high specificity and sensitivity (11), however, there are variations in the types and expression levels of melanocyte markers reported across studies (12). Common myogenic markers include smooth muscle actin, desmin, and heavy calmodulin-binding proteins (caldesmon). Furthermore, malignant PEComas frequently demonstrate TP53, RB1, and ATRX inactivation (13). Other tumor types such as leiomyosarcoma may present with PEComa-like characteristics, necessitating the combination of various types of data, including genomic profiles, for diagnosis (14). Immunohistochemically (Table 3), all tumors were positive for HMB45 and/or melan-A (Figure 1). Additionally, the tumors were positive for at least one myogenic marker, with the positivity rate being the highest for desmin (5/8), followed by caldesmon (3/8), smooth muscle actin (3/8), and calponin (3/8). This finding is slightly different from those reported in previous studies (15). Furthermore, positivity rates for VIM (4/8) and cyclin D1 (3/8) were notably high. One patient with malignant PEComa tested positive for TFE3. Most patients were also positive for the estrogen receptor (5/8) and progesterone receptor (7/8) (Figure 1). Consideration of uterine PEComa as a hormone-dependent disease warrants further investigation. Studies have suggested a cross-interaction between the mTOR pathway and estrogen receptor signaling, where estrogen E2 binding to the receptor activates Akt/mTOR, thereby mediating PEComa resistance to mTOR inhibitors. Sanfilippo et al. retrospectively evaluated seven patients treated with a combination of an mTOR inhibitor (sirolimus) and an anti-estrogen therapy; the results showed

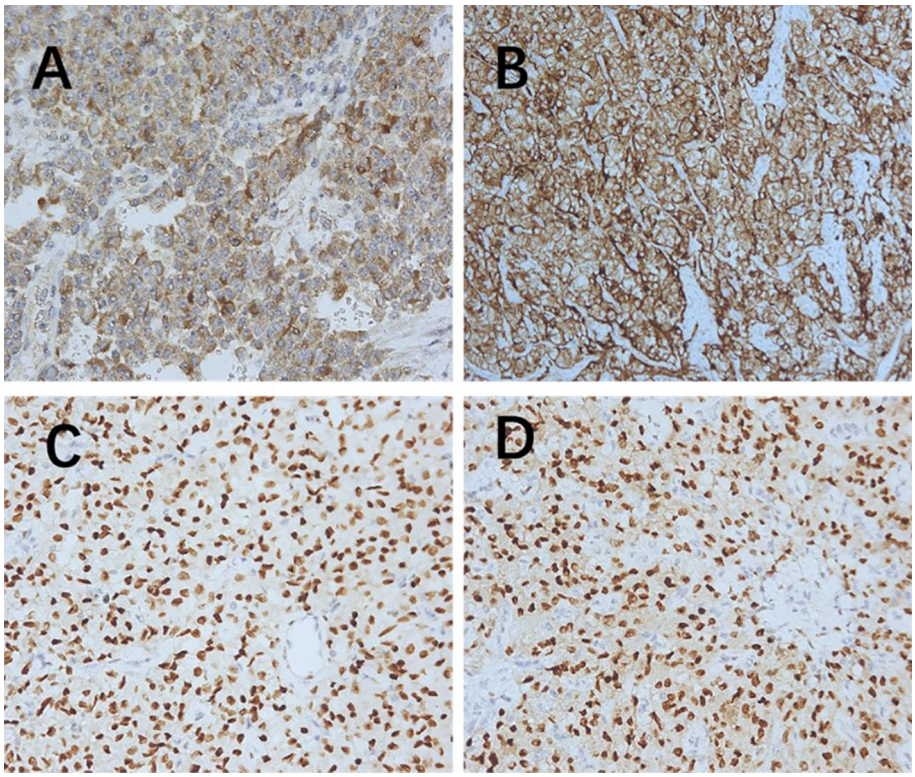

FIGURE 1
Immunohistochemistry (200× magnification). **(A)** Melanoma positive. **(B)** HMB45 positive. **(C)** Estrogen receptor positive. **(D)** Progesterone receptor positive. HMB45, human melanoma black 45.

significant clinical efficacy, with a disease control rate of 86% (16). Additionally, our study found that malignant tumors and PEComas of UMP exhibited high Ki67 values. This suggests a correlation between the Ki67 value and PEComa risk, as well as the degree of malignancy, warranting further investigation. The pathological differential diagnosis of PEComas of the uterus and pelvic cavity includes all mesenchymal neoplasms showing spindle and/or epithelioid cell features, such as smooth muscle tumors and endometrial stromal sarcomas. Compared with smooth muscle tumors, PEComas have key features of eosinophilic to clear cytoplasm, round to oval nuclei, a prominent capillary network, and strong immunoreactivity for melan-A, HMB45, melanocyte-inducing transcription factor, and cathepsin K. Furthermore, PEComas commonly stain negatively for epithelial membrane antigen and cytokeratin, unlike epithelioid smooth muscle tumors. Endometrial stromal sarcomas can resemble PEComas,

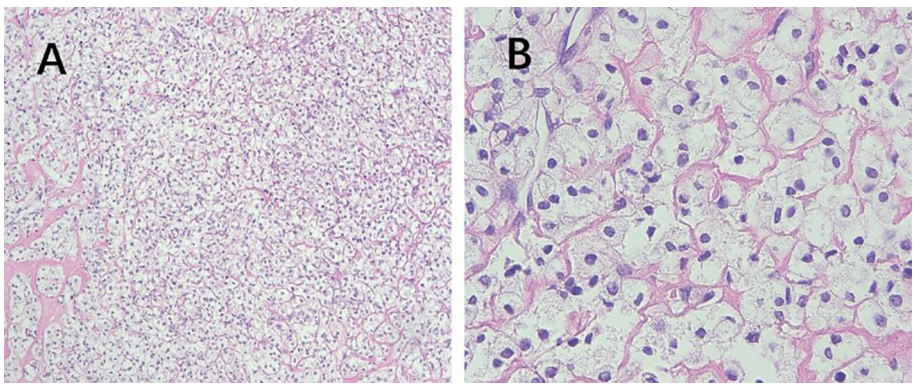

FIGURE 2
Pathological features of PEComa. **(A)** The epithelioid cells are arranged in nests or sheets, with clear cytoplasm, and delicate thin-walled small blood vessels are observed between the cell nests (100× magnification). **(B)** Absence of cell atypia, coagulative necrosis, or mitotic signs (400× magnification). PEComa, perivascular epithelioid cell tumor.

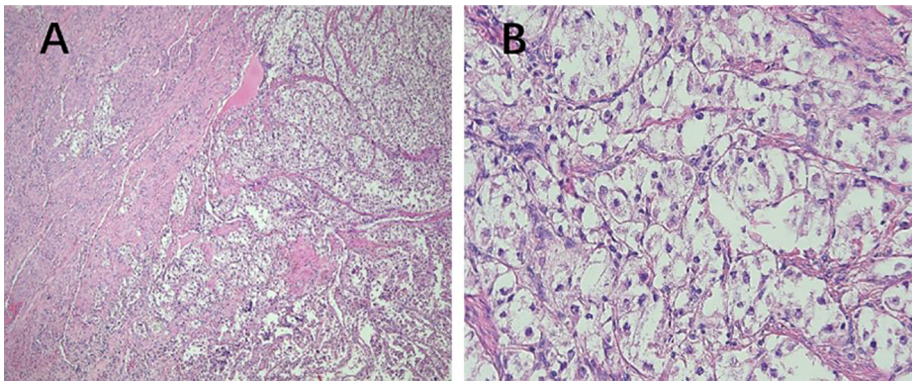

FIGURE 3
Pathological features of PEComa of UMP. **(A)** The tumor exhibits poorly defined borders, with no clear demarcation from the muscle layer (40× magnification). **(B)** The cells are arranged in nests, displaying clear cytoplasm with no evidence of cellular atypia (400× magnification). PEComa, perivascular epithelioid cell tumor; UMP, uncertain malignant potential.

particularly the epithelioid variants, because both tumors may exhibit similar infiltrative patterns within the myometrium. However, endometrial stromal sarcomas exhibit morphological features, such as endometrial involvement and stromal differentiation. Additionally, immunohistochemical markers such as CD10+, HMB45-, melan-A-, and melanocyte-inducing transcription factor help to differentiate them from PEComas (6).

In 2005, Folpe et al. proposed the following criteria to assess the risk level of PEComa (17), where two or more of the following criteria were required for malignant diagnosis: tumor diameter >5.0 cm, infiltration, high nuclear grade, mitotic count of >1 mitosis/50 mm^2, necrosis, and vascular invasion. A benign PEComa was considered if the following characteristics were found: tumor diameter <5 cm, non-infiltrative, non-high nuclear grade, mitotic count ≤1 mitosis/50 mm^2, no necrosis, and no vascular invasion. If only nuclear pleomorphism/multinucleated giant cells were present or if the maximum diameter of the tumor was >5 cm, the classification was a PEComa of UMP. Thereafter, the revised risk assessment system (15) proposed five clinicopathological features to predict the biological behavior of PEComa: tumor diameter ≥5 cm, high nuclear grade, mitotic count >1 mitosis/50 mm^2, necrosis, and vascular invasion. When a tumor exhibits three or more features, it is classified as malignant, whereas a tumor with two or fewer features is considered as a PEComa of UMP. As recommended, the use of the term "benign" should be minimized. These criteria were adopted in the 2020 World Health Organization classification of tumors of the female reproductive system (5). The current study shows the typical pathological manifestations of PEComa (Figure 2), PEComa of UMP (Figure 3), and malignant PEComa (Figure 4), presenting the distinctive characteristics and differences among the three types. Pathologists should carefully differentiate, as the pathologic diagnosis will influence the treatment plan.

PEComas of the female reproductive tract pose challenges during tumor biological behavior assessment. The primary treatment approach for PEComa of the female reproductive tract involves complete resection with negative incisional margins. TH is currently the primary treatment modality for uterine PEComas. In theory, PEComas primarily metastasize hematologically, suggesting the limited significance of lymphadenectomy (18). Currently, lymphadenectomy is not a routine component of surgical treatment for PEComa, but it is recommended for patients with lymph node metastasis (19). Given the limited number of PEComa cases, further studies are warranted to establish a basis for treatment

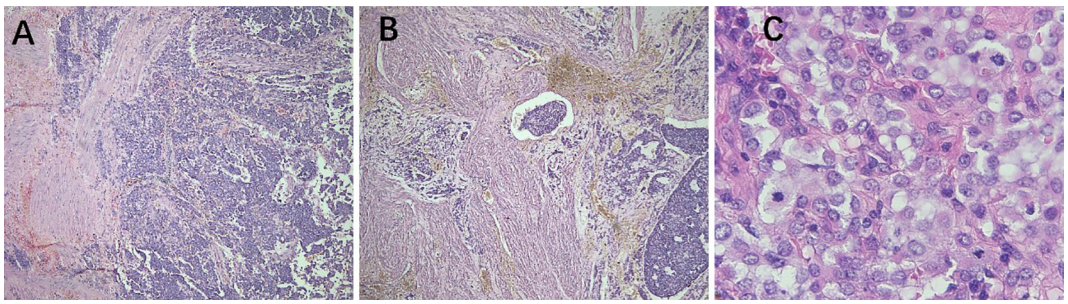

FIGURE 4
Pathological features of malignant PEComa. **(A)** The tumor exhibits unclear borders and infiltrates the muscle layer (40× magnification). **(B)** The tumor exhibits infiltrative growth within the muscle wall, with tumor emboli observed in the blood vessels (40× magnification). **(C)** Atypical epithelioid tumor cells and pathological nuclear division (400× magnification). PEComa, perivascular epithelioid cell tumor.

TABLE 4 Diagnosis and treatment of the patients.

Cases	Initial surgery	Initial pathological diagnosis	Final surgery	Final pathological diagnosis	Postoperative chemoradiotherapy	Follow-up Duration (Months)	Survival status	Recent follow-up result
1	single-incision laparoscopic myomectomy	intraoperative frozen section pathological examination: a mesenchymal tumor? an epithelioid smooth muscle tumor or a perivascular epithelioid cell tumor?	single-incision laparoscopic myomectomy (a)	PEComa	no	9	survive	ultrasound revealed a 2.3 × 2.1 cm mass within the uterus at another hospital
2	hysteroscopic lesion resection	PEComa	TH+bilateral adnexectomy (LAP)	PEComa	no	19	survive	no evidence of recurrence
3	bilateral oophorectomy and resection of pelvic mass	intraoperative frozen section pathological examination: hyperplastic fibrovascular tissue with widespread infiltration of inflammatory cells	bilateral oophorectomy and pelvic mass resection	PEComa	no	26	survive	ultrasound revealed a 3.6 x 1.2 x 1.7 cm lesion in the left pelvic cavity. CT revealed multiple nodules of varying sizes in both lungs.
4	curettage	PEComa	TH+bilateral adnexectomy (LAP)	PEComa	no	58	survive	No signs of recurrence were observed in the pelvis. The patient reported undergoing surgery for a pulmonary nodule (details unspecified).
5	curettage	PEComa	hysteroscopic lesion resection	PEComa	no	68	survive	ultrasound revealed a uterine mass measuring 5 cm. CT revealed enlargement of subpleural nodules in the right lung to varying degrees, along with multiple new nodular lesions in both lungs, suggestive of lung metastasis. Mediastinal and right hilar lymph node metastases were also considered possible.
6	hysteroscopic lesion resection	PEComa	TH+bilateral adnexectomy (LAP)	PEComa of UMP	no	9	survive	no evidence of recurrence
7	hysteroscopic lesion resection	intraoperative frozen section pathological examination: the tumor predominantly exhibits epithelioid morphology, with visible mitotic figures (accurately counting the number of mitotic figures in frozen sections is difficult). Focal nuclear atypia is observed. Epithelioid leiomyoma is primarily considered, at least as epithelioid leiomyoma of uncertain malignant potential. Other tumors, such as PEComa and endometrial stromal tumors, also need to be excluded	TH+bilateral adnexectomy (LAP)	malignant PEComa	epirubicin + IFO 6 cycles	19	survive	no evidence of recurrence
8	curettage (b)	neoplastic lesions, PEComa with mitotic count of >1 mitosis/50mm2	TH+bilateral adnexectomy (LAP) in the other hospital	malignant PEComa	radiotherapy 28 times, chemotherapy: IFO+ADM 1 cycle and PTX+IFO 3 cycles (c)	26	survive	no evidence of recurrence

TH total hysterectomy, LAP laparoscope.

a. the patient's family requested preservation of the uterus during the operation.

b. the patient declined surgery during the initial visit, but underwent total hysterectomy (TH) along with bilateral adnexectomy one year later.

c. postoperative CT revealed lymph node enlargement in the right obturator region, suggesting potential lymph node metastasis.

10.3389/fonc.2024.1449936

decision making. In addition, chemoradiotherapy should be considered when managing malignant PEComas (20). The staging of malignant PEComas should follow that of uterine sarcomas. In patients with inoperable or residual lesions, single or combination chemotherapy with dacarbazine, isocyclophosphamide, doxorubicin, vincristine, or other antitumor drugs may be considered (6, 19). Owing to the limited number of clinical cases and lack of long-term follow-up data, the efficacy of chemotherapy regimens remains unclear.

Recurrence and metastasis can manifest locally or distantly, affecting organs such as the liver, lungs, intestines, bones, and lymph nodes (21), and may emerge months or even decades after surgery (22). The management of recurrent and/or distant metastatic PEComa remains uncertain, but surgery is the optimal treatment modality for isolated recurrent lesions in patients in good physical condition. Chemotherapy may be attempted, and targeted therapies, such as the mTOR inhibitors sirolimus and everolimus (7, 23), also appear to be promising (24). Immunotherapy using programmed cell death 1 inhibitors and vascular endothelial growth factor receptor inhibitors may be used as second-line or subsequent-line treatments, particularly for patients experiencing resistance to mTOR inhibitors and disease progression (25, 26). In young women requiring fertility preservation, meticulous consideration should be given to simple tumor resection if the tumor is small or benign or exhibits UMP. However, in our study, two patients experienced recurrence of uterine masses shortly after simple tumor resection, whereas two patients diagnosed with malignant PEComa who underwent TH and bilateral adnexectomy followed by chemotherapy, with or without radiotherapy, exhibited favorable prognoses without recurrence. This indicates that preservation of the uterus in patients with PEComa should involve strict patient selection and detailed counseling regarding the risks of recurrence and metastasis. Moreover, with appropriate treatment, satisfactory outcomes can be achieved for malignant PEComas.

5 Conclusion

PEComa of the female reproductive tract is a rare tumor that often presents with atypical signs and symptoms; thus, it is frequently misdiagnosed as other uterine tumors preoperatively. Diagnosis primarily relies on pathology, which poses challenges for early identification. The low incidence rates and limited availability of clinical data hinder a comprehensive understanding of the risk and invasiveness of uterine or pelvic PEComa. Although the current criteria are generally effective in assessing tumor invasiveness, emphasizing the significance of complete lesion resection is crucial. Inadequate treatment significantly increases the risks of recurrence and metastasis. Additionally, the prevalence of pulmonary metastases may have been underestimated. Refining risk stratification to prevent the overtreatment of low-grade malignancies and overlooking highly aggressive tumors is a pertinent research avenue.

Data availability statement

The original contributions presented in the study are included in the article/supplementary material. Further inquiries can be directed to the corresponding author.

Ethics statement

The studies involving humans were approved by West China Second University Hospital (2016020). The studies were conducted in accordance with the local legislation and institutional requirements. Written informed consent for participation was not required from the participants or the participants' legal guardians/next of kin in accordance with the national legislation and institutional requirements. Written informed consent was obtained from the individual(s) for the publication of any potentially identifiable images or data included in this article.

Author contributions

XY: Data curation, Formal analysis, Investigation, Methodology, Writing – original draft. RD: Conceptualization, Formal analysis, Funding acquisition, Methodology, Writing – review & editing. BY: Investigation, Validation, Writing – original draft. LH: Data curation, Supervision, Writing – original draft. MH: Methodology, Writing – review & editing. MQ: Conceptualization, Investigation, Writing – review & editing.

Funding

The author(s) declare financial support was received for the research, authorship, and/or publication of this article. This work was supported by the National Natural Science Fund of China (grant No.61505126), the Natural Science Foundation of Sichuan Province (grant No. 2024NSFSC1875).

Conflict of interest

The authors declare that the research was conducted in the absence of any commercial or financial relationships that could be construed as a potential conflict of interest.

Publisher's note

All claims expressed in this article are solely those of the authors and do not necessarily represent those of their affiliated organizations, or those of the publisher, the editors and the reviewers. Any product that may be evaluated in this article, or claim that may be made by its manufacturer, is not guaranteed or endorsed by the publisher.

References

1. Utpatel K, Calvisi DF, Köhler G, Kühnel T, Niesel A, Verloh N, et al. Complexity of PEComas: Diagnostic approach, molecular background, clinical management. *Der Pathologe*. (2020) 41:9–19. doi: 10.1007/s00292-019-0612-5

2. Agaram NP, Sung YS, Zhang L, Chen CL, Chen HW, Singer S, et al. Dichotomy of genetic abnormalities in PEComas with therapeutic implications. *Am J Surg pathology*. (2015) 39:813–25. doi: 10.1097/PAS.0000000000000389

3. Chang HY, Dermawan J, Sharma A, Dickson B, Turashvili G, Torrence D, et al. Sarcomas with RAD51B fusions are associated with a heterogeneous phenotype. *Modern Pathol*. (2024) 37:100402. doi: 10.1016/j.modpat.2023.100402

4. Pecorino B, Scibilia G, Galia A, Scollo P. A very rare case of uterine PEComa HMB45 negative: Primitive or relapse? *Ital J Gynaecology Obstetrics Off Publ Societa Italiana Di Ginecologia E Ostetricia*. (2015) 27:111. doi: 10.14660/2385-0868-024

5. Bennett JA, Oliva E. Perivascular epithelioid cell tumors (PEComa) of the gynecologic tract. *Genes Chromosomes cancer*. (2021) 60:168–79. doi: 10.1002/gcc.22908

6. Gadducci A, Zannoni GF. Perivascular epithelioid cell tumors (PEComa) of the female genital tract: A challenging question for gynaecologic oncologist and pathologist. *Gynecologic Oncol Rep*. (2020) 33:100603. doi: 10.1016/j.gore.2021.100705

7. Liu CH, Chao WT, Lin SC, Lau HY, Wu HH, Wang PH. Malignant perivascular epithelioid cell tumor in the female genital tract: Preferred reporting items for systematic reviews and meta-analyses. *Medicine*. (2019) 98:e14072. doi: 10.1097/MD.0000000000014072

8. Dashraath P, Sidek NA, Kalaichelvan V, Makmur A, Lim DGS, Low JJH, et al. Malignant perivascular epithelioid cell tumor (PEComa) of uterus. *Ultrasound obstetrics gynecology*. (2022) 59:826–8. doi: 10.1002/uog.24794

9. Folpe AL, Kwiatkowski DJ. Perivascular epithelioid cell neoplasms: pathology and pathogenesis. *Hum pathology*. (2010) 41:1–15. doi: 10.1016/j.humpath.2009.05.011

10. Fadare O. Perivascular epithelioid cell tumor (PEComa) of the uterus: an outcome-based clinicopathologic analysis of 41 reported cases. *Adv anatomic pathology*. (2008) 15:63–75. doi: 10.1097/PAP.0b013e31816613b0

11. Valencia-Guerrero A, Pinto A, Anderson WJ, Trevisan G, Nucci MR, Hirsch MS. PNL2: A useful adjunct biomarker to HMB45 in the diagnosis of uterine perivascular epithelioid cell tumor (PEComa). *Int J gynecological Pathol*. (2020) 39:529–36. doi: 10.1097/PGP.0000000000000653

12. Bennett JA, Ordulu Z, Pinto A, Wanjari P, Antonescu CR, Ritterhouse LL, et al. Uterine PEComas: correlation between melanocytic marker expression and TSC alterations/TFE3 fusions. *Modern Pathol*. (2022) 35:515–23. doi: 10.1038/s41379-021-00855-1

13. Anderson WJ, Dong F, Fletcher CDM, Hirsch MS, Nucci MR. A clinicopathologic and molecular characterization of uterine sarcomas classified as Malignant PEComa. *Am J Surg pathology*. (2023) 47:535–46. doi: 10.1097/PAS.0000000000002028

14. Natsume T, Yoshida H, Nishikawa T, Kikkawa N, Naka T, Kobayashi-Kato M, et al. Uterine leiomyosarcoma masquerading as a Malignant perivascular epithelioid cell tumor: A diagnostic challenge. *Int J Surg pathology*. (2023) 31:778–84. doi: 10.1177/10668969221133348

15. Bennett JA, Braga AC, Pinto A, Van de Vijver K, Cornejo K, Pesci A, et al. Uterine PEComas: A morphologic, immunohistochemical, and molecular analysis of 32 tumors. *Am J Surg pathology*. (2018) 42:1370–83. doi: 10.1097/PAS.0000000000001119

16. Sanfilippo R, Fabbroni C, Fucà G, Fumagalli E, Morosi C, Sbaraglia M, et al. Addition of antiestrogen treatment in patients with Malignant PEComa progressing to mTOR inhibitors. *Clin Cancer Res*. (2020) 26:5534–8. doi: 10.1158/1078-0432.CCR-20-1191

17. Folpe AL, Mentzel T, Lehr HA, Fisher C, Balzer BL, Weiss SW. Perivascular epithelioid cell neoplasms of soft tissue and gynecologic origin: a clinicopathologic study of 26 cases and review of the literature. *Am J Surg pathology*. (2005) 29:1558–75. doi: 10.1097/01.pas.0000173232.22117.37

18. Shan W, Shi Y, Zhu Q, Yang B, Xie L, Li B, et al. Five cases of uterine perivascular epithelioid cell tumors (PEComas) and review of literature. *Arch gynecology obstetrics*. (2019) 299:185–90. doi: 10.1007/s00404-018-4920-4

19. Liu JL, Lin YM, Lin MC, Yeh KT, Hsu JC, Chin CJ. Perivascular epithelioid cell tumor (PEComa) of the uterus with aggressive behavior at presentation. *Hematology/oncology Stem Cell Ther*. (2009) 2:426–30. doi: 10.1016/s1658-3876(09)50013-1

20. Jeon IS, Lee SM. Multimodal treatment using surgery, radiotherapy, and chemotherapy in a patient with a perivascular epithelioid cell tumor of the uterus. *J Pediatr hematology/oncology*. (2005) 27:681–4. doi: 10.1097/01.mph.0000193475.06870.d5

21. Armah HB, Parwani AV. Malignant perivascular epithelioid cell tumor (PEComa) of the uterus with late renal and pulmonary metastases: a case report with review of the literature. *Diagn pathology*. (2007) 2:45. doi: 10.1186/1746-1596-2-45

22. Ascione A, Martignoni G, d'Amati G, Della Rocca C, Graziano P, Pernazza A. Extremely late-onset pulmonary metastasis from uterine PEComa. *Pathologica*. (2022) 114:312–5. doi: 10.32074/1591-951X-762

23. Wagner AJ, Malinowska-Kolodziej I, Morgan JA, Qin W, Fletcher CD, Vena N, et al. Clinical activity of mTOR inhibition with sirolimus in Malignant perivascular epithelioid cell tumors: targeting the pathogenic activation of mTORC1 in tumors. *J Clin Oncol*. (2010) 28:835–40. doi: 10.1200/JCO.2009.25.2981

24. Sanfilippo R, Jones RL, Blay JY, Le Cesne A, Provenzano S, Antoniou G, et al. Role of Chemotherapy, VEGFR Inhibitors, and mTOR inhibitors in advanced perivascular epithelioid cell tumors (PEComas). *Clin Cancer Res*. (2019) 25:5295–300. doi: 10.1158/1078-0432.CCR-19-0288

25. Lattanzi M, Deng FM, Chiriboga LA, Femia AN, Meehan SA, Iyer G, et al. Durable response to anti-PD-1 immunotherapy in epithelioid angiomyolipoma: a report on the successful treatment of a rare Malignancy. *J immunotherapy cancer*. (2018) 6:97. doi: 10.1186/s40425-018-0415-x

26. Liapi A, Mathevet P, Herrera FG, Hastir D, Sarivalasis A. VEGFR inhibitors for uterine metastatic perivascular epithelioid tumors (PEComa) resistant to mTOR inhibitors. A case report and review of literature. *Front Oncol*. (2021) 11:641376. doi: 10.3389/fonc.2021.641376

frontiers | Frontiers in Oncology

TYPE Original Research
PUBLISHED 07 November 2024
DOI 10.3389/fonc.2024.1458968

Check for updates

OPEN ACCESS

EDITED BY
Dragos Eugen Georgescu,
Carol Davila University of Medicine and Pharmacy, Romania

REVIEWED BY
Giuseppe Marino,
University of Milano-Bicocca, Italy
Mladen Anđić,
University of Belgrade, Serbia

*CORRESPONDENCE
Huaijun Zhou
Zhouhj2007@126.com
Xiaofeng Xu
xuxiaofeng@njglyy.com

RECEIVED 03 July 2024
ACCEPTED 18 October 2024
PUBLISHED 07 November 2024

CITATION
Liu L, Xiao Z, Li Z, Zheng J, Xu X and Zhou H (2024) Uterine smooth muscle tumors of uncertain malignant potential: a 13-year retrospective study.
Front. Oncol. 14:1458968.
doi: 10.3389/fonc.2024.1458968

COPYRIGHT
© 2024 Liu, Xiao, Li, Zheng, Xu and Zhou. This is an open-access article distributed under the terms of the Creative Commons Attribution License (CC BY). The use, distribution or reproduction in other forums is permitted, provided the original author(s) and the copyright owner(s) are credited and that the original publication in this journal is cited, in accordance with accepted academic practice. No use, distribution or reproduction is permitted which does not comply with these terms.

Uterine smooth muscle tumors of uncertain malignant potential: a 13-year retrospective study

Liuliu Liu [1], Zhendong Xiao [1], Zhiwen Li [2], Jinyu Zheng [2], Xiaofeng Xu [1*] and Huaijun Zhou [1*]

[1]Department of Gynecology, Nanjing Drum Tower Hospital, The Affiliated Hospital of Nanjing University Medical School, Nanjing, China, [2]Department of Pathology, Nanjing Drum Tower Hospital, The Affiliated Hospital of Nanjing University Medical School, Nanjing, China

Objective: The primary objective of this study was to provide valuable evidence for the management of patients diagnosed with uterine smooth muscle tumors of uncertain malignant potential (STUMP), with a focus on those with reproductive aspirations.

Methods: We conducted a retrospective analysis of clinical and pathological data from the medical records and slides of STUMP patients treated at Drum Tower Hospital, affiliated with Nanjing University Medical School, from January 2009 to December 2021.

Results: Thirty-four patients were included in the study, with a median follow-up duration of 76 months (range: 13-157 months). After slide review, the diagnosis agreement rate was 77.3% (34/44 among initially considered cases). The consistency rate between our hospital's diagnosis and those of other institutions was 75% (15/20). The accuracy rate of intraoperative frozen section diagnosis was low, at 21.4% (3/14). Half of the patients (17) underwent myomectomy, while the other half (17) received hysterectomy, including one subtotal hysterectomy. Two recurrences were observed (5.9%), one as STUMP and the other as leiomyosarcoma, with one recurrence in each surgical group. Notably, 4 of 9 patients with reproductive aspirations successfully underwent cesarean deliveries. Patients with single lesions appeared to exhibit potentially favorable fertility outcomes compared to those with multiple lesions.

Conclusion: The diagnosis of STUMP was difficult. Myomectomy potentially could serve as an alternative for patients with reproductive needs. In selected cases with single lesions, it may indicate potentially favorable fertility outcomes.

KEYWORDS

pathological diagnosis, myomectomy, hysterectomy, recurrence, fertility outcome

1 Introduction

Uterine smooth muscle tumors are the most prevalent neoplasms in the female genitourinary system. The prognosis of these tumors is determined by three pivotal factors: cytologic atypia, tumor cell necrosis, and mitotic index. Benign leiomyoma is typically characterized by a low mitotic index and the absence of moderate to severe cytologic atypia or necrosis. Conversely, tumors exhibiting any two or all three of the following features diffuse moderate to severe cytologic atypia, tumor cell necrosis, and a high mitotic index are usually classified as leiomyosarcomas. Uterine smooth muscle tumors of uncertain malignant potential (STUMP) refer to tumors that exceed the morphological criteria for leiomyoma or its variants but do not fulfill the diagnostic criteria for leiomyosarcoma (1). This type of tumor is particularly concerning, particularly for young women who have been diagnosed with STUMP following myomectomy and wish to preserve their reproductive function, as it may progress or potentially represent a missed sarcoma. The incidence of STUMP is relatively low, and the scarcity of large-scale studies has limited the data available for effective management. Therefore, the aim of this research is to investigate the clinical and pathological characteristics of STUMP in our institution, in order to provide valuable insights and evidence for the management of women with reproductive needs.

2 Materials and methods

2.1 Case selection

We retrospectively analyzed the data of the patients who were diagnosed with STUMP and underwent surgical treatment at the Gynecology Department of Drum Tower Hospital, a tertiary referral center affiliated to Nanjing University Medical School, between January 2009 and December 2021.

2.2 Slide review process

All slides were reviewed independently by two senior pathologists specializing in gynecologic oncology. The pathologists were blinded to the patient's age, original diagnosis, treatments, and recurrence status. The review process was performed using conventional hematoxylin and eosin-stained slides, excluding supplementary immunohistochemical investigations. Tumor cellularity, cytologic atypia, mitotic activity, the presence of any necrosis, epithelioid/myxoid differentiation, atypical mitotic figures, vascular invasion, and infiltrative margins were observed during the slide review. The degree of cellularity and cytologic atypia was categorized as mild, moderate, or severe. The tumor mitotic activity was determined using the highest count method in 10 high-power fields (HPFs) at 400 times magnification. Necrosis was classified as coagulative tumor cell necrosis (CTCN), hyaline necrosis, and uncertain type necrosis.

According to the 2020 World Health Organization (WHO) guideline on STUMP classification (1) and our interpretation of relevant literature (2), the following subcategories were adopted for the diagnosis of STUMP: 1)tumors exhibiting focal/multifocal or diffuse nuclear atypia, with 2-4 mitoses per square millimeter (equivalent to 6-9 mitoses per 10 HPFs), without necrosis; 2) tumors displaying necrosis, such as unequivocal tumor cell necrosis or uncertain type necrosis, but lacking any other concerning features; 3)tumors with mitoses exceeding 6 per square millimeter (equal to ≥15 mitoses per 10 HPFs), but lacking cytologic atypia and tumor cell necrosis; 4)epithelioid or myxoid differentiated tumors falling below the threshold for leiomyosarcoma, yet exceeding the criteria for leiomyoma; 5) tumors infiltrating the myometrium without exhibiting other features of malignancy; and 6) tumors with atypical mitotic figures without any features of malignancy.

2.3 Clinical and follow-up data

The patient's age, parity history, surgical history, symptoms, maximum tumor diameter, surgical procedure, pathological features, recurrence status, and other pertinent information were extracted from medical records. Additionally, all patients underwent pelvic ultrasound examination within six months prior to the study and chest computed tomography (CT) scans within twelve months. Recurrence was defined as the local or distant reappearance of the tumor (either as STUMP or leiomyosarcoma) subsequent to myomectomy or hysterectomy. Importantly, the emergence of benign lesions was not classified as recurrence. Consequently, recurrence must be pathologically confirmed, and new lesions solely detected by imaging studies, without pathological confirmation, were not considered as recurrent disease.

2.4 Statistical analysis

S Statistical analysis was conducted using SPSS version 26.0 software. The Kolmogorov-Smirnov test was applied to assess the normality of the data. The nonnormal distribution parameters were expressed as the median and range for continuous variables. Categorical variables were presented as numbers and percentages.

3 Results

A total of 68 cases were retrieved from the Department of Pathology. Among them, 24 cases were lost to follow-up, leaving 44 cases available for the slide review process. After the slide review, ten patients were excluded due to not meeting the diagnostic criteria for STUMP. Ultimately, 34 patients were enrolled in the study, and their clinicopathological data were meticulously collected. The specific process of the pathological review is illustrated in Figure 1.

3.1 Clinical characteristics

The patients' demographic and clinical characteristics are presented in Table 1. The median age of the patients was 43.5

years (range: 26–51 years). One patient (2.9%) was in the postmenopausal state, while the remainder were premenopausal. There were 6 nulliparous women (17.6%) and 28 parous women (82.4%). Six patients (17.6%) had a history of previous uterine surgery. None of the patients had a documented history of hormone therapy. Menstrual disorders were the predominant manifestation of STUMP, affecting 16 patients (47.1%). The median maximum tumor diameter was 8 centimeters (range: 3.5-16 cm). Additionally, 23 patients (67.6%) had multiple tumor lesions (including leiomyoma lesions), and 15 patients (44.1%) had multiple STUMP lesions. The median follow-up duration was 76 months (range: 13-157 months). Two patients (5.9%) experienced recurrence as STUMP and leiomyosarcoma, respectively, with no deaths reported. Among the 9 patients with reproductive needs, 4 successfully delivered live babies.

3.2 Pathological characteristics

In this study, the agreement rate of the initial diagnosis after slide review was 77.3% (34/44). Among the 34 enrolled patients, 25 (73.5%) underwent intradepartmental discussions within the Pathology Department prior to diagnosis. Twenty patients (58.8%) sought pathological consultations in other hospitals, of

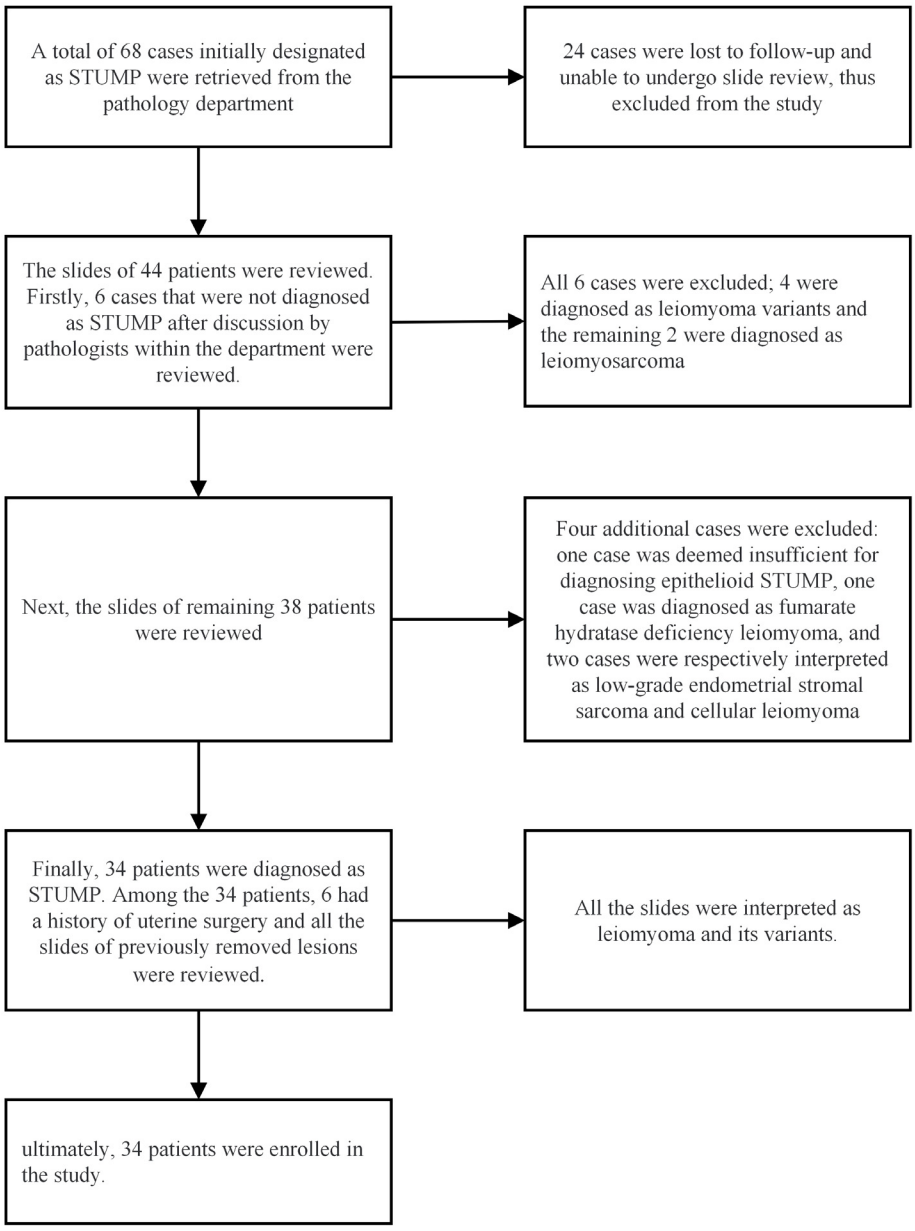

FIGURE 1
The process of pathological review and case enrollment for the study.

which 15 (75%) received a diagnosis consistent with ours. Fourteen patients (56%) underwent intraoperative frozen section examination, but only 3 (21.4%) received a diagnosis that concurred with the permanent section diagnosis. Table 2 summarizes the pathological characteristics of the patients. According to the statistics, 13 cases (38.2%) showed significant cytologic atypia alone, 5 (14.7%) exhibited necrosis alone, 1 (2.9%) demonstrated a high mitotic index alone, 8 (23.5%) displayed at least two Stanford parameters, and 7 (20.6%) did not exhibit any of the three parameters. Consequently, the majority (approximately 79.4%) of STUMP diagnoses were still reliant on these three criteria. The microscopic findings of the primary and recurrent lesions in the patient with four recurrences were illustrated in Figure 2. Notably, the microscopic analysis of the lesions obtained during the fourth surgery is not available for presentation, as the surgical procedure was performed at a separate hospital.

3.3 Treatment and oncologic outcomes

Initially, 13 patients underwent hysterectomy, while 21 patients underwent myomectomy. Shortly after being diagnosed with STUMP, five patients underwent a second operation, and in one patient, residual STUMP lesions were observed. Ultimately, the treatment distribution was even, with 17 patients (50%) undergoing myomectomy and 17 patients (50%) undergoing hysterectomy. Among the 17 patients who underwent hysterectomy, 16 (94.1%) underwent total hysterectomy, while one (5.9%) underwent subtotal hysterectomy. One patient, due to postmenopausal status, underwent additional bilateral salpingo-oophorectomy, and another underwent additional bilateral salpingo-oophorectomy and lymphadenectomy following an intraoperative frozen section diagnosis of sarcoma. One patient, who was considered to have uterine sarcoma during consultation at an external hospital, underwent six courses of chemotherapy there. The remaining patients did not receive chemotherapy, radiotherapy, or endocrine therapy as part of their initial treatment.

Table 3 summarizes the clinical characteristics of patients in both the myomectomy and hysterectomy groups. Notably, patients in the myomectomy group tend to be relatively younger, with a higher proportion of those who have not yet given birth. Among the 17 patients who underwent myomectomy, 8 underwent morcellation, whereas 6 of the 17 patients in the hysterectomy group underwent similar morcellation procedures. In terms of recurrence, one recurrence case was observed in both the myomectomy and hysterectomy groups, and currently, no statistically significant difference in recurrence rates can be discerned.

During the study period, 2 patients (5.9%) relapsed with STUMP and leiomyosarcoma, respectively. Their clinical courses are detailed in Table 4. Additionally, the clinicopathological characteristics of patients without and with recurrence are presented in Table 5. We have not yet observed any statistically significant difference in the surgical approach between recurrent and non-recurrent patients. However, it is noteworthy that both recurrent patients had undergone morcellation. Furthermore, imaging studies detected new uterine lesions in four patients (11.8%), although these lesions

TABLE 1 Demographic and clinical characteristics of patients (n = 34).

Clinical characteristics	Values
Age (years)	43.5 (26–51)
20-29	5 (14.7%)
30-39	7 (20.6%)
40-49	19 (55.9%)
≥50	3 (8.8%)
Parity (number)	1 (0-3)
Nullipara	6 (17.6%)
Pluripara	28 (82.4%)
Postmenopausal state	
Yes	1 (2.9%)
No	33 (97.1%)
Hormone therapy history	0 (0%)
Previous uterine surgery	6 (17.6%)
Symptoms	
Menstrual disorders	16 (47.1%)
Health examination	11 (32.4%)
Pain	3 (8.8%)
Abdominal mass	1 (2.9%)
Increased urination frequency	1 (2.9%)
Increased stool frequency	1 (2.9%)
Incidentally detected	1 (2.9%)
Maximum diameter (cm)	8 (3.5–16)
Tumor number[a]	4 (1-14)
Single tumor[a]	11(32.4%)
Multiple tumor[a]	23(67.6%)
Multiple STUMP (before a second surgery)	14 (41.2%)
Multiple STUMP (after a second surgery)	15 (44.1%)
A second surgery (within a short interval)	5(14.7%)
Surgical procedure	
Total Hysterectomy+BS	3 (8.8%)
Total Hysterectomy+BSO+lymphadenectomy	1 (2.9%)
Hysteroscopic Myomectomy	1 (2.9%)
Interval between the two operations (days)	9-47
Surgical procedure (after the second surgeries)	
Myomectomy	17 (50%)
Laparotomic myomectomy	10 (29.4%)
Myomectomy+ partial rectectomy	1 (2.9%)
Myomectomy	9 (26.5%)
Laparoscopic Myomectomy	6 (17.6%)

(Continued)

TABLE 1 Continued

Clinical characteristics	Values
Surgical procedure (after the second surgeries)	
Hysteroscopic Myomectomy	1 (2.9%)
Hysterectomy	17 (50%)
Subtotal Hysterectomy +BS (Laparoscopic)	1 (2.9%)
Total hysterectomy +/- BS or BSO	16(47.1%)
Laparotomic Hysterectomy	6 (17.6%)
Laparoscopic Hysterectomy	9 (26.5%)
Transvaginal hysterectomy	1 (2.9%)
Morcellation	14 (41.2%)
Laparotomic Myomectomy	1 (7.1%)
Laparoscopic Myomectomy	6 (42.9%)
Hysteroscopic Myomectomy	1 (7.1%)
Subtotal Hysterectomy (Laparoscopic)	1 (7.1%)
Total Hysterectomy (Laparoscopic)	5 (35.7%)
Morcellation methods	14 (41.2%)
Power morcellation	10 (71.4%)
Scalpel morcellation	4 (28.6%)
Oophorectomy	2 (5.9%)
Lymphadenectomy	1 (2.9%)
Chemotherapy	1 (2.9%)
Outcome	
Recurrent	2 (5.9%)
STUMP	1 (50%)
Leiomyosarcoma	1 (50%)
New lesions on imaging (no pathological evidence)	4 (11.8%)
Alive with no evidence of disease	28(82.4%)
Death	0(0%)
Fertility Outcome	4/9(44.4%)
Follow-up duration (median, months)	76 (13-157)

Data are n, median (range), or n (%).
BSO, Bilateral Salpingo-oophorectomy; BS, Bilateral Salpingectomy.
[a]The term tumor number referred to the number of all tumors, including benign leiomyomas and STUMPs.

TABLE 2 The pathological Characteristics of patients (n = 34).

Pathological Characteristics	Value
Discussion within pathology department	25 (73.5%,25/34)
Consultation in other hospitals	20 (58.8%,20/34)
Consistent diagnosis	15 (75%,15/20)
Intraoperative frozen procedure	14 (41.2%,14/34)
Consistent diagnosis	3 (21.4%,3/14)
Cellularity	
Mild	14 (41.2%)
Moderate	8 (23.5%)
Severe	12 (35.3%)
Atypia	
Mild	13 (38.2%)
moderate	10 (29.4%)
Severe	11 (32.4%)
Mitosis	
0-4	17 (50%)
5–9	13 (38.2%)
10 -14	3 (8.8%)
15-19	0 (0%)
≥20	1 (2.9%)
Necrosis	
No necrosis	23 (67.6%)
Necrosis of uncertain type	9 (26.5%)
Coagulative tumor cell necrosis	2 (5.9%)
Atypical mitotic figures	3 (8.8%)
Tumor infiltrates the myometrium	5 (14.7%)
Epithelioid differentiated	6 (17.6%)
Epithelioid STUMP	0 (0%)
Myxoid differentiated	4 (11.%)
Myxoid STUMP	1 (2.9%)

Data are n, median (range), or n (%).

(Continued)

were not confirmed pathologically. The remaining 28 patients (82.4%) are alive with no evidence of disease.

3.4 Reproductive outcomes

During the entire follow-up observation period, 4 out of 9 patients with reproductive needs successfully delivered live babies. All 4 of these patients underwent cesarean section deliveries. Among them, one patient experienced an iatrogenic premature delivery at 36 weeks gestation due to complications stemming from the recurrence of STUMP. The remaining three deliveries were full-term cesarean sections. The clinical and pathological characteristics of these 4 patients are presented in Table 6. Additionally, among the 9 patients with reproductive needs, 5 had single lesions, while 4 had multiple lesions (specifically, 2, 6, 8, and 10 lesions, respectively). Notably, the live birth rate among patients with single lesions was 80% (4/5), whereas the live birth rate among patients with multiple lesions was 0% (0/4).

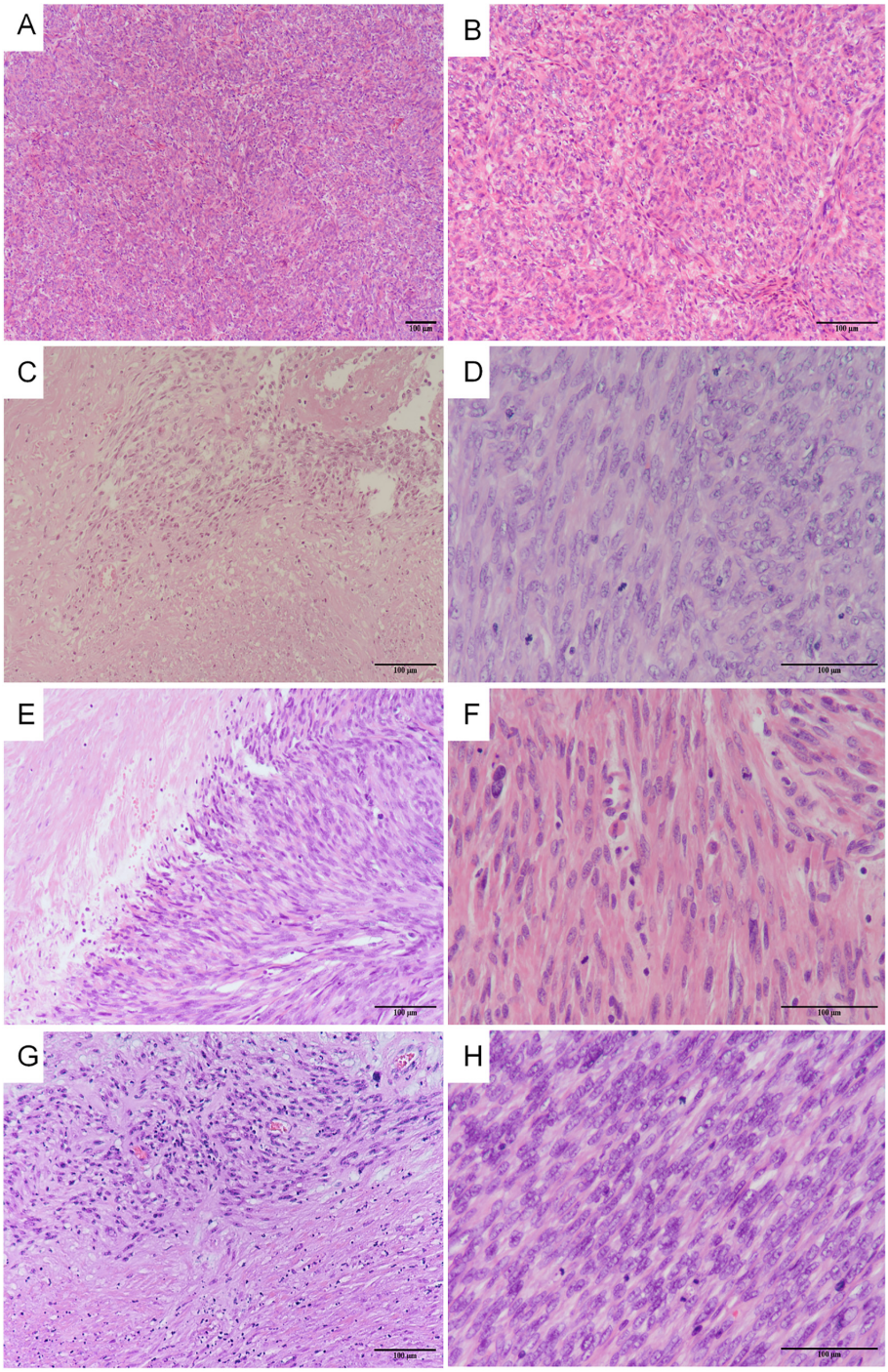

FIGURE 2
The microscopic findings of the primary and recurrent lesions in the patients with four relapses. The first surgery: **(A)** severe cellularity was found (H&E x 100), **(B)** moderate atypia was found (H&E x 200); The second surgery: **(C)** coagulative tumor cell necrosis was found (H&E x 200), **(D)** mitotic index 10-15 mitoses per 10 HPFs (H&E x 400); The third surgery: **(E)** coagulative tumor cell necrosis was found (H&E x 200), **(F)** mitotic index 10-15 mitoses per 10 HPFs (H&E x 400); The fifth surgery: **(G)** coagulative tumor cell necrosis was found (H&E x 200), **(H)** mitotic index 15-20 mitoses per 10 HPFs (H&E x 400).

4 Discussion

In this 13-year retrospective study, we conducted a thorough analysis of the clinicopathological features of patients diagnosed with STUMP, revealing several meaningful findings. The diagnosis of STUMP poses challenges, characterized by a certain level of variability in pathological diagnoses among different pathologists and institutions, and the intraoperative frozen section accuracy rate remains very low. It appears that myomectomy may not increase the risk of recurrence, and myomectomy potentially could serve as

TABLE 3 Differences between hysterectomy and myomectomy groups.

	Myomectomy (n=17)	Hysterectomy (n =17)
Age (years)	37 (26-46)	46 (34-51)
Max tumor diamiter(cm)	7.0 (5-10)	8 (3.5-16)
Parity		
Nullipara	6	0
Parous	11	17
Tumor number [a]		
Single	7	4
Multiple	10	13
Surgical approach		
Open	10	6
No-open	7	11
Morcellation		
Yes	8	6
No	9	11
Recurrence		
Yes	1	1
No	16	16

Data are n, median (range), or n (%).
[a]The term tumor number referred to the number of all tumors, including benign leiomyomas and STUMPs.

an alternative for patients with fertility aspirations. Patients with a single lesion seem to exhibit potentially favorable fertility outcomes.

The term "STUMP" was first proposed by Kempson et al. to denote a specific group of tumors that exhibit concerning clinical malignant behaviors, yet do not meet the criteria for classification as sarcomas (3). In 1994, researchers at Stanford University conducted a study on 213 cases of suspected uterine smooth muscle tumors, where they initially proposed four histopathological diagnostic criteria for STUMP (4). Subsequently, other researchers proposed their own sets of pathological diagnostic criteria for STUMP (2, 5, 6). Gupta emphasized that histological parameters, including atypical mitosis, epithelioid differentiation, infiltrative or irregular margins, and vascular intrusion, suggest a poor prognosis and should be incorporated into the diagnostic framework for STUMP (2). The latest WHO guidelines have elaborated on the diagnostic criteria for STUMP but emphasized that these criteria were not meant to be taken as doctrine (1). Currently, there exists no uniform histopathological diagnostic criteria for STUMP. Therefore, the diagnosis of STUMP poses a significant challenge, and the reproducibility of diagnoses among different pathologists or institutions remains low. In the largest study conducted to date, which initially included 103 patients, 87 cases met the STUMP diagnostic criteria upon pathological review, yielding a preliminary diagnostic agreement rate of 87.9% (87/99, with 4 cases unavailable for pathological review) (7). In contrast, Basaran et al. reported a lower preliminary diagnostic agreement rate of 71.4% after pathologist review, with 21 patients ultimately diagnosed with STUMP (8). Furthermore, in a European study involving 12 tertiary centers, 29 patients initially diagnosed with STUMP underwent central review by two experienced gynecological pathologists, and only 7 (24.1%) patients ultimately met the diagnostic criteria for STUMP, highlighting an even lower rate of reproducibility (9). In our case series, the majority of cases underwent intra-departmental discussions, resulting in a preliminary diagnostic agreement rate of 77.3% (34/44) after slide review. Among the 20 patients who had prior consultations in other hospitals, 75% (15/20) had consistent diagnostic results with ours, which underscores the difficulties in diagnosing STUMP. The difficulties in pathological identification of these tumors may lead to misdiagnoses, potentially resulting in unnecessary interventions, anxiety, or missed diagnoses of sarcomas. Consequently, we believe that multi-center consultations are worthwhile for STUMP patients due to the significant variations in actual diagnoses.

The diagnostic accuracy and clinical significance of frozen section procedures in the diagnosis of uterine smooth muscle tumors have been evaluated in some studies, but few studies have assessed their application in STUMP (10). Ha et al. reported that among patients with STUMP, 54.5% (6/11) were misdiagnosed as having benign leiomyoma by frozen section procedures, 18.2% (2/11) were misdiagnosed as uterine leiomyosarcoma, and only 27.3% (3/11) were accurately diagnosed as STUMP (11). In our case series, 14 patients underwent intraoperative frozen section procedures. Among them, 9 patients (64.3%) were misdiagnosed as having benign leiomyoma, 2 (14.3%) were misdiagnosed as leiomyosarcoma, and only 3 (21.4%) were correctly diagnosed as STUMP. The accuracy of intraoperative frozen section is very low, and its results should not be used as a basis for hysterectomy, especially for patients who desire to preserve their reproductive function. Furthermore, even in cases with permanent pathological outcomes, seeking pathology consultation from experienced centers should be considered as the first step in the management of the stump.

In addition to multicenter consultation, the expression of immunohistochemical markers, such as estrogen receptor (ER), progesterone receptor (PR), p53, p16, and Ki67, is helpful for pathologists to differentiate leiomyosarcoma, leiomyoma, and STUMPs. Several studies have noted that PR and ER expression are frequently present in STUMP and LM but occurre much less frequently in LMS (12–14). Multiple immunohistochemical studies have observed Ki-67, P53, P16 at high levels in LMS, but it was significantly less frequent or weakly positive in STUMP and LM (15–19). The results of the above studies indicated that the expression of the immunohistochemical markers in STUMP are more comparable to that of LM and LM variants than to that of LMS. The major contribution of immunohistochemical studies may thus be limited in differentiating STUMP from LMS. Inrecent years,

TABLE 4 The clinicopathological characteristics of the recurrent patients.

Case	Age	Parity	Time interval since last surgery (month)	Tumor location	Surgery procedure	Adjuvant therapy	Morcellation	Pathological features					Outcome	Follow up (month)
								Diagnosis	Cellularity	Atypia	Mitotic counts	Necrosis		
1	46	2	Initial	Uterus	LSH	No	Yes	STUMP	Severe	Moderate	5-7	uncertain type		
			32	PC	BSO PMR Trachelectomy	No	No	LMS	Severe	Moderate	10-15	CTCN		
			22	PC Omentum	PMR Omentectomy	CT	No	LMS	Severe	Severe	10-15	CTCN		
			18	PC	PMR	CT	No	LMS[a]	–	–	–	–		
			24	PC Sigmoid colon	partial Sigmoidectomy PMR	CT	No	LMS	Severe	Moderate	15-20	CTCN	Alive	110
2	26	0	Initial	Uterus	Myomectomy partial rectectomy	No	Yes	STUMP	Severe	Moderate	1-2	Absent		
			14	Uterus PC AC Omentum	CS, SAH USO PMR Omentectomy	No	No	STUMP	Severe	Severe	1-3	Absent	Alive	56

PC Pelvic cavity, AC Abdominal cavity, LSH Laparoscopic subtotal hysterectomy, BSO Bilateral salpingo-oophorectomy, PMR Pelvic mass resection, CS cesarean section, SAH subtotal abdominal hysterectomy, USO Unilateral salpingo-oophorectomy, CT Chemotherapy, LMS leiomyosarcoma, CTCN coagulative tumor cell necrosis.

[a]The microscopic findings of lesions from the forth surgery was not presented, because the procedure was performed in another hospital.

10.3389/fonc.2024.1458968

TABLE 5 Differences of the clinical and pathological features between no recurrence and recurrence groups.

Characteristics	No recurrence (n = 32)	Recurrence (n =2)
Age (years)	43.5 (27, 51)	36(26, 46)
Parity		
Nullipara	5	1
Pluripara	27	1
Menopausal state		
Yes	1	0
No	31	2
Uterine history		
Yes	6	0
No	26	2
Max tumor diameter	8 (3.5,13)	12.5(9,16)
Tumor number		
Single tumor	10	1
Multiple tumor	22	1
Surgical procedure		
myomectomy	16	1
Hysterectomy	16	1
Morcellation		
Yes	12	2
No	20	0
oophorectomy		
Yes	2	0
No	30	2
Follow-up (months)	76(13,157)	83(56,110)
Cellularity		
Mild	14	0
Moderate	8	0
severe	10	2
Atypia		
Mild	13	0
Moderate	8	2
severe	11	0
Mitosis		
0-4	16	1
5–9	12	1
10–14	3	0
15-19	0	0
≥20	1	0
Necrosis		
No	22	1
Uncertain type	8	1
CTCN	2	0

Data are n, median (range), or n (%).
CTCN, coagulative tumor cell necrosis.

molecular studies of uterine smooth muscle tumors have achieved remarkable progress and it may provide a reliable basis for our diagnosis in the future (9, 20–23).

In the current study, the median age of patients diagnosed with STUMP was 43.5 years old, indicating that STUMP tends to occur in relatively younger patients, a finding that aligns with previous literature (7, 24–26). Consequently, uterine-preserving surgery emerges as a potentially favorable option for a substantial proportion of patients, particularly those with reproductive aspirations. Our analysis revealed that among 17 cases of myomectomy and an equal number of hysterectomies, one recurrence was recorded in each group, which appears to indicate that there may be no significant difference in recurrence rates between the two surgical modalities. Similarly, a study conducted by Guntupalli et al. at M.D. Anderson Cancer Center in 2009 observed comparable recurrence rates between their myomectomy group (0/10) and hysterectomy group (3/31) (6). Furthermore, another investigation encompassing 57 patients found that, while 2 recurrences were documented among 30 patients undergoing hysterectomy, 6 recurrences were noted in the 27 patients who underwent myomectomy, however, statistical analysis failed to detect a significant difference in recurrence rates between these two surgical strategies (25). A systematic review involving 189 patients showed that 15 of 62 patients who underwent myomectomy experienced recurrence, and 22 of 127 patients who underwent hysterectomy had recurrence (24). However, no statistically significant difference in recurrence rates was found between the two groups. It appears that myomectomy may not increase the risk of recurrence, and myomectomy potentially could serve as an alternative for patients with fertility aspirations. Currently, after fully evaluating the trade-off between the risk of recurrence and the possibility of fertility, we believe that myomectomy could be a feasible treatment option for young women with reproductive needs.

Numerous studies have been conducted in an effort to identify high-risk factors associated with recurrence. Shim et al. demonstrated that a previous history of myomectomy for leiomyoma was the sole independent risk factor for recurrence (27). Sahin et al. found that the location of the tumor was closely related to recurrence, with the risk of recurrence for subserosal STUMP being 5.72 times higher than that for STUMP located between the muscular walls and the submucosa (25). Travaglino et al. considered significant atypia and CTCN as independent risk factors for recurrence of STUMP (28). Huo et al. showed that

10.3389/fonc.2024.1458968

TABLE 6 Clinicopathological characteristics of patients with obstetrics outcomes.

Case	Age	Tumor number	Maximum tumor diameter	Parity	Surgical procedure	Pathological features				Timing of delivery	Mode of delivery	Outcome	Supplementary instruction
						Cellularity	Atypia	Mitosis	Necrosis				
1	37	1	10	1	Laparoscopic myomectomy	Moderate	Mild	3-4	Absent	Mature	CS	ANED	A second child was delivered after surgery
2	29	1	5	0	Hysteroscopic myomectomy	Severe	Mild	7	Absent	Mature	CS	ANED	
3	26	1	9	0	Laparotomic myomectomy and partial rectectomy	Severe	Moderate	1-2	Absent	Premature	CS	ANED	Recurrence of disseminated stump during pregnancy
4	29	1	5	0	Laparotomic myomectomy	Moderate	Severe	6	Absent	Mature	CS	ANED	

CS cesarean section, ANED alive with no evidence of disease.

mitosis in the initial pathology (mitotic index > 10/10 HPFs) was the only independent risk factor for recurrence (26). Travaglino et al. found that an abnormal p53 expression and a diffuse p16 expression were significantly associated with the risk of recurrence of STUMP (29). To date, no consensus has been reached regarding the specific risk factors associated with relapse. However, a systematic review published in 2022 showed that unprotected morcellation of lesions was significantly associated with disease recurrence (24). Actually, as early as 2014, the United States Food and Drug Administration issued an alert that focused the entire world's attention on the relevant risks. My study did not identify any significant high-risk factors for recurrence, but the fact that both recurrent cases underwent morcellation suggests that morcellation may be a potential risk factor for recurrence. Therefore, based on existing literature, we recommend avoiding unprotected morcellation due to its association with increased risks of recurrence and metastasis (7, 24, 30–32). Given the challenges in preoperative and intraoperative diagnosis of STUMP, we advise against unprotected morcellation for all patients with uterine smooth muscle tumors.

Among STUMP patients who underwent fertility-sparing surgery, the reported successful pregnancy rate ranged from 20% to 80%, with favorable maternal and infant outcomes (33). Our study revealed that patients with STUMP had a decent chance of fertility (44.4%, 4/9). Sahin reported that ten of 27 patients who underwent myomectomy for uterine myoma had fertility desire, with seven(70%,7/10) recorded pregnancies (25). While Huo reported a successful pregnancy rate of 20% (7/35) among patients attempting to conceive (26). In our study, the live birth rate among patients with single lesions was 80% (4/5), whereas the live birth rate among patients with multiple lesions was 0% (0/4). It seems that patients with a single lesion exhibit potentially favorable fertility outcomes and may therefore be more suitable candidates for uterine preservation surgery. We suggest that caution should be exercised when choosing fertility-sparing surgery for patients with multiple lesions.

5 Strengths and limitations

The most definitive advantage of our study is that the pathology of all lesions has been reviewed, thereby ensuring the homogeneity of case quality. Secondly, the follow-up period is relatively long. We particularly paid attention to the concordance rate of pathological results among different centers, as well as the concordance rate between intraoperative frozen sections and permanent sections. The main limitations of this study lie in its retrospective nature, relatively small sample size, and the wide span of follow-up time.

6 Conclusion

In conclusion, the diagnosis of STUMP was difficult, and multicenter consultation was recommended to distinguish malignant sarcoma. Myomectomy appears an alternative for

patients with fertility aspirations. Patients with a single lesion seem to exhibit potentially favorable fertility outcomes.

Data availability statement

The data analyzed in this study is subject to the following licenses/restrictions: The datasets for this article are not publicly available due to patient privacy concerns. Requests to access the datasets should be directed to liu679626@163.com.

Ethics statement

This study was approved by the Ethics Committee of The Affiliated Drum Tower Hospital of Nanjing University Medical School. Written informed consent was obtained from the individual (s) for the publication of any potentially identifiable images or data included in this article.

Author contributions

LL: Data curation, Formal analysis, Investigation, Methodology, Writing – original draft, Writing – review & editing. ZX: Data curation, Investigation, Writing – original draft, Formal analysis, Writing – review & editing. ZL: Conceptualization, Writing – original draft, Funding acquisition, Resources, Writing – review & editing. JZ: Conceptualization, Writing – review & editing, Data curation, Investigation, Methodology, Writing – original draft. XX: Conceptualization, Data curation, Investigation, Methodology, Writing – original draft, Writing – review & editing. HZ: Conceptualization, Funding acquisition, Supervision, Visualization, Writing – original draft, Writing – review & editing, Project administration, Resources.

Funding

The author(s) declare financial support was received for the research, authorship, and/or publication of this article. This work was supported by the General Medical Research Project of Jiangsu Health Committee (Grant No. H2019012) and Natural Science Youth Foundation of Jiangsu Province (Grant No. BK20210024), which play an important role in data collection and data analysis.

Conflict of interest

The authors declare that the research was conducted in the absence of any commercial or financial relationships that could be construed as a potential conflict of interest.

Publisher's note

All claims expressed in this article are solely those of the authors and do not necessarily represent those of their affiliated organizations, or those of the publisher, the editors and the reviewers. Any product that may be evaluated in this article, or claim that may be made by its manufacturer, is not guaranteed or endorsed by the publisher.

References

1. Ip PPC, Croce S, Gupta M. Smooth muscle tumour of uncertain Malignant potential of the uterine corpus. In: *WHO Classification of Tumours Editorial Board, WHO Classification of Tumours of Female Reproductive Organs, 5th ed*. IARC Press, Lyon (2020). p. 279–80.

2. Gupta M, Laury AL, Nucci MR, Quade BJ. Predictors of adverse outcome in uterine smooth muscle tumours of uncertain Malignant potential (STUMP): a clinicopathological analysis of 22 cases with a proposal for the inclusion of additional histological parameters. *Histopathology*. (2018) 73:284–98. doi: 10.1111/his.2018.73.issue-2

3. Kempson RL. Sarcomas and related neoplasms. In: Norris HJ, Hertig AT, Abell MR, editors. *The Uterus*. Williams & WIlkins, Baltimore (1973). p. 301–14.

4. Bell SW, Kempson RL, Hendrickson MR. Problematic uterine smooth muscle neoplasms. A clinicopathologic study of 213 cases. *Am J Surg Pathol*. (1994) 18:535–58. doi: 10.1097/00000478-199406000-00001

5. Ip PP, Cheung AN, Clement PB. Uterine smooth muscle tumors of uncertain Malignant potential (STUMP): a clinicopathologic analysis of 16 cases. *Am J Surg Pathol*. (2009) 33:992–1005. doi: 10.1097/PAS.0b013e3181a02d1c

6. Guntupalli SR, Ramirez PT, Anderson ML, Milam MR, Bodurka DC, Malpica A. Uterine smooth muscle tumor of uncertain Malignant potential: a retrospective analysis. *Gynecol Oncol*. (2009) 113:324–6. doi: 10.1016/j.ygyno.2009.02.020

7. Borella F, Cosma S, Ferraioli D, Ray-Coquard I, Chopin N, Meeus P, et al. Clinical and histopathological predictors of recurrence in uterine smooth muscle tumor of uncertain Malignant potential (STUMP): A multicenter retrospective cohort study of tertiary centers. *Ann Surg Oncol*. (2022) 29:8302–14. doi: 10.1245/s10434-022-12353-y

8. Basaran D, Usubutun A, Salman MC, Narin MA, Boyraz G, Turkmen O, et al. The clinicopathological study of 21 cases with uterine smooth muscle tumors of uncertain Malignant potential: centralized review can purify the diagnosis. *Int J Gynecol Cancer*. (2018) 28:233–40. doi: 10.1097/IGC.0000000000001178

9. Croce S, Ribeiro A, Brulard C, Noel JC, Amant F, Stoeckle E, et al. Uterine smooth muscle tumor analysis by comparative genomic hybridization: a useful diagnostic tool in challenging lesions. *Mod Pathol*. (2015) 28:1001–10. doi: 10.1038/modpathol.2015.3

10. Lok J, Tse KY, Lee EYP, Wong RWC, Cheng ISY, Chan ANH, et al. Intraoperative frozen section biopsy of uterine smooth muscle tumors: A clinicopathologic analysis of 112 cases with emphasis on potential diagnostic pitfalls. *Am J Surg Pathol*. (2021) 45:1179–89. doi: 10.1097/PAS.0000000000001746

11. Ha HI, Choi MC, Heo JH, Kim KA, Jung SG, Park H, et al. A clinicopathologic review and obstetric outcome of uterine smooth muscle tumor of uncertain Malignant potential (STUMP) in a single institution. *Eur J Obstet Gynecol Reprod Biol*. (2018) 228:1–5. doi: 10.1016/j.ejogrb.2018.06.003

12. Zhang Q, Kanis MJ, Ubago J, Liu D, Scholtens DM, Strohl AE, et al. The selected biomarker analysis in 5 types of uterine smooth muscle tumors. *Hum Pathol*. (2018) 76:17–27. doi: 10.1016/j.humpath.2017.12.005

13. Leitao MM Jr, Hensley ML, Barakat RR, Aghajanian C, Gardner GL, Jewell EL, et al. Immunohistochemical expression of estrogen and progesterone receptors and outcomes in patients with newly diagnosed uterine leiomyosarcoma. *Gynecol Oncol*. (2012) 124:558–62. doi: 10.1016/j.ygyno.2011.11.009

14. Hewedi IH, Radwan NA, Shash LS. Diagnostic value of progesterone receptor and p53 expression in uterine smooth muscle tumors. *Diagn Pathol*. (2012) 7:1. doi: 10.1186/1746-1596-7-1

15. Delgado B, Dreiher J, Braiman D, Meirovitz D, Shaco-Levy D, et al. P16, Ki67, P53, and WT1 expression in uterine smooth muscle tumors: An adjunct in confirming the diagnosis of Malignancy in ambiguous cases. *Int J Gynecol Pathol*. (2021) 40:257–62. doi: 10.1097/PGP.0000000000000688

16. Kanayama S, Oi H, Kawaguchi R, Furukawa N. Immunohitochemical analysis of p16 expression in uterine smooth muscle tumors. *Open J Obstet Gynecol*. (2015) 5:688–97. doi: 10.4236/ojog.2015.512097

17. Atkins KA, Arronte N, Darus CJ, Rice LW. The Use of p16 in enhancing the histologic classification of uterine smooth muscle tumors. *Am J Surg Pathol*. (2008) 32:98–102. doi: 10.1097/PAS.0b013e3181574d1e

18. Schaefer IM, Hornick JL, Sholl LM, Quade BJ, Nucci MR, Parra-Herran C, et al. Abnormal p53 and p16 staining patterns distinguish uterine leiomyosarcoma from inflammatory myofibroblastic tumour. *Histopathology*. (2017) 70:1138–46. doi: 10.1111/his.2017.70.issue-7

19. Ip PP, Lim D, Cheung ANY, Oliva E. Immunoexpression of p16 in uterine leiomyomas with infarct-type necrosis: an analysis of 35 cases. *Histopathology*. (2017) 71:743–50. doi: 10.1111/his.2017.71.issue-5

20. Makinen N, Kampjarvi K, Frizzell N, Butzow R, Vahteristo P. Characterization of MED12, HMGA2, and FH alterations reveals molecular variability in uterine smooth muscle tumors. *Mol Cancer*. (2017) 16:101. doi: 10.1186/s12943-017-0672-1

21. Slatter TL, Hsia H, Samaranayaka A, Sykes P, Clow WB, Devenish C, et al. Loss of ATRX and DAXX expression identifies poor prognosis for smooth muscle tumours of uncertain Malignant potential and early stage uterine leiomyosarcoma. *J Path: Clin Res*. (2015) 1:95–105. doi: 10.1002/cjp2.v1.2

22. Croce S, Ducoulombier A, Ribeiro A, Lesluyes T, Noel JC, Amant F, et al. Genome profiling is an efficient tool to avoid the STUMP classification of uterine smooth muscle lesions: a comprehensive array-genomic hybridization analysis of 77 tumors. *Mod Pathol*. (2018) 31:816–28. doi: 10.1038/modpathol.2017.185

23. Conconi D, Redaelli S, Alberto Lissoni A, Cilibrasi C, Perego P, Gautiero E, et al. Genomic and epigenomic profile of uterine smooth muscle tumors of uncertain Malignant potential (STUMPs) revealed similarities and differences with leiomyomas and leiomyosarcomas. *Int J Mol Sci*. (2021) 22:15. doi: 10.3390/ijms22041580

24. Di Giuseppe J, Grelloni C, Giuliani L, DelliCarpini G, Giannella L, Ciavattini A. Recurrence of uterine smooth muscle tumor of uncertain Malignant potential: A systematic review of the literature. *Cancers (Basel)*. (2022) 14:2323. doi: 10.3390/cancers14092323

25. Şahin H, Karatas F, Coban G, Özen Ö, Erdem Ö, Onan MA, et al. Uterine smooth muscle tumor of uncertain Malignant potential: fertility and clinical outcomes. *J Gynecol Oncol*. (2019) 30:e54. doi: 10.3802/jgo.2019.30.e54

26. Huo L, Wang D, Wang W, Cao D, Yang J, Wu M, et al. Oncologic and reproductive outcomes of uterine smooth muscle tumor of uncertain Malignant potential: A single center retrospective study of 67 cases. *Front Oncol*. (2020) 10:647. doi: 10.3389/fonc.2020.00647

27. Shim JI, Han AKW, Jeon HJ, Kim M, Jung YW, Yun BS, et al. Clinical experience of uterine smooth muscle tumor of uncertain Malignant potential in two gynecological centers: Oncological and obstetrical aspects. *Eur J Obstet Gynecol Reprod Biol*. (2020) 246:7–13. doi: 10.1016/j.ejogrb.2020.01.002

28. Travaglino A, Raffone A, Gencarelli A, Caldarelli C, Granata M, Santoro A, et al. Stanford parameters stratify the risk of recurrence in gynecologic smooth muscle tumors of uncertain Malignant potential. *APMIS*. (2021) 129:283–90. doi: 10.1111/apm.v129.6

29. Travaglino A, Raffone A, Gencarelli A, Neola D, Oliviero DA, Alfano R, et al. p53, p16 and ki67 as immunohistochemical prognostic markers in uterine smooth muscle tumors of uncertain Malignant potential (STUMP). *Pathol Res Pract*. (2021) 226:153592. doi: 10.1016/j.prp.2021.153592

30. Mowers EL, Skinner B, McLean K, Reynolds RK. Effects of morcellation of uterine smooth muscle tumor of uncertain Malignant potential and endometrial stromal sarcoma: case series and recommendations for clinical practice. *J Minim Invasive Gynecol*. (2015) 22:601–6. doi: 10.1016/j.jmig.2015.01.007

31. Oduyebo T, Rauh-Hain AJ, Meserve EE, Seidman MA, Hinchcliff E, George S, et al. The value of re-exploration in patients with inadvertently morcellated uterine sarcoma. *Gynecol Oncol*. (2014) 132:360–5. doi: 10.1016/j.ygyno.2013.11.024

32. Raspagliesi F, Maltese G, Bogani G, Fucà G, Lepori S, De Iaco P, et al. Morcellation worsens survival outcomes in patients with undiagnosed uterine leiomyosarcomas: A retrospective MITO group study. *Gynecol Oncol*. (2017) 144:90–5. doi: 10.1016/j.ygyno.2016.11.002

33. Gadducci A, Zannoni GF. Uterine smooth muscle tumors of unknown Malignant potential: A challenging question. *Gynecol Oncol*. (2019) 154:631–7. doi: 10.1016/j.ygyno.2019.07.002

Glossary

STUMP	smooth muscle tumors of uncertain malignant potential	BSO	Bilateral Salpingo-oophorectomy
HPFs	High-power fields	BS	Bilateral Salpingectomy
CTCN	Coagulative tumor cell necrosis	PC	Pelvic cavity
WHO	World Health Organization	AC	Abdominal cavity
CT	Computed tomography	LSH	Laparoscopic subtotal hysterectomy
LMS	Leiomyosarcomas	PMR	Pelvic mass resection
LM	Leiomyoma	CS	Cesarean section
PR	Progesterone receptor	SAH	Subtotal abdominal hysterectomy
ER	estrogen receptor	USO	Unilateral salpingo-oophorectomy
H&E	Hematoxylin and eosin-stained	ANED	alive with no evidence of disease.

frontiers | Frontiers in Oncology

TYPE Review
PUBLISHED 13 November 2024
DOI 10.3389/fonc.2024.1471978

Check for updates

OPEN ACCESS

EDITED BY
Dragos Eugen Georgescu,
Carol Davila University of Medicine and Pharmacy, Romania

REVIEWED BY
Sabahattin Cömertpay,
Kahramanmaras Sütçü Imam University, Türkiye
Aditi Bhatt,
Zydus Hospitals, India

*CORRESPONDENCE
Jing Xiong
jingxiong@hust.edu.cn

†These authors have contributed equally to this work

RECEIVED 28 July 2024
ACCEPTED 18 October 2024
PUBLISHED 13 November 2024

CITATION
Yao Y, Yan H, Xiong J and Duan Y (2024) A case of ovarian mesothelioma with VHL mutation diagnosed by immunohistochemistry and literature review. *Front. Oncol.* 14:1471978. doi: 10.3389/fonc.2024.1471978

COPYRIGHT
© 2024 Yao, Yan, Xiong and Duan. This is an open-access article distributed under the terms of the Creative Commons Attribution License (CC BY). The use, distribution or reproduction in other forums is permitted, provided the original author(s) and the copyright owner(s) are credited and that the original publication in this journal is cited, in accordance with accepted academic practice. No use, distribution or reproduction is permitted which does not comply with these terms.

A case of ovarian mesothelioma with VHL mutation diagnosed by immunohistochemistry and literature review

Ye Yao[1†], Hao Yan[2†], Jing Xiong[1*] and Yaqi Duan[3]

[1]Department of Nephrology, Union Hospital, Tongji Medical College, Huazhong University of Science and Technology, Wuhan, China, [2]Department of Gynecologic Oncology, Hubei Cancer Hospital, Wuhan, Hubei, China, [3]Department of Pathology, Tongji Hospital, Tongji Medical College, Huazhong University of Science and Technology, Wuhan, China

The malignant mesothelioma mainly develops in the pleura and peritoneum, while primary ovarian mesothelioma is very rare. Here, we report the first case of primary ovarian mesothelioma (clear cell variant) with VHL mutations in the world based on the results of histomorphology, immunohistochemistry, and genetic testing. This is an extremely rare type of tumor that has not been reported so far. Through the literature search, we reviewed primary ovarian mesothelioma, focusing on its differential diagnosis and molecular genetics. The purpose of this paper is to deepen the flexible selection and application of immunohistochemical markers in mesothelioma, so as to reduce missed diagnosis and misdiagnosis.

KEYWORDS

ovarian mesothelioma, ovarian clear cell tumor, differential diagnosis, VHL gene, immunohistochemistry

1 Background

Malignant mesothelioma(MM) originates from the mesothelium, which is a single flat epithelium distributed on the surface of the pleura, peritoneum, and pericardium, mainly occurring in the pleura and peritoneum, while primary ovarian malignant mesothelioma (OMM) is very rare. The first report of malignant mesothelioma was made by Miller and Wynn in 1908 (1), and it was not until 1983 that Addis and Fox proposed the concept of "primary ovary" (2). Compared with epithelial ovarian tumors in gynecology, OMM is difficult to identify. Due to its diverse morphology and great heterogeneity, it is easy to be confused with other tumors under hematoxylin and eosin staining. According to histological characteristics, mesothelioma can be divided into three basic types: epithelioid, sarcomatoid, and biphasic (mixed type). Epithelioid MM is the most common type and includes polygonal, oval, cubic, clear cell-like, and signet-ring-like subtypes (3, 4). The clear cell variant of

mesothelioma is very rare. The earliest one is a case of clear cell variant of pleural mesothelioma reported by Nelson G. Ordóñez in 1996 (5). Subsequent reports were limited to the peritoneal, peritonea, uterus, and testes scabbard film (6–9). There has been no report on OMM with clear cell variants so far. After a complex and tortuous diagnostic process, taking into full consideration the results of histology, immunohistochemistry, and gene sequencing, and conducting multi-team consultations, we hereby report the first case of primary ovarian mesothelioma (clear cell variant) with Von Hippel–Lindau (VHL) gene mutation in the world.

2 Case report

2.1 Initial diagnosis and treatment

Early April 2022, a 40-year-old female patient was diagnosed with right ovarian isodensity occupying lesion by computed tomography (CT) in a local hospital (Figure 1), and serum carbohydrate antigen 125 (CA125) was slightly elevated (62 U/ml). The patient had no special menstrual history, no family history of tumors, and no history of asbestos exposure. After weighing the benefits and drawbacks, the patient agreed to have surgery at the local hospital. During the surgery, the omentum was found to be widely adherent to the pelvis and abdominal wall. The uterus was normal in size and attached to the bladder, abdominal wall, and intestinal canal. The pelvic cavity contained approximately 300 ml of pale-yellow liquid. The right ovary measured 5 cm × 4 cm × 4 cm. It had a smooth exterior and some hard parts. No obvious abnormality in the appearance of the bilateral fallopian tubes or the left ovary was observed. The quick freezing of intraoperative specimens revealed an ovarian tumor on the right side. A borderline ovarian tumor was highly probable, and the presence of a low-grade malignant tumor could not be excluded. Consequently, a comprehensive staging operation for the ovarian tumors was performed: total hysterectomy + bilateral adnophorectomy + pelvic lymph node dissection + para-aortic lymph node dissection + bilateral ovarian artery and vein high ligation + omentum resection.

2.2 Histological

The postoperative pathological examination showed that the right ovarian tumor was 2 cm in diameter and located in the ovary, with a diameter of 0.5 cm nodule in the greater omentum. The boundary of the two lesions was clear, the tumor cells were small, and there was no obvious nuclear division. No tumor tissue was found in the uterus, left adnexa, right fallopian tube, vaginal fornies, and pelvic lymph nodes (Figure 2).

2.3 Similarities and differences of three immunohistochemical tests

The immunohistochemical results of postoperative specimens from local hospitals were as follows: Calretinin (partly+), Wilms tumor gene-1 (WT-1) (−), D2-40 (+), Vimentin (+), GATA-3 (partly+), Paired box gene 8 (PAX-8) (+), Estrogen receptor (ER) (−), Progesterone receptor (PR) (−), Arcinoembryonic antigen (CEA) (−), and Thyroid transcription factor-1 (TTF-1) (−) (Figure 3). Considering the clear cell appearance of the ovarian tumor with positive PAX-8 nuclei and negative WT-1, a diagnosis of ovarian clear cell carcinoma was made in the local hospital.

Nonetheless, some MM markers showed positive results (Calretinin, D2-40, and GATA-3). The diagnosis was still uncertain; therefore, pathological consultation was performed in another hospital, the Affiliated Hospital of Tongji Medical College. On April 17, another hospital reported that the re-staining of WT-1 was positive (the local hospital was negative), and four new markers were added. They included CK5/6(+), Hector Battifora Mesothelial-1 (HBME-1) (+), BRCA-associated protein 1 (BAP1) (weakly +), and NapsinA(−) (Figure 3), indicating a high possibility of mesothelioma.

The diagnosis differed between the two hospitals, and the patient was further seen at a Shanghai hospital in March of the following year. Three new markers were stained by immunohistochemistry: MOC31 (+), Ber-EP4 (+), and hepatocyte nuclear factor-1β (HNF-1β) (−). In addition, further gene testing using a targeted next generation sequencing showed that the first exon of the VHL gene was mutated, p. N78S (c.233A>G) (mutant abundance, 29.36%), p.S65L (c.194C>T) (27.38%). The diagnosis was changed to clear cell papillary cystadenoma of the ovary, related to VHL syndrome.

In view of the twists and turns in the pathological diagnosis (Table 1), the patient returned to the Affiliated Hospital of Tongji Medical College. After carefully reading the pathological slides and searching the literature, the multidisciplinary treatment from the departments of pathology, gynecology, oncology, and other related departments concluded that the specificity of PAX-8, MOC-31, and Ber-EP4 in mesothelioma was not 100%, while the patient was positive for multiple MM markers. The immunohistochemical results of the patient were consistent with the diagnosis of mesothelioma, and the final diagnosis was ovarian mesothelioma (clear cell type) with VHL gene mutation.

2.4 Treatment and follow-up

After surgical treatment in the local hospital, the patient received six cycles of intravenous chemotherapy with pemetrexed 500 mg/m^2 combined with cisplatin 70–75 mg/m^2 in the cancer hospital from May to September 2022. The patient's postoperative

Abbreviations: MM, malignant mesothelioma; OMM, ovarian malignant mesothelioma; VHL, Von Hippel–Lindau; CT, computed tomography; CA125, carbohydrate antigen 125; WT-1, Wilms tumor gene-1; PAX-8, paired box gene 8; ER, estrogen receptor; PR, progesterone receptor; CEA, carcinoembryonic antigen; TTF-1, thyroid transcription factor-1; HBME-1, Hector Battifora Mesothelial-1; BAP1, BRCA-associated protein 1; HNF-1β, hepatocyte nuclear factor-1β; PMM, peritoneal malignant mesothelioma; OCCC, ovarian clear cell carcinoma; ccRCC, clear cell renal cell carcinoma; HIF1α, hypoxia-inducible factor 1α; COSMIC, Catalogue of Somatic Mutations in Cancer.

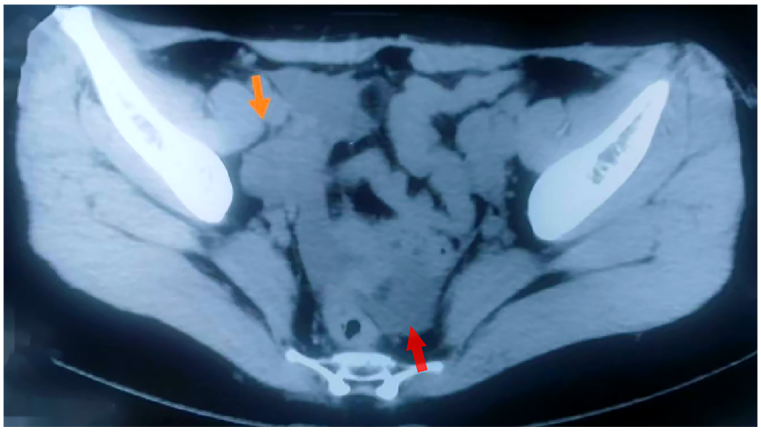

FIGURE 1
Imaging of the tumor. CT showed an isodense mass in the right ovary (orange arrow), with a small amount of fluid in the Douglas cavity (red arrow).

survival period has reached more than 20 months, and no tumor recurrence, metastasis, or ascites was found in regular CT follow-up.

3 Discussion and review

3.1 Epidemiology and clinical manifestations of OMM

Based on the rarity of this diagnosis, we first conducted a literature review on OMM. MM accounts for 0.3% of global cancer deaths, mainly occurring in the pleura (65%–70%), peritoneum (30%), and pericardium (1%–2%) (10). Peritoneal malignant mesothelioma (PMM) can metastasize to the ovary, but is usually limited to the ovarian cortical surface with microscopic infiltration. MM originating from the ovary is extremely rare. According to the review of relevant literature at home and abroad, only 26 cases of OMM have been reported so far (Table 2) (2, 10–22). The 26 OMM patients had an age of onset of 16–74 years, with a median age of 50.5 years. Typical symptoms were abdominal distension and abdominal pain, and some patients had no obvious symptoms and were found by chance during surgery. The tumor diameter was 1–40 cm, and the incidence of bilateral ovarian was 31% (8/26). The pathological types were 14 cases of epithelioid type and two cases of biphasic type. Among the 26 patients, only nine cases had the level of ovarian tumor marker CA125 recorded, of which seven cases were elevated and two cases were normal. Among the seven OMM patients with elevated CA125, three had bilateral mesothelioma lesions. There was no significant correlation between CA125 level and the size of ovarian mesothelioma. The elevated CA125 level may be caused by pelvic inflammation caused by the tumor microenvironment.

The combination of IHC selected by previous OMM is different. The most common markers included calretinin, CK5/6, WT-1, D2-40, Vimentin, HBME-1, ER, PR, CEA, Ber-EP4, B72.3, and HNF-1β (Table 3), and the first six were mesothelioma markers with high sensitivity. The latter six markers are mostly based on the differential diagnosis of ovarian epithelial tumors, and all of them have high specificity for OMM except Ber-EP4.

Calretinin, CK5/6, WT-1, D2-40, Vimentin, and HBME-1, which had high staining rates and sensitivity of OMM, were all positive in this case. Of the six other markers for differential diagnosis, ER, PR, CEA, and HNF-1β were negative, and B72.3

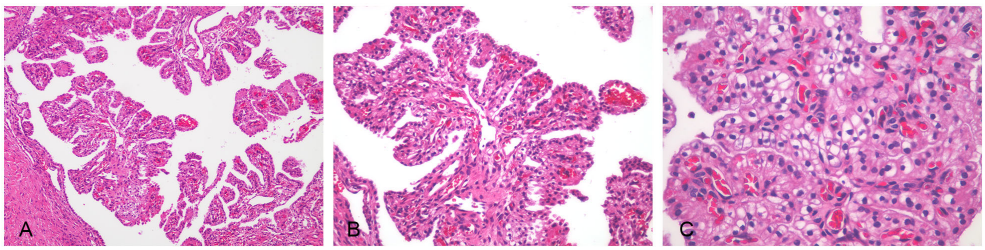

FIGURE 2
Ovarian malignant mesothelioma was seen in hematoxylin–eosin-stained sections. The tumor cells had small atypia; no obvious mitosis, focal well-differentiated papillary mesothelial tumor conformation, complex papillary structure, and interstitial infiltration of the axis of the papilla were observed in some areas. **(A)** Papillary structure (×100). **(B)** Tumor cells were cubic and oval (×200). **(C)** Tumor cells were uniform in size, with clear cytoplasm, small atypia, and no obvious mitoses (×400).

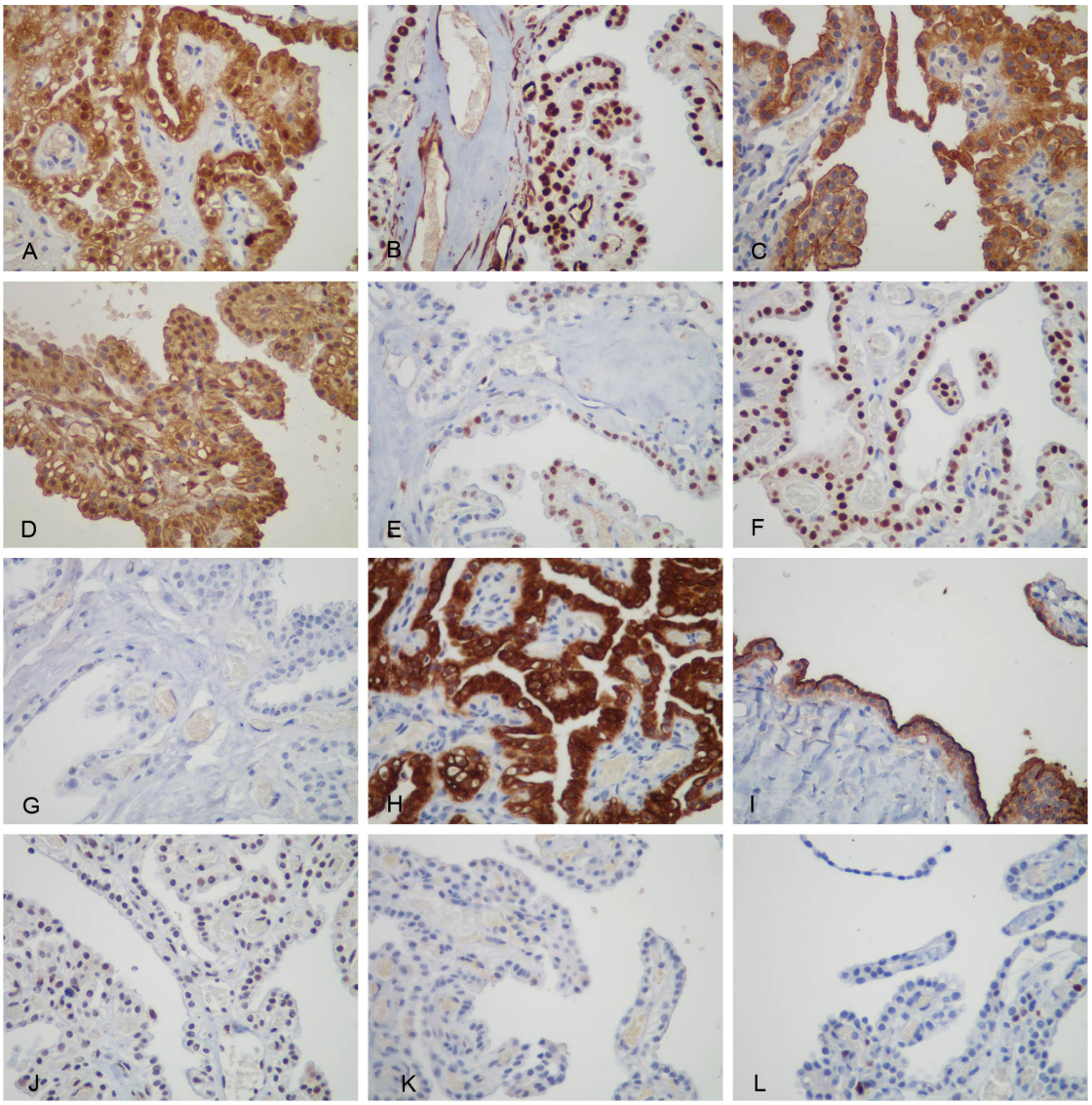

FIGURE 3
Immunohistochemical staining of the tumor cells. **(A)** Both cytoplasmic and nuclear were positive for Calretinin, **(B)** only nuclear was positive for WT-1, **(C)** membranous was positive for D2-40, **(D)** both cytoplasmic and nuclear were positive for Vimentin, **(E)** nuclear was positive for GATA-3 positive, **(F)** nuclear was positive for PAX-8, **(G)** TTF-1, **(H)** membranous was positive for CK5/6, **(I)** membranous was positive for mesothelin (HBME -1), **(J)** nuclear was weakly positive for BAP1, **(K)** Napsin A, and **(L)** Ki-67 positive rate of approximately 5%.

TABLE 1 IHC marker testing institution and time.

Hospital	Time	Positive markers in support of MM	Negative markers in support of MM	Positive markers of MM were excluded	Negative markers of MM were excluded	Diagnosis
The local hospital	2022.4.10	D2-40(+), Calretinin (partly+), GATA-3 (partly+)	ER(−), PR(−), TTF-1(−), CEA(−)	PAX-8(+)	WT-1 (−)*	Ovarian clear cell carcinoma
The Affiliated Hospital of Tongji Medical College#	2022.4.17	WT-1(+)*, CK5/6(+), mesothelin(+), Calretinin (+), GATA-3(+)	NapsinA(−)	BAP1(weakly+)		Ovarian malignant mesothelioma
A Shanghai hospital#	2023.3		HNF-1β(−)	MOC-31(+), Ber-EP4(+)		Ovarian clear cell papillary cystadenoma

MM, malignant mesothelioma.
*Inverted IHC.
#The same IHC is omitted.

TABLE 2 The characteristics of 26 cases of OMM reported internationally.

Case number	Publication (year)	Age (years)	Ovary site	Size (cm)	Clinical manifestations	Histological subtype	Immunohistochemistry	CA125 (U/mL)	Reference number
1	1979	42	Right	1.5	Found during surgery	Epithelioid	NK	NK	(11)
2	1979	74	Left	15	NK	Biphasic	NK	NK	(11)
3	1983	67	Left	9	Found during surgery	Epithelioid	NK	NK	(2)
4	1995	38	Bilateral	NK	Increased abdominal circumference	NK	PCK(+); CEA,B72.3,Leu-M1,Ber-EP4(−)	NK	(12)
5	1995	58	Bilateral	NK	Abdominal pain	NK	PCK(+); CEA,B72.3,Leu-M1,Ber-EP4(−)	NK	(12)
6	1995	71	Left	NK	Abdominal pain	NK	PCK(+); CEA,B72.3,Leu-M1,Ber-EP4(−)	NK	(12)
7	1995	47	Bilateral	NK	Increased abdominal circumference	NK	PCK(+); CEA,B72.3,Leu-M1,Ber-EP4(−)	NK	(12)
8	1995	72	Bilateral	NK	Uterine prolapse	NK	PCK,Ber-EP4(+); CEA,B72.3,Leu-M1(−)	NK	(12)
9	1996	52	Left	3	NK	NK	B72.3,Leu-M1,CEA,Ber-EP4,PLAP(−)	NK	(13)
10	1996	16	Bilateral	10 (left) 1 (left)	Found during surgery	NK	B72.3,Leu-M1,CEA,Ber-EP4,PLAP(−)	NK	(13)
11	2000	47	Right	7	Abdominal pain	Biphasic	PCK,Ber-EP4,thrombomodulin,Calretinin,CK5/6(+); CEA,Leu-M1(−)	NK	(14)
12	2000	61	Left	NK	Weight loss	Epithelioid	PCK,Ber-EP4,Calretinin,CK5/6(+); CEA,Leu-M1,thrombomodulin(−)	NK	(14)
13	2000	66	Left	1	Ascites	Epithelioid	PCK,thrombomodulin,Calretinin,CK5/6(+); CEA,Leu-M1,Ber-EP4(−)	NK	(14)
14	2000	66	Right	3	Ascites	Epithelioid	PCK,Ber-EP4,Calretinin,CK5/6(+); CEA,Leu-M1,thrombomodulin(−)	NK	(14)
15	2001	49	Left	NK	fever	Epithelioid	Vimentin,mesothelial(+); Calretinin partly(+); AFP,CD34(−)	82	(15)
16	2006	46	Right	6	Abdominal pain and distension	NK	CK7,CK,mesothelial,Calretinin(+); CK20,Vimentin(−)	>600	(16)
17	2012	55	Bilateral	6 (both sides)	Frequent urination Abdominal distension	NK	PCK,CA125,CK7,(+); Calretinin(±); CK20,AFP,CEA,Vimentin(−)	1083	(17)
18	2015	50	Left	8	Abdominal pain	Epithelioid	CK,vimentin (+); CEA(−)	Normal*	(10)
19	2015	50	Bilateral	11 (left) 9 (left)	Increased abdominal circumference, Abdominal distension	Epithelioid	PCK,vimentin,WT-1(+); mesothelial,EMA partly(+); D2-40,Calretinin,CK5/6,CK7 focally (+); PLAP,inhibin-α,AFP,CD117,p53,CEA(−); ER positive rate 5%, PR positive rate 10%	3023	(18)

(Continued)

10.3389/fonc.2024.1471978

TABLE 2 Continued

Case number	Publication (year)	Age (years)	Ovary site	Size (cm)	Clinical manifestations	Histological subtype	Immunohistochemistry	CA125 (U/mL)	Reference number
20	2016	39	Right	NK	Abdominal pain	Epithelioid	Calretinin,CK5/6,vimentin,WT-1(+); CEA,P53,ER,PR(-)	Normal*	(19)
21	2017	51	Bilateral	NK	Physical examination found	Epithelioid	WT-1,HBME-1,CK5/6,Calretinin,D2-40,vimentin,CK7,PR(+); CEA,HNF-1β,ER,Ber-EP4(−)	Elevated*	(20)
22	2017	47	Left	NK	Abdominal distension	Epithelioid	WT-1,HBME-1,CK5/6,Calretinin,D2-40,vimentin,CK7(+); CEA,HNF-1β, ER,PR,Ber-EP4(−)	NK	(20)
23	2017	56	Left	3	Abdominal distension	Epithelioid	WT-1,HBME-1,CK5/6,Calretinin,D2-40,vimentin,CK7(+); CEA,HNF-1β,ER,PR,Ber-EP4(−)	NK	(20)
24	2017	69	Right	NK	Abdominal distension	Epithelioid	WT-1,HBME-1,CK5/6,Calretinin,D2-40,vimentin,CK7(+); CEA,HNF-1β,ER,PR,Ber-EP4(−)	NK	(20)
25	2019	35	Left	5	Abdominal distension	Epithelioid	PCK,WT-1,Vimentin,D2-40,CK5/6,Calretinin,IMP-3,HBME-1(+); ER,PR,P53,P16,PAX-8(−)	1045	(21)
26	2021	50	Left	40	NK	NK	CK7,Calretinin,Vimentin,P53,CK8/18,CK19,CK20(+); Ber-EP4 weakly(+) CD30,S100,TTF-1,CD56,EMA,CK5/6,WT-1,TFE3(−)	233	(22)

NK, not known; PCK, pan cytokeratin; PLAP, placental alkaline phosphatase; AFP, alpha fetoprotein; EMA, epithelial membrane antigen; IMP3, insulin-like growth factor II mRNA binding protein 3; TFE3, transcription factor binding to IGHM enhancer 3
*The exact value is not clear.

10.3389/fonc.2024.1471978

10.3389/fonc.2024.1471978

TABLE 3 Specific biomarkers of OMM in this patient and 26 previously reported cases.

	Calretinin	WT-1	D2-40	CK5/6	Vimentin	HBME-1	ER	PR	CEA	Ber-EP4	B72.3	HNF-1β	NapsinA	TTF-1	MOC-31	PAX-8	BAP1	GATA3
The patient	+	+	+	+	+	+	–	–	–	+	NK	–	–	–	+	+	Partly +	+
OMM	+	+	+	+	+	+	–	–	–	–	–	–	–	–	–	–	–	+
Sensitivity in 26 case reports	14/15	7/8	5/6	11/12	10/12	4/4	7/7	6/7	19/19	11/17	7/7	4/4	1/1	NK	NK	1/1	NK	NK

The shaded sections represent contradictory results.

was not stained, while Ber-EP4 achieved the opposite result. In addition to Ber-EP4, MOC-31, PAX-8, and BAP1 listed in Table 3 were not consistent with the usual staining results of MM. Can the diagnosis of OMM be established in this patient?

3.2 Process of diagnosis establishment based on immunohistochemistry

The local hospital considered that the tumor was a right ovarian mass, and the tumor cells were clear cell type. Thus, the diagnosis was ovarian clear cell carcinoma (OCCC). OCCC showed ER(−), PR(−), WT1(−), and PAX-8(+), all of which were consistent with the immunohistochemistry of this case (23), but HNF-1β and NapsinA, which are more specific for OCCC, were not mentioned (24). However, the diagnosis of OCCC depends on morphological features, such as hyaline degeneration of the papillary axis. OCCC also always had cells with significant nuclear atypia even though most of the cells had only mild nuclear atypia. These were not consistent with the pathological sections in this case. There was also no good explanation for the MM-positive markers Calretinin, D2-40, and GATA-3. Calretinin and D2-40 are two mesothelioma markers recommended by the NCCN Clinical Practice Guidelines in Oncology (25). GATA3 is positive in 58% of mesotheliomas, and its expression in adenocarcinomas of the digestive tract, endometrium, ovary, and prostate is often <10% (26).

Pathological sections from the second hospital, Affiliated Hospital of Tongji Medical College, showed focally well-differentiated papillary mesothelial tumor conformation, with complex papillary structures and stromal invasion of the papillary axis in some areas, which was consistent with ovarian malignant mesothelioma. However, the diagnosis of MM is very difficult. In 2017, the International Mesothelioma Interest Group formulated the diagnostic criteria for MM (3, 27): Immunohistochemical results conform to a set of markers, including two mesothelial positive markers and two other tumor markers considered according to morphology. Re-staining for WT-1, a common marker of MM and OCCC, at the second hospital showed the opposite result, which was positive and supported the diagnosis of MM. The MM markers Calretinin, D2-40, and GATA-3, which were positive in the initial hospital, were also positive. The MM markers CK5/6, HBME-1, and BAP1 were also added. The former two mesenchymal markers were positive in MM, which was consistent with the case. BAP1 is a tumor suppressor gene expressed in normal tissues, showing nuclear denudation in >50% of malignant pleural mesothelioma and two-thirds of PMM cases (28). However, the patient was weakly positive for BAP1. However, BAP1 has high specificity and low sensitivity. Accordingly, the absence of BAP1 in the nucleus strongly supports the diagnosis of MM, but the preservation of BAP1 cannot exclude the diagnosis of MM.

The above MM markers are more than two, and the other tumor markers for morphological considerations are worthy of ovarian clear cell carcinoma related markers. Therefore, OCCC-specific markers were added, such as NapsinA, which was negative, and NapsinA showed cytoplasmic granular staining in clear cell

tumors of the ovary (29), which was negative in this case. Unfortunately, Napsin A and HNF-1β are currently two relatively reliable immune antibodies for the diagnosis of OCCC (24). The latter is not shown at this time.

In March of the following year, a pathology consultation was performed in a Shanghai family, and HNF-1β was negative as expected. However, the diagnosis of ovarian clear cell papillary cystadenoma was made based on the positive MOC31 and Ber-EP4. As is known, Ber-EP4 is expressed in epithelial cells but not in mesothelial cells. On the contrary, the statistical analysis of the above 26 cases of OMM reported internationally found that the positive rate of Ber-EP4 was as high as 11/17 (65%), so even if Ber-EP4 is positive, the possibility of OMM cannot be excluded (Table 3). MOC-31 is a cell surface protein with carcinogenic characteristics, expressed in healthy epithelial cells and corresponding malignant tumors, often positive in breast cancer, gastrointestinal tumors, and ovarian mucinous carcinoma, not a specific marker of clear cell ovarian tumors, and can also be positively expressed in 5% of PMM (3). Therefore, even if the patient has positive MOC-31 staining, OMM cannot be excluded.

A retrospective review of the patient's controversial PAX-8 expression was positive, which largely interfered with the judgment of the local hospital. PAX-8 is a specific marker of Mullerian duct epithelium-derived tumors discovered in recent years. During embryonic development, PAX-8 plays a key role in the formation of the thyroid, kidney, part of the central nervous system, inner ear, eye, and Mullerian duct organs. The nuclei of clear cell tumor of the ovary diffusely express PAX-8, so PAX-8 is often used in the differential diagnosis of mesothelioma. The patient also showed strong positive PAX-8 staining; for this reason, some pathological experts did not agree with the diagnosis of mesothelioma. Through a literature search, Chapel and Husain reported 27 cases of peritoneal mesothelioma, of which five cases were positive for PAX-8, including three female patients with diffuse (>50% of the tumor nuclei) staining and two male patients with focal (<50% of the tumor nuclei) staining (30). They believed that PAX-8 could also be positive in MM because PAX-8 and calretinin were co-expressed in the epithelium of the ovary surface, a transitional area known as the tubal–peritoneal junction, where the PAX-8(+) epithelium might sometimes differentiate along the mesothelial lineage, resulting in a series of PAX-8(+) mesothelial lesions. Unfortunately, PAX-8 staining analysis was performed in 1 of the previous 26 cases of OMM (Table 3), which also suggested that we could improve PAX-8 staining rate in patients with mesothelioma as much as possible in the future, providing more accurate information for the formulation of future guidelines or consensus.

The onset of mesothelioma was insidious, the clinical manifestations were nonspecific, and the imaging was atypical. It is difficult to distinguish it from other tissues due to its diverse morphology. Although markers with slightly higher specificity and sensitivity in the diagnosis of MM are emerging, it is difficult for any single molecular marker to definitively diagnose mesothelioma. None of the immunohistochemical markers had 100% sensitivity or specificity. The main reason for the inaccurate diagnosis of MM appears to be the use of incomplete immunostaining and incorrect interpretation of staining. A retrospective study on the pathological diagnosis of 92 MM cases in eastern China found that only 56.5% or 52/92 have confirmed diagnosis of cases, 17.4% excluded, and remained uncertain in 26% of cases (31). The results of this study are similar to those of Goldberg in 2006, confirming the diagnosis in 67% of cases and ruling out indeterminate in 13% and 20% of cases (32). Therefore, the problem of MM diagnostic accuracy is not limited to China. For controversial cases, it is necessary to rely on more experienced pathologists to make a second diagnosis, which requires the centralized diagnosis and management of mesothelioma and the formation of a multidisciplinary team to reduce misdiagnosis and missed diagnosis.

Another confusing diagnosis was PMM. Diffuse PMM often involves the ovary, while malignant mesothelioma originating from the ovary is extremely rare. PMM and OMM are easily confused, and the differential diagnosis between them requires observation of the extent of tumor involvement and ovarian condition during operation. In this case, the presence of omental tumor lesions may indicate the seeding of primary ovarian tumors, or they may originate from the peritoneum, which we suggest to be the first possibility. First, the careful examination of the tumor involvement range during the operation could generally only confirm the involvement of the right ovary, and no obvious lesions in the peritoneum were found. Postoperative pathology showed that the tumor was 2 cm in diameter and located in the ovary, and there were nodules with a diameter of 0.5 cm in the greater omentum. Ovarian enlargement is rare in PMM. Even if the tumor metastasized to the ovary, the involvement of the tumor

TABLE 4 Mesothelioma with VHL mutations.

Publication (year)	Case number	Site	Mutations in genes	Reference number
2019	1	Peritoneal clear cell mesothelioma	VHL exon2, p.F136Nfs 25	(37)
2020	2	Peritoneal clear cell mesothelioma	VHL Y98fs*24	(38)
2021	3	Peritoneal clear cell mesothelioma	VHL exon 1 c.254dupT	(39)
2023	4	Peritoneal clear cell mesothelioma	p.E94Sfs*63	(40)
2023	5	Peritoneal clear cell mesothelioma	p.F136fs*25	(40)
2023	6	Peritoneal clear cell mesothelioma	HD	(40)
2023	7	Pleural clear cell mesothelioma	p.V181fs*18	(40)

was mostly confined to the serosa and cell cortex, with no invasion of the ovarian parenchyma or only minimal surface invasion and usually a large extra-ovarian space occupying (13).

3.3 Clear cell subtype of MM with VHL mutations

The clear cell subtype is a rare variant of epithelioid mesothelioma (25). The most common cause of cytoplasmic hyalinization is the accumulation of large amounts of intracellular glycogen. Another but less common factor is the accumulation of large amounts of lipids, which occurs alone or in combination with glycogen (33). Tumors that are easily confused with clear cell mesothelioma are metastatic renal cell carcinoma, lung adenocarcinoma with clear cell features, and OCCC (6). Inactivation of VHL is common in clear cell renal cell carcinoma (ccRCC), and it has been reported that up to 90% of ccRCC have loss-of-function mutations in VHL (34). Interestingly, this patient presents with the clear cell subtype. The gene testing of this patient showed two missense mutations VHL p.N78S, c.233A>G, VHL p.S65L, and c.194C>T in the first exon of the VHL gene, and both are mutations with potential clinical significance. The product of the VHL gene, pVHL, is involved in the formation of the VCB-CR complex. This complex catalyzes the polyubiquitination of specific proteins and makes them degraded by proteasome. The dysfunction of pVHL leads to the accumulation of downstream hypoxia-inducible factor 1α (HIF 1α) subunits, activates a variety of hypoxia-inducible genes, and promotes the occurrence of tumors under normoxic conditions (35, 36). Screening of the Catalogue of Somatic Mutations in Cancer (COSMIC) database showed that the same missense mutation in this case is highly correlated with renal cancer. For example, the second missense mutation p. S65l has been reported in COSMIC database in 26 cases, all of which were related to the clinical phenotype of renal clear cell carcinoma. Through literature retrieval, a total of seven cases of mesothelioma with VHL gene mutations were reported, including six cases of peritoneal mesothelioma and one case of pleural mesothelioma (37–40) (Table 4), and no ovarian mesothelioma has been reported. The types of mutations include frameshift mutations and repetitive mutations. It is interesting to note that even though there are different types of mutations, these patients are characterized by clear cell variant mesothelioma. Therefore, further studies on genetic and epigenetic changes are needed to determine whether there is a relationship between VHL genotype and clear cell phenotype.

4 Conclusion

We report the first case of primary ovarian mesothelioma (clear cell variant) with VHL gene mutation in the world. Mesothelioma is common in the peritoneum and the pleural, and primary mesothelioma in the ovary is very rare. In addition, this patient presents with a unique subtype of clear cell variant, which has not been reported so far. Even more interesting is that the VHL gene mutation was also detected in this patient. The disease is easily confused with OCCC, so it is necessary to expand the immunohistochemical marker panel. In a word, both primary ovarian mesothelioma and clear cell variant of mesothelioma with VHL mutations are extremely rare, and a careful diagnosis needs to be made by combining histomorphology, immunohistochemistry, and genetic testing.

Author contributions

HY: Data curation, Methodology, Writing – review & editing. YY: Investigation, Software, Visualization, Writing – original draft. JX: Conceptualization, Funding acquisition, Supervision, Visualization, Writing – review & editing. YD: Methodology, Writing – review & editing.

Funding

The author(s) declare financial support was received for the research, authorship, and/or publication of this article. The work was supported by the Chinese Cardiovascular Association-Natural lipid-lowering drugs fund (grant numbers. 2023-CCA-NLD-742) and Scientific research project of Traditional Chinese Medicine Department of Hubei Province Administration of Traditional Chinese Medicine (grant numbers. ZY2023F026).

Acknowledgments

Thanks to Huixia Liu and Yujuan Li for the translation correction.

Conflict of interest

The authors declare that the research was conducted in the absence of any commercial or financial relationships that could be construed as a potential conflict of interest.

Publisher's note

All claims expressed in this article are solely those of the authors and do not necessarily represent those of their affiliated organizations, or those of the publisher, the editors and the reviewers. Any product that may be evaluated in this article, or claim that may be made by its manufacturer, is not guaranteed or endorsed by the publisher.

References

1. Miller J, Wynn WH. A Malignant tumour arising from the endothelium of the peritoneum, and producing a mucoid ascitic fluid. *J Pathol Bacteriol*. (1908) 12:267–78. doi: 10.1002/path.1700120212

2. Addis BJ, Fox H. Papillary mesothelioma of ovary. *Histopathology*. (1983) 7:287–98. doi: 10.1111/j.1365-2559.1983.tb02242.x

3. Husain AN, Colby TV, Ordonez NG, Allen TC, Attanoos RL, Beasley MB, et al. Guidelines for pathologic diagnosis of Malignant mesothelioma 2017 update of the consensus statement from the international mesothelioma interest group. *Arch Pathol Lab Med*. (2018) 142:89–108. doi: 10.5858/arpa.2017-0124-RA

4. Liu B, Zhou X. Pathological diagnosis of Malignant mesothelioma. *Chin J Diagn Pathol*. (2014) 21:1–3.

5. Ordonez NG, Myhre M, Mackay B. Clear cell mesothelioma. *Ultrastruct Pathol*. (1996) 20:331–6. doi: 10.3109/01913129609016333

6. Ordóñez NG. Clear cell mesothelioma presenting as an incarcerated abdominal hernia. *Virchows Arch*. (2005) 447:823–7. doi: 10.1007/s00428-005-0023-2

7. Hayashi H, Kawata T, Shimokawa I. Malignant peritoneal mesothelioma, clear cell variant, in a female and its differentiation from clear cell carcinoma. *Pathol Res Pract*. (2017) 213:580–4. doi: 10.1016/j.prp.2016.12.025

8. Pongsuvareeyakul T, Saipattranusorn K, Sukpan K, Suprasert P, Khunamornpong S. Clear-cell mesothelioma of uterine corpus: diagnostic challenges in intraoperative frozen sections. *Diagnostics (Basel)*. (2023) 13(6):1119. doi: 10.3390/diagnostics 13061119

9. Mishra A, Shet T. Clear cell mesothelioma of the testis with deciduoid areas–a case report. *Indian J Pathol Microbiol*. (2004) 47:544–6.

10. Kapoor R, Kuttikat PG, Vaiphei K, Rai B, Patel FD. A case report of peritoneal Malignant mesothelioma presenting as primary ovarian mass. *J Cancer Res Ther*. (2015) 11:654. doi: 10.4103/0973-1482.139382

11. Russell P. The pathological assessment of ovarian neoplasms. III: The Malignant "epithelial" tumours. *Pathology*. (1979) 11:493–532. doi: 10.3109/00313027909059027

12. Goldblum J, Hart WR. Localized and diffuse mesotheliomas of the genital tract and peritoneum in women. A clinicopathologic study of nineteen true mesothelial neoplasms, other than adenomatoid tumors, multicystic mesotheliomas, and localized fibrous tumors. *Am J Surg Pathol*. (1995) 19:1124–37. doi: 10.1097/00000478-199510000-00003

13. Clement PB, Young RH, Scully RE. Malignant mesotheliomas presenting as ovarian masses. *A Rep nine cases including two primary Ovarian mesotheliomas. Am J Surg Pathol*. (1996) 20:1067–80. doi: 10.1097/00000478-199609000-00004

14. Attanoos RL, Gibbs AR. Primary Malignant gonadal mesotheliomas and asbestos. *Histopathology*. (2000) 37:150–9. doi: 10.1046/j.1365-2559.2000.00942.x

15. Hu H, Ning G, Yang H. Malignant mesothelioma of ovarian epithelium: a case report. *Hainan Med J*. (2001) 07:90.

16. Sun L, Guan YM, Kang ZH, Fu H, Du BT. One case of Malignant mesothelioma of bilateral ovary, oviduct and omentum misdiagnosed as ovarian cancer. *Chin J Misdiagnostics*. (2006) 18:3573–5.

17. Liu Y, Huang X. Malignant ovarian mesothelioma complicated with increased amylase: a case report. *J Pract Gynecol*. (2012) 28:316.

18. Hu LN, Li L, Wang XQ, Liu LL, Li YQ. Ovarian Malignant mesothelioma of both sides:a clinicopathological analysis. *Chin J Diagn Pathol*. (2015) 22:287–289 + 293.

19. Lin J, Wang Q, Gu Y, Pei XJ, Deng YJ, Ding YQ. Ovarian Malignant mesothelioma with endometrial cyst: a case report and review of literature. *Int J Clin Exp Patho*. (2016) 9:2594–8.

20. Zhang S, Yu W, Wang L. Epithelioid Malignant mesothelioma of ovary: a clinicopathological analysis of 4 cases. *J Clin Exp Pathol*. 354. (2017) 33:1135–7. doi: 10.13315/j.cnki.cjcep.2017.10.018

21. Wang M, Ma S, Zhan Z, Wang YJ, Zhao SH, Yang SL. A case report of ovarian epithelioid Malignant mesothelioma and literature review. *Int Reprod Health/Fam Plan*. (2019) 38:438–40.

22. Ouafki I, Nouiakh L, Boujarnija R, Amarti A, Amaadour L, Oualla K, et al. Malignant mesothelioma of the ovary: a case report. *Pan Afr Med J*. (2021) 38:92. doi: 10.11604/pamj.2021.38.92.24462

23. Fujiwara K, Shintani D, Nishikawa T. Clear-cell carcinoma of the ovary. *Ann oncology: Off J Eur Soc Med Oncol*. (2016) 27 Suppl 1:i50–i2. doi: 10.1093/annonc/mdw086

24. Butler H, Saulat O, Guinn BA. Identification of biomarkers for the diagnosis and targets for therapy in patients with clear cell ovarian cancer: a systematic literature review. *Carcinogenesis*. (2022) 43:183–9. doi: 10.1093/carcin/bgac012

25. Ettinger DS, Wood DE, Stevenson J, Aisner DL, Akerley W, Bauman JR, et al. Mesothelioma: peritoneal, version 2.2023, NCCN clinical practice guidelines in oncology. *J Natl Compr Cancer Network: JNCCN*. (2023) 21:961–79. doi: 10.6004/jnccn.2023.0045

26. Miettinen M, McCue PA, Sarlomo-Rikala M, Rys J, Czapiewski P, Wazny K, et al. GATA3: a multispecific but potentially useful marker in surgical pathology: a systematic analysis of 2500 epithelial and nonepithelial tumors. *Am J Surg Pathol*. (2014) 38:13–22. doi: 10.1097/PAS.0b013e3182a0218f

27. Kusamura S, Kepenekian V, Villeneuve L, Lurvink RJ, Govaerts K, De Hingh I, et al. Peritoneal mesothelioma: PSOGI/EURACAN clinical practice guidelines for diagnosis, treatment and follow-up. *Eur J Surg Oncol*. (2021) 47:36–59. doi: 10.1016/j.ejso.2020.02.011

28. Devins KM, Zukerberg L, Watkins JC, Hung YP, Oliva E. BAP1 and claudin-4, but not MTAP, reliably distinguish borderline and low-grade serous ovarian tumors from peritoneal mesothelioma. *Int J Gynecol Pathol*. (2023) 42:159–66. doi: 10.1097/PGP.0000000000000877

29. Iwamoto M, Nakatani Y, Fugo K, Kishimoto T, Kiyokawa T. Napsin A is frequently expressed in clear cell carcinoma of the ovary and endometrium. *Hum Pathol*. (2015) 46:957–62. doi: 10.1016/j.humpath.2015.03.008

30. Chapel DB, Husain AN, Krausz T, McGregor SM. PAX8 expression in a subset of Malignant peritoneal mesotheliomas and benign mesothelium has diagnostic implications in the differential diagnosis of ovarian serous carcinoma. *Am J Surg Pathol*. (2017) 41:1675–82. doi: 10.1097/PAS.0000000000000935

31. Guo Z, Carbone M, Zhang X, Su D, Sun W, Lou J, et al. Improving the accuracy of mesothelioma diagnosis in China. *J Thorac oncology: Off Publ Int Assoc Study Lung Cancer*. (2017) 12:714–23. doi: 10.1016/j.jtho.2016.12.006

32. Goldberg M, Imbernon E, Rolland P, Gilg Soit Ilg A, Savès M, de Quillacq A, et al. The french national mesothelioma surveillance program. *Occup Environ Med*. (2006) 63:390–5. doi: 10.1136/oem.2005.023200

33. Ordóñez NG. Mesothelioma with clear cell features: an ultrastructural and immunohistochemical study of 20 cases. *Hum Pathol*. (2005) 36:465–73. doi: 10.1016/j.humpath.2005.02.014

34. Hsieh JJ, Le VH, Oyama T, Ricketts CJ, Ho TH, Cheng EH. Chromosome 3p loss-orchestrated VHL, HIF, and epigenetic deregulation in clear cell renal cell carcinoma. *J Clin oncology: Off J Am Soc Clin Oncol*. (2018) 36:Jco2018792549. doi: 10.1200/JCO.2018.79.2549

35. Tarade D, Ohh M. The HIF and other quandaries in VHL disease. *Oncogene*. (2018) 37:139–47. doi: 10.1038/onc.2017.338

36. Dagogo-Jack I, Madison RW, Lennerz JK, Chen KT, Hopkins JF, Schrock AB, et al. Molecular characterization of mesothelioma: impact of histologic type and site of origin on molecular landscape. *JCO Precis Oncol*. (2022) 6:e2100422. doi: 10.1200/PO.21.00422

37. Smith-Hannah A, Naous R. Primary peritoneal epithelioid mesothelioma of clear cell type with a novel VHL gene mutation: a case report. *Hum Pathol*. (2019) 83:199–203. doi: 10.1016/j.humpath.2018.07.033

38. Saeed OAM, Armutlu A, Zhang X, Saxena R. Primary peritoneal mesothelioma with clear cell morphology presenting with multiple liver masses: report of a case with a unique VHL Y98fs*24 mutation and indolent clinical course. *Ajsp-Rev Rep*. (2020) 25:295–7. doi: 10.1097/PCR.0000000000000392

39. Du XM, Wei YP, Gao Y, Li Z, Zhang JM, Chang H, et al. Clinicopathological characteristics of primary peritoneal epithelioid mesothelioma of clear cell type: A case report. *Med (Baltimore)*. (2021) 100:e25264. doi: 10.1097/MD.0000000000025264

40. Michal M, Kravtsov O, Ross JS, Skanderova D, Martinek P, Mosaieby E, et al. Clear cell mesotheliomas with inactivating VHL mutations and near-haploid genomic features. *Genes Chromosomes Cancer*. (2023) 62:267–74. doi: 10.1002/gcc.23119

frontiers | Frontiers in Oncology

TYPE Case Report
PUBLISHED 18 November 2024
DOI 10.3389/fonc.2024.1449270

Check for updates

OPEN ACCESS

EDITED BY
Dragos Eugen Georgescu,
Carol Davila University of Medicine and Pharmacy, Romania

REVIEWED BY
Giuseppe Angelico,
Agostino Gemelli University Polyclinic (IRCCS), Italy
Choon Chiat Oh,
SingHealth Duke-NUS Institute of Precision Medicine (PRISM), Singapore

*CORRESPONDENCE
Jun Niu
niujun06@126.com

RECEIVED 14 June 2024
ACCEPTED 18 October 2024
PUBLISHED 18 November 2024

CITATION
Sun Y, Liu Y, Li C, Zhang X, Yin L and Niu J (2024) Case report: Metastatic endocrine mucin-producing sweat gland carcinoma with features of mucinous carcinoma. *Front. Oncol.* 14:1449270. doi: 10.3389/fonc.2024.1449270

COPYRIGHT
© 2024 Sun, Liu, Li, Zhang, Yin and Niu. This is an open-access article distributed under the terms of the Creative Commons Attribution License (CC BY). The use, distribution or reproduction in other forums is permitted, provided the original author(s) and the copyright owner(s) are credited and that the original publication in this journal is cited, in accordance with accepted academic practice. No use, distribution or reproduction is permitted which does not comply with these terms.

Case report: Metastatic endocrine mucin-producing sweat gland carcinoma with features of mucinous carcinoma

Yuehua Sun, Yingchun Liu, Chuntao Li, Xiaodong Zhang, Lu Yin and Jun Niu*

Department of Dermatology, General Hospital of Northern Theater Command, Shenyang, China

Endocrine mucin-producing sweat gland carcinoma is a rare neoplasm of the skin appendages. The tumor typically exhibits slow growth and rarely metastasizes to distant sites. Herein, we report a case of a 77-year-old male who presented with a skin lesion on the right anterior chest wall 23 years ago. Fifteen years later, surgical excision was performed, and the pathological diagnosis was endocrine mucin-producing sweat gland carcinomas. However, the histopathological examination revealed a coexistence of endocrine mucin-producing sweat gland carcinomas and mucinous carcinoma components. Over the past 2 years, the patient developed lymph node metastasis in the right axilla, local recurrence on the right chest wall, and distant skin metastasis. The histopathological type of the lymph node metastasis was consistent with the primary tumor, while the recurrent and skin metastatic lesions exhibited mucinous carcinoma. To our knowledge, this is the first reported case of endocrine mucin-producing sweat gland carcinoma with distant skin metastasis, characterized by two distinct carcinoma components in the histopathological morphology.

KEYWORDS

endocrine mucin-producing sweat gland carcinoma, mucinous carcinoma, neoplasm, metastases, immunohistochemistry

Introduction

Malignant sweat gland tumors are rare neoplasms that occur in sweat glands and are characterized by substantial malignancy, infiltration, and metastasis. They account for approximately 1% of primary cutaneous lesions (1). Malignant sweat gland tumors exhibit various pathological types and often possess both eccrine and apocrine differentiation. Endocrine mucin-producing sweat gland carcinoma (EMPSGC) is a rare subtype that typically arises in the eyelid skin and follows a slow clinical course (2). The main histopathological feature is the presence of mucin within the cytoplasm and extracellularly. EMPSGC can progress to mucinous carcinoma. To date, there have been no reports of skin metastasis in patients with EMPSGC. Here, we report a case in which an

EMPSGC was located on the right anterior chest wall and was characterized by the simultaneous presence of an EMPSGC and mucinous carcinoma. The patient experienced recurrent disease after 5 years, with lymph nodes and distant skin metastasis.

Case presentation

The patient is a 77-year-old male with no significant past medical history, no known chronic diseases, and no documented familial or genetic predispositions. In 2000, the patient presented with a painless, slow-growing mass on the right anterior chest wall, approximately measuring the size of a bean. In June 2015, an ultrasound examination revealed a hypoechoic lesion measuring approximately 3.8 cm×3.6 cm and located subcutaneously to the dermal layer, 2.9 cm from the skin surface. The lesion exhibited no distinct capsule, had unclear boundaries, and had heterogeneous echoes. Color ultrasound examination revealed linear color flow signals within the lesion, while no significant lymphadenopathy was observed in the bilateral axillary regions. In September 2015, the lesion increased to approximately 2 cm in diameter and protruded from the skin surface, exhibiting surface keratinization, roughness, and crusting (Figure 1A). Upon palpation, a subcutaneous mass approximately 11.5 cm×4 cm×3 cm in size was detected. Surgical excision of the cutaneous lesion was performed. Histopathological examination revealed numerous clusters of epithelioid tumor cells, some of which exhibited glandular differentiation and infiltrated the subcutaneous and deep tissues. The tumor cells displayed abundant, pale-staining cytoplasm with cellular atypia. The stroma exhibited mucinous material with transparent degeneration, fibrous tissue proliferation, and scattered chronic inflammatory cell infiltration (Figure 1B). This pathological morphology represents a transitional stage from EMPSGC to mucinous carcinoma. The immunohistochemical results were as follows: chromogranin (+), synaptophysin (-), CK7 (+), CK5/6 (-), p63 (-), CK20 (-), CK-P (+), CK8/18 (+), ER (+) 90%, PR (+) 75%, S-100 (-), cerbB2 (1+), EMA (+), CEA (+), CAM5.2 (+), and Ki67 (35%+). (Typical representative histology photos of positive IHC stains are provided in the Supplementary Material). Four weeks after local surgical excision, wide excision was performed. Histopathological examination revealed a squamous epithelial lining over the tissue and abundant mucin lakes within the subcutaneous adipose tissue. Floating cancer nests were observed within the mucin, some exhibiting a sieve-like pattern and others forming solid nests. The cancer cells were small, had visible nucleoli, and were relatively uniform in size (Figure 1C).

In 2017, the patient presented with enlarged right axillary lymph nodes measuring approximately 2.0 cm×1.0 cm, with a soft consistency, unclear boundaries, rough surface, and poor mobility. In 2020, an ultrasound examination revealed multiple hypoechoic lesions in the right axilla, the largest of which measured 2.15 cm×1.47 cm, and rich color flow within the mass. No significant lymphadenopathy was observed in the left axilla. A plain computed tomography (CT) scan of the lungs revealed no signs of metastatic lesions; however, multiple enlarged lymph nodes were detected in the right axilla. In September 2020, these axillary lymph nodes were surgically removed. Histopathological examination disclosed the presence of various components within the tumor tissue: mucinous, solid nests, and glandular structures (Figure 2). The histopathological features aligned with those of the primary tumor.Combined with the patient's medical history, these findings suggested lymph node metastasis. Immunohistochemistry yielded the following results: CK8/18 (++), D2-40 (+), ER (+90%), PR (+80%), AR (-), cerbB2 (0), GATA3 (+), GCDFP-15 (+/-), Ki-67 (+30%), calponin (-), P63 (-), CD34 (- (blood vessels +)), and CK5/6 (-).

In March 2021, a 0.5 cm×0.5 cm recurrent lesion appeared on the right chest wall. In September of the same year, an ultrasound examination of the right chest wall revealed a 0.62 cm×0.7 cm×0.81 cm ill-defined hypoechoic lesion within the subcutaneous soft tissue above the surgical site. The lesion exhibited uneven echogenicity, a crab-like appearance, and colour flow signals. The deepest part of the lesion was approximately 0.9 cm from the skin surface, indicating a solid lesion in the right chest wall. Subsequent surgical excision was performed, and histopathological examination revealed the findings depicted in Figure 3. Immunohistochemistry revealed the following results: ER (+90%), PR (+90%), AR (-), S-100 (-), cerbB2 (0), (SMA) (-), EMA (+), GATA3 (+), GCDFP-15 (-/+), Ki-67 (+40%), calponin (-), CK7 (-), P63 (-), PSA (-), and CKH (-).

In November 2021, a subcutaneous mass appeared in the left scapular region (Figure 4A), measuring approximately 1.7 cm×0.8 cm, with a smooth surface and hard consistency. In February 2022, an ultrasound examination revealed a lesion measuring approximately 1.7 cm×0.7 cm, with indistinct borders, heterogeneous echogenicity, and peripheral colour flow signals. Plain lung CT revealed no metastatic lesions. Surgical excision was performed, and histopathological examination revealed the presence of multiple tumor cell clusters within the dermal collagen fibres. The tumor cells exhibited solid and cord-like distributions with clear boundaries from the surrounding tissues. The tumor cells were enlarged and epithelioid in appearance, with some exhibiting deep nuclear staining and visible intercellular spaces. The cytoplasm was abundant and pale, with multiple mitotic figures and keratinization (Figure 4B). Immunohistochemistry revealed the following results: CK8/18 (+), ER (90% moderate intensity+), PR (90% strong+), GATA3 (+), GCDFP15 (+), cerbB2 (0), Ki-67 (30%), CK7 (-), P63 (-), and CK5/6 (-), indicating recurrence of EMPSGC.

In October 2023, a positron emission tomography CT scan revealed an increased linear distribution of radioactivity in the left seventh rib, suggesting a high likelihood of malignant lesions with pathological fracture. These findings indicate the possibility of bone metastasis from the EMPSGC. Throughout the course of the disease, the patient did not experience fever or systemic symptoms of discomfort in any body system. At this time, the patient is not receiving any specific active treatment for the metastatic disease. Instead, the patient is under regular surveillance with scheduled follow-up visits to monitor the progression of the condition.

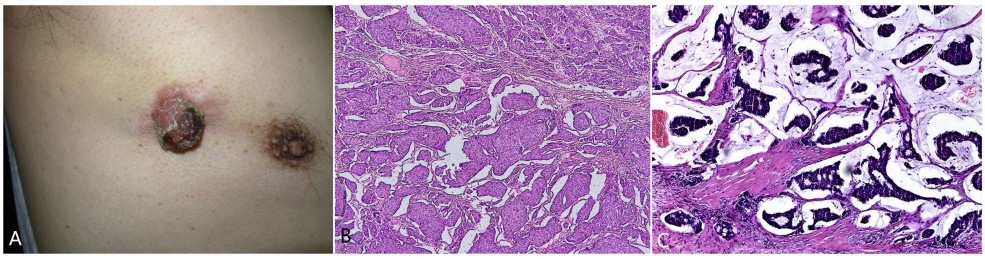

FIGURE 1
(A) A reddish-brown tumor measuring approximately 2 centimeters in diameter on the right anterior chest, with a surface that is keratinized and rough. **(B)** Abundant clusters and cords of epithelioid tumor cells, some exhibiting glandular differentiation, infiltrating the subcutaneous and deep tissues. The tumor cells had abundant, pale-staining cytoplasm with cellular atypia. The stroma contains mucinous material with transparent degeneration, fibrous tissue proliferation, and scattered chronic inflammatory cell infiltration.200×. **(C)** Microscopic view showing the squamous epithelial lining, abundant mucin lakes within the subcutaneous adipose tissue, and floating cancer nests within the mucin. Some nests exhibit a sieve-like pattern, while others form solid nests. The cancer cells are small with visible nucleoli and are relatively uniform in size. Hematoxylin and eosin staining,200×.

Discussion

Malignant sweat gland tumors originate from sweat glands and are classified into 17 different types based on their histopathological features. These include mucinous carcinoma, EMPSGC, and adenoid cystic carcinoma (3). In this case, the patient presented with an initial tumor diagnosed as EMPSGC, which is a rare low-grade carcinoma that produces mucin and typically presents as flesh-colored papules or nodules, predominantly in elderly women. Its histological features include neuroendocrine differentiation and mucin production (4). Interestingly, pathological examination of the EMPSGC tissue in this patient revealed the presence of another cancer component, mucinous carcinoma. Primary cutaneous mucinous carcinoma (PCMC) is an extremely rare low-grade tumor characterized by nests of epithelial cells floating in extracellular pools of mucin. Both EMPSGC and PCMC rarely metastasize (5, 6), and EMPSGC is considered an early manifestation of mucinous carcinoma (7). Multiple recurrences and metastases in this case of EMPSGC are exceptionally rare. Studies have indicated that 50% of EMPSGC recurrences are associated with lesions containing PCMC components, while EMPSGC without PCMC components has a relatively lower recurrence rate (5), which may explain the multiple recurrences observed in this patient.

In this case, lymph node metastasis was observed, and the histopathological findings indicated a transitional stage from EMPSGC to mucinous carcinoma, with both cancer components present. Pathology revealed chest wall recurrence on the right side and skin metastasis on the left scapula, indicating a predominance of EMPSGC with minimal mucin content. Besides,there are common features seen in all the ultrasound scans performed: hypoechoic nature,absence of a capsule,indistinct margins, heterogeneous echotexture,and presence of color doppler flow signals.These consistent features in all ultrasound scans provide valuable information for diagnostic assessment and contribute to a better understanding of the lesion characteristics.

P63 is a marker for basal cells in the epidermis and is expressed in myoepithelial cells of the breast and sweat glands. Several studies suggest that P63 may aid in distinguishing primary cutaneous mucinous carcinoma from metastatic mucinous carcinoma, as it is preferentially expressed in primary appendageal tumors, although only a small subset of primary cutaneous mucinous carcinomas

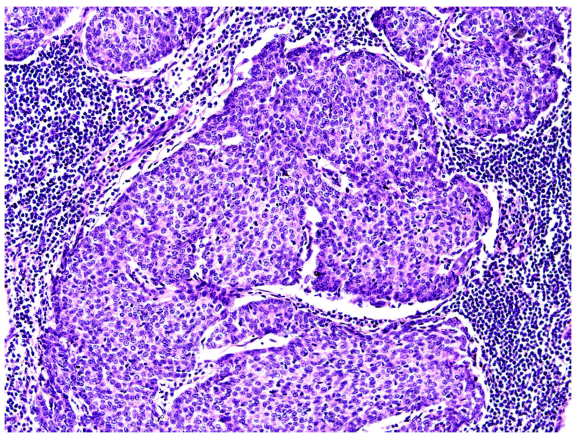

FIGURE 2
Pathological picture of lymph node biopsy. Hematoxylin and eosin staining,200×.

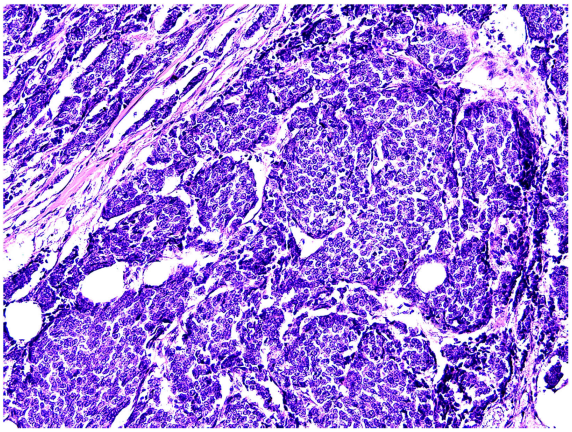

FIGURE 3
Histopathological morphology of recurrent tumor:solid and glandular cancer nests. Hematoxylin and eosin staining,200×.

display P63 expression (8). In this case, the tumors of primary cutaneous mucinous carcinoma, as well as the recurrent and metastatic tumors, were negative for P63. Primary cutaneous mucinous carcinoma showed positive expression for cerbB2, suggesting a propensity for recurrence, while the later recurrent and distant metastatic cancer tissues were negative for cerbB2 in immunohistochemistry. Expression of P63 and cerbB2 may support the diagnosis of primary carcinoma over metastatic carcinoma. GATA-binding protein 3, a transcription factor, is commonly expressed in various sweat gland carcinomas, such as clear cell adenocarcinoma and porocarcinoma (9, 10), but its diagnostic value in differentiation is limited (11). GCDFP-15 is expressed positively in sweat gland tumors as well as breast carcinomas, thus cannot serve as a specific antibody for differential diagnosis (12). All the PCMCs showed positive staining for ER, and PR (8). Lymph nodes in the region are the most common site of metastasis in sweat gland carcinomas. PR and ER are observable in tumors at the primary site, as well as in recurrent and metastatic lesions, suggesting these hormone receptors may play a potential role in the pathogenesis of metastatic lesions.

In this case, the patient with sweat gland carcinoma experienced recurrence, lymph node invasion, and distant skin metastasis over a total duration of 23 years, and the prognosis appears relatively favorable at present. Studies have indicated that factors such as primary site, sex, age, histological grade, and surgery are not associated with the survival rate or prognosis of sweat gland carcinoma patients (13). Currently, the literature on sweat gland carcinoma mainly consists of single case reports (7), and reports of skin metastasis are rare. The unique aspect of this case lies in the long duration of recurrence and skin metastasis, as well as the pathological transition from EMPSGC to mucinous carcinoma.

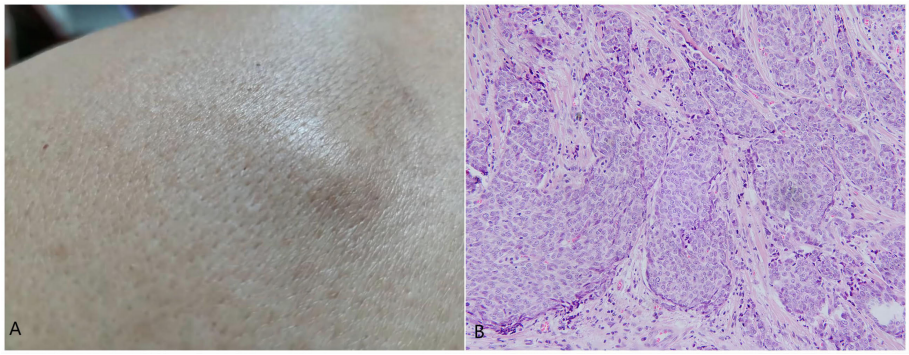

FIGURE 4
(A) Subcutaneous mass in the left scapular region measuring approximately 1.7 cm × 0.8 cm with a smooth surface and hard consistency. **(B)** Multiple tumor cell clusters within the dermal collagen fibres, exhibiting a solid and cord-like distribution with clear boundaries from the surrounding tissues. The tumor cells were enlarged and epithelioid in appearance, with some exhibiting deep nuclear staining, visible intercellular spaces, abundant and pale-staining cytoplasm, multiple mitotic figures, and keratinization. Hematoxylin and eosin staining,200×.

Data availability statement

The original contributions presented in the study are included in the article/Supplementary Material. Further inquiries can be directed to the corresponding author.

Ethics statement

Written informed consent was obtained from the individual(s) for the publication of any potentially identifiable images or data included in this article.

Author contributions

YS: Conceptualization, Writing – original draft. YL: Resources, Writing – review & editing. CL: Data curation, Writing – review & editing. XZ: Conceptualization, Writing – review & editing. LY: Writing – review & editing. JN: Writing – review & editing.

Funding

The author(s) declare that no financial support was received for the research, authorship, and/or publication of this article.

Acknowledgments

The authors would like to thank all the people involved in this work.

Conflict of interest

The authors declare that the research was conducted in the absence of any commercial or financial relationships that could be construed as a potential conflict of interest.

Publisher's note

All claims expressed in this article are solely those of the authors and do not necessarily represent those of their affiliated organizations, or those of the publisher, the editors and the reviewers. Any product that may be evaluated in this article, or claim that may be made by its manufacturer, is not guaranteed or endorsed by the publisher.

Supplementary material

The Supplementary Material for this article can be found online at: https://www.frontiersin.org/articles/10.3389/fonc.2024.1449270/full#supplementary-material

References

1. Khaleeq T, Ishaq N, Khaliq T. Sweat gland carcinoma with lymphadenopathy. *J Ayub Med Coll Abbottabad.* (2016) 28:614–6.

2. Mulay K, Menon V, Lahane S, Sharma M, Honavar SG. Endocrine mucin-producing sweat gland carcinoma (EMPSGC) of the eyelid: Clinicopathologic features, immunohistochemical findings and review of literature. *Indian J Ophthalmol.* (2019) 67:1374–7. doi: 10.4103/ijo.IJO_1745_18

3. Ahn CS, Sangueza OP. Malignant sweat gland tumors. *Hematol Oncol Clin North Am.* (2019) 33:53–71. doi: 10.1016/j.hoc.2018.09.002

4. Quattrochi B, Russell-Goldman E. Utility of insulinoma-associated protein 1 (INSM1) and mucin 2 (MUC2) immunohistochemistry in the distinction of endocrine mucin-producing sweat gland carcinoma from morphologic mimics. *Am J Dermatopathol.* (2022) 44:92–7. doi: 10.1097/DAD.0000000000001990

5. Au RTM, Bundele MM. Endocrine mucin-producing sweat gland carcinoma and associated primary cutaneous mucinous carcinoma: Review of the literature. *J Cutan Pathol.* (2021) 48:1156–65. doi: 10.1111/cup.13983

6. Freeman T, Russell AJ, Council ML. Primary cutaneous mucinous carcinoma: A review of the literature. *Dermatol Surg.* (2023) 49:1091–5. doi: 10.1097/DSS.0000000000003921

7. Ravi PY, Walsh NM, Archibald C, Pasternak S. Endocrine mucin-producing sweat gland carcinoma: emerging evidence of multicentric cutaneous origin and occasional concurrence with analogous breast tumors. *Am J Dermatopathol.* (2022) 44:321–6. doi: 10.1097/DAD.0000000000002132

8. Chung J, Rico-Castillo J, Sebastiano C, Lee JB. Expression of p40 in primary cutaneous mucinous carcinoma versus primary mucinous carcinomas of the breast and colon. *Am J Dermatopathol.* (2021) 43:e175–e80. doi: 10.1097/DAD.0000000000001973

9. Hudacko R, Anderson P, Guerrieri C. Perineal clear cell hidradenoma: A GATA3-positive neoplasm with potential for misdiagnosis. *Int J Gynecol Pathol.* (2021) 40:465–9. doi: 10.1097/PGP.0000000000000713

10. Goto K, Ishikawa M, Hamada K, Muramatsu K, Naka M, Honma K, et al. Comparison of immunohistochemical expression of cytokeratin 19, c-KIT, berEP4, GATA3, and NUTM1 between porocarcinoma and squamous cell carcinoma. *Am J Dermatopathol.* (2021) 43:781–7. doi: 10.1097/DAD.0000000000001901

11. Chou YH, Chang YC, Huang YL, Wu CT. Endocrine mucin-producing sweat gland carcinoma with GATA3 expression: report of two cases. *Pathology.* (2017) 49:805–8. doi: 10.1016/j.pathol.2017.08.018

12. Ansai SI. Topics in histopathology of sweat gland and sebaceous neoplasms. *J Dermatol.* (2017) 44:315–26. doi: 10.1111/jde.2017.44.issue-3

13. Gao T, Pan S, Li M, Su R. Prognostic analysis of hidradenocarcinoma: a SEER-based observational study. *Ann Med.* (2022) 54:454–63. doi: 10.1080/07853890.2022.2032313

Glossary

EMPSGC	endocrine mucin-producing sweat gland carcinoma
PCMC	primary cutaneous mucinous carcinoma
CK-P	C-Kit protein
CK8/18	Cytokeratin 8/18
ER	estrogen receptor
PR	progesterone receptor
cerbB2/HER2	human epidermal growth factor receptor 2, also called cerbB2
EMA	epithelial membrane antigen
CEA	carcinoembryonic antigen
CAM5.2	calmodulin5.2
AR	androgen receptor
GATA3	GATA-binding protein 3
GCDFP-15	gross cystic disease fluid protein 15
CK5/6	cytokeratin5/6
SMA	smooth muscle actin
EMA	epithelial membrane antigen
CK7	cytokeratin 7
PSA	prostate-specific antigen
CKH	human cytokeratin high molecular weight.

frontiers | Frontiers in Oncology

TYPE Case Report
PUBLISHED 22 November 2024
DOI 10.3389/fonc.2024.1440246

Check for updates

OPEN ACCESS

EDITED BY
Dragos Eugen Georgescu,
Carol Davila University of Medicine and Pharmacy, Romania

REVIEWED BY
Nayara Tessarollo,
ICESP, Brazil
Shitong Lin,
Huazhong University of Science and Technology, China

*CORRESPONDENCE
Qiong-Ying Hu
qiongyinghu@tzc.edu.cn

†These authors have contributed equally to this work

RECEIVED 29 May 2024
ACCEPTED 18 October 2024
PUBLISHED 22 November 2024

CITATION
Wang Y, Zheng Y-T, Zhang L, Cao X-Q, Lin Z, Liu H-Y and Hu Q-Y (2024) Undifferentiated endometrial carcinoma diagnosed during perimenopausal hormone therapy: a case report and literature review.
Front. Oncol. 14:1440246.
doi: 10.3389/fonc.2024.1440246

COPYRIGHT
© 2024 Wang, Zheng, Zhang, Cao, Lin, Liu and Hu. This is an open-access article distributed under the terms of the Creative Commons Attribution License (CC BY). The use, distribution or reproduction in other forums is permitted, provided the original author(s) and the copyright owner(s) are credited and that the original publication in this journal is cited, in accordance with accepted academic practice. No use, distribution or reproduction is permitted which does not comply with these terms.

Undifferentiated endometrial carcinoma diagnosed during perimenopausal hormone therapy: a case report and literature review

Ying Wang†, Yu-Tong Zheng†, Ling Zhang†, Xue-Quan Cao, Zhu Lin, Hong-Yu Liu and Qiong-Ying Hu*

The Taizhou Central Hospital (Taizhou University Hospital), School of Medicine, Taizhou University, Taizhou, Zhejiang, China

Uterine corpus endometrial carcinoma, one of the three most frequent cancers of the female reproductive system, primarily affects women who are perimenopausal or postmenopausal. Moreover, it is an epithelial cancer that develops in the endometrium, which is classified as either estrogen-dependent (type I) or non-estrogen-dependent (type II). Non-estrogen-dependent endometrial cancers include plasma cell carcinoma and undifferentiated/dedifferentiated endometrial carcinoma. Undifferentiated endometrial carcinoma is a rare but aggressive endometrial epithelial cancer that lacks any histologic differentiation and is classified as a high-grade endometrial cancer. This case presents that a patient had uterine corpus endometrial carcinoma during perimenopausal hormone therapy, and the patient was treated with sequential estrogen–progestin treatment for 3 years. During that period, she did not undergo a follow-up examination for the last 2 years due to the pandemic. Undifferentiated endometrial carcinoma is a special type of endometrial cancer that is not hormone-dependent, and whether the occurrence of this case is related to perimenopausal hormone therapy needs to be verified by more evidence-based clinical cases and further studies.

KEYWORDS

UEC, perimenopause, hormone, curettage, ultrasound, MRI, pathology

1 Introduction

Uterine corpus endometrial carcinoma (UCEC), one of the three most frequent cancers of the female reproductive system, is an epithelial cancer that develops in the endometrium (1). It primarily affects women who are perimenopausal or postmenopausal (2). The morbidity of this condition makes it the sixth most common cancer among women

worldwide, with a global age-standardized morbidity rate of 8.4/100,000 in 2022. Meanwhile, there were 97,723 cancer deaths from UCEC among women, and a global age-standardized mortality rate of 1.7/100,000 in 2022 (3). Additionally, an estimated 320,000 new cases are diagnosed annually (4). By contrast, the morbidity rate of UCEC in China was 6.8/100,000, accounting for 3.39% of the total morbidities of cancers among women, with a mortality rate of 1.1/100,000 in 2022 (5).The morbidity and mortality rates of UCEC have steadily increased, with a trend toward younger ages for the past 20 years (3, 6, 7), according to the data from the World Health Organization (WHO). The morbidity of UCEC has made it the most prevalent gynecological cancer in some developed countries, along with the decreased incidence of cervical cancer (8–12).

Based on pathogenesis and biological characteristics, UCEC is classified as either estrogen-dependent (type I) or non-estrogen-dependent (type II). The majority of estrogen-dependent UCEC cases are endometrioid adenocarcinoma, with mucinous adenocarcinoma making up a minority (13). Non-estrogen-dependent endometrial cancers include serous carcinoma, clear cell carcinoma, carcinosarcoma, mixed adenocarcinoma, undifferentiated endometrial carcinoma (UEC) or dedifferentiated endometrial carcinoma (DEC), mesonephric adenocarcinoma, squamous cell carcinoma, and gastric-type endocervical adenocarcinoma (14–16). As we know, UEC has only been reported a few times (17–20). UEC is rare and invasive and tends to be diagnosed at an advanced stage according to the International Federation of Gynecology and Obstetrics (FIGO) classification. Moreover, it is resistant to conventional chemotherapy (21, 22). Previously published papers have demonstrated a high risk of locoregional and distant recurrence in UEC compared with differentiated cancers (23); however, it has been published that the pathological and immunohistochemical features of these rare tumors received more attention. In addition, there is a lack of literature on their associated management and survival outcomes (24). This means that patients with UEC may face the dilemma of having to undergo only more invasive surgery.

Here, we presented a rare case of UEC that was diagnosed during perimenopausal hormone therapy. This is a rare case that was seldom reported before. At the same time, it is suggested that the long-term use of estrogen and progestin may influence the development of UEC. On the other hand, Dusp6 can be used as a biomarker to predict the effect of progesterone, and targeting MMR or SWI/SNF may become a trend in the development of UEC-targeted chemotherapeutics to provide a new strategy for the conservative treatment for UEC. The current report is expected to help us understand better the rare UEC and improve the treatment for UEC.

2 Case description

A 51-year-old female patient was admitted in September 2023 for experiencing “irregular and continuous vaginal bleeding for more than 2 months”. Her menstrual period stayed for 5~6 days, with a cycle of 28 days, and her last period was 30 August 2023. In addition, intermittent pain in the lower abdomen also occurred, but with no headache and dizziness, overflow of breast milk, difficulty in urinating, and/or other discomforts. Any additional treatment was not received during her period, but femoston (estradiol and dydrogesterone tablet, 1 mg/tablet) had been given orally 3 years before July for the reason of “perimenopausal hot flashes”. In addition, the patient did not have standardized follow-up examinations, because of inability to see a doctor due to the pandemic and personal situations. She underwent a “lower uterine cesarean section” in another hospital in 2000, accompanied by a spontaneous-labor, no-preterm birth. Moreover, any histories of genetic disease, mental illness, infectious disease, psychosocial history, or similar disease in the second or third generation of the family were denied. This was the first case of a patient who had UEC during the perimenopausal hormone therapy in this hospital (Figure 1).

Outpatient service was received. To diagnose the cause of the disease, we used ultrasound. The ultrasound showed a “long strip,” which was the echo of the intrauterine device in the uterine cavity, whereas the echo in the myometrium was not clear when the pressure was given, and that in the endometrium was not clear either (Figure 2A). Color Doppler flow imaging (CDFI) showed abundant blood flow signals in the area of the uterine cavity. The ovaries on both sides were slightly smaller than the average size, and the internal echogenicity was solid (Figures 2B–G). More details are shown in Figures 2B–G. The results of the spectral Doppler ultrasound presented a blood flow frequency spectrum like pulsation in the veins next to the uterus, which was possibly related to arteriovenous fistula.

Then, we used magnetic resonance imaging (MRI) to explore the abnormality in the uterine cavity. The MRI results of the pelvis showed an increased uterine volume, a thickened uterine wall (significant left side) and cervix, an irregular mass shadow and some small lymph node shadows next to the iliac vessels on both sides, along with approximately 10 mm in length for the large one, and uniform enhancement. In addition, the lesion invaded the endometrium and grew into the uterine cavity (Figures 2H–J). Analysis of computed tomography (CT) plain scan and CT enhancement on the whole abdomen showed the same phenomenon (Figures 2K, L). Given these findings, the mass may be classified as endometrial cancer.

To establish whether the uterine foreign body was indeed a malignant tumor, we performed a pathological examination after diagnostic scraping. The results of the pathology test suggest that the phenomenon of uterine cavity biopsy cells having much coagulative necrosis and a nuclear division is common, which is considered a malignant tumor (Figures 3A, B). Moreover, it was preliminarily considered as squamous cell carcinoma. Then, a surgery of abdominal hysterectomy + bilateral salpingo-oophorectomy + pelvic lymph node dissection + para-aortic lymphadenectomy + presacral lymph node dissection + greater omentum resection was performed. The adnexa of the whole uterus that underwent hysterectomy had the size of 13.0 cm*10.0 cm*5.5 cm and the tumor size was 11.5 cm*10.5 cm*5.0 cm. During the operation, some observations were obtained. First, the uterus was enlarged to a size greater than that of 2 months of pregnancy, and the cervix was thickened and hard, but the paracervical tissues were soft bilaterally. Second, scattered cauliflower-like tissues could be seen on the surface of the uterus. Third, there was a swollen lymph

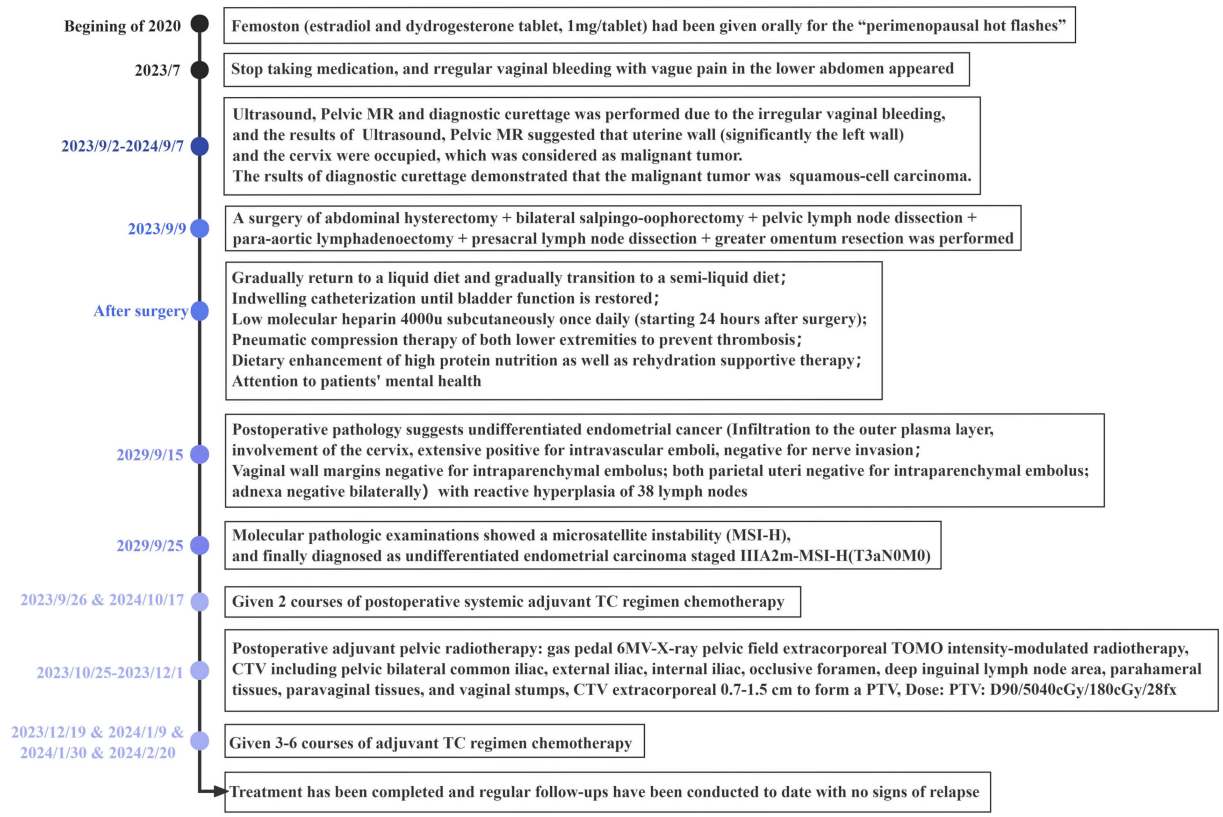

FIGURE 1
Clinical course timeline.

node in front of the sacrum and multiple swollen lymph nodes next to the abdominal aorta (Figures 3C–E).

After that, further pathological examination was performed to explore the type and stage of this endometrial cancer. The results of the immunohistochemistry test suggested that proteins P16, P63, CK5/6, CK-7, Vim, CK-20, and P40 showed positive expressions in minority of the lesion, CKpan and Ki-67 showed positive expressions in majority of the lesion, and WT1, P53 (wild-type), MLH1, MSH2, MSH6, PMS2, E-cad, and PAX-8 showed positive expressions. These suggested that the hysterectomy results showed cancer, specifically UEC (25). A molecular pathological examination showed microsatellite instability (MSI-H). Combined with the outcome of the postoperative pathological diagnosis and molecular pathological examination, it suggested that the stage of the UEC was IIIA2 m-MSI-H (T3aN0M0) (Figures 3F–J).

After surgery, the patient was treated with paclitaxel and carboplatin combined with systemic external beam radiation therapy. Right now, the patient is in good condition with the adjunctive treatment.

3 Discussion

During the course of perimenopausal hormone therapy for perimenopausal hot flashes for almost 3 years, the patient presented with typical symptoms of irregular vaginal bleeding for more than 2 months. The results of ultrasound, CT, and MRI showed that there was a foreign object in the uterine cavity and the endometrium became abnormally thick, which led to a preliminary diagnosis of endometrial cancer. Afterward, surgery was performed. Pathological analysis of the surgical specimen revealed that it was UEC, and it recovered well with subsequent paclitaxel/carboplatin adjuvant therapy. The rigorous adjuvant diagnostic measures and traditional diagnostic protocols in this diagnostic protocol led to a good prognosis for the patient. However, there were certain problems, for example, endometrial cancer types are difficult to differentiate, the surgery was more traumatic, the long-term use of paclitaxel and carboplatin may have led to the development of drug resistance in UEC, or the perimenopausal hormone therapy may have been linked to the emergence of UEC.

Based on this case, we summarize three experiences of diagnostic and management. (1) The first is medical imaging. If the uterine lesion has a wide range, invades the endometrium, and protrudes into the cavity to form mass-like changes with uneven enhancement, it will be initially considered as a malignant tumor of endometrial origin. That is exactly what happened in this case. Moreover, diagnostic imaging should focus more on the stage of the lesion, its relationship with neighboring tissues, the presence or absence of lymph node metastasis, distant metastasis, and other factors to provide detailed diagnostic reports to the clinic. As in this case, before surgery, comprehensive and systematic imaging examination was performed to determine the staging of the patient's lesion, which is one of the reasons why the patient's prognosis is favorable in this case. (2) Second is pathology.

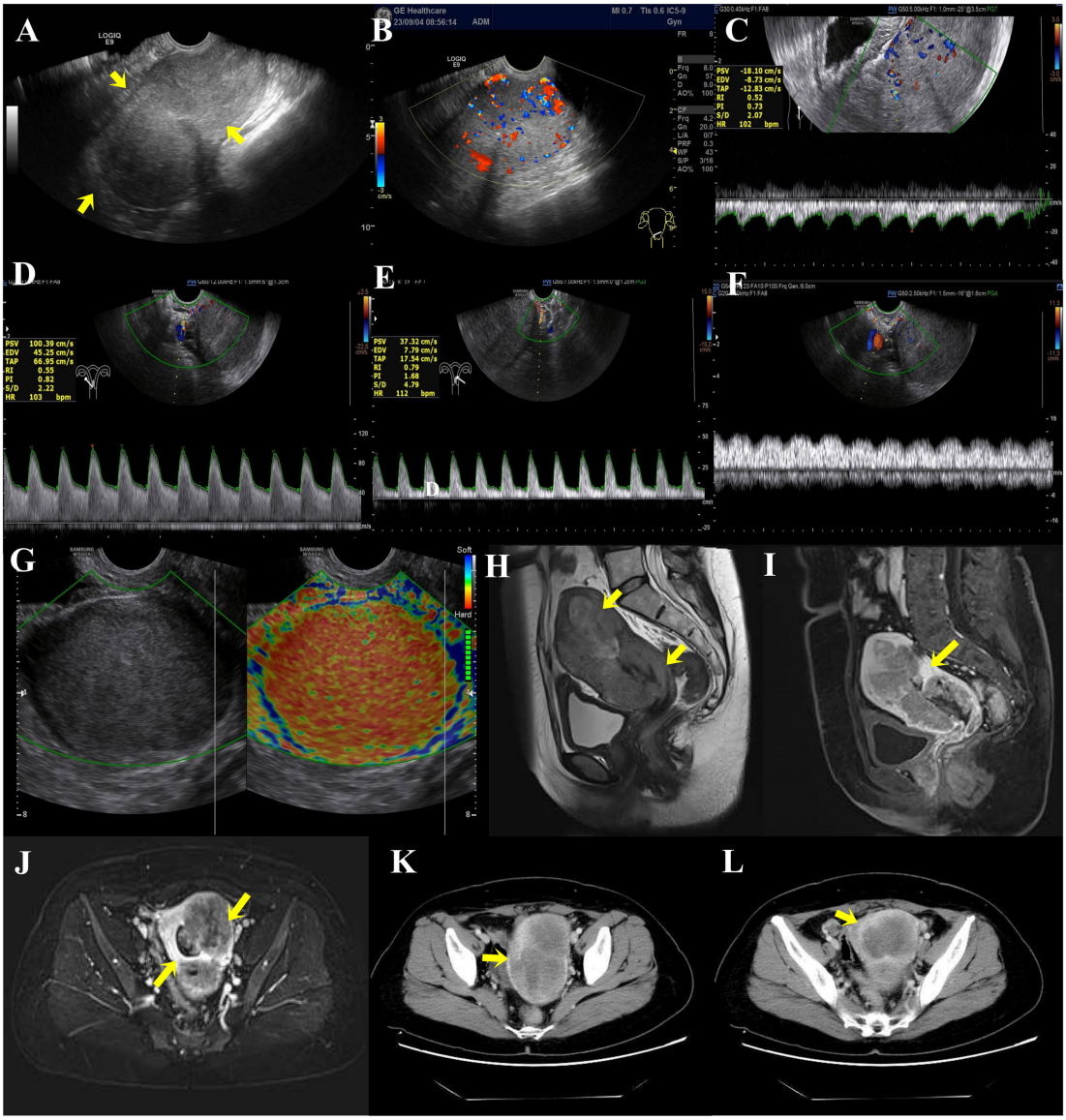

FIGURE 2
(A) Preoperative transvaginal color Doppler ultrasound sonogram of endometrial cancer lesions. Full uterine morphology, unclear cervical and uterine structures, and diffuse lesions in the myometrium (arrows show the location of infiltration of lesions). **(B–G)** Blood flow in and around the lesion. **(B)** Color Doppler ultrasound showed abundant blood flow signals in the interior and margins of the lesion. **(C)** Spectral Doppler ultrasound showed a low resistance type arterial flow spectrum detected within the lesion. RI: 0.52 (The general resistance index RI is less than 0.4, whereas the RI of this case is higher.) **(D)** The right uterine artery has increased blood flow and decreased vascular resistance. **(E)** Decreased vascular resistance of the left uterine artery. **(F)** Spectral Doppler ultrasound defined that the veins next to the uterus show a blood flow frequency spectrum like pulsation. **(G)** Transvaginal ultrasonography E-cervix elastosonography shows the lesion area in red, representing hard tissue. **(H–J)** MRI scanning and MRI enhancement. **(H)** Uneven abnormal signal mass in the cervix and left lateral wall of the uterus. **(I)** Uneven enhancement in the lesion of the myometrium and uterine cavity. **(J)** The local endometrial structures are poorly demonstrated, and the intrauterine lesion is poorly demarcated from the myometrial lesion. **(K, L)** CT plain scan and CT enhancement on the whole abdomen. **(K)** The uterus is enlarged in shape, with marked heterogeneous enhancement of the myometrium, predominantly in the left wall. **(L)** The lesion is poorly demarcated from the uterine cavity and endometrium.

The morphology of undifferentiated endometrial carcinoma is similar to that of squamous cell carcinoma, serous carcinoma, or endometrioid adenocarcinoma, which is easy to be misdiagnosed. This is a problem that exists in all current endometrial cancer staging diagnostic procedures (15). However, further immunohistochemistry analysis can help in avoiding misdiagnosis and improving accuracy. Different treatment strategies exist for different pathological compartments of endometrial cancer (26); new biomarkers and well-defined pathological features can advance the diagnostic and therapeutic regime for undifferentiated endometrial cancer. (3) Third is clinics. There is a relationship between perimenopausal hormone therapy and the development of endometrial malignancy, which requires regular follow-up during hormone therapy. The patient was unable to see the doctor due to the pandemic, and therefore, she did not have

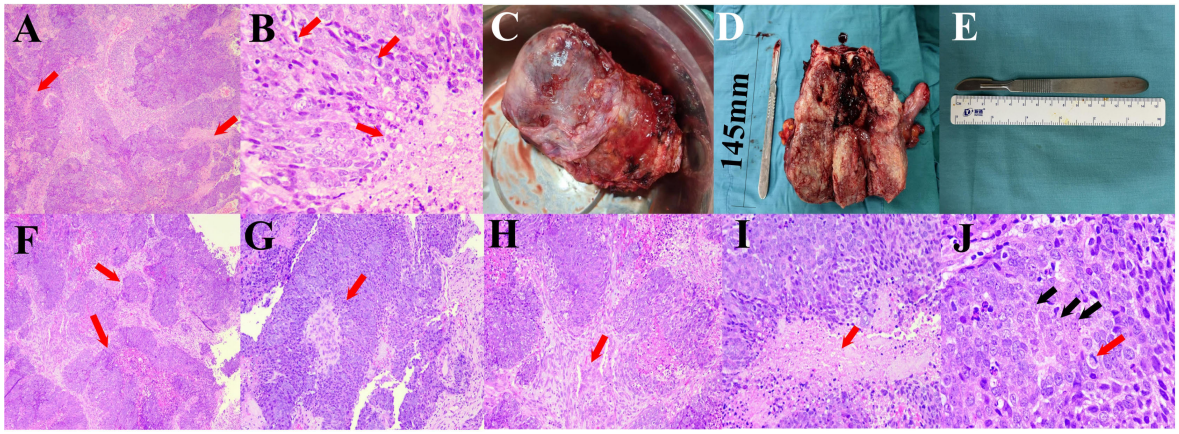

FIGURE 3
(A, B) Pathological results of diagnostic scraping. **(A)** The tumor has a nested structure with multiple coagulative necrosis (red arrows, 50×). **(B)** Coagulative necrosis is seen in the cancer nests (black arrows), the cells are round or polygonal, the nuclei are round and ovoid, the nucleoli are obvious, and nuclear division is common (red arrows, 400×). **(C–E)** The specimen of oophorectomy. **(C)** Enlarged uterus with lesion invading the surface of plasma. **(D)** The dissection specimen showed that the lesion invaded and grew into the entire uterus. **(E)** Length of the scalpel. **(F–J)** Pathological results of oophorectomy. **(F)** The tumor grows infiltratively, forming nested structures of varying sizes (red arrows, 50×). **(G)** Papillary structure with a fibrovascular core in the center (red arrow, 100×). **(H)** The cancer nests are of different sizes, and a desmoplastic response could be seen in the stroma (red arrows, 100×). **(I)** Coagulative necrosis is seen in the center of the cancer nest (red arrow, 200×. **(J)** Cells are large, round, or polygonal, with vacuolated nuclei and distinct nucleoli (black arrows), and nuclear division is common (red arrows, 400×).

standardized follow-up examinations, and this may have affected the progression of the disease.

Typical UEC is similar to lymphoma, high-grade endometrial stromal sarcoma, or small-cell carcinoma on morphology (27). The cells of UEC are almost uniform, medium-sized, poorly adhesive, and distributed in solid patches (23, 28–30). The molecular characteristics of UEC include inactivation of mismatch repair (MMR), the switch/sucrose nonfermentable chromatin remodeling (SWI/SNF) complex (28), and polymerase-epsilon exonuclease domain mutations (POLE-EDM) (31). Inactivation of the SWI/SNF complex is invasive in cases of UEC (28), but patients with POLE-EDM show a more favorable prognosis (31). It suggests that histologic diagnosis should be combined with molecular classification (32, 33). Excessive estrogen could induce UEC by inhibiting Succinate Dehydrogenase Complex Iron Sulfur Subunit B (SDHB) expression (34). Progestogens could increase the expression of progesterone receptor (PR), which is associated with abnormal regulation of MMR and the SWI/SNF (35–37). Recent studies have reported that the long-term use of progesterone may result in the absence of MMR (36) and that the transcription factor NF-E2-related factor 2 (Nrf2) is highly expressed during progestin treatment (38, 39). PR is also able to interact with hexanucleotide repeat expansion (HRE) exposed on the surface of nucleosomes and drive chromatin remodeling, which is a prerequisite for the activation of subsequent genes and determines the remodeling of nucleosomes by SWI/SNF (37). Additionally, it has also been reported that dual-specific phosphatase 6 (Dusp6) is useful for predicting progesterone response in endometrial hyperplasia, and its lack of expression significantly means the failure of potential treatment (40). It may serve as a biomarker for predicting response to progestin treatment. Due to the rarity, current treatment for UEC remains conventional, with practical experience limited to regular paclitaxel and carboplatin chemotherapy and/or radiotherapy (17, 41) and full-staged surgery (42). However, this case suggests that targeting MMR or SWI/SNF may be a strategy for developing targeted chemotherapy drugs for UEC in the presence of progestogens, providing a new approach for the conservative treatment of UEC.

4 Conclusion

Clear imaging features and pathological biomarkers help in diagnosis. In addition, it is necessary to measure the risks and benefits of surgery, radiotherapy, and chemotherapy for each patient. The case clarifies the impact of the prolonged exposure to estrogen and progestin on the development of UEC and suggests using Dusp6 as a biomarker to assess the effect of progesterone therapy. Moreover, targeting MMR or the SWI/SNF complex may emerge as a promising approach for developing conservative chemotherapeutic treatments for UEC.

Data availability statement

The original contributions presented in the study are included in the article/supplementary material. Further inquiries can be directed to the corresponding author.

Ethics statement

The work have been approved by the Institutional Review Board (IRB) of Taizhou Central Hospital, and have been conducted according to the principles expressed in the Declaration of Helsinki. The individual in this manuscript has given written informed consent to publish these case details. Written informed

consent was obtained from the participant/patient(s) for the publication of this case report.

Author contributions

YW: Data curation, Methodology, Writing – original draft. YZ: Writing – review & editing, Conceptualization, Visualization, Writing – original draft. LZ: Project administration, Resources, Supervision, Writing – original draft, Funding acquisition. XC: Data curation, Methodology, Writing – review & editing. ZL: Data curation, Methodology, Writing – review & editing. HL: Data curation, Methodology, Writing – review & editing. QH: Project administration, Resources, Supervision, Writing – review & editing, Funding acquisition.

Funding

The author(s) declare financial support was received for the research, authorship, and/or publication of this article. The work was granted from the Basic Public Welfare Research Program of Zhejiang Province (LGF21H280002), the Science and Technology Plan Project of Taizhou (22gya02), and the Medical Key Discipline of Taizhou.

Conflict of interest

The authors declare that the research was conducted in the absence of any commercial or financial relationships that could be construed as a potential conflict of interest.

Publisher's note

All claims expressed in this article are solely those of the authors and do not necessarily represent those of their affiliated organizations, or those of the publisher, the editors and the reviewers. Any product that may be evaluated in this article, or claim that may be made by its manufacturer, is not guaranteed or endorsed by the publisher.

References

1. Li H, Zhou Q, Wu Z, Lu X. Identification of novel key genes associated with uterine corpus endometrial carcinoma progression and prognosis. *J Ann Trans Med*. (2023) 11(2). doi: 10.21037/atm-22-6461

2. Wu Q, Wang Z, He C, Guo J, Xu C, Gao Y, et al. Protein and transcript expression levels of TRIP13 signify worse prognosis in endometrioid carcinoma. (2023). doi: 10.21203/rs.3.rs-3563302/v1

3. World Health Organization. *International agency for research on cancer*. (2019).

4. Amant Frédéric, Mirza MR, Koskas M, Creutzberg CL. Cancer of the corpus uteri. *J Int J Gynecology Obstetrics*. (2018) 143:37–50. doi: 10.1002/ijgo.2018.143.issue-S2

5. Chhikara BS, Parang K. Global Cancer Statistics 2022: the trends projection analysis. *J Chem Biol Lett*. (2023) 10:451–1.

6. Krämer P, Talhouk A, Brett MA, Chiu DS, Cairns ES, Scheunhage DaniëllaA, et al. Endometrial cancer molecular risk stratification is equally prognostic for endometrioid ovarian carcinoma. *J Clin Cancer Res*. (2020) 26:5400–10. doi: 10.1158/1078-0432.CCR-20-1268

7. Kurman RJ. *Blaustein's pathology of the female genital tract*. Springer Science & Business Media (2013).

8. Zhang YD, Hurson AN, Zhang H, Choudhury PP, Easton DF, Milne RL, et al. Assessment of polygenic architecture and risk prediction based on common variants across fourteen cancers. *J Nat Commun*. (2020) 11:3353. doi: 10.1038/s41467-020-16483-3

9. Wang P-H, Yang S-T, Liu C-H, Chang W-H, Lee F-K, Lee W-L. Endometrial cancer: part I. Basic concept. *J Taiwanese J Obstetrics Gynecol*. (2022) 61:951–9. doi: 10.1016/j.tjog.2022.09.001

10. Lei P, Wang H, Yu L, Xu C, Sun H, Lyu Y, et al. A correlation study of adhesion G protein-coupled receptors as potential therapeutic targets in Uterine Corpus Endometrial cancer. *J Int Immunopharmacol*. (2022) 108:108743. doi: 10.1016/j.intimp.2022.108743

11. Miller KD, Nogueira L, Devasia T, Mariotto AB, Yabroff KR, Jemal A, et al. Cancer treatment and survivorship statistic. *J CA: Cancer J Clin*. (2022) 72:409–36.

12. Abu-Rustum N, Yashar C, Arend R, Barber E, Bradley K, Brooks R, et al. Uterine neoplasms, version 1.2023, NCCN clinical practice guidelines in oncology. *J J Natl Compr Cancer Network*. (2023) 21:181–209. doi: 10.6004/jnccn.2023.0006

13. Tafe LJ, Garg K, Chew I, Tornos C, Soslow RA. Endometrial and ovarian carcinomas with undifferentiated components: clinically aggressive and frequently underrecognized neoplasms. *J Modern Pathol*. (2010) 23:781–9. doi: 10.1038/modpathol.2010.41

14. Stewart CJR, Doherty DA, Havlat M, Koay MHE, Leung YC, Naran A, et al. Transtubal spread of endometrial carcinoma: correlation of intra-luminal tumour cells with tumour grade, peritoneal fluid cytology, and extra-uterine metastasis. *J Pathol*. (2013) 45:382–7. doi: 10.1097/PAT.0b013e328360b6e7

15. Bartosch C, Lopes JoséM, Oliva E. Endometrial carcinomas: a review emphasizing overlapping and distinctive morphological and immunohistochemical features. *J Adv Anatomic Pathol*. (2011) 18:415–37. doi: 10.1097/PAP.0b013e318234ab18

16. Wu D, Hacking S, Cao J, Nasim M. Understanding the role of indoleamine-2, 3-dioxygenase and stromal differentiation in rare subtype endometrial cancer. *J Rare Tumors*. (2021) 13:20363613211044690. doi: 10.1177/20363613211044690

17. Pfaendler KS, Randall LM. Rapid progression of disease in two cases of undifferentiated endometrial carcinoma. *J Gynecologic Oncol Rep*. (2019) 27:65–8. doi: 10.1016/j.gore.2019.01.004

18. Gao J, Fan R, Chen D, Hou J, Chen H, Lu M. Pathological characteristics and immune microenvironment of SMARCA4-deficient undifferentiated uterine sarcoma. *J Diagn Pathol*. (2023) 18:62. doi: 10.1186/s13000-023-01347-3

19. Giordano G, D'Adda T, Bottarelli L, Lombardi M, Brigati F, Berretta R, et al. Two cases of low-grade endometriod carcinoma associated with undifferentiated carcinoma of the uterus (dedifferentiated carcinoma): a molecular study. *J Pathol Oncol Res*. (2012) 18:523–8. doi: 10.1007/s12253-011-9386-7

20. Ishii T, Takayama S, Abe M, Kuroda H, Tanaka J, Numata T, et al. Spontaneous regression of recurrent undifferentiated carcinoma of the endometrium. *J Internal Med*. (2019) 58:1649–53. doi: 10.2169/internalmedicine.0376-17

21. Tung H-J, Wu R-C, Lin C-Y, Lai C-H. Rare subtype of endometrial cancer: undifferentiated/dedifferentiated endometrial carcinoma, from genetic aspects to clinical practice. *J Int J Mol Sci*. (2022) 23:3794. doi: 10.3390/ijms23073794

22. Al-Hussaini M, Lataifeh I, Jaradat I, Abdeen G, Otay L, Badran O, et al. Undifferentiated endometrial carcinoma, an immunohistochemical study including PD-L1 testing of a series of cases from a single cancer center. *J Int J Gynecological Pathol*. (2018) 37:564–74. doi: 10.1097/PGP.0000000000000449

23. Santoro A, Angelico G, Travaglino A, Inzani F, Arciuolo D, Valente M, et al. New pathological and clinical insights in endometrial cancer in view of the updated ESGO/ESTRO/ESP guidelines. *J Cancers*. (2021) 13:2623. doi: 10.3390/cancers13112623

24. Murali R, Davidson B, Fadare O, Carlson JA, Crum CP, Gilks CB, et al. High-grade endometrial carcinomas: morphologic and immunohistochemical features, diagnostic challenges and recommendations. *J Int J Gynecological Pathol*. (2019) 38: S40–63. doi: 10.1097/PGP.0000000000000491

25. Zhang X, Yu M. Undifferentiated endometrial carcinoma: A selected immunohistochemical panel including PAX-8 and E-cadherin for aiding distinction from other endometrial carcinomas. *J Ann Diagn Pathol*. (2019) 39:36–41. doi: 10.1016/j.anndiagpath.2019.01.001

26. Murali R, Delair DF, Bean SM, Abu-Rustum NR, Soslow RA. Evolving roles of histologic evaluation and molecular/genomic profiling in the management of endometrial cancer. *J J Natl Compr Cancer Netw*. (2018) 16:201–9. doi: 10.6004/jnccn.2017.7066

27. Giordano G, Ferioli E, Guareschi D, Tafuni A. Dedifferentiated endometrial carcinoma: A rare aggressive neoplasm-clinical, morphological and immunohistochemical features. *J Cancers*. (2023) 15:5155. doi: 10.3390/cancers15215155

28. Stewart CJR, Crook ML. SWI/SNF complex deficiency and mismatch repair protein expression in undifferentiated and dedifferentiated endometrial carcinoma. *J Pathol*. (2015) 47:439–45. doi: 10.1097/PAT.0000000000000270

29. Xu Z, Saikia K, Yuan L. Dedifferentiated endometrial carcinoma arising from serous carcinoma: Diagnostic challenges and recommendations. *J Gynecologic Oncol Rep*. (2023) 47. doi: 10.1016/j.gore.2023.101188

30. Matsumoto M, Natsugoe S, Nakashima S, Shimada M, Nakano S, Kusano C, et al. Biological evaluation of undifferentiated carcinoma of the esophagus. *J Ann Surg Oncol*. (2000) 7:204–9. doi: 10.1007/BF02523655

31. Zhang K, Liu Y, Liu X, Du J, Wang Y, Yang J, et al. Clinicopathological significance of multiple molecular features in undifferentiated and dedifferentiated endometrial carcinomas. *J Pathol*. (2021) 53:179–86. doi: 10.1016/j.pathol.2020.07.015

32. McConechy MK, Talhouk A, Leung S, Chiu D, Yang W, Senz J, et al. Endometrial carcinomas with POLE exonuclease domain mutations have a favorable prognosis. *J Clin Cancer Res*. (2016) 22:2865–73. doi: 10.1158/1078-0432.CCR-15-2233

33. Köbel M, Hoang LN, Tessier-Cloutier B, Meng Bo, Soslow RA, Stewart CJR, et al. Undifferentiated endometrial carcinomas show frequent loss of core switch/sucrose nonfermentable complex proteins. *J Am J Surg Pathol*. (2018) 42:76–83. doi: 10.1097/PAS.0000000000000941

34. Gu C, Yang H, Chang K, Zhang B, Xie F, Ye J, et al. Melatonin alleviates progression of uterine endometrial cancer by suppressing estrogen/ubiquitin C/SDHB-mediated succinate accumulation. *Cancer Lett*. (2020) 476:34–47. doi: 10.1016/j.canlet.2020.02.009

35. Reyes HD, Carlson MJ, Devor EJ, Zhang Y, Thiel KW, Samuelson MI, et al. Downregulation of FOXO1 mRNA levels predicts treatment failure in patients with endometrial pathology conservatively managed with progestin-containing intrauterine devices. *J Gynecologic Oncol*. (2016) 140:152–60. doi: 10.1016/j.ygyno.2015.10.023

36. Giampaolino P, Cafasso V, Boccia D, Ascione M, Mercorio A, Viciglione F, et al. Fertility-sparing approach in patients with endometrioid endometrial cancer grade 2 stage IA (FIGO): a qualitative systematic review. *J BioMed Res Int*. (2022) 2022. doi: 10.1155/2022/4070368

37. Vicent GP, Zaurin R, Ballaré C, Silvina Nacht A, Beato M. Erk signaling and chromatin remodeling in MMTV promoter activation by progestins. *J Nucl receptor Signaling*. (2009) 7:07008. doi: 10.1621/nrs.07008

38. Wang H, Tang Z, Li T, Liu M, Li Y, Xing B. CRISPR/Cas9-mediated gene knockout of ARID1A promotes primary progesterone resistance by downregulating progesterone receptor B in endometrial cancer cells. *J Oncol Res*. (2019) 27:1051. doi: 10.3727/096504019X15561873320465

39. Fan W, Li J, Chen J, Zhu L, Wang Y, Sun B, et al. Aspirin inhibits the proliferation of synovium-derived mesenchymal stem cells by arresting the cell cycle in the G0/G1 phase. *J Am J Trans Res*. (2017) 9:5056.

40. Zhang H, Yan L, Bai Y, Li C, Guo Q, Wang C, et al. Dual-specificity phosphatase 6 predicts the sensitivity of progestin therapy for atypical endometrial hyperplasia. *J Gynecologic Oncol*. (2015) 136:549–53. doi: 10.1016/j.ygyno.2014.11.008

41. Han J, Ki EY, Rha SE, Hur S, Lee A. Dedifferentiated endometrioid carcinoma of the uterus: report of four cases and review of literature. *J World J Surg Oncol*. (2017) 15:1–9. doi: 10.1186/s12957-016-1093-0

42. Concin N, Matias-Guiu X, Vergote I, Cibula D, Mirza MR, Marnitz S, et al. ESGO/ESTRO/ESP guidelines for the management of patients with endometrial carcinoma. *J Int J Gynecologic Cancer*. (2021), 31(1). doi: 10.1136/ijgc-2020-002230

frontiers | Frontiers in Oncology

TYPE Case Report
PUBLISHED 11 December 2024
DOI 10.3389/fonc.2024.1461216

Check for updates

OPEN ACCESS

EDITED BY
Dragos Eugen Georgescu,
Carol Davila University of Medicine and Pharmacy, Romania

REVIEWED BY
Ahmad Mustafa Metwalley,
Women's Health Fertility Clinic, Saudi Arabia
Alessandra Gallo,
Federico II University Hospital, Italy

*CORRESPONDENCE
Xu Chen
chenxu196301@163.com

†These authors share first authorship

RECEIVED 08 July 2024
ACCEPTED 25 November 2024
PUBLISHED 11 December 2024

CITATION
Fan Y, Song H, Chen X, Zhang P, Si J and Dong H (2024) Case report: A successful live birth after *in vitro* fertilization and embryo transfer in a patient with endometrial cancer who was treated conservatively.
Front. Oncol. 14:1461216.
doi: 10.3389/fonc.2024.1461216

COPYRIGHT
© 2024 Fan, Song, Chen, Zhang, Si and Dong. This is an open-access article distributed under the terms of the Creative Commons Attribution License (CC BY). The use, distribution or reproduction in other forums is permitted, provided the original author(s) and the copyright owner(s) are credited and that the original publication in this journal is cited, in accordance with accepted academic practice. No use, distribution or reproduction is permitted which does not comply with these terms.

Case report: A successful live birth after *in vitro* fertilization and embryo transfer in a patient with endometrial cancer who was treated conservatively

Yifan Fan[1,2,3†], Hui Song[1,2,3†], Xu Chen[1,2,3*], Pei Zhang[1], Jingwen Si[1] and Hui Dong[1,2,3]

[1]Department of Obstetrics and Gynecology, School of Medicine, Nankai University, Tianjin, China, [2]Department of Obstetrics, Tianjin Central Hospital of Gynecology Obstetrics, Tianjin, China, [3]Tianjin Key Laboratory of Human Development and Reproductive Regulation, Tianjin, China

Objective: To describe a patient conceiving with *in vitro* fertilization and embryo transfer(IVF-ET) after conservative treatment of early stage endometrial cancer.

Patient: A 31-year-old multiparous woman diagnosed with highly-differentiated (G1) endometrial adenocarcinoma (grade IA).

Intervention(s): After four courses of conservative treatment each followed by hysteroscopic biopsy and endometrial curettage,assisted reproductive technology was performed.

Main outcome measure(s): Successful pregnancy and delivery without residual endometrial cancer.

Results(s): A healthy normal female infant with a birth weight of 3,690 g was born by cesarean section at 38 + 2 weeks' gestation. No residual malignant cells was detected on a biopsy during cesarean section.

Conclusion(s): Conservative fertility-sparing treatment are crucial for young patients with early stage endometrial cancer. Assisted reproductive technologies may be considered to assist such patients to conceive as soon as possible.

KEYWORDS

early-stage endometrial cancer, fertility-sparing treatment, conservative treatment, *in vitro* fertilization and embryo transfer, pregnancy

1 Introduction

Endometrial cancer is a prominent cause of mortality among gynecological malignancies worldwide. The latest data reports 420,242 new cases of endometrial cancer globally in 2022, ranking it as the 15th most prevalent type of cancer, with 97,704 new deaths, placing it at the 19th position (1). In China during the same year, the incidence rate of endometrial cancer was 11.25 per 100,000 individuals with a corresponding mortality rate of 1.96 per 100,000 individuals.Furthermore, there has been a continuous increase in the incidence rate of endometrial cancer from 2000 to 2018 in China along with a trend towards younger onset cases (2). Notably, a significant proportion of these young patients diagnosed with endometrial cancer have not given birth.

In cases of early-stage endometrial cancer confined to the uterine body, the standard surgical approach involves hysterectomy with bilateral adnexectomy and lymph node evaluation (3); however, this procedure results in loss of female fertility. On the one hand,due to the increasing age of women's first childbirth and the progressively younger onset of endometrial cancer, some women have not completed their childbearing prior to diagnosis. On the other hand, in light of China's three-child policy implemented since 2021, even those who have completed their first childbearing may still have a strong desire to preserve their fertility. Consequently, the fertility-sparing treatment of patients with endometrial carcinoma has become increasingly crucial.

Fertility preservation therapy necessitates comprehensive evaluation and strict screening of patients with fertility needs due to the potential risks of residual tumor lesions, disease recurrence and progression (1). Therefore, it is exclusively suitable for young patients with early-stage endometrial carcinoma without metastasis (4, 5). Typically, these patients exhibit adenocarcinoma tissue type characterized by highly differentiated tumor cells that express PR/ER positively. Consequently, the risk of metastasis is relatively low while the prognosis remains favorable. However, active conception should be pursued promptly following complete remission to minimize estrogen stimulation and avoid the heightened risk of recurrence.

Successful pregnancies have been documented in the literature following fertility preservation therapy in nulliparous females with endometrial cancer (6–8). In this particular case,we report a woman who was diagnosed with endometrial cancer two years after she had given birth to a baby. Due to her persistent desire for future fertility, we performed fertility preservation therapy following comprehensive multidisciplinary consultation and evaluation.Subsequently, she successfully achieved conception through assisted reproductive technology and delivered a healthy baby via cesarean section at full term.

2 Case description

The patient was a 31-year-old multiparous woman who underwent D&C in November 2021 due to abnormal uterine bleeding. The postoperative pathology revealed endometrial atypical hyperplasia with polypoid growth and suspicious focal cancer (Figure 1). And immunohistochemistry indicated ER positive (90%), PR positive (90%), p53 (wild type), Pax-2 negative (local). Following the D&C procedure, a MRI of the pelvic region was performed to fully assess the uterine cavity which showed that the lesion was confined to the uterine cavity without myometrial invasion or cervical involvement (Figure 2). Eventually she was diagnosed with a highly-differentiated (G1) endometrial adenocarcinoma (grade IA). Notably, the patient's body mass index was 27.2 kg/m2 (weight 75 kg, height 166 cm), and she had an irregular menstrual cycle of 30-40 days. Her grandfather died of lung cancer and she denied other family history of tumors and family history of diabetes.

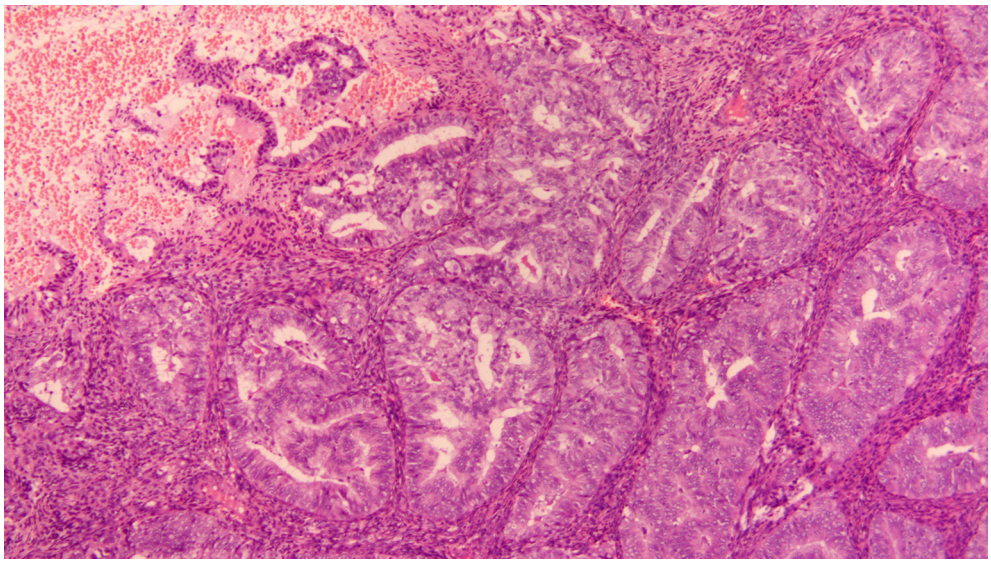

FIGURE 1
HE staining of the pathology section at diagnosis (10X).

FIGURE 2
MRI at diagnosis.

3 The therapeutic intervention, follow-up and outcomes

After counseling, the patient desired to preserve her fertility, thus high-dose progestin therapy was recommended. The timeline is shown in Figure 3. She underwent a 12-week course of oral megestrol acetate at a dosage of 160 mg daily as the initial treatment, followed by hysteroscopic biopsy and endometrial curettage. The postoperative pathology showed decidual-like changes in the endometrial stromal tissue with glandular atrophy observed in some areas (70%), consistent with medication-induced alterations. Immunohistochemistry analysis demonstrated positive estrogen receptor expression (60%), weakly positive progesterone receptor expression (5%), and localized Pax-2 positivity. In addition to the first course, Tamoxifen supplementation at a daily dose of 20mg was administered during the second course along with subsequent hysteroscopic biopsy and endometrial curettage procedures. The postoperative pathology showed decidual-like changes in the endometrial stromal tissue with glandular atrophy observed in some areas (90%). And immunohistochemistry indicated positive estrogen receptor expression (60%-70%) and individual cells showing progesterone receptor positivity. The third course involved an additional daily dose of 750mg metformin on top of the second course, resulting in extensive decidual-like changes in the endometrial stromal tissue along with glandular atrophy observed in approximately 85-90% of areas according to postoperative pathology findings. Immunohistochemistry analysis showed positive estrogen receptor expression (70%) and individual cells displaying progesterone receptor positivity. For the fourth course, medication was switched to monthly intramuscular injections of leuprorelin acetate at a dosage of 3.75mg combined with daily letrozole tablets at a dosage of 2.5mg while continuing oral administration of metformin at a daily dose of 750mg for three months. The follow-up pathology of hysteroscopic biopsy and endometrial curettage revealed that the majority of the glands in the endometrial tissue exhibited atrophy with secretory reaction and stromal decidual-like changes, demonstrating significant remission following treatment. Additionally, immunohistochemistry analysis indicated positive expression of ER and PR. The molecular test showed no mutation in the POLE gene and the molecular subtype was classified as non-specific molecular signature type (NMSP).

In order to expedite conception, the patient chose to conceive by assisted reproductive technology. Her husband was 33 years old with a body mass index of 25.3 kg/m2 (weight 73 kg,height 170 cm). The husband's semen analysis was normal.A mild stimulation protocol for ovulation induction was administered with letrozole at dose of 7.5mg daily from MC3 (artificial menstruation cycle Day3) and human menopausal gonadotrophin (HMG, Livzon, China) at dose of 225 IU daily from MC4 for 9 days in total. The follicular growth was monitored by transvaginal ultrasonography from the 5th day since gonadotropin administration by 2 days interval.When two or more follicles' diameter reached 18 mm, human chorionic gonadotropin (hCG, Merck Serono, Germany) at dose of 6500 IU was administrated. The endometrial thickness was 7.5 mm at the time of hCG administration with following hormonal levels: LH 1.9 IU/L, P 0.8 ng/dL, E2 249 pg/mL. And 36 hours later, oocytes aspiration was performed under the guidance of transvaginal ultrasonography. Twelve oocytes were retrieved, and seven of them were fertilized and then cultured *in vitro*. A high-quality 10-cell embryo was transferred into the uterus 3 days after.The level of serum-hCG was 10887 mIU/mL 21 days after embryo transfer, and a single gestational sac was seen in the uterine cavity by transvaginal ultrasonography 35 days after embryo transfer. Routine prenatal examinations during pregnancy were normal. Considering the patient's previous cesarean section delivery of a male infant in 2019, the pregnancy was terminated by cesarean section this time after multidisciplinary consultation and informed consent. Finally she delivered a live female infant by

Timeline

2021-11-05	The patient underwent D&C due to abnormal uterine bleeding.The postoperative pathology revealed endometrial atypical hyperplasia with polypoid growth and suspicious focal cancer.
2021-12-02	A MRI of the pelvic region was performed which showed that the lesion was confined to the uterine cavity without myometrial invasion or cervical involvement. She was diagnosed with a highly-differentiated (G1) endometrial adenocarcinoma
2021-12-07	She started taking a 12-week course of oral megestrol acetate at a dosage of 160 mg daily as the initial treatment
2022-03-08	Hysteroscopic biopsy and endometrial curettage were performed following the first course.
2022-03-15	She started taking a 12-week course of oral megestrol acetate of 160 mg plus tamoxifen of 20mg daily as the second course.
2022-07-15	Hysteroscopic biopsy and endometrial curettage were performed following the second course.
2022-07-26	She started taking a 12-week course of oral megestrol acetate of 160 mg plus tamoxifen of 20mg plus metformin of 750mg daily as the third course.
2022-11-10	Hysteroscopic biopsy and endometrial curettage were performed following the third course.
2022-11-15	She started taking intramuscular injections of leuprorelin acetate at a dosage of 3.75mg monthly combined with daily letrozole tablets at a dosage of 2.5mg while continuing oral administration of metformin at a daily dose of 750mg for three months.
2023-02-24	Hysteroscopic biopsy and endometrial curettage were performed following the forth course.
2023-07-18	The patient underwent a fresh embryo transferand achieved successful pregnancy.
2024-03-26	The patient delivered a live female infant by cesarean section at 38+2 weeks of gestation in March 2024,with birth weight of 3690 g, length of 52cm and Apgar score of 10.

FIGURE 3
the timeline of diagnosis and treatment.

cesarean section at 38 + 2 weeks of gestation in March 2024,with birth weight of 3690 g, length of 52cm and Apgar score of 10. Meanwhile, curettage and endometrial biopsy was performed during the cesarean section.On one hand, the pelvic MRI in 2021 indicated that the endometrial cancer lesion was located near the uterine corner on the left wall of the uterus. On the other hand, the ultrasound images during current pregnancy suggested that placental placement occurred on the right wall of the uterus. Therefore, tissues from both uterine walls as well as both uterine corners were submitted for histopathology examination. The postoperative pathology report revealed minimal decidual tissue presence alongside abundant thick-walled vessels without significant atypical hyperplasia or malignant lesions (Figure 4).

4 Discussion

Endometrial cancer is one of the most common gynecological malignancies in developed countries (9), primarily observed during menopause. In recent years, there has been an increasing proportion of endometrial cancer cases diagnosed in individuals under the age of 40, accounting for approximately 2% to 14% of all reported cases (10). Previous successful conservative treatment cases for young endometrial cancer have predominantly involved nulliparous women. However, this particular case involves a young multiparous patient who underwent cesarean section delivery two years ago and subsequently received a diagnosis of endometrial cancer.

The uniqueness of this case lies in the absence of any identifiable risk factors for endometrial cancer, such as exposure to unopposed oestrogen, obesity, diabetes, advanced age, nulliparity, polycystic ovarian syndrome, and use of tamoxifen.A comprehensive umbrella review encompassing 171 meta-analyses from 1354 individual studies on 53 risk factors indicated that multiparity was associated with a reduced risk of endometrial cancer (11). However, the patient did not fit any of the above characteristics.Notably, she presented with endometrial polyps. Previous case series have reported varying malignancy risks in endometrial polyps (ranging from 0% to 15%), while one meta-analysis reported an overall prevalence of malignancy in endometrial polyps at 2.7% (12). Nevertheless, it remains unclear how long the patient had uterine polyps prior to diagnosis and whether her abnormal uterine bleeding was attributed to either the presence of polyps or underlying endometrial cancer.

The standards of each guideline are relatively unified on whether patients with early endometrial cancer can be treated with conservative treatment (1). In this case, the patient meets the following criteria for fertility-preservation treatment: 1. Young and

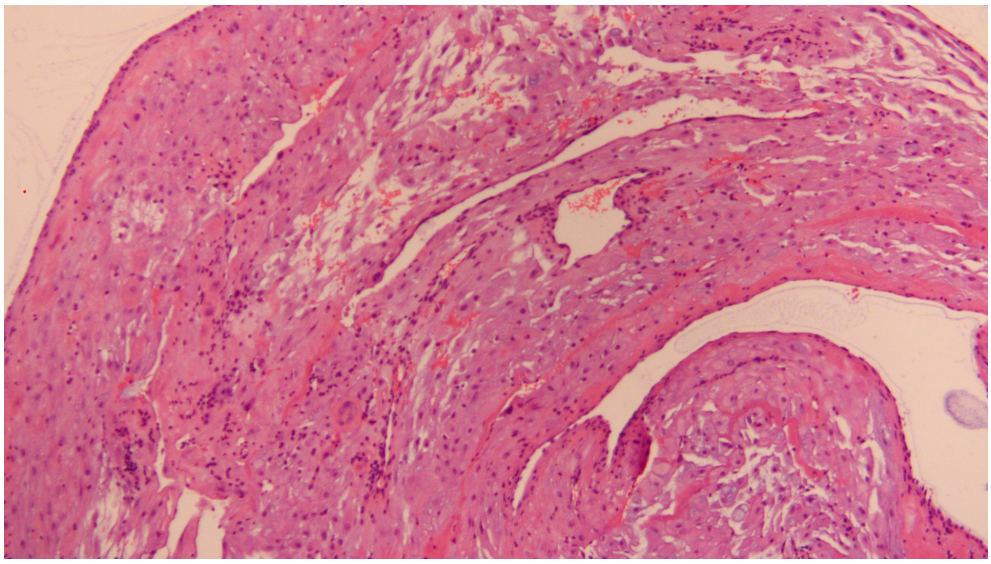

FIGURE 4
HE staining of the pathology section during cesarean section after treatment (10X).

strong fertility intention; 2. highly differentiated endometrioid adenocarcinoma; 3. imaging examination confirms localized lesion confined to the endometrium without invasion or metastasis; 4. positive expression of ER/PR; 5. molecular typing has no specific molecular characteristic (NMSP).

For patients with early endometrial cancer requiring fertility preservation and eligible for endocrine therapy, progesterone is the clinical first choice, and its therapeutic efficacy is highly related to the expression status of hormone receptors, especially the expression level of PR (13, 14). However, certain PR-positive patients are not sensitive to progesterone therapy (15). Although the pre-treatment PR positivity rate in this case was approximately 90%, it significantly declined to weakly positive (about 5%) after the initial course of treatment (oral administration of 12 weeks of megestrol acetate), indicating the development of progesterone resistance.

Tamoxifen, a selective estrogen receptor modulator (SERMs), is currently employed in the treatment of advanced and recurrent endometrial cancer. It exhibits tissue-specific actions by acting as an antagonist of estrogen in breast cancer tissue while displaying weak estrogenic characteristics in endometrial cancer tissue, thereby inducing PR expression (16). Additionally, a study conducted by Mao et al. (17) demonstrated that high-dose TAM also exerts regulatory effects on ERRα, which can inhibit the proliferation of endometrial cancer cells *in vitro*. Therefore, we incorporated tamoxifen into megestrol acetate in the second and third courses to enhance oral progesterone sensitivity while minimizing its side effects. However, despite these interventions, complete remission was not achieved based on pathological assessments and PR expression further decreased (with only individual cells showing positivity). Consequently, we contemplated discontinuing the progesterone treatment regimen.

The anti-tumor effects of gonadotropin-releasing hormone agonists (GnRH-a) are partially attributed to their ability to reduce estrogen levels in the body. Additionally, it binds to GnRH-R to effectively inhibit endometrial cancer cell proliferation (18, 19). Most of the endometrial cancer tissues express GnRH-R, suggesting that GnRH-aholds potential for treating PR-negative endometrial cancer. Current guidelines recommend combining GnRH-a with other drugs. Letrozole, an aromatase inhibitor, reduces estrogen production by inhibiting aromatase activity in ovarian and peripheral tissues; however, it is generally not administered as a standalone treatment option. Therefore, we discontinued the progesterone plus tamoxifen regimen in the fourth course and transitioned to a combination therapy involving GnRH-a and letrozole. Pathological examination following this course demonstrated significant remission.

It is worth mentioning that we have added metformin to the patients since the third course of treatment. Metformin, a conventional insulin sensitizer, was recently found to have both direct and indirect inhibition of EC and synergistic effects with progesterone (20–22). Patients with endometrial cancer often present with comorbidities such as polycystic ovary syndrome, overweight or obesity, and diabetes mellitus.Obesity and insulin resistance are independent adverse factors that not only compromise fertility preservation efficacy in endometrial cancer but also impact pregnancy outcomes (23). Therefore, proactive management of insulin resistance and body composition is imperative. Although the patient in this case did not meet the diagnostic criteria for obesity(BMI≥28.0kg/m2 according to Chinese standards), her BMI was 27.2kg/m2 —approaching the threshold for obesity diagnosis. Considering all these factors collectively, we introduced metformin into the therapeutic approach starting from the third course.

The recommended treatment duration for patients with endometrial cancer is 6-12 months, during which complete remission should be achieved (1). However, in our case, the patient did not achieve complete remission after 12 months of treatment but showed significant remission. Considering her strong desire to

conceive, we decided to discontinue the treatment and assist her in achieving pregnancy as soon as possible after a multidisciplinary consultation. On the one hand, shortening the conception time can reduce estrogen stimulation and minimize the risk of endometrial cancer recurrence. On the other hand, pregnancy itself provides protection against endometrial cancer, which may be attributed to the female potential fertility or the biological process occurring early in pregnancy (24). Therefore, in order to improve the success rate, shorten the conception interval, and mitigate the higher risk of recurrence, we recommend the patients to conceive by assisted reproductive technology. Endometrial cancer is a hormone-dependent tumor, while the development of multiple follicles can significantly increase estrogen levels, potentially increasing the risk of recurrence. Therefore, we implemented a mild stimulation protocol using low doses of gonadotropin and letrozole to achieve an optimal balance between clinical pregnancy rates and recurrence rates.In early-stage endometrial cancer patients, long-term oral progesterone administration may exacerbate endometrial gland atrophy and stromal decidualization. Concurrently, hysteroscopy and curettage are typically required every 3-6 months during treatment. However repeated intrauterine procedures may cause damage to the functional layer of the endometrium, resulting in uterine adhesions and thin endometrium, etc. These factors are detrimental to successful implantation of fertilized eggs, potentially impacting subsequent pregnancies (25). The patient underwent a total of 36 weeks of oral progesterone treatment along with five hysteroscopic procedures and curettages within nearly two years from diagnosis until completion of treatment. Fortunately, she successfully conceived following one single embryo transfer.

Despite completion of childbirth, endometrial cancer patients remain at risk for recurrence and progression; therefore, surgical resection of the uterus is recommended (3). Upon the patient's strong request for uterine preservation, a multidisciplinary consultation was conducted, leading to the decision of implementing close follow-up as a temporary measure.

5 Patient perspective

As a cancer survivor, it was not easy for my family or me to defeat it and have a second child. I was shocked when I was first diagnosed with cancer, because I had just had a baby two years ago. Fortunately, my doctors sincerely listened to my opinions, respected my choice of preserving the uterus, and showing the professionalism in every step of diagnosis and treatment. I am very grateful to doctors in various disciplines for their help in this process, which could not be achieved without them. Now I cherish my hard-won precious child and my own life.

Data availability statement

The original contributions presented in the study are included in the article/Supplementary Material. Further inquiries can be directed to the corresponding author.

Ethics statement

Ethical approval was not required for this article in accordance with the local legislation and institutional requirements. Written informed consent was obtained from the individual(s)for the publication of any potentially identifiable images or data included in this article.

Author contributions

YF: Project administration, Validation, Writing – original draft, Writing – review & editing. HS: Project administration, Validation, Writing – original draft, Writing – review & editing. XC: Funding acquisition, Resources, Validation, Visualization, Writing – review & editing. PZ: Data curation, Investigation, Methodology, Validation, Visualization, Writing – review & editing. JS: Formal analysis, Software, Writing – review & editing. HD: Formal analysis, Software, Writing – review & editing.

Funding

The author(s) declare financial support was received for the research, authorship, and/or publication of this article. This work was supported by Grants from the National Key Research and Development Program of China (Grant No. 2021YFC2701500) and Tianjin Key Medical Discipline(Specialty) Construction Project(TJYXZDXK-034A).

Acknowledgments

The authors extend their gratitude to all doctors, nurses and staff members who contributed significantly to the case.

Conflict of interest

The authors declare that the research was conducted in the absence of any commercial or financial relationships that could be construed as a potential conflict of interest.

Publisher's note

All claims expressed in this article are solely those of the authors and do not necessarily represent those of their affiliated organizations, or those of the publisher, the editors and the reviewers. Any product that may be evaluated in this article, or claim that may be made by its manufacturer, is not guaranteed or endorsed by the publisher.

Supplementary material

The Supplementary Material for this article can be found online at: https://www.frontiersin.org/articles/10.3389/fonc.2024.1461216/full#supplementary-material

References

1. Rodolakis GSA, Planchamp F, Acien M, Di Spiezio Sardo A, Farrugia M. ESGO/ESHRE/ESGE Guidelines for the fertility-sparing treatment of patients with endometrial carcinoma. *Int J Gynecological Cancer*. (2023). doi: 10.1093/hropen/hoac057

2. Han B, Zheng R, Zeng H, Wang S, Sun K, Chen R, et al. Cancer incidence and mortality in China, 2022. *J Natl Cancer Center*. (2024) 4:47–53. doi: 10.1016/j.jncc.2024.01.006

3. Abu-Rustum N, Yashar C, Arend R, Barber E, Bradley K, Brooks R, et al. Uterine neoplasms, version 1.2023, NCCN clinical practice guidelines in oncology. *J Natl Compr Canc Netw*. (2023) 21:181–209. doi: 10.6004/jnccn.2023.0006

4. Bourou MZ, Matsas A, Vrekoussis T, Mastorakos G, Valsamakis G, Panoskaltsis T. Conservative treatment of endometrial cancer in women of reproductive age (Review). *Mol Clin Oncol*. (2023) 19:55. doi: 10.3892/mco.2023.2651

5. Uccella S, Zorzato PC, Dababou S, Bosco M, Torella M, Braga A, et al. Conservative management of atypical endometrial hyperplasia and early endometrial cancer in childbearing age women. *Medicina (Kaunas)*. (2022) 58(9):1256. doi: 10.3390/medicina58091256

6. Kim SW, Kim H, Ku SY, Suh CS, Kim SH, Choi YM. A successful live birth with *in vitro* fertilization and thawed embryo transfer after conservative treatment of recurrent endometrial cancer. *Gynecol Endocrinol*. (2018) 34:15–9. doi: 10.1080/09513590.2017.1342239

7. Yarali H, Bozdag G, Aksu T, Ayhan A. A successful pregnancy after intracytoplasmic sperm injection and embryo transfer in a patient with endometrial cancer who was treated conservatively. *Fertil Steril*. (2004) 81:214–6. doi: 10.1016/j.fertnstert.2003.05.031

8. Eriksson AG, Fallaas Dahl G, Nesbakken AJ, Lund KV, Amant F. Endometrial cancer during pregnancy: management strategies. *Int J Gynecol Cancer*. (2019) 29:1221–4. doi: 10.1136/ijgc-2019-000756

9. Siegel RL, Giaquinto AN, Jemal A. Cancer statistics, 2024. *CA Cancer J Clin*. (2024) 74:12–49. doi: 10.3322/caac.21820

10. Zhao S, Li G, Yang L, Li L, Li H. Response-specific progestin resistance in a newly characterized Ishikawa human endometrial cancer subcell line resulting from long-term exposure to medroxyprogesterone acetate. *Oncol Lett*. (2013) 5:139–44. doi: 10.3892/ol.2012.975

11. Raglan O, Kalliala I, Markozannes G, Cividini S, Gunter MJ, Nautiyal J, et al. Risk factors for endometrial cancer: An umbrella review of the literature. *Int J Cancer*. (2019) 145:1719–30. doi: 10.1002/ijc.v145.7

12. Uglietti A, Buggio L, Farella M, Chiaffarino F, Dridi D, Vercellini P, et al. The risk of Malignancy in uterine polyps: A systematic review and meta-analysis. *Eur J Obstet Gynecol Reprod Biol*. (2019) 237:48–56. doi: 10.1016/j.ejogrb.2019.04.009

13. Neal AS, Nunez M, Lai T, Tosevska A, Morselli M, Amneus M, et al. Expression of stromal progesterone receptor and differential methylation patterns in the endometrium may correlate with response to progesterone therapy in endometrial complex atypical hyperplasia. *Reprod Sci*. (2020) 27:1778–90. doi: 10.1007/s43032-020-00175-w

14. Yu K, Huang Z-Y, Xu X-L, Li J, Fu X-W, Deng S-L. Estrogen receptor function: impact on the human endometrium. *Front Endocrinol*. (2022) 13. doi: 10.3389/fendo.2022.827724

15. Zhou S, Xu Z, Yang B, Guan J, Shan W, Shi Y, et al. Characteristics of progestin-insensitive early stage endometrial cancer and atypical hyperplasia patients receiving second-line fertility-sparing treatment. *J Gynecologic Oncol*. (2021) 32(4):e57. doi: 10.3802/jgo.2021.32.e57

16. Emons G, Mustea A, Tempfer C. Tamoxifen and endometrial cancer: A janus-headed drug. *Cancers (Basel)*. (2020) 12(9):2535. doi: 10.3390/cancers12092535

17. Mao X, Dong B, Gao M, Ruan G, Huang M, Braicu EI, et al. Dual targeting of estrogen receptor alpha and estrogen-related receptor alpha: a novel endocrine therapy for endometrial cancer. *Onco Targets Ther*. (2019) 12:6757–67. doi: 10.2147/OTT.S216146

18. Emons G, Grundker C. The role of gonadotropin-releasing hormone (GnRH) in endometrial cancer. *Cells*. (2021) 10(2):2921. doi: 10.3390/cells10020292

19. Desaulniers AT, White BR. Role of gonadotropin-releasing hormone 2 and its receptor in human reproductive cancers. *Front Endocrinol (Lausanne)*. (2023) 14:1341162. doi: 10.3389/fendo.2023.1341162

20. Mitsuhashi A, Habu Y, Kobayashi T, Kawarai Y, Ishikawa H, Usui H, et al. Long-term outcomes of progestin plus metformin as a fertility-sparing treatment for atypical endometrial hyperplasia and endometrial cancer patients. *J Gynecol Oncol*. (2019) 30:e90. doi: 10.3802/jgo.2019.30.e90

21. Mu N, Dong M, Li L, Xia M, Qv L, Wang Y, et al. Synergistic effect of metformin and medroxyprogesterone 17–acetate on the development of endometrial cancer. *Oncol Rep*. (2018) 39:2015–21. doi: 10.3892/or.2018.6236

22. Xie Y, Wang YL, Yu L, Hu Q, Ji L, Zhang Y, et al. Metformin promotes progesterone receptor expression via inhibition of mammalian target of rapamycin (mTOR) in endometrial cancer cells. *J Steroid Biochem Mol Biol*. (2011) 126:113–20. doi: 10.1016/j.jsbmb.2010.12.006

23. Park J-Y, Seong SJ, Kim T-J, Kim JW, Bae D-S, Nam J-H. Significance of body weight change during fertility-sparing progestin therapy in young women with early endometrial cancer. *Gynecologic Oncol*. (2017) 146:39–43. doi: 10.1016/j.ygyno.2017.05.002

24. Husby A, Wohlfahrt J, Melbye M. Pregnancy duration and endometrial cancer risk: nationwide cohort study. *Bmj*. (2019) 366:14693. doi: 10.1136/bmj.l4693

25. Fan Y, Li X, Wang J, Wang Y, Tian L, Wang J. Analysis of pregnancy-associated factors after fertility-sparing therapy in young women with early stage endometrial cancer or atypical endometrial hyperplasia. *Reprod Biol Endocrinol*. (2021) 19(1):118. doi: 10.1186/s12958-021-00808-y

frontiers | Frontiers in Oncology

TYPE Original Research
PUBLISHED 11 December 2024
DOI 10.3389/fonc.2024.1451175

Check for updates

OPEN ACCESS

EDITED BY
Dragos Eugen Georgescu,
Carol Davila University of Medicine and Pharmacy, Romania

REVIEWED BY
Abderrahman Ouban,
Alfaisal University, Saudi Arabia
Kaijian Hou,
Shantou University, China
Mangala Hegde,
Indian Institute of Technology Guwahati, India

*CORRESPONDENCE
Hongyi Li
lihongyich@126.com

RECEIVED 18 June 2024
ACCEPTED 25 November 2024
PUBLISHED 11 December 2024

CITATION
Zhang Z, Wu W, Lin J and Li H (2024) Unveiling the hidden causal links: skin flora and cutaneous melanoma.
Front. Oncol. 14:1451175.
doi: 10.3389/fonc.2024.1451175

COPYRIGHT
© 2024 Zhang, Wu, Lin and Li. This is an open-access article distributed under the terms of the Creative Commons Attribution License (CC BY). The use, distribution or reproduction in other forums is permitted, provided the original author(s) and the copyright owner(s) are credited and that the original publication in this journal is cited, in accordance with accepted academic practice. No use, distribution or reproduction is permitted which does not comply with these terms.

Unveiling the hidden causal links: skin flora and cutaneous melanoma

Zexin Zhang[1], Wenfeng Wu[1], Jiajia Lin[1] and Hongyi Li[2]*

[1]The Second Clinical School of Guangzhou University of Chinese Medicine, Guangzhou, China, [2]Department of Dermatology, The Second Affiliated Hospital of Guangzhou University of Chinese Medicine, Guangzhou, China

Objective: The presence of skin flora (SF) has been identified as a significant factor in the onset and progression of cutaneous melanoma (CM). However, the vast diversity and abundance of SF present challenges to fully understanding the causal relationship between SF and CM.

Methods: A Two Sample Mendelian Randomization (TSMR) analysis was conducted to investigating the causal relationship between SF and CM. The Inverse-Variance Weighted (IVW) method was utilized as the primary approach to assess the causal relationship under investigation. Furthermore, an independent external cohort was employed to validate the initial findings, followed by a meta-analysis of the consolidated results. To address potential confounding factors related to the influence of SF on CM, a Multivariate Mendelian Randomization (MVMR) analysis was also conducted. Finally, a Reverse Mendelian Randomization (RMR) was conducted to further validate the causal association.

Results: TSMR results showed that 9 SF have a causal relationship with CM in the training cohort. Although these 9 SF weren't confirmed in the testing cohort, 4 SF remained significant in the meta-analysis after integrating results from both cohorts. MVMR analysis indicated that 3 SF were still significantly associated with CM after accounting for the interactions between different SF in the training cohort. No reverse causal relationship was identified in RMR analysis.

Conclusion: A total of 9 SF were identified as having a potential causal relationship with CM; however, a large randomized controlled trial is needed to verify these results.

KEYWORDS

causal relationship, skin flora, cutaneous melanoma, mendelian analysis, meta-analysis

Introduction

Cutaneous melanoma (CM) is a highly malignant tumor that originates from melanocytes in the basal layer of the epidermis, often presenting as irregular, dark-pigmented lesions on the skin surface (1). Globally, the incidence and mortality rates of CM are rising each year. In 2020, approximately 325,000 new cases of melanoma and 57,000 deaths were reported worldwide (2, 3). The prognosis of CM can vary significantly depending on factors such as age of onset, tumor location, and pathological type (4). Research shows that lymphatic metastasis can occur in the early stages of CM, drastically reducing survival rates. As the number of affected lymph nodes increases, the 5-year survival rate for patients plummets to around 10% (5). CM is highly aggressive and invasive, accounting for up to 90% of skin cancer-related deaths, making it the most lethal skin malignancy (6). Given its profound public health and economic impact, it is essential to identify prognostic risk factors for CM and explore novel treatment strategies.

At present, the specific pathogenesis of CM has not been elucidated. Related studies have shown that ultraviolet radiation exposure (Ultraviolet Radiation, UVR, including natural sunlight and artificial lighting systems) is the main risk factor for the occurrence of CM. Additional factors such as age, genetics, geographical location, and a history of skin cancer also contribute to CM incidence (7). The skin, as the largest organ of the human body, hosts a vast ecological niche for diverse microorganisms (8). Skin flora (SF) refers to the microbiome of bacteria, fungi, and viruses that colonize the skin, influencing human health to varying degrees (9). Disruption in the balance and homeostasis of SF have been kinded to several skin diseases, such as psoriasis (10) and acne (11). Consequently, alterations in SF composition hold potential for new diagnostic and therapeutic approaches for skin diseases (12).

Although SF has been showed to be closely related to certain diseases, its relationship with CM remains underexplored. UVR exposure, including ultraviolet A (UVA) and ultraviolet B (UVB), alters the composition of the skin microbiota. Among them, the bacterial group dominated by *Cyanobacteria* and *Fusobacteria* increased significantly, while *Lactic acid bacteria* and other bacterial groups decreased. This may be related to the physical effects that UVR brought about (13). A small sample study by Wang et al. found that *Propionibacterium acnes* can inhibit the survival of UVB-irradiated melanocytes by increasing cell apoptosis. At the same time, the skin commensal bacteria *Staphylococcus epidermidis* and its by-product Lipoteichoic Acid (LTA) induce the upregulation of TRAF1, CASP14, CASP5 and TP73 promoting melanocyte survival (14). In contrast, Nakatsuji et al. found that intravenous infusion of 6-N-hydroxyaminopurine (6-HAP) produced by *Staphylococcus epidermidis* in mice can inhibit the growth of B16F10 melanoma (15). The results of another small sample study suggested that there are differences in the skin microbiota of CM. Among them, acnes (*formerly Propionibacterium*), *Staphylococcus* and *Corynebacterium* are the most common bacterial genera, and the study showed that the diversity of microorganisms of melanoma samples decreased slightly (16). Michael et al. demonstrated the value of skin flora in the treatment of CM by constructing *Staphylococcus epidermidis* expressing tumor antigens and inducing T cell responses to limit melanoma growth (17). These findings suggest a possible association between CM and skin microbiota, yet no epidemiological or clinical studies have definitively established a causal link. Thus, exploring the causal relationship between skin microbiota and CM is crucial.

However, observational studies are limited in their ability to control for confounding factors and cannot fully avoid the effects of reverse causality, making it challenging to determine true associations between exposures and outcomes (18). While randomized controlled trials (RCTs) are the gold standard for establishing causal relationships, they often face obstacles such as high costs and implementation difficulties (19). Mendelian randomization (MR) is an epidemiological research method based on Mendel's law of independent distribution, which uses genetic variation (usually single nucleotide polymorphisms, SNPs) as a tool for natural random assignment. Simulated randomized controlled trials have been widely used in recent years to reveal causal relationships between environmental exposures and disease outcomes (20, 21). In this study, a Two-Sample Mendelian Randomization (TSMR) analysis was performed using a large-scale genome-wide association study (GWAS) dataset to investigate the role of skin flora in the development of CM. The goal was to explore potential causal relationships between skin flora and CM, providing new insights into CM prevention and treatment.

Materials and methods

Data acquire and process

The SNP data of skin flora (SF) and cutaneous melanoma (CM) were obtained from European population. The GWAS summary data of SF was derived from the data published by Moitinho-Silva L et al. in 2022 (9). In this study, the authors conducted a large-scale Genome-Wide Association Study (GWAS) on two population-based German cohorts. These 296 SF originate from different parts of the body and are divided by skin properties into dry, moist and sebaceous skin. The flow of this study was showed in Figure 1.

Screening of instrumental variables

Initially, by setting the threshold of P1 5e-6 was for single nucleotide polymorphisms (SNPs), instrumental variables (IVs) strongly correlated with SF were screened. SNPs demonstrating higher levels of significance were considered to be closely linked to the heritability of SF. Additionally, an F test was performed on each IV to eliminate those with weak correlations. The F test equation, given by F = (Beta/Se)^2, includes the impact size (Beta) of independent variables on SF and the standard error (Se) linked to Beta. The study did not include IVs with F test values lower than 10. Furthermore, an assessment of linkage disequilibrium was performed on the IVs. Linkage disequilibrium in genetics refers to the probability of alleles from multiple gene loci co-occurring on a single chromosome at a frequency higher than expected by chance.

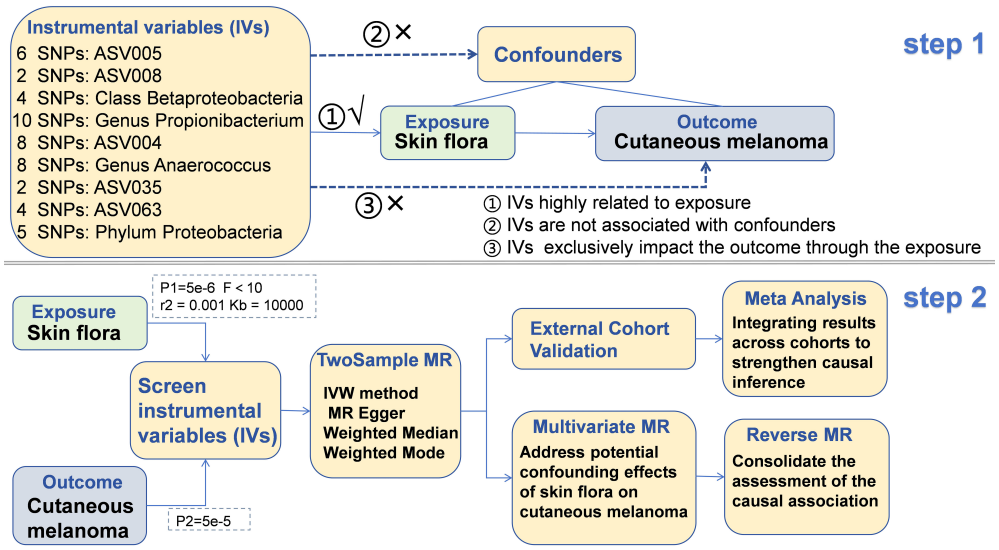

FIGURE 1
The flow of this study.

These occurrences are not conducive to MR analysis. To address this potential bias, a threshold of r2 = 0.001 and Kb = 10000 was set.

The IVs of CM are extracted simultaneously using the IVs of the SF after undergoing a screening process. A significance threshold of P2 = 5e-5 is established for the IVs of the outcome to remove highly correlated variables. Proxy tools are not introduced for IVs that are absent in the CM dataset to uphold the precision and dependability of the findings. Following this, the data of IVs from the SF and CM are merged, and palindromic SNPs are excluded.

Two sample MR analysis

The TwosampleMR package in the R language was employed to perform a comprehensive MR analysis on the combined dataset. The MR analysis incorporated four different methods, namely the Inverse Variance Weighted (IVW), MR Egger, Weighted Median, and Weighted Mode. The findings derived from the IVW method were predominantly utilized for assessment. It is worth noting that the IVW method is advantageous for detecting bias even when invalid instrumental variables (IVs) are present (22). On the other hand, the MR Egger method incorporates an intercept to evaluate and address horizontal pleiotropy in IVs (23). For Weighted median, this estimate is consistent even if up to 50% of the information comes from invalid tool variables. In the simulation analysis, it is proved that it has better class 1 error rate than IVW method (24). The weighted mode model employs the reciprocal of the result variance as weights, thereby assigning greater significance to SNPs with smaller variances in the estimation process (25). In order to ensure the reliability of the findings, only results exhibiting consistent Beta direction across all four analysis methods were included.

Multivariate Mendelian Randomization analysis

In order to improve comprehension of the role of different SF in CM and strengthen the credibility of TSMR results, Multivariate Mendelian Randomization (MVMR) analysis was utilized to investigate the potential association between SF and CM (26). Initially, shared SNPs present in multiple SF types were identified and subsequently extracted from the dataset. After removing linkage disequilibrium, the isolated SNP data underwent MVMR analysis. The IVW method, similar to TSMR, serves as a tool for assessing the primary outcome of MVMR. In addition, Supplementary Methods such as MR Egger, Lasso, and Weighted median are utilized to bolster the reliability of the IVW method. Heterogeneity assessment is performed using the IVW method, while the detection of pleiotropic effects is achieved through the analysis of the Egger intercept and MR Presso.

Verification based on testing cohort and meta-analysis

In order to reduce the bias impact of individual study results on the findings of MR analyses, a meta-analysis was performed using data from two separate cohorts of CM patients to ascertain the magnitude of the association between SF and CM. The meta-analysis predominantly utilized the IVW method for the analysis of the relationship between SF and CM. The presence of heterogeneity in the meta-analysis was evaluated through the I2 statistic, with a fixed effects model applied for I2 values of 50% or less and a random effects model utilized for I2 values exceeding 50%.

Statistic analysis

Horizontal pleiotropy significantly impacts the validity of MR analysis findings by introducing the possibility of IVs exerting effects on outcomes through multiple genetic pathways, thereby contravening fundamental MR analysis principles. To identify and address horizontal pleiotropy, we employed Presso (27) and MR Egger methodologies to assess IVs for potential pleiotropic effects. IVs that passed both tests simultaneously were regarded as not having horizontal pleiotropy, and those with pleiotropic effects were excluded from the study. Heterogeneity testing was also carried out on IVs using the IVW and MR Egger methods, with IVs that showed heterogeneity being excluded from the analysis. Furthermore, heterogeneity testing was conducted on IVs using the IVW and MR Egger methods. After identifying heterogeneity, those IVs were excluded from the analysis.

Each independent variable underwent a leave-one-out sensitivity analysis to determine the potential effect of individual SNPs on the outcome. The Steiger test was employed to detect and remove SNPs demonstrating reverse causality, which could introduce bias into the interpretation of the association between exposure and outcome variables. Furthermore, a Reverse Mendelian randomization (RMR) analysis was conducted to confirm the results by examining the relationship between CM and SF.

Results

Characteristics of SNPs

A total of 2 CM queues were obtained from the GWAS summary data, and their IDs were finngen_R10_C3_MELANOMA_SKIN_EXALLC and ukb-saige-172.11 respectively. Among them, finngen_R10_C3_MELANOMA_SKIN_EXALLC was used as the training cohort, and ukb-saige-172.11 was used as the testing cohort.

ukb-saige-172.11 contains more than 400 million detected variants and 397, 762 sample sizes, including 2, 691 cases and 395, 071 controls. The populations are from European, and the gender includes males and females.

Screening of instrumental variables

Based on the selection criteria mentioned earlier, SNPs were extracted from the exposure and outcome variables for this analysis. In the end, 9 SF were identified as having a causal relationship with CM. 6 SNPs came from ASV005, 2 SNPs came from ASV008, 4 SNPs came from Class Betaproteobacteria, 10 SNPs came from Genus Propionibacterium, 8 SNPs came from ASV004, 8 SNPs came from Genus Anaerococcus, 2 SNPs came from ASV035, 4 SNPs came from ASV063, 5 SNPs came from Phylum Proteobacteria were finally included in the MR analysis. The instrumental variables had F values greater than 10, which indicates they were not weak. The detailed information of IVs was showed in Supplementary Table S1.

TSMR analysis

The IVW results indicated that a total of 9 SF are causally associated with CM, which included 3 protective factors and 6 risk factors. Specially, we found that ASV005 (OR: 0.952, 95% CI: 0.91 to 0.997, P value: 0.036), ASV008 (OR:0.948, 95% CI: 0.902 to 0.997, P value: 0.038) and Genus Anaerococcus (OR: 0.965, 95% CI: 0.931 to 0.999, P value:0.044) were the protective factors on CM, while Class Betaproteobacteria (OR: 1.095, 95% CI: 1.029 to 1.166, P value: 0.004), Genus Propionibacterium (OR: 1.048, 95% CI: 1.003 to 1.094, P value: 0.035), ASV004 (OR: 1.043, 95% CI: 1.001 to 1.088, P value: 0.047), ASV035 (OR: 1.093, 95% CI: 1.006 to 1.187, P value: 0.037), ASV063 (OR: 1.042, 95% CI: 1.002 to 1.084, P value: 0.039) and Phylum Proteobacteria (OR: 1.056, 95% CI: 1.002 to 1.112, P value: 0.043) were the risk factors for CM. Exposure factors are represented by their corresponding ID, the blue line segment represents the 95% confidence interval (CI) of the exposure factor, and the dot on the line segment represents the corresponding OR value. (Figure 2A, Supplementary Table S2). This outcome was also evident in the scatter plot generated from MR analysis. The scatter plot illustrates the influence of each SNP on 9 SF and CM, allowing for a visual representation of the impact of exposure on the outcome. The different colored lines represent different approaches, and they sum up all of the SNPs' contributions to CM, depicting an upward OR downward trend according to the size of the OR value. If the line extends from the bottom left to the top right, SF is a risk factor for CM; if the line extends from the top left to the bottom right, SF is a protective factor for CM (Supplementary Figure S1). The Forest plot presented the MR effect size of the 9 SF and CM for each IVs. MR Egger and IVW methods were used to calculate the MR effect sizes of all IVs, which were then displayed in red line segment (Supplementary Figure S2). Heterogeneity testing indicated that the included IVs were homogeneous, and the distribution on the funnel plot was symmetrical based on the method of IVW and MR Egger (Supplementary Figure S3, Supplementary Table S3). A leave-one-out sensitivity analysis, which systematically eliminated each independent variable, demonstrated the robustness of the results (Supplementary Figure S4). Additionally, no evidence of a reverse causal relationship was observed between 9 SF and CM.

Verification based on testing cohort

In order to verify the reliability of the training cohort results, TSMR analysis was performed using the same parameters in the testing cohorts. Similar to Figure 1A, the exposure factor is displayed by its corresponding ID, the blue line segment

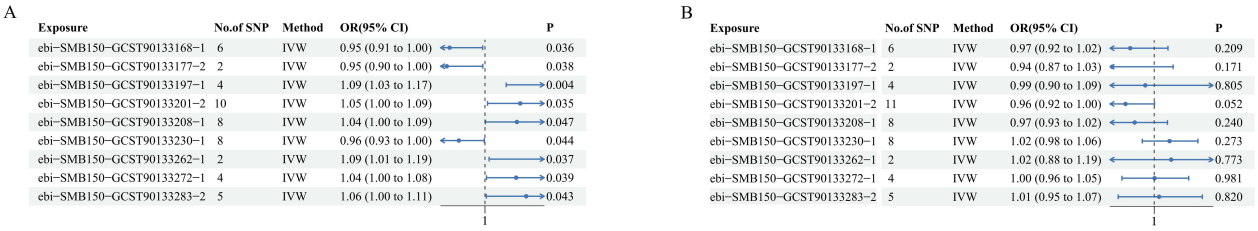

FIGURE 2
The IVW results of 9 skin flora against CM in training cohort and testing cohort. **(A)** finngen_R10_C3_MELANOMA_SKIN_EXALLC; **(B)** ukbsaige-172.11.

represents the 95% CI of the exposure factor, and the dot on the line segment represents the corresponding OR value. However, none of the SF in the testing cohort has been verified to be causally associated with CM (Figure 2B).

Meta-analysis based on inverse-variance weighted method of training cohort and testing cohort

Although none of the SF in testing cohorts has been verified to be causally associated with CM, after integrated the results of IVW method to conduct meta-analysis, a total of 5 SF showed potential causal relationship on CM with significant differences. Source 1 refers to finngen_R10_C3_MELANOMA_SKIN_EXALLC, Source 2 refers to ukb-saige-172.11. Similar to Figure 1, the exposure factor is displayed by its corresponding ID, the black line segment represents 95% CI of the exposure factor, and the diamond represents 95% CI obtained by integrating the training group and the testing group (Figure 3).

MVMR analysis

In order to further clarify the role of 9 SF in CM and consolidate the reliability of TSMR and meta-analysis results, MVMR was used to analyze SF with positive results. 47 shared IVs were extracted among the 9 SF. The results of TSMR from 3 SF remained stable in the MVMR analysis in training group. Among them, *ASV005* (IVW OR: 0.951, 95% CI: 0.911-0.993, P value:0.022) was a protective factor for CM, while *ASV004* (IVW OR: 1.045, 95% CI: 1.004-1.087, P value:0.03) and *ASV063* (IVW OR: 1.058, 95% CI: 1.017-1.101, P value:0.005) were the risk factors for CM (Figure 4). MR Egger and IVW analyses showed no heterogeneity in the instrumental variables. The Egger intercept was close to zero, and the P value was above 0.05, which indicates a lack of horizontal pleiotropy

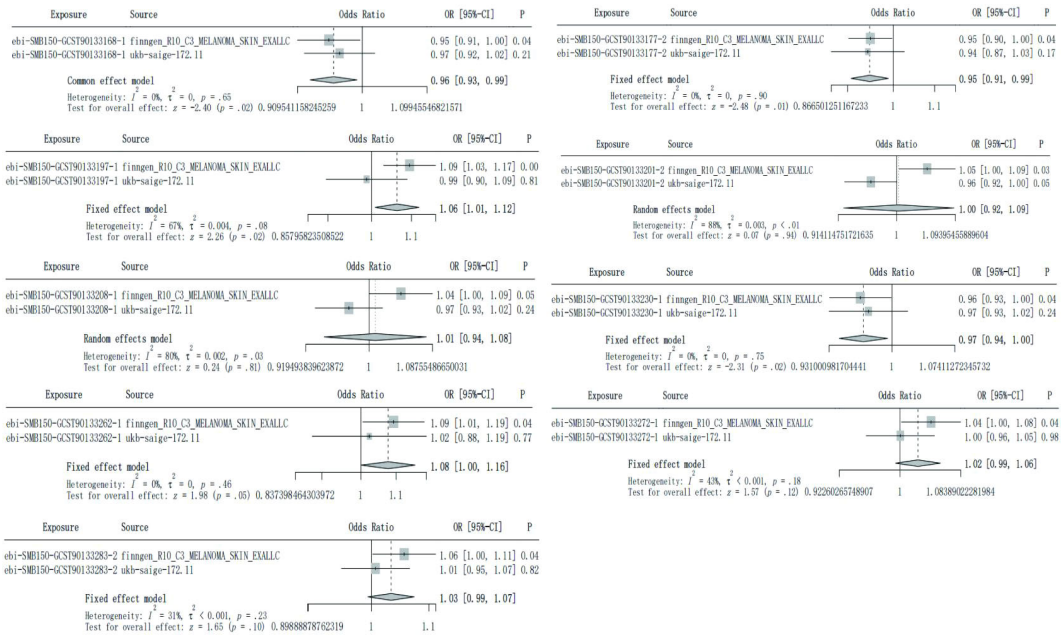

FIGURE 3
Meta-analysis integrated the IVW results of 9 skin flora against CM in training cohort and testing cohort.

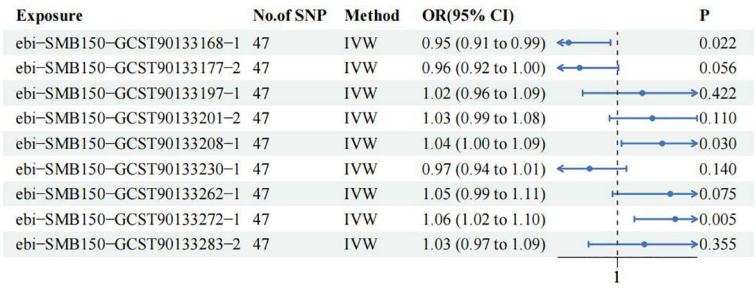

FIGURE 4
Multivariate Mendelian Randomization analysis among 9 skin flora against CM in training cohort.

(Supplementary Table S4). This results were confirmed in MR Presso test (Supplementary Table S5).

Discussion

The skin acts as a physical barrier between the human body and the external environment. It offers a niche for the commensal microbiota while simultaneously shielding against the incursion of alien pathogens (28). Disruptions in the skin flora (SF) could potentially influence the development of skin tumors through direct cellular damage (29), modulation of host defense mechanisms (29), and alterations in the tumor immune microenvironment (30). Additionally, toxins secreted by the SF have the capacity to induce oncogenic mutations via DNA damage (31). The research by Hoste et al. (32)demonstrated that SF induces the production of the inflammatory factor HMGB1 through the pathway of Toll-like receptor 5 (TLR-5) recognition of bacterial flagellin. This process may facilitate the transition from skin injury or chronic inflammation to cutaneous malignancy. SF impacts the formation and stability of the skin barrier (33), and its imbalance may exacerbate UV radiation-induced DNA damage and reactive oxygen species (ROS) production (34). This leads to an enhanced inflammatory response and increased cell proliferation, ultimately disrupting the skin barrier and promoting skin tumorigenesis (34). In conclusion, the role of the skin microbiota should not be overlooked in investigations into the pathogenesis of skin tumors. CM, as a skin malignancy with a high risk, exhibits associations between their onset and progression with dysregulation of the SF ecosystem (35, 36). However, the precise causal relationships remain to be elucidated.

A total of 9 SF showed causal relationship with CM in TSMR results in this study. The results showed that ASV005, ASV008 and *Genus Anaerococcus* were the protective factors on CM, while *Class Betaproteobacteria*, *Genus Propionibacterium*, ASV004, ASV035, ASV063 and *Phylum Proteobacteria* were the risk factors on CM. *Staphylococcus* has a bidirectional regulation of the occurrence risk of CM.

Proteobacteria and *β-Proteobacteria* are considered risk factors for CM (35). They all belong to the group of Gram-negative bacteria, characterized by an outer wall containing a specific component known as lipopolysaccharide (LPS). Currently, there is limited research on the role of *Proteobacteria* and *β-Proteobacteria* in skin diseases. However, some studies have suggested that their proliferation may promote inflammation or facilitate the invasion of external pathogens (37, 38). Furthermore, an increase in *Proteobacteria* abundance has been proposed as a potential diagnostic marker for flora imbalance and disease susceptibility (39). LPS derived from these bacteria can activate intestinal mucosal immunity, leading to local and systemic inflammation as well as metabolic dysfunction (40). Toll-like receptor 4 (TLR4) expression has been observed in 90% of human primary melanoma lesions and 93% of metastatic lesions (41). As a ligand for TLR4, LPS promotes the proliferation and migration of TLR4-positive melanoma cells through signal transduction mediated by transcriptional activator 3 (STAT3) activation (42). Therefore, it is plausible that *Proteobacteria* and *β-Proteobacteria* indirectly activate STAT3 via LPS signaling pathway exacerbating CM progression.

Corynebacterium is considered a significant risk factor for CM (43). According to statistical data, *Corynebacterium* is the most frequently detected or second most frequently detected bacterial genus in stage III/IV melanoma patients. Additionally, coryne-positive patients exhibit higher levels of IL-17 positive cells compared to coryne-negative patients (43). IL-17 can stimulate the production of IL-6, which subsequently activates STAT3 and upregulates genes associated with cell survival and angiogenesis (44). Therefore, it is possible that *Corynebacterium* may contribute to the progression of CM by promoting the IL-6-STAT3 pathway.

According to the analysis, we considered *Fingolderia magnus* to be a risk factor for CM. Formerly known as *peptostreptococcus magnus*, *Fingolderia magnus* is considered one of the most pathogenic opportunistic pathogens capable of causing severe infections in various anatomical sites including bone, joint, lung, skin and soft tissue, as well as infective endocarditis (45, 46). The key virulence factors associated with *E. grandis* pathogenesis encompass protein L, Surface-associated protein F. magna adhesion factor (FAF), Subtilisin-like extracellular serine protease (SufA), Sortase dependent pili, Peptostreptococcal albumin-binding protein (PAB). Its pathogenic mechanisms involve inhibiting biofilm formation, evading host immune defense mechanisms and inducing secretion of pro-inflammatory factors (47, 48). It is

plausible that *Fingoldelia magnus* may augment the risk of CM through similar immune evasion and proinflammatory pathways.

Propionibacterium granulosa, *Propionibacterium acnes*, and *Propionibacterium Feideri* all belong to the *genus Propionibacterium* and *Cutibacterium* (49). The findings of this study suggested that *propionibacteria* are a risk factor for the pathogenesis of CM, while *granular propionibacterial species* have a protective effect on CM, which may be attributed to their differential mechanisms of action. *Propionibacterium acnes* promotes the synthesis of pro-inflammatory cytokines such as IL-1, IL-6, TNF-α, IL-12 and IL-18, leading to an inflammatory response (50, 51). Previous studies have indicated the involvement of *proinflammatory* mechanisms by *propionibacteria* in prostate cancer pathogenesis and its high abundance in prostate cancer (52, 53). It is plausible that *propionibacteria* exacerbate CM pathogenesis through similar proinflammatory reactions. Genomic studies have demonstrated distinct separations between *propionicbaterrium granulosus* and other species within the *genus Propionicbaterrium* suggesting significant differences in their potential functions on skin health (54). Currently limited research exists regarding the mechanism of action for *Propionicbaterrium granulosus*. However, some studies have reported the discovery of an endogenous extracellular nuclease BmdE secreted by this bacterium which can degrade biofilms produced by *Propionicbaterrium acnes* both *in vivo* and *in vitro* (55). These results propose a potential novel competitive mechanism between *P. acnes* and *P. granulosus* possibly related to diverse effects exerted by *P. granulosus* compared with other members within the genus.

The findings of this study demonstrated that *staphylococcus* exerts a bidirectional regulatory effect on the risk of CM (56). *Staphylococcus epidermidis* is commonly considered as a commensal microorganism in the skin microbiota, contributing to the maintenance of skin barrier homeostasis, promotion of wound healing, enhancement of skin immunity, and inhibition of pathogen infection through the production of protective ceramides (57). 6-HAP, a molecule produced by *Staphylococcus epidermidis* that inhibits DNA polymerase activity, exhibits selective growth inhibition against tumor cell lines. Intravenous administration of 6-HAP in mice has been shown to suppress B16F10 melanoma growth, suggesting a potential protective role for Staphylococcus in CM (15). However, both *Staphylococcus epidermidis* and its by-product LTA can promote melanocyte survival by inducing upregulation of TRAF1, CASP14, CASP5 and TP73 genes. This suggested that *staphylococcus* may exacerbate disease progression in CM (14). Introduction of *Staphylococcus epidermidis* into germ-free mice has been demonstrated to restore normal IL-17A production - a chemokine potentially involved in tumor growth and anti-tumor immunity (58). In conclusion, the impact of *staphylococcus* on CM may be mediated through different metabolites; however, further investigation is required to elucidate the specific mechanisms involved.

The breast microbiome of healthy tissues and cancer-related tissues has been compared in studies, revealing a higher abundance of *anaerobes* in the former (59). A high level of bile acid metabolism generally indicates a better prognosis for breast cancer, with the high bile acid metabolism group exhibiting a greater abundance of anaerobes compared to the low bile acid metabolism group (60). These findings suggested potential disease protection mechanisms associated with *anaerobic* coccus. However, the current understanding of its protective mechanism in diseases remains unexplored. Therefore, the conclusions drawn from this study may offer new directions for future research on CM.

As we listed earlier, many studies have shown that there is a certain relationship between SF and CM. This study further provides a basis for consolidating this relationship by combining TSMR, MVMR and RMR. However, there are some limitations in this study, such as the heterogeneity of population background in different research cohorts. Some stratification factors, such as age and gender, were not disclosed in detail in the original study. Therefore, further randomized controlled trials are necessary to prove this conclusion.

Conclusion

In conclusion, our study revealed that 9 SF have causal relationship with CM. Further large randomize control trail to verify this results is needed.

Data availability statement

The original contributions presented in the study are included in the article/Supplementary Material. Further inquiries can be directed to the corresponding author.

Author contributions

ZZ: Conceptualization, Methodology, Writing – original draft. WW: Writing – original draft. JL: Writing – original draft. HL: Writing – review & editing.

Funding

The author(s) declare financial support was received for the research, authorship, and/or publication of this article. This work was funded by Central Government Transfer Payment to Local Projects: Traditional Chinese Medicine Evidence-Based Capacity Enhancement Project; State Administration of Traditional Chinese Medicine's Academic School of Traditional Chinese Medicine Inheritance Project–Lingnan Dermatology School Inheritance Workshop (Project No. LP0119045); Clinical Efficacy Observation of Professor Xuan Guowei's Prescription "Xiao Cuo Decoction" in Granule Form and Traditional Decoction for the Treatment of Mild to Moderate Acne (Project No. 2021A1515220147).

Conflict of interest

The authors declare that the research was conducted in the absence of any commercial or financial relationships that could be construed as a potential conflict of interest.

Publisher's note

All claims expressed in this article are solely those of the authors and do not necessarily represent those of their affiliated organizations, or those of the publisher, the editors and the reviewers. Any product that may be evaluated in this article, or claim that may be made by its manufacturer, is not guaranteed or endorsed by the publisher.

Supplementary material

The Supplementary Material for this article can be found online at: https://www.frontiersin.org/articles/10.3389/fonc.2024.1451175/full#supplementary-material

SUPPLEMENTARY FIGURE 1
The scatter plot of the effect distribution of all SNPs in training cohort.

SUPPLEMENTARY FIGURE 2
The forest plot of MR effect size of 9 skin flora against CM in training cohort.

SUPPLEMENTARY FIGURE 3
The funnel plot of distribution of all SNPs in training cohort.

SUPPLEMENTARY FIGURE 4
The Leave-one-out sensitivity analysis showed that no single SNP was found to have a significant impact on the outcome in training cohort.

SUPPLEMENTARY TABLE 1
The detail of the characteristics of SNPs in training cohort.

SUPPLEMENTARY TABLE 2
All MR results of 9 skin flora against CM in training cohort.

SUPPLEMENTARY TABLE 3
Heterogeneity test of 9 skin flora against CM in training cohort.

SUPPLEMENTARY TABLE 4
Pleiotropy test of 9 skin flora against CM on MR Egger in training cohort.

SUPPLEMENTARY TABLE 5
Pleiotropy test of 9 skin flora against CM on MR presso in training cohort.

References

1. Long GV, Swetter SM, Menzies AM, Gershenwald JE, Scolyer RA. Cutaneous melanoma. *Lancet Lond Engl*. (2023) 402:485–502. doi: 10.1016/S0140-6736(23)00821-8

2. Siegel RL, Miller KD, Wagle NS, Jemal A. Cancer statistics, 2023. *CA Cancer J Clin*. (2023) 73:17–48. doi: 10.3322/caac.21763

3. Arnold M, Singh D, Laversanne M, Vignat J, Vaccarella S, Meheus F, et al. Global burden of cutaneous melanoma in 2020 and projections to 2040. *JAMA Dermatol*. (2022) 158:495–503. doi: 10.1001/jamadermatol.2022.0160

4. Tímár J, Ladányi A. Molecular pathology of skin melanoma: epidemiology, differential diagnostics, prognosis and therapy prediction. *Int J Mol Sci*. (2022) 23:5384. doi: 10.3390/ijms23105384

5. Balch CM, Gershenwald JE, Soong S-J, Thompson JF, Ding S, Byrd DR, et al. Multivariate analysis of prognostic factors among 2,313 patients with stage III melanoma: comparison of nodal micrometastases versus macrometastases. *J Clin Oncol Off J Am Soc Clin Oncol*. (2010) 28:2452–9. doi: 10.1200/JCO.2009.27.1627

6. Garbe C, Amaral T, Peris K, Hauschild A, Arenberger P, Basset-Seguin N, et al. European consensus-based interdisciplinary guideline for melanoma. Part 1: Diagnostics: Update 2022. *Eur J Cancer Oxf Engl 1990*. (2022) 170:236–55. doi: 10.1016/j.ejca.2022.03.008

7. Strashilov S, Yordanov A. Aetiology and pathogenesis of cutaneous melanoma: current concepts and advances. *Int J Mol Sci*. (2021) 22:6395. doi: 10.3390/ijms22126395

8. Yang Y, Qu L, Mijakovic I, Wei Y. Advances in the human skin microbiota and its roles in cutaneous diseases. *Microb Cell Factories*. (2022) 21:176. doi: 10.1186/s12934-022-01901-6

9. Moitinho-Silva L, Degenhardt F, Rodriguez E, Emmert H, Juzenas S, Möbus L, et al. Host genetic factors related to innate immunity, environmental sensing and cellular functions are associated with human skin microbiota. *Nat Commun*. (2022) 13:6204. doi: 10.1038/s41467-022-33906-5

10. Olejniczak-Staruch I, Ciążyńska M, Sobolewska-Sztychny D, Narbutt J, Skibińska M, Lesiak A. Alterations of the skin and gut microbiome in psoriasis and psoriatic arthritis. *Int J Mol Sci*. (2021) 22:3998. doi: 10.3390/ijms22083998

11. Li C-X, You Z-X, Lin Y-X, Liu H-Y, Su J. Skin microbiome differences relate to the grade of acne vulgaris. *J Dermatol*. (2019) 46:787–90. doi: 10.1111/1346-8138.14952

12. Smythe P, Wilkinson HN. The skin microbiome: current landscape and future opportunities. *Int J Mol Sci*. (2023) 24:3950. doi: 10.3390/ijms24043950

13. Burns EM, Ahmed H, Isedeh PN, Kohli I, van der Pol W, Shaheen A, et al. Ultraviolet radiation, both UVA and UVB, influences the composition of the skin microbiome. *Exp Dermatol*. (2019) 28:136–41. doi: 10.1111/exd.13854

14. Wang Z, Choi J-E, Wu C-C, Di Nardo A. Skin commensal bacteria Staphylococcus epidermidis promote survival of melanocytes bearing UVB-induced DNA damage, while bacteria Propionibacterium acnes inhibit survival of melanocytes by increasing apoptosis. *Photodermatol Photoimmunol Photomed*. (2018) 34:405–14. doi: 10.1111/phpp.12411

15. Nakatsuji T, Chen TH, Butcher AM, Trzoss LL, Nam S-J, Shirakawa KT, et al. A commensal strain of Staphylococcus epidermidis protects against skin neoplasia. *Sci Adv*. (2018) 4:eaao4502. doi: 10.1126/sciadv.aao4502

16. Salava A, Aho V, Pereira P, Koskinen K, Paulin L, Auvinen P, et al. Skin microbiome in melanomas and melanocytic nevi. *Eur J Dermatol EJD*. (2016) 26:49–55. doi: 10.1684/ejd.2015.2696

17. Chen YE, Bousbaine D, Veinbachs A, Atabakhsh K, Dimas A, Yu VK, et al. Engineered skin bacteria induce antitumor T cell responses against melanoma. *Science*. (2023) 380:203–10. doi: 10.1126/science.abp9563

18. Sessler DI, Imrey PB. Clinical research methodology 2: observational clinical research. *Anesth Analg*. (2015) 121:1043–51. doi: 10.1213/ANE.0000000000000861

19. Pihlstrom BL, Curran AE, Voelker HT, Kingman A. Randomized controlled trials: what are they and who needs them? *Periodontol 2000*. (2012) 59:14–31. doi: 10.1111/j.1600-0757.2011.00439.x

20. Sekula P, Del Greco MF, Pattaro C, Köttgen A. Mendelian randomization as an approach to assess causality using observational data. *J Am Soc Nephrol JASN*. (2016) 27:3253–65. doi: 10.1681/ASN.2016010098

21. Davies NM, Holmes MV, Davey Smith G. Reading Mendelian randomisation studies: a guide, glossary, and checklist for clinicians. *BMJ*. (2018) 362:k601. doi: 10.1136/bmj.k601

22. Burgess S, Scott RA, Timpson NJ, Davey Smith G, Thompson SG, EPIC-InterAct Consortium. Using published data in Mendelian randomization: a blueprint for efficient identification of causal risk factors. *Eur J Epidemiol*. (2015) 30:543–52. doi: 10.1007/s10654-015-0011-z

23. Bowden J, Davey Smith G, Burgess S. Mendelian randomization with invalid instruments: effect estimation and bias detection through Egger regression. *Int J Epidemiol*. (2015) 44:512–25. doi: 10.1093/ije/dyv080

24. Bowden J, Davey Smith G, Haycock PC, Burgess S. Consistent estimation in mendelian randomization with some invalid instruments using a weighted median estimator. *Genet Epidemiol*. (2016) 40:304–14. doi: 10.1002/gepi.21965

25. Hartwig FP, Davey Smith G, Bowden J. Robust inference in summary data Mendelian randomization via the zero modal pleiotropy assumption. *Int J Epidemiol*. (2017) 46:1985–98. doi: 10.1093/ije/dyx102

26. Burgess S, Thompson SG. Multivariable Mendelian randomization: the use of pleiotropic genetic variants to estimate causal effects. *Am J Epidemiol*. (2015) 181:251–60. doi: 10.1093/aje/kwu283

27. Verbanck M, Chen C-Y, Neale B, Do R. Detection of widespread horizontal pleiotropy in causal relationships inferred from Mendelian randomization between complex traits and diseases. *Nat Genet*. (2018) 50:693–8. doi: 10.1038/s41588-018-0099-7

28. Byrd AL, Belkaid Y, Segre JA. The human skin microbiome. *Nat Rev Microbiol*. (2018) 16:143–55. doi: 10.1038/nrmicro.2017.157

29. Woo YR, Cho SH, Lee JD, Kim HS. The human microbiota and skin cancer. *Int J Mol Sci*. (2022) 23:1813. doi: 10.3390/ijms23031813

30. Wong-Rolle A, Wei HK, Zhao C, Jin C. Unexpected guests in the tumor microenvironment: microbiome in cancer. *Protein Cell*. (2021) 12:426–35. doi: 10.1007/s13238-020-00813-8

31. Sherwani MA, Tufail S, Muzaffar AF, Yusuf N. The skin microbiome and immune system: potential target for chemoprevention? *Photodermatol Photoimmunol Photomed*. (2018) 34:25–34. doi: 10.1111/phpp.12334

32. Hoste E, Arwert EN, Lal R, South AP, Salas-Alanis JC, Murrell DF, et al. Innate sensing of microbial products promotes wound-induced skin cancer. *Nat Commun*. (2015) 6:5932. doi: 10.1038/ncomms6932

33. Harris-Tryon TA, Grice EA. Microbiota and maintenance of skin barrier function. *Science*. (2022) 376:940–5. doi: 10.1126/science.abo0693

34. Bosman ES, Albert AY, Lui H, Dutz JP, Vallance BA. Skin exposure to narrow band ultraviolet (UVB) light modulates the human intestinal microbiome. *Front Microbiol*. (2019) 10:2410. doi: 10.3389/fmicb.2019.02410

35. Mekadim C, Skalnikova HK, Cizkova J, Cizkova V, Palanova A, Horak V, et al. Dysbiosis of skin microbiome and gut microbiome in melanoma progression. *BMC Microbiol*. (2022) 22:63. doi: 10.1186/s12866-022-02458-5

36. Mrázek J, Mekadim C, Kučerová P, Švejstil R, Salmonová H, Vlasáková J, et al. Melanoma-related changes in skin microbiome. *Folia Microbiol (Praha)*. (2019) 64:435–42. doi: 10.1007/s12223-018-00670-3

37. Maharshak N, Packey CD, Ellermann M, Manick S, Siddle JP, Huh EY, et al. Altered enteric microbiota ecology in interleukin 10-deficient mice during development and progression of intestinal inflammation. *Gut Microbes*. (2013) 4:316–24. doi: 10.4161/gmic.25486

38. Walujkar SA, Dhotre DP, Marathe NP, Lawate PS, Bharadwaj RS, Shouche YS. Characterization of bacterial community shift in human Ulcerative Colitis patients revealed by Illumina based 16S rRNA gene amplicon sequencing. *Gut Pathog*. (2014) 6:22. doi: 10.1186/1757-4749-6-22

39. Shin N-R, Whon TW, Bae J-W. Proteobacteria: microbial signature of dysbiosis in gut microbiota. *Trends Biotechnol*. (2015) 33:496–503. doi: 10.1016/j.tibtech.2015.06.011

40. Sun P, Wang M, Liu Y-X, Li L, Chai X, Zheng W, et al. High-fat diet-disturbed gut microbiota-colonocyte interactions contribute to dysregulating peripheral tryptophan-kynurenine metabolism. *Microbiome*. (2023) 11:154. doi: 10.1186/s40168-023-01606-x

41. Takazawa Y, Kiniwa Y, Ogawa E, Uchiyama A, Ashida A, Uhara H, et al. Toll-like receptor 4 signaling promotes the migration of human melanoma cells. *Tohoku J Exp Med*. (2014) 234:57–65. doi: 10.1620/tjem.234.57

42. Fu X-Q, Liu B, Wang Y-P, Li J-K, Zhu P-L, Li T, et al. Activation of STAT3 is a key event in TLR4 signaling-mediated melanoma progression. *Cell Death Dis*. (2020) 11:246. doi: 10.1038/s41419-020-2440-1

43. Mizuhashi S, Kajihara I, Sawamura S, Kanemaru H, Makino K, Aoi J, et al. Skin microbiome in acral melanoma: corynebacterium is associated with advanced melanoma. *J Dermatol*. (2021) 48:e15–6. doi: 10.1111/1346-8138.15633

44. Wang L, Yi T, Kortylewski M, Pardoll DM, Zeng D, Yu H. IL-17 can promote tumor growth through an IL-6-Stat3 signaling pathway. *J Exp Med*. (2009) 206:1457–64. doi: 10.1084/jem.20090207

45. Tang S, Prem A, Tjokrosurjo J, Sary M, Van Bel MA, Rodrigues-Hoffmann A, et al. The canine skin and ear microbiome: a comprehensive survey of pathogens implicated in canine skin and ear infections using a novel next-generation-sequencing-based assay. *Vet Microbiol*. (2020) 247:108764. doi: 10.1016/j.vetmic.2020.108764

46. Liu Y, Su Y, Cui Z, Guo Y, Zhang W, Wu J. Clinical and microbiological features of anaerobic implant-related infection in 80 patients after orthopedic surgery. *Anaerobe*. (2021) 71:102413. doi: 10.1016/j.anaerobe.2021.102413

47. Boyanova L, Markovska R, Mitov I. Virulence arsenal of the most pathogenic species among the Gram-positive anaerobic cocci, Finegoldia magna. *Anaerobe*. (2016) 42:145–51. doi: 10.1016/j.anaerobe.2016.10.007

48. Murphy EC, Frick I-M. Gram-positive anaerobic cocci–commensals and opportunistic pathogens. *FEMS Microbiol Rev*. (2013) 37:520–53. doi: 10.1111/1574-6976.12005

49. Corvec S. Clinical and biological features of cutibacterium (Formerly propionibacterium) avidum, an underrecognized microorganism. *Clin Microbiol Rev*. (2018) 31:e00064–17. doi: 10.1128/CMR.00064-17

50. Tsuji H, Mukaida N, Harada A, Kaneko S, Matsushita E, Nakanuma Y, et al. Alleviation of lipopolysaccharide-induced acute liver injury in Propionibacterium acnes-primed IFN-gamma-deficient mice by a concomitant reduction of TNF-alpha, IL-12, and IL-18 production. *J Immunol Baltim Md 1950*. (1999) 162:1049–55.

51. Smith SR, Calzetta A, Bankowski J, Kenworthy-Bott L, Terminelli C. Lipopolysaccharide-induced cytokine production and mortality in mice treated with Corynebacterium parvum. *J Leukoc Biol*. (1993) 54:23–9. doi: 10.1002/jlb.54.1.23

52. Cavarretta I, Ferrarese R, Cazzaniga W, Saita D, Lucianò R, Ceresola ER, et al. The microbiome of the prostate tumor microenvironment. *Eur Urol*. (2017) 72:625–31. doi: 10.1016/j.eururo.2017.03.029

53. Shinohara DB, Vaghasia AM, Yu S-H, Mak TN, Brüggemann H, Nelson WG, et al. A mouse model of chronic prostatic inflammation using a human prostate cancer-derived isolate of Propionibacterium acnes. *Prostate*. (2013) 73:1007–15. doi: 10.1002/pros.22648

54. Li Z, Ju Y, Xia J, Zhang Z, Zhen H, Tong X, et al. Integrated human skin bacteria genome catalog reveals extensive unexplored habitat-specific microbiome diversity and function. *Adv Sci Weinh Baden-Wurtt Ger*. (2023) 10:e2300050. doi: 10.1002/advs.202300050

55. Bronnec V, Eilers H, Jahns AC, Omer H, Alexeyev OA. Propionibacterium (Cutibacterium) granulosum Extracellular DNase BmdE Targeting Propionibacterium (Cutibacterium) acnes Biofilm Matrix, a Novel Inter-Species Competition Mechanism. *Front Cell Infect Microbiol*. (2021) 11:809792. doi: 10.3389/fcimb.2021.809792

56. Xu Z, Wang Z, Yuan C, Liu X, Yang F, Wang T, et al. Dandruff is associated with the conjoined interactions between host and microorganisms. *Sci Rep*. (2016) 6:24877. doi: 10.1038/srep24877

57. Zheng Y, Hunt RL, Villaruz AE, Fisher EL, Liu R, Liu Q, et al. Commensal Staphylococcus epidermidis contributes to skin barrier homeostasis by generating protective ceramides. *Cell Host Microbe*. (2022) 30:301–313.e9. doi: 10.1016/j.chom.2022.01.004

58. Kumar P, Brazel D, DeRogatis J, Valerin JBG, Whiteson K, Chow WA, et al. The cure from within? a review of the microbiome and diet in melanoma. *Cancer Metastasis Rev*. (2022) 41:261–80. doi: 10.1007/s10555-022-10029-3

59. Tzeng A, Sangwan N, Jia M, Liu C-C, Keslar KS, Downs-Kelly E, et al. Human breast microbiome correlates with prognostic features and immunological signatures in breast cancer. *Genome Med*. (2021) 13:60. doi: 10.1186/s13073-021-00874-2

60. Wu R, Yu I, Tokumaru Y, Asaoka M, Oshi M, Yan L, et al. Elevated bile acid metabolism and microbiome are associated with suppressed cell proliferation and better survival in breast cancer. *Am J Cancer Res*. (2022) 12:5271–85.

frontiers | Frontiers in Oncology

TYPE Case Report
PUBLISHED 11 December 2024
DOI 10.3389/fonc.2024.1406098

Check for updates

OPEN ACCESS

EDITED BY
Giuseppe Giaccone,
Cornell University, United States

REVIEWED BY
Alessio Vagliasindi,
Oncological Center of Basilicata (IRCCS), Italy
Sanja Stifter-Vretenar,
Skejby Sygehus, Denmark

*CORRESPONDENCE
Cheng Zhang
cz1791@163.com

RECEIVED 24 March 2024
ACCEPTED 18 November 2024
PUBLISHED 11 December 2024

CITATION
Tong D, Li J, Gao G and Zhang C (2024) Postoperative unexplained sigmoid stenosis in a patient with rectal cancer complicated with connective tissue disease: a case report and literature review. *Front. Oncol.* 14:1406098. doi: 10.3389/fonc.2024.1406098

COPYRIGHT
© 2024 Tong, Li, Gao and Zhang. This is an open-access article distributed under the terms of the Creative Commons Attribution License (CC BY). The use, distribution or reproduction in other forums is permitted, provided the original author(s) and the copyright owner(s) are credited and that the original publication in this journal is cited, in accordance with accepted academic practice. No use, distribution or reproduction is permitted which does not comply with these terms.

Postoperative unexplained sigmoid stenosis in a patient with rectal cancer complicated with connective tissue disease: a case report and literature review

Deming Tong, Jian Li, Guangrong Gao and Cheng Zhang*

Department of General Surgery, General Hospital of Northern Theater Command, Shenyang, China

It is well established that host immunity plays a critical role in defending against colorectal cancer (CRC) progression. Connective tissue disease (CTD) encompasses a group of heterogeneous, immune-mediated disorders that present with diverse and often non-specific initial symptoms. Raynaud's phenomenon is a common feature, complicating early diagnosis. As CTD progresses, it can damage the skin, muscles, and blood vessels and may extend to the lungs, heart, kidneys, and other abdominal organs. Several studies have reported that CTD can lead to intestinal vascular occlusion and related inflammation, but the occurrence of related complications after intestinal surgery has been reported rarely. In this study, an elderly female patient with rectal cancer complicated with CTD was found to have unexplained proximal anastomotic stenosis during an attempt at fistula restoration 3 months after laparoscopy-assisted transanal total mesorectal excision (TaTME) and preventive terminal ileostomy, resulting in fistula failure. This case study aims to serve as a reference for clinicians in their future practice.

KEYWORDS

rectal cancer (RC), TaTME, CTD (connective tissue disease), anastomotic stenosis, temporary ileostomy

Introduction

Host immunity plays a crucial role in preventing the development and progression of cancer. Connective tissue disease (CTD) is a systemic immune disorder that includes manifestations such as rheumatoid arthritis (RA), systemic sclerosis (SSc), systemic lupus erythematosus (SLE), primary Sjogren's syndrome (pSS), idiopathic inflammatory myopathy (IIM), and mixed connective tissue disease (MCTD) (1, 2). CTD affects multiple organs (skin, heart, lungs, kidneys, joints, muscles, blood vessels, etc.) and leads to various functional impairments (3–5). In addition to CTD itself, secondary vascular inflammatory changes are also a factor of adverse prognosis of the disease, which can occur

in different degrees of ischemia, ulceration, and necrosis on the basis of the severity of the involved vessels (6). The intestine is also one of the target organs of CTD patients, especially in patients with SSc. Characteristics of colon involvement in SSc patients include dyskinesia, telangiectasia, and diverticulosis (7). Furthermore, CTD-related vasculitis affects intestinal blood supply, altering intestinal activity, especially postoperatively, potentially exacerbating ischemia (Figure 1). Presently, there are few reports on CTD patient recovery and complications after intestinal surgery. This study reported a patient with low rectal cancer with CTD who developed colonic stenosis approximately 2 cm proximal to the anastomosis 3 months after laparoscopy-assisted transanal total mesorectal excision (TaTME) and prophylactic terminal ileostomy. Due to the limited reports on the possible complications of CTD combined with intestinal surgery and the lack of established treatment guidelines, this case report aims to provide valuable insights for future clinical research and practice.

Case presentation

A 65-year-old female patient was admitted to our hospital on Mar. 15, 2023, due to rectal cancer discovered during a routine physical examination by fiberoptic colonoscopy with no digestive system symptoms. A polyp approximately 0.6 * 0.8 cm in size was found 20 cm from the anus in the sigmoid colon, which was resected and sent for pathology (Figure 2A). Another polypoid lesion, approximately 1.5 * 2 cm in size, was observed 5 cm from the anus. This lesion had a broad base, a sunken surface, a slightly hard texture, and yellow granular changes around it. A specimen was also taken for pathology (Figure 2B). The pathological report indicated that the polyp in the sigmoid colon (20 cm) was a colonic tubular adenoma (Figure 2C), while the lesion in the rectum (5 cm) was a moderately differentiated adenocarcinoma (Figure 2D).

The patient has a medical history of CTD for 2 years. Due to the progressively worsening nature of her condition, she has been treated multiple times in the rheumatology and immunology department of our hospital over the past 2 years. Her long-term oral medications include methylprednisolone 4 mg daily (QD), cyclophosphamide tablets 0.2 mg weekly (QW), and *Tripterygium wilfordii* glycoside tablets 20 mg three times daily (TID). She is currently in a stable condition. Additionally, she has a 3-year history of diabetes mellitus, for which she takes metformin sustained-release tablets orally to manage hypoglycemia, aiming for fasting blood glucose levels of approximately 5.0 mmol/L. The patient also has a 2-year history of hypertension, managed with oral amlodipine besylate tablets to maintain blood pressure within the normal range. The primary diagnoses were as follows: rectal cancer, CTD, Grade II hypertension, and diabetes mellitus. Upon admission, the patient's physical examination revealed the following findings: body temperature at 36.8°C, pulse rate at 84 bpm, respiratory rate at 18 bpm, and blood pressure at 137/98 mmHg. The physical examination indicated swelling and pain in the knee and finger joints, with restricted movement and morning stiffness lasting over 1 hour. During the digital rectal examination, a mass was palpated on the posterior wall of the rectum, approximately 5 cm from the anal margin. The mass was soft and painless and exhibited good mobility. Laboratory tests showed the following results: red blood cell (RBC) count at 3.51 * 10^{12}/L, hemoglobin at 86 g/L, lymphocyte percentage (LY%) at 17.2%, total protein at 61.5 g/L, albumin at 31.1 g/L, C-reactive protein (CRP) at 61.2 mg/L, and glycated hemoglobin (HbA1c) at 7.35%. Antinuclear antibody (ANA) titer was 1:100. Imaging examination included lung CT, revealing interstitial changes in both lungs and mediastinal lymph node enlargement, and abdominal enhanced CT, which showed no thickening of the lower rectal wall or enlargement of lymph nodes in the mesorectum or at the root of mesenteric vessels. Rectoscopy identified a broadly based mass, approximately 1.8 * 1.5 cm in size, with an uplifted surface and good mobility. The mass exhibited no firmness under white light amplification and lacked bleeding points on its surface, and its shape changed after air injection. Endoscopic examination using the NBI International Colorectal Endoscopic (NICE) Classification categorized the mass as Type 2. Considering the patient's history of connective tissue disease, a rheumatology consultation was obtained for preoperative evaluation. It was recommended to switch the patient's medication from *T. wilfordii* to hydrocortisone 50 mg Q8h IV during the fasting period.

The preoperative evaluation indicated that the malignant rectal lesions were likely confined to the mucosa or had invaded the superficial submucosa without evidence of distant or regional lymph node metastasis. Preoperative TNM staging was determined to be Tis-1N0M0. On Mar. 23, 2023, diagnostic transanal rectal mass resection was performed under combined spinal-epidural anesthesia (CSEA). The surgery lasted 50 minutes, with an estimated blood loss of approximately 5 mL. The postoperative pathological report revealed moderately differentiated adenocarcinoma of the rectum invading the submucosal layer. No cancer was detected at the base, though the surgical margin could not be evaluated. No clear vascular tumor thrombus or nerve invasion was observed (Figures 2E, F). Given the tumor's submucosal invasion and the indeterminate status of the surgical margin, coupled with the risk of regional lymph node metastasis, further surgical intervention was warranted. To accurately determine the distal resection margin, avoid incomplete distal rectal anastomosis, and enhance surgical safety, laparoscopy-assisted TaTME and a preventive terminal ileostomy were performed under general anesthesia on Mar. 30, 2023. The operation lasted 150 minutes, with a blood loss volume of approximately 50 mL. Oral methylprednisolone at a dose of 4 mg/day was resumed on the second postoperative day. The patient was discharged in a stable condition on Apr. 9, 2023. Postoperative pathology showed no residual cancer tissue in the tumor bed and no lymph node metastasis (0/12) (Figures 2G, H).

Abbreviations: CTD, connective tissue disease; RA, rheumatoid arthritis; SSc, systemic sclerosis; SLE, systemic lupus erythematosus; pSS, primary Sjogren's syndrome; IIM, idiopathic inflammatory myopathy; MCTD, mixed connective tissue disease; NICE, NBI International Colorectal Endoscopic Classification; TaTME, transanal total mesorectal excision; QD, quaque die; TID, ter in die; QW, quaque week; LARS, low anterior resection syndrome.

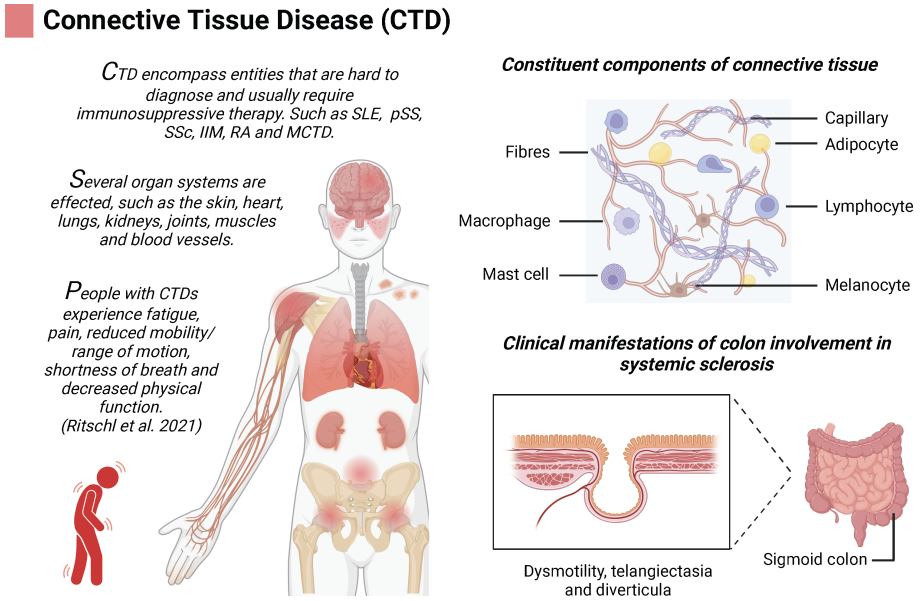

FIGURE 1
Connective tissue disease (CTD) is complex disease that involves multiple organs; created using BioRender.com.

Under postoperative guidance, the patient consistently performed Kegel exercises to enhance anal sphincter function. At the stoma, defecation was satisfactory, with only a small amount of discharge and gas passing through the anus. Digital rectal examinations conducted at 1 and 2 months post-surgery revealed no signs of anastomotic stenosis.

Three months later, the patient was re-hospitalized for the closure of a temporary ileostomy on Jul. 4, 2023. A digital rectal examination revealed the anastomotic site 3 cm from the anus and a narrowed intestine segment approximately 2 cm above it, indicating potential obstruction. Subsequent colonoscopy showed that the rectal anastomosis was unobstructed, but numerous white, scar-like changes and local annular constrictions with lumen occlusion were observed 2 cm into the lateral cavity. Colonoscopic inspection through the abdominal wall stoma revealed multiple mucosal strips covered with a white plaque near the sigmoid colon, with significant luminal obstruction impeding further endoscopic passage. A biopsy from the ulcer edge (Figures 3A–C) revealed necrotic mucosal

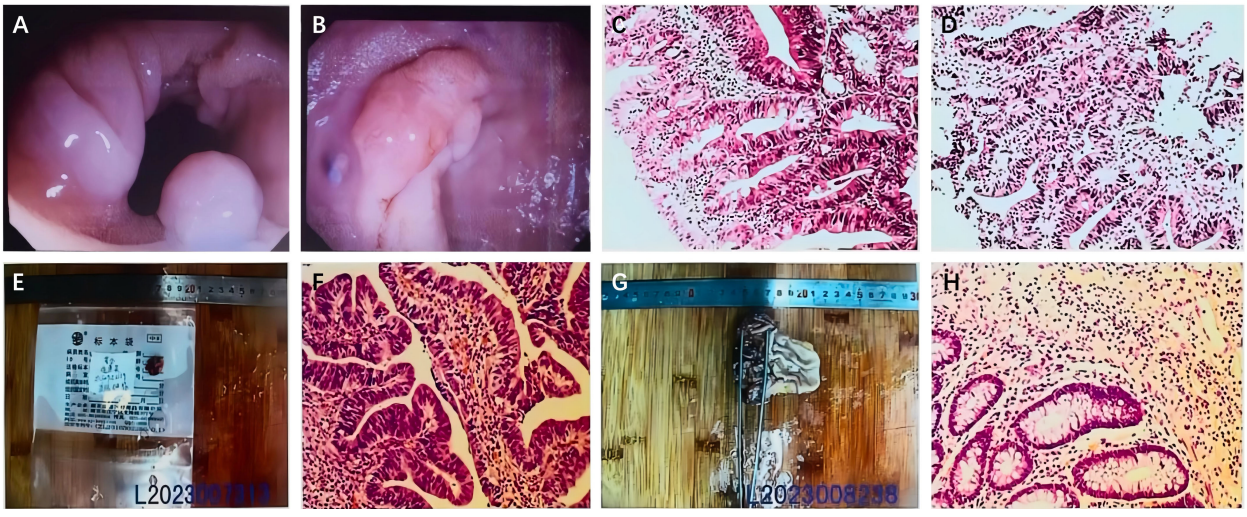

FIGURE 2
(A) A 0.6 * 0.8 cm polyp is seen in the sigmoid colon. **(B)** A 1.5 * 2 cm polyp-like protrusion is seen in the rectum. Pathological findings. **(C)** Tubular adenoma of the sigmoid colon (20 cm). **(D)** Moderately differentiated adenocarcinoma of the rectum (5 cm). **(E, F)** Pathological findings after the initial surgery: moderately differentiated adenocarcinoma of the rectum (5 cm from the anus). **(G, H)** The second operation's pathological findings: no residual cancer tissue.

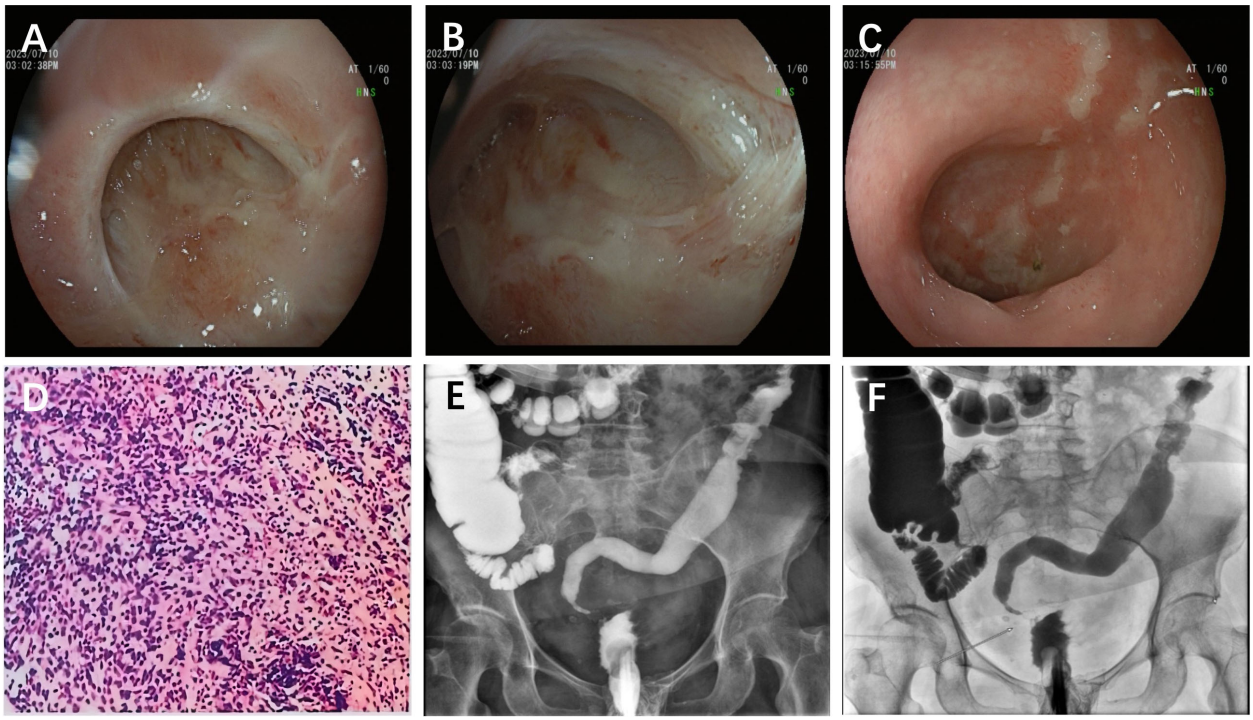

FIGURE 3
(A) Fiberoptic colonoscopy at second admission. The normal anastomosis by fiberoptic colonoscopy through anus. **(B)** A narrow even block intestinal cavity 3 cm from the anus by fiberoptic colonoscopy through anus. **(C)** A narrow intestinal cavity near the sigmoid colon with white moss covered by fiberoptic colonoscopy through abdominal wall. **(D)** Pathological findings of fiberoptic colonoscopy showed inflammatory granulation tissue with a small number of mildly heterotrophic cells. **(E, F)** Iodiography of the lower anal digestive tract showed tubular stenosis of the sigmoid colon.

epithelium and underlying inflammatory granulation tissue with a few mildly atypical cells (Figure 3D). Lower gastrointestinal imaging indicated poor elasticity and slightly tubular narrowing of the sigmoid colon, with luminal obliteration. The junction between the sigmoid colon and rectum appeared ring-shaped and narrow, allowing only minimal contrast medium passage (Figures 3E, F). The unexplained intestinal stenosis posed significant treatment challenges. While redoing the anastomosis was considered, the patient's advanced age, existing medical conditions, and nutritional status suggested elevated perioperative risks. Re-anastomosis was complex, raising concerns about whether sufficient colon length remained post-resection. Additionally, the elderly female patient's compromised anal function and sphincter laxity increased the risk of low anterior resection syndrome (LARS) post-re-anastomosis. After discussion and decision-making, no further stoma reconstruction was performed due to the intestinal stenosis, and the patient was discharged. Relevant laboratory data are presented in Table 1.

Due to unexplained stenosis of the sigmoid colon, the closure of temporary ileostomy was unsuccessful, adversely affecting the patient's mood. We provided psychological intervention and conducted follow-ups at 6, 9, and 12 months postoperatively. The patient continued medication treatment for connective tissue disease during this period. We observed no signs of tumor recurrence in the postoperative follow-ups, and the stoma was well maintained without needing further reconstruction. The patient's quality of life remained largely unaffected. No other adverse or unanticipated events occurred. We discussed with the patient the option of additional examinations to assess the alleviation of stenosis for potential ileostomy reversal. However, due to the patient's age, numerous medical conditions, high risk of complications, and relatively unaffected quality of life, the patient and family members declined further testing. The timeline with relevant data from the episode of care is shown in Figure 4.

Discussion

In this study, we report an elderly female patient with low rectal cancer complicated with CTD who had visited the internal medicine clinic of our hospital for connective tissue disease repeatedly. She was treated with prednisone, cyclophosphamide, and *T. wilfordii* to control the disease as her condition gradually deteriorated. After rectal cancer was found and TaTME was performed, a stricture developed in the colon 2 cm above the anastomosis. To date, no research or case reports have addressed the potential complications of gastrointestinal surgery in patients with CTD, making diagnosis and treatment challenging.

The etiology of intestinal stenosis is frequently linked to ischemic intestinal diseases, often resulting from other medical conditions or medication use, such as ischemic enteritis, diverticulosis, inflammatory bowel disease, intestinal tumors, and

TABLE 1 The relevant laboratory data of the patient in hospital.

Date (2023)	WBC (*10^9/L)	NEU (%)	PCT (ng/mL)	CRP (mg/L)	HB (g/L)	P-AlbG (mg/L)	AlbG (g/L)	TP (g/L)	
	3.5–9.5	40.0–75.0	0–0.05	0–3	115–150	180–350	40–55	65–85	Standard range
3.16	6.9	73.7	0.02	24.9	86.0	191.3	33.1	61.5	Be hospitalized
3.24	6.4	74.0	0.02	21.7	81.0	122.4	29.0	57.4	Day 1 after transanal tumor resection
3.26	8.8	80.2	0.02	22.1	87.0	147.6	32.3	63.6	Day 3 after transanal tumor resection
3.31	9.4	81.5	0.02	40.9	87.0	180.4	31.3	62.1	Day 1 after TaTME
4.01	18.7	88.3	0.16	54.9	80.0	110.1	27.7	55.4	Day 2 after TaTME, complicated with intrapulmonary infection
4.02	19.9	92.4	0.42	78.2	76.0	84.5	27.0	53.6	Day 3 after TaTME
4.04	10.4	84.8	0.24	61.7	85.0	109.8	31.3	60.5	Day 5 after TaTME
4.06	9.2	80.7	0.13	32.1	89.0	135.7	29.6	60.7	Day 7 after TaTME
4.09	7.5	75.6	0.05	18.6	88.0	143.1	30.2	61.0	Discharge

WBC, white blood cell; NEU, neutrophils; PCT, procalcitonin; CRP, C-reactive protein; HB, hemoglobin; TP, total protein; TaTME, transanal total mesorectal excision; P-AlbG, prealbumin; AlbG, albumin.

radiation enteritis (8). A study utilizing a national registry database in China found that among 1,926 TaTME surgery cases, the overall incidence of complications was 15.4%. Specifically, the incidences of postoperative anastomotic leakage, fever, intestinal obstruction, urinary retention, and incision complications were 5.9%, 4.3%, 2.1%, 1.5%, and 0.8%, respectively. Additionally, 2.8% of the patients experienced pelvic abscess (seven cases), deep vein thrombosis (three cases), cardiopulmonary failure (three cases), and ostomy ischemia or necrosis (three cases). However, proximal anastomotic colonic stenosis was not mentioned (9). The incidence rate of postoperative anastomotic stenosis in TaTME has been reported to be approximately 3.6% (10). Although anastomotic stenosis is often secondary to anastomotic fistula, no such fistula was observed in this patient during the perioperative period, thereby excluding proximal colonic stenosis caused by anastomotic fistula. For this patient, we regularly performed digital rectal examination postoperatively to dilate the anastomosis and prevent stenosis, although proximal stenosis remains rare. A thorough review of the patient's medical history and perioperative treatment revealed no cause of intestinal stenosis other than CTD. We hypothesize that the surgery disrupted the homeostasis of the local intestinal tissue and exacerbated the inflammatory response associated with CTD, leading to inflammatory narrowing due to altered blood supply to the intestine post-surgery.

CTDs are associated with multiple etiologies, with immune factors being one of the important factors. The presence of autoantibodies in the serum and chronic inflammation in tissues are characteristic manifestations of CTDs, and autoantibodies serve as crucial tools for these conditions (2, 11). The main organ involved in CTDs is the lung (12), but CTDs can also result in gastrointestinal issues such as gastroesophageal reflux, esophageal stenosis, chronic intestinal obstruction, eosinophilic enteritis, and characteristic diverticular changes (7, 13). The occurrence and progression of some CTDs are closely related to intestinal flora. Studies have reported that patients with RA and SLE typically

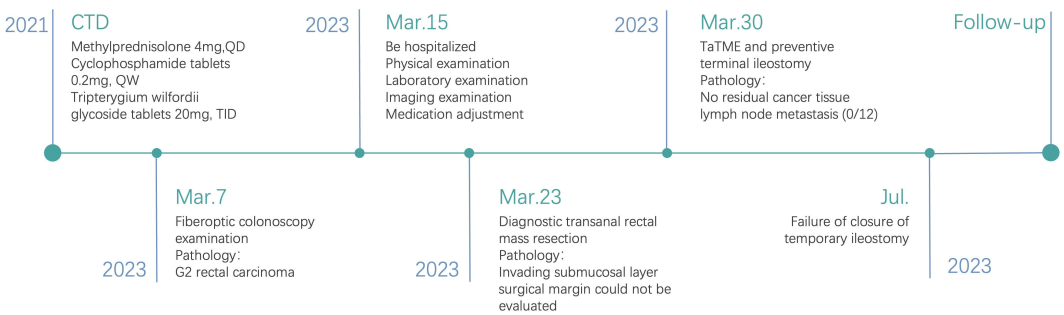

FIGURE 4
A timeline with relevant data from the episode of care.

exhibit intestinal flora dysbiosis, characterized by a reduced number of probiotics in the local mucosal flora. The excessive growth of harmful microorganisms and the decreased abundance of beneficial bacteria lead to changes in intestinal mucosal permeability and chronic inflammation (14, 15). This will aggravate the postoperative inflammatory response around the anastomosis, leading to the occurrence of inflammatory stenosis.

In addition to CTD itself, we also discussed the therapeutic drugs associated with CTD. Cyclophosphamide and glucocorticoid are commonly used to treat CTD (16). Cyclophosphamide, a cytotoxic immunosuppressive agent, has no significant toxicity on the gastrointestinal tract. However, Yang et al. reported a case of cyclophosphamide-related severe enteritis involving both the small intestine and the entire colon. The pathology reported severe intestinal mucosal ulcers and granulation tissue formation, which resembled our pathological findings. This case is strongly suspected to be related to cyclophosphamide treatment, but the cause and specific mechanism remain unidentified (17). At the same time, high doses of cyclophosphamide can increase intestinal permeability, alter the balance of intestinal flora, and elevate harmful bacteria counts (18), potentially contributing to inflammation.

Secondary vascular inflammation is commonly observed as a symptom of CTD, with rheumatoid vasculitis (RV) being the most susceptible to secondary vasculitis. Intestinal involvement may present as ischemic colitis (6) and even gangrene. Lupus mesangial vasculitis, one of the most severe gastrointestinal complications secondary to SLE, often leads to gastrointestinal perforation and sepsis. The small intestine (particularly the jejunum and ileum) is most affected (80%–85%), while the rectum is less affected (14%) (6, 19). The patient in this case also presented with Raynaud's syndrome, which usually affects small arteries in the fingertips and rarely involves the gastrointestinal tract, making the potential inflammatory changes in the intestinal vasculature uncertain. Due to the low location of the tumor, with poor blood supply around the collateral rectal artery, compounded by hypertension, type II diabetes, and other risk factors, the occurrence of ischemic reaction is further aggravated in the presence of secondary vasculitis.

This case report describes the occurrence of sigmoid stenosis above the anastomotic site in a low rectal cancer patient complicated with CTD following surgery. The specific mechanism and risk factors are still unclear. While CTD predominantly targets the lung and is associated with poor prognosis, its impact on the gastrointestinal tract has not been studied widely. Due to the rarity of postoperative complications in CTD patients with concurrent rectal cancer, there is a lack of reliable research conclusions. This report systematically analyzes the potential causes of postoperative proximal anastomotic colonic stenosis in a patient undergoing TaTME surgery complicated with CTD. This case discussion, the first of its kind, expands the scope of CTD-related research in gastrointestinal surgery and aims to guide the clinical management of similar patients.

Data availability statement

The original contributions presented in the study are included in the article/supplementary material. Further inquiries can be directed to the corresponding author.

Ethics statement

Written informed consent was obtained from the individual(s) for the publication of any potentially identifiable images or data included in this article.

Author contributions

DT: Conceptualization, Data curation, Writing – original draft, Writing – review & editing. JL: Software, Writing – original draft. GG: Formal Analysis, Writing – original draft. CZ: Conceptualization, Funding acquisition, Writing – review & editing.

Funding

The author(s) declare financial support was received for the research, authorship, and/or publication of this article. This research received support from a "Scientific research funding project of the Liaoning Provincial Department of Science and Technology (No. 2021JH2/10300106)".

Acknowledgments

We thank the General Hospital of Northern Theater Command for its support and the patient for permitting us to use her case to complete this article.

Conflict of interest

The authors declare that the research was conducted in the absence of any commercial or financial relationships that could be construed as a potential conflict of interest.

Publisher's note

All claims expressed in this article are solely those of the authors and do not necessarily represent those of their affiliated organizations, or those of the publisher, the editors and the reviewers. Any product that may be evaluated in this article, or claim that may be made by its manufacturer, is not guaranteed or endorsed by the publisher.

References

1. Kouchit Y, Morand L, Martis N. Mortality and its risk factors in critically ill patients with connective tissue diseases: A meta-analysis. *Eur J Intern Med*. (2022) 98:83–92. doi: 10.1016/j.ejim.2022.02.006

2. Decker P, Moulinet T, Pontille F, Cravat M, De Carvalho Bittencourt M, Jaussaud R. An updated review of anti-Ro52 (TRIM21) antibodies impact in connective tissue diseases clinical management. *Autoimmun Rev*. (2022) 21:103013. doi: 10.1016/j.autrev.2021.103013

3. Ritschl V, Ferreira RJO, Santos EJF, Fernandes R, Juutila E, Mosor E, et al. Suitability for e-health of non-pharmacological interventions in connective tissue diseases: scoping review with a descriptive analysis. *RMD Open*. (2021) 7:e001710. doi: 10.1136/rmdopen-2021-001710

4. Rose J. Autoimmune connective tissue diseases: systemic lupus erythematosus and rheumatoid arthritis. *Emerg Med Clin North Am*. (2022) 40:179–91. doi: 10.1016/j.emc.2021.09.003

5. Asif MI, Kalra N, Sharma N, Jain N, Sharma M, Sinha R. Connective tissue disorders and eye: A review and recent updates. *Indian J Ophthalmol*. (2023) 71:2385–98. doi: 10.4103/ijo.IJO_286_22

6. Sharma A, Dhooria A, Aggarwal A, Rathi M, Chandran V. Connective tissue disorder-associated vasculitis. *Curr Rheumatol Rep*. (2016) 18:31. doi: 10.1007/s11926-016-0584-x

7. Kumar S, Singh J, Rattan S, DiMarino AJ, Cohen S, Jimenez SA. Review article: pathogenesis and clinical manifestations of gastrointestinal involvement in systemic sclerosis. *Aliment Pharmacol Ther*. (2017) 45:883–98. doi: 10.1111/apt.13963

8. Cain BT, Huang LC. Benign colonic strictures. *Dis Colon Rectum*. (2021) 64:1041–4. doi: 10.1097/DCR.0000000000002179

9. Li Y, Ren M, Zhang H, Wang Q, Xu Q, Yu G, et al. Intraoperative difficulties/accidents and postoperative complications of transanal total mesorectal excision: A nationwide registry study. *Chin J Pract Surg*. (2022) 42(11):1260–4.

10. Penna M, Hompes R, Arnold S, Wynn G, Austin R, Warusavitarne J, et al. Incidence and risk factors for anastomotic failure in 1594 patients treated by transanal total mesorectal excision: results from the international taTME registry. *Ann Surg*. (2019) 269:700–11. doi: 10.1097/SLA.0000000000002653

11. Atalar E, Yurdakul FG, Gök K, Güler T, Erten Ş, Yaşar E, et al. Motor neuron disease in a patient with overlap syndrome (rheumatoid arthritis; systemic lupus erythematosus, Sjogren's syndrome). *Rheumatol Int*. (2023) 43:367–72. doi: 10.1007/s00296-022-05207-z

12. De Zorzi E, Spagnolo P, Cocconcelli E, Balestro E, Iaccarino L, Gatto M, et al. Thoracic involvement in systemic autoimmune rheumatic diseases: pathogenesis and management. *Clin Rev Allergy Immunol*. (2022) 63:472–89. doi: 10.1007/s12016-022-08926-0

13. Lecouffe-Desprets M, Groh M, Bour B, Le Jeunne C, Puéchal X. Eosinophilic gastrointestinal disorders associated with autoimmune connective tissue disease. *Joint Bone Spine*. (2016) 83:479–84. doi: 10.1016/j.jbspin.2015.11.006

14. Guo X, Yang X, Li Q, Shen X, Zhong H, Yang Y. The microbiota in systemic lupus erythematosus: an update on the potential function of probiotics. *Front Pharmacol*. (2021) 12:759095. doi: 10.3389/fphar.2021.759095

15. Li M, Wang F. Role of intestinal microbiota on gut homeostasis and rheumatoid arthritis. *J Immunol Res*. (2021) 2021:8167283. doi: 10.1155/2021/8167283

16. Oliveira RP, Ribeiro R, Melo L, Grima B, Oliveira S, Alves JD. Connective tissue disease-associated interstitial lung disease. *Pulmonology*. (2022) 28:113–8. doi: 10.1016/j.pulmoe.2020.01.004

17. Yang LS, Cameron K, Papaluca T, Basnayake C, Jackett L, McKelvie P, et al. Cyclophosphamide-associated enteritis: A rare association with severe enteritis. *World J Gastroenterol*. (2016) 22:8844–8. doi: 10.3748/wjg.v22.i39.8844

18. Bai Y, Zeng Z, Xie Z, Chen G, Chen D, Sun Y, et al. Effects of polysaccharides from Fuzhuan brick tea on immune function and gut microbiota of cyclophosphamide-treated mice. *J Nutr Biochem*. (2022) 101:108947. doi: 10.1016/j.jnutbio.2022.108947

19. Lee JR, Paik CN, Kim JD, Chung WC, Lee KM, Yang JM. Ischemic colitis associated with intestinal vasculitis: histological proof in systemic lupus erythematosus. *World J Gastroenterol*. (2008) 14:3591–3. doi: 10.3748/wjg.14.3591

frontiers | Frontiers in Oncology

TYPE Case Report
PUBLISHED 18 December 2024
DOI 10.3389/fonc.2024.1462353

Check for updates

OPEN ACCESS

EDITED BY
Dragos Eugen Georgescu,
Carol Davila University of Medicine and Pharmacy, Romania

REVIEWED BY
Apurva Patel,
Gujarat Cancer & Research Institute, India
Chiara Ripepi,
University of Trieste, Italy

*CORRESPONDENCE
Ting Liu
tingliu20082007@hotmail.com

RECEIVED 10 July 2024
ACCEPTED 25 November 2024
PUBLISHED 18 December 2024

CITATION
Wu J and Liu T (2024) Primary uterine non-Hodgkin's lymphoma:a rare case report and review of the literature.
Front. Oncol. 14:1462353.
doi: 10.3389/fonc.2024.1462353

COPYRIGHT
© 2024 Wu and Liu. This is an open-access article distributed under the terms of the Creative Commons Attribution License (CC BY). The use, distribution or reproduction in other forums is permitted, provided the original author(s) and the copyright owner(s) are credited and that the original publication in this journal is cited, in accordance with accepted academic practice. No use, distribution or reproduction is permitted which does not comply with these terms.

Primary uterine non-Hodgkin's lymphoma:a rare case report and review of the literature

Jing Wu and Ting Liu*

Department of Radiology, the Affiliated Hospital of inner Mongolia Medical University, Hohhot, China

Primary uterine non-Hodgkin lymphoma (NHL) is rarely reported, as its incidence is extremely low. We describe a 72 year old patient with primary uterine non-Hodgkin's lymphoma stage IV, diffuse B-cell large cells, who responded well to cytotoxic chemotherapy (R-CHOP). Radiological investigations exhibited certain characteristics, including magnetic resonance T2 weighted imaging, enhanced scanning, diffusion weighted imaging and apparent diffusion coefficient values. The lesion in the anterior wall of the uterine body was relatively large, with a size of about 34mm×47mm×43mm. The gold standard for diagnosis is still the pathological examination of a biopsy specimen, which revealed diffuse large cell of B lineage. This article reviews data collected from 141 patients in the literature.

KEYWORDS

non Hodgkin lymphoma (NHL), diffuse large b-cell lymphoma (DLBCL), diffusion weighted imaging, magnetic resonance (MR) imaging, primary uterine non-Hodgkin lymphoma (NHL)

Introduction

Diffuse large B-cell lymphoma (DLBCL) is an invasive and most common pathological type of non-Hodgkin lymphoma, accounting for approximately 30% to 40% of all cases. However, it is rare for the uterus and reproductive organs to be affected, which has not been well documented. Primary lymphomas of the female genital tract account for 0.2% to 1.1% of all extranodal lymphomas (1). Most cases of uterine lymphoma are caused by secondary involvement of the disease (2). Due to its rarity and non-specific clinical presentation, the diagnosis of uterine DLBCL is difficult. There are few studies at present, and therefore, there is currently no standard treatment for uterine DLBCL. However, several studies on DLBCL have investigated the efficacy of various treatment regimens, which were not specific to the female reproductive tract. For patients with DLBCL, the current standard treatment regimen is rituximab, doxorubicin, cyclophosphamide, vincristine and prednisone (R-CHOP), which has a cure rate of about 60%-70% and a relapse/refractory rate of 30%-40% (3, 4).

Results

Case report

In this case a 72-year-old woman experienced abdominal pain and urinary tract obstruction due to a large tumor in the uterus. The woman was in good general conditions had no hypertension, diabetes and dyslipidemia in her past medical History. Ultrasonography showed the presence of a large uterine mass, without clear evidence of local infiltration or lymphadenopathy. Magnetic resonance imaging (MRI) scan revealed that significant increase in uterine volume and slightly longer T1 and T2 signals were seen in the anterior wall and bottom of the uterine body. The lesion in the anterior wall of the uterine body was relatively large, with a size of about 34mm×47mm×43mm. After enhanced scanning, the arterial phase enhancement of the lesion was significantly uneven, the degree of venous phase enhancement was lower than that of the normal uterine myometrium, the boundary was clear, and the leading edge of the lesion was incomplete. Diffusion weighted imaging showed a significant high signal, which is due to the tight arrangement of tumor cells, small extracellular space, and limited cytoplasm, resulting in limited diffusion of water molecules inside and outside the cell. The apparent diffusion coefficient (ADC) value of 0.751×10^{-3} mm^2/s was significantly decreased (Figure 1). Computed tomography (CT) showed that the uterine volume increased, soft tissue density shadow could be seen in the anterior wall of the uterus, with unclear boundary, the size was about 34mmx47mm, and the enhanced scan showed uneven enhancement, lower than the myometrium, and liquid density shadow could be seen in the pelvic cavity (Figure 2). An incisional biopsy was taken from the anterior wall of the uterus. Histological examination showed a diffuse large B-cell lymphoma of the uterus. Immunohistological examination revealed CD20(+), Bcl6(+), CD10(+),P40(-), CK7(-), P16(+), ER(-), PR(-), Vim(+), P53(mutant type, +), Ki67approximately 90%(+), HNF1-β(-), CK(-), WT1(-), NapsinA (-), PAX8(-), CA125(-), LCA(+), CD3(-), PAX5 (+), P504S(-), Desmin(-), Caldesmon(-), EBV(-), MUM(+), Bcl2(+) and c-Myc approximately 30-40%(+) suggested a diffuse large B-cell lymphoma from the uterus (Figure 3). A bone marrow biopsy was performed, and the results showed normal bone marrow cells without evidence of lymphoma involvement. The patient's International Prognosric Index (IPI) score was 2. Under the supervision of the hematology department, a series of chemotherapy treatments including rituximab, cyclophosphamide, doxorubicin, vincristine, and prednisone (R-CHOP) were initiated. According to the National Comprehensive Cancer Network (NCCN) guideline, the patients in stage IV was planned to receive 6 cycles of RCHOP chemotherapy, and intrathecal methotrexate (IT-MTX) was given for Central Nervous System (CNS) prophylaxis, which were monitored every 3-6 monthly. A comparative CT scan was performed, and the results showed that after 3 courses of chemotherapy, all tumor locations significantly regressed. Before CT enhancement, the lesion density was relatively uniform, and obvious enhanced nodular shadow of about 6mm in diameter in the anterior wall of the uterus after the enhanced scan. The uterus is of normal shape and size. A small amount of fluid-like density shadow is seen in the pelvic cavity. Unfortunately, the patient died of heart failure after 3 cycles of RCHOP chemotherapy. The limitation is that interim positron emission tomography (PET)/CT scan was not done for the patient.

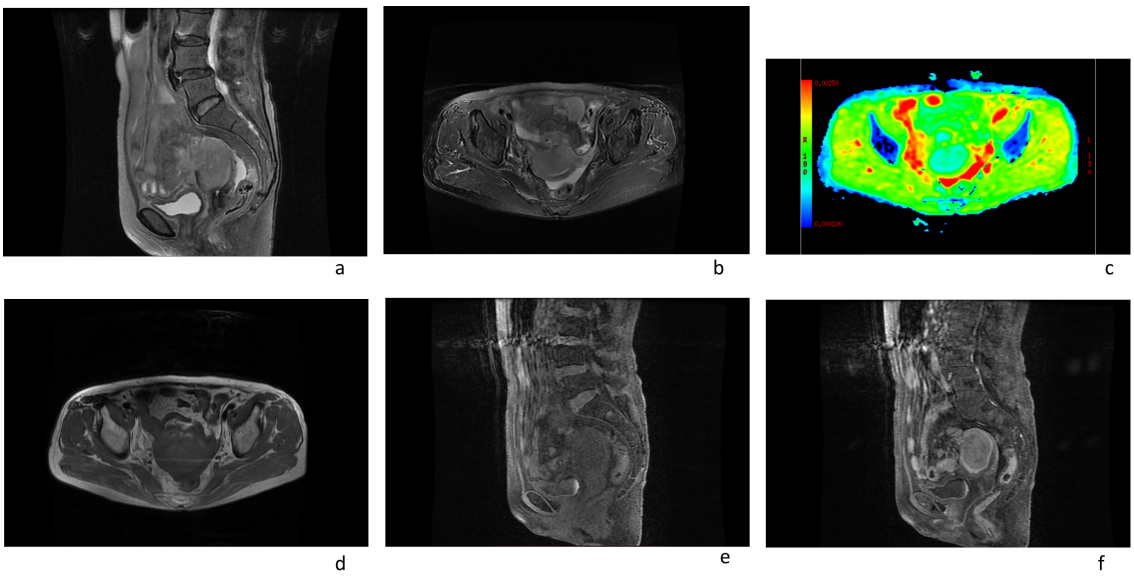

FIGURE 1
Magnetic resonance imaging scans of an 72-year-old female patient with a pelvic mass showed the following: **(A, B, D, E)** an enlarged uterus; **(F)** the arterial phase enhancement of the lesion was significantly uneven, the degree of venous phase enhancement was lower than that of the normal uterine myometrium. **(C)** The apparent diffusion coefficient (ADC) value of uterine mass was 0.751×10^{-3} mm^2/s.

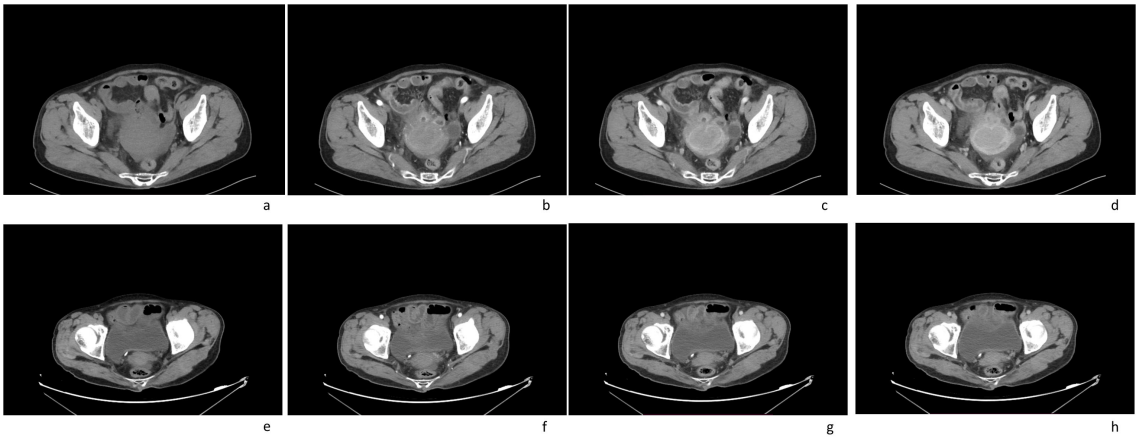

FIGURE 2
Computed tomography (CT) imaging scans of an 72-year-old female patient with a pelvic mass for more than 1 month: **(A)** plain CT imaging showed an enlarged uterine volume, soft tissue density shadow in the anterior wall of the uterus, with unclear boundary; **(B–D)** enhanced CT imaging(arterial phase[b]; venous phase[c]; delay phase[d]) showed that the lesion were slightly enhanced, the boundary was clear; **(E–H)** after treatment, enhanced CT imaging(arterial phase[f]; venous phase[g]; delay phase[h]) showed that the volume of the uterus had significantly reduced(plain CT imaging[e]).

Discussion

The table displays detailed information of 141 patients with primary uterine lymphoma (2, 10–63).

The uterine body, cervix, and vagina are rarely the origin sites of non-Hodgkin lymphoma (NHL). Primary Non-Hodgkin's Lymphomas (NHL) of the uterus is a very rare disease, with non-specific clinical manifestations. Fox and More (4) defined three criteria for primary uterine lymphoma: (1) clinical limitation to the uterus; (2) There is no evidence of leukemia; (3) The interval between primary uterine lymphoma and secondary tumors is very long. If diagnosed with lymphoma, bone marrow biopsy must be performed to rule out leukemia.

Primary uterine and vaginal lymphoma usually present with non-specific symptoms such as abnormal vaginal or uterine bleeding, perineal discomfort, persistent vaginal discharge, abdominal pain, and urinary obstruction. These symptoms occur in many more diseases, such as cervical or endometrial carcinoma, adenomyosis, endometriosis and uterine fibroids, complicating the determination of a definitive differential diagnosis. The appearance of symptoms is not a characteristic of uterine lymphoma, therefore, making a correct diagnosis may take longer.

The age and pathological type of patients with uterine lymphoma are related, and diffuse large B-cell lymphoma is most common in women aged 35 to 45; Follicular lymphoma is more likely to occur in women over the age of 50 (1). Burkitt's lymphoma usually occurs most often in children aged 5 and 10 (5). The current patients are elderly individuals with diffuse large B-cell lymphoma, which is relatively rare in clinical practice.

Magnetic resonance (MR) imaging is the most effective method for distinguishing lymphoma from cervical carcinoma, due to the fact that uterine DLBCL is a stromal rather than epithelial disease. The signal intensity of the uterine stroma and mucosa is usually intact and not invaded, which is different from cervical cancer. The Uterine lymphoma presents as a large mass within the uterus, and has similar signal intensity with that of other tumors, which is of low signal on T1 -weighted images, and high signal on T2 -weighted images. The contrast enhancement is common. The apparent diffusion coefficient values showed certain characteristics, which showed its ability to make a definitive differential diagnosis. The ADC of primary uterine lymphoma (0.696×10^{-3} mm^2/s) (6) was much lower than uterine fibroids and cervical cancer ($1.15\pm 0.18\times 10^{-3}$ mm^2/s and $0.99\pm 0.18\times 10^{-3}$ mm^2/s, respectively) (7).

CT is usually the preferred method for detecting and staging non Hodgkin lymphoma. The size and extent of the tumor can be accurately measured by CT. Moreover, CT can develop appropriate treatment plans and track treatment responses. CT can not only detect the lesions in the cervix, but also the involvement of the vagina, bladder, rectum and adjacent lymph nodes, which often presented as a large enhanced mass within the cervix, invasion of the vagina, bladder, rectum, and enlarged lymph nodes. No calcification is detected. CT is valuable for evaluating response to treatment, identifying active residual masses and assessing recurrence. Diagnosis invariably requires a core biopsy.

Currently, rituximab has been approved for monotherapy and when used in combination with CHOP, they are commonly referred to as R-CHOP (8). In several studies, the adding rituximab to CHOP therapy can improved complete response rate and prolonged event-free survival and overall survival (OS) in DLBCL patients (9) Szanto et al. found that using chemotherapy instead of radiotherapy can protect ovarian function, prevent micro metastasis (10). This has been proven to be effective in our patient.

In conclusion, elderly patients with primary uterine non Hodgkin lymphoma are relatively rare in clinical practice. When elderly patients develop pelvic masses, the physicians should consider the possibility of lymphoma and make a differential diagnosis.

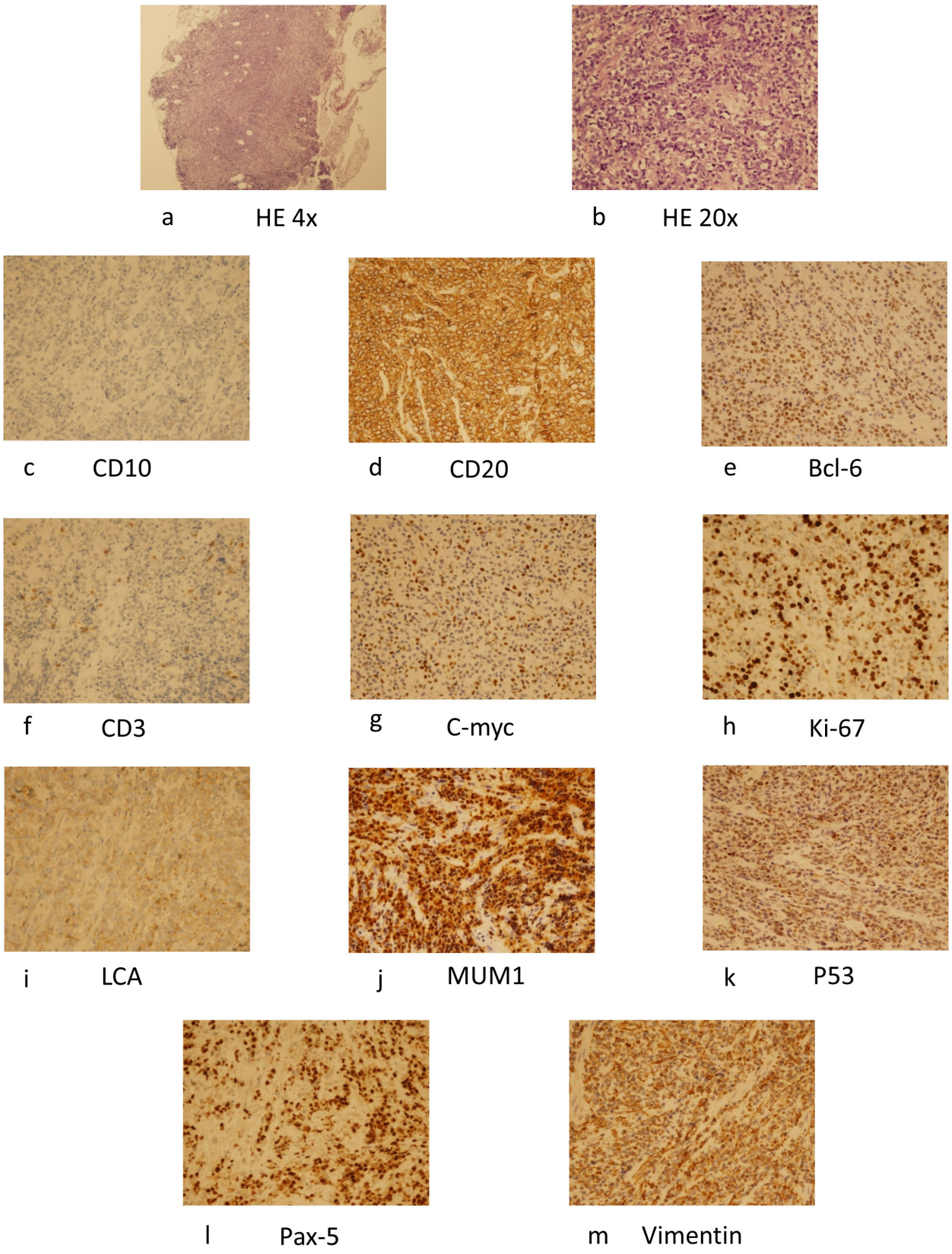

FIGURE 3
HE staining of the specimen (x40) **(A)**, (x200) **(B)**, and immunohistochemical examination revealed CD10 (+) **(C)**, CD20 (+) **(D)**, Bcl-6 (+) **(E)**, CD3(+) **(F)**, C-myc(+) **(G)**, Ki-67(+) **(H)**, LCA(+) **(I)**, MUM1(+) **(J)**, P53(+) **(K)**, Pax-5(+) **(L)**, Vimentin(+) **(M)** and suggested a diffuse large B-cell lymphoma. HE, hematoxylin.

Data availability statement

The original contributions presented in the study are included in the article/Supplementary Material. Further inquiries can be directed to the corresponding author/s.

Ethics statement

Ethical approval was not required for the study involving humans in accordance with the local legislation and institutional requirements. Written informed consent to participate in this study was not required from the participants or the participants' legal guardians/next of kin in accordance with the national legislation and the institutional requirements. Written informed consent was obtained from the individual(s) for the publication of any potentially identifiable images or data included in this article.

Author contributions

JW: Conceptualization, Data curation, Formal analysis, Funding acquisition, Investigation, Methodology, Writing – review & editing. TL: Conceptualization, Data curation, Formal analysis, Funding acquisition, Investigation, Methodology, Writing – review & editing, Supervision, Visualization, Writing – original draft.

Funding

The author(s) declare financial support was received for the research, authorship, and/or publication of this article. We were supported by Natural Science Foundation of Inner Mongolia Autonomous Region of china (No.2024MS08006, No.2020MS08128).

Conflict of interest

The authors declare that the research was conducted in the absence of any commercial or financial relationships that could be construed as a potential conflict of interest.

Publisher's note

All claims expressed in this article are solely those of the authors and do not necessarily represent those of their affiliated organizations, or those of the publisher, the editors and the reviewers. Any product that may be evaluated in this article, or claim that may be made by its manufacturer, is not guaranteed or endorsed by the publisher.

Supplementary material

The Supplementary Material for this article can be found online at: https://www.frontiersin.org/articles/10.3389/fonc.2024.1462353/full#supplementary-material

References

1. Nasioudis D, Kampaktsis PN, Frey M, Witkin SS, Holcomb K. Primary lymphoma of the female genital tract: an analysis of 697 cases. *Gynecol Oncol.* (2017) 145:305–9. doi: 10.1016/j.ygyno.2017.02.043

2. Frey NV, Svoboda J, Andreadis C, Tsai DE, Schuster SJ, Elstrom R, et al. Primary lymphomas of the cervix and uterus: the University of Pennsylvania's experience and a review of the literature. *Leuk Lymphoma.* (2006) 47:1894–901. doi: 10.1080/10428190600687653

3. Li S, Young KH, Medeiros LJ. Diffuse large B-cell lymphoma. *Pathology.* (2018) 50:74–87. doi: 10.1016/j.pathol.2017.09.006

4. Hamlin PA, Satram-Hoang S, Reyes C, Hoang KQ, Guduru SR, Skettino S. Treatment patterns and comparative effectiveness in elderly diffuse large B-cell lymphoma patients: a surveillance, epidemiology, and end results-medicare analysis. *Oncologist.* (2014) 19:1249–57. doi: 10.1634/theoncologist.2014-0113

5. Pinto E, Batista S, Lourenc C, Gonçalves J, Ramalho G. Gynecological lymphomas Linfomas ginecologicos. *Acta Obstet Ginecol Port.* (2014) 8:201–5.

6. Mabray MC, Cohen BA, Villanueva-Meyer JE, Valles FE, Barajas RF, Rubenstein JL, et al. Performance of apparent diffusion coefficient values and conventional MRI features in differentiating tumefactive demyelinating lesions from primary brain neoplasms. *AJR Am J Roentgenol.* (2015) 205:1075–85. doi: 10.2214/AJR.14.13970

7. Lee EY, Yu X, Chu MM, Ngan HY, Siu SW, Soong IS, et al. Perfusion and diffusion characteristics of cervical cancer based on intraxovel incoherent motion MR imaging – a pilot study. *Eur Radiol.* (2014) 24:1506–13. doi: 10.1007/s00330-014-3160-7

8. Salles G, Barrett M, Foà R, Maurer J, O'Brien S, Valente N, et al. Rituximab in B-cell hematologic Malignancies: a review of 20 years of clinical experience. *Adv Ther.* (2017) 34:2232–73. doi: 10.1007/s12325-017-0612-x

9. Coiffier B, Lepage E, Brière J, Herbrecht R, Tilly H, Bouabdallah R, et al. CHOP chemotherapy plus rituximab compared with CHOP alone in elderly patients with diffuse large-B-cell lymphoma. *N Engl J Med.* (2002) 346:235–42. doi: 10.1056/NEJMoa011795

10. Szánthó A, Bálega JJ, Csapó Z, Sréter LL, Matolcsy A, Papp Z. Primary non -Hodgkin's lymphoma of the uterine cervix successfully treated by neoadjuvant chemotherapy: case report. *Gynecol Oncol.* (2003) 89:171–4. doi: 10.1016/s0090-8258(03)00057-x

11. Chorlton I, Karnei RF Jr, King FM, Norris HJ. Primary Malignant reticuloendothelial disease involving the vagina, cervix, andcorpus uteri. *Obstet Gynecol.* (1974) 44:735–8.

12. Harris NL, Scully RE. Malignant lymphoma and granulocytic sarcoma of the uterus and vagina. A clinicopathologic analysis of 27cases. *Cancer.* (1984) 53:2530–45. doi: 10.1002/1097-0142(19840601)53:11<2530::AID-CNCR2820531127>3.0.CO;2-J

13. Komaki R, Cox J, Hansen R, Gunn W, Greenberg M. Malignant lymphoma of the uterus and cervix. *Cancer.* (1984) 54:1699–704. doi: 10.1002/1097-0142(19841015)54:8<1699::AID-CNCR2820540836>3.0.CO;2-E

14. Muntz HG, Ferry JA, Flynn D, Fuller AF Jr, Tarraza HM. StageIE primary Malignant lymphomas of the uterine cervix. *Cancer.* (1991) 68:2023–32. doi: 10.1002/1097-0142(19911101)68:9<2023::AID-CNCR2820680930>3.0.CO;2-V

15. Broekmans FJ, Swartjes JM, van der Valk P, Schutter EM. Primary Malignant lymphoma of the uterus: localization in a cervicalpolyp. *Eur J Obstet Gynecol Reprod Biol.* (1993) 48:215–9. doi: 10.1016/0028-2243(93)90090-Y

16. Kuo HC, Chou CY, Chang CH, Liu MT, Tzeng CC, Huang KE. Primary Malignant lymphoma of the uterine cervix shows favorable response to neoadjuvant chemotherapy. *Gynecol Oncol.* (1994) 52:408–10. doi: 10.1006/gyno.1994.1070

17. Awwad JT, Khalil AM, Shamseddine AI, Mufarrij AA. Primarymalignant lymphoma of the uterine cervix: is radiotherapy thebest therapeutic choice for stage IE? *Gynecol Oncol.* (1994) 52:91–3. doi: 10.1006/gyno.1994.1017

18. Stroh EL, Besa PC, Cox JD, Fuller LM, Cabanillas FF. Treatment of patients with lymphomas of the uterus or cervix with combination chemotherapy and radiation therapy. *Cancer.* (1995) 75:2392–9. doi: 10.1002/1097-0142(19950501)75:9<2392::AID-CNCR2820750932>3.0.CO;2-Y

19. Chandy L, Kumar L, Dawar R. Non-Hodgkin's lymphoma presenting as a primary lesion in uterine cervix: case report. *J Obstet Gynaecol Res.* (1998) 24:183–7. doi: 10.1111/j.1447-0756.1998.tb00073.x

20. Lee KM, Seah ES, Sethi VK. Primary non-Hodgkin's lymphoma of the uterine cervix: case report of long-term survival of two patients treated with surgery and radiotherapy. *Australas Radiol.* (1998) 42:126–7. doi: 10.1111/j.1440-1673.1998.tb00587.x

21. Nasu K, Yoshimatsu J, Urata K, Miyakawa I. A case of primary non-Hodgkin's lymphoma of the uterine cervix treated by combination chemotherapy (THP-COP). *J Obstet Gynaecol Res*. (1998) 24:157–60. doi: 10.1111/j.1447-0756.1998.tb00068.x

22. Grace A, O'Connell N, Byrne P, Prendiville W, O'Donnell R, Royston D, et al. Malignant lymphoma of the cervix: an unusual presentation and a rare disease. *Eur J Gynaecol Oncol*. (1999) 20:26–8.

23. Cheong IJ, Kim SH, Park CM. Primary uterine lymphoma: a case report. *Korean J Radiol*. (2000) 1:223–5. doi: 10.3348/kjr.2000.1.4.223

24. Vang R, Medeiros LJ, Ha CS, Deavers M. Non-Hodgkin's lymphomas involving the uterus: a clinicopathologic analysis of 26cases. *Mod Pathol*. (2000) 13:19–28. doi: 10.1038/modpathol.3880005

25. Pham DC, Guthrie TH, Ndubisi B. HIV-associated primarycervical non-Hodgkin's lymphoma and two other cases of primary pelvic non-Hodgkin's lymphoma. *Gynecol Oncol*. (2003) 90:204–6. doi: 10.1016/S0090-8258(03)00223-3

26. Venizelos ID, Zafrakas M, Dragoumis K, Mandala E, Bondis J. Non-Hodgkin's lymphoma involving the uterine cervix after treatment for Hodgkin disease. *Leuk Lymphoma*. (2003) 44:2155–7. doi: 10.1080/1042819031000116643

27. Gabriele A, Gaudiano L. Primary Malignant lymphoma of the cervix. A case report. *J Reprod Med*. (2003) 48:899–901.

28. Au WY, Chan BC, Chung LP, Choy C. Primary B-cell lymphomaand lymphoma-like lesions of the uterine cervix. *Am J Hematol*. (2003) 73:176–9. doi: 10.1002/ajh.10334

29. Engin H, Türker A, Abali H, Uner A, Günalp S. Successful treatment of primary non-Hodgkin's lymphoma of the vagina with chemotherapy. *Arch Gynecol Obstet*. (2004) 269:208–10. doi: 10.1007/s00404-002-0350-3

30. Chan JK, Loizzi V, Magistris A, Hunter MI, Rutgers J, Disaia PJ, et al. Clinicopathologic features of six cases of primary cervicallymphoma. *Am J Obstet Gynecol*. (2005) 193:866–72. doi: 10.1016/j.ajog.2005.04.044

31. Garavaglia E, Taccagni G, Montoli S, Panacci N, Ponzoni M, Frigerio L, et al. Primary stage I-IIE non-Hodgkin's lymphoma of uterine cervix and upper vagina: evidence for a conservative approach in a study on three patients. *Gynecol Oncol*. (2005) 97:214–8. doi: 10.1016/j.ygyno.2004.07.065

32. Heredia F, Bravo M, Pierotic M, Majlis A, Carmona L. Neoadjuvant combined chemotherapy followed by external whole pelvicirradiation in two cases of primary extranodal non-Hodgkin's lymphoma of the uterine cervix. *Gynecol Oncol*. (2005) 97:285–7. doi: 10.1016/j.ygyno.2004.12.018

33. Dursun P, Gultekin M, Bozdag G, Usubutun A, Under A, Celik NY, et al. Primary cervical lymphoma: Report of two cases and review of the literature. *Gynecol Oncol*. (2005) 98:484–9. doi: 10.1016/j.ygyno.2005.04.040

34. Hariprasad R, Kumar L, Bhatla N, Kukreja M, Papaiah S. Primary uterine lymphoma: Report of 2 cases and review of literature. *Am J Obstet Gynecol*. (2006) 195:308–13. doi: 10.1016/j.ajog.2006.04.002

35. Semczuk A, Skomra D, Korobowicz E, Balon B, Rechberger T. Primary non-Hodgkin's lymphoma of the uterine cervix mimicking leiomyoma: Case report and review of the literature. *Pathol Res Pract*. (2006) 202:61–4. doi: 10.1016/j.prp.2005.10.009

36. González-Cejudo C, Martínez-Maestre MA, Peregrín-Álvarez I, Daza-Manzano C. Primary lymphoma of the cervix: Unusual location for a common disease. *Eur J Obstet Gynecol Reprod Biol*. (2006) 125:268–9. doi: 10.1016/j.ejogrb.2005.09.020

37. Lorusso D, Ferrandina G, Pagano L, Gagliardi ML, Scambia G. Successful pregnancy in stage IE primary non-Hodgkin's lymphoma of uterine cervix treated with neoadjuvant chemotherapy and conservative surgery. *Oncology*. (2007) 72:261–4. doi: 10.1159/000113018

38. Signorelli M, Maneo A, Cammarota S, Isimbaldi G, Garcia Parra R, Perego P, et al. Conservative management in primary genital lymphomas: The role of chemotherapy. *Gynecol Oncol*. (2007) 104:416–21. doi: 10.1016/j.ygyno.2006.08.024

39. Ferreri AJ, Verona C, Bolognesi A, Taccagni G, Ponzoni M, Ferrari S. Successful pregnancy after chemo-immuno-radiation therapy for aggressive lymphoma of the uterus. *Br J Haematol*. (2008) 142:141–3. doi: 10.1111/j.1365-2141.2008.07083.x

40. Wuntakal R, Janga D, Satyanarayana D, Reynolds K, Hollingworth A. An unusual cause of postmenopausal bleeding. *J Low Genit Tract Dis*. (2008) 12:130–3. doi: 10.1097/LGT.0b013e3181571ae2

41. Ab Hamid S, Wastie ML. Primary non -Hodgkin's lymphoma presenting as a uterine cervical mass. *Singapore Med J*. (2008) 49:e73.

42. Baijal G, Vadiraja BM, Fernandes DJ, Vidyasagar MS. Diffuse large B-cell lymphoma of the uterine cervix: A rare case managed novelly. *J Cancer Res Ther*. (2009) 5:140–2. doi: 10.4103/0973-1482.52784

43. Upanal N, Enjeti A. Primary lymphoma of the uterus and cervix: two case reports and review of the literature. *Aust New Z J Obstetrics Gynaecology*. (2011) 51:559–62. doi: 10.1111/j.1479-828X.2011.01365.x

44. Samama M, Poelgeest MV. Primary Malignant lymphoma of the uterus: A case report and review of the literature. *Case Rep Oncol*. (2011) 4:560–3. doi: 10.1159/000334852

45. Parva M, Lamb K, Savior DC, Gilman P, Belden M. Full-term pregnancy and vaginal delivery after treatment for nonHodgkin's lymphoma of the cervix and lower uterine segment: A case report. *J Obstet Gynaecol Can*. (2011) 33:620–4. doi: 10.1016/S1701-2163(16)34911-8

46. Binesh F, Karimi Zarchi M, Vahedian H, Rajabzadeh Y. Primary Malignant lymphoma of the uterine cervix. *BMJ Case Rep*. (2012) 24:bcr2012006675. doi: 10.1136/bcr-2012-006675

47. Parnis J, Camilleri DJ, Babic D, Degaetano J, Savona-Ventura C. Lymphoma of the cervix. *Case Rep Hematol*. (2012) 2012:326127. doi: 10.1155/2012/326127

48. Vasudev DS, Kaler AK. Non-hodgkin's lymphoma of the uterine cervix. *Online J Health Allied Sci*. (2012) 11:13.

49. Mouhajir N, Diakité A, Toulba A, Hemmich M, Saadi I. Primary non-hodgkin's lymphoma of the uterine cervix: case report of long-term survival patient. *J Obstet Gynecol India*. (2014) 64:S145–7. doi: 10.1007/s13224-013-0483-2

50. Cao XX, Li J, Zhang W, Duan MH, Shen T, Zhou DB. Patients with primary diffuse large B-cell lymphoma of female genital tract have high risk of central nervous system relapse. *Ann Hematol*. (2014) 93:1001–5. doi: 10.1007/s00277-013-2003-y

51. Chen R, Yu Z, Zhang H, Ding J, Chen B. Primary malignant lymphoma of the uterus and broad ligament: a case report and review of literature. *OncoTargets Ther*. (2015) 8:265–8. doi: 10.2147/OTT.S78171

52. Pósfai É, Nagy K, Marton I, Bánfalvi A, Kocsis L, Cserni G. Incidentally discovered diffuse large B-cell lymphoma limited to the endocervical mucosa in a young female patient. *Gynecol Obstet Investig*. (2015) 80:134–8. doi: 10.1159/000369388

53. Cubo AM, Soto ZM, Cruz MÁ, Doyague MJ, Sancho V, Fraino A, et al. Primary diffuse large B cell lymphoma of the uterine cervix successfully treated by combined chemotherapy alone: A case report. *Medicine*. (2017) 96:e6846. doi: 10.1097/MD.0000000000006846

54. Boussios S, Zerdes I, Vassou A, Bareta E, Seraj E, Papoudou-Bai A, et al. Extranodal diffuse large B-cell lymphomas: A retrospective case series and review of the literature. *Hematol Rep*. (2018) 10:7070. doi: 10.4081/hr.2018.7070

55. Roberts MB, Cottrill HM. A case of primary lymphoma in a patient with abnormal uterine bleeding. *Gynecol Oncol Rep*. (2018) 26:105–7. doi: 10.1016/j.gore.2018.10.014

56. Gui W, Li J, Zhang Z, Wang L, Zhao J, Ma L, et al. Primary hematological Malignancy of the uterine cervix: A case report. *Oncol Lett*. (2019) 18:3337–41. doi: 10.3892/ol.2019.10652

57. Goda JS, Gaikwad U, Narayan A, Kurkure D, Yadav S, Khanna N, et al. Primary diffuse large B cell lymphoma of Uterine Cervix: Treatment outcomes of a rare entity with literature review. *Cancer Rep*. (2020) 3:e1264. doi: 10.1002/cnr2.1264

58. Akkour K, Alhulwah M, Alhalal H, Alqahtani N, Arafah M. Primary extranodal diffuse large B-cell lymphoma of the uterine cervix. *Malays J Pathol*. (2021) 43:327–31.

59. Stabile G, Sancin L, Bailo PB, Ripepi C, Romano A, Carlucci S, et al. Hysteroscopic resection followed by adjuvant radiotherapy: report of a new therapeutic approach to primary cervical diffuse large B-cell lymphoma. *Int J Environ Res Public Health*. (2022) 19:11779. doi: 10.3390/ijerph191811779

60. Quaresima P, Saccone G, Zuccalà V, Guarascio G, Leo L, Amendola G, et al. Successful vaginal delivery after induction of labour in a patient treated for non-hodgkin's lymphoma of the cervix: A case report and literature review. *Case Rep Obstet Gynecol*. (2022) 2022:3541046. doi: 10.1155/2022/3541046

61. Capsa C, Calustian LA, Antoniu SA, Bratucu E, Simion L, Prunoiu VM. Primary non-hodgkin uterine lymphoma of the cervix: A literature review. *Medicina*. (2022) 58:106. doi: 10.3390/medicina58010106

62. Gao Y, Wang Y, Wang T, Han L, Zhang H. A rare case report of primary uterine and vaginal lymphoma in the elderly. *J Int Med Res*. (2023) 51(3):1–6. doi: 10.1177/03000605221147192

63. Stabile G, Ripepi C, Sancin L, Restaino S, Mangino FP, Nappi L, et al. Management of primary uterine cervix B-cell lymphoma stage IE and fertility sparing outcome: A systematic review of the literature. *Cancers (Basel)*. (2023) 15:3679. doi: 10.3390/cancers15143679

frontiers | Frontiers in Oncology

TYPE Case Report
PUBLISHED 29 January 2025
DOI 10.3389/fonc.2024.1391393

Check for updates

OPEN ACCESS

EDITED BY
Daniel Reis Waisberg,
Hospital das Clinicas da Faculdade de Medicina da USP (HC-FMUSP), Brazil

REVIEWED BY
Nektarios I. Koufopoulos,
University General Hospital Attikon, Greece
Hanen Bouaziz,
Salah Azaiez Institute, Tunisia

*CORRESPONDENCE
Weiwei Gao
weiwei_gao2023@163.com
Fengming Xie
fengming_xie@163.com

†These authors have contributed equally to this work

RECEIVED 22 April 2024
ACCEPTED 27 December 2024
PUBLISHED 29 January 2025

CITATION
Li H, Yang L, Sun X, Wang Z, Qin S, Li C, Liu G, Xie F and Gao W (2025) Changes in hormone receptor when breast cancer metastasizes to the colon: case report and literature review.
Front. Oncol. 14:1391393.
doi: 10.3389/fonc.2024.1391393

COPYRIGHT
© 2025 Li, Yang, Sun, Wang, Qin, Li, Liu, Xie and Gao. This is an open-access article distributed under the terms of the Creative Commons Attribution License (CC BY). The use, distribution or reproduction in other forums is permitted, provided the original author(s) and the copyright owner(s) are credited and that the original publication in this journal is cited, in accordance with accepted academic practice. No use, distribution or reproduction is permitted which does not comply with these terms.

Changes in hormone receptor when breast cancer metastasizes to the colon: case report and literature review

Huimeng Li[1†], Liying Yang[2†], Xiqiang Sun[3], Zhuquan Wang[1], Shuangwei Qin[1], Chengcheng Li[1], Gongwu Liu[3], Fengming Xie[1*] and Weiwei Gao[4*]

[1]Department of Thyroid and Breast Surgery, Southern Central Hospital of Yunnan Province, The First People's Hospital of Honghe State, Honghe Hospital Affiliated to Kunming Medical University, Gejiu, Yunnan, China, [2]Department of Pathology, Southern Central Hospital of Yunnan Province, The First People's Hospital of Honghe State, Honghe Hospital Affiliated to Kunming Medical University, Gejiu, Yunnan, China, [3]Department of Hepatobiliary Surgery, Southern Central Hospital of Yunnan Province, The First People's Hospital of Honghe State, Honghe Hospital Affiliated to Kunming Medical University, Gejiu, Yunnan, China, [4]Department of Rheumatology and Immunology, Southern Central Hospital of Yunnan Province, The First People's Hospital of Honghe state, Honghe Hospital Affiliated to Kunming Medical University, Gejiu, Yunnan, China

The metastasis of breast cancer to the colon is a rare occurrence, especially in the presence of changes in estrogen and progesterone receptors. To date, literature has only reported two cases of invasive ductal carcinoma and two cases of invasive lobular carcinoma metastasizing to the colon with concurrent changes in hormone receptors. This report describes a 65-year-old woman with a history of left breast cancer, who presented with symptoms of bloody stools and abdominal pain. CT and colonoscopy results revealed a malignant tumor in the ascending colon, and the patient underwent surgery. Pathological results post-surgery indicated changes in hormone receptors, differing from the previous breast cancer pathology, ultimately leading to the diagnosis of breast cancer metastasis to the colon. The patient was found to have liver metastasis 14 months after right hemicolectomy, and systemic metastases in various locations were discovered at the 19-month mark.

KEYWORDS

colon metastasis, progesterone receptor, estrogen receptor, non-specific types of breast cancer, breast cancer

Introduction

Breast cancer is the most common malignant tumor in women. Recurrence and distant metastasis often pose challenges in treatment. Common sites of metastasis include bones, liver, and lungs, while gastrointestinal metastases are extremely rare. Previous reports have shown that the pattern of metastasis differs between lobular carcinoma and ductal carcinoma of the

breast. Gastrointestinal, gynecologic, and peritoneal metastases are more common in lobular carcinoma (1, 2). ILC (invasive lobular carcinoma) has an increased tendency to metastasize to the GI (gastrointestinal) tract compared with breast carcinomas of NST (non-special type) (40% vs. 2%) (3). We report a case of infiltrating ductal carcinoma that metastasized to the ascending colon, with changes in estrogen receptor (ER), progesterone receptor (PR), and human epidermal growth factor receptor-2 (HER2) status. To our knowledge, there have been only two similar cases reported previously.

Case presentation

A 65-year-old woman presented to our center with intermittent abdominal pain and hematochezia for several months. She had a previous diagnosis of ER- and PR-positive (Figure 1), HER2 ++ (no

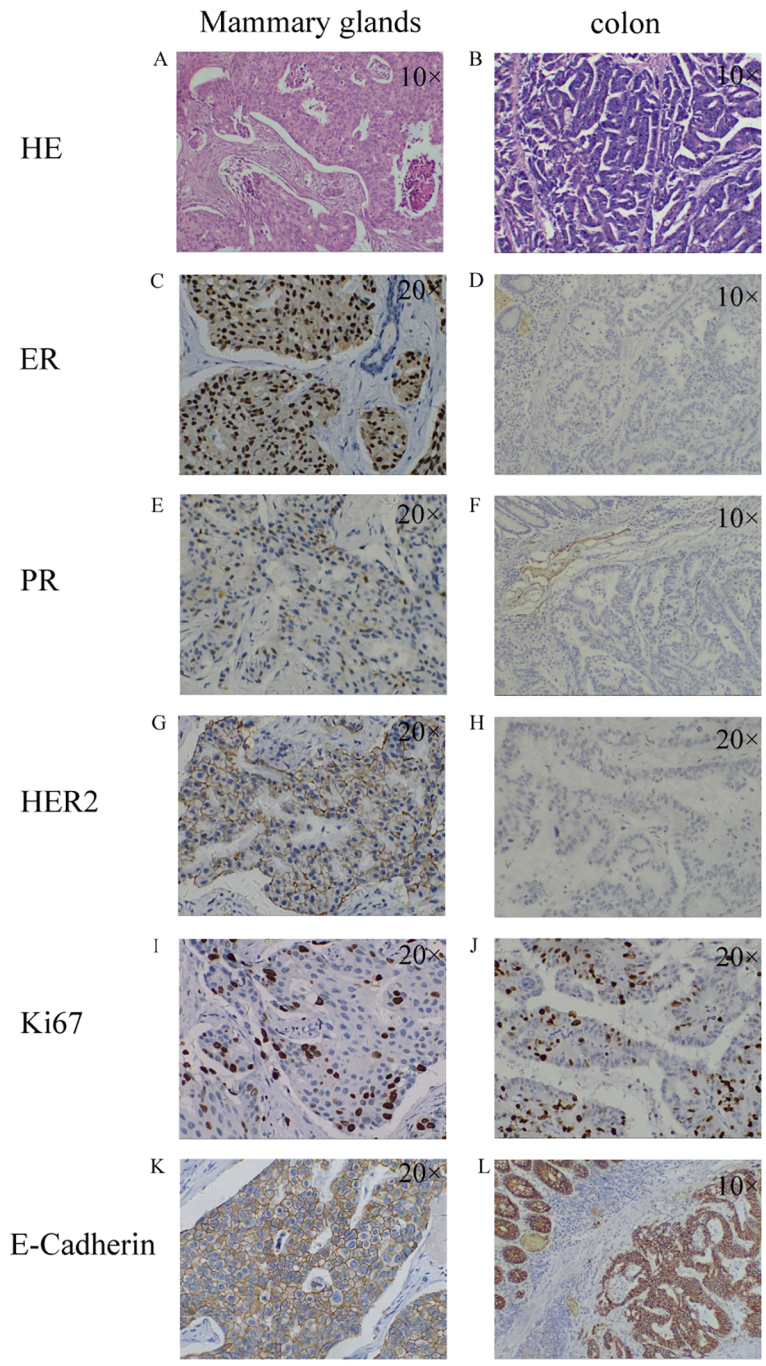

FIGURE 1
Pathological findings of breast malignancy and colon malignancy. breast malignancy: HE staining **(A)**; ER+ **(C)**; PR+ **(E)**; HER2+ **(G)**; Ki67 15%+ **(I)**; E-Cadherin + **(K)**; colon malignancy: HE staining **(B)**; ER- **(D)**; PR- **(F)**; HER2- **(H)**; Ki67 50%+ **(J)**; E-Cadherin+ **(L)**. HE staining: Hematoxylin-Eosin staining; ER: estrogen receptor; PR: progesterone receptor; HER2: human epidermal growth factor receptor-2; Ki67: nuclear-associated antigen Ki67.

further testing was done) invasive ductal carcinoma of the left breast 5 years before. She underwent modified radical mastectomy for breast cancer. The pathological examination did not indicate the presence of axillary lymph node metastasis and received chemotherapy with anthracycline and cyclophosphamide, followed by taxanes. Subsequently, she received 5 years of endocrine therapy with letrozole until she presented to our center. The patient denied having smoked or consumed alcohol in the past.

During colonoscopy, a mass was found in the ascending colon (Figure 2). Biopsy results confirmed metastasis of breast cancer to the colon, which was negative for ER, PR, and HER2. However, no local lesions or enlarged lymph nodes were detected in the contralateral breast, chest wall, or axilla through ultrasound, magnetic resonance imaging, and clinical palpation.

After receiving a transfusion of six units of red blood cells to correct anemia, the patient underwent a right hemicolectomy. Intraoperatively, it was observed that the tumor had invaded the right renal fascia. Two lymph node metastases were found on pathological examination after palliative surgery for colonic malignancy. The postoperative pathological examination confirmed the colonoscopy biopsy findings. Further immunohistochemical staining revealed positive results for Cytokeratin 7 (CK7), negative results for Cytokeratin 20 (CK20), and positive results for GATA 3 binding protein (GATA3) and E-Cadherin (Figure 3).

Considering the rarity of this case, we sought opinions from pathologists in different centers to confirm the diagnosis. After considering the majority of expert opinions, it was confirmed as breast cancer metastasis to the colon. The patient was prescribed oral capecitabine at a dosage of 650-mg/m^2 twice daily for chemotherapy treatment.

Follow-up imaging studies performed 6 months after the operation did not show any tumor metastasis or recurrence. However, the patient discontinued medication due to severe hand–foot syndrome. In a 14-month postoperative computed tomography (CT) scan, a solitary nodule was detected in the liver, indicating a metastatic lesion (Figure 4). The patient refused intravenous chemotherapy and opted for a second course of oral capecitabine treatment. Nineteen months after surgery, multiple metastases were discovered, including the liver, abdominal lymph nodes, adrenal glands, thoracolumbar spine, lungs, and mediastinal lymph nodes, accompanied by widespread cancer-related pain. The patient declined medication treatment. During the entire follow-up, no local recurrence of breast malignancy or new tumors of the opposite breast were found. The patient was lost to follow-up at 20 months after right hemicolectomy. Treatment and follow-up are organized into a timeline (Figure 5).

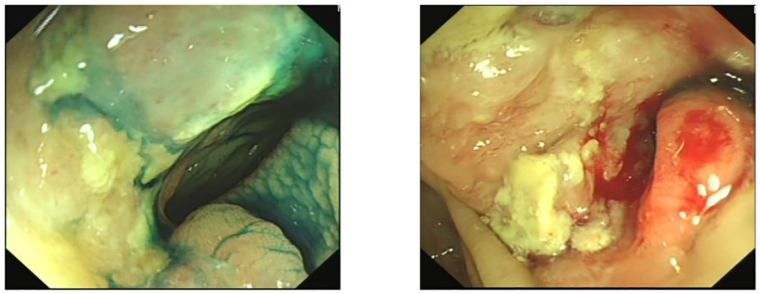

FIGURE 2
Colonoscopy revealed a mass of ascending colon.

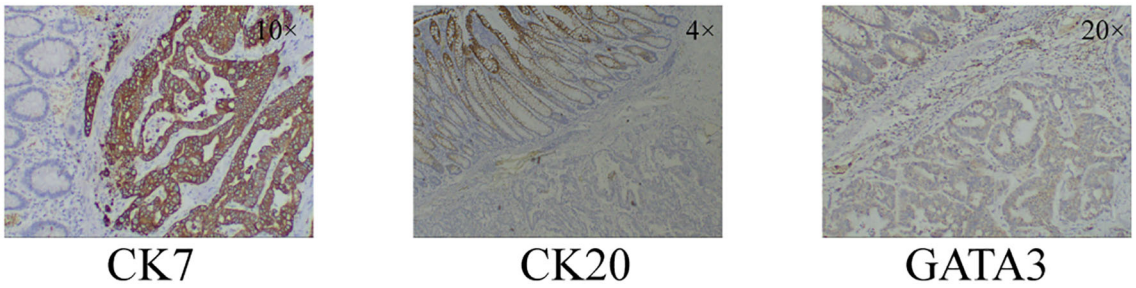

FIGURE 3
Immunohistochemical staining results of colonic malignancies. CK7+, CK20-, GATA3+. CK7: Cytokeratin 7; CK20: Cytokeratin 20; GATA3: GATA 3 binding protein.

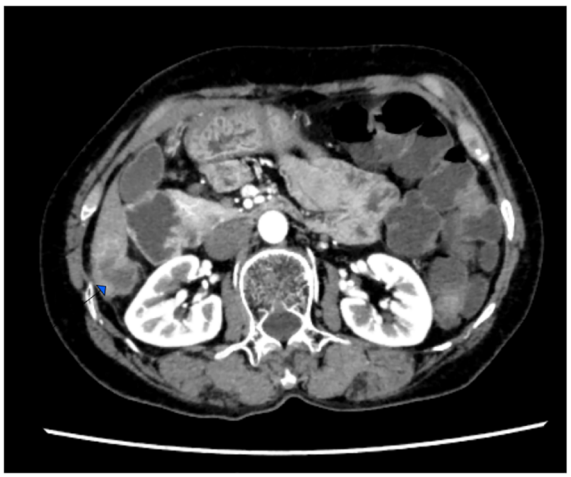

FIGURE 4
Computedtomography (CT) scan, a solitary nodule was detected in the liver, indicating a metastatic lesion.

Discussion

Breast cancer metastases to the gastrointestinal tract is extremely rare. Previous reports have shown that the most common sites of metastases in breast cancer are the bones, lungs, liver, and brain, while gastrointestinal metastases, especially to the colon, is very rare. The incidence of breast cancer metastases to the gastrointestinal tract, particularly to the colon, is estimated to be around 1%, with a rate of approximately 0.1% specifically for metastases to the colon (4). The patterns of metastases differ between lobular carcinoma and ductal carcinoma of the breast, with gastrointestinal metastases being more common in lobular carcinoma (1, 2). In this case, it was the ductal carcinoma of the breast that had colon metastases.

Due to the final diagnosis of breast cancer metastasis to the colon with receptor changes, this case presents significant challenges in terms of diagnosis and treatment. We performed a search in the PubMed database and gathered relevant literature, as detailed in Table 1. Our findings reveal the fourth documented case of ductal carcinoma of breast metastasizing to the colon, accompanied by changes in receptor status. Additionally, there have been two cases where receptor changes were observed when lobular carcinoma metastasized to the colon (5, 6).

In this case, there was a mismatch between the receptors in the primary breast lesion and the colon metastases. Incompatible receptors between the primary and secondary lesions of breast cancer have been reported, with frequencies of alterations in ER, PR, and HER2 being approximately 16.4%–32.4%, 30.9%–37.78%, and 10.2%–14.5%, respectively (7–10). Emilia Montagna reported in 2017 that approximately 82% of breast cancer metastases in the gastrointestinal tract have positive hormone receptor expression (11). In the dozens of case reports we have collected, the majority of patients were found to be hormone receptor positive. Among these patients, most did not exhibit any changes in the hormone receptor status. Previous reports have indicated that the instability of hormone receptors in breast cancer is associated with a poorer prognosis (12, 13), Women whose ER-positive primary tumors transform into ER-negative tumors experience a significant 48% increase in the risk of death (7). In this case report, liver metastases were found at 14 months after surgery, and multiple metastases throughout the body were found at 19 months with subsequent rapid disease progression.

CK7, CK20, and GATA3 are commonly used in pathology for tumor diagnosis and classification. These markers can provide information about the type and origin of the tumor. CK7 was expressed in 89%–98% of non-specified breast cancers (14). Most gastrointestinal, pancreaticobiliary, and ovarian mucinous adenocarcinomas are CK20 positivity, in adenocarcinoma, positivity of CK20 strongly indicates a non-breast origin, and CK7−/CK20+ immunoprofile strongly suggests colorectal origin (15). Based on previous research reports, CK7+/CK20 should be considered indicative of a tumor originating from the breast. GATA3 is also thought to be often positive in primary breast disease (16, 17). It was based on the immunohistochemical staining results of CK7 positive, CK20 negative, and GATA3 positive, combined with the opinions of multicenter pathologists, showing that the case was finally diagnosed as breast cancer with colon metastasis. Even though this case is very rare, we should still pay attention to the occurrence of colon metastasis in the diagnosis and treatment of breast cancer.

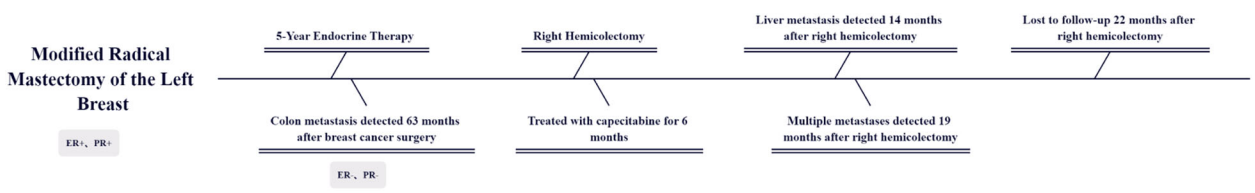

FIGURE 5
Timeline depicting the treatment and follow-up of the patient.

TABLE 1 Case reports of breast carcinomas with colonic metastases.

Author	Year	Age	Primary(breast)			Treatment	Time since first diagnosis (years)	Metastasis	
			Site	Pathological types	Biomarkers			Site	Biomarkers
Takeuchi H (18)	2012	38	left	ILC	ER+,PR-,HER2-	Surgery, Chemotherapy, Radiation therapy, Endocrine Therapy	3	Stomach and Colon	ER+,PR-, HER2- -
Jansen van Rensburg A (19)	2021	74	left	DC	ER+,PR-	Surgery, Radiation therapy, Endocrine Therapy	27	Bone,ovary, sigmoid colon	ER +, PR+ E-cadherin+, GATA3+,CK20-
Sheen-Chen SM (20)	2008	41	right	IDC	–	–	Simultaneous	ovary and omentum	- CK7+、CEA+、CK20-
Higley C (21)	2020	74	right	–	–	breast-conserving surgery and radiation therapy, Endocrine Therapy	40	transverse colon.	ER-、PR-、HER2- CDX-2-、CK20-、GATA3+、E-cadherin-、PD-L1-
Khan I (22)	2017	56	right	ring cell adenocarcinoma	–	–	Simultaneous	stomach, small intestine, and colon	–
Noor A (23)	2020	68	–	ILC	ER+,PR+,HER2-	Surgery, Radiation therapy, Endocrine Therapy	30	Bone、 sigmoid colon	ER+、PR+、HER2-,CK7+, CK20-,CDX2-,CA19-9-
Bering J (5)	2020	67	left	ILC	ER+,PR+,HER2-	Endocrine Therapy	Simultaneous	transverse colon	ER-,PR-,HER2+ GATA3+,CK7+,CDX2-,CK20-,E-cadherin-,GCDFP-15+
Abid A (24)	2013	59	left	LC	ER+,PR+,HER2-	–	Simultaneous	stomach, duodenum, and colon	ER+、PR+ GCDFP-15+
Takedomi H (4)	2019	76	right	ILC	–	Chemotherapy	Simultaneous	descending colon	- GCDFP-15+,mammaglobin+
Abu Zaanona MI (25)	2020	73	–	–	–	Endocrine Therapy	–	colon	ER+,PR-,HER2-,Pancytokeratin+, GATA3 +, E-cadherin-, CDX2-, SOX10-
Inoue H (26)	2022	63	right			Chemotherapy, Endocrine Therapy	15		ER+,PR-,HER2+,CK7+, GATA3+, ER+, HER2+, CK20-, PR-, E-cadherin-, GCDFP15- ,caudal-related homeobox 2
Mostafa A (27)	2002	56	–	IDC	ER+,PR+	Surgery, Radiation therapy, Endocrine Therapy	5	descending colon	ER-,PR–
Tsujimura K (28)	2017	51	left	ILC	ER+,PR+	–	Simultaneous	ileocecal	ER+,PR+,HER2-
Feng CL (29)	2009	49	right	IDC	–	–	2	Colon	CK7+, CK20-
Kobayashi M (30)	2020	74	–	ILC	–	surgery	23	stomach and colon	CAM5.2+,ER+, E-cadherin-
Théraux J (31)	2008	69	bilateral	IDC	–	Surgery, Endocrine Therapy	28	transverse colon	ER+,PR+, HER2-, CK7+, CK20-
Malhotra A (32)	2009	71	–	–	–	–	–	bone, transverse colon	–

(Continued)

10.3389/fonc.2024.1391393

TABLE 1 Continued

Author	Year	Age	Primary(breast)			Treatment	Time since first diagnosis (years)	Metastasis	
			Site	Pathological types	Biomarkers			Site	Biomarkers
Villa Guzmán JC (33)	2017	58	–	ILC	ER+,PR+,HER2-	Surgery, Chemotherapy, Radiation therapy, Endocrine Therapy	3	stomach	cytokeratin-19+,ER+
Gerova VA (34)	2012	56	left	ILC	PR+	Surgery, Chemotherapy, Radiation therapy, Endocrine Therapy	5	stenotic, stomach	–
		42	left	–	ER+,PR+	Surgery, Chemotherapy, Radiation therapy, Endocrine Therapy	7	stomach	ER+,PR+,CK7+, E-cadherin+,S-100+, GCFP15-,CDX2-
Wang G (35)	2014	70	left	IDC	E-cadherin+、34βE12-、ER+、PR+、CK19+、CK20+	Surgery, Radiation therapy, Endocrine Therapy	10	ascending colon	CK7+、E-cadherin+、34βE12-、ER+、GCDFP-15+、CK19+、CK20+
Cho DH (36)	2011	46	bilateral	IDC	ER+,PR+,HER2-	Surgery, Chemotherapy, Radiation therapy, Endocrine Therapy	2	terminal ileum	ER+,PR-,HER2+,
Algethami NE (37)	2022	47	bilateral	ILC	ER+,PR+,HER2-	Surgery, Radiation therapy, Endocrine Therapy	4	rectum	ER+、HER2+、Pan-cytokeratin +
Zhou XC (38)	2012	54	right	IDC	ER+,PR+,P53+, HER2-	Surgery, Chemotherapy, Radiation therapy, Endocrine Therapy	8	sigmoid colon	CDX2-, Villin-, TTF-1-, -CK20-, HER2-, ER- ,PR-, CK7+,p53+
Andriola V (39)	2014	63	left	IDC,LC	–	Surgery, Chemotherapy, Radiation therapy, Endocrine Therapy	23	colon and terminal ileum	CK19+, GCFDP-15+,HER2+
Motos-Micó J (40)	2014	69	right	ILC	–	Surgery, Chemotherapy	18	sigmoid colon	ER-,PR-,HER2-,CK7+
Abdallah H (41)	2020	59	right	ILC	ER+,PR+,HER2-	–	Simultaneous	endometrium, myometrium, fibroid and cervix	CK7+,GATA3+,ER+,PR+, desmin-, CD10-, actin-,Caldesmon-
		66	right	ILC	CK+,ER+,PR+,HER2-	–	Simultaneous	Colon	CK7+,GATA-3+,ER+,CK20-,CDX2-
		53	right	ILC	–	–	Simultaneous	intestine, omentum, and peritoneal wall, bilateral ovarian, stomach	CK7+、GATA-3+,ER+,E-cadherin+,CK20-,CDX2-
Michalopoulos A (42)	2004	55	left	IDC	–	Surgery, Chemotherapy	4	transverse colon	CK7+,milk-fat globule protein+,
		57	left	ILC	–	Surgery, Chemotherapy, Radiation therapy	10	transverse colon	CK7+,milk-fat globule protein+, CEA+,ER+, weakly positive for cytokeratin 20 and Breast II.
Schellenberg AE (43)	2018	69	left	IDC	E-cadherin+,ER+,PR+, HER2+	Surgery, Chemotherapy, Radiation therapy, Endocrine Therapy	2	rectosigmoid	CK-7+, E-cadherin+, GCDFP+, mammoglobin+,ER+,PR+,CK-20-,CDX-2–

(Continued)

10.3389/fonc.2024.1391393

TABLE 1 Continued

Author	Year	Age	Primary(breast)			Treatment	Time since first diagnosis (years)	Metastasis	
			Site	Pathological types	Biomarkers			Site	Biomarkers
Matsuda I (44)	2012	62	left	ILC	–	Surgery	24	ascending colon and rectum	CK7+,ER+,CK20-,E-cadherin-
Koleilat I (45)	2010	54	right	IDC	–	Surgery, Chemotherapy, Radiation therapy, Endocrine Therapy	13	colon	ER+,PR+,HER2-
Mistrangelo M (46)	2011	80	left	ILC	–	Surgery, Endocrine Therapy	25	sigmoid colon	–
Razzetta F (47)	2011	77	bilateral	ILC(left),IDC(right)	–	–	Simultaneous	right, transverse and left colon	ER+,PR-
Cervi G (48)	2001	59	–	ILC	–	Surgery	8	rectum	ER+,PR+
Amin AA (49)	2011	61	right	ILC	–	Surgery, Endocrine Therapy	17	rectum	CK 20-,ER+,CK7+,PR+
López Deogracias M (6)	2009	67	left	ILC	ER+,PR+	Surgery	15	rectum	ER-,PR-,CK20-,CDX2-
Law WL (50)	2003	49	left	IDC	ER+	Surgery, Endocrine Therapy	5	descending colon	ER+
Samra B (51)	2019	64	–	–	–	–	–	colon,right sacral iliac	CK-7+,GATA-3+,ER+,MOC31+,CK-20-,CD-X2-, PR-,PAX-8-,SOX-10-,CD4-5,chromogranin-, synaptophysin-, TTF-1-
Kim HW (52)	2014	46	right	metaplastic	ER-,PR-,HER2-	Surgery, Chemotherapy, Radiation therapy	2	sigmoid colon	CK20-,CK5/6-,ER-,PR-,HER2-,CK7+
Signorelli C (53)	2005	62	right	ILC	–	Surgery	12	right chest wall, colon	ER+,PR+,P53-,HER2-
Gizzi G (54)	2015	72	–	–	ER+,PR+	Surgery, Chemotherapy, Radiation therapy, Endocrine Therapy	11	sigmoid colon	CK7+,GATA3+, ER+,PR+,HER2-
Dhar S (55)	2003	75	left	–	ER+	Surgery	6	sigmoid colon	ER+,CK7+,CK20-
Maekawa H (56)	2012	52	right	IDC	ER+,PR+	Surgery, Chemotherapy, Radiation therapy, Endocrine Therapy	16	ascending colon	–
Koufopoulos N (57)	2018	87	–	–	–	–	–	Colonic serosa	CK-20-,CDX-2-,CK7-,r GATA-3+, mammaglogin+, ER+,PR+, E-cadherin-, Chromogranin- ,synaptophysin-
Critchley AC (58)	2011	62	–	IDC	–	Surgery, Chemotherapy, Radiation therapy, Endocrine Therapy	8	stomach, ascending colon	ER+,PR+,HER2-,CK7+,CK20-
Kachi A (59)	2019	58	left	ILC	–	Surgery, Chemotherapy, Radiation therapy, Endocrine Therapy	6	sigmoid colon, appendix, and ovaries.	ER+,PR+
Blachman-Braun R (60)	2018	73	bilateral	–	–	Surgery, Chemotherapy,	15	colon	ER+,PR-,HER2-

(Continued)

10.3389/fonc.2024.1391393

TABLE 1 Continued

Author	Year	Age	Primary(breast)			Treatment	Time since first diagnosis (years)	Metastasis	
			Site	Pathological types	Biomarkers			Site	Biomarkers
Jia J (61)	2023	67	right	IDC	ER+,PR+,HER2-	Surgery, Chemotherapy, Endocrine Therapy	10	Appendix, colon	GATA-3+,GCDFP-15+,ER+,PR+,HER2+, E-cadherin+,p120+,CK7+,CK20-,SATB-2-,Villin-syn-, CgA-,CD56-
Arif FZ (62)	2023	65	bilateral	IDC	triple-negative (left), HER2+(right)	-	-	descending colon	-

ILC, Invasive lobular carcinoma; IDC, Invasive ductal carcinoma; DC, ductal carcinoma; LC, lobular carcinoma; ER, estrogen receptor; PR, progesterone receptor; HER2, human epidermal growth factor receptor-2; CK7, Cytokeratin 7; CK20, Cytokeratin 20; GATA3, GATA 3 binding protein. CEA, Carcinoembryonic antigen; CDX2, caudal-related homeobox transcription factor 2; GCDFP, Gross cystic disease fluid protein; CAM5.2, cytokeratin CAM5.2; S-100, closely related, small, acidic Ca2+-binding proteins; 34βE12, cytokeratin 34βE12; P53, tumour suppressor gene p53; PAX-8, a nephric cell lineage transcription factor; SOX-10, SRY-related HMG-box 10; CD45, receptor-like protein tyrosine phosphatase; TTF-1, Thyroid transcription factor 1; CK5/6, cytokeratin 5/6; p120, p120-catenin; SATB-2, special AT-rich sequence-binding protein 2; syn, Synuclein; CgA, Chlorogenic acid; CD56, Neural cell adhesion molecule; SOX10, transcription factors SOX10.

Conclusions

This case serves as a reminder to clinicians that they should consider rare sites of metastases and different receptor expression patterns in breast cancer patients in order to make more accurate treatment decisions. However, further research is needed to explore the mechanisms of this metastatic pattern and related treatment strategies.

Data availability statement

The datasets presented in this article are not readily available due to participant privacy. Requests to access the datasets should be directed to the corresponding authors.

Ethics statement

The studies involving humans were approved by Ethics Review Committee of Southern Central Hospital of Yunnan Province. The studies were conducted in accordance with the local legislation and institutional requirements. The participants provided their written informed consent to participate in this study. Written informed consent was obtained from the individual(s) for the publication of any potentially identifiable images or data included in this article.

Author contributions

HL: Investigation, Resources, Writing – original draft, Writing – review & editing. LY: Investigation, Writing – original draft. XS: Investigation, Writing – original draft. GL: Investigation, Writing – original draft. WG: Resources, Writing – original draft. FM: Writing – review & editing. ZW: Writing – review & editing. SQ: Writing – review & editing. CL: Writing – review & editing.

Funding

The author(s) declare financial support was received for the research, authorship, and/or publication of this article. The present study was supported by the Scientific Research Project of Southern Central Hospital of Yunnan Province (grant no.KY202401).

Conflict of interest

The authors declare that the research was conducted in the absence of any commercial or financial relationships that could be construed as a potential conflict of interest.

Publisher's note

All claims expressed in this article are solely those of the authors and do not necessarily represent those of their affiliated organizations, or those of the publisher, the editors and the reviewers. Any product that may be evaluated in this article, or claim that may be made by its manufacturer, is not guaranteed or endorsed by the publisher.

References

1. Borst MJ, Ingold JA. Metastatic patterns of invasive lobular versus invasive ductal carcinoma of the breast. *Surgery*. (1993) 114:637–41; discussion 641-2.

2. Kennecke H, Yerushalmi R, Woods R, Cheang MC, Voduc D, Speers CH, et al. Metastatic behavior of breast cancer subtypes. *J Clin Oncol*. (2010) 28:3271–7. doi: 10.1200/JCO.2009.25.9820

3. Kioleoglou Z, Georgaki E, Koufopoulos N, Kostek O, Volakakis N, Dimitriadou A, et al. Gastrointestinal metastases from lobular breast carcinoma: A literature review. *Cureus*. (2024) 16:e65852. doi: 10.7759/cureus.65852

4. Takedomi H, Akutagawa T, Sakata Y. Colon metastasis of breast cancer with a unique endoscopic finding. *Clin Gastroenterol Hepatol*. (2020) 18:e74. doi: 10.1016/j.cgh.2019.04.014

5. Bering J, Ryan M, Gurudu SR. Breast cancer metastasis presenting as colonic polyps. *ACG Case Rep J*. (2020) 7:e00411. doi: 10.14309/crj.0000000000000411

6. López Deogracias M, Flores Jaime L, Arias-Camisón I, Zamacola I, Murillo Guibert J, Suescun García R, et al. Rectal metastasis from lobular breast carcinoma 15 years after primary diagnosis. *Clin Transl Oncol*. (2010) 12:150–3. doi: 10.1007/S12094-010-0481-0

7. Lindström LS, Karlsson E, Wilking UM, Johansson U, Hartman J, Lidbrink EK, et al. Clinically used breast cancer markers such as estrogen receptor, progesterone receptor, and human epidermal growth factor receptor 2 are unstable throughout tumor progression. *J Clin Oncol*. (2012) 30:2601–8. doi: 10.1200/JCO.2011.37.2482

8. Matsumoto A, Jinno H, Murata T, Seki T, Takahashi M, Hayashida T, et al. Prognostic implications of receptor discordance between primary and recurrent breast cancer. *Int J Clin Oncol*. (2015) 20:701–8. doi: 10.1007/s10147-014-0759-2

9. Yang Z, Li N, Li X, Lei L, Wang X. The prognostic impact of hormonal receptor and HER-2 expression discordance in metastatic breast cancer patients. *Onco Targets Ther*. (2020) 13:853–63. doi: 10.2147/OTT.S231493

10. Zhao W, Sun L, Dong G, Wang X, Jia Y, Tong Z. Receptor conversion impacts outcomes of different molecular subtypes of primary breast cancer. *Ther Adv Med Oncol*. (2021) 13:17588359211012982. doi: 10.1177/17588359211012982

11. Montagna E, Pirola S, Maisonneuve P, De Roberto G, Cancello G, Palazzo A, et al. Lobular metastatic breast cancer patients with gastrointestinal involvement: features and outcomes. *Clin Breast Cancer*. (2018) 18:e401–401e405. doi: 10.1016/j.clbc.2017.07.003

12. Yang YF, Liao YY, Yang M, Peng NF, Xie SR, Xie YF. Discordances in ER, PR and HER2 receptors between primary and recurrent/metastatic lesions and their impact on survival in breast cancer patients. *Med Oncol*. (2014) 31:214. doi: 10.1007/s12032-014-0214-2

13. Yamanouchi K, Kuba S, Eguchi S. Hormone receptor, human epidermal growth factor receptor-2, and Ki-67 status in primary breast cancer and corresponding recurrences or synchronous axillary lymph node metastases. *Surg Today*. (2020) 50:657–63. doi: 10.1007/s00595-019-01831-8

14. Lu S, Yakirevich E, Wang LJ, Resnick MB, Wang Y. Cytokeratin 7-negative and GATA binding protein 3-negative breast cancers: Clinicopathological features and prognostic significance. *BMC Cancer*. (2019) 19:1085. doi: 10.1186/s12885-019-6295-8

15. Lerwill MF. Current practical applications of diagnostic immunohistochemistry in breast pathology. *Am J Surg Pathol*. (2004) 28:1076–91. doi: 10.1097/01.pas.0000126780.10029.f0

16. Gown AM, Fulton RS, Kandalaft PL. Markers of metastatic carcinoma of breast origin. *Histopathology*. (2016) 68:86–95. doi: 10.1111/his.12877

17. Davies T, Chouari T, Ray C, Elgammal S. Appendiceal adenocarcinoma with breast metastases. *BMJ Case Rep*. (2021) 14. doi: 10.1136/bcr-2020-240808

18. Takeuchi H, Hiroshige S, Yoshikawa Y, Kusumoto T, Muto Y. A case of synchronous metastasis of breast cancer to stomach and colon. *Anticancer Res*. (2012) 32:4051–5.

19. Jansen van Rensburg A, Riddell A. A case report of ductal carcinoma of the breast metastasizing to the bowel. *J Surg Case Rep*. (2021) 2021:rjab471. doi: 10.1093/jscr/rjab471

20. Sheen-Chen SM, Liu YW, Sun CK, Lin SE, Eng HL, Huang WT, et al. Abdominal carcinomatosis attributed to metastatic breast carcinoma. *Dig Dis Sci*. (2008) 53:3043–5. doi: 10.1007/s10620-008-0529-y

21. Higley C, Hsu A, Park BU, Pang M. Back to basics: history and physical examination uncover colonic metastasis in a patient with remote history of breast cancer. *ACG Case Rep J*. (2020) 7:e00494. doi: 10.14309/crj.0000000000000494

22. Khan I, Malik R, Khan A, Assad S, Zahid M, Sohail MS, et al. Breast cancer metastases to the gastrointestinal tract presenting with anemia and intra-abdominal bleed. *Cureus*. (2017) 9:e1429. doi: 10.7759/cureus.1429

23. Noor A, Lopetegui-Lia N, Desai A, Mesologites T, Rathmann J. Breast cancer metastasis masquerading as primary colon and gastric cancer: A case report. *Am J Case Rep*. (2020) 21:e917376. doi: 10.12659/AJCR.917376

24. Abid A, Moffa C, Monga DK. Breast cancer metastasis to the GI tract may mimic primary gastric cancer. *J Clin Oncol*. (2013) 31:e106–7. doi: 10.1200/JCO.2012.44.6393

25. Abu Zaanona MI, Gulati A, Rowland K. Colon metastases as first clinical manifestation of lobular breast carcinoma with no subsequent evidence of breast disease. *BMJ Case Rep*. (2020) 13. doi: 10.1136/bcr-2020-236225

26. Inoue H, Arita T, Kuriu Y, Shimizu H, Kiuchi J, Yamamoto Y, et al. Colonic metastasis from breast cancer: A case report and review of the literature. *In Vivo*. (2022) 36:522–7. doi: 10.21873/invivo.12733

27. Mostafa A, Carpenter R. Colonic metastasis from a breast cancer a case report and a few questions. *Eur J Surg Oncol*. (2002) 28:462. doi: 10.1053/ejso.2002.1174

28. Tsujimura K, Teruya T, Kiyuna M, Higa K, Higa J, Iha K, et al. Colonic metastasis from breast carcinoma: a case report. *World J Surg Oncol*. (2017) 15:124. doi: 10.1186/s12957-017-1193-5

29. Feng CL, Chou JW, Huang SF. Colonic metastasis from carcinoma of the breast presenting with colonic erosion. *Endoscopy*. (2009) 41 Suppl 2:E276–7. doi: 10.1055/s-0029-1215066

30. Kobayashi M, Tashima T, Nagata K, Sakuramoto S, Osaki A, Ryozawa S. Colorectal and gastric metastases from lobular breast cancer that resembled superficial neoplastic lesions. *Clin J Gastroenterol*. (2021) 14:103–8. doi: 10.1007/s12328-020-01285-3

31. Théraux J, Bretagnol F, Guedj N, Cazals-Hatem D, Panis Y. Colorectal breast carcinoma metastasis diagnosed as an obstructive colonic primary tumor. A case report and review of the literature. *Gastroenterol Clin Biol*. (2009) 33:1114–7. doi: 10.1016/j.gcb.2009.05.015

32. Malhotra A, Guturu P, Basim MS, Raju GS. A rare case of breast cancer metastasis presenting as linitis plastica of the stomach and colon (with videos). *Gastrointest Endosc*. (2009) 70:552–3; discussion 553. doi: 10.1016/j.gie.2009.04.029

33. Villa Guzmán JC, Espinosa J, Cervera R, Delgado M, Patón R, Cordero García JM. Gastric and colon metastasis from breast cancer: case report, review of the literature, and possible underlying mechanisms. *Breast Cancer (Dove Med Press)*. (2017) 9:1–7. doi: 10.2147/BCTT.S79506

34. Gerova VA, Tankova LT, Mihova AA, Drandarska IL, Kadian HO. Gastrointestinal metastases from breast cancer: report of two cases. *Hepatogastroenterology*. (2012) 59:178–81. doi: 10.5754/hge10681

35. Wang G, Wang T, Jiang J, Zhou L, Zhao H. Gastrointestinal tract metastasis from tubulolobular carcinoma of the breast: a case report and review of the literature. *Onco Targets Ther*. (2014) 7:435–40. doi: 10.2147/OTT.S57831

36. Cho DH, Jeon YS, Choi MY, Lee SK, Kim SM, Hur SM, et al. Ileal metastasis of breast cancer in a patient with a BRCA2 gene mutation: report of a case. *Surg Today*. (2011) 41:1665–9. doi: 10.1007/s00595-011-4503-5

37. Algethami NE, Althagafi AA, Aloufi RA, Al Thobaiti FA, Abdelaziz HA. Invasive lobular carcinoma of the breast with rectal metastasis: A rare case report. *Cureus*. (2022) 14:e23666. doi: 10.7759/cureus.23666

38. Zhou XC, Zhou H, Ye YH, Zhang XF, Jiang Y. Invasive ductal breast cancer metastatic to the sigmoid colon. *World J Surg Oncol*. (2012) 10:256. doi: 10.1186/1477-7819-10-256

39. Andriola V, Piscitelli D, De Fazio M, Altomare DF. Massive colonic metastasis from breast cancer 23 years after mastectomy. *Int J Colorectal Dis*. (2015) 30:427–8. doi: 10.1007/s00384-014-1992-x

40. Motos-Micó J, Ferrer-Márquez M, Belda-Lozano R, Reina-Duarte Á, Rosado-Cobián R. Metastasis of lobular breast carcinoma in the sigmoid colon. *Rev Esp Enferm Dig*. (2014) 106:366–7.

41. Abdallah H, Elwy A, Alsayed A, Rabea A, Magdy N. Metastatic breast lobular carcinoma to unusual sites: A report of three cases and review of literature. *J Med Cases*. (2020) 11:292–5. doi: 10.14740/jmc3538

42. Michalopoulos A, Papadopoulos V, Zatagias A, Fahantidis E, Apostolidis S, Haralabopoulos E, et al. Metastatic breast adenocarcinoma masquerading as colonic primary. Report of two cases. *Tech Coloproctol*. (2004) 8 Suppl 1:s135–7. doi: 10.1007/s10151-004-0135-8

43. Schellenberg AE, Wood ML, Baniak N, Hayes P. Metastatic ductal carcinoma of the breast to colonic mucosa. *BMJ Case Rep*. (2018) 2018. doi: 10.1136/bcr-2018-224216

44. Matsuda I, Matsubara N, Aoyama N, Hamanaka M, Yamagishi D, Kuno T, et al. Metastatic lobular carcinoma of the breast masquerading as a primary rectal cancer. *World J Surg Oncol*. (2012) 10:231. doi: 10.1186/1477-7819-10-231

45. Koleilat I, Syal A, Hena M. Metastatic male ductal breast cancer mimicking obstructing primary colon cancer. *Int J BioMed Sci*. (2010) 6:66–70. doi: 10.59566/IJBS.2010.6066

46. Mistrangelo M, Cassoni P, Mistrangelo M, Castellano I, Codognotto E, Sapino A, et al. Obstructive colon metastases from lobular breast cancer: report of a case and review of the literature. *Tumori*. (2011) 97:800–4. doi: 10.1177/030089161109700619

47. Razzetta F, Tassara E, Saro F, Sironi M, D'Ambrosio G. Rare abdominal metastases from occult lobular breast cancer: report of two cases. *Updates Surg*. (2011) 63:129–33. doi: 10.1007/s13304-011-0047-x

48. Cervi G, Vettoretto N, Vinco A, Cervi E, Villanacci V, Grigolato P, et al. Rectal localization of metastatic lobular breast cancer: report of a case. *Dis Colon Rectum*. (2001) 44:453–5. doi: 10.1007/BF02234749

49. Amin AA, Reddy A, Jha M, Prasad K. Rectal metastasis from breast cancer: an interval of 17 years. *BMJ Case Rep*. (2011) 2011. doi: 10.1136/bcr.01.2011.3683

50. Law WL, Chu KW. Scirrhous colonic metastasis from ductal carcinoma of the breast: report of a case. *Dis Colon Rectum*. (2003) 46:1424–7. doi: 10.1007/s10350-004-6762-3

51. Samra B, Ghanem S, Ilyas G, Taiwo E. Screening colonoscopy unmasking colonic metastasis from an occult breast ductal carcinoma: A case report and review of the literature. *Case Rep Oncol Med*. (2019) 2019:8432079. doi: 10.1155/2019/8432079

52. Kim HW, Moon DH. Sigmoid colon metastasis from metaplastic breast carcinoma mimicking primary sigmoid colon cancer. *Rev Esp Med Nucl Imagen Mol*. (2015) 34:211–2. doi: 10.1016/j.remn.2014.09.002

53. Signorelli C, Pomponi-Formiconi D, Nelli F, Pollera CF. Single colon metastasis from breast cancer: a clinical case report. *Tumori*. (2005) 91:424–7. doi: 10.1177/030089160509100509

54. Gizzi G, Santini D, Guido A, Fuccio L. Single colonic metastasis from breast cancer 11 years after mastectomy. *BMJ Case Rep*. (2015) 2015:bcr2015211193. doi: 10.1136/bcr-2015-211193

55. Dhar S, Kulaylat MN, Gordon K, Lall P, Doerr RJ. Solitary papillary breast carcinoma metastasis to the large bowel presenting as primary colon carcinoma: case report and review of the literature. *Am Surg*. (2003) 69:799–803. doi: 10.1177/000313480306900914

56. Maekawa H, Fujikawa T, Tanaka A. Successful laparoscopic investigation and resection of solitary colonic metastasis from breast cancer (with video). *BMJ Case Rep*. (2012) 2012. doi: 10.1136/bcr-2012-007187

57. Koufopoulos N, Goudeli C, Pigadioti E, Balalis D, Manatakis DK, Antoniadou F, et al. Synchronous colonic adenocarcinoma and metastatic lobular carcinoma in a colectomy specimen: A rare finding. *Cureus*. (2018) 10:e3207. doi: 10.7759/cureus.3207

58. Critchley AC, Harvey J, Carr M, Iwuchukwu O. Synchronous gastric and colonic metastases of invasive lobular breast carcinoma: case report and review of the literature. *Ann R Coll Surg Engl*. (2011) 93:e49–50. doi: 10.1308/147870811X582800

59. Kachi A, Nicolas G, Semaan DB, Hashem M, Abou Sleiman C. Unusual pattern of invasive lobular carcinoma metastasis: A case report. *Am J Case Rep*. (2019) 20:1659–63. doi: 10.12659/AJCR.917237

60. Blachman-Braun R, Felemovicius I, Barker K, Kehrberg E, Khan F. Widespread metastatic breast cancer to the bowel: an unexpected finding during colonoscopy. *Oxf Med Case Rep*. (2019) 2019:omy133. doi: 10.1093/omcr/omy133

61. Jia J, Huang Y, Li X. Ascending colon metastasis after breast cancer surgery: a case report and literature review. *Gland Surg*. (2023) 12:309–16. doi: 10.21037/gs-22-642

62. Arif FZ, Breese RO, Burke R. Breast cancer metastasis to colon. *Am Surg*. (2023) 89:3873–4. doi: 10.1177/00031348231173979

frontiers | Frontiers in Oncology

TYPE Case Report
PUBLISHED 30 January 2025
DOI 10.3389/fonc.2025.1500785

Check for updates

OPEN ACCESS

EDITED BY
Vladimir Spiegelman,
Penn State Milton S. Hershey Medical Center, United States

REVIEWED BY
Gianluca Nazzaro,
IRCCS Ca 'Granda Foundation Maggiore Policlinico Hospital, Italy
Andrey A. Yurchenko,
INSERM U981 Prédicteurs moléculaires et nouvelles cibles en oncologie (PMNCO), France
Cosimo Di Raimondo,
Policlinico Tor Vergata, Italy

*CORRESPONDENCE
Wolfram Samlowski
wsamlowski1@gmail.com

RECEIVED 23 September 2024
ACCEPTED 13 January 2025
PUBLISHED 30 January 2025

CITATION
Lambert-Swainston C, Samlowski W, Reynolds B and Hedayat A (2025) Case report: Complete response of recurrent locally advanced basal cell carcinoma following addition of vismodegib to neoadjuvant cemiplimab therapy. *Front. Oncol.* 15:1500785. doi: 10.3389/fonc.2025.1500785

COPYRIGHT
© 2025 Lambert-Swainston, Samlowski, Reynolds and Hedayat. This is an open-access article distributed under the terms of the Creative Commons Attribution License (CC BY). The use, distribution or reproduction in other forums is permitted, provided the original author(s) and the copyright owner(s) are credited and that the original publication in this journal is cited, in accordance with accepted academic practice. No use, distribution or reproduction is permitted which does not comply with these terms.

Case report: Complete response of recurrent locally advanced basal cell carcinoma following addition of vismodegib to neoadjuvant cemiplimab therapy

Chalette Lambert-Swainston[1], Wolfram Samlowski[1,2,3]*, Brandon Reynolds[4] and Amin Hedayat[5,6]

[1]Kirk Kerkorian School of Medicine, Department of Internal Medicine, University of Nevada Las Vegas (UNLV), Las Vegas, NV, United States, [2]Comprehensive Cancer Centers of Nevada, Las Vegas, NV, United States, [3]Department of Internal Medicine, University of Nevada School of Medicine, Reno, NV, United States, [4]Reynolds Plastic Surgery, Las Vegas, NV, United States, [5]Quest Diagnostics, Associated Pathologists Chartered, Las Vegas, NV, United States, [6]American Melanoma Institute, Las Vegas, NV, United States

Locally advanced basal cell carcinoma (laBCC) remains a significant management challenge. Historically, surgery or radiotherapy represented the major treatment options. Recently, hedgehog inhibitors and checkpoint inhibitors have demonstrated significant activity. The optimal sequencing of these approaches is not yet known. We describe a case of laBCC that recurred after definitive radiotherapy. This patient was treated with neoadjuvant cemiplimab with minimal response. Cautious addition of vismodegib with ongoing cemiplimab treatment was well tolerated and resulted in significant tumor regression. A wide excision demonstrated a pathologic complete response. Further evaluation of cemiplimab and hedgehog inhibitor combination therapy in la BCC appears warranted.

KEYWORDS

hedgehog inhibitor, checkpoint inhibitor, targeted therapy, immunotherapy, keratinocyte carcinoma

Background

Basal cell carcinoma (BCC) represents the most common form of skin cancer in the United States, with 3.3-5.4 million individuals affected per year (1). A small percentage of patients neglect a developing BCC, which can become large and deeply invasive. The frequency of locally advanced basal cell (laBCC) carcinoma is not well characterized but is estimated to be 1.28/100,000 individuals in the US each year, resulting in 7940 annual cases (2). Historically, radical surgery or radiotherapy were the major treatment options for laBCC patients. Unfortunately, these treatments resulted in a high recurrence rate.

The "hedgehog" signaling pathway was identified as a key regulatory pathway for epidermal cell growth and development (3). Mutations in this pathway occur in the majority of patients with either sporadic or inherited forms of BCC (e.g., Gorlin's syndrome). These mutations lead to constitutive activation of the pathway, resulting in progressive cell growth (4). Oral small-molecule hedgehog inhibitors (HHI), such as vismodegib and sonidegib have significant activity in la BCC and can induced rapid and deep responses in many patients with modest systemic toxicity (5, 6). Unfortunately, most patients eventually progress despite continued HHI therapy (7, 8).

The PD-1 antibody cemiplimab has also been evaluated in patients with laBCC, who were not candidates for curative surgery or radiation, and who had progressed after HHI therapy. These studies demonstrated that cemiplimab has a significant clinical response rate in HHI refractory patients, with about 1/3 of patients achieving long-term responses or remissions (9). More recently, neoadjuvant cemiplimab has been tested prior to definitive local therapy in keratinocyte-derived skin cancers (10).

Case report

A 43-year-old Caucasian man presented with a large 8 x 8 cm ulcerated basal cell carcinoma located at the base of the neck overlying the right trapezius (Figure 1A). The patient had been diagnosed with laBCC four years previously that had been treated with external beam radiotherapy with 73.8 cGy in 40 fractions. The patient was lost to follow-up for two years, but eventually sought medical attention due to the rapidly increasing size to 8x5 cm of a recurrent lesion, associated with pain and bleeding.

As the patient had previously received maximal radiotherapy, a surgical consultant suggested a wide surgical excision. Due to size of the lesion, there were concerns about potential deep tissue invasion and proximity to cranial nerve XI. A large skin graft or flap reconstruction were considered necessary as part of the post-operative reconstruction. Due to his perception of potential side-effects, the patient declined prolonged hedgehog inhibitor therapy. After multidisciplinary discussion the patient was treated with neoadjuvant cemiplimab therapy, with the goal of cytoreduction. After three doses of cemiplimab (350mg fixed dose) given intravenously three weeks apart, there was little clinical change in the lesion (8 x 5 cm). At the time of the third dose, oral vismodegib was cautiously added (150 mg p.o. daily), to try to increase the clinical response. After this modification of treatment, the lesion decreased in size and began to re-epithelialize. The patient received a total of 6 doses of cemiplimab (350 mg every 3 weeks) and 11 weeks of daily oral vismodegib (150 mg/d), with a progressive reduction in size of the lesion to approximately 2-2.5 cm. The patient subsequently underwent excision of the previously involved area with a skin graft repair (Figure 1B). Evaluation of the resection specimen by pathology confirmed a complete remission (Figure 2).

Vismodegib treatment was well tolerated with side effects. The patient described minimal loss of taste and mild hair thinning, which resolved after drug discontinuation. There was no apparent cemiplimab associated immune adverse events, either during monotherapy or following addition of vismodegib. The patient currently continues to be disease free at 24 months post resection. A graphic schema to the treatment course is provided (Figure 3).

Discussion

We evaluated a young man with a large laBCC that had recurred after primary radiotherapy. Multidisciplinary discussion recommended initial systemic therapy.

We considered the use of HHI therapy. While this treatment has been shown to have a high response rate, eventual progression

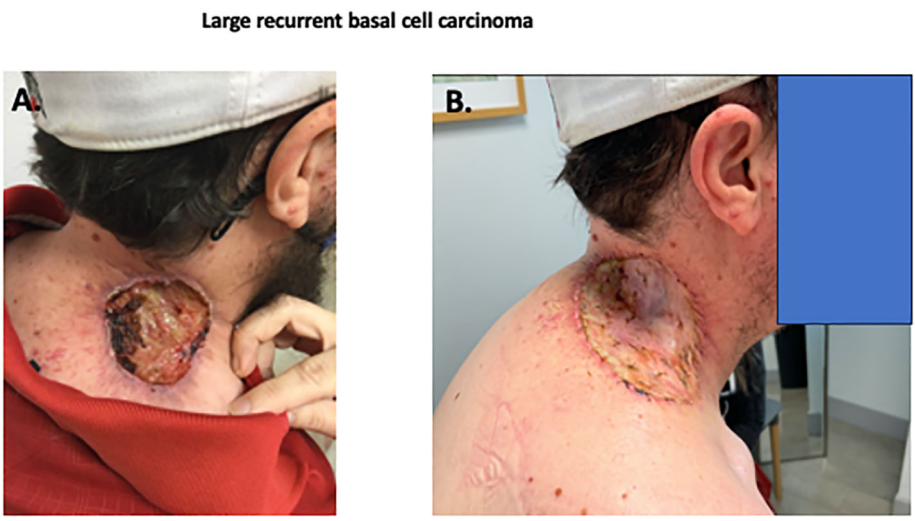

FIGURE 1
Photographs of recurrent BCC. Initial skin lesion **(A)** demonstrating a deeply invasive nodular basal cell carcinoma, Resection of skin lesion with skin graft **(B)** with no residual BCC.

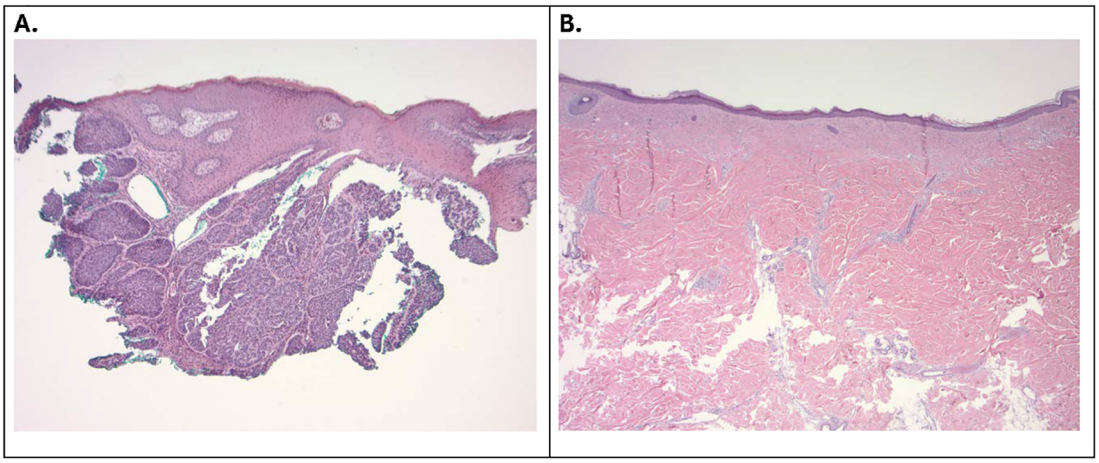

FIGURE 2
(A) The micrograph (100x) shows a nodular basal cell presenting as islands and nodules of basaloid cells with a peripheral palisading arrangement, embedded in a fibrous stroma. A noticeable cleft or retraction artifact separates the tumor islands from the surrounding stroma. The dermis shows a sparse inflammatory infiltrate. **(B)** The photomicrograph (20x) confirms the successful surgical removal of the site of the original basal cell carcinoma, with clear margins and satisfactory wound healing. The histological section illustrates a region of dense fibrous connective tissue, indicative of scar formation, with no evidence of residual basaloid cell nests. Collagen bundles are tightly packed and aligned parallel to the skin surface, characteristic of a reparative process.

appeared likely. Vismodegib has produced objective response rates of 43-68.5% (7, 11), with a median duration of response of 26.2 months in laBCC (7). Sonidegib has produced an objective response rate of 56% in la BCC, with a median duration of response of 26.1 months (8). In addition, these clinical trials reported high rates of adverse events, resulting in frequent treatment discontinuation.

We therefore initiated cemiplimab therapy. Cemiplimab was initially tested in advanced BCC as salvage therapy after initial surgery, radiotherapy and HHI therapy. A phase II study in 84 laBCC patients described a response rate of 32% in patients who had previously failed or were intolerant HHI therapy with an adverse event rate of 20.4% (9). Based on this phase II study, cemiplimab was subsequently approved by the US Food and Drug Administration (FDA) in 2021 for patients with locally advanced basal cell carcinoma (laBCC) previously treated with a hedgehog pathway inhibitor (HHI) or for whom a HHI is not appropriate.

Several reports have suggested significant clinical activity of cemiplimab and other PD-1 antibodies as a neoadjuvant therapy for locally advanced cutaneous squamous cell carcinoma (10). There is less data concerning neoadjuvant PD-1 antibody therapy in laBCC. One recent case series has demonstrated successful treatment of advanced BCC with neoadjuvant PD-1 inhibitors (12). A significant percentage of durable complete pathological responses was reported. The theoretical advantage of neoadjuvant therapy is potential for tumor cytoreduction, reducing the scope of necessary surgery. Individualized response assessment is possible, allowing subsequent tailored therapy. It appears likely that neoadjuvant therapy also results in a stronger and broader T cell response.

After two cycles of treatment, it became apparent that our patient had a very minimal response to cemiplimab. We considered cautious addition of HHI treatment based on three case reports that suggested clinical activity of this combination (13–15). In addition, recent data suggested that HHI may decrease immunosuppressive features of tumor microenvironment, in a manner that may potentiate checkpoint inhibitor treatment (16). The combination of cemiplimab therapy with vismodegib was well tolerated. The patient described minimal loss of taste and mild hair thinning, which resolved after drug discontinuation. This combined treatment induced substantial tumor regression. Complete surgical resection of the affected skin (avoiding deeper tissue

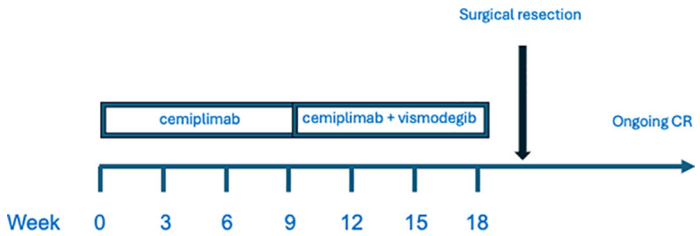

FIGURE 3
Treatment schema.

resection) demonstrated a pathologic complete response. This unmaintained response has continued for 24 months after treatment discontinuation.

In conclusion, this case demonstrates a novel treatment option for the locally advanced BCC. This patient did not respond to cemiplimab alone. The addition of HHI to PD-1 therapy led to a marked reduction in the locally advanced tumor. There was no apparent added toxicity from combination therapy. Upon resection, it was determined that the patient had achieved a pathologic complete remission. This case suggests a rationale to further evaluate cemiplimab with HHI to improve pathologic responses and curability of large laBCC lesions.

Data availability statement

The original contributions presented in the study are included in the article/supplementary material, further inquiries can be directed to the corresponding author/s.

Ethics statement

Ethical approval was not required for the study involving humans in accordance with the local legislation and institutional requirements. Written informed consent to participate in this study was not required from the participants or the participants' legal guardians/next of kin in accordance with the national legislation and the institutional requirements. Written informed consent was obtained from the individual(s) for the publication of any potentially identifiable images or data included in this article.

Author contributions

CL-S: Conceptualization, Data curation, Formal analysis, Investigation, Methodology, Writing – original draft, Writing – review & editing. WS: Conceptualization, Data curation, Formal analysis, Funding acquisition, Investigation, Methodology, Project administration, Resources, Supervision, Validation, Writing – original draft, Writing – review & editing. BR: Data curation, Formal analysis, Investigation, Visualization, Writing – review & editing. AH: Data curation, Formal analysis, Investigation, Visualization, Writing – review & editing.

Funding

The author(s) declare financial support was received for the research, authorship, and/or publication of this article. This study was funded in part by US National Institutes of Health (NIH) grant 5U10CA035421. The publication fees for this article were supported by the Kirk Kerkorian School of Medicine @ UNLV Open Article Fund.

Acknowledgments

We appreciate the patients, families, clinic staff, and referring physicians who made this case report possible. The helpful editorial suggestions of Suzanne Samlowski, M. Arch. are also appreciated.

Conflict of interest

The authors declare that the research was conducted in the absence of any commercial or financial relationships that could be construed as a potential conflict of interest.

Publisher's note

All claims expressed in this article are solely those of the authors and do not necessarily represent those of their affiliated organizations, or those of the publisher, the editors and the reviewers. Any product that may be evaluated in this article, or claim that may be made by its manufacturer, is not guaranteed or endorsed by the publisher.

References

1. Rogers HW, Weinstock MA, Feldman SR, Coldiron BM. Incidence estimate of nonmelanoma skin cancer (Keratinocyte carcinomas) in the U.S. Population, 2012. *JAMA Dermatol.* (2015) 151:1081–6. doi: 10.1001/jamadermatol.2015.1187

2. Goldenberg G, Karagiannis T, Palmer JB, Lotya J, O'Neill C, Kisa R, et al. Incidence and prevalence of basal cell carcinoma (BCC) and locally advanced BCC (LABCC) in a large commercially insured population in the United States: A retrospective cohort study. *J Am Acad Dermatol.* (2016) 75:957–966 e2. doi: 10.1016/j.jaad.2016.06.020

3. Amakye D, Jagani Z, Dorsch M. Unraveling the therapeutic potential of the Hedgehog pathway in cancer. *Nat Med.* (2013) 19:1410–22. doi: 10.1038/nm.3389

4. Iwasaki JK, Srivastava D, Moy RL, Lin HJ, Kouba DJ. The molecular genetics underlying basal cell carcinoma pathogenesis and links to targeted therapeutics. *J Am Acad Dermatol.* (2012) 66:e167–78. doi: 10.1016/j.jaad.2010.06.054

5. Sekulic A, Migden MR, Lewis K, Hainsworth JD, Solomon JA, Yoo S, et al. Pivotal ERIVANCE basal cell carcinoma (BCC) study: 12-month update of efficacy and safety of vismodegib in advanced BCC. *J Am Acad Dermatol.* (2015) 72:1021–6 e8. doi: 10.1016/j.jaad.2015.03.021

6. Dummer R, Ascierto PA, Basset-Seguin N, Dreno B, Garbe C, Gutzmer R, et al. Sonidegib and vismodegib in the treatment of patients with locally advanced basal cell carcinoma: a joint expert opinion. *J Eur Acad Dermatol Venereol.* (2020) 34:1944–56. doi: 10.1111/jdv.16230

7. Sekulic A, Migden MR, Basset-Seguin N, Garbe C, Gesierich A, Lao CD, et al. Long-term safety and efficacy of vismodegib in patients with advanced basal cell carcinoma: Final update of the pivotal ERIVANCE BCC study. *BMC Cancer.* (2017) 17:332. doi: 10.1186/s12885-017-3286-5

8. Dummer R, Guminksi A, Gutzmer R, Lear JT, Lewis KD, Chang ALS, et al. Long-term efficacy and safety of sonidegib in patients with advanced basal cell carcinoma: 42-month analysis of the phase II randomized, double-blind BOLT study. *Br J Dermatol.* (2020) 182:1369–78. doi: 10.1111/bjd.18552

9. Stratigos AJ, Sekulic A, Peris K, Bechter O, Prey S, Kaatz M, et al. Cemiplimab in locally advanced basal cell carcinoma after hedgehog inhibitor therapy: an open-label, multi-centre, single-arm, phase 2 trial. *Lancet Oncol.* (2021) 22:848–57. doi: 10.1016/S1470-2045(21)00126-1

10. Gross ND, Miller DM, Khushalani NI, Divi V, Ruiz ES, Lipson EJ, et al. Neoadjuvant cemiplimab for stage II to IV cutaneous squamous-cell carcinoma. *N Engl J Med*. (2022) 387:1557–68. doi: 10.1056/NEJMoa2209813

11. Basset-Seguin N, Hauschild A, Grob JJ, Kunstfeld R, Dreno B, Mortier L, et al. Vismodegib in patients with advanced basal cell carcinoma (STEVIE): a pre-planned interim analysis of an international, open-label trial. *Lancet Oncol*. (2015) 16:729–36. doi: 10.1016/S1470-2045(15)70198-1

12. Ligtenberg KG, Hu JK, Damsky W, Olino K, Kluger H, Clune J, et al. Neoadjuvant anti-programmed cell death 1 therapy for locally advanced basal cell carcinoma in treatment-naive patients: A case series. *JAAD Case Rep*. (2020) 6:628–33. doi: 10.1016/j.jdcr.2020.05.010

13. Colombo E, Gurizzan C, Ottini A, Caspani F, Bergamini C, Locati LD, et al. The association of cemiplimab plus sonidegib for synchronous cutaneous squamous cell carcinoma and basal cell carcinoma of the head and neck: Two case reports. *Front Oncol*. (2023) 13:1111146. doi: 10.3389/fonc.2023.1111146

14. Weis J, Grote C, Weichenthal M, Hauschild A. Complete response of advanced cutaneous squamous cell and basal cell carcinomas with sequential cemiplimab and sonidegib therapy. *J Eur Acad Dermatol Venereol*. (2022) 36:66–9. doi: 10.1111/jdv.17403

15. Pirruccello J, Afzal MZ, Voudouri M, Shirai K. Complete response of a large basosquamous carcinoma following treatment with cemiplimab and vismodegib. *BMJ Case Rep*. (2023) 16(7):e251273. doi: 10.1136/bcr-2022-251273

16. Gambini D, Passoni E, Nazzaro G, Beltramini G, Tomasello G, Ghidini M, et al. Basal cell carcinoma and hedgehog pathway inhibitors: focus on immune response. *Front Med (Lausanne)*. (2022) 9:893063. doi: 10.3389/fmed.2022.893063

frontiers | Frontiers in Oncology

TYPE Case Report
PUBLISHED 06 February 2025
DOI 10.3389/fonc.2025.1486688

Check for updates

OPEN ACCESS

EDITED BY
Giuseppe Giaccone,
Cornell University, United States

REVIEWED BY
Dilyara Kaidarova,
Kazakh Institute of Oncology and Radiology, Kazakhstan
Federica Perelli,
Azienda USL Toscana Centro, Italy

*CORRESPONDENCE
Weiyong Gu
liujingfengbaobao@126.com
Mei Wang
wangmei@shpdph.com

RECEIVED 26 August 2024
ACCEPTED 15 January 2025
PUBLISHED 06 February 2025

CITATION
Zhou A, Gu W, Yang Y, Chen X, Ye W and Wang M (2025) High-grade serous cancer of left fallopian tube with right inguinal lymph node enlargement: a case report.
Front. Oncol. 15:1486688.
doi: 10.3389/fonc.2025.1486688

COPYRIGHT
© 2025 Zhou, Gu, Yang, Chen, Ye and Wang. This is an open-access article distributed under the terms of the Creative Commons Attribution License (CC BY). The use, distribution or reproduction in other forums is permitted, provided the original author(s) and the copyright owner(s) are credited and that the original publication in this journal is cited, in accordance with accepted academic practice. No use, distribution or reproduction is permitted which does not comply with these terms.

High-grade serous cancer of left fallopian tube with right inguinal lymph node enlargement: a case report

Aizhi Zhou[1], Weiyong Gu[2*], Yumei Yang[1], Xin Chen[1], Wenfeng Ye[1] and Mei Wang[1*]

[1]Department of Obstetrics and Gynecology, Shanghai Pudong New Area People's Hospital, Shanghai, China, [2]Department of Pathology, Hospital of Obstetrics and Gynecology, Fudan University, Shanghai, China

A 47-year-old woman with a two-month history of right inguinal lymphadenopathy visited Shanghai Pudong New Area People's Hospital for a biopsy. Histopathological and immunohistochemical analyses revealed a metastasis of high-grade serous carcinoma, likely of gynecological origin. A PET-CT scan identified a tumor in the left adnexa, with no other organ involvement. The patient underwent primary cytoreduction, including laparoscopy, hysterosalpingo-oophorectomy, omentectomy, and resection of the right deep inguinal lymph nodes at the Hospital of Obstetrics and Gynecology. No residual disease was found post-surgery. Pathological examination revealed high-grade serous cancer in the fimbria of the left fallopian tube and left ovary, while the right deep inguinal lymph nodes were negative. The patient received standard chemotherapy (Carboplatin and Taxol) and showed no new lesions after three cycles, as confirmed by imaging.

KEYWORDS

HGSOC, ovarian cancer, lymphadenopathy, metastasis, inguinal lymph node

Introduction

Ovarian cancer remains the most lethal reproductive system cancer, with an estimated 55,000 new cases and 38,000 deaths in China in 2020 (1). According to the Chinese Cause of Death Surveillance, the crude mortality rate of ovarian cancer increased from 1.42 per 100,000 to 2.87 per 100,000 from 2006 to 2020 (2). Common symptoms in ovarian cancer patients include abdominal discomfort or distension, abdominal or pelvic pain, constipation or early satiety, weight loss, and asthenia. Inguinal lymphadenopathy is a rare initial presentation of ovarian cancer (3). Due to the usual lack of symptoms associated with early-stage disease, most cases are diagnosed only after the cancer has progressed. Epithelial ovarian cancer may metastasize intraperitoneally, lymphatically, or hematogenously (4, 5). Lymphatic

dissemination from the ovary typically involves the para-aortic and pelvic areas (6), with an estimated incidence of such lesions ranging between 14% and 70% (7). Metastases to pelvic lymph nodes are less frequent than those in the para-aortic region (8–10).

The exact mechanism by which tumor cells spread to the inguinal lymph nodes remains unclear. One possibility is that tumor cells may follow the round ligament of the uterus (11) or the external iliac artery and vein. However, it has been argued that spread to the inguinal lymph nodes should only occur after the blockage of pelvic and para-aortic lymph node stations (12). Considering the peculiarity of this route of spread, the aim of this report is to describe a rare case of high-grade serous cancer of the left fallopian tube with right inguinal lymph node enlargement, with the right deep inguinal lymph nodes negative.

Case presentation

The patient presented with an enlarged right inguinal lymph node for at least 2 months, which was evaluated at another medical institution. She reported no other symptoms apart from occasional dull pain in the lower abdomen over the past two months. Her medical history included chronic nephritis in 2014 and the resection of a benign cervical vertebral tumor in 2021. Her family history was negative for malignancy, and she had no known occupational or environmental exposure to hormones, particularly estrogens. Clinical examination confirmed the enlarged right inguinal lymph node, which was further evaluated by abdominal ultrasound. The result revealed a heterogeneous solid mass with intrinsic vascularization, measuring 28 × 19 mm. It also showed several smaller reactive lymphadenopathies locoregionally but was otherwise normal. Laboratory analysis was normal except for an elevated CA 125 level of 46 kU/L.

A lymph node resection at the first institution revealed metastasis of high-grade serous cancer, likely from the reproductive system. A PET-CT was requested to check for other abnormalities. It confirmed a likely malignant tumor in the left adnexa, showed postoperative fluid accumulation in the right inguinal region, and revealed no other suspicious lesions or ascites. Laparoscopy showed a solid mass on the surface of the left ovary, measuring 30 × 30 × 25 mm (Figure 1A). The right ovary and bilateral fallopian tubes appeared normal, and no other macroscopic lesions were found in the abdominal and pelvic cavities (Figure 1B). There were no enlarged lymph nodes in the para-aortic or pelvic areas, and no ascites. The pathological examination revealed high-grade serous cancer in the fimbria of the left fallopian tube, which involved the left ovary, but the right deep inguinal lymph nodes were negative (Figure 1C–H). Germline and somatic BRCA1/2 testing showed no BRCA1 or BRCA2 mutations. The homologous recombination deficiency (HRD) status was positive, with a score of 53.44 (threshold value: 30).

According to the NCCN guidelines updated in 2024, the patient underwent six cycles of chemotherapy with Carboplatin and Taxol, administered every three weeks for the first four cycles. Bevacizumab was added to the last two cycles as her chronic nephritis was stable and her urine protein turned negative. She was subsequently placed on maintenance therapy with bevacizumab. After four cycles of chemotherapy, imaging showed no lesions. The initially elevated CA 125 level (46 kU/L) declined to 11 kU/L and remained stable.

Discussion

In this report, we described a rare case of high-grade serous cancer of the left fallopian tube with right inguinal lymph node enlargement, with the right deep inguinal lymph nodes negative. Patients with ovarian cancer typically present with metastatic disease, with the most common site of metastasis being the peritoneum. Diagnosing ovarian cancer based on a metastatic inguinal lymph node is extremely rare (13). The literature reveals only a few cases where patients with ovarian carcinoma had positive inguinal lymph nodes at onset (14). Our patient initially sought medical attention for an enlarged right inguinal lymph node, and a diagnosis of high-grade serous carcinoma was made after its excision.

Metastasis to the inguinal region in ovarian cancer may occur through hematogenous spread or lymphatic spread via the round ligament (15). The lymphogenic-only spread in this case suggests a specific biological metastatic behavior. Some researchers proposed that host immune defense mechanisms may destroy the primary tumor without affecting lymphatic metastasis (16, 17), whereas others suggested that spread to the inguinal region might occur through the peritoneum after previous surgery (11), but our patient had no prior surgeries. Isolated lymph node disease in ovarian cancer appears to represent a less aggressive relapse pattern, associated with relatively mild behavior and few symptoms. According to some literature, this pattern may be related to the tumor cells' low proliferation rate and initial lack of peritoneal spread (18). The lymph node microenvironment might keep cells dormant due to the presence of cytokines and T-cells (19). This metastatic pattern often shows higher lymphocyte infiltration, particularly of CD3 and CD8 cells, compared to extra-nodal ovarian cancer relapses. However, it does not show significant differences regarding known genomic subtypes, such as BRCA1/2 mutations or increased CCNE1 (20).

There are some limitations of the study. The current study is a single-case analysis, which restricts its broader applicability. Also, this case showed no germline or somatic BRCA1/2 mutations, and the homologous recombination deficiency (HRD) score was 53.44 (threshold value: 30). Homologous recombination deficiency may be one of the factors associated with isolated lymph node metastasis. Therefore, further research is needed to identify other genetic factors linked to this phenomenon. Specifically, the reasons for the left fallopian tube tumor presenting with right inguinal lymph node enlargement and the explanation for lymphatic drainage from

10.3389/fonc.2025.1486688

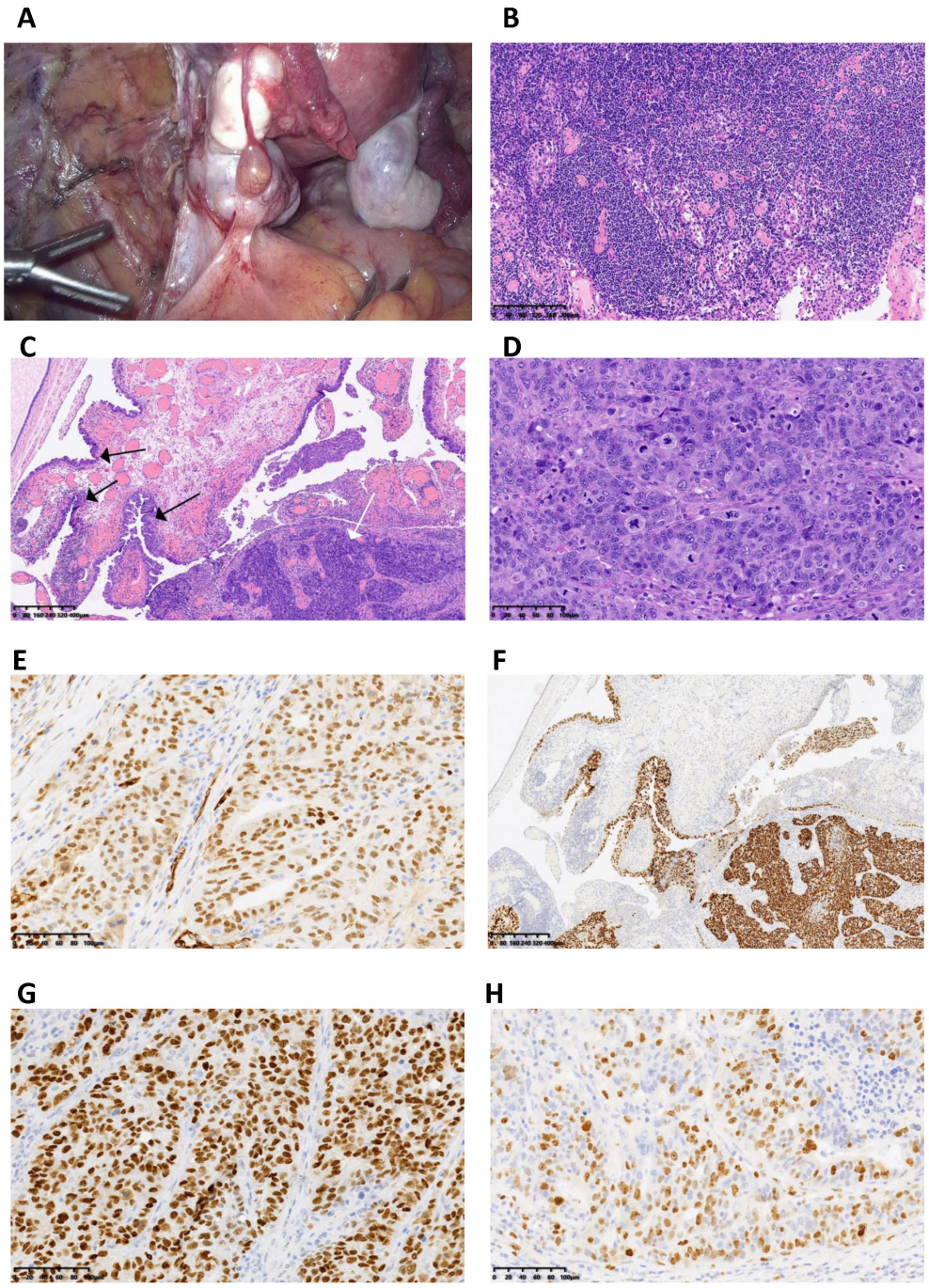

FIGURE 1
Information of the cancer. **(A)** A solid mass on the surface of the left ovary (size 30×30×25mm). **(B)** No cancer metastasis observed in the right deep inguinal lymph nodes. **(C)** Serous intraepithelial carcinoma (STIC) (indicated by the black arrow) and invasive carcinoma (indicated by the white arrow) observed in the left fallopian tube fimbria. **(D)** High-grade serous carcinoma of the left ovary with mitotic figures observed. **(E)** Immunohistochemical staining shows positive expression of WT1 in the high-grade serous carcinoma of the left ovary. **(F)** Immunohistochemical staining shows diffuse strong positive mutant-type expression of p53 in the lesion of the left fallopian tube fimbria. **(G)** Immunohistochemical staining shows diffuse strong positive mutant-type expression of p53 in the high-grade serous carcinoma of the left ovary. **(H)** Immunohistochemical staining shows a Ki67 proliferation index of 60% in the high-grade serous carcinoma of the left ovary.

the primary tumor to only the right inguinal lymph node require urgent investigation. Previous research suggests that the prognosis for this type of primary fallopian tube carcinoma (PFTC) appears to be good (14). Consequently, the patient will be followed up for a long time for clinical outcome.

Conclusions

The literature reports a rare case of isolated ovarian metastases to the inguinal lymph nodes, and the mechanism by which fallopian tube cancer metastasizes to the contralateral groin lymph nodes

remains unclear. Homologous recombination deficiency may play an important role in this type of primary fallopian tube carcinoma (PFTC). Therefore, patients like the one in this case may benefit from PARP inhibitor (PARPi) therapy.

Data availability statement

The original contributions presented in the study are included in the article/supplementary material. Further inquiries can be directed to the corresponding authors.

Ethics statement

The studies involving humans were approved by Shanghai Pudong New Area People's Hospital Ethics Committee. The studies were conducted in accordance with the local legislation and institutional requirements. The participants provided their written informed consent to participate in this study. Written informed consent was obtained from the participant/patient(s) for the publication of this case report.

Author contributions

AZ: Conceptualization, Investigation, Writing – original draft. WG: Data curation, Writing – review & editing. YY: Conceptualization, Validation, Writing – review & editing. XC: Writing – review & editing. WY: Data curation, Writing – review & editing. MW: Formal analysis, Methodology, Writing – review & editing.

Funding

The author(s) declare financial support was received for the research, authorship, and/or publication of this article. The author(s) declare that this article was supported by the Key Discipline Project of the Shanghai Pudong New Area Health Commission (PWZxk2022-28).

Conflict of interest

The authors declare that the research was conducted in the absence of any commercial or financial relationships that could be construed as a potential conflict of interest.

Publisher's note

All claims expressed in this article are solely those of the authors and do not necessarily represent those of their affiliated organizations, or those of the publisher, the editors and the reviewers. Any product that may be evaluated in this article, or claim that may be made by its manufacturer, is not guaranteed or endorsed by the publisher.

References

1. Sung H, Ferlay J, Siegel RL, Laversanne M, Soerjomataram I, Jemal A, et al. Global cancer statistics 2020: GLOBOCAN estimates of incidence and mortality worldwide for 36 cancers in 185 countries. *CA Cancer J Clin*. (2021) 71:209–49. doi: 10.3322/caac.21660

2. Han X, Wang Z, Huang D, Deng K, Wang Q, Li C, et al. Analysis of the disease burden trend of Malignant tumors of the female reproductive system in China from 2006 to 2020. *BMC Womens Health*. (2022) 22:504. doi: 10.1186/s12905-022-02104-2

3. Rose PG, Piver MS, Tsukada Y, Lau TS. Metastatic patterns in histologic variants of ovarian cancer. *autopsy study. Cancer*. (1989) 64:1508–13. doi: 10.1002/1097-0142(19891001)64:7<1508::AID-CNCR2820640725>3.0.CO;2-V

4. Panici PB, Angioli R. Role of lymphadenectomy in ovarian cancer. *Best Pract Res Clin Obstet Gynaecol*. (2002) 16:529–51. doi: 10.1053/beog.2002.0301

5. Vizzielli G, Costantini B, Tortorella L, Petrillo M, Fanfani F, Chiantera V, et al. Influence of intraperitoneal dissemination assessed by laparoscopy on prognosis of advanced ovarian cancer: an exploratory analysis of a single-institution experience. *Ann Surg Oncol*. (2014) 21:3970–7. doi: 10.1245/s10434-014-3783-6

6. Fournier M, Stoeckle E, Guyon F, Brouste V, Thomas L, MacGrogan G, et al. Lymph node involvement in epithelial ovarian cancer: sites and risk factors in a series of 355 patients. *Int J Gynecol Cancer*. (2009) 19:1307–13. doi: 10.1111/IGC.0b013e3181b8a07c

7. Ulker V, Kuru O, Numanoglu C, Akbayır O, Polat I, Uhri M. Lymph node metastasis in patients with epithelial ovarian cancer macroscopically confined to the ovary: review ofa single-institution experience. *Arch Gynecol Obstet*. (2014) 289:1087–92. doi: 10.1007/s00404-013-3078-3

8. Benedetti-Panici P, Greggi S, Maneschi F, Scambia G, Amoroso M, Rabitti C, et al. Anatomical and pathological study of retroperitoneal nodes in epithelial ovarian cancer. *Gynecol Oncol*. (1993) 51:150–4. doi: 10.1006/gyno.1993.1263

9. Maggioni A, Benedetti Panici P, Dell'Anna T, Landoni F, Lissoni A, Pellegrino A, et al. Randomised study of systematic lymphadenectomy in patients with epithelial ovarian cancer macroscopically confined to the pelvis. *Br J Cancer*. (2006) 95:699–704. doi: 10.1038/sj.bjc.6603323

10. Colombi I, D'Indinosante M, Lazzeri L, Zupi E, Pisaneschi S, Giusti M, et al. Tubal cancer clinical management: two exceptional scenarios and a review of the literature. *J Clin Med*. (2024) 13:5075. doi: 10.3390/jcm13175075

11. Metwally IH, Zuhdy M, Hassan A, Alghandour R, Megahed N. Ovarian cancer with metastatic inguinal lymphadenopathy: A case series and literature review. *J Egypt Natl Canc Inst*. (2017) 29:109–14. doi: 10.1016/j.jnci.2017.01.003

12. Kleppe M, Kraima AC, Kruitwagen RF, Van Gorp T, Smit NN, van Munsteren JC, et al. Understanding lymphatic drainage pathways of the ovaries to predict sites for sentinel nodes in ovarian cancer. *Int J Gynecol Cancer*. (2015) 25:1405–14. doi: 10.1097/IGC.0000000000000514

13. Giancontieri P, Turetta C, Barchiesi G, Pernazza A, Pignataro G, D'Onghia G, et al. High-grade serous carcinoma of unknown primary origin associated with STIC clinically presented as isolated inguinal lymphadenopathy: a case report. *Front Oncol*. (2024) 13:1307573. doi: 10.3389/fonc.2023.1307573

14. Maeda M, Hisa T, Matsuzaki S, Ohe S, Nagata S, Lee M, et al. Primary fallopian tube carcinoma presenting with a massive inguinal tumor: A case report and literature review. *Medicina*. (2022) 58:581. doi: 10.3390/medicina58050581

15. Ang D, Ng KY, Tan HK, Chung AY, Yew BS, Lee VK. Ovarian carcinoma presenting with isolated contralateral inguinal lymph node metastasis: a case report. *Ann Acad Med Singap*. (2007) 36:427–30. doi: 10.47102/annals-acadmedsg.

16. Kehoe S, Luesley D, Rollason T. Ovarian carcinoma presenting with inguinal metastatic lymphadenopathy 33 months prior to intraabdominal disease. *Gynecol Oncol*. (1993) 50:128–30. doi: 10.1006/gyno.1993.1177

17. Preston CC, Goode EL, Hartmann LC, Kalli KR, Knutson KL. Immunity and immune suppression in human ovarian cancer. *Immunotherapy*. (2011) 3:539–56. doi: 10.2217/imt.11.20

18. Restaino S, Mauro J, Zermano S, Pellecchia G, Mariuzzi L, Orsaria M, et al. CUP-syndrome:Inguinal high grade serous ovarian carcinoma lymph node metastases with unknown primary origin – A case report and literature review. *Front Oncol*. (2022) 12:987169. doi: 10.3389/fonc.2022.987169

19. Legge F, Petrillo M, Adamo V, Pisconti S, Scambia G, Ferrandina G. Epithelial ovarian cancer relapsing as isolated lymph node disease: natural history and clinical outcome. *BMC Cancer*. (2008) 8:367. doi: 10.1186/1471-2407-8-367

20. Hollis RL, Carmichael J, Meynert AM, Churchman M, Hallas-Potts A, Rye T, et al. Clinical and molecular characterization of ovarian carcinoma displaying isolated lymph node elapse. *Am J Obstet Gynecol*. (2019) 221:245.e1–245.e15. doi: 10.1016/j.ajog.2019.04.035

frontiers | Frontiers in Oncology

TYPE Case Report
PUBLISHED 13 February 2025
DOI 10.3389/fonc.2025.1472017

Check for updates

OPEN ACCESS

EDITED BY
Giuseppe Giaccone,
Cornell University, United States

REVIEWED BY
Muhammad Babar Khawar,
Chinese Academy of Sciences (CAS), China
Teng Li,
Air Force Medical University, China

*CORRESPONDENCE
Zhixing Cao
635572402@qq.com

RECEIVED 28 July 2024
ACCEPTED 24 January 2025
PUBLISHED 13 February 2025

CITATION
Sun D, Li Y and Cao Z (2025) Gastric-type endocervical adenocarcinoma, superficial myofibroblastoma, sex cord-stromal tumors, and HSIL in Peutz–Jeghers syndrome: a rare case report, genetic characterization, and review of literature.
Front. Oncol. 15:1472017.
doi: 10.3389/fonc.2025.1472017

COPYRIGHT
© 2025 Sun, Li and Cao. This is an open-access article distributed under the terms of the Creative Commons Attribution License (CC BY). The use, distribution or reproduction in other forums is permitted, provided the original author(s) and the copyright owner(s) are credited and that the original publication in this journal is cited, in accordance with accepted academic practice. No use, distribution or reproduction is permitted which does not comply with these terms.

Gastric-type endocervical adenocarcinoma, superficial myofibroblastoma, sex cord-stromal tumors, and HSIL in Peutz–Jeghers syndrome: a rare case report, genetic characterization, and review of literature

Dongjin Sun[1], Yumei Li[2] and Zhixing Cao[3]*

[1]Department of Pathology, Sir Run Run Shaw Hospital, Zhejiang University School of Medicine, Hangzhou, Zhejiang, China, [2]Department of Pathology, the Fifth Affiliated Hospital of Sun Yat-sen University, Zhuhai, China, [3]Department of Pathology, Zhuhai People's Hospital, Zhuhai/Zhuhai Hospital Affiliated with Jinan University, Zhuhai, China

Peutz-Jeghers syndrome (PJS) is characterized by an increased risk of gynecologic tumors. Gastric-type endocervical adenocarcinoma (GEA) is a rare non-human papillomavirus (HPV)-related tumor. We reported an uncommon case of a 39-year-old woman with PJS who developed GEA, superficial cervical vaginal myofibroblastoma, sex cord-stromal tumors with annular tubules of the ovaries, and cervical and vaginal high-grade squamous interepithelial neoplasia (HSIL). Before being verified GEA, the patient had been experiencing suspicious symptoms for over 9 years, with nabothian cysts and vaginitis being misdiagnosed. HSIL displayed widespread p16 immunostaining, and HPV DNA screening confirmed HPV-18 infection, although GEA was negative. Further, we verified *TP53* mutation and *HER2* amplification of GEA by fluorescence *in situ* hybridization (FISH). *TP53* was the most commonly mutated gene. The therapy with the anti-HER2 antibody trastuzumab was suggested based on HER2 amplification. We also analyzed the somatic mutations of GEA by whole genome sequencing (WES). There were 157 single nucleotide variations (SNVs) and 215 indels, with all of them being heterozygotes. Nonsynonymous and frameshift insertions were the most common kinds of mutations. The germine *STK11* gene mutation was found, which may play an important role in tumor development. According to gene function enrichment analyses, the genomic changes primarily implicated general transcription or expression pathways and cell cycle pathways. In addition, the JAK2/STAT3 pathway could be a major focus of targeted therapy for GEA patients with PJS. Our findings show that the patient with PJS can have a variety of unusual gynecologic tumors. Patients with PJS must have routine gynecological, ultrasonographic, and cytological examinations to detect precursor or early-stage lesions. The patient's abnormal symptoms must be treated early with caution. A comprehensive

genomic study reveals the potential causative genetic factors, therapeutic targets, and chemotherapy resistance of GEA. Further research will focus on the main driving genes, molecular mechanisms, and molecular target therapy in more patients.

KEYWORDS

somatic mutations, gene enrichment analysis, whole-genome sequencing, gastric-type endocervical adenocarcinoma, Peutz-Jeghers syndrome

Introduction

Peutz-Jeghers syndrome (PJS) is a rare autosomal dominant disorder caused by germline mutations in the *STK11/LKB1* gene on chromosome 19p13.3 (1). The *STK11/LKB1* gene is involved in cell polarity, apoptosis, metabolism, and proliferation by activating the AMP-activated serine/threonine protein kinase (AMPK) pathway (1, 2). The reduction in *STK11/LKB1* expression in normal cells leads to the development of cancer (3). Patients with PJS are characterized by gastrointestinal hamartomatous polyps, mucocutaneous pigmentation, and have a high incidence of malignancies, especially in the lower gastrointestinal tract and female reproductive system (4). Gastric-type endocervical adenocarcinoma (GEA) of the cervix and sex cord-stromal tumors with annular tubules (SCTAT) of the ovary are common gynecological tumors (5).

GEA of the cervix is a rare tumor, which is a human papillomavirus (HPV)-independent adenocarcinoma that accounts for 10%-15% of all cervical adenocarcinomas (6). P16 immunoreactivity and HPV DNA detection are generally negative (7). Patients with PJS may be diagnosed with GEA and other multiple neoplastic lesions, including mucinous tumors of the fallopian tube or ovary, SCTAT of the ovary, and serous tubal intraepithelial lesions (5, 8).

To understand the pathogenesis and therapeutic targets of GEA, gene detection has been reported. By next-generation sequencing (NGS) performed on 21, 15, and 14 cases, *TP53* was found to be the most frequently mutated gene, followed by STK11 (9–11). The mutated genes are mainly involved in DNA damage repair, cell cycle, epithelial-mesenchymal transition (EMT), PI3K/AKT signaling pathways, and so on (9–11). Selenica et al. (12) performed massively parallel sequencing analysis on 68 GEA patients, identifying the most frequent pathways involved in the cell cycle (*TP53, CDKN2A*), PI3K-AKT (*PIK3CA, STK11*), and Notch (*FBXW7, NOTCH2, CREBBP, SPEN*). In the therapeutic target, ERBB3, ERBB2, and BRAF were detected. With the development of sequencing technologies, whole-exome sequencing (WES) was performed on 25 pairs of GEA tumors and matched normal samples, and the common *TP53*, *CDKN2A*, and *SKT11* were discovered, as well as the new somatic copy number alteration (SCNA) of *APOBEC3B* (13).

Here, we present a case of a PJS patient who also has GEA, superficial cervical vaginal myofibroblastoma (SCVM), and SCTAT of the bilateral ovary. SCVM was first reported in patients with PJS. More interestingly, we found high-grade squamous intraepithelial neoplasia (HSIL) in the cervix and vagina, and P16 was diffuse and strongly positive. Furthermore, we performed WES on paired GEA tumors and peripheral blood samples to explore the potential causative genetic factors and therapeutic targets of GEA with PJS, primarily through somatic mutation genes and functional enrichment analysis.

Case presentation

Clinical characteristics

A 39-year-old female with mucocutaneous pigmentation on her digits, feet, and lips (Figures 1A, B) and multiple hamartomatous polyps in the gastrointestinal tract (Figures 1C, D) was diagnosed with PJS at the age of 21 years in 2004. She had undergone bowel resection due to intestinal obstruction caused by intestinal polyps in 2015. Her father had also been diagnosed with PJS. Her menstrual cycles prolonged to between 30 and 180 days approximately one decade ago. So far, she was not pregnant.

Sonographic findings revealed a significantly enlarged cervix (4.2×6.7×6.4 cm), and Nabothian cysts were considered during a physical examination 9 years ago. This situation was not emphasized. The patient complained of thin and mucoid vaginal discharge and vaginal odor, but this situation had been diagnosed with vaginitis and treated correspondingly many times 7 years ago. However, her symptoms were hardly relieved and recurred frequently. In this period, a plain CT scan showed larger cervical cysts than before in the lower abdomen, but further treatment was not performed. In 2021, a little hemorrhage after intercourse occurred for 2 to 3 days. Sonographic findings suggested a pelvic cystic mass, but a further measurement had not been made. The woman came to our hospital in 2022 with a vaginal hemorrhage (no clear reason). A gynecological examination revealed a thin, watery discharge and an enlarged cervix, as well as an 8×7×8 cm cystic mass posterior to the uterus. Contrast-enhanced magnetic

Abbreviations: GEA, gastric-type endocervical adenocarcinoma; AMPK, AMP-activated serine/threonine protein kinase; SCTAT, sex cord-stromal tumors with annular tubules; SCVM, superficial cervical vaginal myofibroblastoma; MDA, minimum deviation adenocarcinoma.

FIGURE 1
The main clinical characteristics of PJS patients. **(A, B)** Pig pigmentation on her digits and feet. **(C, D)** Multiple polyps in the stomach and intestinal tract. **(E)** Contrast-enhanced magnetic resonance imaging showed multiple cystic/solid lesions in the pelvis.

resonance imaging (MRI) in the lower abdomen revealed multiple cystic/solid lesions with sizes of 8.6×9.5×9.1 cm in the pelvis (Figure 1E), which were closely related to the cervix. Sonography showed an 11.4×8.6×11cm area surrounding the cervix with uneven anechoic patches, suggesting hydrosalpinx. Both sides of the ovary were indistinct. The serum levels of CA125 and CA199 were within normal limits.

The biopsy of the cervical tumor and pelvic cyst via laparoscopic surgery was certified as HPV-unrelated GEA; however, the polyp at the junction of the uterine body and cervix was diagnosed as superficial cervicovaginal myofibroblastoma.

Subsequently, PET-CT indicated the residual tumor tissue and suspected lymph node metastasis in the pelvic cavity. The FIGO stage was classified as II B according to the clinical staging standard of the International Federation of Obstetrics and Gynecology (FIGO, 2018). The patient underwent a total hysterectomy, bilateral uterine adnexectomy, pelvic lymphadenectomy, and pelvic adhesionlysis in May 2022. The maximum invasion depth was around 2.9 cm, with cancer tissues visible on the uterine serosal surface, paracervical region, and no lymph node metastasis. The patient received neoadjuvant chemoradiotherapy, including cisplatin/paclitaxel combination chemotherapy.

In December 2023, the patient was readmitted to the hospital because of abdominal pain, distension, and nausea. PET-CT revealed disease progression, including several regional lymph node metastases as well as metastases in the abdominal cavity, pelvic cavity, and abdominal wall. She also developed severe small bowel fistulae. Finally, she died as a result of tumor recurrence and serious complications, despite receiving Candonilimab therapy. The disease-free survival time of this patient after receiving surgery and chemoradiation therapy was about 19 months.

Pathological examination and FISH analysis

A gross specimen of gastric cancer displayed the barrel-shaped morphology of the cervix (Figure 2A). Microscopically, multiple cysts and glands of varying sizes in fibrous tissues were lined by columnar cells with abundant, pale, or weak eosinophilic cytoplasm and clear cell boundaries, and no significant cytological atypia was observed in larger regions (Figure 2B). In certain areas, the tumor cells displayed hyperchromatic and enlarged nuclei, as well as necrosis, strong eosinophilic cytoplasm, goblet cell differentiation, and abortive mucin production (Figure 2C). The tumor cells showed positive expression of MUC-6, CAIX, MUC5AC, HNF-1β, MUC-1, CK7, and Pax-8. P16 immunoreactivity was focal and weak. The Ki67 proliferation index was approximately 15%. It was negative for ER, PR, PAX-2, CK20, CDX-2, and NKX3.1. Mismatch repair proteins, including PMS2, MSH2, MSH6, and MLH1, have expression indices ranging from 10% to 90%. HER2 staining was determined as 2+ in some areas when evaluated by IHC (Figure 2D). Furthermore, *HER2* amplification was identified by FISH, and the ratio of red to green signals was approximately 2.42. (Figure 3A). P53 was categorized as a mutation type because its positive index was almost 70% in the region with the most atypia (Figure 2E); otherwise, it was wild-type in the MDA regions by IHC. The tumor cells stained pinkish-red with AB-PAS, indicating neutral mucus (Figure 2F). The tumor's HPV DNA test was

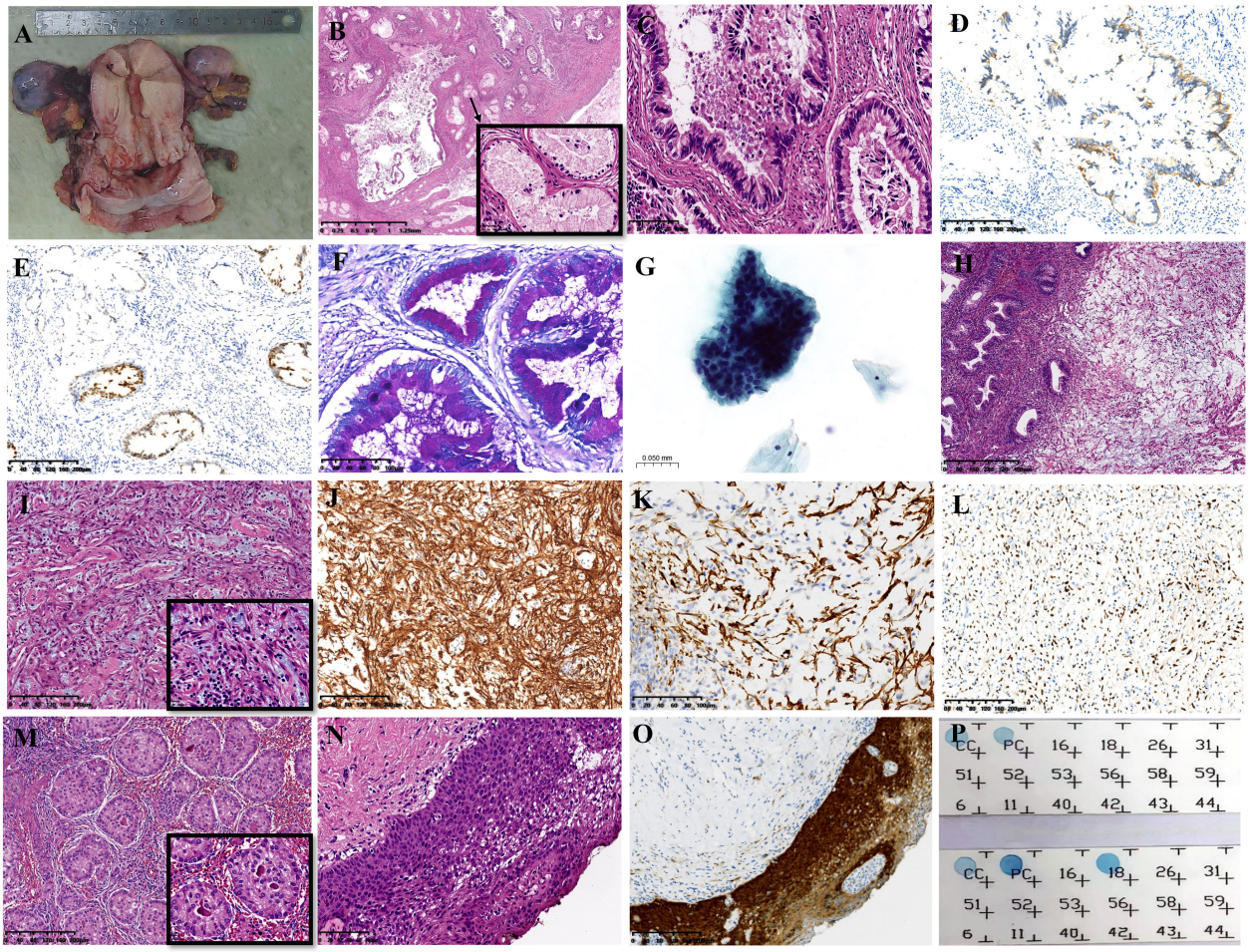

FIGURE 2
The distinct features of multiple tumors. **(A)** The gross feature showed a barrel-shaped cervix. **(B)** GEA was composed of variable shapes and sizes of glands (HE: ×16). **(C)** The tumor cells had prominent eosinophilic cytoplasm, hyperchromatic and enlarged nuclei, localized necrosis, and goblet cell development in certain regions (HE: ×200). **(D)** Positive staining for HER2 by immunohistochemistry (IHC: ×100). **(E)** P53 staining (IHC: ×100). **(F)** AB-PAS staining showed pink–red (×200). **(G)** Cytology test results (HE: ×400). **(H)** SCVM was under normal glands (HE: ×50). **(I)** Small to medium-sized vascular proliferation with hyaline degeneration (HE: ×100). **(J)** Focal positivity of Desmin staining (IHC: ×100). **(K)** Diffuse positivity of CD34 staining (IHC: ×200). **(L)** The positive index of PR was approximately 30% (IHC: ×100). **(M)** SCTAT in bilateral ovaries (HE: ×100). **(N)** HSIL of the vagina (IHC: ×200). **(O)** Diffuse positive immunoreaction of p16 in HSIL (IHC: ×100). **(P)** HPV DNA detection results. The upper panel displays the negative GEA results; the lower panel displays the HPV-18 infection of HSIL. GEA: A-G; SMFGT: H-L.

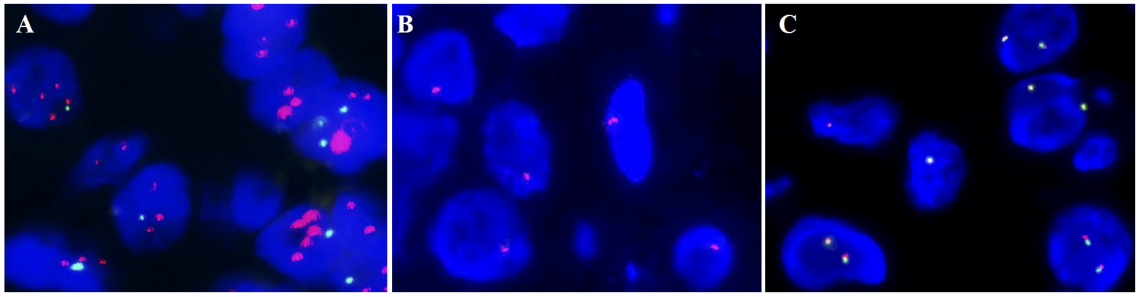

FIGURE 3
Fluorescence *in situ* hybridization (FISH) results. **(A)** *HER2* amplification. **(B)** The 1 red signal represents the heterozygous deletion; the 0 red signals suggest the homozygous deletion of *RB1*. **(C)** *HMGA2* rearrangement was negative.

negative (Figure 2P). A few glandular cells with plentiful cytoplasm and mild to moderate atypical hyperplasias were detected by the cervical liquid-based cytology test (Figure 2G), but due to the well-differentiated cell structure, it was easily overlooked.

There was a polypoid protrusion with stellate cells and long spindle cells at the uterocervical junction under the endometrium and cervical glands (Figure 2H). These cells had mild to moderate nuclear atypia and red cytoplasmic staining. Intercellular thin collagen fibrils, mucinous degeneration, lymphocyte and mast cell infiltration, and small- to medium-sized vascular proliferation with hyaline degeneration were among the interstitial histologic characteristics (Figure 2I). Desmin had localized positivity (Figure 2J). The diffuse, strong positive was exhibited by vimentin, SMA, and CD34 (Figure 2K). Ki67 had a positive rate of approximately 5%. ER and PR immunostaining was observed in approximately 30% of the cells (Figure 2L). Mast cells were identified by CD117. The expression of Rb was absent. Subsequently, we confirmed the monoallelic deletion of *13q14 (RB1)* (Figure 3B), and FISH results for the *HMGA2* broken gene were negative (Figure 3C). Our analysis revealed that it was SCVM.

Under microscopy, SCTAT linked to PJS was discovered in the bilateral ovaries. The hyaline basement membrane-like substance was surrounded by tumor cells, which were organized in rosette-like patterns (Figure 2M). The tumor cells expressed calretinin, WT-1, CD99, and inhibin-α.

The accompanying lesions included endometrial adenomyomatous polyps and HSILs of the cervix and vagina (Figure 2N). P16 displayed diffuse positivity for HSIL (Figure 2O), and infection with high-risk HPV-18 was discovered by HPV DNA testing (Figure 2P).

Whole-exome sequencing and data analysis of GEA

We took a sample of control peripheral blood and formalin-fixed paraffin-embedded (FFPE) GEA tissues from this patient and performed WES with sequencing depths of 70.74× and 138.12×, respectively.

On tumor tissues, we discovered the germline STK11 gene nonframeshift deletion on exotic 5 on Chr19. Additionally, the tumor displayed common *TP53* and *ERBB2* nonsynonymous SNVs. We verified *HER-2* amplification by FISH, and P53 immunohistochemistry revealed the mutation type in some areas. In addition, we discovered some hotspot SNVs, including *POLE*, *BRCA1*, *BRCA2*, *CDX-2*, *MUC-6*, *CAIX*, *EGFR*, *APC*, *PDGFRa*, *BCL-6*, *USP6*, *Fli-1*, *NOTCH1*, *NOTCH2*, *PAX-5*, *TTF-1*, *ALK*, and *ROS1*, as well as Indels, such as *MUC-6*, *MUC-4*, *MUC-2*, *MAML-2*, and AR (Supplymentary Tables S1, S2).

Identification of somatic mutations

We sequenced and analyzed the patient's tumor tissues and the control peripheral blood sample at the same time. Mutect2 and Varscan2 were utilized to identify somatic mutations and copy numbers. The number of passed SNVs and indels was 157 and 215, respectively, with all of them being heterozygotes (Supplementary Table S3). The tumor mutation burden (TMB) value was 2.98 mutations/Mb. We also examined the spectrum of base substitutions. C to T and G to T were the frequent transversions in somatic mutations, accounting for 15% and 14%, respectively. All percentages are displayed in Figure 4A.

The mutant-filter variants were obtained by screening the protein-coding areas for mutations and eliminating synonymous and unidentified mutations. It was chosen to include 149 mutations, including 59 nonsynonymous SNVs, 49 frameshift insertions, 17 frameshift deletions, 12 stop-gain mutations, 6 nonframeshift insertions, 5 nonframeshift deletions, and 1 stop-loss mutation. Nonsynonymous and frameshift insertion mutations, which made up approximately 40% and 31% of the total, were the most common forms. Furthermore, we obtained 116 genes from trustworthy sites and used Cytoscape to create the network interaction, which is shown in Figure 4B. The top core gene in the network interaction was JAK2.

We evaluated mutation frequency statistics on genes that passed somatic mutations in the tumor and then chose genes with a relatively high mutation frequency to draw the oncoprint. Figure 4C displays the mutation types and rates for the genes with mutation sites higher than or equal to 2. The majority of genes have two different types of mutations. Nonsynonymous SNV was the most prevalent mutation type, followed by frameshift insertion and nonsynonymous SNV. There were four SNV mutation sites in ZNF43.

We evaluated the somatic mutation using the Circos image, which exhibited the mutation's frequency and distribution, as well as the somatic copy number variation (CNV) details (Figure 4D). The inner tracks display the SNV and Indel distribution in various chromosomes. The number of indels was higher than SNVs, and the majority of the mutations were found in chr1, chr2, chr7, and chr16, as indicated by the red histogram, which represents the functional alterations.

Gene enrichment analysis

We performed a gene ontology enrichment study utilizing the passed somatic mutation genes via the gene ontology database from molecular function, cellular component, and biological process (Supplementary Figure 1A). The dynein complex was the most important cellular component, followed by the biological process of protein localization to the Golgi apparatus. Many associated genes were enriched by the biological control of biosynthetic processes, ion binding, cellular biosynthetic processes, RNA biosynthetic processes, and the molecular function of cation binding and metal ion binding. The degree of gene enrichment in phospholipid efflux was greatest when the rich factor was approximately 0.25.

Furthermore, we performed pathway enrichment using the KEGG pathway database, Reactome pathway database, BioCyc pathway database, and PANTHER (Supplementary Figure 1B). The generic transcription pathway was the most noticeable. There were approximately 40 genes in the pathway for gene expression. The

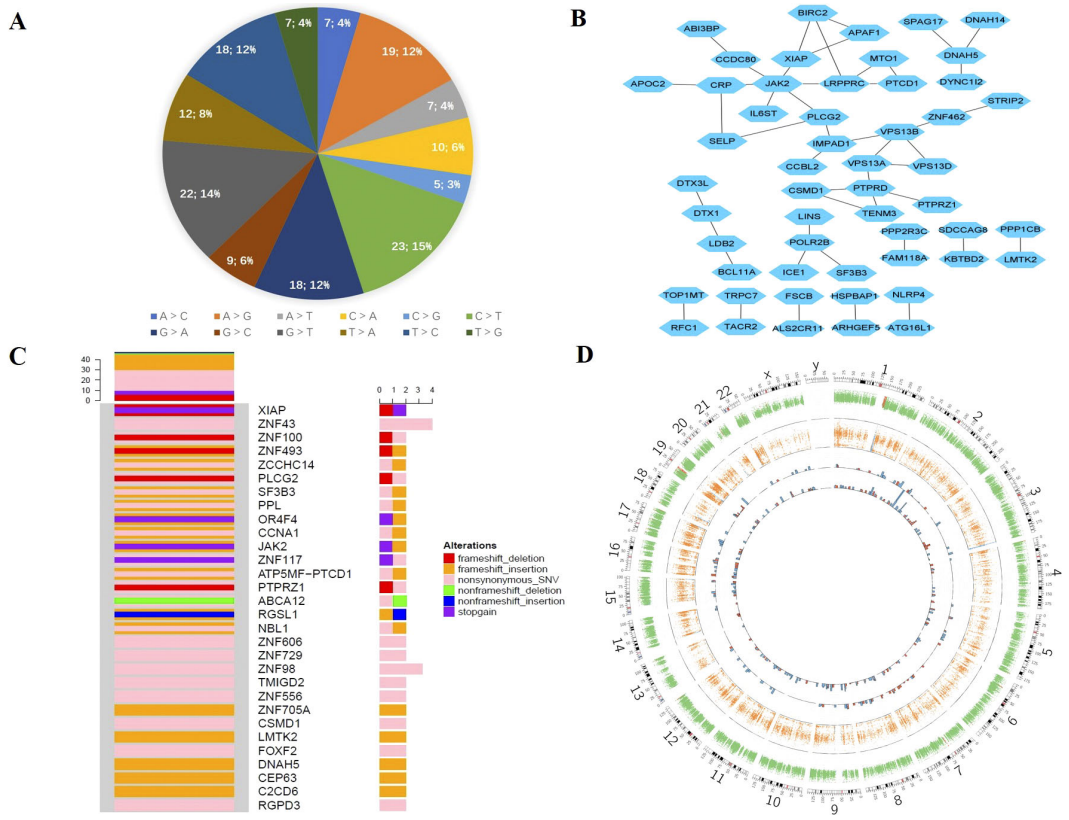

FIGURE 4
Somatic mutation of GEA. **(A)** The proportion of base substitutions in somatic mutations. **(B)** The network interaction of the main somatic mutation genes. **(C)** Oncoprint for the genomic mutation profile. **(D)** Circos plot of somatic mutations displaying the mutation frequencies, distributions, and CNV results. From the outside to the inside: the first circle represents the genome karyotype (24 chromosomes and the corresponding number); the second circle represents somatic CNV; the third circle represents LOH; the fourth circle represents somatic mutation SNV; and the last circle represents somatic mutation Indel. The red histogram column indicates mutations with functional effects, including stop gain, nonsynonymous, and frameshift effects; the blue histogram column indicates mutations without functional effects. The mutation frequencies are represented by the height of the column.

enrichment degree of differential genes on apoptotic factor-mediated response and downregulation of the *ERBB4* signaling pathway was the highest. In the top 30 pathways, gene expression (transcription), cell cycle pathway, programmed cell death, signal transduction, and biosynthesis pathways played essential roles. Other affected pathways included developmental biology, the immune system, transport of non-small molecules, cellular processes, lipid metabolism, the circulatory system, and drug resistance. In addition, we also found the Notch signaling pathway (*DTX3L*, *DTX1*, *MAML1*), TNF signaling pathway (*BIRC2*), Ras pathway (*PDPK1*, *RAF1*, *PAK2*), p53 pathway (*APAF1*, *PDPK1*, *CDKN2A*, *PIK3C2B*), NF-kappa B signaling pathway (BIRC2, XIAP, PLCG2), JAK/STAT signaling pathway (*JAK2*, *RAF1*, *IL23R*, *IL6ST*), and PI3K-Akt signaling pathway (*JAK2*, *PDPK1*, *PPP2R3C*, *LAMA1*, *PPP2R2B*, *RAF1*, *PPP2R5A*). Some pathways were related to pancreatic cancer (*RAF1*, *CDKN2A*, *ARHGEF6*) and endometrial cancer (*PDPK1*, *RAF1*) (Supplementary Table S4).

In addition, we explored the disease enrichment in the patient's somatic mutation genes using the GWAS Catalog, NHGRI GWAS Catalog, OMIM, and KEGG disease databases (Supplementary Figure 1C). The response to taxane treatment (docetaxel) was quite significant. Schizophrenia, schizoaffective disorder, bipolar disorder, and myeloproliferative neoplasms showed relatively higher degrees of gene enrichment.

In addition, we used MSIsensor to examine somatic microsatellite variation and determined that this tumor was the non-MSI-H type.

Discussion

In this study, we thoroughly investigated a patient with PJS who also had GEA, bilateral ovary SCTAT, SCVM, and vaginal HSIL from clinical, histological, and molecular perspectives.

GEA often appeared in the middle and upper regions of the endocervical canal, with bigger masses producing a "barrel-shaped" cervix with no evident exterior lesions. The tumor cells of well-differentiated areas have no significant cytological atypia and are classified as minimum deviation adenocarcinoma (MDA), which is regarded as a highly differentiated type within the differentiation spectrum of GEA, but the term MDA is no longer recommended in WHO 2020 (14). These characteristics can also easily lead to missed diagnoses. A pattern of infiltrative growth, an irregular glandular

structure, and neural mucus in pale or weak eosinophilic cytoplasm indicate GEA (5). The neural mucus, which is gastric mucus, is revealed by the pinkish-red staining of AB-PAS. ER, PR, P16, and Pax-2 are commonly negative (15). However, only a few instances display widespread p16 expression despite negative oncogenic HPV molecular testing, showing that diffuse p16 immunoreactivity is not necessarily an indication of a high-risk HPV-related tumor (16). The loss of Pax-2 expression can help to exclude lobular endocervical glandular hyperplasia (15, 17). MUC-6, MUC5AC, CAIX, and HNF-1 were immunoreactive, and we discovered germline mutations of *MUC-6* and *CAIX* in tumor tissue. When only a few well-differentiated glands are seen in cytology and endocervical curettage specimens, the GEA is easily ignored, and the useful clue is the pale and abundant cytoplasm.

We detected the germline alterations STK11 gene non-frameshift deletion in our GEA tumor by WES. Germline mutations of the STK11 gene are the leading cause of PJS and were detected in around 80% of patients (1). According to one study, endogenous *STK11/LKB1* knockdown accelerated cell cycle progression from G1 to the S phase, which was at least partially mediated by the decrease in the p53 and p16 pathways (3). We detected *STK11* gene nonframeshift deletion in our GEA tumor. This mechanism may explain the loss or decline of P16 expression in GEA and negative HPV DNA detection results. But we found cervical and vaginal HISL with diffuse P16 immunostaining and HPV-18 infection in our case. Several researchers have also observed this occurrence (18). The rarity of GEA coexisting with HPV infection emphasizes the importance of continuing research and close monitoring in the field of gynecological oncology.

Women with PJS have an increased risk for gynecologic tumors (2, 5). Our patient with PJS was diagnosed with GEA, SCVM, and SCTAT of the bilateral ovary. SCVM is a rare benign mesenchymal tumor. Magro et al. (19) validated the chromosome abnormalities linked to the loss of the 13q14 area in the lower female genital tract myofibroblastoma. We also found the RB1(13q14) deletion in SCVM. SCVM has been identified to be unrelated to HPV infection (20), and it has a tumor-hormone relationship due to the presence of estrogen and progesterone receptors. SCTAT is also an uncommon and distinct tumor that is present in approximately one-third of PJS patients (21). SCTAT with PJS is typically bilateral and visible under a microscope (21), with just a few instances indicating malignant tendencies (22, 23). However, SCTAT without PJS is frequently unilateral, massive, and malignant (21). The primary treatment for these tumors is surgical removal (20, 21).

Using immunohistochemistry and FISH, we first identified the *TP53* mutation and *ERBB2* amplification. Further, we also found germline alterations in the *TP53* and *ERBB2* genes by WES. *TP53* was the gene that was most often altered in GEA tumors. A study discovered that *HER2* overexpression and amplification were linked to poor progression-free survival, whereas mutant-type *p53* has no prognostic value (24). Some researchers have also observed *HER2* amplification, indicating that therapy with a monoclonal antibody against HER2 may be a potential therapeutic option for GEA expressing HER2 (24–26). Ehmann et al. (27) proposed excellent clinical outcomes with adjusted trastuzumab. Besides, one trial demonstrated that trastuzumab exhibited durable responses in heavily pretreated patients with HER2-expressing solid tumors, including cervical cancers (28).

Furthermore, we performed a somatic mutation analysis of GEA with PJS by comparing the patient's GEA tumor tissues and the control peripheral blood sample. In this patient, we detected 372 mutations, all of which were heterogeneous at the mutational level. Nonsynonymous and frameshift insertions were the most frequent types of mutations. Liao et al. (13) performed WES on 25 Chinese patients with GEA and compared the prior genetic profiles. The most altered genes were found to be *TP53*, *CDKN2A*, *STK11*, *BRCA2*, *SMAD4*, *ERBB2*, *FRMPD4*, *TELO2*, *NOP2*, *ELF3*, *FGF1*, *DNAL1*, and *NRIP3*, and the enrichment of the *APOBEC* signature was significant. In our case, we discovered *CDKN2A* and *KMT2D* somatic mutations. *CDKN2A* is a common mutation that affects the cell cycle. The *KMT2D* mutation has been described in two GEA cases thus far, both of which were gastric adenocarcinomas with a poor prognosis and involved cell proliferation and differentiation (9).

In our case, *JAK2* was the top core gene in network interaction by Cytoscape, and it was widely dispersed in the cytoplasm of somatic cells. The activated *JAK2/STAT3* pathway is involved in the pathologies of cancer and inflammatory diseases, and it promotes carcinogenesis, tumor development, cancer cell survival, and the spread of solid tumors (29). In addition, it can be involved in mediating resistance to traditional cancer therapy, including cervical cancer (29). The STK11/LKB1 promoter contains a STAT binding/interferon gamma-activated sequence, and PRL-mediated increases in promoter activity require signaling through STAT3 and STAT5A, also involving JAK2 (2, 30). Some researchers claimed that IL-11-mediated activation of JAK/STAT3 was crucial in gastrointestinal carcinogenesis following *LKB1* mutations and that targeting this pathway offers therapeutic potential in PJS (31). However, the mechanism of the JAK2/STAT3 pathway in GEA remains unknown, which could be a key focus of targeted therapy for GEA patients with PJS.

In gene enrichments, generic transcription or expression pathways and cell cycle pathways played important roles in the pathogenesis of GEA. This result was consistent with Selenica's findings (12). The response to taxane treatment (docetaxel) was the most significant in disease enrichment, which might indicate chemotherapy resistance. Park et al. [9] came to the view that EMT-related pathways may have a role in GEA aggression and chemoresistance. Some researchers (9–13) found the unique genomic changes of GAS, mainly involving cell cycle and PI3K/AKT signaling pathways. Currently, a phase II interventional trial is underway to investigate the safety, tolerability, and effectiveness of WX390, a PI3K-mTOR cell cycle inhibitor, in combination with toripalimab, a PD-L1 inhibitor, in patients with advanced GEAS and confirmed STK11 mutations (32, 33).

In our case, the GEA tumor was the non-MSI-H type. Garg et al. (11) showed MSH6, MLH1, MSH2, and PMS2 aberrations, but mismatch repair marker expression was intact in every instance. Only one Lynch syndrome patient had MSH6 staining deletion as of yet (16). Most likely, GEA did not arise via the MMR pathway.

GEA patients with PJS have poor outcomes, short progression-free survival (PFS), and overall survival (OS) (5, 34). Nine years ago,

our patient had an ultrasound that showed an enlarged cervix, and seven years earlier, she complained of vaginal discharge. However, nabothian cysts and vaginitis were incorrectly identified as the cause of these symptoms. Our patient was diagnosed with IIB GEA after nine years. GEA can easily be misdiagnosed and missed due to the lack of typical clinical manifestation, hidden lesion location, negative high-risk HPV screening, and mild cytological atypia. Clinicians and pathologists must furthermore enhance a high level of awareness and vigilance for GEA. Clinicians should pay high attention to patients with long-term abnormal vaginal discharge. For patients with high suspicion of GEA, particularly PJS patients, the cervical multiple-point biopsy or conization of the cervix should be performed (35). PJS patients should have annual gynecological ultrasonography, gynecological exams, and cervical cytologic (including sexual life history) testing to detect precursor or early-stage lesions beginning at the age of 18-20, according to National Comprehensive Cancer Network (NCCN) guidelines. Given its rarity and little information on treatment results, the best therapeutic technique for GEA is unknown. Experts now advocate adhering to the most recent NCCN guidelines for cervical carcinoma (32). For early-stage high-risk disease, these guidelines recommend primary radical hysterectomy and pelvic lymphadenectomy ± para-aortic lymph node sampling and advise against fertility-sparing surgery. They also recommend removal of the appendix, greater omentum, bilateral adnexa, and any metastatic lesions in the pelvic and abdominal cavity. In addition, postoperative concurrent chemoradiation was administered to high-risk patients, defined as those with at least one major risk factor, including positive nodes, parametrial involvement, and positive surgical margin (Chinese Expert Consensus on Clinical Diagnosis and Treatment of gastric-type endocervical adenocarcinoma, 2023 edition). Our case followed these rules. Surgical resection or radiation combination was an effective form of treatment. However, chemotherapy may not be a suitable adjuvant therapy for GEA (9, 34).

We thoroughly investigated this complex case. However, there are certain limitations to this study. We were unable to evaluate the GEA driver genes with PJS since we only sequenced one case by WES and detected two equivalent somatic mutations compared to the previous genetic profiles. At present, our case is the first to report SCVM with PJS; more instances are needed to investigate the link between unusual SCVM and SCTAT with PJS.

In conclusion, it was extremely rare for GEA with PJS to occur alongside the rare SCVM, bilateral ovarian SCTAT, and cervical and vaginal HISL with infection with high-risk HPV 18. Patients with PJS require routine gynecological, ultrasound, and cytological tests to detect precursor or early-stage lesions. Gynecologists must handle PJS patients carefully to obtain early clinical detection and diagnosis. We also thoroughly investigated the GEA gene characteristics using WES. The *STK11/LKB1* mutation may play an important role in tumor development. *TP53* and *HER2* mutations were found. The patient is most likely to benefit from the use of the anti-HER2 antibody trastuzumab in the future. The somatic mutations mainly involved general transcription or expression pathways and cell cycle pathways, which revealed the potential causative genetic factors and chemotherapy resistance of GEA. In addition, the JAK2/STAT3 pathway could be a major focus of targeted therapy for GEA patients with PJS. However, more cases are needed to investigate the pathogenesis of GEA with PJS.

Data availability statement

The datasets presented in this study can be found in online repositories. The names of the repository/repositories and accession number(s) can be found in the article/Supplementary Material.

Ethics statement

The studies involving humans were approved by Sir Run Run Shaw Hospital of Zhejiang University School of Medicine. The studies were conducted in accordance with the local legislation and institutional requirements. The human samples used in this study were acquired from gifted from another research group. Written informed consent for participation was not required from the participants or the participants' legal guardians/next of kin in accordance with the national legislation and institutional requirements. Written informed consent was obtained from the individual(s) for the publication of any potentially identifiable images or data included in this article.

Author contributions

DS: Conceptualization, Data curation, Formal analysis, Investigation, Methodology, Project administration, Resources, Software, Supervision, Validation, Visualization, Writing – original draft, Writing – review & editing. ZC: Funding acquisition, Resources, Writing – review & editing. YL: Data curation, Resources, Writing – review & editing.

Funding

The author(s) declare that no financial support was received for the research, authorship, and/or publication of this article.

Acknowledgments

We acknowledge the technique supported by Shanghai Bohao Biotechnology Company.

Conflict of interest

The authors declare that the research was conducted in the absence of any commercial or financial relationships that could be construed as a potential conflict of interest.

Publisher's note

All claims expressed in this article are solely those of the authors and do not necessarily represent those of their affiliated organizations, or those of the publisher, the editors and the reviewers. Any product that may be evaluated in this article, or claim that may be made by its manufacturer, is not guaranteed or endorsed by the publisher.

Supplementary material

The Supplementary Material for this article can be found online at: https://www.frontiersin.org/articles/10.3389/fonc.2025.1472017/full#supplementary-material

SUPPLEMENTARY FIGURE 1
Gene enrichment analysis in GEA. **(A)** Gene ontology enrichment analysis results. **(B)** Pathway enrichment analysis results. **(C)** Disease enrichment analysis results.

References

1. Hemminki A, Markie D, Tomlinson I, Avizienyte E, Roth S, Loukola A, et al. A serine/threonine kinase gene defective in Peutz–Jeghers syndrome. *Nature*. (1998) 391:184–7. doi: 10.1038/34432

2. Peña CG, Castrillón DH. LKB1 as a tumor suppressor in uterine cancer: mouse models and translational studies. *Adv Exp Med Biol*. (2017) 943:211–41. doi: 10.1007/978-3-319-43139-0_7

3. Liang X, Wang P, Gao Q, Xiang T, Tao X. Endogenous LKB1 knockdown accelerates G (1)/S transition through p53 and p16 pathways. *Cancer Biol Ther*. (2010) 9:156–60. doi: 10.4161/cbt.9.2.10452

4. Chen HY, Jin XW, Li BR, Zhu M, Li J, Mao GP, et al. Cancer risk in patients with Peutz–Jeghers syndrome: A retrospective cohort study of 336 cases. *Tumor Biol*. (2017) 39:1010428317705131. doi: 10.1177/1010428317705131

5. Gordhandas SB, Kahn R, Sassine D, Aviki EM, Baltich Nelson B, Catchings A, et al. Gastric-type adenocarcinoma of the cervix in patients with Peutz–Jeghers syndrome: a systematic review of the literature with proposed screening guidelines. *Int J Gynecol Cancer*. (2022) 32:79–88. doi: 10.1136/ijgc-2021-002997

6. Stolnicu S, Barsan I, Hoang L, Patel P, Terinte C, Pesci A, et al. International endocervical adenocarcinoma criteria and classification (IECC): A new pathogenetic classification for invasive adenocarcinomas of the endocervix. *Am J Surg Pathol*. (2018) 42:214–26. doi: 10.1097/PAS.0000000000000986

7. Radomska A, Lee D, Neufeld H, Korte N, Torlakovic E, Agrawal A, et al. A retrospective study on incidence, diagnosis, and clinical outcome of gastric-type endocervical adenocarcinoma in a single institution. *Diagn Pathol*. (2021) 16:68. doi: 10.1186/s13000-021-01129-9

8. Neyaz A, Husain N, Deodhar M, Khurana R, Shukla S, Arora A. Synchronous cervical minimal deviation adenocarcinoma, gastric type adenocarcinoma and lobular endocervical glandular hyperplasia along with STIL in peutz–Jeghers syndrome: eliciting oncogenesis pathways. *Turk Patoloji Derg*. (2019) 35:247–53. doi: 10.5146/tjpath.2017.01406

9. Park E, Kim SW, Kim S, Kim HS, Lee JY, Kim YT, et al. Genetic characteristics of gastric-type mucinous carcinoma of the uterine cervix. *Mod Pathol*. (2021) 34:637–46. doi: 10.1038/s41379-020-0614-0

10. Lu S, Shi J, Zhang X, Kong F, Liu L, Dong X, et al. Comprehensive genomic profiling and prognostic analysis of cervical gastric-type mucinous adenocarcinoma. *Virchows Arch*. (2021) 479:893–903. doi: 10.1007/s00428-021-03080-y

11. Garg S, Nagaria TS, Clarke B, Freedman O, Khan Z, Schwock J, et al. Molecular characterization of gastric-type endocervical adenocarcinoma using next-generation sequencing. *Mod Pathol*. (2019) 32:1823–33. doi: 10.1038/s41379-019-0305-x

12. Selenica P, Alemar B, Matrai C, Talia KL, Veras E, Hussein Y, et al. Massively parallel sequencing analysis of 68 gastric-type cervical adenocarcinomas reveals mutations in cell cycle-related genes and potentially targetable mutations. *Mod Pathol*. (2021) 34:1213–25. doi: 10.1038/s41379-020-00726-1

13. Liao X, Xia X, Su W, Yan H, Ma Y, Xu L, et al. Association of recurrent APOBEC3B alterations with the prognosis of gastric-type cervical adenocarcinoma. *Gynecol Oncol*. (2022) 165:105–13. doi: 10.1016/j.ygyno.2022.01.036

14. Herrington CS, Kim KR, Kong CS, Longacre TA, McCluggage WG, Mikami Y. *Tumors of the cervix. WHO classification of tumors of female genital organs. 5th ed*. Lyon: IARC Press (2020) p. 336–89.

15. Nishio S. Current status and molecular biology of human papillomavirus-independent gastric-type adenocarcinoma of the cervix. *J Obstet Gynecol Res*. (2023) 49:1106–13. doi: 10.1111/jog.15578

16. Carleton C, Hoang L, Sah S, Kiyokawa T, Karamurzin YS, Talia KL, et al. A detailed immunohistochemical analysis of a large series of cervical and vaginal gastric-type adenocarcinomas. *Am J Surg Pathol*. (2016) 40:636–44. doi: 10.1097/PAS.0000000000000578

17. Rabban JT, McAlhany S, Lerwill MF, Grenert JP, Zaloudek CJ. PAX2 distinguishes benign mesonephric and mullerian glandular lesions of the cervix from endocervical adenocarcinoma, including minimal deviation adenocarcinoma. *Am J Surg Pathol*. (2010) 34:137–46. doi: 10.1097/PAS.0b013e3181c89c98

18. Sun Y, Lin W, Zou Q, Zheng W, Zhang H, Zhou F. Gastric type endocervical adenocarcinoma with concurrent high-grade squamous intraepithelial lesion: A clinicopathologic study of three patients. *Int J Surg Pathol*. (2024) 1:10668969241241637. doi: 10.1177/10668969241241637

19. Magro G, Righi A, Casorzo L, Antonietta T, Salvatorelli L, Kacerovská D, et al. Mammary and vaginal myofibroblastomas are genetically related lesions: fluorescence in situ hybridization analysis shows deletion of 13q14 region. *Hum Pathol*. (2012) 43:1887–93. doi: 10.1016/j.humpath.2012.01.015

20. Liu JL, Su TC, Shen KH, Lin SH, Wang HK, Hsu JC, et al. Vaginal superficial myofibroblastoma: a rare mesenchymal tumor of the lower female genital tract and a study of its association with viral infection. *Med Mol Morphol*. (2012) 45:110–4. doi: 10.1007/s00795-011-0566-z

21. Young RH, Welch WR, Dickersin GR, Scully RE. Ovarian sex cord tumor with annular tubules: review of 74 cases including 27 with Peutz–Jeghers syndrome and four with adenoma Malignum of the cervix. *Cancer*. (1982) 50:1384–402. doi: 10.1002/1097-0142(19821001)50:7<1384::aid-cncr2820500726>3.0.co;2-5

22. Barker D, Sharma R, McIndoe A, Blair E, Hall M, Gabra H, et al. An unusual case of sex cord tumor with annular tubules with Malignant transformation in a patient with Peutz-Jeghers syndrome. *Int J Gynecol Pathol*. (2010) 29:27–32. doi: 10.1097/PGP.0b013e3181b6a7c2

23. Lele SM, Sawh RN, Zaharopoulos P, Adesokan A, Smith M, Linhart JM, et al. Malignant ovarian sex cord tumor with annular tubules in a patient with Peutz–Jeghers syndrome: a case report. *Mod Pathol*. (2000) 13:466–70. doi: 10.1038/modpathol.3880079

24. Shi H, Shao Y, Lu W, Lu B. An analysis of HER2 amplification in cervical adenocarcinoma: correlation with clinical outcomes and the International Endocervical Adenocarcinoma Criteria and Classification. *J Pathol Clin Res*. (2021) 7:86–95. doi: 10.1002/cjp2.184

25. Murakami R, Abiko K, Hamanishi J, Kondoh E, Baba T, Mandai M, et al. Mucinous adenocarcinoma, gastric type of the uterine cervix: clinical features and HER2 amplification. *Med Mol Morphol*. (2019) 52:52–9. doi: 10.1007/s00795-018-0202-2

26. Wang S, Zhou X, Niu S, Chen L, Zhang H, Chen H, et al. Assessment of HER2 in gastric-type endocervical adenocarcinoma and its prognostic significance. *Mod Pathol*. (2023) 36:100148. doi: 10.1016/j.modpat.2023.100148

27. Ehmann S, Sassine D, Straubhar AM, Praiss AM, Aghajanian C, Alektiar KM, et al. Gastric-type adenocarcinoma of the cervix: Clinical outcomes and genomic drivers. *Gynecol Oncol*. (2022) 167:458–66. doi: 10.1016/j.ygyno.2022.10.003

28. AstraZeneca. A phase 2 study of T-DXd in patients with selected HER2 expressing tumors (DPT02) ClinicalTrials.gov.NCT04482309. *U.S. Natl Library Med*. (2023). Available online at: https://clinicaltrials.gov/study/NCT04482309

29. Mengie Ayele T, Tilahun Muche Z, Behaile Teklemariam A, Bogale Kassie A, Chekol Abebe E. Role of JAK2/STAT3 signaling pathway in the tumorigenesis, chemotherapy resistance, and treatment of solid tumors: A systemic review. *J Inflammation Res*. (2022) 15:1349–64. doi: 10.2147/JIR.S353489

30. Linher-Melville K, Singh G. The transcriptional responsiveness of LKB1 to STAT-mediated signaling is differentially modulated by prolactin in human breast cancer cells. *BMC Cancer*. (2014) 14:415. doi: 10.1186/1471-2407-14-415

31. Ollila S, Domènech-Moreno E, Laajanen K, Wong IP, Tripathi S, Pentinmikko N, et al. Stromal Lkb1 deficiency leads to gastrointestinal tumorigenesis involving the IL-11-JAK/STAT3 pathway. *J Clin Invest*. (2018) 128:402–14. doi: 10.1172/JCI93597

32. Chalif J, Kistenfeger Q, Fulton J, Morton M, DeVengencie I, Weldemichael W, et al. Diagnosis and management of gastric-type endocervical adenocarcinoma: A case report and review of the literature. *Gynecol Oncol*. (2024) 185:165–72. doi: 10.1016/j.ygyno.2024.02.024

33. Shanghai Jiatan Pharmatech Co., Ltd. A study of WX390 combined with toripalimab in patients with advanced gastric-type endocervical adenocarcinoma with STK11 mutations. ClinicalTrials.gov.NCT06124963. *U.S. Natl Library Med*. (2023). Available online at: https://clinicaltrials.gov/study/NCT06124963

34. Nishio S, Matsuo K, Nasu H, Murotani K, Mikami Y, Yaegashi N, et al. Analysis of postoperative adjuvant therapy in 102 patients with gastric-type mucinous carcinoma of the uterine cervix: A multi-institutional study. *Eur J Surg Oncol*. (2022) 48:2039–44. doi: 10.1016/j.ejso.2022.03.007

35. Li G, Jiang W, Gui S, Xu C. Minimal deviation adenocarcinoma of the uterine cervix. *Int J Gynaecol Obstet*. (2010) 110:89–92. doi: 10.1016/j.ijgo.2010.03.016

frontiers | Frontiers in Oncology

TYPE Case Report
PUBLISHED 27 February 2025
DOI 10.3389/fonc.2025.1464446

Check for updates

OPEN ACCESS

EDITED BY
Ronald M Bukowski,
Cleveland Clinic, United States

REVIEWED BY
Andrea Guttilla,
Azienda ULSS 6 Euganea, Italy
Angelo Naselli,
MultiMedica Holding SpA (IRCCS), Italy

*CORRESPONDENCE
Junqing Hou
hjq0418@sina.com

RECEIVED 15 July 2024
ACCEPTED 10 February 2025
PUBLISHED 27 February 2025

CITATION
Chang B, Zhang M, Hou Y, Li W, Li S, Zhang J, Wang C, Zhang Q and Hou J (2025) Solitary testicular metastasis post-prostatectomy for prostatic ductal adenocarcinoma: case report and literature review. *Front. Oncol.* 15:1464446. doi: 10.3389/fonc.2025.1464446

COPYRIGHT
© 2025 Chang, Zhang, Hou, Li, Li, Zhang, Wang, Zhang and Hou. This is an open-access article distributed under the terms of the Creative Commons Attribution License (CC BY). The use, distribution or reproduction in other forums is permitted, provided the original author(s) and the copyright owner(s) are credited and that the original publication in this journal is cited, in accordance with accepted academic practice. No use, distribution or reproduction is permitted which does not comply with these terms.

Solitary testicular metastasis post-prostatectomy for prostatic ductal adenocarcinoma: case report and literature review

Bo Chang[1], Manqing Zhang[2], Yifan Hou[3], Wenbin Li[4], Song Li[1], Jianhua Zhang[4], Chenyang Wang[1], Qiangqiang Zhang[1] and Junqing Hou[4]*

[1]Department of Urology, Huaihe Hospital of Henan University, Kaifeng, Henan, China, [2]Department of General Medicine, the First Affiliated Hospital of Henan University, Kaifeng, Henan, China, [3]Medical College of Henan University, Kaifeng, Henan, China, [4]Department of Urology, Kaifeng 155th Hospital, Kaifeng, Henan, China

Background and Purpose: Prostatic ductal adenocarcinoma (PDA) constitutes a rare and notably aggressive histological subtype within the spectrum of prostate malignancies, distinguished by a heightened propensity for recurrence and metastasis compared to prostatic acinar adenocarcinoma (PAA). Testicular metastasis in PDA is exceptionally rare. Despite sporadic reports in the literature, a consensus regarding the optimal therapeutic approach remains elusive. This study retrospectively analyzes a singular case of PDA manifesting with solitary testicular metastasis after laparoscopic radical prostatectomy (LRP), consolidating insights into clinical, histopathological, molecular, and therapeutic aspects, alongside existing scholarly discourse.

Methods: We present the case of a 63-year-old gentleman diagnosed with pure PDA (pT3aN0, Gleason score 4 + 4 = 8), exhibiting a serum prostate-specific antigen (PSA) level exceeding 100 ng/ml. Subsequently, the patient underwent androgen deprivation therapy (ADT) followed by LRP. Subsequently, at 17 months post-LRP, local recurrence and a right testicular mass emerged, prompting pelvic radiotherapy and docetaxel chemotherapy. Ultimately, the patient underwent right orchiectomy 65 months post-LRP, with pathological findings confirming metastatic PDA. Four months post-orchiectomy, PSA levels declined to 1.77 ng/ml. Additionally, a comprehensive review of published literature concerning PDA complicated by testicular metastasis was conducted.

Results: The patient derived therapeutic benefits from ADT, LRP, radiation therapy, and orchiectomy, resulting in objective symptom alleviation and a reduction in PSA. Nevertheless, docetaxel proved inefficacious. The literature review indicated variability in outcomes across diverse treatment modalities.

Conclusions: Prolonged surveillance is imperative for patients diagnosed with PDA. Urologists must remain vigilant regarding uncommon sites of metastasis, particularly in instances of elevated PSA.

KEYWORDS

prostatic ductal adenocarcinoma, metastatic testicular tumor, solitary metastasis, laparoscopic radical prostatectomy, orchiectomy

Introduction

Prostate cancer (PC) stands as the second most prevalent malignancy among men worldwide (1). Prostatic epithelial tumors exhibit various histological subtypes, including acinar adenocarcinoma (AA), ductal adenocarcinoma (DA), intraductal carcinoma (IDC), squamous cell carcinoma, and basal cell carcinoma. Among these, prostatic ductal adenocarcinoma (PDA) ranks second in incidence, comprising 2.6% of cases (2, 3). PDA is delineated into pure type and mixed type (mixed with AA); pure ductal adenocarcinoma accounts for merely 0.2% to 0.4% of all prostate cancers (2). The description of ductal adenocarcinoma of the prostate dates back to 1967, attributed to Melicow and Pachter (4). Predominant clinical manifestations of PDA include lower urinary tract symptoms and hematuria. Diagnosis of PDA relies on histopathological evaluation, revealing characteristic morphological features such as papillary, cribriform, and solid structures (5, 6).

The long-term prognosis of PDA primarily hinges upon the presence or absence of metastasis, typically affecting bone, lymph nodes, and viscera, while testicular metastasis is a rare occurrence (7). Testicular tumors are predominantly primary germ cell neoplasms, with secondary metastases being exceedingly rare (8, 9). While clinical evidence indicates that metastatic tumors in the testis primarily arise from the prostate, there exists a paucity of robust research and substantial clinical data concerning the metastasis of PDA to the testis (10). This article presents a rare case of PDA with solitary testicular metastasis occurring 17 months post-laparoscopic radical prostatectomy, accompanied by a comprehensive review of published literature detailing the clinical characteristics and treatment strategies for this disease.

Case report

In March 2018, a 63-year-old male patient was admitted with a chief complaint of intermittent dysuria and initial hematuria for two years. His medical history included 20 years of bronchitis and 10 years of hypertension. Upon admission, the patient declined a digital rectal examination. Serum prostate-specific antigen (PSA) was found to be >100 ng/mL. Color Doppler ultrasound revealed a residual urine volume of 1100 mL, and pelvic magnetic resonance imaging (MRI) indicated a prostatic mass with minor hemorrhagic foci, suggestive of prostate cancer (Figures 1A, B). Chest and abdominal computed tomography (CT) scans, as well as a whole-body bone scan, showed no evidence of distant metastasis. Transrectal prostate biopsy confirmed PDA, characterized by a Gleason score of 4 + 4 = 8. Immunohistochemistry demonstrated positivity for P504S and PSA, with a Ki-67 index of 20%, while 34BE12 and P63 were negative. Following comprehensive discussions with the patient regarding treatment options, including their benefits and anticipated outcomes, the patient opted for neoadjuvant endocrine therapy to reduce tumor volume, enhance local control, and reduce the likelihood of positive surgical margins. Subsequently, the patient underwent a planned 12-week course of androgen deprivation therapy (ADT) to maximize androgen blockade, utilizing a goserelin acetate sustained-release implant (10.8 mg every 12 weeks) and bicalutamide (50 mg daily). This constituted the preoperative neoadjuvant endocrine therapy. However, one month later, the patient was readmitted due to intolerable discomfort from the indwelling urinary catheter. At this time, his serum PSA level was 36.36 ng/mL. At his request, a laparoscopic radical prostatectomy (LRP) was performed. Postoperative pathological examination revealed PDA staged as pT3aN0, with a Gleason score of 4 + 4 = 8. The tumor exhibited diffuse invasive growth, extensively infiltrating the left and right lobes, middle and posterior lobes, constituting approximately 80% of the tissue. Local invasion of the urethral mucosa and prostate capsule, with no cancer involvement observed in the bilateral seminal vesicle glands, vas deferens, or at the upper and lower urethral incisal margins (Figures 2A–C).

Seventeen months post-LRP, the serum PSA level measured 16.50 ng/ml, while pelvic MRI revealed a dubious nodule in the left perineal region (Figure 1C). Color ultrasonography detected a solid mass within the right testicular parenchyma (Figure 1E). Testicular tumor markers indicated human chorionic gonadotropin at 3.73 mIU/ml, while lactate dehydrogenase, alpha-fetoprotein, and carcinoembryonic antigen levels remained within normal limits. We recommended the patient undergo testicular biopsy or orchiectomy. However, due to economic constraints, the patient declined. Subsequently, the patient underwent pelvic radiotherapy (72.9Gy/27f) in conjunction with ADT (goserelin acetate plus bicalutamide). Five months post-pelvic radiotherapy, reassessment revealed a serum PSA level of 4.03 ng/ml, accompanied by the resolution of suspicious nodules on the left perineal side as evidenced by pelvic MRI (Figure 1D).

At 41 months post-LRP, the serum PSA level measured 13.43 ng/ml, prompting a transition from bicalutamide to abiraterone (1g, once daily). However, after one month of treatment, the patient independently ceased the medication. By 54 months post-LRP, the serum PSA level exceeded 100ng/ml, leading to the initiation of oral abiraterone and docetaxel (75mg/m2, every 4 weeks) chemotherapy. Despite completing 6 cycles of chemotherapy, the serum PSA level remained elevated (> 100ng/ml), and the painless swelling of the right scrotum worsened. At 65 months post-LRP, the patient experienced intolerable pain in the right testicle, with a serum PSA level >100 ng/mL. Scrotal MRI revealed enlargement of the right testis with multiple nodules, along with a large cyst-like structure in the right scrotum indicative of hemorrhagic changes (Figures 1F-H). Extensive investigations found no evidence of distant metastasis, and testicular tumor markers remained within the normal range. Consequently, a right orchiectomy was performed, unveiling metastatic PDA with a 2.7×2.5×1.5cm tumor invading the rete testis. No carcinoma was detected at the spermatic cord stump. Immunohistochemistry indicated negativity for P504S and positivity for PSA, with a Ki67 index of 10% (Figures 2D-I). In the third month post-orchiectomy, the patient's PSA level decreased to 3.066 ng/ml. In the fourth month, the PSA level further declined to 1.77 ng/ml (Figure 3). The patient presently maintains good physical condition and leads a normative lifestyle.

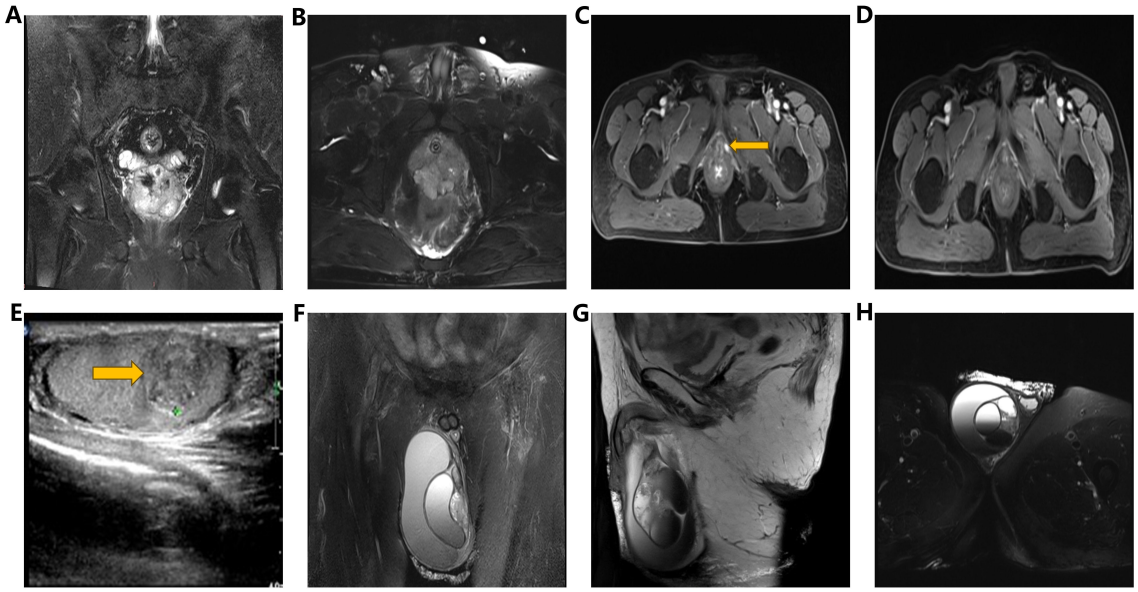

FIGURE 1
(A, B) Pelvic MRI images (coronal view, transverse view): Demonstrating an enlarged prostate volume with irregular shape and indistinct boundary between peripheral zone and urethral periphery zone, along with multiple T2WI low signal nodules and masses, accompanied by focal areas of hemorrhage. **(C)** Pelvic enhanced MRI image (transverse view): Revealing a nodular lesion (1.3cm) on the left perineum, exhibiting significant enhancement upon contrast administration. **(D)** Pelvic enhanced MRI (transverse view): Illustrating resolution of pelvic nodules five months post-radiotherapy. **(E)** Testicular ultrasound: Identifying multiple heterogeneous hypoechoic lesions (1.3×1.0×1.2cm) within the right testicular parenchyma. **(F–H)** Scrotal MRI images (coronal, sagittal, and transverse views): Demonstrating volumetric enlargement of the right testis with multiple intratesticular nodules, accompanied by a large cystic lesion in the right scrotum, suggestive of hemorrhagic changes.

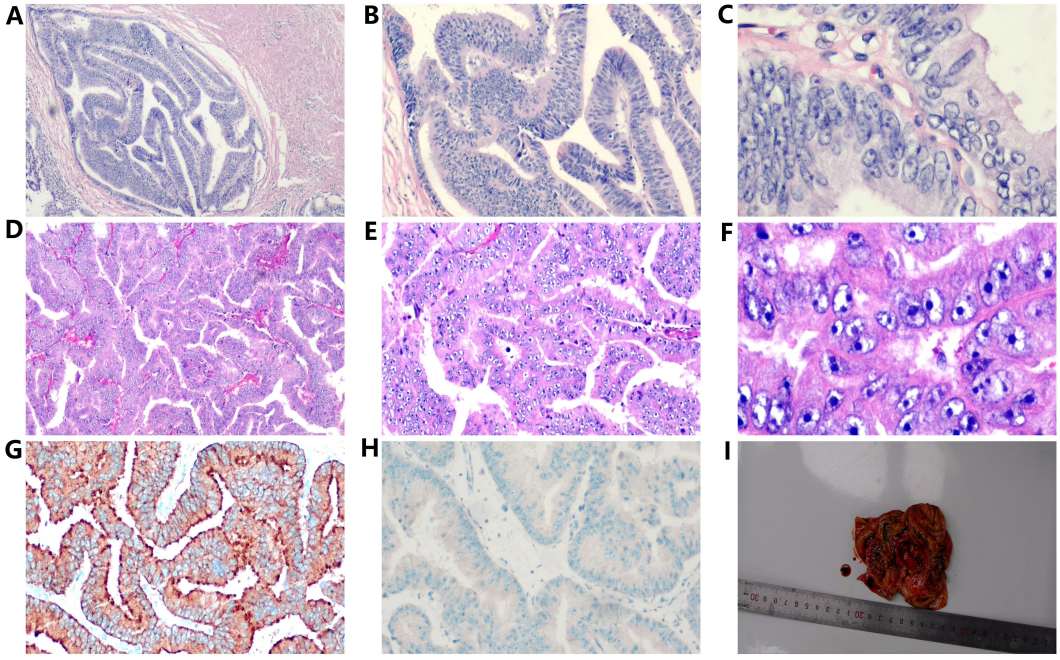

FIGURE 2
Histopathological examination of prostatic ductal adenocarcinoma **(A–C** and a testicular tumor **(D–F)**, revealing characteristic papillary and cribriform structures with enlarged and hyperchromatic nuclei (H&E, ×40, ×100, ×400). Immunohistochemical results of testicular tumors, **(G)** positive prostate specific antigen (PSA) in the cytoplasm (×100). **(H)** P504S(negative, ×100). **(I)** The gross specimen of the right testis exhibited a gray-white nodule (2.7×2.5×1.5cm) surrounded by cystic fibrous tissue upon sectioning.

Literature review

To explore the rarity of this case, we utilized specific keywords in PubMed, Web of Science, and Google Scholar databases. The search terms included "Prostatic ductal adenocarcinoma," "Ductal adenocarcinoma of the prostate," "Testicular metastasis," "Prostatic carcinoma with testicular metastases," "Prostate cancer metastasis to testis," and "Prostate cancer spread to testis." The search was conducted up to April 2024, excluding duplicate articles and reviews. After meticulous screening, a total of three articles were included: one case series and two case reports. Merely six cases of PDA with metastasis to the testis, including this instance, have been elucidated in the literature (11–13). As delineated in Table 1.

The average age was 66 years, with a median age of 68 years. The predominant age of onset ranged from 65 to 70 years (50%), while occurrences at the age of 45 were rare. Among these cases, 2 were located on the left side, 1 on the right side, and 3 lacked side-specific reporting. Gleason scores were 9 in 2 cases, 8 in 3 cases, and not reported in 1 case. The time interval from the initial diagnosis of PDA to testicular metastasis was 4 years in 2 cases, 17 months in 1 case, and undisclosed in 3 cases. PSA levels were < 4 ng/ml in 2 patients and ≥4 ng/ml in 4 patients (with levels exceeding 100 ng/ml in this instance). Among the reported cases, 5 exhibited bone metastases, 2 bladder metastases, and 2 lymph node metastases. Treatment modalities included ADT for all patients, orchiectomy in 5 cases, docetaxel chemotherapy in 2 cases, transurethral resection of the prostate in 2 cases, radiotherapy in 2 cases, and LRP in 1 case. Two patients achieved prolonged survival, spanning 243 and 181 months, respectively, while one survived for 34 months, one received palliative care, and one lacked reported outcomes. None of the previously documented patients underwent radical prostatectomy, and all had bone metastases, with three experiencing at least three metastatic sites. The solitary testicular metastasis observed in the present case, following LRP, represents the first reported instance.

Histopathological characteristics

The standard of excellence for diagnosing PDA is histopathological analysis. Initially denoted as "prostatic endometrioid adenocarcinoma" due to its distinctive histological traits reminiscent of endometrial cancer in females, it is now established that PDA originates from the major prostatic ducts and their secondary counterparts (5, 14). Previously encompassing papillary, cribriform, solid, and PIN-like carcinoma morphologies, the recent WHO classification of prostate cancer redefines PIN-like carcinoma as a subtype of AA (2).

The papillary structure stands out as the hallmark for diagnosing PDA, typified by tall columnar tumor cells arranged pseudostratified amidst fibrovascular bundles. These cells exhibit conspicuous nuclear atypia, elongated oval or ovoid shapes, prominent nucleoli, frequent mitotic figures, and typically dichromatic abundant cytoplasm. Conversely, the cribriform structure, comprising columnar epithelial cells, features slit-like lumens distinct from the round lumens in acinar prostate cancer. Solid structure, albeit rare in PDA, manifests as densely packed columnar epithelial cells in solid formations. It is generally posited that papillary structures predominate in the larger ducts encircling the urethra, while cribriform structures prevail in the smaller surrounding ducts; however, these two morphologies are often intertwined. A Gleason score of 4 + 4 = 8 is designated in the presence of papillary or/and cribriform structures. Immunohistochemical profiles of PDA closely mirror those of AA, frequently exhibiting positive expression of prostate tissue-specific markers (prostate-specific antigen and prostate-specific acid phosphatase). The Ki-67 proliferation index of PDA surpasses that of AA, indicating its heightened biological aggressiveness.

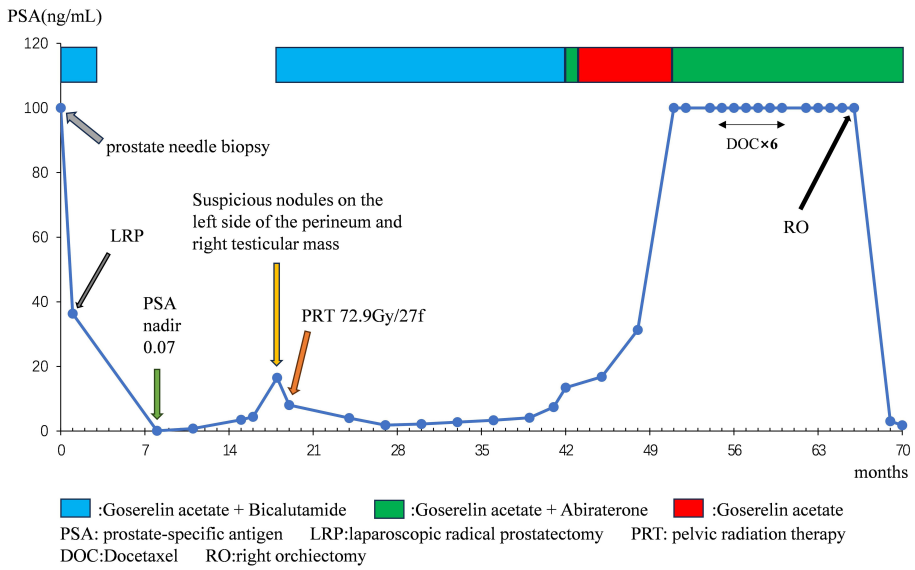

FIGURE 3
PSA change curves throughout treatment.

TABLE 1 Profiles of 6 cases of PDA with testicular metastasis in contemporary literature.

Author/year of publication	Number of cases	Age/ years	Side	Gleason score	Time from PDA diagnosis to testicular metastasis	PSA at Testicular Metastasis (ng/ml)	Site of metastasis	Treatment	Outcomes
Tu et al., 2002 (11)	3	45	Unreported	9	Unreported	<4	Testis, bone, LN	ADT, Orchiectomy, Estramustine/docetaxel	The survival time was 243 months
		59	Unreported	9	Unreported	≥4	Testis, bone, lung, bladder, adrenal gland	ADT, TURP, Ketoconazole/ doxorubicin and estramustine/ vinblastine	The survival time was 181 months
		68	Unreported	8	Unreported	<4	Testis, bone, bladder, gluteal muscle, LN	Testis, bone, bladder, gluteal muscle, LN	The survival time was 34 months
Anila et al., 2012 (12)	1	68	Left	Unreported	4 years	75	Testis, bone	TURP,RT, ADT, Orchiectomy	Multiple bone metastases were treated with palliative care
Mortensen et al., 2014 (13)	1	89	Left	8 (4 + 4)	4 years	41.6	Testis, bone	ADT, Orchiectomy	Unreported
Our csae (2024)	1	69	Right	8 (4 + 4)	17 months	>100	Testis	ADT, LRP, RT, docetaxel, Orchiectomy	There were no signs of disease after orchiectomy

PDA, prostatic ductal adenocarcinoma; PSA, prostate-specific antigen; LN, lymph node; ADT, androgen deprivation therapy; TURP, transurethral resection of the prostate; RT, radiotherapy; LRP, laparoscopic radical prostatectomy.

10.3389/fonc.2025.1464446

Discussion

The median age of onset among individuals diagnosed with PDA spans from 60 to 80 years, marginally surpassing that of those afflicted with AA (15). Originating from the periurethral prostatic ducts, PDA manifests chiefly through lower urinary tract symptoms (such as urinary tract obstruction, diminished urine flow, or urinary retention) and hematuria (either microscopic or gross). Hematospermia may ensue upon tumor infiltration into the seminal vesicle glands or urethra (16). Owing to the nonspecific symptomatology, benign prostatic hyperplasia (BPH) often emerges as the initial clinical diagnosis for such cases. The patient in question endured dysuria and initial hematuria persisting for over two years, concomitant with a residual urine volume of 1100ml upon initial assessment. The distinctive growth pattern of tumor cells in PDA culminates in elevated luminal PSA secretion juxtaposed with diminished serum PSA secretion. Consequently, patients with this subtype are 2.4 times more prone to exhibit PSA levels below 4.0 ng/ml compared to those with AA, with a substantial proportion of PDA patients registering PSA levels below this threshold upon diagnosis (17). The PSA level of the patient surpassed 100 ng/ml during the initial hospital visit and fluctuated throughout subsequent treatment. Fifty months post-LRP, the PSA level once again exceeded 100 ng/ml. However, the alteration in PSA sensitivity enables us to more accurately gauge disease progression. Four months after the orchiectomy, the PSA level dropped to 1.77 ng/ml. Despite this significant reduction from over 100 ng/ml to 1.77 ng/ml indicating the efficacy of the orchiectomy, the PSA level did not fall below 0.2 ng/ml. Possible reasons include: first, the presence of a small number of prostate cancer cells that continue to secrete PSA; second, PDA is an aggressive subtype of prostate cancer that often exhibits partial resistance to conventional castration therapy, which may limit the extent of PSA reduction post-treatment. Therefore, we have devised the following clinical management measures for this patient: first, continue regular monitoring of PSA levels and other imaging examinations to assess tumor progression or residual disease; second, consider further treatment based on the patient's overall condition and response to therapy; third, conduct multidisciplinary team discussions as needed to develop a personalized treatment plan to optimally control the condition.

PDA exhibits greater aggressiveness compared to prostatic acinar adenocarcinoma (PAA). At the time of diagnosis, PDA is three times more prone to metastasize than AA and demonstrates a predilection for metastasizing to uncommon sites such as the brain, skin, penis, and testes (5). Testicular metastasis from any primary site is uncommon, with the testes often termed a "tumor sanctuary" due to the presence of the blood-testis barrier and the unfavorable low temperature of the scrotum for metastatic tumor survival (18, 19). Currently, most instances of prostate cancer with testicular metastasis are documented through autopsy or examination of testicular castration specimens (20). Given that PDA originates from the periurethral prostatic ducts, there exists an elevated risk of prostatic urethral invasion by tumor cells, potentially leading to testicular dissemination via arterial embolization, retrograde venous spread, retrograde lymphatic metastasis, or direct metastasis through the vas deferens (12). In this particular case, no cancer cells were detected in the vas deferens, indicating a likelihood of venous or lymphatic metastasis.

A consensus regarding the optimal management of PDA remains elusive, with treatment modalities resembling those utilized for AA. Radical prostatectomy or radiotherapy represents the primary selection for local intervention, while ADT or chemotherapy constitutes the principal option for systemic management (21). Superior survival outcomes are associated with radical prostatectomy (RP) (22, 23). However, PDA is correlated with an increased propensity for local recurrence following radical prostatectomy. Following RP, patients exhibiting inadequate PSA control, unfavorable pathological characteristics, or a high risk of recurrence may be candidates for postoperative adjuvant radiotherapy. In this instance, the patient underwent radiotherapy 18 months following LRP, resulting in the disappearance of a suspicious nodule in the left perineum and a decrease in PSA levels, thereby validating the efficacy of radiotherapy. Several studies have documented the effectiveness of docetaxel in managing metastatic PDA (11, 24, 25). Nonetheless, the administration of docetaxel chemotherapy in this patient ceased due to exacerbation of scrotal enlargement following six cycles of treatment. A study involving 228 patients with PDA revealed that ADT was less effective in preventing recurrence compared to AA, with over 85% of patients progressing following initial treatment (26). Nonetheless, a similar high expression of androgen receptor was demonstrated in both PDA and AA (27, 28). Given the patient's rapid PSA elevation following discontinuation of abiraterone after a month of goserelin acetate plus abiraterone, incorporating abiraterone in addition to ADT could be beneficial for patients with PDA.

The incidence of metastatic testicular tumors ranges from 0.02% to 2.5%, with the prostate being the most prevalent primary site, constituting approximately 15% (29). In cases where a patient with PDA presents with a testicular mass and elevated PSA levels, the possibility of testicular metastases should be considered, even post-prostatectomy. Solitary testicular metastases warrant prompt orchiectomy, a simple and efficacious procedure that diminishes the tumor burden in patients. In this particular case, due to financial constraints, the patient was unable to actively engage in treatment. The interval from the discovery of an asymptomatic testicular mass to the eventual orchiectomy, prompted by pain from an enlarged testicular metastasis, was 48 months. Based on these findings, orchiectomy is most optimally performed upon initial identification of the testicular mass.

PDA exhibits a graver prognosis compared to AA (30). The 5-year overall survival (OS) rate for metastatic PDA ranges from 19.4% to 72%, with a median survival time of 77 months. Despite undergoing multiple systemic treatments, 87% of men with newly diagnosed metastases still experience progression (7). Wu et al. analyzed 511 PDA cases from the SEER database, finding that T3 and T4 stages were significantly more common in PDA patients than in AA patients (22.5% vs. 15.8%, respectively). The 5-year cancer-specific survival rate for PDA increased to 72%, yet it remains 20% lower than that for AA (31). In another study involving 581 PDA patients, PDA demonstrated higher aggressiveness and poorer prognosis compared to AA, regardless of the stage (32).Testicular metastasis signifies an advanced stage of PDA, often accompanied by widespread metastases throughout the body. However, the prognosis

of PDA with solitary testicular metastasis remains unreported. Studies indicate that many patients with metastases in rare sites experience stable disease, maintain relatively good quality of life, and remain asymptomatic, except for urinary system-related symptoms, before the progression of bone and visceral metastases (11). In this instance, rapid PSA reduction followed testicular resection, yielding apparent clinical benefits. Nonetheless, owing to the highly aggressive nature of PDA, the long-term prognosis remains uncertain, necessitating diligent monitoring.

It is noteworthy that while PSA presently serves as the sole biomarker for prostate cancer, a retrospective analysis of the existing literature indicates that PSA levels may not consistently correlate with the severity of PDA. Therefore, PSA may not be a reliable indicator for evaluating the treatment effect and prognosis of PDA and should be evaluated in combination with clinical symptoms and imaging findings. Compared with conventional imaging, prostate-specific membrane antigen-positron emission tomography/computed tomography (PSMA-PET/CT) can detect metastatic prostate cancer in some uncommon sites with better results than CT, bone scans, and MRI, especially at lower PSA levels (33). However, recent studies have unearthed unsatisfactory results regarding the effectiveness of PSMA-PET/CT in the context of PDA (34–36). One study revealed that this discrepancy stemmed from significantly lower PSMA expression in PDA compared to AA. Additionally, the study noted higher GLUT1 expression in PDA, particularly in membrane GLUT1 expression. Targeting membrane GLUT1 may emerge as a novel anticancer strategy for PDA in the future (37). Furthermore, the high cost of utilizing PSMA-PET/CT must be taken into consideration. Consequently, novel biomarkers are imperative for assessing PDA in the future.

The genomic and transcriptomic characteristics of PDA are similar to AA, but several pathways driving the aggressive phenotype are upregulated in PDA. DNA damage repair (DDR) alterations are more prevalent in metastatic PCa compared to localized PCa (38). DDR alterations are also frequently observed in ductal adenocarcinoma patients. Reports indicate these alterations occur not only in somatic mutations (20%–49%) but also in autosomal dominant germline mutations (20%), with a higher incidence than in metastatic castration-resistant prostate cancer (mCRPC) (39). Thus, germline testing for PDA is recommended to identify therapeutic targets. A study of 51 PDA patients found that DDR gene mutation rates in PDA were higher than in other tumors, twice that of mCRPC (40–42). Compared to AA, mismatch repair (MMR) defects are more common in PDA. In a study of 10 PDA patients, 4 (40%) exhibited MMR gene alterations, with 3 (75%) showing high mutation rates (43). Given the high incidence of MMR defects, molecular profiling, including immunohistochemistry (IHC) for MMR proteins, holds significant predictive relevance. Precision oncology necessitates treatment decisions based on the tumor's molecular characteristics. In this case of solitary testicular metastasis post-LRP, comprehensive molecular analysis could elucidate the tumor's genetic landscape. MMR defects, indicated by the loss of expression of proteins such as MLH1, MSH2, MSH6, and PMS2, suggest a high microsatellite instability (MSI-H) status, known to correlate with better responses to immunotherapy, particularly PD-1/PD-L1 inhibitors (44). This molecular characterization aids in understanding tumor biology and potential progression pathways, and is crucial for targeted therapy. IHC detection of MMR protein expression can guide personalized treatment, potentially improving the prognosis and management of metastatic PDA. Therefore, incorporating routine molecular profiling in the diagnostic evaluation of PDA patients is recommended to enhance predictive and therapeutic precision.

Conclusion

Due to the rarity of PDA, establishing large-scale prospective studies poses a challenge. Present investigations predominantly rely on limited case series and individual case reports. In this study, we present the inaugural case of pure PDA with solitary testicular metastasis after LRP. We aim to synthesize pertinent literature, providing valuable insights for the diagnosis and management of this condition. However, this study has certain limitations. For instance, the patient's financial constraints precluded the use of advanced imaging modalities such as PET-CT, which may have enhanced the precision of staging and the detection of occult metastases. Accurate diagnosis stands paramount for effective disease management. Healthcare practitioners must heighten their awareness of this condition. Even post-prostatectomy, patients diagnosed with PDA necessitate comprehensive evaluation. This evaluation may include testicular assessment when clinically indicated, particularly in cases with suspected metastasis or unusual clinical presentations. To avoid unnecessary treatment, it is essential to accurately diagnose testicular metastases. In cases where testicular metastases are confirmed, timely orchiectomy should be considered to manage symptoms and prevent complications.

Data availability statement

The original contributions presented in the study are included in the article/supplementary material. Further inquiries can be directed to the corresponding author.

Ethics statement

The studies involving humans were approved by Ethics Committee of Huaihe Hospital, Henan University. The studies were conducted in accordance with the local legislation and institutional requirements. The participants provided their written informed consent to participate in this study. Written informed consent was obtained from the individual(s) for the publication of any potentially identifiable images or data included in this article.

Author contributions

BC: Conceptualization, Data curation, Formal analysis, Writing – original draft, Writing – review & editing. MZ: Writing – original draft, Investigation. YH: Data curation, Writing – review & editing. WL: Writing – review & editing, Methodology. SL:

Writing – review & editing, Formal analysis. JZ: Writing – review & editing, Supervision. CW: Investigation, Writing – review & editing. QZ: Investigation, Writing – review & editing. JH: Conceptualization, Supervision, Writing – review & editing.

Funding

The author(s) declare that financial support was received for the research, authorship, and/or publication of this article. This project was supported by the Henan Province Medical Science and Technology Research Program (LHGJ20230435); Henan Province Key Scientific Research Project Plan for Higher Education Institutions (23A320039); Henan Province Medical Science and Technology Research Program (LHGJ20230425); Henan Province Science and Technology Research Program (232102310416); Henan Provincial Medical Science and Technology Research Program (LHGJ20220667).

Conflict of interest

The authors declare that the research was conducted in the absence of any commercial or financial relationships that could be construed as a potential conflict of interest.

Publisher's note

All claims expressed in this article are solely those of the authors and do not necessarily represent those of their affiliated organizations, or those of the publisher, the editors and the reviewers. Any product that may be evaluated in this article, or claim that may be made by its manufacturer, is not guaranteed or endorsed by the publisher.

References

1. Bray F, Laversanne M, Sung H, Ferlay J, Siegel RL, Soerjomataram I, et al. Global cancer statistics 2022: globocan estimates of incidence and mortality worldwide for 36 cancers in 185 countries. *CA: Cancer J Clin*. (2024) 74(3):229–63. doi: 10.3322/caac.21834

2. Surintrspanont J, Zhou M. Prostate pathology: what is new in the 2022 who classification of urinary and male genital tumors? *Pathologica*. (2022) 115:41–56. doi: 10.32074/1591-951x-822

3. Netto GJ, Amin MB, Berney DM, Compérat EM, Gill AJ, Hartmann A, et al. The 2022 world health organization classification of tumors of the urinary system and male genital organs-part B: prostate and urinary tract tumors. *Eur Urol*. (2022) 82:469–82. doi: 10.1016/j.eururo.2022.07.002

4. Melicow MM, Pachter MR. Endometrial carcinoma of proxtatic utricle (Uterus masculinus). *Cancer*. (1967) 20:1715–22. doi: 10.1002/1097-0142(196710)20:10<1715::AID-CNCR2820201022>3.0.CO;2-E

5. Kench JG, Amin MB, Berney DM, Compérat EM, Cree IA, Gill AJ, et al. Who classification of tumours fifth edition: evolving issues in the classification, diagnosis, and prognostication of prostate cancer. *Histopathology*. (2022) 81:447–58. doi: 10.1111/his.14711

6. Seipel AH, Delahunt B, Samaratunga H, Amin M, Barton J, Berney DM, et al. Diagnostic criteria for ductal adenocarcinoma of the prostate: interobserver variability among 20 expert uropathologists. *Histopathology*. (2014) 65:216–27. doi: 10.1111/his.12382

7. Ranasinghe WKB, Brooks NA, Elsheshtawi MA, Davis JW, Bathala TK, Tang C, et al. Patterns of metastases of prostatic ductal adenocarcinoma. *Cancer*. (2020) 126:3667–73. doi: 10.1002/cncr.32957

8. Gilligan T, Lin DW, Aggarwal R, Chism D, Cost N, Derweesh IH, et al. Testicular cancer, version 2.2020, nccn clinical practice guidelines in oncology. *J Natl Compr Cancer Network: JNCCN*. (2019) 17:1529–54. doi: 10.6004/jnccn.2019.0058

9. Hermi A, Boussaffa H, Saadi A, Blel A, Chakroun M, Ben Slama MR. Prostate adenocarcinoma metastasis to the testis: A new case report. *Urol Case Rep*. (2023) 48:102392. doi: 10.1016/j.eucr.2023.102392

10. Nova-Camacho LM, Acosta AM, Trpkov K, Sangoi AR, Pierre A, Chou A, et al. Metastatic solid tumors to the testis: A clinicopathologic evaluation of 157 cases from an international collaboration. *Hum Pathol*. (2023) 139:37–46. doi: 10.1016/j.humpath.2023.06.002

11. Tu SM, Reyes A, Maa A, Bhowmick D, Pisters LL, Pettaway CA, et al. Prostate carcinoma with testicular or penile metastases. Clinical, Pathologic, and Immunohistochemical Features. *Cancer*. (2002) 94:2610–7. doi: 10.1002/cncr.10546

12. Anila KR, Somanathan T, Mathews A, Jayasree K. An unusual variant of prostatic adenocarcinoma with metastasis to testis. *A Case Rep Gulf J Oncol*. (2012) 12:73–6.

13. Mortensen MA, Engvad B, Geertsen L, Svolgaard N, Lund L. Metastasis in testis from prostate cancer. *Ugeskrift laeger*. (2014) 176(13):V10130632.

14. Ning H, Song Y, Wu H, Gao D, Lyu J. Ductal adenocarcinoma of the prostate or seminal vesicle adenocarcinoma: an multi-disciplinary team (Mdt) case report and literature review. *Curr Urol*. (2022) 16:107–13. doi: 10.1097/cu9.0000000000000084

15. Seipel AH, Delahunt B, Samaratunga H, Egevad L. Ductal adenocarcinoma of the prostate: histogenesis, biology and clinicopathological features. *Pathology*. (2016) 48:398–405. doi: 10.1016/j.pathol.2016.04.001

16. Rubinowicz DM, Soloway MS, Lief M, Civantos F. Hemospermia and expressed tumor in the urethra: an unusual presentation of ductal carcinoma of the prostate. *J Urol*. (2000) 163:915. doi: 10.1016/s0022-5347(05)67841-x

17. Morgan TM, Welty CJ, Vakar-Lopez F, Lin DW, Wright JL. Ductal adenocarcinoma of the prostate: increased mortality risk and decreased serum prostate specific antigen. *J Urol*. (2010) 184:2303–7. doi: 10.1016/j.juro.2010.08.017

18. Oka S, Hara T, Ito S, Hayashida M, Sakaguchi K, Urakami S. Metastatic sites in rare genitourinary Malignancies and primary cancer sites in genitourinary organ metastases: A secondary analysis using the Japanese pathological autopsy registry database. *Eur Urol Open Sci*. (2024) 59:78–89. doi: 10.1016/j.euros.2023.12.004

19. Woortman C, van Leenders G, Hugen N, van Oijen MGH, Nagtegaal ID. Origin and outcome of metastatic tumours to the testes: A nationwide study. *BJU Int*. (2024) 133:305–13. doi: 10.1111/bju.16212

20. Gibas A, Sieczkowski M, Biernat W, Matuszewski M. Isolated testicular metastasis of prostate cancer after radical prostatectomy: case report and literature review. *Urologia internationalis*. (2015) 95:483–5. doi: 10.1159/000368720

21. Ranasinha N, Omer A, Philippou Y, Harriss E, Davies L, Chow K, et al. Ductal adenocarcinoma of the prostate: A systematic review and meta-analysis of incidence, presentation, prognosis, and management. *BJUI compass*. (2021) 2:13–23. doi: 10.1002/bco2.60

22. Liu M, Jin K, Qiu S, Xu P, Zhang M, Cai W, et al. Oncological outcomes of patients with ductal adenocarcinoma of the prostate receiving radical prostatectomy or radiotherapy. *Asian J Urol*. (2021) 8:227–34. doi: 10.1016/j.ajur.2020.05.005

23. Zhao J, Sun G, Zhao F, Chen J, Zhu S, Xu N, et al. The therapeutic efficacy of radical prostatectomy and external beam radiation therapy in patients with different pathological patterns of prostate cancer. *Asian J Surg*. (2023) 46:4178–85. doi: 10.1016/j.asjsur.2022.11.004

24. Kumar A, Mukherjee SD. Metastatic ductal carcinoma of the prostate: A rare variant responding to a common treatment. *Can Urological Assoc J = J l'Association Des urologues du Canada*. (2010) 4:E50–4. doi: 10.5489/cuaj.830

25. Fujiwara R, Kageyama S, Tomita K, Hanada E, Tsuru T, Yoshida T, et al. Metastatic prostatic ductal adenocarcinoma successfully treated with docetaxel chemotherapy: A case report. *Case Rep Oncol*. (2015) 8:339–44. doi: 10.1159/000438785

26. Ranasinghe W, Shapiro DD, Hwang H, Wang X, Reichard CA, Elsheshtawi M, et al. Ductal prostate cancers demonstrate poor outcomes with conventional therapies. *Eur Urol*. (2021) 79:298–306. doi: 10.1016/j.eururo.2020.11.015

27. Sanati S, Watson MA, Salavaggione AL, Humphrey PA. Gene expression profiles of ductal versus acinar adenocarcinoma of the prostate. *Modern pathology: an Off J United States Can Acad Pathology Inc*. (2009) 22:1273–9. doi: 10.1038/modpathol.2009.103

28. Seipel AH, Samaratunga H, Delahunt B, Wiklund F, Wiklund P, Lindberg J, et al. Immunohistochemical profile of ductal adenocarcinoma of the prostate. *Virchows Archiv: an Int J Pathol*. (2014) 465:559–65. doi: 10.1007/s00428-014-1636-0

29. Ahmed SA, Nawaz MM, Masood Y, Maqbool H, Mir K. Metastatic prostate tumor to testes: sign of advance disease. *Urol Case Rep*. (2023) 50:102410. doi: 10.1016/j.eucr.2023.102410

30. Marra G, van Leenders G, Zattoni F, Kesch C, Rajwa P, Cornford P, et al. Impact of epithelial histological types, subtypes, and growth patterns on oncological outcomes for patients with nonmetastatic prostate cancer treated with curative intent: A systematic review. *Eur Urol*. (2023) 84:65–85. doi: 10.1016/j.eururo.2023.03.014

31. Wu YP, Chen SH, Wang ST, Li XD, Cai H, Lin YZ, et al. Prognostic values of clinicopathological characteristics and survival outcomes in prostate infiltrating ductal carcinoma: A population-based study. *Oncotarget*. (2017) 8:29048–55. doi: 10.18632/oncotarget.16070

32. Knipper S, Preisser F, Mazzone E, Mistretta FA, Tian Z, Briganti A, et al. Contemporary comparison of clinicopathologic characteristics and survival outcomes of prostate ductal carcinoma and acinar adenocarcinoma: A population-based study. *Clin genitourinary Cancer*. (2019) 17:231–7.e2. doi: 10.1016/j.clgc.2019.04.009

33. Tsechelidis I, Vrachimis A. Psma pet in imaging prostate cancer. *Front Oncol*. (2022) 12:831429. doi: 10.3389/fonc.2022.831429

34. Zhao Q, Dong A, Bai Y, Zuo C. Prostate-specific membrane antigen uptake heterogeneity in mixed ductal-acinar adenocarcinoma of the prostate. *Clin Nucl Med*. (2023) 48:750–2. doi: 10.1097/rlu.0000000000004742

35. Pepe P, Pepe L, Curduman M, Pennisi M, Fraggetta F. Ductal prostate cancer staging: role of psma pet/ct. *Archivio italiano di urologia andrologia: organo ufficiale [di] Societa italiana di ecografia urologica e nefrologica*. (2024) 96:12132. doi: 10.4081/aiua.2024.12132

36. Qiu S, Dong A, Zhu Y, Zuo C. 68 ga-psma-11 and 18 F-fdg pet/ct in a case of ductal adenocarcinoma of the prostate. *Clin Nucl Med*. (2022) 47:836–8. doi: 10.1097/rlu.0000000000004230

37. Wang X, Zhou L, Qi L, Zhang Y, Yin H, Gan Y, et al. High glut1 membrane expression and low psma membrane expression in ductal adenocarcinoma and intraductal carcinoma of the prostate. *Prostate Cancer prostatic Dis*. (2023) 27 (4):720–7. doi: 10.1038/s41391-023-00759-y

38. Cancer Genome Atlas Research Network. The molecular taxonomy of primary prostate cancer. *Cell*. (2015) 163:1011–25. doi: 10.1016/j.cell.2015.10.025

39. Kobayashi H, Kosaka T, Nakamura K, Kimura T, Nishihara H, Oya M. Genomic analysis of aggressive ductal adenocarcinoma of the prostate. *Cancer Med*. (2023) 12:8445–51. doi: 10.1002/cam4.5573

40. Schweizer MT, Antonarakis ES, Bismar TA, Guedes LB, Cheng HH, Tretiakova MS, et al. Genomic characterization of prostatic ductal adenocarcinoma identifies a high prevalence of DNA repair gene mutations. *JCO Precis Oncol*. (2019) 3:1–9. doi: 10.1200/po.18.00327

41. Pritchard CC, Mateo J, Walsh MF, De Sarkar N, Abida W, Beltran H, et al. Inherited DNA-repair gene mutations in men with metastatic prostate cancer. *New Engl J Med*. (2016) 375:443–53. doi: 10.1056/NEJMoa1603144

42. Heeke AL, Pishvaian MJ, Lynce F, Xiu J, Brody JR, Chen WJ, et al. Prevalence of homologous recombination-related gene mutations across multiple cancer types. *JCO Precis Oncol*. (2018) 2018:1–13. doi: 10.1200/po.17.00286

43. Schweizer MT, Cheng HH, Tretiakova MS, Vakar-Lopez F, Klemfuss N, Konnick EQ, et al. Mismatch repair deficiency may be common in ductal adenocarcinoma of the prostate. *Oncotarget*. (2016) 7:82504–10. doi: 10.18632/oncotarget.12697

44. Le DT, Durham JN, Smith KN, Wang H, Bartlett BR, Aulakh LK, et al. Mismatch repair deficiency predicts response of solid tumors to pd-1 blockade. *Sci (New York NY)*. (2017) 357:409–13. doi: 10.1126/science.aan6733

frontiers | Frontiers in Oncology

TYPE Case Report
PUBLISHED 17 March 2025
DOI 10.3389/fonc.2025.1468266

Check for updates

OPEN ACCESS

EDITED BY
Liang Qiao,
The University of Sydney, Australia

REVIEWED BY
Bojan Stojanovic,
University of Kragujevac, Serbia
Sara Massironi,
Vita-Salute San Raffaele University, Italy

*CORRESPONDENCE
Qingjun Dong
shdongqingjun@163.com
Chen Wang
wangchen_longhua@163.com

RECEIVED 21 July 2024
ACCEPTED 24 February 2025
PUBLISHED 17 March 2025

CITATION
Dong R, Lu J, Zhou H, Dong Q and Wang C (2025) Rectal neuroendocrine tumor during anorectal surgery: three case reports and a review of the literature. *Front. Oncol.* 15:1468266. doi: 10.3389/fonc.2025.1468266

COPYRIGHT
© 2025 Dong, Lu, Zhou, Dong and Wang. This is an open-access article distributed under the terms of the Creative Commons Attribution License (CC BY). The use, distribution or reproduction in other forums is permitted, provided the original author(s) and the copyright owner(s) are credited and that the original publication in this journal is cited, in accordance with accepted academic practice. No use, distribution or reproduction is permitted which does not comply with these terms.

Rectal neuroendocrine tumor during anorectal surgery: three case reports and a review of the literature

Ruoxi Dong, Jingen Lu, Hao Zhou, Qingjun Dong* and Chen Wang*

Department of Anorectal Surgery, LongHua Hospital, Shanghai University of Traditional Chinese Medicine, Shanghai, China

Background: Rectal neuroendocrine tumors (NET) are thought to originate from the diffuse neuroendocrine system. The lack of apparent signs of illness and the patient's non-specific presentations often cause a delay in diagnosis, until in their final stages of cancer. Thus, rectal NETs pose a significant challenge to most physicians.

Case presentation: This article presents three cases of rectal NETs discovered during anorectal surgery. Owing to their atypical symptoms, they were initially diagnosed as mixed hemorrhoids or perianal fistulas. However, the patients were diagnosed with rectal NETs and thus underwent endoscopic dissection or transanal endoscopic microsurgery. Histological analysis revealed three rectal NETs, one G1 and two G2. All patients were followed-up for more than 6 months, with excellent outcomes without recurrence.

Conclusions: The etiology, pathogenesis, therapeutic methods, prevention, and prognosis of rectal NETs remain challenging. Given the variable understanding of the most appropriate operative approaches for rectal NETs, our objective was to broaden the perspective of this infrequent disease by delivering distinctive individual experiences and emphasizing the therapeutic significance of delicate surgery.

KEYWORDS

rectal neuroendocrine tumors, surgery, diagnosis, treatment, case report

Introduction

Rectal neuroendocrine tumors (NET), which are thought to originate from the diffuse neuroendocrine system, are a fusion of neurologic and endocrine features (1). Most of rectal-NETs are asymptomatic, a possibly cause for the increase of incidence rate may be a consequence of more elaborate and numerous screening colonoscopies with widespread use of endoscopy for detecting colorectal cancers (2). Despite diagnostic modalities, the

diagnosis of rectal NETs is not straightforward; it may present with symptoms such as bleeding or changes in bowel habits, or without any at all (3). Several techniques are available for resecting rectal NETs, including the endoscopic, trans-anal and surgical therapies (4). Endoscopically resecting consists of endoscopic mucosal resection, endoscopic submucosal dissection (ESD), and endoscopic full-thickness resection (5). But the lack of apparent signs of illness and the patient's non-specific presentations often result in delayed diagnosis, until in their advanced disease stages (6). Furthermore, the macroscopic appearance of rectal NETs resembles that of hyperplastic or adenomatous polyps, making the differential diagnosis from other polypoid lesions challenging (7). Thus, rectal NETs pose a significant challenge to most physicians. Herein, we present three cases of rectal NETs. Our objective was to further emphasize the diagnostic value of endoscopy and digital rectal examination for detecting rectal NETs as well as to enhance patient cognition of this disease, thereby providing insights and high reference values for both imaging radiologists and clinicians.

Case report

The first case

A 46-year-old male presented with lumps and pain in the perianal and -rectal regions. The lump ruptured with spontaneous drainage for 1 year. Physical and laboratory examinations showed no obvious abnormality. An indentation, located 1 cm above the dentate line at the 12 o'clock direction in the bladder lithotomy position, was associated with slight tenderness as well as with a soft, subcutaneous induration extending to the rectum. Before the surgery, a colonoscopy was done, showing a 5mm×5mm longitudinal, protruding mass in the lower posterior rectal wall. Colonoscopic examination had also shown the lesion region, shape, and scope. Thus, surgeons have chosen proper operative schemes, wherein endoscopic resection was an effective treatment for mass resection without impairing the functional anatomy and biochemical of the anorectal physiological condition. After obtaining patient consent, ESD was performed, wherein the tumor was excised en bloc using a disposable, high-frequency knife. To date, doctors remain unaware of any adverse events associated with this dissection. Histologic hematoxylin and eosin (HE) staining confirmed a rectal NET, having a tumor stage of G1 (WHO 2019), revealing atypical epithelial cells. Immunohistochemistry (IHC) also demonstrated the diagnosis of a rectal NET, as the pathologic tissue section was positive for Synaptophysin(Syn), negative for chromogranin A(CgA), and with approximately 2% Ki-67 expression (Figure 1). Long-term follow-up over 5 years showed no recurrence, with an excellent outcome.

The second case

A 29-year-old female initially presented with occasional, reducible prolapses during defecation with a 3 year-long progression, later progressing to recurrent, irreducible prolapse. The patient was diagnosed with mixed hemorrhoids. The patient had no family history of colorectal cancer, a past medical history of hashimoto thyroiditis for 15 years, and a medication history of thyroxine intake.

Laboratory tests, including routine blood work, liver and kidney function tests, coagulation function, and electrocardiography, were all unremarkable. Serum tumor marker findings, such as carcinoembryonic antigen(CEA), squamous cell carcinoma, carbohydrate antigen 72-4(CA72-4),19-9(CA19-9), 50(CA50), 242 (CA242), 211, alpha-fetoprotein(AFP), and neuron-specific enolase (NSE) were all negative. Pre-operative colonoscopy findings were also unremarkable. Physical examination revealed mixed stage III hemorrhoids and rectal polyps. The patient underwent mixed hemorrhoidectomy and rectal polypectomy. Engorged hemorrhoidal cushions were observed at the 12-, 6-, and 7-to 8 o'clock positions in the bladder lithotomy position. During hemorrhoidectomy, a gray, 5 mm×5 mm×3 mm, hyperplastic lesion located at the dentate line at the 6 o'clock position. The surgeon then incised the rectal mucous membrane and carefully separated the lesion from the rectal muscle stratum. Finally, the intact hyperplastic lesion was completely resected using a high-frequency electrotome. A shuttle-like incision was designed to be incorporated to avoid creating narrow skin bridges and to protect the rectal muscle, in order to maintain the integrity of the rectal mucosa. Then, the muscular layer of the rectum was closed by the surgeons via a horizontal mattress suture.

The final pathologic findings included a tumor measuring 3 mm× 3 mm × 3 mm in size as well as atypical epithelial cells in the rectal submucosa and rectal muscle, but with tumor-free margins. HE staining confirmed a rectal NET, having a tumor stage of G2. Several mitotic figures and necrotic images were observed in the pathologic sections. IHC indicated that the tumor cells were positive for neuroendocrine markers, including Syn, somatostafin receptor 2 (SSTR2), and insulinoma-associated protein1(INSM1), and with an approximately 8% Ki67 expression, but were negative for CgA and CDx2 (Figure 2). After surgery, the patient underwent delayed positron emission tomography-computed tomography (PET-CT) examination, wherein the tumor was then staged as T1aN0M0, phase I, with no distant metastases. Therefore, surgery alone was sufficient enough to cure the cancer without the need for subsequent adjuvant therapies. Over the 6-month follow-up period post-surgery, the patient did not experience any anal dysfunction or evidence of tumor recurrence.

The third case

A 74-year-old male was admitted with anal and rectal lumps for 1 month, worsening over 3 days without hematochezia. The patient was initially diagnosed with rectal polyps. Family history for colorectal cancer was negative. Recurrent episodes of anal fistulas were present in the three patients, all of whom had a prior history of anal fistula surgery. However, this patient had no history of surgery nor trauma.

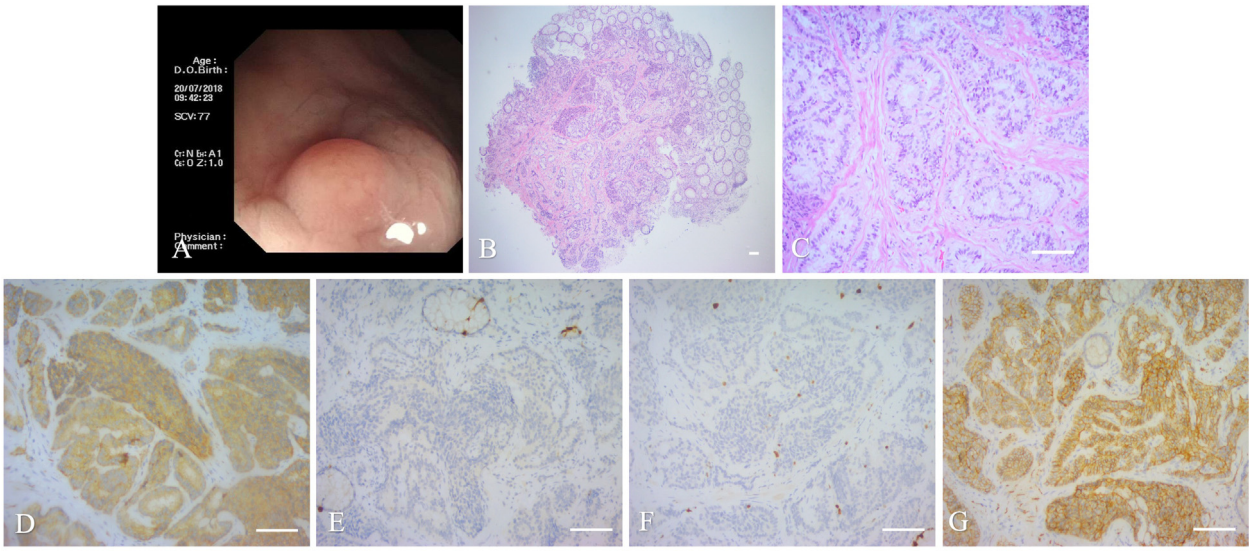

FIGURE 1
Imaging and histopathology of the biopsy specimen of the first case. **(A)**: Colonoscopy showing a mass approximately 0.5×0.5 cm in size. **(B, C)**: Histopathology of the mass (magnification, ×40 and ×200, scale bar of 100 μm). **(D–G)**: IHC of the mass, scale bar of 100 μm). **(D)** Cancer cells positive for Syn (Syn; ×200). **(E)** Cancer cells negative for CgA (CgA; ×200). **(F)** Cancer cells positive for Ki-67 (Ki-67, ×200). **(G)** Cancer cells positive for CD56(CD56; ×200).

Laboratory tests revealed a hemoglobin concentration of 128 g/L,WBC count of $10.70*10^9$/L, platelet count of 282 × 10^9/L, and normal C-reactive protein levels. Hepatic, renal, and blood coagulation functions were also unremarkable. Standard serum tumor markers, AFP, CA19-9, CA72-4, CA50, and CA242 were also unremarkable. However, CEA (6.1 ng/mL) and NSE were elevated (25.30 ng/mL).

After admission to our hospital, a series of surveys were performed, including colonoscopy, endoscopic ultrasonography, transrectal ultrasound, and perianal magnetic resonance imaging (MRI). Transrectal ultrasound showed a 26 × 11-mm, solid, hypoechoic lesion in the lower rectal segment. Endoscopic ultrasonography revealed a solid nodule at the right wall of the rectal mucosa with associated rectal muscularis propria thickening, for which endoscopic ultrasound-guided fine needle aspiration was performed as necessary. Iso-intense, perianal MRI showed a 95-mm oval tumor, located at the upside canal mucosa and about 3.5 cm from the anus, and a 2.2×1.5-cm irregular tumor, located at the right rectal mucosal wall and about 7-8 cm from the anus. The canal lesion showed iso-intense signals on T1- and T2-WI, while the rectal lesion showed a hypointense signal on T1WI and a slightly hyperintense one on T2WI. The lesions showed significantly low or inhomogeneous enhancement after perianal MRI reinforcement.

Enhanced MRI of the lower abdomen revealed a malignant tumor in the right rectal wall with multiple lymph node metastases. The patient underwent colonoscopy and biopsy and was then diagnosed with a rectal NET. PET-CT scan was also performed before the surgery to understand the delayed uptake of ^{18}F-fluoro-2-deoxy-D-glucose by the mass over-time. The goal of PET-CT was to further clarify the location and characteristics of the mass, as well as to detect long-distance metastasis appropriate tumor staging. Right lower rectal wall radioactivity and adjacent lymph node swelling increased, with multiple liver metastases.

The patient underwent laparoscopic tumor resection with rectal lymph node dissection under general anesthesia. During surgery, the surgeons found that the mass compressed the adjacent bowel, with contracture of the sigmoid colon mesentery. To improve the patient's quality of life and to prolong survival, the primary tumor was completely resected to prevent recurrence, wherein subsequent stenosis or an ileal stoma was then constructed. HE staining of the tumor on post-operative pathological examination revealed atypical epithelial cells. IHC staining showed a positive reaction for Syn, SSTR2, INSM1, and CgA, an approximately 10% Ki-67 expression, and a negative reaction for CDx2 (Figure 3). Based on these pathologic and imaging characteristics, a diagnostic staging of a pT4N1Mx rectal NET was established. Post-operatively, the patient underwent a 5-day course of antibiotic treatment. The patient recovered without complications and was discharged on post-operative day 14.

Given this advanced stage with a high degree of malignancy and a non-functioning tumor behavior, the physicians recommended a treatment strategy using first-line targeted therapy, Surufatinib 300mg daily for days 1 to 28. Over the 6-month follow-up period, there were no significant side effects, clinical or radiological manifestations of local recurrence, nor distant metastases (Figure 4).

Discussion

NETs, originating from sensory and secretory neuroendocrine cells, can arise in multiple organs and are the most common endocrine tumors of the gastrointestinal (GI) tract (8, 9). NETs

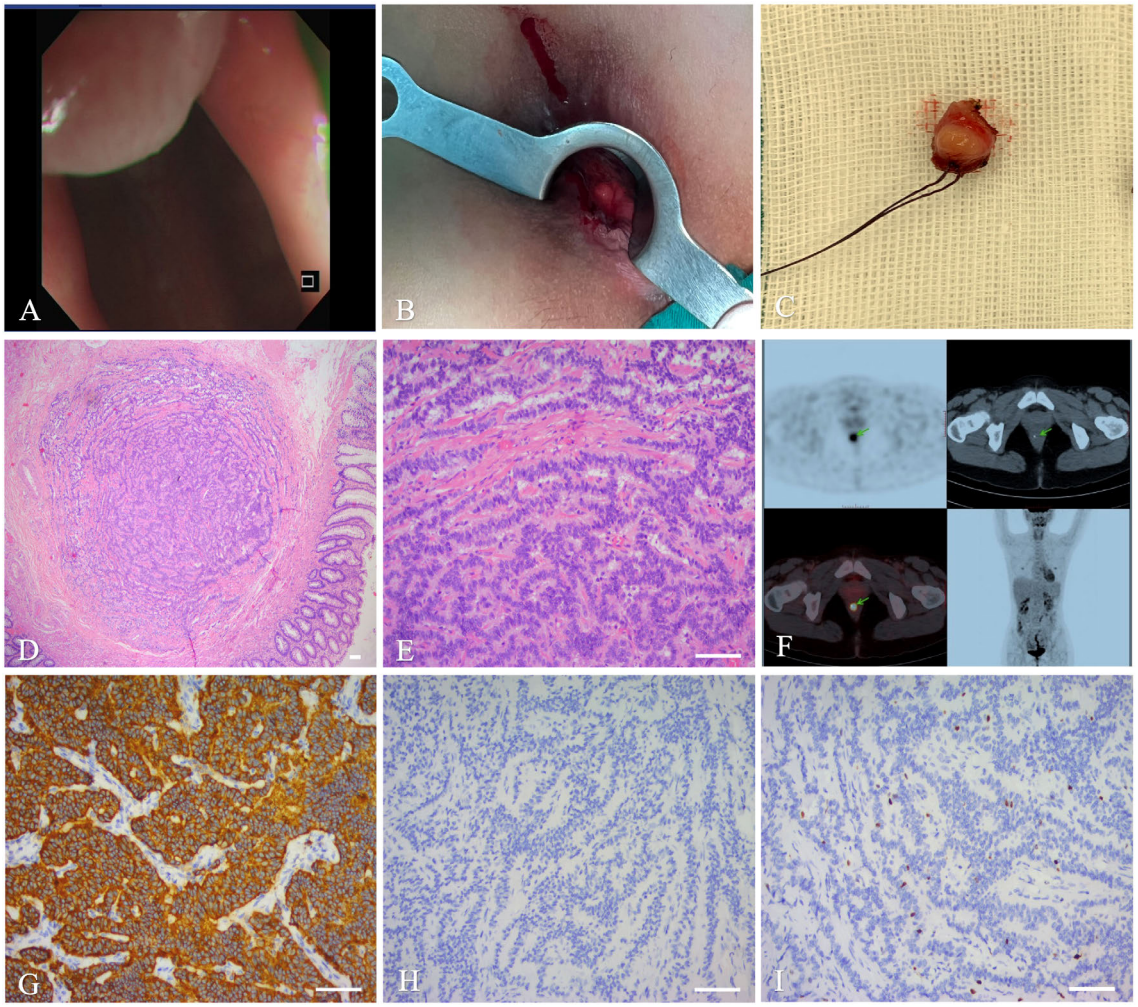

FIGURE 2
Imaging and histopathology of the biopsy specimen of the second case. **(A)**: Colonoscopy. **(B)**: Intra-operative photographs. **(C)**: Operative specimen. **(D, E)**: Histopathology of the mass (magnifications,×40, ×200, scale bar of 100 μm). **(F)**: PET-CT. **(G–I):** IHC showing Syn **(G)**, CgA **(H)**, and Ki-67 **(I)**, scale bar of 100 μm.

were once called carcinoids, and carcinoid tumors were first described by Langhans in 1867 (10). However, almost half a century later in 1914, Gosset and Mason recognized that although the structure and histology of carcinoids were similar to those of cancer, their biological behavior was completely different. Carcinoids show slow progression of pathological changes and are essentially endocrine-related tumors (11).

NETs stems from the neural crest cells—a group of cells that can differentiate into various cell types, including the specialized neuroendocrine cells. The principal reason for NET incidence correlates strongly with the distribution density of neuroendocrine cells because these tumors originate from neuroendocrine cell compartments. Several transcribed genes are implicated in tumor development, metastasis and hormone secretion and can be useful in defining primary NETs and predicting metastasis occurrence. These genes include Ki-67 proliferation index, nucleosome assembly protein 1- like, CgA, INSM1 (12). Serum CgA has been the general biomarker for well-differentiated NETs for a long time. Its diagnostic accuracy is now under debate. However, it is useful in follow-up. A new immunohistochemical marker is the transcription factor INSM1, which is more specific for the differentiation of NETs of the pancreas and rectum (13).

The intestines, considered as the body's largest endocrine organ, may arise nearly 60% of NETs. The region in the human body with the highest NET incidence rate is the GI tract (67.5%), followed by the bronchopulmonary system (25.3%); the remaining 10% occur in the liver, kidneys, and other endocrine glands. Researches show that within the GI tract, the small intestine (41.8%) is the most common location, followed by the rectum (27.4%) and stomach (8.7%) (14). NETs are usually considered rare. 1%–2% of all rectal tumors are neuroendocrine (15).However, over the past decades, their incidence has increased in most countries (16). According to the Surveillance, Epidemiology, and End Results (SEER) database in the US, showed a 10-fold increase of incidence in rectal NETs over the past 30 years in the United States

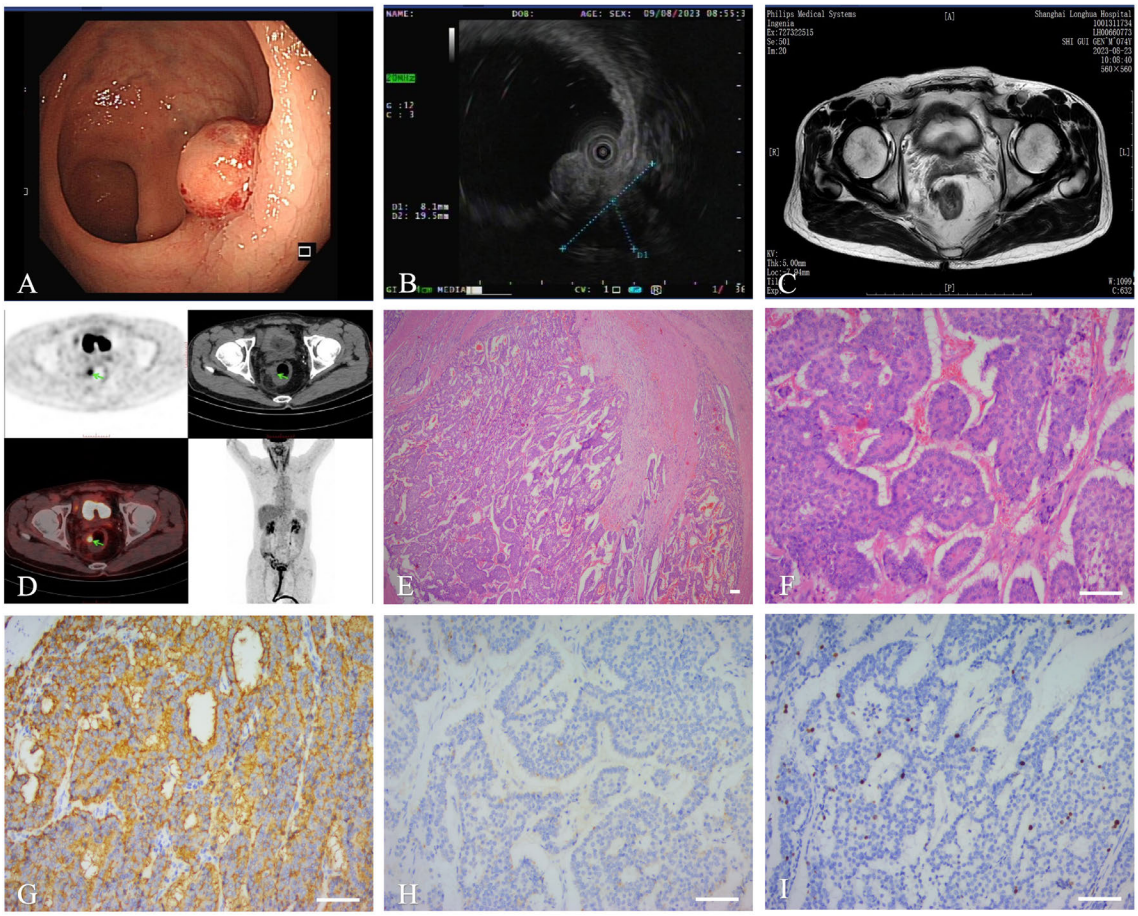

FIGURE 3
Imaging and histopathology of the biopsy specimen of the third case. **(A)**: Colonoscopy. **(B)**: Ultrasound colonoscope. **(C)**: MRI. **(D)**: PET-CT. **(E, F)**: Histopathology showed that differentiated(magnifications,×40, ×200, scale bar of 100 μm). **(G–I)**: IHC showing Syn **(G)**,CgA **(H)**, Ki-67 **(I)**, scale bar of 100 μm.

(17), the same trend was also confirmed in the German registry (18), as well as in the Asian registers (19).

The US research data indicated that the greatest incidence of pathogenic sites for all gastro-entero-pancreatic NETs (GEP-NETs) are the rectum (29.2%) and small intestines (28.4%); in China, GEP-NETs were most frequently found in the pancreas (31.5%) and rectum (29.6%). The total number of rectal NET cases has also progressively improved by approximately 8%. Significant sex differences also exist in the incidence of rectal NETs, with rectal and pancreatic NETs occurring more commonly in men (20, 21).

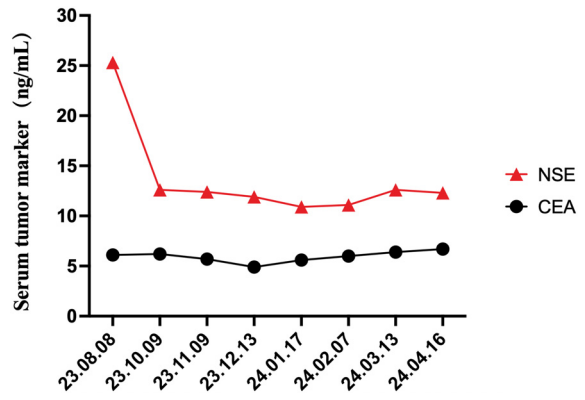

FIGURE 4
Changes in the serum tumor markers, NSE and CEA, during the treatment and throughout the 6-month follow-up periods.

The basic classification of NETs is based on the mitotic count and Ki-67 index, and is classified into three grades (G1, G2, and G3) that can be applied to almost any part of the GI tract: well-differentiated NETs with benign or uncertain behavior, well-differentiated neuroendocrine carcinomas with low-grade malignancy, and poorly differentiated neuroendocrine carcinomas. According to their degree of Ki-67 labeling index, malignant tumors can be categorized into three pathological grades: 1% to 3% as low risk; 3% to 20% as intermediate risk; more than 20% as high risk.

CgA, a member of the neuropeptide family, may assess the activities of the neuroendocrine system and is widely distributed in the neuroendocrine system. Several documentations indicated that CgA may be regarded as a tumor marker because its expression among patients could be increased to 70% to 90% (22). Among two

present cases in this series, the specimens were all positive for CgA. Irregular mitosis are closely connected with the degree of cellular differentiation (23). Pathological and immunohistochemical analyses remain as the gold standard for diagnosis, whereas CgA and Syn are often selected as biological NET markers owing to their sensitivity and specificity (24).

Research has shown that rectal NETs are usually, but not exclusively, small and generally of low-to-intermediate grades (G1 or G2) (25). Given the substantial differences between common GI adenocarcinomas and NETs in terms of pathological physiology and prognosis, clinicians have instituted into account the individualized therapeutic methods that consider the biology of NET lesions (14). Currently, if there is no evidence of invasion beyond submucosa and presence of locoregional disease, endoscopic treatment for rectal NETs is indicated (26), usually complete tumor resection remains as the best curative option for patients with NETs (27, 28).

According to the 2016 European Neuroendocrine Tumor Society (ENETS) and 2020 National Comprehensive Cancer Network (NCCN) guidelines, treatment protocols for rectal NETs should vary according to their size, grade, and stage. For example, for G1 or G2 and stage T1 lesions with a diameter of 1–2 cm, the 2016 ENETS guidelines suggest minimally invasive surgery, whereas the NCCN guidelines recommend endoscopic resection. For those with a diameter of less than 1 cm, the ENETS guidelines recommend endoscopic resection as an effective treatment. R0 resection is an effective method for primary tumors and does not require follow-up for patients, which received support from the NCCN guidelines. Furthermore, for R0 lesions with a diameter of less than 1 cm, current guidelines are capable of creating treatment benefits for patients without further follow-up monitoring (29). Guidelines from the ENETS recommend local excision via a transanal or endoscopic approach for rectal NETs of less than 1 cm, and radical resection for those greater than 2 cm (25).

In these three cases, we found that the symptoms of rectal NETs were atypical, making misdiagnosis inevitable (Table 1). Therefore, there is greater demand for the physicians' clinical skills. Ultrasonic contrast can also be used for further evaluating rectal NETs, if necessary. Based on our experiences, we recommend complete resection for all rectal-NETs. For rectal-NETs <1 cm without muscularis propria invasion, endoscopic resection may be a viable treatment option. For the rectal-NETs >2 cm, or with lymph node involvement, or grade 3 histology require radical surgical resection. Although our case report is based on three patients, compared with relevant guidelines, both our surgical methods and treatment procedurals of the of rectal NETs have some defects that need perfecting. Even the patient was diagnosed as anorectal disease, it is still necessary to perform colonoscopy preoperatively. Even when colonoscopy is performed preoperatively, digital rectal examination before surgery is indispensable and can provide more intuitive information regarding the NET location, size, shape, density, margins, and relationship with its surrounding tissues, which are important for operation schemes. We believe that there are different surgical methods in effective tumor control and could also improve the overall health of these patients. As reported in these cases, those different size of NETs require collaboration between different departments for better treatment. In our case report, endoscopic resection is enough for smaller rectal-NETs, bigger one should receive surgery therapy from anorectal surgery department. In addition, according to rectal NET grading and genotyping tests, molecular targeted therapy, chemotherapy, peptide receptor radionuclide therapy, and immune checkpoint inhibitor therapy may also enhance therapeutic potential. We also need more photo/video documentation to describe rectal NETs in more detail. Moreover, because the surgery number are few, we still have to accumulate more case of rectal NETs and the experience, to further observe its forward curative effect.

From the lungs to the gastrointestinal tract and the pancreas, neuroendocrine tumors can emerge in almost any body part, each

TABLE 1 Clinical characteristics of reported cases of rectal-NETs.

Variable	Patient 1	Patient 2	Patient 3
Sex	Male	Female	Male
Age(y)	46	29	74
Symptoms	Lumps and pain in the perianal and -rectal regions	Recurrent, irreducible prolapse during defecation	Anal and rectal lumps for 1 month, worsening over 3 days without hematochezia.
Laboratory tests	Normal	Normal	Hb:128g/L,WBC:10.70*10^9/L, PLT:282×10^9/L, CEA:6.1ng/mL,NSE:25.30ng/mL
Imaging tests	Colonoscopy showing a 5mm×5mm longitudinal, protruding mass in the lower posterior rectal wall	Direct vision shows a gray 5mm×5mm ×3mm, hyperplastic lesion located at the dentate line at the 6 o'clock position	PET-CT shows that right lower rectal wall radioactivity and adjacent lymph node swelling increased, with multiple liver metastases
Tumor stage	G1, T1aN0M0 phase I	G2, T1aN0M0 phase I	G2, pT4N1Mx
Treatment	Endoscopic submucosal dissection (ESD)	Transanal resection	Laparoscopic tumor resection with rectal lymph node dissection,with targeted therapy(Surufatinib)
Outcome	Survive with no recurrence	Survive with no anal dysfunction or evidence of tumor recurrence	Survive with no significant side effects, clinical or radiological manifestations of local recurrence, nor distant metastases.

site offering its unique challenges and management paradigms (30). A clear understanding of the tumor's organ of origin and its inherent characteristics is indispensable for determining the most suitable therapeutic approach. Moreover, the highlighted controversies, especially in the importance of accurate diagnosis and tailored management strategies that require further exploration and consensus-building. Ultimately, the goal is to provide personalized, effective care that enhances patients' quality of life and survival outcomes.

Conclusion

Rectal NETs are often accompanied by symptoms of bleeding or disruption of bowel habits. However, almost half of the patients produce very few noticeable symptoms. It is easily misdiagnosed as a benign anorectal disease; therefore, it is crucial to perform colonoscopy preoperatively. Endoscopic or transanal resection of rectal NETs has a good overall prognosis. Recent studies have suggested that a histological grade of G2 may be rated as an independent risk factor for R1 resection. Further follow-up management after rectal NET R0 resection is also necessary.

Data availability statement

The original contributions presented in the study are included in the article/supplementary material. Further inquiries can be directed to the corresponding authors.

Ethics statement

The studies involving humans were approved by Ethics Committee of LongHua Hospital, Shanghai University of Traditional Chinese Medicine. The studies were conducted in accordance with the local legislation and institutional requirements. The participants provided their written informed consent to participate in this study. Written informed consent was obtained from the participant/patient(s) for the publication of this case report.

Author contributions

RD: Conceptualization, Data curation, Investigation, Visualization, Writing – original draft. JL: Funding acquisition, Project administration, Supervision, Writing – review & editing. HZ: Formal Analysis, Project administration, Validation, Writing – review & editing. QD: Funding acquisition, Project administration, Supervision, Validation, Writing – review & editing. CW: Funding acquisition, Resources, Supervision, Validation, Writing – review & editing.

Funding

The author(s) declare that financial support was received for the research and/or publication of this article. This work was supported by the National Natural Science Foundation of China (Nos. 82004374 and 82074441), Shanghai Municipal Hospital Clinical Competence Promotion and Enhancement Specialty Alliance for Traditional Chinese Medicine Surgery (SHDC22021316-A), National Administration of Traditional Chinese Medicine (2023 Anorectal Disease), Shanghai City's Key Research Center Construction Project (2023ZZ02003), and the National Administration of Traditional Chinese Medicine Key Discipline Project-Traditional Chinese Medicine of Anorectal Disease (ZYYZDXK-2023064).

Conflict of interest

The authors declare that the research was conducted in the absence of any commercial or financial relationships that could be construed as a potential conflict of interest.

Publisher's note

All claims expressed in this article are solely those of the authors and do not necessarily represent those of their affiliated organizations, or those of the publisher, the editors and the reviewers. Any product that may be evaluated in this article, or claim that may be made by its manufacturer, is not guaranteed or endorsed by the publisher.

References

1. Asmundo L, Ambrosini V, Anderson MA, Fanti S, Bradley WR, Campana D, et al. Clinical intricacies and advances in neuroendocrine tumors: an organ-based multidisciplinary approach. *J Comput Assist Tomogr*. (2024) 48:614–27. doi: 10.1097/RCT.0000000000001596

2. Volante M, Grillo F, Massa F, Maletta F, Mastracci L, Campora M, et al. Neuroendocrine neoplasms of the appendix, colon and rectum. *Pathologica*. (2021) 113:19–27. doi: 10.32074/1591-951X-230

3. Anthony LB, Strosberg JR, Klimstra DS, Maples WJ, O'Dorisio TM, Warner RR, et al. The NANETS consensus guidelines for the diagnosis and management of gastrointestinal neuroendocrine tumors (nets): well-differentiated nets of the distal colon and rectum. *Pancreas*. (2010) 39:767–74. doi: 10.1097/MPA.0b013e3181ec1261

4. de Mestier L, Lorenzo D, Fine C, Cros J, Hentic O, Walter T, et al. Endoscopic, transanal, laparoscopic, and transabdominal management of rectal neuroendocrine tumors. *Best Pract Res Clin Endocrinol Metab*. (2019) 33:101293. doi: 10.1016/j.beem.2019.101293

5. Panzuto F, Parodi MC, Esposito G, Massironi S, Fantin A, Cannizzaro R, et al. Endoscopic management of gastric, duodenal and rectal NETs: Position paper from the Italian Association for Neuroendocrine Tumors (Itanet), Italian Society of Gastroenterology (SIGE), Italian Society of Digestive Endoscopy (SIED). *Dig Liver Dis*. (2024) 56:589–600. doi: 10.1016/j.dld.2023.12.015

6. Modlin IM, Champaneria MC, Chan AKC, Kidd M. A three-decade analysis of 3,911 small intestinal neuroendocrine tumors: the rapid pace of no progress. *Am J Gastroenterol*. (2007) 102:1464–73. doi: 10.1111/j.1572-0241.2007.01185.x

7. Maione F, Chini A, Milone M, Gennarelli N, Manigrasso M, Maione R, et al. Diagnosis and management of rectal neuroendocrine tumors (NETs). *Diagnostics (Basel)*. (2021) 11. doi: 10.3390/diagnostics11050771

8. Jetmore AB, Ray JE, Gathright JJ, McMullen KM, Hicks TC, Timmcke AE. Rectal carcinoids: the most frequent carcinoid tumor. *Dis Colon Rectum*. (1992) 35:717–25. doi: 10.1007/BF02050318

9. Cives M, Strosberg JR. Gastroenteropancreatic neuroendocrine tumors. *Ca-Cancer J Clin*. (2018) 68:471–87. doi: 10.3322/caac.21493

10. Langhans T. Ueber einen drusenpolyp im ileum [Over one glandular polyp in the ileum. *Virchow Arch Pathol Anat Physiol Klin Med*. (1867) 38:559–60. doi: 10.1007/BF02114017

11. Gosset A, Masson P. Tumeurs endocrines de 1'appendice. *Presse Med*. (1914) 25:237–9.

12. Drozdov I, Kidd M, Nadler B, Camp RL, Mane SM, Hauso O, et al. Predicting neuroendocrine tumor (carcinoid) neoplasia using gene expression profiling and supervised machine learning. *Cancer*. (2009) 115:1638–50. doi: 10.1002/cncr.v115:8

13. Fernandez CJ, Agarwal M, Pottakkat B, Haroon NN, George AS, Pappachan JM, et al. Gastroenteropancreatic neuroendocrine neoplasms: A clinical snapshot. *World J Gastrointest Surg*. (2021) 13(3):231–55. doi: 10.4240/wjgs.v13.i3.231

14. Modlin IM, Lye KD, Kidd M. A 5-decade analysis of 13,715 carcinoid tumors. *Cancer*. (2003) 97:934–59. doi: 10.1002/cncr.11105

15. Gallo C, Rossi RE, Cavalcoli F, Barbaro F, Boškoski I, Invernizzi P, et al. Rectal neuroendocrine tumors: Current advances in management, treatment, and surveillance. *World J Gastroenterol*. (2022) 28:1123–38. doi: 10.3748/wjg.v28.i11.1123

16. Valent F, Tullio A, Kara E, Cipri C, Sciannimanico SM, Vescini F, et al. A retrospective cohort study of histology-proven neuroendocrine neoplasms in the Italian area of udine. *Endocr Metab Immune Disord Drug Targets*. (2021) 21:448–57. doi: 10.2174/1871530320666200713093533

17. Dasari A, Shen C, Halperin D, Zhao B, Zhou SH, Xu Y, et al. Trends in the incidence, prevalence, and survival outcomes in patients with neuroendocrine tumors in the United States. *JAMA Oncol*. (2017) 3:1335–42. doi: 10.1001/jamaoncol.2017.0589

18. Ploeckinger U, Kloeppel G, Wiedenmann B, Lohmann R, representatives of 21 German NET Centers. The German NET registry: an audit on the diagnosis and therapy of neuroendocrine tumors. *Neuroendocrinology*. (2009) 90:349–63. doi: 10.1159/000242109

19. Chang JS, Chen LT, Shan YS, Chu PY, Tsai CR, Tsai HJ. An updated analysis of the epidemiologic trends of neuroendocrine tumors in Taiwan. *Sci Rep*. (2021) 11:7881. doi: 10.1038/s41598-021-86839-2

20. Fan JH, Zhang YQ, Shi SS, Chen YJ, Yuan XH, Jiang LM, et al. A nation-wide retrospective epidemiological study of gastroenteropancreatic neuroendocrine neoplasms in China. *Oncotarget*. (2017) 8:71699–708. doi: 10.18632/oncotarget.17599

21. Fraenkel M, Kim M, Faggiano A, De Herder WW, Valk GD, et al. Incidence of gastroenteropancreatic neuroendocrine tumours: a systematic review of the literature. *Endocr Relat Cancer*. (2014) 21:R153–63. doi: 10.1530/ERC-13-0125

22. Al-Gahtany M, Horvath E, Kovacs K. Pituitary hyperplasia. *Hormones (Athens)*. (2003) 2:149–58. doi: 10.14310/horm.2002.1195

23. Klimstra DS. Pathology reporting of neuroendocrine tumors: essential elements for accurate diagnosis, classification, and staging. *Semin Oncol*. (2013) 40:23–36. doi: 10.1053/j.seminoncol.2012.11.001

24. Hochwald SN, Zee S, Conlon KC, Colleoni R, Louie O, Brennan MF, et al. Prognostic factors in pancreatic endocrine neoplasms: an analysis of 136 cases with a proposal for low-grade and intermediate-grade groups. *J Clin Oncol*. (2002) 20:2633–42. doi: 10.1200/JCO.2002.10.030

25. Ramage JK, De Herder WW, Delle Fave G, Ferolla P, Ferone D, Ito T, et al. ENETS consensus guidelines update for colorectal neuroendocrine neoplasms. *Neuroendocrinology*. (2016) 103:139–43. doi: 10.1159/000443166

26. Rossi RE, Elvevi A, Gallo C, Palermo A, Invernizzi P, Massironi S, et al. Endoscopic techniques for diagnosis and treatment of gastro-entero-pancreatic neuroendocrine neoplasms: Where we are. *World J Gastroenterol*. (2022) 28:3258–73. doi: 10.3748/wjg.v28.i26.3258

27. Woltering EA, Voros BA, Beyer DT, Wang YZ, Thiagarajan R, Ryan P, et al. Aggressive surgical approach to the management of neuroendocrine tumors: A report of 1,000 surgical cytoreductions by a single institution. *J Am Coll Surg*. (2017) 224:434–47. doi: 10.1016/j.jamcollsurg.2016.12.032

28. Lambert R. Gastric and rectal carcinoids. *Endoscopy*. (2010) 42:661–3. doi: 10.1055/s-0030-1255592

29. Li Y, Pan F, Sun G, Wang ZK, Meng K, Peng LH, et al. Risk factors and clinical outcomes of 54 cases of rectal neuroendocrine tumors with incomplete resection: A retrospective single-center study. *Ther Clin Risk Manag*. (2021) 17:1153–61. doi: 10.2147/TCRM.S332838

30. Rizen EN, Phan AT. Neuroendocrine tumors: a relevant clinical update. *Curr Oncol Rep*. (2022) 24:703–14. doi: 10.1007/s11912-022-01217-z

frontiers | Frontiers in Oncology

TYPE Case Report
PUBLISHED 28 March 2025
DOI 10.3389/fonc.2025.1403881

Check for updates

OPEN ACCESS

EDITED BY
Vladimir Spiegelman,
Penn State Milton S. Hershey Medical Center, United States

REVIEWED BY
Dharmendra Kumar Yadav,
Gachon University, Republic of Korea
Giovanni Scarzello,
Veneto Institute of Oncology (IRCCS), Italy

*CORRESPONDENCE
Young-Joon Jun
joony@catholic.ac.kr

RECEIVED 20 March 2024
ACCEPTED 04 March 2025
PUBLISHED 28 March 2025

CITATION
Choi J, Park H, Ko EJ, Choi JY, Moon S-H, Oh DY and Jun Y-J (2025) Cutaneous histiocytic sarcoma arising from soft tissue filler injections: a case report.
Front. Oncol. 15:1403881.
doi: 10.3389/fonc.2025.1403881

COPYRIGHT
© 2025 Choi, Park, Ko, Choi, Moon, Oh and Jun. This is an open-access article distributed under the terms of the Creative Commons Attribution License (CC BY). The use, distribution or reproduction in other forums is permitted, provided the original author(s) and the copyright owner(s) are credited and that the original publication in this journal is cited, in accordance with accepted academic practice. No use, distribution or reproduction is permitted which does not comply with these terms.

Cutaneous histiocytic sarcoma arising from soft tissue filler injections: a case report

Jangyoun Choi, Heeyang Park, Eun Jeong Ko, Jong Yun Choi, Suk-Ho Moon, Deuk Young Oh and Young-Joon Jun*

Department of Plastic and Reconstructive Surgery, Seoul St. Mary's Hospital, The Catholic University of Korea, Seoul, Republic of Korea

Background: The administration of soft-tissue fillers is a popular aesthetic procedure. Nonetheless, it can result in complications such as foreign-body reactions, infections, skin necrosis, granulomas, and even malignant transformation. This case study documents an unusual occurrence of sarcoma following a prior cosmetic injection.

Case report: A male patient, aged 76, presented with facial swelling. He received filler injections from a non-professional aesthetician twenty-five years ago. The patient reported a slow downward movement of the injected material, recurring inflammation, and the development of multiple nodules. An excisional biopsy and tissue culture were conducted, which did not identify any microorganisms but did reveal a dense infiltration of large polygonal cells with pleomorphic nuclei. The diagnosis of histiocytic sarcoma(HS) was confirmed through immunohistochemistry. A comprehensive systemic examination, including contrast MRI and PET-CT, identified multiple nodular soft tissue lesions in the subcutaneous layer of the face and intense metabolic activity in the same nodular lesions. Metabolic activities were also observed in the abdominal wall, indicating a potential migration of the injected material. Following diagnosis, all remaining lesions in the forehead, nose, and abdomen were surgically excised. Due to the complete nature of the excision, adjuvant chemoradiation was not administered.

Conclusion: This case underscores the serious complication that can result from unauthorized filler injections, including the extremely rare histiocytic sarcoma. It emphasizes the necessity of cautious follow-up and patient education in aesthetic procedures.

KEYWORDS

histiocytic sarcoma, foreign-body reaction, fillers, tumorigenesis, injection site reaction

Introduction

Soft-tissue filler injection is an essential part of cosmetic practice. Because of its high demand and case volume, its post-procedure follow-up is mainly neglected. However, serious complications can arise from a foreign-body reaction inciting local inflammatory reaction. The most common presentation is Cellulitis, secondary bacterial infection, skin necrosis, and

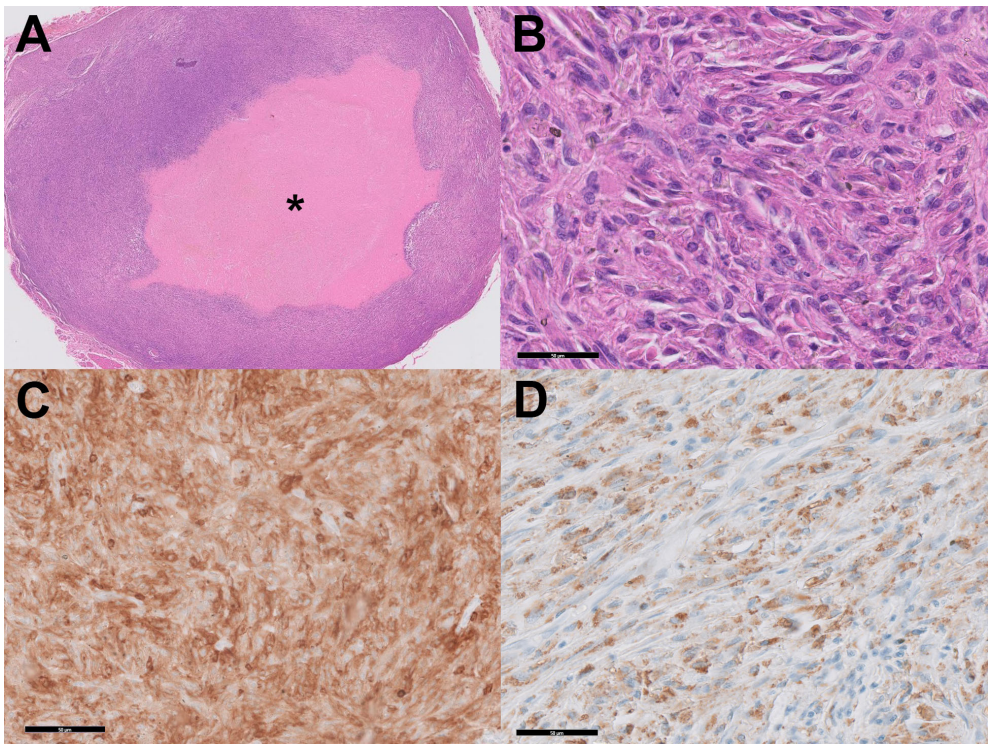

FIGURE 1
Histologic analysis. **(A)** Proliferation of histiocytes around the injected material shows a gel-pool-like accumulation (asterisk). **(B)** High-power magnification shows the epitheloid configuration, eosinophilic cytoplasm, and prominent nucleoli. (HE Stain, x400) **(C)** Immunohistochemical stain for CD4 shows diffuse immunoreactivity. **(D)** Immunohistochemical stain for CD68 shows positivity.

granuloma. A chronic state of inflammation may trigger the malignant transformation of the injected soft tissue but is underreported. In this case report, we report an exceedingly rare case of primary cutaneous histiocytic sarcoma(HS) arising from a previous cosmetic injection. Distant filler migration was also observed, with concurrent development of the same disease.

Case presentation

A 76-year-old male patient with diabetes first visited our clinic ten years ago with facial swelling. He had a history of filler injections on his forehead and both cheeks by an unlicensed individual twenty-five years ago. He had not been informed of the chemical properties

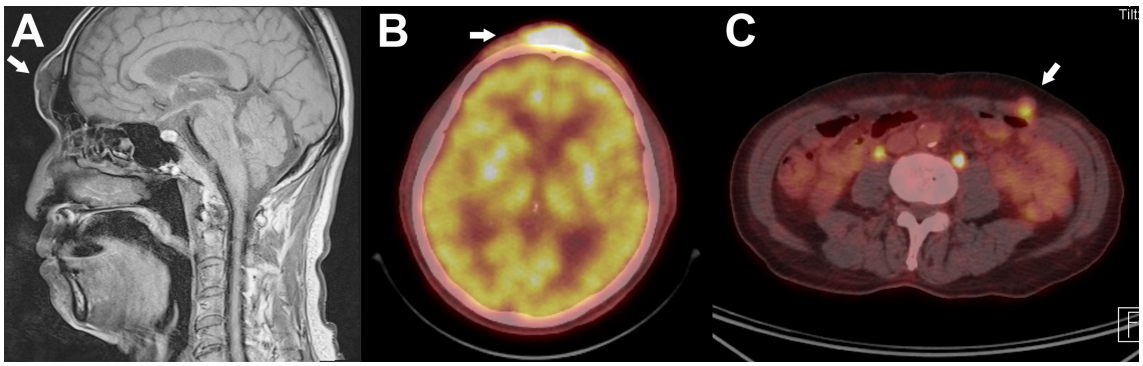

FIGURE 2
Magnetic Resonance Imaging(MRI) and positron Emission tomography(PET) Scan. **(A)** T1-Weighted sagittal view shows nodular accumulation of foreign body material in the subcutaneous layer of the forehead. **(B)** PET-CT scan shows high metabolic activity (SUVmax=15) in the same region as shown in **(A)**. **(C)** Hypermetabolic activity was also noted in the anterior abdominal wall, suggesting distant migration of the injected material. Biopsy confirmed the same pathology with the lesion in **(A)**.

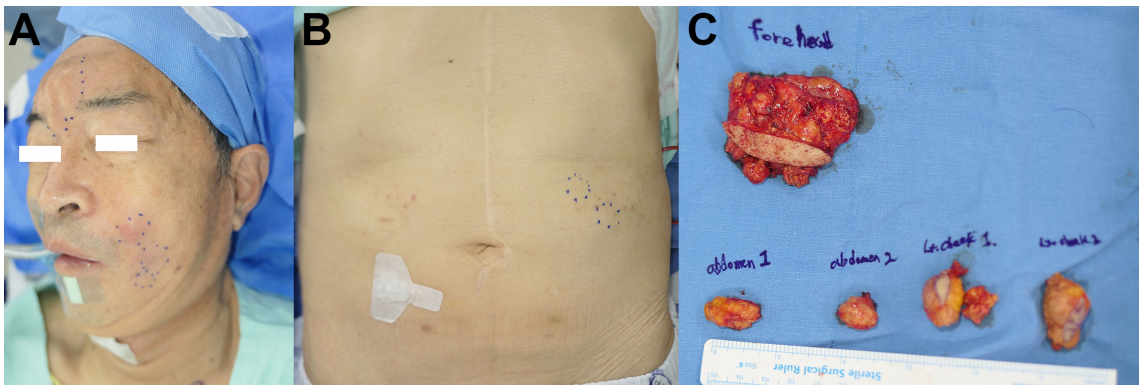

FIGURE 3
Clinical photo of the patient. **(A)** Enlarged nodular lesions in the nasolabial, forehead area are noted. The uppermost nodule in the nasolabial fold area shows erythematous change, indicating infection. **(B)** Similar nodular lesion in the abdominal wall suggests distant migration of the injected material. **(C)** Specimens resected *en bloc*.

of the filler. A few years after receiving the injection, the patient started to experience a gradual, descent of the injected material from the original area of treatment. Intermittent rubor and swelling of the injection site occurred repeatedly, which was only temporarily resolved with anti-inflammatory agents and oral antibiotics. The severity of symptoms continued to worsen, and the frequency of symptom occurrence increased. The patient visited our institution seeking surgical treatment for his condition.

On physical exam, multiple nodules were palpable along the bilateral nasolabial fold and forehead, which corresponded to the location of the past injections. The nodules were about 2-centimeter-sized, firm, and immobile. Since the lesion on the nasolabial fold area was the most disturbing, excision of the cheek nodules was planned. Under the impression of chronic foreign body reaction, excisional biopsy and tissue culture were performed.

The tissue culture did not reveal any microorganisms. However, histology showed dense infiltration of large polygonal cells with epithelioid-to-pleomorphic morphology with pleomorphic nuclei, which needs to be differentiated from cancerous entities such as sarcoma (Figures 1A, B). Immunohistochemistry revealed high nuclear atypia, positivity in CD68 and CD15, and negativity in S100 and CD1a (Figures 1C, D). Based on these results, the diagnosis of HS was made.

Further systemic workup was performed. Contrast MRI showed multiple nodular soft tissue lesions in the subcutaneous layer of the glabella, nasolabial fold, and lower face. (Figure 2A) Positron emission tomogram computed tomography (PET-CT) showed intense metabolic activity in the same nodular lesions. (Figure 2B) Interestingly, metabolic activities were also noted in the abdominal wall, raising the possibility of migration of the injected material (Figure 2C).

After the confirmed diagnosis of histiocytic sarcoma, subsequent removal of all remaining lesions in the forehead, nasolabial area, and abdomen were performed (Figures 3A-C). Adjuvant chemoradiation was not administered owing to the complete nature of the excision. The patient is being followed up disease free, with thorough physical exams for unusual formation of nodules, and PET-CT scans at 6-month intervals (Figure 4).

Discussions and conclusions

HS is an extremely rare non-Langerhans histiocyte disorder that presents as a unifocal or multifocal disease affecting various organ systems. Here, we presented an even more unique case of histiocytic sarcoma, which arose from a previously injected foreign material, which we think is the first to be reported.

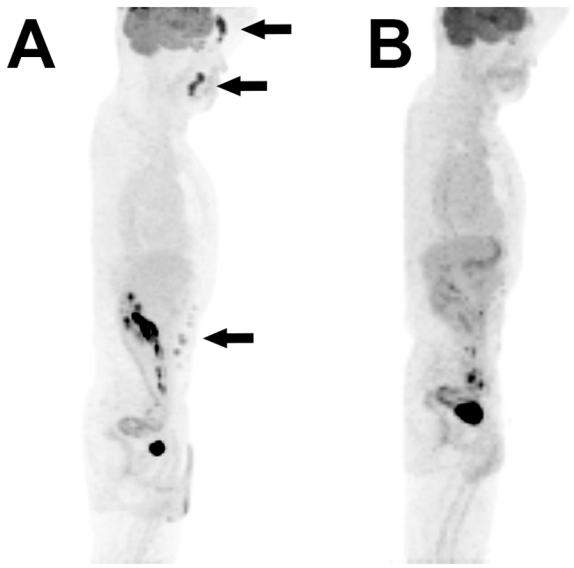

FIGURE 4
Pre- and post-operative PET scans. **(A)** Preoperative maximum intensity projection reconstituted PET scan shows increased metabolic activity in the forehead, nasolabial fold, and abdominal wall. **(B)** Postoperative PET image of the same reconstitution shows no activity in the corresponding regions.

Regardless of the location or chemical composition, malignancy arising from injected foreign material is possible but uncommon. The most relevant clinical scenario can be derived from the cosmetic injection of polyacrylamide hydrogel (PAAG), more commonly known as 'AmazingGel' or 'Aquamid', to the public (1). PAAG is a non-resorbable, synthetic material composed of approximately 2.5% cross-linked polyacrylamide and 97.5% water. It was widely used as an injectable filler for soft tissue augmentation, particularly for breast enhancement, from 1997 until its ban in 2006 (1). It has gained popularity due to its suggested biocompatibility due to its chemically hydrophilic nature. Through PAAG injection to the face and breast had been widely performed for augmentation purposes, Various complications followed, most related to inflammation, infection, asymmetry, and migration to other anatomical locations (2–4).

Few literature reported occurrence of malignancy after PAAG injection to the breast (5–7). Once considered biocompatible, questions were raised from its potential degradation into acrylamide, a probable human carcinogen. The exact carcinogenic mechanism of PAAG is not clearly identified, but *c-myc* overexpression may play a role (5, 8). When included in dietary form, exposure to acrylamide is well known to cause neurotoxicity, genotoxity, and carcinogenicity, and thus has been classified as group 2A substance by the International Agency for Research on Cancer (IARC) (9).

The injected material can migrate along the fascial tissue plane of the body, which is a hallmark of long-term complication in PAAG injections (3). Similarly, remote migration of the injected material to the abdominal wall was also found in our case. The reason for such a high migration rate of PAAG is thought to be originating from the initial high inflammatory response with the surrounding tissues, rather than formation of a capsule. This may decompose the normal tissue structures and subsequently make way for migration along tissue planes (10).

Due to its infrequent occurrence, the type of malignancy in our case is a noteworthy feature. Given the history of cosmetic injection, differential diagnosis usually points to benign conditions such granuloma or abscess. However in this case, high uptake values in PET CT suggested otherwise and led us to perform a thorough pathologic investigation. Pathogenesis of HS is unknown and has not been reported to be produced by a foreign material. Primary cutaneous HS is exceedingly rare and occupies a minor proportion of all HS etiologies. In theory, longstanding deposition and cellular aberration of histiocytes around the foreign material may have played a role in tumorigenesis of the neighboring tissue, as has also been suggested in animal models (11). Rather than systemic progression, a multifocal but circumscribed development of HS in spots where the injection was performed supports this claim.

HS is notable for its broad overlapping features with other myeloid neoplasms (12). Its major differential diagnoses include anaplastic large-cell lymphoma, myeloid sarcoma, and Langerhans cell histiocytosis (13). Immunohistochemistry is vital in differential diagnosis, especially positive expression in CD68, CD163, lysozyme, CD4, and CD45. Expression of at least 2 of the above markers has been recommended in diagnosing HS from other differentials (14). Similarly, our case showed positive expression in CD68 and CD4, which fulfills the diagnostic criteria. In HS, negative expression for CD1a (for Langerhans cell) and CD35(for follicular dendritic cell) is expected, which also parallels the immunohistochemical marker expression of our case.

Due to its rarity and aggressive clinical course, there is currently no standard treatment regimen for patients with HS (15). Extracutaneous HS especially presents at an advanced stage and shows limited response to chemoradiation (13). However, some reports claim that primary cutaneous HS may show a better prognosis than other types of extranodal HS if complete resectability is guaranteed (16, 17). Similarly, we achieved complete resection in all lesions localized in PET-CT, and the patient is showing excellent disease course without adjuvant therapy. To establish a more confident treatment plan for this rare disease, a multidisciplinary approach including pathology, hematology, and radiation oncology is crucial (18). The decision not to start adjuvant therapy was made by the interdisciplinary tumor board team, which was guided by the achieved complete resection, absence of progressive lesions, and the long-standing localized nature of the sarcoma. Until now, the patient is remaining disease-free with meticulous physical examination and imaging.

Conclusion

This case is the first reported instance of histiocytic sarcoma induced by foreign material, emphasizing the need for careful observation of the disease's progression through long-term follow-up. The association between soft tissue augmentation procedures and the development of sarcomas is not well-established, making this case particularly noteworthy.

Data availability statement

The original contributions presented in the study are included in the article/supplementary material. Further inquiries can be directed to the corresponding author.

Ethics statement

The studies involving humans were approved by Institutional Review Board of The Catholic University of Korea (IRB No. KC24ZISI0182). The studies were conducted in accordance with the local legislation and institutional requirements. The human samples used in this study were acquired from a by- product of routine care or industry. Written informed consent for participation was not required from the participants or the participants' legal guardians/next of kin in accordance with the national legislation and institutional requirements. Written informed consent was obtained from the individual(s) for the publication of any potentially identifiable images or data included in this article.

Author contributions

JC: Conceptualization, Visualization, Writing – original draft, Writing – review & editing. HP: Visualization, Writing – original draft. EK: Visualization, Writing – original draft, Writing – review & editing. JC: Validation, Writing – review & editing. SM: Writing – review & editing. DO: Supervision, Writing – review & editing. YJ: Conceptualization, Supervision, Writing – review & editing.

Funding

The author(s) declare that financial support was received for the research and/or publication of this article. This work was supported by the National Research Foundation of Korea (NRF) grant funded by The Ministry of Education. (NRF-2021R1I1A1A01049056).

Conflict of interest

The authors declare that the research was conducted in the absence of any commercial or financial relationships that could be construed as a potential conflict of interest.

Publisher's note

All claims expressed in this article are solely those of the authors and do not necessarily represent those of their affiliated organizations, or those of the publisher, the editors and the reviewers. Any product that may be evaluated in this article, or claim that may be made by its manufacturer, is not guaranteed or endorsed by the publisher.

References

1. Jin R, Luo X, Wang X, Ma J, Liu F, Yang Q, et al. Complications and treatment strategy after breast augmentation by polyacrylamide hydrogel injection: summary of 10-year clinical experience. *Aesthetic Plast Surg*. (2018) 42:402–9. doi: 10.1007/s00266-017-1006-9

2. Winter J, Shiga S, Islur A. The complications of polyacrylamide hydrogel augmentation mammoplasty. *Plast Surg Case Stud*. (2017) 3. doi: 10.1177/2513826X17693821

3. Choi J, Kim YS, Oh DY. Remote migration of breast filler to the inguinal area: a case report. *Arch Aesthetic Plast Surgery*. (2021) 27:149–52. doi: 10.14730/aaps.2021.00206

4. Mo YW, Lee DL, Shin HK, Jung GY. Polyacrylamide hydrogel (Aquamid) filler removal after a decade. *Arch Aesthetic Plast Surg*. (2019) 25:115–8. doi: 10.14730/aaps.2019.01697

5. Yang Y, Li S, He J, Zhao X, Chen W, Dai X, et al. Clinicopathological analysis of 90 cases of polyacrylamide hydrogel injection for breast augmentation including 2 cases followed by breast cancer. *Breast Care (Basel)*. (2020) 15:38–43. doi: 10.1159/000499832

6. Qian B, Xiong L, Guo K, Wang R, Yang J, Wang Z, et al. Comprehensive management of breast augmentation with polyacrylamide hydrogel injection based on 15 years of experience: a report on 325 cases. *Ann Transl Med*. (2020) 8:475. doi: 10.21037/atm.2020.03.68

7. Chen G, Wang Y, Huang JL. Breast cancer following polyacrylamide hydrogel injection for breast augmentation: A case report. *Mol Clin Oncol*. (2016) 4:433–5. doi: 10.3892/mco.2016.731

8. Xi TF, Fan CX, Feng XM, Wan ZY, Wang CR, Chou LL. Cytotoxicity and altered c-myc gene expression by medical polyacrylamide hydrogel. *J BioMed Mater Res A*. (2006) 78:283–90. doi: 10.1002/jbm.a.v78a:2

9. Dybing E, Farmer PB, Andersen M, Fennell TR, Lalljie SP, Müller DJ, et al. Human exposure and internal dose assessments of acrylamide in food. *Food Chem Toxicol*. (2005) 43:365–410. doi: 10.1016/j.fct.2004.11.004

10. Wen J, Li Z, Chi Y, Chen B, Hong T, Liu Z, et al. Vulvar migration of injected polyacrylamide hydrogel following breast augmentation: a case report and literature review. *BMC Women's Health*. (2024) 24:152. doi: 10.1186/s12905-024-02998-0

11. Kirkpatrick CJ, Alves A, Köhler H, Kriegsmann J, Bittinger F, Otto M, et al. Biomaterial-induced sarcoma: A novel model to study preneoplastic change. *Am J Pathol*. (2000) 156:1455–67. doi: 10.1016/S0002-9440(10)65014-6

12. Jiang M, Bennani NN, Feldman AL. Lymphoma classification update: T-cell lymphomas, Hodgkin lymphomas, and histiocytic/dendritic cell neoplasms. *Expert Rev Hematol*. (2017) 10:239–49. doi: 10.1080/17474086.2017.1281122

13. Hung YP, Qian X. Histiocytic sarcoma. *Arch Pathol Lab Med*. (2020) 144:650–4. doi: 10.5858/arpa.2018-0349-RS

14. Emile JF, Abla O, Fraitag S, Horne A, Haroche J, Donadieu J, et al. Revised classification of histiocytoses and neoplasms of the macrophage-dendritic cell lineages. *Blood*. (2016) 127:2672–81. doi: 10.1182/blood-2016-01-690636

15. Skala SL, Lucas DR, Dewar R. Histiocytic sarcoma: review, discussion of transformation from B-cell lymphoma, and differential diagnosis. *Arch Pathol Lab Med*. (2018) 142:1322–9. doi: 10.5858/arpa.2018-0220-RA

16. Sato N, Arai E, Nakamura Y, Yazawa Y, Yasuda M. Primary cutaneous localized/clearly-outlined true histiocytic sarcoma: Two long-term follow-up cases. *J Dermatol*. (2020) 47:651–3. doi: 10.1111/1346-8138.15315

17. Magro CM, Kazi N, Sisinger AE. Primary cutaneous histiocytic sarcoma: A report of five cases with primary cutaneous involvement and review of the literature. *Ann Diagn Pathol*. (2018) 32:56–62. doi: 10.1016/j.anndiagpath.2017.10.004

18. Wehrmann S, Rudolph H, Ernst D, Siepmann T, Kaltofen D, Hanel M, et al. Case report: eighteen month relapse- free survival following radical multidisciplinary oncological treatment in a 68-year-old male patient with histiocytic sarcoma. *Front Oncol*. (2021) 11:633215. doi: 10.3389/fonc.2021.633215

frontiers | Frontiers in Oncology

TYPE Original Research
PUBLISHED 15 May 2025
DOI 10.3389/fonc.2025.1487812

Check for updates

OPEN ACCESS

EDITED BY
Sharon R. Pine,
University of Colorado Anschutz Medical Campus, United States

REVIEWED BY
Przemyslaw Karol Wolak,
Jan Kochanowski University, Poland
Omar Hamdy,
Mansoura University, Egypt

*CORRESPONDENCE
Shengmin Zhang
nbsmzhang@163.com

RECEIVED 28 August 2024
ACCEPTED 22 April 2025
PUBLISHED 15 May 2025

CITATION
Chen M, Liao S, Xu Y, Ye X, Jia X and Zhang S (2025) Clinicopathological and imaging features of struma ovarii: a retrospective study.
Front. Oncol. 15:1487812.
doi: 10.3389/fonc.2025.1487812

COPYRIGHT
© 2025 Chen, Liao, Xu, Ye, Jia and Zhang. This is an open-access article distributed under the terms of the Creative Commons Attribution License (CC BY). The use, distribution or reproduction in other forums is permitted, provided the original author(s) and the copyright owner(s) are credited and that the original publication in this journal is cited, in accordance with accepted academic practice. No use, distribution or reproduction is permitted which does not comply with these terms.

Clinicopathological and imaging features of struma ovarii: a retrospective study

Mei Chen[1], Shusheng Liao[2], Youfeng Xu[1], Xianwang Ye[3], Xiupeng Jia[4] and Shengmin Zhang[1]*

[1]Department of Ultrasonography, The First Affiliated Hospital of Ningbo University, Ningbo, Zhejiang, China, [2]Department of Ultrasound, The First Affiliated Hospital of Wenzhou Medical University, Wenzhou, Zhejiang, China, [3]Department of Radiology, The First Affiliated Hospital of Ningbo University, Ningbo, Zhejiang, China, [4]Department of Pathology, The First Affiliated Hospital of Ningbo University, Ningbo, Zhejiang, China

Objectives: The struma ovarii (SO) is a rare disease, presenting significant challenges in achieving an accurate diagnosis. This study aims to delineate the clinicopathological and multimodal imaging characteristics of SO, enabling the precise diagnosis of this entity.

Methods: A retrospective analysis was conducted of the clinicopathological manifestations, laboratory examination results, and imaging data (including ultrasound and MRI) of 40 SO patients who received treatment at the First Affiliated Hospital of Ningbo University over the period from January 2010 to February 2024.

Results: The pathological results of 40 patients showed 21 pure SO, including 20 benign and one malignant; 19 patients had mixed SO, composed of 17 benign and two malignant. Three malignant cases were thyroid carcinoid. According to the ultrasound image, 40 SO patients were divided into three types: 22 cases were cystic, which had mainly single room or separations; 12 cases were mainly cystic-solid mixed, which had multiple septations and hyperechoic nodules; and six solid cases showed regular or irregular mass and rich blood supply. Five patients underwent contrast-enhanced ultrasound (CEUS) examination. The cystic wall and septation showed equal enhancement and slow regression. Two patients showed low enhancement in the protrusion and with slow regression. The MRI manifestations of SO are various. In this cohort, T1-weighted imaging (T1WI) showed hypo-intensity in six cases and heterogeneity in six cases; T2-weighted imaging (T2WI) showed hypo-intensity in two cases, heterogeneity in five cases, and hyper-intensity in four cases; diffusion-weighted imaging (DWI) showed hypo-intensity in two cases, heterogeneity in three cases, and hyper-intensity in four cases.

Conclusions: The incidence of SO is low, but there are some features in imaging. There were cystic, cystic-solid, or solid lesions in the appendage area; CEUS showed separations and solid components with rich blood flow and slow enhancement; MRI showed high signal on T2WI and multiple cysts and heterogeneous signal on T1WI, which were the imaging markers for SO. A comprehensive understanding of imaging manifestations can help radiologists identify this disease and provide a basis for an appropriate therapeutic regime.

KEYWORDS

struma ovarii, ovarian teratoma, imaging, ultrasound, pathology

Introduction

Struma ovarii (SO) is a rare highly specific mature teratoma originating from ovarian primordial germ cells. Although the thyroid tissue component is observed in 5%–15% of ovarian teratomas, the diagnosis of SO can be established when the thyroid tissue component exceeds 50% (1). SO contributes approximately 3% of ovarian teratoma, 2% of ovarian germ cell tumors, and merely 0.5% of all ovarian tumors (2). Most of the SO cases were benign, but still 0.3%–5% of them were malignant (3). SO can occur at any age, but the majority age of patients ranged from 40 to 50 years (4). The clinical manifestations of the disease, including asymptomatic pelvic mass, abdominal discomfort, thyrotoxicosis, ascites, and elevated Cancer antigen 125 (CA125), lack specificity and often resemble those of other ovarian tumors (5). The biological behavior of SO is difficult to predict, and even benign cases can transfer to malignant growth of peritoneum and omental dissemination (6), while malignant SO can develop distant metastasis (7). Overlap in the imaging manifestations with other ovarian malignancies (8) creates difficulties in the diagnosis of SO and affects the choice of surgery, especially considering the protection of the fertility of women of childbearing age (9). Therefore, early diagnosis is very important for the management and prognosis of patients. Most previous works of literature focused only on ultrasound or CT and MRI diagnosis (6, 9, 10), and there were no reports of multimodal imaging for systematic description of this disease. This study retrospectively analyzed the clinicopathological and imaging data of 40 SO patients and subdivided their ultrasound features, aiming to achieve a better understanding of imaging findings and enhance the diagnostic precision of this rare entity.

Materials and methods

Study subjects

This study included 40 patients diagnosed with SO at our hospital from January 2010 to February 2024. The ages of these patients ranged from 23 to 78 years, with an average age of 45 ± 15.4 years. We conducted a comprehensive retrospective analysis of the clinical data, laboratory results, and imaging findings for these patients. Our study was approved by the Medical Ethics Committee of our institution (No. 2024-041RS-01).

Ultrasound examination

The equipment for this study included the GE E8 (Voluson E8, GE Healthcare, Chicago, IL, USA), Toshiba Aplio 500 (Tokyo, Japan), and Philips IU22 (Philips, Bothell, WA, USA) color Doppler ultrasound diagnostic systems. Transvaginal sonography and transabdominal ultrasound used a probe with a frequency range of 5–9 MHz and 3.5–5.0 MHz, respectively. The two-dimensional ultrasound evaluated the lesions' location, size, shape, boundaries, internal echo characteristics, and the presence of pleuritic and abdominal effusion. Color Doppler flow imaging (CDFI) was utilized to analyze the blood flow within the lesions. Additionally, five patients underwent contrast-enhanced ultrasound (CEUS). This procedure involved the administration of a contrast agent (SonoVue, Bracco, Italy) in a 1.8-mL dose via the median antecubital vein. Throughout the contrast-enhanced phase, continuous observation was made of the enhancement pattern, timing, intensity, and washout of the contrast agent within the lesions.

MRI inspection method

MRI examinations were conducted using a GE Signa HDxt 1.5T superconducting MRI scanner. A phased array body coil was utilized with the following scan parameters: for sagittal T2-weighted imaging (T2WI) with fat suppression, the repetition time (TR) was 5,300 ms, and the echo time (TE) was 102 ms; for T1-weighted imaging (T1WI), the TR was set to 600 ms and the TE to 7 ms; T2WI with lipid suppression had a TR of 4,900 ms and a TE of 108 ms; T2WI in the coronal position featured a TR of 4,940 ms and a TE of 102 ms; T1WI with fat suppression in the axial plane had a TR of 760 ms and a TE of 3.6 ms; slice thickness ranged from 5.6 to 6.0 mm, with a slice gap of 2 mm. For enhanced scanning, a transverse and sagittal T1WI sequence with lipid suppression was used, employing gadolinium gluconate (Gd-DTPA) as the contrast agent at a dose of 0.2 mmol/kg and an injection rate of 2–3 mL/s. The parameters for this phase were adjusted accordingly. Diffusion-weighted imaging (DWI) was performed in the axial plane using a single-shot echo-planar imaging sequence with a TR of 5,125 ms, a TE of 98 ms, b-values of 0 and 1,000 s/mm^2, a slice thickness of 6 mm, an interslice gap of 2 mm, and an acquisition number of 4.

Statistical method

Statistical analyses were conducted utilizing SPSS version 23.0. Continuous variables are reported as either mean or median values, measurement data are expressed as $\bar{x} \pm s$, and categorical variables are described using frequencies and percentages.

Results

General medical history

Among the 40 patients, 25 (62.5%) patients were premenopausal, and 15 (37.5%) were postmenopausal. Of the patients, 28 (70.0%) were asymptomatic, and 12 (40.0%) had different symptoms, such as abdominal swelling, vaginal bleeding, pelvic pain, or digestive symptoms. Of the cases, 15 (37.5%) had

Abbreviations: CDFI, color Doppler flow imaging; CEUS, contrast-enhanced ultrasound; DWI, diffusion-weighted imaging; MRI, magnetic resonance imaging; SO, struma ovarii.

minimal ascites, three cases (7.5%) had moderate ascites, and 17 (42.5%) had no ascites. There were thyroid nodules in five patients (12.5%) who had undergone scans of their thyroid. In this cohort, 20 cases performed laparoscopic ovarian cyst removal, 10 cases underwent salpingo-oophorectomy laparoscopy, three cases underwent laparoscopic salpingectomy, and seven cases underwent total transabdominal adnexectomy. Compared to menstruation, the symptomatology, ascites, surgery, and pathology between the pure and impure groups had no statistically significant differences (Table 1).

Laboratory test results

1) Tumor markers: The level of CA125 was higher than 118.9 U/mL (normal, <30 U/mL) in four cases (10.8%). Two cases had higher human chorionic gonadotropin (HCG) levels for pregnancy, and one had also a higher serum alpha-fetoprotein (AFP) of 162 U/mL (normal, <5 U/mL). The level of Cancer antigen 724 (CA724) in two cases was slightly high at 10.89 U/mL (normal, <7 U/mL). In three cases, Cancer antigen 199 (CA-199) was slightly high at 31.3 U/mL (normal, <30 U/mL). One case had a high serum carcinoembryonic antigen (CEA) at 6.4 ng/mL (normal, <5 ng/mL). 2) Serum sex hormones: Five cases had high E2, one case had high prolactin (PRL), and four cases had high TT. 3) Serum thyroid hormone: The thyroid indicators in most patients were in the normal range (Table 2).

TABLE 1 Clinical characteristics and surgical management of the 40 patients with SO.

Parameters		Pure (n = 21)	Impure (n = 19)
Age at surgery (years)		44 (29–71)	45 (23-78)
Menstruation	Premenopausal	30.0% (12/40)	32.50% (13/40)
	Postmenopausal	22.5% (9/40)	10.0% (4/40)
Symptomatology	Asymptomatic	37.5% (15/40)	32.5% (13/40)
	symptomatic	15.0% (6/40)	15.0% (6/40)
Ascites	Mild	17.50% (7/40)	20.0% (8/40)
	Moderate	7.50% (3/40)	0
	Severe	0	0
	No	25.0% (10/40)	17.50% (7/40)
Surgery	Laparoscopic oophorocystectomy	25.0% (10/40)	25.0% (10/40)
	Salpingo-oophorectomy laparoscopy	12.50% (5/40)	12.50% (5/40)
	Total laparoscopic hysterectomy	2.50% (1/40)	5.0% (2/40)
	Total abdominal hysterectomy	12.50% (5/40)	5.0% (2/40)
Pathology	Benign	50.0% (20/40)	42.50% (17/40)
	Malignant	2.50% (1/40)	5.0% (2/40)

Values are expressed as median (range) or n (%).
SO, struma ovarii.

Pathological and immunohistochemical examination results

In pathology, 21 (52.5%) patients had pure SO (Figure 1A), and 19 (47.5%) patients had impure SO (Figures 1C, D). The majority of 37 (92.5%) patients were benign, only three (7%) patients were malignant, and the pathological subtypes of malignant were strumal carcinoid (Figure 1B). In these malignant cases, one had pure SO, and the other two had impure SO. The postoperative follow-up of three malignant patients was 8, 20, and 141 months, and there was no metastasis or death. The 37 benign patients had no recurrence during the follow-up period. The immunohistochemical examination was further carried out for three malignant patients, and the expression of tumor cell immune markers across them is detailed in Supplementary Table. Notably, there was a high expression of chromogranin A (CgA), synaptophysin (Syn), and cytokeratin 5/6 (CD56) in all three malignant patients and thyroglobulin (TG) in two patients, with Ki-67 between 1% and 2% (Figure 2). In contrast, the results revealed no expression of calcitonin in all three patients and TG in two patients.

Ultrasound features of SO

2D and color Doppler ultrasound manifestations of 40 SO patients

1) Lesion site: All patients were unilateral, including 25 patients on the left side and 15 patients on the right side. 2) Size: The diameter of the mass ranged from 2.6 to 16.2 cm. 3) Morphology and boundary: All patients had clear boundaries. Of the cases, 31 (77.5%) were round or circular, and the morphology was regular. Nine cases (22.5%) had irregular morphology. 4) Internal echo manifestations and blood flow: According to ultrasound features, the patients were subdivided into three types: 22 (55.0%) were cystic type, 12 (30.0%) were cystic-solid type, and six (15.0%) were solid type. Among the 22 cystic cases, single room and thick septations were the features (Figures 3A, D). There were eight cases that showed papillary protrusion on the cystic wall (Figure 3B) and an "amniotic fat ball" floating inside the cyst (Figure 3C), and some had a "catkins" sign hanging on the wall. Twelve cases of cystic-solid (Figure 3G), light spots, and separations were seen in most cases. In particular, there were "strum pearls" (Figures 3E, F) in seven cases, which were seen as hyperechoic nodules with different sizes and rich blood flow within them (Figure 3H). Among the six solid ones, there were regular or irregular nodules with clear boundaries (Figures 3I, K), which demonstrated rich blood flow in both peripheral and internal areas (Figures 3J, L), with moderate resistance index (RI). Among this

TABLE 2 Laboratory results of 40 patients.

Parameters			Pure (n = 21)	Impure (n = 19)
Serum tumor marker	Serum CA125 level (U/mL) Reference range (0–30)	<30	45.95% (17/37)	43.24% (16/37)
		>30	5.41% (2/37)	5.41% (2/37)
	Serum CA-724 level (U/mL) Reference range (0–7)	<7	48.48% (16/33)	45.45% (15/33)
		>7	3.03% (1/33)	3.03% (1/33)
	Alpha-fetoprotein (AFP) level (ng/mL) Reference range (0–25)	<25	50.0% (18/36)	47.22% (17/36)
		>25		2.78% (1/36)
	Carcinoembryonic antigen (CEA) Level (ng/mL) Reference range (0–5)	<5	41.94% (13/31)	54.84% (17/31)
		>5		3.23% (1/31)
	Serum CA-199 level (U/mL) Reference range (0–25)	<37	42.42% (14/33)	48.48% (16/33)
		>37	6.06% (2/33)	3.03% (1/33)
Serum sex hormone	Estrogen levels (E2) (IU/L)	Normal	46.67% (14/30)	36.67% (11/30)
		Abnormal	6.67% (2/30)	10.0% (3/30)
	Prolactin (PRL)	Normal	56.61% (16/31)	45.16% (14/31)
		Abnormal	3.23% (1/31)	
	Testosterone (TT)	Normal	42.86% (12/28)	42.86% (12/28)
		Abnormal	3.57% (1/28)	10.71% (3/28)
Serum thyroid hormone levels and antibodies	Triiodothyronine (T3)	Normal	43.33% (13/30)	46.67% (14/30)
		Abnormal	3.33% (1/30)	6.67% (2/30)
	Thyroxine (T4)	Normal	44.83% (13/29)	48.28% (14/29)
		Abnormal		6.70% (2/29)
	Thyroid-stimulating hormone (TSH)	Normal	39.29% (11/28)	53.57% (15/28)
		Abnormal	7.14% (2/28)	
	Thyroid peroxidase antibody (TPO)	Normal	44.44% (4/9)	33.33% (3/9)
		Abnormal	22.22% (2/9)	

cohort, only two cases had concurrent presence of myoma or polyp. According to the International Ovarian Tumor Analysis (IOTA) system classification, 14 (35%) cases were diagnosed to be benign, 13 (32.5%) cases were borderline, and 13 (32.5%) cases were malignant (Table 3).

CEUS features of SO

Five patients in this group underwent a CEUS examination. Among them, four cases were cystic with papillary protrusion and separations. After injecting the contrast agent, the cystic wall and septations were enhanced, ranging from 13 to 19 s and showing equal enhancement (compared to the degree of uterine enhancement) and subsequently with slow regression (Figures 4A, B, E). In two cases, contrast agent perfusion was visible at the intracapsular protrusion (Figures 4D, F), which showed slow enhancement and then slow regression, and the other two cases showed no contrast perfusion at the intracapsular protrusion. In one case of cystic-solid type, contrast perfusion was seen in the cyst wall and septa after injection of contrast agent; however, there was no contrast perfusion in the heterogeneous moderate echo components ("amniotic fat ball") within the capsule (Figure 4C).

The MRI performance

Twelve patients in this study underwent an MRI examination. T1WI showed hypo-intensity in six cases and heterogeneity in six cases (Figures 5A, E, I). T2WI showed hypo-intensity in two cases, heterogeneity in five cases, and hyper-intensity in four cases (Figures 5B, F, J). DWI showed hypo-intensity in two cases, heterogeneity in three cases, and hyper-intensity in four cases (Figures 5D, H, L). All the 10 cases with enhanced scans showed obvious enhancement (Figures 5C, G, K). Half of these 12 patients were finally confirmed to have simple SO by pathology (Table 4).

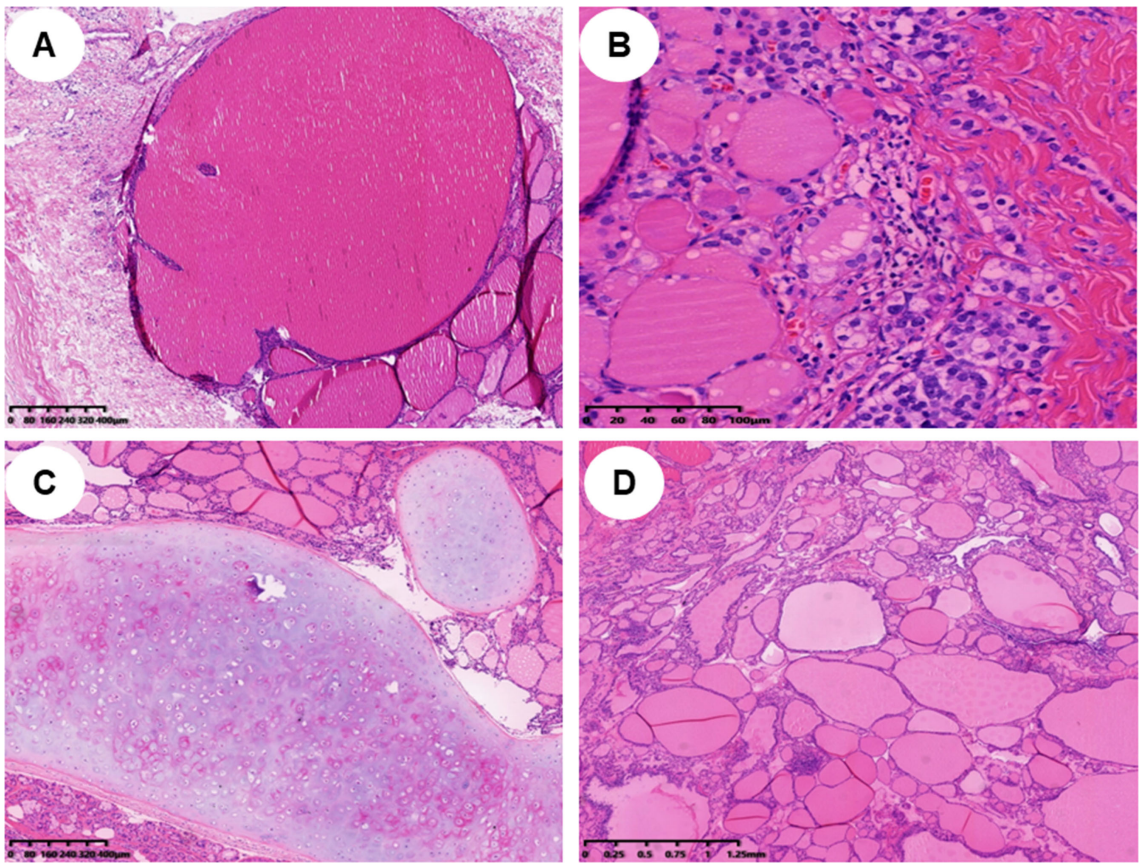

FIGURE 1
Histopathological findings of different types of struma ovarii (H&E staining). **(A)** Histopathological findings of a pure struma ovarii (×40). **(B)** Histopathological findings of a struma carcinoid (×200). **(C, D)** Histopathological findings of an impure struma ovarii; mature teratoma component can be found in panel C (×40), and struma ovarii tissue is displayed in panel D (×40).

Discussion

SO was defined by the WHO in the early 20th century as a monodermal teratoma, which was composed mainly or only of the thyroid tissue (1). Previous studies have shown that SO can occur at any age (7), but mostly during menopause. A few studies have also reported that SO is visible during pregnancy (11), which may be related to the transient increase of thyroid cancer risk in this situation (12). This was mainly due to the structural similarity between HCG and thyroid hormone. HCG can stimulate the thyroid-stimulating hormone (TSH) receptor in ovarian tumors and promote tumor growth during pregnancy (13). Two cases in this study also occurred during pregnancy, and tumor resection was performed during a cesarean section. The majority of SO patients had no special clinical symptoms; previous studies have reported that abdominal pain was the main clinical symptom, and it was believed that the symptoms of pain were caused by increased pressure in the pelvis (5). In this study, 12 (30.0%) patients had the clinical symptoms of abdominal pain and distension, which slightly increased, compared with the previous studies. A few patients with SO may have pseudo-Meigs syndrome, which can disappear after tumor resection (4, 14). Peyron (15) suggested that the increased CA125 may be related to the stimulation of the peritoneal, omentum, and mesentery mesothelial cells. In this study, the variable occurrence of ascites was found in 18 (45%) patients, and abdominal effusion disappeared after the lesions were resected.

Pathologically, benign SO is the most common. However, there have approximately 5% of cases of malignant SO (3). In this study, 37 (92.5%) patients were benign, and only three patients were malignant, which coincided with previous studies (3, 16–18). Carcinoid tumors are similar to well-differentiated neuroendocrine tumors in other organs (19), usually asymptomatic, and a small number present with constipation, abdominal distension, and pain, which are due to the production of YY peptides (20). In malignant tumors, metastasis and recurrence are positively correlated with the Ki-67 proliferation index and tumor volume (19–22). In our study, the three malignant patients were asymptomatic with a long history and classified at the stage of International Federation of Gynecology and Obstetrics (FIGO) I. Two of them had a Ki-67 index of less than 2%, and the average tumor diameter was small at approximately 0.3 cm. No metastasis occurred during follow-up, which is consistent with previous studies (23, 24).

Immunohistochemistry is an important basis for the diagnosis and differential diagnosis of tumors. In our study, all three patients with thyroid carcinoid were positive for CgA, Syn, and CD56, which

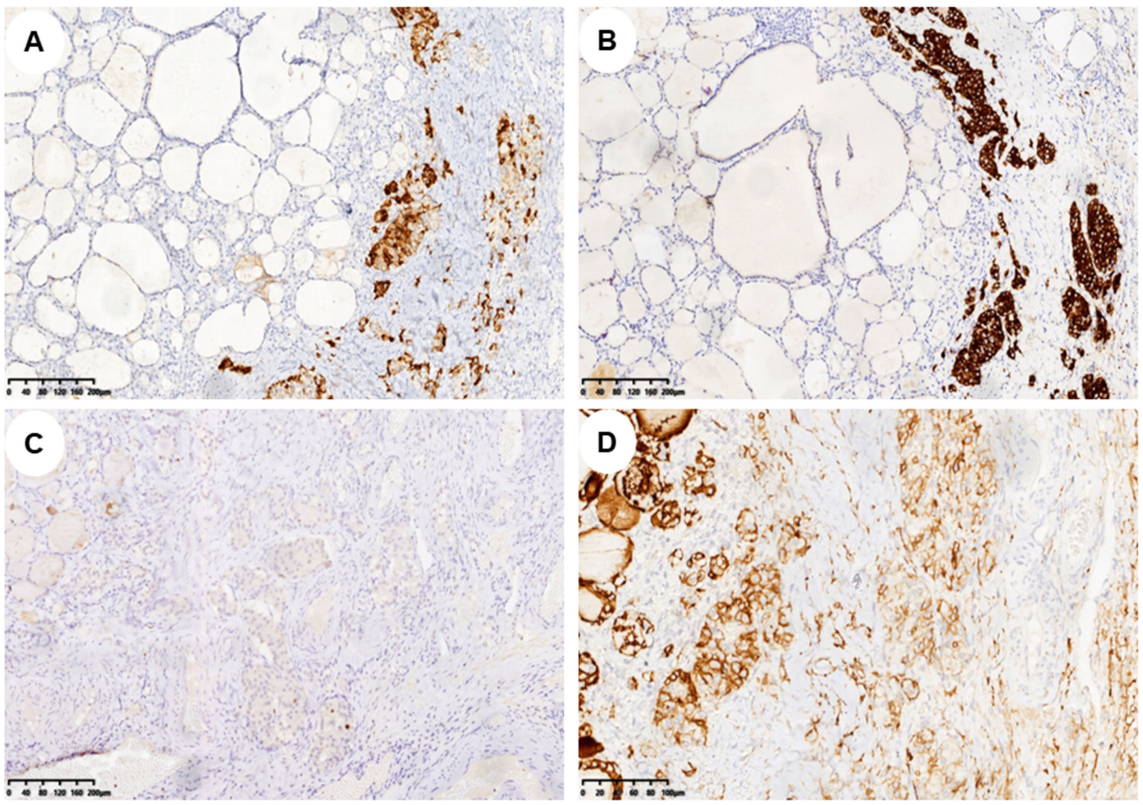

FIGURE 2
Immunohistochemical markers of struma carcinoid. **(A–D)** Immunohistochemistry showed CgA, Syn, Ki-67, and CD56 expression in struma carcinoid cells, respectively (**A–C**, ×100; **D**, ×200). CgA, chromogranin A; Syn, synaptophysin; CD56, cytokeratin 5/6.

is consistent with the previous literature (25, 26). All of them were excluded from the diagnosis of medullary thyroid carcinoma due to negative calcitonin staining. One of them was diagnosed with a follicular variant of papillary thyroid carcinoma due to positive CD56 and negative HBME1. Another one was confirmed as mucinous cystadenoma because of positive TTF-1, which was marked with epithelial-origin gynecological tumors (26).

Regarding tumor markers, the levels of CA125, CA724, and CA-199 were slightly elevated in some patients, which is consistent with a previous study (4). In this study, the levels of sex hormones and thyroid hormones, such as E2, TT, and free triiodothyronine (T3), were elevated in some patients. It is speculated that as a neuroendocrine tumor, carcinoids can cause abnormal levels of estrogen and thyroid hormones (27). However, T3 and thyroxine

TABLE 3 Two-dimensional and color Doppler ultrasound findings of the 40 patients of SO.

Ultrasonic classification		Cyst (n = 22)	Cystic-solid (n = 12)	Solid (n = 6)
Number		55.0% (22/40)	30.0% (12/40)	15.0% (6/40)
Position	Left	32.50% (13/40)	22.50% (9/40)	7.50% (3/40)
	Right	22.50% (9/40)	7.50% (3/40)	7.50% (3/40)
Maximum diameter (cm)		2.7–12.5	2.6–16.2	3.7–7.8
Shape	Regular	50.0% (20/40)	17.5% (7/40)	10.0% (4/40)
	Irregular	5.0% (2/40)	12.5% (5/40)	5.0% (2/40)
Cystic fluid	Clear	15.0% (6/40)	11.76% (4/40)	
	Unclear	40.0% (16/40)	20.0% (8/40)	
	No			15.0% (6/40)
Separation	Yes	25.0% (10/40)	20.0% (8/40)	

(Continued)

TABLE 3 Continued

Ultrasonic classification		Cyst (n = 22)	Cystic-solid (n = 12)	Solid (n = 6)
	No	30.0% (12/40)	10.0% (4/40)	15.0% (6/40)
Parenchymal echo and blood flow in the sac	Yes	20.0% (8/40)	17.5% (7/40)	0
	No	35.0% (14/40)	12.5% (5/40)	15.0% (6/40)
Comet tail sign	Yes	15.0% (6/40)	22.50% (9/40)	
	No	40.0% (16/40)	7.5% (3/40)	15.0% (6/40)
Ultrasound diagnosis (IOTA system)	Benign	30.0% (12/40)	12.5% (5/40)	
	Uncertain	15.0% (6/40)	10.0% (4/40)	
	Malignant	10.0% (4/40)	7.50% (3/40)	15.0% (6/40)

Values are expressed as n (%).
SO, struma ovarii.

(T4) were elevated in some cases with a normal TSH, which may be ascribed to thyroid tissue in SO. Some literature reported that 5%–8% of SO may be accompanied by hyperthyroidism (1). Therefore, if a female patient has abnormal thyroid function, the ovary should be routinely examined to rule out SO.

SO ultrasonic manifestations were varied. In this study, we classified SO patients into cystic, cystic-solid, and solid types. Among them, the cystic type was the most common, accounting for approximately 55%. Most of them can be seen with thick walls and separations, also with "comet tail" signs of glial deposition. The

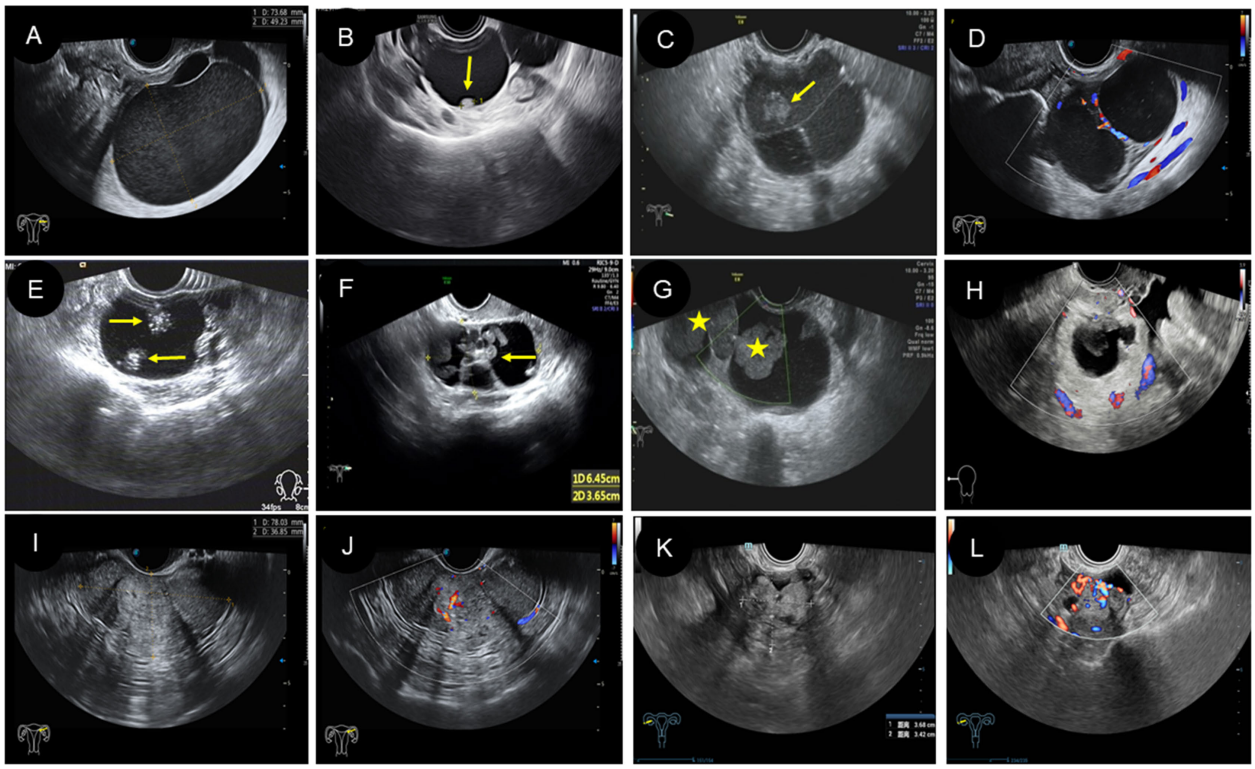

FIGURE 3
Two-dimensional and color Doppler ultrasound manifestations of different types of struma ovarii. **(A–D)** The ultrasound manifestations of cystic type of SO. **(A)** Two-dimensional ultrasound showed a large cyst with regular morphology and clear boundary, and the cyst is filled with weak echoes. **(B)** Two-dimensional ultrasound revealed a unilocular cyst with a papillary protrusion (arrow) in the cystic wall. **(C)** Two-dimensional ultrasound revealed multilocular cyst with several septations and "amniotic fat ball" (arrow) within the cyst. **(D)** On color Doppler flow imaging, blood flow signals were visible in the cystic wall and septa. **(E–H)** The ultrasound features of cystic-solid-type SO. **(E, F)** Two-dimensional ultrasound showed cystic-solid SO with several hyperechoic and different-sized nodules (arrow) in the cystic area (known as "strum pearls"). In addition, thick septa can be found in panel **(F, G)** The "amniotic fat ball" (asterisk) also can be found in the cystic area of cystic-solid SO patients. **(H)** On CDFI, blood flow signals were visible in the solid component. **(I–L)** The ultrasound characteristics of solid type of SO. **(I, J)** A solid-type SO patient showed regular morphology with rich blood flow. **(K, L)** A solid-type SO patient showed irregular morphology with rich blood flow. SO, struma ovarii; CDFI, color Doppler flow imaging.

formation mechanism of the comet tail sign may be similar to that of a thyroid glial cyst (25). Solid-cystic type was often larger, which may be related to the secretory function of thyroid tissue, and the continuous secretion of glial cells leads to the enlargement of tumor mass (25). More internal compartments and nodular or papillary protrusions were seen in the capsule wall and compartments. This nodular or papillary protrusion was also called "thyroid pearl" (28), which was a special ultrasonic manifestation. The size of the "thyroid pearl" was generally small, and it could be single or multiple, and CDFI showed rich blood flow within it. However, some components were similar to "amniotic fat ball", which were floating in the sac; CDFI did not show obvious blood flow, and most of them were colloids secreted by thyroid tissue. More interesting, most of the capsule walls had a "comet tail" too. The solid type was characterized by a well-defined boundary and moderate internal echo, and CDFI showed rich blood flow. This type overlapped with many other ovarian malignancies. According to the IOTA system (29), cystic with multiple septa, solid-cystic, and solid types of SO could be easily misdiagnosed. In this study, all the cases had clearly boundaries; even 26 cases were diagnosed as malignant or unclear type by ultrasound, but only three cases were finally malignant. A review of the ultrasound images revealed that the tumor had clear boundaries and a moderate internal echo similar to thyroid tissue, which may be the difference between SO and other ovarian malignancies (25). The rich blood flow in tumors was related to the abundant fibrovascular matrix (30). The ultrasonographic manifestations of solid-cystic and solid SO are complex and often misdiagnosed, which leads to unnecessary laparotomy and extensive operation.

The advantage of CEUS was that it could show low-velocity blood flow (31), which had been widely used. In this study, two patients of cystic type had "thyroid pearls" visible on the cyst wall, and color Doppler showed no obvious blood flow signal. However, contrast perfusion was seen by CEUS with slow and equal enhancement. The "thyroid pearl" was considered to be composed of thyroid tissue and matrix with rich blood vessels and fibers (30), which had endocrine functions. It can be found that the display of microcirculation by CEUS was superior to CDFI. In the other case, the cystic-solid type showed an "amniotic fat ball" sign on 2D ultrasound, and no contrast perfusion was observed even when using CEUS. This was because these "amniotic fat balls" were actually colloids secreted by thyroid tissue, concentrated in cysts, and without vessels inside. They looked like "thyroid pearls". Therefore, CEUS can obtain more imaging information and help to deeply understand the pathological features of this lesion. At the same time, the visualization of intra-tumoral microcirculation by CEUS can improve the identification of benign and malignant (32). Some scholars have found the discrepancy in microcirculation density in benign and malignant tumors (33) and revealed that the solid part of ovarian cancer was characterized by high enhancement with rapid perfusion and fast regression (32, 34). In contrast, the ovarian physiological luteal hematoma showed circular enhancement on the thick wall and without contrast perfusion in the internal area (34). Benign ovarian sex cord stromal tumors showed sparse or no enhancement, while malignant tumors showed rapid and high enhancement (35). The results of this study show that SO is characterized by slow enhancement and regression on CEUS, which is more consistent with the manifestations of benign tumors.

The MRI manifestations of SO were complex. Multiple cysts and heterogeneous signals usually show low signals in T1WI. However, they change with the increase of mature fat components. In this cohort, half of the patients showed hypo-

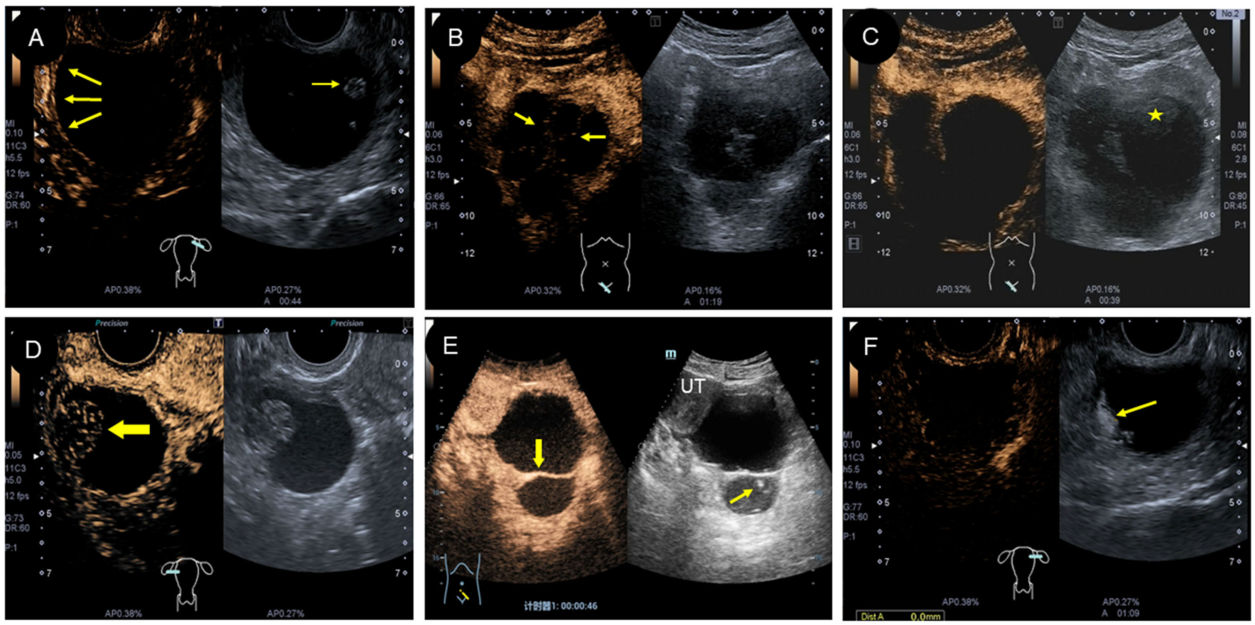

FIGURE 4
Characteristics of CEUS in different types of struma ovarii. **(A)** CEUS showed low enhancement of the cyst wall and papillary protrusion (arrow). **(B)** and **(E)** Different forms of septations in cyst were enhanced, but the light spot was unenhanced. **(C)** The "amniotic fat ball" (asterisk) in cyst showed no contrast agent perfusion on CEUS. **(D)** CEUS displayed that the solid area (arrow) was low enhanced in a cystic-solid-type SO. **(F)** CEUS showed that the irregular protrusion in cyst wall (arrow) was low enhanced, which was verified as a struma carcinoid pathologically. CEUS, contrast-enhanced ultrasound; SO, struma ovarii.

TABLE 4 Magnetic resonance imaging (MRI) features of the 12 patients of SO.

MRI Project	Pure SO (n = 6)			Impure SO (n = 6)		
	Hypo-intensity	Heterogeneity	Hyperintensity	Hypo-intensity	Heterogeneity	Hyperintensity
T1WI	2 (16.67%)	4 (33.33%)		4 (33.33%)	2 (16.67%)	
T2WI		3 (25.0%)	2 (16.67%)	2 (16.67%)	2 (16.67%)	2 (16.67%)
DWI	2 (16.67%)		3 (25.0%)		3 (25.0%)	1 (8.33%)

Values are expressed as n (%).
SO, struma ovarii; T1WI, T1-weighted imaging; T2WI, T2-weighted imaging; DWI, diffusion-weighted imaging.

intensity in T1WI, but the other half showed heterogeneity for containing mature fat components. T2WI showed a high signal and/or very low signal, depending on the protein content of SO. The signal can gradually decrease with the increase of the viscosity in the lesions (8, 9). If there was jelly-like material in the capsule, T2WI could show a very low signal, which was the characteristic MRI appearance of SO (36). Moreover, hemorrhage in the cyst can increase the signal in the cyst (8). In this study, T2WI showed almost all cases of heterogeneity and hyperintensity for less content of jelly-like material. Diffusion-weighted imaging was capable of reflecting the diffusion patterns of water molecules within living tissue. Where the protein content and viscosity within the lesions were minimal, DWI typically demonstrated unrestricted diffusion as in previous studies (8, 37). In this study, there was no enhancement observed in the cystic portion of the tumor. However, the cystic wall, septa, and "struma pearls" exhibited prominent enhancement for abundant blood vessels and fibers. Consistently, all cases in our study exhibited marked enhancement. The presence of imaging findings that were indicative of multiple signal patterns on T1WI and T2WI reflecting the content of thyroid colloids, hypervascularity, and restricted diffusion within the solid component on DWI collectively suggest the presence of a specific condition. These comprehensive imaging features contributed to a more accurate diagnosis and understanding of the pathophysiology of SO.

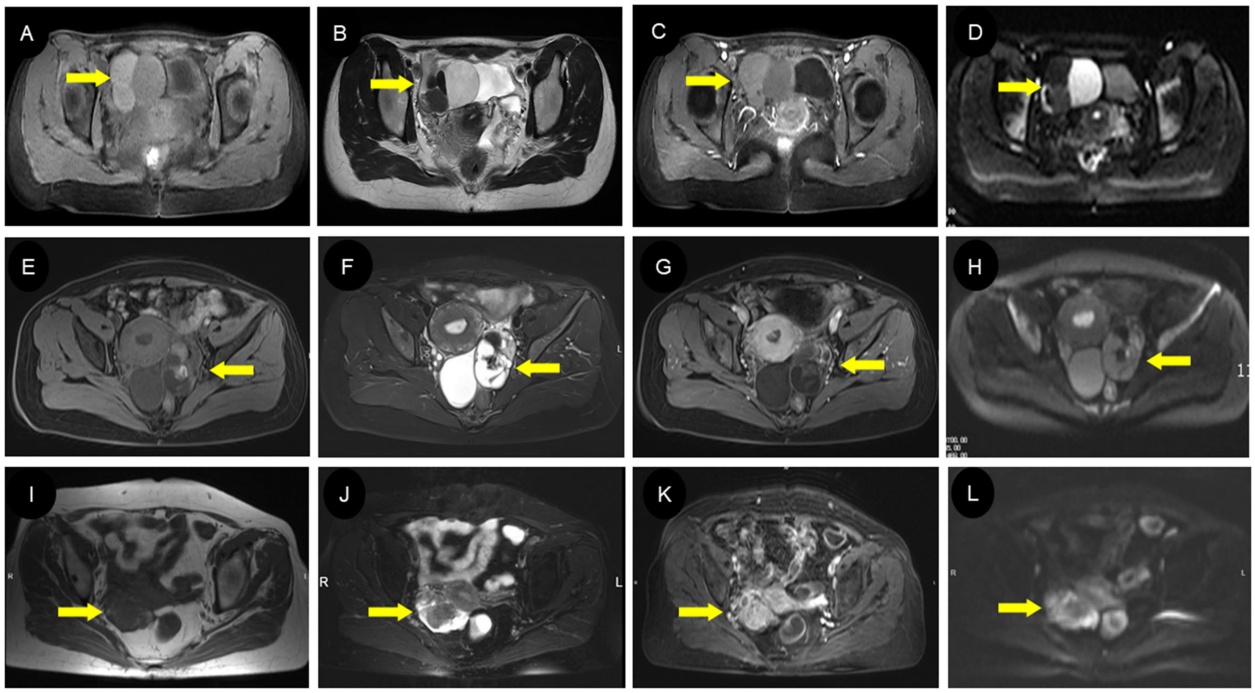

FIGURE 5
MRI findings of different types of struma ovarii. **(A–D)** A 23-year-old woman with cystic-type SO with multiple circular signal shadows in the right ovary. The cyst had slightly low signal in axial T1WI **(A)** and high/low signal in T2WI **(B)** with enhanced internal septa **(C)**. The DWI images **(D)** exhibited diverse cyst signals, suggestive of the varying viscosity of the cyst fluid, which can be indicative of a diagnosis of SO. The extremely low signal on T2WI **(B)** represents the colloidal substances consisting of thyroglobulin, thyroid hormones, and so on, which is of great value in diagnosing SO. **(E–H)** A 44-year-old woman with mixed-type SO with a solid and cystic mass in the left ovary. There was heterogeneous signal intensity on both T1WI **(E)** and T2WI **(F)** owing to regions of fluid, hemorrhage, and calcification; prominent contrast enhancement was seen in the solid part **(G)**. Locally hyperintense regions on the DWI **(H)** are presented on the DWI images, suggesting a higher concentration of thyroglobulin within the lesion. **(I–L)** A 71-year-old woman with solid-type SO with a heterogeneous lesion in the right ovary. Most parts of the lesion showed iso-intensity on both T1WI **(I)** and T2WI **(J)** with vivid uneven enhancement **(K)**, while the surrounding wreath-like cystic part presented slightly hyperintense signals on T1WI **(I)**, markedly hyperintense signals on T2WI **(J)**, and hyperintense signals on DWI **(L)**. SO, struma ovarii; T1WI, T1-weighted imaging; T2WI, T2-weighted imaging; DWI, diffusion-weighted imaging.

Study limitations

Several limitations of this study should be noted. First, because it is a retrospective study, some clinical and imaging data are incomplete, and only 12 patients underwent MRI examination in our study, so the contrastive analysis of different imaging in all patients is unavailable. Second, this research was derived from a single center with a relatively small sample size, so a multicenter, large sample, prospective study is needed to further increase the understanding of this rare entity.

Conclusion

SO is a clinically rare disease and may be easily misdiagnosed. However, there are some characteristic manifestations in imageology. In cystic or cystic-solid lesions with clear boundary located in the adnexa, 2D ultrasound presents "thyroid pearl", "amniotic fat ball", and "comet tail" in the cystic area; CEUS shows blood flow in papillary protrusion or septation. MRI shows a high signal or confounding signal in T2WI and a low signal in T1WI but with enhanced nodules. An accurate understanding of the imaging manifestations of SO can help radiologists identify this disease and provide a basis for an appropriate clinical therapeutic regime.

Data availability statement

The raw data supporting the conclusions of this article will be made available by the authors, without undue reservation.

Ethics statement

This study was approved by the Medical Ethics Committee of Ningbo First Hospital (No. 2024-041RS-01). All patients provided their written informed consent to participate in this study.

Author contributions

MC: Conceptualization, Data curation, Writing – original draft, Writing – review & editing. SL: Data curation, Formal analysis, Writing – review & editing. YX: Investigation, Resources, Writing – review & editing. XY: Data curation, Writing – review & editing. XJ: Formal analysis, Writing – review & editing. SZ: Formal analysis, Validation, Writing – original draft, Writing – review & editing.

Funding

The author(s) declare that no financial support was received for the research and/or publication of this article.

Conflict of interest

The authors declare that the research was conducted in the absence of any commercial or financial relationships that could be construed as a potential conflict of interest.

Publisher's note

All claims expressed in this article are solely those of the authors and do not necessarily represent those of their affiliated organizations, or those of the publisher, the editors and the reviewers. Any product that may be evaluated in this article, or claim that may be made by its manufacturer, is not guaranteed or endorsed by the publisher.

Supplementary material

The Supplementary Material for this article can be found online at: https://www.frontiersin.org/articles/10.3389/fonc.2025.1487812/full#supplementary-material

References

1. Podfiguma A, szeliga A, Horwat P, Maciejewska-Jeske M, Meczekalski B. Hyperthyroidism associated with struma ovarii - a case report and review of literature. *Gynecol Endocrino*. (2021) 37:1143–50. doi: 10.1080/09513590.2021.1963953

2. Devaney K, Snyder R, Norris HJ, Tavassoli FA. Proliferative and histologically Malignant struma ovarii: a clinicopathologic study of 54 cases. *Int J Gynecol Patho*. (1993) 12:333–43. doi: 10.1097/00004347-199310000-00008

3. Li S, Hong R, Yin M, ZhangT , Zhang X, Yang J. Incidence, clinical characteristics, and survival outcomes of ovarian strumal diseases: a retrospective cohort study. *BMC Women's Healt*. (2023) 23:497. doi: 10.1186/s12905-023-02624-5

4. Jiang W, Lu X, Zhu ZL, Liu XS, Xu CJ. Struma ovarii associated with pseudo-Meigs' syndrome and elevated serum CA 125: a case report and review of the literature. *J Ovarian Re*. (2010) 3:18. doi: 10.1186/1757-2215-3-18

5. Yoo SC, Chang KH, Lyu MO, Chang SJ, Ryu HS, Kim HS. Clinical characteristics of struma ovarii. *J Gynecol Onc*. (2008) 19:135–8. doi: 10.3802/jgo.2008.19.2.135

6. Li Z, Wang J, Chen Q. Struma ovarii and peritoneal strumosis during pregnancy. *BMC Pregnancy Childbirt*. (2021) 21:347. doi: 10.1186/s12884-021-03815-4

7. Ayhan S, Kilic F, Ersak B, Aytekin O, Akar S, Turkmen O, et al. Malignant struma ovarii: From case to analysis. *J Obstet Gynaecol R*. (2021) 47:3339–51. doi: 10.1111/jog.14902

8. Yamauchi S, Kokabu T, Kataoka HC, Yoriki K, Takahata A, Mori T, et al. Computed tomography, magnetic resonance imaging, and positronemission tomography/computed tomography findings for the diagnosis of Malignant struma ovarii: A case report. *J Obstet Gynaecol R*. (2023) 49:1456–61. doi: 10.1111/jog.15619

9. Tamura N, Murakami K, Ozaki R, Takeuchi S, Ochiai A, Kawasaki Y, et al. Current state of management of struma ovarii and preoperative imaging features: A retrospective case series study of 18 patients at a single institution. *J Obstet Gynaecol Re*. (2023) 49:1007–11. doi: 10.1111/jog.15545

10. Lei X, Zhou Y, Kong L, Kong Z. A rare case of struma ovarii: Typical CT imaging. *Asian J Sur*. (2024) 47:1265–6. doi: 10.1016/j.asjsur.2023.11.060

11. Mancuso A, Triolo O, Leonardi I, De Vivo A. Struma ovarii: a rare benign pathology which may erroneously suggest Malignancy. *Acta Obstet Gynecol Scan*. (2001) 80:1075107–6. doi: 10.1034/j.1600-0412.2001.801121.x

12. Horn-Ross PL, Canchola AJ, Ma H, Reynolds P, Bernstein L. Hormonal factors and the risk of papillary thyroid cancer in the California Teachers Study cohort. *Cancer Epidemiol Biomarkers Pre*. (2011) 20:1751–9. doi: 10.1158/1055-9965.EPI-11-0381

13. Kennedy RL, Darne J. The role of hCG in regulation of the thyroid gland in normal and abnormal pregnancy. *Obstet Gynecol*. (1991) 78:298–307.

14. Robboy SJ, Shaco-Levy R, Peng RY, Snyder MJ, Donahue J, Bentley RC, et al. Malignant struma ovarii: an analysis of 88 cases, including 27 with extraovarian spread. *Int J Gynecol Patho*. (2009) 28:405–22. doi: 10.1097/PGP.0b013e3181a27777

15. Peyron N, Coulon A. Struma ovarii pseudo-Meigs'syndrome and raised CAl25, a rare association. *Diagn Interv Imagin*. (2012) 93:643–7. doi: 10.1016/j.diii.2012.03.012

16. Shou L, Lu J, Yang J, Wang H, Sun L, Dong H, et al. Follicular carcinoma originating from struma ovarii: A case report. *Medicine*. (2023) 102:e32658. doi: 10.1097/MD.0000000000032658

17. Cui Y, Yao J, Wang S, Zhao J, Dong J, Liao L. The clinical and pathological characteristics of Malignant struma ovarii: an analysis of 144 published patients. *Front Onco*. (2021) 5:645156. doi: 10.3389/fonc.2021.645156

18. Li S, Yang T, Xiang Y, Li X, Zhang L, Deng S, et al. Clinical characteristics and survival outcomes of malignant struma ovarii confined to the ovary. *BMC Cance*. (2021) 21:383. doi: 10.1186/s12885-021-08118-7

19. Choi HY, Pak MG, Park JW. Fortuitously detected primary ovarian carcinoid tumor: A case report. *Medicine*. (2023) 102:e34391. doi: 10.1097/MD.0000000000034391

20. Muller KE, Tafe LJ, Gonzalez JL, West LA, Schned AR. Ovarian strumal carcinoid producing peptide YY associated with severe constipation: a case report and review of the literature. *Int J Gynecol Patho*. (2015) 34:30–5. doi: 10.1097/PGP.0000000000000117

21. Zhang PJ, Gao HG, Pasha TL, Litzky L, Livolsi VA. TTF-1 expression in ovarian and uterine epithelial neoplasia and its potential significance, an immunohistochemical assessment with multiple monoclonal antibodies and different secondary detection systems. *Int J Gynecol Patho*. (2009) 28:10–8. doi: 10.1097/PGP.0b013e3181804bc6

22. Turla A, Zamparini M, Milione M, Grisanti S, Amoroso V, Pedersini R, et al. Ovarian strumal carcinoid: case report, systematic literature review and pooled analysis. *Front Endocrino*. (2022) 13:871210. doi: 10.3389/fendo.2022.871210

23. Robboy SJ, Scully RE. Strumal carcinoid of the ovary: An analysis of 50 cases of a distinctive tumor composed of thyroid tissue and carcinoid. *Cancer*. (1980) 46:2019–34. doi: 10.1002/1097-0142(19801101)46:9<2019::AID-CNCR2820460921>3.0.CO;2-W

24. Li S, Wang X, Sui X, Zhang X, Yin M, Yang J. Clinical characteristics and survival outcomes in patients with ovarian strumal carcinoid. *BMC Cancer*. (2022) 22:1090. doi: 10.1186/s12885-022-10167-5

25. Hoang VT, Trinh CTA. Review of the pathology, diagnosis and management of colloid goitre. *Eur Endocrino*. (2020) 16:131–5. doi: 10.17925/EE.2020.16.2.131

26. Ciobanu DG, BuȚureanu TA, Socolov DG, Scripcaru DC, Rosin OL, Lozneanu L. Ovarian strumal carcinoid - case report. *Rom J Morphol Embryo*. (2017) 58:1035–40.

27. Yuan Y, Li H, Yang H. Clinicopathological observation of mature teratoma with Malignant transformation, a single center retrospective study. *Indian J Pathol Micr*. (2022) 65:369–73. doi: 10.4103/IJPM.IJPM_828_20

28. Weinberger V, Kadlecova J, Minář L. Struma ovarii - ultrasound features of a rare tumor mimicking ovarian cancer. *Med Ultrason*. (2018) 20:355–61. doi: 10.11152/mu-1526

29. Carballo EV, Maturen KE, Li Z. Surgical outcomes of adnexal masses classified by IOTA ultrasound simple rules. *Sci Re*. (2022) 12:21848. doi: 10.1038/s41598-022-26441-2

30. Dujardin MI, Sekhri P, Turnbull LW. Struma ovarii: role of imaging? *Insights Imagin*. (2014) 5:41–51. doi: 10.1007/s13244-013-0303-3

31. Sun M, Zhang B. Contrast-enhanced ultrasound of ovarian steroid cell tumor, not otherwise specified: A case report. *Oncol Let*. (2022) 24:370. doi: 10.3892/ol.2022.13490

32. Xun L, Zhai L, Xu H. Comparison of conventional, doppler and contrast-enhanced ultrasonography in differential diagnosis of ovarian masses: a systematic review and meta-analysis. *BMJ Ope*. (2021) 11:e052830. doi: 10.1136/bmjopen-2021-052830

33. Liu C, Li Y, Zhu Y, Lu M. The value of IOTA simple rules combined with CEUS scoring system in the diagnosis of benign and Malignant ovarian masses and its correlation with MVD and VEGF: A preliminary study. *J Ultras Me*. (2022) 41:2983–92. doi: 10.1002/jum.15999

34. Lu B, Liu C, Qi J, He W, Shi T, Zhu Y, et al. Comparison of contrast-enhanced ultrasound, IOTA simple rules and O-RADS for assessing the Malignant risk of sonographically appearing solid ovarian masses. *J Gynecol Obstet Hum Repro*. (2023) 52:102564. doi: 10.1016/j.jogoh.2023.102564

35. Xu Y, Xue N, Zhang S, Wei Z. The value of contrast-enhanced ultrasonography in differential diagnosis of benign and Malignant ovarian sex cord stromal tumors. *Gland Sur*. (2022) 11:1086–93. doi: 10.21037/gs-22-301

36. Ikeuchi T, Koyama T, Tamai K, et al. CT and MR features of struma ovarii. *Abdom Imaging*. (2012) 37:904–10. doi: 10.1007/s00261-011-9817-7

37. Takeshita T, Nino T, Maebayashi T, Mniki Y, Hashimoto S, Mniki Y. Diffusion-weighted magnetic resonance imaging findings in a patient with struma ovarii. *Osaka City Med*. (2014) 60:45–52.

frontiers | Frontiers in Oncology

TYPE Case Report
PUBLISHED 29 May 2025
DOI 10.3389/fonc.2025.1480730

Check for updates

OPEN ACCESS

EDITED BY
Robert Fruscio,
University of Milano Bicocca, Italy

REVIEWED BY
Giuseppe Scibilia,
Gynecology and Obstetrics Department, Italy
Raghunadharao Digumarti,
MNJ Institute of Oncology & Regional Cancer Centre, India

*CORRESPONDENCE
Hongjing Wang
whjscdx@163.com

RECEIVED 14 August 2024
ACCEPTED 07 May 2025
PUBLISHED 29 May 2025

CITATION
Li T, Jiang W and Wang H (2025) Fertility-sparing surgery in primary peritoneal serous borderline tumor: a case report. *Front. Oncol.* 15:1480730. doi: 10.3389/fonc.2025.1480730

COPYRIGHT
© 2025 Li, Jiang and Wang. This is an open-access article distributed under the terms of the Creative Commons Attribution License (CC BY). The use, distribution or reproduction in other forums is permitted, provided the original author(s) and the copyright owner(s) are credited and that the original publication in this journal is cited, in accordance with accepted academic practice. No use, distribution or reproduction is permitted which does not comply with these terms.

Fertility-sparing surgery in primary peritoneal serous borderline tumor: a case report

Tingting Li[1,2], Wei Jiang[3] and Hongjing Wang[1,2]*

[1]Department of Gynecology and Obstetrics, West China Second University Hospital, Sichuan University, Sichuan, Chengdu, China, [2]Key Laboratory of Birth Defects and Related Diseases of Women and Children (Sichuan University), Ministry of Education, Sichuan, Chengdu, China, [3]Department of Pathology, West China Second University Hospital, Sichuan University, Sichuan, Chengdu, China

Primary peritoneal serous borderline tumor (PPSBT) is a rare, low-malignant-potential neoplasm arising from the peritoneum, diagnosed only after excluding ovarian involvement. While typically discovered incidentally during surgery, it often presents with infertility or abdominal pain in young women. Due to its favorable prognosis and the desire to preserve fertility, fertility-sparing surgery (FSS) is a critical consideration. We report a case of PPSBT in a reproductive-aged woman who underwent three FSS procedures, demonstrating the feasibility of this approach. Our findings support FSS as a viable option for PPSBT patients after thorough exclusion of ovarian malignancy. This case underscores the importance of comprehensive surgical staging and multidisciplinary evaluation to optimize oncological and reproductive outcomes. Further research is needed to standardize management strategies for this rare condition.

KEYWORDS

PPSBT: primary peritoneal serous borderline tumor, FSS: fertility-sparing surgery, SBT: ovarian serous borderline tumors, ovarian lesion, case report

Introduction

Extra-ovarian peritoneal implants are observed in 30–50% of women with ovarian serous borderline tumors (SBTs) (1). However, similar peritoneal lesions have been reported in cases with no ovarian involvement or only minimal surface involvement. These lesions have been described using various terms, including atypical endosalpingiosis, primary papillary peritoneal neoplasia, serous micropapillomatosis of low malignant potential, and serous papillary borderline tumors of the peritoneum (2). Currently, the most widely accepted terminology is PPSBT (3), which emphasizes its histological resemblance to non-invasive implants of SBTs. PPSBT is a rare, low-malignant-potential neoplasm arising from the peritoneum. It is diagnosed only when ovarian involvement is absent, distinguishing it from secondary peritoneal implants of ovarian SBTs (4). Most reported cases of PPSBT were incidentally detected during laparotomy or laparoscopy (2, 4, 5). The majority of affected women (>80%) are premenopausal, typically between 30 and 40 years of age (2). Common clinical presentations include infertility and abdominal pain.

Although standardized treatment guidelines for PPSBT are lacking, surgical debulking of peritoneal lesions remains the primary approach. Given its excellent prognosis and frequent occurrence in young women of reproductive age, FSS should be considered after excluding an ovarian primary tumor. Here, we present a case of PPSBT in a patient who underwent three FSS procedures.

Case report

The patient was a 33-year-old nulliparous woman presenting with secondary infertility, admitted to West China Second University Hospital, Sichuan University. Hysterosalpingography revealed intrauterine adhesions and bilateral fallopian tube adhesions. The patient denied any personal or family history of malignancy. Her medical history was significant for two failed *in vitro* fertilization-embryo transfer (IVF-ET) cycles due to infertility, both resulting in spontaneous abortions. These procedures necessitated repeated intrauterine manipulations, which subsequently led to the formation of intrauterine and tubal adhesions. Serum tumor marker levels were within normal limits. Transvaginal ultrasound confirmed intrauterine adhesions, while hysterosalpingography demonstrated bilateral tubal occlusion. Given the patient's strong reproductive desire, she underwent combined hysteroscopic and laparoscopic adhesiolysis as the primary surgical intervention. Laparoscopic exploration revealed multiple disseminated miliary nodules on the posterior uterine wall, anterior rectal wall, bilateral fallopian tubes, and pelvic sidewalls surrounding the ovaries. Surgical management included hysteroscopic adhesiolysis, laparoscopic salpingolysis, and excision of pelvic lesions. Notably, post-adhesiolysis examination showed no macroscopic evidence of ovarian or tubal neoplasia. Intraoperative frozen section analysis of the posterior uterine wall lesions showed serous tumors with extensive psammomatous calcification. Final histopathological examination confirmed non-invasive implants of a serous borderline tumor with psammoma bodies (Figure 1A). The primary origin of these lesions remained undetermined. Following multidisciplinary consultation and thorough discussion of the risks, the patient elected for conservative management with close surveillance. The follow-up protocol included regular transvaginal ultrasonographic evaluation of the uterus and adnexa, along with serial tumor marker assessment.

Notably, the second surgery was performed 16 months after the initial procedure. The patient was admitted to Xinan Gynecological Hospital in Chengdu for in IVF-ET. Preoperative ultrasound findings indicated hydrosalpinx, prompting a combined hysteroscopy and laparoscopy. Due to limited exposure of the right fallopian tube, a left salpingectomy and right tubal ligation were performed. During laparoscopy, a well-demarcated, grayish-white nodule (approximately 1 cm in diameter) was observed near the right pelvic sidewall. Additionally, multiple small miliary nodules were identified in the right paracolic gutter and upper abdominal region. Given these findings, the patient's family was consulted intraoperatively, and a biopsy of the pelvic nodule was performed. Histopathological examination confirmed the presence of both invasive and non-invasive implants of a serous borderline tumor with psammoma bodies.

One month after the second surgery, the patient returned to West China Second University Hospital, Sichuan University, for evaluation of suspected tumor progression. Pathological consultation revealed disseminated pelvic lesions and right fallopian tube involvement, characterized by invasive and non-invasive implants of a serous borderline tumor with psammoma bodies (Figures 1B, C). Peritoneal lavage cytology further confirmed a serous borderline tumor, likely of adnexal origin. Intriguingly, laparoscopy showed no macroscopic ovarian tumors. Given these findings, the patient was diagnosed with advanced serous borderline ovarian tumor, prompting cytoreductive surgery with comprehensive staging. After obtaining detailed informed consent, the procedure included: Pelvic lymph node dissection, Para-aortic lymph node sampling, Left salpingectomy, Omentectomy, Appendectomy, Tumor debulking (achieving no visible residual disease). Since prior surgeries had not performed ovarian biopsies, bilateral ovarian biopsies were conducted to assess occult lesions. Histopathology confirmed serous borderline tumor implants with psammoma bodies in the omentum, appendix, and pelvic peritoneum (Figures 1D, E).

According to World Health Organization (WHO) criteria, the tumor was classified as borderline malignancy. Due to the absence of ovarian involvement, this case was defined as PPSBT. The patient received four cycles of chemotherapy (cyclophosphamide + cisplatin) and remained disease-free for 8 years post-surgery. However, 6 years after FSS, she underwent bilateral oophorectomy due to encapsulated ovarian effusions, resulting in permanent loss of reproductive function.

Discussion and conclusions

PPSBT is a rare neoplasm of the peritoneal cavity with potential malignant behavior, hypothesized to arise from remnants of the secondary Müllerian system embedded within or adjacent to the peritoneum (6). Typically, PPSBT is discovered incidentally during surgical procedures. While it predominantly affects women of reproductive age, isolated cases have been reported in postmenopausal individuals (7). Clinically, PPSBT most commonly manifests with two primary symptoms: infertility and abdominal pain. Limited research exists on its risk factors, though current evidence suggests an association with nulliparity and infertility; however, the role of hereditary factors remains unclear (2).

In our case, PPSBT was incidentally discovered during diagnostic laparoscopy for infertility. Laparoscopic examination revealed pelvic peritoneal involvement, manifesting as diffuse adhesions, small nodules, or miliary granularity. Histologically, PPSBT exhibits features resembling non-invasive implants of low malignant potential serous ovarian neoplasms.

Abbreviations: PPSBT, primary peritoneal serous borderline tumor; FSS, fertility-sparing surgery; WHO, World Health Organization; SBT, ovarian serous borderline tumors; IVF-ET, *in vitro* fertilization-embryo transfer; CT, computed tomography; MRI, magnetic resonance imaging; PET, positron emission tomography.

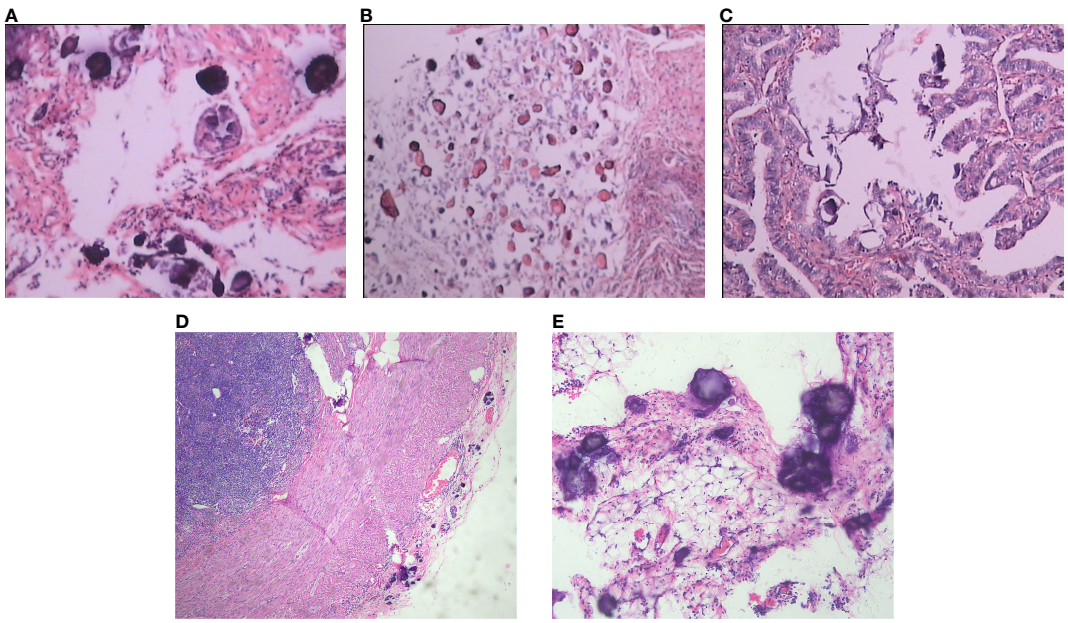

FIGURE 1
Pathological findings of the specimens obtained from the three surgeries. **(A)** The nodules on the posterior uterine wall (HEx200). **(B)** The tumors on the pelvic region showed Invasive and non-invasive implant foci of borderline serous adenoma with sand formation (HEx200). **(C)** The tumors on the right fallopian tube showed Invasive and non-invasive implant foci of borderline serous adenoma with sand formation (HEx200). **(D)** Appendix demonstrated a large number of sand grains and borderline serous tumors(HEx40). **(E)** Omentum demonstrated a large number of sand grains and borderline serous tumors (HEx100).

The definitive diagnosis was confirmed by pathological examination, which identified epithelial and desmoplastic non-invasive lesions without ovarian involvement. Notably, psammoma bodies and endosalpingiosis were observed in up to 88% of cases (1). As pathological examination remains the gold standard for diagnosing gynecological tumors, the differential diagnosis of PPSBT is critical. Key considerations include: Endometriosis and endosalpingiosis; Benign reactive mesothelial proliferations (e.g., adenomatoid tumor or florid mesothelial hyperplasia); Borderline mesothelial proliferations with overlapping histological features, such as benign or well-differentiated papillary mesothelioma (5, 8). Among neoplastic differentials, primary ovarian papillary serous borderline tumor with peritoneal implants and high-grade primary peritoneal papillary serous carcinoma are the most clinically significant (9). To date, no comparative studies have systematically distinguished PPSBT from primary ovarian serous borderline tumors. Thus, conventional histomorphological analysis combined with microscopic evaluation remains the cornerstone of diagnosis.

Standardized therapeutic guidelines for PPSBT remain undefined. Historically, the recommended treatment involved total abdominal hysterectomy with bilateral salpingo-oophorectomy and omentectomy; however, the clinical benefits of this aggressive approach lack robust evidence. Currently, the primary management for PPSBT consists of surgical debulking of peritoneal lesions. For young women desiring fertility preservation, fertility-sparing surgery (FSS) may be considered after thorough exclusion of an ovarian primary tumor. The role of adjuvant therapy in PPSBT remains controversial. Chemotherapy demonstrates limited efficacy, with only a minority of patients exhibiting a response (10). In a study by Janna et al. (2), adjuvant chemotherapy or radiation was administered in 15.3% of cases, yet no significant prognostic improvement was observed, suggesting that such interventions may be unnecessary. Notably, PPSBT is associated with an excellent prognosis, characterized by a low risk of recurrence or malignant transformation to low-grade serous carcinoma. Long-term survival rates mirror those of women with serous borderline ovarian tumors and non-invasive peritoneal implants, with a 95% survival rate over a mean follow-up period of 6.6 years (11). Furthermore, successful pregnancies following conservative treatment have been documented, highlighting the feasibility of fertility preservation in select cases (4).

Although FSS is a viable treatment option for young patients with PPSBT, its clinical application poses significant challenges in disease management. A key difficulty lies in the initial diagnosis of PPSBT, as these cases are often detected incidentally during laparotomy or laparoscopy, typically in the context of infertility and extensive pelvic adhesions. In this report, we present the case of a female patient with PPSBT who underwent FSS on three separate occasions. Notably, despite repeated interventions, the patient did not achieve a successful pregnancy, a outcome likely influenced by multiple contributing factors.

The preoperative evaluation was constrained by two key factors: (i) the patient's prior IVF-ET treatment at an external institution obscured clinical suspicion of malignancy, and (ii) the absence of computed tomography(CT)/magnetic resonance imaging(MRI) before both surgical interventions due to the unexpected tumor diagnosis. This lack of cross-disciplinary consultation particularly manifested in three aspects: First, diagnostic monitoring proved inadequate during follow-up. While serial transvaginal ultrasounds and tumor marker assays were performed, advanced imaging surveillance (CT/MRI) was omitted. Second, the assisted reproduction team exclusively addressed hydrosalpinx management prior to the second surgery without comprehensive oncological

evaluation. Third, no individualized treatment plan was established through tumor board discussion post-diagnosis, despite the patient's unique profile of having undergone two failed IVF-ET cycles with consequently limited natural conception potential.

The case highlights the growing imperative for multimodal treatment approaches in fertility-preserving oncology care. A notable opportunity existed during the initial FSS: prophylactic bilateral salpingectomy could have potentially averted subsequent hydrosalpinx-related adhesions while simultaneously reducing cumulative surgical trauma to the pelvic environment. This strategy finds support in Marchette et al.'s (12) findings that while surgical approach (conservative vs. radical) does not affect recurrence rates or fertility outcomes in serous borderline ovarian tumors, repeated surgical interventions demonstrably compromise residual fertility potential.

In the present case, the patient primarily exhibited extraovarian implants, and PPSBT was not initially considered due to the absence of an identifiable primary lesion. This diagnostic oversight is not uncommon and may lead to delayed recognition of PPSBT, ultimately influencing surgical decision-making. Given the patient's strong desire for fertility preservation and the potential risks associated with repeated surgeries, close postoperative surveillance was implemented following the first FSS. Subsequent pathological analysis from the second FSS suggested an adnexal origin of the tumor. Notably, no distinct lesions were detected in the bilateral ovaries during any of the three FSS procedures, including the third surgery, in which ovarian biopsies also revealed no evidence of tumor involvement. This absence of ovarian pathology may have contributed to the initial misdiagnosis, complicating the differentiation between PPSBT and serous borderline ovarian tumor.

Finally, restaging surgery was not performed in a timely manner. Although no gross lesions were detected in the bilateral ovaries, restaging—along with the identification of the primary lesion based on the initial FSS pathology—remained a critical step. Notably, preoperative positron emission tomography (PET) imaging was not conducted for this patient, which could have aided in surgical staging. Due to the unclear origin of the primary lesion, a definitive diagnosis could not be established. Moreover, complete surgical staging was omitted, and not all potential peritoneal lesions were resected. Importantly, however, the patient remained relapse-free after undergoing comprehensive surgical staging.

The findings of this study highlight the importance of considering FSS for young patients with PPSBT. Future research should prioritize multidisciplinary collaboration to optimize diagnostic and therapeutic strategies. Additionally, this study emphasizes that comprehensive surgical staging plays a pivotal role in fertility preservation and management for this patient population.

Data availability statement

The original contributions presented in the study are included in the article/Supplementary Material. Further inquiries can be directed to the corresponding author.

Ethics statement

The studies involving humans were approved by Ethics Committee of West China Second Hospital. The studies were conducted in accordance with the local legislation and institutional requirements. The participants provided their written informed consent to participate in this study. Written informed consent was obtained from the individual(s) for the publication of any potentially identifiable images or data included in this article.

Author contributions

TL: Conceptualization, Data curation, Project administration, Writing – original draft, Writing – review & editing. WJ: Data curation, Investigation, Writing – original draft, Writing – review & editing. HW: Conceptualization, Supervision, Writing – original draft, Writing – review & editing.

Funding

The author(s) declare that no financial support was received for the research and/or publication of this article.

Conflict of interest

The authors declare that the research was conducted in the absence of any commercial or financial relationships that could be construed as a potential conflict of interest.

Publisher's note

All claims expressed in this article are solely those of the authors and do not necessarily represent those of their affiliated organizations, or those of the publisher, the editors and the reviewers. Any product that may be evaluated in this article, or claim that may be made by its manufacturer, is not guaranteed or endorsed by the publisher.

Supplementary material

The Supplementary Material for this article can be found online at: https://www.frontiersin.org/articles/10.3389/fonc.2025.1480730/full#supplementary-material

References

1. Bell DA, Scully RE. Serous borderline tumors of the peritoneum. *Am J Surg Pathol*. (1990) 14:230–9. doi: 10.1097/00000478-199003000-00004

2. Janna P, Eleftherios Pierre S, Matthias C, Daniel F, Patrick I. Primary peritoneal serous borderline tumors as a therapeutic challenge: a systematic review of the literature. *SN Compr Clin Med*. (2020) 2:316–26. doi: 10.1007/s42399-020-00232-0

3. Couto D, Motal F, Silva T, de Oliveira C. Primary peritoneal borderline tumour: report of an unusual case. *Eur J Gynaecol Oncol*. (2007) 28:54–6.

4. Go HS, Hong HS, Kim JW, Woo JY. CT appearance of primary peritoneal serous borderline tumour: a rare epithelial tumour of the peritoneum. *Br J Radiol*. (2012) 85:e22–5. doi: 10.1259/bjr/26458228

5. Tinelli A, Malvasi A, Pellegrino M. An incidental peritoneal serous borderline tumor during laparoscopy for endometriosis. *Eur J Gynaecol Oncol*. (2009) 30:579–82.

6. Fox H. Primary neoplasia of the female peritoneum. *Histopathology*. (1993) 23:103–10. doi: 10.1111/j.1365-2559.1993.tb00467.x

7. Biscotti CV, Hart WR. Peritoneal serous micropapillomatosis of low Malignant potential (serous borderline tumours of the peritoneum): a clinicopathologic study of 17 cases. *Am J Surg Pathol*. (1992) 16:467–75. doi: 10.1097/00000478-199205000-00005

8. Lin PY, Ueng SH, Tseng MJ. Primary peritoneal serous borderline tumor presenting as an 'adnexal torsion' gynecologic emergency. *Taiwan J Obstet Gynecol*. (2007) 46:308. doi: 10.1016/S1028-4559(08)60043-1

9. Couto D, Motal F, Silva T, de Oliveira C. Primary peritoneal borderline tumour: report of an unusual case. *Eur J Gynaecol Oncol*. (2007) 28:54.

10. Gandhi H, Bickerton NJ. Primary borderline serous neoplasia of the peritoneum. *J Obstet Gynaecol*. (2004) 24:187–8. doi: 10.1080/01443610410001653371

11. Bell DA, Weinstock MA, Scully RE. Peritoneal implants of ovarian serous borderline tumors. Histologic features and prognosis. *Cancer*. (1988) 62:2212–22. doi: 10.1002/1097-0142(19881115)62:10<2212::AID-CNCR2820621024>3.0.CO;2-W

12. Guo LL, Kang XY, Su Y, Liu XY, Wu X, Xie W. Is there re-staging surgery necessity for borderline ovarian tumors. *Curr Med Sci*. (2023) 43:822–30. doi: 10.1007/s11596-023-2775-9

Frontiers in Oncology

Advances knowledge of carcinogenesis and tumor progression for better treatment and management

The third most-cited oncology journal, which highlights research in carcinogenesis and tumor progression, bridging the gap between basic research and applications to imrpove diagnosis, therapeutics and management strategies.

Discover the latest Research Topics

See more →

Frontiers

Avenue du Tribunal-Fédéral 34
1005 Lausanne, Switzerland
frontiersin.org

Contact us

+41 (0)21 510 17 00
frontiersin.org/about/contact